





**MBL**



# THE BIOLOGICAL BULLETIN



41° 00' N

40° 00' N



Published by the Marine Biological Laboratory

[www.biolbull.org](http://www.biolbull.org)



# THE BIOLOGICAL BULLETIN ONLINE

The Marine Biological Laboratory is pleased to announce that the full text of *The Biological Bulletin* is available online at

<http://www.biolbull.org>

*The Biological Bulletin* publishes outstanding experimental research on the full range of biological topics and organisms, from the fields of Neurobiology, Behavior, Physiology, Ecology, Evolution, Development and Reproduction, Cell Biology, Biomechanics, Symbiosis, and Systematics.

Published since 1897 by the Marine Biological Laboratory (MBL) in Woods Hole, Massachusetts, *The Biological Bulletin* is one of America's oldest peer-reviewed scientific journals.

The journal is aimed at a general readership, and especially invites articles about those novel phenomena and contexts characteristic of intersecting fields.

*The Biological Bulletin Online* contains the full content of each issue of the journal, including all figures and tables, beginning with the February 2001 issue (Volume 200, Number 1). The full text is searchable by keyword, and the cited references include hyperlinks to Medline. PDF files are available beginning in February 1990 (Volume 178, Number 1), some abstracts are available

beginning with the October 1976 issue (Volume 151, Number 2), and some Tables of Contents are online beginning with the October 1965 issue (Volume 129, Number 2).

Each issue will be placed online approximately on the date it is mailed to subscribers; therefore the online site will be available prior to receipt of your paper copy. Online readers may want to sign up for the eTOC (electronic Table of Contents) service, which will deliver each new issue's table of contents *via* e-mail. The web site also provides access to information about the journal (such as Instructions to Authors, the Editorial Board, and subscription information), as well as access to the Marine Biological Laboratory's web site and other *Biological Bulletin* electronic publications.

The free trial period for access to *The Biological Bulletin* online has ended. Individuals and institutions who are subscribers to the journal in print or are members of the Marine Biological Laboratory Corporation may now activate their online subscriptions. All other access (*e.g.*, to Abstracts, eTOCs, searching, Instructions to Authors) remains freely available. Online access is included in the print subscription price.

For more information about subscribing or activating your online subscription, visit [www.biolbull.org/subscriptions](http://www.biolbull.org/subscriptions).

---

<http://www.biolbull.org>

# SEEKERS IN THE SOCIETY OF CELLS.

At Dr. Simon Watkins' lab, they look at cells the way anthropologists look at human culture: as communities of good guys and bad guys, of traders and communicators, of connections and relationships. "We are the observers,"

Simon says. "We never jump to conclusions. We let the conclusions jump to us." His mantra? "Imaging is everything." Which is why the best and the brightest of tomorrow's seekers and solvers find their way to Pittsburgh and the Watkins Lab.

**OLYMPUS MICROSCOPES. ROCKET SCIENCE™**

Find out more about Olympus microscopes at [www.olympusamerica.com/microscopes](http://www.olympusamerica.com/microscopes) 800-455-8236

## OLYMPUS®

(From L to R)

Ana Bursick - Research Specialist

Stuart Shand - Research Specialist

Simon C. Watkins, Ph.D. - Director

Glenn Papwarth - Research Associate

Ramesh Draviam - Graduate Student

Center for Biologic Imaging,  
University of Pittsburgh Medical School,  
Pittsburgh, PA

AUG 25 2003



## Cover

---

The deep sea is, in general, sparsely occupied; but in restricted areas and under unusual conditions, such as cold seeps, vents, and seamounts, dense communities do exist and persist for generations. Sparse populations also aggregate temporarily to facilitate mating, breeding, and brooding, and such reproductive aggregations are well known in various habitats—but not in the deep sea, where only three such aggregations have previously been documented.

In this issue of *The Biological Bulletin* (p. 1), Jeffrey C. Drazen and colleagues at the Monterey Bay Aquarium Research Institute (MBARI, California) describe, for the first time in the deep sea, a multi-species reproductive aggregation—or reproductive hot spot—with an unusually high population density and biomass. This aggregation is featured on the cover; it is located in 1500–1600 meters of water on the Gorda Escarpment, a submarine plateau off Cape Mendocino in northern California. The site was discovered in the course of 15 exploratory dives by MBARI's remotely operated vehicle (ROV) *Tiburon* (top left image on the cover); the vehicle's two main cameras are identifiable by the white protective collars around their glass domes. The map on the cover locates the hot spot (red circle), Cape Mendocino (red dot), and the ROV dives (the line of small, irregular black areas extending westward).

Reproductive aggregations of two species—an octopus (*Graneledone* sp.), and a fish, the blob sculpin (*Psychrolutes phrictus*)—co-occurred at this site. The bottom left image shows three octopuses (body width, ~16 cm) in a characteristic brooding position; their eggs are underneath them, attached to the rock outcrop. Also attached are several anemones of

various species; the crab is *Chionocetes* sp. The image at the top right shows octopus eggs (length, 40 mm) being sampled by the suction sampler on the ROV. Many of the eggs hatched during sampling; one hatchling appears in the sampler tube, and another is swimming away.<sup>1</sup> In the lower right image—watching from behind a rock, which is covered in brisingid sea stars and anemones—is a blob sculpin (length, ~60 cm) with a nest of large, pinkish eggs behind it. Another fish is just visible in the upper left corner of the image. Most blob sculpins were seen attending to their egg masses (e.g., Fig. 3A, p. 4), the first direct observations of parental care by an oviparous deep-sea fish.

The particular location of this reproductive hot spot could be due to environmental heterogeneity; that is, the animals were concentrated at the crest of the local topography and near cold seeps. In these situations, they might benefit from enhanced current flow and local productivity, critical resources for reproductive success in the deep sea, where oxygen tension is very low and food is in short supply. Thus, for some deep-sea species, the fortuitous occurrence of critical environmental features may be essential for reproduction.

The four images are frames selected from videos taken during dives in 2001 and 2002. The videos were produced collaboratively by the crew of the support ship *R/V Western Flyer*, the ROV *Tiburon* pilots, and the scientists. Photo credit is to MBARI. Jeffrey C. Drazen contributed to the cover and legend. The final cover was designed by Beth Liles (Marine Biological Laboratory, Woods Hole, Massachusetts).

<sup>1</sup> The octopus hatchlings are being described by Janet Voight (Chicago Field Museum), an MBARI collaborator.

# THE BIOLOGICAL BULLETIN

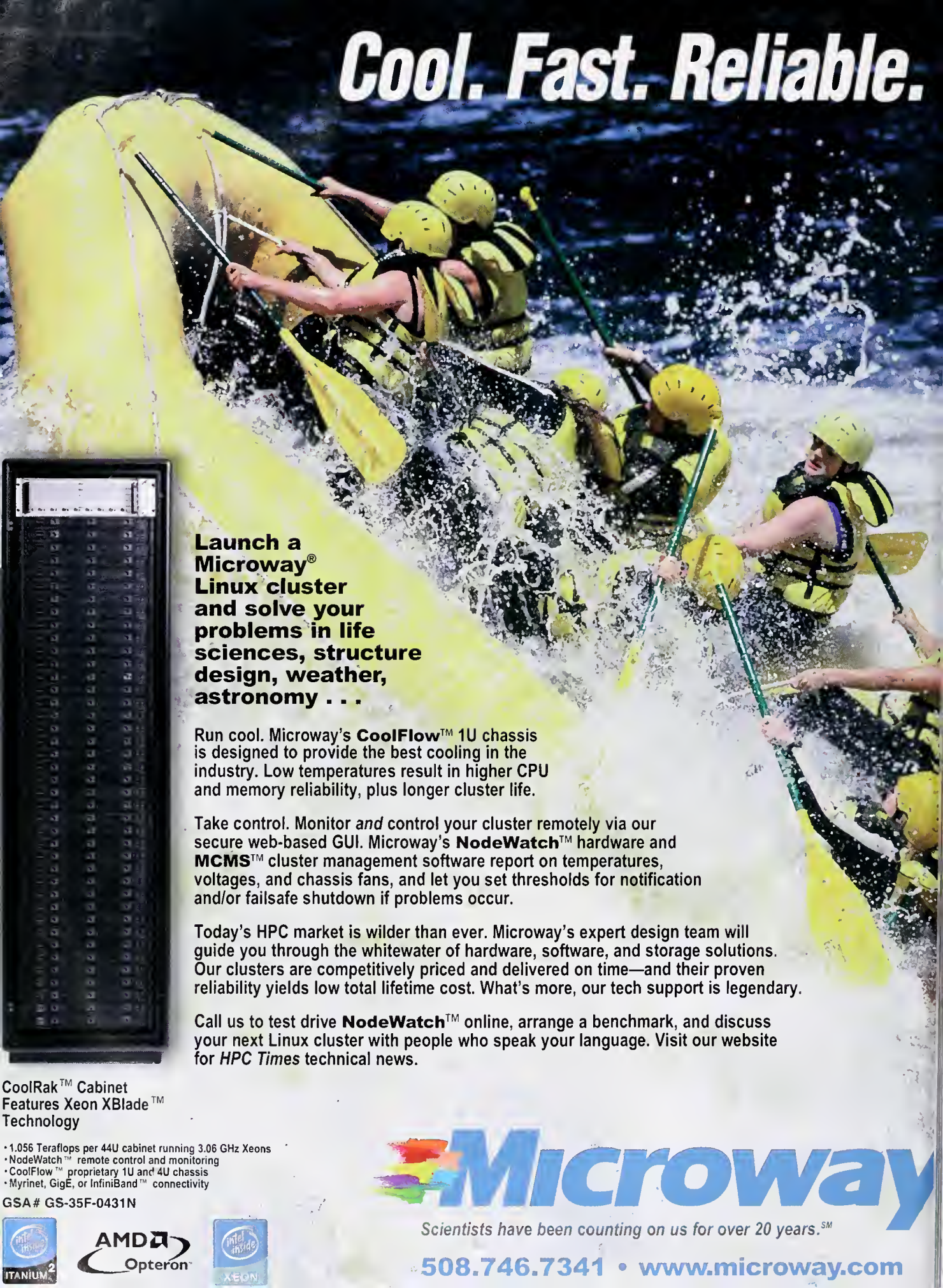
## AUGUST 2003

<b>Editor</b>	MICHAEL J. GREENBERG	The Whitney Laboratory, University of Florida
<b>Associate Editors</b>	LOUIS E. BURNETT R. ANDREW CAMERON CHARLES D. DERBY MICHAEL LABARBERA	Grice Marine Laboratory, College of Charleston California Institute of Technology Georgia State University University of Chicago
<b>Section Editor</b>	SHINYA INOUÉ, <i>Imaging and Microscopy</i>	Marine Biological Laboratory
<b>Online Editors</b>	JAMES A. BLAKE, <i>Keys to Marine Invertebrates of the Woods Hole Region</i> WILLIAM D. COHEN, <i>Marine Models Electronic Record and Compendia</i>	ENSR Marine & Coastal Center, Woods Hole Hunter College, City University of New York
<b>Editorial Board</b>	PETER B. ARMSTRONG JOAN CERDÁ ERNEST S. CHANG THOMAS H. DIETZ RICHARD B. EMLET DAVID EPEL KENNETH M. HALANYCH GREGORY HINKLE NANCY KNOWLTON MAKOTO KOBAYASHI ESTHER M. LEISE DONAL T. MANAHAN MARGARET MCFALL-NGAI MARK W. MILLER TATSUO MOTOKAWA YOSHITAKA NAGAHAMA SHERRY D. PAINTER J. HERBERT WAITE RICHARD K. ZIMMER	University of California, Davis Center of Aquaculture-IRTA, Spain Bodega Marine Lab., University of California, Davis Louisiana State University Oregon Institute of Marine Biology, Univ. of Oregon Hopkins Marine Station, Stanford University Auburn University, Alabama Millennium Pharmaceuticals, Cambridge, Massachusetts Scripps Inst. Oceanography & Smithsonian Tropical Res. Inst. Hiroshima University of Economics, Japan University of North Carolina Greensboro University of Southern California Kewalo Marine Laboratory, University of Hawaii Institute of Neurobiology, University of Puerto Rico Tokyo Institute of Technology, Japan National Institute for Basic Biology, Japan Marine Biomed. Inst., Univ. of Texas Medical Branch University of California, Santa Barbara University of California, Los Angeles
<b>Editorial Office</b>	PAMELA CLAPP HINKLE VICTORIA R. GIBSON CAROL SCHACHINGER WENDY CHILD	Managing Editor Staff Editor Editorial Associate Subscription & Advertising Administrator

Published by  
MARINE BIOLOGICAL LABORATORY  
WOODS HOLE, MASSACHUSETTS

<http://www.biolbull.org>

# Cool. Fast. Reliable.



**Launch a  
Microway<sup>®</sup>  
Linux cluster  
and solve your  
problems in life  
sciences, structure  
design, weather,  
astronomy . . .**

Run cool. Microway's **CoolFlow<sup>™</sup>** 1U chassis is designed to provide the best cooling in the industry. Low temperatures result in higher CPU and memory reliability, plus longer cluster life.

Take control. Monitor *and* control your cluster remotely via our secure web-based GUI. Microway's **NodeWatch<sup>™</sup>** hardware and **MCMS<sup>™</sup>** cluster management software report on temperatures, voltages, and chassis fans, and let you set thresholds for notification and/or failsafe shutdown if problems occur.

Today's HPC market is wilder than ever. Microway's expert design team will guide you through the whitewater of hardware, software, and storage solutions. Our clusters are competitively priced and delivered on time—and their proven reliability yields low total lifetime cost. What's more, our tech support is legendary.

Call us to test drive **NodeWatch<sup>™</sup>** online, arrange a benchmark, and discuss your next Linux cluster with people who speak your language. Visit our website for *HPC Times* technical news.

CoolRak<sup>™</sup> Cabinet  
Features Xeon XBlade<sup>™</sup>  
Technology

- 1.056 Teraflops per 44U cabinet running 3.06 GHz Xeons
- NodeWatch<sup>™</sup> remote control and monitoring
- CoolFlow<sup>™</sup> proprietary 1U and 4U chassis
- Myrinet, GigE, or InfiniBand<sup>™</sup> connectivity

GSA # GS-35F-0431N



# Microway

Scientists have been counting on us for over 20 years.<sup>SM</sup>

508.746.7341 • [www.microway.com](http://www.microway.com)

# CONTENTS

VOLUME 205, No. 1: AUGUST 2003

## RESEARCH NOTE

**Drazen, Jeffrey C., Shana K. Goffredi, Brian Schlining, and Debra S. Stakes**

Aggregations of egg-brooding deep-sea fish and cephalopods on the Gorda Escarpment: a reproductive hot spot . . . . . 1

## EVOLUTION

**Zigler, Kirk S., and H. A. Lessios**

250 million years of bindin evolution . . . . . 8

## NEUROBIOLOGY AND BEHAVIOR

**Painter, Sherry D., Bret Clough, Sara Black, and Gregg T. Nagle**

Behavioral characterization of attractin, a waterborne peptide pheromone in the genus *Aplysia* . . . . . 16

**Bergman, Daniel A., and Paul A. Moore**

Field observations of intraspecific agonistic behavior of two crayfish species, *Orconectes rusticus* and *Orconectes virilis*, in different habitats . . . . . 26

## PHYSIOLOGY AND BIOMECHANICS

**Etnier, Shelley A.**

Twisting and bending of biological beams: distribution of biological beams in a stiffness mechano-space . . . . . 36

**Eyster, L. S., and L. M. van Camp**

Extracellular lipid droplets in *Idiosepius notoides*, the Southern pygmy squid . . . . . 47

**Christensen, Ana Beardsley, James M. Colacino, and Celia Bonaventura**

Functional and biochemical properties of the hemoglobins of the burrowing brittle star *Hemipholis elongata* Say (Echinodermata, Ophiuroidea) . . . . . 54

## SYMBIOSIS AND PARASITOLOGY

**Davy, Simon K., and John R. Turner**

Early development and acquisition of zooxanthellae in the temperate symbiotic sea anemone *Anthopleura ballii* (Cocks) . . . . . 66

## DEVELOPMENT AND REPRODUCTION

**Neumann, Dietrich, and Heike Kappes**

On the growth of bivalve gills initiated from a lobule-producing budding zone . . . . . 73

**Beninger, Peter G., Gaël Le Pennec, and Marcel Le Pennec**

Demonstration of nutrient pathway from the digestive system to oocytes in the gonad intestinal loop of the scallop *Pecten maximus* L. . . . . 83

\* \* \*

**Annual Report of the Marine Biological Laboratory . . . R1**

## THE BIOLOGICAL BULLETIN

THE BIOLOGICAL BULLETIN is published six times a year by the Marine Biological Laboratory, 7 MBL Street, Woods Hole, Massachusetts 02543.

Subscriptions and similar matter should be addressed to Subscription Administrator, THE BIOLOGICAL BULLETIN, Marine Biological Laboratory, 7 MBL Street, Woods Hole, Massachusetts 02543. Subscription includes both print and online journals. Subscription per year (six issues, two volumes): \$280 for libraries; \$105 for individuals. Subscription per volume (three issues): \$140 for libraries; \$52.50 for individuals. Back and single issues (subject to availability): \$50 for libraries; \$20 for individuals.

Communications relative to manuscripts should be sent to Michael J. Greenberg, Editor-in-Chief, or Pamela Clapp Hinkle, Managing Editor, at the Marine Biological Laboratory, 7 MBL Street, Woods Hole, Massachusetts 02543. Telephone: (508) 289-7149. FAX: 508-289-7922. E-mail: pclapp@mbledu.

---

<http://www.biolbull.org>

---

THE BIOLOGICAL BULLETIN is indexed in bibliographic services including *Index Medicus* and MEDLINE, *Chemical Abstracts*, *Current Contents*, *Elsevier BIOBASE/Current Awareness in Biological Sciences*, and *Geo Abstracts*.

Printed on acid free paper,  
effective with Volume 180, Issue 1, 1991.

---

POSTMASTER: Send address changes to THE BIOLOGICAL BULLETIN, Marine Biological Laboratory, 7 MBL Street, Woods Hole, MA 02543.

Copyright © 2003, by the Marine Biological Laboratory

Periodicals postage paid at Woods Hole, MA, and additional mailing offices.  
ISSN 0006-3185

---

## INSTRUCTIONS TO AUTHORS

*The Biological Bulletin* accepts outstanding original research reports of general interest to biologists throughout the world. Papers are usually of intermediate length (10–40 manuscript pages). A limited number of solicited review papers may be accepted after formal review. A paper will usually appear within four months after its acceptance.

Very short, especially topical papers (less than 9 manuscript pages including tables, figures, and bibliography) will be published in a separate section entitled "Research Notes." A Research Note in *The Biological Bulletin* follows the format of similar notes in *Nature*. It should open with a summary paragraph of 150 to 200 words comprising the introduction and the conclusions. The rest of the text should continue on without subheadings, and there should be no more than 30 references. References should be referred to in the text by number, and listed in the Literature Cited section in the order that they appear in the text. Unlike references in *Nature*, references in the Research Notes section should conform in punctuation and arrangement to the style of recent issues of *The Biological Bulletin*. Materials and Methods should be incorporated into appropriate figure legends. See the article by Lohmann *et al.* (October 1990, Vol. **179**: 214–218) for sample style. A Research Note will usually appear within two months after its acceptance.

The Editorial Board requests that regular manuscripts conform to the requirements set below; those manuscripts that do not conform will be returned to authors for correction before review.

1. **Manuscripts.** Manuscripts, including figures, should be submitted in quadruplicate, with the originals clearly marked. (Xerox copies of photographs are not acceptable for review purposes.) If possible, please include an electronic copy of the text of the manuscript. Label the disk with the name of the first author and the name and version of the wordprocessing software used to create the file. If the file was not created in some version of Microsoft Word, save the text in rich text format (rtf). The submission letter accompanying the manuscript should include a telephone number, a FAX number, and (if possible) an E-mail address for the corresponding author. The original manuscript must be typed in no smaller than 12 pitch or 10 point, using double spacing (including figure legends, footnotes, bibliography, etc.) on one side of 16- or 20-lb. bond paper, 8 by 11 inches. Please, no right justification. Manuscripts should be proofread carefully and errors corrected legibly in black ink. Pages should be numbered consecutively. Margins on all sides should be at least 1 inch (2.5 cm). Manuscripts should conform to the *Council of Biology Editors Style Manual*, 5th Edition (Council of Biology Editors, 1983) and to American spelling. Unusual abbreviations should be kept to a minimum and should be spelled out on first reference as well as defined in a footnote on the title page. Manuscripts should be divided into the following components: Title page, Abstract (of no more than 200 words), Introduction, Materials and Methods, Results, Discussion, Acknowledgments, Literature Cited, Tables, and Figure Legends. In addition, authors should supply a list of words and phrases under which the article should be indexed.

2. **Title page.** The title page consists of a condensed title or running head of no more than 35 letters and spaces, the manuscript title, authors' names and appropriate addresses, and footnotes listing present addresses, acknowledgments or contribution numbers, and explanation of unusual abbreviations.

3. **Figures.** The dimensions of the printed page, 7 by 9 inches, should be kept in mind in preparing figures for publication. We recommend that figures be about 1 times the linear dimensions of the final printing desired, and that the ratio of the largest to the smallest letter or number and of the thickest to the thinnest line not exceed 1:1.5. Explanatory matter generally should be included in legends, although axes should always be identified on the illustration itself. Figures should be prepared for reproduction as either line cuts or halftones. Figures to be reproduced as line cuts should be unmounted glossy photographic reproductions or drawn in black ink on white paper, good-quality tracing cloth or plastic, or blue-lined coordinate paper. Those to be reproduced as halftones should be mounted on board, with both designating numbers or letters and scale bars affixed directly to the figures. All figures should be numbered in consecutive order, with no distinction between text and plate figures and cited, in order, in the text. The author's name and an arrow indicating orientation should appear on the reverse side of all figures.

**Digital art:** *The Biological Bulletin* will accept figures submitted in electronic form; however, digital art must conform to the following guidelines. Authors who create digital images are wholly responsible for the quality of their material, including color and halftone accuracy.

**Format.** Acceptable graphic formats are TIFF and EPS. Color submissions must be in EPS format, saved in CMKY mode.

**Software.** Preferred software is Adobe Illustrator or Adobe Photoshop for the Mac and Adobe Photoshop for Windows. Specific instructions for artwork created with various software programs are available on the Web at the Digital Art Information Site maintained by Cadmus Professional Communications at <http://cpc.cadmus.com/da/>

**Resolution.** The minimum requirements for resolution are 1200 DPI for line art and 300 for halftones.

**Size.** All digital artwork must be submitted at its actual printed size so that no scaling is necessary.

**Multipanel figures.** Figures consisting of individual parts (e.g., panels A, B, C) must be assembled into final format and submitted as one file.

**Hard copy.** Files must be accompanied by hard copy for use in case the electronic version is unusable.

**Disk identification.** Disks must be clearly labeled with the following information: author name and manuscript number; format (PC or Macintosh); name and version of software used.

**Color:** *The Biological Bulletin* will publish color figures and plates, but must bill authors for the actual additional cost of printing in color. The process is expensive, so authors with more than one color image should—consistent with editorial concerns, especially citation of figures in order—combine them into a single plate to reduce the expense. On request, when supplied with a copy of a color illustration, the editorial staff will provide a pre-publication estimate of the printing cost.

4. **Tables, footnotes, figure legends, etc.** Authors should follow the style in a recent issue of *The Biological Bulletin* in

preparing table headings, figure legends, and the like. Because of the high cost of setting tabular material in type, authors are asked to limit such material as much as possible. Tables, with their headings and footnotes, should be typed on separate sheets, numbered with consecutive Arabic numerals, and placed after the Literature Cited. Figure legends should contain enough information to make the figure intelligible separate from the text. Legends should be typed double spaced, with consecutive Arabic numbers, on a separate sheet at the end of the paper. Footnotes should be limited to authors' current addresses, acknowledgments or contribution numbers, and explanation of unusual abbreviations. All such footnotes should appear on the title page. Footnotes are not normally permitted in the body of the text.

5. **Literature cited.** In the text, literature should be cited by the Harvard system, with papers by more than two authors cited as Jones *et al.*, 1980. Personal communications and material in preparation or in press should be cited in the text only, with author's initials and institutions, unless the material has been formally accepted and a volume number can be supplied. The list of references following the text should be headed Literature Cited, and must be typed double spaced on separate pages, conforming in punctuation and arrangement to the style of recent issues of *The Biological Bulletin*. Citations should include complete titles and inclusive pagination. Journal abbreviations should normally follow those of the U. S. A. Standards Institute (USASI), as adopted by BIOLOGICAL ABSTRACTS and CHEMICAL ABSTRACTS, with the minor differences set out below. The most generally useful list of biological journal titles is that published each year by BIOLOGICAL ABSTRACTS (BIOSIS List of Serials; the most recent issue). Foreign authors, and others who are accustomed to using THE WORLD LIST OF SCIENTIFIC PERIODICALS, may find a booklet published by the Biological Council of the U.K. (obtainable from the Institute of Biology, 41 Queen's Gate, London, S.W.7, England, U.K.) useful, since it sets out the WORLD LIST abbreviations for most biological journals with notes of the USASI abbreviations where these differ. CHEMICAL ABSTRACTS publishes quarterly supplements of additional abbreviations. The following points of reference style for THE BIOLOGICAL BULLETIN differ from USASI (or modified WORLD LIST) usage:

A. Journal abbreviations, and book titles, all underlined (for italics)

B. All components of abbreviations with initial capitals (not as European usage in WORLD LIST e.g., *J. Cell. Comp. Physiol.* NOT *J. cell. comp. Physiol.*)

C. All abbreviated components must be followed by a period, whole word components *must not* (i.e., *J. Cancer Res.*)

D. Space between all components (e.g., *J. Cell. Comp. Physiol.*, not *J.Cell.Comp.Physiol.*)

E. Unusual words in journal titles should be spelled out in full, rather than employing new abbreviations invented by the author. For example, use *Rit Vísindafélags Íslendinga* without abbreviation.

F. All single word journal titles in full (e.g., *Veliger*, *Ecology*, *Brain*).

G. The order of abbreviated components should be the same as the word order of the complete title (*i.e.*, *Proc.* and *Trans.* placed where they appear, not transposed as in some BIOLOGICAL ABSTRACTS listings).

H. A few well-known international journals in their preferred forms rather than WORLD LIST or USASI usage (*e.g.*, *Nature*, *Science*, *Evolution* NOT *Nature, Lond.*, *Science, N.Y.*; *Evolution, Lancaster, Pa.*)

6. *Sequences.* By the time a paper is sent to the press, all nucleotide or amino acid sequences and associated alignments should have been deposited in a generally accessible database

(*e.g.*, GenBank, EMBL, SwissProt), and the sequence accession number should be provided.

7. *Reprints, page proofs, and charges.* Authors may purchase reprints in lots of 100. Forms for placing reprint orders are sent with page proofs. Reprints normally will be delivered about 2 to 3 months after the issue date. Authors will receive page proofs of articles shortly before publication. They will be charged the current cost of printers' time for corrections to these (other than corrections of printers' or editors' errors). Other than these charges for authors' alterations, *The Biological Bulletin* does not have page charges.

# Aggregations of Egg-Brooding Deep-Sea Fish and Cephalopods on the Gorda Escarpment: a Reproductive Hot Spot

JEFFREY C. DRAZEN\*, SHANA K. GOFFREDI, BRIAN SCHLINING, AND DEBRA S. STAKES

*Monterey Bay Aquarium Research Institute, 7700 Sandholdt Road,  
Moss Landing, California 95039-9644*

*Localized areas of intense biological activity, or hot spots, in the deep sea are infrequent but important features in an otherwise sparsely occupied habitat (1). Hydrothermal vents, methane cold seeps, and the tops of seamounts are well documented areas where dense communities persist for generations (2–5). Reproductive aggregations where conspecifics concentrate for the purposes of spawning or egg brooding could be thought of as transient hot spots. It is likely that they occur in populations with low densities to maximize mate location and increase reproductive success (6). However, only a few deep-sea reproductive aggregations have ever been documented (7–9), demonstrating the paucity of present-day information regarding reproductive behavior of deep-sea animals. In this paper we describe a unique multispecies reproductive aggregation located on the Gorda Escarpment, California. We document some of the highest fish and octopus densities ever reported in the deep sea, with most individuals of both species brooding eggs. We describe the nesting behavior of the blob sculpin, *Psychrolutes phrictus*, and the egg-brooding behavior of an octopus, *Graneledone* sp. observed during annual dives of a remotely operated vehicle (ROV) on the Gorda Escarpment. The animals are concentrated at the crest of the local topography and near cold seeps where they may benefit from enhanced current flow and local productivity. These findings provide new information on the reproductive behaviors of deep-sea animals. More importantly, they highlight how physical and bathymetric heterogeneity in the environment can result in reproductive hot spots, which*

*may be a critical resource for reproductive success in some deep-sea species.*

Fifteen ROV dives were conducted on the Gorda Escarpment and Mendocino Ridge during three visits in August 2000, August 2001, and July 2002 (Fig. 1). The Gorda Escarpment is a submarine plateau offshore of northern California. The Mendocino Ridge extends westward from its northern edge at 40.35° N. The Escarpment's northern side is characterized by steep topography, frequent rocky outcrops and talus fields, sediment slumps, and drainage channels (10). The depth of investigation ranged from 1300 to 3000 m.

Reproductive aggregations of both blob sculpin and octopus were present at Site 1 (Fig. 1). The biomass of *P. phrictus* alone at this site was equivalent to the average total biomass of fishes on the continental slope. Likewise, the density of *Graneledone* sp. was considerably greater than previously published estimates (Fig. 2). Eighty-four individuals of *P. phrictus* and 64 nests (Fig. 3A) were observed. They were present at two sites, with the highest density occurring at Site 1 in both August 2000 and August 2001 (Fig. 1). The fish were found over the steepest topography and at a topographic break between the steep northern side of the ridge and the more gently sloping top (Fig. 4). *P. phrictus* and associated nests were absent in July 2002. Two hundred and thirty-two individuals of *Graneledone* sp. (Fig. 3B) were observed across all locations, with the highest densities observed at Site 1 during all three visits (Fig. 1). The octopus co-occurred with the blob sculpin, with 51% of the octopus observed within 5 m of sculpin adults or nests in 2001. Smaller aggregations of brooding blob sculpin and octopus were observed at Site 2.

Site 1 (depth 1547–1603 m; dives T208, T349, T448) was

Received 14 February 2003; accepted 12 May 2003.

\* To whom correspondence should be addressed. E-mail: jdrazen@mbari.org

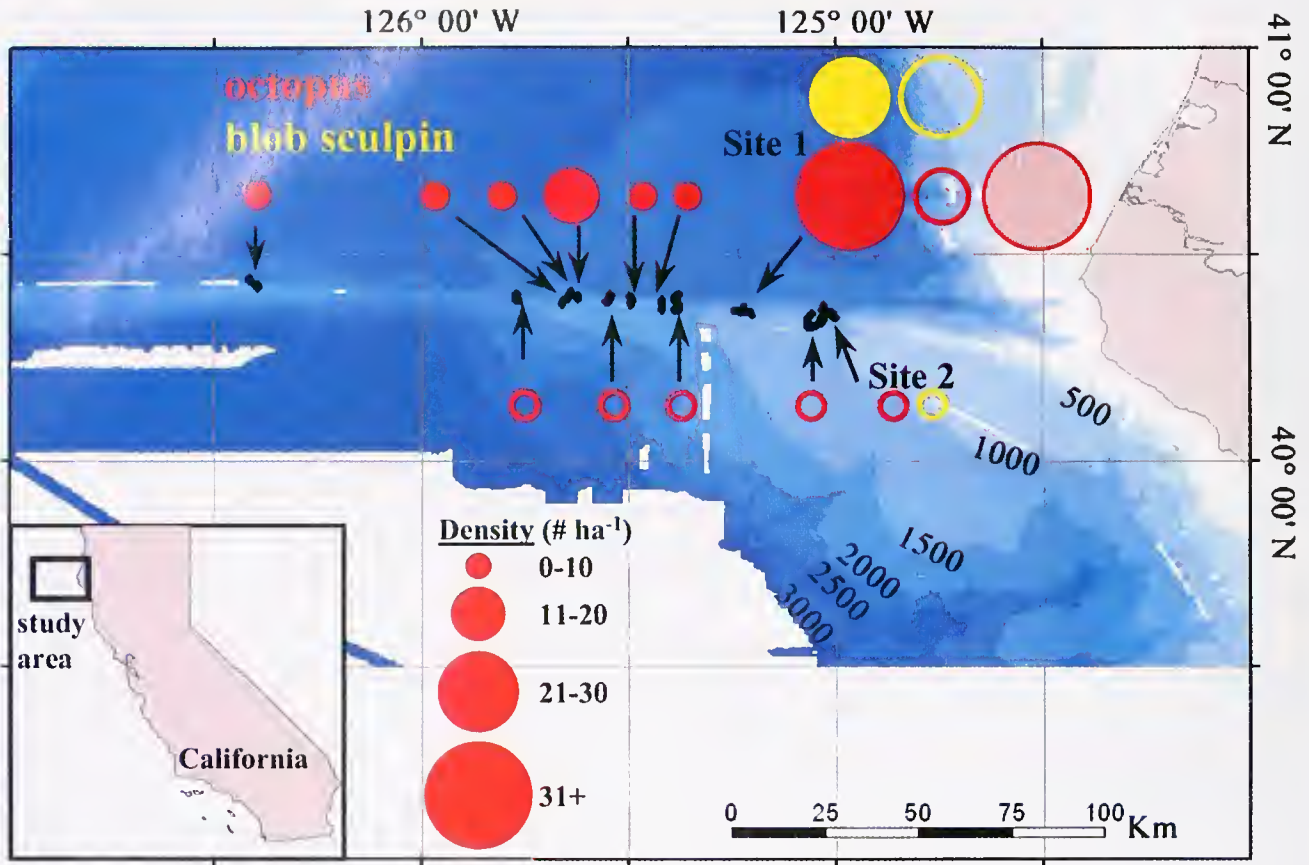


**Figure 1.** Bathymetric map of the Mendocino Ridge and Gorda Escarpment, showing all dive sites. Depths are in meters. One hundred and fourteen hours of video from ROV bottom time was recorded, annotated, and analyzed. Annotations of all occurrences of discernible animals and geologic features were stored in a searchable database with corresponding environmental (CTDO), observational (time, position), and system (camera zoom) data. Bathymetry is derived from a hull-mounted EM300 sonar system with 20-m pixel resolution. Ultrashort baseline Transponders (Sonardyne, Houston, TX) mounted on the ROV and the ship determine position. Tracklines are derived in a real-time ArcView-based (Environmental Systems Research Institute) navigation system. Closed circles, open circles, and hatched circles are densities ( $\# \text{ ha}^{-1}$ ) of blob sculpin (yellow) and octopus (red) from dives in 2000, 2001, and 2002 respectively. For each dive the densities reflect the number of animals observed over the surveyed area of seafloor. Areas for density estimates were calculated using the navigation to determine track length and assuming an average observational width of 4 m. Overlap of the dive track was accounted for in the calculations.

characterized by small rocky cliffs and bouldered slopes that shoaled to a sloping talus field in which the gravel and boulders were interspersed with sediment. Site 2 (depth 1534–1583 m; dive T351; Fig. 1) was on a shallowly sloping mud and sand bottom interspersed by boulders, talus, and small rock outcrops. Diffuse cold seeps at the base of several bouldered slopes at both sites were evident by the presence of small patches of vestimentiferan tube worms and vesicomyid clams (10). Sites 1 and 2 were characterized by an average bottom water temperature of 2.4 °C (range = 2.3 – 2.7 °C) and very low oxygen concentration (mean = 1.07 ml  $l^{-1}$ ; range = 0.73–1.46 ml  $l^{-1}$ ). The temperature at Site 1 was slightly elevated above

ambient ( $\sim 0.1$ – $0.2$  °C) due to local subsurface fluid seepage from the substrate (10).

Blob sculpin attended nests of large ( $4.0 \pm 0.6$  mm;  $n = 50$ ) pinkish eggs (Fig. 3A). The majority of the nests had fish in close attendance (within 3 m), often sitting directly on or touching the eggs. Some nests and fish were observed by themselves primarily in the roughest terrain where it was difficult to see behind nearby rocks and ledges. Eggs were free of sediment, suggesting that the adults cleaned or fanned their nest sites. Brooding fish were almost always found very close to each other, and nests were often on neighboring boulders separated by only 1–2 m. Generally the parent fish did not move when the ROV approached;

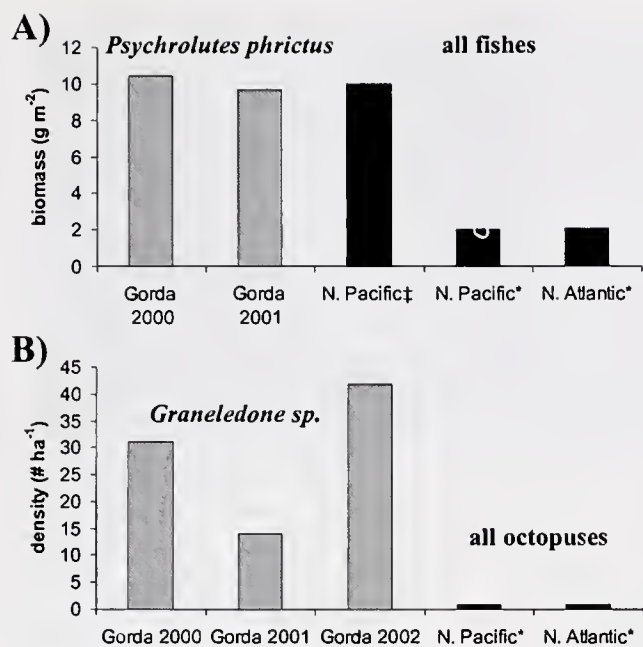


**Figure 2.** Biomass of blob sculpin (*Psychrolutes phricus*) and density of octopus (*Graneledone* sp.) at Site 1 (grey bars) compared to “background” averages for total fishes and total octopuses at similar depths elsewhere (black bars). (A) Biomass (g m<sup>-2</sup>; the metric typically used for fish) of blob sculpin was estimated by assuming an average adult size of 4.5 kg (26). (B) Density of octopuses (# ha<sup>-1</sup>; typically used for cephalopods). Data from other locations are from trawling\* (16, 27, 28; J. R. Voight, pers. comm.) or camera surveys‡ (29).

however, this was also true for fish without eggs, which precluded any conclusions about nest-guarding behavior. The sex of the fish could not be determined from video observations. Fecundity was estimated for four egg masses and ranged from 9375 to 108,125 eggs. The eggs were generally laid on the flat exposed surfaces of large boulders and rock outcrops. Of the 64 egg masses, 57 (89%) had been laid on single rocks; the other seven were each strewn across as many as three neighboring rocks or across large fissures in a flat rock face.

This study presents the first direct evidence of parental care (11) in an oviparous deep-sea fish. It is likely that members of the families Zoarcidae and Liparidae also exhibit parental care, but this has not been confirmed. The zoarcid *Melanostigma atlanticum* was captured in a burrow with its eggs by a box core at 350 m depth (12). The developmental stage of the eggs was not determined; thus, it is unknown whether the parents were in the process of egg laying (one female still retained her eggs) or whether they were staying to guard and ventilate the eggs. Many liparids have large eggs and very low fecundities, suggesting some form of parental care, but no direct evidence has been described (13). Reviews of reproduction in other diverse deep-sea fishes make no note of parental care (1, 14–16).

Individuals of *Graneledone* sp. were observed brooding

eggs under their bodies while sitting vertical and motionless with arms curled outwards on boulders, rock outcrops, and ledges (Fig. 3C). An adult specimen of *Graneledone boreopacifica* was collected in July 2002 with 51 eggs. The eggs were 40 mm in length, and many began hatching prematurely when collected; these juveniles still retained egg sacs. Site 1 was revisited in July 2002, and 63 individuals of *Graneledone* sp. were observed in the curled position. Nine of ten individuals in this position were confirmed to be in the process of brooding eggs. In August 2001, 43 eggs of a specimen of *Benthoctopus* sp. were collected from Site 2. This octopus, unlike the others observed, was underneath a small rock with its eggs out of plain view; it was also much smaller than the *Graneledone* sp. (mantle length ~10 cm), and its eggs were only 16 mm long. It was only observed during the course of collecting the rock for geologic examination.

Our observations provide the first evidence of a multi-species reproductive aggregation in the deep sea. To our knowledge, the only other reproductive aggregations described from deep-sea environments are for spawning aggregations of orange roughy (7); another brooding aggregation of octopuses, including a species of *Graneledone*, in the North Pacific (8); and small (2–6 individuals) aggregations of an echinoid (9). In addition, there are reports of aggregations of two echinoderm species in the North Atlantic (17, 18) that may have been for the purpose of reproduction, and pair formation has been documented in a holothuroid (19). Observations over 3 years indicate that the aggregation at Site 1 is either long-lived or recurs at the same location perhaps every year. The aggregations of blob sculpin and octopus exhibit densities and biomass among the highest recorded in the deep sea (Fig. 2). Localized aggregations of this magnitude could have profound influences on local food webs and fauna.

There are several possible explanations for the presence of the dense aggregations of animals on the Gorda Escarpment. For instance, the presence of brooding aggregations of *Benthoctopus* sp. and *Graneledone* sp. in the North Pacific have been explained previously by the availability of both rocky substrate for egg attachment and bivalve prey from nearby cold seeps (8). Rocky substrate for egg attachment is an obvious requisite for spawning by both sculpin and octopus. Rocky substrate, however, occurred at all dive locations yet reproductive aggregations were present at only two locations, suggesting that substrate is not the only criterion involved in site selection for brooding. Furthermore, aggregations of sculpin or octopuses have not been observed on other rocky features, including some within our dive areas on the Gorda Escarpment and Mendocino Ridge and on the Davidson, Guide, and Gumdrop seamounts in the North Pacific. These seamounts have been observed using the Monterey Bay Aquarium Research Institute’s ROV at various times of the year, but no aggregations such as we

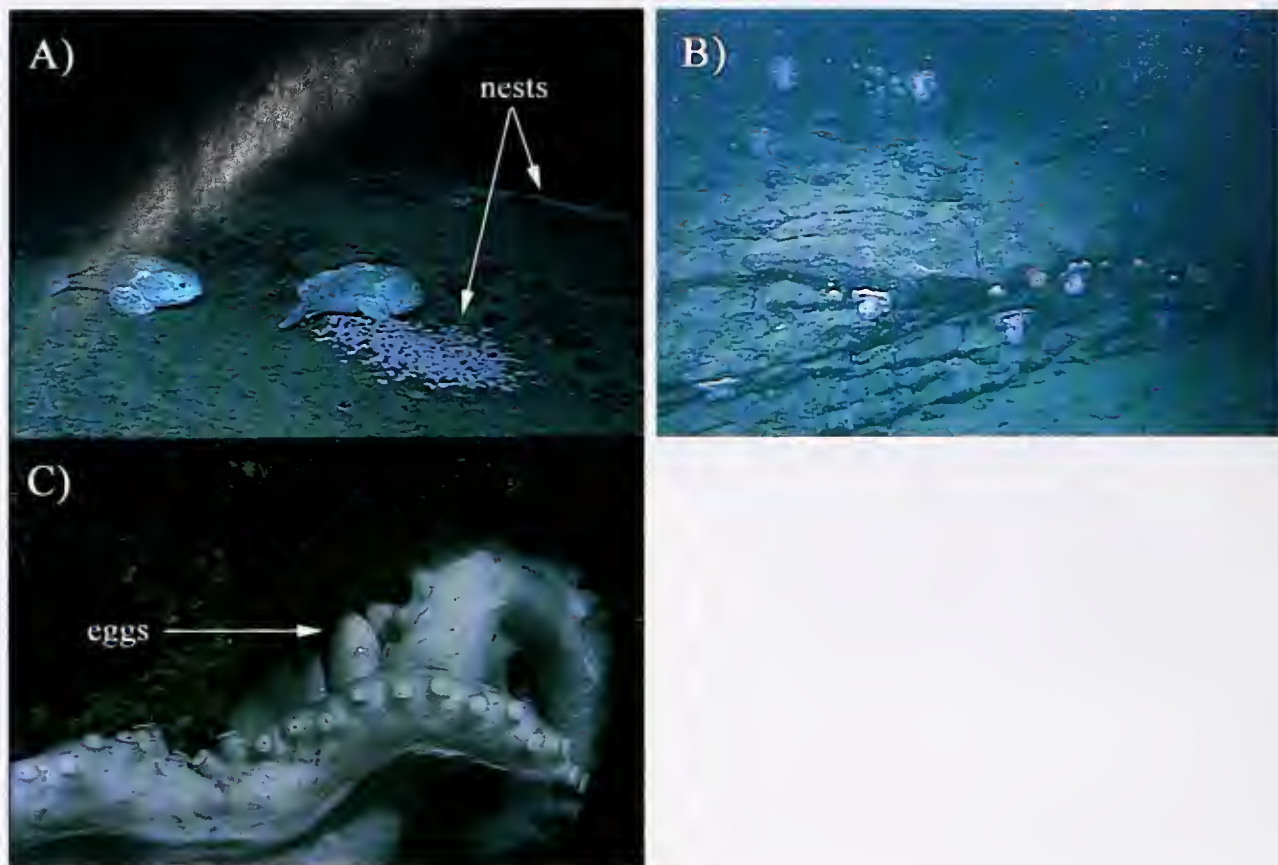


**Figure 3.** Egg-brooding fish and octopus. (A) Three blob sculpin, *Psychrolutes phrictus*, attending nests. The fish on the left has a nest just outside of the field of view. Size-calibrated images were used to determine fish egg size and fecundity. When the camera had zoomed such that the plane of focus was narrow, then the horizontal dimension of the field of view (field width) could be determined (30). From the resulting calibrated images, Optimas image analysis software (ver. 6) (Optimas Corporation, Bothell, WA) was used to measure fish egg diameters. Occasionally when field width could be used to calibrate the size of objects in the video, the Optimas software was used to calculate the area of fish egg masses. The eggs appeared to be laid in a thin layer across the rocks, and in a few cases they were piled on top of each other near the center of the mass. Consequently, egg numbers were estimated by assuming that a single layer of eggs was placed across the nest area as closely together as possible. (B) Eight egg-brooding individuals of *Graneledone* sp. on a rock outcrop. (C) A specimen of *Graneledone* sp. showing eggs protected under arms and mantle.

describe have been found (J. Drazen, unpubl. data). Likewise, on more than 200 dives in the Monterey Bay area at depths greater than 1000 m and often in areas of rocky substrate (*i.e.*, canyon walls and slopes), no brooding octopuses were observed (although octopuses are common) and only 13 blob sculpin were seen, none with eggs.

The presence of cold seeps can dramatically influence the local productivity of surrounding deep-sea communities by transfer of organic nutrients (2). Diffuse cold seeps were observed at both sites of sculpin and octopus aggregations, suggesting that enhanced local productivity from cold seeps on the Gorda Escarpment may also influence the aggregations. This is unconfirmed, however, because only six octopuses were seen in the immediate vicinity of seep organisms

and the distribution of nesting blob sculpin was much broader than that of the seeps (Fig. 4).

Cold seeps are related to the upward flow of warm, methane-rich pore fluids from depth; this flow has also generated slight increases in temperature (0.1–0.2 °C above ambient) at Site 1 (10). Increases in temperature could shorten egg development times, which would be an advantage to species that invest parental care. Assuming a  $Q_{10}$  of 2, an increase of 1.5 °C would be required for a 10% reduction in incubation time. Similar conclusions were drawn for benthic octopus brooding near cold seeps at the Baby Bare site off of Washington State (8). However, temperature elevations of this magnitude around cold seeps are very unlikely. Furthermore, animal occurrences did not

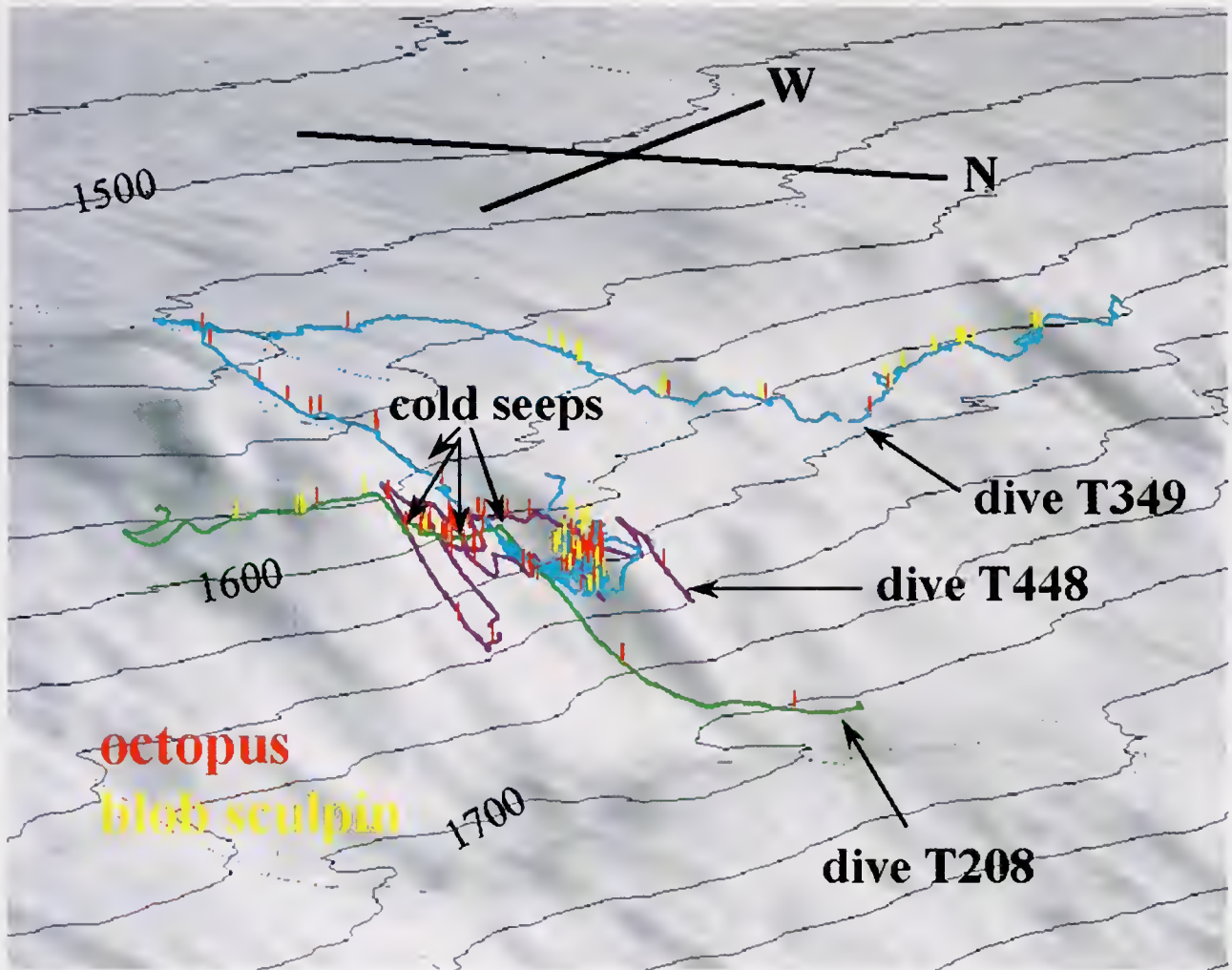


**Figure 4.** Three-dimensional sunshaded map of dive tracks and locations of all sightings of blob sculpin, octopus, and cold seeps at Site 1. Contours are in meters. Mapping information was generated as for Figure 1. The compass is also a scale bar with each arm equivalent to 500 m. Note that, due to the typical perspective of a three-dimensional rendering, the apparent distances for each axis are not equal.

correlate with the highest temperature anomalies. Therefore, we conclude that cold seeps do not benefit these animals physically, but they may provide a food source that could play a role in the location of the animal aggregations.

In addition, elevated currents may influence site selection by brooding aggregations. All blob sculpin and most octopus were observed near the ridge crest where exposure to elevated currents is likely (1, 3, 20). As on seamount crests, abundant suspension feeders such as brisingid sea stars, tunicates, gorgonians, and venus flytrap anemones were found at the crest of the Gorda Escarpment, providing evidence of accelerated current speeds. Some shallow-living sculpins have a strong preference for nesting sites that are exposed to the current; this exposure aids in gas exchange and waste removal and accelerates embryogenesis (21, 22). At Site 1, where oxygen concentrations are very low, enhanced water movement may be required to deliver

adequate oxygen for embryogenesis. A reduction in the need to ventilate or fan the eggs could be an energetic benefit to the adults. In addition, benthic egg brooding and hatching implies a demersal larval/juvenile phase (23). Bottom currents in the deep sea are generally low, so these organisms may take advantage of intensified currents at this site to enhance the dispersal of larvae or juveniles within the demersal habitat.

At one time the deep sea was thought to be a sparsely populated and homogenous environment (1). Today, dense localized communities such as the chemosynthetic communities of hydrothermal vents and methane cold seeps (2) and the suspension-feeding communities of seamounts (3) are well known. Our study site on the Gorda Escarpment is another unique type of biological hot spot in the deep sea. The site is connected to the continental margin but topographically exhibits characteristics of a seamount environ-

ment. In addition, small cold seeps are present. We hypothesize that the local topography interacting with the physical and geologic setting has created a localized reproductive hot spot in the deep sea utilized by at least two very different animals.

This information has several important implications. The reproductive hot spot on the Gorda Escarpment (and future sites determined to be similar) might qualify as an area to be protected from fishing. The protection of habitats associated with vulnerable life stages, notably spawning aggregations, is a main objective of marine reserves (24). Our study site could be threatened by commercial trawling and long-lining operations. In the last two decades, the world has seen a rapid development of deep-sea fisheries to depths of 2000 m, and currently fishers regularly operate at depths of 1000 m off of the west coast of the United States (25). From an ecological perspective, our findings contribute to our understanding of habitat heterogeneity within the broader deep-sea ecosystem as well as providing sites where scientists can predictably observe reproductive biology in deep-sea animals, a prospect that is exciting for the study of these elusive species.

### Acknowledgments

Special thanks to Linda Kuhn, Kyra Schlining, Susan Von Thun, and Kris Walz for video annotation. Dan Davis provided helpful advice and software for measuring egg and nest sizes from video framegrabs. We are indebted to Dave Clague, Robert Young, and Jenny Paduan for their assistance with dive T448. Janet Voight also provided assistance on that dive and helped to confirm the octopus identity. Bob Vrijenhoek was the principal investigator on dives T349 and T351. Thanks to the pilots of the ROV *Tiburion* and the crew of the RV *Western Flyer*. Thanks to Jim Barry, Brad Seibel, Bruce Robison, and Greg Cailliet for discussion and comments. Waldo Wakefield, Eric Hochberg, and an anonymous reviewer provided valuable insight and revisions. Dives T348, T350, and T352 were funded by a grant from the National Undersea Research Program awarded to Robert Duncan (Oregon State University). J. C. Drazen was supported by a postdoctoral fellowship from MBARI.

### Literature Cited

- Gage, J. D., and P. A. Tyler. 1991. *Deep-Sea Biology: a Natural History of Organisms at the Deep-Sea Floor*. Cambridge University Press, Cambridge.
- Tunnicliffe, V., A. G. McArthur, and D. McHugh. 1998. A biogeographical perspective of the deep-sea hydrothermal vent fauna. *Adv. Mar. Biol.* **34**: 353–442.
- Genin, A., P. K. Dayton, P. F. Lonsdale, and F. N. Spiess. 1986. Corals on seamount peaks provide evidence of current acceleration over deep-sea topography. *Nature* **322**: 59–61.
- Van Dover, C. L., C. R. German, K. G. Speer, L. M. Parson, and R. C. Vrijenhoek. 2002. Evolution and biogeography of deep-sea vent and seep invertebrates. *Science* **295**: 1253–1258.
- Wilson, R. R., Jr., and R. S. Kaufmann. 1987. Seamount biota and biogeography. Pp. 355–377 in *Seamounts, Islands, and Atolls*, B.H. Keating, P. Fryer, R. Batiza, and G.W. Boehlert, eds. Geophysical Monograph 43, American Geophysical Union, Washington DC.
- Domeier, M. L., and P. L. Colin. 1997. Tropical reef fish spawning aggregations: defined and reviewed. *Bull. Mar. Sci.* **60**: 698–726.
- Pankhurst, N. W. 1988. Spawning dynamics of orange roughy, *Hoplostethus atlanticus*, in mid-slope waters of New Zealand. *Environ. Biol. Fishes* **21**: 101–116.
- Voight, J. R., and A. J. Grehan. 2000. Egg brooding by deep-sea octopuses in the North Pacific Ocean. *Biol. Bull.* **198**: 94–100.
- Young, C. M., P. A. Tyler, J. L. Cameron, and S. G. Rumrill. 1992. Seasonal breeding aggregations in low-density populations of the bathyal echinoid *Stylocidaris lineata*. *Mar. Biol.* **113**: 603–612.
- Stakes, D. S., A. M. Trehu, S. K. Goffredi, T. H. Naehr, and R. A. Duncan. 2002. Mass wasting, methane venting, and biological communities on the Mendocino transform fault. *Geology* **30**: 407–410.
- Smith, C., and R. J. Wootton. 1995. The costs of parental care in teleost fishes. *Rev. Fish Biol. Fish.* **5**: 7–22.
- Silverberg, N., H. M. Edenborn, G. Ouellet, and P. Beland. 1987. Direct evidence of a mesopelagic fish, *Melanostigma atlanticum* (Zoaridae) spawning within bottom sediments. *Environ. Biol. Fishes* **20**: 195–202.
- Stein, D. L. 1980. Aspects of reproduction of liparid fishes from the continental slope and abyssal plain off Oregon, with notes on growth. *Copeia* 687–699.
- Mead, G. W., E. Bertelsen, and D. M. Cohen. 1964. Reproduction among deep-sea fishes. *Deep-Sea Res.* **11**: 569–596.
- Merrett, N., and R. L. Haedrich. 1997. *Deep-Sea Demersal Fish and Fisheries*. Chapman and Hall, London.
- Haedrich, R. L. 1997. Distribution and population ecology. Pp. 79–114 in *Deep-Sea Fishes*, D. J. Randall and A. P. Farrell, eds. Academic Press, San Diego.
- Grassle, J. F., H. L. Sanders, R. R. Hessler, G. T. Rowe, and T. McLellan. 1975. Pattern and zonation: a study of the bathyal megafauna using the research submersible *Alvin*. *Deep-Sea Res.* **22**: 457–481.
- Billett, D. S. M., and B. Hansen. 1982. Abyssal aggregations of *Kolga hyalina* Danieltssen and Koren (Echinodermata: Holothuroidea) in the Northeast Atlantic Ocean: a preliminary report. *Deep-Sea Res.* **29**: 799–818.
- Tyler, P. A., C. M. Young, D. S. M. Billett, and L. A. Giles. 1992. Pairing behaviour, reproduction and diet in the deep-sea holothurian genus *Paroriza* (Holothuroidea: Synallactidae). *J. Mar. Biol. Assoc. UK* **72**: 447–462.
- Fock, H., F. Uiblein, F. Koster, and H. von Westernhagen. 2002. Biodiversity and species-environment relationships of the demersal fish assemblage at the Great Meteor Seamount (subtropical NE Atlantic), sampled by different trawls. *Mar. Biol.* **141**: 185–199.
- DeMartini, E. E. 1978. Spatial aspects of reproduction in buffalo sculpin, *Enophrys bison*. *Environ. Biol. Fishes* **3**: 331–336.
- DeMartini, E. E., and B. G. Patten. 1979. Egg guarding and reproductive biology of the red Irish lord, *Hemilepidonus hemilepidonus* (Tilesius). *Syesis* **12**: 41–55.
- Hochberg, F. G., M. Nixon, and R. B. Toll. 1992. Order Octopoda Leach, 1818. Pp. 213–280 in *"Larval" and Juvenile Cephalopods: A Manual for Their Identification*, M. J. Sweeney, C. F. E. Roper, K. M. Mangold, M. R. Clarke, and S. v. Boletzky, eds. Smithsonian Contributions to Zoology 513, Smithsonian Institution Press, Washington, DC.
- Roberts, C. M., S. Andelman, G. Branch, R. H. Bustamante, J. C. Castilla, J. Dugan, B. S. Halpern, K. D. Lafferty, H. Leslie, and J. Lubchenco. 2003. Ecological criteria for evaluating candidate sites for marine reserves. *Ecol. Appl.* **13**: S199–214.

25. **National Research Council. 2002.** *Effects of Trawling and Dredging on Seafloor Habitat*. National Academy Press, Washington, DC.
26. **Matarese, A. C., and D. L. Stein. 1980.** Additional records of the sculpin *Psychrolutes phricus* in the eastern Bering Sea and off Oregon. *Fish. Bull.* **78**: 169–171.
27. **Alton, M. S. 1972.** Characteristics of the demersal fish fauna inhabiting the outer continental shelf and slope off the northern Oregon coast. Pp. 583–634 in *The Columbia River Estuary and Adjacent Ocean Waters*. A. T. Pruter and D. L. Alverson, eds. University of Washington Press, Seattle.
28. **Collins, M. A., C. Yau, L. Allcock, and M. H. Thurston. 2001.** Distribution of deep-water benthic and bentho-pelagic cephalopods from the north-east Atlantic. *J. Mar. Biol. Assoc. UK* **81**: 105–117.
29. **Wakefield, W. W. 1990.** Patterns in the distribution of demersal fishes on the upper continental slope off central California with studies on the role of ontogenetic vertical migration in particle flux. Ph.D. dissertation, Scripps Institution of Oceanography, University of California, San Diego, La Jolla, CA.
30. **Davis, D. L., and C. H. Pilskaln. 1993.** Measurements with underwater video: camera field width calibration and structured light. *Mar. Technol. Soc. J.* **26**: 13–19.

## 250 Million Years of Bindin Evolution

KIRK S. ZIGLER<sup>1,2,\*</sup> AND H. A. LESSIOS<sup>1</sup>

<sup>1</sup> *Smithsonian Tropical Research Institute, Balboa, Panamá; and* <sup>2</sup> *Department of Biology, Duke University, Durham, North Carolina*

**Abstract.** Bindin plays a central role in sperm-egg attachment and fusion in sea urchins (echinoids). Previous studies determined the DNA sequence of bindin in two orders of the class Echinoidea, representing 10% of all echinoid species. We report sequences of mature bindin from five additional genera, representing four new orders, including the distantly related sand dollars, heart urchins, and pencil urchins. The six orders in which bindin is now known include 70% of all echinoids, and indicate that bindin was present in the common ancestor of all extant sea urchins more than 250 million years ago. Over this span of evolutionary time there has been (1) remarkable conservation in the core region of bindin, particularly in a stretch of 29 amino acids that has not changed at all; (2) conservation of a motif of basic amino acids at the cleavage site between preprobindin and mature bindin; (3) more than a twofold change in length of mature bindin; and (4) emergence of high variation in the sequences outside the core, including the insertion of glycine-rich repeats in the bindins of some orders, but not others.

### Introduction

Various studies have shown that molecules involved in reproduction (and particularly in gamete interactions) evolve rapidly, often under the influence of positive selection (reviewed in Swanson and Vacquier, 2002). Among these proteins there are examples of both high (Metz and Palumbi, 1996) and low (Metz *et al.*, 1998b) levels of intraspecific variation. In some cases a single molecule displays domains that are highly conserved and other domains that are highly variable (Vacquier *et al.*, 1995). Variation in such proteins is usually studied at a low taxonomic

level, often within species, sometimes within genera, but rarely across an entire class. There are good reasons for this focus: such studies are likely to uncover mutational changes that are important in mate recognition and in speciation. However, comparisons across broad taxonomic levels can offer insights into the evolution of such molecules. They can reveal which features of these molecules are conserved (and are thus essential for basic functions) and which features are free to vary. For the parts that do vary, such comparisons can determine common features of evolution. Most of all, the comparisons can address the question of the universality of a particular molecule by asking how far back in evolution one needs to search to find the point at which a completely different molecule has taken over the essential functions involved in gamete binding and fusion.

Echinoids (sea urchins, heart urchins, and sand dollars), with their readily obtainable gametes, have long been model organisms for fertilization studies. Because fertilization is external, the molecules involved in gamete recognition and fusion are associated exclusively with the gametes. Biochemical studies in sea urchins identified the first “gamete recognition protein,” bindin (Vacquier and Moy, 1977). Bindin is the major insoluble component of the sperm acrosomal vesicle and has been implicated in three molecular interactions (Hofmann and Glabe, 1994). First, after the acrosomal reaction, bindin self-associates, coating the acrosomal process. Second, it functions in sperm-egg attachment by binding to carbohydrates in the vitelline layer on the egg surface. Third, it is involved in the fusion of sperm and egg membranes (Ulrich *et al.*, 1998, 1999).

Bindin is translated as a larger precursor, from which the N-terminal preprobindin portion is subsequently cleaved to produce mature bindin (Gao *et al.*, 1986). The mature bindin molecule contains an amino acid core of about 55 residues that is highly conserved among all bindins characterized to date (Vacquier *et al.*, 1995). An 18 amino acid section of this conserved core (B18) has been shown to fuse lipid

Received 25 February 2003; accepted 3 June 2003.

\* To whom correspondence should be addressed. Current address: Friday Harbor Laboratories, University of Washington, 620 University Road, Friday Harbor, WA 98250. E-mail: ziglerk@u.washington.edu

vesicles *in vitro*, suggesting that this region functions in sperm-egg membrane fusion (Ulrich *et al.*, 1998, 1999). Thus far, bindin is known only from echinoids; no homologous molecules have been identified in any other organism (Vacquier, 1998).

To date, the nucleotide sequence of bindin has been determined in six genera of sea urchins. In *Echinometra* (Metz and Palumbi, 1996), *Strongylocentrotus* (Gao *et al.*, 1986; Minor *et al.*, 1991; Biermann, 1998; Debenham *et al.*, 2000), and *Heliocidaris* (Zigler *et al.*, 2003), there are many sequence rearrangements among individuals and species, and indications of positive selection in regions on either side of the core. In *Arbacia* (Glabbe and Clark, 1991; Metz *et al.*, 1998a) and *Tripneustes* (Zigler and Lessios, 2003), there are fewer sequence rearrangements and no evidence for positive selection. In *Lytechinus*, only one sequence has been published (Minor *et al.*, 1991), so the mode of evolution of the molecule remains unknown.

The five genera in which bindin was previously sequenced belong to two echinoid orders, the Echinoida and the Arbacioida. These two orders contain only 10% of all extant echinoid species (Kier, 1977; Smith, 1984; Littlewood and Smith, 1995). The molecular structure of bindin in the other 13 orders of the class Echinoida has not been studied. The only evidence that bindin is present outside the Echinoida and Arbacioida comes from Moy and Vacquier (1979), who reported that an antibody to bindin of *Strongylocentrotus purpuratus* reacted with sperm from one species of the order Phymosomatoida and two species of the order Clypeasteroida. As Vacquier (1998) has pointed out, molecules that mediate fertilization—in contrast to those central to other basic life processes—often differ between taxa. For example, in the molluscan class Bivalvia, completely different proteins are involved in gamete recognition of oysters (Brandriff *et al.*, 1978) and of mussels (Takagi *et al.*, 1994). It is, therefore, not safe to assume without empirical evidence that bindin is present in all orders of echinoids, or that it has the same general structure as in the taxa in which it has already been characterized.

As a first step in determining which orders of echinoids possess bindin and, if they do, how its structure varies, we cloned and sequenced mature bindin from five genera of sea urchins, four of which belong to orders in which bindin was previously unknown. We combined our data with those of previous studies of bindin in genera belonging to the orders Echinoida and Arbacioida. The final data set includes bindin from 10 genera of sea urchins, pencil urchins, sand dollars, and heart urchins, and the results indicate that the molecule was present in the common ancestor of all extant echinoids that diverged from each other over 250 million years ago. The core sequence has remained remarkably unchanged over this period of time, whereas the areas flanking the core have undergone substantial modification, resulting in great

differences in molecular size, amino acid sequence, and number of repeats.

## Materials and Methods

### Samples

The pencil urchins (order Cidaroida) were represented in our study by *Eucidaris tribuloides*, collected on the Atlantic coast of Panamá; the order Diadematoida by *Diadema antillarum*, also from the Atlantic coast of Panamá. The sand dollars (order Clypeasteroida) were represented by *Encope stokesii* from the Pacific coast of Panamá; the heart urchins (order Spatangoida) by *Moira clotho* collected at the Perlas Islands in the Bay of Panamá. *Heliocidaris erythrogramma* (order Echinoida) was collected near Sydney, Australia.

### DNA isolation and sequencing

We injected various individuals of each species with 0.5 M KCl until we encountered one that produced sperm. The testes of this ripe male were removed and used either directly for mRNA extraction, or after preservation in either RNALater (Ambion Inc.) or in liquid nitrogen. The methods for mRNA isolation, reverse transcription reactions, initial polymerase chain reactions, 3' and 5' rapid amplification of cDNA ends (RACE) reactions, and DNA sequencing were as described in Zigler and Lessios (2003), with the following modifications. (1) A fragment of the core region of bindin was amplified from the reverse transcriptase reaction product or from genomic DNA, using primers MB1130+ (5'-TGCTSSGGTGCSSACSAAAGATTGA-3') and either core200- (5'-TCYTCYTCYTCYTGCATIGC-3') or core157- (5'-CIGGRTCCCHATTRTTIGC-3'). These primers correspond to amino acids VLGATKID, ANIGDP, and AMQEEEE, respectively (Vacquier *et al.*, 1995). (2) When complete 5' mature bindin sequences were not obtained during the first round of 5' RACE, new primers were designed at the 5' end of the obtained sequence; then a second round of RACE amplification was conducted. (3) A 5' preprobindin primer was designed based on a comparison of preprobindin sequences of *Moira clotho* (this study) to preprobindin sequences of *Arbacia* (Glabbe and Clark, 1991), *Strongylocentrotus* (Gao *et al.*, 1986; Minor *et al.*, 1991), and *Lytechinus* (Minor *et al.*, 1991). This primer, pro180 (5'-AAGMGIKCIAGYSCIMGIAAGGG-3'), which corresponds to the conserved amino acids KR(A/S)S(A/P)RKG of the preprobindin, was used in combination with exact primers from the bindin core to amplify mature bindin sequences 5' of the core from *Eucidaris tribuloides* testis cDNA. (4) Bindin sequences obtained from RACE were subsequently confirmed by amplification, cloning, and sequencing of full mature bindin sequences from testis cDNA.

Sequencing of both DNA strands was performed on an ABI 377 automated sequencer, and sequences were

edited using Sequencher 4.1 (Gene Codes Corp.). Sequences have been deposited in GenBank (Accession numbers AY126482-AY126485, AF530406). Published mature bindin sequences from a single exemplar from each of the five genera in which bindin had been previously sequenced were taken from GenBank. These representatives were *Strongylocentrotus purpuratus* (Accession number: M14487, Gao *et al.*, 1986), *Lytechinus variegatus* (M59489, Minor *et al.*, 1991), *Arbacia punctulata* (X54155, Glabe and Clark, 1991), *Echinometra oblonga* (U39503, Metz and Palumbi, 1996), and *Tripneustes ventricosus* (AF520222, Zigler and Lessios, 2003). Three amino acids of the core region of the bindin of *Lytechinus variegatus* [numbers 367 (N), 368 (L), and 385 (Y) in the alignment of Vacquier *et al.* (1995)] were changed to A, V, and D, respectively, based on our own sequence data of *Lytechinus* bindin from 25 individuals representing 5 species; all 25 sequences had these amino acids at the 3 sites (Zigler and Lessios, unpub.). In *Echinometra oblonga*, sequences for the extreme 3' end of preprobindin are not in GenBank. They were inferred from the primer sequences used by Metz and Palumbi (1996) to amplify mature bindin sequences.

#### Sequence analysis

We aligned the mature bindin amino acid sequences with ClustalX ver. 1.81 (Thompson *et al.*, 1997), and adjusted the alignment by eye in Se-A1 (ver. 2.0a5, Rambaut, 1996). We characterized the amino acid changes observed in the core region of bindin as either radical or conservative with respect to charge and polarity (Taylor, 1986; Hughes *et al.*, 1990). The PROTPARAM tool of the EXPASY proteomics server of the Swiss Institute for Bioinformatics (<http://www.expasy.org>) was used to calculate Kyte and Doolittle (1982) hydrophobicity plots (window size = 11 amino acids) for each mature bindin sequence. The PROTSSCALE tool of the same server was used to calculate amino acid composition

for the mature bindins both for the core region (10 sequences, 55 amino acids per sequence) and for mature bindin sequences outside the core (10 sequences of varying length for a total of 1909 amino acids). The program CODONS (Lloyd and Sharp, 1992) was used to calculate the effective number of codons (ENC), a measure of codon usage bias (Wright, 1990), for each sequence. ENC values can range from 20 to 61, with 61 indicating that all synonymous codons are used in equal frequency (no codon bias), and 20 indicating that only a single codon is used for each amino acid (maximum codon bias). The statistical analysis of protein sequences (SAPS, [http://www.isrec.isb-sib.ch/software/SAPS\\_form.html](http://www.isrec.isb-sib.ch/software/SAPS_form.html)) program was used to identify separated repeats, simple tandem repeats, and periodic repeats in each mature bindin sequence (Brendel *et al.*, 1992).

### Results and Discussion

Figure 1 shows the phylogenetic relationships among the echinoid orders from which bindin was sequenced, as they have been reconstructed from molecular, morphological, and fossil evidence (Littlewood and Smith, 1995; Smith *et al.*, 1995). As the figure indicates, bindin is present not only in the Echinoidea and the Arbacioida (from which it was previously known), but also in the sand dollars (Clypeasteroidea) and the heart urchins (Spatangoida), as well as the phylogenetically much more distant Diadematoidea and Cidaroida. Along with the sequence of *Heliocidaris*, reported in this paper, and the previously known sequences from *Arbacia*, *Strongylocentrotus*, *Tripneustes*, *Lytechinus*, and *Echinometra*, the data set covers orders that contain more than 70% of all extant echinoid species (Kier, 1977). The Cidaroida, the only extant order of the subclass Perischochinoidea, is the lineage most divergent from all other echinoids. It was separated from the Euechinoidea approximately 250 mya. Bindin's presence in both extant subclasses of the Echinoidea indicates that it was present in



**Figure 1.** Phylogenetic relationships, divergence times, and systematic position of genera in which bindin has been sequenced. Echinoid phylogeny and divergence times are from Smith (1988) and Smith *et al.* (1995). Source of bindin sequence data is also indicated.

their common ancestor and that it has been evolving along each of the branches of the sea urchin phylogenetic tree for more than 250 my. Whether bindin is present in other echinoderms remains uncertain. Moy and Vacquier (1979) found that their antibody to *Strongylocentrotus purpuratus* bindin did not react with sperm from three species of sea stars, and "zoo blots" using *S. purpuratus* bindin sequences to probe genomic DNAs of a sea cucumber and a sea star were negative (Minor *et al.*, 1991). No attempt has been made to determine bindin's presence in the ophiuroids or crinoids.

Figure 2 indicates that the aligned mature bindin sequences are a mosaic of highly conserved and highly diver-

gent regions. Over the past 250 my, the 55 residues of the core (amino acids 155–209) have been remarkably conserved. This region does not contain any insertions or deletions in any echinoid lineage. Of the 55 amino acids, 45 are conserved across all of the 10 exemplars, including a stretch of 29 residues in a row (amino acids 164–192). The B18 sequence of 18 amino acids implicated in membrane fusion (Ulrich *et al.*, 1998, 1999) is part of this perfectly conserved section. Seven amino acid sites in the core region exhibit a singleton amino acid change (*i.e.*, a change found in only one of the sequences). Four of these changes are conservative with respect to charge and polarity (amino

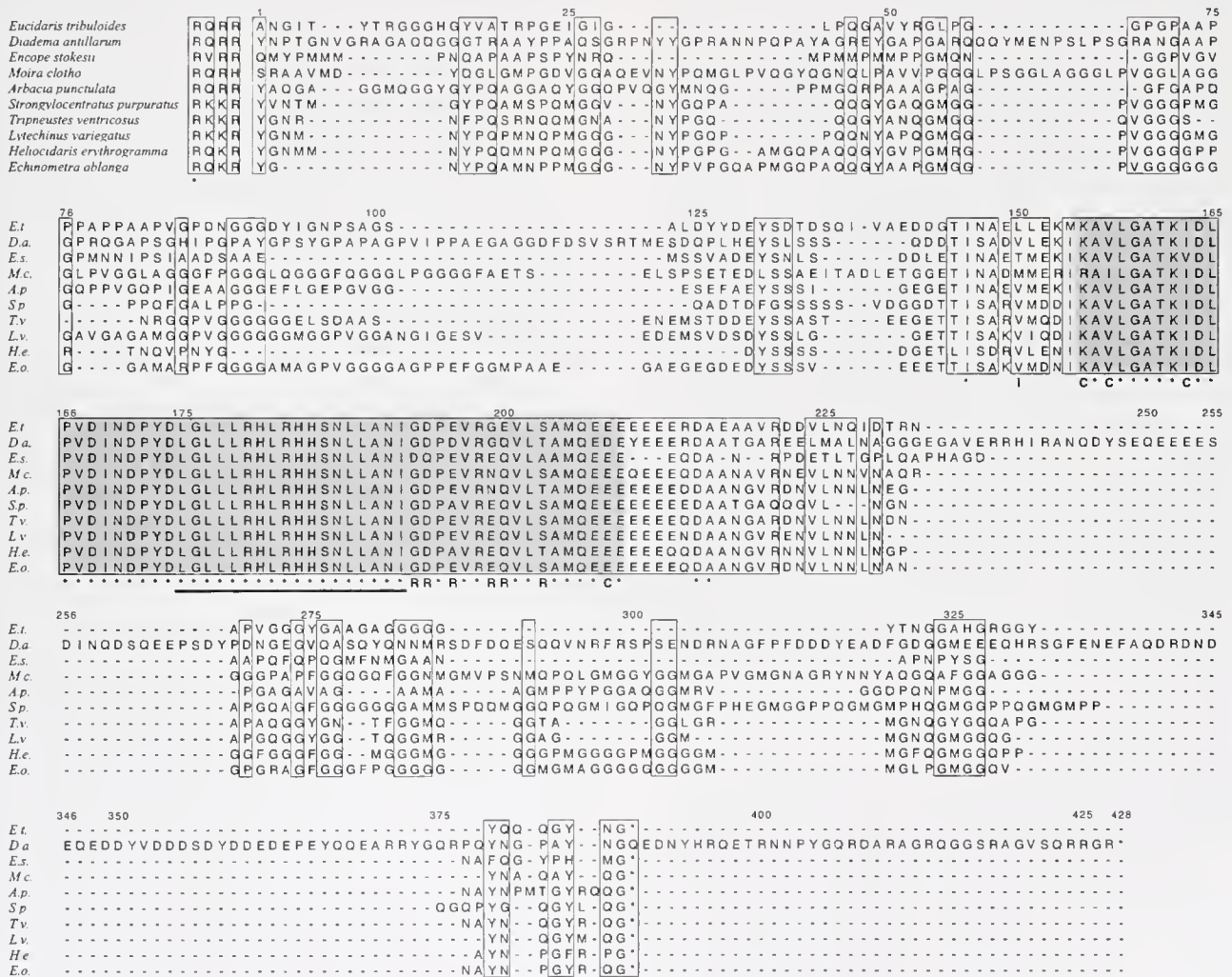


**Figure 2.** Mature bindin amino acid alignment. The first four amino acids are the presumed cleavage site from preprobindin. Sites at which amino acids are identical in more than 50% of the genera are enclosed in boxes. Conservation across all 10 genera is indicated by an asterisk below the site. Dashes indicate deletions. The site for which an intron is known to exist in *Echinometra*, *Arbacia*, *Strongylocentrotus*, *Lytechinus*, *Tripeustes*, *Heliocidaris*, and *Diadema* is indicated by an "I" under the alignment. The core region is shaded. The B18 region of the core is indicated by a bar beneath the alignment. Sites in the core where radical amino acid changes have occurred are marked with an 'R' under the alignment; sites in the core where only conservative amino acid changes have occurred are marked with a 'C'. Stop codons are indicated by an asterisk after the last amino acid.

acids at positions 155, 157, 164, and 208), and three are radical (positions 193, 194, and 200). Each of positions 196, 199, and 203 contain three amino acids across the 10 genera, indicating that there have been at least two changes at each of these sites. At least one of the changes at each site must have been a radical change. Thus, radical changes are observed in only six amino acid positions of the core region, all of them concentrated in a small portion of the core close to the C terminus (amino acids 193, 194, 196, 199, 200, and 203). The rest of the core (amino acids 155 through 192 and 204 through 209) contains only four conservative singleton amino acid substitutions.

A second conserved region is the cleavage site at the border between preprobindin and mature bindin (Fig. 2). In *Strongylocentrotus purpuratus*, the cleavage site is marked by a motif of four basic amino acids (RKKR) (Gao *et al.*, 1986). Multibasic motifs are also present in the other nine genera (Fig. 2). Such multibasic motifs typically mark the cleavage sites of proproteins from the mature molecule during the secretory process through the action of proprotein convertases (Steiner, 1998; Seidah and Chretien, 1999). The conservation of this multibasic motif in bindin reinforces the idea that it functions as a signal for the cleavage of preprobindin from mature bindin in all echinoids.

In contrast to the core and to the cleavage site, the rest of the molecule is so variable between orders that we have little confidence that the alignment of these regions depicted in Figure 2 is correct. There is a great amount of variation in the length of mature bindin both on the 5' and on the 3' side of the molecule (Table 1). This study identifies both the longest and the shortest bindins described to date. Bindin in *Diadema antillarum* (418 amino acids) is more than twice as long as bindin in *Encope stokesii* (193 amino acids). Bindin length 5' of the core ranges from 78 to 148 amino acids, while bindin length 3' of the core ranges from 56 to 215 amino acids. There seems to be no discernible evolutionary trend in bindin length. Closely related orders do not

tend to have bindins that are of similar length. Indeed, it cannot be assumed that the genera we have included in the study are representative of their orders in this respect. The regions on either side of the core were found to confer species-specificity in *Strongylocentrotus* (Lopez *et al.*, 1993). If their variation reflects the requirements of this function, they can be expected to vary in a phylogenetically unpredictable fashion.

An intron located at a conserved position just 5' of the core region has been identified in the mature bindins of *Echinometra* (Metz and Palumbi, 1996), *Arbacia* (Metz *et al.*, 1998a), *Strongylocentrotus* (Biermann, 1998), and *Triploneustes* (Zigler and Lessios, 2003). In each of these genera, the intron is located at a conserved valine (amino acid 150 in Fig. 2). Comparison of sequences derived from both cDNA and from genomic DNA in *Heliocidaris* (Zigler *et al.*, 2003), *Lytechinus*, and *Diadema* revealed that in these genera the intron also exists at the same location and that its point of insertion is also a valine. We have made no attempt to amplify bindin from genomic DNA in *Eucidaris*, *Moira*, and *Encope*, so we do not know whether this intron is a universal feature of all bindins. These three genera do not have a valine in the site at which the intron is known to exist in the others, but the significance of this pattern cannot be evaluated with the present data.

Previous studies have identified both bindins with glycine-rich repeat structures and bindins that lack such structure. Glycine-rich repeats were found in the bindins of *Lytechinus* (Minor *et al.*, 1991), *Strongylocentrotus* (Biermann, 1998), *Echinometra* (Metz and Palumbi, 1996), and *Triploneustes* (Zigler and Lessios, 2003), all members of the order Echinoidea. Consistent with the phylogenetic position of *Heliocidaris*, its bindin also contains glycine-rich repeat sequences, with MGGGN and VGGGGP on the 5' side of its core, and the series MGGG-MGGGGP-MGGGGP-MGGGGM-MGFQG-MGGQPP on the 3' side. Although *Moira* belongs to a different order, its bindin also contains extensive glycine-rich repeats, with the sequence PGGGL-PSGGL-AGGGL-PVGGL-AGGGL-PVGGL-AGGGF-PGGGL-QGGGF-QGGGL-PGGGG found 5' of the core. Glabe and Clark (1991) noted that bindin from *Arbacia punctulata* lacked significant repeat structure, and this observation was extended to three other species of *Arbacia* (Metz *et al.*, 1998a). *Eucidaris*, *Encope*, and *Diadema* resemble *Arbacia* in containing only minimal tandem or separated repeats, the longest of which is PAAP-PPAP-PAAP in the region flanking the 5' side of the core in *Eucidaris*. Thus, glycine-rich repeat structure remains a common trait of the bindin of the Echinoidea, although, as the data from the spatangoid *Moira* indicate, it is not a characteristic limited to this order or even to a closely aligned clade.

There are no cysteine or tryptophan residues in any mature bindin. Disulfide bonds formed between cysteine residues are often critical for protein structure, and in rap-

Table 1

Number of amino acids in three regions of the mature bindin in 10 genera

	5'	Core	3'	Total
<i>Eucidaris</i>	101	55	60	216
<i>Diadema</i>	148	55	215	418
<i>Encope</i>	82	55	56	193
<i>Moira</i>	138	55	94	287
<i>Arbacia</i>	105	55	73	233
<i>Lytechinus</i>	103	55	60	218
<i>Triploneustes</i>	88	55	68	211
<i>Strongylocentrotus</i>	82	55	99	236
<i>Heliocidaris</i>	78	55	73	206
<i>Echinometra</i>	111	55	75	241

5' and 3' regions are defined relative to the conserved core.

idly evolving proteins—such as toxins of cone snails (Duda and Palumbi, 1999) and pheromones of the marine ciliate *Euplotes* (Luporini *et al.*, 1995)—cysteine residues are often among the most conserved amino acids, serving as guides for aligning sequences. Thus, the lack of cysteine residues in bindin may have important structural consequences. When all sequences are pooled, glycine is by far the most common amino acid outside the core, constituting nearly a quarter of all residues. If the orders that possess glycine-rich repeats (Echinoida and Spatangoida) are separated from those that do not, glycine remains the most common amino acid in both categories, constituting 29.6% of the non-core amino acids in the former and 16.4% of non-core residues in the latter. The six most common residues outside the core (G, A, P, Q, N, and E) compose 63.9% of all non-core residues. Leucine is the most common amino acid in the core, present in 10 completely conserved amino acid positions, including 6 of the 18 amino acids in the B18 region. There is a much higher proportion of charged residues in the core (31.8%) than in the rest of the molecule (15.6%). Each of the five charged amino acids (E, D, R, H, and K) is more common in the core.

Another common feature of all bindins is their lack of codon usage bias. ENC values among the 10 genera range from 61 (for *Eucidaris* and *Diadema*) to 48.1 (for *Arbacia*), with an average of 56.4. Low levels of codon usage bias have also been observed in sex-related genes in *Drosophila* (Civetta and Singh, 1998) and in the *Chlamydomonas* mating-type locus genes *Mid* and *Fus1* (Ferris *et al.*, 2002).

Given the large divergence in amino acid sequence and length (and the uncertainties in alignments), it is not surprising that hydrophobicity plots (Fig. 3) from these bindins are diverse. The conserved amino acid sequence of the core and its flanking regions causes all plots to be similar through the middle of the molecule. Plots of the closely related *Triplaneustes ventricosus*, *Lytechinus variegatus*, *Heliocidaris erythrogramma*, and *Echinometra oblonga* bindins are similar throughout their lengths. The rest of the hydrophobicity plots are not clearly similar. One particularly distinct region is the long hydrophilic stretches in *Diadema* bindin along its extended length. A second is the highly hydrophobic region 3' of the core of *Arbacia* bindin, noted by Glabe and Clark (1991).

The only other gamete recognition protein that has been studied in marine invertebrates separated for as long as 250 my is the gastropod sperm protein lysin. Lysin opens a hole in the vitelline envelope of free-spawning snails and thus enables sperm to penetrate to the plasma membrane of the egg. It has been studied in the abalones (*Haliotis*) (Lee and Vacquier, 1992; Lee *et al.*, 1995; Yang *et al.*, 2000; reviewed in Kresge *et al.*, 2001) and in two genera of turban snails, *Tegula* and *Norrisia* (Hellberg and Vacquier, 1999). Abalones and turban snails diverged 250 mya, roughly the same time the cidaroids separated from the euechinoids. The

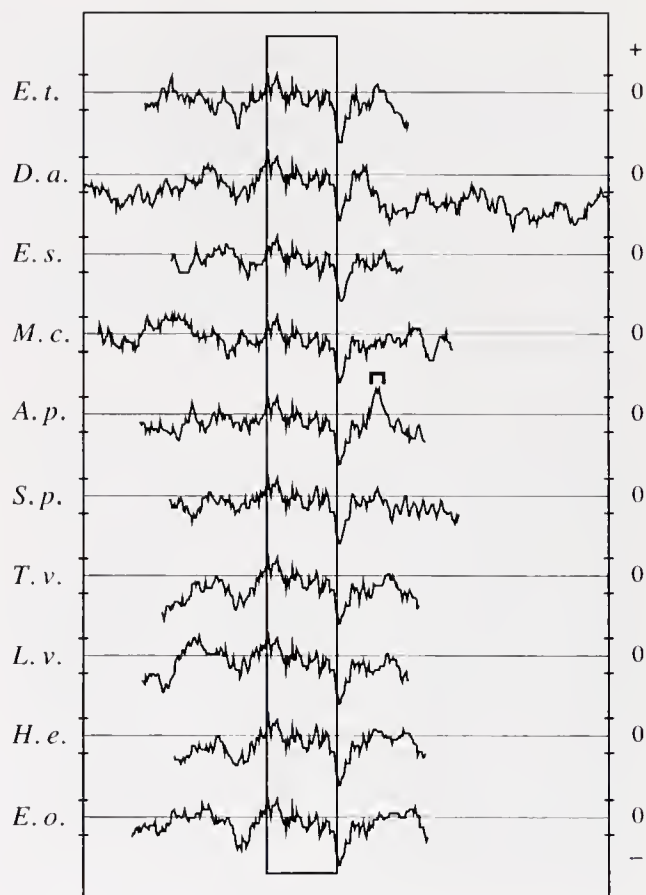


**Figure 3.** Hydrophobicity plots of mature bindin in 10 genera. The genera are presented in the same order as in Figure 1 and abbreviated as follows: *E.t.*: *Eucidaris tribuloides*, *D.a.*: *Diadema antillarum*, *E.s.*: *Encopse stokesii*, *M.c.*: *Moira clotha*, *A.p.*: *Arbacia punctulata*, *S.p.*: *Strongylocentrotus purpuratus*, *T.v.*: *Triplaneustes ventricosus*, *L.v.*: *Lytechinus variegatus*, *H.e.*: *Heliocidaris erythrogramma*, and *E.o.*: *Echinometra oblonga*. A box encloses the core, and a bracket indicates the hydrophobic region in *Arbacia*. The scale bars above and below each zero line mark +1 and -1, respectively.

additional bindin sequences reported here reinforce the conclusions of Hellberg and Vacquier (1999) from comparisons between the modes of evolution of these two proteins. Although they are both involved in gamete recognition and both lack cysteine residues, they evolve in different fashions. There is no equivalent of a bindin core region in lysin: amino acid substitutions are spread throughout the molecule, with only three amino acids conserved between all *Haliotis* species and the two teguline genera. Instead of conserving a section of the molecule, lysin has maintained its function by conserving secondary structure through conservative amino acid substitutions (Hellberg and Vacquier, 1999). Length variation is another obvious difference. Mature bindin length varies from 193 to 418 amino acids, but lysin length (at least in the two groups studied to date) only from 126 to 138 amino acids.

## Conclusions

The comparisons of bindin from 10 genera of echinoids reveal the results of long-term evolution under two opposing selective forces acting on gamete recognition molecules. The sections of the molecule involved in the basic functions of gamete fusion and post-translational cleaving of the preprobindin have been remarkably conserved over 250 my of evolution, presumably through purifying selection. The sections involved in species recognition have been evolving rapidly in seemingly unpredictable directions, presumably under diversifying selection; such changes are likely to be specific to each species.

A number of features identified by these comparisons are in need of functional explanations. Among the conserved features, the lack of change in the core region is the only one that can be easily explained. We do not yet know whether there is a particular reason for the low codon usage bias of all bindins, for the absence of tryptophan or cysteine residues, or for the absence of major hydrophobic regions in all bindins except that of *Arbacia*. The differences between the orders are equally puzzling. Is there a functional reason for the length variation of the regions outside the core? Why do the Echinozoa and the Spatangoida have glycine-rich repeats in the regions flanking the core, while other orders do not? Comparisons alone cannot provide answers to these questions; but they can identify features of the molecule that are worthy of functional study.

## Acknowledgments

We are grateful to A. and L. Calderón for providing support in the laboratory, to M. McCartney for primer design and advice on the RACE technique, to T. Duda for collecting *Moira clotho*, and to E. Popodi for providing testis RNA from *Heliocidaris erythrogramma*. Comments from C. Cunningham, D. McClay, R. Sponer, W. Swanson, V. Vacquier, and two anonymous reviewers improved the manuscript. This work was supported by National Science Foundation and Smithsonian predoctoral fellowships to KSZ, by the Duke University Department of Zoology, and by the Smithsonian Molecular Evolution Program.

## Literature Cited

- Biermann, C. H. 1998. The molecular evolution of sperm bindin in six species of sea urchins (Echinozoa: Strongylocentrotidae). *Mol. Biol. Evol.* **15**: 1761–1771.
- Brandriff, B., G. W. Moy, and V. D. Vacquier. 1978. Isolation of sperm bindin from the oyster (*Crassostrea gigas*). *Gamete Res.* **89**: 89–99.
- Brendel, V., P. Bucher, I. Nourbakhsh, B. E. Blaisdell, and S. Karlin. 1992. Methods and algorithms for statistical analysis of protein sequences. *Proc. Natl. Acad. Sci. USA* **89**: 2002–2006.
- Civetta, A., and R. S. Singh. 1998. Sex-related genes, directional sexual selection, and speciation. *Mol. Biol. Evol.* **15**: 901–909.
- Debenham, P., M. A. Brzezinski, and K. R. Foltz. 2000. Evaluation of sequence variation and selection in the bindin locus of the red sea urchin, *Strongylocentrotus franciscanus*. *J. Mol. Evol.* **51**: 481–490.
- Duda, T. F., and S. R. Palumbi. 1999. Molecular genetics of ecological diversification: duplication and rapid evolution of toxin genes of the venomous gastropod *Conus*. *Proc. Natl. Acad. Sci. USA* **96**: 6820–6823.
- Ferris, P. J., E. V. Armbrust, and U. W. Goodenough. 2002. Genetic structure of the mating-type locus of *Chlamydomonas reinhardtii*. *Genetics* **160**: 181–200.
- Gao, B., L. E. Klein, R. J. Britten, and E. H. Davidson. 1986. Sequence of mRNA coding for bindin, a species-specific sperm protein required for fertilization. *Proc. Natl. Acad. Sci. USA* **83**: 8634–8638.
- Glabe, C. G., and D. Clark. 1991. The sequence of the *Arbacia punctulata* bindin cDNA and implications for the structural basis of species-specific sperm adhesion and fertilization. *Dev. Biol.* **143**: 282–288.
- Hellberg, M. E., and V. D. Vacquier. 1999. Rapid evolution of fertilization selectivity and lysin cDNA sequences in teguline gastropods. *Mol. Biol. Evol.* **16**: 839–848.
- Hofmann, A., and C. G. Glabe. 1994. Bindin, a multifunctional sperm ligand and the evolution of new species. *Semin. Dev. Biol.* **5**: 233–242.
- Hughes, A. L., T. Ota, and M. Nei. 1990. Positive Darwinian selection promotes charge profile diversity in the antigen-binding cleft of class I major-histocompatibility-complex molecules. *Mol. Biol. Evol.* **7**: 515–524.
- Kier, P. M. 1977. The poor fossil record of the regular echinoid. *Paleobiology* **3**: 168–174.
- Kresge, N., V. D. Vacquier, and C. D. Stout. 2001. Abalone lysin: the dissolving and evolving sperm protein. *Bioessays* **23**: 95–103.
- Kyte, J., and R. F. Doolittle. 1982. A simple method for displaying the hydrophobic character of a protein. *J. Mol. Biol.* **157**: 105–132.
- Lee, Y.-H., and V. D. Vacquier. 1992. The divergence of species-specific abalone sperm lysins is promoted by positive Darwinian selection. *Biol. Bull.* **182**: 97–104.
- Lee, Y.-H., T. Ota, and V. D. Vacquier. 1995. Positive selection is a general phenomenon in the evolution of abalone sperm lysin. *Mol. Biol. Evol.* **12**: 231–238.
- Littlewood, D. T. J., and A. B. Smith. 1995. A combined morphological and molecular phylogeny for sea urchins (Echinozoa: Echinodermata). *Philos. Trans. R. Soc. Lond. B* **347**: 213–234.
- Lloyd, A. T., and P. M. Sharp. 1992. CODONS: A microcomputer program for codon usage analysis. *J. Hered.* **83**: 239–240.
- Lopez, A., S. J. Miraglia, and C. G. Glabe. 1993. Structure/function analysis of the sea-urchin sperm adhesive protein bindin. *Dev. Biol.* **156**: 24–33.
- Luporini, P., A. Vallesi, C. Miceli, and R. A. Bradshaw. 1995. Chemical signaling in ciliates. *J. Eukaryot. Microbiol.* **42**: 208–212.
- Metz, E. C., and S. R. Palumbi. 1996. Positive selection and sequence rearrangements generate extensive polymorphism in the gamete recognition protein bindin. *Mol. Biol. Evol.* **13**: 397–406.
- Metz, E. C., G. Gomez-Gutierrez, and V. D. Vacquier. 1998a. Mitochondrial DNA and bindin gene sequence evolution among allopatric species of the sea urchin genus *Arbacia*. *Mol. Biol. Evol.* **15**: 185–195.
- Metz, E. C., R. Robles-Sikisaka, and V. D. Vacquier. 1998b. Nonsynonymous substitution in abalone sperm fertilization genes exceeds substitutions in introns and mitochondrial DNA. *Proc. Natl. Acad. Sci. USA* **95**: 10,676–10,681.
- Minor, J. E., D. R. Fromson, R. J. Britten, and E. H. Davidson. 1991. Comparison of the bindin proteins of *Strongylocentrotus franciscanus*, *S. purpuratus*, and *Lytechinus variegatus*: sequences involved in the species specificity of fertilization. *Mol. Biol. Evol.* **8**: 781–795.
- Moy, G. W., and V. D. Vacquier. 1979. Immunoperoxidase localization of bindin during the adhesion of sperm to sea urchin eggs. *Curr. Top. Dev. Biol.* **13**: 31–44.
- Rambaut, A. 1996. Se-AL: Sequence Alignment Editor. University of

- Oxford, Oxford [Online]. Available: <http://evolve.zoo.ox.ac.uk/> [accessed June 2003].
- Seidah, N. G., and M. Chretien. 1999.** Proprotein and prohormone convertases: a family of subtilases generating diverse bioactive polypeptides. *Brain Res.* **848**: 45–62.
- Smith, A. B. 1984.** *Echinoid Paleobiology*. George Allen and Unwin, London. 190 pp.
- Smith, A. B. 1988.** Phylogenetic relationship, divergence times, and rates of molecular evolution for camarodont sea urchins. *Mol. Biol. Evol.* **5**: 345–365.
- Smith, A. B., D. T. J. Littlewood, and G. A. Wray. 1995.** Comparing patterns of evolution: larval and adult life history stages and ribosomal RNA of post-Paleozoic echinoids. *Philos. Trans. R. Soc. Lond. B* **349**: 11–18.
- Steiner, D. F. 1998.** The proprotein convertases. *Curr. Opin. Chem. Biol.* **2**: 31–39.
- Swanson, W. J., and V. D. Vacquier. 2002.** Reproductive protein evolution. *Annu. Rev. Ecol. Syst.* **33**: 161–179.
- Takagi, T., A. Nakamura, R. Deguchi, and K. Kyojuka. 1994.** Isolation, characterization, and primary structure of three major proteins obtained from *Mytilus edulis* sperm. *J. Biochem.* **116**: 598–605.
- Taylor, W. R. 1986.** The classification of amino acid conservation. *J. Theor. Biol.* **119**: 205–218.
- Thompson, J. D., T. J. Gibson, F. Plewniak, F. Jeanmougin, and D. G. Higgins. 1997.** The ClustalX windows interface: flexible strategies for multiple sequence alignment aided by quality analysis tools. *Nucleic Acids Res.* **24**: 4876–4882.
- Ulrich, A. S., M. Otter, C. G. Glabe, and D. Hoekstra. 1998.** Membrane fusion is induced by a distinct peptide sequence of the sea urchin fertilization protein bindin. *J. Biol. Chem.* **273**: 16,748–16,755.
- Ulrich, A. S., W. Tichelaar, G. Forster, O. Zschornig, S. Weinkauff, and H. W. Meyer. 1999.** Ultrastructural characterization of peptide-induced membrane fusion and peptide self-assembly in the lipid bilayer. *Biophys. J.* **77**: 829–841.
- Vacquier, V. D. 1998.** Evolution of gamete recognition proteins. *Science* **281**: 1995–1998.
- Vacquier, V. D., and G. W. Moy. 1977.** Isolation of bindin: the protein responsible for adhesion of sperm to sea urchin eggs. *Proc. Natl. Acad. Sci. USA* **74**: 2456–2460.
- Vacquier, V. D., W. J. Swanson, and M. E. Hellberg. 1995.** What have we learned about sea urchin sperm bindin? *Dev. Growth Differ.* **37**: 1–10.
- Wright, F. 1990.** The “effective number of codons” used in a gene. *Gene* **87**: 23–29.
- Yang, Z., W. J. Swanson, and V. D. Vacquier. 2000.** Maximum likelihood analysis of molecular adaptation in abalone sperm lysin reveals variable selective pressures among lineages and sites. *Mol. Biol. Evol.* **17**: 1446–1455.
- Zigler, K. S., and H. A. Lessios. 2003.** Evolution of bindin in the pantropical sea urchin *Tripneustes*: comparisons to bindin of other genera. *Mol. Biol. Evol.* **20**: 220–231.
- Zigler, K. S., E. C. Raff, E. Popodi, R. A. Raff, and H. A. Lessios. 2003.** Adaptive evolution of bindin is correlated with the shift to direct development in the genus *Heliocidaris*. *Evolution* (In press).

## Behavioral Characterization of Attractin, a Water-Borne Peptide Pheromone in the Genus *Aplysia*

SHERRY D. PAINTER\*, BRET CLOUGH, SARA BLACK, AND GREGG T. NAGLE

*The Marine Biomedical Institute and the Department of Anatomy and Neurosciences,  
University of Texas Medical Branch, Galveston, Texas 77555-1069*

**Abstract.** Pheromones play a significant role in coordinating reproductive activity in many animals, including opisthobranch molluscs of the genus *Aplysia*. Although solitary during most of the year, these simultaneous hermaphrodites gather into breeding aggregations during the reproductive season. The aggregations contain both mating and egg-laying animals and are associated with masses of egg cordons. The egg cordons are a source of pheromones that attract other *Aplysia* to the area, reduce their latency to mating, and induce egg laying. One of these water-borne egg cordon pheromones ("attractin") has been characterized and shown to be attractive in T-maze assays. Attractin is the first water-borne peptide pheromone characterized in invertebrates.

In the current studies, behavioral assays were used to better characterize the attraction, and to examine whether attractin can induce mating. Although the two activities could be related (*i.e.*, attraction occurring because animals were looking for a partner), this was not tested. T-maze assays showed that attractin works as part of a bouquet of odors: the peptide is attractive only when *Aplysia brasiliiana* is part of the stimulus. The animal does not need to be a conspecific, perhaps explaining why multiple species may be associated with one aggregation. Native and recombinant attractin are equally attractive, verifying that *N*-glycosylation at residue 8 is not required for attraction.

Mating studies showed that both native and recombinant

attractin reduce the latency to mating. The effects are larger when hermaphroditic mating is considered: in addition to reducing latency, attractin doubles the number of pairs mating as hermaphrodites. The effect may result from attractin stimulating both animals to mate as males and would be consistent with behaviors previously seen in the T-maze. Attractin may thus be contributing to the formation of copulatory chains and rings seen in aggregations in the field.

These results may be interpreted in two ways: (1) attractin has multiple activities that contribute to the establishment and maintenance of the aggregation; or (2) the induced desire to mate may make attractin attractive when it is presented in conjunction with an animal. In either case, the results open the door for cellular and molecular studies of mechanism of action.

### Introduction

Chemical communication is the most ancient form of communication and is used by most, if not all, animals examined. The organisms include, for example, ciliated protozoans (Luporini *et al.*, 1995), yeast (Kodama *et al.*, 2003), insects (Monsma and Wolfner, 1988; Roelofs *et al.*, 2002; Saudan *et al.*, 2002), molluscs (Painter *et al.*, 1998), worms (Ram *et al.*, 1999), fish (Li *et al.*, 2002), amphibians (Kikuyama *et al.*, 1995; Rollmann *et al.*, 1999; Wabnitz *et al.*, 1999), rodents (Stowers *et al.*, 2002; Novotny, 2003) and humans (Savic *et al.*, 2001.). The number of pheromones characterized in each species depends, at least in part, on the chemical nature of the pheromones and on whether the pheromones are water-borne.

Opisthobranch molluscs of the genus *Aplysia* are simultaneous hermaphrodites that do not normally fertilize their own eggs. Field studies (Kupfermann and Carew, 1974; Audesirk, 1979; Susswein *et al.*, 1983, 1984) have shown that they are solitary animals that move into breeding ag-

Received 8 October 2002; accepted 16 April 2003.

\* To whom correspondence should be addressed. Marine Biomedical Institute, 2.138 Medical Research Building, University of Texas Medical Branch, 301 University Blvd., Galveston, Texas 77555-1069. E-mail: sdpainter@houston.rr.com

*Abbreviations:* ASW, artificial seawater; Att, attractin; CH<sub>3</sub>CN, acetonitrile; HFBA, heptafluorobutyric acid; M-REP, Marine Research and Educational Products; RP-HPLC, reversed-phase high performance liquid chromatography.

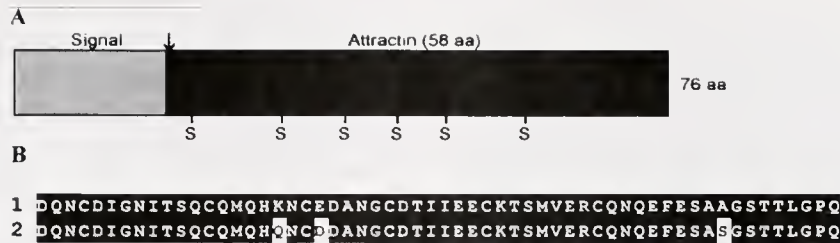


**Figure 1.** (A) Schematic diagram of the precursor to the attractin pheromone from the albumen gland of *Aplysia californica*. Cleavage of the signal sequence (arrow) generates the 58-residue pheromone attractin. The disulfide-bonding pattern of cysteine residues (S) is I–IV, II–V, and III–IV, where the Roman numeral indicates the order of occurrence in the primary sequence (Schein *et al.*, 2001). Unlike attractin, the precursors for pheromones that act as part of a group of scents often contain sequences of more than one scent. (B) The amino acid sequences of attractin from the two species of *Aplysia* used in the current studies, *A. californica* and *A. brasiliana* (Painter *et al.*, 1998, 2000). Amino acid residues that are identical to those in *A. californica* attractin are indicated by the black background.

gregations during the reproductive season. The aggregations typically contain both mating and egg-laying animals and are associated with masses of recently deposited egg cordons, often deposited one on top of another. Most of the egg-laying animals mate simultaneously as females even though mating does not cause reflex ovulation (Blankenship *et al.*, 1983), suggesting that egg laying precedes mating in the aggregation and that egg laying may release pheromones that establish and maintain the aggregation.

Similar observations have been made in the laboratory when animals were not individually caged (Audesirk, 1979; Blankenship *et al.*, 1983; Susswein *et al.*, 1983, 1984), and behavioral studies have shown that egg-laying animals with cordons are more attractive than sexually mature but non-laying conspecifics (Aspey and Blankenship, 1976; Jahan-Parwar, 1976; Audesirk, 1977; Painter *et al.*, 1989). T-maze assays show that at least some of the attractants derive from the egg cordon and are waterborne: (1) recent egg-layers without egg cordons are no more attractive than non-laying conspecifics; (2) recently deposited egg cordons are attractive, with or without a non-laying conspecific, but sham egg cordons are not; and (3) both recently deposited egg cordons and their eluates increase the attractiveness of non-laying conspecifics when placed in the surrounding seawater (Painter *et al.*, 1991; Painter, 1992).

One of the water-borne pheromonal attractants has been isolated from eluates of the egg cordon and characterized. Named attractin, it is a 58-residue peptide that has six cysteines that form three intramolecular disulfide bonds (Fig. 1; Painter *et al.*, 1998; Schein *et al.*, 2001). Attractin was isolated from a Pacific Coast species (*A. californica*) and bioassayed in a species from the Gulf of Mexico (*A. brasiliana*). This was done because individuals of *A. californica* tend to crawl out of T-maze chambers before they are exposed to the stimulus. *A. californica* attractin was attractive to *A. brasiliana* and produced behaviors that were suggestive of mating (Painter *et al.*, 1998), but these behaviors were not further analyzed. The amount of attrac-

tin that was attractive to conspecifics and induced the potential mating behaviors (1–10 pmol in 6 l artificial seawater) was in the range of concentrations normally observed with pheromones, demonstrating that attractin has pheromonal activity.

There is no geographical overlap between the distributions of the two species, suggesting that attractin or an attractin-related peptide is a pheromonal attractant in *A. brasiliana*. A peptide was subsequently isolated from the *A. brasiliana* albumen gland and sequenced. It is 58 amino acids in length and differs from *A. californica* attractin at only 3 amino acids (Fig. 1; Painter *et al.*, 2000). It is deposited on the egg cordon and elutes into the seawater following deposition. It could thus serve a pheromonal function in *A. brasiliana*, but its pheromonal activities have yet to be tested.

In the present study, behavioral assays were used to better characterize the attraction and to examine whether mating is induced. The current T-maze assays showed that attractin works as part of a bouquet of water-borne odors: the peptide is attractive only when individuals of *A. brasiliana* or *A. californica* are part of the stimulus. The animal does not need to be a conspecific, perhaps explaining why multiple species of *Aplysia* may be associated with one aggregation—for example, *A. vaccaria* with *A. californica* aggregations (Kupfermann and Carew, 1974; Pennings, 1991); *A. californica* with *A. vaccaria* aggregations (S. LePage, Marine Research and Educational Products (M-REP), pers. comm.); and *A. depilans* with *A. fasciata* aggregations (Achituv and Susswein, 1985). Recombinant attractin was also tested for two reasons: (1) to see whether *N*-glycosylation at Asn<sup>8</sup> is necessary for attraction (native attractin is glycosylated and recombinant attractin is not); and (2) to see whether the two are equally attractive, so that recombinant attractin could be used in 3D nuclear magnetic resonance solution structure studies (Garimella *et al.*, 2003) and for future studies of mechanism of action at the receptor level.

A series of mating assays was performed because behav-

iors in earlier T-maze assays suggested that both the stimulus and test animals wanted to mate (Painter *et al.*, 1998). The assays showed that attractin reduces the latency to mating at concentrations consistent with a pheromone. Attractin also reduces the latency to hermaphroditic mating and doubles the number of pairs mating as hermaphrodites. This effect may result from attractin stimulating both animals to mate as males and would be consistent with behaviors seen in earlier T-maze assays (Painter *et al.*, 1998). These results suggest that attractin, acting in an aggregation where there are more animals, could be at least partially responsible for the copulatory chains and rings that have been observed. Recombinant attractin also induces mating, both one-way and as a hermaphrodite, showing that *N*-glycosylation is not required for the induction of either type of mating. The attraction and mating data demonstrate that attractin may contribute to the establishment and maintenance of breeding aggregations, and to successful reproduction.

## Materials, Methods, and Results

### Animals

Specimens of *Aplysia brasiliana* (Rang), ranging in weight from 100 to 500 g, were collected from South Padre Island, Texas, and were used in experiments between June and September. *A. brasiliana* was used as the experimental animal in the T-maze and mating experiments because it is more reproductively active than *A. californica* (see fig. 2 in Painter *et al.*, 1998), does not crawl out of T-mazes, makes fewer false choices, and can be collected in large numbers from the south Texas coast during the reproductive season. Previous T-maze assays (Painter *et al.*, 1998) showed that an individual of *A. brasiliana* is attracted to a non-laying conspecific and displays behaviors suggestive of mating when 10 pmol of attractin is placed in the adjacent artificial seawater, even though attractin is a product of the *A. californica* albumen gland.

The animals were housed in individual plastic cages in one of five aquaria containing recirculating artificial seawater (ASW; Instant Ocean Marine Salt, Longhorn Pet Supply, Houston, Texas). Water was maintained at room temperature ( $20^{\circ} \pm 2^{\circ}\text{C}$ ); the salinity ranged from 30 to 32 ppt. A 14:10 light:dark cycle was maintained in the aquarium facility, with the light period starting at 0600. Animals were fed dried laver in the late afternoon (1600–1800) after experiments were completed.

Egg-laying activity was checked twice every day (0800–0900, 1600–1800), egg-laying activity was recorded, and egg cordons were removed. All animals used in assays were sexually mature, as defined by the ability to lay eggs spontaneously or in response to injection of atrial gland extracts (made as described in Painter *et al.*, 1991).

Specimens of *A. californica* (Cooper) were obtained from

Alacrity Marine Biological Services (Redondo Beach, California) and M-REP (Escondido, California). They were maintained as described above, except that the water temperature was  $14^{\circ} \pm 2^{\circ}\text{C}$ . This species was used as a stimulus animal in one set of T-maze assays and as the source of albumen glands for purification of native attractin.

### Purification of native and recombinant attractin

**Procedures.** Attractin from the albumen gland of *A. californica* was purified by analytical C18 reversed-phase high performance liquid chromatography (RP-HPLC) as previously described (Painter *et al.*, 1998). To prepare recombinant attractin, the *A. californica* albumen-gland attractin cDNA (Fan *et al.*, 1997) was subcloned into the baculovirus expression vector pFastBac 1, and recombinant virus was generated using the Bac-to-Bac Baculovirus Expression System (Invitrogen). Attractin was expressed in Sf9 insect cells grown at 27–28 °C in Sf-900 II serum-free medium (Invitrogen).

Expressing Sf9 cells were centrifuged, and the pellet was resuspended in 20 ml of ice-cold 0.1% heptafluorobutyric acid (HFBA) and sonicated. The resulting lysates were purified on C18 Sep-Pak Vac cartridges (5 g; Waters Corp.) that were pretreated with 10 ml of 100% acetonitrile ( $\text{CH}_3\text{CN}$ ) containing 0.1% HFBA and rinsed with 20 ml of 0.1% HFBA. The peptides were loaded, eluted with 15 ml of 50%  $\text{CH}_3\text{CN}$  containing 0.1% HFBA, and lyophilized. The lyophilizate was resuspended in 2.5 ml of 0.1% HFBA and applied to a Vydac analytical C18 RP-HPLC column ( $4.6 \times 250$  mm).

The column was eluted with a two-step linear gradient of 0.1% HFBA in water and 100%  $\text{CH}_3\text{CN}$  containing 0.1% HFBA. The first step was 0%–10%  $\text{CH}_3\text{CN}$  in 5 min, followed by a shallower gradient from 10% to 34%  $\text{CH}_3\text{CN}$  in 85 min. The column eluate was monitored at 215 nm, and 1-min (1 ml) fractions were collected. The attractin-containing fractions were combined, lyophilized, and repurified by Vydac C18 RP-HPLC. The same gradient conditions were used as described above, except that 0.1% trifluoroacetic acid was the counterion.

**Results.** The RP-HPLC peak fractions containing *A. californica* recombinant attractin, identified by comparison to the elution time of native attractin, were characterized by amino acid compositional and microsequence analyses; the 58-residue peptide sequence was identical to *A. californica* albumen-gland attractin except that, according to matrix-assisted laser desorption/ionization mass spectrometry, the native peptide is *N*-glycosylated at Asn<sup>8</sup> and the recombinant peptide is not.

### Pheromonal attraction

**Procedures.** The T-maze, and its associated cages, is illustrated in Figure 2. Before each assay, 6 l of ASW was

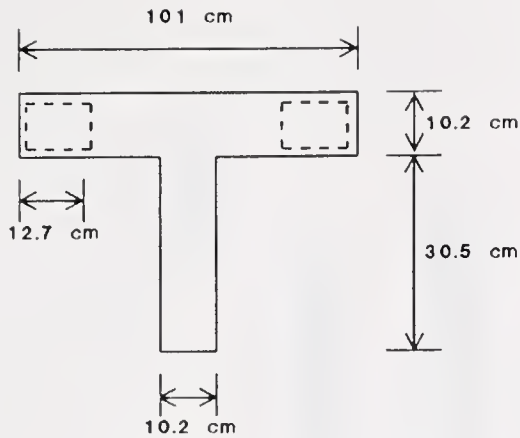


**Figure 2.** Schematic diagram of the T-maze with removable stimulus cages (dashed outlines) in place. T-maze depth: 10.2 cm.

put into the maze; the ASW was stationary during experiments. To minimize the amount of stress experienced by the animals during transfer to the maze, the ASW was similar in temperature and salinity to that in the aquarium from which the animals were taken. The ASW placed in the maze had not previously contacted *A. californica* or *A. brasiliensis*, because there are animal-derived factors that make a non-laying conspecific attractive (Painter *et al.*, 1991).

A non-laying conspecific was placed in one of the stimulus cages and a potential attractant added to the adjacent ASW; this is the stimulus animal. After 5 min, a non-laying animal, known as the test animal, was placed in the base of the maze and watched for up to 20 min. In most cases, the test animal moved directly to the top of the maze and exhibited one of two patterns of behavior. (1) It stopped, moved its head from side to side, then either moved into one arm or returned to the base of the maze and remained there. (2) It swam around in the maze, often visiting both cages before deciding where to stop. A response was considered to be positive if the test animal traveled to the stimulus within 20 min, and then maintained contact with the stimulus cage for 5 min. It was negative if the test animal traveled to the cage in the opposite arm and maintained contact for 5 min. The response was considered to be no choice if the test animal did neither. Ten assays were performed for every potential attractant, and the attractant was alternated between arms in consecutive assays. Statistical significance was assessed by chi-square analysis. In each case, test animals were choosing between a stimulus in one arm and no stimulus in the other.

Animals for each assay were selected on the basis of three criteria. First, the animals must have been sexually mature but not have laid eggs or been used in a bioassay during the preceding 24 h. Second, the test animal must not have been exposed previously to the fraction being tested. Third, stimulus and test animals must have been housed in the same aquarium (Painter *et al.*, 1998). An exception was made to

the third criterion in one set of assays, when *A. californica* was used as the stimulus animal. *A. brasiliensis* was always used as the test animal (Painter *et al.*, 1998).

Several series of experiments were performed. The first compared the attractiveness of a non-laying specimen of *A. brasiliensis* with 1 pmol of either native or recombinant attractin in the adjacent ASW to a non-laying conspecific with nothing added. We were asking several questions. Are smaller amounts of native attractin attractive? Is recombinant attractin as attractive? Would it be feasible to use recombinant attractin in future behavioral, molecular, or 3D structural studies? The second series examined whether a non-laying conspecific was needed for 1 pmol attractin to be attractive. We were asking: does attractin function alone or as part of a "bouquet of scents," as other pheromones do in many systems? The third series examined whether the non-laying animal must be a conspecific. We were asking: could the presence of multiple species at one breeding aggregation be due, partially or completely, to attractin? If animal-derived factors are necessary, do they differ among species?

**Results.** The results of the experiments comparing the attractiveness of native and recombinant attractin are shown in Figure 3. In the negative control (non-laying conspecific with nothing placed in the adjacent ASW), two animals (20%) traveled to the right arm and remained, two (20%) traveled to the left arm and remained, and six (60%) did neither. Of the four animals making a choice, only two went to the stimulus animal, one of which was in the right arm and the other of which was in the left arm of the maze. These bioassays verify that there is no directional bias in the maze and establish chance levels of attraction at two animals.

The response pattern changed when 1 pmol of either native or recombinant attractin was placed in the seawater adjacent to the stimulus animal (Fig. 3): 9 of 10 animals (90%) were attracted to recombinant attractin, and 8 of 10 animals (80%) were attracted to native attractin; in both cases, fewer animals went to the opposite arm and fewer failed to make a choice. The response patterns for each differed significantly from that for a non-laying conspecific alone [recombinant:  $\chi^2(2) = 13.75$ ;  $P < 0.005$ ; native:  $\chi^2(2) = 10.44$ ,  $0.05 < P < 0.1$ ], but did not differ significantly from each other [ $\chi^2(2) = 2.1$ ,  $0.25 < P < 0.5$ ].

The results of the experiment examining whether an animal is needed for attraction are shown in Figure 3. When 1 pmol recombinant attractin was placed in the seawater without a stimulus animal, 3 of 10 animals (30%) were attracted to recombinant attractin, two animals (20%) went to the opposite arm, and five animals (50%) did neither (Fig. 3). The response pattern to 1 pmol recombinant attractin alone differed significantly from that to 1 pmol recombinant attractin with an animal [ $\chi^2(2) = 6.00$ ;  $0.025 < P < 0.05$ ], but did not differ from that to a non-laying conspecific alone [ $\chi^2(2) = 0.277$ ;  $0.95 < P < 0.975$ ].

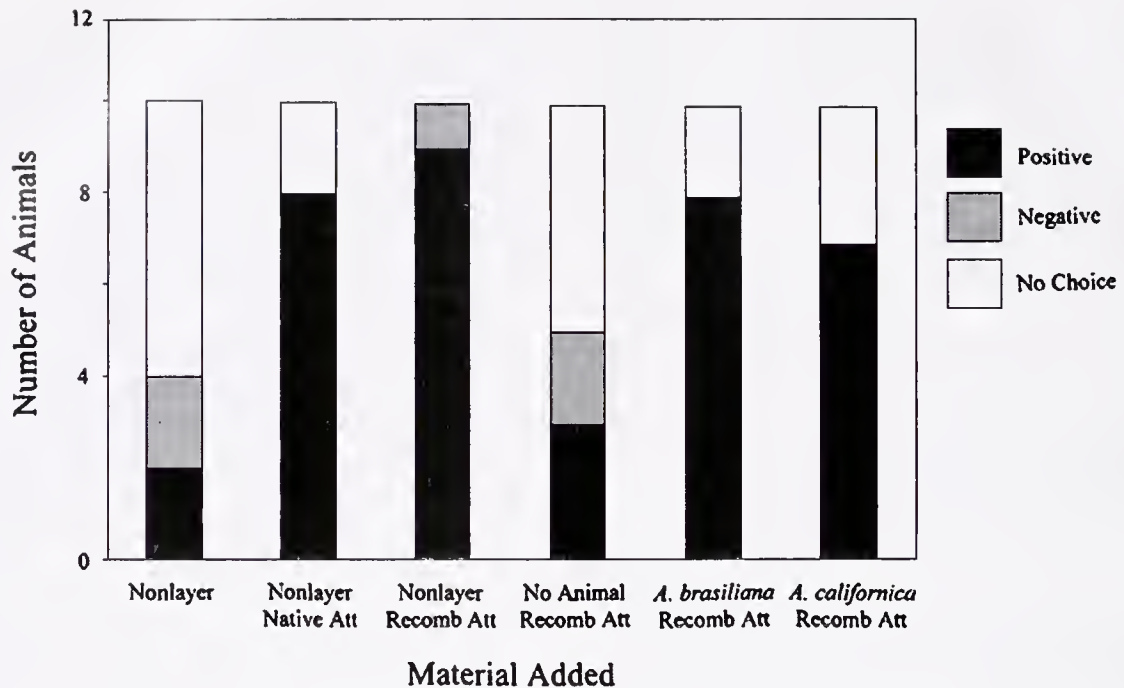


**Figure 3.** Both native and recombinant attractin are attractive; attractin acts in conjunction with other odors; and the animal-derived factor is not species-specific. The number of *Aplysia brasiliiana* individuals attracted to a non-laying conspecific (Nonlayer) was increased by placing 1 pmol of either native attractin (Nonlayer Native Att) or recombinant attractin (Nonlayer Recomb Att) in the adjacent seawater. In each assay, animals chose between a stimulus in one arm and no stimulus in the other. Fewer *A. brasiliiana* individuals were attracted to recombinant attractin when the stimulus did not contain a non-laying conspecific (No Animal Recomb Att; 1 pmol). About the same number of *A. brasiliiana* individuals were attracted to the specimen of *A. californica* with recombinant attractin (*A. californica* Recomb Att; 1 pmol) as were attracted to the specimen of *A. brasiliiana* with recombinant attractin (*A. brasiliiana* Recomb Att; 1 pmol).

Animals do not release attractin unless they are laying eggs; therefore, the combined odor of a non-laying animal and attractin produces a qualitatively different stimulus from attractin alone. The data confirm that attractin functions as part of a bouquet of scents and led us to ask, Does the animal-derived pheromone have to come from a conspecific or can it come from a different species of *Aplysia*, perhaps accounting for the presence of multiple species at an aggregation? This would also be consistent with reports of multiple species showing up at one aggregation in the field.

The results of experiments examining whether the stimulus animal needs to be a conspecific in order for attractin to be attractive are shown in Figure 3. When 1 pmol of recombinant attractin was placed in the seawater adjacent to *A. brasiliiana*, 8 of 10 *A. brasiliiana* (80%) were attracted to the non-laying conspecific. When 1 pmol of recombinant attractin was placed in the seawater adjacent to *A. californica*, 7 of 10 *A. brasiliiana* (70%) were attracted to the non-laying *A. californica*. The response patterns for the two species did not differ significantly from each other [ $\chi^2(2) = 0.265$ ;  $0.75 < P < 0.9$ ], but each differed significantly from

that for a non-laying *A. brasiliiana* alone [*A. brasiliiana*,  $\chi^2(2) = 10.44$ ;  $0.005 < P < 0.01$ ; *A. californica*,  $\chi^2(2) = 7.50$ ;  $0.005 < P < 0.01$ ].

#### *Pheromonal induction of mating activity*

**Procedures.** As in the T-maze bioassays, three criteria were used to select animals for each experiment. First, the animals must have been sexually mature but not have laid eggs or been used in a bioassay during the previous 24 h. Second, the animals must not have been exposed previously to the fraction being tested or have been paired with the same animal twice. Third, both animals must have been housed in the same aquarium (Painter *et al.*, 1998).

Each assay was performed in 3 l of aerated ASW in a 4-l plastic beaker. The ASW had approximately the same osmolarity and temperature as the ASW in the aquarium from which the animals were removed, and had not previously contacted *A. brasiliiana*. Animal-conditioned ASW not only increases the attractiveness of a non-laying conspecific, but also reduces the latency to mating (Painter *et al.*, 1991).

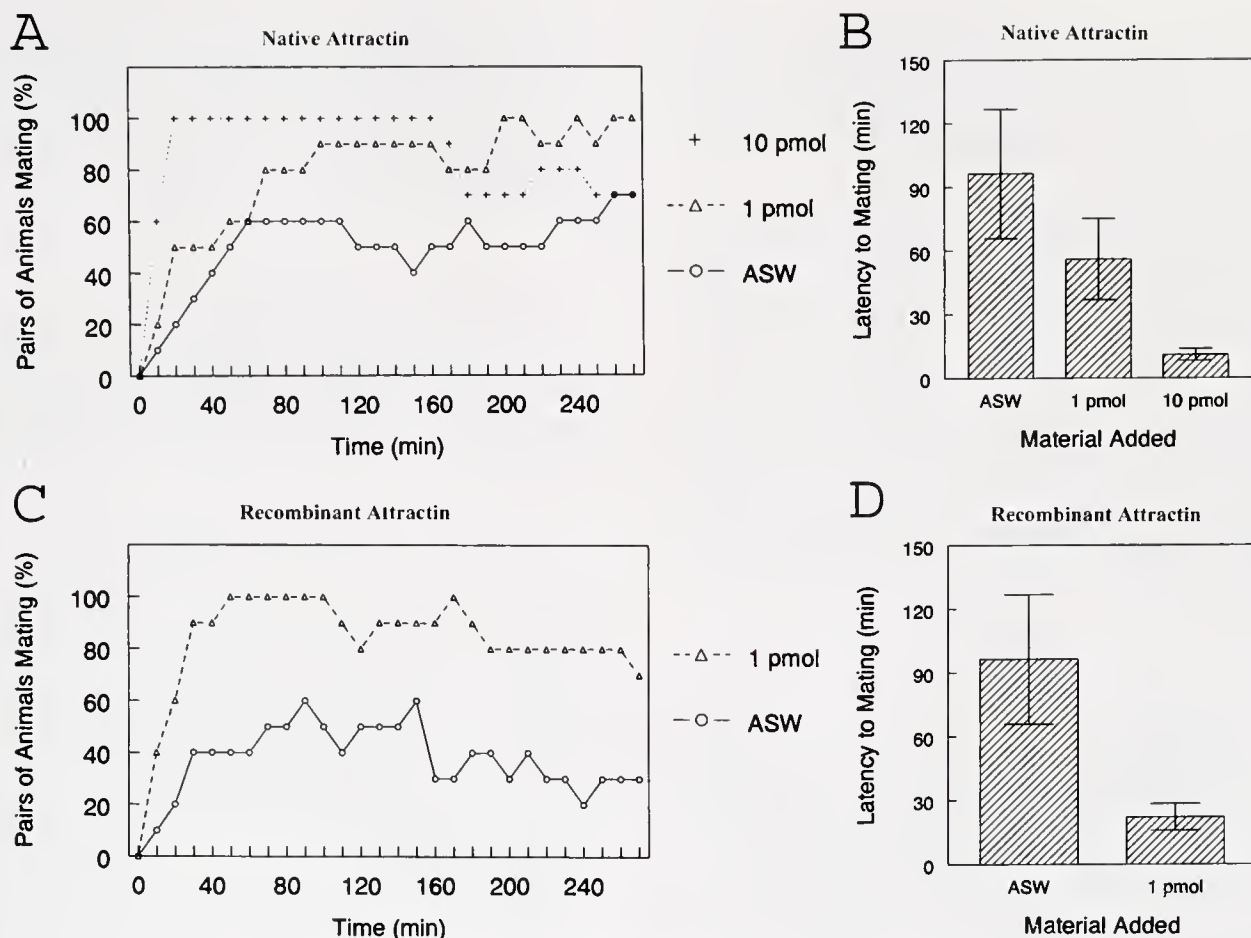


**Figure 4.** Both native and recombinant attractin reduce the latency to mating in *Aplysia brasiliiana*. (A) The percentage of animals mating at early time periods was increased when native attractin was placed in the adjacent seawater. (B) The latency to mating was reduced by placing either 1 pmol or 10 pmol native attractin in the seawater. (C) The percentage of animals mating at early time periods was increased when recombinant attractin was placed in the adjacent seawater. (D) The latency to mating was reduced by placing 1 pmol recombinant attractin in the seawater.

Animals were rinsed in fresh non-conditioned ASW before being introduced into the experimental beaker.

Two individuals of *A. brasiliiana* and a test sample were added to a beaker, and behaviors were assessed at 10-min intervals for 270 min. Three categories of behavior were identified: (1) mating as a female or male (one-way mating), (2) mating as a hermaphrodite, and (3) laying eggs. Since an egg cordon is a source of multiple contact and water-borne pheromones that modify reproductive behaviors, egg-laying activity was noted and the bioassay stopped; the bioassay for that sample was repeated with other animals. Egg laying occurred rarely with any stimulus.

Test samples included ASW with nothing added (negative control), ASW with 1 or 10 pmol native attractin added, and ASW with 1 pmol recombinant attractin added. The statistical significance of the differences between time points was determined by chi-square analysis; the statistical

significance of differences in mean latency was determined by one-way analysis of variance. The same number of assays was performed for each treatment.

*Results (native attractin).* When 1 or 10 pmol of native attractin was placed in ASW containing two non-laying specimens of *A. brasiliiana*, the percentage of animals mating at each time point (10-min intervals) was recorded. The percentage of animals mating was significantly increased for 10 pmol attractin at 10, 20, 30, and 40 min, and there was a nonsignificant trend in this direction for 1 pmol attractin (Fig. 4A). The mean latency to mating was significantly reduced for 10 pmol attractin ( $\chi^2(1) > 3.84$  for each;  $P < 0.05$ ;  $n = 10$ ), and there was a nonsignificant trend in this direction for 1 pmol (Fig. 4B). Although the latency to mating was reduced, the overall percentage of animal pairs mating during the 270-min period was not affected (negative controls: 90% mated; native attractin: 100% mated),

perhaps reflecting the long duration of the assay or animal housing in individual cages. In these experiments, nearly all animal pairs eventually mated during the 270-min time period, regardless of whether attractin was present. Nevertheless, the results suggest that attractin facilitates, but does not induce, mating.

**Results (recombinant attractin).** When 1 pmol of recombinant attractin was placed in ASW containing two non-laying specimens of *A. brasiliana*, the percentage of animals mating at 10, 20, 170, and 240 min was significantly increased compared to negative controls [ $\chi^2(1) > 3.84$  for each;  $P < 0.05$ ;  $n = 10$ ; Fig. 4C]. The mean latency to mating was significantly reduced for 1 pmol recombinant attractin ( $P < 0.05$ ; one-way analysis of variance; Fig. 4D). Although the latency to mating was reduced, the total percentage of animal pairs that mated during the entire 270-min period was similar (negative controls: 90% mated; recombinant attractin: 100% mated), suggesting again that attractin facilitates, rather than induces, mating.

#### *Pheromonal induction of hermaphroditic mating*

**Procedure.** This is a re-analysis of the data collected in the mating assays, focusing on whether attractin can induce or facilitate hermaphroditic mating. As noted above, hermaphroditic mating was recorded during the mating assays.

**Results (native attractin).** When native attractin was placed in the ASW surrounding two non-laying specimens of *A. brasiliana*, the percentage of animal pairs mating as hermaphrodites was significantly increased for 10 pmol attractin at every time point between 20 and 170 min and for 190, 200, 230, and 250 min ( $\chi^2(1) > 3.84$  for each;  $P < 0.05$ ;  $n = 10$ ); the same was true for 1 pmol attractin at 230, 240, and 250 min ( $\chi^2(1) > 3.84$  for each;  $P < 0.05$ ;  $n = 10$ ) (Fig. 5A). The mean latency to hermaphroditic mating was significantly reduced for 10 pmol attractin ( $P < 0.05$ ; one-way analysis of variance), and there was a nonsignificant trend in this direction for 1 pmol attractin (Fig. 5B). Compared to control assays, the percentage of animal pairs that mated as hermaphrodites during the 270-min period was about doubled (negative controls: 40%; 1 pmol: 70%; 10 pmol: 80%). This suggests that attractin induces, rather than facilitates, hermaphroditic mating, perhaps by stimulating both animals to mate as males. This induction could be responsible for copulatory rings and chains in the field, which may result because there are usually more than two animals in an aggregation.

**Results (recombinant attractin).** The percentage of animals mating as hermaphrodites at any given time point and the latency to hermaphroditic mating were not significantly increased upon addition of 1 pmol of recombinant attractin, although there were trends in this direction (Fig. 5 C, D). Although the percentage of animals mating as hermaphro-

dites was not significantly increased at any particular time point, the percentage of animal pairs that mated as hermaphrodites at some point during the assay did increase (negative controls: 40% mated as hermaphrodites; recombinant attractin: 70% mated as hermaphrodites). A dose of 10 pmol was not tested, which may account for the lack of statistical significance.

## Discussion

We purified native attractin from extracts of *Aplysia californica* albumen gland (Painter *et al.*, 1998) and recombinant attractin from insect cells to better characterize the biological activity of the peptide and to see whether recombinant attractin could be used in future molecular studies.

#### *Pheromonal attraction*

In the T-maze, the attractiveness of a stimulus animal was significantly increased when 1 pmol of either native or recombinant attractin was placed in the adjacent seawater, verifying that both peptides are attractive in amounts consistent with pheromonal activity, and confirming that *N*-glycosylation is not required for attraction. The response patterns for the two peptides do not differ significantly from each other, demonstrating that either could be used in future studies. Recombinant attractin was therefore used in subsequent T-maze bioassays. Since it was not *N*-glycosylated, recombinant attractin was also used to determine the solution structure of the pheromone by 3D nuclear magnetic resonance (Garimella *et al.*, 2003).

Fewer individuals of *A. brasiliana* were attracted to recombinant attractin when the stimulus did not contain a non-laying conspecific, demonstrating that attractin acts in concert with other unidentified odors to stimulate attraction. These results, combined with earlier observations (the egg cordon is attractive without a stimulus animal, Painter *et al.*, 1991; attractin elutes from the egg cordon, Painter *et al.*, 1998), suggest that the composition of the bouquet of scents can vary. To identify other attractive chemical factors in the egg-cordon bouquet of scents, we have begun isolating other peptides/proteins that elute from the cordon for bioassay.

To begin looking for animal-derived attractants, we tested whether the stimulus animal needs to be a conspecific. It does not. *A. californica* with attractin and *A. brasiliana* with attractin each attracted a similar number of *A. brasiliana*. This pairing may seem inappropriate since the two species do not overlap in their geographic distributions (*A. californica*, Pacific Coast; *A. brasiliana*, Gulf of Mexico), but it may help explain why multiple *Aplysia* species are sometimes associated with one aggregation. For example, *A. californica* and *A. vaccaria* have been observed in the same breeding aggregations off the coast of California (Kupfermann and Carew, 1974; S. LePage, M-REP, pers.

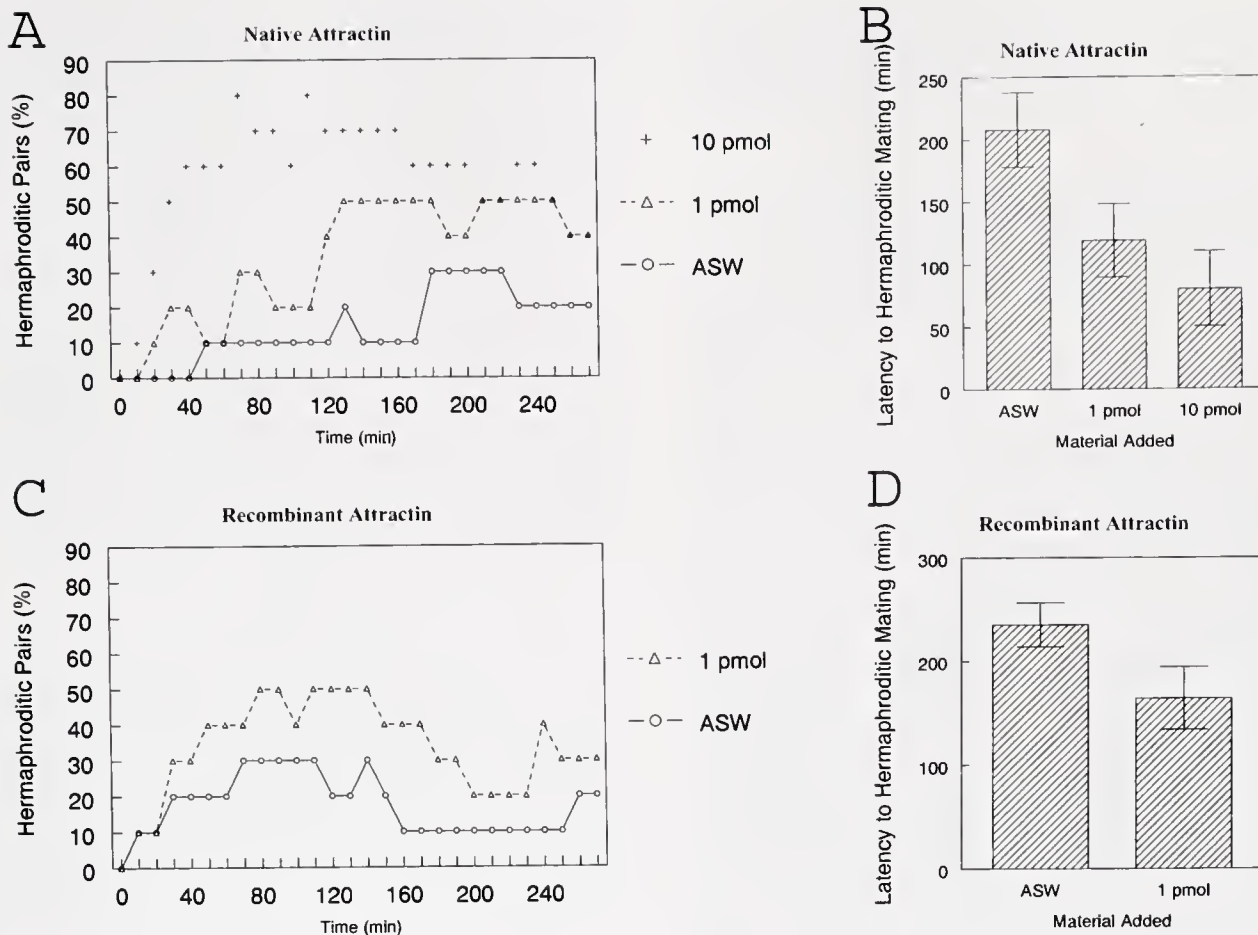


**Figure 5.** Both native and recombinant attractin induce hermaphroditic mating in *Aplysia brasiliiana*. (A) The percentage of animals mating as hermaphrodites was increased when native attractin was placed in the adjacent seawater. (B) The latency to hermaphroditic mating was reduced by placing either 1 pmol or 10 pmol native attractin in the seawater. (C and D) The percentage of animal pairs mating as hermaphrodites was increased when 1 pmol recombinant attractin was placed in the adjacent seawater. The mean latency to hermaphroditic mating was also reduced.

comm.), and have been seen mating with each other in the aggregation (S. LePage, M-REP, pers. comm.). *A. fasciata* and *A. depilans* have also been seen associated with the same aggregation (Achituv and Susswein, 1985), but mating has not been observed because their reproductive cycles are not entirely synchronized. Audesirk (1977) previously found that *A. californica* was not attracted to conspecifics in Y-maze assays, and Audesirk and Audesirk (1977) showed that there was no seasonal effect on the sensitivity to conspecifics. Furthermore, experimental perfusion of the *A. californica* rhinophore nerve with seawater that had bathed *A. californica*, *A. vaccaria*, or *Pleurobranchia californica* evoked about the same increase in afferent activity, suggesting that aggregations of *Aplysia* species in the field are not determined by species-specific chemical cues (Chase, 1979).

*Pheromonal induction of mating*

Mating assays were performed because behaviors seen in earlier T-maze assays suggested that exposure to attractin could stimulate behaviors suggestive of mating as a male (Painter *et al.*, 1998). The current studies showed that when attractin is added to the seawater adjacent to a pair of *A. brasiliiana*, the latency to mating is reduced relative to controls. However, the overall percentage of animal pairs mating during the prolonged assay period was not significantly different, suggesting that attractin facilitates, but does not induce, mating.

Attractin also significantly reduces the latency to hermaphroditic mating when added to the seawater surrounding a pair of *A. brasiliiana*. The percentage of animal pairs mating as hermaphrodites during the assay period was about doubled, suggesting that attractin induces hermaphroditic

mating. This effect may result from attractin stimulating both animals to mate as males, as suggested by T-maze behaviors. Overall, these data suggest that attractin contributes to the establishment and maintenance of breeding aggregations.

#### *Attractin does not stimulate species-specific attraction*

The attractins appear to be a structurally diverse family of peptides, each of which is sequence-specific for a given species. Attractin has recently been characterized from *A. brasiliensis*, *A. fasciata*, *A. vaccaria*, *A. depilans*, and *Bursatella leachii* and found to be 95%, 91%, 43%, 41%, and 21% identical to *A. californica* attractin, respectively (Painter *et al.*, 2000, and unpubl. data). Nevertheless, attractin is attractive to all aquatic gastropods tested to date: (1) *A. californica* attractin is attractive to *A. brasiliensis* (Painter *et al.*, 1998); (2) *A. vaccaria* attractin is attractive to *A. brasiliensis* (unpubl. data); and (3) *A. californica* attractin is attractive to the freshwater pulmonate *Lymnaea stagnalis* (A. ter Maat, Free University, Amsterdam, pers. comm.). Although the primary structures of attractin-related peptides are divergent, their 3D structures may be similar to *A. californica* attractin (Garimella *et al.*, 2003). To our knowledge, the attractins are the first peptide pheromone family in invertebrates that is not species-specific. In contrast, waterborne peptide pheromonal attractants in amphibians are species-specific (Kikuyama *et al.*, 2002).

There may be advantages to attracting multiple species to the same breeding aggregation. If members of a second species lay eggs on those of a different species, the mixed egg mass becomes larger, which might in some way protect the eggs of both species. Another possibility is that egg laying by one *Aplysia* species attracts a second species that then lays eggs and releases attractin, which may eventually attract members of the first species. Because attractin is continuously degraded from the C-terminus after its release (Painter *et al.*, 1998, and unpubl. obs.), it may be advantageous to attract as many individual *Aplysia* as possible, regardless of species, to lay eggs and maintain the elevated attractin concentrations needed to recruit new individuals to the breeding aggregation.

Chemical communication frequently involves the use of blends of pheromones rather than single-compound pheromones. Blends of airborne pheromones are important for species-specific signaling in many organisms, including arthropods. Mate finding in most moth species, for example, involves the release of long-distance airborne sex pheromones, which are produced in specialized female abdominal glands, generally *via* unsaturated fatty-acid precursors produced by desaturases (Roelofs *et al.*, 2002). A great diversity of pheromone structures is used throughout the Lepidoptera, even among closely related species, and the blend ratio is important for species-specific signaling. There is

strong selection pressure against novel blends and response preferences (Roelofs *et al.*, 2002). Although airborne sex pheromones capable of inducing spatial orientation of conspecifics "downwind" are well established in insects (Carde and Minks, 1996), this is not the case in vertebrates, whose identified sex pheromones tend to have a small range of effectiveness; in fish, the known sex pheromones are gonadal steroids, prostaglandins, or bile acids (Li *et al.*, 2002).

Mate attraction in the genus *Aplysia*, and perhaps in other gastropods, appears to involve long-distance signaling *via* waterborne pheromone blends. Attractin by itself is not attractive to *Aplysia* species, but egg cordons alone are sufficient to attract *Aplysia* species "downstream," indicating that the cordons themselves contain a blend of pheromones. Once aggregations of multiple *Aplysia* species form, appropriate intraspecific mating may be achieved through the use of specific proximal cues involving contact chemoreception and mechanoreception (Chase, 1979).

#### Acknowledgments

We thank Drs. A. Susswein, A. ter Maat, and M. Miller for their interesting comments and acknowledge the University of Texas Medical Branch (UTMB) Protein Chemistry Laboratory, which is supported by the UTMB Educational Cancer Center, for compositional and microsequence analyses. This work was supported by NSF Grant IBN-9985778 (S.D.P.), and John Sealy Memorial Endowment Fund for Biomedical Research Development Grant 2579-02R (G.T.N.).

#### Literature Cited

- Achituv, Y., and A. Susswein. 1985. Habitat selection by two Mediterranean species of *Aplysia*: *A. fasciata* Poiret and *A. depilans* Gmefin (Mollusca: Opisthobranchia). *J. Exp. Mar. Biol. Ecol.* **85**: 113–122.
- Aspey, W. P., and J. E. Blankenship. 1976. *Aplysia* behavioral biology. II. Induced burrowing in swimming *A. brasiliensis* by burrowed conspecifics. *Behav. Biol.* **17**: 301–312.
- Audesirk, T. E. 1977. Chemoreception in *Aplysia californica*. III. Evidence for pheromones influencing reproductive behavior. *Behav. Biol.* **20**: 235–243.
- Audesirk, T. E. 1979. A field study of growth and reproduction in *Aplysia californica*. *Biol. Bull.* **157**: 407–421.
- Audesirk, T. E., and G. J. Audesirk. 1977. Chemoreception in *Aplysia californica*. II. Electrophysiological evidence for detection of the odor of conspecifics. *Comp. Biochem. Physiol.* **56A**: 267–270.
- Blankenship, J. E., M. K. Rock, L. C. Robbins, C. A. Livingston, and H. K. Lehman. 1983. Aspects of copulatory behavior and peptide control of egg laying in *Aplysia*. *Fed. Proc.* **42**: 96–100.
- Carde, R. T., and A. K. Minks. 1996. Molecular mechanisms of pheromone reception in insect antennae. Pp. 115–130 in *Insect Pheromone Research*, H. Breer, ed. Chapman and Hall, New York.
- Chase, R. 1979. An electrophysiological search for pheromones of *Aplysia californica*. *Can. J. Zool.* **57**: 781–784.
- Fan, X., B. Wu, G. T. Nagle, and S. D. Painter. 1997. Molecular cloning of a cDNA encoding a potential water-borne pheromonal attractant released during *Aplysia* egg laying. *Mol. Brain Res.* **48**: 167–170.

- Garimella, R., Y. Xu, C. H. Schein, K. Rajarathnam, G. T. Nagle, S. D. Painter, and W. Braun. 2003. NMR solution structure of attractin, a water-borne protein pheromone from the mollusk *Aplysia californica*. *Biochemistry*. (In press).
- Jahan-Parwar, B. 1976. Aggregation pheromone from the egg-mass of *Aplysia californica*. *Physiologist* **19**: 240.
- Kikuyama, S., F. Toyoda, Y. Ohmiya, K. Matsuda, S. Tanaka, and H. Hayashi. 1995. Sodefrin: a female-attracting peptide pheromone in newt cloacal glands. *Science* **267**: 1643–1645.
- Kikuyama, S., K. Yamamoto, T. Iwata, and F. Toyoda. 2002. Peptide and protein pheromones in amphibians. *Comp. Biochem. Physiol. B* **132**: 69–74.
- Kodama, T., T. Hisatomi, T. Kanemura, K. Mokubo, and M. Tsuboi. 2003. Molecular cloning and DNA analysis of a gene encoding alpha mating pheromone from the yeast *Saccharomyces naganishii*. *Yeast* **20**: 109–115.
- Kupfermann, I., and T. Carew. 1974. Behavior patterns of *Aplysia californica* in its natural environment. *Behav. Biol.* **12**: 317–337.
- Li, W., A. P. Scott, M. J. Siefkes, H. Yan, Q. Liu, S.-S. Yun, and D. A. Gage. 2002. Bile acid secreted by male sea lamprey that acts as a sex pheromone. *Science* **296**: 138–140.
- Luporini, P., A. Vallesi, C. Miceli, and R. A. Bradshaw. 1995. Chemical signaling in ciliates. *J. Eukaryot. Microbiol.* **42**: 208–212.
- Monsma, S. A., and M. F. Wolfner. 1988. Structure and expression of a *Drosophila* male accessory gland gene whose product resembles a peptide pheromone precursor. *Genes Dev.* **2**: 1063–1073.
- Novotny, M. V. 2003. Pheromones, binding proteins and receptor responses in rodents. *Biochem. Soc. Trans.* **31**: 117–122.
- Painter, S. D. 1992. Coordination of reproductive activity in *Aplysia*: peptide neurohormones, neurotransmitters, and pheromones encoded by the egg-laying hormone family of genes. *Biol. Bull.* **183**: 165–172.
- Painter, S. D., A. R. Gustavson, V. K. Kalman, G. T. Nagle, R. A. Zuckerman, and J. E. Blankenship. 1989. Induction of copulatory behavior in *Aplysia*: atrial gland factors mimic the excitatory effects of recently deposited egg cordons. *Behav. Neural Biol.* **51**: 222–236.
- Painter, S. D., M. G. Chong, M. A. Wong, A. Gray, J. G. Cormier, and G. T. Nagle. 1991. Relative contributions of the egg layer and egg cordon to pheromonal attraction and the induction of mating and egg-laying behavior in *Aplysia*. *Biol. Bull.* **181**: 81–94.
- Painter, S. D., B. Clough, R. W. Garden, J. V. Sweedler, and G. T. Nagle. 1998. Characterization of *Aplysia* attractin, the first water-borne peptide pheromone in invertebrates. *Biol. Bull.* **194**: 120–131.
- Painter, S. D., D.-B. G. Akalal, B. Clough, A. J. Susswein, M. Levy, and G. T. Nagle. 2000. Characterization of four new members of the attractin family of peptide pheromones in *Aplysia*. *Soc. Neurosci. Abstr.* **26**: 1166.
- Pennings, S. C. 1991. Reproductive behavior of *Aplysia californica* Cooper: diel patterns, sexual roles and mating aggregations. *J. Exp. Mar. Biol. Ecol.* **149**: 249–266.
- Ram, J. L., C. T. Muller, M. Beckmann, and J. D. Hardege. 1999. The spawning pheromone cysteine-glutathione disulfide ('nereithione') arouses a multicomponent nuptial behavior and electrophysiological activity in *Nereis succinea* males. *FASEB J.* **13**: 945–952.
- Roelofs, W. L., W. Liu, G. Han, H. Jiao, A. P. Rooney, and C. E. Linn, Jr. 2002. Evolution of moth sex pheromones via ancestral genes. *Proc. Natl. Acad. Sci. USA* **99**: 13621–13626.
- Rollmann, S. M., L. D. Houck, and R. C. Feldhoff. 1999. Proteinaceous pheromone affecting female receptivity in a terrestrial salamander. *Science* **285**: 1907–1909.
- Saudan, P., K. Hauck, M. Soller, Y. Choffat, M. Ottiger, M. Sporri, Z. Ding, D. Hess, P. M. Gehrig, S. Klausner, P. Hunziker, and E. Kubli. 2002. Ductus ejaculatorius peptide 99B (DUP99B), a novel *Drosophila melanogaster* sex-peptide pheromone. *Eur. J. Biochem.* **269**: 989–997.
- Savic, I., H. Berglund, B. Gulyas, and P. Roland. 2001. Smelling of odorous sex hormone-like compounds causes sex-differentiated hypothalamic activations in humans. *Neuron* **31**: 661–668.
- Schein, C. H., G. T. Nagle, J. S. Page, J. V. Sweedler, Y. Xu, S. D. Painter, and W. Braun. 2001. *Aplysia* attractin: biophysical characterization and modeling of a water-borne pheromone. *Biophysical J.* **81**: 463–472.
- Stowers, L., T. E. Holy, M. Meister, C. Dulac, and G. Koentges. 2002. Loss of sex discrimination and male-male aggression in mice deficient for TRP2. *Science* **295**: 1493–1500.
- Susswein, A. J., S. Gev, E. Feldman, and S. Markovitch. 1983. Activity patterns and time budgeting of *Aplysia fasciata* in field and laboratory conditions. *Behav. Neural Biol.* **39**: 203–220.
- Susswein, A. J., S. Gev, Y. Aчитuv, and S. Markovitch. 1984. Behavioral patterns of *Aplysia fasciata* along the Mediterranean coast of Israel. *Behav. Neural Biol.* **41**: 203–220.
- Wabnitz, P. A., J. H. Bowie, M. J. Tyler, J. C. Wallace, and B. P. Smith. 1999. Aquatic sex pheromone from a male tree frog. *Nature* **401**: 444–445.

# Field Observations of Intraspecific Agonistic Behavior of Two Crayfish Species, *Orconectes rusticus* and *Orconectes virilis*, in Different Habitats

DANIEL A. BERGMAN AND PAUL A. MOORE\*

*Laboratory for Sensory Ecology, Department of Biological Sciences and the J. P. Scott Center for Neuroscience, Mind, and Behavior, Bowling Green State University, Bowling Green, Ohio 43403; and University of Michigan Biological Station, 9008 Biological Road, Pellston, Michigan 49769*

**Abstract.** Agonistic behavior is a fundamental aspect of ecological theories on resource acquisition and sexual selection. Crustaceans are exemplary models for agonistic behavior within the laboratory, but agonistic behavior in natural habitats is often neglected. Laboratory studies do not achieve the same ecological realism as field studies. In an attempt to connect laboratory results to field data and investigate how habitat structure affects agonistic interactions, the nocturnal behavior of two crayfish species was observed by scuba diving and snorkeling in two northern Michigan lakes. Intraspecific agonistic interactions were analyzed in three habitats: two food resources—macrophytes and detritus—and one sheltered habitat. The overall observations reinforce the concept that resources influence agonistic bouts. Fights in the presence of shelters were longer and more intense, suggesting that shelters have a higher perceived value than food resources. Fights in the presence of detritus patches had higher average intensities and ended with more tailflips away from an opponent, suggesting that detritus was a more valuable food resource than macrophytes. In addition, observations of aggressive behavior within a natural setting can add validity to laboratory studies. When fights in nature are compared with laboratory fights, those in nature are shorter, less intense, and less likely to end with a tailflip, but do show the fundamental fight dynamics associated with laboratory studies. Extrinsic and intrinsic factors affect intraspecific aggression in many ways, and both should always be recognized as having the potential to alter agonistic behavior.

## Introduction

Many observations of crayfish behavior have been made under controlled laboratory conditions. These studies generally focus on intraspecific aggressive behavior in terms of shelter acquisition (Capelli and Hamilton, 1984; Peeke *et al.*, 1995; Figler *et al.*, 1999), chemical communication (Bovbjerg, 1956; Zulandt Schneider *et al.*, 1999, 2001), mating (Hill and Lodge, 1999), food preferences (Capelli and Munjal, 1982), and starvation (Hazlett *et al.*, 1975; Stocker and Huber, 2001). Laboratory experiments have been invaluable in clarifying the extrinsic and intrinsic factors that affect agonistic interactions. Intrinsic factors that have been shown to affect aggression are size, sex, reproductive state, hunger state, and social experience, while extrinsic factors are status and individual recognition, resource availability, prior residence, and shelter presence.

Asymmetries in fighting ability may be produced by some intrinsic features or extrinsic circumstances that favor one contestant (Parker, 1974; Maynard Smith and Parker, 1976). Intrinsic asymmetries are accurate predictors of dominance during interactions between pairs of decapod crustaceans; they include physical body size (Bovbjerg, 1953, 1970; Rubenstein and Hazlett, 1974; Berrill and Arsenault, 1984; Pavey and Fielder, 1996), chelae size (Garvey and Stein, 1993; Rutherford *et al.*, 1995), and sex (Stein, 1976; Peeke *et al.*, 1995, 1998). Extrinsic asymmetries such as prior residence (Peeke *et al.*, 1995, 1998), differing fight strategies (Guiasu and Dunham, 1997), and previous history in agonistic encounters (Rubenstein and Hazlett, 1974; Daws *et al.*, 2002; Bergman *et al.*, 2003) contribute to the outcome of agonistic interactions. Seasonal variations in food availability can also increase activity levels that lead to

Received 16 December 2002; accepted 19 May 2003.

\* To whom correspondence should be addressed. E-mail: pmoore@bgsu.net

increased social contact and consequently to increased aggressive interactions (Hazlett *et al.*, 1975). Laboratory experiments are an invaluable aid to understanding behavioral mechanisms, but they have limitations in their applicability to natural ecosystems (Bovbjerg, 1953, 1956; Peeke *et al.*, 1995). One severe constraint on laboratory studies of aggression is the restriction of space, which reduces an animal's ability to escape from an opponent.

Dominance hierarchies, territorial defense, mate selection, substrate preferences, and escalation of fight behavior observed under laboratory conditions may not be representative of behaviors in a natural setting (Karnofsky *et al.*, 1989). These changes in agonistic behavior observed within the laboratory may largely be caused by an inability to escape an agonistic conflict (Hediger, 1950). To circumvent this artifact, studies have been conducted in artificial ponds or streams that are less restrictive than the aquaria used in standard laboratory experiments. By increasing the complexity of the experimental environment, studies in these semi-natural settings attempt to obtain a more natural repertoire of behavior. They provide useful information about agonistic interactions, foraging, mating, orientation, shelter acquisition, and molting (Abrahamsson, 1966; Ranta and Lindström, 1992; Tomba *et al.*, 2001). However, even studies in semi-natural environments cannot illustrate the "true" behavioral ecology of the crayfish. Because of this shortcoming, field studies are invaluable to the understanding of crayfish behavior. They minimize laboratory bias and allow for an integration of behaviors observed in laboratories with those in a natural setting.

Crustaceans, particularly crayfish, have been used as a model system to study aggression (Dingle, 1983; Hyatt, 1983) because of the ritualized nature of their agonistic bouts (Bruski and Dunham, 1987), the presence of formidable chelipeds (Garvey and Stein, 1993; Schroeder and Huber, 2001), and the use of sensory information during such encounters (Zulandt Schneider *et al.*, 1999, 2001; Bergman *et al.*, 2003). The ultimate goal of any aggressive encounter is to obtain an elevated social status that gives an individual an advantage in obtaining a resource, such as food, mates, and shelters (Wilson, 1975; Atema, 1986). Conversely, a subordinate individual may lose access to resources through unsuccessful bouts, but may obtain a net benefit by avoiding costs such as increased energy expenditure, injury from a conspecific, or increased predation risk (Wilson, 1975; Edsman and Jonsson, 1996). If a subordinate does not gain a benefit, then the lower status will have a negative effect on fitness. Consequently, a subordinate will have less food and shelter and fewer mating opportunities.

Extrinsic environmental factors can have a profound effect on aggressive activities; thus a connection between extrinsic factors in the laboratory and their effects in nature need further validation. Agonistic behavior has been studied extensively in the laboratory and in semi-natural conditions,

but less emphasis has been placed on agonistic behavior in a natural setting. For this reason, we examined agonistic behavior under natural nocturnal conditions in two northern Michigan lakes. The study was conducted in three different habitats within the lakes to provide a global view of intraspecific agonistic behavior in nature that could be correlated to laboratory results on aggression. The results of this study also allowed us to examine differences in agonistic behavior that may be correlated to differing extrinsic factors in the laboratory and nature.

## Materials and Methods

### Study site

The study was sited in two remnant glacial lakes in the northern part of the lower peninsula of Michigan: Douglas Lake (lat. 45°33' N, long. 84°57' W) and Burt Lake (lat. 45°28' N, long. 84°40' W). The Burt Lake substrate is predominantly sand and small gravel. Water depth ranges from 0.4 (shallow) to 2.0 m (deep). A mixture of sand and gravel containing intermittent patches of detritus dominates the shallow-water substrates. The deep water contains a sand substrate with a population of macrophytes (dominated by *Potamogeton* sp. and *Vallisneria* sp.) and their associated epiphytes. Water temperatures range from 14 to 23 °C. Observation points were accessed by snorkeling. The Douglas Lake substrate is sand that contains a small band of iron substrata forming natural holes that crayfish use as shelters (burrows). This site ranges from 7.5 to 18.0 m in depth and is devoid of macrophytes. The water temperature ranges from 10 to 15 °C. Observation points were accessed through scuba diving.

### Study animals

Both the Burt Lake and Douglas Lake sites contained two species of crayfish, *Orconectes rusticus* and *Orconectes virilis*. Crayfish species were determined by the color of the periopods (chelae and legs), which are bright blue in *O. virilis* and brownish-green in *O. rusticus*. The determination of species allowed for an analysis of conspecific fights. In Douglas Lake, only *O. rusticus* conspecific fights were observed in the shelter habitat. In the Burt Lake population conspecific interactions for *O. virilis* were observed only on the macrophyte beds and not on the detritus patches, even although both species were present in the two regions. The observers took care to avoid physically disturbing any of the animals; they remained as motionless as possible by using intermittent kick strokes to drift over the observation areas (Karnofsky *et al.*, 1989). None of the animals were handled before or captured after behavioral observations. Consequently, male and female crayfish could not be distinguished when aggressive interactions were analyzed, but the relative size difference between crayfish was determined on

a video screen (Sony Trinitron color monitor; model # PVM-1315Q) by calculating the percent size difference of the opponents.

#### Behavioral observations

Observations were made during July and August between the hours of 2230 and 0100 (nocturnal activity period) from 1996 to 2002 (no observations were made in the summer of 1999). All observations were made on clear, calm nights when the water surf was below 8.0 cm. Interactions were recorded on a video camera (Sony Hi-8 Handycam; model # CCD-TR700) that was illuminated with white lights mounted on an underwater housing (Stingray video housing; model # SR-700) that contained the camera. Animals were filmed from a minimum distance of 0.4 m. Slow swimming motions were made to follow animals, and when the lights on the underwater housing noticeably disturbed an animal, the interaction was removed from the analysis. Crayfish are primarily nocturnal animals, and any behavioral alterations caused by the sudden exposure to white light could not be determined from this study. For this reason, any animal that tailflipped away or used a meral spread in the absence of an interaction was removed from the data analysis; however, this does not take into account any unnoticeable changes in behavior in response to the artificial light. Crayfish do appear to alter their behavior when light intensities are altered (Bruski and Dunham, 1987); however, since uniform white lighting was used in all observations, there should be no differential effects on the behavior.

Two sampling techniques were used. The first technique was to follow a single crayfish until it had an agonistic interaction with a conspecific. The second method was to scan detritus patches (Burt Lake), macrophyte beds (Burt Lake), and the shelter areas (Douglas Lake) for two crayfish that were within two body lengths of one another. When agonistic interactions were observed with either of these sampling techniques, the encounter was videotaped from initiation to termination of the fight and the interactions were later analyzed by playing the tape on a Panasonic VHS recorder (model # AG-7530-P) onto the Sony Trinitron monitor.

#### Analysis of fight behavior

All videotaped fight trials were analyzed using an ethogram modified from Bruski and Dunham (1987) (Table 1). An agonistic encounter in a laboratory setting with no resources available typically begins when an individual approaches a potential opponent (intensity 1). The encounter may then progress to a series of agonistic threat displays using a meral spread (intensity 2). If neither individual retreats, the bout gradually increases in fight intensity, starting with chelae contact and progressing to pushing with

Table 1

#### Crayfish ethogram codes

Intensity Level	Description
-2	Tailflip away from opponent or fast retreat
-1	Slowly back away from opponent
0	Ignore opponent with no response or threat display
1	Approach without a threat display
2	Approach with threat display using meral spread and/or antennal whip
3	Initial claw use by boxing, pushing, or touching with closed claws
4	Active claw use by grabbing opponent with open claws
5	Unrestrained fighting by grasping and pulling opponent's claws or appendages

closed chelae (intensity 3). When the chelae are opened and used to grab an opponent, a new intensity level is reached (intensity 4). The most intense interactions have periods of unrestrained fighting in which an individual appears to attempt to injure an opponent by grasping at chelae, legs, or antennae (intensity 5). A conflict is concluded when one individual retreats (intensity -1), usually signified by a tailflip away from the opponent (intensity -2), and usually followed by a submissive posture (Bruski and Dunham, 1987). A subordinate will retreat consistently and assume a posture in which the cephalothorax, abdomen, and claws are near the substrate. Typically, crayfish did not respond to each other when separated by greater than two body lengths (intensity 0). The temporal dynamics of these changes in behavior were recorded to include the total duration of the encounter and the time it took to reach the different intensity levels. Duration, time to different intensities, maximum intensity level reached, and average maximum intensity levels were analyzed using a one-way MANOVA and a Tukey honestly significant difference (hsd) *post hoc* test. The retreating animals (tailflip away) and maximum intensity achieved during an encounter were recorded and analyzed using a multiple comparisons for proportions contingency table ( $q_{0.05,\infty,4} = 3.633$ ) that allows for testing analogous to the Tukey or Student-Newman-Keuls tests (Zar, 1999). Significant results are represented by giving a  $q_{0.05,\infty,4}$  value  $> 3.314$  from the multiple comparisons test and a  $P$  value  $< 0.05$ . An additional power analysis (Power =  $1 - \beta$ ) was included for the ANOVA and multiple comparisons for proportions contingency table tests. The size differences of agonistic opponents were obtained in 117 of the fights. Size differences are presented as a percentage of the larger animal in the pairing. Thus, a value of 20% means that the smaller animal is 20% smaller than the larger animal. A regression analysis between size difference in percentage and fight duration was analyzed using an exponential regression using the least-squares method.

## Results

### Qualitative description of fight dynamics

In general, as in the laboratory, crayfish quickly approached one another and immediately began to interact (Bruski and Dunham, 1987; Bergman *et al.*, 2003). In most instances, fights, unlike those in the laboratory, were relatively short and did not always show a stepwise progression in intensities (Stocker and Huber, 2001; Zulandt Schneider *et al.*, 2001; Bergman *et al.*, 2003). Crayfish retreated quickly from opponents by moving away in a different direction. Fights rarely progressed to the high intensities seen in the laboratory (Stocker and Huber, 2001; Bergman *et al.*, 2003), but did seem to include many of the stereotypical agonistic behaviors (Huber and Kravitz, 1995). Surprisingly, the number of fights ending in tailflips was low (45%) compared to fights in a laboratory (>90% for laboratory fights; Moore, pers. obs.). In addition, multiple interactions between the same opponents within a short time were virtually nonexistent, which may be due to social recognition (Daws *et al.*, 2002).

### Quantitative description of all fights

Two hundred and forty-six encounters were included in the data analysis. Statistical tests were performed on conspecific fights for *O. rusticus* for the three habitat types. Conspecific fights for *O. virilis* were observed only in the macrophyte habitat, and all statistical tests were done on these animals. Within the macrophyte bed habitat, no significant differences were found for any of the following statistical tests. For this reason, the data for the macrophyte habitat fights were pooled to provide a more global description of the parameters of average agonistic encounters in nature. In the subsequent statistical tests, encounters were separated on the basis of the habitat in which the encounter occurred. The mean duration of all encounters was  $5.3 \pm 0.4$  s (mean  $\pm$  SE); ( $n = 246$ ; Fig. 1A), and 0.45 (111 of 246 encounters) of the conflicts ended with the behavior "tailflips away from an opponent" (Fig. 2). Intensity 2 was reached in 0.49 of the encounters (121 of 246; Fig. 3A), intensity 3 was reached in 0.39 (95 of 246; Fig. 3A), and intensity 4 was reached in 0.12 (29 of 246; Fig. 3A). The average maximum intensity of all encounters was  $2.6 \pm 0.04$  on the crayfish ethogram scale (Table 1; Fig. 3B). The rate of escalation is a measure of time to different levels of intensity and averaged  $1.5 \pm 0.1$  s for escalation to intensity 2 (246 of 246 encounters; Fig. 4),  $3.9 \pm 0.2$  s to intensity 3 (124 of 246 encounters; Fig. 4), and  $9.5 \pm 0.9$  s to intensity 4 (28 of 246 encounters).

### Fight duration

The overall fight duration in the three habitats for the collective pool of crayfish showed a significant difference

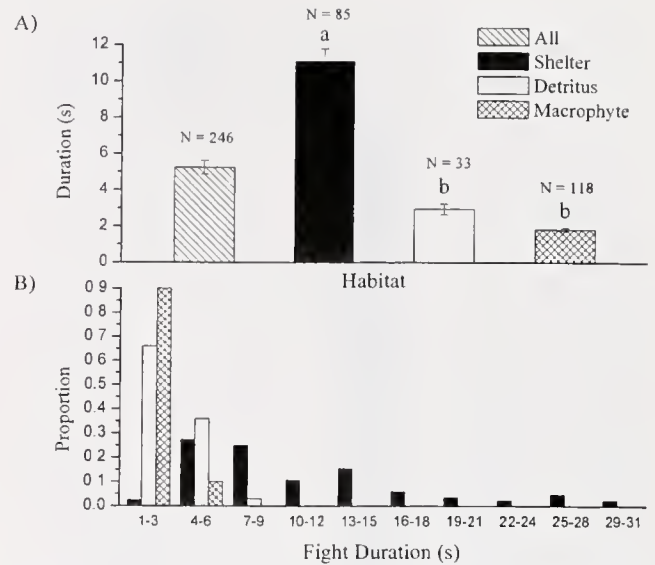


**Figure 1.** (A) The mean ( $\pm$ SEM) fight duration of all fights (hatched), fights near shelters (black), fights on detritus patches (white), and fights among macrophytes beds (crosshatch). Values above bars ( $N =$ ) indicate numbers used for the statistical calculations. The letters above the bars denote a significant difference between the habitat types (one-way ANOVA, Tukey-hsd *post hoc* test;  $P < 0.05$ ). (Note: Nine interactions were not categorized into a habitat type and are only included in the "All" category). (B) Frequency histogram showing the proportion of fight durations in the shelter, macrophyte, and detritus habitats in 3-s bins.

using a one-way MANOVA with a Tukey *post hoc* analysis (Fig. 1A). The fight duration in the shelter habitat ( $11.1 \pm 0.7$  s;  $n = 85$ ) significantly differed from both the detritus patch ( $2.9 \pm 0.3$  s;  $n = 33$ ) and macrophyte bed interactions ( $1.8 \pm 0.1$  s;  $n = 118$ ; Power = 1.00) ( $P < 0.05$ ). There was no significant difference in fight duration between the conflicts occurring on detritus patches and on macrophyte beds ( $P > 0.05$ ). Fight durations for encounters in the shelter habitat ranged between 1 and 31 s, whereas the duration of encounters on macrophyte beds and detritus patches did not exceed 6 s (Fig. 1B).

### Tailflip-away

A contingency table for multiple comparisons of proportions demonstrated that agonistic encounters ended in a tailflip significantly more often when the fight was in the shelter ( $61/85 = 0.72$ ;  $q = 19.01$ ; Power = 0.84) and detritus patch habitats ( $20/33 = 0.61$ ;  $q = 10.36$ ; Power = 0.14) than when in macrophyte bed habitats ( $30/118 = 0.25$ ; Power = 0.98) ( $P < 0.05$ ; Fig. 2). No significant difference was found between conflicts in the shelter and detritus habitats ( $q = 3.29$ ;  $P > 0.05$ ).

### Fight intensity

A significantly greater proportion of agonistic encounters on macrophyte beds (0.85; Power = 1.00) reached a max-

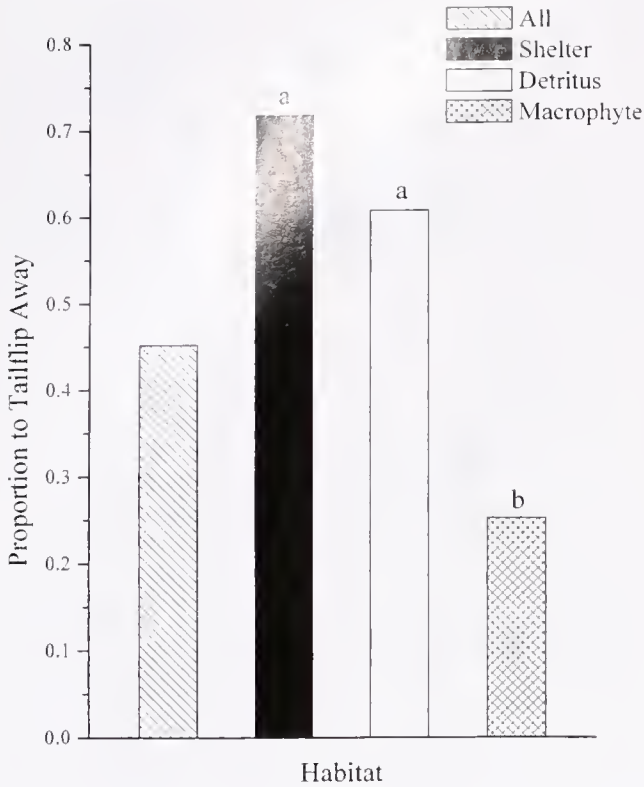


**Figure 2.** Frequency histogram showing the proportion of fights that ended in a tailflip for all fights (hatched), fights near shelters (black), fights on detritus patches (white), and fights among macrophytes beds (cross-hatch). The letters above the bars denote a significant difference between the habitat types (contingency table for multiple comparisons of proportions;  $P < 0.05$ ).

imum intensity level of 2 (meral spread display) than either encounters in the shelter ( $0.0$ ;  $q = 44.31$ ; Power = 1.00) or detritus habitat ( $0.36$ ;  $q = 14.86$  Power = 0.21) ( $P < 0.05$ ; Fig. 3A). A significantly greater proportion of encounters on detritus patches reached the maximum intensity of 2 than did encounters in the shelter habitat ( $q = 16.57$ ;  $P < 0.05$ ; Fig. 3A). A maximum intensity of 3 (pushing with chelae) was reached in a significantly greater proportion of fights when in the shelter ( $0.67$ ;  $q = 22.01$ ; Power = 0.62) and detritus habitats ( $0.61$ ;  $q = 13.99$ ; Power = 0.11) than in macrophyte beds ( $0.15$ ; Power = 0.62) ( $P < 0.05$ ; Fig. 3A). There was no significant difference between fights in the detritus and macrophyte habitats ( $q = 1.89$ ;  $P > 0.05$ ). In addition, maximum intensity 4 (open chelae use by grabbing) was reached by a greater proportion of conflicts in the shelter habitat ( $0.33$ ; Power = 0.24) than by interactions on detritus patches ( $0.03$ ;  $q = 11.23$ ; Power = 0.15) or macrophyte beds ( $0.0$ ;  $q = 20.0$ ) ( $P < 0.05$ ; Fig. 3A). There was no significant difference between the detritus and macrophyte fights ( $q = 2.83$ ;  $P > 0.05$ ). No fights in any habitat achieved intensity 5 (unrestrained fighting). Encounters in the shelter habitat had a significantly higher average maxi-

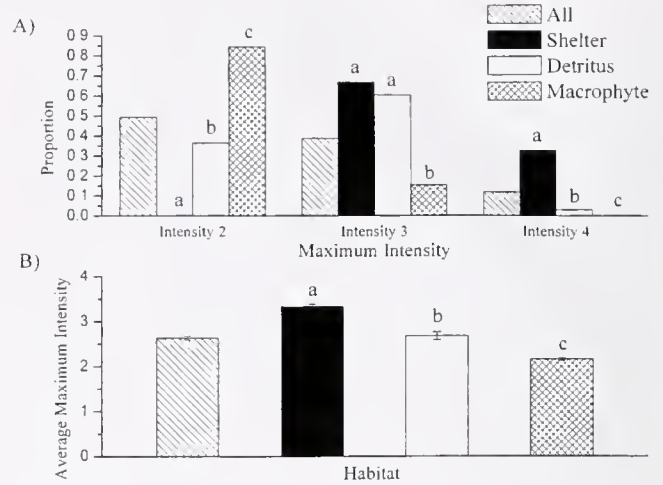


**Figure 3.** (A) Frequency histogram showing the proportion of fights that achieved each maximum intensity level for all fights (hatched), fights near shelters (black), fights on detritus patches (white), and fights among macrophytes beds (cross-hatch). The letters above the bars denote a significant difference between the habitat intensities (contingency table for multiple comparisons of proportions;  $P < 0.05$ ). (B) The average maximum fight intensity level achieved per habitat type. The letters above the bars denote a significant difference between the average maximum intensity per habitat ( $P < 0.05$ ).

imum intensity ( $3.33 \pm 0.05$ ) than encounters in either of the other two habitats ( $P < 0.05$ ; Fig. 3B). Interactions on detritus patches had a significantly higher average maximum intensity ( $2.67 \pm 0.09$ ) than encounters on macrophyte beds (average maximum intensity of  $2.16 \pm 0.03$ ) ( $P < 0.05$ ; Fig. 3B).

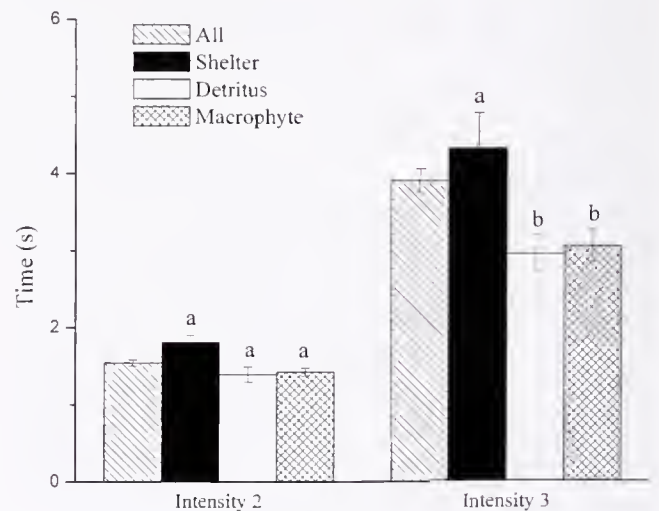


**Figure 4.** The mean ( $\pm$ SEM) time to intensity levels of all fights (hatched), fights near shelters (black), fights on detritus patches (white), and fights among macrophytes beds (cross-hatch). The letters above the bars denote a significant difference for the time to reach intensity levels for each habitat (one-way ANOVA Tukey hsd *post hoc* test;  $P < 0.05$ ).

### Rate of escalation

The average time to intensity 3 was significantly longer in the shelter habitat ( $4.3 \pm 0.5$  s) than on the detritus patches ( $3.0 \pm 0.2$  s) or macrophyte beds ( $3.1 \pm 0.2$  s) ( $P < 0.05$ ; Power = 1.00; Fig. 4). Intensity 2 showed no significant difference among the habitats, whereas intensity 4 was primarily achieved in the shelter habitat; however, no statistical test could be performed because of the lack of fights in the macrophyte ( $n = 0$ ) and detritus ( $n = 1$ ) habitats.

### Effect of size differential on fight duration

A significant exponential regression analysis using the least-squares method demonstrated that the duration of agonistic interactions ( $n = 117$ ) was longer when the size differential between opponents was smaller ( $P < 0.05$ ; Fig. 5). Encounters were longer when opponents were size-matched within 10%, whereas fights with a size difference greater than 10% did not exceed 4 s.

## Discussion

### Extrinsic and intrinsic factors of agonistic behavior

Crayfish agonistic interactions were longer (Fig. 1A), more intense (Fig. 3A, 3B, 4), and more likely to end with a tailflip (Fig. 2) when the interaction took place near a shelter (burrow) than on or near food-resource habitats (detritus and macrophytes). Interactions in the shelter habitat were more likely to reach higher intensities, but they also took longer to reach those intensities (Fig. 4). These results indicate that shelters were more valuable than either

macrophytes or detritus patches. Shelters may be alluring because of their use to attract mates or in defense from predators (Hill and Lodge, 1999). Conflicts were more intense (Fig. 3A, B) and ended more often with a tailflip (Fig. 2) when they occurred on detritus patches as opposed to macrophyte beds.

Extrinsic factors, such as the availability of a shelter or a food resource, seem to influence aggressive fighting behavior in crayfish. With reference to food resources, when crayfish are fed a strictly macrophyte diet (*Ammicola* sp. and *Lymnaea* sp.) they have slower growth rates and higher levels of mortality than crayfish fed detritus (Hill *et al.*, 1993). Physiologically, it appears as if detritus is more nutritious and thus a more valuable resource than macrophytes. Moreover, crayfish have been observed foraging on both species of macrophyte (*Potamogeton* sp. and *Vallisneria* sp.) and on detritus, suggesting that all three are viable food resources (Lodge and Lorman, 1987; Hill *et al.*, 1993; Cronin *et al.*, 2002). Among these food resources, detritus was located in distinct patches, whereas the macrophytes and their associated epiphytes were far more abundant and consistently distributed in Burt Lake. Moreover, shelters and detritus patches are limited resources, hence more easily defended. Conversely, macrophyte beds are usually an easily accessible and abundant food source (Capelli, 1982), and defense becomes difficult and unnecessary when they are widely available. Given the increased nutritional value and limited distribution of detrital food sources, we predict that intraspecific encounters on detritus patches would be more intense and longer than fights in a macrophyte habitat. Indeed, in our sample, intraspecific fights lasted longer, reached a higher average maximum intensity, and ended more often with a tailflip. These results may be caused by the relative scarcity and temporal unpredictability of detritus patches within Burt Lake. Patches are often destroyed or moved overnight by physical wave action. Detrital patch heterogeneity may limit this potential nutritional resource, and when a crayfish finds a rare patch, the interactions become more intense in defense of it. In contrast, the macrophyte beds and their associated epiphytes had a more homogeneous distribution and greater temporal stability than detrital patches. As a result, macrophytes interactions were the least intense of the habitat types.

Our results for the crayfish interactions in the macrophyte and detritus habitats are consistent with the idea that detritus is more valuable than macrophytes because of its increased nutritional value (Hill *et al.*, 1993). However, no definitive conclusion about the relative merits of detritus and macrophyte diets can be drawn from our study due to the unknown and varying composition of the detritus. Nevertheless, both macrophyte and detritus food resources appear to be less valuable than shelters. Shelters have been shown to have an effect on agonistic outcomes in that the previous owner is more likely to retain a shelter and initiate more interactions

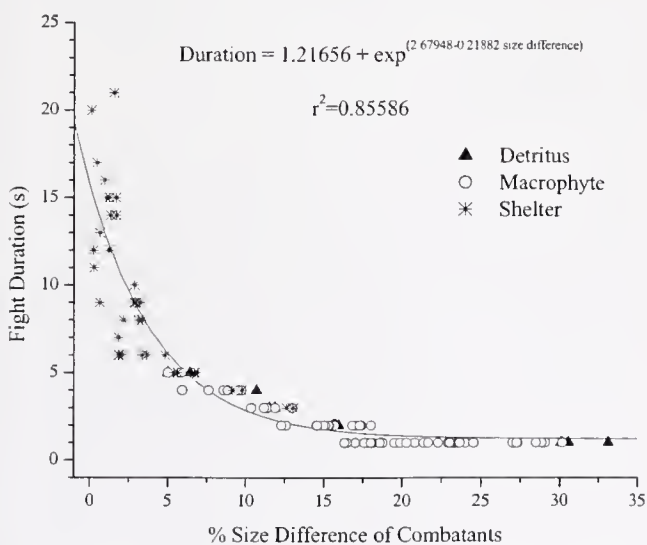


**Figure 5.** The percentage size differences of agonistic opponents analyzed with an exponential regression using the least-squares method. Size-matched fights lasted longer than fights between unevenly sized opponents ( $P < 0.05$ ).

(Peeke *et al.*, 1995; Edsman and Jonsson, 1996). Capelli and Hamilton (1984) have shown that food and prior residencies affect agonistic behavior in a simplified laboratory environment. They reported that aggressive activity decreases with the increased availability of both shelters and food. In addition, they show that the increase in shelter availability reduces aggression more than an increase in food availability. Thus, high food availability, more macrophytes than detrital patches, and low shelter availability would lead to more intense conflict over shelters, followed by detritus patches, and then macrophyte beds.

Conspecific conflicts can usually be thought of as a "limited war," in which serious injury is avoided (Maynard Smith and Price, 1973). However, conspecific conflicts between crayfish involve potentially lethal chelae that allow for an "unlimited war" with the possibility for more intense and lethal fights. High-intensity fights are common in a laboratory environment, largely because the opponents have been closely matched for size of carapace and chelae (Huber and Kravitz, 1995; Karavanich and Atema, 1998a, b). In nature, an advantage in size directly confers an advantage in resource holding power (RHP) to the larger individual. Parker (1974) noted that as RHP disparity (size difference) increases, conflicts become less intense and shorter. Both combatants may increase their overall fitness by minimizing the chance for injury and reducing energy expenditure from long and intense fights. The winners of such interactions gain access to more valuable resources such as mates, food, or shelters, while the losers reduce their risk of predation, minimize energy costs, and emigrate to find a new resource.

Our results are typical for asymmetric contests (Maynard Smith and Parker, 1976) in which a larger individual holds more valuable resources (shelters), and conflicts are longer when the opponents are size-matched. Moreover, when resource availability is asymmetrical, conflicts will generally be shorter when the least valuable resource—macrophytes in this study—is in dispute. The shelter habitat appears to have some significance tied to it because the longest fights were in this habitat, and these fights were the most closely size-matched (Fig. 5). The longest fights in all three habitats occurred when the opponents were within 10% of each other in size (Bruski and Dunham, 1987; Schroeder and Huber, 2001; Stocker and Huber, 2001; Bergman *et al.*, 2003). However, the shelter habitat appears to be more closely matched than the food resource habitats; consequently, the valuable resource (shelter) may attract larger individuals, which causes smaller individuals to move to the periphery or into other habitats (detritus and macrophyte). Moreover, a hierarchy has likely been established in the stable shelter habitat, whereas the macrophyte and detritus habitats do not provide the same temporal stability and do not function to decrease predation. The recognition of hierarchical status is probably reinforced by visual or chemical

social or individual recognition of conspecifics (Bruski and Dunham, 1987; Karavanich and Atema, 1998a, b). Intrinsic factors, such as size and recognition, and extrinsic factors, such as environmental surroundings, are important in determining intraspecific agonistic outcomes. However, the extent of the role each intrinsic and extrinsic factor plays is yet to be conclusively determined.

#### *Cursory review of laboratory studies in relation to field observations*

Intraspecific aggressive behavior between decapod crustaceans can be influenced by a myriad of extrinsic factors. For example, an extrinsic factor such as small aquarium size will sometimes elicit a "critical reaction" (Hediger, 1950). A critical reaction occurs when antagonists are crowded together in an aquarium with no possibility of escape. The inability to escape a competitor can cause changes in fight duration, retreat behavior, and intensity levels reached in fights (Peeke *et al.*, 2000). The presence of a defendable extrinsic resource can also cause an escalation in fight intensities in small aquaria. When shelters are present, fights will be more intense than when they are absent (Peeke *et al.*, 1995). Intrinsic factors such as size, sex, and social experience can also affect aggressive activities. Size-matched large crayfish escalate more slowly to high intensities and have longer fight durations than size-matched small crayfish (Schroeder and Huber, 2001). Generally, male crayfish are more aggressive than females (Bruski and Dunham, 1987), and social experiences in the form of winner and loser effects influence the likelihood of success in subsequent fights (Daws *et al.*, 2002; Bergman *et al.*, 2003). These extrinsic and intrinsic factors change the dynamics of fights in the laboratory so that they do not necessarily show the same characteristics as fights in a natural setting.

In general, fights were shorter ( $5.3 \pm 0.4$  s; Fig. 1) and had lower average maximum intensities (2.6; Fig. 3B) in the field than in laboratory studies (Table 2). The average maximum fight intensity in the field was lower than in laboratory fights seen by both Schroeder and Huber (2001) (2.7 and 2.8) and Bergman *et al.*, (2003) (4.2 and 3.5) (Table 2). In addition, the time to different intensity levels has been used as a measure of the rate of escalation in violence during fights and was considerably shorter for all intensities in the field than in the laboratory fights of Stocker and Huber (2001) and Bergman *et al.* (2003) (Table 2).

Within a laboratory environment, all aspects of a confrontation can be controlled to lengthen conflicts or increase fight intensities. Sex, species, size of opponents, size of aquarium, reproductive state, status/individual recognition, social experience, and hierarchy establishment can all be controlled in the laboratory. An example of a controlled variable is size-matched opponents (Bruski and Dunham, 1987; Rutherford *et al.*, 1995; Stocker and Huber, 2001;

Table 2

*Cursory review of crustacean agonistic experiments in the laboratory*

Reference	Animal	Treatment	Duration (s)	Avg. Intensity Value	Time to Intensity 2	Time to Intensity 3	Time to Intensity 4
Bergman and Moore (This study)	Crayfish	Field observations	5.3	2.6	1.5	3.9	9.5
Bergman <i>et al.</i> , 2003	Male crayfish	Previous win experience vs. size-matched opponent	127.0	4.2	4.6	8.6	18.0
	Male crayfish	Previous win experience vs. size-matched anosmic opponent	452.0	3.5	87.0	72.0	336.0
Stocker and Huber, 2001	Satiated male crayfish	Food odor present; Size-matched	—	—	85.0	135.0	210.0
	Starved male crayfish	Food odor present; Size-matched	—	—	60.0	90.0	125.0
Zulandt <i>et al.</i> , 2001	Familiar male crayfish	Urine present; Fight 1/Fight 2	80/70	1.9/1.8	—	—	—
	Familiar male crayfish	Urine absent; Fight 1/Fight 2; Size-matched	230/80	2.4/2.0	—	—	—
Schroeder and Huber, 2001	Male crayfish	Small; Size-matched	16.7	2.7	—	—	—
	Male crayfish	Large; Size-matched	30.6	2.8	—	—	—
Guiasu and Dunham, 1998	Male crayfish	First fight/Last fight; Size-matched	95.3/46.2	—	—	—	—
Guiasu and Dunham, 1997	Male crayfish	First fight/Last fight; Size-matched	115.6/26.2	—	—	—	—
Bruski and Dunham, 1987	Male crayfish	Dark; Size-matched	42.0	—	—	—	—
	Male crayfish	Light; Size-matched	17.0	—	—	—	—
	Female crayfish	Dark; Size-matched	29.0	—	—	—	—
	Female crayfish	Light; Size-matched	11.0	—	—	—	—
Karavanich and Atema, 1998a	Male lobster	Control; Day 1 Size-matched	510.0	—	—	—	—
	Male lobster	Control; Day 2 Size-matched	150.0	—	—	—	—
	Male lobster (anosmic)	Anosmic; Day 1 Size-matched	350.0	—	—	—	—
	Male lobster (anosmic)	Anosmic; Day 2 Size-matched	525.0	—	—	—	—
Huber and Kravitz, 1995	Male and female lobster	Day 1; Size-matched; Laboratory-raised juveniles	568.0	—	—	—	—
	Male and female lobster	Day 2; Size-matched; Laboratory-raised juveniles	365.0	—	—	—	—

Bergman *et al.*, 2003). Size matching increases the likelihood that fights will be longer and more intense than usually observed in the field. Field encounters had an average fight duration of 5.3 s (Fig. 1), whereas crayfish fight durations in the laboratory ranged from an average of 11.0 to 452.0 s (Bruski and Dunham, 1987; Bergman *et al.*, 2003) and lobster interactions took longer yet, ranging from 350.0 to 568.0 s (Huber and Kravitz, 1995; Karavanich and Atema, 1998a) (Table 2). This study does show that the fights of closely size-matched individuals are longer than those of unmatched opponents (Fig. 5), but they are not as long as fights seen in the laboratory. A possible extrinsic influence on this increased duration of fights is confinement of animals within an aquarium. Within the laboratory, a push to use larger aquaria will reduce the “critical reaction” effect

on fights by providing space for a possible escape that signifies the end of a conflict. Generally, the dynamics of laboratory fights tends to mimic field observations. However, Guiasu and Dunham (1997, 1998), using relatively large aquaria, showed average fight durations of 115.6 and 95.3 s, times that are considerably longer than those seen in this study (Table 2). The light regime also affects the duration of crayfish fights. Crayfish fights are shorter in the light than in the dark (Bruski and Dunham, 1987; Table 2). However, under different circumstances, fights can reach very long durations under lighted conditions, as was observed by Zulandt Schneider *et al.* (2001) and Bergman *et al.* (2003) (Table 2). One cannot discount the fact that laboratory conditions may have an unknown effect on agonistic behavior.

### Summary

These field observations suggest that the environmental surroundings have a significant effect on intraspecific agonistic bouts in crayfish. As suggested by Parker (1974), asymmetries in resource-based power can be an important factor in fight progression. Conflicts in the presence of shelters were longer and more intense, suggesting that shelters have a higher fitness value than detritus or macrophyte food resources. A shelter's protective value may outweigh the value of the food sources when the threat of predation is especially high. Detrital food sources are likely more valuable than macrophyte food sources because of their patchy distribution and the nutritional inadequacy of macrophytes (Hill *et al.*, 1993). It is quite evident from this study's results that extrinsic resources are an intricate influence on the agonistic interactions of crayfish.

Moreover, we conclude that aggressive behavior must be examined both in the laboratory and in the field to better understand the factors that influence crayfish aggression. Each experimental environment has unique benefits and problems. Observations in nature contribute to an understanding of habitat usage, movement patterns, shelter occupation, and food availability. Laboratory experiments are invaluable in elucidating the behavioral mechanisms and the environmental components that affect aggression. By controlling different aspects of agonistic interactions, such as size, sex, food preferences, and shelter accessibility, a researcher can test facets of agonistic behavior that are not easily controlled in a natural setting. However, such investigations do not answer the question of whether the behavior is an artifact of laboratory confinement or a behavior that is displayed in nature. Consequently, one must be hesitant when using laboratory results to explain agonistic behaviors in the wild. Laboratory and field observations show considerable differences in fight dynamics. A combination of the two is needed to develop a realistic picture of aggressive behavior.

### Acknowledgments

The authors thank the Laboratory for Sensory Ecology for comments on the manuscript and the University of Michigan Biological Station for the use of their facilities. Thanks also to Robert Schneider, Rebecca Zulantz Schneider, and Mary Wolf for help in collecting the data. Support for this research was supplied by the National Science Foundation (DAB 9874608, IBN-9514492, and IBN-0131320).

### Literature Cited

- Abrahamsson, S. A. A. 1966. Dynamics of an isolated population of the crayfish *Astacus astacus* Linné. *Oikos* 17: 96–107.
- Atema, J. 1986. Review of sexual selection and chemical communication in the lobster, *Homarus americanus*. *Can. J. Fish. Aquat. Sci.* 43: 2283–2290.
- Bergman, D. A., C. P. Kozłowski, J. C. McIntyre, R. Huber, A. G. Daws, and P. A. Moore. 2003. Temporal dynamics and communication of winner-effects in the crayfish, *Orconectes rusticus*. *Behaviour* (In Press).
- Berrill, M., and M. Arsenault. 1984. The breeding behaviour of the northern temperate orconectid crayfish, *Orconectes rusticus*. *Anim. Behav.* 32: 333–339.
- Bovbjerg, R. V. 1953. Dominance order in the crayfish *Orconectes virilis* (Hagen). *Physiol. Zool.* 26: 173–178.
- Bovbjerg, R. V. 1956. Some factors affecting aggressive behavior in crayfish. *Physiol. Zool.* 29: 127–136.
- Bovbjerg, R. V. 1970. Ecological isolation and competitive exclusion in two crayfish (*Orconectes virilis* and *Orconectes immunitis*). *Ecology* 51: 225–236.
- Bruski, C. A., and D. W. Dunham. 1987. The importance of vision in agonistic communication of the crayfish *Orconectes rusticus*. *Behaviour* 103: 83–107.
- Capelli, G. M. 1982. Displacement of northern Wisconsin crayfish by *Orconectes rusticus* (Girard). *Limnol. Oceanogr.* 27: 741–745.
- Capelli, G. M., and P. A. Hamilton. 1984. Effects of food and shelter on aggressive activity in the crayfish *Orconectes rusticus* (Girard). *J. Crustac. Biol.* 4: 252–260.
- Capelli, G. M., and B. L. Munjal. 1982. Aggressive interactions and resource competition in relation to species displacement among crayfish of the genus *Orconectes*. *J. Crustac. Biol.* 2: 486–492.
- Cronin, G., D. M. Lodge, M. E. Hay, M. Miller, A. M. Hill, T. Hovath, R. C. Bolser, N. Lindquist, and M. Wahl. 2002. Crayfish feeding preferences for freshwater macrophytes: the influence of plant structure and chemistry. *J. Crustac. Biol.* 22: 708–718.
- Daws, A. G., J. L. Grills, K. Konzen, and P. A. Moore. 2002. Previous experiences alter the outcome of aggressive interactions between males in the crayfish, *Procambarus clarkii*. *Mar. Freshw. Behav. Physiol.* 35: 139–148.
- Dingle, H. 1983. Strategies of agonistic behavior in Crustacea. Pp. 85–111 in *Studies in Adaptation: The Behavior of Higher Crustacea*, S. Rebach and D. W. Dunham, eds. John Wiley and Sons, New York.
- Edsman, L., and A. Jonsson. 1996. The effect of size, antennal injury, ownership, and ownership duration on fighting success in male signal crayfish, *Pacifastacus leniusculus* (Dana). *Nord. J. Freshw. Res.* 72: 80–87.
- Figler, M. H., H. M. Cheverton, and G. S. Blank. 1999. Shelter competition in juvenile red swamp crayfish (*Procambarus clarkii*): the influences of sex differences, relative size, and prior residence. *Aquaculture* 178: 63–75.
- Garvey, J., and R. A. Stein. 1993. Evaluating how chela size influences the invasion potential of an introduced crayfish (*Orconectes rusticus*). *Am. Nat.* 129: 172–181.
- Guíasu, R. C., and D. W. Dunham. 1997. Initiation and outcome of agonistic contests in male Form I *Cambarus robustus* Girard, 1852 crayfish (Decapoda, Cambaridae). *Crustaceana* 70: 480–496.
- Guíasu, R. C., and D. W. Dunham. 1998. Inter-form agonistic contests in male crayfishes, *Cambarus robustus* (Decapoda, Cambaridae). *Invertebr. Biol.* 117: 144–154.
- Hazlett, B., D. Rubenstein, and D. Rittschof. 1975. Starvation, energy reserves, and aggression in the crayfish *Orconectes virilis* (Hagen, 1870) (Decapoda, Cambaridae). *Crustaceana* 28: 11–16.
- Hediger, H. 1950. *Wild Animals in Captivity*. Butterworths, London.
- Hill, A. M., and D. M. Lodge. 1999. Replacement of resident crayfishes by an exotic crayfish: the roles of competition and predation. *Ecol. Appl.* 9: 678–690.
- Hill, A. M., D. M. Sinars, and D. M. Lodge. 1993. Invasion of an

- occupied niche by the crayfish *Orconectes rusticus*: potential importance of growth and mortality. *Oecologia* **94**: 303–306.
- Huber, R., and E. A. Kravitz. 1995.** A quantitative analysis of agonistic behavior in juvenile American lobsters (*Homarus americanus* L.). *Brain Behav. Evol.* **46**: 72–83.
- Hyatt, G. W. 1983.** Qualitative and quantitative dimensions of crustacean aggression. Pp. 113–139 in *Studies in Adaptation: The Behavior of Higher Crustacea*, S. Rebach and D. W. Dunham, eds. John Wiley and Sons, New York.
- Karavanich, C., and J. Atema. 1998a.** Olfactory recognition of urine signals in dominance fights between male lobster, *Homarus americanus*. *Behaviour* **135**: 719–730.
- Karavanich, C., and J. Atema. 1998b.** Individual recognition and memory in lobster dominance. *Anim. Behav.* **56**: 1553–1560.
- Karnofsky, E. B., J. Atema, and R. H. Elgin. 1989.** Field observations of social behavior, shelter use, and foraging in the lobster, *Homarus americanus*. *Biol. Bull.* **176**: 239–246.
- Lodge, D. M., and J. G. Lorman. 1987.** Reductions in submersed macrophyte biomass and species richness by the crayfish *Orconectes rusticus*. *Can. J. Fish Aquat. Sci.* **44**: 591–597.
- Maynard Smith, J., and G. A. Parker. 1976.** The logic of asymmetric contests. *Anim. Behav.* **24**: 159–175.
- Maynard Smith, J., and G. R. Price. 1973.** The logic of animal conflict. *Nature* **246**: 15–18.
- Parker, G. A. 1974.** Assessment strategy and the evolution of fighting behavior. *J. Theor. Biol.* **47**: 223–243.
- Pavey, C. R., and D. R. Fielder. 1996.** The influence of size differential on agonistic behaviour in the freshwater crayfish, *Cherax cuspidatus*. *J. Zool.* **238**: 445–457.
- Peeke, H. V. S., J. Sippel, and M. H. Figler. 1995.** Prior residence effects in shelter defense in adult signal crayfish (*Pacifastacus leniusculus*) results in same- and mixed-sex dyads. *Crustaceana* **68**: 873–881.
- Peeke, H. V. S., M. H. Figler, and E. S. Chang. 1998.** Sex differences and prior residence effects in shelter competition in juvenile lobsters, *Homarus americanus* Milne-Edwards. *J. Exp. Mar. Biol. Ecol.* **229**: 149–156.
- Peeke, H. V. S., G. S. Blank, M. H. Figler, and E. S. Chang. 2000.** Effects of exogenous serotonin on a motor behavior and shelter competition in juvenile lobsters (*Homarus americanus*). *J. Comp. Physiol. A* **186**: 575–582.
- Ranta, E., and K. Lindström. 1992.** Power to hold sheltering burrows by juveniles of the signal crayfish, *Pacifastacus leniusculus*. *Ethology* **92**: 217–226.
- Rubenstein, D. I., and B. A. Hazlett. 1974.** Examination of the agonistic behaviour of the crayfish *Orconectes virilis* by character analysis. *Behaviour* **50**: 193–216.
- Rutherford, P. L., D. W. Dunham, and V. Allison. 1995.** Winning agonistic encounters by male crayfish *Orconectes rusticus* (Girard) (Decapoda, Cambaridae): chela size matters but chela symmetry does not. *Crustaceana* **68**: 526–529.
- Schroeder, L., and R. Huber. 2001.** Fight strategies differ with size and allometric growth of claws in crayfish, *Orconectes rusticus*. *Behaviour* **138**: 1437–1449.
- Steele, C., C. Skinner, P. Alberstadt, and J. Antonelli. 1997.** Importance of adequate shelters for crayfishes maintained in aquaria. *Aquar. Sci. Conserv.* **1**: 189–192.
- Stein, R. A. 1976.** Sexual dimorphism in crayfish chelae: functional significance linked to reproductive activities. *Can. J. Zool.* **54**: 220–227.
- Stocker, A. M., and R. Huber. 2001.** Fighting strategies in crayfish *Orconectes rusticus* (Decapoda, Cambaridae) differ with hunger state and the presence of food cues. *Ethology* **107**: 727–736.
- Tomba, A. M., T. A. Keller, and P. A. Moore. 2001.** Foraging in complex odor landscapes: chemical orientation strategies during stimulation by conflicting chemical cues. *J. North Am. Benthol. Soc.* **20**: 211–222.
- Wilson, E. O. 1975.** *Sociobiology*. Belknap Press, Cambridge, MA.
- Zar, J. H. 1999.** Multiple comparisons for proportions. Pp. 563–565 in *Biostatistical Analysis*, 4<sup>th</sup> ed. Prentice Hall, Englewood Cliffs, NJ.
- Zulandt Schneider, R. A., R. W. S. Schneider, and P. A. Moore. 1999.** Recognition of dominance status by chemoreception in the red swamp crayfish. *Procambarus clarkii*. *J. Chem. Ecol.* **25**: 781–794.
- Zulandt Schneider, R. A., R. Huber, and P. A. Moore. 2001.** Individual and status recognition in the crayfish, *Orconectes rusticus*: the effects of urine release on fight dynamics. *Behaviour* **138**: 137–153.

# Twisting and Bending of Biological Beams: Distribution of Biological Beams in a Stiffness Mechanospace

SHELLEY A. ETNIER\*

*Department of Biology, Duke University, Durham, North Carolina 27708-0338*

**Abstract.** Most biological beams bend and twist relatively easily compared to human-made structures. This paper investigates flexibility in 57 diverse biological beams in an effort to identify common patterns in the relationship between flexural stiffness and torsional stiffness. The patterns are investigated by mapping both ideal and biological beams into a mechanospace defined by flexural and torsional stiffness. The distribution of biological beams is not random, but is generally limited to particular regions of the mechanospace. Biological beams that are stiff in bending are stiff in torsion, while those that bend easily also twist easily. Unoccupied regions of the mechanospace represent rare combinations of mechanical properties, without proving that they are impossible. The mechanical properties of biological beams closely resemble theoretical expectations for ideal beams. Both distributions are potentially being driven by the interdependence of the material and structural properties determining stiffness. The mechanospace can be used as a broadly comparative tool to highlight systems that fall outside the general pattern observed in this study. These outlying beams may be of particular interest to both biologists and engineers due to either material or structural innovations.

## Introduction

Flexibility, or the ability to deform in response to a load, is a property of most biological beams (Vogel, 1984; Denny, 1988), yet the biological consequences of flexibility vary widely. In motile organisms, flexibility permits the relative movements of structural elements in response to

internal forces generated by muscular contractions or hydrostatic pressures. The flexibility of a fish backbone influences the mechanical behavior of the body during undulatory swimming (McHenry *et al.*, 1995; Long and Nipper, 1996), while the flexibility of mammalian backbones has been implicated in locomotor differences between species (Gäl, 1993). In many sessile organisms, flexibility allows structures to passively adjust their posture relative to the forces experienced (Wainwright *et al.*, 1976; Vogel, 1984). Leaf petioles (Vogel, 1989; Niklas, 1991) and herbaceous plants (Ennos, 1993; Etnier and Vogel, 2000) reduce flow-induced drag by bending or twisting in response to wind, and similar drag-reducing mechanisms have been found in hydroid colonies (Harvell and LaBarbera, 1985) and anemones (Koehl, 1977a). Other flexible organisms take advantage of external forces to passively orient their filter-feeding structures in response to ever-changing flow (Wainwright and Dillon, 1969; Koehl, 1977b; Harvell and LaBarbera, 1985; Best, 1988). Thus, the ability to deform in response to loads is observed in both motile and sessile organisms living in either an aquatic or a terrestrial environment, apparently independent of phylogenetic affiliations. Such convergence may be viewed as a red flag indicating the tremendous importance of flexibility in the design of biological organisms (Lauder, 1982; Vogel, 1998).

Flexibility is measured in terms of stiffness, where flexural stiffness ( $EI$  in  $\text{N} \cdot \text{m}^2$ ) represents the resistance of a beam (a structure that is long relative to its width) to bending, and torsional stiffness ( $GJ$  in  $\text{N} \cdot \text{m}^2$ ) represents the resistance of a beam to twisting. Flexural stiffness and torsional stiffness are composite variables that are influenced both by material and structural properties (Wainwright *et al.*, 1976). Every beam is characterized by a combination of flexural stiffness and torsional stiffness, and the relationship between these two variables determines

Received 14 February 2003; accepted 21 May 2003.

\*Present address: University of North Carolina at Wilmington, 601 S. College Road, Wilmington, NC 28403. E-mail: etniers@uncwil.edu

how the beam responds to a given load. The ratio of flexural stiffness to torsional stiffness, commonly termed the twist-to-bend ratio, has been used as a dimensionless (and, thus, size invariant) index describing the relationship between these two variables (Niklas, 1992; Vogel, 1992, 1995; Etner and Vogel, 2000). The twist-to-bend ratio indicates the relative resistance of a beam to bending *versus* twisting. More intuitively, a higher twist-to-bend ratio indicates a structure that twists more readily than it bends, without reference to the magnitude of either variable.

While flexibility is a common property of a phylogenetically diverse group of organisms, are there any common patterns or trends in the relationship between flexural stiffness and torsional stiffness in biological beams? This paper investigates such patterns with a mechanospace defined by values of flexural and torsional stiffness. The mechanospace, similar to Raup's (1966) classic morphospace, is a broadly comparative tool used to visualize the relationships between mechanical variables in biological beams. The concept is based on the premise that the mechanical properties of flexural and torsional stiffness are common to all biological beams. Three variations of this mechanospace will be used to compare the patterns of flexibility seen in a large diversity of biological structures. First, material and structural properties will be used in combination to predict, on the basis of principles of engineering beam theory, the theoretical relationships between bending and twisting in ideal beams. Second, experimentally measured values of flexural stiffness and torsional stiffness for biological structures will be examined within the context of the theoretical distribution. Finally, the relative contribution of overall size to the mechanical properties of biological beams will be explored. The results suggest that the distribution of biological beams within the mechanospace is not random, due to the interdependence of material and structural properties determining stiffness.

## Materials and Methods

### *Distribution of ideal beams*

The distribution of ideal beams was determined using principles from engineering beam theory. Importantly, this distribution is limited to structures built of a single, isotropic material (*i.e.*, the material properties are not directionally variable), with precise specifications for the cross-sectional shape of the beam in question (Roark, 1943). Additionally, engineering beam theory stipulates that the material is linearly elastic, and that the beam is straight and does not vary in size or shape along its length, nor does the beam undergo deflections greater than 10% of total length (Roark, 1943). More complex solutions are required for beams that undergo larger deflections (*e.g.*, Morgan and Cannell, 1987; Morgan, 1989).

*Material properties.* The material properties influencing flexural stiffness and torsional stiffness are Young's modulus ( $E$  in  $\text{N} \cdot \text{m}^{-2}$ ) and the shear modulus ( $G$  in  $\text{N} \cdot \text{m}^{-2}$ ), respectively. Young's modulus and the shear modulus are related to one another by Poisson's ratio ( $\nu$ ), which is the dimensionless ratio of the induced strain, causing lateral contraction of the specimen, to the applied strain, causing the specimen to elongate (Vincent, 1990). Poisson's ratios can vary from 0 to 0.50 for naturally occurring isotropic materials. Mollusc shell has a Poisson's ratio of about 0.10, while rubber has a ratio closer to 0.50 (Denny, 1988) and materials such as cornstalks have moderate ratios around 0.23 (Prince and Bradway, 1969). Commonly occurring metals have Poisson's ratios between 0.25 and 0.30 (Niklas, 1992).

For isotropic materials, the shear modulus is related to Young's modulus (Roark, 1943) by:

$$G = \frac{E}{2(1 + \nu)} \quad (1)$$

Thus, the Young's modulus for a typical isotropic material will range from 2 to 3 times its shear modulus as Poisson's ratio varies from 0 to 0.50 (Wainwright *et al.*, 1976; Niklas, 1992).

*Structural properties.* The structural variables influencing flexural stiffness and torsional stiffness are the second moment of area ( $I$  in  $\text{m}^4$ ) and the polar moment of area ( $J$  in  $\text{m}^4$ ), respectively. These variables reflect the geometry of a cross section of a beam and are influenced by size, shape, and orientation (Roark, 1943). The relationship between  $I$  and  $J$  depends upon the cross-sectional shape of the structure in question (Roark, 1943). Formulas for the calculation of  $I$  and  $J$  for most simple shapes can be found in any basic engineering handbook (*e.g.*, Gere and Timoshenko, 1984).  $I$  and  $J$  are both proportional to radius to the fourth power, hence radius is a very strong determinant of stiffness (Roark, 1943). For example, for a beam with a circular cross-sectional area

$$I = \frac{\pi r^4}{4} \quad \text{and} \quad J = \frac{\pi r^4}{2} \quad (2)$$

the value of  $I/J$  is 0.50. Small changes in the cross-sectional shape of a beam can greatly influence the values of  $I$  and  $J$ ; thus, the value  $I/J$  for noncircular cross sections can be much higher (Table 1). Note that there may be several values of  $I/J$  for a beam with an asymmetric cross-sectional shape, depending on its orientation with respect to the applied load (Table 1).

*Relationship between flexural and torsional stiffness.*  $EI$  and  $GJ$  are dependent variables, with Poisson's ratio linking the material properties ( $E$  and  $G$ ), and geometry linking the structural properties ( $I$  and  $J$ ). Theoretically, the relationship between flexural stiffness and torsional stiff-

Table 1

Theoretical relationships between flexural and torsional stiffness

Cross-sectional shape	$I/J$	Ratio of $EI/GJ$	
		If $\nu = 0$ , then $E/G = 2$	If $\nu = 0.50$ , then $E/G = 3$
Circle	0.50	1.00	1.50
Ellipse 4:1 major:minor axis	0.27	0.54	0.81
Ellipse 4:1 major:minor axis	4.25	8.50	12.75

The ratio of  $I/J$  was determined from beam-theory equations (Niklas, 1992) and represents the structural contributions to stiffness in these beams. For the ellipses,  $I$  is calculated about the axis indicated by the dashed line. The ratio of  $E/G$  represents the material contribution to beam stiffness as Poisson's ratio was allowed to vary from 0 to 0.50. The chosen cross-sectional shapes are broadly representative of biological beams (Wainwright, 1988).

ness can vary only slightly, based on this interdependence. The relationships between flexural stiffness and torsional stiffness can be calculated for beams of different shapes and materials (Table 1). The ratio of  $EI/GJ$  for a given circular beam can range between 1 and 1.5 as Poisson's ratio varies from 0 to 0.5. In contrast, an elliptical beam with a major to minor axis ratio of 4:1 has a range of  $EI/GJ$  (with  $EI$  measured about the minor axis) from 8.50 to 12.75 for the same range in Poisson's ratio (Niklas, 1992). These particular cross-sectional shapes are presented because they are broadly representative of biological beams (Wainwright, 1988). Note that two beams can have the same  $EI/GJ$  ratio despite vast differences in size, shape, and material because the ratio is determined by the relative magnitudes of flexural stiffness to torsional stiffness, not by their absolute values.

The relationship between  $EI$  and  $GJ$  for ideal beams can be mapped into a mechanospace defined by these variables (Fig. 1). Each quadrant of the mechanospace represents different combinations of flexural stiffness and torsional stiffness, ranging from the upper left, where beams twist easily but do not bend, to the lower right, where beams bend easily but do not twist. The dashed line in Figure 1 represents a circular beam with a moderate Poisson's ratio of 0.25. The solid lines in Figure 1 represent the two orientations of a beam with a 4:1 elliptical cross-sectional shape as Poisson's ratio is maximized ( $\nu = 0.5$ ) or minimized ( $\nu = 0$ ). An elliptical beam of this form was chosen because such an ellipse has a large  $I/J$  ratio and likely represents an extreme shape for biological structures. Thus, the area between the two solid lines represents the range of values for beams with moderate to extreme material values, with shapes that are broadly representative of biological beams (Wainwright, 1988). Importantly, the solid lines do not represent absolute theoretical limits, but rather identify the expected extremes for ideal beams composed of a single,

isotropic material. Greater shape modification will slightly alter these limits.

#### Distribution of biological beams

Although biological beams are commonly modeled using beam theory (*e.g.*, Koehl, 1977b; Carrier, 1983; Vogel, 1992; Baumiller, 1993; Ennos, 1993; Vogel, 1995; Niklas, 1998; Etnier and Vogel, 2000; Etnier, 2001), they are rarely, if ever, made up of a single, isotropic material. More typically, they are made up of multiple materials, whose distribution varies both across the cross section of the beam and along its length. Yet, in practice, flexural stiffness and torsional stiffness are measured experimentally using basic engineering formulas for beams. In general, a known load is applied to a beam, causing it to deform, either by bending or by twisting. The exact equation used is dependent on how the beam is loaded. For example, for end-loaded cantilever beams (one end fixed and the other end free to deform), flexural stiffness is calculated as:

$$EI = \frac{FL^3}{3y} \quad (3)$$

where  $F$  is the applied force,  $L$  is the length of the specimen, and  $y$  is the deflection of the free end of the specimen (Gere and Timoshenko, 1984). Similarly, torsional stiffness is calculated using the following formula:

$$GJ = \frac{Fd}{\theta/L} \quad (4)$$

where  $F$  is the force applied at a moment arm  $d$ ,  $L$  is the length of the specimen, and  $\theta$  is the rotation of the free end in radians (Gere and Timoshenko, 1984).

Data were compiled from the literature and from the

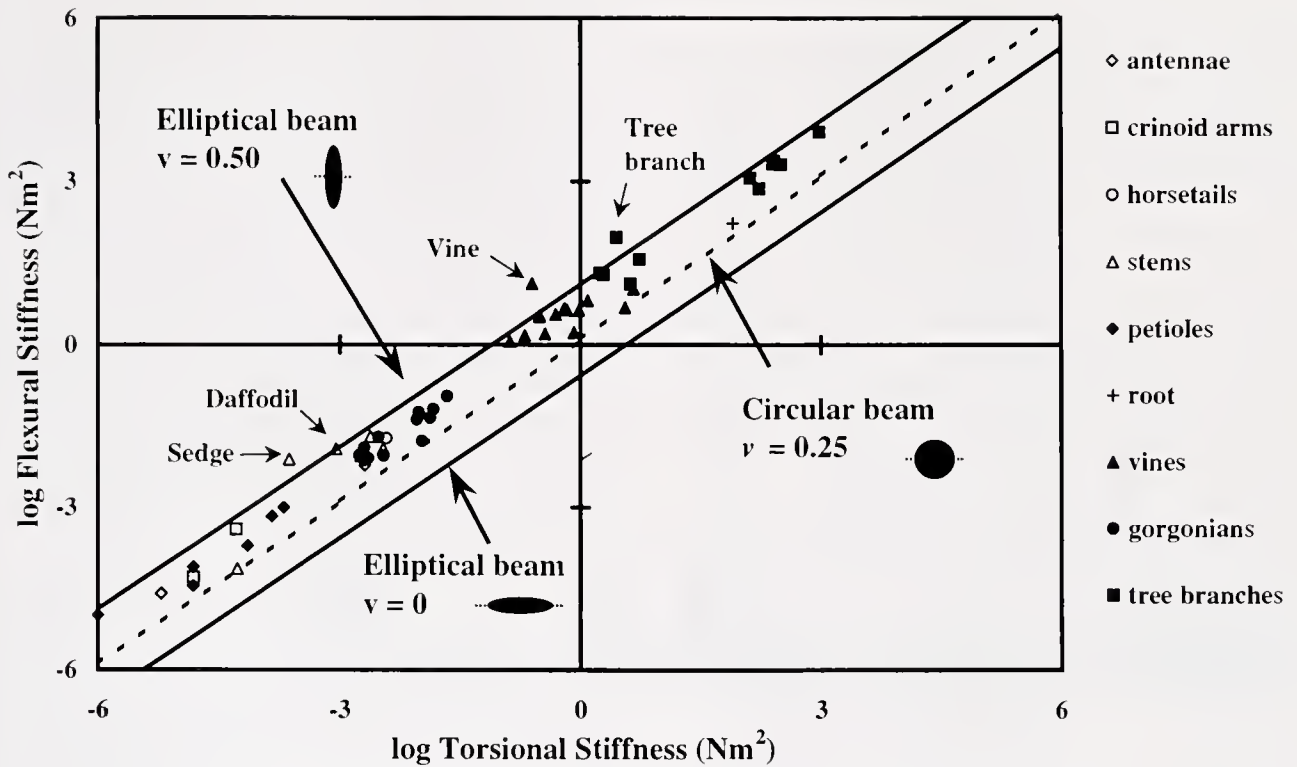


**Figure 1.** The mechanospace defined by values of flexural stiffness and torsional stiffness. The lines represent the distribution of ideal beams based upon an assumed cross-sectional shape and Poisson's ratio. The symbols represent the nine groups (Table 2), with each individual point representing an average value for a species (appendix). The upper line represents an elliptical beam (4:1 major to minor axis) with  $I/J$  calculated about the short axis and a Poisson's ratio of  $\nu = 0.50$ . The lower line represents that same beam with  $I/J$  calculated about the long axis and a Poisson's ratio of  $\nu = 0$ . The dashed line represents a circular beam with a Poisson's ratio of  $\nu = 0.25$ .

author's research to obtain average flexural stiffness and torsional stiffness measures for 25 species of plants and animals (see appendix). These data were obtained following protocols similar to those discussed above. In other cases ( $n = 32$ ), published data consisted only of measures of  $E$  and  $G$ . In these cases, the researchers experimentally determined  $EI$  and  $GJ$ , but then factored out  $I$  and  $J$  based on the cross-sectional size and shape of the structures. But note that the experimental data were still based on the overall mechanical behavior of the beam (*i.e.*, deformation due to a load), rather than direct measures of material properties. In cases where published data consisted only of measures of  $E$  and  $G$ , both size and shape were estimated to determine values for  $I$  and  $J$  (appendix). Flexural stiffness and torsional stiffness were then calculated, based on these estimates. The estimates of beam diameter were deliberately conservative, while cross-sectional shape was always assumed to be circular. For example, for 14 of the 16 vines and 5 of the 11 tree branches included in the mechanospace, the beam was assumed to have a circular cross section with a diameter of 0.02 m. The reported diameters for these species were 0.02–0.05 m (Putz and Holbrook, 1991). Sim-

ilar assumptions were made for the gorgonian corals, with an estimated diameter of 0.002 m (Jeyasuria and Lewis, 1987). The assumption of a relatively small diameter will affect the overall magnitudes of flexural stiffness and torsional stiffness, but will not affect the ratio of the two. The assumption of a circular cross-sectional shape will result in lower estimated values of  $I/J$  than would be seen in noncircular beams (Table 1).

The species (total  $n = 57$ ) were divided into nine groups based upon broad morphological similarities (Table 2). Structures varied greatly in size, with diameters ranging from 0.001 m (red maple petioles) to 0.05 m (small tree branches). Average values for  $\log GJ$  versus  $\log EI$  for all species ( $n = 57$ ) were plotted in the mechanospace (Fig. 1). Note that each point represents an average value for a species, and thus does not reflect individual variation in size and material properties. For asymmetric beams, such as the daffodils, crinoid arms, and crustacean antennae, flexural stiffness is reported as the average of the different orientations. Coefficients of variation for these organisms varied between 35% and 196% for flexural stiffness, and from 36% to 110% for torsional stiffness (Etnier and Vogel, 2000;

Table 2

Basic group characteristics for beams analyzed in this study

Groups	Basic characteristics
Crustacean antennae	Multi-jointed beam. Antennae used for sensory information and in some cases, for aggressive interactions. Not loaded gravitationally. Aquatic animal.
Crinoid arms	Multi-jointed beam. Arms used for passive filter feeding. Not loaded gravitationally. Aquatic animal.
Horsetails	Multi-jointed beam. Stem must maintain upright position for photosynthesis, so self-supporting. Terrestrial plant.
Herbaceous stems	Continuous beam. Stem must maintain upright position for photosynthesis, so self-supporting. Terrestrial plant.
Leaf petioles	Continuous beam. Petiole must support leaf against gravity and withstand wind, so self-supporting. Terrestrial plant.
Tree roots	Continuous beam. Root is not self-supporting. Loaded in tension. Terrestrial plant.
Vines	Continuous beam. Vine is not self-supporting. Loaded in tension. Terrestrial plant.
Gorgonian corals	Continuous beam. Support individual polyps against water flow. Not loaded gravitationally. Aquatic animal.
Tree branches	Continuous beam. Tree must maintain upright position for photosynthesis, so self-supporting. Terrestrial plant.

The biological beams investigated were divided into nine groups, based on broad differences in morphology and function.

Etnier, 2001), reflecting the individual variation noted above.

The twist-to-bend ratio for each species was calculated and compared to the predicted values as an additional descriptor of flexibility in biological beams (Fig. 2). Standard deviations for the twist-to-bend ratios, when available, are reported in the appendix.

#### Size-normalized mechanospace

Size greatly influences the stiffness of a biological beam, both in twisting and in bending. The structural variables,  $I$  and  $J$ , are both proportional to radius to the fourth power; thus, small increases in size will greatly increase beam stiffness, regardless of cross-sectional shape or material composition. Values of  $EI$  and  $GJ$  were normalized for size by dividing by radius to the fourth power to determine if size alone was driving the observed patterns. These values were then mapped into a size-normalized mechanospace (Fig. 3). This normalization accounts for size alone, rather than equating to calculations of  $E$  or  $G$  for a given beam.

## Results

The lines shown in Figure 1 are based upon the assumptions of engineering beam theory and represent values for ideal beams. The distribution of biological beams closely matched that of the ideal beams, with 93% (53 of 57) of the points falling within the bounded region (Fig. 1). The boundaries reflect possible extremes for biological beams, based on assumed material values and chosen cross-sectional shapes. Flexural stiffness and torsional stiffness changed concurrently in the biological beams. Thus, beams that bent easily also twisted easily, while those that were hard to bend were also hard to twist. Overall, flexural stiffness and torsional stiffness each varied over 9 orders of magnitude. Species within the defined groups occupied similar regions of the mechanospace, implying that the flexural stiffness and torsional stiffness of group members were of similar magnitude.

Due to the finite nature of the data set, the unoccupied regions of the mechanospace suggest that other combinations of mechanical values are rare without proving that they are impossible. Biological beams may exist within these unoccupied regions, given sufficient variation in material or structural design. The four samples falling outside of the predicted boundaries for ideal circular and elliptical beams included two herbaceous stems (daffodils *Narcissus pseudonarcissus* and sedges *Carex acutiformis*), a tree branch (*Dendropanax arboreus*), and a tropical vine (*Marcgravia rectiflora*). These systems were all characterized by high flexural stiffness relative to torsional stiffness—that is, they twisted more easily than they bent (Fig. 2).

Twist-to-bend ratios varied dramatically among different species (Fig. 2), with both the maximum (52.9) and the minimum (1.4) occurring in tropical vines. The average twist-to-bend ratio for all groups combined was 7.2, which falls between the predicted values for ideal beams that are circular or elliptical in cross-sectional shape.

When the data were normalized for size (Fig. 3), the observed distribution changed slightly. In particular, the relative position of the antennae, horsetail rushes, and gorgonian corals shifted up and to the right relative to the other beams. This result suggests that these structures are all relatively stiff for their size. While the position of groups changed slightly, structures that were stiffer in bending were also stiffer in torsion, regardless of their overall size.

## Discussion

The close resemblance in the distribution of ideal and biological beams suggests that both are limited by the interdependence between the material properties,  $E$  and  $G$ , and between the geometric properties,  $I$  and  $J$ . Yet, keep in mind the assumptions of beam theory, which are violated almost universally by biological beams. The theoretical relationships apply only to beams consisting of a single,

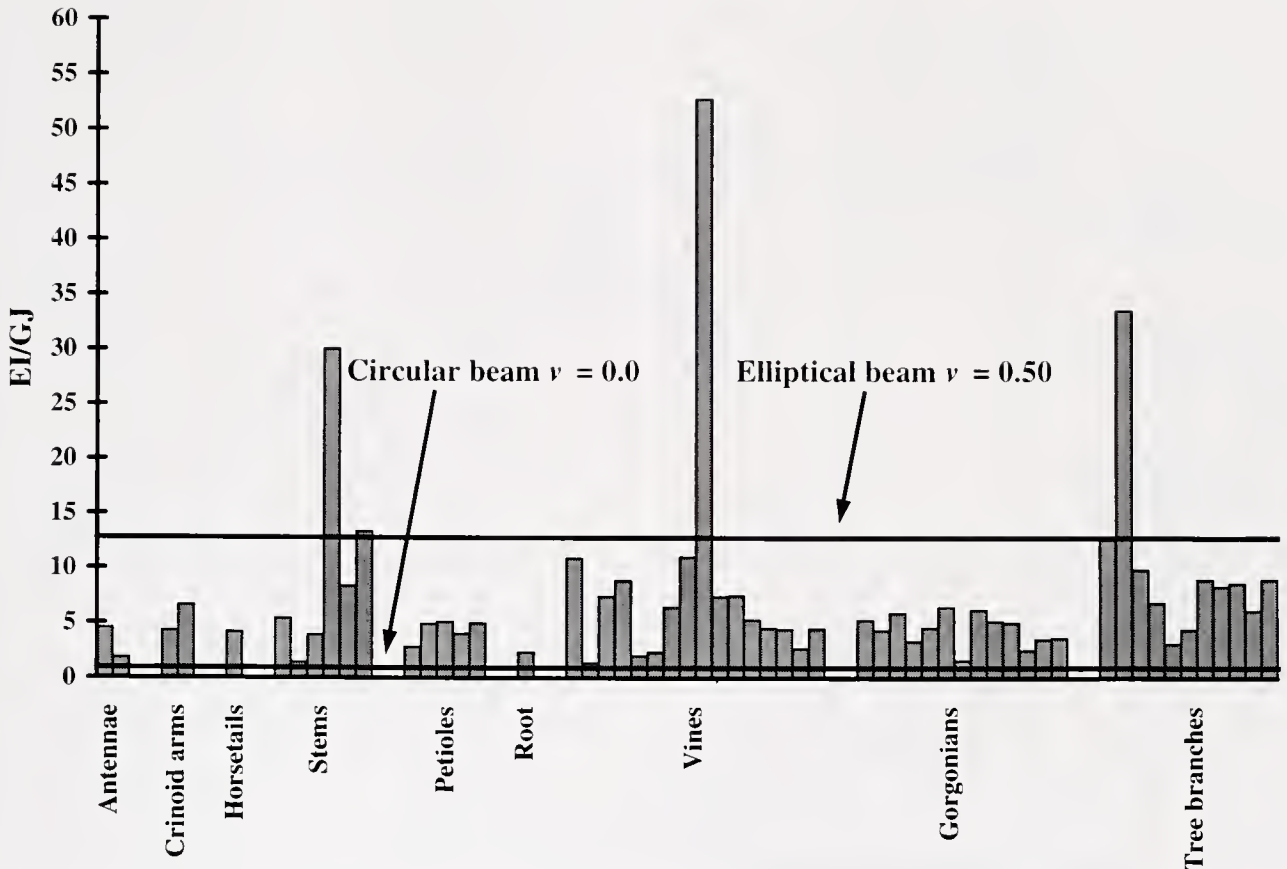


**Figure 2.** Twist-to-bend ratios for the nine groups. The horizontal lines indicate the predicted values for ideal beams with circular ( $EI/GJ = 1.00$ ,  $\nu = 0$ ) and elliptical ( $EI/GJ = 12.75$ ,  $\nu = 0.50$ ) cross sections. The beams are arranged by size within each group, with the smallest diameter beam to the left. Standard deviations for the twist-to-bend ratios, when available, are reported in the appendix.

isotropic material (Roark, 1943). Biological materials are more typically anisotropic, and values for Poisson's ratio can vary greatly from the theoretical expectations (Vincent, 1990). More importantly, biological beams are almost always composite structures built of multiple materials that differ greatly in their mechanical properties. Thus, it is not obvious that  $EI$  and  $GJ$  would be highly interdependent in biological beams, particularly in the beams that deviate most from the theoretical assumptions, such as the jointed crinoid arms or crustacean antennae.

The four samples falling outside of the predicted boundaries are all characterized by high flexural stiffness relative to torsional stiffness—that is, they will twist more easily than bend (Fig. 2). The two herbaceous stems have flowers or seed heads that extend perpendicular to the long axis of the stem, potentially causing the stem to bend or twist when the wind blows. Rather than resisting this load with a high torsional stiffness, daffodils (*Narcissus pseudonarcissus*) and sedges (*Carex acutiformis*) have a low torsional stiffness, which allows them to twist in the wind. Daffodils reduce flow-induced drag with this action (Etnier and Vo-

gel, 2000), and a similar function has been suggested for sedges (Ennos, 1993). The functional relevance of the high ratios of flexural stiffness to torsional stiffness in the tree trunk and vine has not been explored.

Conservative estimates of size and shape were made for many of the tree branches, vines, and gorgonian corals (appendix). Beam size affects  $EI$  and  $GJ$  equally; thus, errors in the size estimates will not affect the position of data points relative to the predicted boundaries (Fig. 4). Rather, an increase or decrease in diameter will cause these points to shift parallel to the boundaries. In contrast, shape estimates will differentially affect  $EI$  and  $GJ$ , causing data points to shift relative to the predicted boundaries (Fig. 4). Although branches and vines are fairly circular in cross section, this assumption may not be valid for the gorgonian corals, whose cross-sectional shape can be circular, elliptical, or even triangular (Jeyasuria and Lewis, 1987). The assumption of a circular cross section potentially underestimates the range of values seen in the gorgonian corals. For example, if the cross-sectional shape of the gorgonians is assumed to be a 4:1 ellipse rather than circular, then all of

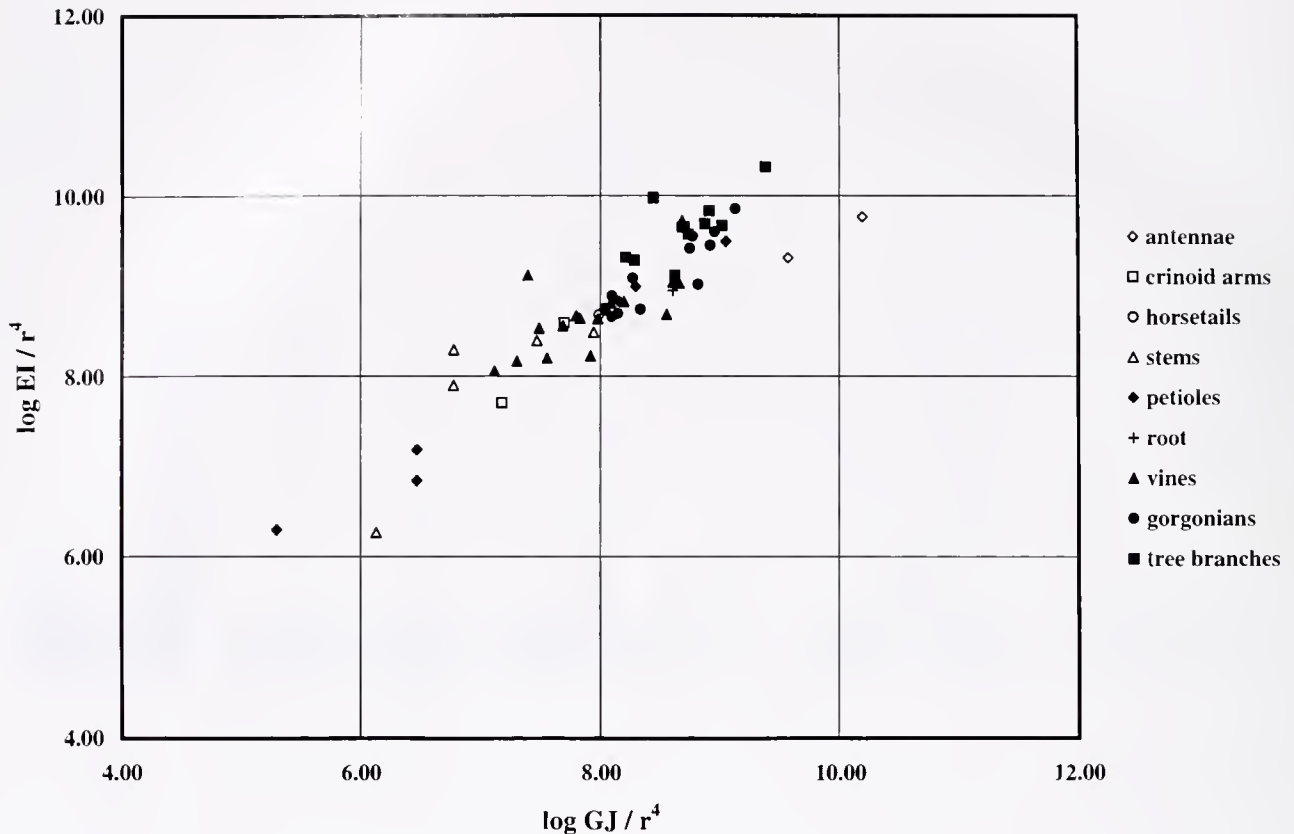


**Figure 3.** Flexural and torsional stiffness normalized by size for all groups (Table 2). The data points were normalized by dividing by radius to the fourth power.

these beams will fall outside of the predicted boundaries. Future studies that include the cross-sectional shape of the gorgonian corals may identify group members that are of particular mechanical and functional interest within a biological context.

Flexural stiffness and torsional stiffness are both highly dependent on the size of the structure in question. While the pattern seen in the stiffness mechanospace is driven in part by size increases alone, the size-normalized mechanospace (Fig. 3) suggests a robust pattern. Even with differences in size removed from the comparison, there is still a strong relationship between how a beam bends and how it twists. The size-normalized mechanospace suggests some interesting comparisons between the different groups. For example, the antennae have a size-normalized flexural stiffness similar to that of tree branches, while exhibiting a higher size-normalized torsional stiffness. Again, the biological implications of such variation have not been sufficiently explored in the literature.

The size, shape, and function of a beam may change during development (Wainwright and Dillon, 1969; Carrier, 1983; Katz and Gosline, 1992; Gallenmüller *et al.*, 2001). Such changes potentially influence both flexural stiffness and torsional stiffness, thus affecting how the beam re-

sponds to a given load. The mechanospace introduced in this study is well suited for investigations relating the morphology, mechanics, and functional demands of biological beams during ontogeny. A systematic study of the relationship between  $EI$  and  $GJ$  over a developmental series can reveal clues to the changing functional demands on a system during growth (Gallenmüller *et al.*, 2001). Concurrent morphological studies could determine whether mechanical changes are due to variation in material or structural properties, potentially identifying the mechanisms that different systems use to modulate mechanical properties.

Species within a group occupy a similar region of the mechanospace, signifying that the flexural stiffness and torsional stiffness of group members are of similar magnitude. The same pattern is true for the size-normalized mechanospace. While group members tend to occupy similar regions of the mechanospace, there is still variation within each group. Interspecific variation in shape and material may permit different combinations of flexural and torsional stiffness that may subtly influence how each species functions in its environment.

Despite clear differences in design, no obvious mechanical differences distinguish jointed beams from continuous beams. In continuous biological beams, the observed me-

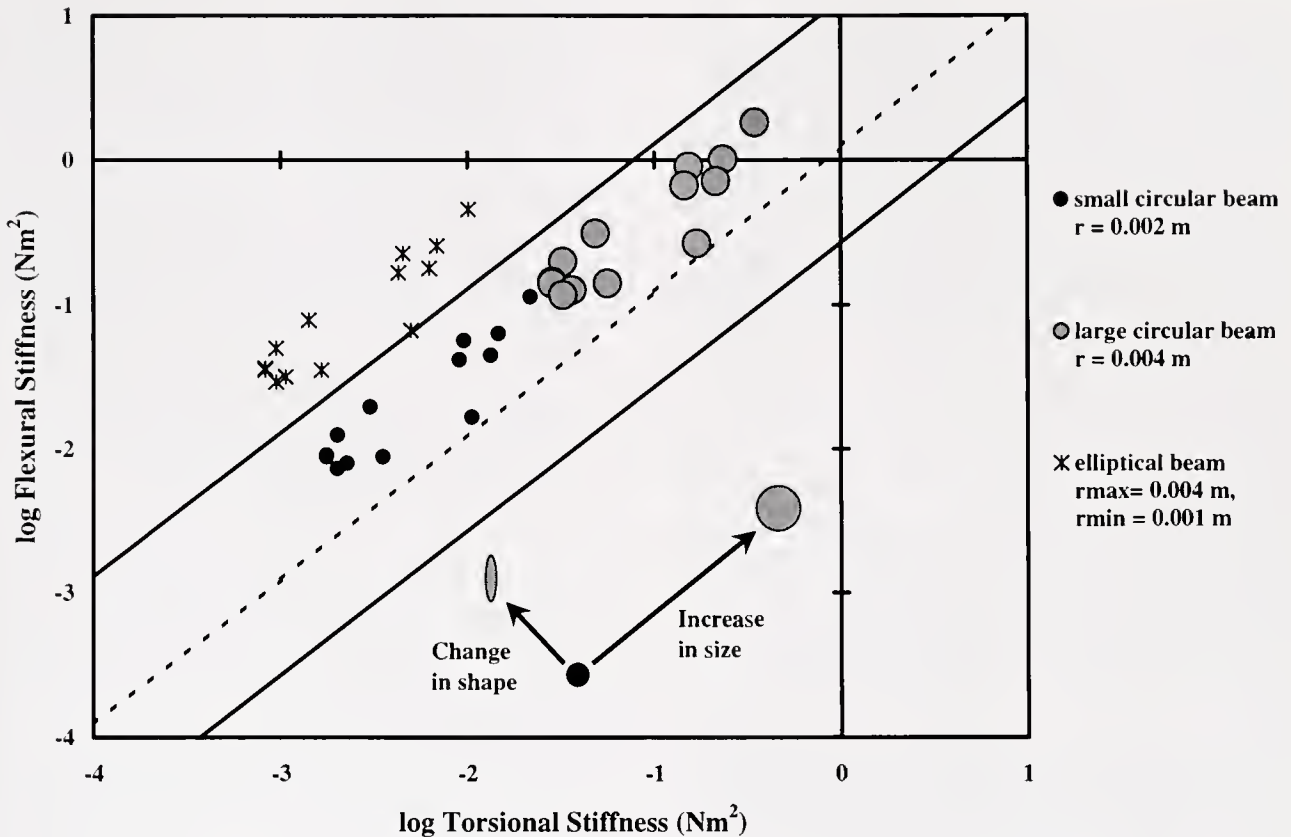


**Figure 4.** Changes in the assumptions of size and shape of beams will affect their distribution in the mechanospace. The small filled circles are the gorgonian values graphed in Figure 1 and were based on an assumed radius of 0.002 m. The lines represent the predicted values for ideal beams discussed previously. Changes in radius will affect the magnitude of  $I$  and  $J$  equally; thus, an increase or decrease in radius will cause these points to shift parallel to the predictions. For example, increasing the radius from  $r = 0.002$  m to  $r = 0.004$  m shifts the distribution up and to the right (large circles). In contrast, shape estimates differentially affect  $I$  and  $J$ . If the cross-sectional shape is assumed to be a 4:1 ellipse ( $r_{\max} = 0.004$  m,  $r_{\min} = 0.001$  m) rather than a circle, and  $I$  is calculated about the short axis, the data points move outside of the upper boundary (stars). Note that the cross-sectional area of the elliptical beams is equivalent to that of the small, circular beams; thus, these changes do not reflect an increase in the total amount of material, but rather a change in its distribution.

chanical properties may be attributed to materials that extend the entire length of the beam, but this explanation is inadequate for the jointed beams, which have no materials extending uninterruptedly along their entire length. The similarity in values for flexural stiffness and torsional stiffness for both jointed and continuous systems suggests that these beams may represent alternative designs to meet the functional need for flexibility in biological structures. Two of the jointed systems, horsetails and antennae, are relatively stiff for their size, suggesting that the presence of joints does not necessarily equate with increased flexibility.

Neither the ideal beams nor the biological beams are distributed uniformly throughout the mechanospace (Fig. 1). Unoccupied regions of the mechanospace correspond to beams that bend but do not twist and beams that twist but do not bend. The distribution within the mechanospace may be

determined by inherent principles governing the relationships between  $E$  and  $I$ , as well as  $G$  and  $J$ . Conversely, empty areas within the distribution may not be an indication of physical impossibility, but of evolutionary history. There may be an absence of environmental patterns of change causing natural selection for particular combinations of mechanical properties (Raup and Stanley, 1971). Alternatively, once an evolutionary pathway has been initiated, phylogenetic canalization may limit future options for change (Lauder, 1982). Finally, empty spaces within the mechanospace may reflect temporal, rather than physical, limitations to those areas (Raup, 1966). The empty spaces will eventually be occupied, given enough time. Although the identification of boundaries within this mechanospace may not reveal their ultimate source, the boundaries do identify factors that may influence the observed pattern (Lessa and Patton, 1989).

Despite the structural diversity of the samples used in this study, they are merely a subset of the biological possibilities. A notable limitation is the absence of fiber-wrapped beams in the mechanospace. Internally pressurized, hydrostatic skeletons are typically wrapped with reinforcing fibers (Wainwright *et al.*, 1978). The fibers may be arranged orthogonally with the fibers parallel and perpendicular to the long axis of the structure, or they may be in a helical array with fibers running in right- and left-handed helices around the long axis. Orthogonal arrays offer little resistance to twisting, while being relatively stiff in bending (Wainwright *et al.*, 1978). Thus, these beams would potentially fall into the upper left-hand corner of the mechanospace. In contrast, helical fiber arrays allow pressurized beams to bend smoothly without kinking, while resisting torsional deformations (Wainwright *et al.*, 1978), potentially positioning these beams in the lower right of the mechanospace. Fibrous support systems may decouple the relationship between *EI* and *GJ*, permitting novel combinations of mechanical properties. Thus, their inclusion in the mechanospace may greatly expand the observed distribution.

The mechanospace presented here is a useful approach for investigating patterns of flexibility in biological beams. Importantly, the mechanospace does not imply that flexibility has critical functional relevance in each system. Rather, it should be used as a broadly comparative tool to highlight systems in which flexibility may be biologically important. Biological beams that do not follow the basic pattern seen in the mechanospace may be of particular interest to both biologists and engineers, either due to material or structural innovation.

### Acknowledgments

I am grateful for the comments of Dr. Steve Vogel, Dr. Steve Wainwright, and Dr. Bill Hoesle on early drafts of this manuscript, as well as informative and invaluable discussions with Dr. John Gosline and Dr. D. A. Pabst. This manuscript was greatly improved by the comments of the reviewers.

### Literature Cited

- Baumiller, T. K. 1993. Crinoid stalks as cantilever beams and the nature of the stalk ligament. *Neues Jahrb. Geol. Palaeontol. Abh.* **190**: 279–297.
- Best, B. A. 1988. Passive suspension feeding in a sea pen: effects of ambient flow on volume flow rate and filtering efficiency. *Biol. Bull.* **175**: 332–342.
- Carrier, D. R. 1983. Postnatal ontogeny of the musculo-skeletal system in the black-tailed jack rabbit (*Lepus californicus*). *J. Zool.* **201**: 27–55.
- Denny, M. W. 1988. *Biology and the Mechanics of the Wave-swept Environment*. Princeton University Press, Princeton, NJ.
- Ennos, A. R. 1993. The mechanics of the flower stem of the sedge *Carex acutiformis*. *Ann. Bot.* **72**: 123–127.
- Etnier, S. A. 1999. Flexural and torsional stiffness in biological beams: the morphology and mechanics of multi-jointed structures. Ph.D. dissertation. Duke University, Durham, NC. 147 pp.
- Etnier, S. A. 2001. Flexural and torsional stiffness in multi-jointed biological beams. *Biol. Bull.* **200**: 1–8.
- Etnier, S. A., and S. Vogel. 2000. Reorientation of daffodil (*Narcissus*: Amaryllidaceae) flowers in wind: drag reduction and torsional flexibility. *Am. J. Bot.* **87**: 29–32.
- Gál, J. 1993. Mammalian spinal biomechanics. II. Intervertebral lesion experiments and mechanisms of bending resistance. *J. Exp. Biol.* **174**: 281–297.
- Gallenmüller, F., U. Müller, N. Rowe, and T. Speck. 2001. The growth form of *Croton pullei* (Euphorbiaceae)—functional morphology and biomechanics of a neotropical liana. *Plant Biol.* **3**: 50–61.
- Gere, J. M., and S. P. Timoshenko. 1984. *Mechanics of Materials*. Brooks/Cole Engineering Division, Monterey, CA.
- Harvell, C. D., and M. LaBarbera. 1985. Flexibility: a mechanism for control of local velocities in hydroid colonies. *Biol. Bull.* **168**: 312–320.
- Jeyasuria, P., and J. C. Lewis. 1987. Mechanical properties of the axial skeleton in gorgonians. *Coral Reefs* **5**: 213–219.
- Katz, S. L., and J. M. Gosline. 1992. Ontogenetic scaling and mechanical behaviour of the tibiae of the African desert locust (*Schistocerca gregaria*). *J. Exp. Biol.* **168**: 125–150.
- Koehl, M. A. R. 1977a. Effects of sea anemones on the flow forces they encounter. *J. Exp. Biol.* **69**: 87–105.
- Koehl, M. A. R. 1977b. Mechanical organization of cantilever-like sessile organisms: sea anemones. *J. Exp. Biol.* **69**: 127–142.
- Lauder, G. V. 1982. Historical biology and the problem of design. *J. Theor. Biol.* **97**: 57–67.
- Lessa, E. P., and J. L. Patton. 1989. Structural constraints, recurrent shapes and allometry in pocket gophers genus *Thomomys*. *Biol. J. Linn. Soc.* **36**: 349–364.
- Long, J. H., Jr., and K. S. Nipper. 1996. The importance of body stiffness in undulatory propulsion. *Am. Zool.* **36**: 678–694.
- McHenry, M. J., C. A. Pefl, and J. H. Long, Jr. 1995. Mechanical control of swimming speed: stiffness and axial wave form in undulating fish models. *J. Exp. Biol.* **198**: 2293–2305.
- Morgan, J. 1989. Analysis of beams subject to large deflections. *Aeronautical J.* **93**: 356–360.
- Morgan, J., and M. G. R. Cannel. 1987. Structural analysis of tree trunks and branches: tapered cantilever beams subject to large deflections under complex loading. *Tree Physiol.* **3**: 365–374.
- Niklas, K. J. 1991. The elastic moduli and mechanics of *Populus tremuloides* (Salicaceae) petioles in bending and torsion. *Am. J. Bot.* **78**: 989–996.
- Niklas, K. J. 1992. *Plant Biomechanics: An Engineering Approach to Plant Form and Function*. University of Chicago Press, Chicago.
- Niklas, K. J. 1998. The mechanical roles of clasping leaf sheaths: evidence from *Arundinaria tecta* (Poaceae) shoots subjected to bending and twisting forces. *Ann. Bot.* **81**: 23–34.
- Prince, R. P., and D. W. Bradway. 1969. Shear stress and modulus of selected forages. *Am. Soc. Agr. Eng. Trans.* **12**: 426–428.
- Putz, F. E., and N. M. Holbrook. 1991. Biomechanical studies of vines. Pp. 73–97 in *The Biology of Vines*, F. E. Putz and H. A. Mooney, eds. Cambridge University Press, New York.
- Raup, D. M. 1966. Geometric analysis of shell coiling: general problems. *J. Paleontol.* **40**: 1178–1190.
- Raup, D. M., and S. M. Stanley. 1971. *Principles of Paleontology*. W. H. Freeman, San Francisco.
- Roark, R. J. 1943. *Formulas for Stress and Strain*, 2nd ed. McGraw-Hill, New York.

- Vincent, J. 1990.** *Structural Biomaterials*. Princeton University Press, Princeton, NJ.
- Vogel, S. 1984.** Drag and flexibility in sessile organisms. *Am. Zool.* **24**: 37–44.
- Vogel, S. 1989.** Drag and reconfiguration of broad leaves in high winds. *J. Exp. Bot.* **40**: 941–948.
- Vogel, S. 1992.** Twist-to-bend ratios and cross-sectional shapes of petioles and stems. *J. Exp. Bot.* **43**: 1527–1532.
- Vogel, S. 1995.** Twist-to-bend ratios of woody structures. *J. Exp. Bot.* **46**: 981–985.
- Vogel, S. 1998.** Convergence as an analytical tool in evaluating design. Pp. 13–20 in *Principles of Animal Design: The Optimization and Symmorphosis Debate*, E. R. Weibel, C. R. Taylor, and L. Bolis, eds. Cambridge University Press, Cambridge.
- Wainwright, S. A. 1988.** *Axis and Circumference: The Cylindrical Shape of Plants and Animals*. Harvard University Press, Cambridge, MA.
- Wainwright, S. A., and J. R. Dillon. 1969.** On the orientation of sea fans. *Biol. Bull.* **136**: 130–139.
- Wainwright, S. A., W. D. Biggs, J. D. Currey, and J. M. Gosline. 1976.** *Mechanical Design in Organisms*. Princeton University Press, Princeton, NJ.
- Wainwright, S. A., F. Vosburgh, and J. H. Hebrank. 1978.** Shark skin: function in locomotion. *Science* **202**: 747–749.

## Appendix

Species ( $n = 57$ ) used in the mechanospace, along with their source, diameter, flexural stiffness ( $EI$ ), torsional stiffness ( $GJ$ ), and the ratio  $EI/GJ$ . Species for which assumptions were made about their size and shape are marked with an asterisk. The standard deviations for  $EI/GJ$  are given in parenthesis, when available

Group	Species	Diameter (m)	$EI$ (Nm <sup>2</sup> )	$GJ$ (Nm <sup>2</sup> )	$EI/GJ$	Source
Crustacean antennae $n = 2$	<i>Procambarus</i> sp. Crayfish	0.004	2.50E-05	6.00E-06	4.5 (3.7)	Etnier, 2001
	<i>Panulirus argus</i> Lobster	0.002	5.83E-03	2.04E-03	1.8 (1.3)	Etnier, 2001
Crinoid arms $n = 2$	<i>Comactinia echinoptera</i>	0.002	5.00E-05	1.50E-05	4.3 (3.8)	Etnier, 2001
	<i>Florometra serratissima</i>	0.002	3.92E-04	5.10E-05	6.6 (2.7)	Etnier, 2001
Horsetails $n = 1$	<i>Equisetum hyemale</i>	0.005	1.87E-02	3.83E-03	4.1 (1.8)	Etnier, 1999
Herbaceous stems $n = 6$	<i>Cucumis sativus</i> Cucumber	0.004	8.73E-03	1.83E-03	5.4 (1.2)	Vogel, 1992
	<i>Helianthus annuus</i> Sunflower	0.005	7.30E-05	5.30E-05	1.4 (0.4)	Vogel, 1992
	<i>Lycopersicon esculentum</i> Tomato	0.005	1.20E-02	3.46E-03	3.9 (1.1)	Vogel, 1992
	<i>Carex acutiformis</i> sedge	0.005	7.70E-03	2.34E-04	36.0 (11.3)	Ennos, 1993
	Tulips	0.006	2.02E-02	2.40E-03	8.3 (3.2)	Etnier and Vogel, 2000
	<i>Narcissus pseudonarcissus</i> Daffodil	0.007	1.19E-02	8.90E-04	13.3 (1.0)	Etnier and Vogel, 2000
Leaf petioles $n = 5$	<i>Acer rubrum</i> Red maple	0.001	1.94E-04	7.10E-05	2.8 (1.2)	Vogel, 1992
	<i>Liquidambar styraciflua</i> Sweet gum	0.002	9.84E-04	1.99E-04	5.1 (1.3)	Vogel, 1992
	<i>Phaseolus vulgaris</i> Green bean	0.002	6.77E-04	1.43E-04	4.9 (2.1)	Vogel, 1992
	<i>Populus alba</i> White poplar	0.003	7.75E-05	1.50E-05	4.95	Vogel, 1992
	<i>Populus tremuloides</i>	0.003	1.00E-05	1.00E-06	4	Niklas, 1991
Tree roots $n = 1$	<i>Pinus taeda</i> Loblolly pine	0.05	1.72E+02	7.90E+01	2.3 (0.8)	Vogel, 1995
Vines $n = 16$	<i>Croton pullei</i> juvenile	0.01*	3.30E+00	3.04E-01	10.9	Gallenmüller <i>et al.</i> , 2001
	<i>Cissampelos pareira</i>	0.02*	3.63E+00	4.90E-01	7.4	Putz and Holbrook, 1991
	<i>Cissus sicyoides</i>	0.02*	1.15E+00	1.30E-01	8.8	Putz and Holbrook, 1991
	<i>Forsteronia portoricensis</i>	0.02*	1.67E+00	8.30E-01	2.0	Putz and Holbrook, 1991
	<i>Heteropteris laurifolia</i>	0.02*	1.07E+01	4.60E+00	2.3	Putz and Holbrook, 1991
	<i>Hippocratea vulbilis</i>	0.02*	4.38E+00	6.80E-01	6.4	Putz and Holbrook, 1991
	<i>Ipomoea repanda</i>	0.02*	3.41E+00	3.10E-01	11.0	Putz and Holbrook, 1991
	<i>Marcgravia rectiflora</i>	0.02*	1.32E+01	2.50E-01	52.8	Putz and Holbrook, 1991
	<i>Mikania fragilis</i>	0.02*	1.48E+00	2.00E-01	7.4	Putz and Holbrook, 1991
	<i>Paullinia pinnata</i>	0.02*	4.71E+00	6.30E-01	7.5	Putz and Holbrook, 1991
	<i>Rourea surinamensis</i>	0.02*	6.48E+00	1.23E+00	5.3	Putz and Holbrook, 1991
	<i>Schlegelia brachyantha</i>	0.02*	4.34E+00	9.60E-01	4.5	Putz and Holbrook, 1991
	<i>Securidaca virgata</i>	0.02*	1.59E+00	3.60E-01	4.4	Putz and Holbrook, 1991
	<i>Croton pullei</i> mature	0.02*	4.87E+00	3.61E+00	1.4	Gallenmüller <i>et al.</i> , 2001
	<i>Vitis rotundifolia</i> Grape	0.046	3.08E+02	1.14E+02	2.7 (0.3)	Vogel, 1995
	<i>Wisteria sinensis</i> Wisteria	0.051	2.85E+02	6.70E+01	4.5 (2.1)	Vogel, 1995
Gorgonian corals $n = 13$	<i>Ellisella barbadensis</i>	0.004*	1.14E-01	2.16E-02	5.3	Jeyasuria and Lewis, 1987
	<i>Eunicea calyculata</i>	0.004*	9.07E-03	1.76E-03	5.1	Jeyasuria and Lewis, 1987
	<i>Eunicea clavigera</i>	0.004*	7.94E-03	2.26E-03	3.5	Jeyasuria and Lewis, 1987
	<i>Gorgonia ventalina</i>	0.004*	1.66E-02	1.05E-02	1.6	Jeyasuria and Lewis, 1987
	<i>Leptogorgia virgulata</i>	0.004*	4.47E-02	1.33E-02	3.3	Jeyasuria and Lewis, 1987
	<i>Lophogorgia cardinalis</i>	0.004*	6.35E-02	1.46E-02	4.3	Jeyasuria and Lewis, 1987
	<i>Muriceopsis flavida</i>	0.004*	8.82E-03	3.51E-03	2.5	Jeyasuria and Lewis, 1987
	<i>Plexaura flexuosa</i>	0.004*	1.25E-02	2.01E-03	6.2	Jeyasuria and Lewis, 1987
	<i>Plexaurella grisea</i>	0.004*	5.66E-02	9.54E-03	5.9	Jeyasuria and Lewis, 1987
	<i>Pseudoplexaura crucis</i>	0.004*	7.31E-03	2.01E-03	3.6	Jeyasuria and Lewis, 1987
	<i>Pseudopterogorgia bipinnata</i>	0.004*	4.17E-02	9.04E-03	4.6	Jeyasuria and Lewis, 1987
	<i>Pterogorgia citrina</i>	0.004*	1.95E-02	3.01E-03	6.5	Jeyasuria and Lewis, 1987
	<i>Swiftia exserta</i>	0.004*	8.82E-03	1.76E-03	5.0	Jeyasuria and Lewis, 1987
Tree branches $n = 11$	<i>Brunellia comocladifolia</i>	0.02*	2.08E+01	1.65E+00	12.6	Putz and Holbrook, 1991
	<i>Dendropanax arboreus</i>	0.02*	9.42E+01	2.81E+00	33.5	Putz and Holbrook, 1991
	<i>Guarea trichilioides</i>	0.02*	1.92E+01	1.95E+00	9.9	Putz and Holbrook, 1991
	<i>Inga vera</i>	0.02*	3.74E+01	5.47E+00	6.8	Putz and Holbrook, 1991
	<i>Ocotea floribunda</i>	0.02*	1.31E+01	4.23E+00	3.1	Putz and Holbrook, 1991
	<i>Juniperus virginiana</i> E. red cedar	0.04	7.44E+02	1.68E+02	4.4 (0.7)	Vogel, 1995
	<i>Liriodendron tulipifera</i> Tulip poplar	0.045	1.16E+03	1.30E+02	8.9 (1.4)	Vogel, 1995
	<i>Acer rubrum</i> Red maple	0.047	2.07E+03	2.50E+02	8.3 (0.9)	Vogel, 1995
	<i>Phyllostachys</i> sp. Bamboo	0.05	8.03E+03	9.50E+02	8.6 (1.3)	Vogel, 1995
	<i>Pinus taeda</i> Loblolly pine	0.051	2.06E+03	3.19E+02	6.1 (0.9)	Vogel, 1995
	<i>Liquidambar styraciflua</i> Sweet gum	0.054	2.38E+03	2.60E+02	8.9 (1.6)	Vogel, 1995

# Extracellular Lipid Droplets in *Idiosepius notoides*, the Southern Pygmy Squid

L. S. EYSTER\* AND L. M. VAN CAMP

*School of Biological Sciences, Flinders University, Adelaide, South Australia 5001, Australia*

**Abstract.** Cephalopod metabolism typically involves carbohydrates and proteins, so that the lipid content of the mantle and all internal organs except the digestive gland is very low. Despite clear evidence of nonlipoid metabolic trends in cephalopods, we observed extracellular spheres, or droplets, in the cecum and digestive gland of newly collected juvenile, male, and female individuals of *Idiosepius notoides*, the southern pygmy squid. Prior to staining, the droplets were various shades of yellow and were often large enough to detect at 7× magnification. The droplets were less dense than water, hydrophobic, and sudanophilic, staining positively with Sudan III, Sudan IV, and Sudan Black B. We conclude that these spheres are lipid and that they derive from the squid's normal field diet. When newly collected squid were starved in the laboratory, the droplets disappeared in 7–8 d and then reappeared in the cecum about 3 h after feeding.

## Introduction

Although cephalopods require considerable energy for rapid movement, growth, and reproduction, they apparently have limited capacity to metabolize or store lipids (Hochachka *et al.*, 1975; Storey and Storey, 1983; O'Dor and Webber, 1986; Moltschaniwskyj and Semmens, 2000). In 1975, cephalopod metabolism was described as poorly understood, and squid storage substrates were "a well known mystery in marine biochemistry" (Hochachka *et al.*, 1975). That mystery arises because lipids, efficient energy storage molecules due to their high per-gram energy content, are typically not abundant in cephalopods (Hochachka *et al.*, 1975; Castro *et al.*, 1992; Clarke *et al.*, 1994).

Received 24 September 2002; accepted 12 June 2003.

\* To whom correspondence should be addressed. Current address: Science Department, Milton Academy, Milton, Massachusetts, 02186. E-mail: Linda\_Eyster@Milton.edu

Abbreviation: ML = mantle length.

Despite evidence of limited lipid metabolism in cephalopods, lipid storage has been reported for the digestive gland, the only cephalopod organ consisting of more than a few percent lipid. The cecum is not reported to be a typical lipid storage site, although cecal cells have been ascribed a variety of functions, including fat absorption in several species (Bidder, 1966; Boucaud-Camou and Boucher-Rodoni, 1983; O'Dor *et al.*, 1984; Westermann and Schipp, 1998).

*Idiosepius notoides* Berry 1921 is a small sepioid found in seagrass beds in southern Australian waters, from Cockburn Sound in Western Australia to Morton Bay, Queensland (Shepard and Thomas, 1989). We report the existence and retention of yellow spheres within the cecal lumen and digestive gland of field-collected specimens of *I. notoides* subjected to starvation, and explore the possible lipid nature of these droplets. We also speculate on the origin, function, and fate of the droplets.

## Materials and Methods

*Idiosepius notoides* was collected by seining over seagrass beds (18 °C, 39 ppt salinity) near the mouth of the Port River, Adelaide, South Australia, on 29 March 2002 (Day 0). All squid were recognized by their small size (about 10 mm dorsal mantle length), by a pair of rounded fins near the rear of the body, and by their attachment to seagrasses and *Ulva* sp. using dorsal duoadhesive glands (Norman and Reid, 2000). Because idiosepiids are morphologically unusual, they historically have been placed with the teuthids but are currently classified as sepiids (Berry, 1932; Hylleberg and Natewathana, 1991); despite their cuttlefish alliances, they are commonly called pygmy "squid" and will be referred to as squid in this paper.

Squid that died on collection ( $n = 2$ ) were examined on Day 0. Live squid were kept unfed in an aquarium connected to the recirculating seawater system (~16 °C, 40 ppt salinity, 12 h light:12 h dark cycle) until natural death or

sacrifice on Days 4–15. To investigate whether “starved” squid ate small organisms (e.g., copepods present in the recirculating seawater), three squid were videotaped individually (2.5 h total, 25 frames per second) in a tank measuring 19.3 × 7 cm (containing one liter of unfiltered seawater from the recirculating system).

Before sacrifice, each squid (chosen at random) was observed at about 10× magnification in a small, flat dish for 15 min in an attempt to locate droplets prior to anesthesia or dissection. The dark-pigmented mantle of active, stressed animals often hid droplets. However, during the squids’ occasional flashes of transparency, we could see through the mantle tissue and determine droplet location.

At sacrifice, squid were transferred (in seawater) to a freezer for terminal anesthesia, measured (dorsal mantle length = ML), and then decapitated (Boyle, 1991). (Although cold water may be analgesic rather than anesthetic [Boyle, 1991], in this paper the treatment is referred to as cold anesthesia.) The mantle was cut open to expose but not damage internal organs. We recorded gender, stage of sexual maturation (based on Lipiński’s maturation scale as interpreted by Moltschaniwskyj, 1995), droplet presence, and sometimes droplet diameter. Droplets to be tested for lipid content were obtained by puncturing the cecum. Because it is unknown if handling of squid may break drops into smaller droplets (and we wanted larger drops for stain testing), we minimized handling of squid prior to anesthesia and during dissection.

Droplets were tested for lipid content using three stains: Sudan III, Sudan IV, and Sudan Black B (one stain per squid). Because these stains have very low water solubilities (ranging from <0.1 mg/ml for Sudan III to 0.7 mg/ml for Sudan IV; Green, 1990) compared to solubility in ethanol, staining solutions were prepared as saturated solutions in 70% ethanol. Staining solutions were prepared only a few days before use to avoid the deterioration that can occur in Sudan/alcohol solutions (Gurr, 1962).

We tried three approaches to cecal droplet staining (one method per squid). For ceca cut open unsubmerged, stain was pipetted directly onto the body. For ceca punctured submerged, filtered stain was added to the seawater (i.e., drops were stained floating on the water surface). Additional droplets collected from the water surface by patting with strips of filter paper were flooded with stain for about 10 min, followed by ethanol rinses to de-stain the paper. Control tests were conducted using food-grade vegetable oil. Positive stain for lipid includes yellow-orange for Sudan III, orange-red for Sudan IV, and blue-black for Sudan Black B (Conn, 1961; Gurr, 1962, 1965).

To determine if changes in extracellular lipid volume or location could be detected after feeding, we fed one squid and then repeatedly examined it for droplets. This squid (see 9.7-mm-ML male on Day 7, Table 1) was chosen because it seemed less stressed by handling: compared to most of our

other squid, its movements were less vigorous in the small observation dish, and it seemed to have a transparent mantle more frequently. No anesthesia was used on the day of feeding, but it had to be used on the second and third days after feeding. Before feeding, the squid had no cecal drops but did have two small, equal-sized drops at the anterior end of the digestive gland, one on the left and one on the right side. After it caught the live shrimp provided (*Hippolyte* sp., ~19 mm long), the squid was left undisturbed until it discarded the intact but almost empty exoskeleton 45 min later. No effort was made to locate oil droplets during feeding because preliminary work showed that disturbed squid tended to abandon their prey. We examined the squid for droplets immediately after its meal, at hourly intervals for the next 7 h, and then up to twice daily until no drops were detected at a magnification of about 30×. We measured the cecal droplets if the squid remained stationary and was transparent during observations.

To address the possibility of droplet expulsion, we kept four immature squid (4.4–6.9 mm ML) in individual glass bowls (colorless) until their oil droplets were undetectable. We used small bowls (100 ml of filtered seawater, 16 °C) to decrease the surface area we would have to search for oil. These squid, from a separate collection made in late April 2002 near Noarlunga (south of Adelaide), all had oil drops when collected and when placed in the glass bowls. Prior to use in this experiment they were maintained in an aquarium connected to the recirculating seawater system and fed field-collected mysid shrimp for 1 week. After placement in individual dishes, these squid were kept without food and were examined with a dissecting microscope once per day to determine whether droplets were present in the digestive system. Prior to the daily cleaning and refilling of the bowls, the water surface was examined with a dissecting microscope for floating droplets and then was patted with white paper toweling, which was also examined for droplets.

## Results

Of the 16 squid collected in March, 11 were males, 3 were juveniles, and 2 were females. Dorsal mantle length ranged from 6.5 to 16.5 mm. Females tended to be larger than males, as previously recorded (Norman and Reid, 2000); mantle length was  $15.4 \pm 1.1$  mm (mean  $\pm$  SD) in females,  $8.4 \pm 0.9$  mm in males, and  $6.8 \pm 0.3$  mm in juvenile squid.

Droplets were easiest to locate in dissected, fresh squid or in healthy, stationary squid in transparent phase. Opaque mantle tissue in preserved and moribund squid hid the droplets. For active squid, it was difficult or impossible to obtain accurate droplet counts or measurements.

In the first week after collection, we examined one juvenile, nine male, and two female squid. Of these 12 un-fed squid, 11 had droplets (Table 1). Droplets were not detected

**Table 1**

Gender, reproductive maturity stage, and dorsal mantle length of starved *Idiosepius notoides* individuals examined Days 0–15 post-collection for extracellular droplets in the digestive tract

Days (post-collection)	Gender & maturity stage		Mantle length (mm)	Droplets seen?
0	J	1	6.5	+
0	M	3	9.0	+
4	M	3	9.1	+
4	M	3	8.7	+
4	M	3	8.1	+
4	F	5	16.5	–
5	M	3	8.0	+
5	M	3	8.0	+
5	M	3	8.0	+
7	M	5	9.8	+
7	F <sup>a</sup>	nd	14.3	+
7	M <sup>b</sup>	nd	9.7	+
9	J	1	nd	–
9	J <sup>c</sup>	1	nd	–
10	F <sup>a</sup>	nd	13.7	–
10	J <sup>c</sup>	1	7.0	–
14	M	3	8.6	–
15	M	3	6.5	–

J, juvenile; M, male; F, female; nd, no data.

<sup>a</sup> Same squid examined Days 7 and 10.

<sup>b</sup> This squid was used in a feeding experiment beginning later on Day 7.

<sup>c</sup> Same squid examined Days 9 and 10.

in the largest squid, a female. During Days 9–15 after collection, we found no droplets in any of the unfed squid (Table 1).

Drops were most obvious in the cecum (Fig. 1a), a digestive sac near the rear of the body. The cecum wall was transparent, and the lumen of the organ contained a clear greenish or bluish fluid without obvious particles (Fig. 1a, b), all of which made the droplets conspicuous. We did not notice any distinct progression of color changes in cecal fluid (Lipiński, 1990). Cecal droplets moved around, apparently due to ciliary currents and cecal contractions. Because the drops floated, they were easily detectable in the cecum whether we removed a dorsal or ventral piece of mantle (Fig. 1a, b). Unlike the luminal oil droplets described in the loliginid squids *Septoteuthis lessoniana* and *Photololigo* sp. (Semmens, 1998), the droplets in *Idiosepius notoides* apparently are not membrane-bound; when pushed together with a microprobe, droplets could readily fuse.

We also saw droplets in the anterior end of the digestive gland, just under the edge of the uncut mantle, but these were often harder to detect than cecal drops. Drops were seen in the left, right, or both sides of the digestive gland simultaneously. We never found drops outside the cecum or digestive gland when we carefully cut only mantle tissue.

Droplet color varied among squid but typically looked like some shade of yellow. It was difficult to be sure of color

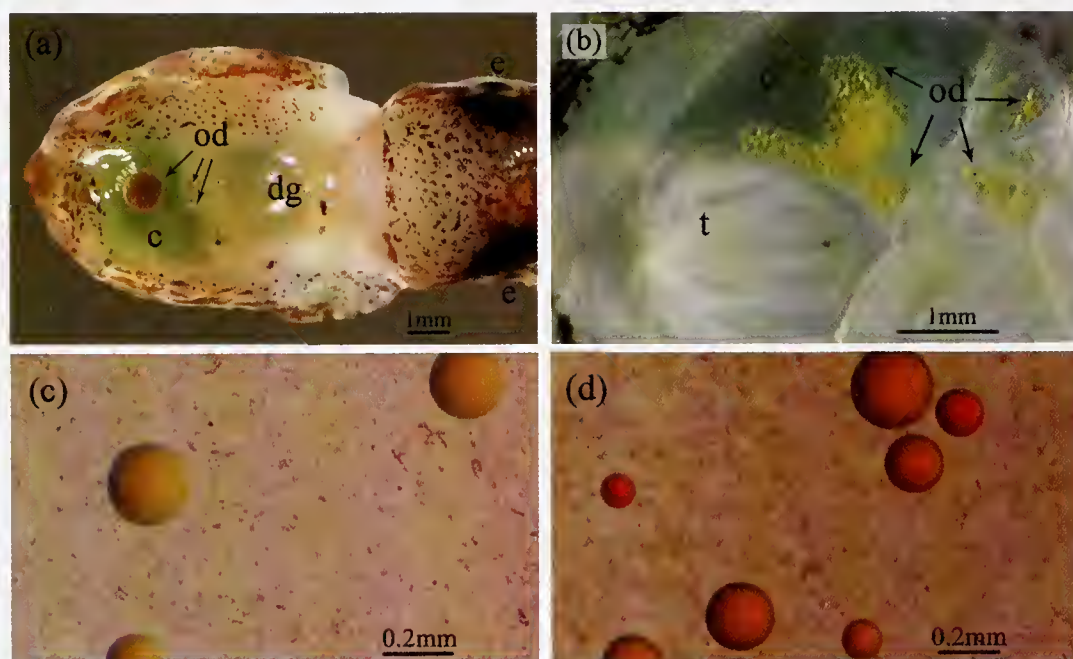


**Figure 1.** Cecal lipid droplets in *Idiosepius notoides*. Tissue was cut from dorsal (a) or ventral (b) mantle to expose the cecum and its yellow droplets. All oil drops shown are from starved male squid sacrificed Days 4–5 after collection (8–9 mm ML). The floating drops in c and d are from a cecum punctured under water. Filtered Sudan IV (in 70% ethanol) was added to the seawater. Photographs were taken every 5 min for 1 h on an Olympus DP10 digital camera attached to an Olympus SZH microscope. Shown are droplets at 5 min (c) and 60 min (d) staining. c = cecum, dg = digestive gland, e = eye, od = oil droplets, t = testis

comparisons for cecal droplets because the variable blue-green hues of the cecal fluid (e.g., Fig. 1a vs. 1b) probably altered our color perception. Larger drops of yellow food oils (almond, olive, sunflower, vegetable) all appeared colorless floating in seawater under the same lighting conditions. Unstained droplets collected onto white filter paper from two Port River squid were conspicuous at 10 $\times$  due to their brilliant lemon yellow color, while droplets from three of the four Noarlunga squid looked colorless in the cecum.

Number and size of droplets varied among squid. For example, one squid had a huge cecal drop (~0.9 mm in diameter; Fig. 1a), and another had dozens of tiny droplets (Fig. 1b). However, on Days 0–7 after collection, most starved squid had 2–14 droplets with a typical diameter of 0.05–0.2 mm per droplet.

Evidence supporting the lipid nature of the droplets is summarized in Table 2 and in Figure 1c and d. The yellow droplets were hydrophobic, typically forming small spheres in the cecum. When we cut a submerged cecum, droplets rapidly escaped and floated to the water surface. On hitting the air-water interface, larger drops "popped" from a sphere into a thin disk on the water surface. One large drop pipetted onto a piece of thin brown-paper bag and pressed onto the paper using Parafilm left a translucent window (11 mm in diameter) in the paper for a 48-h observation period, whereas other random fluids from the same squid did not. Floating droplets collected onto filter paper changed from yellow (before staining) to orange with Sudan III, orange-red with Sudan IV, and blue-black with Sudan Black B. Floating droplets exposed to Sudan IV changed from yellow (Fig. 1c) to orange (Fig. 1d).

There was no evidence of feeding in any "starved" squid. All squid were accounted for, so no cannibalism occurred. Two of the videotaped squid explored the aquarium walls with their arms for about 10% of the filmed time, and they sometimes made motions as if catching something, but frame-by-frame viewing of those times gave no conclusive evidence of feeding.

In the squid fed the large shrimp, no cecal droplets were seen until 3 h after feeding ended (Table 3). Cecal droplet volume increased on the day of feeding, then decreased, becoming negligible by 3 d later. When cecal drop total

volume was largest (6 h to 2 d after feeding), no drops were seen on either side of the digestive gland (Table 3). Digestive gland droplets were seen more often on the left side (12 times) than on the right side (6 times) (Table 3). Droplets persisted for about 5 d after the squid ate that one shrimp. No droplets were detectable 7 d after feeding (Table 3).

No evidence of droplet expulsion was obtained from squid held in individual bowls. We saw no oil on the water surface, or on paper toweling that was used to wipe the water surface. Droplets disappeared in all four squid sometime between the third and fourth day of starvation.

## Discussion

Despite the limited storage or usage of lipids in cephalopods, we show in this work that droplets in the cecal lumen of *Idiosepius notoides* are lipid. To our knowledge, these extracellular droplets have not been reported in any other cephalopod. We believe these droplets are common in this species and that droplets persist for up to 7 d in starved squid as a result of slow absorption, slow expulsion, or both. Our preliminary evidence suggests that expulsion of large drops was not occurring in the laboratory, but expulsion of small droplets could have been undetected.

Because droplets appear to be free and not membrane-bound in the cecal lumen, lipases could have ready access to them. Perhaps droplets can persist in the cecal sac for a week after a meal because no, or few, lipases are consistently present or active there. The digestive gland and cecum both produce various digestive enzymes (Boucaud-Camou and Boucher-Rodoni, 1983), but few studies have demonstrated lipase activity in any cephalopod digestive tract fluids or extracts (Bidder, 1966). Lipases probably occur in cephalopod digestive organs, including those of paralarvae (Boucaud-Camou and Roper, 1995), but oily feces in animals that were fed a diet high in lipids, and the accessibility of lipids in *Octopus vulgaris* for several days after feeding support the conclusion that cephalopod lipid metabolism is "slow and inefficient" (O'Dor *et al.*, 1984). A study of lipase activity in various regions of the digestive tract of *Idiosepius notoides* before, during, and after meals should be informative.

Droplets seemed easier to see in the cecum than in the digestive gland, probably because of the opaque brownish color and tubular structure of the latter organ. In addition, larger droplets may form more readily in the cecum because small droplets might meet and coalesce into larger spheres more easily in the cecal lumen than in the digestive gland, whose structure may interfere with contact between droplets.

We observed movement of small droplets along the length of both the left and right halves of the digestive gland in live squid, but never saw movement of droplets between the two sides. The digestive gland of the congener *I. pygmaeus* is a

Table 2

Summary of evidence supporting the lipid nature of cecal droplets in southern pygmy squid, *Idiosepius notoides*.

Criterion	Observation	Consistent with lipid?
Color	yellow	+
Solubility	insoluble in water	+
Density	less than water	+
Paper bag test	translucent mark	+
Sudan stains	sudanophilic	+

Table 3

Number of extracellular lipid drops seen in the cecum and in both sides of the digestive gland of one *Idiosepius notoides* squid over a 7-day period after feeding; the squid was starved in the laboratory for one week before feeding

Time (after feeding)*	Cecum		Digestive Gland			Totals	
	Number of cecal drops	Diameter of cecal drops (mm)†	No. of drops on left side	No. of drops on right side	Location of largest drop‡	Total number of drops	Total cecal drop volume (mm <sup>3</sup> × 10 <sup>-2</sup> )§
-1 h	0	0	1	1	dg	2	0.0
0 h	0	0	1	1	dg	2	0.0
1 h	0	0	1	1	dg	2	0.0
2 h	0	0	1	1	ldg	2	0.0
3 h	2	nd	1	1	ldg	4	> 0.0
4 h	2	nd	1	0	ldg	3	> 0.0
5 h	2	0.2, 0.3	1	0	ldg	3	1.8
6 h	4	0.2, 0.25, 0.35, 0.45	0	0	cecum	4	8.3
7 h	4	0.1, 0.1, 0.2, 0.55	0	0	cecum	4	9.2
2 d	2	0.1, 0.5	0	0	cecum	2	6.6
3 d	0	0	6	0	ldg	6	0.0
4 d a.m.	3	nd	1	1	dg	5	> 0.0
4 d p.m.	1	0.1	1	0	ldg	2	0.05
5 d a.m.	0	0	1	0	ldg	1	0.0
5 d p.m.	1	0.05	1	0	ldg	2	0.007
7 d	0	0	0	0	—	0	0.0

\* 0 h signifies the end of the meal.

† nd = no data.

‡ dg = digestive gland; ldg = left side of digestive gland.

§ Total volume of cecal drops was calculated from the number of drops and their diameter. Digestive gland drops were not measured.

“single unilobed organ” that is “ventrally bilobed with an incomplete dorsal septum” (Semmens *et al.*, 1995). If a digestive gland septum occurs in *I. notoides*, it might explain this apparent separation and separate movement of left and right drops. It does not explain why we saw droplets more frequently on the left side of the digestive gland in the one squid examined repeatedly over a 7-d period (Table 3).

Mantle length seemed irrelevant to either the presence or size of oil droplets, but we could find only two large squid for our study. The fact that the only squid without droplets in Week 1 of starvation was also the only gravid female suggests that further records of reproductive stage *versus* droplets are warranted.

Cephalopods are active carnivores, typically catching crustaceans, molluscs, and fish that are relatively large—often as long as two-thirds of the predators' mantle length (Bidder, 1966; Wells and Clarke, 1996). However, members of *Idiosepius* are the world's smallest cephalopods (Norman and Reid, 2000) and may also be able to feed on small organisms that are not readily apparent to the unaided eye. We observed “nibbling” behavior (Moynihan, 1983) in our squid but no definite feeding during nibbling. Although our “unfed” squid may have fed on small organisms like copepods that were present in the recirculating seawater system, we consider it unlikely that this potential feeding affects any of our conclusions.

Most of the carbon in cephalopod meals is in protein

molecules, and growth in cephalopods is primarily through protein formation (O'Dor *et al.*, 1984). A typical squid body is about 80% muscle, but only 1%–1.5% lipid, and less than 0.4% carbohydrate (O'Dor and Webber, 1986). In line with their proteo-metabolic capabilities, all cephalopod organs, except the digestive gland, are also high in protein and low in lipid (*e.g.*, 10%–17% protein *versus* 1%–2% lipid dry mass in squid mantle, head, testis, or spermatophoric complex [Hochachka *et al.*, 1975; Clarke *et al.*, 1994], and 3% lipid in cuttlefish gonad [Blanchier and Boucaud-Camou, 1984]). The only cephalopod organ containing abundant lipid is the digestive gland (called liver or hepatopancreas in older literature). Content of that organ varies from one species to another: reported values for lipid content are 4%–6% in *Photololigo* sp. (Semmens, 1998; Moltschanivskyj and Semmens, 2000), 8%–11% in *Sepia officinalis* (Blanchier and Boucaud-Camou, 1984), about 30% in *Illex argentinus* (Clarke *et al.*, 1994), and 27%–56% in *Moroteuthis ingens* (Brachi, 1953; Phillips *et al.*, 2001).

Food in a typical cephalopod travels through the buccal mass and down the esophagus to the stomach for initial extracellular digestion, probably aided by salivary and digestive gland enzymes (Boucaud-Camou and Boucher-Rodoni, 1983). Smaller food materials move to the digestive gland or the cecum for further digestion, and wastes travel the intestine to the anus (Bidder, 1966). The cecum, connected to the digestive tract between the stomach and anus,

receives and processes fine particles, has its own sphincter to isolate contents, and is the primary site of absorption from food fluids (Bidder, 1966; Boucaud-Camou and Boucher-Rodoni, 1983; O'Dor and Webber, 1986). Perhaps the cecum of *I. notoides* can absorb dietary lipids, as reported for *Octopus*, *Loligo*, *Sepia*, and *Nautilus* (Bidder, 1966; Boucaud-Camou and Boucher-Rodoni, 1983; O'Dor *et al.*, 1984; Westermann and Schipp, 1998).

In this study, we saw extracellular lipid in two organs: the cecum and the digestive gland. In other cephalopods, the only organ with significant lipid (reported as cellular deposits) is the digestive gland; therefore, it has been considered the only storage site for lipid molecules. These lipid molecules might be oxidized during reproductive maturation or starvation, as in other marine organisms (Voogt, 1983; Boucaud-Camou, 1971, cited in Blanchier and Boucaud-Camou, 1984; Kreuzer, 1984, cited in Castro *et al.*, 1992; Clarke *et al.*, 1994). Besides storing lipids, the digestive gland may be absorptive in some but not all species (Bidder, 1966; Boucaud-Camou and Boucher-Rodoni, 1983). In fact, lipid seen inside digestive gland cells of two squid species appears to be packaged for expulsion, not storage (Semmens, 1998); because expulsion would be energetically wasteful and would make the squid denser, perhaps some lipid is moved to the cecum rather than expelled from the organism. Although very few cephalopods produce and store lipids for buoyancy (Clarke, 1988; O'Dor, 2002), perhaps the cecal lipid in *I. notoides* aides in the support of this small but negatively buoyant cephalopod.

It is clear from our study that retention of extracellular lipid occurs in *I. notoides*; it is less clear whether retention for 7 to 8 days qualifies as "storage." The term storage is used in the literature without reference to length of retention, without evidence of retention *versus* replacement of molecules, and with the implication of future use. Labeling studies may be useful in determining if "storage" of extracellular lipid in the cecum and digestive gland of *I. notoides* is due to slow utilization and/or slow elimination, either or both coupled with the addition of new molecules from the next meal.

During our laboratory study with *I. notoides*, luminal oil droplets disappeared slowly, over a period of days (7–8 days in our field-fed squid; 3–4 days in our mysid-fed squid), not hours or minutes. This slow disappearance of lipid suggests slow absorption, slow expulsion, or both in starved squid. We cannot rule out rapid expulsion of large drops in the field. It is also unknown if this species makes rapid vertical movements in the field. In the laboratory, these squid spent most of their time sitting on aquarium walls or on the undersurface of plastic plants, and movements were mostly horizontal. Anesthetized squid sank to the bottom, indicating that even with lipid droplets in the cecum, these squid are negatively buoyant. Rapid expulsion of large lipid drops by these small cephalopods might pro-

vide a quick increase in negative buoyancy during a dive, and new drops could apparently be formed at the next meal. Our squid could not deep dive in our expulsion study because the water was only a couple of centimeters deep; the water level in our holding tank was about 10 cm deep, and the tank contained no predators that might induce swimming up and down in the water column.

Extracellular lipid droplets have not been previously reported in *Idiosepius* species. Perhaps the drops are specific to *I. notoides*, which is not a well-researched species. Perhaps droplet presence and color vary with lipid content of the field diet; less fatty prey might not lead to droplets, and some prey might lead to paler droplets that are harder to see. Perhaps droplets were overlooked in previous studies of *I. notoides* because tiny droplets in live squid can resemble the yellow chromatophores in size and color, or because the droplets were obscured or extracted by preservatives (*e.g.*, alcohol can turn the cecum opaque white).

We considered using chemical anesthesia on *I. notoides* to help us locate and measure droplets in live squid, but this can move material from organ to organ in the digestive tract of cephalopods (Bidder, 1966). Decapitation and dissection can also cause movement of material between organs (Bidder, 1966). Although movement or breakage of drops due to handling cannot be ruled out in our study, we minimized post-collection handling and confirmed for some squid that droplets were in the cecum before chilling.

We provide preliminary evidence that cecal oil droplets originate from food a few hours after consumption. Although droplets were admittedly less obvious in the digestive gland than in the cecum, the amount of lipid in the cecum at 3–7 h after feeding far exceeded the amount detected in the digestive gland before feeding. Thus, the "new" cecal lipid probably derived from the latest meal.

Cephalopod digestion times (defined as time from food capture to return of stomach and cecum to "hunger condition") include 15–20 h in *Octopus* and *Sepia* and 4–12 h in *Loligo* (Bidder, 1966; Lipiński, 1990). Although cephalopods "digest quickly, convert efficiently, and grow but do not store energy during their 'live fast, die young' lives" (O'Dor and Webber, 1986), we cannot say with certainty that the digestive gland of *I. notoides* was empty after 7 d of starvation. However, because digestive gland lipid in *Octopus* dropped from 0.3% to 0.06% of body weight with a 6-d starvation (O'Dor *et al.*, 1984), 7-d starvation in *I. notoides* may deplete most non-membrane lipid from its digestive gland. The large volume of "new" cecal lipid after feeding, coupled with a week of prior starvation, leads us to conclude that the post-meal cecal lipid seen in *I. notoides* was produced in a few hours from the recent meal. Both the reappearance of lipid drops in the squid fed after a 7-d starvation and the continued absence of drops in all squid starved more than 7 d support this conclusion.

This study describes extracellular lipid droplets in *I.*

*notoides* but leaves unanswered whether these tiny cephalopods expel the material over time, whether they are metabolically capable of obtaining energy from the lipid, and whether the drops confer a buoyant advantage. The fact that lipid droplets did not disappear until the eighth or ninth day of starvation in field-fed animals suggests that these squid may use the droplets as an energy source. However, slow expulsion of the lipid as a dietary waste cannot yet be ruled out.

### Acknowledgments

We are grateful to Jon N. Havenhand for use of his laboratory facilities, to J. Robertson and A. R. Dyer for the use of their boats, to O. A. Pechenik for typing and data entry, and to Cat Darrow for technical help in preparing the digital color plate. Research was supported by a sabbatical leave and research grant from Milton Academy to L. S. Eyster.

### Literature Cited

- Berry, S. S. 1932. Cephalopods of the genera *Sepioloidea*, *Sepiadarium*, and *Idiosepius*. *Rec. South Austral. Mus.* **47**: 39–55.
- Bidder, A. M. 1966. Feeding and digestion in cephalopods. Pp. 97–124 in *Physiology of Mollusca*, Vol II, K. M. Wilbur and C. M. Yonge, eds. Academic Press, New York.
- Blanchier, B., and E. Boucaud-Camou. 1984. Lipids in the digestive gland and the gonad of immature and mature *Sepia officinalis* (Mollusca: Cephalopoda). *Mar. Biol.* **80**: 39–43.
- Boucaud-Camou, E. 1971. Constituants lipidiques du foie de *Sepia officinalis*. *Mar. Biol.* **8**: 66–69. (Cited in Blanchier and Boucaud-Camou, 1984.)
- Boucaud-Camou, E., and R. Boucher-Rodoni. 1983. Feeding and digestion in cephalopods. Pp. 149–187 in *The Mollusca*, P. R. Boyle, ed. Academic Press, New York.
- Boucaud-Camou, E., and C. Roper. 1995. Digestive enzymes in paralarval cephalopods. *Bull. Mar. Sci.* **57**: 313–327.
- Boyle, P. R. 1991. *The UFAW Handbook on the Care and Management of Cephalopods in the Laboratory*. Universities Federation for Animal Welfare, Potters Bar, UK. 62 pp.
- Brachi, R. M. 1953. Examination of some components of cephalopod and sperm-whale liver oils by the chromatographic method. *Biochem. J.* **54**: 459–465.
- Castro, B. G., J. L. Garrido, and C. G. Sotelo. 1992. Changes in composition of digestive gland and mantle muscle of the cuttlefish *Sepia officinalis* during starvation. *Mar. Biol.* **114**: 11–20.
- Clarke, A., P. G. Rodhouse, and D. J. Gore. 1994. Biochemical composition in relation to the energetics of growth and sexual maturation in the ommastrephid squid *Illex argentinus*. *Philos. Trans. R. Soc. Lond. B.* **344**: 201–212.
- Clarke, M. R. 1988. Evolution of buoyancy and locomotion in recent cephalopods. Pp. 203–213 in *The Mollusca*, M. R. Clarke and E. R. Trueman, eds. Academic Press, New York.
- Conn, H. J. 1961. *Biological Stains: a Handbook on the Nature and Uses of the Dyes Employed in the Biological Laboratory*. Williams and Wilkins, Baltimore, MD. 350 pp.
- Green, F. J. 1990. *The Sigma-Aldrich Handbook of Stains, Dyes, and Indicators*. Aldrich Chem. Co., Milwaukee, WI. 776 pp.
- Gurr, E. 1962. *Staining Animal Tissues: Practical and Theoretical*. Leonard Hill Ltd., London. 631 pp.
- Gurr, E. 1965. *The Rational Use of Dyes in Biology and General Staining Methods*. Leonard Hill Ltd., London. 422 pp.
- Hochachka, P. W., T. W. Moon, T. Mustafa, and T. W. Storey. 1975. Metabolic sources of power for mantle muscle of a fast swimming squid. *Comp. Biochem. Physiol.* **52B**: 151–158.
- Hyllberg, J., and A. Nateewathana. 1991. Redescription of *Idiosepius pygmaeus* Steenstrup, 1881 (Cephalopoda: Idiosepiidae), with mention of additional morphological characters. *Phuket Mar. Biol. Cent. Res. Bull.* **55**: 33–42.
- Kreuzer, R. 1984. Cephalopods: handling, processing and products. *FAO Fish. Tech. Pap.* **254**: 1–108. (Cited in Castro *et al.*, 1992.)
- Lipiński, M. R. 1990. Changes in pH in the caecum of *Loligo vulgaris reynaudii* during digestion. *S. Afr. J. Mar. Sci.* **9**: 43–51.
- Moltschanivskyj, N. A. 1995. Multiple spawning in the tropical squid *Photololigo* sp.: What is the cost in somatic growth? *Mar. Biol.* **124**: 127–135.
- Moltschanivskyj, N. A., and J. M. Semmens. 2000. Limited use of stored energy reserves for reproduction by the tropical loliginid squid *Photololigo* sp. *J. Zool. Lond.* **251**: 307–313.
- Moynihan, M. 1983. Notes on the behaviour of *Idiosepius pygmaeus* (Cephalopoda: Idiosepiidae). *Behaviour* **85**: 42–57.
- Norman, M. D., and A. Reid. 2000. *A Guide to Squid, Cuttlefishes and Octopuses of Australasia*. CSIRO Publishing and the Gould League of Victoria, Melbourne, Australia. 96 pp.
- O'Dor, R. K. 2002. Telemetered cephalopod energetics: swimming, soaring, and blimping. *Integ. Comp. Biol.* **42**: 1065–1070.
- O'Dor, R. K., and D. M. Webber. 1986. The constraints on cephalopods: Why squid aren't fish. *Can. J. Zool.* **64**: 1591–1605.
- O'Dor, R. K., K. Mangold, R. Boucher-Rodoni, M. J. Wells, and J. Wells. 1984. Nutrient absorption, storage and remobilization in *Octopus vulgaris*. *Mar. Behav. Physiol.* **11**: 239–258.
- Phillips, K. L., G. D. Jackson, and P. D. Nichols. 2001. Predation on myctophids by the squid *Moroteuthis ingens* around Macquarie and Heard Islands: stomach contents and fatty acid analyses. *Mar. Ecol. Prog. Series* **215**: 179–189.
- Semmens, J. M. 1998. An examination of the role of the digestive gland of two loliginid squids, with respect to lipid: storage or excretion? *Proc. R. Soc. Lond. B.* **265**: 1685–1690.
- Semmens, J. M., N. A. Moltschanivskyj, and C. G. Alexander. 1995. Effect of feeding on the structure of the digestive gland of the tropical sepioid *Idiosepius pygmaeus*. *J. Mar. Biol. Assoc. UK* **75**: 885–897.
- Shepard, S. A., and I. M. Thomas. 1989. *Marine Invertebrates of Southern Australia, Part II*. SA Government Printing Division, Adelaide.
- Storey, K. B., and J. M. Storey. 1983. Carbohydrate metabolism in cephalopod molluscs. Pp. 92–137 in *The Mollusca I. Metabolic Biochemistry and Molecular Biomechanics*, P. W. Hochachka, ed. Academic Press, London.
- Voogt, P. A. 1983. Lipids: their distribution and metabolism. Pp. 329–370 in *The Mollusca I. Metabolic Biochemistry and Molecular Biomechanics*, P. W. Hochachka, ed. Academic Press, London.
- Wells, M. J., and A. Clarke. 1996. Energetics: the costs of living and reproducing for an individual cephalopod. *Philos. Trans. R. Soc. Lond.* **351**: 1083–1104.
- Westermann, B., and R. Schipp. 1998. Cytological and enzyme-histochemical investigations on the digestive organs of *Nautilus pompilius* (Cephalopoda, Tetrabranchiata). *Cell Tissue Res.* **293**: 327–336.

# Functional and Biochemical Properties of the Hemoglobins of the Burrowing Brittle Star *Hemipholis elongata* Say (Echinodermata, Ophiuroidea)

ANA BEARDSLEY CHRISTENSEN<sup>1,\*</sup>, JAMES M. COLACINO<sup>2</sup>, AND CELIA BONAVENTURA<sup>3</sup>

<sup>1</sup>Biology Department, Lamar University, PO Box 10037, Beaumont, Texas 77710; <sup>2</sup>Department of Biology, Clemson University, 132 Long Hall, Clemson, South Carolina 29634; and <sup>3</sup>Marine Biomedical Laboratory, Duke Marine Laboratory, Duke University, 135 Duke Marine Lab Road, Beaufort, North Carolina 28516

**Abstract:** The burrowing brittle star *Hemipholis elongata* (Say) possesses hemoglobin-containing coelomocytes (RBCs) in its water vascular system. The RBCs, which circulate between the arms and body, are thought to play a role in oxygen transport. The hemoglobin of adult animals has a moderate affinity for oxygen ( $P_{50} = 11.4$  mm Hg at pH 8, 20 °C, measured *in cellulose*) and exhibits cooperativity (Hill coefficient > 1.7). The hemoglobin of juveniles has a higher affinity ( $P_{50} = 2.3$  mmHg at pH 8.0, 20 °C) and also exhibits cooperativity. The oxygen-binding properties of the hemoglobin are relatively insensitive to pH, temperature, and hydrogen sulfide. Adult hemoglobin is a heterogeneous mixture composed of three major fractions. The combined results of electrospray mass spectrometry and oxygen-binding experiments performed on purified fractions indicate that the native hemoglobin is in the form of homopolymers. A partial amino acid sequence (about 40 amino acids) of adult hemoglobin reveals little homology with holothurian hemoglobins.

## Introduction

The hemoglobin of the burrowing brittle star *Hemipholis elongata* Say (Echinodermata, Ophiuroidea) is contained in anucleate coelomocytes (red blood cells, RBCs) present in the water vascular system (WVS) (Hajduk and Cosgrove,

1975; Hajduk, 1992; unpubl. data). The presence of RBCs in the WVS imparts a bright red color to the tube feet, which are external projections of the WVS, and readily distinguishes *H. elongata* from other burrowing ophiuroids (family Amphiruridae) occurring in the same locations. RBCs and the fluid of the WVS are circulated throughout the body by a series of synchronous contractions of the tube feet (Beardsley and Colacino, 1998). *H. elongata* does not ventilate its burrow, and it has been hypothesized that hemoglobin in the WVS transports oxygen from arms extended into the water column to buried body parts (Beardsley and Colacino, 1998).

*H. elongata* is often found in the lower intertidal zone in protected, low-energy areas of the southeast coast of the United States (Hendler *et al.*, 1995), and the sediments it inhabits are often soft, poorly oxygenated and may contain hydrogen sulfide (Windom and Kendall, 1979; Camargo, 1982; unpubl. data). The distribution of *H. elongata* is sporadic, but densities in a given area may be as high as 2000/m<sup>2</sup> (Valentine, 1991a). The juveniles of *H. elongata* often settle out onto the arms of the adults (adult disc diameter 5 to 12 mm) (Mortensen, 1920; Valentine, 1991a, b), crawl down the arms of the adult, and grow in the burrow until they reach a size at which they can establish their own burrows. Recently settled juveniles (disc diameter  $\geq 0.48$  mm) also possess RBCs. Although juveniles smaller than 0.43 mm apparently do not have RBCs (unpubl. data), the stage at which they start producing RBCs is unknown.

Only three of the approximately 2000 species of brittle stars possess hemoglobin: *Ophiactis virens* (Foettinger,

Received 4 September 2002; accepted 27 May 2003.

\* To whom correspondence should be addressed. E-mail: christenab@hal.lamar.edu

List of abbreviations: RBCs, red blood cells; WVS, water vascular system.

1880; Cuenot, 1891), *Hemipholis elongata* (Hajduk and Cosgrove, 1975; Heatwole, 1981; Beardsley *et al.*, 1993), and *Ophiactis simplex* (Christensen, 1998). Of these three, only *H. elongata* burrows; the other species inhabit the fouling communities of rock jetties and pilings. As for the functional and biochemical properties of ophiuroid hemoglobins, very little has been reported in the literature (Hajduk and Cosgrove, 1975; Beardsley *et al.*, 1993; Christensen, 1998; Weber and Vinogradov, 2001). Hajduk and Cosgrove (1975) reported that the hemoglobin of *H. elongata* has a high affinity for oxygen ( $P_{90} = 9$  mmHg) and is composed of five components separable by acrylamide gel electrophoresis. They also reported two components with molecular weights of 19,000 and 23,000 Da separable by SDS gel electrophoresis. The hemoglobins of the holothurians, the other group of extant echinoderms possessing the iron-containing pigment, have been more thoroughly investigated (Terwilliger and Terwilliger, 1988 [review]; Suzuki, 1989; Mauri *et al.*, 1991; McDonald *et al.*, 1992; Baker and Terwilliger, 1993; Kitto *et al.*, 1998).

The goal of the present study was to characterize the functional, biochemical, and structural properties of the hemoglobins of *Hemipholis elongata* in more detail. Comparisons were made with the findings of Hajduk and Cosgrove (1975), and the functional and structural properties observed in this study were compared to those of the holothurian hemoglobins.

## Materials and Methods

### *Collection and care of animals*

Animals were collected with a shovel and sieve during low tide from Johnson Creek, Hunting Island, South Carolina. Animals were transported to the laboratory and kept at room temperature (24 °C) in an aquarium containing sediments from the collection site and aerated natural seawater. All experiments using whole animals or RBCs were conducted within 6 weeks of collection. Unless otherwise noted, all experiments used hemoglobin or RBCs from adult animals.

### *Preparation of hemolysates and determination of total hemoglobin per animal*

RBCs were extracted by cutting the animal into small fragments in a small quantity of buffered seawater (50 mM TRIS, pH 8.0 at 20 °C) and then rinsing the fragments until no red color was visible. The body fragments were removed and the cell/buffer mixture was placed on ice. The cells were washed three times in fresh buffer. After a final wash, the supernatant was removed and the cell pellet frozen and thawed to lyse the cells. The thawed pellet was resuspended in about 1 ml of 50 mM TRIS, pH 8 at 20 °C in distilled water and centrifuged at  $14,000 \times g$  for 5 min to remove

cell remnants and debris. The hemolysate was diluted with appropriate buffer to an absorbance of 0.4 to 0.5 OD units at 540 nm to minimize photometric error (van Assendelft, 1970).

For determination of total hemoglobin, the absorption spectrum of the solution was recorded in a Beckman DU-65 spectrophotometer. The hemoglobin concentration, as heme, was calculated using the Beer-Lambert law and the extinction coefficient for human hemoglobin at 542 nm (van Assendelft, 1970). This concentration was multiplied by the total sample volume to give total hemoglobin (as heme) in millimoles, and then divided by animal wet weight to obtain total hemoglobin per gram of wet weight.

Hemolysates used in the oxygen-binding equilibria and the sulfide sensitivity experiments were prepared as above, but with RBCs taken only from excised arms with the aim of avoiding potential interfering effects due to enzymes released from the gut and gonads. Such material may have increased the formation of methemoglobin in the whole animal hemolysates (see Discussion for methemoglobin effects).

### *Intracellular heme concentration*

RBCs collected from an animal as described above were resuspended in isotonic filtered seawater buffered to pH 8.0 at 20 °C with 50 mM TRIS. A few drops of a suspension of polystyrene microbeads (Polysciences, Inc.) of  $5.85 \mu\text{m} \pm 0.13 \mu\text{m}$  diameter were added to the cell suspension. A small drop of this mixture was placed on a glass microscope slide, and a glass coverslip was placed on top of the drop. Excess water was wicked away with a tissue until the coverslip was resting on the microbeads, and the cells were flattened between the coverslip and the slide. This technique serves to set the pathlength for the subsequent absorbance measurements (Colacino and Kraus, 1984). The slide was then placed on the stage of the microspectrophotometer (Mangum *et al.*, 1989). The light transmission spectrum through an area of the slide containing only buffer was collected as a reference. Cells were picked at random on the slide, and the transmission spectrum was recorded through each. The absorbance at 540 nm, 560 nm, and 577 nm was computed from light transmission data. The intracellular hemoglobin concentration was calculated as heme concentration using the Beer-Lambert Law and the extinction coefficients for human hemoglobin at the chosen wavelengths (van Assendelft, 1970). Concentrations calculated at the three wavelengths were averaged for each cell. A total of 48 cells were measured (12 cells on each of four slides prepared from the same cell suspension).

### *Separation of hemoglobins*

The presence of multiple hemoglobins was determined using a Pharmacia fast protein liquid chromatography

(FPLC) system. Crude hemolysates were collected as previously described and resuspended in 50 mM TRIS, pH 8.0, at 20 °C. Hemolysates from 7–10 individuals were pooled due to the small quantities of hemoglobin collected from each animal. The pooled samples were equilibrated with 50 mM TRIS, pH 8.0, by dialysis. The hemolysates were then loaded onto a DEAE Q Sepharose Hi-Load 2610 column, 60-ml column volume. The resin had been equilibrated with four volumes of 50 mM, pH 8.0, TRIS buffer. A linear salt gradient (50 mM TRIS to 0.075 M NaCl + 50 mM TRIS) was used for elution. The total gradient volume was 300 ml. Fractions were collected at a rate of 6 min per fraction, and absorbance was read at 280 nm (for protein) and 415 nm (hemoglobin peak).

The fractions showing peak absorbance were electrophoresed on a Pharmacia Phast system using a native gel. Samples were run on a 10% acrylamide gel with pH 8.3 electrophoresis buffer and stained with Coomassie blue. A low-porosity stacking gel (upper fraction) was used to sharpen the banding pattern. Samples contained 5–25 µg of protein. Crude hemolysate and human hemoglobin A were electrophoresed as references.

#### *Determination of molecular weight*

The molecular weights of the purified hemoglobin fractions were determined by electrospray ionization mass spectrometry. Samples were prepared by the method described by Stevens *et al.* (1994). Measurements were made on a Fissons-VG BIO-Q triple quadrupole mass spectrometer equipped with a pneumatically assisted electrospray ionization source operating at atmospheric pressure (supplied by VG Biotech, Altrincham, UK).

#### *Hemoglobin spectra and oxygen-binding equilibria in cellulose*

A small portion ( $\leq 5$  mm) of the distal end of an arm was excised from an unanesthetized animal and rinsed in buffer to remove any adhering mud. The arm tip was placed in a large depression slide containing a small amount of 0.45-µm filtered isotonic seawater buffered with 50 mM TRIS of the desired experimental pH (7, 8, or 9). The tube feet were manually stimulated to contract, forcing the RBCs out of the cut end of the radial canal. About 50 µl of the buffer/RBC mixture was transferred to a specially designed gas slide (Colacino and Kraus, 1984). The gas slide was placed on the microscope stage of a diode array microspectrophotometer (Mangum *et al.*, 1989). The slide was maintained at a constant temperature ( $20^\circ \pm 0.5$  °C) with water pumped from a refrigerated water bath (Forma Scientific). The internal gas tension of the slide was controlled by a gas-mixing flowmeter (Cameron Instrument Co.). The gases were humidified and brought to experimental temperature before flowing through the sample chamber of the gas slide

at 100 ml/min. A total of 60 cells taken from 47 animals were used in these experiments.

To examine the equilibrium oxygen-binding characteristics of the hemoglobin *in cellulose*, cells were exposed to gases at nine oxygen tensions, ranging from 0 to  $> 150$  mmHg (room air). Fractional saturation values were computed from transmitted light intensities (540 nm, 560 nm, and 580 nm) using a two-wavelength modification of a standard analysis (Rossi-Fanelli and Antonini, 1958). The effect of pH on oxygen affinity was determined from oxygen equilibrium experiments conducted at pH 7.0, 8.0, and 9.0. Temperature effects on oxygen binding were determined from oxygen affinity experiments conducted at 10 °C, pH 8.0, and 20 °C, pH 8.0. The heat of oxygenation ( $\Delta H$ ) was calculated from the van't Hoff equation.

#### *Oxygen-binding equilibria in vitro*

For measurements on crude hemolysates, about 50 µl of the hemolysate was placed in the working chamber of the gas slide along with a 0.5-cm<sup>2</sup> piece of monofilament nylon mesh (105-µm mesh opening) (Small Parts, Inc.). A freshly prepared hemolysate solution was used in each experiment because repeated freezing and thawing increased methemoglobin formation (see Discussion for methemoglobin effects). The nylon mesh served to ensure a stable pathlength for light transmission measurements. Oxygen-binding equilibria were measured as previously described for *in cellulose* measurements at 20 °C. Measurements on purified FPLC fractions were made using standard tonometric techniques at pH 7 at 20 °C.

#### *Oxygen-binding equilibria of juvenile hemoglobin*

Oxygen-binding equilibria for hemoglobins of juvenile *H. elongata* were measured on both isolated cells and intact animals. For the isolated-cell measurements, cells were collected from individuals of disc diameter  $\leq 1$  mm ( $n = 5$ ) by excising a small portion of an arm in a small quantity of buffer, 50 mM TRIS, pH 8.0, at 20 °C. The cells were loaded onto the gas slide, and the oxygen binding was measured by the method previously described for the adult cells.

For the whole-animal measurements, an intact juvenile was loaded onto the gas slide. The juvenile was anesthetized by placing it in a small quantity of buffer ( $< 200$  µl) containing a few drops of 7% MgCl<sub>2</sub>. The individual was then placed centrally in the gas slide chamber in a small drop of buffer/MgCl<sub>2</sub>. Hemoglobin spectra were taken through a tube foot with RBCs in it. Oxygen-binding experiments were conducted as before. Four individuals were measured in this manner.

### *Hemoglobin sensitivity to sulfide*

The effects of hydrogen sulfide on oxygen-binding equilibria were examined using hemolysates prepared as described earlier (hemoglobin 50 mM TRIS in distilled water, pH 8.0 at 20 °C, adjusted to give an absorbance reading of 0.4–0.5 at 540 nm in an 0.5-cm cuvette). Four milliliters of this solution were placed into each of two glass tonometers equipped with 0.5-cm pathlength cuvettes. The initial oxygenated spectra were recorded from 650 nm to 400 nm on a Beckman DU 65 spectrophotometer. The samples were deoxygenated with 99.999% N<sub>2</sub>, and a deoxygenated spectrum was taken. Then 100 µl of 10 mM Na<sub>2</sub>S solution was injected into one tonometer with a syringe; 100 µl of deoxygenated buffer was added to the control tonometer. The spectrum was again recorded. Oxygen was gradually introduced in a stepwise fashion by the injection of room air samples after an equal volume had been removed from the tonometers, and the spectra were measured after a 10-min equilibration. This experiment was repeated three times with freshly prepared hemolysates pooled from three to five individuals.

### *Stopped-flow measurements of ligand kinetics*

Kinetics of the hemoglobin-oxygen reaction were estimated using the stopped-flow technique on the crude cell hemolysates suspended in 50 mM HEPES, pH 7, at 20 °C; the crude hemolysates represent pooled samples. Measurements were made for the O<sub>2</sub> "off" reaction (dissociation) and the CO "on" reaction (association). The CO "on" reaction was also examined using flash photolysis. The presence of modulator effects was determined by performing the above reactions in the presence of ATP.

Experiments were performed on a Gibson-Durrum stopped-flow apparatus that consists of a Durrum model 13000 light source and monochromator and Durrum model 110 stopped-flow instrument with pneumatic drive. The dissociation constant,  $k_{\text{off}}$ , was determined by reacting oxy-hemoglobin, from crude hemolysates, with sodium dithionite (Na<sub>2</sub>S<sub>2</sub>O<sub>4</sub>) (about 0.5%). The time course of the reaction was monitored by measuring transmitted light intensities.

Light intensity data were collected by a DASAR data acquisition, storage, and retrieval system with a DW-2 interface to a Tektronix 4052 computer. Initial data analyses were carried out with the ASYST program (Macmillan Software Co.) prior to curve-fitting analysis by a nonlinear least-squares program (Johnson *et al.*, 1981).

The carbon monoxide (CO) association reaction was monitored by the stopped-flow technique and flash photolysis. Flash photolysis was performed with dual fast extinguishing (approximately 30 µs) flash tubes and a Xenon Corp. model B micropulser. The subsequent association of CO and the hemoglobin was then monitored as before.

### *Amino acid sequence of hemoglobin fractions*

Partial amino acid sequences of each purified hemoglobin fraction were determined by the automated Edman method using a Porton Instruments PI 2090 integrated micro-sequencing system. The amino acids were identified by visual inspection of hardcopy plots, using retention times from a standard of PTH amino acids.

Proteins were not digested with proteases prior to sequencing. Each analysis used 150–200 pmol of protein. Samples of fractions 1 and 2 were processed for 40 cycles, at which time it became difficult to distinguish the amino acid peaks from the background noise. Fraction 3 was run for 21 cycles.

The partial sequence for fraction 1 was compared to other protein sequences using the MacVector sequence analysis software (Oxford Molecular Group PLC) and the *Entrez* database (National Center for Biotechnology Information).

## Results

### *Total hemoglobin per individual*

The average wet weight of the adult animals used for this measurement was 0.39 g ± 0.16 g (mean ± SD,  $n = 9$ ). These individuals contained  $8.5 \times 10^{-5}$  mmol ±  $4.4 \times 10^{-5}$  mmol of hemoglobin, measured as heme. Using a hemoglobin subunit molecular mass of 16,000 Da, this figure translates into 0.35% of the total body mass accounted for by the hemoglobin.

### *Intracellular hemoglobin concentration and estimation of hematocrit*

The RBC hemoglobin concentration, as heme, was  $19.5 \pm 5.0$  mM (mean ± SD,  $n = 48$  cells). Using a mean cell diameter of 9 µm (Hajduk and Cosgrove, 1975; Heatwole, 1981; unpubl. data) and an intracellular hemoglobin concentration of 19.5 mM, the volume of a single cell is  $3.8 \times 10^{-7}$  mm<sup>3</sup> and contains  $7.4 \times 10^{-12}$  mmol hemoglobin. If an animal has a total of  $8.5 \times 10^{-5}$  mmol of hemoglobin, it has approximately  $1 \times 10^7$  cells. The total cell volume is equal to 4.3 mm<sup>3</sup>; and for an animal with a total WVS volume of 18.1 mm<sup>3</sup> (Beardsley and Colacino, 1994), the fraction of the WVS taken up by cells is 0.24.

### *Separation of the hemoglobins*

The hemoglobin is a heterogeneous mixture. Separation of oxygenated crude cell hemolysates by DEAE Q Sepharose FPLC resulted in three fractions that absorb at 280 and 415 nm (Fig. 1). Native gel electrophoresis of the crude hemolysates yielded five bands, two of the major bands corresponding to FPLC fractions 1 and 2, a third major band of uncertain identity, and two minor bands (Fig. 2). Lack of

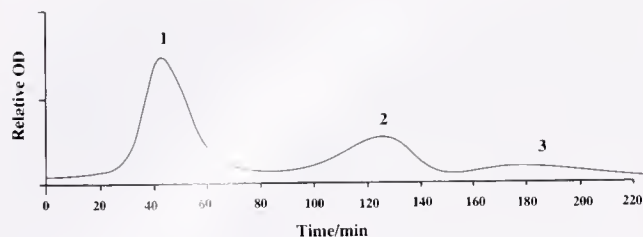


**Figure 1.** Chromatogram of crude hemolysates from *Hemipholis elongata*, separated by FPLC ion exchange chromatography. Separation was achieved using a DEAE Q Sepharose Hi-Load 2610 column, 60-ml column volume. A linear salt gradient was established from 50 mM Tris to 0.75 M NaCl + 50 mM Tris; gradient volume was 300 ml. The profile represents absorbance at 280 nm and 415 nm.

banding in lane 5 (FPLC fraction 3) is attributed to low concentration applied to the gel.

As the sample placed on the column was a pooled sample, it is unknown if all of the FPLC fractions are found in a single individual or in separate individuals. However, the separation was performed on two occasions using animals from different collections, and both experiments yielded the same results.

#### Molecular weight of hemoglobin subunits

The technique used to determine molecular weight, electrospray mass spectrometry, breaks polymeric hemoglobins into monomeric subunits and causes the heme to dissociate from the protein. The signals for FPLC fractions 1 and 2 indicated that each was composed of a single protein and a heme peak. The molecular weights of the subunits were as follows: fraction 1—16,080, fraction 2—16,119, and fraction 3—16,143. The hemes all had a molecular weight of 616. The differences in the protein weight indicate differences in amino acid composition for the three subunits.

The mass spectrum generated by the third FPLC fraction indicated the possibility of more than one subunit. However, the low concentration of this sample resulted in high-noise mass spectrometry data, making this conclusion uncertain.

#### Oxygen-binding equilibria in cellulo and in vitro

The hemoglobin of *Hemipholis elongata* has a moderate affinity for oxygen ( $P_{50} = 11.4$  mmHg at pH 8.0, 20 °C) (Table 1). The  $P_{50}$  at pH 8.0 is similar to those reported for holothurian hemoglobins (Table 1). The Hill numbers ( $n$ ) were greater than 1 for both *in cellulo* and *in vitro* measurements, indicating cooperativity and functional hemoglobin composed of at least two subunits (a dimer) (Table 1). Then  $n$  values are greater for the *in cellulo* measurements ( $n = 2.81$ ) than for the crude hemolysates ( $n = 1.91$ ). The difference in Hill coefficients may be due to concentration differences (19.5 mM *in cellulo* vs. 0.1 mM *in vitro*) (see Discussion for concentration effects).

The  $P_{50}$  values measured on the FPLC fractions are lower than those measured on the crude hemolysates and *in cellulo*.  $P_{50}$  at pH 7.0 at 20 °C for fraction 1 is 6.1 mmHg and that for fraction 2 is 2.5 mmHg. These low values may be due to the formation of methemoglobin (see Discussion). The Hill numbers for the purified FPLC fractions 1 and 2 are greater (about 1.8) (Table 1).

Values for  $P_{50}$  measured at the three pHs are significantly different from one another (Student's  $t$  test,  $P = 0.05$ ) (Table 1). Oxygen affinity increases slightly as pH decreases. This is opposite to the usual pH effect. The slope of the Bohr plot is 0.072. The temperature dependence of the oxygen affinity is small ( $P_{50} = 8.9$  mmHg at 10 °C vs. 11.4 mmHg at 20 °C). The heat of oxygenation ( $\Delta H$ ) is  $-4.1$  kcal/mol.

#### Oxygen-binding equilibria of juvenile hemoglobin

The hemoglobin of juveniles (disc diameter 0.48 to 0.8 mm) has a higher affinity ( $P_{50} = 2.3$  mmHg *in cellulo* and 4.0 mmHg in tube feet of intact animals, pH 8.0 at 20 °C) for oxygen than the adult hemoglobin ( $P_{50} = 11.4$  mmHg, disc diameter 5 to 12 mm) (see Table 1). This was true for both isolated RBCs and intact animal measurements. The greater apparent  $P_{50}$  for measurements using intact animals may be explained by oxygen consumption of the animal. The  $P_{O_2}$  within the tissues is lower than the external  $P_{O_2}$  due to oxygen consumption by the tissues. The difference in  $P_{O_2}$  can lead to an overestimation of the  $P_{50}$ . Even with the



**Figure 2.** Native gel electrophoresis of crude hemolysates and purified FPLC fractions of *Hemipholis elongata* hemoglobin. Samples were run on a 10% acrylamide gel with pH 8.3 electrophoresis buffer and stained with Coomassie blue. A low-porosity stacking gel (upper fraction) was used to sharpen the banding pattern. Lack of banding in lane 5 is attributed to low concentration applied to the gel, since mass spectrometry results showed fraction 3 to contain hemoglobin. Lane 1: Human hemoglobin A; lane 2: Crude hemolysate; lane 3: FPLC fraction 1; lane 4: FPLC fraction 2; lane 5: FPLC fraction 3.

Table 1

Oxygen  $P_{50}$  values and Hill numbers of echinoderm hemoglobins (mean  $\pm$  SE)

Species	$P_{50}$ mmHg	Hill number ( <i>n</i> )	# of measurements (# of individuals)*	Study
<b>Ophiuroids</b>				
<i>Hemipholis elongata</i>				
<i>in cellulo</i>				
pH 7.0, 20 °C	9.5 $\pm$ 1.2	2.35 $\pm$ 0.07	15 (11)	Present study
pH 8.0, 10 °C	8.9 $\pm$ 1.1	3.20 $\pm$ 0.10	12 (8)	
pH 8.0, 20 °C	11.4 $\pm$ 1.2	2.81 $\pm$ 0.08	17 (14)	
pH 9.0, 20 °C	13.1 $\pm$ 1.2	2.67 $\pm$ 0.09	16 (14)	
<i>in vitro</i> crude hemolysates				
pH 7.0, 20 °C	8.2 $\pm$ 1.1	1.78 $\pm$ 0.04	6	Present study
pH 8.0, 20 °C	10.5 $\pm$ 1.1	1.91 $\pm$ 0.05	4	
pH 9.0, 20 °C	11.3 $\pm$ 1.2	1.73 $\pm$ 0.06	4	
<i>in vitro</i> purified				
fraction 1, pH 7.0, 20 °C	6.1	1.83	2	Present study
fraction 2, pH 7.0, 20 °C	2.5	1.41	2	
juvenile				
<i>in vitro</i> , pH 8.0, 20 °C	4.0 $\pm$ 1.2	3.28 $\pm$ 0.37	4	Present study
<i>in cellulo</i> , pH 8.0, 20 °C	2.3 $\pm$ 1.5	1.76 $\pm$ 0.51	5 (4)	
<i>Ophiactis simplex in cellulo</i> , pH 8.0, 20 °C	22.3 $\pm$ 1.2	3.04 $\pm$ 0.18	15 (12)	Christensen, 1998
<b>Holothuroids†</b>				
<i>Cucumaria miniata</i>	8.0 $\pm$ 1.5	1.86 $\pm$ 0.07		Terwilliger, 1975
<i>Cucumaria curata</i>	7.1	1.6		Roberts <i>et al.</i> , 1984
<i>Thyonella gemmata</i>	2.6	1.4		Steinmeier & Parkhurst, 1979
<i>Molpadia oolitica</i>	4.0	1.6		Terwilliger & Read, 1972
<i>Molpadia intermedia</i>	2.0	<1.0		Manwell, 1966
<i>Caudina arenicola</i>	3.5	1.5		Bonaventura <i>et al.</i> , 1976
<i>Sclerodactyla (Thyone) briareus</i>	8.1	1.08		Colacino, 1973
<i>Paracaudina chilensis</i>	1.5	1.3		Baker & Terwilliger, 1993

\* The numbers in # of measurements reflect the number of cells measured; the number in parentheses reflects the number of individuals represented in the experiment. No animal was used more than twice.

† All holothurian  $P_{50}$  values were measured *in vitro*.

overestimation of the juvenile  $P_{50}$ , the value is significantly less than that of the adult, indicating distinct functional differences.

#### Hemoglobin sensitivity to sulfide

Exposure to sulfide caused no changes in the absorption spectrum, and there was no peak at 620 nm; this peak is characteristic of human sulphemoglobin in the visible region of the spectrum (van Assendelft, 1970; Carrico *et al.*, 1978). There was also no change in the oxygen affinity of the hemolysates in the presence of sulfide (Fig. 3).

#### Kinetics of ligand binding

Both of the ligand reactions with the crude hemolysates were biphasic, with the two components in each reaction accounting for about 50% of the reacting species ( $134.6 \pm 2.2$  (SD)  $s^{-1}$  and  $22.3 \pm 0.3 s^{-1}$  for the  $O_2$  "off" reaction and  $5.2 \times 10^4 M^{-1}s^{-1}$  and  $2.8 \times 10^4 M^{-1}s^{-1}$  for the CO "on" reaction). These data are consistent with the heteroge-

neity of the crude hemolysate. Given that FPLC reveals three distinct hemoglobins with two (fractions 1 and 2) accounting for the majority of the protein, one might expect to see two distinct reaction components in ligand-binding experiments. A third kinetic component representing the third FPLC fraction was not seen, either due to the small amount of it present in the crude hemolysates or to a lack of difference in rate constants.

There was no effect of ATP on the CO "on" reaction. However, the presence of ATP caused a small, but statistically significant ( $P = 0.05$ ) increase in the dissociation rate constant for both phases of the biphasic oxygen "off" reaction of *H. elongata* hemoglobin ( $144.3 \pm 2.4 s^{-1}$  and  $24.2 \pm 0.2 s^{-1}$ ).

#### Amino acid sequence of the protein

Figure 4 shows the partial amino acid sequences for the three FPLC fractions of the hemoglobin. The sequences for

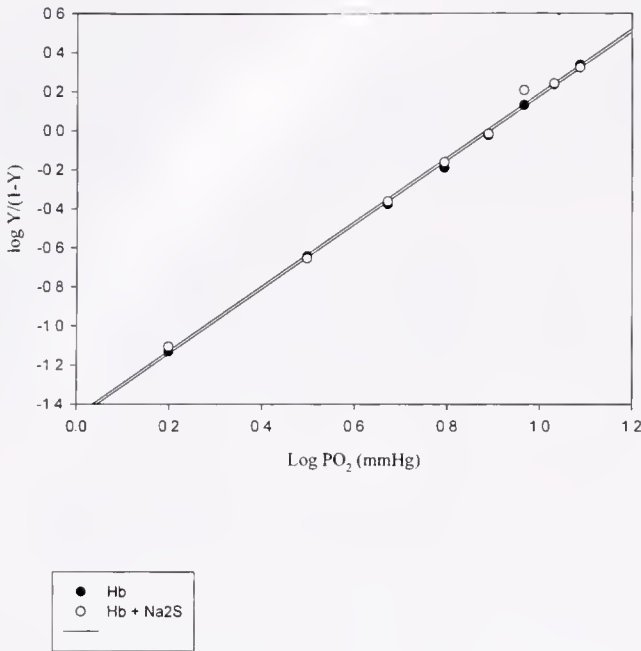


**Figure 3.** Hill plots for the oxygen-binding equilibria of *Hemipholis elongata* hemoglobin in the absence (●) and presence of Na<sub>2</sub>S (○). Hemoglobin is crude hemolysate suspended in 50 mM Tris, pH 8.0, at 20 °C.

fractions 1 and 2 differ by eight amino acids. The partial sequence for fraction 3 was identical to that of fraction 2.

Neither hemoglobin fraction appears to be blocked at the N-terminus of the globin, unlike the hemoglobins of many holothurians (Terwilliger and Terwilliger, 1988). Proteins blocked at the N-terminus are resistant to the Edman reaction used in protein sequencing (Kitto *et al.*, 1976). No modification (*e.g.*, digestion with proteases) of the *H. elongata* protein was necessary to obtain amino acid sequences.

## Discussion

### Intracellular hemoglobin concentrations and hematocrit

The intracellular heme concentration of *Hemipholis elongata* (19.5 mM) is comparable to the values reported for

holothurian RBCs (12.5 mM for *Sclerodactyla (Thyone) briareus* [Colacino, 1973] and 15.8 mM for *Cucumaria miniata* [from data in Manwell, 1959, and Terwilliger and Read, 1972]). These values are similar to those of human RBCs (20 mM heme) (calculated from Guyton, 1991) and phoronid (*Phoronis architecta*) RBCs (14 mM heme) (Vandergon and Colacino, 1989). If the hemoglobin of *H. elongata* exists as dimers, this would mean that the intracellular hemoglobin concentration is 9.8 mM.

The computed hematocrit value of *H. elongata* (0.24) is comparable to the tube foot hematocrits of the holothurian *S. briareus* (0.24, by direct measurement) (Colacino, 1973). These values are greater than the reported hematocrits of the perivisceral fluids of the holothurians *Cucumaria pseudocurata* (0.032) (Roberts *et al.*, 1984) and *Paracaudina chilensis* (0.015) (Baker and Terwilliger, 1993), but less than those for humans (0.4) (Guyton, 1991) and other mammals ( $\geq 0.4$ ) (Schmidt-Nielsen, 1990).

### Structural properties of the hemoglobin

The hemoglobins of *H. elongata* are a heterogeneous mixture of three components, as evidenced by FPLC. Because the samples were pooled from several individuals, it is not known whether hemoglobin heterogeneity is a normal characteristic of *H. elongata* blood or an artifact of sample mixing. However, the identical results (*e.g.*, same ratio of fractions) obtained on two separate occasions suggest that all three fractions are present within an individual. Hajduk and Cosgrove (1975) reported only two components separable by gel filtration, one apparently composed of monomers and the other of dimers. The difference in number of fractions may be attributable to difference in separation techniques. Gel filtration separates on the basis of size and shape; DEAE Q Sepharose FPLC (ion exchange) separates molecules on the basis of charge.

Both the present study and Hajduk and Cosgrove (1975) obtained five bands by acrylamide gel electrophoresis. Two of the major bands reported here correspond to FPLC fractions 1 and 2. Because this sample was a crude hemolysate, the two minor bands may have been due to proteins other

**F1:** val ile ser ala gly glu lys thr leu ile arg asp ser trp ala pro val tyr ala gly asp  
**F2:** val ile ser ala asp glu lys asn leu ile arg ser ? trp phe thr val tyr ser gly asp  
**F3:** val ile ser ala asp glu lys asn leu ile arg ser ? trp phe thr val tyr ser

### Fractions, continued

**F1:** arg phe gln ile gly val asn val phe thr asn phe ? ? ala tyr pro ala  
**F2:** arg phe gln val gly val asp val phe thr asn phe ? ? ala tyr

**Figure 4.** Partial amino acid sequences for the three FPLC fractions of *Hemipholis elongata* hemoglobin. Amino acids in hold type represent differences in primary sequence; ? represents amino acids that could not be definitively identified. F1 = fraction 1, F2 = fraction 2, F3 = fraction 3.

than hemoglobin, found within or associated with the RBCs. Due to the presence of heme at high relative concentration, two of the major bands from the crude hemolysate were visible on the gel prior to staining with Coomassie blue. The two minor bands were not visible. If the minor bands do represent hemoglobins, the low concentration, as evidenced by the faintness of the bands on the gel, could explain why these fractions were not isolated by FPLC.

The molecular masses of the various fractions (approximately 16,000 Da) are comparable to human  $\beta$  chain (15,860 Da) (Dickerson and Geis, 1980) and holothurian hemoglobin monomers (17,000–18,000 Da) (Terwilliger and Terwilliger, 1988). These values are smaller than those reported by Hajduk and Cosgrove (1975) (19,000 and 23,000 Da). Differences between the previously reported weights and those of the present study may be attributed to differences in techniques. Mangum (1992) remarked that many of the early studies on holothurian hemoglobin reported similarly large molecular weights that were later found to be smaller ( $\sim$ 17,000 Da). She attributed these differences to refinement of molecular techniques.

The cooperative binding of oxygen, both *in cellulo* and *in vitro* (Hill number  $\geq$  1), indicates that the functional hemoglobin exists as a polymer. Many of the holothurian hemoglobins are known to exist as dimers (Terwilliger and Terwilliger, 1988) and possibly tetramers (Baker and Terwilliger, 1993). The purified fractions, 1 and 2, of *H. elongata* hemoglobin have only one globin chain type but exhibit cooperativity in oxygen binding, suggesting that both are able to form cooperative homodimers. The Hill numbers typically observed at low concentrations, somewhat less than 2, are consistent with the formation of cooperative homodimers. Larger assemblies may form under some circumstances, as evidenced by Hill numbers greater than 3 that were observed under some conditions (*e.g.*, *in cellulo*).

The normally existing homopolymers of several invertebrate hemoglobins exhibit cooperativity (*Scapharca inaequivalvis* [Chiancone *et al.*, 1981; Royer *et al.*, 1985]; holothurians [Terwilliger and Read, 1972; Bonaventura *et al.*, 1976]), although homodimers and homotetramers of human (and other vertebrate) hemoglobins do not. In fact, the mechanism for cooperativity in invertebrates is thought to be different from that utilized by vertebrates (Riggs, 1998). Cooperativity is thought to be due to interactions between the E and F helices of the hemoglobin subunits, first described in the arcid clam *Scapharca inaequivalvis* (Royer *et al.*, 1985, 1990). This same association has been described for the innkeeper worm, *Urechis caupo* (Kolatkhar *et al.*, 1994) and a sea cucumber, *Caudina arenicola* (Mitchell *et al.*, 1995). However, Kitto *et al.* (1998) believe that the cooperativity mechanism in *C. arenicola* differs from that in *S. inaequivalvis* as the residues involved at the crucial contact points are different for the two species. Further

structural studies on *H. elongata* hemoglobin are needed to investigate the nature of the interactions of its subunits.

Comparison of the amino acid sequence of fraction 1 from *H. elongata* with sequences reported for the globins of the holothurians *Caudina arenicola* (Mauri *et al.*, 1991; McDonald *et al.*, 1992) and *Paracaudina chilensis* (Suzuki, 1989) reveals little homology. The lack of homology between the ophiuroid and holothurian globins has contributed to the inability to identify the brittle star globin gene by using holothurian primers (Kitto, pers. comm.). Furthermore, no successful primers for the hemoglobin gene have been generated based on the 39 amino acid sequence of the ophiuroid (Kitto, pers. comm.).

#### Oxygen-binding characteristics of the hemoglobin

The hemoglobin of *H. elongata* has a moderate affinity for oxygen, both *in cellulo* and *in vitro*. It is not certain at this time whether all of the FPLC fractions exist in the same cell, in separate cell populations, or even within the same animal. However, a large number of cells from many individuals were examined microspectrophotometrically and little variation was seen within the measured  $P_{50}$  values observed within each treatment. This suggests that the different hemoglobins represented by the purified FPLC fractions are present within a single cell. The ratio of this mixture is unknown.

The oxygen affinity results of the present study differ greatly from those reported by Hajduk and Cosgrove (1975) ( $P_{90} = 9$  mmHg). On the basis of the Hill numbers from the present study, a hemoglobin with a  $P_{90}$  of 9 mmHg (pH 7.2) should have a  $P_{50}$  of about 3 mmHg. The *in cellulo* and *in vitro* analysis in the present study demonstrated a  $P_{50}$  between 8 and 9 mmHg at pH 7.0, 20 °C. This difference in oxygen affinities may be attributable to the formation of methemoglobin. The oxygen affinity of mammalian hemoglobin increases with increasing percentages of methemoglobin in the sample (Darling and Roughton, 1942)

Several of the holothurian hemoglobins are prone to oxidation and denaturation at pH 7.0 (Terwilliger and Read, 1972; Bonaventura *et al.*, 1976; Steinmeier and Parkhurst, 1979). When the crude hemolysates of *H. elongata* were repeatedly frozen and thawed, the  $P_{50}$  decreased. Tests for the presence of methemoglobin showed an increase in the amount present in the sample. Freshly prepared *H. elongata* hemolysates were typically 5%–7% methemoglobin as determined by the ferrocyanide method (van Assendelft, 1970). In one experiment, the methemoglobin fraction was 13% initially and rose to 45% by the end. The  $P_{50}$  calculated for this run was 3.6 mmHg. This corresponds to the  $P_{50}$  value estimated from the data of Hajduk and Cosgrove (1975).

The formation of methemoglobin may explain the low  $P_{50}$  of the purified fractions. Although it is not unusual for

different hemoglobins within an individual to have different binding affinities, the apparent  $P_{50}$  of the mixture usually lies between those of the separate fractions, not above them. During oxygen-binding experiments on the purified fractions, methemoglobin rose from 10% to 16% of the total in fraction 1 and from 32% to 42% in fraction 2. While the large proportion of methemoglobin, particularly in fraction 2, makes comparisons of  $P_{50}$  difficult, the importance of this experiment is the demonstration of the cooperative binding of homopolymers.

Another explanation for the difference in oxygen affinities may be the presence of intracellular modulators that would have been removed during the purification of the fractions. However, many invertebrate hemoglobins, including the holothurian hemoglobins, are insensitive to organic phosphates (Terwilliger and Terwilliger, 1988; Scholnick and Mangum, 1991; Baker and Terwilliger, 1993). The rate constant for the oxygen "off" reaction of *H. elongata* crude hemolysates exhibited a small, but significant, increase in the presence of ATP.

The differences in apparent cooperativity between the *in cellulo* and *in vitro* measurements may be due to concentration effects. Dilute preparations may be less aggregated than concentrated ones, with the consequence that the Hill coefficient increases due to subunit interactions as the concentration of hemoglobin increases. This may account for the fact that the hemoglobins of capitellid worms were reported to have greater cooperativity *in cellulo* than *in vitro* (Mangum *et al.*, 1992).

Other than those reported here, no data on ligand-binding kinetics are available for the brittle star hemoglobins. The smaller of the two dissociation rate constants for *H. elongata* hemoglobin is similar to those of human ( $\sim 40 \text{ s}^{-1}$ , Antonini and Brunori, 1971) and holothurian hemoglobin (*S. briareus*,  $4.8 \text{ s}^{-1}$  [Colacino, 1973]; *Thyonella gemmata*,  $3.6$  to  $8 \text{ s}^{-1}$  [Steinmeier and Parkhurst, 1979]). The larger of the two dissociation rate constants ( $134.6 \text{ s}^{-1}$ ) is among the largest reported. The CO association rate constant of *H. elongata* is between those of holothurian hemoglobin (*S. briareus*,  $\sim 10^3 \text{ M}^{-1}\text{s}^{-1}$  [Colacino, 1973]; *T. gemmata*,  $10^3$  to  $10^4 \text{ M}^{-1}\text{s}^{-1}$  [Steinmeier and Parkhurst, 1979]) and human hemoglobins ( $30 \times 10^5 \text{ M}^{-1}\text{s}^{-1}$  [Antonini and Brunori, 1971]).

Most hemoglobins exhibit a decrease in oxygen affinity as the pH decreases (Weber, 1980). It is generally accepted that most holothurian hemoglobins are insensitive to pH (Terwilliger and Terwilliger, 1988). A weak pH dependence (normal direction) on the oxygen affinity of hemoglobin has only been reported for two holothurians, *Paracauding chilensis* (Baker and Terwilliger, 1993) and *Molpadia arenicola* (Bonaventura *et al.*, 1976). The hemoglobin of *H. elongata*, however, shows a slight increase in its oxygen affinity, both *in cellulo* and *in vitro*, with a decrease in pH (Table 1). The magnitude of the Bohr shift of *H. elongata* hemoglobin,

however, is very small and may not have any adaptive significance under physiological conditions.

There is not a large temperature dependence, as evidenced by the small change in affinity with a change in temperature. The heat of oxygenation,  $\Delta H = -4.1 \text{ kcal/mol}$ , is smaller than that reported for other hemoglobins,  $-6 \text{ kcal/mol}$  to  $-8 \text{ kcal/mol}$  (Antonini and Brunori, 1971; Colacino, 1973). The possession of a hemoglobin with a small temperature dependence may be adaptive to an intertidal organism, because it would make it relatively insensitive to the large temperature changes that can occur in the intertidal environment (Cochran and Burnett, 1996; unpubl. data).

The high affinity of the hemoglobin of juvenile brittle stars is clearly different from that of the adults. This functional difference could be adaptive in their normal habitat. The planktonic larvae often settle out onto the extended arms of the adults. The juveniles then crawl down the arm into the burrow of the adult, where they move around within the burrow (pers. obs). Small juveniles (disc diameter  $< 1 \text{ mm}$ ) do not extend their arms into the water column as the adults do; therefore, they must obtain oxygen from the burrow environment or from the adult. The measured  $P_{O_2}$  of the burrow water is very low (undetectable with FOXY system [Ocean Optics, Inc.]; unpubl. data), but some oxygen must escape into the environment from the adult, as evidenced by the fact that the sediments lining the burrow are oxidized. The possession of high-affinity hemoglobin by the juveniles would aid them in the acquisition of oxygen from this low-oxygen environment. The switch from high-affinity hemoglobin in the fetus/juvenile to lower affinity hemoglobin in the adult has been documented in many animals (Barcroft, 1935; Riggs, 1951). The time in development in *H. elongata* when the switch from high-affinity to low-affinity hemoglobin occurs is not known. Also unknown is whether the hemoglobin present in the juvenile RBCs is one of the hemoglobins found in the adults or an entirely different one. Due to the small size of the juveniles and the small numbers collected, insufficient hemoglobin has been isolated to make comparisons with adult hemoglobin by gel electrophoresis.

The hemoglobins of *H. elongata* have a higher affinity for oxygen than those of another ophiuroid species, *Ophiactis simplex* (Christensen, 1998) (see Table 1). The differences in the oxygen-binding properties could be related to differences in their lifestyles. *H. elongata* burrows in anoxic mud, does not ventilate its burrow, and lacks genital bursae, structures known to serve as sites of gas exchange in ophiuroids. *O. simplex* is epibenthic and commonly occurs in fouling communities associated with rock jetties and wharf pilings. The oxygen levels in these environments may not be as limiting as in the mud. The function of hemoglobin in *O. simplex* is not known, but is under investigation.

*Effects of sulfide on oxygen binding*

Vertebrate and many invertebrate hemoglobins bind with sulfide to form sulphemoglobin. In human hemoglobin A, the binding of sulfide takes place at the heme, but not to the iron, and is effectively irreversible (Berzofsky *et al.*, 1971; Carrico *et al.*, 1978). This also decreases oxygen affinity so much as to render the hemoglobin functionless under normal conditions (Carrico *et al.*, 1978). Many invertebrate hemoglobins show reversible binding with sulfide (Arp and Childress, 1983; Childress *et al.*, 1984; Doeller *et al.*, 1988; Somero *et al.*, 1989). In many cases the binding of sulfide is vital to the organism because it harbors endosymbionts that require sulfide as an energy source (Felbeck, 1983; Hand and Somero, 1983; Powell and Somero, 1986). No such endosymbionts have been observed in *H. elongata* (unpubl. data.)

No abnormal spectral changes were observed during the oxygen equilibrium experiments on *H. elongata* hemoglobin exposed to sulfide. This indicates that either the hemoglobin is insensitive to sulfide or there are detoxifying enzymes present. However, due to the nature of the hemolysate solution, any enzymes present would be greatly diluted, thus decreasing their efficiency. The lack of abnormal spectra points toward a hemoglobin that is insensitive to sulfide. The hemoglobins of the phoronid *Phoronis architecta* (Vandergon and Colacino, 1991) and the polychaete *Abarenicola affinis* (Wells and Pankhurst, 1980) also appear to be insensitive to sulfide. If sulfide does bind to the hemoglobin of *H. elongata*, it does so in a way that does not alter oxygen affinity or the visible absorption spectra. For organisms that live in sulfide-rich environments but do not rely on sulfide-requiring symbionts, it would be highly adaptive to possess hemoglobin whose function is not disrupted by exposure to sulfide.

**Summary**

It appears that the hemoglobins of *Hemipholis elongata* are well suited to the habitat and lifestyle of the animal. *H. elongata* does not ventilate its burrow, and its aerobic metabolism must be supported by circulation of the WVS fluid and RBCs between arms exposed to the water column and buried body parts. The moderate  $P_{50}$  (11.4 mmHg, pH 8.0, at 20 °C) and cooperativity (Hill number  $\geq 1.7$ ) of the hemoglobin would allow it to extract oxygen from the overlying water column and deliver it to buried body parts over a wide range of external and internal  $P_{O_2}$  values. The relative insensitivity of the hemoglobins to changes in temperature and pH preserve hemoglobin function when conditions change, as they frequently do in an intertidal environment. The insensitivity to hydrogen sulfide ensures that the hemoglobins continue to function below the sediment surface where the animal is situated and sulfide levels may be high.

**Acknowledgments**

We thank the following people for their contributions to this research: Ed Ruppert for his aid in animal collections and discussions on brittle stars; Barry Kitto and Pei Thomas for their work in trying to identify the brittle star hemoglobin gene; Robert Cashion for his analysis of the hemoglobin kinetics; Bob Stevens for the electrospray mass spectrometry work; Ellen Beedle for operation of the protein sequencer; Gerald Godette and Shirley Tesh for their help in purification of the hemoglobins and oxygen binding of purified fractions; Steve Stancyk for his discussions on *H. elongata*; John Wourms for his help in DAPI staining and fluorescence microscopy to look for the presence of nuclei in the RBCs; Will Johnson for his measurements made at 10 °C; William C. Bridges for his help in the statistical analysis; and Jim Schindler and Stuart Mellinchamp for their instruction and use of the Coulter Counter to determine RBC size.

**Literature Cited**

- Antonini, E., and M. Brunori. 1971. *Hemoglobin and Myoglobin in Their Reactions with Ligands: Frontiers of Biology*, Vol. 21. North-Holland Publishing, Amsterdam. 436 pp.
- Arp, A. J., and J. J. Childress. 1983. Sulfide binding by the blood of the hydrothermal vent tube worm *Riftia pachyptila*. *Science* **219**: 295–297.
- Baker, S. M., and N. B. Terwilliger. 1993. Hemoglobin structure and function in the rat-tailed sea cucumber, *Paracaudina chilensis*. *Biol. Bull.* **185**: 115–122.
- Barcroft, J., 1935. Foetal respiration. *Proc. R. Soc. Lond. B.* **118**: 242–263.
- Beardsley, A. M., and J. M. Colacino. 1994. Red blood cell circulation and oxygen transport in *Hemipholis elongata* (Ophiuroidea, Echinodermata). *Am. Zool.* **34**: 35A.
- Beardsley, A. M., and J. M. Colacino. 1998. System-wide oxygen transport by the water vascular system of the burrowing ophiuroid, *Hemipholis elongata* (Say). Pp. 323–328 in *Echinoderms: San Francisco. Proceedings of the 9th International Echinoderm Conference*, R. Mooi, and M. Telford, eds. Balkema, Rotterdam.
- Beardsley, A. M., J. M. Colacino, R. Cashion, and C. J. Bonaventura. 1993. The hemoglobins of the brittlestar, *Hemipholis elongata* (Say) (Ophiuroidea, Echinodermata): biochemical and ligand binding properties. *Am. Zool.* **33**: 43A.
- Berzofsky, J. A., J. Peisach, and W. E. Blumberg. 1971. Sulphemoglobin proteins. II. The reversible oxygenation of ferrous sulphemoglobin. *J. Biol. Chem.* **246**: 7366–7372.
- Bonaventura, C., J. Bonaventura, G. B. Kitto, M. Brunori, and E. Antonini. 1976. Functional consequences of ligand-linked dissociation in hemoglobin from the sea cucumber *Molpadia arenicola*. *Biochim. Biophys. Acta* **428**: 779–786.
- Carrico, R. J., W. E. Blumberg, and J. Peisach. 1978. The reversible binding of oxygen to sulphemoglobin. *J. Biol. Chem.* **253**: 7212–7215.
- Chiancone, E., P. Vecchini, D. Verzili, F. Ascoli, and E. Antonini. 1981. Dimeric and tetrameric hemoglobins from the mollusc *Scapharca inaequivalvis*. *J. Mol. Biol.* **152**: 577–592.
- Childress, J. J., A. J. Arp, and C. R. Fisher, Jr. 1984. Metabolic and blood characteristics of the hydrothermal vent tube-worm *Riftia pachyptila*. *Mar. Biol.* **83**: 109–124.
- Christensen, A. B. 1998. The properties of the hemoglobins of *Ophiactis simplex* (Echinodermata, Ophiuroidea). *Am. Zool.* **38**: 120A.

- Cochran, R. E., and L. E. Burnett. 1996. Respiratory responses of the salt marsh animals, *Fundulus heteroclitus*, *Leiostomus xanthurus*, and *Palaemonetes pugio* to environmental hypoxia and hypercapnia and to the organophosphate pesticide, azinphosmethyl. *J. Exp. Mar. Biol. Ecol.* **195**: 125–144.
- Colacino, J. M. 1973. A mathematical model of oxygen transport in the tube foot-ampullary system of the sea-cucumber, *Thyone briareus* L. Ph.D. dissertation. State University of New York at Buffalo. 143 pp.
- Colacino, J. M., and D. W. Kraus. 1984. Hemoglobin-containing cells of *Neodasyx* (Gastrotricha, Chaetodontida) II. Respiratory significance. *Comp. Biochem. Physiol.* **79A**: 363–369.
- Cuénot, L. 1891. Etudes sur le sang et les glandes lymphatiques dans la série animale. II. Invertebrates. *Arch. Zool. Exp. Gen.* **9**: 595–670.
- Darling, R. C., and F. J. W. Roughton. 1942. The effect of methemoglobin on the equilibrium between oxygen and hemoglobin. *Am. J. Physiol.* **137**: 56–68.
- de Camargo, T. M. 1982. Changes in the echinoderm fauna in a polluted area on the coast of Brazil. *Papers from the Echinoderm Conference. The Australian Museum Sydney, 1978*, F. W. E. Rowe, ed. *Aust. Mus. Syd. Mem.* **16**: 165–173.
- Dickerson, R. E., and I. Geis. 1980. *Hemoglobin: Structure, Function, Evolution and Pathology*. Benjamin/Cummings, Menlo Park, NJ. 176 pp.
- Doeller, J. E., D. W. Kraus, J. M. Colacino, and J. B. Wittenberg. 1988. Gill hemoglobin may deliver sulfide to bacterial symbionts of *Solemya vellum* (Bivalva, Mollusca). *Biol. Bull.* **175**: 388–396.
- Felbeck, J. 1983. Sulfide oxidation and carbon fixation by the gutless clam *Solemya reidi*: an animal-bacteria symbiosis. *J. Comp. Physiol.* **152**: 3–11.
- Foettinger, A. 1880. Sur l'existence de l'hémoglobine chez les échinodermes. *Arch. Biol. Paris* **1**: 405–415.
- Guyton, A. C. 1991. *Textbook of Medical Physiology*, 8th ed. W.B. Saunders, Philadelphia. 1014 pp.
- Hajduk, S. L. 1992. Ultrastructure of the tube-foot of an ophiuroid echinoderm, *Hemiphysalis elongata*. *Tissue Cell* **24**: 111–120.
- Hajduk, S. L., and W. B. Cusgrove. 1975. Hemoglobin in an ophiuroid, *Hemiphysalis elongata*. *Am. Zool.* **15**: 808.
- Hand, S. C., and G. N. Somero. 1983. Energy metabolism pathways of hydrothermal vent animals: adaptations to a food-rich and sulfide-rich deep-sea environment. *Biol. Bull.* **165**: 167–181.
- Heatwole, D. W. 1981. Spawning and respiratory adaptations of the ophiuroid, *Hemiphysalis elongata* (Say) (Echinodermata). M.S. thesis. University of South Carolina. 84 pp.
- Hendler, G. L., J. E. Miller, D. L. Pawson, and P. M. Kier. 1995. *Sea Stars, Sea Urchins, and Allies: Echinoderms of Florida and the Caribbean*. Smithsonian Institution Press, Washington, DC. 390 pp.
- Johnson, M. L., J. J. Correia, D. A. Yphantis, and H. R. Halvorson. 1981. Analysis of data from the analytical ultracentrifuge by nonlinear least-squares technique. *Biophys. J.* **36**: 575–588.
- Kitto, G. B., D. Erwin, R. West, and J. Omnaas. 1976. N-terminal substitution of some sea cucumber hemoglobin. *Comp. Biochem. Physiol.* **55B**: 105–107.
- Kitto, G. B., P. W. Thomas, and M. L. Hackert. 1998. Evolution of cooperativity in hemoglobins: what can invertebrate hemoglobins tell us? *J. Exp. Zool.* **282**: 120–126.
- Kolatkhar, P. R., M. L. Hackert, and A. F. Riggs. 1994. Structural analysis of *Urechis caupo* hemoglobin. *J. Mol. Biol.* **237**: 87–97.
- Mangum, C. P. 1992. Respiratory function of the red blood cell hemoglobins of six animal phyla. Pp. 117–149 in *Blood and Tissue Oxygen Carriers, Adv. Comp. Env. Physiol.*, vol. 13, C. P. Mangum, ed. Springer-Verlag, Heidelberg.
- Mangum, C. P., J. M. Colacino, and T. L. Vandergon. 1989. Oxygen binding of single red blood cells of the annelid bloodworm *Glycera dibranchiata*. *J. Exp. Zool.* **249**: 144–149.
- Mangum, C. P., J. M. Colacino, and J. P. Grassle. 1992. Red blood cell oxygen binding in caprellid polychaetes. *Biol. Bull.* **182**: 129–134.
- Manwell, C. 1959. Oxygen equilibrium of *Cucumaria miniata* hemoglobin and the absence of the Bohr effect. *J. Cell Comp. Physiol.* **53**: 75–83.
- Manwell, C. 1966. Sea cucumber sibling species: polypeptide chain types and oxygen equilibrium of hemoglobin. *Science* **152**: 1393–1395.
- Mauri, F., J. Omnaas, L. Davidson, C. Whitfill, and G. B. Kitto. 1991. Amino acid sequence of a globin from the sea cucumber *Caudina (Molpadia) arenicola*. *Biochim. Biophys. Acta.* **1078**: 63–67.
- McDonald, G. D., L. Davidson, and G. B. Kitto. 1992. Amino acid sequence of the coelomic C globin from the sea cucumber *Caudina (Molpadia) arenicola*. *J. Protein Chem.* **11**: 29–37.
- Mitchell, D. T., G. B. Kitto, and M. L. Hackert. 1995. Structural analysis of monomeric hemichrome and dimeric cyanomet hemoglobins from *Caudina arenicola*. *J. Mol. Biol.* **251**: 412–431.
- Mortensen, T. 1920. On hermaphroditism in viviparous ophiuroids. *Acta Zool.* **1**: 1–19.
- Powell, M. A., and G. N. Somero. 1986. Adaptations to sulfide by hydrothermal vent animals: sites and mechanisms of detoxification and metabolism. *Biol. Bull.* **171**: 274–290.
- Riggs, A. 1951. The metamorphosis of hemoglobin in the bullfrog. *J. Gen. Physiol.* **35**: 23–44.
- Riggs, A. 1998. Self-association, cooperativity and supercooperativity of oxygen binding by hemoglobins. *J. Exp. Biol.* **201**: 1073–1084.
- Roberts, M. S., R. C. Terwilliger, and N. B. Terwilliger. 1984. Comparison of sea cucumber hemoglobin structures. *Comp. Biochem. Physiol.* **77B**: 237–243.
- Rossi-Fanelli, A., and E. Antonini. 1958. Studies on the oxygen and carbon monoxide equilibria of human hemoglobin. *Arch. Biochem. Biophys.* **77**: 478–492.
- Royer, W. E., W. E. Love, and F. F. Fenderson. 1985. Cooperative dimeric and tetrameric clam hemoglobins are novel assemblages of myoglobin folds. *Nature* **316**: 277–280.
- Royer, W. E., W. A. Hendrickson, and E. Chiancone. 1990. Structural transitions upon ligand binding in a cooperative dimeric hemoglobin. *Science* **249**: 518–521.
- Schmidt-Neilsen, K. 1990. *Animal Physiology: Adaptation and Environment*. Cambridge University Press, Cambridge. 602 pp.
- Scholnick, D. A., and C. P. Mangum. 1991. Sensitivity of hemoglobins to intracellular effectors: primitive and derived features. *J. Exp. Zool.* **259**: 32–42.
- Somero, G. N., J. J. Childress, and A. E. Anderson. 1989. Transport, metabolism, and detoxification of hydrogen sulfide in animals from sulfide-rich marine environments. *Rev. Aquat. Sci.* **1**: 591–614.
- Steinmeier, R. C., and L. Parkhurst. 1979. Oxygen and carbon monoxide equilibria and the kinetics of oxygen binding by the cooperative dimeric hemoglobin of *Thyonella gemmata*. *Biochemistry* **18**: 4645–4656.
- Stevens, R. D., J. Bonaventura, C. Bonaventura, T. R. Fennel, and D. S. Millington. 1994. Application of electrospray ionization mass spectrometry for analysis of hemoglobin adducts with acetonitrile. *Biochem. Soc. Trans.* **22**: 543–548.
- Suzuki, T. 1989. Amino acid sequences of a major globin from the sea cucumber *Paracaudina chilensis*. *Biochim. Biophys. Acta* **998**: 292–296.
- Terwilliger, R. C. 1975. Oxygen equilibrium and subunit aggregation of a holothurian hemoglobin. *Biochim. Biophys. Acta* **386**: 62–68.
- Terwilliger, R. C., and K. Read. 1972. Hemoglobin of the holothurian echinoderm, *Molpadia oolitica* Pourtales. *Comp. Biochem. Physiol.* **42**: 65–72.
- Terwilliger, R. C., and N. B. Terwilliger. 1988. Structure and function of holothurian hemoglobins. Pp. 589–595 in *Echinoderm Biology: Proceedings from the Sixth International Echinoderm Conference*,

- R. D. Burke, P. V. Mladenov, P. Lambert, and R. L. Parsley, eds., Balkema, Rotterdam.
- Valentine, J. F. 1991a.** Temporal variation in populations of the brittlestars *Hemipholis elongata* (Say, 1825) and *Microphiopholis atra* (Stimpson, 1852) (Echinodermata: Ophiuroidea) in eastern Mississippi Sound. *Bull. Mar. Sci.* **48**: 597–605.
- Valentine, J. F. 1991b.** The reproductive periodicity of *Microphiopholis atra* (Stimpson, 1852) and *Hemipholis elongata* (Say, 1825) (Echinodermata: Ophiuroidea) in eastern Mississippi Sound. *Ophelia* **33**: 121–129.
- van Assendelft, O. W. 1970.** *Spectrophotometry of Hemoglobin Derivatives*. Charles C. Thomas, Springfield, MA. 152 pp.
- Vandergon, T. L., and J. M. Colacino. 1989.** Characterization of hemoglobin from *Phoronis architecta* (Phoronida). *Comp. Biochem. Physiol. B.* **94**: 31–39.
- Vandergon, T. L., and J. M. Colacino. 1991.** Hemoglobin function in the lophophorate *Phoronis architecta* (Phoronida). *Physiol. Zool.* **64**: 1561–1577.
- Weber, R. E. 1980.** Functions of invertebrate hemoglobins with some special reference to adaptation to environmental hypoxia. *Am. Zool.* **20**: 79–101.
- Weber, R. E., and S. N. Vinogradov. 2001.** Nonvertebrate hemoglobins: functions and molecular adaptations. *Physiol. Rev.* **81**: 569–628.
- Wells, R. M. G., and N. W. Pankhurst. 1980.** An investigation into the formation of sulfide and oxidation compounds from the haemoglobin of the lugworm *Abarenicola affinis* (Ashworth). *Comp. Biochem. Physiol.* **66C**: 255–259.
- Windom, H. L., and D. R. Kendall. 1979.** Accumulation and biotransformation of mercury in coastal and marine biota. Pp. 303–323 in *The Biogeochemistry of Mercury in the Environment*. J. O. Nriagu, ed. Elsevier/North-Holland Biomedical Press, Amsterdam.

# Early Development and Acquisition of Zooxanthellae in the Temperate Symbiotic Sea Anemone *Anthopleura ballii* (Cocks)

SIMON K. DAVY<sup>1,\*</sup> AND JOHN R. TURNER<sup>2</sup>

<sup>1</sup> *Institute of Marine Studies, University of Plymouth, Drake Circus, Plymouth PL4 8AA, UK; and*

<sup>2</sup> *School of Ocean Sciences, University of Wales - Bangor, Marine Science Laboratories,  
Menai Bridge, Anglesey LL59 5EY, UK*

**Abstract.** The ova of *Anthopleura ballii* become infected with zooxanthellae (endosymbiotic dinoflagellates) of maternal origin just prior to spawning. After fertilization, the zygotes undergo radial, holoblastic cleavage, and then gastrulate by invagination to form ciliated planulae. Because the zooxanthellae are localized on one side of the ovum—and later, within the blastomeres at one end of the embryo—invagination leads to the zooxanthellae being restricted to the planular endoderm and hence to the gastrodermal cells of the adult anemone. We propose that maternal inheritance of zooxanthellae plays an important part in the success of these temperate sea anemones, which live in regions where potential sources of zooxanthellae are scarce.

## Introduction

Associations between marine invertebrates and endosymbiotic dinoflagellates (zooxanthellae) are abundant in nutrient-poor tropical seas, where the zooxanthellae supply photosynthetically fixed carbon to their hosts and facilitate the conservation and recycling of essential nutrients (Muscatine, 1990; Davies, 1992). These nutritional advantages are not immediately obvious in temperate waters, which show marked seasonal fluctuations in irradiance, high levels of nutrients, and seasonal abundance of planktonic food (Davy *et al.*, 1996, 1997; Muller-Parker and Davy, 2001). Indeed, associations between invertebrates and zooxanthellae are uncommon at temperate latitudes (Turner, 1988; Davy *et al.*, 1996; Muller-Parker and Davy, 2001).

Hosts may acquire zooxanthellae either by maternal inheritance or from the surrounding seawater. Maternal inheritance is probably the rarer mechanism in the tropics. For example, while some reef corals inherit their symbionts (Lewis, 1974; Kojis and Quinn, 1981; Richmond, 1981; Babcock *et al.*, 1986; Glynn *et al.*, 1991), the vast majority of coral species spawn gametes that lack zooxanthellae (Babcock *et al.*, 1986).

In contrast to tropical symbioses, for temperate symbioses transmission modes have been identified in only a few cases. These include the soft coral *Capnella gaboensis*, which inherits zooxanthellae from the parent colony (Farrant, 1986); the scleractinian coral *Astrangia danae*, which spawns zooxanthella-free gametes (Szmant-Froelich *et al.*, 1980); and a small number of sea anemones, the majority of whose ova contain algal symbionts (reviewed by Shick, 1991; Muller-Parker and Davy, 2001). Moreover, the cellular events leading to the acquisition of zooxanthellae and their eventual restriction to the host's endodermal cells have been reported for tropical scleractinian corals (Hirose *et al.*, 2000, 2001), soft corals (Benayahu *et al.*, 1988, 1992; Benayahu and Schleyer, 1998), and jellyfish (Montgomery and Kremer, 1995), but not for temperate corals or sea anemones.

The sea anemone *Anthopleura ballii* (Cocks) is locally abundant along the southwestern coasts of Europe, where it is found from intertidal regions to depths of about 25 m (Manuel, 1988; Turner, 1988; Davy *et al.*, 1996, 1997). The zooxanthellae harbored by *A. ballii* belong to the genus *Symbiodinium* (Davy *et al.*, 1997), though they have yet to be subjected to molecular characterization. In this study, we documented cellular events from gametogenesis through to planula development in *A. ballii*, paying particular attention

Received 7 August 2002; accepted 11 May 2003.

\* Author for correspondence and current address: School of Biological Sciences, Victoria University of Wellington, PO Box 600, Wellington, New Zealand.

to the transmission and distribution of zooxanthellae within the host's tissues.

## Materials and Methods

### *Experimental organisms*

Specimens of the zooxanthellate sea anemone *Anthopleura ballii* were collected, from between 0 and 25 m depth, in the Lough Hyne Marine Nature Reserve, Eire. Anemones were then maintained for up to one year in 30-l recirculating seawater tanks at 10–15 °C. Irradiance of 96  $\mu\text{mol photons m}^{-2} \text{s}^{-1}$  was provided on a 12-h light:12-h dark regime, and the anemones were fed twice weekly with *Artemia* sp. nauplii.

### *Microscopical examination*

Spawning of *A. ballii*, which is dioecious, was induced during summer. This was done by exposing anemones to air for between 3 and 5 h. The expelled gametes were collected by pipette and maintained in 100-ml sterile flasks containing artificial seawater at 15 °C. Fertilization occurred within hours and, every second day, the embryos were pipetted into new flasks, which also contained artificial seawater. This procedure ensured that the only possible source of zooxanthellae was the adult anemone.

Gametes, fertilization, and subsequent early development were examined by taking samples, first at hourly intervals and later once daily, for microscopical observation. A careful search for zooxanthellae was made, using interference contrast microscopy, by optical sectioning at each developmental stage. A Leitz Dialux 20 microscope with Vario-orthomat photographic system was employed, and a photographic record of early development was produced. In addition, cellular events occurring during gametogenesis were documented, again using interference contrast microscopy. This was made possible by anesthetizing anemones in equal parts artificial seawater and 7.5%  $\text{MgCl}_2 \cdot 6\text{H}_2\text{O}$  for 12 to 24 h, and then teasing gametes out of the gonads.

## Results

### *Gametogenesis and gametes*

Dissection occasionally revealed germ cells in the gonadal tissue on the mesentery. The mesenterial tissue was densely packed with zooxanthellae, and the tissues around the oocytes contained many zooxanthellae, but the oocytes themselves were never observed to contain zooxanthellae (Fig. 1A).

Unfertilized ova, examined by interference phase microscopy immediately upon release from the adult anemone, were spherical, yellow-brown, and 300  $\mu\text{m}$  in diameter (Figs. 1B, 2A). The surface of each ovum was covered in fine translucent cytopines (stiffened bundles of long mac-

rovilli that are characteristic of actinarians; Larkman, 1980), about 23  $\mu\text{m}$  in length. The cytoplasm was heterogeneous, dense and granular, and no nuclei were visible under low power in unstained preparations. When the ova were optically sectioned by interference contrast microscopy, the zooxanthellae could be observed in the cytoplasm, just inside the cell membrane. Moreover, the zooxanthellae were concentrated in one hemisphere of the ovum (Fig. 1B). Out of a total of 380 ova examined, only one aposymbiotic ovum was observed.

Spermatozoa were examined under high power ( $\times 1000$ ) in a live preparation. The head was rectangular, 3.5  $\mu\text{m}$  in length and 2.3  $\mu\text{m}$  across, with dense cytoplasm and a large, dark nucleus. No basal body was visible. The tail was about 50  $\mu\text{m}$  long.

### *Fertilization*

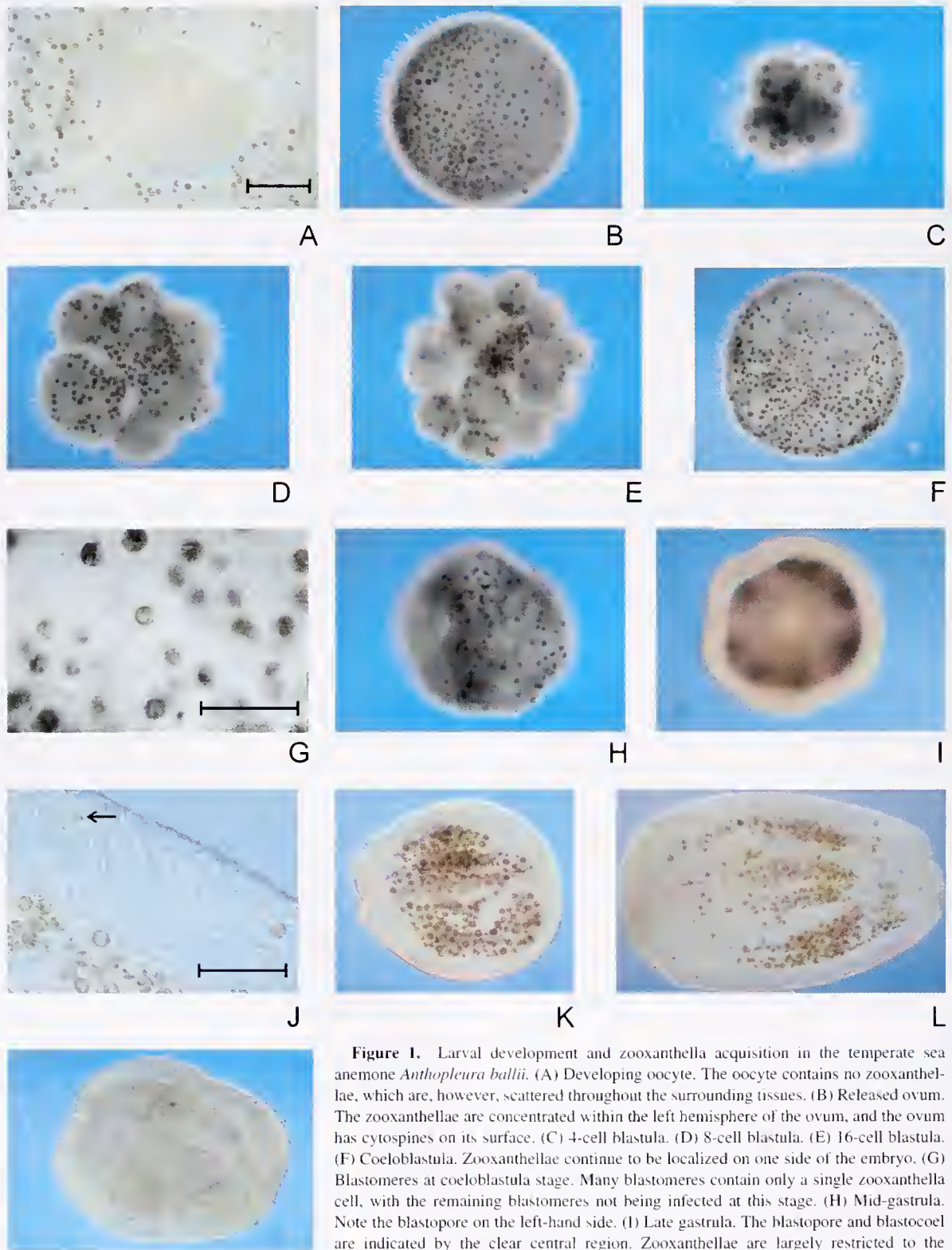
The gametes were shed into open water, where fertilization occurred. Each released ovum was surrounded by numerous sperm, which were aggregated between the cytopines. Fertilization usually occurred within 3.5 h of spawning, and unfertilized ova disintegrated after about 7 h, liberating their zooxanthellae. Spermatozoa were still active at this stage and became inactive after 20–32 h.

### *Cleavage*

About 3.5 h after spawning, 2-, 4-, 8-, and 16-cell blastulas were observed (4- to 16-cell stages shown in Fig. 1C–1E; 2-cell stage not shown). Cleavage was equal, radial, complete (*i.e.*, holoblastic), and rapid, dividing the embryo into a ball of cells (blastomeres). Due to the initial localization of the zooxanthellae, symbionts were distributed unevenly in the blastomeres, being concentrated in those cells at only one end of the embryo. The zooxanthellae remained just inside the cell membrane of each blastomere. Blastulas of 32 cells were observed after about 5.5 h, and blastulas of 64 cells or more were apparent after 6 h. The blastomeres became ever smaller due to repeated cleavage, and after 8 h, a coeloblastula consisting of many cells and one cell layer was formed (Figs. 1F, 2B). The blastomeres were now 20–30  $\mu\text{m}$  in diameter, even in size, and rarely contained more than one zooxanthella each (Fig. 1G). The cytopines were resorbed and replaced by cilia, which soon began to exhibit the characteristic metachronal rhythm that rendered the coeloblastula motile.

### *Gastrulation*

Few gastrulae (Figs. 1H–I, 2C–E) were seen, suggesting that this developmental stage is very short. Twenty hours after spawning, the motile coeloblastulas began to show a slight depression at the pole about which the algae were



M

**Figure 1.** Larval development and zooxanthella acquisition in the temperate sea anemone *Anthopleura ballii*. (A) Developing oocyte. The oocyte contains no zooxanthellae, which are, however, scattered throughout the surrounding tissues. (B) Released ovum. The zooxanthellae are concentrated within the left hemisphere of the ovum, and the ovum has cytopines on its surface. (C) 4-cell blastula. (D) 8-cell blastula. (E) 16-cell blastula. (F) Coeloblastula. Zooxanthellae continue to be localized on one side of the embryo. (G) Blastomeres at coeloblastula stage. Many blastomeres contain only a single zooxanthella cell, with the remaining blastomeres not being infected at this stage. (H) Mid-gastrula. Note the blastopore on the left-hand side. (I) Late gastrula. The blastopore and blastocoel are indicated by the clear central region. Zooxanthellae are largely restricted to the endoderm, while the ectoderm is largely zooxanthella-free. (J) Cell layers of gastrula, showing distribution of zooxanthellae. Most zooxanthellae are in the endoderm, but two can be seen in the ectoderm. One of these zooxanthellae (see arrow) appears to be degenerating. (K) Early planula. (L) Late planula. Zooxanthellae are distributed along the mesenteries. (M) Aposymbiotic mid-planula. Scale bar in A applies to all images except G and J and represents about 100  $\mu\text{m}$ ; scale bars for G and J represent about 50  $\mu\text{m}$ .

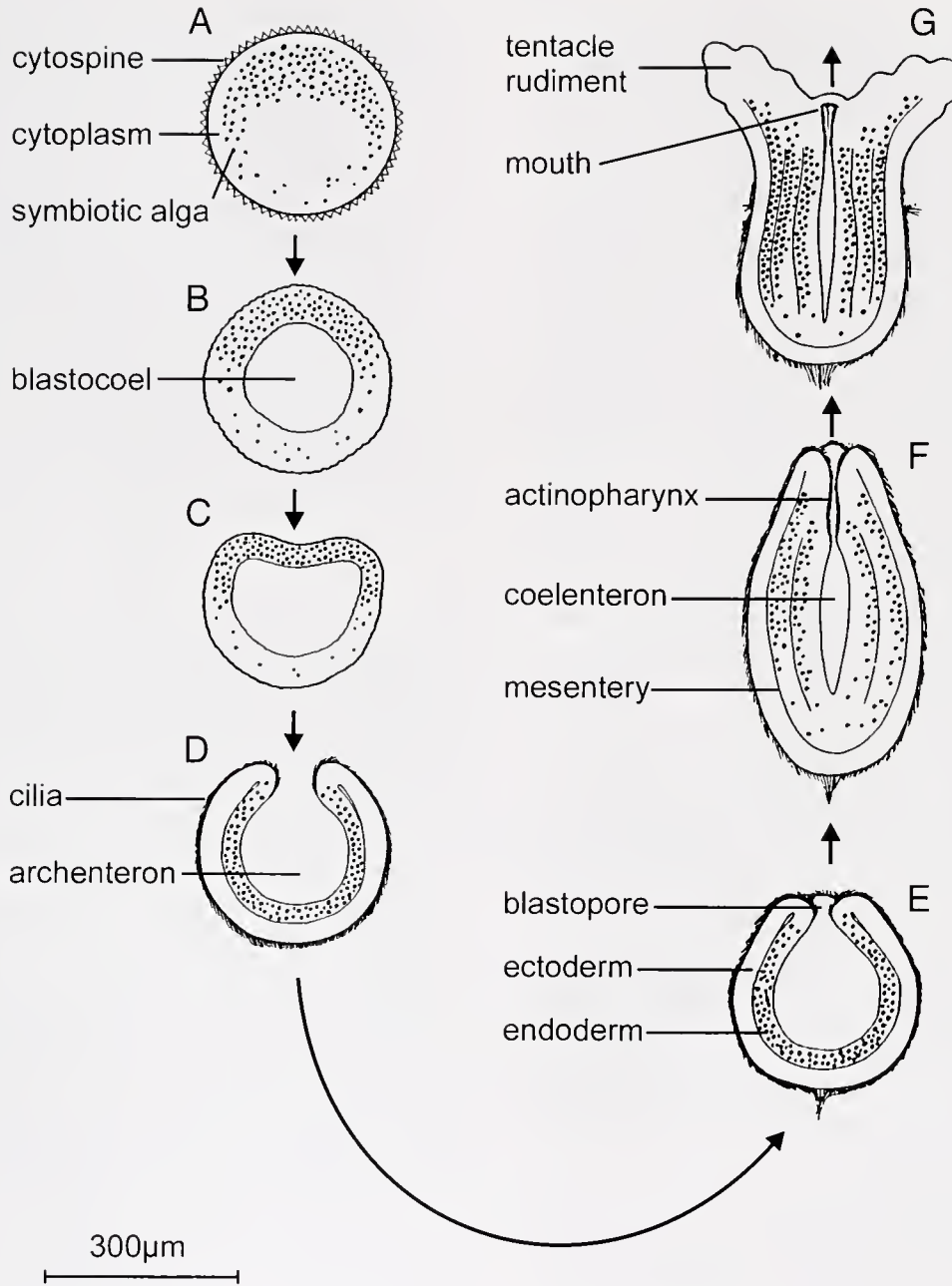


**Figure 2.** Localization of zooxanthellae during early development of *Anthopleura ballii*. (A) Ovum, showing localization of zooxanthellae. (B) Coeloblastula. (C) Early gastrula, showing invagination. (D) Mid-gastrula, showing localization of zooxanthellae in the endoderm. (E) Late gastrula-early planula. (F) Mid-planula, showing zooxanthellae distributed along the mesenteries. (G) Late planula, prior to settlement.

concentrated. Gastrulation by invagination (and perhaps epiboly) followed (Figs. 1H, 2C), with the blastomeres aggregated, at first, around the blastopore. Gastrulation led to the formation of an embryo with two cell layers encompassing a central cavity—the archenteron (Figs. 1I, 2D). During gastrulation, almost all of the blastomeres containing zooxanthellae moved into the endoderm from around the blastopore region. Only very occasionally were zooxan-

thellae seen in the ectoderm, and many of these cells appeared to disintegrate (Fig. 1J).

#### Planulation

After 27 h, most embryos had become late gastrulae or early planulae (Figs. 1K, 2E). By this stage, the developing larvae had shown no growth, remaining about 300  $\mu\text{m}$  in

diameter. However, after 2 days, most planulae began to elongate along their vertical axis, tapering slightly towards the posterior end. The zooxanthellae were clearly visible, aggregated in striations running the length of the endoderm. The surface of each larva was completely ciliated, and an apical tuft of longer cilia was visible. After 3 days, the larvae began to exhibit signs of differentiation (Figs. 1L, 2F), with the development of nematocysts, and a ciliated actinopharynx, which replaced the blastopore. Between 3 and 5 days, the planulae began to grow to about 400–600  $\mu\text{m}$  in length and 300  $\mu\text{m}$  in diameter, even though they were not fed. The number of zooxanthellae also increased (not quantified), and dividing zooxanthellae were seen frequently. As the mesenteries developed, it became clear that most zooxanthellae were located along these structures. Interestingly, only one aposymbiotic planula was observed throughout the course of this work (Fig. 1M), which is consistent with the absence of aposymbiotic *A. ballii* at the field site (Lough Hyne). Tentacle rudiments were seen very occasionally in some planulae (Fig. 2G). Although care was taken to isolate the surviving planulae, they could not be kept alive for more than 7 days and so settlement was not observed.

### Discussion

Gametogenesis, spawning, and early development in *Anthopleura ballii* follows the pattern exemplified by many anemone species (Siebert, 1973; Chia, 1976; Jennison, 1979, 1981). All these species are dioecious, shedding their gametes into open water where fertilization occurs. The zygote then undergoes radial, holoblastic cleavage and forms a hollow coeloblastula. Gastrulation follows by invagination to form a ciliated, pelagic planula larva. This mode of development is notably different from that shown by the larger, yolky, meroblastic ova of the anemones *Tealia crassicornis* (Chia and Spaulding, 1972) and *Cribrinopsis fernaldi* (Siebert and Spaulding, 1976), in which cleavage is incomplete, unequal, and relatively slow. The sequence and timing of events in *A. ballii* were very similar to those described for the temperate zooxanthellate or zoochlorellate anemones *Anthopleura elegantissima* and *Anthopleura xanthogrammica* (Siebert, 1973). However, unlike these anemones, *A. ballii* spawned ova that contained zooxanthellae. In *A. ballii*, concentration of the zooxanthellae in one hemisphere of the ovum, and invagination (and perhaps epiboly) during the gastrula stage, led to the localization of symbionts within the host's endoderm; this same process occurs in the temperate anemone *Anemonia viridis* (Turner, 1988).

#### *Gametogenesis and zooxanthella acquisition*

In *A. ballii*, the endodermal tissue surrounding the developing oocytes was heavily laden with zooxanthellae, though

infected oocytes were never observed. In contrast, spawned ova almost always harbored zooxanthellae, indicating that infection must occur at, or just prior to, release. We could not ascertain whether infection occurs in the gonadal tissue or after the ova have been released into the coelenteron. But, as the anemones were kept in artificial (and so zooxanthella-free) seawater in sterile flasks, and as spawning occurred in air, we can be certain that the zooxanthellae were of maternal origin, and that infection occurs prior to release into the surrounding seawater and hence prior to fertilization.

While the mode of zooxanthella acquisition has been determined in relatively few species of cnidarians, early indications are that infection prior to fertilization is quite uncommon. For example, the vast majority of scleractinian corals investigated do not harbor zooxanthellae in their eggs (Szmant-Froelich *et al.*, 1980; Babcock *et al.*, 1986; Harrison and Wallace, 1990), though some species of *Pocillopora* and *Montipora* do release zooxanthellate ova (Babcock *et al.*, 1986; Harrison and Wallace, 1990; Glynn *et al.*, 1991; Hirose *et al.*, 2001). Of note, the eggs of the hard coral *Montipora digitata* become infected just 24 h prior to spawning (Harrison and Wallace, 1990), suggesting that the delayed infection seen in *A. ballii* eggs also occurs in some other hosts. Furthermore, in brooding species like the soft corals *Xenia umbellata* and *Anthelia glauca*, where zooxanthellae are transmitted maternally, infection does not occur until the later stages of embryogenesis or larval development (Benayahu *et al.*, 1988; Benayahu and Schleyer, 1998).

The mechanism of entry into the ovum is unknown, but may well be similar to that described for the soft coral *Litophyton arboreum* (Benayahu *et al.*, 1992). In *L. arboreum*, zooxanthellae pass through gaps in the mesogloea covering of the oocytes, accumulate in the perioocytic zone, and ultimately bulge through the oolema and enter the mature oocyte. A similar "phagocytosis" of algal symbionts has been reported for the oocytes of several scleractinian corals (Hirose *et al.*, 2001), as well as for the freshwater *Hydra viridissima* (Campbell, 1990).

#### *Spawning, early development, and the localization of zooxanthellae*

The sperm of *A. ballii* are similar to those of other *Anthopleura* spp. (Siebert, 1973). Moreover, as in other symbiotic Anthozoa, the heads are too small ( $3.5 \times 2.3 \mu\text{m}$ ) to act as vectors for paternal transmission of zooxanthellae; zooxanthellae in *A. ballii* are about 10  $\mu\text{m}$  in diameter (Turner, 1988; Davy *et al.*, 1996).

During the early stages of development, and throughout cleavage, the zooxanthellae remain localized at one end of the embryo. By the time a coeloblastula forms, most zooxanthellae are located in individual blastomeres, at one end of the coeloblastula. That this positioning is of paramount importance for the ultimate localization of the zooxanthellae

becomes evident during gastrulation, when zooxanthellae are situated within invaginating blastomeres and so become localized within the endoderm. Indeed, the mechanism is so successful that "stray" zooxanthellae, which end up in the ectoderm, are rare (Fig. 1J).

The initial localization of zooxanthellae seen here is similar to that seen in the corals *Pocillopora verrucosa* and *P. eydouxi* (Hirose *et al.*, 2000). However, as in some other coral species (Szmant-Froelich *et al.*, 1980, 1985), gastrulation in *P. verrucosa* and *P. eydouxi* occurs via delamination rather than invagination. This means that, in marked contrast to events observed in *A. ballii*, blastomeres containing zooxanthellae move into the blastocoel of developing embryos, eventually filling the space and forming a stereogastrula (Hirose *et al.*, 2000). The precise mechanism by which the zooxanthellae move into the blastocoel is unknown.

#### Planulation

As stated above, the position of zooxanthellae in the embryo, and the subsequent localization of zooxanthellae in the endodermis by invagination, means that "stray" zooxanthellae in the epidermal cells of planulae are very rare. A similar paucity of stray zooxanthellae was also reported for the reef corals *Pocillopora verrucosa* and *P. eydouxi* (Hirose *et al.*, 2000). However, the planulae of some scleractinian corals (Szmant-Froelich *et al.*, 1985; Schwarz *et al.*, 1999), soft corals (Farrant, 1986; Benayahu *et al.*, 1988, 1992; Benayahu and Schleyer, 1998), and jellyfish (Montgomery and Kremer, 1995) may contain zooxanthellae in their epidermal cells more frequently. In these cases, the zooxanthellae infect either the planulae or, as in the jellyfish *Linuche unguiculata*, both the embryos and planulae (Montgomery and Kremer, 1995), as opposed to the gametes. The zooxanthellae may then be transferred to the endodermal tissue via cell migration (Montgomery and Kremer, 1995) or trans-mesogloaeal passages (Benayahu, 1997; Benayahu and Schleyer, 1998). Alternatively, stray zooxanthellae may degrade in the host or be expelled as a result of being harbored by an inappropriate cell type. Degrading zooxanthellae have been observed in planulae of the scleractinian corals *Stylophora pistillata*, *Seriatopora caliendrum*, and *Pocillopora verrucosa*, though always in the endodermis, rather than the epidermis (Titlyanov *et al.*, 1998).

#### Mode of transmission as a function of latitude

Symbiotic invertebrates are abundant in tropical seas and regularly release zooxanthellae into the surrounding seawater (Hoegh-Guldberg *et al.*, 1987); viable zooxanthellae are also released in the feces of numerous corallivorous predators (Muller-Parker, 1984). This may result in low selective pressure for the evolution of maternal inheritance in tropical regions, as zooxanthellae are readily available from exoge-

nous sources to infect potential hosts (Buddemeier and Fautin, 1993; Kinzie *et al.*, 2001).

In contrast, while transmission mechanisms have been investigated in relatively few species of zooxanthellate invertebrate, initial observations (including those presented here) suggest that maternal transmission of zooxanthellae is more likely to occur in temperate regions than in the tropics (reviewed by Muller-Parker and Davy, 2001). A predominance of maternal transmission mechanisms at high latitudes would not be surprising, as it could be related to a scarcity of exogenous sources of zooxanthellae and, therefore, selection against hosts that acquire their symbionts from exogenous supplies (Muller-Parker and Davy, 2001). Indeed, a scarcity of sources of zooxanthellae could explain why the temperate coral *Astrangia danae*, which does not acquire its zooxanthellae maternally, is sometimes found devoid of these symbionts (Szmant-Froelich *et al.*, 1980). In addition, maternal transmission, combined with the ability of temperate algal-invertebrate symbioses to tolerate a wide range of environmental variables (Kevin and Hudson, 1979; Squire, 2000; Howe and Marshall, 2001), could explain the persistence of zooxanthellate organisms at high latitudes (Davy *et al.*, 1997; Muller-Parker and Davy, 2001). More analyses of zooxanthellar transmission mechanisms at different latitudes, and of the ecological advantages conveyed by symbioses in nutrient-rich temperate waters, will help resolve this matter.

#### Acknowledgments

This work was funded by a NERC award to JRT and was conducted, in part, at the University of Oxford. JRT thanks Professor Sir David Smith FRS FRSE for support. SKD thanks the Institute of Marine Studies, University of Plymouth for financial assistance.

#### Literature Cited

- Babcock, R. C., G. D. Bull, P. L. Harrison, A. J. Heyward, J. K. Oliver, C. C. Wallace, and B. L. Willis. 1986. Synchronous spawnings of 105 scleractinian coral species on the Great Barrier Reef. *Mar. Biol.* **90**: 379–394.
- Benayahu, Y. 1997. Developmental episodes in reef soft corals: ecological and cellular determinants. *Proc. 8<sup>th</sup> Int. Coral Reef Symp.* **2**: 1213–1218.
- Benayahu, Y., and M. H. Schleyer. 1998. Reproduction in *Anthelia glauca* (Octocorallia: Xeniidae). II. Transmission of algal symbionts during planular brooding. *Mar. Biol.* **131**: 433–442.
- Benayahu, Y., Y. Aчитov, and T. Berner. 1988. Embryogenesis and acquisition of algal symbionts by planulae of *Xenia umbellata* (Octocorallia: Alcyonacea). *Mar. Biol.* **100**: 93–101.
- Benayahu, Y., D. Weil, and Z. Malik. 1992. Entry of algal symbionts into oocytes of the coral *Litophyton arboreum*. *Tissue Cell* **24**: 473–482.
- Buddemeier, R. W., and D. G. Fautin. 1993. Coral bleaching as an adaptive mechanism: a testable hypothesis. *Bioscience* **43**: 320–325.
- Campbell, R. D. 1990. Transmission of symbiotic algae through sexual

- reproduction in hydra: movement of algae into the oocyte. *Tissue Cell* **22**: 137–147.
- Chia, F.-S. 1976.** Sea anemone reproduction: patterns and adaptive radiations. Pp. 261–270 in *Coelenterate Ecology and Behaviour*, D.D. Mackie, ed. Plenum Press, London.
- Chia, F.-S., and J. G. Spaulding. 1972.** Development and juvenile growth of the sea anemone, *Tealia crassicornis*. *Biol. Bull.* **142**: 206–218.
- Davies, P. S. 1992.** Endosymbiosis in marine cnidarians. Pp. 511–540 in *Plant-Animal Interactions in the Marine Benthos*, D. M. John, S. J. Hawkins, and J. H. Price, eds. Clarendon Press, Oxford.
- Davy, S. K., I. A. N. Lucas, and J. R. Turner. 1996.** Carbon budgets in temperate anthozoan-dinoflagellate symbioses. *Mar. Biol.* **126**: 773–783.
- Davy, S. K., J. R. Turner, and I. A. N. Lucas. 1997.** The nature of temperate anthozoan-dinoflagellate symbioses. *Proc. 8th Int. Coral Reef Symp.* **2**: 1307–1312.
- Farrant, P. A. 1986.** Gonad development and the planulae of the temperate Australian soft coral *Capnella gaboensis*. *Mar. Biol.* **92**: 381–392.
- Glynn, P. W., N. J. Gassman, C. M. Eakin, J. Cortes, D. B. Smith, and H. M. Guzman. 1991.** Reef coral reproduction in the eastern Pacific: Costa Rica, Panama, and Galapagos Islands (Ecuador). I. Pocilloporidae. *Mar. Biol.* **109**: 355–368.
- Harrison, P. L., and C. C. Wallace. 1990.** Reproduction, dispersal and recruitment of scleractinian corals. Pp. 133–207 in *Ecosystems of the World: Coral Reefs*, Vol. 25, Z. Dubinsky, ed. Elsevier, Amsterdam.
- Hirose, M., R. A. Kinzie III, and M. Hidaka. 2000.** Early development of zooxanthella-containing eggs of the corals *Pocillopora verrucosa* and *P. eydouvi* with special reference to the distribution of zooxanthellae. *Biol. Bull.* **199**: 68–75.
- Hirose, M., R. A. Kinzie III, and M. Hidaka. 2001.** Timing and process of entry of zooxanthellae into oocytes of hermatypic corals. *Coral Reefs* **20**: 273–280.
- Hoegh-Guldberg, O., L. R. McCloskey, and L. Muscatine. 1987.** Expulsion of zooxanthellae by symbiotic cnidarians from the Red Sea. *Coral Reefs* **5**: 201–204.
- Howe, S. A., and A. T. Marshall. 2001.** Thermal compensation of metabolism in the temperate coral, *Plesiastrea versipora* (Lamarck, 1816). *J. Exp. Mar. Biol. Ecol.* **259**: 231–248.
- Jennison, B. L. 1979.** Gametogenesis and reproductive cycles in the sea anemone *Anthopleura elegantissima* (Brandt, 1835). *Can. J. Zool.* **57**: 403–411.
- Jennison, B. L. 1981.** Reproduction in three species of sea anemones from Key West, Florida. *Can. J. Zool.* **59**: 1708–1719.
- Kevin, K. M., and R. C. L. Hudson. 1979.** The role of zooxanthellae in the hermatypic coral *Plesiastrea versipora* (Milne Edwards and Haime) from cold waters. *J. Exp. Mar. Biol. Ecol.* **36**: 157–170.
- Kinzie, R. A. III, M. Takayama, S. R. Santos, and M. A. Coffroth. 2001.** The adaptive bleaching hypothesis: experimental tests of critical assumptions. *Biol. Bull.* **200**: 51–58.
- Kojis, B. L., and N. J. Quinn. 1981.** Reproductive strategies in four species of *Porites* (Scleractinia). *Proc. 4th Int. Coral Reef Symp.* **2**: 145–152.
- Larkman, A. U. 1980.** Ultrastructural aspects of gametogenesis in *Actinia equina*. Pp. 61–66 in *Development and Cellular Biology of Coelenterates*, P. Tardent and R. Tardent, eds. Elsevier, Amsterdam.
- Lewis, J. B. 1974.** The settlement behaviour of planulae larvae of the hermatypic coral *Favia fragum* (Esper). *J. Exp. Mar. Biol. Ecol.* **15**: 165–172.
- Mannel, R. L. 1988.** *British Anthozoa*. Academic Press, London.
- Montgomery, M. K., and P. M. Kremer. 1995.** Transmission of symbiotic dinoflagellates through the sexual cycle of the host scyphozoan *Linuche unguiculata*. *Mar. Biol.* **124**: 147–155.
- Muller-Parker, G. 1984.** Dispersal of zooxanthellae on coral reefs by predators on cnidarians. *Biol. Bull.* **167**: 159–167.
- Muller-Parker, G., and S. K. Davy. 2001.** Temperate and tropical algal-sea anemone symbioses. *Invertebr. Biol.* **120**: 104–123.
- Muscatine, L. 1990.** The role of symbiotic algae in carbon and energy flux in reef corals. Pp. 75–87 in *Ecosystems of the World: Coral Reefs*, Vol. 25, Z. Dubinsky, ed. Elsevier, Amsterdam.
- Richmond, R. 1981.** Energetic considerations in the dispersal of *Pocillopora damicornis* (Linnaeus) planulae. *Proc. 4th Int. Coral Reef Symp.* **2**: 153–156.
- Schwarz, J. A., D. A. Krupp, and V. M. Weis. 1999.** Late larval development and onset of symbiosis in the scleractinian coral *Fungia scutaria*. *Biol. Bull.* **196**: 70–79.
- Shick, J. M. 1991.** *A Functional Biology of Sea Anemones*. Chapman and Hall, New York.
- Siebert, A. E. 1973.** A description of the embryology, larval development, and feeding of the sea anemones *Anthopleura elegantissima* and *A. xanthogrammica*. *Can. J. Zool.* **52**: 1383–1388.
- Siebert, A. E., and J. G. Spaulding. 1976.** The taxonomy, development and brooding behavior of the anemone, *Cribrinopsis fernaldi* sp. nov. *Biol. Bull.* **150**: 128–138.
- Squire, L. R. 2000.** Natural variations in the zooxanthellae of temperate symbiotic Anthozoa. Ph.D. thesis, University of Wales, Bangor.
- Szmant-Froelich, A., P. Yevich, and M. E. Q. Pilson. 1980.** Gametogenesis and early development of the temperate coral *Astrangia danae* (Anthozoa: Scleractinia). *Biol. Bull.* **158**: 257–269.
- Szmant-Froelich, A., M. Reutter, and L. Riggs. 1985.** Sexual reproduction of *Favia fragum* (Esper): lunar patterns of gametogenesis, embryogenesis and planulation in Puerto Rico. *Bull. Mar. Sci.* **37**: 880–892.
- Titlyanov, E. A., T. V. Titlyanova, V. Loya, and K. Yamazato. 1998.** Degradation and proliferation of zooxanthellae in planulae of the hermatypic coral *Stylophora pistillata*. *Mar. Biol.* **130**: 471–477.
- Turner, J. R. 1988.** The ecology of temperate symbiotic Anthozoa. D. Phil. thesis, University of Oxford.

# On the Growth of Bivalve Gills Initiated From a Lobule-Producing Budding Zone

DIETRICH NEUMANN\* AND HEIKE KAPPES

*Zoological Institute, University of Cologne, D-50923 Köln, Germany*

**Abstract.** The growth of bivalve gills proceeds at the posterior end of the gill from a meristem-like budding zone, that is, an undifferentiated terminal organ, which continuously proliferates new gill elements in growing bivalves. In representatives of protobranch, filibranch, and eulamellibranch gills (13 species from Protobranchia, Pteriomorpha, Palaeoheterodonta, and Heterodonta), the first growth steps demonstrate a uniform basic pattern. The budding zone produces either transverse folds that split after a transition zone into parallel pairs of lobules (which themselves later differentiate into the inner and outer demibranchs), or it produces the lobules directly, without first forming a transition zone. The lobules elongate, differentiate into lobes, and transform into leaflet-like structures (protobranchs) or into filaments (filibranchs and eulamellibranchs). The filaments represent the differentiated outer margins of each lobe, of which the central tissue (interlamellar septum) becomes incised or fenestrated, or transformed by tissue junctions. A distally located main growth zone for each lobe is suggested. With regard to the delayed onset of the differentiation of the outer demibranch in juvenile unionids, an additional temporary growth zone for filaments is suggested to exist at the anterior end of the outer demibranch.

## Introduction

Bivalve gills are unique organs that show a continuous terminal growth by adding new elements in correlation with the lifelong increase in shell size. The gills consist of two plate-like demibranchs that are extended anterior-posteriorly on each side of the visceral mass (the only exception: Lucinidae with only one demibranch; Ridewood, 1903). In the case of the phylogenetically primitive protobranch gill, the demibranchs are comparatively small and consist of a

series of ciliated leaf-like discs. In filibranch gills, the demibranchs are considerably longer and consist of extended parallel structures—the filaments—rather than parallel disks. The filament structure also appears on the surface of the demibranch in eulamellibranch gills; however, their demibranchs are much more complex organs, because the filaments are connected by various tissue junctions (see Ridewood, 1903).

These gills all share two functional elements: a peripheral ciliary pump that creates a flow of oxygenated water over and through the demibranchs, and an internal circulatory system that carries the oxygenated hemolymph to the heart. During the evolution of filibranch and eulamellibranch bivalves, the size of the gills increased in relation to body mass and mantle cavity, and two additional functions evolved: feeding on inhaled particles, facilitated by mucous secretion and followed by food-string transport along food grooves; and in some taxa, brood care within the interlamellar spaces (for reviews, see Purchon, 1968; Bayne *et al.*, 1976; Morton, 1996).

Bivalve gills develop new elements from their posterior end as they grow (Wasserloos, 1911; Ansell, 1962; Kornushin, 1997). In the past, however, studies on gill growth processes focused only on the early organogenesis of the gill during the postlarval development (for review of the older literature, see Raven, 1966). In all subclasses except Protobranchia, these early stages start with a short row of unidirectional slender filaments of only the inner demibranch (Jackson, 1890; Drew, 1901; Wasserloos, 1911; Ansell, 1962; Waller, 1981; Gros *et al.*, 1998; Chaparro *et al.*, 2001). The row of filaments extends in anterior-posterior sequence. Detailed studies of postlarval stages of the eulamellibranch Veneridae revealed that the unidirectional filaments first display knob-like thickenings at their distal ends and then transform to widened, roughly V-shaped filaments; no bending or reflexion was involved in this process (Ansell, 1962; Mouëza *et al.*, 1999). At the end of

Received 29 August 2002; accepted 30 April 2003.

\* To whom correspondence should be addressed. E-mail: dietrich.neumann@uni-koeln.de

this postlarval development, the new filaments of the inner demibranch arise from the posterior end of the gill base in the form of V-shaped elements (Ansell, 1962).

In contrast to these developmental results on postlarvae and early juveniles, this study is focused on the continual growth of the differentiated bivalve gill from its posterior growth zone, where new filaments are added. Bivalves of different subclasses were examined. For juvenile unionids, we further describe the beginning of the outer demibranch, which lags behind the early formation of the inner demibranch. The results offer new insights into the increase in filament number, the differentiation of the filaments, and bivalve gill growth in general.

## Materials and Methods

### Material

To examine gill development in bivalves possessing protobranch gills, we studied three *Nucula* species (subclass Protobranchia) preserved in ethanol (Museum Senckenberg, Frankfurt a.M., FRG): *Nucula nucleus* Linnaeus (Helgoland ex Wolf/2, Coll.-No. SMF 320968/2), *N. sulcata* Bronn (Me5/51 Ku/3, Coll.-No. SMF 320966/3), and *N. tenuis* (Montagu) (Gauss-St. 101 Ku/6, Coll.-No. SMF 320967/6).

As examples of filibranch gills, we examined species belonging to the subclass Pteriomorphia: *Mytilus edulis* Linnaeus (sampled at Grömitz on the shore of the Baltic Sea, Schleswig-Holstein, Germany), *M. galloprovincialis* Lamarck (Ria de Vigo, Galicia, Spain), and *Anadara* sp. (Kakinada Bay, Andhra Pradesh, India; soft body directly preserved in Bouin's fluid).

Eulamellibranch gills from the subclasses Palaeoheterodonta [*Unio pictorum* (Linnaeus), *U. tumidus* (Philipsson)] and Heterodonta [*Dreissena polymorpha* (Pallas), *Corbicula fluminea* (O.F. Müller), and *Pisidium casertanum* (Poli)] were studied. *Corbicula* was collected from the Rhine River near Cologne (Rh.-km 683); the other species from waters of the flood plain of the Lower Rhine (Hafensche Landwehr near Rees, Rh.-km 840). We also inspected *Mya arenaria* (L.) from Grömitz and *Venerupis decussata* (L.) from Ria de Vigo.

### Scanning electron microscopy

Fresh gills (posterior sections) of *U. pictorum*, *C. fluminea*, *D. polymorpha*, and *P. casertanum* were fixed in 2% glutaraldehyde in 0.133 mol phosphate buffer (pH 7.2) for 2 h. This material, as well as prefixed gills from *Anadara* sp., *N. sulcata*, and *N. tenuis*, were then dehydrated in ethanol. After two rinses in pure acetone for 2 h each, the gills were stored overnight in pure acetone, then dried with CO<sub>2</sub>, mounted, and sputtered (ca. 140-nm gold layer).

### Histology of subadult *Unio* gills

For histological analysis of the budding zone, two specimens of *U. pictorum* (shell lengths 4.85 mm and 20.1 mm) were fixed in Bouin-Allen's fluid (2 h, 37 °C). After rinsing in 70% ethanol followed by standard dehydration, the tissues were embedded *via* Rotihistol (15 h) and Rotihistol-Rotiplast 1:1 (1.5 h at 61 °C) in Rotiplast (paraffin, melting point 58 °C). Serial 10- $\mu$ m microtome sections were stained with Domagk's stain (Romeis, 1968).

### Dissection of juvenile gills

Early juvenile eulamellibranchs possess only slender filaments of the inner demibranch. We estimated the shell size at which the outer demibranchs first developed. Specimens of *U. pictorum* and *U. tumidus* (shell length between 3.5 and 16.95 mm) preserved in ethanol were dissected for this purpose. The gills were placed on slides (after dehydration in ethanol) and embedded in Rotihistokitt (Roth, Karlsruhe-FRG). The longest filament of each demibranch was then measured from its dorsal base to its ventral tip with an image analyzing system attached to a CCD-camera linked to a Leitz microscope. With a pointer on the monitor, the length could be measured to the nearest 0.01 mm. Linear regression lines were calculated using SPSS 7.5 and Statgraphics 4.0.

### Terms used for gill structures

Various anatomical terms have been used for the description of bivalve gills (Mitsukuri, 1881; Ridewood, 1903; Yonge, 1947; Kiliyas, 1956; Beninger *et al.*, 1988; and others). To avoid terminological confusion, we summarize most of these terms and mark (by single quotation marks and italics) those that we will use in this study. In most aspects we follow Ridewood (1903). However, with regard to the posterior growth zone of the gill, we will introduce new terms.

When juvenile filibranch and eulamellibranch bivalves have passed the early period of gill differentiation, they possess two '*demibranchs*' (also gill plates) in an anterior-posterior extension on each side of the foot. These two demibranchs, that is, the '*inner*' and '*outer*' ones (Fig. 1b, right side: id and od), are attached by a '*gill base*' (also gill axis, gill root) on the dorsal side of the '*mantle cavity*' (also pallial cavity) between the visceral mass and the mantle. Each dorsoventrally lengthened demibranch is formed into two '*lamella*'-like structures (also membrane plates, leaves) consisting of vertically ciliated '*filaments*' in parallel (also gill bars, ciliated discs) (Fig. 1a). The terms '*descending limb*' of the filament (also descending portion of the filament, *i.e.*, that part of the filament connected to the gill base) and '*ascending limb*' (the other part of the filament dorsally unattached or fused with foot or mantle) will be circumvented as far as possible because of developmental

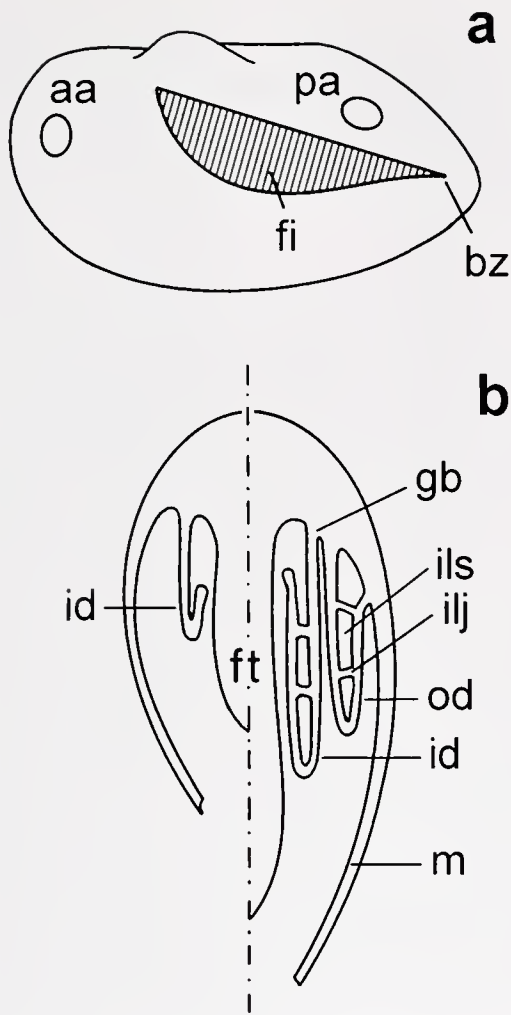


**Figure 1.** (a) Schematic view of shell shape and the relative position of the two adductor muscles (aa: anterior adductor, pa: posterior adductor) and the gill in *Unio tumidus*. The budding zone (bz) of the successively increasing number of filaments (fi) is located at the posterior end. The filaments lengthen during shell growth. (b) Schematic view of a transverse section showing the age-dependent difference in gill organization between juvenile unionids of shell length 3.5 mm (left half) and 8.1 mm (right half). id: inner demibranch, showing early differentiation and later differentiation on the left and right sides, respectively (in most parts of the gill, not yet attached to the foot), od: outer demibranch, gb: gill base, ils: interlamellar space, ilj: interlamellar junction, m: mantle, ft: foot.

and functional connotations. 'Interlamellar junctions' may stabilize the elongated filibranch filaments, and adjacent filaments are held together by 'ciliated knobs' (also ciliated discs), which are arranged dorsoventrally, and more or less equidistantly (Fig. 2). Eulamellibranchs possess two types of tissue bridges: 'interlamellar junctions' (also septa) between the descending and ascending limbs of the filaments, and 'interfilamentar junctions' between adjacent filaments. The variety of tissue junctions increases the complexity of the branchial architecture, with 'interlamellar spaces' or 'gaps' (also suprabranchial chambers, vertical water tubes, interlamellar cavity) and 'interfilamentar pores' (also ostia,

slits) through which the inhaled water passes. The filaments of each demibranch are strengthened by skeletal rods and are joined at their ventrodorsal margins, thus forming the ciliated 'food groove' (also marginal groove). As the central structures of the lamellae increase in complexity, two general types of gills—homorhabdic and heterorhabdic—become evident in different species. Homorhabdic gills contain only 'ordinary filaments', whereas heterorhabdic gills contain both 'ordinary' and 'principal' filaments (Ridewood, 1903).

Gills of protobranch bivalves are smaller, restricted to the posterior part of the mantle cavity, and characterized by a simple anatomy. However, the gross design is the same as that of the filibranch and eulamellibranch types, that is, two demibranchs on each side. Each consists of a series of extended leaflets (also discs), ciliated and attached to each other by ciliated knobs.

## Results

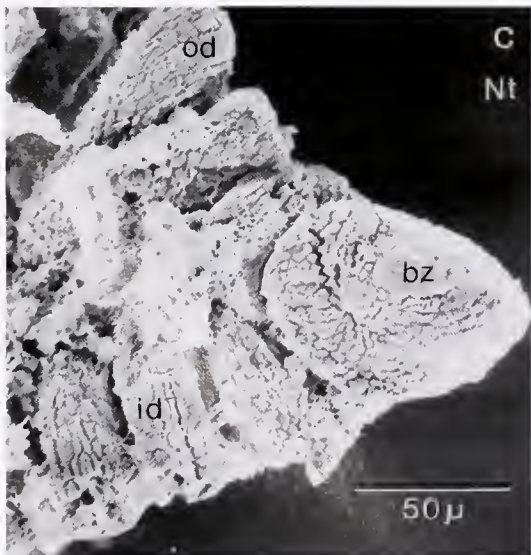
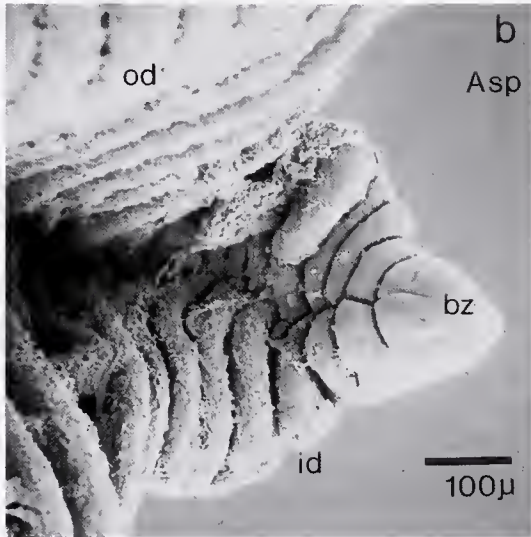
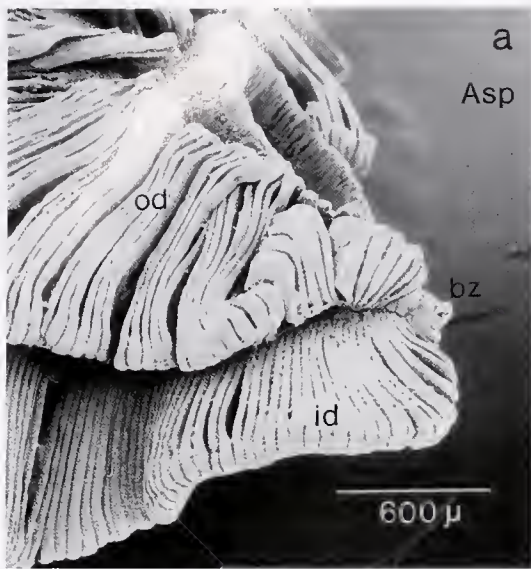
### *Budding zones of protobranch and filibranch gills*

On the basis of our material, the posterior growth zone of these two gill types can be demonstrated best in the filibranch gill of *Anadara* (Pteriomorpha) (Fig. 2a). In this species, the posterior part of the gill base ends in a small, rounded projection of undifferentiated cells, from which the separation of new filaments starts (Fig. 2b). We name this meristem-like cell complex the 'budding zone'.

As was observed in all dissections, the budding zone of *Anadara* is not attached to the mantle but projects into the mantle cavity. The budding zone of the specimen presented (Fig. 2b) is already marked on its ventral side by a fine medial line. This is the onset of the deep longitudinal groove that separates the inner and outer demibranchs. The second step of early differentiation is the appearance of transverse folds which form undifferentiated 'lobules' of the inner and the outer demibranchs in a characteristic 1:1 relationship.

We were able to confirm the 1:1-ratio of demibranch lobules in the filibranch mussel *Mytilus* (not shown). However, the undifferentiated budding zone of *Mytilus* is followed by a 'transition zone' characterized by a number of transverse folds that have not yet split medially into the lobules of the two demibranchs (as in *Unio*, compare Fig. 4a). The length of the transition zone differed among specimens. In *M. galloprovincialis* from Vigo ( $n = 12$ ), small specimens (0.5–0.7 cm) and larger ones (1.0–3.3 cm) revealed 4–6 and 8–12 transverse folds, respectively (exception: one 3.7-cm specimen with only four folds). In *M. edulis* ( $n = 7$ ) from Grömitz, the length of the transition zone had no relation to shell length (2 folds in specimens of 1.7 and 2.1 cm shell length, 5 folds for sizes of 1.8 and 2.1 cm, 7 for a 1.2-cm specimen, 9 and 10 folds for sizes of 3.2 cm and 2.0 cm, respectively). It is possible that such variations are correlated with different rates of gill increase.

Similar to *Anadara*, in *Nucula tenuis* (Protobranchia) the



tiny budding zone of the gill is represented by the posterior apex of the gill base and has no contact to the mantle (Fig. 2c). The same was observed in dissected specimens of the other two *Nucula* species. In *Nucula*, both the transverse folds and the separation of inner and outer demibranchs occur simultaneously. Thus, the lobules appear from the very beginning.

#### *Lobule differentiation in protobranchs and filibranchs*

In the protobranch *Nucula*, the lobules of the demibranchs extend laterally and dorsoventrally and form the leaf-like lobes. Part of the margin of each lobe becomes thickened and ciliated, whereas the expanded inner portion of the lobe—its 'lamina' (also interlamellar septum)—remains unchanged. These are then the differentiated leaflets.

The lobules in the filibranchs *Anadara* and *Mytilus* mainly increase dorsoventrally and form elongated lobes. Their margins differentiate into descending and ascending limbs of the filament, as already described for Arcidae and Mytilidae (Ridewood, 1903). Simultaneously, the lamina of each lobe becomes transformed. In *Anadara*, a gap (interlamellar space) occurs within the lamina and separates the filament's margins (Fig. 3a). The length of the gap may be as little as 50% or as much as 90% of the filament's length. The outer margins of the filament now resemble descending and ascending limbs. Adjacent filaments are attached to each other by nearly equidistant ciliated knobs that are arranged in vertical rows, one on either side of the two ciliated margins. Lateral views of the lamellae reveal that the equidistant knobs on adjacent filaments are aligned, and that the number of equidistant lines of knobs increases as the filaments elongate. It was obvious that, during elongation, new lines of knobs appeared stepwise near the filament's distal end. Thus, a main growth zone of each filament must be localized in this distal area (Fig. 3a). However, it can also be seen that a new line of knobs becomes inserted in a few areas along the length of the lamellae after the distance between two rows has increased (not shown). This fact suggests that, in *Anadara* gills, some incremental elongation of the filaments also occurs all along the dorsoventral length of the lamina.

In *Mytilus*, the lobules occur after the medial splitting of the transition zone into inner and outer demibranchs (see above). Each lobule elongates and forms a lobe. Then, its lamina becomes transformed. A few interlamellar junctions

**Figure 2.** Scanning electron micrographs of the differentiating demibranchs in the filibranch *Anadara* sp. (Asp; full-grown specimen) and the protobranch *Nucula tenuis* (Nt; 6.5 mm). (a) Overview of the posterior end of the left gill of an adult *Anadara* specimen showing the budding zone (bz). (b) Budding zone of *Anadara* differentiating into lobules of the inner and outer demibranch (id, od). (c) Budding zone and separating inner and outer demibranchs of *Nucula*; the lobules are partly covered by mucus and cilia.

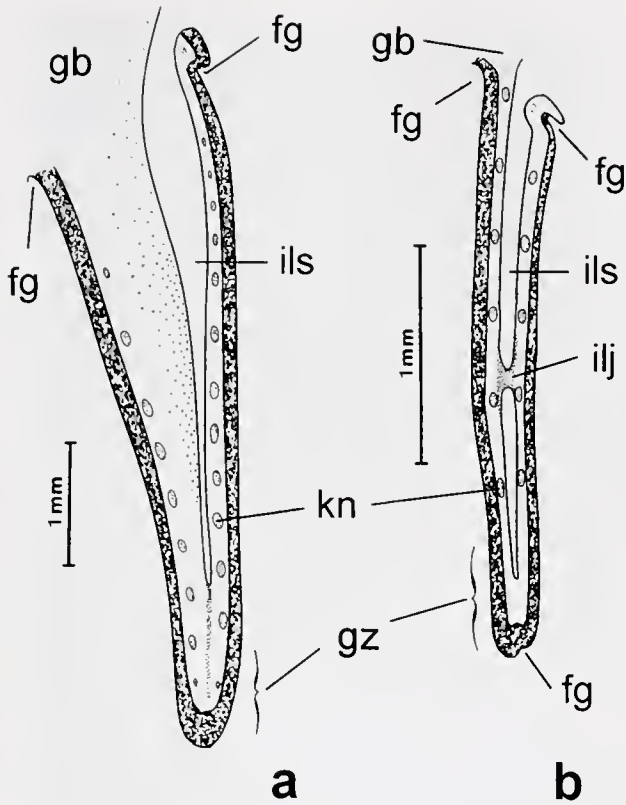


**Figure 3.** Gill filaments of two filibranch bivalves demonstrating the lengthened lobules with the equidistantly arranged ciliated knobs (kn), which increase in number from the distal end. The proposed distal growth zone (gz) is indicated. (a) *Anadara* sp. (shell size about 5 cm); (b) *Mytilus edulis* (shell size of 2.2 cm). fg: food groove, gb: gill base, ilj: interlamellar junction, ils: interlamellar space.

remain and stabilize the small distance between the outer margins (Fig. 3b); the first ones appeared at about the 30th filament (counted anteriorly from the budding zone). Again, the margins strongly resemble filamentary structures. All adjacent filaments are attached to each other by equidistant ciliated knobs (Fig. 3b). In dissections of the gills of adult *Mytilus*, we observed that the ciliated knobs form equidistant lines, which are arranged parallel to the gill base along the whole gill. The number of lines increased with the size of the demibranchs and the length of their filaments. In contrast to *Anadara*, *Mytilus* shows new lines of knobs only near the ventral end of the filaments. No inserted lines of knobs were detected in lateral views of the lamina. Thus, unlike growth in *Anadara*, the main growth zone responsible for elongation must be restricted to this area.

#### *Budding zones of eulamellibranch gills*

The four representatives of the Palaeoheterodonta (*Unio*) and Heterodonta (*Dreissena*, *Corbicula*, and *Pisidium*) studied possess eulamellibranch gills. Again, an undifferentiated budding zone lies at the posterior end of each species' gills (Fig. 4). In each example, the transverse folds form in a way

similar to that of protobranchs and filibranchs: the folds split into inner and outer demibranchs. Apart from these common differentiation events, species-specific differences exist in the relative size of the budding zone and in the extension of a segmented transition zone before the two parallel rows of lobules begin to emerge (Fig. 4). Cilia already occur on the early lobules.

*Unio* (Fig. 4a): Only the growing left gill and the adjacent mantle epithelium are visible; the right gill is obscured. The budding zone is located on the posterior process of the gill base, which is curved inwards. At least six transverse folds extend from it; this is the transition zone. These folds then become separated by the prospective dorsal food groove into two parallel rows of further enlarged lobules. The lobules become ciliated as they grow ventrally. As can be seen in the outer demibranch (Fig. 4a), the outer edges of the lobules (later forming the outer lamellae) are attached to the mantle tissue from the very beginning. The corresponding processes occur on the other side of the foot, on the growing right gill.

*Dreissena* (Fig. 4b): In this view from the ventral side, only the left gill is horizontally positioned, so that the details of the transitions between the budding zone and the transverse folds can be seen. The budding zone is smaller than in *Unio* and is followed by a short transition zone. No exceptions to the 1:1 relationship in lobule number between developing inner and outer demibranchs was found. As was demonstrated during dissections, the budding zone is not attached to the mantle.

*Corbicula* (Fig. 4c): The separation of the transverse folds follows the same principles as described above. The budding zones of the left and right gills lie close together and seem to be attached to the mantle. The dorsal margins of the outer demibranch lobes are also attached to the mantle from the beginning on. However, two peculiarities can be noticed in this species. Firstly, the first transverse fold starts at the inner demibranch of each gill. Secondly, a transition zone, such as is found in *Unio* and *Dreissena*, does not exist.

*Pisidium* (Fig. 4d): The convergent budding zones were as short as in *Corbicula*. The separation of lobules and their early differentiation appear to be somewhat advanced in the most recent section of the inner demibranch, without disturbing the 1:1 relationship of the older inner and outer lobules (compare idl and odl in Fig. 4d).

Dissection of two other lamellibranchs revealed a differentiation of new lobules more or less identical to that shown in Figure 4. In adult *Venerupis decussata* specimens, neither the budding zone nor the transition zone was fused to the mantle; and the transition zone extended over only two or three transverse folds. When the demibranchs were separated, the most posterior lobules of both demibranchs were still solid, lacking any transformation. A small specimen of *Mya arenaria* (shell length 3.8 mm) showed a similar pat-

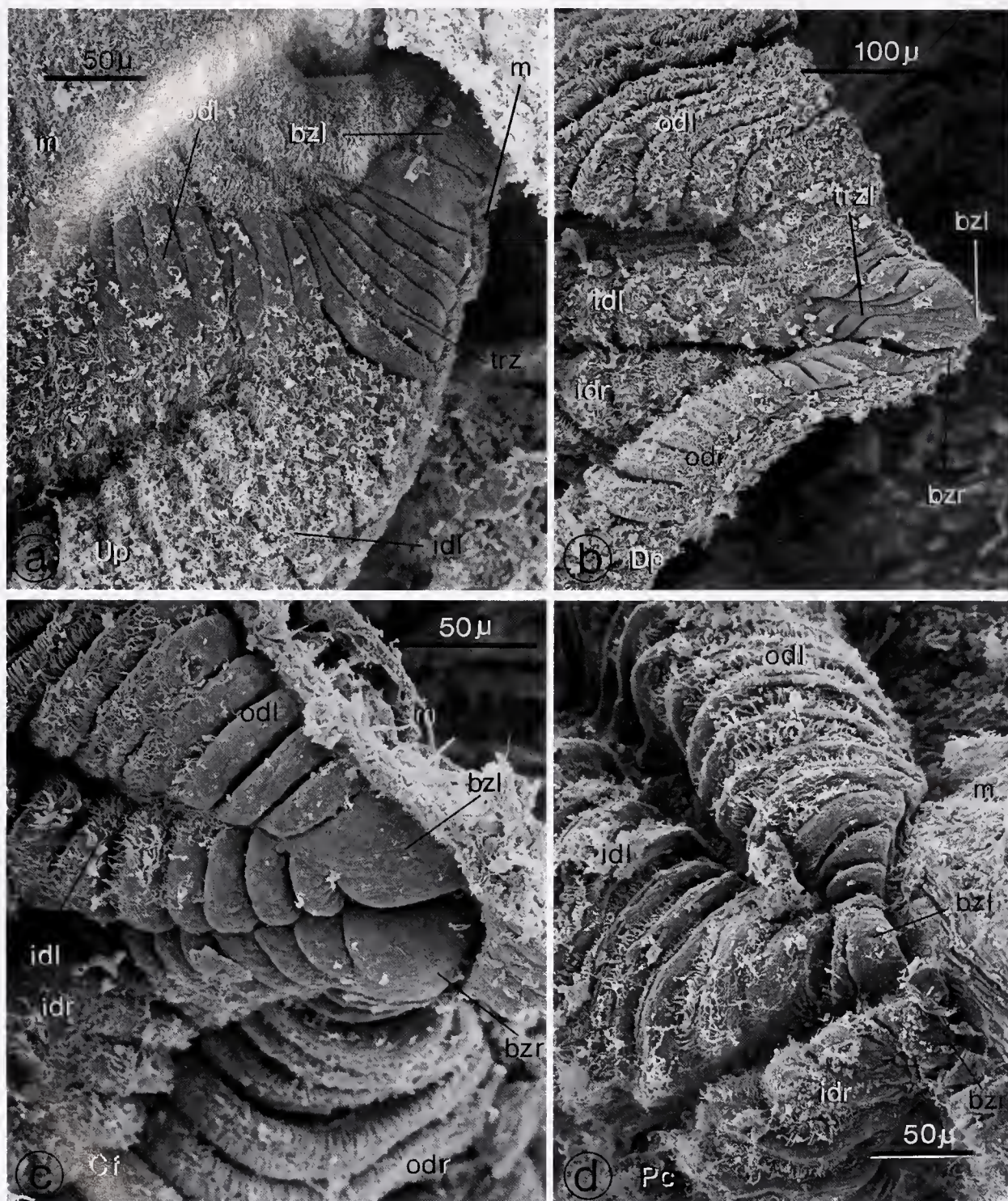


Figure 4. Scanning electron micrographs of the budding zones and the start of both lobule and demibranch differentiation in four eulamellibranch bivalves. (a) *Unio pictorum* (Up; shell length 1.7 cm); (b) *Dreissena polymorpha* (Dp; 1.8 cm); (c) *Corbicula fluminea* (Cf; 0.9 cm); and (d) *Pisidium casertanum* (Pc; 2.1 mm). The budding zones of the left and right gills (bzl, bzl) may lie next to each other, as in Dp, Cf, and Pc. Each is differentiating into the lobules of the separating inner and outer demibranchs (idl, odl, and idr, odr). In *Unio*, a transition zone (trz) of about six transverse folds is shown. m: mantle.

tern. The transition zone consisted of three folds at this stage.

#### *Lobule differentiation in eulamellibranchs*

Histological sections of a subadult specimen of *Unio* (Fig. 5) were examined to follow the differentiation of the lobules into the filaments of eulamellibranch gills. The posterior end of the gill, that is, the budding zone, reveals the character of an undifferentiated tissue with a high density of nuclei (Fig. 5a). New transverse folds are added to the already differentiated gill from the budding zone. The longitudinal splitting of the folds into two rows of lobules (representing the inner and outer demibranch) is clearly visible in Figure 5b. The development of these lobules into extended lobes (still unfenestrated) is followed by those differentiations that continuously transform the lengthening lobes into the complexly structured filaments of the eulamellibranchs. Three processes can be distinguished during this development. As they cannot be followed in only one frontal section, we present sections of different levels (Fig. 5a–c).

The first skeletal rods (grayish opaque, no nuclei) are formed in the late transition zone during the beginning of demibranch formation. At first, these rods seem to be confined to the gill base between the inner and outer demibranchs (Fig. 5a); later they extend into the filaments.

The other processes of lobule differentiation can be seen in Figure 5c. Tissue bridges representing interfilament junctions occur between adjacent lobes (ifj in Fig. 5c). As documented further, interlamellar spaces appear in the laminae of most lobes (ils in Fig. 5c). In some lobes, the lamina remains unchanged and constitutes an interlamellar junction (ilj in Fig. 5c). When the demibranchs of eulamellibranchs are observed *in situ*, the lamellae appear filamentous because the outer ciliated margins of the lobes have differentiated into the descending and ascending limbs of the so-called filament. However, this filamentary appearance is due to no more than the outermost 50  $\mu\text{m}$  of the tissue, which bears the ciliary machinery and the vertical hemolymph vessels of the gill.

#### *Outer demibranch formation in juvenile unionids*

The dorsal mantle cavity of a 3.5-mm-long specimen of *Unio pictorum* revealed no indication of filaments of the outer demibranch (Fig. 1b). However, six short filaments of the outer demibranch were identified in frontal sections of a *U. pictorum* specimen of 4.9-mm shell length. Apart from the anterior one, these were already differentiated in that they were fused at their outer margins with the mantle epithelium.

Because the development of the outer demibranch lags behind that of the inner, the two demibranchs differ in filament number, in gill-base length, and in demibranch height (as expressed by the length of the longest filament in

the row; Fig. 1a). In Figure 6 the height of the demibranch in juveniles is plotted against shell length, up to 17 mm (years 1–3, based on the number of growth rings). The data for both *Unio* species were pooled because no species-specific deviation was found when they were tested separately ( $P > 0.1$ ). The linear regressions of maximum filament length *versus* shell length were significantly different with respect to the intercepts for the inner and outer demibranchs ( $P < 0.001$ ). The slopes differed only marginally ( $P = 0.051$ ).

In the case of the smallest *Unio* specimen in which an outer demibranch was observed (shell length 4.9 mm), the anteriormost filament of the outer demibranch was located next to the 27th filament of the inner demibranch. In larger specimens, we never found such a large difference in filament number at the anterior margins of inner and outer demibranchs; usually the difference was 10–12 filaments ( $n = 10$  specimens with shell lengths between 6.9 and 14.6 mm). Along the whole gill axis, the skeletal rods of parallel filaments of inner and outer demibranchs touched each other at the gill base, resulting in the strict 1:1-arrangement of filaments already shown in Figure 5a.

### Discussion

The terminal growth zone of bivalve gills was described based on dissections, scanning electron micrographs, and histological sections. Despite the anatomical differences of the three main gill types (protobranchs, filibranchs, and eulamellibranchs), gill formation in juveniles and adults of 13 species shows a common and uniform pattern. The increase in the number of leaflets in protobranchs, and of filaments in filibranchs and eulamellibranchs, starts from an undifferentiated cell complex that we termed the 'budding zone'. This growth zone generates a series of transverse, paired lobules that constitute, in a 1:1-relationship, both the inner and outer demibranch. The lobules grow into extended and elongated lobes that become transformed into leaflets in protobranch gills and into filaments in filibranch and eulamellibranch gills.

The budding zone should be seen as a specific, undifferentiated complex of dividing cells that is active in growing bivalves. This terminal zone can be characterized as meristem-like because it produces new gill elements during the whole life of these animals, similar to the formation of new leaves from a shoot apical meristem in higher plants, or the development of new polyps from a terminal cell complex in the elongating stems or stolons of thecate hydrozoans (Berking *et al.*, 2002).

One may assume that this terminal growth zone is a projection of the postlarval gill axis composed of peripheral ectodermic and internal mesodermic cells. The budding zone either first produces transversal folds (in cases of delayed splitting into inner and outer demibranch lobules, as in *Mytilus*, *Unio*, *Dreissena*, *Venerupis*, *Mya*) or it directly

forms lobules (in cases of simultaneous splitting of the demibranchs: *Nucula*, *Anadara*, *Corbicula*, *Pisidium*). The segregation may resemble the first steps of somitic segmentation in the early embryology of segmented animals (Wolpert *et al.*, 1998), accompanied by a change in cell adhesion between distinct blocks of ectodermic cells.

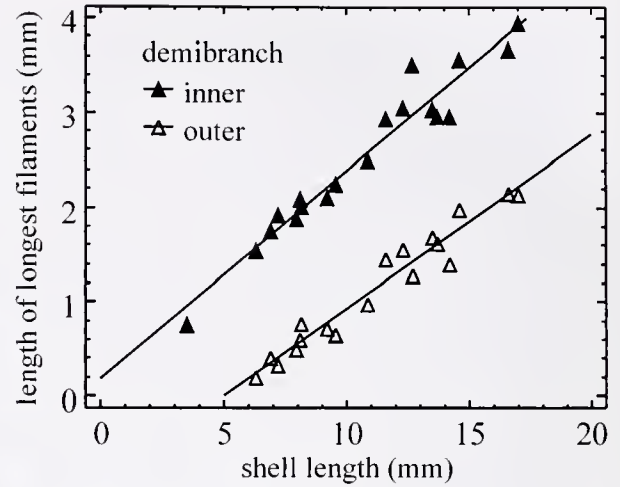
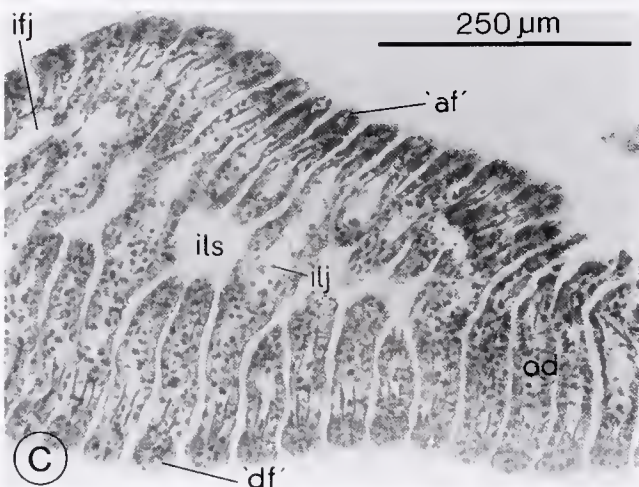
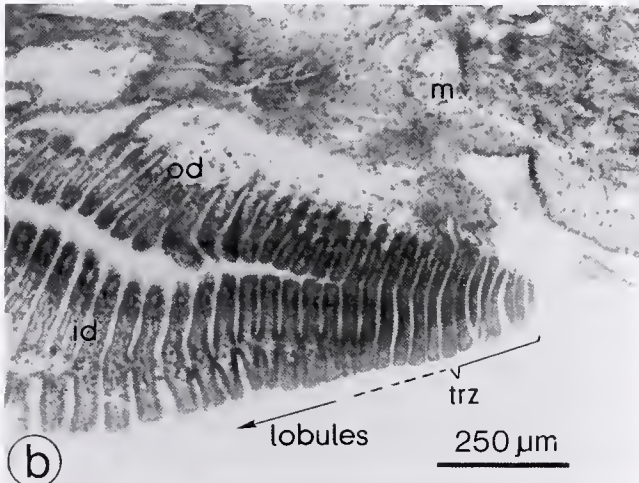
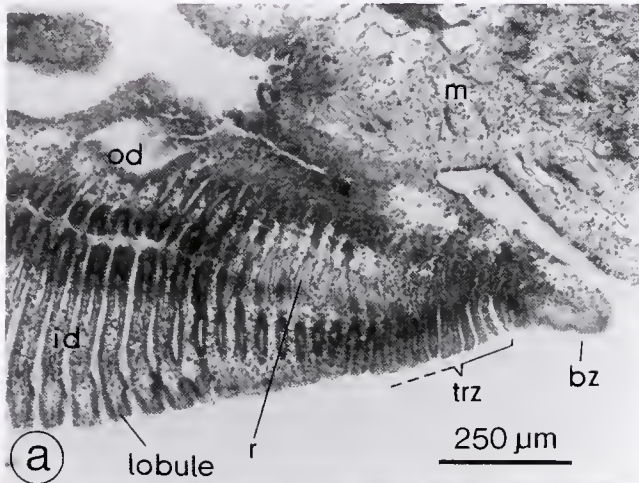


**Figure 6.** Length of the longest filaments of the inner and outer demibranchs (solid and open triangles, respectively) in *Unio pictorum* and *U. tumidus* specimens of different shell lengths (pooled data of both species). The regression lines are  $y_{id} = 0.22(\pm 0.01)x + 0.17(\pm 0.15)$ , ( $r = 0.97$ ) in the case of the inner demibranchs; and  $y_{od} = 0.19(\pm 0.01)x - 0.93(\pm 0.13)$ , ( $r = 0.97$ ) in the case of the outer demibranchs.

The conformity of initial lobule formation in all bivalves tested supports the monophyly of this class. In *Nucula*, the protobranch gill closely resembles the ctenidia of prosobranch gastropods, because both consist of a series of leaflets along a gill axis (Yonge, 1947). This simple gill structure is distinct from the more complex gills in the rest of the bivalves. Based on morphological and molecular data sets, the Protobranchia are therefore considered to be a sister group to the other bivalves, which are grouped as Autobranchia (Hoeh *et al.*, 1998; Giribet and Wheeler, 2002).

In the Autobranchia, the gills are adapted to additional functions, such as feeding and breeding. The decisive evolutionary step was the strong elongation of the lobe. The lobe's transformation into filibranch or eulamellibranch filaments can be understood as a series of developmental steps correlated with increasing efficiencies of the gill's various functions. Fossil records (Cope, 1996) as well as morphological and molecular data (Hoeh *et al.*, 1998; Giribet and Wheeler, 2002) indicate that the filibranch gill represents

**Figure 5.** Frontal (horizontal) sections (slightly slanted) through the posterior end of the left gill of a subadult *Unio pictorum* (shell-length 20 mm). (a) Section near the gill base with the undifferentiated budding zone (bz), and with a transition zone (trz) and the beginning of lobe differentiation via lobules. (b) The same section (about 30  $\mu\text{m}$  ventral of section a), showing the increasing gap between inner and outer demibranch (id, od). (c) Section of the outer demibranch, ventral to the left part of section b, revealing further details of the differentiation of lobules into early filaments with interfilamentar junctions (ifj), interlamellar spaces (ils), and interlamellar junctions (ilj). 'af': ascending limb of filament, 'df': descending limb of filament, m: mantle tissue, r: rod structure inside the gill base connecting the inner and outer demibranchs.

the plesiomorphic type, and that the eulamellibranch gill characters evolved polyphyletically.

Because lobules and lobes are the primary structural elements, it is interesting to follow their successive transformation into the so-called filaments. The present study confirms that neither bending nor folding of filamentary structures occurs in juvenile and adult bivalves. The final V-shape of the filaments results from the continuous transformation of a lobular anlage *via* lobes into filaments by a dominating ventral growth zone near the tip of the filaments. Evidence of high mitotic activities in this zone was observed in adult filibranchs (*Crenomytilus*, *Mytilus*) by H<sup>3</sup>-thymidine autoradiographical labeling (Leibson and Movchan, 1975). This result perfectly correlates with our conclusion, which is based on the pattern of equidistant lines of ciliated knobs. Leibson and Movchan (1975) detected two additional areas of DNA-synthesizing activities in *Mytilus*. Both were situated close to the dorsal food grooves, one at the gill base, the other one at the dorsal apex of the filament's ascending limb. As these authors already stated, further studies are needed to investigate whether these two areas represent additional growth zones of the filaments or a higher renewal rate of epithelium cells. In any event, during the transformation of lobes into filaments and the succeeding elongation, no bending or reflection occurs; as declared by Yonge (1947, p. 501): "this mode of origin is impossible." The convenient terms '*descending limb*' and '*ascending limb*' are referring neither to the direction of growth of the filaments, nor to the direction of hemolymph flows, because both arterial and venous lacunae (separated by an intrafilamentar septum; Ridewood, 1903) are located inside the limbs (Yonge, 1947; Kiliyas, 1956; our observations on *Anadara*).

In the early development of the unidirectional slender filaments in postlarvae, developmental processes similar to those described above seem to occur. One could term them '*pro-filaments*' because they strongly differ from the filaments in adults. Based on scanning electron microscopy figures of juveniles of the pseudolamellibranch *Ostrea chilensis* (Chaparro *et al.*, 2001) it may be inferred that growth occurs without bending; the gill rudiments (*e.g.*, pp. 201–203; Fig. 1c, Fig. 2a) perfectly correspond to compact transverse structures, *i.e.*, lobules. During postlarval development of the eulamellibranch Veneridae, the unidirectional filaments of the inner demibranch display a thickened distal end and transform into V-shaped filaments without any bending (Ansell, 1962; Mouëza *et al.*, 1999). This thickened end may be recognized as a kind of lobule. Corresponding conclusions may be derived from the thickened ends of the filaments presented in figures of *Pecten* (Beninger *et al.*, 1994), freshly metamorphosed *Unio* (Herbers, 1913) and juvenile *Sphaerium* (Wasserloos, 1911, figs. K, L).

The onset of the outer demibranch formation and its delay in the Autobranchia reveals two further interesting developmental aspects, as shown in *Unio pictorum* and *U. tu-*

*midus*. Firstly, a certain body size must be reached before outer demibranch development is initialized. In the *Unio* population we studied, differentiation of the outer demibranch started at shell lengths of about 4–4.5 mm. Specimens of this size showed one growth ring, indicating the cessation of growth during the first winter. In contrast, Korniushin (1997) found the first filaments in 2.4-mm *Unio* specimens. Whether such a difference in the start of outer demibranch formation is due to environmental or genetic factors remains unclear. Secondly, at the anterior end of the gill axis, the number of filaments in inner and outer demibranchs differs. The difference is size-dependent and decreases in larger juveniles. Such a decrease in the difference of anterior filament number was also observed in several other eulamellibranch species (Korniushin, 1997). A reduction of the foremost filaments of the inner demibranch seems to be unlikely, because all filaments were completely differentiated at the 4.9-mm stage; *i.e.*, they were fused to the foot and were functionally integrated. We hypothesize that the outer demibranch also extends its range at its anterior end where—during a short developmental period—a limited number of lobules differentiate from the gill axis in parallel to the filaments of the inner demibranch.

In summary, the generation of simply structured lobules from the posterior budding zone and their differentiation into protobranch leaflets, filibranch filaments (interlamellar junctions and ciliated knobs between adjacent filaments), or more intricate structures (with complex interfilamentar junctions, as in pseudolamellibranchs and eulamellibranchs) may be an interesting model for further developmental studies, which may also offer insight into the evolution of the various gill types that occurred during the phylogeny of bivalves.

### Acknowledgments

Our sincere thanks are due to Dr. Ronald Janssen (Forschungsinstitut und Naturmuseum Senckenberg, Frankfurt a. M.) for lending *Nucula* specimens from the museum collection; to Prof. Gerard Van de Velde (Dept. of Ecology, University of Nijmegen) for acquiring the *Anadara* specimens from India; to Hans-Peter Bollhagen, Helmut Wratil (University of Cologne), and Dr. Markus Weitere (Dept. of Biology, Free University of Berlin) for SEM assistance; to Frederic Bartlett for linguistic comments; and to Prof. M. J. Greenberg and anonymous referees for valuable suggestions for improving the text.

### Literature Cited

- Ansell, A. D. 1962. The functional morphology of the larva, and the postlarval development of *Venus striatula* (Da Costa). *J. Mar. Biol. Assoc. UK* 42: 419–443.
- Bayne, B. L., J. Widdows, and R. J. Thompson. 1976. Physiology: feeding and digestion. Pp. 121–206 in *Marine Mussels: Their Ecology and Physiology*. B. L. Bayne, ed. Cambridge University Press, Cambridge.

- Beninger, P. G., M. Le Pennec, and M. Salaün. 1988.** New observations of the gills of *Placopecten magellanicus* (Mollusca: Bivalvia), and implications for nutrition 1. General anatomy and surface micro-anatomy. *Mar. Biol.* **98**: 61–70.
- Beninger, P. G., S. A. P. Dwiono, and M. Le Pennec. 1994.** Early development of the gill and implications for feeding in *Pecten maximus* (Bivalvia: Pectenidae). *Mar. Biol.* **119**: 405–412.
- Berking, S., M. Hesse, and K. Herrmann. 2002.** A shoot meristem-like organ in animals: monopodial and sympodial growth in Hydrozoa. *Int. J. Dev. Biol.* **46**: 301–308.
- Chaparro, O. R., J. A. Videla, and R. J. Thompson. 2001.** Gill morphogenesis in the oyster *Ostrea chilensis*. *Mar. Biol.* **138**: 199–207.
- Cope, J. C. W. 1996.** The early evolution of the Bivalvia. Pp. 361–370 in *Origin and Evolutionary Radiation of the Mollusca*, J. Taylor, ed. Oxford University Press, Oxford.
- Drew, G. A. 1901.** The life-history of *Nucula delphinodonta* (Mighels). *Q. J. Microsc. Sci.* **44**: 313–391.
- Giribet, G., and W. Wheeler. 2002.** On bivalve phylogeny: a high-level analysis of the Bivalvia (Mollusca) based on combined morphology and DNA sequence data. *Invertebr. Biol.* **121**: 271–324.
- Gros, O., L. Frenkiel, and M. Mouëza. 1998.** Gill filament differentiation and experimental colonization by symbiotic bacteria in aposymbiotic juveniles of *Codakia orbicularis* (Bivalvia: Lucinidae). *Invertebr. Reprod. Dev.* **34**: 219–231.
- Herbers, K. 1913.** Entwicklungsgeschichte von *Anodonta cellensis* Schröt. *Z. Wiss. Zool.* **108**: 1–174.
- Hoeh, W. R., M. B. Black, R. Gustafson, A. E. Bogan, R. A. Lutz, and R. C. Vrijenhoek. 1998.** Testing alternative hypotheses of *Neotrigonia* (Bivalvia: Trigonioidea) phylogenetic relationships using cytochrome c oxidase subunit I DNA sequences. *Malacologia* **40**: 267–278.
- Jackson, R. T. 1890.** Phylogeny of the Pelecypoda: the Aviculidae and their allies. *Mem. Bost. Soc. Nat. Hist.* **4**: 277–394.
- Kilius, R. 1956.** Über die Kieme der Teichmuschel (*Anodonta* Lam.) (Ein Beitrag zur Anatomie). *Mitt. Zool. Mus. Berl.* **32**: 151–174.
- Korniushin, A. V. 1997.** Patterns of gill structure and development as taxonomic characters in bivalve molluscs (Mollusca Bivalvia). *Ann. Zoologici* **46**: 245–254.
- Leibson, N. L., and O. T. Movchan. 1975.** Cambial zones in gills of Bivalvia. *Mar. Biol.* **31**: 175–180.
- Mitsukuri, K. 1881.** On the structure and significance of some aberrant forms of lamellibranch gills. *Q. J. Microsc. Sci.* **21**: 595–608.
- Morton, B. 1996.** The evolutionary history of the Bivalvia. Pp. 337–359 in *Origin and Evolutionary Radiation of the Mollusca*, J. D. Taylor, ed. Oxford University Press, Oxford.
- Mouëza, M., O. Gros, and L. Frenkiel. 1999.** Embryonic, larval and postlarval development of the tropical clam, *Anomalocardia brasiliiana* (Bivalvia, Veneridae). *J. Molluscan Stud.* **65**: 73–88.
- Purchon, R. D. 1968.** *The Biology of the Mollusca*. Pergamon Press, Oxford.
- Raven, Chr. P. 1966.** *Morphogenesis: The Analysis of Molluscan Development*. Pergamon Press, Oxford.
- Ridewood, W.G. 1903.** On the structure of the gills of the Lamelli-branchia. *Philos. Trans. R. Soc. Lond. B* **1905**: 147–284.
- Romeis, B. 1968.** *Mikroskopische Technik*. Oldenburg, Munich.
- Waller, T. R. 1981.** Functional morphology and development of the veliger larvae of the european oyster, *Ostrea edulis* Linné. *Smithson. Contrib. Zool.* **328**: 1–70.
- Wasserloos, E. 1911.** Die Entwicklung der Kiemen bei *Cyclas cornea* und anderen Acephalen des süßen Wassers. *Zool. Jahrb. Anat.* **31**: 171–284.
- Wolpert, L., R. Beddington, J. Brockes, Th. Jessell, P. Lawrence, and E. Meyerowitz. 1998.** *Principles of Development*. Current Biology, London.
- Yonge, C. M. 1947.** The pallial organs in the aspidobranch gastropoda and their evolution throughout the mollusca. *Philos. Trans. R. Soc. Lond. B* **232**: 443–518.

# Demonstration of Nutrient Pathway From the Digestive System to Oocytes in the Gonad Intestinal Loop of the Scallop *Pecten maximus* L.

PETER G. BENINGER<sup>1\*</sup>, GAËL LE PENNEC<sup>2</sup>, AND MARCEL LE PENNEC<sup>2</sup>

<sup>1</sup>Laboratoire de Biologie Marine, Faculté des Sciences, Université de Nantes, 44322 Nantes Cédex, France; and <sup>2</sup>Institut Universitaire Européen de la Mer, Université de Bretagne Occidentale, Site Technopôle Brest-Iroise, 29280 Plouzané, France

**Abstract.** The mechanism of nutrient transfer from the digestive system to the gonad acini and developing oocytes was investigated in the gonad-intestinal loop system of the queen scallop *Pecten maximus* L. Ferritin was injected directly into the purged intestine of specimens from the wild. Subsequently, a histochemical reaction and transmission electron microscopy were used to localize ferritin in various cell types. Ferritin was rapidly absorbed by the intestinal epithelium, and then appeared in hemocytes in the surrounding connective tissue. In the hemocytes, ferritin was stored in variously sized inclusions, as well as in the general cytoplasm. In all sections examined for the 12 experimental individuals, hemocytes were always found in association with connective tissue fibers extending from the base of the intestinal epithelium to gonad acini. After 30-min incubation, ferritin appeared inside the acini of all individuals. Ferritin-bearing cells were rarely found in association with male acini or gametes, nor with mature female gametes, but often with developing female gametes. Not all individuals showed the same temporal dynamics of ferritin transport, suggesting that nutrient transfer to oocytes is either not a continuous process, or that among individuals, transfer is not synchronized on short time scales. This is the first demonstration of a pathway of nutrient transfer from the intestine, and more generally the digestive system, to developing oocytes in the Bivalvia.

## Introduction

In the Bivalvia, the digestive and reproductive systems are closely situated and often intertwined, either within the visceral mass (the majority of bivalves), or more distinctly separated from the visceral mass, as in the Pectinidae (Galtsoff, 1964; Morales-Alamo and Mann, 1989; Beninger and Le Pennec, 1991; Morse and Zardus, 1997). The ultrastructural characteristics of gametogenesis have only recently begun to be elucidated in this class (Pipe, 1987a, b; Dorange and Le Pennec, 1989; Eckelbarger and Davis, 1996a, b). However, gametogenesis must rely on the transfer of nutrients, which are acquired almost exclusively by other tissues or organs and transferred to the gonad.

Transfer of nutrients from storage or digestive sites to the gonad has been inferred or demonstrated in a number of bivalve species (Goddard and Martin, 1966; Vassallo, 1973; Ansell, 1974; Comely, 1974; Gabbott, 1975, 1983; Adachi, 1979; Zaba, 1981; Lubet *et al.*, 1987; Le Pennec *et al.*, 1991a, b). Although successful gamete production relies on such transfers, very little is known about the underlying pathways and mechanisms. The elaboration of oocyte reserves has been the subject of considerable research in many invertebrates, but is largely lacking in bivalves (see Eckelbarger and Davis, 1996a, for review). Regardless of whether bivalve gametes ultimately elaborate vitelline reserves using autotrophic (Suzuki *et al.*, 1992) or heterotrophic pathways (as suggested by Eckelbarger and Davis, 1996a), or both, it is clear that nutrients must be made available, largely from the diet, for the synthesis of the gametes and their reserves.

A summary of known or inferred pathways that transfer nutrients to the gonad acini and gametes has been outlined

Received 21 November 2000; accepted 4 June 2003.

\* To whom correspondence should be addressed. E-mail: Peter.Beninger@Isomer.univ-nantes.fr

for the queen scallop, *Pecten maximus*, based on anatomical, ultrastructural, and histochemical observations (Le Pennec *et al.*, 1991a). In particular, transfer of nutrients from the intestine to the developing gametes was proposed. Although it has long been known that both extracellular and intracellular digestion take place in the intestine of bivalves (Zacks, 1955; Reid, 1966; Payne *et al.*, 1972; Mathers, 1973; Teo and Sabapathy, 1990), the persistence of the "conventional wisdom" that the intestine merely serves as a conduit for undigested matter prompted Purchon (1971) to call for a reexamination of the role of this organ. In the family Pectinidae, the intestine loops within the otherwise anatomically distinct gonad, and indeed Le Pennec *et al.* (1991a) provided data suggesting that nutrients are transferred from this structure to developing gametes. They also proposed a transfer mechanism and pathway involving hemocytes. Enzymatic and detailed ultrastructural studies subsequently showed that the scallop intestinal loop is capable of digestion and assimilation (Le Pennec *et al.*, 1991b). This research provided a framework for the demonstration of transfer pathways using direct physiological techniques such as labeling. In this study, therefore, we have used ferritin as a marker to examine the proposed transfer pathway from the gonad intestinal loop to gonadal tissue in the scallop *Pecten maximus*.

Ferritin is an iron-containing transfer protein, consisting of a core of up to 4300 iron cations in the form of ferric oxyhydroxide and ferric phosphate, and a protein shell of approximately 450,000 Da (Miksys and Saleuddin, 1986). In the specific tissues of living organisms which contain ferritin, the molecules are often grouped into variously sized clusters, with a near-crystalline appearance (Bottke and Sinha, 1979; Miksys and Saleuddin, 1986). A specific stain for iron can therefore be used to distinguish it from other proteins (Bockman and Winborn, 1966; Heneine *et al.*, 1969; Block *et al.*, 1981; Bottke *et al.*, 1982; Boucher-Rodoni and Boucaud-Camou, 1987; Paar *et al.*, 1992; Ito *et al.*, 1992). Ferritin is also visible in uncontrasted transmission electron microscopy (TEM) sections as small, variously sized electron-dense clusters (Bottke and Sinha, 1979; Miksys and Saleuddin, 1986). Ferritin has been used both to demonstrate intestinal absorption mechanisms (Bockman and Winborn, 1966; Boucher-Rodoni and Boucaud-Camou, 1987) and to study mechanisms of uptake into the ferritin-rich yolk of snail oocytes (Bottke *et al.*, 1982). In this study we use ferritin as a substrate model with which to follow the transfer of nutrient molecules from the intestine to the gonadal tissue of *Pecten maximus*. Although hemoglobin is present in the hemocytes of some bivalve families (see reviews by Reid, 1966; Bonaventura and Bonaventura, 1983), none has yet been reported in the pectinids, and in any event, this substance cannot confound histochemical detection of injected ferritin since the iron of hemoglobin cannot be demonstrated histochemically without total de-

struction of histochemical sections (Kiernan, 1990). Control for the eventual presence of naturally occurring ferritin can be accomplished through the use of control subjects.

Pectinids are ideal candidates for such experiments, because the gonad-intestinal complex is well-separated from the other organs. *Pecten maximus* was chosen in part because it is a simultaneous hermaphrodite, thus allowing investigation of both male and female components within the same individual under identical experimental conditions. The gonad intestinal loop of pectinids also presents the advantage of being easily visible throughout most of the reproductive cycle. No respiratory function has yet been ascribed to bivalve hemocytes, and bivalve plasma generally lacks circulating respiratory pigments (Booth and Mangum, 1978), obviating possible artifacts.

### Materials and Methods

Twelve specimens of *Pecten maximus* (size range 9–10 cm shell length, antero-posterior axis) were collected from the Bay of Brest (Finistère, France). The valves of each scallop were kept open with a wedge in the posterior dorsal region, and the proximal part of the descending intestinal loop was located by directing a cold light source at the male portion of the translucent gonad (see Fig. 1). Into this portion of the intestine in each scallop, 1 ml of a 4 mg ml<sup>-1</sup> solution of cadmium-free ferritin (Sigma horse spleen Type

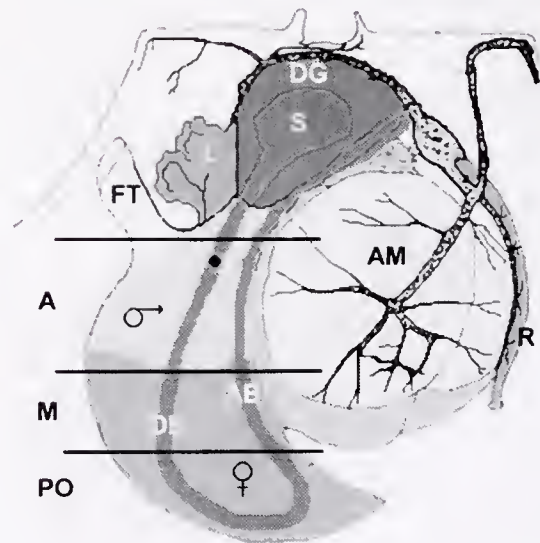


**Figure 1.** *Pecten maximus*. Schematic diagram to show planes of section in anterior (A), median (M), and posterior (PO) gonad levels. Histological sections were performed on these planes, such that the region of the median level surrounding the descending branch of the intestinal loop (DB) contained predominantly male acini, whereas the region of the median level surrounding the ascending branch of intestinal loop (AB) contained predominantly female acini. AM, adductor muscle; DG, digestive gland; FT, foot; L, lips; R, rectum; S, stomach; ♂, male, and ♀, female parts of gonad.

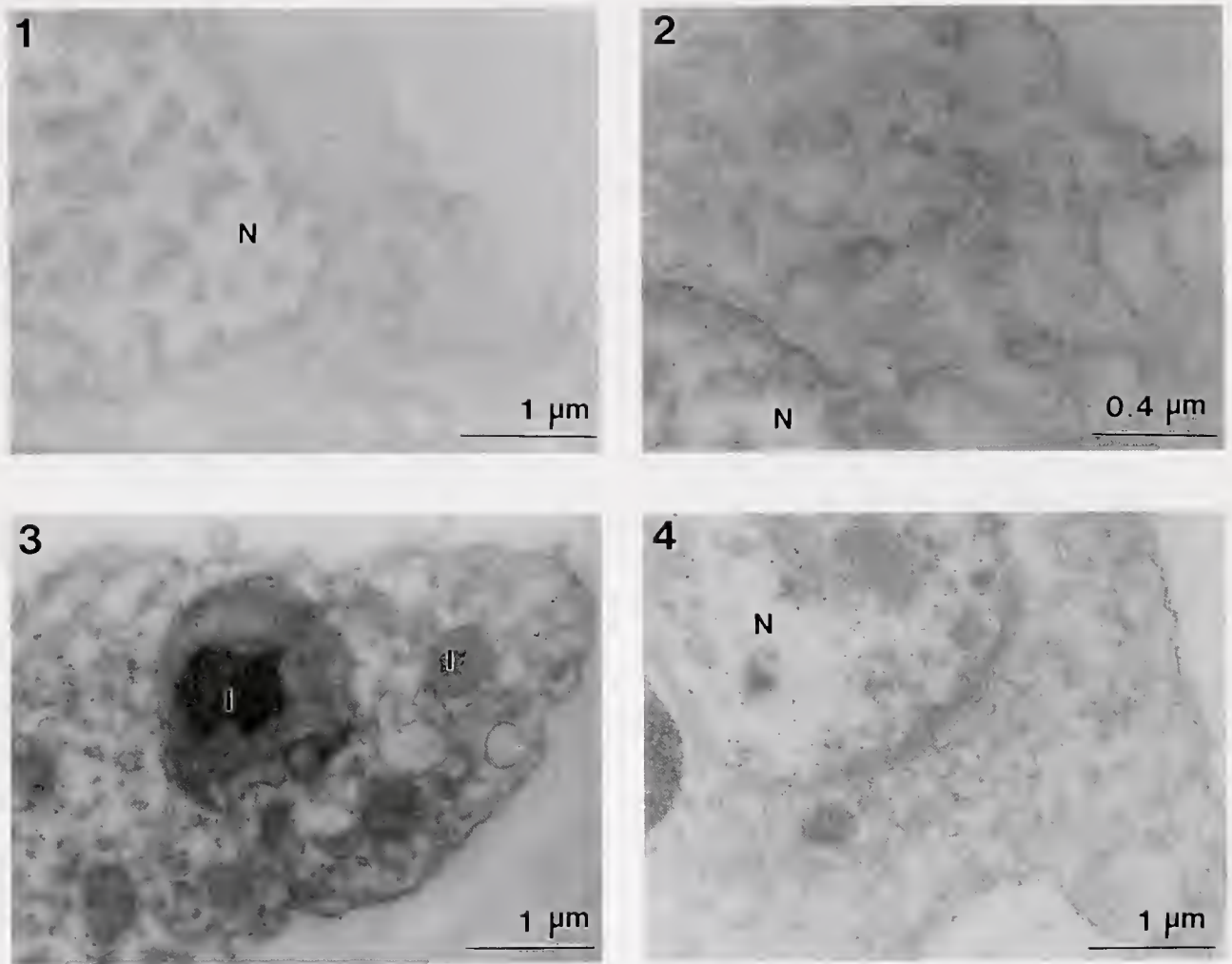


**Figure 2.** Transmission electron micrographs of uncontrasted oocytes and hemocytes in posterior (female) region of gonad, from individuals which had not been injected with ferritin. **2.1, 2.2** Details of early-developing oocytes at two magnifications (20,000 and 40,000  $\times$ , respectively). **2.3** Detail of rounded hemocyte, showing non-ferritin-containing inclusions (I); **2.4** Detail of pseudopod-bearing hemocyte. Note absence of ferritin clusters in all micrographs. N, nucleus.

1, 10–12 nm diameter molecules) was slowly injected. Complete distribution of ferritin throughout the length of the intestinal lumen was monitored visually by the appearance of the colored solution in the ascending branch. The scallops were divided into four groups of three individuals each, corresponding to 10, 30, 120, and 300 min of exposure to the ferritin solution. Exposure was carried out in 15°C filtered seawater, which was aerated with a pump and airstone. Following the designated period of exposure, the scallops were immediately dissected. Transverse slices of the gonad (about 1–2 mm thick) were removed at three levels along the antero-posterior axis of the gonad as shown in Figure 1, and immediately processed for histology and electron microscopy. To control for the eventual presence of clusters of endogenic ferritin molecules or other electron-dense particles, a control group of three individuals was

injected with 0.8  $\mu\text{m}$  filtered seawater, and processed for histology as detailed below.

#### Histology

Slices of gonad were fixed for histology in aqueous Bouin's solution (24 h), dehydrated in an ascending ethanol-xylene series, and embedded in paraffin. Transverse sections corresponding to each exposure time and gonad level were cut at 5  $\mu\text{m}$ , and each exposure series for a given level were positioned on a single microscope slide. The slides were then immersed in 35% ammonium sulfite for 2 h and rinsed with Milli-Q-filtered ultrapure water (all glassware at this stage was also prerinsed with ultrapure water). Sections were stained using the Turnbull blue protocol,

Exposure time (min)		10					30					120					300				
Distribution stage		1	2	3	4	5	1	2	3	4	5	1	2	3	4	5	1	2	3	4	5
♂	A	[Thick line]																			
	AB	[Thick line]																			
	M DB	[Thick line]																			
♀	AB	[Thick line]																			
	PO DB	[Thick line]																			
	AB	[Thick line]																			

**Figure 3.** Dynamics of ferritin distribution in the *Pecten maximus* gonad for the three individuals at each exposure time. A, anterior region of gonad; M, median region of gonad; PO, posterior region of gonad; ♂, male portion of gonad; ♀, female portion of gonad; AB, tissues of ascending branch of intestine-gonad complex; DB, tissues of descending branch of intestine-gonad complex; 1, uptake into intestinal epithelium; 2, appearance in hemocytes within connective tissue surrounding intestine; 3, appearance in hemocytes at the outer faces of the acini; 4, appearance in hemocytes within the acini; 5, appearance in hemocytes/follicle cells appressed to oocytes. Thin line represents one individual; medium line represents two individuals; thick line represents three individuals.

counterstained with nuclear red (Gabe, 1968; Vacca, 1985), dehydrated, and mounted under coverslips for photography.

#### Transmission electron microscopy

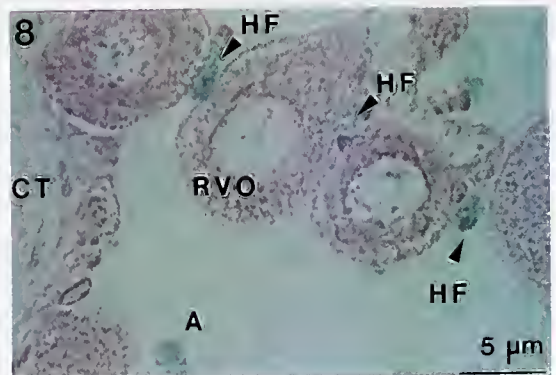
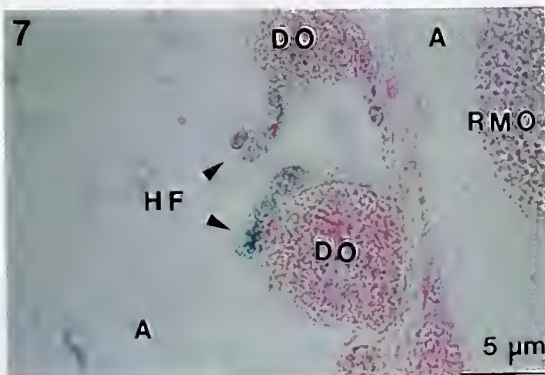
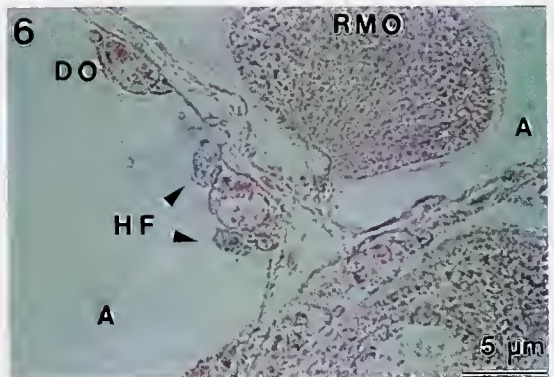
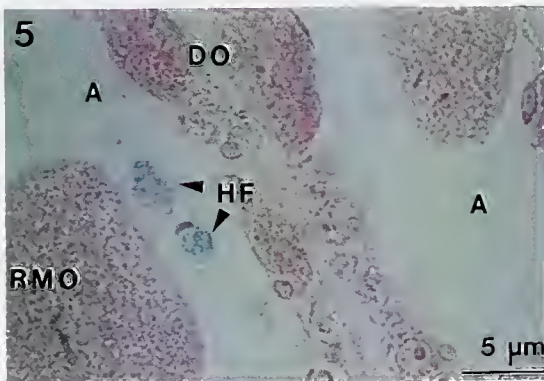
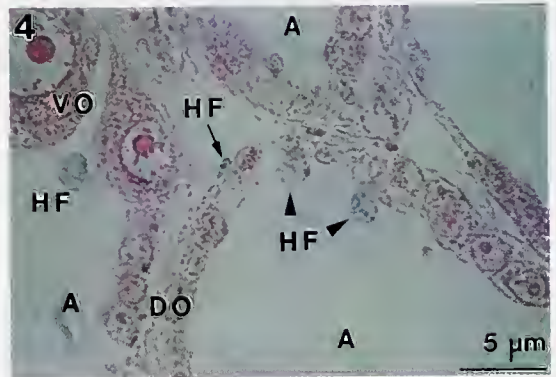
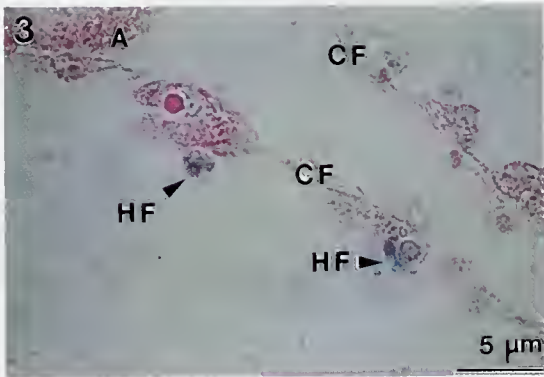
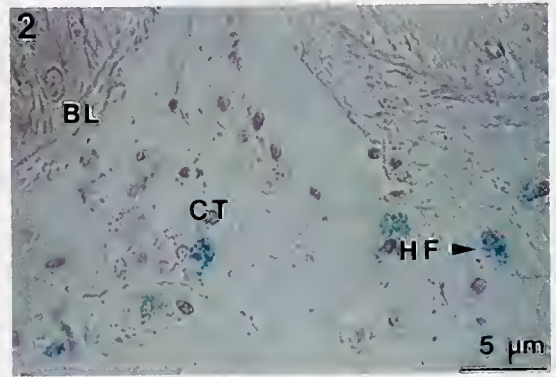
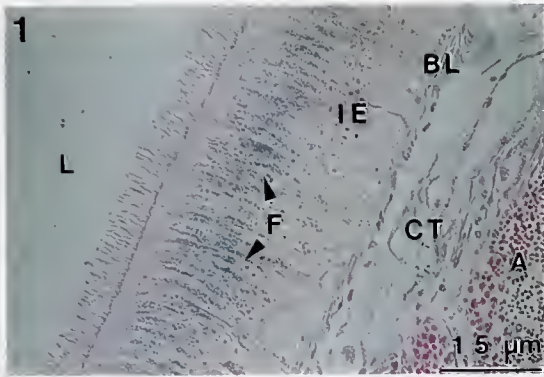
For transmission electron microscopy (TEM), the gonad slices were fixed for 10 h in cold (4°C) 2.5% glutaraldehyde–0.1 M sodium cacodylate buffer at pH 7.3 and 1100 mOsm. They were then cut into pieces of about 1 mm<sup>3</sup>, rinsed twice with the sodium cacodylate buffer solution, and post-fixed in cold 1% osmium tetroxide in buffer for 1 h. The tissue pieces were then rinsed with 70% ethanol, dehydrated in an ascending ethanol-xylene series, and embedded in Epon 812 resin. Transverse sections (400–600 nm)

were cut with a Reichert ultracut-S ultramicrotome and examined without further contrast using a JEOL 100CX transmission electron microscope. The lack of further contrasting allowed ferritin granules to be identified without ambiguity in the resulting micrographs. However, lack of contrast and the very small size of the free ferritin molecules and masses render observation *via* the fluorescent TEM screen somewhat challenging.

#### Results

As will be shown below, it is important to distinguish between oocytes in different states. Oocytes may be in development (previtellogenic and vitellogenic oocytes), or

**Figure 4.** *Pecten maximus*. Histological sections showing the presence of ferritin in the intestine and gonad. Turnbull blue-neutral red staining protocol. **4.1** Low-magnification view, after 120-min incubation, of ciliated intestinal epithelium (IE) in the anterior (male) gonad level with assimilated ferritin (F), surrounding connective tissue (CT), and adjacent acini (A) in the male region of the gonad. BL, basal lamina; L, lumen of intestine. **4.2** Basal region of intestine, in median (male + female) level of gonad after 10-min incubation, showing ferritin-containing hemocytes (HF) associated with connective tissue (CT) surrounding basal lamina (BL) of intestine. **4.3** Ferritin-containing hemocytes (HF) associated with connective tissue fibers (CF) leading from the basal lamina of the intestine to gonad acinus (A) in median (male + female) level of gonad. Incubation time: 120 min. **4.4** Ferritin-containing hemocytes (HF) positioned both at the base (→) and on the inside of gonad acini (▶), in posterior (female) level of gonad. Note proximity and association of hemocytes with developing (DO) and vitellogenic oocytes (VO) within the acinus (A). Incubation time: 30 min. **4.5** Ferritin-containing hemocytes (HF) within acinus (A) of posterior (female) level of gonad. DO, developing oocyte; RMO, residual mature oocyte. Incubation time: 30 min. **4.6** Ferritin-containing hemocytes (HF) attached to developing oocyte (DO) within acinus (A) of posterior (female) level of gonad. RMO, residual mature oocyte. Incubation time: 30 min. **4.7** Multiple large, round, ferritin-containing hemocytes (HF) attached to developing oocytes (DO) within acinus (A) in posterior (female) level of gonad. RMO, residual mature oocyte. Incubation time: 30 min. **4.8** Residual vitellogenic oocytes (RVO, late-developing stage) within an acinus (A) in posterior (female) level of gonad. Note attached large, round, ferritin-containing hemocytes/follicle cells (HF). CT, inter-acinal connective tissue. Incubation time: 120 min.



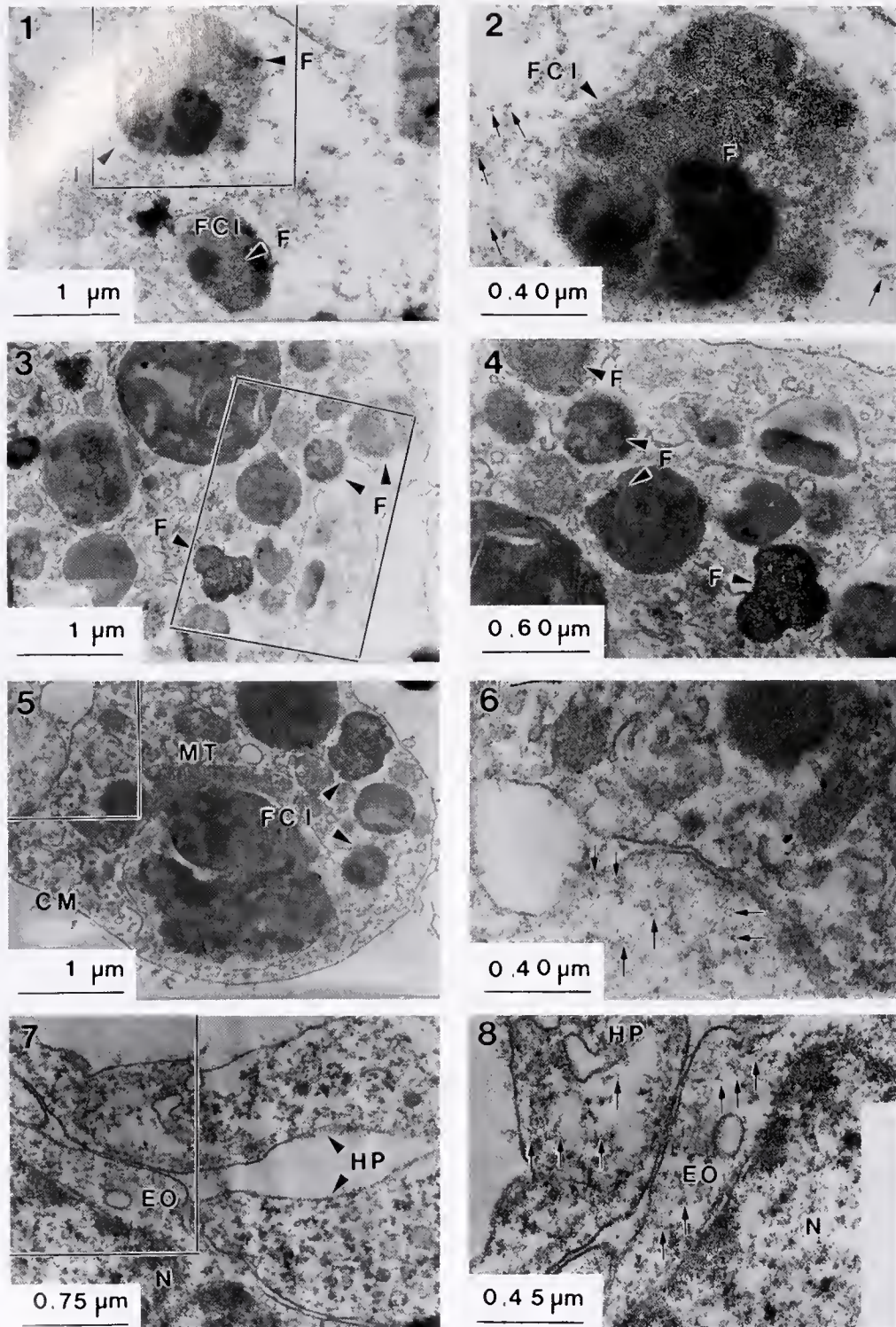


Figure 5. *Pecten maximus*. Uncontrasted transmission electron micrographs of cells in the intestine-gonad complex following ferritin injection in the intestinal lumen. 5.1 Detail of cytoplasm of absorptive cell from intestinal epithelium, in median (male + female) level of gonad showing ferritinating clusters (F) in inclusions (FCI). 5.2 Enlargement of indicated region in Fig. 4.1. Note presence of ferritin both within the inclusions and distributed freely in the cytoplasm ( $\rightarrow$ ). 5.3 Detail of a large, rounded hemocyte in the connective tissue surrounding the acini in median (male + female) level of gonad. Note presence of ferritin (F) in various sized inclusions. 5.4 Enlargement of region indicated in Fig. 4.3., showing ferritin (F) in inclusions. 5.5, 5.6 Portion

they may be mature (detached from the acinal wall). Following spawning, some oocytes of both types may remain in the acinus; these are termed residual oocytes. We will thus adopt this terminology in the present paper.

No ferritin was detected using either the Turnbull method or TEM observation (Fig. 2) in any of the control individuals; we may thus conclude that the ferritin observed in our histological and electron microscopical sections was injected.

The histological observations of the entire set of individuals and gonad levels revealed that the distribution of ferritin in the sampled tissues could be divided into 5 sequential steps: (1) uptake into intestinal epithelium, (2) appearance in hemocytes among the connective tissue surrounding the intestine, (3) appearance in hemocytes at the exterior faces of acini, (4) appearance in hemocytes within the acini, and (5) appearance in hemocytes/follicle cells appressed to oocytes. It is not possible to ascertain whether these cells were hemocytes or follicle cells in the histological sections (only TEM profiles can distinguish these cell types). The TEM profiles of these cells described below do not correspond to follicle cells, which are rich in rough endoplasmic reticulum (Dorange and Le Pennec, 1989), absent in the two pectinid hemocyte types (Beninger and Le Pennec, 1991) and in the cells observed appressed to the oocytes; however, as the TEM sections were uncontrasted, it is not possible to distinguish these cells with certainty. Although ferritin-containing hemocytes were very rarely observed associated with male spermatogonia, they were never observed appressed to developing male gametes. The distribution of ferritin among the sections is summarized in Figure 3, which presents each step in the sequence, for each gonad level, and each intestinal branch (ascending and descending), for each exposure time.

Light microscopy of the histological sections showed that ferritin was distributed in cells of the intestinal epithelium at all three antero-posterior levels of the gonad-intestinal complex, from the apex to the basal region of the columnar intestinal cells (Fig. 4). Ferritin appeared very rapidly in the intestinal cells, and was observed in all preparations, even after 10 min of exposure. TEM micrographs revealed that ferritin appeared predominantly in variously sized inclusions of the intestinal cells, although isolated granules could also be found in the cytoplasm (Fig. 5.1, 5.2). Large, round, ferritin-containing hemocytes were also detected beneath the intestinal basal lamina within the surrounding connective tissue after only a 10-min exposure (Fig. 4.2). Ferritin

appeared in these hemocytes in variously sized inclusions, as well as being generally distributed within the cytoplasm (Fig. 5.3–5.6). In all sections examined for the 12 experimental individuals, ferritin-containing hemocytes were always observed in close association with connective tissue fibers extending from the basal lamina of the intestinal epithelium and the acini (Fig. 4.2, 4.3).

Further transport of ferritin to the gonad acini and oocytes appeared to be somewhat independent of exposure time (Fig. 3). Specimens in which further ferritin transport was observed showed ferritin-containing hemocytes/follicle cells both at the outside faces of gonad acini (including those which were remote from the intestine) and inside the gonad acini (Fig. 4.3–4.8). These hemocytes/follicle cells were typically found appressed to developing oocytes (Fig. 4.3–4.8). Although no positive Turnbull blue reaction was observed in female gametes, transmission electron micrographs revealed dispersed ferritin clusters within the cytoplasm of oocytes to which ferritin-containing hemocytes/follicle cells were appressed (Fig. 5.7, 5.8).

The localization and distribution of ferritin within the various cell types involved in the transfer sequence presented notable differences, which also explains the absence of a visibly positive Turnbull reaction in some cell types. Both the intestinal cells and the transport hemocytes possessed variously sized inclusions with considerable concentrations of ferritin, and these cells presented visibly positive Turnbull reactions.

Upon histological examination, 3 of the 12 experimental scallops were observed to be mature and ready to spawn, while the remaining 9 had already spawned and had begun producing a new cohort of female gametes. Although ferritin appeared in the intestinal epithelium and surrounding connective tissue of the mature scallops, ferritin-containing hemocytes were virtually never observed, either in the acini, or appressed to the oocytes of these individuals. Moreover, despite the presence of mature residual oocytes in the acini of the individuals which had spawned previously, ferritin-containing hemocytes/follicle cells were never observed appressed to them. Ferritin-containing hemocytes/follicle cells were, however, observed appressed to late-developing residual oocytes in these individuals (Fig. 4.8).

## Discussion

The uptake of ferritin in the intestinal epithelium of *Pecten maximus*, observed in the present study, demon-

---

of a large, rounded hemocyte within an acinus in posterior (female) level of gonad, showing ferritin-containing inclusions (FCI), as well as ferritin molecules and clusters distributed freely in the cytoplasm (→). CM, cell membrane; MT, mitochondria. 5.7, 5.8 Detail of association between early developing oocyte (EO) and pseudopods of hemocyte/follicle cell (HP), in posterior (female) level of gonad. Note ferritin freely distributed in cytoplasm of both cells (→). N, nucleus.

strates that proteinaceous substrates are absorbed by the scallop intestinal epithelium, at least some of which subsequently appear in hemocytes at the cell bases. The rapidity and ubiquity of this uptake, observed in the present study, as well as the cytological and enzymatic equipment of the intestinal epithelium (Le Penneec *et al.*, 1991b), suggest that the scallop intestine is well-adapted for both a digestive and a transfer function. This result is consistent with the view of the intestine as a digestive organ in bivalves (Zacks, 1955; Reid, 1966; Payne *et al.*, 1972; Mathers, 1973; Teo and Sabapathy, 1990). The development of the gonad around the intestine optimizes the potential for the transfer of nutrients to developing gametes.

The results of the present study allow us to identify the various cell categories and pathways that mediate the entero-gonadal transfer system in bivalves: intestine epithelial cells; large hemocytes which concentrate ferritin in cytoplasmic inclusions, in addition to that present freely in the cytoplasm; and connective fibers which are often associated with the hemocytes. Previous studies have shown that hemocytes may move across the intestinal epithelium: those containing material of little or no nutritional value move toward the lumen, while those containing nutritionally valuable material move from the lumen to the tissues surrounding the intestinal epithelium (see Cheng, 1996, for review of bivalve hemocyte types and functions). The present study shows that the scallop intestinal cells may, themselves, move nutrients from the lumen to the basal lamina; hemocytes subsequently act as transport vectors to the surrounding gonad tissue. This line of investigation does not seem to have been pursued previously, despite long-held anatomical knowledge of the scallop intestine-gonad relationship.

The pathway of intestine-oocyte transfer seems to conform largely to that postulated by Le Penneec *et al.*, based on detailed histological observations (1991a). These authors proposed that nutrients assimilated by the intestinal epithelium are transferred to hemocytes at the base of the basal lamina, as observed in the present study. They further proposed that the efficiency of this transport relied upon connective tissue fibers linking the basal lamina to the acini, such that incorporated nutrients could be directed specifically to acini. In the present study, ferritin-containing hemocytes were always observed in association with connective tissue fibers between the base of the intestinal epithelium and the bases of the acini.

The asymmetry in ferritin distribution between the male and female parts of the simultaneous hermaphroditic gonad is consistent with the difference in the composition and consequent energetic demand of male and female gametes. While ferritin-containing hemocytes/follicle cells were readily observed appressed to developing oocytes, which elaborate substantial vitelline reserves, they were rarely observed within male gonad acini, which produce small

spermatozoa with few energy reserves (see Beninger and Le Penneec, 1991, for the sizes of spermatozoa and oocytes in pectinids, and Beninger and Le Penneec, 1997, for the sizes of spermatozoa and oocytes in bivalves generally); and ferritin-containing hemocytes were never observed appressed to developing male gametes. This asymmetry suggests that the entero-gonadal pathway is specific to female gametes. Another such possible distinction is described below.

The fact that ferritin-containing hemocytes/follicle cells were always found in association with developing oocytes, and never in association with mature oocytes, suggests that the ferritin-containing cells might be able to distinguish between these two states, and can supply nutrients to the oocytes most in need, *i.e.*, developing oocytes. It should be noted that the follicle cells detach from the mature oocytes of *Pecten maximus* (Dorange and Le Penneec, 1989). Although both residual mature and residual developing oocytes were observed in individuals that had recently spawned, ferritin-containing cells were only observed appressed to the residual developing oocytes, and never to the residual mature oocytes. This finding suggests that the spawning status (*i.e.*, pre-spawning or post-spawning) does not influence nutrient transport; rather, the oocyte developmental stage appears to be the determining feature of such transport, even when these gametes are destined for atresia and metabolic recycling (Pipe, 1987b; Dorange and Le Penneec, 1989; Le Penneec *et al.*, 1991a). The data of Figure 3 show that ferritin transfer to developing oocytes does not occur at a uniform rate for all individuals; indeed, after 300 min, some individuals had no ferritin-containing cells appressed to developing oocytes. While this could be due to the stress induced by the experimental procedure, it could also indicate that nutrient transfer from the intestine is not a continuous physiological activity, or that among individuals, transfer is not synchronous on such short time scales. We are unaware of any studies that present the dynamics of oogenesis on such short time scales, but this is an interesting physiological question.

While the particular scallop gonad-intestine anatomical relationship is not common in bivalves, the digestive system and gonad are generally closely associated and intertwined, with loose connective tissue containing abundant fibers between these epithelia (Galtsoff, 1964; Morales-Alarno and Mann, 1989; Morse and Zardus, 1997). These similarities to the pectinid system suggest that transfer from digestive epithelia to developing oocytes *via* a pathway similar to that described above may be a general feature of bivalve physiology.

#### Acknowledgments

The authors wish to thank Dr. Ita Widowati, Diponegoro University, Semarang, Indonesia, for having carried out

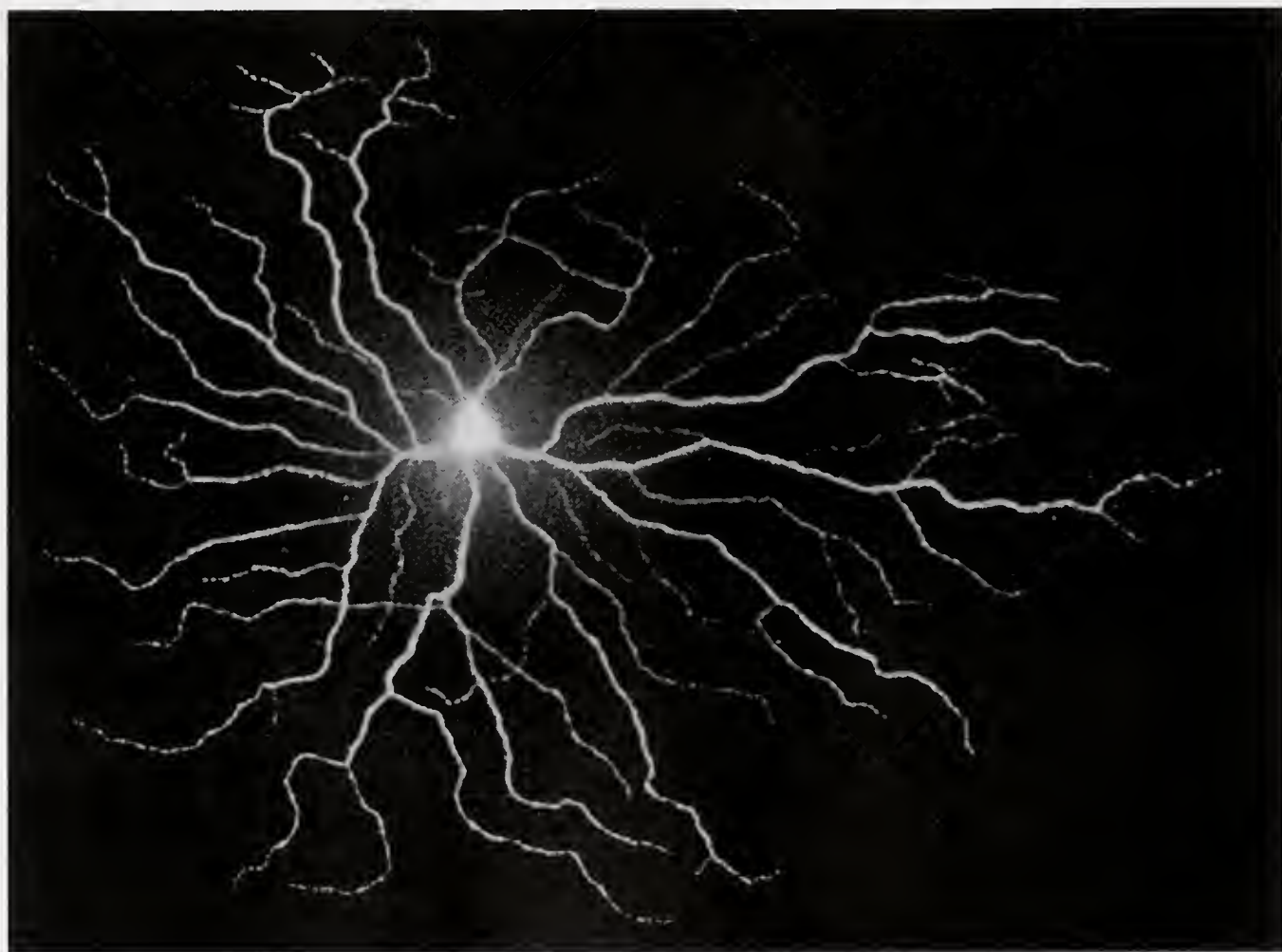
previous unpublished experiments on this subject, which guided the methodology of the present work. We are indebted to the staff of *The Biological Bulletin* for their very rigorous editorial work on this paper, which allowed us to substantially improve earlier versions of the manuscript. As a study of no direct economic or medical impact on humans, it is not possible to acknowledge funding from any of the French funding agencies.

### Literature Cited

- Adachi, K. 1979. Seasonal changes of the protein level in the adductor muscle of the clam, *Tapes philippinarum* (Adams and Reeves) with reference to the reproductive season. *Comp. Biochem. Physiol.* **64A**: 85–89.
- Ansell, A. D. 1974. Seasonal changes in the biochemical composition of the bivalve *Chlamys septemradiata* from the Clyde Sea area. *Mar. Biol.* **25**: 85–99.
- Beninger, P. G., and M. Le Pennec. 1991. Functional anatomy of scallops. Pp. 133–223 in *Scallops: Biology, Ecology and Aquaculture*, S. E. Shumway, ed. Elsevier Science Publishers B. V., Amsterdam.
- Beninger, P. G., and M. Le Pennec. 1997. Reproductive characteristics of a primitive bivalve from a deep-sea reducing environment: giant gametes and their significance in *Acharax aline* (Cryptodonta: Solemyidae). *Mar. Ecol. Prog. Ser.* **157**: 195–206.
- Block, J., A. A. Mulder-Stapel, L. A. Ginsel, and W. T. Daems. 1981. Endocytosis in absorptive cells of cultured human small-intestinal tissue: horse-radish peroxidase, lactoperoxidase and ferritin as markers. *Cell Tissue Res.* **216**: 1–13.
- Bockman, D. E., and W. B. Winborn. 1966. Light and electron microscopy of intestinal ferritin absorption. Observations in sensitized and non-sensitized hamsters (*Mesocricetus auratus*). *Anat. Rec.* **155**: 603–622.
- Bonaventura, C., and J. Bonaventura. 1983. Respiratory pigments: structure and function. Pp. 1–50 in *The Mollusca, Vol. 2: Environmental Biochemistry and Physiology*, P. W. Hochachka, ed. Academic Press, New York.
- Booth, C. E., and C. P. Mangum. 1978. Oxygen uptake and transport in the lamellibranch mollusc *Modiolus demissus*. *Physiol. Zool.* **51**: 17–32.
- Bottke, W., and I. Sinha. 1979. Ferritin as an exogenous yolk protein in snails. *Wilhelm Roux's Arch.* **186**: 71–75.
- Bottke, W., I. Sinha, and I. Kiel. 1982. Coated vesicle-mediated transport and deposition of vitellogenic ferritin in the rapid growth phase of snail oocytes. *J. Cell Sci.* **53**: 173–191.
- Boucher-Rodoni, R., and E. Boucaud-Camou. 1987. Fine structure and absorption of ferritin in the digestive organ of *Loligo vulgaris* and *L. forbesi* (Cephalopoda, Teuthoidea). *J. Morphol.* **193**: 173–184.
- Cheng, T. C. 1996. Hemocytes: forms and functions. Pp. 299–333 in *The Eastern Oyster Crassostrea virginica*, V. S. Kennedy, R. I. E. Newell, and A. F. Eble, eds. Maryland Sea Grant College, College Park, MD.
- Comely, C. A. 1974. Seasonal variations in the flesh weights and biochemical content of the scallop *Pecten maximus* L. in the Clyde Sea area. *J. Cons. Cons. Int. Explor. Mer* **35**: 281–295.
- Dorange, G., and M. Le Pennec. 1989. Ultrastructural study of oogenesis and oocytic degeneration in *Pecten maximus* from the Bay of St Brieuc. *Mar. Biol.* **103**: 339–348.
- Eckelbarger, K. J., and C. V. Davis. 1996a. Ultrastructure of the gonad and gametogenesis in the eastern oyster, *Crassostrea virginica*. I. Ovary and oogenesis. *Mar. Biol.* **127**: 79–87.
- Eckelbarger, K. J., and C. V. Davis. 1996b. Ultrastructure of the gonad and gametogenesis in the eastern oyster, *Crassostrea virginica*. II. Testis and spermatogenesis. *Mar. Biol.* **127**: 89–96.
- Gabbott, P. A. 1975. Storage cycles in marine bivalve molluscs: a hypothesis concerning the relationship between glycogen metabolism and gametogenesis. Pp. 191–211 in *Proceedings of the 9<sup>th</sup> European Marine Biological Symposium*, H. Barnes, ed. Aberdeen University Press, Aberdeen, Scotland.
- Gabbott, P. A. 1983. Development and seasonal metabolic activities in marine molluscs. Pp. 165–217 in *The Mollusca*, Vol. 2, P. W. Hochachka, ed. Academic Press, London.
- Gabe, M. 1968. *Techniques Histologiques*. Masson & Cie, Paris.
- Galtsoff, P. S. 1964. The American oyster *Crassostrea virginica* Gmelin. *Fish. Bull.* **64**: 1–480.
- Goddard, C. K., and A. W. Martin. 1966. Carbohydrate metabolism. Pp. 275–308 in *Physiology of Mollusca*, Vol. 2, K. M. Wilbur and C. M. Yonge, eds. Academic Press, New York.
- Heneine, I. F., G. Gazzinelli, and W. L. Tafuri. 1969. Iron metabolism in the snail *Biomphalaria glabrata*: uptake, storage and transfer. *Comp. Biochem. Physiol.* **28**: 391–399.
- Ito, T., H. Kitamura, Y. Inayama, A. Nazawa, and M. Kanisawa. 1992. Uptake and intracellular transport of cationic ferritin in the brachiolar and alveolar epithelia of the rat. *Cell Tissue Res.* **268**: 335–340.
- Kiernan, J. A. 1990. *Histological and Histochemical Methods: Theory and Practice*, P. 226. Academic Press, New York.
- Le Pennec, M., P. G. Beninger, G. Dorange, and Y. M. Pualet. 1991a. Trophic sources and pathways to the developing gametes of *Pecten maximus* (Bivalvia Pectinidae). *J. Mar. Biol. Assoc. UK* **71**: 451–463.
- Le Pennec, M., G. Dorange, P. G. Beninger, A. Donval, and I. Widawati. 1991b. Les relations trophiques anse intestinale-gonade chez *Pecten maximus* (Mollusque, Bivalve). *Haliotis* **21**: 57–69.
- Lubet, P., J. Y. Besnard, R. Faveris, and I. Robbins. 1987. Physiologie de la reproduction de la coquille Saint Jacques (*Pecten maximus*). *Oceanis* **13**: 265–290.
- Mathers, N. F. 1973. A comparative histochemical survey of enzymes associated with the processes of digestion in *Ostrea edulis* and *Crassostrea angulata* (Mollusca: Bivalvia). *J. Zool. Lond.* **169**: 169–179.
- Miksys, S., and A. S. M Saleuddin. 1986. Ferritin as an exogenously derived yolk protein in *Heliosoma duryi* (Mollusca: Pulmonata). *Can. J. Zool.* **64**: 2678–2682.
- Morales-Alamo, R., and R. Mann. 1989. Anatomical features in histological sections of *Crassostrea virginica* (Gmelin, 1791), as an aid in measurements of gonad area for reproductive assessment. *J. Shellfish Res.* **8**: 71–82.
- Morse, M. P., and J. D. Zardus. 1997. Bivalvia. Pp. 7–118 in *Microscopic Anatomy of Invertebrates*, Vol. 6A. F. W. Harrison and A. J. Kohn, eds. Wiley-Liss, New York.
- Paar, M., E. M. Liebler, and J. F. Pohlenz. 1992. Uptake of ferritin by follicle-associated epithelium in the colon of calves. *Vet. Pathol.* **29**: 120–128.
- Payne, D. W., N. A. Thorpe, and E. Donaldson. 1972. Cellulolytic activity and a study of the bacterial population in the digestive tract of *Scrobicularia plana* (Da Costa). *Proc. Malacol. Soc. Lond.* **40**: 147–160.
- Pipe, R. K. 1987a. Ultrastructural and cytochemical study on interaction between nutrient storage cells and gametogenesis in mussel *Mytilus edulis*. *Mar. Biol.* **96**: 519–528.
- Pipe, R. K. 1987b. Oogenesis in the marine mussel *Mytilus edulis*: an ultrastructural study. *Mar. Biol.* **95**: 405–414.
- Purchon, R. D. 1971. Digestion in filter feeding bivalves—a new concept. *Proc. Malacol. Soc. Lond.* **39**: 253–262.
- Read, K. R. H. 1983. Molluscan hemoglobin and myoglobin. Pp. 209–232 in *Physiology of Mollusca*, Vol. 2, K. M. Wilbur and C. M. Yonge, eds. Academic Press, New York.

- Reid, R. G. B. 1966.** Digestive tract enzymes in the bivalve *Lima hians* Gmelin and *Mya arenaria* L. *Comp. Biochem. Physiol.* **17**: 417–433.
- Suzuki, T., A. Hara, K. Matsuuchi, and K. Mori. 1992.** Purification and immunolocalization of a vitellin-like protein from the Pacific oyster *Crassostrea gigas*. *Mar. Biol.* **113**: 239–245.
- Teo, L. H., and U. K. Ghosh. 1990.** Preliminary report on the digestive enzymes present in the digestive gland of *Perna viridis*. *Mar. Biol.* **106**: 403–407.
- Vacca, L. 1985.** *Laboratory Manual of Histochemistry*. Raven Press, New York. 578 pp.
- Vassallo, M. T. 1973.** Lipid storage and transfer in the scallop *Chlamys hericia* Gould. *Comp. Biochem. Physiol.* **44A**: 1169–1175.
- Zaba, B. M. 1981.** Glycogenolytic pathways in the mantle tissue of *Mytilus edulis* L. *Mar. Biol. Lett.* **2**: 67–74.
- Zacks, S. I. 1955.** The cytochemistry of the amoebocytes and intestinal epithelium of *Venus mercenaria* (Lamellibranchiata), with remarks on a pigment resembling ceroid. *Q. J. Microsc. Sci.* **96**: 57–71.

# **MBL** annual report 2002



**MARINE BIOLOGICAL LABORATORY**  
Woods Hole, Massachusetts

---

The Marine Biological Laboratory does not discriminate in employment or in access to any of its activities or programs on the basis of race, color, religion, sex, sexual orientation, national origin, ancestry, age, marital status, pregnancy, physical or mental disability, or veteran status. In addition, the MBL is committed to the prevention and elimination of sexual harassment, as well as other forms of unlawful harassment, in the workplace. Through training programs and disseminated information, MBL strives to educate its employees, students, faculty, and visitors on these important issues.

| ON THE COVER: Alpha ganglion cell retina, Peter Koulen

---

The MBL Annual Report 2002 is published by the Marine Biological Laboratory. Although the greatest possible care has been taken in the preparation of this record, the Marine Biological Laboratory recognizes the possibility of omissions or inaccuracies. If any are noted, please accept our apology and advise us of any corrections to be made.

Office of Communications and Public Affairs  
Marine Biological Laboratory  
7 MBL Street  
Woods Hole, MA 02543  
Phone: (508) 289-7423  
Fax: (508) 289-7934  
[www.mbl.edu](http://www.mbl.edu)



## TABLE OF CONTENTS

R2	REPORT OF THE DIRECTOR & CEO
R7	RESEARCH
R44	EDUCATION
R63	MBL/WHOI LIBRARY
R66	FINANCIAL INFORMATION
R69	GIFTS
R85	GOVERNANCE & ADMINISTRATION

# report of the director and CEO

---



I am pleased to share with you highlights from the Marine Biological Laboratory for the year 2002. I've now served as Director and CEO of the MBL for nearly three years. I continue to be impressed with the breadth of the science

being done here, the impact that our basic research continues to have on human health as well as the environment, and the remarkable commitment our scientists, faculty, and staff have to their work and to the Marine Biological Laboratory itself.

## | Developing a Strategic Plan

Much of my time in 2002 was devoted to directing, with MBL President John Dowling and the aid of the consulting firm McKinsey & Company, a planning effort aimed at developing a strategic roadmap for the Laboratory over the next five to ten years. This process, and the recommendations emerging to date, are outlined in detail on our web site ([www.mbl.edu/inside/what/planning/index.html](http://www.mbl.edu/inside/what/planning/index.html)). Although we continue to fine-tune the plan, the initial phases of the process are largely complete.

As a result of this effort, we are already undertaking a number of key initiatives. These include developing a graduate program with Brown University, hiring a Chief Academic and Scientific Officer, establishing a new resident research program in Cellular Dynamics and Imaging, expanding the Board of Trustees, preparing for major renovations of the Whitman Building for summer and visiting research, and working with a site planner to help us further reconfigure and renovate space to meet the emerging needs of the strategic plan.

Developing the Laboratory's first strategic plan has been an exciting and illuminating process involving participation at all levels of the organization. I'm most grateful to everyone who has contributed to the experience.

## | Establishing the Program in Global Infectious Diseases

One of the highlights of the year was establishing our newest resident research program in Global Infectious Diseases. Funded by a \$5 million grant from the Ellison Medical Foundation, the Program links scientists who study disease-causing organisms with experts in molecular biology, phylogenetics, and environmental microbiology and creates a one-of-a-kind international center for research and training dedicated to studying pathogens and the complex relationships they have with their hosts.

We were fortunate to recruit leading parasitologist and molecular biologist Stephen L. Hajduk to direct the Program. Steve comes to the MBL from the University of Alabama at Birmingham where he was a Professor in the Department of Biochemistry and Molecular Genetics and Senior Scientist in the AIDS Center and the Comprehensive Cancer Center. Steve brings with him a number of students, postdocs, and technicians. In addition, we welcomed two new Assistant Scientists—Robert Sabatini and Andrew McArthur—to the Program in early 2003.

Steve's research program is broadly based in the area of molecular and biochemical basis of pathogenesis. Many of his studies focus on African trypanosomes, which cause human sleeping sickness, a fatal disease that has reemerged as a major health problem in sub-Saharan Africa.

The importance of research in infectious disease cannot be overstated. No single reason can explain our inability to eradicate or minimize the global impact of infectious agents on human health. In total, 25% of all deaths worldwide are caused by bacterial, viral, fungal, and parasitic pathogens. Every year, one to three million people die from malaria, a disease caused by the organism *Plasmodium*. Tuberculosis infects one person every second, and over the coming decade, at least 30 million will die from the disease.

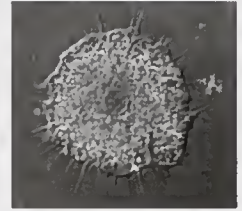
The Global Infectious Disease Program is part of the MBL's Josephine Bay Paul Center for Comparative Molecular Biology and Evolution. Directed by Mitchell Sogin, the Bay Paul Center has an active research program with strong ties to infectious disease. Bay Paul Center scientists have contributed many important insights about the evolution of parasitic protists using modern genomic approaches. Recently they embarked upon the sequence analysis of the *Giardia* genome. Excluding bacterial pathogens, *Giardia* is a principal cause of diarrheal disease in children and adults and therapeutic treatments for the parasite are almost as devastating as the disease itself. The availability of the *Giardia* genome may lead to the identification of novel treatments that have minimal side effects.

The technology necessary to sequence entire genomes is found at very few institutions. The MBL's Global Infectious Diseases Program will build on the unique expertise of the Bay Paul Center to provide more traditional parasitologists the opportunity to expand their research and better apply genomics to their research areas. This blending of genomics and parasitology will create a uniquely productive research environment and provide the catalyst for exciting new discoveries on the important pathogens.

The MBL has a rich history in studying the basic science of parasitism and infectious disease. Twenty years ago, the laboratory launched the field of molecular parasitology with the establishment of its Biology of Parasitism course, which continuously reinvents itself as it trains new investigators in this ever-expanding field. The Global Infectious Diseases Program includes a strong training component that will allow tropical health and infectious disease scientists from the world to conduct research they would be unable to do at their home institutions. The Program's unique strengths lie within its capability to integrate visiting scientists into the lab and give them access to instruments and technology that would otherwise be unavailable to them. The broad impact that the training component will have on the field of infectious diseases globally is very exciting.

#### | Other Resident Research Highlights

The MBL's resident research program grew in other areas during 2002 as well. We welcomed Frederick Goetz in January, when he joined the staff of the Marine Resources Center (MRC) as Director of the Program in Scientific Aquaculture. Through exploring factors such as an organism's nutritional and water quality requirements, physiological characteristics, reproductive biology, diseases, and genetic background, the MBL's Scientific Aquaculture Program is developing novel research techniques and addressing problems faced by both scientific and commercial aquaculture interests. Rick is spearheading the Program's efforts to use DNA technology as a tool to understand the growth, reproduction, and disease resistance in commercially important fish and shellfish. He is also focusing on enhancing the MRC's culture and husbandry of biomedical models such as squid, clams, toadfish, and zebrafish.



Heliozoan, Linda Amaral Zettler and Erik Zettler



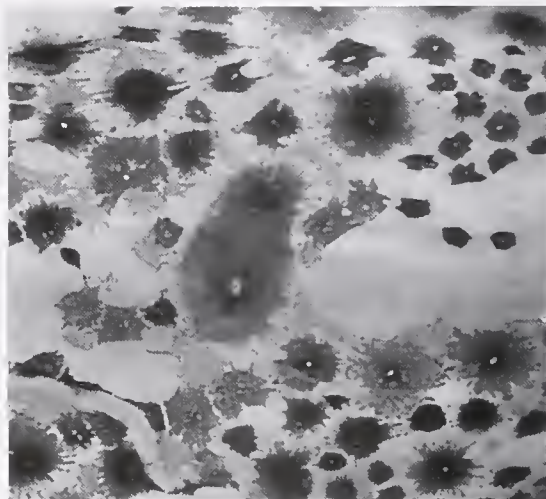
Clam egg, Robert Palazzo

Continued...



*Woods Hole aerial, Doug Weisman*

*Pigment cells on the surface of the cunner spinal cord, Steven Zottoli*



Gabriele Gerlach also joined the staff of the MRC in 2002 as an Associate Scientist. A specialist in behavioral ecology and population genetics, Gabby is using the zebrafish facilities at the MRC to explore the genetic basis of behavior.

Scientists at The Ecosystems Center received strong support from the National Science Foundation through the competitive peer-review grant process again this year. Of special note is the \$2.7 million, multi-year award in support of the Long-Term Ecological Research project at Plum Island Sound, a research site located north of Boston. Here scientists are studying the effects of land-use change on watersheds. The Center also received \$850,000 from the Andrew W. Mellon Foundation to support research on nitrogen transformation in terrestrial landscapes.

### [Summer and Visiting Research

During a typical Woods Hole summer, MBL researchers look for basic principles of life in organisms from squid to surf clams to zebrafish. They ask how nerve cells communicate, how cells regulate their complex processes, and how they proliferate. They explore how organisms reproduce and develop, how they fight disease, how sense organs gather information, and how brains process it. The investigators who gather each summer bring a diversity of approaches and questions to their research. In 2002 we welcomed 129 principal investigators and 237 other researchers from 124 institutions representing 12 countries.

The MBL's summer and visiting research program was further strengthened in 2002 with a remarkable and farsighted gift of \$2.3 million from long-time summer investigators Laura and Arthur Colwin. Their gift established the Laura and Arthur Colwin Endowed Summer Research Fellowship Fund, which, when mature, will provide full support for approximately 10 independent investigators conducting research in the fields of cell and developmental biology at the MBL for a minimum of two months during the summer. The MBL is committed to ensuring that the very best scientists have the opportunity to conduct research here each summer. We can help do this by providing financial support in the form of fellowships like these.

On the recommendation of the Science Council, the Laboratory reinstated the MBL Awards for outstanding presentations at the annual General Scientific Meetings in 2002. During the meeting, which was held in the Lillie Auditorium August 12 to 14, 56 presentations were made. After peer-review of all papers and talks, four awards and two honorable mentions were presented in the categories of Senior Investigator (Peter Armstrong), Junior Investigator (Michael Smotherman), Graduate Student (Beate Mittman), and Undergraduate Student (Jane La Du).

## | Education

The 2002 Education Program provided 499 graduate and advanced-level students from 288 institutions and 31 countries an opportunity to study a range of biological topics with some of the leading scientists in the world serving as course faculty and lecturers. The Laboratory welcomed 554 faculty members and staff and 203 lecturers to the courses in 2002. They represented 175 institutions and 33 countries.

The MBL offered two new courses in 2002. "Advances in Genome Technology and Bioinformatics," was co-directed by Mitchell Sogin, director of the MBL's Bay Paul Center, and Claire M. Fraser of The Institute of Genomic Research. Twenty-four students from the U.S. and Europe participated in the inaugural course, held October 6 to November 1, 2002. The course integrates bioinformatics with the latest laboratory techniques for genome sequencing, genome analysis, and high-throughput gene expression.

The second course, "Neuroinformatics," was directed by Partha Mitra of Lucent Technologies and Emery Brown of Massachusetts General Hospital. Twenty-six students participated in that course, which was held August 17 to September 1.

In addition to our programs for graduate students, the MBL also offers a "Semester in Environmental Science" program for undergraduates each fall. In 2002, 19 undergraduates from 14 colleges and small universities around the country participated in the program, which is hosted by The Ecosystems Center. The goal of the SES program, now in its 6<sup>th</sup> year, is to help prepare the next generation of leaders in environmental science and policymaking.

## | MBL/WHOI Library

The MBL/WHOI Library continues to grow in non-traditional directions. More and more information is being delivered directly to scientists' desktops via the Internet. In early 2002, the Library was delivering approximately 52% of its serials and 100% of its databases electronically, extending the Library's reach beyond its walls to wherever its patrons may be at any time of the day or night.

In addition, the Library is actively involved in the development of new electronic research tools. Thanks to a grant of \$500,000 from the Andrew W. Mellon Foundation, Library and IT staff are developing the Universal Biological Indexer and Organizer (uBio), an exciting new database and Internet tool that provides an innovative means of accessing, sorting, and collating taxonomic information contained in databases distributed throughout the Internet.

A portion of the Library's archival collection was also featured during the summer of 2002 in the "Wall Charts as Art" exhibit in the Meigs Room. The exhibit showcased 15 life-size reproductions of the 116 charts produced by Rudolf Leukart between 1877 and 1892. Noted for their detail, these charts were used as teaching aids in universities around the world. The Archives has one of the few remaining complete collections of the original chromolithographs. We are grateful to Ann Weissmann for curating this outstanding exhibit.

## | Outreach

During the fall of 2002, the MBL worked with Avari Studios to reorganize and redesign the MBL's web site. The new site was launched in January 2003 to very positive reviews. Early data show that the site is being visited by nearly 50,000 unique users a month. We are continuing to build and enhance the site, which is becoming an increasingly important tool for institutional advancement, marketing, communications, and outreach. If you haven't seen the new site, I invite you to visit it at <[www.mbl.edu](http://www.mbl.edu)>.



Continued...

## | Construction and Facilities

We were fortunate in 2002 to be able to continue to fund depreciation and upgrade our facilities. Lab and office space in both the Marine Resources Center and the Crane Wing of the Lillie building were substantially renovated for new Marine Resources and Global Infectious Disease program staff. The Grass Fellows also enjoyed 1400 square feet of newly renovated laboratory space in the Whitman Building during the summer of 2002. This fully modernized space was designed to meet the Fellows' research needs and also foster the cooperative and collegial nature of the program. Educational programs displaced by this renovation, including SPINES and a program for undergraduates from Williams College, were moved to the Loeb teaching building.

The MBL also purchased a five-acre farm in Newbury, MA. The property will enable the expansion of the MBL's Plum Island Research Program, which focuses on understanding how coastal ecosystems are affected by changing land cover, climate, and sea level. Upon the departure of Ecosystems Center staff to the C.V. Starr Building, the Homestead Building was gutted and renovated for use by the administrative departments of Financial Services, Human Resources, Education, and *The Biological Bulletin*. The Candle House, now home to the Director's Office, Development Office, Associates Office, and Communications and Public Affairs Office, also received a modest facelift in 2002.

## | Trustees

The Board of Trustees elected five new members whose terms began in 2002. Margaret C. Bowles of Woods Hole, MA; Martha W. Cox of Hobe Sound, FL; Walter E. Massey of Atlanta, GA; Marcia C. Morris of Boston, MA; and Gerald Weissmann, M.D., of New York, NY, are all serving four-year terms as members of the Class of 2006. In addition, John E. Dowling, Mary B. Conrad, and

Thomas S. Crane were elected to serve as President of the Corporation, Treasurer, and Clerk, respectively. Sheldon Segal was also elected to serve a final year as Chair of the Board.

On November 8, 2002, Shelly stepped down as Chair of the Board and handed his virtual gavel to Al Zeien, the former Chairman and CEO of the Gillette Company, who assumed the duties of Chair at the February 2003 meeting of the Board. Shelly has served as a member of the Board for 20 years, 10 as its Chair. He will now serve as an Honorary Trustee.

Shelly has been, and will continue to be, a vital force at the MBL. On behalf of the MBL community, I thank Shelly for all his efforts over these many years. I know we can count on his guidance and wisdom in the future.

## | Conclusion

We are living in challenging times, and the Marine Biological Laboratory is not immune to the impact that the downturn in the national economy is having on businesses, foundations, and state and local governments. Like everyone, we've had to tighten our belts and carefully consider the impact new initiatives may have on our budget. So far, the MBL has been able to weather the economic storm and continue to work in positive ways towards achieving the goals we've begun to establish through the strategic planning process.

This is an exciting time for the Marine Biological Laboratory. I look forward to working with you as we further build upon the strengths of this vital institution to ensure that the Marine Biological Laboratory continues to have a disproportionate impact on the biological, biomedical, and environmental sciences long into the future.

—William T. Speck



Eel Pond through the front doors of Ebert Hall



# research



*Zebrafish cardiovascular system, Jonathan Muyskens*

Throughout its history, the MBL has been a place where the world's top biologists can focus on their research, not distracted by departmental affairs, committee work, or other aspects of university life. The MBL provides both the resource support and the intellectual environment that enables many scientists to do their best work.

Today 47 principal investigators and their staff conduct research at the Laboratory year-round in areas such as cellular, developmental, and reproductive biology; molecular biology and evolution; neurobiology and sensory physiology; ecology and ecosystems studies; global infectious diseases; and marine biotechnology and aquaculture.

The population of investigators grows dramatically each summer when hundreds of distinguished scientists from around the world gather here to do research. During a typical MBL summer, researchers look for basic principles of life in organisms from squid to surf clams to zebrafish. They ask how nerve cells communicate, how cells regulate their complex processes, and how they proliferate. They explore how organisms reproduce and develop, how they fight disease, how sense organs gather information, and how brains process it. The investigators who gather each summer bring a diversity of approaches and questions. Along with the large number of faculty associated with the summer courses, they make the MBL the largest and most exciting biological laboratory in the world.

## THE ECOSYSTEMS CENTER

The Ecosystems Center, founded in 1975, is a collegial association of scientists led by co-directors John Hobbie and Jerry Melillo. Its mission is to understand how ecosystems are structured and how they function, to predict their response to changing environments, to apply the best scientific knowledge to the preservation and management of natural resources, and to educate scientists and citizens of the future.



*The Ecosystems Center's C.V. Starr Building*

In 2002, the Center continued the Semester in Environmental Science. This program brings undergraduates from a consortium of nearly 60 small liberal arts colleges and universities to the MBL campus for an intensive introduction to environmental sciences.

The complex nature of modern ecosystems research requires a multi-disciplinary collaborative approach to address a variety of questions. Accordingly, Center scientists collaborate on more than 60 projects. We conduct our field studies in many locations, from the North

American and European Arctic to Brazil, from the temperate forests of New England to the estuaries of the eastern U.S.

One question addressed in 2002 was the effect that a warmer climate will have on the high amounts of organic matter accumulated in forest soils over the centuries. If microbes decompose most of the organic matter, the forests would switch from a global sink of carbon dioxide gas to a source causing an acceleration of global warming. Jerry Melillo and Paul Steudler of the Center have collaborated with University of New Hampshire scientists in a decade-long experiment in which the soil of 6 x 6 m plots was heated 5° above the temperature of similar control plots. They found that soil warming did accelerate soil organic matter decay and carbon dioxide fluxes to the atmosphere but that the response was small and short-lived because microbes were able to decompose only a small proportion of the total organic matter.



*Eel grass, Rick Crawford*

### CO-DIRECTORS

John E. Hobbie  
Jerry M. Melillo

### SENIOR SCIENTISTS

John E. Hobbie  
Charles S. Hopkins  
Jerry M. Melillo  
Knut J. Nadelhoffer  
Bruce J. Peterson  
Edward B. Rastetter  
Gaius R. Shaver

### ASSOCIATE SCIENTISTS

Linda A. Deegan  
Anne E. Giblin

### ASSISTANT SCIENTISTS

Christopher Neill  
Joseph J. Vallino

### SENIOR RESEARCH

SPECIALIST  
Paul A. Steudler



Robert Holmes at the Yenisey River, Russia

### International Study Shows River Discharge in Arctic Ocean is Increasing

Another question investigated microbes in nature. These are responsible for many of the transformations in the carbon and nitrogen cycles that control important ecological processes such as carbon storage and nutrient recycling. This study looked at the link between the structure of the microbial populations in an Arctic lake and seasonal changes. This research, carried out by Byron

Crump and John Hobbie of the Center, could only be done with the assistance in molecular techniques from Mitch Sogin of the Bay Paul Center. New techniques allowed the identification of microbes and species changes, which is the first step towards the long-term goal of linking species to



An Ecosystems scientist collects samples from the Kuparuk River in Alaska

ecological function. The study, the first of its kind for lakes, revealed that there was a resident population of bacterial species throughout the year. However, a distinctly different group of species appeared when large amounts of organic matter entered the lake during the spring meltwater runoff. This organic matter, and perhaps the bacteria, came from the plant litter and soil in the surrounding watershed.

Researchers from The Ecosystems Center, along with an international team of hydrologists and oceanographers, have documented that the flow of freshwater from Arctic rivers into the Arctic Ocean has increased significantly over recent decades. If the trend continues, some scientists predict this could impact the global climate, perhaps leading to the cooling of Northern Europe.

Ecosystems Center researchers Bruce Peterson, Robert (Max) Holmes, and James McClelland led the team of scientists from the United States, Russia, and Germany. They analyzed discharge data from the six largest Eurasian rivers that drain into the Arctic Ocean. These rivers, all located in Russia, account for more than 40% of total riverine freshwater inputs to the Arctic Ocean.

Peterson and his colleagues found that combined annual discharge from the Russian rivers increased by 7% from 1936 to 1999. They contend that this measured increase in runoff is an observed confirmation of what climatologists have been saying for years—that freshwater inputs to the Arctic Ocean and North Atlantic will increase with global warming. “If the observed positive relationship between global temperature and river discharge continues into the future, Arctic river discharge may increase to levels that impact Atlantic Ocean circulation and climate within the 21st century,” says Peterson.

*Continued...*

---

*This project was funded by the Arctic System Science Program of the National Science Foundation.*

A significant increase of freshwater flow to the Arctic Ocean could slow down or shut off the formation in the North Atlantic Deep Water. The driving force behind the great underwater "conveyor belt" current known as thermohaline circulation. Thermohaline circulation is responsible for moving great amounts of thermal energy around the globe, influencing the planet's climate. One of the potential effects could be cooling of Northern Europe.

Data analyzed in this study, published in the December 13, 2002, issue of *Science* magazine, is important because it represents net precipitation (precipitation minus evapotranspiration) over a vast area, in contrast to point measurements of precipitation and evapotranspiration which are difficult to extrapolate to a large area.

"These data are a unique measure of an environmental trend both in terms of how long the time series is and in that it integrates over a vast area rather than just measuring a precipitation trend at a few locations," says co-author Stefan Rahmstorf of the Potsdam Institute for Climate Impact Research.

Project scientists are hopeful that this study, which links the work of hydrologists and oceanographers, will stimulate the two fields of science to better communicate their scientific findings with each other. The group will focus their future work on the links between the atmospheric, continental, and oceanic components of the Arctic hydrologic cycle and on the biogeochemical tracers that allow scientists to follow the circulation of riverine freshwater throughout the northern oceans. This research is needed to better understand the current functioning of the linked land-ocean-atmosphere hydrologic system and improve confidence in predictions of the future behavior of the system.

A researcher from *The Ecosystems Center* collects water from a stream in the Ipswich River watershed in the Plum Island Ecosystem Long Term Ecological Research site in northeastern Massachusetts. Investigators study different land uses and their impacts on nutrient loading into the estuaries of Plum Island Sound.

## Staff

### RESEARCH STAFF

Toby Ahrens, Research Assistant  
 Michele P. Bahr, Research Assistant  
 Jonathan P. Benstead, Postdoctoral Scientist  
 Neil D. Betzet, Research Assistant  
 Zy F. Biesinger, Research Assistant  
 Mary S. Booth, Postdoctoral Scientist  
 Laura C. Broughton, Postdoctoral Scientist  
 Donald W. Burnette, Research Assistant  
 Elizabeth H. Burrows, Research Assistant  
 Alvarus S. K. Chan, Postdoctoral Scientist  
 Benjamin P. Colman, Research Assistant  
 Christopher P. Crockett, Research Assistant  
 Byron Crump, Postdoctoral Scientist  
 Jeffrey A. Evans, Research Assistant  
 Benjamin Felzer, Research Associate  
 Solange Filoso, Postdoctoral Scientist  
 Robert H. Garritt, Research Assistant  
 Marcus O. Gay, Research Assistant  
 Joshua H. Goldstein, Research Assistant  
 Adrian C. Green, Research Assistant  
 Heather Haas, Postdoctoral Scientist  
 Diana C. Garcia-Montiel, Staff Scientist  
 Darrell A. Herbert, Staff Scientist  
 Robert M. Holmes, Staff Scientist  
 Shaomin Hu, Research Assistant  
 Jeffrey E. Hughes, Staff Scientist  
 Samuel Kelsey, Research Assistant  
 David W. Kicklighter, Research Associate  
 Bonnie L. Kwiatkowski, Research Assistant  
 James A. Laundre, Research Assistant  
 Corey R. Lawrence, Research Assistant  
 John M. Logan, Research Assistant  
 Ann L. Lezberg, Research Assistant  
 Heidi Lux, Research Assistant  
 Roxanne Marino, Staff Scientist  
 James W. McClelland, Postdoctoral Scientist  
 Patricia Micks, Research Assistant  
 Sarah Morrisseau, Research Assistant  
 Marshall L. Otter, Research Assistant  
 Suzanne Randazzo, Research Assistant  
 Heather M. Rueth, Postdoctoral Scientist  
 Diane M. Sanzone, Postdoctoral Scientist  
 Carol Schwamb, Laboratory Assistant  
 Karie A. Slavik, Research Assistant

Martin Sommerkom, Postdoctoral Scientist  
 Erica L. Stieve, Research Assistant  
 Kristin S. Tholke, Research Assistant  
 Suzanne M. Thomas, Research Assistant  
 Craig R. Tobias, Postdoctoral Scientist  
 Jane Tucker, Research Assistant  
 Zhenwen Wan, Postdoctoral Scientist  
 Ian J. Washbourne, Research Assistant  
 Michael R. Williams, Postdoctoral Scientist  
 Yuriko Yano, Postdoctoral Scientist  
 Qianlai Zhuang, Postdoctoral Scientist

### ADJUNCT SCIENTISTS

Robert W. Howarth, Cornell University  
 Paul A. Colinvaux, Smithsonian Tropical Research Institute (retired)

### VISITING SCIENTISTS

James Galloway, University of Virginia  
 Robert Naiman, University of Washington

### ADMINISTRATIVE STAFF

Kenneth H. Foreman, Associate Director, Semester in Environmental Science Program  
 Dorothy J. Berthel, Administrative Assistant  
 Anthony J. Cave, Research Administrator  
 Suzanne J. Donovan, Executive Assistant  
 Frances Johnson-Horman, Administrative Assistant  
 Guillermo Nuñez, Research Administrator  
 Deborah G. Scanlon, Executive Assistant  
 Mary Ann Seifert, Administrative Assistant

### CONSULTANTS

Francis P. Bowles, Research Designs  
 Margaret C. Bowles



Boardwalks protect vegetation from disturbance at research sites in the Arctic heath and mountain birch ecosystem around the Abisko Naturvetenskapliga Station in northern Sweden. Plots shown here are part of a pilot soil-warming project begun during 1993 at Abisko, Rose Crabtree





The Ecosystems Center's Long-Term Ecological Research site at Toolik Lake, Alaska, Knute Nadelhoffer

## Publications

- Barron, S., C. F. Weber, R. Marino, E. A. Davidson, G. Tomasky, and R. W. Howarth. 2002. Effects of varying salinity on phytoplankton growth in a low-salinity coastal pond under two nutrient conditions. *Biol. Bull.* 203: 260-261.
- Bashkin, V. N., and R. W. Howarth. 2002. *Modern Biogeochemistry*. Kluwer, Dordrecht. 561 pp.
- Bettez, N., P. Rublee, W. J. O'Brien, and M. C. Miller. 2002. Changes in abundance, composition and controls within the plankton of a fertilized arctic lake. *Freshw. Biol.* 47: 303-311.
- Boyer, E. W., and R. W. Howarth, eds. 2002. *Global and Regional Synthesis of the Nitrogen Cycle*. Kluwer, Dordrecht. 561 pp.
- Boyer, E. W., C. L. Goodale, N. A. Jaworski, and R. W. Howarth. 2002. Anthropogenic nitrogen sources and relationships to riverine nitrogen export in the northeastern U.S.A. *Biogeochemistry* 57/58: 137-169.
- Bret-Harte, M. S., G. R. Shaver, and F. S. Chapin, III. 2002. Primary and secondary stem growth in arctic shrubs: implications for community response to environmental change. *J. Ecol.* 90: 251-267.
- Bush, M. B., M. C. Miller, P. E. De Oliveira, and P. A. Colinvaux. 2002. Orbital forcing signal in sediments of two Amazonian lakes. *J. Paleolimnol.* 27: 341-352.
- Clein, J. S., A. D. McGuire, X. Zhang, D. W. Kicklighter, J. M. Melillo, S. C. Wofsy, P. G. Jarvis, and J. M. Massheder. 2002. Historical and projected carbon balance of mature black spruce ecosystems across North America: the role of carbon-nitrogen interactions. *Plant Soil* 242: 15-32.
- Currie, W. S., and K. J. Nadelhoffer. 2002. The imprint of land use history: patterns of carbon and nitrogen in downed woody debris at the Harvard Forest. *Ecosystems* 5: 446-460.
- Currie, W. S., K. J. Nadelhoffer, and B. Colman. 2002. Long-term movement of  $^{15}\text{N}$  tracers into fine woody debris under chronically elevated N inputs. *Plant Soil* 238: 313-323.
- Dargaville, R. J., M. Heimann, A. D. McGuire, I. C. Prentice, D. W. Kicklighter, F. Joos, J. S. Clein, G. Esser, J. Foley, J. Kaplan, R. A. Meier, J. M. Melillo, B. Moore III, N. Ramankutty, T. Reichenau, A. Schloss, S. Sitch, H. Tian, L. J. Williams, and U. Wittenberg. 2002. Evaluation of terrestrial carbon cycle models with atmospheric  $\text{CO}_2$  measurements: results from transient simulations considering increasing  $\text{CO}_2$ , climate and land-use effects. *Global Biogeochem. Cycles* 16: 1092. DOI:10.1029/2001GM001426.
- Deegan, L. A. 2002. Lessons learned: the effects of nutrient enrichment on the support of nekton by seagrass and salt marsh ecosystems. Special SCOR Volume. *Estuaries* 25: 727-742.
- Deegan, L. A., A. Wright, S. G. Ayvazian, J. T. Finn, H. Golden, R. R. Merson, and J. Harrison. 2002. Nitrogen loading alters seagrass ecosystem structure and support of higher trophic levels. *Aquat. Conserv. Mar. Freshw. Ecosyst.* 12: 193-212.
- Driscoll, C., D. Whittall, J. Aber, E. Boyer, M. Castro, C. Cronan, C. Goodale, P. Groffman, K. Lambert, G. Lawrence, C. Hopkinson, and S. Ollinger. 2002. *Nitrogen Pollution: From the Sources to the Sea*. Science Links – Hubbard Brook Research Foundation, Hanover, NH.
- Felzer, B. S., D. W. Kicklighter, J. M. Melillo, C. Wang, Q. Zhuang, and R. G. P. Prinn. 2002. *Ozone Effects on Net Primary Production and Carbon Sequestration in the Conterminous United States Using a Biogeochemistry Model*. Report No. 90, MIT Joint Program on the Science and Policy of Global Change, Cambridge, MA.
- Garcia-Montiel, D. C. 2002. Legacy of human activity in the present neotropical forests. Pp. 97-116 in *Ecology and Conservation of Neotropical Forests*, M.R. Guariguata and G.H. Kattan, eds. Libro Universitario Regional, Cartago, Costa Rica, (In Spanish).
- Garcia-Montiel, D. C., J. Melillo, P. A. Steudler, and C. Neill. 2002. Relationship between  $\text{N}_2\text{O}$  and  $\text{CO}_2$  emissions from the Amazon Basin. *Geophys. Res. Lett.* 29: 14.1-14.3.
- Goodale, C. L., K. Lajtha, K. J. Nadelhoffer, E. W. Boyer, and N. A. Jaworski. 2002. Forest nitrogen sinks in large eastern U. S. watersheds: inventory and modeled estimates. *Biogeochemistry* 57/58: 239-266.
- Gough, L., P. A. Wookey, and G. R. Shaver. 2002. Dry heath arctic tundra responses to long-term nutrient and light manipulation. *Arct. Antarct. Alp. Res.* 34: 211-218.
- Grams, T. E. E., A. R. Kozovits, I. M. Reiter, J. B. Winkler, M. Sommerkorn, H. Blaschke, K.-H. Häberle, and R. Matyssek. 2002. Quantifying competitiveness in woody plants. *Plant Biol.* 4: 153-158.
- Hobbie, S. E., K. J. Nadelhoffer, and P. Höglberg. 2002. A synthesis: the role of nutrients as constraints on carbon balances in boreal and arctic regions. *Plant Soil* 242: 163-170.

- Holmes, R. M., J. W. McClelland, B. J. Peterson, I. A. Shiklomanov, A. I. Shiklomanov, A. V. Zhulidov, V. V. Gordeev, and N. N. Bobrovitskaya. 2002. A circumpolar perspective on fluvial sediment flux to the Arctic Ocean. *Global Biogeochem. Cycles* 16: 10.1029/2001 GB001849.
- Hopkinson, C. S., J. J. Valiela, and J. Nriagu. 2002. Decomposition of dissolved organic matter from the continental margin. *Deep-Sea Res. II* 49: 4461-4478.
- Howarth, R. W. 2001. The nitrogen cycle. Pp. 429-435 in *Encyclopedia of Global Environmental Change. Vol. 2, The Earth System: Biological and Ecological Dimensions of Global Environmental Change*, H. A. Mooney and J.G. Canadell, eds. Wiley, Chichester.
- Howarth, R. W. 2002. *Nutrient Over-Enrichment of Coastal Waters in the United States: Steps Toward a Solution*. Pew Oceans Commission, Washington, DC.
- Howarth, R. W., E. W. Boyer, W. J. Pabich, and J. N. Galloway. 2002. Nitrogen use in the United States from 1961-2000 and potential future trends. *Ambio* 31: 88-96.
- Howarth, R. W., and D. M. Rielinger. 2002. *Nitrogen From the Atmosphere: Understanding and Reducing a Major Cause of Degradation of our Coastal Waters*. Science and Policy Bulletin No. 8, Waquoit Bay National Estuarine Research Reserve, Waquoit, MA.
- Howarth, R. W., D. Scavia, and R. Marino. 2002. *Nutrient Pollution in Coastal Waters: Priority Topics for an Integrated National Research Program for the United States*. National Oceanic and Atmospheric Administration, Silver Springs, MD.
- Howarth, R. W., D. Walker, and A. Sharpley. 2002. Sources of nitrogen pollution to coastal waters of the United States. *Estuaries* 25: 656-676.
- Hughes, J. E., L. A. Deegan, J. C. Wyda, and A. Wright. 2002. An index of biotic integrity based on fish community structure applied to Rhode Island and Connecticut estuaries. Pp. 49-58 in *Proceedings of the Fifth Biennial Long Island Sound Research Conference 2000*, M. Van Patten, ed. Connecticut Sea Grant Publication CTSG-01-02, Stamford, CT.
- Hughes, J. E., L. A. Deegan, M. J. Weaver, and J. E. Costa. 2002. Regional application of an index of estuarine biotic integrity based on fish communities. *Estuaries* 25: 250-263.
- Hughes, J. E., L. A. Deegan, J. C. Wyda, M. J. Weaver, and A. Wright. 2002. The effects of eelgrass habitat loss on estuarine fish communities of southern New England. *Estuaries* 25: 235-249.
- Hunter-Thomson, K., J. Hughes, and B. Williams. 2002. Estuarine-open-water comparison of fish community structure in eelgrass (*Zostera marina* L.) habitats of Cape Cod. *Biol. Bull.* 203: 247-248.
- Koop-Jakobsen, K., and A. Giblin. 2002. Tidal flushing of ammonium from intertidal salt marsh sediments: The relative importance of adsorbed ammonium. *Biol. Bull.* 203: 258-259.
- LaMontagne, M. G., A. E. Giblin, and I. Valiela. 2002. Denitrification and the stoichiometry of nutrient regeneration in Waquoit Bay, MA. *Estuaries* 25: 272-281.
- Levine, U. Y., and B. C. Crump. 2002. Bacterioplankton community composition in flowing waters of the Ipswich River watershed. *Biol. Bull.* 203: 251-252.
- Marino, R., F. Chan, R. W. Howarth, M. Pace, and G. E. Likens. 2002. Ecological and biogeochemical interactions constrain planktonic nitrogen fixation in estuaries. *Ecosystems* 5: 719-725.
- Mayer, B., E. W. Boyer, C. Goodale, N. A. Jaworski, N. van Breemen, R. W. Howarth, S. P. Seitzinger, G. Billen, K. Lajtha, K. Nadelhoffer, D. van Dam, L. J. Hetling, M. Nosil, K. Paustian, and R. Alexander. 2002. Sources of nitrate in rivers draining sixteen watersheds in the northeastern US: isotopic constraints. *Biogeochemistry* 57/58: 171-197.
- Mayer, B., N. Jaworski, E. Boyer, R. Howarth, C. Goodale, L. Hetling, S. Seitzinger, G. Billen, R. Alexander, N. van Breemen, K. Paustian, D. van Dam, K. Lajtha, and K. Nadelhoffer. 2002. On the feasibility of using the nitrogen and oxygen isotope ratios of nitrate for describing the origin of riverine nitrate and N transformations in large watersheds. *Biogeochemistry* 57/58: 238-266.
- McClelland, J. W., and J. P. Montoya. 2002. Trophic relationships and the nitrogen isotopic composition of amino acids in plankton. *Ecology* 83: 2173-2180.
- McGuire, A. D., C. Wirth, M. Apps, J. Beringer, J. Clein, H. Epstein, D. W. Kicklighter, J. Bhatti, F. S. Chapin III, B. de Groot, D. Efremov, W. Eugster, M. Fukuda, T. Gower, L. Hinzman, B. Huntley, G. J. Jia, E. Kasischke, J. Melillo, V. Romanovsky, A. Shvidenko, E. Vaganov, and D. Walker. 2002. Environmental variation, vegetation distribution, carbon dynamics and water/energy exchange at high latitudes. *J. Veg. Sci.* 13: 301-314.
- McKane, R. B., L. C. Johnson, G. R. Shaver, K. J. Nadelhoffer, E. B. Rastetter, B. Fry, A. E. Giblin, K. Kielland, B. L. Kwiatkowski, J. A. Laundre, and G. Murray. 2002. Resource-based niches provide a basis for plant species diversity and dominance in arctic tundra. *Nature* 415: 68-71.
- Melillo, J. M. 2002. How camest thou in this pickle? Pp. 23-31 in *Engineering and Environmental Challenges: Technical Symposium on Earth Systems Engineering*. National Academy Press, Washington, DC.
- Melillo, J. M., and E. B. Cowling. 2002. Reactive nitrogen and public policies for environmental protection. *Ambio* 31: 150-158.
- Melillo, J. M., O. Sala, et al. 2002. Ecosystem services. Pp. 13-18 in *Biodiversity: Its Importance to Human Health*, E. Chivian, ed. Center for Health and the Global Environment, Harvard Medical School, Boston, MA.



Bruce Peterson looks for bryophytes and filamentous algae in the mountain stream at the Ivishak  $^{15}\text{N}$  addition site in the Arctic National Wildlife Refuge, Laura Broughton

- Melillo, J. M., P. A. Steudler, J. D. Aber, K. Newkirk, H. Lux, F. P. Bowles, C. Catricala, A. Magill, T. Ahrens, and S. Morrisseau. 2002. Soil warming and carbon-cycle feedbacks to the climate system. *Science* 298: 2173-2176.
- Mulholland, P. J., J. L. Tank, J. R. Webster, W. B. Bowden, W. K. Dodds, S. V. Gregory, N. B. Grimm, S. K. Hamilton, S. L. Johnson, E. Marti, W. H. McDowell, J. L. Merriam, J. L. Meyer, B. J. Peterson, H. M. Valett, and W. M. Wollheim. 2002. Can uptake length in streams be determined by nutrient addition experiments? Results from an interbiome comparison study. *J. North Am. Benthol. Soc.* 21: 544-560.
- Nadelhoffer K. J., L. Johnson, J. Laundre, A. E. Giblin, and G. R. Shaver. 2002. Fine root production and nutrient use in wet and moist arctic tundras as influenced by chronic fertilization. *Plant Soil* 242: 107-113
- Novak, J. M., and A. S. K. Chan. 2002. Development of P-hyperaccumulator plant strategies to remediate soils with excess P concentrations. *Crit. Rev. Plant Sci.* 21: 493-509
- Pan, Y., A. D. McGuire, J. M. Melillo, D. W. Kicklighter, S. Sitch, and I. C. Prentice. 2002. A biogeochemistry-based successional model and its application along a moisture gradient in the continental United States. *J. Veg. Sci.* 13: 369-382.
- Peterson, B. J., R. M. Holmes, J. W. McClelland, C. J. Vörösmarty, I. A. Shiklomanov, A. I. Shiklomanov, R. B. Lammers, and S. Rahmstorf. 2002. Increasing river discharge to the Arctic Ocean. *Science* 298: 2171-2173.
- Rastetter, E. B., and G. I. Ågren. 2002. Changes in individual allometry can lead to species coexistence without niche separation. *Ecosystems* 5: 789-801.
- Rueth, H. H., and J. S. Baron. 2002. Differences in Englemann spruce forest biogeochemistry east and west of the Continental Divide in Colorado, USA. *Ecosystems* 5: 45-57.
- Rueth, H. M., J. S. Baron, and L. A. Joyce. 2002. Natural resource extraction: past, present and future. Pp. 85-112 in *Rocky Mountain Futures: An Ecological Perspective*, J. S. Baron, ed. Island Press, Washington, DC.
- Scavia, D., J. C. Field, D. Boesch, R. Buddemeier, V. Burkett, D. Canyon, M. Fogarty, M. A. Harwell, R. W. Howarth, C. Mason, D. J. Reed, T. C. Royer, A. H. Sallenger, and J. G. Titus. 2002. Climate change impacts on U.S. coastal and marine ecosystems. *Estuaries* 25: 149-164.
- Schmidt, I. K., S. Jonasson, G. Shaver, A. Michelsen, and A. Nordin. 2002. Mineralization and allocation of nutrients by plants and microbes in four arctic ecosystems: responses to warming. *Plant Soil* 242: 93-106
- Seitzinger, S. P., R. V. Styles, E. W. Boyer, R. Alexander, G. Billen, R. Howarth, B. Mayer, and N. van Breemen. 2002. Nitrogen retention in rivers: model development and application to watersheds in the northeastern U.S. *Biogeochemistry* 57/58: 199-237.
- Steudler, P. A., D. C. Garcia-Montiel, M. C. Piccolo, C. Neill, J. M. Melillo, B. J. Feigl, and C. C. Cerri. Trace gas responses of tropical forest and pasture soils to N and P fertilization. *Global Biogeochem. Cycles* 16: 10.1029/2001GB001394
- Twichell, S., S. Sheldon, L. Deegan, and R. Garritt. 2002. Nutrient and freshwater inputs from sewage effluent discharge alter benthic algal and infaunal communities in a tidal salt marsh creek. *Biol. Bull.* 203: 256-258
- van Breemen, N., E. W. Boyer, C. L. Goodale, N. A. Jaworski, K. Paustian, S. P. Seitzinger, K. Lajtha, B. Mayer, D. van Dam, R. W. Howarth, K. J. Nadelhoffer, M. Eve, and G. Billen. Where did all the nitrogen go? Fate of nitrogen inputs to large watersheds in the northeastern U.S. *Biogeochemistry* 57/58: 267-293
- Vitousek, P. M., K. Cassman, C. Cleveland, T. Crews, C. B. Field, N. B. Grimm, R. W. Howarth, R. Marino, L. Martinelli, E. B. Rastetter, and J. I. Sprent. 2002. Towards an ecological understanding of biological nitrogen fixation. *Biogeochemistry* 57-58: 1-45.
- Weber, C. F., S. Barron, R. Marino, R. W. Howarth, G. Tomasky, and E. A. Davidson. 2002. Nutrient limitation of phytoplankton growth in Vineyard Sound and Oyster Pond, Falmouth, Massachusetts. *Biol. Bull.* 203: 261-263.
- Williams, B. S., J. E. Hughes, and K. Hunter-Thomson. 2002. Influence of epiphytic algal coverage on fish predation rates in simulated eelgrass habitats. *Biol. Bull.* 203: 248-249.
- Williams, M., Y. Shimabokuro, D. A. Herbert, S. Pardi-Lacruz, C. Renno, and E. B. Rastetter. 2002. Heterogeneity of soils and vegetation in eastern Amazonian rain forest: implications for scaling up biomass and production. *Ecosystems* 5: 692-704
- Wyda, J. C., L. A. Deegan, J. E. Hughes, and M. J. Weaver. 2002. The response of fishes to submerged aquatic vegetation complexity in two ecoregions of the mid-Atlantic Bight: Buzzards Bay and Chesapeake Bay. *Estuaries* 25: 86-100.
- Zhuang, Q., A. D. McGuire, J. Harden, K. P. O'Neill, and J. Yane. 2002. Modeling the soil thermal and carbon dynamics of a fire chronosequence in interior Alaska. *J. Geophys. Res.* 107: 8147. DOI: 10.1029/2001JD001244
- Zwart, G., B. C. Crump, M. Agterveld, F. Hagen, and S. K. Han. 2002. Typical freshwater bacteria: an analysis of available 16S rRNA gene sequences from plankton of lakes and rivers. *Aquat. Microb. Ecol.* 28: 141-155.



Scientists collect samples at the spring stream at the Ivishak <sup>15</sup>N addition site in the Arctic National Wildlife Refuge, Laura Broughton

## JOSEPHINE BAY PAUL CENTER FOR MOLECULAR BIOLOGY AND EVOLUTION

---

DIRECTOR  
Mitchell Sogin

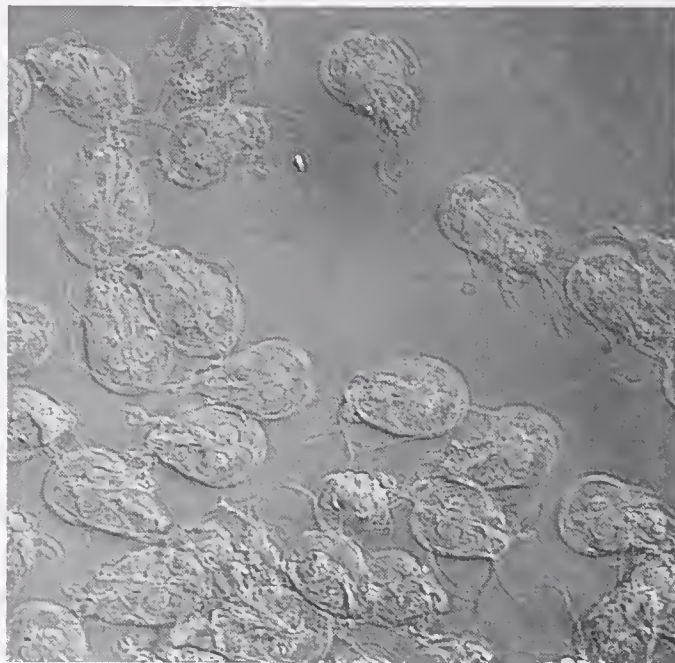
SENIOR SCIENTISTS  
Stephen Hajduk  
Monica Riley

ASSISTANT SCIENTISTS  
Michael Cummings  
Robert Sabatini  
Jennifer Wernegreen

The underlying theme of the Josephine Bay Paul Center is to explore the evolution and interaction of genomes of diverse organisms that play significant roles in environmental biology and human health. This dynamic research program integrates the powerful tools of genome science, molecular phylogenetics, and molecular ecology to advance our understanding of how living organisms are related to each other, to provide the tools to quantify and assess biodiversity, and to identify genes and underlying mechanisms of biomedical importance.

Three interlocking programs define the scope of research in the Bay Paul Center. They are the Program in Global Infectious Diseases, the Program in Molecular Evolution, and the Program in Molecular Microbial Diversity. This past year has marked significant growth in the Bay Paul Center. We attracted Mat Meselson's molecular evolution program to the MBL. Meselson is an esteemed member of the National Academy of Science and in collaboration with David Mark Welch and Jessica Mark Welch, he has established a molecular evolution group in the Bay Paul Center that explores genome evolution in asexual rotifers.

A generous award by the Ellison Medical Foundation allowed us to move forward with a dramatically expanded program in Global Infectious Diseases. This grant provided support for a major renovation that accommodates 24 scientists and visitors to the Bay Paul Center. Dr. Steve Hajduk is the director of this new initiative and has brought six graduate and post doctoral fellows to the MBL. His research emphasizes the post transcriptional processing of RNA in African trypanosomes, the cause of human sleeping sickness. RNA



*Giardia lamblia*, Barb Davids (UCSD)

### *Life at the Extremes—Molecular Technology Uncovers Astonishing Diversity in Spain's "River of Fire"*

Living conditions are tough for bacteria, algae, and other microscopic organisms in the Rio Tinto, the highly acidic, vividly crimson river that flows through the countryside of southwestern Spain. Mined since 3000 B.C., the Rio Tinto contains heavy metal concentrations that are several orders of magnitude higher than those of typical fresh water. New findings from the Rio Tinto, published in the May 9, 2002, issue of the journal *Nature*, present the first molecular description of eukaryotes in a highly acidic, high metal environment and reveal the River's incredible eukaryotic diversity. The results show that adaptation to extreme conditions is much more widespread than originally expected and provide a new understanding of the range of organisms capable of living at life's extremes and perhaps on other planets.

Eukaryota describes those organisms whose genetic material is contained within a membrane-bound nucleus. This includes plants, animals, and humans. Previous studies of the Rio Tinto relied on morphology to describe the river's diversity and alerted scientists to only a few of the evolutionary similarities between its eukaryotic organisms. By examining the DNA of organisms extracted from the Rio Tinto's sediment and biofilm, the slimy substance that coats the surface of the River's water and rocks, scientists have uncovered new eukaryotic lineages



Ocean-dwelling ancantharian,  
Linda Amaral Zettler

editing results in the post-transcriptional insertion or deletion of nucleotides into mRNA, at specific sites, creating functional open reading frames. It has been suggested that the enzymes involved in RNA editing might be potential targets for drug development. As part of this major expansion we have recruited two other new investigators to the GID program. Dr. Andrew McArthur has been a Staff Scientist at the MBL since 2000. Andrew directs NIH-funded programs to explore gene expression during different stages of the life cycle of the parasite *Giardia lamblia* and in *Trypanosoma brucei*. Robert Sabatini studies the role of unusual base modifications in trypanosomes referred to as "X-base." The enzymes involved in these genetic alterations may be unique to Trypanosomes and therefore may serve as valuable targets for drug design.

Finally, we offered a new course titled Advances in Genome Sciences and Bioinformatics, which is co-directed by Mitchell Sogin of the MBL and Claire Fraser from The Institute of Genome Research (TIGR). Important research publications this past year include descriptions of eukaryotic microbial populations that thrive in very acidic environments (pH levels between 1.7 and 2.2) in the presence of iron concentrations that can exceed 20 milligrams/ml; descriptions of eukaryotic diversity in warm, anoxic sediments that are proximal to hydrothermal vents; the discovery of introns in the primitive eukaryote, *Giardia lamblia*; and evidence of lateral transfer of genes from several different bacteria into the genome of *Giardia lamblia*.

*Camponotus nearcticus*, collected in Falmouth, MA. Adam Lazarus



Rio Tinto, J. L. de Lope, J. M. Sánchez

Rio Tinto, continued

that escaped detection by traditional methods. The work, led by Linda Amaral Zettler and Mitchell Sogin of the Josephine Bay Paul Center for Comparative Molecular Biology and Evolution, has also revealed completely new eukaryotes as well as others which have never been seen before in such a highly-acidic environment.



Linda Amaral Zettler, Erik Zettler

In mapping out the evolutionary family tree (or phylogeny) for the Rio Tinto, Amaral Zettler, Sogin, and their colleagues have detected a close relationship between the River's acid-loving eukaryotes and other species that prefer neutral environments. The short evolutionary distance between the two tells the scientists that adaptations are, in addition to being widespread, occurring rapidly when measured on an evolutionary time scale.

---

The project was funded by the National Science Foundation's Life in Extreme Environments (or LexEn) Program and NASA's Astrobiology Institute.

## | Staff

## RESEARCH STAFF

Linda Amaral Zettler, Staff Scientist III  
 David Beaudoin, Research Assistant III  
 Steven J. Biller, Research Assistant II  
 Amy Crump, Research Assistant I  
 Patrick Degnan, Research Assistant I  
 Ashita Dhillon, Postdoctoral Scientist  
 Daniel Golden, Graduate Student  
 Sulip Goswami, Research Assistant II  
 Josh Herbert, Postdoctoral Scientist  
 Jennifer Hsieh, Research Assistant I  
 Ulandt Kim, Research Assistant II  
 Abby Laatsch, Research Assistant I  
 Erica Lasek-Nesselquist, Research Assistant I  
 Adam Lazarus, Research Assistant I  
 Bruce Luders, Research Assistant II  
 Jessica Mark Welch, Postdoctoral Scientist  
 David Mark Welch, Staff Scientist II  
 Andrew McArthur, Assistant Scientist  
 Hilary Morrison, Staff Scientist II  
 Maria Murray, Research Assistant I  
 Daniel Myers, Lab Assistant  
 Laila Nahum, Postdoctoral Scientist  
 Lorraine Olendzenski, Postdoctoral Scientist  
 Bertil Olsson, Senior Research Assistant  
 Sarah Pacochal, Research Assistant II  
 Carmen Palacios, Postdoctoral Scientist  
 Gretta Serres, Staff Scientist I  
 Lynn Sherrer, Graduate Student  
 Jillian Ward, Research Assistant I

## VISITING SCIENTISTS

Maristela Camargo, University of São Paulo,  
 Brazil  
 Robert Campbell, Ares Pharmaceutical  
 Lynne McAnelly, University of Texas, Austin

## ADJUNCT SCIENTISTS

Matthew Meselson, Harvard University  
 Roger Milkman, Professor Emeritus, University  
 of Iowa  
 Harold Zakon, University of Texas, Austin

## HIGH SCHOOL INTERN

Alexandria Papa

## VISITING UNDERGRADUATE

Alissa Cohen

## HHMI SUMMER UNDERGRADUATES

Sarah Biber  
 Marsha Wheeler

## NATIONAL SCIENCE FOUNDATION

## RESEARCH EXPERIENCE FOR

## UNDERGRADUATE STUDENTS

Chad Brock  
 Andrew Magis  
 Amy McCurley  
 John Sander

## ADMINISTRATIVE STAFF

Pauline Lim  
 Tara Nihill

## | Publications

Cross, M., R. Kieft, R. Sabatini, A. Dirks-Mulder,  
 I. Chaves, and P. Borst. 2002. J-binding protein  
 increases the level and retention of the unusual  
 base J in trypanosome DNA. *Mol. Microbiol.*  
 46: 37-47.

Dehal, P., Y. Satou, R. K. Campbell, J. Chapman,  
 B. Degnan, et al. 2002. The draft genome of  
*Ciona intestinalis*: insights into chordate and  
 vertebrate origins. *Science* 298: 2157-2167.

Edgcomb, V. P., D. T. Kysela, A. Teske, A.  
 de Vera GÚmez, and M. L. Sogin. 2002. Benthic  
 eukaryotic diversity in the Guaymas Basin  
 hydrothermal vent environment. *Proc. Natl.  
 Acad. Sci. USA* 99: 7658-7662.

Edgcomb, V. P., A. G. B. Simpson, L. A. Amaral  
 Zettler, T. A. Nerad, D. J. Patterson, M. E.  
 Holder, and M. L. Sogin. 2002. Pelobionts are  
 degenerate protists: insights from molecules and  
 morphology. *Mol. Biol. Evol.* 19: 978-982.

Garcla-Verela, M., M. P. Cummings, G. Pérez-  
 Ponce de León, S. L. Gardner, and J. P. Lacleite  
 2002. Phylogenetic analysis based on 18S  
 ribosomal RNA gene sequences supports the  
 existence of class Polyacanthocephala  
 (Acanthocephala). *Mol. Phylogenet. Evol.*  
 23: 288-292.

Laan, M., H. Richmond, C. He, and R. K.  
 Campbell. 2002. Zebrafish as a model for  
 vertebrate reproduction: characterization of  
 the first functional zebrafish (*Danio rerio*)  
 gonadotropin receptor. *Gen. Comp. Endocrinol.*  
 125: 349-364.

Langford, T. D., J. D. Silberman, M. E.-L.  
 Weiland, S. G. Svard, J. M. McCaffery, M. L.  
 Sogin, and F. D. Gillin. 2002. *Giardia lamblia*  
 identification and characterization of Rab  
 and GDI proteins in a genome survey of the  
 ER to Golgi endomembrane system. *Exp.  
 Parasitol.* 101: 13-24.

Morrison, H. G., G. Zamora, R. K. Campbell,  
 and M. L. Sogin. 2002. Inferring protein function  
 from genomic sequence. *Giardia lamblia*  
 expresses a phosphatidylinositol kinase-related  
 kinase similar to yeast and mammalian TOR.  
*Comp. Biochem. Physiol. B Biochem. Mol. Biol.*  
 133: 477-491.

Nixon, J. E. J., A. Wang, J. Field, H. G. Morrison,  
 A. G. McArthur, M. L. Sogin, B. J. Loftus, and J.  
 Samuelson. 2002. Evidence for lateral transfer of  
 genes encoding ferredoxins, nitroreductases,  
 NADH oxidase, and alcohol dehydrogenase 3  
 from anaerobic prokaryotes to *Giardia lamblia*  
 and *Entamoeba histolytica*. *Eukaryotic Cell*  
 1: 181-190.

Nixon, J. E. J., A. Wang, H. G. Morrison, A. G.  
 McArthur, M. L. Sogin, B. Loftus, and J.  
 Samuelson. 2002. A spliceosomal intron in  
*Giardia intestinalis*. *Proc. Natl. Acad. Sci. USA*  
 99: 3701-3705.

Palacios, C., and J. J. Wernegreen. 2002.  
 A strong effect of AT mutational bias on  
 amino acid usage in *Buchnera* is mitigated at  
 high-expression genes. *Mol. Biol. Evol.* 19:  
 1575-1584.

Podar, M., L. Mullineaux, H.-R. Huang, P. S.  
 Perlman, and M. L. Sogin. 2002. Bacterial  
 Group II introns in a deep-sea hydrothermal  
 vent environment. *Appl. Environ. Microbiol.*  
 68: 6392-6398.

Sabatini, R., N. Meeuwenoord, J. H. van Boom,  
 and P. Borst. 2002. Recognition of base J in  
 duplex DNA by J-binding protein. *J. Biol. Chem.*  
 277: 958-966.

Sabatini, R., N. Meeuwenoord, J. H. van Boom,  
 and P. Borst. 2002. Site-specific interactions of  
 JBP with base and sugar moieties in duplex  
 J-DNA. *J. Biol. Chem.* 277: 28150-28156.

Simpson, A. G. B., L. A. Amaral Zettler, F.  
 Gomez, E. Zettler, B. G. Keenan, R. Amils, and  
 M. L. Sogin. 2002. Heavy-metal, acid-loving  
 eukaryotes from Spain's "River of Fire." *Nature*  
 417: 137.

Simpson, A. G. B., A. J. Roger, J. D. Silberman,  
 D. D. Leipe, V. P. Edgcomb, L. S. Jermin, D. J.  
 Patterson, and M. L. Sogin. 2002. Evolutionary  
 history of "early diverging" eukaryotes: the  
 excavate taxon *Carpediemonas* is a close relative  
 of *Giardia*. *Mol. Biol. Evol.* 19: 1782-1791.

Sun, C.-H., D. Palm, A. G. McArthur, S. G. Svard,  
 and F. G. Gillin. 2002. A novel Myb-related  
 protein involved in transcriptional activation of  
 encystation genes in *Giardia lamblia*. *Mol.  
 Microbiol.* 46: 971-984.

Tamas, I., L. Klasson, B. Canback, A. K. Naslund,  
 A. S. Eriksson, J. Wernegreen, J. P. Sandstrom,  
 N. A. Moran, and S. G. Andersson. 2002. 50  
 million years of genomic stasis in endosymbiotic  
 bacteria. *Science* 296: 2376-2379.

Teske, A., K.-U. Hinrichs, V. Edgcomb, A. de  
 Vera Gómez, D. Kysela, S. P. Sylva, M. L. Sogin,  
 and H. W. Jannasch. 2002. Microbial diversity  
 of hydrothermal sediments in the Guaymas  
 Basin: evidence for anaerobic methanotrophic  
 communities. *Appl. Environ. Microbiol.*  
 68: 1994-2007.

Wernegreen, J. J. 2002. Genome evolution in  
 bacterial endosymbionts of insects. *Nat. Rev.  
 Genet.* 3: 850-861.

Wernegreen, J. J., A. B. Lazarus, and P. H.  
 Degnan. 2002. Small genome of *Candidatus  
 blochmannia*, the bacterial endosymbiont of  
*Camponotus*, implies irreversible specialization  
 to an intracellular lifestyle. *Microbiology* 148:  
 2551-2556.



## ARCHITECTURAL DYNAMICS IN LIVING CELLS PROGRAM

---



*Microtubules radiating in all directions from a centrosome, Rudolf Oldenbourg, with Robert E. Palazzo*

The Architectural Dynamics in Living Cells Program, established at the MBL by Dr. Shinya Inoué in 1992, continues the pioneering research and educational activities in biophysical inquiries directly in living cells that Dr. Inoué started at Princeton University in 1949. The Program focuses on architectural dynamics in living cells — the timely and coordinated assembly and disassembly of macromolecular structures essential for the proper functioning and differentiation of cells, the spatial and temporal organization of these structures, and their physiological and genetic control. The Program is also devoted to the development and application of powerful new imaging tools that permit such studies directly in living cells and functional cell-free extracts. Program members have special expertise in the use of polarized light for analyzing the local arrangement of molecular bonds and fine structure in biological specimens. Unique instrumentation developed by Program members include the universal light microscope, centrifuge polarizing microscope, the liquid-crystal based Pol-Scope, and related technology. Biological phenomena currently under investigation include mitosis/meiosis and related motility, amoeboid movement, microtubule-centrosome interaction, and optical properties of green fluorescent protein. The Architectural Dynamics in Living Cells Program is an active component of the MBL's resident cell research group and promotes interdisciplinary research and training among its resident core researchers, visiting investigators, and collaborating manufacturers.

DISTINGUISHED SCIENTISTS  
Shinya Inoué

SENIOR SCIENTIST  
Rudolf Oldenbourg

STAFF SCIENTIST II  
Michael Shribak

---

*Meiosis II in spermatocyte of the crane fly, recorded with the new Pol-Scope, James R. Lafountain (U. at Buffalo) and Rudolf Oldenbourg*

*Polarized fluorescence of single crystal of GFP rotated between parallel polarizers, Shinya Inoué*



## |Staff

### RESEARCH STAFF

Diane Baraby, Research Assistant  
Grant Harris, Software Engineer  
Robert Knudson, Instrument Development Engineer and Research Associate  
Gwen Szent-Györgyi, Research Assistant

### VISITING INVESTIGATORS

Michael Bennett, Albert Einstein College of Medicine  
Michael Braun, Woods Hole Oceanographic Institution  
Robert Campbell, Serono  
Larry Cohen, Yale University School of Medicine  
Makoto Goda, Japan Biological Informatics Consortium, Tokyo, Japan  
Peter Hepler, University of Massachusetts at Amherst  
Joseph Hoffman, Yale University School of Medicine  
David Keefe, Rhode Island Women & Infants Hospital  
James R. LaFountain, University at Buffalo  
Lin Liu, Rhode Island Women & Infants Hospital  
Jessica Mark Welch, Bay Paul Center, MBL  
Timothy Mitchison, Harvard University  
Robert Palazzo, Rensselaer Polytechnic Institute  
Prem Ponka, McGill University, Montreal  
Edward D. Salmon, University of North Carolina at Chapel Hill  
Orion Vanderlinde, Florida State University

### INDUSTRIAL COLLABORATORS

Cambridge Research and Instrumentation, Inc., Woburn, MA  
Nikon, Japan  
Technical Video, Woods Hole, MA  
Yokogawa Electric, Japan  
Universal Imaging Corporation, Downingtown, PA

### ADMINISTRATIVE STAFF

Jane MacNeil

## |Publications

Inoué, S. 2002. Polarization microscopy. In *Current Protocols in Cell Biology*, Suppl. 13, J. Lippincott-Schwartz, ed. John Wiley & Sons, pp. 4.9.1-4.9.27.

Inoué, S., O. Shimomura, M. Goda, M. Shribak, and P.T. Tran. 2002. Fluorescence polarization of green fluorescent protein (GFP). *Proc. Natl. Acad. Sci. USA* 99(7): 4272-4277.

Inoué, S., and T. Inoué. 2002. Direct-view high-speed confocal scanner—the CSU-10. In *Cell Biological Applications of Confocal Microscopy*, 2nd Edition, B. Matsumoto, ed. Academic Press, pp. 87-123.

Oldenbourg, R. 2002. Retardance measurement method. US Patent, Number 6,501,548. USA, Assignee: Cambridge Research & Instrumentation Inc. (Woburn, MA).

Shribak, M., S. Inoué, and R. Oldenbourg. 2002. Polarization aberrations caused by differential transmission and phase shift in high NA lenses: theory, measurement and rectification. *Opt. Eng.* 41(S): 943-954.

Shribak, M. I., and R. Oldenbourg. 2002. Scanning aperture polarized light microscope: observation of small calcite crystals using oblique illumination. In *Three-Dimensional and Multidimensional Microscopy: Image Acquisition and Processing IX*, J.-A. Conchello, C. J. Cogswell and T. Wilson, eds. San Jose, *Proceedings of SPIE* 4621: 104-109.

Shribak, M., and R. Oldenbourg. 2002. Sensitive measurements of two-dimensional birefringence distributions using near-circularly polarized beam. In *Polarization Analysis, Measurement and Remote Sensing V*, D. H. Goldstein, D. B. Chenault, W. Egan and M. Duggin, eds. Seattle, *Proceedings of SPIE* 4819: 56-67.

Wang, W. H., L. Meng, R. J. Hackett, R. Oldenbourg, and D. L. Keefe. 2002. Rigorous thermal control during intracytoplasmic sperm injection stabilizes the meiotic spindle and improves fertilization and pregnancy rates. *Fertil. Steril.* 77: 1274-1277.



## BOSTON UNIVERSITY MARINE PROGRAM

### | Staff

#### DIRECTOR

Jelle Atema, Professor of Biology

#### FACULTY

Paul Barber, Assistant Professor of Biology  
 John Finnerty, Assistant Professor of Biology  
 Stjepko Golubic, Professor of Biology  
 Les Kaufman, Associate Professor of Biology  
 Phillip Lobel, Associate Professor of Biology  
 Gil Rosenthal, Assistant Professor of Biology  
 Ivan Valiela, Professor of Biology

#### ADJUNCT FACULTY

Roger Hanlon, MBL  
 Gabriele Gerlach, MBL  
 Anne Giblin, MBL  
 Frederick Goetz, MBL  
 Norman Wainwright, MBL

#### SENIOR STAFF COORDINATORS

Sharifa Gulamhussein  
 Jennifer Ripley

#### ADMINISTRATIVE STAFF

Sheri Hall, Program Manager  
 Stefano Mazzilli, Research Assistant, Valiela Lab  
 Michelle McCafferty, Program Coordinator

Continued...

In 2002, the Boston University Marine Program realized its vision for an expanded research focus in behavioral ecology and population genetics. We appointed two new assistant professors, Paul Barber (Berkeley, PhD; Harvard, postdoc) and Gil Rosenthal (University of Texas PhD; UC San Diego, postdoc). In addition, joint planning and advertising with the MBL's Marine Resources Center resulted in additional strength in this area with the appointment of MBL associate scientist Gabi Gerlach (University of Konstanz). Their scientific perspectives complement the sensory and behavioral ecology strengths in the labs of senior faculty Phil Lobel and Jelle Atema and MRC director, Roger Hanlon. Newly appointed MRC senior scientist Rick Goetz further enhances the scientific goals of this research focus. Gerlach and Goetz are both BUMP adjunct professors.

The coastal ecology program headed by Ivan Valiela flourished with a continuous stream of graduate students, postdocs, and international visiting scientists. Its Research Experience for Undergraduates Program continues to bring 10 outstanding undergraduates to Woods Hole doing research that ends up being published regularly. Anne Giblin of the MBL's Ecosystems Center has an adjunct appointment at BUMP.

With the new faculty, the Program immediately took in a graduate class of 17 highly competitive students for both PhD and Masters degrees, continuing its mission to provide exceptional educational opportunities to students in Marine Biology. Several of our current 35 students work directly with scientists at the Woods Hole Oceanographic Institution, and the National Marine Fisheries Service.

The undergraduate program also continued its mission successfully by providing eight challenging research-based courses to 16 students primarily from Boston University. Here too, student research has led to several publications.



Ruth Carmichael, BUMF

## Staff, continued

## RESEARCH TECHNICIANS

Sarah Boyce  
Devin Drown  
Janelle Morano  
David Portnoy

## VISITING FACULTY

Bill Simmons, Sandia  
National Laboratory  
Nathalie Ward, Lecturer

## PHD STUDENTS

Brendan Annett  
Jennifer Bowen  
Ruth Carmichael  
Marc Cole  
Eric Crandall  
Heidi Fisher  
Sara Grady  
Kevin Kroeger  
Carolyn Miller  
Vanessa Miller-Sims  
Elizabeth Neeley  
Jason Philibotte  
Mindy Richlen  
Gregory Skomal  
Molly Steinbach  
Mirta Teichberg  
Gabrielle Tomasky  
Joanna York  
Erik Zettler

## MASTERS STUDENTS

Abby Atkinson  
Andrea Bogomolni  
Lisa Bonacci  
Chelsea Bouchard-Harnish  
Jessica Buckingham  
Michael Cermak  
Pieter deHart  
James Estrada  
Christopher Florio  
Sophia Fox  
Sarah Good  
Dawn Grebner  
Andrea Hsu  
Alison Leschen  
Mark Lever  
Vanessa Malley  
David Martel

Amee Mehta  
Karen Morschauer  
Catherine O'Keefe  
Mollie Oremland  
Aaron Rice  
Deborah Rutecki  
Andrea Shriver  
Elizabeth Soule  
Todd Stueckle  
Erin Summers  
Melissa Sweeney

## UNDERGRADUATE STUDENTS

Alaina Avery  
Colleen Butler  
Sean Dixon  
Yael Erlitz  
Deirdre Grant  
Alfred Huang  
Laura Kloepper  
Heather Marlow  
Melissa Penn  
William Rowan  
Elisse Ruiz  
James Saenz  
Josiah Sewell  
Jami Whitney  
Kristen Wright  
Julia Young  
Chandra Ziegler

## SUMMER REU INTERNS

Stacy Barron  
Emily Gaines  
Kristin Hunter-Thompson  
Jane La Du  
Melissa Millman  
Sarah Rohrkasse  
Dianne Suggs  
Jeremy Testa  
Carolyn Weber  
Bradley Williams

## SUMMER VOLUNTEER

Jillian Barber

SUMMER STUDENT  
RESEARCHERS  
Rachel Allen  
Jillian Barber  
Margaret Johnson

## Publications

- Armstrong, Peter B., Margaret T. Armstrong, R. L. Pardy, Alice Child, and Norman Wainwright. 2002. Immunohistochemical demonstration of a lipopolysaccharide in the cell wall of a eukaryote, the green alga, *Chlorella*. *Biol. Bull.* 203: 203-204.
- Atema, J., M. K. Kingsford, and G. Gerlach. 2002. Larval reef fish could use odour for detection, retention and orientation to reefs. *Mar. Ecol. Prog. Ser.* 241: 151-160.
- Barber, P. H., M. K. Moosa, and S. R. Palumbi. 2002. Rapid recovery of genetic diversity on coral reefs and the temporal and spatial scale of larval dispersal: examples from Krakatau. *Proc. R. Soc. Lond. B* 269: 1591-1597.
- Barber, P. H., S. R. Palumbi, M. V. Erdmann, and M. K. Moosa. 2002. Sharp genetic breaks among populations of a benthic marine crustacean indicate limited oceanic larval transport: patterns, cause, and consequence. *Mol. Ecol.* 11: 659-674.
- Barron, Stacy, Carolyn Weber, Roxanne Marino, Eric Davidson, Gabrielle Tomasky, and Robert Howarth. 2002. Effects of varying salinity on phytoplankton growth in a low-salinity coastal pond under two nutrient conditions. *Biol. Bull.* 203: 260-261.
- Evgenidou, A., and I. Valiela. 2002. Response of growth and density of a population of *Geukensia demissa* to land-derived nitrogen loading, in Waquoit Bay, Massachusetts. *Estuar. Coast. Shelf Sci.* 55: 125-138.
- Gaines, Emily F., Ruth H. Carmichael, Sara P. Grady, and Ivan Valiela. 2002. Stable isotopic evidence for changing nutritional sources of juvenile horseshoe crabs. *Biol. Bull.* 203: 228-230.
- Grasso, F. W., and J. Atema. 2002. Integration of flow and chemical sensing for guidance of autonomous marine robots in turbulent flows. *Environ. Fluid Mech.* 2: 95-114.
- Hunter-Thomson, Kristin, Jeffrey Hughes, and Bradley Williams. 2002. Estuarine-open-water comparison of fish community structure in eelgrass (*Zostera marina* L.) habitats of Cape Cod. *Biol. Bull.* 203: 247-248.
- Millman, Melissa, Mirta Teichberg, Paulina Martinetto, and Ivan Valiela. 2002. Response of shrimp populations to land-derived nitrogen in Waquoit Bay, Massachusetts. *Biol. Bull.* 203: 263-264.
- Philibotte, Jason. 2002. Pelagic larval duration of the Caribbean wrasse, *Thalassoma bifasciatum*. *Biol. Bull.* 203: 245-246.
- Rohrkasse, Sarah M., and Jelle Atema. 2002. Tracking behavior of Busyconinae whelks. *Biol. Bull.* 203: 235-236.
- Rosenthal, G. G., M. J. Ryan, and W. E. Wagner, Jr. 2002. Secondary loss of preference for swords in the pygmy swordtail *Xiphophorus nigrensis* (Pisces: Poeciliidae). *Anim. Behav.* 63: 37-45.
- Shady, S., D. I. A. MacLeod, H. S. Fisher, and J. Y. Liang. 2002. Adaptation from invisible luminance and chromatic flicker. *J. Vision* 2: 68.
- Shriver, A. C., R. H. Carmichael, and I. Valiela. 2002. Growth, condition, reproductive potential, and mortality of bay scallops, *Argopecten irradians*, in response to eutrophic-driven changes in food resources. *J. Exp. Mar. Biol. Ecol.* 279: 21-40.
- Suggs, Dianne N., Ruth H. Carmichael, Sara P. Grady, and Ivan Valiela. 2002. Effects of individual size on pairing in horseshoe crabs. *Biol. Bull.* 203: 225-227.
- Testa, Jeremy M., Matthew A. Charette, Edward R. Sholkovitz, Matt C. Allen, Adam Rago, and Craig W. Herbold. 2002. Dissolved iron cycling in the subterranean estuary of a coastal bay: Waquoit Bay, Massachusetts. *Biol. Bull.* 203: 255-256.
- Valiela, I., and J. L. Bowen. 2002. Nitrogen sources to watersheds and estuaries: Role of land cover mosaics and losses within watersheds. *Environ. Pollut.* 118: 239-248.
- Valiela, I., J. L. Bowen, and K. D. Kroeger. 2002. Assessment of models for estimation of land-derived nitrogen loads to shallow estuaries. *Appl. Geochem.* 17: 935-953.
- Valiela, I., and M. L. Cole. 2002. Comparative evidence that salt marshes and mangroves may protect seagrass meadows from land-derived nitrogen loads. *Ecosystems* 5: 92-102.
- Weber, Carolyn F., Stacy Barron, Roxanne Marino, Robert W. Howarth, Gabrielle Tomasky, and Eric A. Davidson. 2002. Nutrient limitation of phytoplankton growth in Vineyard Sound and Oyster Pond, Falmouth, Massachusetts. *Biol. Bull.* 203: 261-263.
- Weiss, E. T., R. H. Carmichael, and I. Valiela. 2002. The effect of nitrogen loading on the growth rates of quahogs (*Mercenaria mercenaria*) and soft-shell clams (*Mya arenaria*) through changes in food supply. *Aquaculture* 211: 1-4.
- Williams, Bradley S., Jeffrey E. Hughes, and Kristin Hunter-Thomson. 2002. Influence of epiphytic algal coverage on fish predation rates in simulated eelgrass habitats. *Biol. Bull.* 203: 248-249.



## MARINE RESOURCES CENTER PROGRAMS

### Staff

**DIRECTOR/SENIOR  
SCIENTIST**  
Roger Hanlon

**SENIOR SCIENTIST**  
Frederick Goetz

**ASSOCIATE SCIENTISTS**  
Gabriele Gerlach  
Alan Kuzirian

**ASSOCIATE SCIENTIST/  
VETERINARIAN**  
Roxanna Smolowitz

The Marine Resources Center (MRC) is a national center for the development and use of aquatic organisms in basic biological research, biomedical research, aquaculture, and fisheries science. The research programs focus on biological processes integrated at the level of the whole organism.

We made three primary faculty hires in the research ranks during 2002: Frederick Goetz, Senior Scientist; Gabriele Gerlach, Associate Scientist; and Scott Lindell, Research Specialist. In addition, two Assistant Professors affiliated with the MRC were hired by the Boston University Marine Program: Gil Rosenthal and Paul Barber. Collectively, these hires help establish a critical mass of year-round researchers in the MRC.





#### MRC Staff, continued

James Carroll, Life Support Technical Assistant  
 Edward Enos, Aquatic Resources Division Superintendent  
 William Grossman, Marine Specimen Collector/Diving Safety Officer  
 Janice Hanley, Water Quality and Animal Health Technician  
 William Klimm, Licensed Boat Captain - R/V Gemma  
 Scott Lindell, Manager, Aquatic Resource Services and Aquaculture Research Specialist  
 Beth Linnon, Special Projects Coordinator  
 William Mebane, Aquaculture and Engineering Division Superintendent  
 Gabrielle Santore, Executive Assistant  
 Andrew Sexton, Marine Organism Shipper  
 Daniel Sullivan, Boat Captain  
 Eugene Tassinari, Senior Biological Collector  
 Sean Whelan, Diver/Marine Specimen Collector

#### SEASONAL EMPLOYEES AND VOLUNTEERS

Amanda Carroll, Intern, Lawrence School  
 Brienne Como, Intern, University of Massachusetts at Dartmouth  
 Jay Dimond, Diver/Collector  
 George Gannon, Intern, Massachusetts Bay Community College  
 Andrew Sterling, Diver/Collector  
 Christian Sterling, Diver/Collector  
 Monica Weedon, Intern, Pratt Institute

Photos by Elizabeth Armstrong

### Program in Sensory Biology, Behavioral Ecology & Population Genetics

Our studies of the physiological, sensory and genetic mechanisms of behavior bridge neuroscience, behavior, and ecology. Such an approach allows us (1) to study evolutionary processes of natural and sexual selection that shape the lives of animals and humans, and (2) to investigate the genetic consequences of behavioral interactions in an ecological context, including the population level.

In 2002, using DNA fingerprinting, we discovered that there are five genetic stocks of squids in the northwest Atlantic, and that each stock tends to return to certain spawning grounds each summer. This finding will not only revise the federal fishery management plan, but also highlights the sophistication of the squids' sensory and behavioral abilities.

Social signals such as pheromones regulate reproductive behavior in fish as well as in other vertebrates including humans. Using zebrafish, we found that male and female pheromones released during complex behavioral interactions greatly influenced female reproduction. This research will lay the foundation for future analysis of the genetic background of fertility and reproduction in vertebrates.

Learning and memory experiments centered upon defining the different stages of memory formation. Using the marine mollusk *Hermisenda*, we were able to correlate memory acquisition and retention with the animals' responses to an accessory sensory stimulus. By quantifying the immunocytochemistry, we demonstrated that levels of calyculin increase and persist during the formation stages of long-term memory. Calyculin is a key element for regulating internal calcium release in memory acquisition.





## | Program in Scientific Aquaculture

This program focuses on biotechnology research, applied research on biomedical and commercial organisms, and policy development in both of those areas. The biotechnology research is aimed at basic mechanisms that control growth, behavior, reproduction, and disease in commercially important finfish and shellfish. This includes studies on novel regulators of growth and reproduction in fish and shellfish, pathogen-regulated genes in fish, and the development of molecular-based diagnostic techniques.

In 2002, with collaborators in Spain, we established—for the first time in any fish species—a primary cell culture technique to obtain differentiated trout macrophages. We then demonstrated that only these differentiated macrophages can respond to pathogenic antigens by upregulating early response genes such as tumor necrosis factors and interleukins. It will now be possible to use global genomic techniques to obtain all of the macrophage genes that are regulated by antigen exposure and this is being pursued.

We received funding from the Southeastern Massachusetts Aquaculture Center and developed new technology to help commercial shellfish growers overwinter quahog clam seed, which will circumvent the 60-80% “winter-kill” common in field-planted seed.

The Policy Center for Marine Biosciences and Technology, directed by former MBL Director Harlyn Halvorson, has now been aligned jointly with the University of Massachusetts (Boston) and the Marine Resources Center. The Policy Center defines major problems in the fields of marine aquaculture and biotechnology, and conducts international workshops to address these important societal issues.

### AMERICORPS VOLUNTEERS (SENIOR MEMBERS)

Pat Kosky  
Joan Lemieux  
Haskell Maude  
Birgit Nelson  
Joseph Sheehy  
Judith Sheehy  
Joyce Wynne

### Laboratory of Roger Hanlon

#### STAFF

Roger Hanlon, Senior Scientist  
Jean Boal, Adjunct Scientist  
Kendra Buresch, Research Assistant  
Martha Delaney, Research Assistant  
Chris Florio, Graduate Student, Boston University  
Nicole Gilles, Research Assistant  
Mary Beth Saffo, Adjunct Scientist  
Nadav Shashar, Adjunct Scientist  
Mollie Tubbs, Research Assistant

#### VISITING INVESTIGATORS

Chuan-Chin Chiao, Postdoc, Howard Hughes Medical Institute  
Melissa Grable, Graduate Student, Boston University Marine Program  
Nuutti Kangas, Postdoc, Academy of Finland  
Miranda Karson, Graduate Student, Michigan State University  
Allen Mensinger, University of Minnesota at Duluth  
Marie-Jose Naud, Graduate Student, Flinders University  
Andrew Simpson, MMBR Student, University of California, Santa Barbara

#### INTERNS

Angela Abbott, Massachusetts Maritime Academy  
Melissa Cox, Purdue University  
Robert Nobuhara, Colorado State University  
Reshma Patel, Emory University  
Camille Riviere, E.N.S.A.I.A.  
Eric Stone, University of Massachusetts, Dartmouth  
Kate Sweeney, Colby College

### Laboratory of Alan Kuzirian

#### STAFF

Alan Kuzirian, Associate Scientist  
Hemant Chikarmane, Investigator  
Herman Epstein, Investigator

#### VISITING INVESTIGATORS

Frank Child  
John Clay, National Institutes of Health  
Robert Gould, New York State Institute for Basic Research

#### INTERNS

Kimberly Borley, Ohio University  
Alex Hangsterfer, Roger Williams University  
Justin Walker, Massachusetts Maritime Academy

### Laboratory of Roxanna Smolowitz

#### STAFF

Roxanna Smolowitz, Veterinarian  
Kevin Uhlinger, Research Assistant

#### INTERNS

Krystal Baird, AmeriCorps Member  
Amy Hancock, Summer Veterinary Intern  
Jen Hsieh, AmeriCorps Member  
Andrea Hsu, Graduate Student, Boston University  
Kyle Hunt, Mashpee High School

### Laboratory of Frederick Goetz

#### STAFF

Frederick Goetz, Senior Scientist  
Scott Lindell, Manager, Aquatic Resource Services  
and Aquaculture Research Specialist  
Linda McCauley, Research Assistant  
Steven Roberts, Postdoctoral Researcher  
Raquel Sussman  
Andrew Sweetman, Graduate Student, University  
of Bergen  
Dimitar Iliev, Graduate Student, University of Notre Dame

### Laboratory of Gabriele Gerlach

#### STAFF

Gabriele Gerlach, Associate Scientist  
Jenny Lusk-Yablick, Research Assistant

#### VISITING INVESTIGATORS

Thomas Breithaupt, Konstanz University

#### INTERNS

Martha Delaney, University of Massachusetts at Amherst  
Chris Follett, Acton Boxborough Regional High School  
Nick Hanney, Bishop Stang High School  
Nick Ryan, Thayer Academy

### Publications

Atema, J., M. J. Kingsford, and G. Gerlach. 2002. Larval reef fish could use odour for detection, retention and orientation to reefs. *Mar. Ecol. Prog. Ser.* 241: 151-160.

Basil, J. A., G. B. Lazenby, L. Nakanuku, and R. T. Hanlon. 2002. Female *Nautilus* are attracted to male conspecific odor. *Bull. Mar. Sci.* 70: 217-225.

Borley, K. A., H. T. Epstein, and A. M. Kuzirian. 2002. Effects of a sensory block on calcexin levels in the photoreceptors of *Hemissenda crassicornis*. *Biol. Bull.* 203: 197-198.

Clay, John R., and Alan M. Kuzirian. 2002. Trafficking of axonal K<sup>+</sup> channels: potential role of Hsc70. *J. Neurosci. Res.* 67: 745-752.

Delaney, M., C. Follet, N. Ryan, N. Hanney, J. Lusk-Yablick, and G. Gerlach. 2002. Social interaction and distribution of female zebrafish (*Danio rerio*) in a large aquarium. *Biol. Bull.* 203: 240-241.

Gerlach, G., and S. Bartmann. 2002. Reproductive skew, costs and benefits of cooperative breeding in female wood mice (*Apodemus sylvaticus*). *Behav. Ecol.* 13: 408-418.

Grable, M. M., N. Shashar, N. L. Gilles, C.-C. Chiao, and R. T. Hanlon. 2002. Cuttlefish body patterns as a behavioral assay to determine polarization perception. *Biol. Bull.* 203: 232-234.

Hall, K. C., and R. T. Hanlon. 2002. Principal features of the mating system of a large spawning aggregation of the giant Australian cuttlefish *Sepia apama* (Mollusca: Cephalopoda). *Mar. Biol.* 140: 533-545.

Hsieh, J. L., H. M. Chikarmane, R. Smolowitz, K. R. Uhlinger, W. Mebane, and A. M. Kuzirian. 2002. Microbial analysis of ozone disinfection in a recirculating seawater system. *Biol. Bull.* 203: 266-267.

Kusakabe, M., T. Todo, H. J. McQuillan, F. W. Goetz, and G. Young. 2002. Characterization and expression of steroidogenic acute regulatory protein and MLN64 cDNAs in trout. *Endocrinology* 143: 2062-2070.

Roberts, S. B. 2002. Characterization of growth hormone in yellow perch and myostatin in several teleost species. *Diss. Abst. Int. B Sci. Eng.* 63: 1710.

Saffo, M. B. 2002. Themes from variation: probing the commonalities of symbiotic associations. *Integr. Comp. Biol.* 42: 291-294.

Shashar, N., C. A. Milbury, and R. T. Hanlon. 2002. Polarization vision in cephalopods: neuroanatomical and behavioral features that illustrate aspects of form and function. *Mar. Freshwat. Behav. Physiol.* 35: 57-68.

Smolowitz, R., J. Hanley, and H. Richmond. 2002. A three-year retrospective study of abdominal tumors in zebrafish maintained in an aquatic laboratory animal facility. *Biol. Bull.* 203: 265-266.

Sunila, I., N. A. Stokes, R. Smolowitz, R. C. Karney, and E. M. Burreson. 2002. *Haplosporidium costale* (seaside organism), a parasite of the eastern oyster, is present in Long Island Sound. *J. Shellfish Res.* 21: 113-118.



Marine models,  
JoAnna DeNobile,  
Irina Chaikhoutdinov,  
and Lydia Louis



Rat cardiac muscle cell, Peter J. S. Smith

## PROGRAM IN MOLECULAR PHYSIOLOGY

The Program in Molecular Physiology (PMP) brings together a group of resident and visiting scientists who share common interests in the molecular bases of cellular physiology. The several laboratories making up the PMP focus on cellular plasticity and the properties of molecular transport mechanisms. A variety of experimental approaches are used ranging from molecular and biochemical methodologies, through biophysics, to advanced optical and electrochemical imaging techniques. An example of a research area spanning the independent laboratories within PMP is the role of metabolism and the mitochondrion in health and disease. How, for example, does the mitochondrion contribute to insulin secretion, heme synthesis, or channel modulation? Does the aging process, targeting metabolic disorders, contribute to reproductive and neural malfunction, degeneration, and apoptosis?

In addition to our interests in basic biology the laboratories of the PMP carry on a strong tradition within the Marine Biological Laboratory resident programs for instrumentation development. The BioCurrents Research Center—a national bioengineering resource of the National Institutes of Health (NCRR)—has pioneered the use of electrochemical sensors to define cellular activity through monitoring conditions in the extended boundary layer.

A notable characteristic of the PMP is the extensive year-round collaborative outreach to regional universities and hospitals. Members contribute to three Boston based NIH Program Project Grants in protein trafficking, diabetes, and anemia. Collaboration also allows the group to rapidly advance in areas of topical interest—as with an ongoing initiative to study the molecular physiology of the multi-drug resistant transporters, players of critical interest to cancer research and our understanding of infectious diseases. Annually, the member laboratories host more than 40 national and international visitors, taking advantage of the unique combination of scientific and technical expertise concentrated at the Marine Biological Laboratory. Access is provided to experimental platforms, cutting edge imaging techniques, and a diverse array of marine models suitable for studying both basic and biomedical problems. Strong collaborative and joint research projects are also underway with other members of the resident MBL community — notably the Architectural Dynamics Program and the Bay Paul Center.

### |Staff

*BioCurrents Research Center (NIH: NCRR)  
Transport of Bioactive Molecules; Development of  
Electrochemical and Optical Sensors*

DIRECTOR/SENIOR SCIENTIST  
Peter J. S. Smith

RESEARCH ASSISTANTS  
Katherine Hammar  
Laurel Moore  
Richard Sanger

TECHNICIAN  
Robert Lewis

*Laboratory of Peter J.S. Smith: Molecular Physiology  
of Transport and Sensor Development*

SENIOR SCIENTIST  
Peter J. S. Smith

STAFF SCIENTIST  
Mark Messerli

POSTDOCTORAL RESEARCHERS  
Abdoullah Diarra

VISITING SCIENTIST  
Radwan Khawaled

ADJUNCT SCIENTIST  
George Holz

*Laboratory of Stefan McDonough: Channel Biophysics*

ASSISTANT SCIENTIST  
Stefan McDonough

*Laboratory of Orián Shirihai: Molecular Physiology  
of Mitochondria*

ASSISTANT SCIENTIST  
Orián Shirihai

POSTDOCTORAL RESEARCHERS  
Sarah Haigh  
Shana Katzman

*Continued...*

## Staff, continued

## RESEARCH ASSISTANTS

Erica Corson  
Solomon Graf  
Gil Palchik

Laboratory for Reproductive Medicine:  
Molecular Physiology of Reproduction

## DIRECTOR

David L. Keefe, Adjunct Scientist, Brown University

## ADJUNCT SCIENTISTS

Lin Liu, Brown University  
James Trimarchi, Brown University

## POSTDOCTORAL RESEARCHER

Eva Czerwiec, Brown University

Laboratory of Ayse Dosemeci: Synaptic Plasticity

## ADJUNCT SCIENTIST

Ayse Dosemeci

## Publications

Cooper, R. A., and S. Jung. 2002. Single cell electrochemistry. In *Encyclopedia of Electrochemistry: 9 (Biochemistry)*, G. S. Wilson, ed. Wiley & Sons, New York.

Kennedy, R. T., L. M. Kauri, G. M. Dahlgren, and S.-K. Jung. 2002. Metabolic oscillations in  $\beta$ -cells. *Diabetes* 51 (suppl. 1): S152-S161.

Liu, L., and David L. Keefe. 2002. Aging-associated aberration in meiosis of oocytes from Senescence-Accelerated Mouse (SAM). *Hum. Reprod.* 17: 2678-2685.

Liu, L., Maria A. Blasco, James R. Trimarchi, and David L. Keefe. 2002. An essential role for functional telomeres in mouse germ cells during fertilization and early development. *Dev. Biol.* 249: 74-84.

Liu L, J. R. Trimarchi, P. J. S. Smith, and D. L. Keefe. 2002. Checkpoint for DNA integrity at the first mitosis after oocyte activation. *Mol. Reprod. Dev.* 62: 277-288.

Liu, L., Maria A. Blasco, and David L. Keefe. 2002. Requirement of functional telomeres for metaphase chromosome alignments and integrity of meiotic spindles. *EMBO Reports* 3: 230-234.

Liu L., J. R. Trimarchi, and D. L. Keefe. 2002. Haploidy but not parthenogenetic activation leads to increased incidence of apoptosis in mouse embryos. *Biol. Reprod.* 66: 204-210.

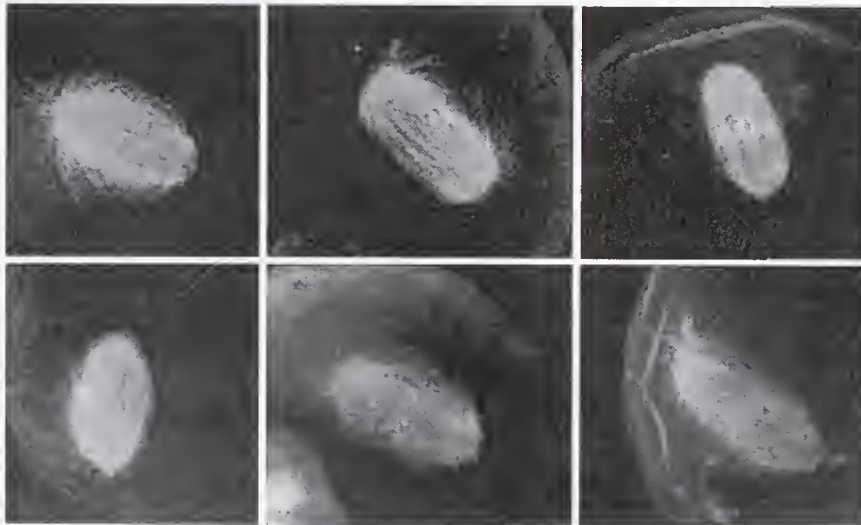
Liu, L., J. R. Trimarchi, P. J. S. Smith, and D. L. Keefe. 2002. Mitochondrial dysfunction leads to telomere attrition and genomic instability. *Aging Cell* 1: 40-46.

McDonough, S. I., L. M. Boland, I. M. Mintz, and B. P. Bean. 2002. Interactions among toxins that inhibit N-type and P-type calcium channels. *J. Gen. Physiol.* 119: 313-328.

Robinson, K. R., and M. A. Messerli. 2002. Pulsating ion fluxes and growth at the pollen tube tip. [Online]. *Science's STKE* 2002 (162): PES1.

Trimarchi, J. R., L. Liu, P. J. S. Smith, and D. L. Keefe. 2002. Apoptosis recruits two-pore domain potassium channels used for homeostatic volume regulation. *Am. J. Physiol. Cell Physiol.* 282: C588-C594.

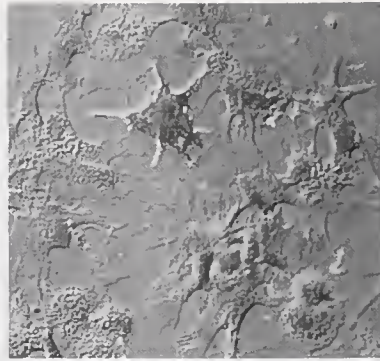
Twig, G., R. P. Malchow, K. Hammar, P. J. S. Smith, H. Levy, and I. Perlman. 2002. A novel turtle retinal preparation for simultaneously measuring light-induced electrical activity and changes in metabolite levels. *Biol. Bull.* 203: 198-200.



Representative immunofluorescence images of spindles (green), actin filaments (red), and chromosomes (blue) of oocytes from young and old mice, Lin Liu

## LABORATORY OF AQUATIC BIOMEDICINE

This laboratory is dedicated to using marine invertebrates as biomedical models to study issues of health at the molecular level. In an embryo model, we are examining how industrial chemicals influence neural development, plasticity, and function. Specifically, polychlorinated biphenyls (PCBs) or chemicals found in the wells of Brick, NJ, a site of autism in children, are added to developing clam embryos and neuronal development assessed. We evaluate how chemicals pinpoint molecular targets such as the p53 gene family. We are dissecting how p53 gene expression and function are altered by chemical exposure. Currently we are focusing on the p73 gene, which is critically important in regulating neuronal development.



A non-adhering clam (*Mya arenaria*) leukemia cell, stained reddish via the monoclonal antibody "1E10", atop a mat of spreading, normal clam hemocytes, Carol Reinisch

### Staff

SENIOR SCIENTIST  
Carol L. Reinisch

ADJUNCT SCIENTIST  
Raymond Stephens, Boston University

POSTDOCTORAL RESEARCHERS  
Rachel Cox  
Jill Kreiling

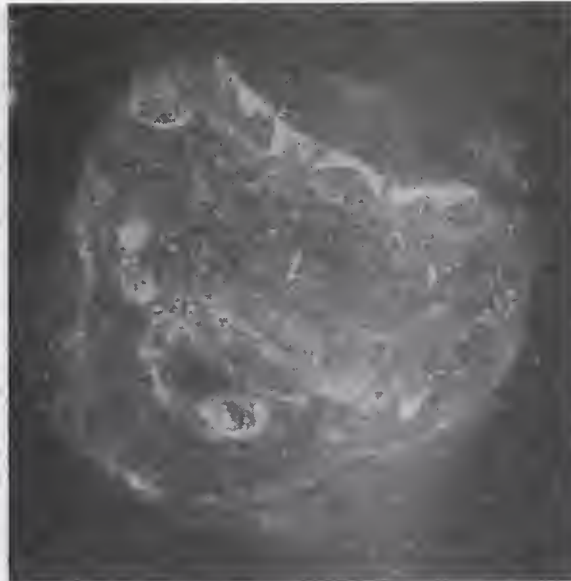
STUDENT  
Daniel Kabat

VISITING SCIENTISTS  
Sylvie St Jean, Division of Fisheries and Oceans, Moncton, Canada  
Greg McCallum, Atlantic Veterinary College, Charlottetown, Prince Edward Island, Canada

The second line of research examines the induction of leukemia in clams or mussels at industrially polluted sites. We have developed *in vitro* technology to grow the tumor cells for genetic analyses. (Supported by the Alternatives Research and Development.) In collaboration with the Division of Fisheries and Oceans (DFO) Canada, we are examining the rate of induction of leukemia in *Mytilus edulis*, the blue mussel. Mussels are placed in both clean and dirty sites in Canadian harbors. Five to six months later, the animals are retrieved and assessed for cancer using a leukemia-specific monoclonal antibody generated by this laboratory. Thus far we have determined that exposure of mussels to PAHs, PCBs, heavy metals, and other industrial compounds increases both the rate and severity of leukemia. This research is funded by DFO, Canada.

### Publication

Jessen-Eller, et al., 2002. A new invertebrate member of the p53 gene family is developmentally expressed and responds to the polychlorinated biphenyls (PCBs). *Environ. Health Perspect.* 110: 377-385.



A 72-hour-old *Spisula solidissima* embryo, stained with an antibody to clam neurofilament/intermediate filament protein (NF/IF), Jill Kreiling



## LABORATORY OF BARBARA FURIE AND BRUCE FURIE

### |Publications

Brown, M., B. Hambe, B. Furie, B. C. Furie, J. Stenflo, and L. M. Stenberg. 2002. Detection of vitamin K-dependent proteins in venoms with a monoclonal antibody specific for  $\beta$ -carboxyglutamic acid. *Toxicon* 40: 447-453.

Czerwiec, E., G. S. Begley, J. Stenflo, K. Taylor, B. C. Furie, and B. Furie. 2002. Structural similarity and functional differences between invertebrate and vertebrate carboxylases: expression and characterization of recombinant vitamin K-dependent  $\beta$ -glutamyl carboxylase from *Conus textile*. *Eur. J. Biochem.* 269: 6162-6172.

$\beta$ -Carboxyglutamic acid is a calcium-binding amino acid that is found in the conopeptides of the predatory marine cone snail, *Conus*. This laboratory has been investigating the biosynthesis of this amino acid in *Conus* and the structural role of  $\beta$ -carboxyglutamic acid in the conopeptides. This satellite laboratory relates closely to the main laboratory, the Center for Hemostasis and Thrombosis Research, on the Harvard Medical School campus in Boston, whose main focus is the synthesis and function of  $\beta$ -carboxyglutamic acid in blood clotting proteins and the role of vitamin K.

Until recently, the marine cone snail had been the sole invertebrate known to synthesize the vitamin K-dependent amino acid,  $\beta$ -carboxyglutamic acid (Gla), but the work of this laboratory and others has shown that this synthetic pathway has been preserved in most animal phyla. The cone snail produces neurotoxic conopeptides, some rich in Gla, which it injects into its prey to immobilize it. To examine the biosynthetic pathway for Gla, we have studied the *Conus* carboxylase which converts glutamic acid to  $\beta$ -carboxyglutamic acid in the presence of vitamin K. We examined the diversity of animal species that maintain vitamin K-dependent carboxylation to generate Gla. We have cloned full length carboxylase from the beluga whale (*Delphinapterus leucas*), the toadfish (*Opsanus tau*), and the cone snail (*Conus textile*) to compare these structures to the known bovine, human, rat, and mouse cDNA sequences. In addition, we have partially cloned the carboxylase gene from chicken (*Gallus gallus*), hagfish (*Myxine glutinosa*), and horseshoe crab (*Limulus polyphemus*). In addition, the *Drosophila* genome contains the  $\beta$ -carboxylase gene. The predicted amino acid sequence of the carboxylase cDNA from *Conus textile* shows most regions are nearly identical to the mammalian sequence, and that there is about 40% sequence similarity. This protein has been expressed, and the recombinant enzyme identified as a carboxylase and epoxidase. These results demonstrate the broad distribution of the vitamin K-dependent carboxylase gene, including a highly conserved motif that is likely critical for enzyme function. The vitamin K-dependent biosynthesis of Gla is a highly conserved function in the animal kingdom and we are now searching for a novel Gla containing protein that is critical for survival of animal species.

### |Staff

ADJUNCT SCIENTISTS  
Barbara C. Furie, Harvard Medical School  
Bruce Furie, Harvard Medical School  
Alan Rigby, Harvard Medical School

VISITING SCIENTIST  
Johan Stenflo, University of Lund

STAFF SCIENTIST II  
Eva Czerwiec

## LABORATORY OF NORMAN WAINWRIGHT



Photo by Volker Steger

### | Staff

DIRECTOR/SENIOR SCIENTIST  
Norman Wainwright

RESEARCH ASSISTANTS  
Alice Child  
Kendra Williams

VISITING SCIENTIST  
Porter Anderson

### | Publication

Armstrong, Peter B., Margaret T. Armstrong, R. L. Pardy, Alice Child, and Norman Wainwright. 2002. Immunohistochemical demonstration of a lipopolysaccharide in the cell wall of a eukaryote, the green alga, *Chlorella*. *Biol. Bull.* 203: 203-204.



Limulus, Volker Steger



Limulus trilobites, Beate Mittmann

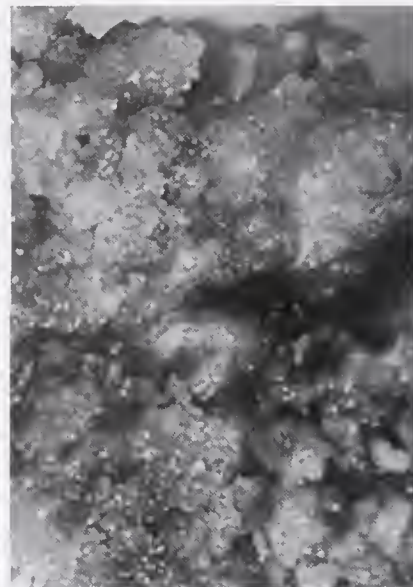
The mission of this laboratory is to understand the molecular defense mechanisms exhibited by marine invertebrates in response to invasion by bacteria, fungi, and viruses. Their primitive immune systems demonstrate unique and powerful strategies for survival in diverse marine environments. The key model has been the horseshoe crab *Limulus polyphemus*. *Limulus* hemocytes exhibit a very sensitive LPS-triggered protease cascade that results in blood coagulation. Several proteins found in the hemocyte and hemolymph display microbial binding properties that contribute to antimicrobial defense. Commensal or symbiotic microorganisms may also augment the antimicrobial mechanisms of macroscopic marine species. Secondary metabolites are being isolated from diverse marine microbial strains in an attempt to understand their role. Microbial participation in oxidation of the toxic gas hydrogen sulfide is also being studied.



Intertidal mats, John Spear



Mat cross section, Jack D. Farmer



Crystalline gypsum, John Spear

## CENTER FOR ADVANCED STUDIES IN THE SPACE LIFE SCIENCES

In 1995, NASA's life sciences programs and the MBL established a cooperative agreement with the formation of the Center for Advanced Studies in the Space Life Sciences (CASSLS at MBL). CASSLS strives to increase awareness of NASA's life sciences interests and to expand NASA's interactions with talented biologists. In support of these goals in 2002, CASSLS had its busiest year ever with the presentation of several meetings and workshops. Scientific meetings ranged in content from information technology to evolutionary biology, and served more than 125 participants. Additionally, in another workshop, 17 East Coast teachers spent four days learning about astrobiology and space life sciences.

### Staff

DIRECTOR  
Diana E. Jennings

ADMINISTRATIVE  
ASSISTANT  
Heather K. Farrell

### Meeting proceedings published in The Biological Bulletin:

"Limits to Self-Organization in Biological Systems." Includes 12 peer-reviewed articles ranging from computational to behavioral studies of self-organizing phenomena. *Biol. Bull.* 202: 243-320. June 2002.

### Three Scientific Conferences were held at the Erik Jonsson Center for the National Academy of Sciences:

April 22-24, 2002. "Combating Uncertainty with Fusion," presented in collaboration with meeting Chair Misha Pavel, Ph.D., of the Oregon Graduate Institute

May 1-3, 2002. "Outcomes of genome-genome interactions," presented in collaboration with meeting Chair Mitchell Sogin, Ph.D., of the Marine Biological Laboratory

September 22-24, 2002. "Understanding Mechanisms of Evolution," presented in collaboration with meeting Chair Eric Davidson, Ph.D., of the California Institute of Technology

### Teacher Enhancement Workshop held at the MBL:

November 22-24, 2002: "Life and Living in Space," co-directed by Diana Jennings and Lorraine Olendzenski

## SUMMER AND VISITING RESEARCHERS

---

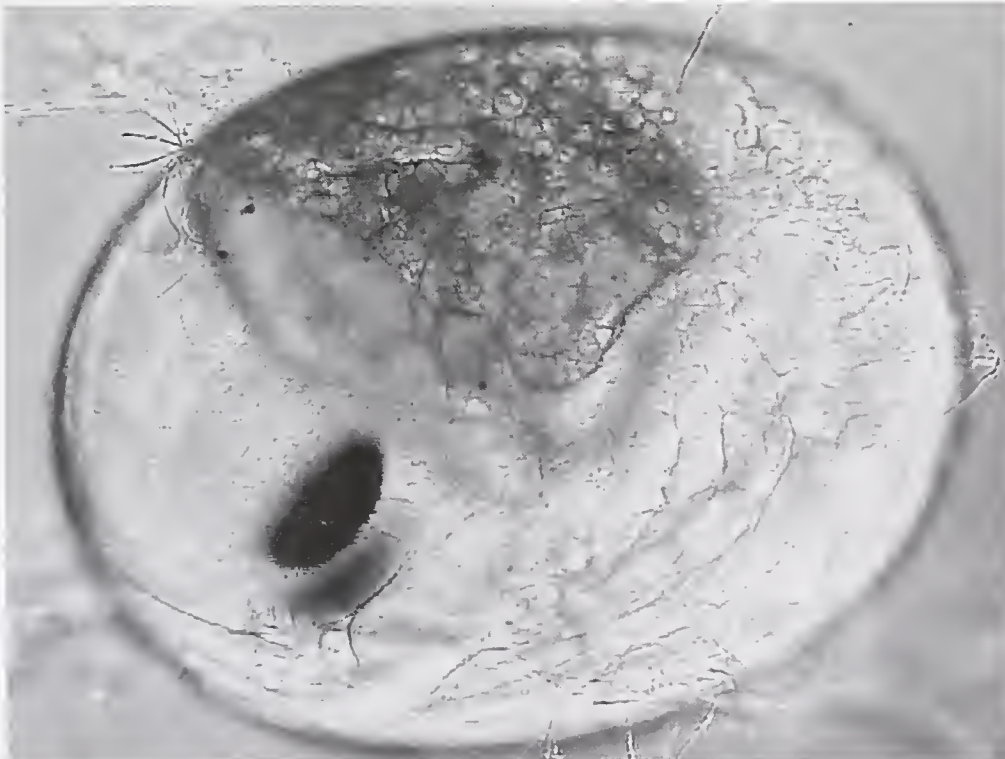


*Sea urchin cell, Philip Presley*

Many visiting MBL investigators use marine organisms as models for studying basic biological processes. Research using squids, sea urchins, horseshoe crabs, dogfish, clams, toadfish, and sea slugs, for example, has increased our fundamental understanding of a broad range of diseases and medical conditions including cancer, diabetes, epilepsy, hypertension, multiple sclerosis, arthritis, and neurological disorders.

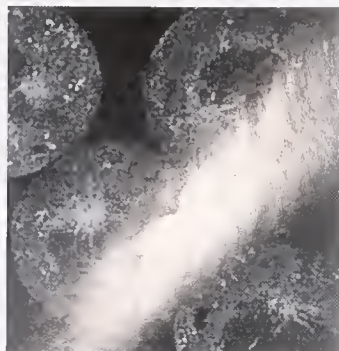
During 2002, the MBL welcomed 129 Principal Investigators and 237 other researchers from 124 institutions, representing 12 countries. Members of the summer community come from Harvard and Howard, from the University of Alabama and the Universitat de Barcelona, from the Food and Drug Administration and the National Institutes of Health, from Canada, Argentina, England, and Switzerland, among many other institutions, universities, agencies and countries.

MBL summer researchers find an infrastructure and an informal, interactive scientific community that allows them to launch into research almost immediately upon their arrival. Advice and equipment always seem available from other researchers or from the summer courses. Free from academic duties at their home institutions, some veteran summer scientists report they do more hands-on research in three months at the MBL than they do during the rest of the year at their home institutions.



---

*Spider crab embryo,  
Gundrun Aspöck*



*Spisula solidissima nuclei*, Anne Goldman



Elizabeth Armstrong

## 2002 Summer Investigators

Armstrong, Clay  
University of Pennsylvania

Armstrong, Peter B.  
University of California, Davis

Augustine, George J.  
Duke University Medical Center

Baker, Robert  
New York University Medical Center

Barlow, Jr., Robert B.  
State University of New York  
Upstate Medical University

Barry, Susan  
Mount Holyoke College

Beaugé, Luis  
Instituto de Investigacion Medica  
"Mercedes y Martin Ferreyra,"  
Argentina

Bennett, Michael V. L.  
Albert Einstein College of Medicine

Bodznick, David  
Wesleyan University

Botto, Florencia  
Universidad Nacional de Mar del  
Plata, Argentina

Boyer, Barbara  
Union College

Brady, Scott T.  
The University of Texas Southwestern  
Medical Center, Dallas

Brown, Joel  
Albert Einstein College of Medicine

Browne, Carole  
Wake Forest University School of  
Medicine

Burbach, Peter  
Rudolf Magnus Institute for  
Neurosciences, The Netherlands

Burger, Max M.  
Novartis International AG,  
Switzerland

Burgess, David  
Boston College

Camargo, Maristela  
University of São Paulo, Brazil

Canessa, Cecilia  
Yale University

Chang, Fred  
Columbia University

Chappell, Richard L.  
Hunter College, City University of  
New York

Clay, John  
National Institutes of Health

Cohen, Lawrence B.  
Yale University School of Medicine

Cohen, William D.  
Hunter College, City University of  
New York

Crawford, Karen  
St. Mary's College of Maryland

De Polavieja, Gonzalo  
University of Cambridge, United  
Kingdom

De Weer, Paul  
University of Pennsylvania School  
of Medicine

Denk, Winfried  
Max-Planck-Institute for Medical  
Research, Germany

Desai, Rooma  
Yale University School of Medicine

Dickinson, Bonny  
Children's Hospital

DiPolo, Reinaldo  
Instituto Venezolano  
Investigaciones Cientificas,  
Venezuela

Dodge, Frederick  
State University of New York  
Upstate Medical University

Douglas, John K.  
University of Arizona

Eckberg, William  
Howard University

Edds-Walton, Peggy  
Parmlly Hearing Institute of  
Loyola University

Ellenberg, Jan  
European Molecular Biology  
Laboratory, Germany

Fay, Richard  
Loyola University of Chicago

Field, Christine  
Harvard University Medical School

Fields, Douglas  
National Institutes of Health

Fishman, Harvey M.  
University of Texas Medical Branch,  
Galveston

Gadsby, David  
The Rockefeller University

Galione, Antony  
Oxford University, United Kingdom

Gandhi, Sunil  
The Salk Institute

Garber, Sarah  
The Chicago Medical School

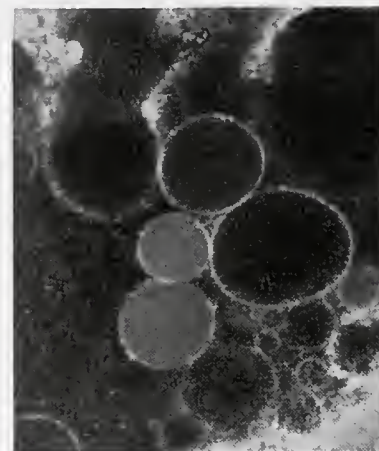
Gerhart, John  
University of California, Berkeley

Giuditta, Antonio  
Universita di Napoli "Federico II,"  
Italy

Goldman, Robert D.  
Northwestern University Medical  
School

Gould, Robert  
New York State Institute for Basic  
Research

- Groden, Joanna  
University of Cincinnati
- Gruenbaum, Yosef  
The Hebrew University of Jerusalem,  
Israel
- Gruhn, Matthias  
Cornell University
- Haimo, Leah  
University of California, Riverside
- Hardege, Jorg  
Hull University, United Kingdom
- Harper, Mary-Ellen  
University of Ottawa, Canada
- Heck, Diane  
Rutgers University
- Hershko, Avram  
Technion-Israel Institute of  
Technology, Israel
- Highstein, Steven M  
Washington University School of  
Medicine
- Hines, Michael  
Yale University School of Medicine
- Holmgren, Miguel  
Harvard University Medical School
- Iribame, Oscar  
Universidad Nacional de Mar del  
Plata, Argentina
- Johnston, Daniel  
Baylor College of Medicine
- Jonas, Elizabeth  
Yale University School of Medicine
- Kaczmarek, Leonard  
Yale University School of Medicine
- Kaplan, Barry  
National Institutes of Mental Health
- Kaplan, Ilene M.  
Union College
- Kauer, Julie  
Brown University
- Kaupp, U.B.  
Institut für Biologische  
Informationsverarbeitung, Germany
- Khodakhah, Kamran  
University of Colorado School of  
Medicine
- Khodjakov, Alexey  
Wadsworth Center
- Kirschner, Marc  
Harvard University Medical School
- Koonce, Michael  
Wadsworth Center
- Kuhns, William  
The Hospital for Sick Children,  
Canada
- Lafer, Eileen M., University of Texas  
Health Science Center, San Antonio
- Lambert, Nevin  
Medical College of Georgia
- Landowne, David  
University of Miami School of  
Medicine
- Langford, George  
Dartmouth College
- Laskin, Jeffrey  
University of Medicine and  
Dentistry of New Jersey
- Laufer, Hans  
University of Connecticut
- LeBaron, Richard  
University of Texas, San Antonio
- Lipicky, Raymond J  
Food and Drug Administration
- Lipscombe, Diane  
Brown University
- Llinás, Rodolfo R.  
New York University Medical Center
- Magee, Jeff  
Louisiana State University Medical  
Center
- Malchow, Robert Paul  
University of Illinois, Chicago
- Martinez, Joe  
University of Texas, San Antonio
- McNeil, Paul  
Medical College of Georgia
- Mensingher, Allen  
University of Minnesota, Duluth
- Mitchison, Timothy  
Harvard University Medical School
- Mittmann, Beate  
Institute für Biologie, Germany
- Moore, John W  
Duke University Medical Center
- Mooseker, Mark  
Yale University
- Nasi, Enrico  
Boston University School of  
Medicine
- Palazzo, Robert  
Rensselaer Polytechnic Institute
- Pant, Harish  
National Institutes of Health
- Parysek, Linda  
University of Cincinnati
- Perlman, Ido  
Technion Israel
- Ponka, Prem  
McGill University, Canada
- Rakowski, Robert F.  
Ohio University
- Ratner, Nancy  
University of Cincinnati
- Reese, Thomas S.  
National Institutes of Health
- Rieder, Conly  
Wadsworth Center
- Rinberg, Dima  
Bell Laboratories
- Ripps, Harris  
University of Illinois College of  
Medicine
- Rodriguez-Contreras, Adrian  
University of California, Davis
- Rome, Larry  
University of Pennsylvania
- Russell, James  
National Institutes of Health
- Salmon, Edward  
University of North Carolina,  
Chapel Hill
- Silver, Robert  
Wayne State University School  
of Medicine
- Sloboda, Roger D  
Dartmouth College
- Sluder, Greenfield  
University of Massachusetts  
Medical School
- Smotherman, Michael  
University of California, Los  
Angeles
- Spiegel, Evelyn  
Dartmouth College
- Spiegel, Melvin  
Dartmouth College
- Steinacker, Antoinette  
University of Puerto Rico
- Stockbridge, Norman  
Food and Drug Administration
- Sugimon, Mutsuyuki  
New York University Medical Center
- Tank, David  
Princeton University
- Telzer, Bruce  
Pomona College
- Tilney, Lewis  
University of Pennsylvania
- Treistman, Steven  
University of Massachusetts Medical  
School
- Tytell, Michael  
Wake Forest University School of  
Medicine



Squid vesicles, Harvey Fishman

Vollrath, Melissa Ann  
Baylor College of Medicine

Weidner, Earl  
Louisiana State University

Wheeler, Damian  
McGill University, Canada

Whittaker, J. Richard  
University of new Brunswick,  
Canada

Zecevic, Dejan P.  
Yale University School of Medicine

Zimmerberg, Joshua  
National Institutes of Health

Zottoli, Steven  
Williams College

Zukin-Bennett, R. Suzanne  
Albert Einstein College of Medicine



Mitochondrial dysfunction and oxidative stress lead to telomere attrition and chromosomal end-to-end fusions (indicated by arrows) in mouse embryos, Lin Liu

## MBL Research Fellows

Twenty-two scientists received awards to conduct research at the MBL in 2002.

Peter Armstrong, Ph.D.  
University of California, Davis  
His research focused on immune defense proteins and defense processes of arthropods that show evolutionary conservation. Dr. Armstrong was funded by The Laura and Arthur Colwin Endowed Summer Research Fellowship Fund.

Florencia Botto, Ph.D.  
Universidad Nacional de Mar del Plata, Mar del Plata, Argentina  
"The role of intertidal burrowing species (e.g., crabs) on the dynamics of organic matter in estuarine environments." Dr. Botto was funded by the MBL Associates, The Catherine Filene Shouse Foundation, and the Lucy B. Lemann Fellowship Fund.

J. Peter H. Burbach, Ph.D.  
Rudolf Magnus Institute for Neurosciences University Medical Center, Utrecht, The Netherlands  
"The stellate ganglion of the squid as a model for neurodevelopment gene cascades." Dr. Burbach was funded by The Stephen W. Kuffler Fellowship Fund and the Baxter Postdoctoral Fellowship Fund.

David Burgess, Ph.D.  
Boston College, Chestnut Hill, Massachusetts  
"Cytokinesis in embryonic cells." Dr. Burgess was funded by the Josiah Macy, Jr. Foundation, the Robert Day Allen Fellowship Fund, and the William Townsend Porter Foundation.

Maristela Camargo, D.V.M., Ph.D.  
University São Paulo, São Paulo, Brazil  
"An evolutive study of Th1/Th2 differentiation." Dr. Camargo was funded by The Catherine Filene Shouse Foundation, The Frederik B. Bang Fellowship Fund, and an MBL Research Fellowship.

Cecilia M. Canessa, M.D.  
Yale University, New Haven, Connecticut  
"Cloning and characterization of ASIC channels in marine vertebrates." Dr. Canessa was funded by The Erik B. Fries Endowed Fellowship, the M.G.F. Fuortes Memorial Fellowship Fund, The Stephen W. Kuffler Fellowship Fund, an MBL Research Fellowship, and the Ann E. Kammer Memorial Fellowship Fund.

Fred Chang, M.D., Ph.D.  
Columbia University College of Physicians and Surgeons, New York, New York  
"Placement of the cell division plane." Dr. Chang was funded by The Universal Imaging Corporation Fellowship Fund.

Karen Crawford, Ph.D.  
St. Mary's College of Maryland, St. Mary's City, Maryland  
"Molecular analysis of B-catenin expression, axes formation and early embryogenesis in the squid, *Loligo pealei*, insights into evolution." Dr. Crawford was funded by the Evelyn and Melvin Spiegel Fellowship Fund, the MBL Associates, and the James A. and Faith Miller Fellowship Fund.

Bonny Dickinson, Ph.D.  
Harvard Medical School and Children's Hospital, Boston  
"Calmodulin and the unconventional myosins play key roles in FcRn trafficking by mediating interaction with the actin cytoskeleton" Dr. Dickinson was funded by The Laura and Arthur Colwin Endowed Summer Research Fellowship, The Frederik B. Bang Fellowship Fund, the MBL Associates, and an MBL Research Fellowship.

John K. Douglass, Ph.D.  
*University of Arizona, Tucson*  
 "An electrophysiological and anatomical study of central visual pathways in *Limulus polyphemus*." Dr. Douglass was funded by the H. Keffer Hartline Fellowship Fund, the Plum Foundation, John E. Dowling Fellowship Fund, and the Herbert W. Rand Fellowship.

Jan Ellenberg, Ph.D.  
*European Molecular Biology Laboratory, Heidelberg, Germany*  
 "Mechanism of nuclear envelope breakdown (NEBD) in echinoderm oocytes and embryos." Dr. Ellenberg was the 2002 Nikon Fellow, funded by Nikon Instruments, Inc.

Sarah Garber, Ph.D.  
*Chicago Medical School, North Chicago, Illinois*  
 "Correlation of ion flux and regulation of cell volume." Dr. Garber was funded by The Erik B. Fries Endowed Fellowship.

Yosef Gruenbaum, Ph.D.  
*Institute of Life Sciences at The Hebrew University of Jerusalem, Jerusalem, Israel*  
 "Molecular and functional dissection of the nuclear lamina in the surf clam." Dr. Gruenbaum was funded by The Gruss Lipper Foundation, The Frank R. Lillie Fund, The Erik B. Fries Endowed Fellowship, the Robert Day Allen Fellowship Fund, and the H. Burr Steinbach Memorial Fellowship Fund.

Leah Haimo, Ph.D.  
*University of California, Riverside*  
 Her research focused on how molecular motors are regulated to control organelle transport. Dr. Haimo was funded by The Laura and Arthur Colwin Endowed Summer Research Fellowship Fund.

Jörg Hardege, Ph.D.  
*Hull University, Hull, United Kingdom*  
 "Do sex pheromone differences in *Nereidid* polychaetes lead to reproductive isolation?" Dr. Hardege was funded by the Lucy B. Lemann Fellowship Fund, The Charles R. Crane Fellowship Fund and The John O. Crane Fellowship Fund.

Mary-Ellen Harper, Ph.D.  
*University of Ottawa, Ontario, Canada*  
 "Use and construction of self-referencing microelectrochemical probes for studies into the role of Uncoupling Protein-3 (UCP3) in myocellular energy metabolism." Dr. Harper was funded by The Laura and Arthur Colwin Endowed Summer Research Fellowship and the H. Burr Steinbach Memorial Fellowship Fund.

Oscar Iribarne, Ph.D.  
*Universidad Nacional de Mar del Plata, Argentina*  
 "The role of the SW Atlantic intertidal burrowing crab *Chasmagnathus granulata* in the dynamics of nutrients." Dr. Iribarne was funded by the Lucy B. Lemann Fellowship Fund.

Diane Lipscombe, Ph.D.  
*Brown University, Providence, Rhode Island*  
 "The identification of novel conus toxins to discriminate among voltage-gated calcium channels and their splice variants." Dr. Lipscombe was funded by The Catherine Filene Shouse Foundation and the MBL Associates.

Ido Perlman, Ph.D.  
*Technion-Israel Institute of Technology, Haifa, Israel*  
 "Nitric oxide synthesis in the vertebrate retina and its physiological and cellular functions." Dr. Perlman was funded by The Gruss Lipper Foundation.

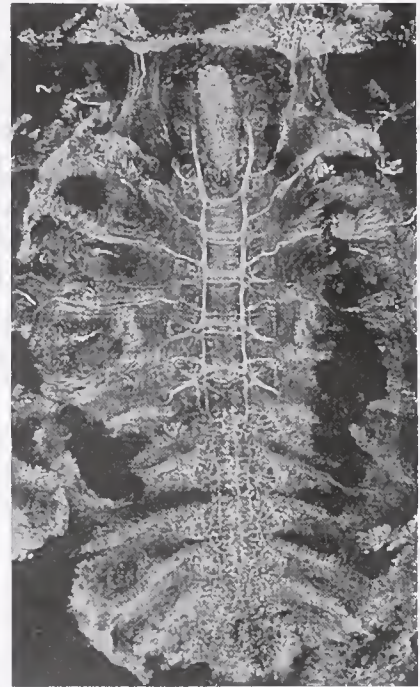
Prem Ponka, M.D., Ph.D.  
*McGill University, Montreal, Canada*  
 "Iron Trafficking in Erythroid Cells: A Collaborative Program." Dr. Ponka was funded by the Frank R. Lillie Fund.

Nancy Ratner, Ph.D.  
*University of Cincinnati College of Medicine, Cincinnati, Ohio*  
 The title of her research project was "Cyclin-dependent kinases in fast axonal transport." Dr. Ratner was funded by the Frank R. Lillie Fund and The Herbert W. Rand Fellowship Fund.

J. Richard Whittaker, Ph.D.  
*University of New Brunswick in Fredericton, New Brunswick, Canada*  
 "The Sea Squirt's Secret: How We Discovered Our Chordate Ancestry." Dr. Whittaker was funded by the Frank A. Brown, Jr. Readership Fund.



Kevin Begos



## | Grass Fellows

Nine scientists participated in the 2002 Grass Fellowship Program in Neuroscience at the Marine Biological Laboratory. The program is sponsored by The Grass Foundation and offers independent research opportunities to young neuroscientists. The 2002 program was directed by Dr. Susan R. Barry of Mount Holyoke College. Dr. Melissa Ann Vollrath of Baylor College of Medicine was the program's Associate Director.

Rooma Desai, Ph.D., Yale School of Medicine, "Isolation of K<sup>+</sup> Currents Underlying the 'Chopper Response' of the Principal Cells of Lateral Superior Olive (LSO)"

Sunil Gandhi, The Salk Institute, "Evanescence Wave Microscopy of Single Vesicle Recycling in Goldfish Retinal Bipolar Terminals"

Matthias Gruhn, Ph.D., Cornell University, "Correlation of Extracellular Nerve Recordings and Behavioral Activity in Live Crayfish Using Implantable Electrodes and High-Speed Video Technology"

Beate Mittmann, Institut für Biologie, "The Development of the Nervous System in the Horseshoe Crab *Limulus polyphemus* (Chelicerata, Ziphosura) and its Implication for Arthropod Relationships"

Gonzalo Garcia de Polavieja, Ph.D., UCLA School of Medicine, "Behavioral Algorithm and Circuitry for Visual Motion Detection in the Leech"

Dima Rinberg, Ph.D., Bell Laboratories Lucent Technologies, "Optical Recording of Multineuron Activity Using Ballistic Delivery of Voltage Sensitive Dyes"

Adrian Rodriguez-Contreras, Ph.D., University of California, Davis, "Intrinsic Properties, Distribution and Morphology of Inhibitory Neurons in the Midbrain Auditory Pathway of Chicken"

Michael S. Smotherman, Ph.D., UCLA, "Descending Control of Chromatophore Motoneurons in the Cephalopod Brain"

Damian G. Wheeler, McGill University, "Multiprotein Complex Signaling from Synapse to Nucleus"

## Other Research Personnel

- Abe, Teruo, Niigata University, Japan  
 Adams, Christina, Williams College  
 Akingbade, Katherine, University of Oxford, United Kingdom  
 Alber, Merry, University of Georgia  
 Alimi, Mariam, Wake Forest University  
 Alliegro, Mark, Louisiana State University Health Sciences Center  
 Arnolds, David, Williams College  
 Artigas, Pablo, Rockefeller University  
 Asomoah, Nikiya, Williams College  
 Ayliffe, Harold, University of Utah
- Banta, Gary, Roskilde University, Denmark  
 Bartels-Hardege, H., Hull University, United Kingdom  
 Beach, Rebecca, Hollins University  
 Bearer, Elaine, Brown University  
 Berberian, Graciela, Instituto de Investigacion Medica "Mercedes y Martin Ferreyra," Argentina  
 Bertetto, Lisa, Wesleyan University  
 Biber, Sarah, Earlham College  
 Binion, Samantha, Emory University  
 Bodily, Jill, Stanford University  
 Bordenstein, Seth, Marine Biological Laboratory  
 Borley, Kimberly, Ohio University  
 Bornstein, Gil, Technion, Israel  
 Braun, Alexander, Hunter College  
 Brewton, Luke, University of Texas Medical Branch  
 Brown, Jeremiah, Dartmouth College  
 Bucior, Iwona, Friedrich Miescher Institut, Switzerland
- Cameron, Lisa, University of North Carolina, Chapel Hill  
 Cameron, Luiz, University of Rio de Janeiro, Brazil  
 Carroll, Amanda, Marine Biology Laboratory  
 Cefaliello, Carolina, University of Naples, Italy  
 Charkhoutdin, Irina, Hunter College  
 Chang, Donald, Kong Kong University, Kong Kong  
 Chen, Xiaobing, National Institutes of Health  
 Chiao, Chuan-Chin, Massachusetts General Hospital  
 Chludzinski, John, National Institutes of Health  
 Churchill, Grant, University of Oxford, United Kingdom  
 Clark, Michael, Medical College of Georgia  
 Collis, Leon, University of Rhode Island  
 Conrad, Mara, Hunter College  
 Coric, Tatjana, Yale University School of Medicine  
 Corson, Erica, Mt Holyoke College  
 Couch, Ernest, Texas Christian University  
 Cox, Melissa, Marine Biological Laboratory
- De Stefano, Rosanna, University of Naples, Italy  
 Delaney, Martha, Marine Biological Laboratory  
 DeNobile, JoAnna, Hunter College  
 Dineen, Shauna, Williams College  
 Djuricic, Maja, Yale University School of Medicine
- Ehsanian, Reza, NASA Ames Research Center  
 Evans, Louise, Harvard Medical School  
 Eyman, Maria, Universita di Napoli "Federico II," Italy
- Fernandez-Busquets, Xavier, Universitat de Barcelona, Spain  
 Ferrara, Eugenia, Universita di Napoli "Federico II," Italy  
 Fevrier, Salem, Williams College  
 Follett, Christopher, Marine Biological Laboratory  
 Franzini-Armstrong, Clara, University of Pennsylvania School of Medicine  
 Frick, Andreas, Baylor College of Medicine
- Gainer, Harold, National Institutes of Health  
 Garnham, Clive, University of Oxford, United Kingdom  
 Garza, John, University of Texas at San Antonio  
 Gaszewska, Anna, Medical College of Georgia
- Ge, Lan, University of California, Riverside  
 Gifford, Raeann, University of Kansas  
 Gilland, Edwin, New York University School of Medicine  
 Gioia, Anthony, National Institutes of Health  
 Goda, Makoto, Japan Biological Information Research Center, Japan  
 Goldman, Anne, Northwestern University Medical School  
 Gomez, Maria del Pilar, Boston University School of Medicine  
 Grant, Philip, National Institutes of Health  
 Gratton, Michael Anne, University of Pennsylvania  
 Greer, Jonathan, Brown University  
 Guo, YiFan, Williams College  
 Gyoeva, Fatima, Institute of Protein Research, Russia
- Hangsterfer, Alexandra, Marine Biological Laboratory  
 Hanney, Nicholas, Marine Biological Laboratory  
 Harrington, John, University of California, Davis  
 Harwood, Claire, University of Pennsylvania  
 Hatoum, Nagi, New York University Medical School  
 Helbig, Annika, Institut für Biologische Informationsverarbeitung, Germany  
 Hellemons, Anita, Rudolf Magnus Institute for Neuroscience, The Netherlands  
 Helm, Jessica, Yale University School of Medicine  
 Hepler, Peter, University of Massachusetts  
 Hernandez, Carlos, New York University School of Medicine  
 Hernandez, Ruben, University of Texas  
 Hess, Sam, National Institutes of Health  
 Hoffman, Mathew, Boston College  
 Holtz, Scott, Northwestern University Medical School  
 Homsy, Sara, Wake Forest University  
 Horseman, Nelson, University of Cincinnati
- Iliev, Dimitar, University of Notre Dame
- Jackson, Ticiana, Howard University  
 Johnson, Michael, University of Connecticut  
 Jurkovicova, Dana, National Institutes of Health
- Katar, Mazkhan, Wayne State University  
 Khavandgar, Simin, Albert Einstein College  
 King, Curtis, University of Utah  
 Knowles, James, Colgate University  
 Koester, Helmut, Baylor College of Medicine  
 Konnerth, Arthur, University of Munich, Germany  
 Koop-Jabobsen, Ketil, Roskilde University, Denmark
- Lee, Kyeng-Gea, Hunter College  
 Levy, Hanna, Technion, Israel  
 Li, YuLong, Duke University Medical Center  
 Lober, Robert, Medical College of Georgia  
 Lockard, Jon, National Institutes of Health  
 Louis, Lydia, Rutgers, The State University of New Jersey  
 Lowe, Chris, University of California, Berkeley
- Maddox, Paul, University of North Carolina  
 Marangoni, Maria Natalia, University of Buenos Aires, Argentina  
 Martinez, Gabriela, University of New Hampshire  
 Masgrau, Roser, Oxford University, United Kingdom  
 Maude, Haskell, Marine Biological Laboratory  
 Mbanu, Chijoke, Wayne State University  
 McAnelly, Lynne, University of Texas, Austin  
 McCurley, Amy, Richmond University  
 Molina, Anthony, University of Illinois at Chicago  
 Momose-Sato, Yoko, Tokyo Medical and Dental University, Japan  
 Montanez, Marlena, Mt Holyoke College  
 Montgomery, John, University of Auckland, New Zealand  
 Moran, Kimberly, New York University School of Medicine  
 Moreira, Jorge, University of São Paulo, Brazil  
 Morfini, Gerardo, University of Texas Southwestern Medical Center  
 Morgan, Anthony, University of Oxford, United Kingdom  
 Morse, Thomas, Yale University

## Domestic Institutions Represented

Najera, Julia, University of Texas  
 Nedoluzhko, Aleksey, Wadsworth Center  
 Ng, Michelle, Boston College  
 Nobuhara, Robert, Colorado State University  
 Nonaka, Mio, Kyoto University  
 Normand, Danielle, University of New Hampshire  
 Nuccitelli, Richard, University of Connecticut Health Center

O'Neal, Jessica, College of Charleston  
 Obata, Shuichi, Yokohama City University, Japan  
 Olsen, Gary, University of Illinois, Urbana  
 Ortiz, Christopher, University of California, Irvine

Palmer, Lucy, University of Minnesota  
 Pascal, Akil, Williams College  
 Passianoto, Caio, Marine Biological Laboratory  
 Patel, Reshma, Marine Biological Laboratory  
 Peacock-Villa, Elizabeth, Dartmouth College  
 Pelletier, Cory, Brown University  
 Petersen, Jennifer, National Institutes of Health  
 Pollema, Sarah, University of Minnesota, Duluth  
 Prasad, Kondury, University of Texas Health Science Center

Quigley, James, Scripps Research Institute

Rabbitt, Richard, University of Utah  
 Radojicic, Mihailo, Yale University  
 Redenti, Stephen, Hunter College  
 Remick, Katherine, University of Texas Medical Branch  
 Rhodes, Paul, New York University Medical School  
 Richmond, Hazel, University of Minnesota  
 Ridings, Corey, Occidental College  
 Rieder, Leila, Albany High School  
 Rinkwitz, Silke, New York University Medical School  
 Ripps, Jeff, Towson University  
 Rummel, John, NASA

Sanchez, Carlos, University of Texas  
 Sato, Katsushige, Tokyo Medical and Dental University, Japan  
 Satpute, Prasanna, Brown University  
 Schnackenberg, Bradley, University of Carolina, Chapel Hill  
 Scotto Lavina, Zeno, National Institutes of Health  
 Short, Michelle, Marine Biological Laboratory  
 Shumaker, Dale, Northwestern University Medical School  
 Simpson, Andrew, University of California, Santa Barbara  
 Smillie, Darren, University of Edinburgh, United Kingdom  
 Smith, Kalmia, Cornell University  
 Steeds, Craig, Kansas University  
 Stone, Eric, Marine Biological Laboratory  
 Sweeney, Catherine, Marine Biological Laboratory

Takahashi, Hajime, Olympus Optical Co., Ltd., Japan  
 Tanner, Geoffrey, Wesleyan University  
 Terasaki, Mark, University of Connecticut Health Center  
 Thompson, Reid, Dartmouth College  
 Tokumar, Hiroshi, Duke University Medical Center  
 Tokumar, Keiko, Duke University Medical Center  
 Twig, Gilad, Technion, Israel  
 Tzur, Yonatan, Hebrew University, Israel

Vautrin, Jean, University of Montpellier, France  
 Vetrano, Anna, Rutgers University  
 Villalba-Galea, Carlos, Duke University Medical Center  
 Vucinic, Dejan, Yale University

Wachowiak, Matt, Yale University School of Medicine  
 Weedon, Monica, Marine Biological Laboratory  
 Wetherington, Jonathan, Medical College of Georgia  
 Weyand, Ingo, Institut für Biologische Informationsverarbeitung,  
 Germany  
 Wheeler, Marsha, Earlham College  
 Williams, Kethurah, Howard University  
 Wollert, Torsten, Universität Rostock, Germany

Yamasaki, Michiko, University of Oxford, United Kingdom  
 Young, Iain, University of Pennsylvania

Zakevicius, Jane, University of Illinois College of Medicine  
 Zakon, Harold, University of Texas, Austin

Albert Einstein College of Medicine  
 Arizona State University

Barnard College  
 Baylor College of Medicine  
 Beth Israel Deaconess Medical Center  
 Boston College  
 Boston University School of Medicine  
 Brown University

California Institute of Technology  
 California, University of, Berkeley  
 California, University of, Davis  
 California, University of, Irvine  
 California, University of, Los Angeles  
 California, University of, Riverside  
 California, University of, San Francisco  
 Cincinnati, University of  
 Colorado School of Medicine, University of  
 Columbia University  
 Connecticut, University of  
 Cornell University  
 Courant Institute

Dartmouth College  
 Duke University  
 Duke University Medical Center



Emory University

Federal Department of Agriculture  
 Flower Garden Banks National Marine Sanctuary  
 Food and Drug Administration

Gladstone Institute of Neurological Disease

Hartford, University of  
 Harvard University  
 Harvard University Medical School  
 Hawaii, University of  
 Howard University  
 Hunter College

Illinois, University of

Kansas, University of

Louisiana State University  
Loyola University of Chicago

Maryland, University of  
Massachusetts, University of  
Medical College of Georgia  
Miami School of Medicine, University of  
Michigan State University  
Millersville University  
Minnesota, University of

NASA  
National Institutes of Health  
National Institutes of Mental Health  
New York State Institute for Basic Research  
New York University  
New York University School of Medicine  
North Carolina State University  
North Carolina, University of  
Northwestern University Medical School

Ohio University

Penn State University  
Pennsylvania, University of  
Pomona College  
Providence College  
Puerto Rico, University of

Rutgers, the State University of New Jersey

Scripps Research Institute  
South Carolina, University of  
St Mary's College of Maryland  
Stanford University  
State University of New York Upstate Medical University  
Syracuse University

Texas Health Science Center, University of  
Texas Southwestern Medical Center, University of  
Texas, University of, Austin  
Texas, University of, San Antonio  
The Rockefeller University

Union College  
Utah, University of

Virginia, University of

Wadsworth Center  
Wake Forest University  
Washington University School of Medicine  
Wayne State University School of Medicine  
Wesleyan University  
Williams College  
Women and Infants Hospital

Yale University  
Yale University School of Medicine

## Foreign Institutions Represented

Auckland, University of, New Zealand

Barcelona, Universitat de, Spain  
Buenos Aires, University of, Argentina

Cambridge, University of, United Kingdom

Edinburgh, University of, United Kingdom  
European Molecular Biology Laboratory, Germany

Friedrich Miescher Institute, Switzerland

Hebrew University of Jerusalem, Israel  
Hong Kong University, Hong Kong  
Hospital for Sick Children, Canada  
Hull University, United Kingdom

Institut für Biologische Informationsverarbeitung, Germany  
Institute of Protein Research, Russia  
Instituto de Investigacion Medica "Mercedes y Martin Ferreyra,"  
Argentina  
Instituto Venezolano Investigaciones Cientificas, Venezuela

Japan Biological Information Research Center, Japan

Kyoto University, Japan

Max-Planck-Institute for Medical Research, Germany  
McGill University, Canada  
Montpellier, University of, France  
Munich, University of, Germany

Napoli "Federico II", Universita di, Italy  
New Brunswick, University of, Canada  
Niigata University, Japan  
Novartis International AG, Switzerland

Olympus Optical Co., Ltd, Japan  
Ottawa, University of, Canada  
Oxford, University of, United Kingdom

Rio de Janeiro, University of, Brazil  
Roskilde University, Denmark  
Rostock, Universitat, Germany  
Rudolf Magnus Institute for Neuroscience, The Netherlands

São Paulo, University of, Brazil  
Technion-Israel Institute of Technology, Israel  
Tokyo Medical and Dental University, Japan

Universidad Nacional de Mar del Plata, Argentina  
University of College London, United Kingdom  
Utrecht, University of, The Netherlands

Yokohama City University, Japan



## General Scientific Meetings Awards

On the recommendation of the Science Council, the MBL reinstated the MBL Award for outstanding presentations at the Laboratory's annual General Scientific Meetings. The award in each category consists is a crystal clock and a \$300 cash prize.

Fifty-six presentations were given during the Meetings, which were held August 12 to 14 in the Lillie Auditorium. After peer-review of all papers and talks, four awards and two honorable mentions were presented.

### Senior Investigator:

Peter Armstrong, Margaret Armstrong, R. L. Pardy, Alice Child, and Norman Wainwright, "Histochemical demonstration of lipopolysaccharide in the cell wall of a eukaryote, the green alga *Chlorella*"

### Junior Investigator:

Michael Smotherman, "Acetylcholine mediates excitatory input to chromatophore motoneurons in the squid, *Loligo pealei*"

### Graduate Student:

Beate Mittmann, "Early neurogenesis in the horseshoe crab *Limulus polyphemus* and its implication for arthropod relationships"

### Undergraduate Student:

Jane La Du, Deana Erdner, Sonya Dyhrman, and Don Anderson, "Molecular approaches to understanding population dynamics of the toxic dinoflagellate *Alexandrium fundyense*"

### Student Honorable Mentions:

Jeremy M. Testa, Matt Charette, Edward Sholkovitz, Matt Allen, Adam Rago, and Craig Herbold, "Dissolved iron cycling in the subterranean estuary of a coastal bay: Waquoit Bay, Massachusetts"

D. E. Arnolds, S. J. Zottoli, C. E. Adams, S. M. Dineen, S. Fevrier, Y. Guo, and A. J. Pascal, "Physiological effects of tricaine on the supramedullary/dorsal neurons of the cunner, *Tautoglabrus adspersus*"

## 2002

### FRIDAY EVENING LECTURES

June 21

Barry Bloom, *Harvard School of Public Health*  
"Economic and Political Implications of Global Infectious Diseases"

June 28

R. Alan B. Ezekowitz, *Massachusetts General Hospital for Children*  
"Fighting Infections from Flies to Man"

July 5

Lang Lecture

Michael J. Ryan, *University of Texas, Austin*  
"Sexual Selection and The Brain"

July 12

Gail K. Naughton, *Advanced Tissue Sciences*  
"Stem Cells and Tissue Engineering: From Science Fiction to Medical Fact"

July 18, 19

Forbes Lectures

William Newsome, *Stanford University*  
I. Thursday, July 18

"Making Decisions: The Brain's Link Between Perception and Action"

II. Friday, July 19

"Seeing Motion: Linking Neurophysiology to Perceptual Psychology"

July 26

Michael Brown, *University of Texas Southwestern Medical Center at Dallas*  
"Genetic Defenses Against Heart Attacks"

August 2

Steven Hyman, *Harvard University*  
"Reflections on Behavior in the Postgenomic Era"

August 9

Dan Barry, *NASA*  
"Sensations of Space Flight"

August 16

Tim Hunt, *Cancer Research UK, Clare Hall Laboratories*  
"What is the Cell Cycle and How is it Controlled?"

## Publications

- Alliegro, M. C. 2002 Coiled body heterogeneity induced by G1 arrest with amiloride + bumetanide. *Exp. Cell Res.* 279 111-117
- Alliegro, M. C., and M. A. Alliegro. 2002. Nuclear injection of anti-pigpen antibodies inhibits endothelial cell division. *J. Biol. Chem.* 277 19,037-19,041.
- Armstrong, Peter B , Margaret T Armstrong, R. L. Pardy, Alice Child, and Norman Wainwright 2002. Immunohistochemical demonstration of a lipopolysaccharide in the cell wall of a eukaryote, the green alga, *Chlorella*. *Biol. Bull.* 203: 203-204
- Arnolds, D E W., S. J. Zottoli, C. E. Adams, S. M. Dineen, S. Fevrier, Y Guo, and A. J. Pascal 2002 Physiological effects of tricaine on the supramedullary/dorsal neurons of the cunner, *Tautoglabrus adspersus*. *Biol. Bull.* 203 188-189
- Bearer, E. L., and P. Satpute-Krishnan 2002 The role of the cytoskeleton in the life cycle of viruses and intracellular bacteria: tracks, motors, and polymerization machines *Curr. Drug Targets Infect. Disord.* 2 247-264
- Borst, Douglas, and Robert Barlow 2002. Circadian rhythms in locomotor activity of juvenile horseshoe crabs. *Biol. Bull.* 203: 227-228
- Boyle R , S. M. Highstein, J. P. Carey, and J. P. Xu 2002. Functional recovery of anterior semicircular canal afferents following hair cell regeneration in birds *JARO* 3 149-166.
- Brown, J. R., E. M. Peacock-Villada, and G. M. Langford 2002 Globular tail fragment of myosin-V displaces vesicle-associated motor and blocks vesicle transport in squid nerve cell extracts *Biol. Bull.* 2 210-211.
- Cermak, Michael J 2002 *Caranx latus* (Carangidae) chooses dock pilings to attack silverside schools. a tactic to interfere with stereotyped escape behavior of prey? *Biol. Bull.* 203 241-243
- Chappell, R. L., E. Schuette, R. Anton, and H. Ripps 2002. GABA<sub>A</sub> receptors modulate the rod-driven ERG b-wave of the skate retina. *Doc. Ophthalmol* 105 179-188.
- Clay, John R , and Alan Kuzirian. 2002. Trafficking of axonal K<sup>+</sup> channels: potential role of Hsc70. *J. Neurosci. Res.* 67 745-752
- Clay, John R , and Alvin Shrier 2002. Temperature dependence of bistability in squid giant axons with alkaline intracellular pH. *J. Membr. Biol.* 187 213-223.
- Claypool S M , B. L. Dickinson, M. Yoshida, W. I. Lencer, and R. S. Blumberg 2002 Functional reconstitution of human FcRn in Madin-Darby canine kidney cells requires co-expressed human beta 2-microglobulin. *J. Biol. Chem.* 277 28,038-28,050
- Cox, B. L., Popa, R , Bazylnski, D A , Lanoil. B , Douglas, S , Belz, A , Engler, D.L and Nealsen, K.H 2002 Organization and elemental analysis of P-, S-, and Fe-rich inclusions in a population of freshwater magnetococci. *Geomicrobiol. J.* 19 387-406
- Crawford, Karen. 2002 Culture method for *in vitro* fertilization to hatching of the squid, *Loligo pealeii*. *Biol. Bull.* 203 216-217
- DeGiorgis, J A , T S Reese, and E. L. Bearer. 2002. Association of myosin II with axoplasmic organelles: implications for axonal transport. *Mol. Biol. Cell.* 13 1046-1057
- Eddleman, C. S., G. D. Bittner, and H. M. Fishman. 2002 SEM comparison of severed ends of giant axons isolated from squid (*Loligo pealeii*) and crayfish (*Procambarus clarkii*). *Biol. Bull.* 203 219-220
- Edds-Walton, P. L , and R. R. Fay 2002 Directional auditory processing by the oyster toadfish, *Opsanus tau*. *Bioacoustics* 12 202-204
- Edds-Walton, P. L , L. A. Mangiamele, and L. C. Rome 2002 Variations of pulse repetition rate in boatwhistle sounds from oyster toadfish (*Opsanus tau*). *Bioacoustics* 13: 153-173
- Fay, R. R 2002 The sense of hearing in fishes. *Bioacoustics* 12: 167-169
- Fay, R. R , and P. L Edds-Walton 2002 Preliminary evidence for interpulse interval selectivity of cells in the torus semicircularis of the oyster toadfish (*Opsanus tau*). *Biol. Bull.* 203 195-196
- Fernandez-Busquets, X , W. J. Kuhns, T. L. Simpson, M. Ho, D. Gerosa, M. Grob, and M. M. Burger. 2002. Cell-adhesion-related proteins as specific markers of sponge cell types involved in allogeneic recognition. *Dev. Comp. Immunol.* 26: 313-323.
- Garber, Sarah S , and Mary M Hoffman. 2002. Cl<sup>-</sup> and glutamate<sup>-</sup> competition for a volume-regulated anion channel. *Biol. Bull.* 203 194-195
- Giuditta, A , M. Eyman, and B. B. Kaplan. 2002 Gene expression in the squid giant axon: neurotransmitter modulation of RNA transfer from periaxonal glia to the axon. *Biol. Bull.* 203 189-190
- Giuditta, A , B. B. Kaplan, J. van Minnen, J. Alvarez, and E. Koenig 2002. Axonal and presynaptic protein synthesis: new insights into the biology of the neuron. *Trends Neurosci.* 25 400-404

Continued..

Golan, A., Y. Yudkovsky, and A. Hershko. 2002. The cyclin-ubiquitin ligase activity of the cyclosome/APC is jointly activated by protein kinases Cdk1-cyclin B and Plk. *J. Biol. Chem.* 277: 15,552-15,557.

Graf, Werner, Edwin Gilland, Matt McFarlane, Laura Knott, and Robert Baker. 2002. Central pathways mediating oculomotor reflexes in an elasmobranch, *Scyliorhinus canicula*. *Biol. Bull.* 203: 236-238.

Hinkle, B., B. Slepchenko, M. M. Rolls, T. C. Walther, P. A. Stein, L. M. Mehlmann, J. Ellenberg, and M. Terasaki. 2002. Chromosomal association of Ran during meiotic and mitotic divisions. *J. Cell Sci.* 115: 4685-4693.

Huffaker, Diana, and R. Gil Pontius, Jr. 2002. Reconstruction of historical land cover in the Ipswich Watershed. *Biol. Bull.* 203: 253-254.

Husted L. B., E. S. Sorensen, P. B. Armstrong, J. P. Quigley, L. Kristensen, L. Sottrup-Jensen. 2002. Localization of carbohydrate attachment sites and disulfide bridges in *Limulus*  $\alpha$ 2-macroglobulin. Evidence for two forms differing primarily in their bait region sequences. *J. Biol. Chem.* 277: 43,698-43,706.

Islas-Flores, I., S. Corrales-Villamar, E. L. Bearer, J. C. Raya, and M.-A. Villanueva. 2002. Isolation of lipoxygenase isoforms from *Glycine max* embryo axes based on cross-reactivity with anti-myosin antibodies. *Biochim. Biophys. Acta* 1571: 64-70.

Jimenez C. J., M. Eyman, Z. Scotto Lavina, A. E. Gioio, K. W. Li, R. van der Schors, W. P. M. Geraerts, A. Giuditta, B. B. Kaplan, and J. van Minnen. 2002. Protein synthesis in synaptosomes: a proteomics analysis. *J. Neurochem.* 81: 735-744.

Kuner, T., H. Tokumaru, and G. J. Augustine. 2002. Peptides as probes of protein-protein interactions involved in neurotransmitter release. Pp 552-570 in *Peptide-Lipid Interactions*, S. A. Simon and T. J. McIntosh, eds. Academic Press, San Diego.

La Du, Jane, Deana Erdner, Sonya Dyhrman, and Don Anderson. 2002. Molecular approaches to understanding population dynamics of the toxic dinoflagellate *Alexandrium fundyense*. *Biol. Bull.* 203: 244-245.

Landowne, D. 2002. Perchlorate prevents sodium channel gating and sodium protects in the squid giant axon. *Biol. Bull.* 203: 190-191.

Langford, G. M. 2002. Myosin-V, a versatile motor for short-range vesicle transport. *Traffic* 3: 859-865.

Lee, K-G., A. Braun, I. Chaikhoutdinov, J. DeNobile, M. Conrad, and W. Cohen. 2002. Rapid visualization of microtubules in blood cells and other cell types in marine model organisms. *Biol. Bull.* 203: 204-206.

Ludlam, John P., David H. Shull, and Robert Buchsbaum. 2002. Effects of haying on salt-marsh surface invertebrates. *Biol. Bull.* 203: 250-251.

Ma, W.-L., and R. R. Fay. 2002. Neural representations of the axis of acoustic particle motion in the auditory midbrain of the goldfish, *Carassius auratus*. *J. Comp. Physiol.* 188: 301-313.

Maddox, P., A. Desai, K. Oegema, T. J. Mitchison, and E. D. Salmon. 2002. Poleward microtubule flux is a major component of spindle dynamics and anaphase A in mitotic *Drosophila* embryos. *Curr. Biol.* 12: 1670-1674.

Megela-Simmons, A., R. R. Fay, and A. N. Popper, eds. 2002. *Springer Handbook of Auditory Research, Vol. 14, Acoustic Communication*. Springer-Verlag, New York.

Mehlmann, L. M., T. L. Z. Jones, and L. A. Jaffe. 2002. Meiotic arrest in the mouse follicle maintained by a Gs protein in the oocyte. *Science*. 297: 1343-1345.

Mensingher, A. F., and M. Deffenbaugh. 2002. Acoustical neural telemetry from free-swimming fish. *Bioacoustics* 12: 333-334.

Mikhailov, A., R. W. Cole, and C. L. Rieder. 2002. DNA damage during mitosis in human cells delays the metaphase/anaphase transition via the spindle assembly checkpoint. *Curr. Biol.* 12: 1797-1806.

Mittmann, Beate. 2002. Early neurogenesis in the horseshoe crab *Limulus polyphemus* and its implication for arthropod relationships. *Biol. Bull.* 203: 221-222.

Montgomery, John, Guy Carton, and David Bodznick. 2002. Error-driven motor learning in fish. *Biol. Bull.* 203: 238-239.

Morgan, J. R., G. J. Augustine, and E. M. Lafer. 2002. Synaptic vesicle endocytosis: the races, places, and molecular faces. *Neuromolecular Med* 2: 101-114.

Pahl, Nicholas, Sara Homsy, Hilary G. Mornson, and Robert M. Gould. 2002. mRNAs located in *Squalus acanthias* (Spiny Dogfish) oligodendrocyte processes. *Biol. Bull.* 203: 217-218.

Piccoli, G., M. Gomez, and E. Nasi. 2002. Role of protein kinase C in light adaptation of molluscan microvillar photoreceptors. *J. Physiol.* 543: 481-494.

Rakowski, R. F., D. C. Gadsby, and P. De Weer. 2002. Single ion occupancy and steady-state gating of Na channels in squid giant axon. *J. Gen. Physiol.* 119: 235-249.

Redenti, S., and R. L. Chappell. 2002. Zinc chelation enhances the zebrafish retinal ERG b-wave. *Biol. Bull.* 203: 200-202.



Stained hippocampal pyramidal neuron (rat), Dan Johnston

- Ridings, C., D. Borst, K. Smith, F. Dodge, and R. B. Barlow. 2002. Visual behavior of juvenile *Limulus* in their natural habitat and in captivity. *Biol. Bull.* 203: 224-225.
- Rieder, C. L., and R. W. Cole. 2002. Cold shock and the mammalian cell cycle. *Cell Cycle* 1: 169-175.
- Ripps, H., H. Qian, and J. Zakevicius. 2002. Blockade of an inward sodium current facilitates pharmacological study of hemi-gap-junctional currents in *Xenopus* oocytes. *Biol. Bull.* 203: 192-194.
- Ripps, H., H. Qian, and J. Zakevicius. 2002. Pharmacological enhancement of hemi-gap-junctional currents in *Xenopus* oocytes. *J. Neurosci. Methods* 121: 81-92.
- Ripps, H. 2002. Cell death in retinitis pigmentosa: gap junctions and the 'bystander' effect. *Exp. Eye Res.* 74: 327-336.
- Shuster, C. B., and D. R. Burgess. 2002. Targeted new membrane addition in the cleavage furrow is a late, separate event in cytokinesis. *Proc. Natl. Acad. Sci. USA.* 99: 3633-3638.
- Shuster, C. B., and D. R. Burgess. 2002. Transitions regulating the timing of cytokinesis in embryonic cells. *Curr. Biol.* 12: 854-858.
- Silver, Robert B., and Marc Bartman. 2002. A metronome-like control of the calcium signal leading to nuclear envelope breakdown and mitosis in sand dollar (*Echinarracnius parma*) cells. *Biol. Bull.* 203: 213-215.
- Smith, K., C. Ridings, F. A. Dodge, and R. B. Barlow. 2002. Development of the lateral eye of juvenile *Limulus*. *Biol. Bull.* 203: 222-223.
- Smotherman, Michael. 2002. Acetylcholine mediates excitatory input to chromatophore motoneurons in the squid, *Loligo pealeii*. *Biol. Bull.* 203: 231-232.
- Sommers, M.G., Dollhopf, M.E. and Douglas, S. 2002. Freshwater ferromanganese stromatolites from Lake Vermilion, Minnesota: microbial culturing and environmental scanning electron microscopy investigations. *Geomicrobiol. J.* 19: 407-427.
- Thompson R. F., and G. M. Langford. 2002. Myosin superfamily evolutionary history. *Anat. Rec.* 268: 276-289.
- Tirnauer, J., Julie C. Canman, E. D. Salmon, and Timothy J. Mitchison. 2002. EB1 targets to kinetochores with attached, polymerizing microtubules. *Mol. Biol. Cell* 13: 4308-4316.
- Tirnauer J. S., S. Grego, E. D. Salmon, and T. J. Mitchison. 2002. EB1-microtubule interactions in *Xenopus* egg extracts: role of EB1 in microtubule stabilization and mechanisms of targeting to microtubules. *Mol. Biol. Cell.* 13: 3614-3626.
- Twig, G., R. P. Malchow, K. Hammar, P. J. S. Smith, H. Levy, and I. Perlman. 2002. A novel turtle retinal preparation for simultaneously measuring light-induced electrical activity and changes in metabolite levels. *Biol. Bull.* 203: 198-200.
- Wachowiak, M., L. B. Cohen, and M. Zochowski. 2002. Distributed and concentration invariant spatial representations of odorants by receptor neuron input to the turtle olfactory bulb. *J. Neurophysiol.* 87: 1035-1045.
- Weeg, M., R. R. Fay, and A. Bass. 2002. Directional response and frequency tuning in saccular nerve fibers of a vocal fish, *Pomichthys notatus*. *J. Comp. Physiol.* 188: 631-641.
- Weidner, Earl, and Ann Findley. 2002. Peroxisomal catalase in extrusion apparatus posterior vacuole of microsporidian spores. *Biol. Bull.* 203: 212.
- Wen, H., D. Jurkovicova, V. M. Pickel, A. E. Gioio, and B. B. Kaplan. 2002. Identification of a novel membrane-associated protein expressed in neurons of the squid and rodent nervous system. *Neuroscience* 114: 995-1004.
- White, T. W., M. Srinivas, H. Ripps, A. Trovato-Salinaro, D. F. Condorelli, and R. Bruzzone. 2002. Virtual cloning, functional expression and gating analysis of human connexin31.9. *Am. J. Physiol. Cell Physiol.* 283: C960-C970.
- Wöllert T., A. S. DePina, R. F. Thompson, and G. M. Langford. 2002. Ca<sup>2+</sup> effects on myosin-II-mediated contraction of pseudo-contractile rings and transport of vesicles in extracts of clam oocytes. *Biol. Bull.* 203: 206-208.
- Wöllert T., A. S. DePina, R. F. Thompson, and G. M. Langford. 2002. GTPase Rho is involved in myosin-II-mediated contraction of pseudo-contractile rings and transport of vesicles in extracts of clam oocytes. *Biol. Bull.* 203: 208-210.



# education

The 2002 Education Program provided 499 students from 288 institutions and 30 countries an opportunity to study a range of biological topics with some of the best and brightest scientists in the world serving as course faculty and lecturers. The Laboratory welcomed 554 faculty members and staff and 203 lecturers to the courses in 2002. They represented 175 institutions and 31 countries. Among the many outstanding lecturers last summer, we were especially pleased to host two Nobel Laureates, Michael Brown and Tim Hunt, who gave the Arthur K. Parpart and the Irvin Isenberg Lectures, respectively, in the Physiology course.

In addition to the MBL's six major summer courses, we offered 14 special topics courses throughout the year, including two exciting new courses: Advances in Genome Technology and Bioinformatics, directed by Claire M. Fraser, TIGR, and Mitchell Sogin, MBL; and Neuroinformatics, directed by Partha Mitra of Lucent Technologies, Emery Brown of Massachusetts General Hospital, and David Kleinfeld of the University of California, San Diego.

At the end of the 2002 season, we bid farewell to Chris Tschudi and Elisabetta Ullu, directors of the Biology of Parasitism course. Jay Bangs of the University of Wisconsin, Madison, will take the helm of that course in 2003. We also said goodbye to Bill Bialek and Rob de Ruyter Van Steveninck of the Computational Neuroscience course. Bard Ermentrout of the University of Pittsburgh and John White of Boston University will assume the directorship of the course in 2003. In addition, Sandra Masur, of Mount Sinai School of Medicine, joined David Papermaster as co-director of the Vision Research course in 2002.

The MBL's educational program once again received a stamp of approval from the National Institutes of Health's competitive peer review process with renewed funding for the Embryology, Neural Systems & Behavior, and Neurobiology courses, and new funding for the inaugural Neuroinformatics course.

## SUMMER COURSES

### Biology of Parasitism: Modern Approaches

June 13- August 10, 2002

#### DIRECTORS

Tschudi, Christian, Yale University Medical School  
Ullu, Elisabetta, Yale University Medical School

#### FACULTY

Bangs, James, University of Wisconsin-Madison  
Grencis, Richard, University of Manchester  
Hajduk, Stephen, University of Alabama-Birmingham  
Matthews, Keith, University of Manchester  
McFadden, Geoff, University of Melbourne  
Parsons, Marilyn, Seattle Biomedical Research Institute  
Rathod, Pradip, University of Washington  
Reiner, Steven, University of Pennsylvania

Tarleton, Rick, University of Georgia

#### LECTURERS

Allen, Judith, University of Edinburgh  
Cross, George, Rockefeller University  
Deitsch, Kirk, Weill Medical College of Cornell University  
Englund, Paul, Johns Hopkins Medical School  
Garside, Paul, University of Glasgow  
Hunter, Christopher, University of Pennsylvania  
Muller, Miklos, The Rockefeller University  
Nutman, Thomas, National Institutes of Health  
Panigrahi, Aswini, Seattle Biomedical Research Institute  
Pearlman, Eric, Case Western Reserve University  
Phillips, Meg, UT Southwestern Medical Center  
Riley, Eleanor, London School of Hygiene & Tropical Medicine  
Rudenko, Gloria, University of Oxford  
Sacks, David, NIAID, NIH  
Scherf, Artur, Institut Pasteur  
Stanley, Sam, Washington University  
Striepen, Boris, University of Georgia  
Waters, Andrew, Leiden University, The Netherlands  
White, Michael, Montana State University  
Wilson, Iain, National Institute for Medical Research  
Wynn, Thomas, National Institutes of Health  
Dobbelaere, Dirk, University of Bern  
Roditi, Isabel, University of Bern  
Soldati, Dominique, Imperial College of Science & Technology

#### TEACHING ASSISTANTS

Jiang, Lei, University of Washington  
Karthikeyan, Ganesan, University of Washington  
Mollard, Vanessa, University of Melbourne  
Arts, David, University of Pennsylvania  
Cummings, Kara, University of Georgia  
Jensen, Bryan, Seattle Biomedical Research Institute  
Mair, Gunnar, Queen's University Belfast  
Martin, Diana, University of Georgia  
Pennock, Joanne, University of Manchester  
Ralph, Stuart, University of Melbourne  
Triggs, Veronica, University of Wisconsin-Madison  
van Deursen, Fredenck, The University of Manchester



Kevin Begos

#### COURSE ASSISTANTS

Bridegam, Patrick, Texas A&M University  
McKinnon, Nicole, University of Victoria, B.C

#### STUDENTS

Avila, Andréa, Inst de Biol Molecular do Paraná-IBMP  
Chamond, Nathalie, Institut Pasteur  
Cockburn, Ian, University of Edinburgh  
Fenn, Katelyn, University of Edinburgh  
Green, Heather, New York University  
Karnataki, Anuradha, University of Washington  
Klotz, Christian, Humboldt-University-Berlin  
Kooij, Taco, Leiden University Medical Centre  
Lee, SooHee, Johns Hopkins School of Medicine  
Li, Hongjie, Yale University  
Meissner, Markus, Imperial College of Science, Technology & Medicine, UK  
Mueller, Ann-Kristin, University School of Medicine, Heidelberg  
Nkinin, Wuyika, University of Yaounde  
Slavin, Ileana, Universidad Nacional de Cordoba  
Stubbs, Janine, Royal Melbourne Hospital

### Embryology: Concepts and Techniques in Modern Developmental Biology

June 16 - July 28, 2002

#### DIRECTORS

Richard Harland, University of California, Berkeley  
Joel Rothman, University of California, Santa Barbara

#### FACULTY

Fraser, Scott, California Institute of Technology  
Levine, Michael, University of California, Berkeley  
Rokhsar, Dan, University of California, Berkeley  
Tabin, Clifford, Harvard University  
Blair, Seth, University of Wisconsin-Madison  
Bronner-Fraser, Marianne, California Institute of Technology  
Collazo, Andres, House Ear Institute  
Ettensohn, Charles, Carnegie Mellon University  
Halpern, Marnie, Carnegie Institution of Washington  
Henry, Jonathan, University of Illinois  
Krumlauf, Robb, Stowers Institute for Medical Research

Martindale, Mark, University of Hawaii  
Niswander, Lee, Sloan-Kettering Institute  
Patel, Nipam, University of Chicago  
Saunders, John, Retired  
Sherwood, David, California Institute of Technology  
Zeller, Robert, San Diego State University

#### LECTURERS

Davidson, Eric, California Institute of Technology  
Keller, Ray, University of Virginia  
Greenwald, Iva, Columbia University  
Joyner, Alexandra, New York University/HHMI  
McGinnis, William, University of California, San Diego  
Robertson, Elizabeth, Harvard University  
Sanes, Joshua, Washington University  
Shankland, Martin, University of Texas at Austin  
Struhl, Gary, Columbia University  
Trainor, Paul, Stowers Institute for Medical Research  
Wieschaus, Eric, Princeton University  
Wray, Gregory, Duke University  
Yelon, Deborah, New York University School of Medicine

#### S. MERYL ROSE LECTURER

Gerhart, John, University of California, Berkeley

#### TEACHING ASSISTANTS

Baker, Clare, University of Cambridge  
Cheeks, Rebecca, University of North Carolina-Chapel Hill  
Gamse, Joshua, Carnegie Institution of Washington  
Gerberding, Matthias, University of Chicago  
Gross, Jeffrey, Duke University  
Khokha, Mustafa, University of California, Berkeley/UCB  
Kuhlman, Julie, University of Oregon  
Lartillot, Nicolas, Centre Genetique Moleculaire  
Liu, Karen, University of California, Berkeley  
Maduro, Morris, University of California, Santa Barbara  
Nederbragt, Alexander, University of Hawaii/PBRC  
Solomon, Keely, Emory University  
Tobey, Allison, Memorial Sloan Kettering Cancer Center  
Wallingford, John, University of California, Berkeley  
Walsh, Emily, Whitehead Institute for Biomedical Research  
Weatherbee, Scott, Memorial Sloan Kettering Cancer Center  
Wiellette, Elizabeth, Whitehead Institute for Biomedical Research  
Wilson, Valene, Centre for Genome Research  
Wolfe, Adam, University of Illinois, Urbana

#### COURSE ASSISTANTS

Balligan, Sarah, University of Missouri-Columbia  
McCluskey, Kathryn, Marine Biological Laboratory  
Tai, Phillip, University of California, Berkeley

Continued...

## STUDENTS

Berry, Katy, University of Sheffield  
 Brown, Ann, Medgar Evers College  
 Caracino, Diana, Emory University School of Medicine  
 Copf, Tijana, University of Crete  
 Crotwell, Patricia, University of South Dakota  
 Dash, Satya, University of East Anglia  
 Delalande, Jean-Marie, University College London  
 Drago, Grazia, Universita Degli Studi di Palermo  
 Extavour, Cassandra, University of Cambridge  
 Guest, Jennifer, National Institute for Medical Research  
 Kee, Yun, California Institute of Technology  
 Kerney, Ryan, Harvard University  
 Koziel, Lydia, Max-Planck-Inst. for Molecular Genetics  
 Livi, Carolina, University of Texas Health Science Center, San Antonio  
 Malartre, Marianne, University of Portsmouth  
 Maslakova, Svetlana, Smithsonian Institution  
 Matus, David, University of Hawaii  
 Mitchell, Tracy, University of Wisconsin-Madison  
 Muyskens, Jonathan, University of Oregon  
 Nouri, Ali, Princeton University  
 Orsborn, April, University of Missouri-Columbia  
 Primus, Alexander, University of Texas, Austin  
 Roche, Daniel, University of California, Berkeley  
 Su, Yi-Hsien, Scripps Inst. of Oceanography, MBRD  
 Van Stry, Melanie, Boston University School of Medicine

## Microbial Diversity

June 16 - August 2, 2002

## DIRECTORS

Harwood, Caroline, University of Iowa  
 Spormann, Alfred, Stanford University

## FACULTY

Buckley, Daniel, University of Connecticut  
 Gibson, Jane, Cornell University (Emerita)  
 Marsh, Terence, Michigan State University

## LECTURERS

Boetius, Antje, MPI für Marine Mikrobiologie  
 Breznak, John, Michigan State University  
 DeLong, Edward, Monterey Bay Aquarium  
 Elhai, Jeff, Virginia Commonwealth University  
 Giovannoni, Stephen, Oregon State University  
 Gottschalk, Gerhard, Institut für Mikrobiologie u Genet  
 Handelsman, Jo, University of Wisconsin  
 Larimer, Frank, Oak Ridge National Laboratory  
 Lory, Stephen, Harvard Medical School  
 Loveley, Derek, University of Massachusetts  
 Meeks, John, University of California  
 Metcalf, William, University of Illinois  
 Rocap, Gabnelie, University of Washington  
 Strous, Marc, University of Nymegen  
 Thauer, Rudolf, MPI für Terrestr. Mikro  
 Wackett, Lawrence, University of Minnesota  
 Wolfe, Ralph, University of Illinois



Kevin Begos

## TEACHING ASSISTANTS

Behrens, Sebastian, MPI for Marine Microbiology  
 Martiny, Adam, Danmark Tekniske Universitet  
 Mueller, Jochen, Stanford University  
 Schaefer, Amy, University of Iowa

## COURSE COORDINATOR

Hawkins, Andrew, University of Iowa

## LAB ASSISTANT

Waterbury, Matthew, Marine Biological Laboratory

## STUDENTS

Boucher, Yan, Dalhousie University  
 Case, Rebecca, University of New South Wales  
 Clement, Barbara, Doane College  
 Deneff, Vincent, Michigan State University  
 Dethlefsen, Les, Michigan State University  
 Dick, Gregory, Scripps Institute of Oceanography  
 Erbs, Marianne, Swiss Fed. Inst. for Environmental Science & Technology  
 Gentile, Margaret, Stanford University  
 Ginder-Vogel, Matthew, Stanford University  
 Graco, Michelle, University of Pierre et Marie Curie  
 Harrison, Faith, University of Iowa  
 Koren, Omry, Tel Aviv University  
 Lostroh, Phoebe, University of Iowa College of Medicine  
 Maresca, Julia, Pennsylvania State University  
 Pinel, Nicolas, University of Washington  
 Rajagopal, Soumitra, University of Nebraska  
 Remold, Susanna, Michigan State University  
 Sharp, Katherine, Scripps Institute of Oceanography  
 Spain, Jim, United States Air Force  
 Walker, Jeffrey, University of Colorado

## Neural Systems &amp; Behavior

June 16 - August 10, 2002

## DIRECTORS

Carr, Catherine, University of Maryland  
 Levine, Richard, University of Arizona

## FACULTY

Baines, Richard, University of Warwick  
 Calabrese, Ronald, Emory University  
 Chitwood, Raymond, Baylor College of Medicine  
 Davis, Graeme, University of California, San Francisco  
 French, Kathleen, University of California, San Diego  
 Glanzman, David, University of California, Los Angeles  
 Golowasch, Jorge, Rutgers University  
 Kristan, William, University of California, San Diego  
 Mooney, Richard, Duke University  
 Nadim, Farzan, Rutgers University  
 Philpot, Ben, Brown University  
 Prusky, Glen, University of Lethbridge  
 Reyes, Alex, New York University  
 Ribera, Angeles, University of Colorado Health Sciences Center  
 Roberts, William, University of Oregon  
 Simon, Jonathan, University of Maryland  
 Stein, Wolfgang, Universitaet Ulm  
 Szczupak, Lidia, Universidad de Buenos Aires  
 Weeks, Janis, University of Oregon  
 Wenning-Exleben, Angela, Emory University  
 Wessel, Ralf, Washington University  
 Wilson, Richard, University of Calgary  
 Wood, Debra, Case Western Reserve University  
 Wood, Emma, University of Edinburgh  
 Zhang, Bing, University of Texas at Austin

## LECTURERS

Augustine, George, Duke Medical Center  
 Bate, Michael, University of Cambridge  
 Feldman, Daniel, University of California, San Diego  
 Finger, Thomas, University of Colorado Health Sciences Center



## Neurobiology

June 16 - August 17, 2002

### DIRECTORS

Faber, Donald, Albert Einstein College of Medicine  
Lichtman, Jeff, Washington University School of Medicine

### SECTION DIRECTOR

DeFranco, Donald, University of Pittsburgh School of Medicine

### FACULTY

Buchanan, JoAnn, Stanford University  
Conchello, Jose-Angel, Washington University Medical School  
Coyle, Joseph, Harvard University  
Denk, Winfried, MPI für Medical Research  
Gan, Wenbiao, New York University  
Hart, Anne, Massachusetts General Hospital  
Heuser, John, Washington University  
Jacob, Michele, Tufts University  
Kaprielian, Zaven, Albert Einstein College of Medicine  
Khodakhah, Kamran, Albert Einstein College of Medicine  
Lambert, Nevin, Medical College of Georgia  
Levinthal, David, University of Pittsburgh  
Lin, Jen-Wei, Boston University  
Littleton, J. Troy, Massachusetts Institute of Technology  
Logothetis, Nikos, MPI for Biological Cybernetics  
McMahon, Lori, University of Alabama  
Pimenta, Aurea, University of Pittsburgh School of Medicine  
Preuss, Thomas, Albert Einstein College of Medicine  
Price, Donald, Johns Hopkins University  
Reese, Tom, NIH  
Schweizer, Felix, University of California, Los Angeles  
Smith, Stephen, Stanford University  
Thompson, Wesley, University of Texas  
Wong, Rachel, Washington University

### LECTURERS

Almers, Wolfhard, Vollum Institute  
Auerbach, Anthony, SUNY at Buffalo  
Bear, Mark, HHMI/Brown University  
Brodin, Lennart, Karolinska Institutet  
Chapman, Ed, University of Wisconsin-Madison  
Harlow, Mark, Stanford University  
Harris, Ken, Rutgers University  
Hoh, Jan, Johns Hopkins School of Medicine  
Hopkins, Nancy, Massachusetts Institute of Technology  
Huguenard, John, Stanford University  
Kernan, Maurice, SUNY at Stony Brook  
Lipscombe, Diane, Brown University  
Magee, Jeffrey, Louisiana State University Health Science Center  
McMahan, Uel J., Stanford University  
Nedivi, Elly, Massachusetts Institute of Technology  
Nicolelis, Miguel, Duke University  
Ogden, David, National Institute for Medical Research  
Ryan, Tim, Weill Medical Cornell  
Sigworth, Fred, Yale University  
Svoboda, Karel, Cold Spring Harbor Laboratory  
Tsien, Roger, University of California, San Diego  
Tully, Tim, Cold Spring Harbor Laboratory  
Yellen, Gary, Harvard Medical School

### TEACHING ASSISTANTS

Allana, Tariq, Boston University  
Chang, Paul, New York University  
Godinho, Leanne, Washington University School of Medicine  
Guan, Zhuo, Massachusetts Institute of Technology  
Misgeld, Thomas, Washington University School of Medicine  
Rosenberg, Madelaine, Tufts University  
Szabo, Theresa, Albert Einstein College of Medicine

### COURSE ASSISTANTS

Hall, David, Marine Biological Laboratory  
Satterlee, Danielle, Texas A & M University

### STUDENTS

Boassa, Daniela, University of Arizona College of Medicine  
Campbell, Susan, University of Alabama, Birmingham  
Ewald, Rebecca, Cold Spring Harbor Laboratory  
Hobbs, Steven, University of Colorado  
Hu, Hailan, University of California, Berkeley  
Ihring, Alexandra, Max-Planck-Institute of Neurobiology  
Koirala, Samir, University of Southern California  
Kozhevnikov, Alexey, Bell Labs/Lucent Technologies  
Montana, Enrico, Massachusetts Institute of Technology  
Petersen, Rasmus, International School for Advanced Study (SISSA)  
Ryan, Amy, University of Virginia Health Systems  
Zhou, Zhaolan (Joe), Harvard Medical School

## Physiology: The Biochemical and Molecular Basis of Cell Signaling

June 16 - July 27, 2002

### DIRECTORS

Garbers, David, UT Southwestern Medical Center/HHMI  
Reed, Randall, Johns Hopkins University/HHMI

### FACULTY

Duncan, Tod, Imperial Cancer Research Fund  
Ehrlich, Barbara, Yale University  
Franco, Peter, University of Minnesota  
Furlow, David, University of California, Davis  
Kao, Ling-Rong, University of Texas Southwestern Medical Center  
Lim, Wayland, University of California, Davis  
Megraw, Timothy, University of Texas Southwestern Medical Center  
Schultz, Nikolaus, University of Texas Southwestern Medical Center

### LECTURERS

Bennett, Anton, Yale Medical School  
Clapham, David, Harvard Medical School  
Comerford, Sarah, University of Texas Southwestern Medical Center  
Devreotes, Peter, Johns Hopkins University School of Medicine  
Dietrich, William, Harvard Medical School  
Gardner, Kevin, University of Texas Southwestern Medical Center

Stewart, Bryan, University of Toronto  
Trussell, Larry, Oregon Health & Science University  
White, Stephanie, University of California, Los Angeles

### TEACHING ASSISTANTS

Beenhakker, Mark, University of Pennsylvania  
Bradford, Yvonne, University of Oregon  
Chen, Shanning, House Ear Institute  
Coleman, Melissa, Duke University  
Ezzeddine, Youssef, University of California, Los Angeles  
Fames, Michael, University of Pennsylvania  
Heiser, Ryan, University of Colorado Health Sciences  
MacLeod, Katrina, University of Maryland, College Park  
Miller, Julie, University of Arizona  
Roberts, Adam, University of California, Los Angeles  
Roy, Arani, Duke University  
Siegel, Jennifer, Bowling Green State University  
Soares, Daphne, University of Maryland  
Svoboda, Kurt, University of Colorado Health Sciences Center  
Villareal, Greg, University of California, Los Angeles  
Zee, M. Jade, University of Oregon

### COURSE ASSISTANTS

Cardon, Aaron, Texas A & M University  
Rodríguez, Elizabeth, University of Oregon  
Shaw, Abigail, Stanford University

### STUDENTS

Chang, Andrew, Oregon State University  
De Labra, Carmen, University College London  
Dellen, Babette, Washington University, St. Louis  
Doiron, Brent, University of Ottawa  
Dulcis, Davide, University of Arizona, Tucson  
Higley, Michael, University of Pennsylvania  
Hughes, Cynthia, Indiana University  
Julian, Glennis, University of Arizona  
Khalil, Mona, Columbia University  
Miranda, Jason, University of Texas at Austin  
Pfeiffer, Keram, Philipps-Universität Marburg  
Renart, Alfonso, Brandeis University  
Rutherford, Mark, University of Oregon  
Sebe, Joy, University of Washington  
Spitzer, Nadja, Georgia State University  
Steinberg, Rebecca, University of Texas  
Sterner, Scott, Rockefeller University  
Witney, Alice, University of Birmingham Medical School  
Wohlgemuth, Sandra, Humboldt-Universität zu Berlin  
Zomik, Erik, Columbia University

## 2002 SPECIAL LECTURE SERIES

## Meryl S. Rose Lecture (June 17)

John Gerhart, University of California, Berkeley  
 "Cells, Embryos, and Evolution: Toward a Cellular and Developmental Understanding of Phenotypic Variation and Evolutionary Adaptability"

## Irvin Isenberg Lecture (June 21)

Timothy Hunt, Nobel Laureate, International Cancer Research Fund, Clare Hall Laboratories  
 "Protein Synthesis and the Control of the Cell Cycle"

## Gertrude Forkosh Waxler Lecture (July 17)

Robert A. Weinberg, Massachusetts Institute of Technology  
 "Rules for Making Human Tumor Cells"

## Teru Hayashi Lecture (July 23)

Melanie H. Cobb, University of Texas Southwestern Medical Center  
 "Information Flow in MAP Kinase Cascades"

## Arthur K. Parpart Lecture (July 26)

Michael Brown, Nobel Laureate, University of Texas Southwestern Medical Center  
 "The SREBP Pathway: How the Membrane Tells the Nucleus What it Needs"

## Ruth Sager Lecture in Genetics (August 30)

Mark Fishman, Massachusetts Hospital and Harvard Medical School  
 "Genetic Modules: Fashioning Organs in Zebrafish"

Hammer, Robert, University of Texas  
 Southwestern Medical Center

Hepler, Peter, University of Massachusetts  
 Mangelsson, David, University of Texas  
 Southwestern Medical Center

Nambu, John, University of Massachusetts  
 Stock, Ann, University of Medicine & Dentistry,  
 New Jersey-RW Johnson Medical School/HHMI  
 Tilney, Lewis, University of Pennsylvania  
 Welsh, Michael, University of Iowa

## IRVIN ISENBERG LECTURER

Hunt, Timothy, International Cancer Research  
 Fund, Clare Hall Laboratories

## GERTRUDE FORKOSH WAXLER LECTURER

Weinberg, Robert, Whitehead Institute

## ARTHUR K. PARPART LECTURER

Brown, Michael, University of Texas  
 Southwestern Medical Center

## TERU HAYASHI LECTURER

Cobb, Melanie, University of Texas  
 Southwestern Medical Center

## TEACHING ASSISTANTS

Anyatonwu, Georgia, Yale University  
 Rengifo, Juliana, Yale University

## COURSE COORDINATOR

Rossi, Kristen, University of Texas Southwestern  
 Medical Center

## COURSE ASSISTANTS

Grellhesl, Dana, University of Texas Southwestern  
 Medical Center  
 Swaney, Sara-Love, University of Texas  
 Southwestern Medical Center

## STUDENTS

Aguilar, Arturo, Instituto Politécnico Nacional,  
 Mexico  
 Amarie, Dragos, University of Notre Dame  
 Chen, Yen-Chin, National Cheng Kung University  
 Medical College  
 Chong, Curtis, Johns Hopkins School of Medicine  
 Davis, Kevin, University of Pittsburgh  
 Dojcinovic, Danijel, Arizona State University  
 Gadea, Bedrick, Harvard Medical School  
 Ge, Lan, University of California, Riverside  
 Goentoro, Lea, Princeton University  
 Kaynar, Murat, Beth Israel Deaconess  
 Medical Center  
 Kelly, Melissa, University of Kentucky College  
 of Medicine  
 Kydd, Alison, University of Calgary  
 LaPointe, Nichole, Northwestern University  
 McVaugh, Cheryl, University of Pennsylvania  
 Oh, Ji-Eun, University of Illinois at Chicago  
 Pace, Margaret, University of Texas  
 Pignatelli, Vincenzo, University of Pisa  
 Pineda, Gabriel, University of Texas  
 Southwestern Medical Center  
 Ramos, Arnolt, Children's Hospital, Boston  
 Rossi, Chiara, University of Pisa  
 Sha, Edward, Indiana University Medical Center  
 Thamatrakoln, Kimberlee, University of California,  
 San Diego  
 Vega, Rebecca, Stanford University

## SPECIAL TOPICS COURSES

Advances in Genome Technology  
& Bioinformatics

October 6 - November 2, 2002

## DIRECTORS

Fraser, Claire, The Institute for Genomic Research  
 Sogin, Mitchell, Marine Biological Laboratory

## FACULTY

Bateman, Alex, Sanger Institute  
 Blake, Judith, Jackson Laboratory  
 Churchill, Gary, Jackson Laboratory  
 Cummings, Michael, Marine Biological Laboratory  
 deJong, Pieter, Children's Hospital Oakland  
 Research Institute  
 DeLong, Edward, Monterey Bay Aquarium  
 Eisen, Jonathan, The Institute for Genomic  
 Research  
 Eisen, Michael, Lawrence Berkeley  
 Feldblyum, Tamara, The Institute for Genomic  
 Research  
 Felsenstein, Joe, University of Washington  
 Florens, Laurence, Scripps Research Institute  
 Gill, Steven, The Institute for Genomic Research  
 Gray, Michael, Dalhousie Institute  
 Heidelberg, John, The Institute for Genomic  
 Research  
 Jaffe, David, Whitehead Institute for Biomedical  
 Research  
 Kent, Jim, University of California, Santa Cruz  
 Kim, Ulandt, Marine Biological Laboratory  
 Lee, Norman, The Institute for Genomic Research  
 Mann, Barbara, University of Virginia Health  
 System  
 McArthur, Andrew, Marine Biological Laboratory  
 Mesirov, Jill, Whitehead Institute for Biomedical  
 Research  
 Morrison, Hilary, Marine Biological Laboratory  
 Myers, Eugene, Celera Genomics  
 Nelson, Karen, The Institute for Genomic  
 Research  
 Nierman, William, The Institute for Genomic  
 Research  
 Nusbaum, Chad, Whitehead Institute for  
 Biomedical Research  
 Ochman, Howard, University of Arizona  
 Olsen, Gary, University of Illinois

Palmer, Jeffrey, Indiana University  
 Pearson, William, University of Virginia  
 Peterson, Scott, The Institute for Genomic Research  
 Pop, Mihai, The Institute for Genomic Research  
 Quackenbush, John, The Institute for Genomic  
 Research  
 Reich, Claudia, University of Illinois  
 Reysenbach, Anna-Louise, Portland State University  
 Ringwald, Martin, Jackson Laboratory  
 Roos, David, University of Pennsylvania  
 Salzberg, Steven, The Institute for Genomic Research  
 Smith, Hamilton, Celera Genomics  
 Tettelin, Herve, The Institute for Genomic Research  
 Venter, Craig, The Institute for Genomic Research  
 Wernegreen, Jennifer, Marine Biological Laboratory  
 White, Owen, The Institute for Genomic Research

## TEACHING ASSISTANTS

Tallon, Luke, The Institute for Genomic Research  
 Radune, Diana, The Institute for Genomic Research  
 Vamathevan, Jessica, The Institute for Genomic  
 Research  
 Davidsen, Tanja, The Institute for Genomic Research  
 Gill, John, The Institute for Genomic Research  
 Bhagabati, Nirmal, The Institute for Genomic Research  
 Saeed, Alexander, The Institute for Genomic Research  
 White, Joseph, The Institute for Genomic Research  
 Thiagarajan, Mathangi, The Institute for Genomic  
 Research  
 Wang, Hong-Ying, The Institute for Genomic Research  
 Gaspard, Renee, The Institute for Genomic Research  
 Frank, Bryan, The Institute for Genomic Research  
 Hasseman, Jeremy, The Institute for Genomic Research

## STUDENTS

Bebout, Brad, NASA Ames Research Center  
 Brodhagen, Marion, Oregon State University  
 Bundy, Becky, University of Georgia  
 Chen, Lishan, University of Washington  
 da Silva, Alexandre, Centers for Disease Control  
 and Prevention  
 Doak, Thomas, University of Utah  
 Duvefelt, Kristina, Karolinska Institutet  
 Fenwick, Brad, Kansas State University  
 Francis, Susan, University of Washington  
 Gilchrist, George, College of William & Mary  
 Golden, Daniel, University of Alabama, Birmingham

Handley, Heather, Woods Hole Oceanographic Institution  
 Hildebrandt, John, Medical University of South Carolina  
 Kanzok, Stefan, Yale University School of Medicine  
 Kiesling, Traci, University of Miami  
 Kimbell, Jennifer, University of Hawaii  
 Kinnersley, Margie, University of Montana  
 Neumann, Tobias, Carl Zeiss  
 Jena-Pineda, Fernando, Johns Hopkins Bloomberg School of Public Health  
 Radniecki, Tyler, Yale University  
 Ranson, Hilary, Liverpool School of Tropical Medicine  
 Sawyer, Sara, Cornell University  
 Thomas, Bolaji, Tufts University  
 Williams, David, Illinois State University

Fitzpatrick, John, Yale University School of Medicine  
 Fleming, Shawna, Brown University  
 Fu, Lianwu, University of Alabama, Birmingham  
 Galko, Michael, Stanford University School of Medicine  
 Glover, Greta, Oregon Health and Sciences University  
 Green, Heather, New York University  
 Gruenbaum, Lore, Boehringer Ingelheim Pharmaceuticals  
 Habdas, Piotr, Emory University

## Molecular Biology of Aging

August 5 - August 24, 2002

### DIRECTORS

Guarente, Lenny, Massachusetts Institute of Technology  
 Wallace, Douglas, University of California, Irvine

### FACULTY

Culotta, Valeria, Johns Hopkins University  
 Kirkwood, Tom, University of Manchester  
 Lambeth, Dave, Emory University

## Analytical and Quantitative Light Microscopy

May 9 - May 17, 2002

### DIRECTORS

Sluder, Greenfield, University of Massachusetts Medical Center  
 Wolf, David, BioHybrid Technologies

### FACULTY

Amos, William, MRC Lab of Molecular Biology  
 Bulseco, Dylan, University of Massachusetts Medical School  
 Cardullo, Richard, University of California  
 Gelles, Jeff, Brandeis University  
 Hinchcliffe, Edward, University of Notre Dame  
 Inoué, Shinya, Marine Biological Laboratory  
 Moomaw, Butch, Hamamatsu Photonic Systems  
 Reichelt, Stefanie, MRC Lab of Molecular Biology  
 Salmon, Edward, University of North Carolina, Chapel Hill  
 Silver, Randi, Weill Medical College Cornell University  
 Spring, Kenneth, National Institutes of Health  
 Swedlow, Jason, University of Dundee  
 Waters Shuler, Jennifer, Harvard Medical School  
 Sears, Kathryn, Sensor Technologies

### LECTURERS

Straight, Aaron, Harvard Medical School  
 Wachowiak, Mel, Smithsonian Institution

### TEACHING ASSISTANT

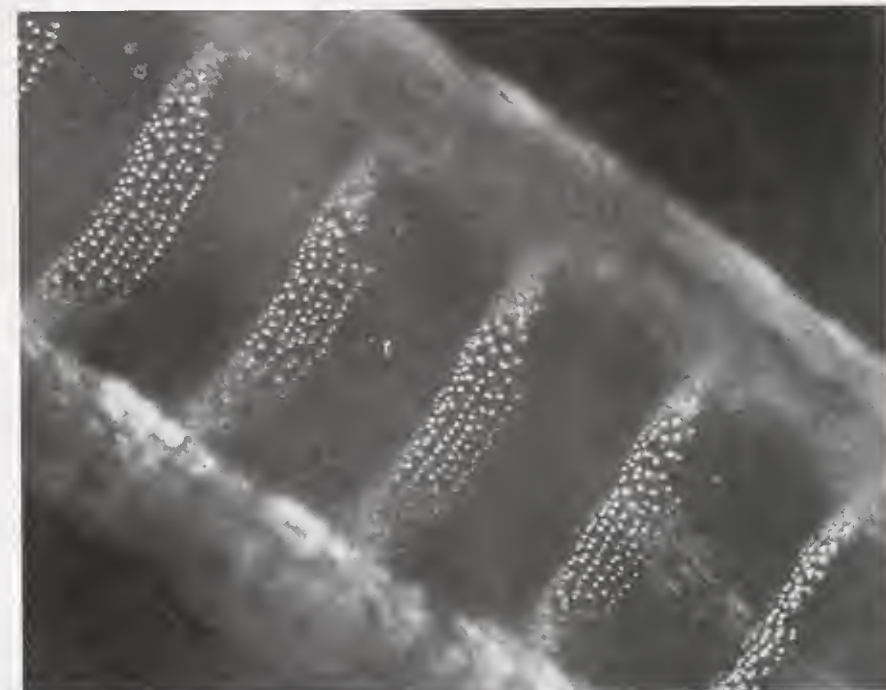
Ehrhardt, Anka, University of Massachusetts Medical School

### COURSE ASSISTANT

Nordberg, Joshua, University of Massachusetts Medical School

### STUDENTS

Chatterjee, Samit, Weill Medical College of Cornell University  
 Cooke, Emma-Louise, AstraZeneca R&D, Charnwood, UK  
 Counterman, Anne, Pennsylvania State University  
 Espinosa Tanguma, Ricardo, University of San Lui Potosi  
 Fischer, Robert, The Scripps Research Institute



*Drosophila*, April Orsbom

Hidalgo, Carlos, Instituto Venezolano de Investig. Cientificas  
 Iszard, Melissa, Raytheon Polar Services  
 Jungnickel, Melissa, University of Massachusetts Medical School  
 Liu, Songtao, Fox Chase Cancer Center  
 Luna, Elizabeth, University of Massachusetts Medical School  
 McKeown, Caroline, University of Utah  
 Paladino, Simona, University of Naples  
 Panetti, Tracee, Temple University School of Medicine  
 Poskanzer, Kira, University of California, San Francisco  
 Powers, Maureen, Emory University  
 Raphael, Marc, The Naval Research Laboratory  
 Rusan, Nasser, University of Massachusetts, Amherst  
 Smyth, Jeremy, University of Massachusetts, Amherst  
 Tam, Jenny, Tufts University  
 Wagener, Michael, Carl Zeiss, Inc.  
 Welch, Jeffrey, Duke University Medical Center  
 Yamamoto, Akihiro, RIKEN, Japan  
 Zandbank-Zucker, Keren, Hebrew University  
 Zhang, LingLi, University of Pennsylvania

Weindruch, Richard, University of Wisconsin  
 Bishop, Nicholas, Massachusetts Institute of Technology  
 Helfand, Stephen, University of Connecticut Health Center  
 Price, Donald, Johns Hopkins University  
 Ruvkun, Gary, Massachusetts General Hospital  
 Wright, Woodring, University of Texas Southwestern Medical Center

### LECTURERS

Pelicci, Pier Giuseppe, European Institute of Oncology  
 Austad, Steven, University of Idaho  
 Bohr, Vilhelm, National Institute on Aging, NIH  
 Campisi, Judith, Lawrence Berkeley National Laboratory  
 Davenport, John, AAAS  
 Donehower, Larry, Baylor College of Medicine  
 Goldberg, Alfred, Harvard Medical School  
 Hanawalt, Philip, Stanford University  
 Harley, Calvin, Geron Corporation  
 Hekimi, Siegfried, McGill University  
 Jones, Dean, Emory University  
 Kim, Stuart, Stanford University  
 Martin, George, University of Washington

Continued...

Partridge, Linda, University College London  
Richardson, Arlan, University of Texas Health  
Science Center at San Antonio  
Tatar, Marc, Brown University  
Tower, John, University of Southern California

#### TEACHING ASSISTANTS

Coskun, Elif Pinar, Emory University  
Kaeberlein, Mark, Massachusetts Institute of  
Technology  
Kerstann, Keith, Emory University  
Kokoszka, Jason, Emory University  
Visithawan, Mo, Massachusetts Institute  
of Technology  
Liszt, Gregory, Massachusetts Institute of  
Technology  
Subramaniam, Vaidya, Emory University

#### COURSE COORDINATOR

Burke, Rhonda, Emory University

#### COURSE ASSISTANT

Wylie, Michael, University of Michigan

#### STUDENTS

Almeida, Cláudia, Weill Medical College  
of Cornell University  
Bishop, Glenda, Case Western Reserve University  
Bokov, Alex, University of Texas Health Science  
Center, San Antonio  
Chen, Lishan, University of Washington  
Dunaief, Joshua, University of Pennsylvania  
Fuller, Kathryn, University of Minnesota  
Harvey, Sarah, Medical College of Virginia  
Hong, Eun-Jin (Erica), Yale University  
Johnston, Janet, Queen's University Belfast  
Lledias, Fernando, Instituto de Biotecnologia,  
UNAM  
Lu, Xiangdong, University of North Carolina,  
Chapel Hill  
Moynihan, Kathryn, Washington University  
Ogle, William, Stanford University  
Powers, Ralph, The University of Washington  
Proctor, Carole, University of Newcastle  
Rea, Shane, University of Colorado  
Rutten, Bart, University of Maastricht  
Shirasawa, Takuji, Tokyo Metropolitan Institute  
of Gerontology  
Tong, Liqi, University of California, Irvine  
Zou, Ying, University of Texas Southwestern  
Medical Center

### Frontiers in Reproduction: Molecular and Cellular Concepts and Applications

May 19 - June 29, 2002

#### DIRECTORS

Fazleabas, Asgerally, University of Illinois at  
Chicago  
Hunt, Patricia, Case Western Reserve University  
Woodruff, Teresa, Northwestern University

#### FACULTY

Albertini, David, Tufts University School of  
Medicine  
Ascoli, Mario, The University of Iowa  
Behringer, Richard, University of Texas  
Cross, James C., University of Calgary  
Croy, B. Anne, University of Guelph  
DeMayo, Francesco, Baylor College of Medicine

Ducibella, Thomas, New England Medical Center  
Hunt, Joan, University of Kansas  
Jaffe, Laurinda, University of Connecticut  
Health Center  
Mayo, Kelly, Northwestern University  
Moore, Karen, University of Florida  
Overstrom, Eric, Tufts University School  
of Veterinary Medicine  
Schatten, Gerald, University of Pittsburgh  
Shupnik, Margaret, University of Virginia  
Medical Center  
Terasaki, Mark, University of Connecticut  
Health Center  
Weigel, Nancy, Baylor College of Medicine

#### Lecturers

Gosden, Roger, Eastern Virginia Medical School  
Guillette, Louis, University of Florida  
Hassold, Terry, Case Western Reserve University  
Miele, Lucio, University of Illinois at Chicago  
Nilson, John, Case Western Reserve University  
Ober, Carole, University of Chicago  
Richards, JoAnne, Baylor College of Medicine  
Sarras Jr., Michael, University of Kansas  
Medical Center  
Schultz, Richard, University of Pennsylvania  
Seminara, Stephanie, Massachusetts General  
Hospital  
Shenker, Andrew, Northwestern University  
Medical School  
Simerly, Calvin, Pittsburgh Development Center  
Suarez-Quian, Carlos, Georgetown University  
Medical School  
Tasca, Richard, NIH  
Wells, Dagan, St. Barnabas Medical Center  
Welt, Corrine, Massachusetts General Hospital  
Yin, Hang, McGill University

#### Teaching Assistants

Agoulnik, Irina, Baylor College of Medicine  
Aldrich, Carrie, Roche Molecular Systems  
Berard, Mark, University of Michigan  
Britton, Chad, Case Western Reserve University  
Brudney, Allison, University of Illinois at Chicago  
Carroll, David, Florida Institute of Technology  
Combelles, Catherine, Tufts University  
Curtin, Denis, University of Virginia  
Galet, Colette, University of Iowa  
Hadsell, Louise, Baylor College of Medicine  
Huntress, Victoria, Tufts University School of  
Veterinary Medicine  
Jackson, Jodi, Case Western Reserve University  
Kalinowski, Rebecca, University of Connecticut  
Health Center  
Kenny, Hilary, Northwestern University  
Kim, Julie, University of Illinois at Chicago  
Kleinhenz, Andrew, Case Western Reserve  
University  
Payne, Christopher, Magee-Womens Research  
Institute  
Petroff, Margaret, University of Kansas  
Medical Center  
Runft, Linda, University of California, Santa  
Barbara  
Santiago, Jose, Northwestern University  
Stein, Paula, University of Pennsylvania  
Susiarjo, Martha, Case Western Reserve University  
Suszko, Magdalena, Northwestern University  
Wang, Min-Kang, Tufts University Veterinary  
School  
Wang, Jie, Baylor College of Medicine

#### COURSE COORDINATOR

Roberts, Sheila, Bridgewater State College

#### COURSE ASSISTANT

Harrison, Emily, Bridgewater State College

#### STUDENTS

Akcali, Kamil, Bilkent University, Turkey  
Bachman, Katherine, Case Western Reserve  
University  
Busso, Dolores, Buenos Aires University  
Gill, Ryan, University of Kansas Medical Center  
Gonsalves, Joanna, University of California,  
San Francisco  
Hallikas, Outi, University of Helsinki  
Ka, Hakhyun, University of Kansas Medical Center  
Kayisli, Umit, Yale University School of Medicine  
Kreeger, Pamela, Northwestern University  
Perez, Christian, University of Pennsylvania  
Prosen, Tracy, University of Pittsburgh  
Sachdeva, Geetanjali, Institute for Research  
in Reproduction  
Torréns, Javier, New Jersey Medical School,  
UMDNJ  
Tou, Janet, NASA Ames Research Center  
Wang, Eileen, Northwestern Medical School

### Fundamental Issues in Vision Research

August 11 - August 24, 2002

#### DIRECTORS

Masur, Sandra, Mount Sinai School of Medicine  
Papermaster, David, University of Connecticut  
Health Center



Limulus eye, Robert Barlow

#### FACULTY

Beebe, David, Washington University  
Bok, Dean, University of California, Los Angeles  
Born, Richard, Harvard Medical School  
Colley, Nansi, University of Wisconsin - Madison  
Gordon, Marion, Rutgers University  
Horwitz, Joseph, Jules Stein Eye Institute, UCLA  
Masland, Richard, Harvard/MGH  
Sugrue, Stephen, University of Florida

## LECTURERS

Barlow, Robert, SUNY Upstate Medical University  
 Barres, Ben, Stanford Medical School  
 Berson, Elliot., Harvard Medical School  
 Besharse, Joseph, Medical College of Wisconsin  
 Birk, David, Jefferson Medical College  
 Bok, Dean, University of California, Los Angeles  
 Colley, Nansi, University of Wisconsin-Madison  
 Dowling, John, Harvard University  
 Green, Carla, University of Virginia  
 Griep, Ann, University of Wisconsin Medical School  
 Hauswirth, William, University of Florida College of Medicine  
 Hernandez, Rosario, Washington University School of Medicine  
 Horton, Jonathan, University of California, San Francisco  
 Hunter, Chyren, National Eye Institute/NIH  
 Lang, Richard, Children's Hospital, Cincinnati  
 Liberman, Ellen, National Eye Institute/NIH  
 LaVail, Jennifer, University of California, San Francisco  
 Moses, Marsha, Harvard Medical School  
 Niederkorn, Jerry, University of Texas Southwestern Medical Center  
 Piatigorsky, Joram, NIH/NEI  
 Raviola, Elio, Harvard Medical School  
 Stepp, Mary Ann, GWU Medical Center  
 Wasson, Paul, Eye Health Services, Weymouth, MA  
 Wiggs, Janey, Massachusetts Eye & Ear Infirmary

## COURSE COORDINATOR

Zekaria, Dania, Mount Sinai School of Medicine

## STUDENTS

Bensingler, Steven, University of Pennsylvania  
 Cusato, Karen, Albert Einstein College of Medicine  
 Dominy, Nathaniel, University of Chicago  
 Ehrlich, Jason, Stanford University School of Medicine  
 Ensslen, Sonya, Case Western Reserve University  
 Katz, Elizabeth, University of Maryland  
 Levy, Hanna, Technion Israel Institute of Technology  
 Lishko, Polina, Massachusetts Eye & Ear Infirmary  
 McCabe, Sarah, Brown University  
 Ortega, Nathalie, University of California, San Francisco  
 Prasad, Dipti, University of California, San Diego  
 Ramsey, David, University of Illinois, Chicago  
 Reiter, Chad, Pennsylvania State University College of Medicine  
 Shepard, Laura, University of Oklahoma Health Science Center  
 Steinle, Jena, Texas A&M University Health Science Center  
 Wei, Echo Shiyi, University of Southern California  
 Wu, David, University of Michigan  
 Yang, Ellen, Mount Sinai School of Medicine  
 Zamora, David, Oregon Health & Science University  
 Zandy, Anna, Washington University in St. Louis

## Medical Informatics I

May 26 - June 2, 2002

## DIRECTOR

Cimino, James, Columbia University

## FACULTY

Ackerman, Michael, National Library of Medicine  
 Bakken, Suzanne, Columbia University  
 Friedman, Charles, University of Pittsburgh  
 Hammond, William, Duke University Medical Center  
 Kingsland, Lawrence, National Library of Medicine  
 Kohane, Issac, Children's Hospital  
 Lindberg, Donald, National Library of Medicine  
 Miller, Perry, Yale University  
 Starren, Justin, Columbia University

## LECTURERS

Canese, Kathi, National Library of Medicine  
 Cimino, Christopher, Albert Einstein College of Medicine  
 McCray, Alexa, National Library of Medicine

## STUDENTS

Alverson, Dale, University of New Mexico  
 Anderson, Karen, University of North Dakota  
 Bergman, Dale, Alberta Research Council  
 Binstock, Mark, Ohio Permanente Medical Group  
 Bowles, Kathy, University of Pennsylvania  
 Bragdon, Lynn, Veterans Affairs Medical Center  
 Brock, Tina, University of North Carolina, Chapel Hill  
 Cheng, Grace, Hospital Authority  
 Chuma, Chomba, Avenue Healthcare Ltd  
 Cowen, Janet, Maine Medical Center  
 Dee, Cheryl, University of South Florida  
 Dhara, Rosaline, Centers for Disease Control & Prevention  
 Erdley, William, University of Buffalo  
 Hayes, Barrie, University of North Carolina, Chapel Hill  
 Henry, Nancy, Pennsylvania State University  
 Kovach, Christine, Kaiser Permanente Northwest  
 Lambert-Lanning, Anita, Toronto West Hospital-University Health Network  
 Luberti, Anthony, The Children's Hospital of Philadelphia  
 Marazzo, Donald, Family Health Council  
 Markland, Mary, University of North Dakota  
 McCabe, Jennifer, James Madison University  
 Pond, Fred, Dartmouth College  
 Prendergast, Neville, Washington University School of Medicine  
 Raglow, Gregory, Good Samaritan Family Practice Center  
 Rangappa, Shantaram, Virginia Commonwealth University  
 Robertson, Nan, Kaiser Permanente-Northwest  
 Ruiz, Jorge, University of Miami School of Medicine  
 Sinha, Sunil, VA Maryland Health Care System  
 Smith, Scott, University of North Carolina  
 Suzewits, Jeffrey, Southern Illinois University School of Medicine

## Medical Informatics II

September 29 - October 6, 2002

## DIRECTOR

Cimino, James, Columbia University

## FACULTY

Friedman, Charles, University of Pittsburgh  
 Kingsland, Lawrence, National Library of Medicine  
 Lindberg, Donald, National Library of Medicine  
 Miller, Perry, Yale University  
 Miller, Randolph, Vanderbilt University Medical Center  
 Nahin, Annette, National Library of Medicine  
 Nesbitt, Thomas, University of California, Davis  
 Ozbolt, Judy, Vanderbilt University  
 Shortliffe, Edward, Columbia University  
 Stead, William, Vanderbilt University

## LECTURERS

McCray, Alexa, National Library of Medicine  
 Ash, Joan, Oregon Health and Sciences University

## STUDENTS

Aarstad, Robert, Louisiana State University Medical School  
 Beaudoin, Denise, Utah Department of Health  
 Beyea, Suzanne, AORN  
 Bird, Geoffrey, Children's Hospital of Philadelphia  
 Bowen, Elizabeth, Morehouse School of Medicine  
 Contini, Janice, University of California, Los Angeles  
 Cuddy, Colleen, New York University School of Medicine  
 Driebeek, Mary, Duke University  
 Hughes, Christopher, Monongahela Valley Hospital  
 James, Veronica, Georgetown University Medical Center Library  
 Just, Melissa, Children's Hospital Los Angeles  
 Long, Susan, Virginia Mason Medical Center  
 Mays, Brynn, Georgetown University Medical Center  
 Meisel, Jim, Massachusetts General Hospital  
 Mittal, Richa, University of Toronto  
 Nagle, Ellen, University of Minnesota  
 Perley, Cathy, Emporia State University  
 Pimental, Sara, Kaiser Permanente  
 Reavie, Keir, University of California, San Francisco  
 Reisinger, Curtis, North Shore Long Island Jewish Health System  
 Schardt, Connie, Duke University  
 Schilling, Lisa, University of Colorado Health Sciences Center  
 Schmidt, Heidi, University of California, San Francisco  
 Sennett, Cary, American College of Cardiology  
 Silverman, Howard, Banner Health System  
 Trimarchi, Michaelleen, The Scripps Research Institute  
 Wax, Diane, University of New Mexico  
 White, Mary, Kaiser Permanente  
 Williams, Annette, Vanderbilt University Medical Center  
 Zuniga, Miguel, Texas A&M University Health Sciences Center

Continued...

## Methods in Computational Neuroscience

August 4 - September 1, 2002

### DIRECTORS

Bialek, William, Princeton University  
de Ruyter van Steveninck, Princeton University

### FACULTY

Abbott, Linda F., Brandeis University  
Aslin, Richard, University of Rochester, New York  
Ermentrout, Bard, University of Pittsburgh  
Fairhall, Adrienne, Princeton University  
Gelpenn, Alan, Monell Chemical Senses Center  
Jensen, Roderick, Wesleyan University  
Koberle, Roland, University of Sao Paulo  
Kopell, Nancy, Boston University  
Lewen, Geoffrey, NEC Research Institute, Inc  
Reinagel, Pamela, Harvard Medical School  
Saffran, Jenny, University of Wisconsin-Madison  
Schneidman, Elad, Princeton University  
Shadmehr, Reza, Johns Hopkins University  
Solla, Sara, Northwestern University  
Sompolinsky, Haim, Hebrew University  
Tank, David, Princeton University  
Tishby, Naftali, The Hebrew University  
White, John, Boston University

### LECTURERS

Alon, Uri, Weizmann Institute  
Ayuera y Arcas, Blaise, Princeton University  
Doupe, Allison, UCSF  
Fetsch, Robert, University of Wisconsin-Madison  
Hopfield, John, Princeton University  
Johnston, Dan, Baylor College of Medicine  
Kennedy, Mary, Cal Tech  
Logothetis, Nikos, Max-Planck-Institute  
Menzel, Rolf, Freie Universität Berlin  
Rieke, Fred, University of Washington  
Saffran, Jenny, University of Wisconsin-Madison  
Seung, Sebastian, Massachusetts Institute of Technology  
Srinivasan, MV, Australian National University  
Zucker, Steven, Yale University

### TEACHING ASSISTANT

Still, Susanne, Princeton University

### COURSE ASSISTANT

Jensen, Kate, Princeton University

### STUDENTS

Barreto, Ernest, George Mason University  
Beck, James, New York University School of Medicine  
Chakraborty, Santanu, Cold Spring Harbor Laboratory  
Chiappe, Eugenia, The Rockefeller University  
Connell, Michael, Harvard University  
Dobbins, Heather, University of Maryland at Baltimore  
Farries, Michael, University of Pennsylvania  
Gaertner, Tara, University of Texas Health Sciences Center  
Herrera-Valdez, Marco, University of Arizona  
Huys, Quentin, Cambridge University  
Lien, Cheng-Chang, Physiology Institute of University Freiburg  
Loebel, Alex, The Weizmann Institute of Science  
Ma, Whee Ky, California Institute of Technology  
Miller, Robyn, Cornell University  
Mirny, Leonid, Massachusetts Institute of Technology

Montgomery, Kimberly, Northwestern University  
Nasir, Sazzad, University of California, San Francisco  
Pinto, Reynaldo, Instituto de Física da Univ of São Paulo  
Raffi, Milena, Rutgers University  
Shahrezaei, Vahid, Simon Fraser University  
Stephens, Greg, Los Alamos National Laboratory  
Werner-Reiss, Uri, Dartmouth College  
Wright, Geraldine, Ohio State University  
Zhou, Yi, Boston University

## Molecular Mycology: Current Approaches to Fungal Pathogenesis

August 12 - August 30, 2002

### DIRECTORS

Edwards, John, Harbor-UCLA Medical Center  
Mitchell, Aaron, Columbia University

### FACULTY

Calderone, Richard, Georgetown University Medical Center  
Casadevall, Arturo, Albert Einstein College of Medicine  
Cole, Gary, Medical College of Ohio  
Filler, Scott, Harbor-UCLA Medical Center  
Heitman, Joseph, Duke University  
Magee, Paul, University of Minnesota  
Rhodes, Judith, University of Cincinnati  
Sanglard, Dominique, University Hospital Lausanne

### LECTURERS

Alspaugh, Andrew, Duke University Medical Center  
Brown, Alistair, University of Aberdeen  
Gale, Cheryl, University of Minnesota  
Goldman, William, Washington University  
Kronstad, Jim, University of British Columbia  
Kumamoto, Carol, Tufts University  
White, Ted, Seattle Biomedical Res. Inst  
Yeaman, Michael, UCLA-Harbor Medical Center

### COURSE COORDINATOR

Rafkin, Wendy, Harbor-UCLA Medical Center

### COURSE ASSISTANT

Mitchell, Hannah, Glen Ridge High School

### STUDENTS

Andes, David, University of Wisconsin  
Berbes, Carlos, Virginia Commonwealth University  
Frank, Charlotte, Yale University  
Heung, Lena, Medical University of South Carolina  
Jabra-Rizk, MaryAnn, University of Maryland, Baltimore  
MacCallum, Donna, University of Aberdeen  
Mayorga, Maria, Microbia Inc.  
Morais, Flavia, Universidade Federal de Sao Paulo  
Nielsen, Kirsten, Duke University Medical Center, HHMI  
Noble, Suzanne, University of California, San Francisco  
Ramon, Ana, Georgetown University Medical Center

Reese, Amy, Washington University School of Medicine  
Steinbach, William, Duke University  
Sturtevant, Joy, Louisiana State University Health Sciences Center  
Vallim, Marcelo, Duke University Medical Center  
Van Dijk, Patrick, Flemish Interuniversity Inst for Biotechnology  
Wozniak, Karen, Louisiana State University Health Sciences Center

## Neural Development and Genetics of Zebrafish

August 18 - August 31, 2002

### DIRECTORS

Moens, Cecilia, Fred Hutchinson Cancer Research Center/HHMI  
Talbot, William, Stanford University

### FACULTY

Chien, Chi-Bin, University of Utah  
Collazo, Andres, House Ear Institute  
Dowling, John, Harvard University  
Fetcho, Joseph, SUNY at Stony Brook  
Granato, Michael, University of Pennsylvania  
Hanlon, Roger, Marine Biological Laboratory  
Kimmel, Charles, University of Oregon  
Lin, Shuo, University of California, Los Angeles  
Link, Brian, Medical College of Wisconsin  
Linnon, Beth, Marine Biological Laboratory  
Mullins, Mary, University of Pennsylvania  
Neuhaus, Stephan, ETH Zurich  
Raible, David, University of Washington  
Wilson, Carole, University College London

### LECTURERS

Astrofsky, Keith, Praecis Pharmaceutical  
Fadool, James, Florida State University  
Hopkins, Nancy, Massachusetts Institute of Technology

### TEACHING ASSISTANTS

Cooke, Julie, Fred Hutchinson Cancer Research Center  
Downes, Gerald, University of Pennsylvania  
Durchanek, Charline, University of Oregon  
Hutson, Lara, University of Utah  
Schumacher, Jennifer, University of Pennsylvania  
Ungos, Josette, University of Washington

### COURSE COORDINATORS

Lawrence, Christian, Harvard University  
Lesko, Suzanna, Case Western Reserve University  
Perkins, Brian, Harvard University  
Wilson, Steven, University College London

### STUDENTS

Ahlgren, Sara, California Institute of Technology  
Campbell, Douglas, University of Cambridge  
Dambly-Chaudiere, Christine, Université Montpellier 2  
Dürr, Katrin, University of Freiburg  
Gerlach, Gabriele, Marine Biological Laboratory  
Hammonds-Odie, Latanya, Spelman College  
Leach, Steven, Johns Hopkins University  
Malaga-Trillo, Edward, University of Konstanz  
Masino, Mark, SUNY, Stony Brook  
Morris, Jacqueline, Cleveland Clinic Foundation  
Panzer, Jessica, University of Pennsylvania

Prober, David, University of Washington  
 Renier, Corinne, Stanford University  
 Stewart, Rodney, Dana Farber Cancer Institute  
 Wang, Weiyi, University of Pennsylvania  
 Westerlund, Johanna, University of Helsinki  
 Young, Rodrigo, Universidad de Chile

## Neuroinformatics

August 17 - September 1, 2002

### DIRECTORS

Brown, Emery, Massachusetts General Hospital  
 Kleinfeld, David, University of California, San Diego  
 Mitra, Partha, Bell Laboratories

### Faculty

Brillinger, David, University of California, Berkeley  
 Bokil, Hemant, California Institute of Technology  
 Fee, Michael, Bell Labs, Lucent Technologies  
 Iyengar, Satish, University of Pittsburgh  
 Mehta, Mayank, Massachusetts Institute of Technology  
 Pesaran, Bijan, California Institute of Technology  
 Purpura, Ketih, Cornell Medical School  
 Richmond, Barry, National Institute of Mental Health  
 Victor, Jonathan, Weill Medical College of Cornell University

### LECTURERS

Dale, Anders, Harvard University  
 Fitch, Tecumseh, Harvard University  
 Gardener, Dan, Cornell Medical School  
 Hu, Xiaoping, University of Minnesota  
 Jacobs, Gwen, Montana State University  
 King, Wayne, Ohio State University  
 Loader, Catherine, Bell Labs, Lucent Technologies  
 Margoliash, Daniel, University of Chicago  
 Miller, John, Montana State University  
 Schiff, Nicholas, Weill Medical College of Cornell University  
 Schmidt, Marc, University of Pennsylvania  
 Strothers, Steven, University of Minnesota  
 Tchernikovski, Ofer, City College of New York  
 Vicario, David, Rutgers University

### STUDENTS

Aldworth, Zane, Montana State University  
 Anderson, Britt, Brown University  
 Baron, Jérôme, Max-Planck-Institute for Brain Research  
 Bauer, Markus, University of Nijmegen  
 Bodelón, Clara, Boston University  
 Boloon, Alireza, Harvard University  
 Buffalo, Elizabeth, National Institutes of Health, NIMH  
 Cimenser, Aylin, Bell Laboratories/Lucent Technologies  
 Diogo, Antonia, Federal University of Rio de Janeiro  
 Fanselow, Erika, Brown University  
 Froud, Karen, Massachusetts Institute of Technology  
 Grün, Sonja, Max Planck Institute for Brain Research  
 Hudson, Andrew, Weill Medical College of Cornell University  
 Jones, Lauren, University of Maryland at Baltimore



Herb Luther

Jones, Matthew, Massachusetts Institute of Technology  
 Knutsen, Per, Weizmann Institute of Science  
 Kronhaus, Dina, University of Edinburgh  
 Litvak, Vladimir, Technion-Israel Institute of Technology  
 McKeehan, Troy, Montana State University  
 Moravcikova, Gabriela, University of Pittsburgh  
 Nicolaou, Nicoletta, University of Reading  
 Reddy, Leila, California Institute of Technology  
 Sanjana, Neville, Massachusetts Institute of Technology  
 Smith, Spencer, University of California, Los Angeles  
 Sripathi, Arun, Johns Hopkins University  
 Yokoo, Takeshi, Mount Sinai School of Medicine

## Optical Microscopy

October 9 - October 18, 2002

### DIRECTOR

Izzard, Colin, University at Albany

### FACULTY

DePasquale, Joseph, New York State Department of Health  
 Hard, Robert, SUNY, Buffalo  
 Keller, H. Ernst, Carl Zeiss, Inc  
 Maxfield, Frederick, Cornell University Medical College  
 Murray, John, University of Pennsylvania School of Medicine  
 North, Allison, The Rockefeller University  
 Pierini, Lynda, Cornell University Medical College  
 Piston, David, Vanderbilt University  
 Spring, Kenneth, National Institutes of Health  
 Swedlow, Jason, The University of Dundee

### TEACHING ASSISTANTS

Hao, Mingming, Cornell University Medical College  
 Oberski, Danial, University of Buffalo  
 Platani, Melpomeni, The University of Dundee  
 Sigurdson, Wade, SUNY, Buffalo  
 Snyder, Kenneth, University at Buffalo

### STUDENTS

Ahir, Alpa, University College London  
 Bauer, Christoph, University of Geneva  
 Boes, Marianne, Harvard Medical School  
 Boxem, Mike, Dana Farber Cancer Institute

Bruce, Ashley, University of Chicago  
 Davenne, Marc, Cold Spring Harbor Laboratory  
 Dorman, Jennie, University of Washington  
 Ferris, Matthew, Los Alamos National Laboratory  
 Gray, Annette, Brown University  
 Hooper, John, The Scripps Research Institute  
 Jenik, Pablo, Carnegie Institution of Washington  
 Kateneva, Anna, Oklahoma Medical Research Foundation  
 Kolb, Robert, Case Western Reserve University  
 McCauley, Anita, Wake Forest University  
 McDonough, Stefan, Marine Biological Laboratory  
 Morgan, Jeffrey, Brown University  
 Murthy, Vinit, Rice University  
 Pfeifer, Andrea, National Institutes of Health  
 Popoola, Joyce, King's College London  
 Prigozhina, Natalie, The Scripps Research Institute  
 Seth, Abhinav, University of Texas Southwestern Medical Center at Dallas  
 Vaishnav, Shipra, University of Georgia  
 Veklich, Yuri, University of Pennsylvania School of Medicine  
 Walters, Katherine, University of Iowa

## Rapid Electrochemical Measurements

May 9 - May 13, 2002

### DIRECTOR

Gerhardt, Greg, University of Kentucky Medical Center

### FACULTY

Allen, Jennifer, University of Kentucky Medical Center  
 Apparsundaram, Subu, University of Kentucky Medical Center  
 Burmeister, Jason, Center For Sensor Technology  
 Currier, Theresa, University of Kentucky Medical Center  
 Davis, Heather, University of Kentucky Medical Center  
 Daws, Lynette, University of Texas Health Sciences Center at San Antonio  
 Hoffman, Alex, National Institute on Drug Abuse  
 Huettl, Peter, University of Kentucky Medical Center  
 Palmer, Michael, University of Colorado Health Sciences Center  
 Pomerleau, Francois, University of Kentucky Medical Center  
 Porterfield, D. Marshall, University of Missouri-Rolla  
 Surgener, Stewart, University of Kentucky Medical Center

### TEACHING ASSISTANTS

Caulder, Tara, NIH/NIDA  
 Knight, Tim, University of Kentucky  
 Parrish, J. Michael, University of Kentucky Medical Center  
 Robinson, Scott, University of Kentucky Medical Center

### COURSE COORDINATOR

Lindsay, Robin, University of Kentucky Medical Center

## STUDENTS

Almeida, Catarina, Universidade Aveiro, Portugal  
 Baccei, Christopher, Merck Research Labs  
 Caldwell, Ray, University of North Carolina,  
 Chapel Hill  
 Cao, Bo-Jin, University of Texas Health Sciences  
 Center  
 Cavus, Idil, Yale University  
 Conour, John, University of Illinois at Urbana-  
 Champaign  
 Douglas, Christopher, University of Michigan  
 French, Kristen, Medical University of South  
 Carolina  
 Galvan, Adriana, Emory University  
 Herzog, Chris, Ohio State University  
 Inglis, Fiona, Tulane University  
 Korzan, Wayne, University of South Dakota  
 Li, Guichu, East Carolina University School of  
 Medicine  
 Martin, Joshua, The Ohio State University  
 Noll, Elizabeth, Brigham & Women's & Children's  
 Hospitals  
 Oldenziel, Weite, University Centre for Pharmacy  
 Overli, Oyvind, University of South Dakota  
 Sarter, Martin, The Ohio State University  
 Schad, Christina, Chicago Medical School  
 Sokoloski, Joshua, University of Pittsburgh  
 Stephens, Jr., Robert, Ohio State University  
 vanHorne, Craig, Brigham & Women's Hospital  
 Wagner, Amy, University of Pittsburgh  
 Willis, Lauren, Medical University of South  
 Carolina  
 Zapata, Agustin, National Institutes of Health

## Summer Program in Neuroscience, Ethics, and Survival (SPINES)

June 15 - July 13, 2002

## DIRECTORS

Martinez, Joseph, University of Texas at San  
 Antonio  
 Townsel, James, Meharry Medical College

## FACULTY

Hernandez, Ruben, University of Texas, San  
 Antonio  
 LeBaron, Richard, University of Texas, San  
 Antonio  
 Zottoli, Steven, Williams College  
 Berger-Sweeney, Joanne, Wellesley College  
 Castaneda, Edward, Arizona State University  
 Etgen, Anne, Albert Einstein College of Medicine  
 Fox, Tom, Harvard Medical School  
 Gonzalez-Lima, Erika, University of Texas  
 at Austin  
 Gonzalez-Lima, Francisco, University of Texas  
 at Austin  
 Hildebrand, John, University of Arizona  
 Jones, James M., American Psychological  
 Association  
 Nickerson, Kim, American Psychological  
 Association

## LECTURERS

Burgess, David, Boston College  
 Kaplan, Barry, NIH/NIMH  
 Langford, George, Dartmouth College  
 Mensinger, Allen, University of Minnesota  
 Palazzo, Robert, University of Kansas  
 Zakon, Harold, University of Texas, Austin  
 Kravitz, Edward A., Harvard Medical School

## TEACHING ASSISTANT

Orfila, James, University of Texas, San Antonio

## STUDENTS

Black, Carlita, University of Virginia  
 Cruz, Nelson, Brandeis University  
 Diaz, Manuel, University of Puerto Rico  
 Dieguez, Jr., Dario, University of Texas at San  
 Antonio  
 Gallegos, Diana, San Jose State University  
 Gutierrez, Tannia, University of Georgia  
 Hyde, Rhonda, Harvard University  
 Jones, Floretta, University of Texas at San Antonio  
 Martinez, Veronica, Texas A&M University  
 Mendes, Shannon, University of Miami  
 Padilla, Mayra, University of California, Berkeley  
 Prather, Richard, Massachusetts Institute of  
 Technology  
 Salas-Ramirez, Kaliris, Michigan State University  
 Sánchez, Javier, Baylor College of Medicine  
 Torres-Reveron, Annelyn, Ponce School of  
 Medicine  
 Wrubel, Kathryn, University of Texas

## Workshop on Molecular Evolution

July 28 - August 9, 2002

## DIRECTOR

Cummings, Michael, Marine Biological  
 Laboratory

## FACULTY

Beerli, Peter, University of Washington  
 Edwards, Scott, University of Washington  
 Eisen, Jonathan, The Institute for Genomic  
 Research  
 Felsenstein, Joseph, University of Washington  
 Kuhner, Mary, University of Washington  
 Lewis, Paul, University of Connecticut  
 Meyer, Axel, University of Konstanz  
 Rand, David, Brown University  
 Swofford, David, Florida State University  
 Thompson, Steven, Florida State University  
 Yang, Ziheng, University College London  
 Yoder, Anne, Yale University

## LECTURERS

Fraser, Claire, The Institute for Genomic Research  
 Pearson, William, University of Virginia  
 Sanderson, Michael, University of California, Davis  
 Voytas, Daniel, Iowa State University  
 Yokoyama, Shozo, Syracuse University

## TEACHING ASSISTANTS

Bowie, Rauri C.K., University of Cape Town  
 Mead, Louise, Oregon State University  
 Rokas, Antonis, University of Wisconsin-Madison  
 Winka, Katarina, Umeå University

## STUDENTS

Banks, Michael, Oregon State University  
 Behrmann, Jasminca, University of Constance  
 Benavides, Edgar, Brigham Young University  
 Borchardt, Mark, Marshfield Medical Research  
 Foundation  
 Boudreau, Ellen, Dalhousie University  
 Boyce, Sarah Lyn, Natural History Museum of  
 Los Angeles County  
 Brown, Joseph, Queen's University  
 Budd, Aidan, European Molecular Biology  
 Laboratory  
 Bumbaugh, Alyssa, Michigan State University

Burk, Robert, Albert Einstein College of Medicine  
 Burleigh, Gordon, University of Missouri-  
 Columbia  
 Buschbom, Jutta, Field Museum of Natural  
 History  
 Caufield, Page, New York University  
 Conley, Catharine, NASA-Ames Research Center  
 Countway, Peter, University of Southern California  
 Dopman, Erik, Cornell University  
 Fehling, Johanna, Dunstaffnage Marine Laboratory  
 Flores-Ramirez, Sergio, Autonomous University  
 of Baja California Sur  
 Ginzel, Matthew, University of Illinois at Urbana-  
 Champaign  
 Goetze, Erica, University of California, San Diego  
 Gonzalez, Francisco, Universidad Autonoma del  
 Estado de Morelos  
 Gopal, Shuba, The Rockefeller University  
 Gormley, Joseph, Massachusetts Biomedical  
 Initiative  
 Hall, Paula, University of New Mexico  
 Hallam, Steven, Monterey Bay Aquarium  
 Research Institute  
 Holder, Mark, University of Connecticut  
 Hudelot, Cendrine, University of Manchester  
 Jennings, Bryan, University of Texas at Austin  
 Jolly, Marc, Université Pierre et Marie Curie  
 Kiontke, Karin, New York University  
 Komadina, Naomi, WHO Influenza Center  
 Lange, Martin, Staatliche Lehr- und  
 Forschungsanstalt für Landwirtschaft  
 Langeland, James, Kalamazoo College  
 Lee, Dan, The Institute for Genomic Research  
 Leonard, Jennifer, University of California,  
 Los Angeles  
 Lim, Grace, Scripps Institution of Oceanography  
 Linse, Katrin, British Antarctic Survey  
 Martinello, Rick, Yale University School of Medicine  
 Merson, Rebekah, Woods Hole Oceanographic  
 Institution  
 Opazo, Juan, P. Universidad Católica de Chile  
 Pearman, Peter, University of Zurich  
 Pie, Marcio, Boston University  
 Presa, Pablo, University of Vigo  
 Raes, Jeroen, University of Gent  
 Rodriguez, Carmina, Universidad Complutense  
 Madrid  
 Rubicz, Rohina, University of Kansas  
 Sakwa, James, University of Pretoria  
 Sievert, Stefan, Woods Hole Oceanographic  
 Institution  
 Sipe, Tavis, Wake Forest University  
 Smith, Catherine, Centers for Disease Control  
 & Prevention  
 Smith, Una, Los Alamos National Laboratory  
 Stahls-Mäkelä, Gunilla, University of Helsinki  
 Storz, Jay, University of Arizona  
 Stuart, Gary, Indiana State University  
 Terry, Rebecca, University of Leeds  
 Thomas, Bolaji, Tufts University  
 Tilley, Stephen, Smith College  
 Wang, Zhenshan, University of Washington  
 Whitford, Tracy, East Stroudsburg University  
 Wojciechowski, Martin, Arizona State University  
 Wu, Martin, The Institute for Genomic Research  
 Zinser, Erik, Massachusetts Institute of Technology  
 Zwickl, Derrick, University of Texas, Austin

## OTHER EDUCATIONAL PROGRAMS

---

### Marine Models in Biological Research Undergraduate Program

#### DIRECTORS

Browne, Carole, Wake Forest University  
Tytell, Michael, Wake Forest University School of Medicine

#### FACULTY

Augustine, George, Duke University  
Eckberg, William, Howard University  
Furie, Barbara, Harvard School of Medicine  
Furie, Bruce, Harvard School of Medicine  
Gould, Robert, New York State Institute for Basic Research  
Hanlon, Roger, Marine Biological Laboratory  
Jonas, Elizabeth, Yale University  
Laufer, Hans, University of Connecticut  
Malchow, R. Paul, University of Illinois, Chicago  
Mensinger, Al, University of Minnesota-Duluth  
Palazzo, Robert, Rensselaer Polytechnic Institute  
Rome, Larry, University of Pennsylvania  
Silver, Robert, Wayne State University  
Wainwright, Norman, Marine Biological Laboratory

#### STUDENTS

Alimi, Mariam, Wake Forest University  
Bodily, Jill, Stanford University  
Borely, Kimberly, Ohio University  
Homsy, Sara, Wake Forest University  
Jackson, Ticaria, Howard University  
Montanez, Marlana, Mount Holyoke College  
Najera, Julia, Univ of Texas, El Paso  
Normand, Danielle, University of New Hampshire  
O'Neal, Jessica, College of Charleston  
Simpson, Andrew, University of California, Santa Barbara  
Steeds, Craig, University of Kansas



### NASA Planetary Biology Internship Program

#### DIRECTORS

Dolan, Michael F., University of Massachusetts Amherst  
Margulis, Lynn, University of Massachusetts Amherst

#### INTERNS

Allen, Michelle, The University of New South Wales, Australia  
Chichon Garcia, Francisco J., Universidad Autonoma de Madrid  
Fike, David, University of Cambridge  
Guarin, Alejandro, The Pennsylvania State University  
Navio, Rubén Peco, Universitätsklinikum Hamburg-Eppendorf  
Rosenfeld, Arie, University of Haifa  
Vaisanen, Katarina, University of Aberdeen  
Wier, Andrew, University of Wisconsin-Milwaukee

#### SPONSORS

Cabrol, Nathalie A., NASA Ames Research Center  
Garland, Jay, NASA Kennedy Space Center  
Hagan, William, College of St. Rose  
Hinkle, C. Ross, NASA Kennedy Space Center  
Margulis, Lynn, University of Massachusetts Amherst  
Summons, Roger, Massachusetts Institute of Technology  
Trent, Jonathan, NASA Ames Research Center  
Wofsy, Steven C., Harvard University

### Science Journalism Program

#### FELLOWS

Bellinghini, Ruth Helena, Science Reporter, Brazil  
Berreby, David, Freelance  
Biskup, Agnes, Freelance  
Bogo, Jennifer, Audubon Magazine  
Carter, Kandice, AAAS Science Update  
Dempsey, Dale, Freelance  
Griffin, Katherine, Freelance  
Hostetler, A. J., *Richmond Times-Dispatch*  
King, Robert, *The Palm Beach Post*  
Manier, Jeremy, *Chicago Tribune*  
Onifade, Diran, Nigerian Television Authority  
Perry, Rebecca, *Los Angeles Times*  
Reker, Mary Lou, Library of Congress  
Valentine, Vikki, National Public Radio Online  
Wisby, Gary, *Chicago Sun-Times*

#### BIOMEDICAL FACULTY

Beach, Dale, UNC Chapel Hill  
Bloom, Kerry, Dale Beach, UNC Chapel Hill  
Palazzo, Robert, University of Kansas  
Pearson, Chad, UNC Chapel Hill  
Schnackenberg, Brad, UNC Chapel Hill

#### ENVIRONMENT FACULTY

Foreman, Kenneth, Marine Biological Laboratory  
Neill, Christopher, Marine Biological Laboratory  
Tholke, Kris, Marine Biological Laboratory

#### CO-DIRECTORS

Goldman, Robert D., Northwestern University  
Rensberger, Boyce, Director, Knight Science Journalism Fellowships, Massachusetts Institute of Technology

#### ADMINISTRATIVE DIRECTOR

Hinkle, Pamela Clapp, Marine Biological Laboratory

## Semester in Environmental Science

September 2 – December 16, 2002

### DIRECTOR

Hobbie, John E

### ASSOCIATE DIRECTOR

Foreman, Kenneth H

### FACULTY

Deegan, Linda A  
Foreman, Kenneth H  
Giblin, Anne E.  
Hobbie, John E  
Hopkinson, Charles S., Jr  
Liles, George  
Melillo, Jerry M.  
Neill, Christopher  
Peterson, Bruce J  
Rastetter, Edward B.  
Shaver, Gaius R.  
Stuedler, Paul A  
Vallino, Joseph J.

### RESEARCH AND TEACHING ASSISTANTS

Bahr, Michele  
Bowen, Jennifer  
Creswell, Joel  
Kwiatkowski, Bonnie  
Micks, Patricia  
Tholke, Kris  
Ziemann, Tori

### Administrative Assistant

Johnson-Horman, Frances

### Students

Adams, Jacqueline M., Ripon College  
Burce, Allison E., Harvey Mudd College  
Copeland, Maureen T., Allegheny College  
Dean, Mary D., Ripon College  
Engelhart, Gabriella J., Lafayette College  
Fila, Laurie A., Mount Holyoke College  
Franklin, Jennifer M., Wheaton College  
Freeman, Christopher J., Connecticut College  
Havassy, Joshua I., Haverford College  
Kang, MoonKoo Simon, Clark University  
Kennedy, Jenny L., Clarkson University  
Leahy, Sarah E., Wheaton College  
Leamy, Claire A., Wellesley College  
Lindell, Joshua S., Dickinson College  
Roberts, Rachael A., Skidmore College  
Shea, Alexandra E., Earlham College  
Stern, Stephanie B., Wellesley College  
Webster, William K., Trinity University  
Wright, Julie A., Wellesley College

## Teachers' Workshop: Living in the Microbial World

August 10–16, 2002

### DIRECTORS

Dorritie, Barbara, Cambridge Rindge and Latin School, Cambridge, Massachusetts  
Olendzenski, Lorraine, University of Connecticut, Storrs

### FACULTY

Gunnard, Jessie, University of Massachusetts  
Offerdahl, Erika, University of Arizona

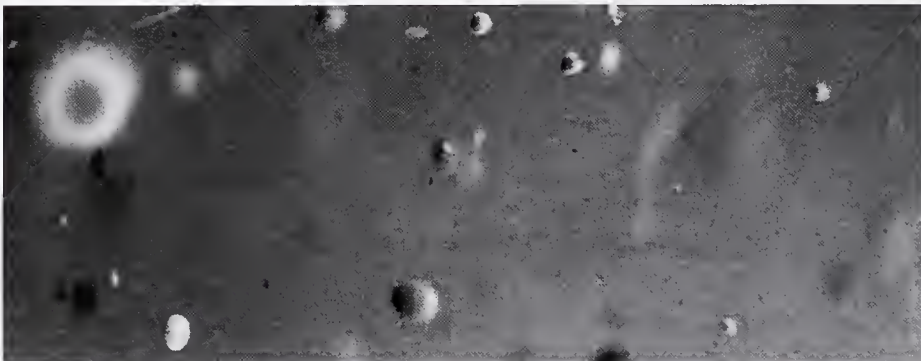
### COURSE ASSISTANT:

Waksman, George, Massachusetts Institute of Technology

### PRESENTERS

Bermudes, David, Vion Pharmaceuticals, New Haven, Connecticut  
Dyer, Betsey, Wheaton College  
Edgcomb, Virginia, Woods Hole Oceanographic Institution  
Guerrero, Ricardo, University of Barcelona, Spain  
Margulis, Lynn, University of Massachusetts, Amherst  
Rogers, Dan, Woods Hole Oceanographic Institute

Eliot, Judith, Middle Years Alternative School for the Humanities, Philadelphia, Pennsylvania  
Freitas, Caroline, Cape Cod Regional Technical High School, Massachusetts  
Golet, Gerie, Salem School, Connecticut  
Gooding, Debbie, Kraemer Middle School, Placentia, California  
Hammond, Christine, Clarendon House Grammar School, Ramsgate, Kent, United Kingdom  
Howie, Charles, Old Rochester Regional High School, Massachusetts  
Knox, Carol, Northfield Mount Hermon School, Massachusetts  
Lee, Marge, Harrington School, Cambridge, Massachusetts  
Lichtenstein, Leslie, Massachusetts Community College, Massachusetts  
Lincoln, Peter, Hingham Public Schools, Massachusetts  
Natoli, Therese, Ledyard Middle School, Gales Ferry, Connecticut  
Potrafka, Renee, Father Gabriel Richard Catholic High School, Ann Arbor, Michigan



### Teacher Participants

Barron, Melanie, Cambridge Public Schools, Massachusetts  
Berrick, Steve, Cape Cod Regional Technical High School, Massachusetts  
Connor, Lynn, Old Rochester Regional High School, Massachusetts  
Crook, Jolene, East Lyme High School, Connecticut  
Diehl, Penny, Hempfield High School, Landisville, Pennsylvania

Pullan, Mary, Fitch Middle School, Groton, Connecticut  
Roark, Eileen, Nathan Hale-Ray High School, Moodus, Connecticut  
Ruston, Steve, King Etherbert School, Birchington, Kent, United Kingdom  
Tanigawa, Joy, El Rancho High School, Pico Rivera, California

## SCHOLARSHIP AWARDS



Elizabeth Armstrong

**THE BRUCE AND BETTY ALBERTS ENDOWED SCHOLARSHIP IN PHYSIOLOGY**  
Aguilar, Arturo, Av. Instituto Politécnic National Kelly, Melissa, University of Kentucky College of Medicine

**AMERICAN SOCIETY FOR CELL BIOLOGY**  
Brown, Ann, Medgar Evers College  
Campbell, Susan, University of Alabama, Birmingham  
Davis, Kevin, University of Pittsburgh  
Gadea, Bedrick, Harvard Medical School  
Gonsalves, Joanna, University of California, San Francisco  
Green, Heather, New York University  
Harrison, Faith, University of Iowa  
Livi, Carolina, University of Texas Health Sciences Center, San Antonio  
Miranda, Jason, University of Texas at Austin  
Pineda, Gabriel, University of Texas Health Sciences Center, Dallas  
TorrEns, Javier, New Jersey Medical School, UMDNJ  
Van Stry, Melanie, Boston University School of Medicine  
Vega, Rebecca, Stanford University

**BIOLOGY CLUB OF THE COLLEGE OF THE CITY OF NEW YORK**  
Zornik, Erik Columbia University

**JOHN AND ELISABETH BUCK SCHOLARSHIP**  
Thamatrakoln, Kimberlee, University of California, San Diego

**IC LALOR BURDICK SCHOLARSHIP**  
Dash, Satya, University of East Anglia  
Gonsalves, Joanna, University of California, San Francisco  
Hallikas, Outi, University of Helsinki  
Prosen, Tracy, University of Pittsburgh

**BURROUGHS WELLCOME FUND - BIOLOGY OF PARASITISM COURSE**  
Chamond, Nathalie, Institut Pasteur  
Cockburn, Ian, University of Edinburgh  
Karnataki, Anuradha, University of Washington  
Klotz, Christian, Humboldt-University-Berlin  
Kooij, Taco Leiden, University Medical Centre  
Lee, SooHee, Johns Hopkins School of Medicine  
Li, Hongjie, Yale University  
Mueller, Ann-Kristin, University School of Medicine, Heidelberg

**BURROUGHS WELLCOME FUND - FRONTIERS IN REPRODUCTION COURSE**  
Akcali, Kamil, Bilkent University  
Bachman, Katherine, Case Western Reserve University  
Gill, Ryan, University of Kansas Medical Center  
Gonsalves, Joanna, University of California, San Francisco  
Hallikas, Outi, University of Helsinki  
Ka, Hakhyun, University of Kansas Medical Center  
Kayisli, Umit, Yale University School of Medicine  
Kreeger, Pamela, Northwestern University  
Perez, Christian, University of Pennsylvania  
Prosen, Tracy, University of Pittsburgh  
TorrEns, Javier, New Jersey Medical School, UMDNJ  
Wang, Eileen, Northwestern Medical School

**BURROUGHS WELLCOME FUND-MOLECULAR MYCOLOGY COURSE**  
Berbes, Carlos, Virginia Commonwealth University  
Brown, Constance, Howard University  
Heung, Lena, Medical University of South Carolina  
MacCallum, Donna, University of Aberdeen  
Morais, Flavia, Universidade Federal de Sao Paulo  
Noble, Suzanne, University of California, San Francisco  
Ramon, Ana, Georgetown University Medical Center  
Reese, Amy, Washington University School of Medicine  
Steinbach, William, Duke University  
Sturtevant, Joy, Louisiana State University Health Science Center  
Vallim, Marcelo, Duke University Medical Center  
Van Dijk, Patrick, Flemish Interuniversity Institute for Biotechnology  
Wozniak, Karen, Louisiana State University Health Science Center

**GARY N. CALKINS MEMORIAL SCHOLARSHIP FUND**  
Bery, Katy, University of Sheffield  
Copf, Tijana, University of Crete

**CONRAD**  
Sachdeva, Geetanjali, Institute for Research in Reproduction, India

**EDWIN GRANT CONKLIN MEMORIAL FUND**  
Caracino, Diana, Emory University School of Medicine  
Copf, Tijana, University of Crete

**BERNARD DAVIS FUND**  
Boucher, Yan, Dalhousie University  
Denef, Vincent, Michigan State University  
Erbs, Marianne, Swiss Fed. Institute for Environmental Science & Technology  
Pinel, Nicolas, University of Washington

**WILLIAM F. AND IRENE C. DILLER MEMORIAL SCHOLARSHIP FUND**  
Davis, Kevin, University of Pittsburgh  
Vega, Rebecca, Stanford University

**THE ELLISON MEDICAL FOUNDATION - BIOLOGY OF PARASITISM COURSE**  
Chamond, Nathalie, Institut Pasteur  
Cockburn, Ian, University of Edinburgh  
Karnataki, Anuradha, University of Washington  
Klotz, Christian, Humboldt-University-Berlin  
Kooij, Taco Leiden, University Medical Centre  
Mueller, Ann-Kristin, University School of Medicine, Heidelberg

**THE ELLISON MEDICAL FOUNDATION - MOLECULAR BIOLOGY OF AGING COURSE**  
Almeida, Claudia, Weill Medical College of Cornell University  
Bishop, Glenda, Case Western Reserve University

continued

Bokov, Alex, University of Texas Health Science Center, San Antonio  
 Chen, Lishan, University of Washington  
 Dunaief, Joshua, University of Pennsylvania  
 Fuller, Kathryn, University of Minnesota  
 Harvey, Sarah, Medical College of Virginia  
 Hong, Eun-Jin (Eric), University of Washington  
 Johnston, Janet, Queen's University Belfast  
 Lledias, Fernando, Instituto de Biociencia, UNAM  
 Lu, Xiangdong, University of North Carolina, Chapel Hill  
 Moynihan, Kathryn, Washington University  
 Ogle, William, Stanford University  
 Powers, Ralph, The University of Washington  
 Proctor, Carole, University of Newcastle  
 Rea, Shane, University of Colorado  
 Rutten, Bart, University of Maastricht  
 Shirasawa, Takuji, Tokyo Metropolitan Institute of Gerontology  
 Tong, Liqi, University of California, Irvine  
 Zou, Ying, University of Texas Southwestern Medical Center

#### CASWELL GRAVE SCHOLARSHIP FUND

Berry, Katy, University of Sheffield  
 Chen, Yen-Chin, National Cheng Kung University Medical College  
 Copf, Tijana, University of Crete  
 Delalande, Jean-Marie, University College London  
 Extavour, Cassandra, University of Cambridge

#### DANIEL S. GROSCH SCHOLARSHIP FUND

Dethlefsen, Les, Michigan State University  
 Ge, Lan, University of California, Riverside  
 McVaugh, Cheryl, University of Pennsylvania

#### WILLIAM RANDOLPH HEARST FOUNDATION

Chong, Curtis, Johns Hopkins School of Medicine  
 Kelly, Melissa, University of Kentucky College of Medicine  
 LaPointe, Nichole, Northwestern University  
 McVaugh, Cheryl, University of Pennsylvania  
 Pace, Margaret, University of Texas  
 Pignatelli, Vincenzo, University of Pisa  
 Sha, Edward, Indiana University Medical Center

#### HOWARD HUGHES MEDICAL INSTITUTE - BIOLOGY OF PARASITISM COURSE

Meissner, Markus, Imperial College of Science, Technology & Medicine, UK  
 Slavin, Ileana, Universidad Nacional de Cordoba  
 Stubbs, Janine, Royal Melbourne Hospital

#### HOWARD HUGHES MEDICAL INSTITUTE

Boassa, Daniela, University of Arizona College of Medicine  
 Dash, Satya, University of East Anglia  
 Dellen, Babette, Washington University in St. Louis  
 Denev, Vincent, Michigan State University  
 Doiron, Brent, University of Ottawa  
 Dulcis, Davide, University of Arizona, Tucson  
 Graco, Michelle, University of Pierre et Marie Curie

Guest, Jennifer, National Institute for Medical Research  
 Ihring, Alexandra, Max-Planck-Institute of Neurobiology  
 Malartre, Marianne, University of Portsmouth  
 Nkinin, Wuyika, University of Yaounde  
 Petersen, Rasmus, International School for Advanced Study (SISSA)  
 Pfeiffer, Keram, Philipps-Universität Marburg  
 Pinel, Nicolas, University of Washington  
 Rajagopal, Soumitra, University of Nebraska  
 Renart, Alfonso, Brandeis University  
 Sharp, Katherine, Scripps Institute of Oceanography  
 Werner-Reiss, Uri, Dartmouth College  
 Witney, Alice, University of Birmingham Medical School  
 Wright, Geraldine, Ohio State University

#### ICRO-UNESCO

Akcali, Kamil, Bilkent University  
 Hallikas, Outi, University of Helsinki

#### INTERNATIONAL BRAIN RESEARCH ORGANIZATION

Chakraborty, Santanu, Cold Spring Harbor Laboratory  
 Chiappe, Eugenia, The Rockefeller University  
 Diogo, Antonia, Federal University of Rio de Janeiro  
 Herrera-Valdez, Marco, University of Arizona  
 Hu, Hailan, University of California, Berkeley  
 Koirala, Samir, University of Southern California  
 Kozhevnikov, Alexey, Bell Laboratories  
 Nasir, Sazzad, University of California, San Francisco  
 Pinto, Reynaldo, Instituto de Física da University of São Paulo  
 Reddy, Leila, California Institute of Technology  
 Shahrezaei, Yahid, Simon Fraser University  
 Sripathi, Arun, Johns Hopkins University  
 Wang, Weiyi, University of Pennsylvania  
 Young, Rodrigo, University of Chile  
 Zhou, Yi, Boston University

#### ARTHUR KLORFEIN SCHOLARSHIP AND FELLOWSHIP FUND

Drago, Grazia, Università Degli Studi di Palermo  
 Extavour, Cassandra, University of Cambridge  
 Kee, Yun, California Institute of Technology  
 Koziel, Lydia, Max-Planck-Institute for Molecular Genetics  
 Malartre, Marianne, University of Portsmouth  
 Maslakova, Svetlana, Smithsonian Institution  
 Su, Yi-Hsien, Scripps Institute of Oceanography, MBRD

#### FRANK R. LILLIE FELLOWSHIP AND SCHOLARSHIP FUND

Aguilar, Arturo, Av Instituto Politécnico Nacional  
 Amarie, Dragos, University of Notre Dame  
 Dojcinovic, Danijel, Arizona State University  
 Ge, Lan, University of California, Riverside  
 Goentoro, Lea, Princeton University  
 Kaynar, Murat, Beth Israel Deaconess Medical Center

Kydd, Alison, University of Calgary  
 Oh, Ji-Eun, University of Illinois at Chicago  
 Pace, Margaret, University of Texas  
 Ramos, Arnolt, Children's Hospital  
 Rossi, Chiara, University of Pisa

#### THE GRUSS LIPPER FOUNDATION SCHOLARSHIP

Keren, Zandbank  
 Koren, Omry, Tel Aviv University  
 Litvak, Vladimir, Technion-Israel Institute of Technology  
 Loebel, Alex, The Weizmann Institute of Science

#### JACQUES LOEB FOUNDERS' SCHOLARSHIP FUND

Amarie, Dragos, University of Notre Dame  
 Dojcinovic, Danijel, Arizona State University  
 Pace, Margaret, University of Texas

#### S. O. MAST MEMORIAL FUND

Ihring, Alexandra, Max-Planck-Institute of Neurobiology  
 Zhou, Zhaolan (Joe), Harvard Medical School

#### MBL ASSOCIATES ENDOWED SCHOLARSHIP FUND

Amarie, Dragos, University of Notre Dame

#### MBL PIONEERS SCHOLARSHIP FUND

Brown, Ann, Medgar Evers College  
 Berry, Katy, University of Sheffield  
 Caracino, Diana, Emory University School of Medicine  
 Copf, Tijana, University of Crete  
 Dash, Satya, University of East Anglia  
 Delalande, Jean-Marie, University College, London  
 Extavour, Cassandra, University of Cambridge  
 Koziel, Lydia, Max-Planck-Institute for Molecular Genetics  
 Livi, Carolina, University of Texas Health Science Center, San Antonio

#### CHARLES BAKER METZ AND WILLIAM METZ SCHOLARSHIP FUND IN REPRODUCTIVE BIOLOGY

Akcali, Kamil, Bilkent University  
 Hallikas, Outi, University of Helsinki  
 Kreeger, Pamela, Northwestern University  
 Prosen, Tracy, University of Pittsburgh

#### FRANK MORRELL ENDOWED MEMORIAL SCHOLARSHIP

Petersen, Rasmus, International School for Advanced Study (SISSA)

#### MOUNTAIN MEMORIAL FUND SCHOLARSHIP

Chong, Curtis, Johns Hopkins School of Medicine  
 Kelly, Melissa, University of Kentucky College of Medicine  
 LaPointe, Nichole, Northwestern University  
 Oh, Ji-Eun, University of Illinois at Chicago  
 Pignatelli, Vincenzo, University of Pisa  
 Ramos, Arnolt, Children's Hospital

**ALBERTO MONROY FOUNDATION**  
Drago, Grazia, Università Degli Studi di Palermo

**PFIZER INC. ENDOWED SCHOLARSHIP**  
Aguilar, Arturo, Av Instituto Politécnico Nacional  
Chong, Curtis, Johns Hopkins School of Medicine  
Pignatelli, Vincenzo, University of Pisa

**PLANETARY BIOLOGY INTERNSHIP SCHOLARSHIPS**  
Maresca, Julia, Pennsylvania State University  
Remold, Susanna, Michigan State University  
Walker, Jeffrey, University of Colorado

**WILLIAM TOWNSEND PORTER FELLOWSHIP AND SCHOLARSHIP FUND**  
Brown, Ann, Medgar Evers College  
Campbell, Susan, University of Alabama, Birmingham  
Davis, Kevin, University of Pittsburgh  
Gadea, Bedrick, Harvard Medical School  
Gonsalves, Joanna, University of California, San Francisco  
Green, Heather, New York University  
Harrison, Faith, University of Iowa  
Livi, Carolina, University of Texas Health Science Center, San Antonio  
Miranda, Jason, University of Texas at Austin  
Pineda, Gabriel, University of Texas Southwestern Medical Center at Dallas

## POST-COURSE RESEARCH AWARDS

Extavour, Cassandra, University of Cambridge (Embryology)  
Chong, Curtis, Johns Hopkins School of Medicine (Physiology)  
Davis, Kevin, University of Pittsburgh (Physiology)  
Ge, Lan, University of California, Riverside (Physiology)  
LaPointe, Nichole, Northwestern University (Physiology)

Torréns, Javier, New Jersey Medical School, UMDNJ  
Van Stry, Melanie, Boston University School of Medicine  
Vega, Rebecca, Stanford University

**HERBERT W. RAND FELLOWSHIP AND SCHOLARSHIP FUND**  
Ahlgren, Sara, California Institute of Technology  
Amarie, Dragos, University of Notre Dame  
Campbell, Douglas, University of Cambridge  
Chen, Yen-Chin, National Cheng Kung University Medical College  
Dojcinovic, Danijel, Arizona State University  
Dürr, Katrin, University of Freiburg  
Gaertner, Tara, University of Texas Health Science Center  
Goentoro, Lea, Princeton University  
Hammonds-Odie, Latanya, Spelman College  
Kaynar, Murat, Beth Israel Deaconess Medical Center



Marine diatom,  
Kalina White

Lien, Cheng-Chang, Physiology Institute of University Freiburg  
Ma, Whee Ky, California Institute of Technology  
Málaga-Trillo, Edward, University of Konstanz  
Masino, Mark, State University of New York at Stony Brook  
Prober, David, University of Washington  
Raffi, Milena, Rutgers University  
Ramos, Arnolt, Children's Hospital  
Rossi, Chiara, University of Pisa  
Sha, Edward, Indiana University Medical Center

**FLORENCE C. ROSE AND S. MERYL ROSE ENDOWED SCHOLARSHIP FUND**  
Caracino, Diana, Emory University School of Medicine

**RUTH SAGER MEMORIAL SCHOLARSHIP**  
Guest, Jennifer, National Institute for Medical Research  
Mitchell, Tracy, University of Wisconsin-Madison

**HOWARD A. SCHNEIDERMAN ENDOWED SCHOLARSHIP**  
Boassa, Daniela, University of Arizona College of Medicine  
Ewald, Rebecca, Cold Spring Harbor Lab  
De Labra, Carmen, University College London  
Doiron, Brent, University of Ottawa

**MILTON L. SHIFMAN ENDOWED SCHOLARSHIP**  
Khalil, Mona, Columbia University  
Kerney, Ryan, Harvard University

**MOSHE SHILO MEMORIAL SCHOLARSHIP FUND**  
Koren, Omry, Tel Aviv University

**CATHERINE FILENE SHOUSE SCHOLARSHIP**  
Avila, Andréa, Instituto de Biologia Molecular do Paran -IBMP  
Boassa, Daniela, University of Arizona College of Medicine  
Brown, Ann, Medgar Evers College  
Caracino, Diana, Emory University School of Medicine  
Ewald, Rebecca, Cold Spring Harbor Lab  
Fenn, Katelyn, University of Edinburgh  
Graco, Michelle, University of Pierre et Marie Curie  
Kreeger, Pamela, Northwestern University  
Orsborn, April, University of Missouri-Columbia  
Sharp, Katherine, Scripps Institute of Oceanography

Spitzer, Nadja, Georgia State University  
Wohlgemuth, Sandra, Humboldt-Universität zu Berlin

**MARJORIE W. STETTEN SCHOLARSHIP FUND**  
Witney, Alice, University of Birmingham Medical School

**HORACE W. STUNKARD SCHOLARSHIP FUND**  
Akcali, Kamil, Bilkent University  
Gill, Ryan, University of Kansas Medical Center

**SOCIETY FOR GENERAL PHYSIOLOGY**  
Brown, Ann, Medgar Evers College  
Dojcinovic, Danijel, Fumio Mekata Scholar, Arizona State University  
Hu, Hailan, University of California, Berkeley  
Wohlgemuth, Sandra, Humboldt-Universität zu Berlin

**SURDNA FOUNDATION SCHOLARSHIP**  
De Labra, Carmen, University College London  
Dellen, Babette, Washington University in St. Louis  
Doiron, Brent, University of Ottawa  
Hobbs, Steven, University of Colorado  
Montana, Enrico, Massachusetts Institute of Technology  
Ryan, Amy, University of Virginia Health Systems  
Zhou, Zhaolan (Joe), Harvard Medical School

**IRVING WEINSTEIN ENDOWED SCHOLARSHIP**  
Berry, Katy, University of Sheffield  
Su, Yi-Hsien, Scripps Institute of Oceanography, MBRD

**WILLIAM MORTON WHEELER FAMILY FOUNDERS' SCHOLARSHIP**  
Ihring, Alexandra, Max-Planck-Institute of Neurobiology

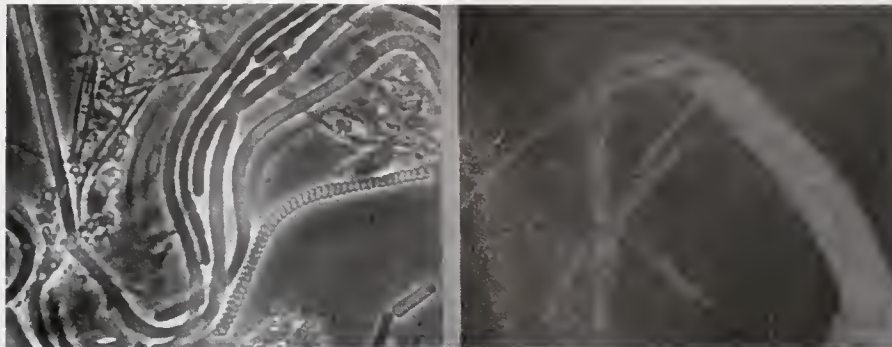
**WALTER L. WILSON ENDOWED SCHOLARSHIP FUND**  
Dojcinovic, Danijel, Arizona State University  
LaPointe, Nichole, Northwestern University

**WORLD ACADEMY OF ARTS AND SCIENCES EMILY MUDD SCHOLARSHIP**  
Akcali, Kamil, Bilkent University  
Bachman, Katherine, Case Western Reserve University  
Hallikas, Outi, University of Helsinki  
Perez, Christian, University of Pennsylvania  
Wang, Eileen, Northwestern Medical School

**WORLD HEALTH ORGANIZATION**  
Busso, Dolores, Buenos Aires University

## INSTITUTIONS REPRESENTED (students)

Albert Einstein College of Medicine  
 Alberta Research Council  
 American College of Cardiology  
 AORN  
 Arizona State University  
 AstraZeneca R&D Charnwood, UK  
 Autonomous University of Baja California Sur  
 Av Instituto Politécnico Nacional #2508  
 Avenue Healthcare Ltd  
  
 Banner Health System  
 Baylor College of Medicine  
 Bell Laboratories/Lucent Technologies  
 Beth Israel Deaconess Medical Center  
 Bilkent University  
 Boehringer Ingelheim Pharmaceuticals  
 Boston University  
 Boston University School of Medicine  
 Brandeis University  
 Brigham & Women's Hospital  
 Brigham Young University  
 British Antarctic Survey  
 Brown University  
 Buenos Aires University  
  
 California Institute of Technology  
 Cambridge University  
 Carl Zeiss  
 Carnegie Institution of Washington  
 Case Western Reserve University  
 Centers for Disease Control & Prevention  
 Chicago Medical School  
 Children's Hospital Boston  
 Children's Hospital of Philadelphia  
 Children's Hospital Los Angeles  
 Cleveland Clinic Foundation  
 Cold Spring Harbor Lab  
 College of William & Mary  
 Columbia University  
  
 Dalhousie University  
 Dana Farber Cancer Institute  
 Dartmouth College  
 Doane College  
 Duke University  
 Duke University Medical Center  
 Dunstaffnage Marine Laboratory  
  
 East Carolina University School of Medicine  
 East Stroudsburg University  
 Emory University  
 Emory University School of Medicine  
 Emporia State University  
 European Molecular Biology Laboratory  
  
 Family Health Council  
 Federal University of Rio de Janeiro  
 Field Museum of Natural History  
 Flemish Interuniversity Institute for  
 Biotechnology  
 Fox Chase Cancer Center  
  
 George Mason University  
 Georgetown University Medical Center  
 Georgia State University  
 Good Samaritan Family Practice Center  
  
 Harvard Medical School  
 Harvard University  
 Hebrew University  
 Hospital Authority  
 Howard University  
 Humboldt-Universität zu Berlin  
  
 Illinois State University  
 Imperial College of Science, Technology  
 & Medicine  
 Indiana State University  
 Indiana University  
 Indiana University Medical Center  
 Instituto Venezolano de Investig. Cientificas  
 Institut Pasteur  
 Institute de Física da Univ of São Paulo  
 Institute for Research in Reproduction  
 Instituto de Biología Molecular do Paraná-IBMP  
 Instituto de Biotecnología, UNAM  
 International School for Advanced Study (SISSA)  
  
 James Madison University  
 Johns Hopkins Bloomberg School of Public  
 Health  
 Johns Hopkins School of Medicine  
 Johns Hopkins University  
  
 Kaiser Permanente  
 Kalamazoo College  
 Kansas State University  
 Karolinska Institutet  
 King's College London  
  
 Leiden University Medical Centre  
 Liverpool School of Tropical Medicine  
 Los Alamos National Laboratory  
 Louisiana State University Health Sciences Center  
 Louisiana State University Medical School  
  
 Maine Medical Center  
 Marine Biological Laboratory  
 Marshfield Medical Research Foundation  
 Massachusetts Biomedical Initiative  
 Massachusetts Eye & Ear Infirmary  
 Massachusetts General Hospital  
 Massachusetts Institute of Technology  
 Max-Planck-Institute for Brain Research  
 Max-Planck-Institute for Molecular Genetics  
 Max-Planck-Institute of Neurobiology  
 Medgar Evers College  
 Medical College of Virginia  
 Medical University of South Carolina  
 MerckResearch Labs  
 Michigan State University  
 Microbia Inc.  
 Monongahela Valley Hospital  
 Montana State University  
 Monterey Bay Aquarium Research Institute  
 Morehouse School of Medicine  
 Mount Sinai School of Medicine  
  
 NASA-Ames Research Center  
 National Cheng Kung University Medical College  
 National Institute for Medical Research  
 National Institutes of Health  
 Natural History Museum of Los Angeles County  
  
 New Jersey Medical School, UMDNJ  
 New York University  
 New York University School of Medicine  
 North Shore Long Island Jewish Health System  
 Northwestern Medical School  
 Northwestern University  
  
 Ohio Permanente Medical Group  
 Ohio State University  
 Oklahoma Medical Research Foundation  
 Oregon Health & Science University  
 Oregon State University  
  
 P Universidad Católica de Chile  
 Pennsylvania State University College  
 of Medicine  
 Pennsylvania State University  
 Philipps-Universität Marburg  
 Physiology Institute of University Freiburg  
 Ponce School of Medicine  
 Princeton University  
  
 Queen's University Belfast  
  
 Raytheon Polar Services  
 Rice University  
 RIKEN, Japan  
 Rockefeller University  
 Royal Melbourne Hospital  
 Rutgers University  
  
 San Jose State University  
 Scripps Institute of Oceanography  
 Simon Fraser University  
 Smith College  
 Smithsonian Institution  
 Southern Illinois University School of Medicine  
 Spelman College  
 Staatliche Lehr-und Forschungsanstalt für  
 Landwirtschaft  
 Stanford University  
 Stanford University School of Medicine  
 State University of New York at Stony Brook  
 Swiss Federal Institute for Environmental Science  
 & Technology  
  
 Technion Israel Institute of Technology  
 Tel Aviv University  
 Temple University School of Medicine  
 Texas A&M University  
 Texas A&M University Health Science Center  
 The Institute for Genomic Research  
 The Naval Research Laboratory  
 The Scripps Research Institute  
 Tokyo Metropolitan Institute of Gerontology  
 Toronto West Hospital-Univ Health Network  
 Tufts University  
  
 UMass Medical School  
 United States Air Force  
 University of Massachusetts, Amherst  
 Universidad Autonoma del Estado de Morelos  
 Universidad Complutense Madrid  
 Universidad de Chile  
 Universidad Nacional de Córdoba  
 Universidade Aveiro



Cyanobacteria, Rolf Schauder

Universidade Federal de Sao Paulo  
 Università Degli Studi di Palermo  
 Université Montpellier 2  
 Université Pierre et Marie Curie-Paris 6  
 University Centre for Pharmacy  
 University College London  
 University of Aberdeen  
 University of Alabama, Birmingham  
 University of Arizona  
 University of Arizona College of Medicine  
 University of Birmingham Medical School  
 University of Buffalo  
 University of Calgary  
 University of California, Los Angeles  
 University of California, Berkeley  
 University of California, Irvine  
 University of California, Riverside  
 University of California, San Diego  
 University of California, San Francisco  
 University of Cambridge  
 University of Chicago  
 University of Colorado  
 University of Colorado Health Sciences Center  
 University of Connecticut  
 University of Constance  
 University of Crete  
 University of East Anglia  
 University of Edinburgh  
 University of Freiburg  
 University of Gent  
 University of Georgia  
 University of Hawaii  
 University of Helsinki  
 University of Illinois at Chicago  
 University of Illinois at Urbana-Champaign  
 University of Iowa  
 University of Iowa College of Medicine  
 University of Kansas  
 University of Kansas Medical Center  
 University of Kentucky College of Medicine  
 University of Konstanz  
 University of Leeds  
 University of Maastricht  
 University of Manchester  
 University of Maryland  
 University of Massachusetts Medical School  
 University of Miami  
 University of Miami School of Medicine  
 University of Michigan  
 University of Minnesota  
 University of Missouri-Columbia  
 University of Montana  
 University of Naples  
 University of Nebraska  
 University of New Mexico  
 University of New South Wales  
 University of Newcastle

University of Nijmegen  
 University of North Carolina  
 University of North Dakota  
 University of Notre Dame  
 University of Oklahoma Health Sciences Center  
 University of Oregon  
 University of Ottawa  
 University of Pennsylvania  
 University of Pennsylvania School of Medicine  
 University of Pierre et Marie Curie  
 University of Pisa  
 University of Pittsburgh  
 University of Portsmouth  
 University of Pretoria  
 University of Puerto Rico  
 University of Reading  
 University of San Luis Potosi  
 University of Sheffield  
 University of South Dakota  
 University of South Florida  
 University of Southern California  
 University of Texas at Austin  
 University of Texas Health Science Center,  
 San Antonio  
 University of Texas Southwestern Medical  
 Center at Dallas  
 University of Toronto  
 University of Utah  
 University of Vigo  
 University of Virginia  
 University of Washington  
 University of Wisconsin  
 University of Wisconsin-Madison  
 University of Yaounde  
 University of Zurich  
 University School of Medicine, Heidelberg  
 University of Geneva  
 Utah Department of Health

VA Maryland Health Care System  
 Vanderbilt University Medical Center  
 Veterans Affairs Medical Center  
 Virginia Commonwealth University  
 Virginia Mason Medical Center

Wake Forest University  
 Washington University in St. Louis  
 Weill Medical College of Cornell University  
 Weizmann Institute of Science  
 WHO Influenza Center  
 Woods Hole Oceanographic Institution

Yale University  
 Yale University School of Medicine

## COUNTRIES REPRESENTED

Argentina  
 Australia  
 Belgium  
 Brazil  
 Cameroon  
 Canada  
 Chile  
 China  
 Finland  
 France  
 Germany  
 Greece  
 India  
 Israel  
 Italy  
 Japan  
 Kenya  
 Mexico  
 Netherlands  
 Portugal  
 Scotland  
 South Africa  
 Spain  
 Sweden  
 Switzerland  
 Taiwan  
 Turkey  
 United Kingdom  
 United States of America  
 Venezuela

## INSTITUTIONS REPRESENTED (faculty)

Albert Einstein College of Medicine  
 American Association for the Advancement  
 of Science  
 American Psychological Association  
 Arizona State University

Baylor College of Medicine  
 Bell Labs, Lucent Technologies  
 BioHybrid Technologies  
 Boston College  
 Boston University  
 Bowling Green State University  
 Brandeis University  
 Bridgewater State College  
 Brown University

California Institute of Technology  
 Carnegie Institution of Washington  
 Carnegie Mellon University  
 Case Western Reserve University  
 CCNY  
 Center For Sensor Technology  
 Centre for Genome Research  
 Centre Genetique Moleculaire  
 Cold Spring Harbor Laboratory  
 Columbia University  
 Cornell Medical School  
 Cornell University

Dartmouth College  
 Danmark Tekniske Universitet  
 Duke University Medical Center  
 Duke University

Eastern Virginia Medical School  
 Emory University  
 ETH Zurich  
 European Institute of Technology

Florida Institute of Technology  
 Florida State University  
 Fred Hutchinson Cancer Research Center  
 Freie Universitaet Berlin

Georgetown University Medical School  
 Geron

Hamamatsu Photonic Systems  
 Harbor-UCLA Medical Center  
 Harvard Medical School  
 Harvard University  
 Hebrew University  
 HHMI/Brown University  
 HHMI/Fred Hutchinson Cancer Research Center  
 HHMI/UMDNJ-RW Johnson Medical School  
 HHMI/UT Southwestern Medical Center  
 HHMI/Johns Hopkins University  
 HHMI/NYU  
 House Ear Institute

ICRF Clare Hall Laboratories  
 Imperial Cancer Research Fund  
 Imperial College of Science Technology  
 Institut Pasteur  
 Iowa State University

Johns Hopkins School of Medicine  
 Johns Hopkins University  
 Jules Stein Eye Institute, UCLA

Karolinska Institutet  
 Kent State University  
 King's College, London

Lawrence Berkeley National Laboratory  
 London School of Hygiene and Tropical Medicine  
 Louisiana State University Health Science Center  
 Leiden University, The Netherlands

Magee-Womens Research Institute  
 Marine Biological Laboratory  
 Massachusetts General Hospital  
 Massachusetts Institute of Technology  
 McGill University  
 Medical College of Georgia  
 Medical College of Ohio  
 Medical College of Wisconsin  
 Meharry Medical College  
 Michigan State University  
 Monell Chemical Senses Center  
 Montana State University  
 Mount Sinai School of Medicine  
 MPI for Medical Research  
 MPI for Biological Cybernetics  
 MPI for Marine Microbiology  
 MRC Lab of Molecular Biology  
 Memorial Sloan Kettering Cancer Center

National Institute on Aging, NIH  
 National Institute for Medical Research  
 National Institute of Mental Health  
 National Institute on Drug Abuse  
 National Institutes of Health  
 National Library of Medicine  
 NEC Research Institute, Inc  
 New England Medical Center  
 New York University

New York University School of Medicine  
 Northwestern University  
 Northwestern University Medical School

Ohio State University  
 Oregon Health & Science University  
 Oregon State University

Praecis Pharmaceuticals  
 Princeton University

Queen's University Belfast

Roche Molecular Systems  
 Rockefeller University  
 Rutgers University

San Diego State University  
 Seattle Biomedical Research Institute  
 Sensor Technologies  
 Smithsonian Institution  
 St. Barnabas Medical Center  
 Stanford Medical School  
 Stanford University  
 Stowers Institute for Medical Research  
 SUNY at Buffalo  
 SUNY at Stony Brook  
 Syracuse University

Texas A&M University  
 The Hebrew University  
 The Institute for Genomic Research  
 The University of Iowa  
 The University of Manchester  
 Tufts University  
 Tufts University School of Medicine  
 Tufts University School of Veterinary Medicine

Umeå University  
 University of Pittsburgh  
 University of Texas Southwestern Medical Center  
 University of Virginia  
 University of Texas at Austin  
 University of California, Davis  
 University of California, San Diego  
 University of California, Santa Barbara  
 University of California, Berkeley  
 University of California, Los Angeles  
 University of California, San Francisco  
 University of North Carolina, Chapel Hill  
 University of Illinois, Chicago  
 University of Kentucky Medical Center  
 University of Maryland, College Park  
 University of Rochester (NY)  
 University of Pittsburgh  
 University of Colorado Health Sciences Center  
 University of British Columbia  
 University of Colorado Health Sciences Center  
 University of Kansas Medical Center  
 University of Oregon  
 University of Pennsylvania  
 University of Sao Paulo  
 University of Southern California  
 University of Pittsburgh School of Medicine  
 Universidad de Buenos Aires  
 Universitaet Ulm  
 University College London  
 University Hospital Lausanne  
 University of Aberdeen  
 University of Alabama  
 University of Arizona  
 University of Bern  
 University of Calgary  
 University of Cambridge  
 University of Cape Town  
 University of Chicago  
 University of Cincinnati

University of Connecticut  
 University of Connecticut Health Center  
 University of Dundee  
 University of Edinburgh  
 University of Florida  
 University of Georgia  
 University of Glasgow  
 University of Guelph  
 University of Hawaii  
 University of Idaho  
 University of Illinois  
 University of Illinois, Chicago  
 University of Illinois, Urbana  
 University of Iowa  
 University of Kansas  
 University of Kentucky  
 University of Kentucky Medical Center  
 University of Konstanz  
 University of Lethbridge  
 University of Manchester  
 University of Maryland  
 University of Massachusetts  
 University of Massachusetts Medical School  
 University of Melbourne  
 University of Michigan  
 University of Minnesota  
 University of Missouri-Columbia  
 University of Missouri-Rolla  
 University of North Carolina, Chapel Hill  
 University of Notre Dame  
 University of Oregon  
 University of Oxford  
 University of Texas  
 University of Texas at Austin  
 University of Toronto  
 University of Utah  
 University of Victoria, B C  
 University of Virginia  
 University of Warwick  
 University of Washington  
 University of Wisconsin  
 University of Wisconsin - Madison  
 UT Health Science Center, San Antonio

Vollum Institute

Washington University  
 Washington University School of Medicine  
 Weill Medical College Cornell University  
 Weizmann Institute  
 Wellesley College  
 Wesleyan University  
 Whitehead Institute for Biomedical Research  
 Williams College

Yale Medical School  
 Yale University

## COUNTRIES REPRESENTED

Argentina	Lebanon
Australia	Mexico
Austria	New Zealand
Brazil	Russia
Canada	South Africa
China	Sweden
Columbia	Switzerland
Denmark	Taiwan
France	The Netherlands
Germany	Turkey
Greece	United Kingdom
India	United States of America
Indonesia	
Ireland	
Israel	
Italy	
Jamaica	

# mbl/whoi library



*The MBL/WHOI Library maintains one of the world's largest print and electronic collections of biomedical, oceanographic, and marine biological literature. It is jointly operated with the Woods Hole Oceanographic Institution. The main library is located in the MBL's Lillie Building, with branches on the campuses of the Woods Hole Oceanographic and the National Marine Fisheries Service in Woods Hole.*



## REPORT OF THE LIBRARIAN

Libraries are the computer-age doorways to information systems worldwide. Today the MBL/WHOI Library uses an integrated set of resources for online cataloging, resource sharing and reference services, with local and regional systems linking Woods Hole with large universities and museums all over the world. Libraries like ours are now essentially borderless. With increases in journal pricing and shrinking budgets, libraries must collaborate with other institutions more and more to deliver information that their users require.

Digitization technology—which enables the one-time transformation of information from print to electronic format—will only increase collaborations and encourage the sharing of information over time. Thanks to this technology, important articles, books, and images once at risk of being lost forever on a dusty shelf can be stored and delivered electronically to users around the world. The MBL/WHOI Library has shown this to be true with the successful digitization of the Leuckart charts, which have been available on the Library's web site since 1996. Over the years, hundred of thousands of people from around the world have rediscovered these 19<sup>th</sup> century teaching charts, which are still very useful today.

The MBL/WHOI Library continues to grow in non-traditional directions. We are developing innovative digitization services and important new research tools, including X-ID, an online taxonomic key, funded by the Jewett Foundation, and uBio, a network taxonomic name server funded by the Andrew W. Mellon Foundation. Through these two pilot projects we have established global alliances with GBIF (Global Biodiversity Information Facility) and ITIS (Information Taxonomic Information Service) and bolstered our relationships with museums. Currently, we are creating a digital archive for the MBL Herbarium of local fauna and marine algae. A very enthusiastic group of MBL Associates is scanning the specimens for the project, which is funded by SeaGrant.

*Continued...*

In 2002, we aggressively moved more Library content and supporting services to the web for direct delivery to the patron. By the end of 2002, the MBL/WHOI Library was delivering approximately 52% of our serials and 100% of our databases in distributed, electronic form extending the Library's reach beyond our walls to wherever our patrons want to be twenty-four hours a day, seven days a week. We continued to improve existing services with the enhancement of our web site ([www.mblwhoilib.org/](http://www.mblwhoilib.org/)). We also continued to invest in the Library's future through major expenditures, projects, technological platforms, support systems and replacement of current infrastructure and computer technology that support existing library services.

The Library hosted 119 Readers taking sabbaticals, working on writing projects, or conducting long-term research projects. The wireless network installed in 2002 brought Internet access to the stacks and reading rooms. Ironically, we have declared the Grass Reading Room to be a "technology free" zone to maintain a quiet, contemplative space in a Library that has resolutely embraced electronic information delivery.



## | Serials

We made a smooth transition to a new serials vendor, EBSCO, and escaped the turmoil our former vendor created when it declared bankruptcy and stranded major academic libraries with loss of access to journals. The Library realigned serial holdings and services to better support current scientific research interests. We analyzed

serial and database usage statistics and surveyed the scientific community about how current subscriptions and exchange programs were meeting their needs. Discussions resulted in substantive changes to the 2003 serial collection, including a cut back of long-standing exchange programs at the MBL and WHOI. These changes reflect input from librarians and members of the community on a number of factors: survey responses; the community's request that we subscribe to the Web of Science database; rising serials prices; expiring ejournal contracts being replaced with higher-cost alternatives; space constraints in the Lillie Building; and a 4% decrease in the MBL-serials budget line.

## | Monographs

We continued to acquire titles for the book and special/named collections using our general budget and specific funds including the Atwood, Aron, and Mullin gift funds. The WHOI ship libraries were updated with the addition of new reference as well as recreational reading materials. The Clark Reading Room was completely dismantled to reorganize staff workspace. Non-duplicate Clark materials were filed with the main book collection (3rd floor Lillie), which was completely shifted. In addition, all stacks were relabeled.

## | Special Collections

Dedicated staff and volunteers continued to make great strides in Special Collections. The MBL Archives processed the reprint collection of Viktor Hamburger, John Burris' Director's papers, James Ebert's scientific and Director's papers, and the Arthur Humes collection of glass plates, slides, and photographs. We also restored and rebound 130 items from Rare Books/Special Collections with the support of the Florence Gould Foundation. The WHOI Data Library & Archives (DLA) continued to process and catalog their extensive collection of technical reports, maps, scientist's papers, ship cruise reports and logs, etc. They spent a considerable amount of time migrating Alvin and other data from old media to newer formats. Both MBL and WHOI Archivists are raising awareness for the need of institutional records management plans.

## LIBRARY READERS

### Courses

Library staff gave 37 general library orientations or department-oriented sessions and taught 25 courses in 2002. Trainers were brought in from several specific databases to do in-depth training sessions. In conjunction with our Spring and Fall Medical Informatics courses, new interactive student web pages were designed, and course packs were made available over the web.

Our staff actively participated in professional development activities and contributed to the profession as a whole. This serves to promote MBL/WHOI Library projects and it exposes our staff to new ideas and methods. DLA staff hosted a meeting of the Marine Technology Society concerning scientific instruments. The Library Director and Associate Director also served on various task forces involved in developing a strategic plan for the MBL.

The MBL/WHOI Library continues to serve as an electronic bridge between Woods Hole and the world providing access to collections at universities, and in public, corporate, private, museum, and laboratory libraries around the globe.

—Catherine N. Norton

Abbott, Jayne, Marine Research, Inc  
Ahmadjian, Vernon, Clark University  
Allen, Garland, Washington University  
Anderson, Everett, Harvard University

Baccetti, Baccio, NRC of Siena, Italy  
Benjamin, Thomas, Harvard Medical School  
Bernhard, Jeffery, University of Massachusetts Medical Center  
Borgese, Thomas, Leaman College, CUNY  
Bower, James, University of Texas, San Antonio  
Boyer, John, Union College

Candelas, Graciela, University of Puerto Rico  
Cariello, Lucio, Stanzione Zoologica "A Dohrn"  
Chang, Donald, Hong Kong University  
Child, Frank, Trinity College  
Clarkson, Kenneth, Bell Labs  
Cohen, Seymour, American Cancer Society  
Cook, Erik, Howard Hughes Medical Center  
Cooperstein, Sherwin, University of Connecticut  
Copeland, Eugene, Woods Hole, MA  
Corwin, Jeffery, University of Virginia  
Couch, Ernest, Texas Christian University

D'Alessio, Giuseppe, Università di Napoli Federico II  
Davis, Jonathan, Lexigen Pharmaceuticals  
Donavan, Erin, Auburn University  
Dube, Francois, St Luc, Canada  
Duncan, Thomas, Nichols College

Epstein, Herman, Brandeis University

Finkelstein, Alan, Albert Einstein College of Medicine

Fraenkel, Dan, Harvard Medical School  
Frenkel, Krystyna, New York University School of Medicine

Galatzer-Levy, Robert, University of Chicago  
Garcia-Blanco, Mariano, Duke University Medical School  
German, James, Cornell University  
Grossman, Albert, New York University Medical School  
Gruner, John, Cephalon, Inc

Halvorson, Harlyn, University of Massachusetts, Boston  
Harrington, John, SUNY New Paltz  
Herskovits, Theodore, Fordham University

Inoué, Sadayuki, McGill University

Jaye, Robert, Boston  
Jacobson, Allan, University of Massachusetts Medical Center  
Josephson, Robert, University of California

Kaltenbach, Jane, Mount Holyoke College  
Karlín, Arthur, Columbia University  
Kelly, Robert, Woods Hole, MA  
Keynan, Alexander, Israel Academy of Sciences & Humanities  
King, Kenneth, Falmouth, MA  
Knox, Carol, Northfield Mount Herman  
Kornberg, Hans, Boston University  
Krane, Stephen, Harvard Medical School

Laczko, Jozsef, New York University  
Laderman, Amilee, Yale University  
Lisman, John, Brandeis University  
Linck, Richard, University of Minnesota  
Llinas, Rudolfo, New York University  
Loewenstein, Werner, Journal of Membrane Biology  
Lorand, Laszlo, Northwestern University Medical School  
Luckenbill, Louise, Ohio University

Menini, Anna, CNR-SISSA  
Milkman, Roger, University of Iowa  
Miller, Andra, NIH  
Mitchell, Ralph, Harvard University  
Morrell, Leyla, Rush Presbyterian St Lukes

Nagel, Ronald, Albert Einstein College of Medicine  
Narahashi, Toshio, Northwestern University  
Naugle, John, NASA

Plummer Cobb, Jewel, California State University  
Prendergast, Robert, Johns Hopkins University



Rabinowitz, Michael, Harvard University  
Rafferty, Nancy, Falmouth, MA  
Reynolds, George, Princeton University  
Rome, Larry, University of Pennsylvania  
Ruderman, Joan, Harvard Medical School

Segal, Sheldon, The Population Council  
Sheng, Morgan, Massachusetts Institute of Technology  
Shepard, Frank, Woods Hole Data Base  
Shimomura, Osamu, Falmouth, MA  
Smith, Tim, Northeast Fisheries Science Center  
Solomon, Dennis, Yarmouth Port, MA  
Spector, Abraham, College of Physicians & Surgeons  
Spotte, Stephen, Mote Marine Lab  
Steinberg, Martin, Boston University School of Medicine  
Stuart, Ann, University of North Carolina  
Sullivan, Gerald, Savio Prep-Boston

Trinkhaus, John, Yale University  
Tweedell, Kenyon, University of Notre Dame  
Tycosinski, Mark, University of Pennsylvania

Walton, Alan, Cavendish Laboratory  
Warren, Leonard, University of Pennsylvania  
Weissmann, Gerald, New York University Medical Center  
Whittaker, J. Richard, University of New Brunswick  
Woods Hole Research Center

# financials



## REPORT OF THE TREASURER

The financial results for 2002 reflected the difficult operating environment in a year where all non-profits were adversely affected by two major trends: the continued decline in the investment markets and a softening of philanthropic support.

The Unrestricted Operating results showed a loss of \$1.76 million, which was a vast improvement over the \$2.9 million loss reported in 2001. This was due to a more rapid increase (14.4%) in Unrestricted Operating Support when compared to Operating Expense growth (9.6%). On the revenue side, Government Grants increased by 8.2%, Lab Rental & Net Tuition increased by 12%, Fees for Conferences and Services rebounded 21.7% from depressed levels in 2001 as a result of cancelled events due to September 11<sup>th</sup>, and Investment and Other Revenues increased by 30%.

On the expense side, Research activities represented two-thirds of the increase, growing by approximately \$2 million (9.7%) as the Laboratory added more than two dozen scientists mainly to gear up for expanded research programs in Scientific Aquaculture and Global Infectious Disease. As a result, grant applications hit an all-time high and grant dollars awarded increased almost 30% over 2001. Looking at the underlying components, double-digit increases were experienced in Salaries (13.6%), Fringe Benefits (16.2%), Supplies (19.4%), Utilities (12.1%), and Depreciation (16.8%).

Philanthropic support fell dramatically from the unusually strong levels the Laboratory had experienced in the three previous years when the MBL received gifts exceeding \$10 million each year. Total Contributions including those to Plant were \$4.6 million, the lowest level since 1995. The long-term investment portfolio, however, performed quite competitively in a year when the average common stock mutual fund declined by 28%. The 3.9% decline in market values was in the top quartile when compared to how a universe of 122 foundations and endowments performed in 2002. The MBL had realized and unrealized investment losses, which totaled \$2 million in 2002.

Taking into account the challenging near-term market environment, in 2002 the Laboratory experienced its first decline in Total Net Assets since 1994. MBL's Net Assets declined \$6.2 million.

The MBL's Balance Sheet Assets reflected this impact, declining by \$7.1 million. The entire decline was concentrated in Short Term Investments and Pledge Receivables. The Endowment held up due to the receipt of new permanently restricted gifts. Property, Plant & Equipment also held steady as \$2.4 million in improvements more than offset the accrued depreciation. Liabilities declined by approximately \$1 million, principally due to the relinquishment of a Unitrust to the benefit of the Laboratory.

Considering some financial performance ratios, our Return on Average Net Assets was a negative 6.7%, which is in line with most non-profits during this period. The MBL's Leverage Ratio (Unrestricted & Temporarily Restricted Net Assets/ Debt) remains sound at 4.48X. Also, both our Debt Service Coverage ratio of 1.72X for 2002 and our non-permanently restricted Cash & Investments of \$25.6 million at year-end are well in excess of the financial covenants of the Letter of Credit supporting the MBL's Long Term Debt.

In summary, it was a challenging year financially mainly due to the effect the third consecutive year of investment market declines had on MBL's philanthropic support and investment portfolio. Coming out of our strategic planning effort we have already started implementing steps that will position the Laboratory for a strong rebound in our Government Grants and to ultimately gear-up for a new capital campaign that should improve our philanthropic support. Our education, summer/visiting scientist, and conference activities remained strong and when combined with the expanded resident research programs should help us continue to improve our operating results in the near future.

— Mary B. Conrad



Lobster eyes, Diane Heck, David Ramsey, Lydia Louis, and Jeff Laskin

## FINANCIAL STATEMENTS

Operating History and Balance Sheet as of December 31, 2002 and 2001.



The financial statements of the Marine Biological Laboratory, for the fiscal year ending December 31, 2002, were audited by PricewaterhouseCoopers, LLP.

Complete financial statements are available upon request from:

Mr. Homer Lane  
Chief Financial Officer  
Marine Biological Laboratory  
7 MBL Street  
Woods Hole, MA  
02543-1015

<b>BALANCE SHEET (In Thousands)</b>	<b>2002</b>	<b>2001</b>
<b>ASSETS:</b>		
Cash and Short Term Investments	\$4,357	\$8,993
Pledges and Other Receivables	8,794	11,265
Assets Held by Bond Trustee	-	269
Other Assets	631	711
Endowment and Similar Investments	42,290	42,181
Property Plant and Equipment (Net)	<u>31,729</u>	<u>31,519</u>
<b>TOTAL ASSETS:</b>	<b><u>87,801</u></b>	<b><u>94,938</u></b>
<b>LIABILITIES:</b>		
Accounts Payable	2,797	3,133
Annuities and Unitrusts Payable	535	1,383
Deferred Revenue and Other Liabilities	2,557	2,318
Long Term Debt	<u>10,200</u>	<u>10,200</u>
<b>Total Liabilities:</b>	<b><u>16,089</u></b>	<b><u>17,034</u></b>
<b>NET ASSETS:</b>		
Unrestricted	20,381	22,261
Temporary Restricted	25,278	29,941
Permanently Restricted	<u>26,053</u>	<u>25,702</u>
<b>Total Net Assets:</b>	<b><u>71,712</u></b>	<b><u>77,904</u></b>
<b>TOTAL LIABILITIES AND NET ASSETS:</b>	<b><u>\$87,801</u></b>	<b><u>\$94,938</u></b>
<b>OPERATING HISTORY (In Thousands)</b>		
<b>OPERATING SUPPORT:</b>		
Government Grants	\$15,849	\$14,648
Private Contracts	1,495	1,675
Lab Rental and Net Tuition	2,188	1,954
Fees for Conferences and Services	5,333	4,383
Contributions	4,522	10,886
Investment and Other Revenues	<u>3,321</u>	<u>2,555</u>
<b>Total Operating Support</b>	<b><u>32,708</u></b>	<b><u>36,101</u></b>
<b>EXPENSES:</b>		
Research	22,371	20,399
Instruction	5,998	5,637
Conferences and Services	1,460	1,133
Other Programs	<u>5,027</u>	<u>4,643</u>
<b>Total Expenses:</b>	<b><u>34,856</u></b>	<b><u>31,812</u></b>
<b>CHANGE IN NET ASSETS BEFORE NON-OPERATING ACTIVITY:</b>	<b>(2,148)</b>	<b>4,289</b>
<b>Non-Operating Activities:</b>		
Contributions to Plant and Other Expenses, Net	(149)	2,244
Total Investment Income and Earnings	(1,994)	(2,930)
Less Investment Earnings Used for Operations	<u>(1,901)</u>	<u>(1,475)</u>
Reinvested (Utilized) Investment Earning	<u>(3,895)</u>	<u>(4,405)</u>
<b>TOTAL CHANGE IN NET ASSETS:</b>	<b><u>\$(6,192)</u></b>	<b><u>\$2,128</u></b>

# gifts

---



*Planktonic sarcodine. The host DNA is located within the dark, central nuclear capsule. The symbionts are the small bright specks radiating outward along the host spines. David Caron*

## REPORT OF THE DEVELOPMENT COMMITTEE

---

As the MBL engaged in institution-wide strategic planning during this past year as described by Dr. Speck earlier in this report, 2002 was a pivotal year for Development efforts. Moving forward after our spectacularly successful *Discovery Campaign* with new research and educational programs now in place, we turned our attention to broadening our outreach and education activities through a series of events and communications.

Last summer, we held an enjoyable and informative Day of Science attended by 92 guests from nearby communities that included presentations by MBL scientists and lab tours. The Council of Visitors meeting drew 80 friends from across the country to learn about *Modern Molecular Approaches to Global Infectious Diseases* and to tour the totally refurbished suite of laboratories for the newly established research program in this area. As in past years, our summer lectures and childrens' programs in Nantucket and Martha's Vineyard spread the word about the MBL. We branched out in 2002 and held our first-ever alumni reception in Chapel Hill, North Carolina, attended by 65 course alumni and faculty, MBL Corporation Members, and friends of the Lab. And, turning to the Internet, Development information is now featured on MBL's web site so we can effectively extend our message to a world-wide community.

In 2002, MBL raised \$4,944,803 in private support. This included \$1,350,000 from the Andrew W. Mellon Foundation in renewed support for terrestrial forest research and support for a new pilot project designed to index and organize information about organisms that is distributed on the Internet. MBL Council of Visitors member, Robert Shifman, provided an additional gift of \$564,502 to the Milton Shifman Endowed Scholarship. The G. Unger Vetlesen Foundation continued its generous and long-standing support for the Bay Paul Center and unrestricted support. The Ellison Medical Foundation, the Grass Foundation, and the Burroughs Wellcome Fund all provided renewed support for MBL's advanced courses in biology and biomedicine.

The 2002 Annual Fund had another strong year with \$553,620 raised from 898 donors—both new records in annual fund giving at the MBL. The amount raised and numbers of donors are both up by 9% over last year. As in past years, the Whitman Society, comprised of donors whose gifts of \$1,000 or more accounted for much of this success. I would like to thank Dr. Peter Armstrong for serving as Annual Fund Chair and Mr. Michael Fenlon for leading the Annual Fund drive for the Associates. We are enormously grateful for this unrestricted support for the Laboratory.

On behalf of the Development Committee, the Board of Trustees, and the entire MBL community, I would like to express my appreciation to the donors whose names appear on the following pages, and to those who requested anonymity. We are all most grateful for their generous support for the Marine Biological Laboratory's research and educational programs.

— Christopher M. Weld, Chair, Development Committee

## HIGHLIGHTS

During 2002, the following foundations and individuals provided major support for the Laboratory.



Ecosystems Center Staff members map out a research plan, Elizabeth Armstrong

Burroughs Wellcome Fund awarded \$170,000 for continuing support of the Molecular Mycology course.

The Ellison Medical Foundation awarded \$282,670 for continuing support of the Molecular Biology of Aging Colloquium for the period 2002 through 2004.

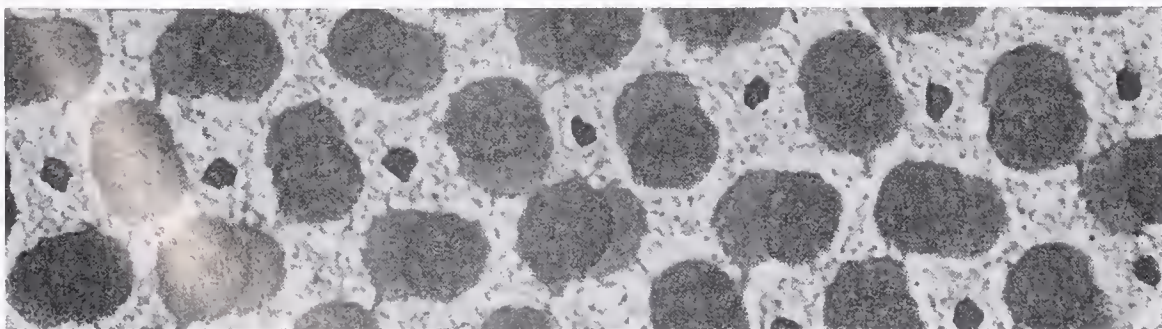
The Grass Foundation awarded \$226,500 in renewed funding for the Neurobiology and Neural Systems and Behavior courses.

Andrew W. Mellon Foundation awarded two grants totaling \$1,350,000: \$850,000 to support research on nitrogen transformation in terrestrial landscapes conducted by The Ecosystems Center and \$500,000 to launch the Universal Biological Indexer and Organizer (uBio), a database and internet tool to provide up-to-date biological information.

Mr. Robert Shifman made an additional gift of \$564,502 to support the Milton L. Shifman Endowed Scholarship. Mr. Shifman was a member of the Council of Visitors.

G. Unger Vetlesen Foundation provided \$150,000 for the Josephine Bay Paul Center in Comparative Molecular Biology and Evolution; \$100,000 in support of the program to develop marine models for biomedical research; and \$100,000 to underwrite veterinary services in the Marine Resources Center.

Neural system cone mosaic, Inigo Novalis Flamarique



## SPECIAL GIFTS



*A variety of foundations, individuals, and companies provided funds for special projects and programs at the Marine Biological Laboratory. We gratefully acknowledge their support.*

### Major Gifts

Anonymous (2)  
 American Society for Cell Biology  
 American Society for Reproductive Medicine  
 Applied Biosystems  
 Cox Foundation, Inc  
 Estate of Emily Ann Cramer  
 Environmental Data Research Institute  
 ExxonMobil Foundation  
 Georgia-Pacific Corporation  
 Mr. William Golden and Dr. Jean Taylor  
 Howard Hughes Medical Institute  
 Dr. and Mrs. Kurt J. Isselbacher  
 Mr. and Mrs. George W. Logan  
 The Mantia Family Trust  
 Massachusetts Environmental Trust  
 The Honorable and Mrs. G. William Miller  
 New York Times Company Foundation  
 Nikon Instruments Inc  
 The Pfizer Foundation  
 Mrs. Robert W. Pierce  
 William Townsend Porter Foundation  
 Dr. and Mrs. John W. Rowe  
 The Schooner Foundation  
 Sholley Foundation, Inc  
 The Catherine Filene Shouse Foundation  
 Alfred P. Sloan Foundation  
 Society for Neuroscience  
 The Seth Sprague Education & Charitable Foundation  
 Drs. William Speck and Evelyn Lipper  
 The Sprague Foundation  
 Drs. Albert Stunkard and Margaret Maurin  
 Mr. and Mrs. Gerard L. Swope  
 Universal Imaging Corporation  
 Mr. Sidney J. Weinberg, Jr.  
 The Irving Weinstein Foundation, Inc.  
 Mr. and Mrs. Christopher M. Weld

### Other Gifts

American Society for Biochemistry & Molecular Biology  
 Mrs. Kimball C. Atwood, III  
 Aquatic Eco-systems, Inc  
 Ms. Susan M. Barnes  
 Josephine Bay Paul & C. Michael Paul Foundation  
 Bio-Rad  
 Dr. Barry R. Bloom  
 Mr. and Mrs. Thomas C. Bolton  
 Mrs. Carolyn S. Carlson  
 Dr. Eloise E. Clark  
 Drs. William and Marion Cohen  
 Dr. Seymour S. Cohen  
 Elsevier Science Ireland Ltd  
 Drs. Lawrence Cohen and Barbara Ehrlich  
 Federation of American Societies for Experimental Biology  
 Fluke Corporation  
 Friendship Fund  
 Dr. and Mrs. Harold Gainer  
 Drs. Robert and Anne Goldman  
 Dr. and Mrs. J. Woodland Hastings  
 Dr. Robert R. Haubrich  
 Mr. and Mrs. Irwin Herskowitz  
 Mrs. Carmela J. Huettner  
 Mr. and Mrs. Richard A. Huettner  
 Dr. and Mrs. Shinya Inoue  
 Mr. David Isenberg and Ms. Paula Blumenthal  
 Invitrogen  
 Dr. Wallace Ip  
 Mr. Daniel Isenberg  
 Dr. and Mrs. Benjamin Kaminer  
 Dr. Andrew Kropinski and Dr. Peggy Pritchard  
 Dr. Kiyoshi Kusano  
 Dr. Hans Laufer  
 Mr. Richard Mawe  
 Merck Research Laboratories  
 Ms. Natalie Miller  
 Dr. Betty C. Moore  
 Ms. Mary Musacchia and Dr. James Faber  
 Mr. Telephone, Inc  
 New England Biolabs, Inc  
 Ms. Catherine N. Norton  
 Novartis  
 Dr. and Mrs. Philip Person  
 Pharmacia & Upjohn Company  
 PhotoArk  
 Estate of Madelene E. Pierce  
 Princeton Day School  
 Promega Corporation  
 Qiagen, Inc  
 Dr. and Mrs. Harris Ripps  
 Dr. Raja Rosenbluth  
 Mr. and Mrs. William Rugh  
 Schering-Plough Research Institute  
 Sinauer Associates Inc., Publishers  
 Dr. Sol Sepsewol  
 Dr. Abraham Spector and Ms. Marguerite Filson  
 Drs. Melvin and Evelyn Spiegel  
 Mrs. Eleanor Steinbach  
 Syngenta  
 Dr. and Mrs. Andrew G. Szent-Gyorgyi  
 Ms. Natalie Trousof  
 United States Geological Survey  
 Dr. Dale A. Webster  
 Dr. and Mrs. Gerald Weissmann  
 Mrs. Clare M. Wilber  
 World Health Organization  
 World Precision Instruments  
 The Worthington Family Foundation, Inc

## THE WHITMAN SOCIETY

Membership in the Whitman Society is open each year to individual donors who contribute \$1,000 or more to the MBL Annual or Alumni Funds.

### Director's Circle

Anonymous

Dr. Porter W. Anderson, Jr.  
Key Largo, Florida

Mr. and Mrs. William C. Cox, Jr.  
Hobe Sound, Florida

Dr. and Mrs. Kurt J. Isselbacher  
Newton Center, Massachusetts

Mr. and Mrs. George W. Logan  
Salem, Virginia

The Honorable G. William Miller  
Washington, DC

Mrs. Robert W. Pierce  
Boca Grande, Florida

Mr. Vin Ryan and Ms. Carla Meyer  
Boston, Massachusetts

Dr. and Mrs. John W. Rowe  
New York, New York

Drs. William Speck and Evelyn Lipper  
West Falmouth, Massachusetts

Mr. Sidney J. Weinberg, Jr.  
New York, New York

Dr. and Mrs. Gerald Weissmann  
New York, New York

Mr. and Mrs. Christopher M. Weld  
Essex, Massachusetts

Mr. and Mrs. Alfred M. Zeien  
Boston, Massachusetts

### Benefactor

Diane and Norman Bernstein  
Washington, DC

Mr. and Mrs. Jonathan Conrad  
New York, New York

Mr. and Mrs. Diarmaid Douglas-Hamilton  
Beverly, Massachusetts

Mr. William T. Golden  
American Museum of Natural History,  
New York, New York

Mr. and Mrs. Amos B. Hostetter Jr.  
Boston, Massachusetts

Dr. Laurie J. Landeau  
Northport, New York

Robert A. Prendergast  
Falmouth, Massachusetts

Mr. and Mrs. Richard Reiss  
New York, New York

Harriet and Sheldon Segal  
Hartsdale, New York

### Patron

Anonymous

Frank and Mardi Bowles  
Woods Hole, Massachusetts

Mr. and Mrs. Malcolm K. Brachman  
Dallas, Texas

Mr. and Mrs. Murray H. Bring  
East Hampton, New York

Drs. Claire Fraser and J. Craig Venter  
Potomac, Maryland

Frances and Howard Jacobson  
Westborough, Massachusetts

Dr. and Mrs. Stephen M. Krane  
Waban, Massachusetts

Catherine C. Lastavica, M.D.  
Manchester, Massachusetts

Dr. and Mrs. Leonard Laster  
Woods Hole, Massachusetts

Dr. Anna Logan Lawson  
Daleville, Virginia

Birgit Rose and Werner R. Loewenstein  
Falmouth, Massachusetts

Ginny and Pete Nicholas  
Boston, Massachusetts

Arthur B. Pardee and Ann B. Goodman  
Cambridge, Massachusetts

Mr. Marius A. Robinson  
Key Biscayne, Florida

Drs. Mitchell Sogin and Laurel Miller  
Falmouth, Massachusetts

Mr. and Mrs. John C. Stegeman  
Ann Arbor, Michigan

Drs. Ann E. Stuart and John W. Moore  
Chapel Hill, North Carolina

### Member

Edward and Marion Adelberg  
New Haven, Connecticut

Dr. Louise Adler  
Falmouth, Massachusetts

Dr. Garland E. Allen  
Saint Louis, Missouri

Mr. and Mrs. Douglas F. Allison  
Bloomfield Hills, Michigan

Drs. Clay and Clara Armstrong  
Philadelphia, Pennsylvania

Peter and Margaret Armstrong  
Davis, California

Dr. Samuel C. Armstrong  
Everett, Washington

Jean and Bob Ashton  
New York, New York

Mr. and Mrs. David Bakalar  
Chestnut Hill, Massachusetts

Mr. and Mrs. Charles A. Baker  
Princeton, New Jersey

Drs. Robert and Harriet Baker  
White Plains, New York

David Baltimore and Alice S. Huang  
Pasadena, California

- Mrs Frederik B Bang  
Woods Hole, Massachusetts
- Hope and Mel Barkan  
Boston, Massachusetts
- Dr. and Mrs Robert B Barlow  
Jamesville, New York
- Fred and Christine Bay  
Landgrove, Vermont
- Bruce Anthony Beal  
Woods Hole, Massachusetts
- Drs Eugene and Millicent Bell  
Boston, Massachusetts
- Drs Michael and R Suzanne Bennett  
New Rochelle, New York
- Mrs Beth Berne  
Woods Hole, Massachusetts
- Jewelle and Nathaniel Bickford  
New York, New York
- Mr. and Mrs Eric F Billings  
Potomac, Maryland
- Dr. and Mrs Elkan R. Blout  
Cambridge, Massachusetts
- Mr. Allen Bragdon  
South Yarmouth, Massachusetts
- Dr. and Mrs Goodwin M Breinin  
New York, New York
- Dr and Mrs John B Buck  
Sykesville, Maryland
- Mr. and Mrs N Harrison Buck  
Princeton, New Jersey
- Dr Max M Burger  
Basel, Switzerland
- Dr and Mrs Mario Burgos  
Mendoza, Argentina
- Rick and Nonnie Burnes  
Butler's Hole Fund  
Boston, Massachusetts
- Mr and Mrs Malcolm Campbell  
Upper Montclair, New Jersey  
Vineyard Haven, Massachusetts
- Dr Graciela C Candelas  
San Juan, Puerto Rico
- Mr and Mrs Frank C Carotenuto  
East Falmouth, Massachusetts
- Dr and Mrs Richard L Chappell  
New York, New York
- Frank and Julie Child  
Woods Hole, Massachusetts
- Dr Eloise E. Clark  
Bowling Green, Ohio
- Mr. and Mrs Hays Clark  
Hobe Sound, Florida
- Mr. and Mrs. James M. Clark  
Palm Beach, Florida
- Arnold and Connie Clark  
Woods Hole, Massachusetts
- Drs Alexander W Clowes and Susan E Detweiler  
Seattle, Washington
- Mrs George H A Clowes  
Dover, Massachusetts
- Dr Jewel Plummer Cobb  
Los Angeles, California
- Drs Arthur L. and Laura H Colwin  
Key Biscayne, Florida
- Dr and Mrs D Eugene Copeland  
Woods Hole, Massachusetts
- Molly N Cornell  
Falmouth, Massachusetts
- Dr William B Cosgrove  
Pittsboro, North Carolina
- Dr Joseph T. Coyle  
Belmont, Massachusetts
- Thomas and Geraldine Crane  
Weston, Massachusetts
- Dr and Mrs Stephen D Crocker  
Bethesda, Maryland
- Mrs Sally Cross  
Falmouth, Massachusetts
- Dr and Mrs. Anthony J Cutaia  
Ballwin, Missouri
- Mr and Mrs Bruce G Daniels  
Lincoln, Massachusetts
- Dr Eric H Davidson  
Pasadena, California
- Mr and Mrs David L Douglass  
Woodside, California
- Judith and John Dowling  
Boston, Massachusetts
- The Jane and Allan Dragone Foundation  
Vero Beach, Florida
- Mr and Mrs George Edmonds  
Osterville, Massachusetts
- Mr and Mrs Hans A. Ege  
Mahwah, New Jersey
- Drs. Herman N Eisen and Natalie Aronson  
Waban, Massachusetts
- Mrs Ariana Fairbanks  
Honolulu, Hawaii
- Dr A Verdi Farmanfarmaian  
Princeton, New Jersey
- Ms Linda Sallop and Mr. Michael Fenlon  
Newton, Massachusetts
- Mrs James J Ferguson Jr  
Chevy Chase, Maryland
- Mr and Mrs Harold E. Foreman, Jr.  
Northbrook, Illinois
- Drs Bruce and Barbara C. Furie  
Wellesley, Massachusetts
- Dr and Mrs David C Gadsby  
New York, New York
- Ms Sallie Giffen  
Falmouth, Massachusetts
- Rebeckah DuBois Glazebrook  
Osprey, Florida
- Dr and Mrs Murray Glusman  
Woods Hole, Massachusetts
- Suzanne and Maynard Goldman  
Boston, Massachusetts
- Drs Robert and Anne Goldman  
Chicago, Illinois
- Drs Timothy and Mary Helen Goldsmith  
Northford, Connecticut
- Dr and Mrs Moise H Goldstein, Jr  
Woods Hole, Massachusetts
- Susan and Tom Goux  
Teaticket, Massachusetts

Continued

- Dick and Eleanor Grace  
*The Brain Center*  
New Seabury, Massachusetts
- Philip Grant  
Washington, DC
- Dr Michael J. and Mrs. Rebecca H. Greenberg  
St. Augustine, Florida
- Dr Mary J. Greer  
New York, New York
- Mr. and Mrs. William H. Greer, Jr  
Chevy Chase, Maryland
- Dr. and Mrs. Thomas C. Gregg  
Falmouth, Massachusetts
- Paul R. and Mona Gross  
Jamaica Plain, Massachusetts
- Dr. and Mrs. Lawrence Grossman  
Baltimore, Maryland
- Dr. and Mrs. Harlyn O. Halvorson  
Woods Hole, Massachusetts
- Ms. Penelope Hare  
West Falmouth, Massachusetts
- Dr. and Mrs. Robert Haselkorn  
Chicago, Illinois
- Woody and Hanna Hastings  
Cambridge, Massachusetts
- Dr. Robert R. Haubrich  
Granville, Ohio
- Synnova Hayes  
Princeton, West Virginia
- Dr. Diane E. Heck  
Rumson, New Jersey
- Dr. and Mrs. Thomas Hedges, Jr  
Moorestown, New Jersey
- Doris and Howard Hiatt  
Cambridge, Massachusetts
- Mr. and Mrs. David Hibbitt  
Bristol, Rhode Island
- Dr. Llewellyn Hillis and Dr. Paul Colinvaux  
Woods Hole, Massachusetts
- Mr. Timothy T. Hilton  
Cambridge, Massachusetts
- Gregory J. and Pamela Clapp Hinkle  
Plymouth, Massachusetts
- Dr. Gertrude W. Hinsch  
Thonotosassa, Florida
- John and Olivann Hobbie  
Falmouth, Massachusetts
- Drs. Joseph F. Hoffman and Elena Citkowitz  
New Haven, Connecticut
- Dr. Francis C. G. Hoskin and  
Elizabeth M. Farnham  
Canton, Massachusetts
- Mrs. Carmela J. Huettner  
Woods Hole, Massachusetts
- Mr. and Mrs. Charles Hunter  
Kansas City, Missouri
- Dr. and Mrs. Hugh E. Huxley  
Concord, Massachusetts
- Dr. and Mrs. Shinya Inoué  
Falmouth, Massachusetts
- Mary D. Janney  
Washington, DC
- Diane and Robert Jaye  
Newton, Massachusetts
- Dr. William R. Jeffery  
Silver Spring, Maryland
- Ms. Barbara W. Jones  
Falmouth, Massachusetts
- Freda and Benjamin Kaminer  
Woods Hole, Massachusetts
- Drs. Darcy B. Kelley and Richard S. Bockman  
Sag Harbor, New York
- Anastasia and Tom Kelly  
River Vale, New Jersey
- Dr. and Mrs. Alexander Keynan  
Jerusalem, Israel
- Mr. and Mrs. A. Sidney Knowles, Jr  
Raleigh, North Carolina
- Sir Hans and Lady Kornberg  
Falmouth, Massachusetts
- Ms. Ellyn V. Korzun  
Chatham, New Jersey
- Dr. William J. Kuhns  
Toronto, Ontario
- Mr. and Mrs. Robert P. Lambrecht  
Boca Grande, Florida
- Mr. and Mrs. Rudy Landry  
Pocasset, Massachusetts
- Homer W. and Mary Cronan Lane  
North Falmouth, Massachusetts
- Mrs. Nancy Norman Lassalle  
New York, New York
- Dr. Hans Laufer  
Storrs, Connecticut
- Mr. Joel A. Leavitt  
Boston, Massachusetts
- Mrs. J. K. Lilly, III  
West Falmouth, Massachusetts
- Dr. and Mrs. Anthony Liuzzi  
Boston, Massachusetts
- Laszlo and Joyce Lorand  
Glencoe, Illinois
- Dr. and Mrs. Robert E. Mainer  
Wayland, Massachusetts
- Walter and Shirley Massey  
Atlanta, Georgia
- Mr. and Mrs. Robert Mastroianni  
Falmouth, Massachusetts
- Luigi Mastroianni, M.D. and  
Elaine Pierson-Mastroianni, M.D., Ph.D.  
Haverford, Pennsylvania
- Mr. Andrew Mattox and Ms. Sandee Parmelee  
Woods Hole, Massachusetts
- Dr. and Mrs. Robert T. McCluskey  
Brookline, Massachusetts
- Mr. and Mrs. Michael Meehan  
Williamstown, Massachusetts
- Dr. and Mrs. Jerry M. Melillo  
Falmouth, Massachusetts
- Mr. Richard P. Mellon  
Laughlintown, Pennsylvania
- Dr. and Mrs. Roger D. Milkman  
Falmouth, Massachusetts
- Mr. Gerrish H. Milliken  
New York, New York

Ralph and Muriel Mitchell  
Cambridge, Massachusetts

Dr and Mrs Merle Mizell  
New Orleans, Louisiana

Dr Leyla deToledo-Morrell  
Chicago, Illinois

Ms Marcia Morris  
Boston, Massachusetts

Professor and Mrs Toshio Narahashi  
Chicago, Illinois

Mr and Mrs Frank L. Nickerson  
Falmouth, Massachusetts



Andrew Hawkins

Ronald P. and Karen E. O'Hanley  
Ipswich, Massachusetts

David and Anastasia Palmer  
Waquoit, Massachusetts

Dr and Mrs George D. Pappas  
Chicago, Illinois

Drs Thoru and Judith Pederson  
Worcester, Massachusetts

Mr and Mrs Joseph Pellegrino  
Boston, Massachusetts

Mrs Nancy Pendleton  
Falmouth, Massachusetts

Bertha and Philip Person  
Flushing, New York

Mr and Mrs Frederick H. Pierce  
Amherst, New Hampshire

Mr and Mrs Robert W. Pierce, Jr  
Boston, Massachusetts

Tom and Patty Pollard  
Branford, Connecticut

Drs Frank and Billie Press  
Washington, DC

Mr and Mrs John S. Price  
Bryn Mawr, Pennsylvania

Charlotte and Irving W. Rabb  
Cambridge, Massachusetts

Lionel and Mildred Rebhun  
Charlottesville, Virginia

Mr and Mrs Peter W. Renaghan  
North Falmouth, Massachusetts

Mr and Mrs Richard Rhoads  
Boston, Massachusetts

Dr Monica Riley  
Falmouth, Massachusetts

Dr and Mrs Harris Ripps  
Chicago, Illinois

Dr and Mrs Jack Rosenbluth  
New Rochelle, New York

Allan and Clare Rosenfield  
Hartsdale, New York

Mr and Mrs Edward S. Rowland  
Hamilton, Massachusetts

Drs Joan and Gerald Ruderman  
Wellesley, Massachusetts

Mr Andrew Sabin  
East Hampton, New York

Dr and Mrs Edward D. Salmon  
Chapel Hill, North Carolina

Dr and Mrs Hidemi Sato  
Toba Mie, Japan

Dr and Mrs John W. Saunders, Jr  
Waquoit, Massachusetts

Mr Morton T. Saunders  
Gladwyne, Pennsylvania

Dr Cecily Cannan Selby  
New York, New York

Dr and Mrs Douglas R. Shanklin  
Memphis, Tennessee

Marilyn and David Sheprow  
Woods Hole, Massachusetts

Mrs Jacqueline N. Simpkins  
Barnstable, Massachusetts

Drs Dorothy M. Skinner and John S. Cook  
Falmouth, Massachusetts

Drs Melvin and Evelyn Spiegel  
Hanover, New Hampshire

Mrs Corinne Steel  
Little Neck, New York

Dr and Mrs Malcolm S. Steinberg  
Princeton, New Jersey

Mr and Mrs James M. Stewart  
Nantucket, Massachusetts

Carol and Joseph T. Stewart, Jr  
Skillman, New Jersey

Mr Richard H. Stowe  
New York, New York

Drs Alfred and Dorothy Stracher  
Roslyn, New York

Gerard and Mary Swope  
Washington, DC

John and Marjory Swope  
Concord, New Hampshire

Andrew G. and Ursula Szent-Gyorgyi  
Waltham, Massachusetts

Mr and Mrs Samuel Thorne  
Manchester, Massachusetts

Mr and Mrs Tom Tierney  
Wellesley, Massachusetts

Mr D. Thomas Trigg  
Westwood, Massachusetts

Elaine and Walter Troll  
New York, New York

Mr and Mrs Edward Tsoi  
Arlington, Massachusetts

Drs Walter Vincent and Dore Butler  
Woods Hole, Massachusetts

Dr and Mrs Byron H. Waksman  
New York, New York

Leonard and Eve Warren  
Bala Cynwyd, Pennsylvania

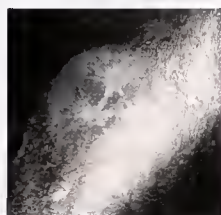
Mr and Mrs Henry Wheeler  
Boston, Massachusetts

Ms Rosalind C. Whitehead  
New York, New York

Mrs Annette L. Williamson  
Fort Worth, Texas

Dr Matthew Winkler  
Austin, Texas

## ANNUAL FUND 2002



*Gifts to the Annual Fund are unrestricted and used immediately where they will best benefit the current activities of the MBL research community.*

## Corporate and Foundation Donors

Aetna Inc  
 Amerigroup Foundation  
 Bay Foundation  
 George Botelho, Inc  
 The Commonwealth Fund  
 Cox Foundation, Inc.  
 ExxonMobil Foundation, Inc  
 Gilbane Building Company  
 The Gillette Company  
 Doreen Grace Fund  
 Harken Foundation  
 Johnson & Johnson  
 The Henry J. Kaiser Family Foundation  
 The Gruss Lipper Foundation  
 McDonald's Corporation  
 National Grid  
 Oracle Corporation  
 The David and Lucile Packard Foundation  
 Josephine Bay Paul and C. Michael Paul  
 Foundation  
 Ralph F. Peo Foundation, Inc  
 Saint-Gobain Corporation Foundation  
 The Schooner Foundation  
 Esther Simon Charitable Trust

The 1888 Club  
\$500 - \$999

Drs. Ted Begenisich and Sherrill Spires  
 Mr and Mrs. Robert O. Bigelow  
 Drs. Colleen Cavanaugh and Philip Gschwend  
 Mr. and Mrs. Gorham L. Cross  
 Drs. Robert and Ellen DeGroof  
 Dr. Philip Dunham and Ms. Gudrun Bjarnarson  
 Mrs. Ruth E. Fye  
 Dr. Joseph Gall and Ms. Diane Dwyer  
 Mr. and Mrs. Charles M. Ganson, Jr.  
 Mr. and Mrs. William Gilbane, Jr.  
 Mr. and Mrs. John G. McMillian  
 Mr. Andrew E. Norman  
 Mr. and Mrs. Jonathan O'Herron  
 Dr. Michael Rabinowitz and Ms. Diane Hoxmeier  
 Dr. Edward B. Rastetter  
 Dr. and Mrs. Frederick R. Rickles  
 Mr. Michael C. Ruettgers  
 Prof. and Mrs. Howard K. Schachman  
 Mr. and Mrs. Hans L. Schlesinger  
 Dr. and Mrs. William Trager  
 Mr. and Mrs. John J. Valois  
 Dr. Dyann and Mr. Peter Wirth

The Sponsors Club  
\$250 - \$499

Dr. and Mrs. Daniel L. Alkon  
 Drs. James and Helene Anderson  
 Mr. and Mrs. Michael Angelini  
 Dr. and Mrs. George P. Baker, Jr.  
 Dr. Andrew Bass and Ms. Margaret Marchaterre  
 Dr. Martha B. Baylor  
 Dr. Miriam F. Bennett  
 Mr. and Mrs. Thomas C. Bolton  
 Drs. Harry Conner and Carol Scott-Conner  
 Mr. John Cromie and Dr. Gloria Gallo-Cromie  
 Dr. and Mrs. Paul J. De Weer  
 Drs. Linda Deegan and Christopher Neill  
 Prof. and Mrs. Frederick A. Dodge  
 Mr. and Mrs. David Fausch  
 Dr. Rachel D. Fink  
 Dr. and Mrs. Harold Gainer  
 Mrs. Mary L. Goldman  
 Dr. Stephen L. Hajduk  
 Dr. and Mrs. John P. Harrington  
 Mr. William A. Haskins  
 Mr. and Mrs. Gary G. Hayward  
 Mrs. Elizabeth Heald  
 Dr. Yukio Hiramoto  
 Mr. and Mrs. Lon Hocker  
 Dr. and Mrs. Daniel Johnston  
 Dr. and Mrs. Morris John Karnovsky  
 Mr. and Mrs. Gilbert King  
 Dr. and Mrs. Edward A. Kravitz  
 Dr. and Mrs. Alan M. Kuzirian  
 Attorney and Mrs. William K. Mackey  
 Ms. Lynn Snyder Mackler  
 Drs. Richard and Hermine Makman  
 Dr. and Mrs. Julian B. Marsh  
 Ms. Jane A. McLaughlin  
 Dr. DeForest Mellon, Jr.  
 Drs. Timothy Mitchison and Christine Field  
 Dr. Peter A. Nickerson  
 Dr. and Mrs. Santo V. Nicosia  
 Mr. and Mrs. William J. Pechilis  
 Dr. Khela Ransier  
 Rev. Michael Robertson and  
 Dr. Emmy Robertson  
 Mr. and Mrs. Phillip S. Robertson  
 Mr. Kenneth Rosenthal  
 Dr. Cynthia V. Stauffacher  
 Dr. Dusan Stefanoski  
 Dr. Andreas C. Stemmer  
 Drs. Maurice and Raquel Sussman  
 Mr. and Mrs. Stephen E. Taylor  
 Drs. William and Mary Telfer  
 Mr. and Mrs. Richard Verney  
 Mr. and Mrs. Lynn H. Wilke  
 Mr. and Mrs. Leslie J. Wilson  
 Dr. Charles Yanofsky  
 Mr. John F. Zietlow, Jr.  
 Dr. Michael J. Zigmund  
 Mr. and Mrs. Hans Zimmer

The Century Club  
\$100 - \$249

Mr. Thomas H. Aal  
 Dr. and Mrs. Donald A. Abt  
 Dr. Nina Stromgren Allen  
 Mr. and Mrs. David S. Ament  
 Mr. and Mrs. Duncan P. Aspinwall  
 Mr. and Mrs. Richard Asthalter  
 Mrs. Kimball C. Atwood, III  
 Mr. Nathaniel Atwood and Ms. Susan Parkes  
 Mr. and Mrs. Donald R. Aukamp  
 Dr. and Mrs. David S. Babin  
 Mr. and Mrs. John M. Baitsell  
 Drs. Barbara-Anne Battelle and James Allgood  
 Dr. and Mrs. Thomas L. Benjamin  
 Mr. and Mrs. Maks Birnbach  
 Dr. and Mrs. Thomas P. Bleck  
 Dr. and Mrs. David A. Bodznick  
 George Botelho, Inc  
 Drs. Barbara and John Boyer  
 Mr. and Mrs. Peter Boyer  
 Mrs. Eleanor D. Bronson  
 Ms. Sarah Dixwell Brown  
 Mr. and Mrs. Darryl A. Buckingham  
 Bufftree Building Co., Inc  
 Drs. William and Madeline Burbanck  
 Mrs. Barbara Gates Burwell  
 Mr. and Mrs. William O. Burwell  
 Mr. and Mrs. Bruce E. Buxton  
 Mr. and Mrs. John L. Callahan, Jr.  
 Mr. and Mrs. David J. Campbell  
 Mr. and Mrs. D. Bret Carlson  
 Mr. Robert J. Carney  
 Father Joseph D. Cassidy, O.P., Ph.D.  
 Dr. and Mrs. Estill L. Caudill  
 Ms. Martha Chen  
 Mrs. Vera S. Clark  
 Dr. Mary Clutter  
 Dr. Carolyn Cohen  
 Dr. and Mrs. Maynard M. Cohen  
 Mr. and Mrs. Alexander Colby  
 Mr. and Mrs. Franz Collaredo-Mansfeld  
 Dr. LeBaron C. Colt, Jr.  
 Mr. and Mrs. Nathaniel S. Coolidge  
 Dr. and Mrs. Sherwin J. Cooperstein  
 Dr. and Mrs. John O. Corliss  
 Dr. Helen M. Costello  
 Mr. and Mrs. William G. Coughlin  
 Mr. Charles Crane and Ms. Wendy Breuer  
 Dr. Karen Crawford  
 Mr. and Mrs. Richard D. Cutler  
 Dr. and Mrs. Giuseppe D'Alessio  
 Dr. and Mrs. Nigel Daw  
 Dr. Martha Bridge Denckla  
 Dr. Wolf-Dietrich Dettbarn  
 Dr. William A. Dickson  
 Mr. and Mrs. David L. Donovan  
 Ms. Dorothy L. Drummy

## Annual Fund Volunteers

### Chairman

Dr. Peter B. Armstrong

### Associates Chairman

Mr. Michael Fenlon

### Volunteers

Dr. Robert B. Barlow, Jr.  
 Dr. A. Verdi Farmanfarmanian  
 Mr. Homer W. Lane, Jr.  
 Dr. Hans Laufer  
 Dr. Anthony Liuzzi  
 Dr. Luigi Mastroianni, Jr.  
 Dr. Merle Mizell  
 Dr. Thoru Pederson  
 Dr. Robert A. Prendergast  
 Dr. Cecily C. Selby  
 Dr. Byron H. Waksman



Elizabeth Armstrong

### Annual Fund, continued

Dr. and Mrs. Thomas K. Duncan  
 Mr. and Mrs. Hoyt Ecker  
 Dr. Frank Egloff  
 Drs. Paul Englund and Christine Schneyer  
 Dr. and Mrs. Herman T. Epstein  
 Mr. Gordon C. Estabrooks  
 Dr. and Mrs. Thomas Evans  
 Dr. Alan Ezekowitz and Ms. Debbie Lunder  
 Dr. Patricia M. Failla  
 Mr. and Mrs. Daniel D. Federman  
 Mr. and Mrs. Howard G. Freeman  
 Dr. Larry Jay Friedman  
 Dr. and Mrs. John J. Funkhouser  
 Dr. and Mrs. Robert M. Galatzer-Levy  
 Dr. and Mrs. Frank Gallagher  
 Miss Eleanor Garfield  
 Ms. Margaret A. Geist  
 Mr. and Mrs. Vincent Geoffroy  
 Dr. and Mrs. Martin Gibbs  
 Mrs. Janet F. Gillette  
 Drs. Alfred and Joan Goldberg  
 Dr. and Mrs. Herbert Graham  
 Dr. and Mrs. Philip Green  
 Mr. Noah Greenberg  
 Dr. Roger L. Greif  
 Dr. and Mrs. Newton H. Gresser  
 Dr. June Harrigan and Mr. Arnold Lum  
 Dr. Glenn W. Harrington  
 Dr. and Mrs. Neils Haugaard  
 Mr. and Mrs. Edmund Hazzard  
 Dr. and Mrs. Peter K. Hepler  
 Dr. and Mrs. Theodore T. Herskovits  
 Mr. and Mrs. William Hobart  
 Dr. Edward G. Horn  
 Dr. and Mrs. James C. Houk  
 Prof. Ruth Hubbard  
 Dr. and Mrs. W. Bruce Hunter  
 Dr. and Mrs. Kurt J. Isselbacher  
 Dr. Marietta Radovic Issidorides  
 Dr. Laurinda A. Jaffe  
 Mr. and Mrs. Ernest G. Jaworski  
 Mrs. Sally S. Joslin  
 Drs. Jane Kaltenbach and Robert Townsend  
 Mrs. Sally Karush  
 Mr. and Mrs. H. Ernst Keller  
 Mr. Louis M. Kerr  
 Mr. and Mrs. Arthur King

Dr. David Klein  
 Mr. Mark Koide  
 Dr. Kiyoshi Kusano  
 Drs. Eugene and Mitsuko Laforet  
 Ms. Judith E. Laster  
 Mr. William Lawrence and Mrs. Barbara Buchanan  
 Dr. and Mrs. John J. Lee  
 Ms. Alice C. Leech  
 Dr. Manan E. LeFevre  
 Dr. David P. Lenzi  
 Dr. and Mrs. Aaron B. Lerner  
 Dr. and Mrs. Jack Levin  
 Dr. and Mrs. Richard B. Levine  
 Mr. and Mrs. David W. Lillie  
 Dr. and Mrs. Daniel M. Lilly  
 Dr. and Mrs. Richard W. Linck  
 Dr. Raymond J. Lipicky  
 Dr. Stephen J. Lipson  
 Dr. and Mrs. John E. Lisman  
 Dr. Robert B. Lofffield  
 Dr. and Mrs. Irving M. London  
 Dr. Louise M. Luckenbill  
 Dr. Richard Lum  
 Mr. Gerald Lynch  
 Drs. Richard and Sylvia Manalis  
 Mr. and Mrs. Ronald Marcks  
 Dr. Andrew C. Marinucci  
 Mr. and Mrs. Lowell V. Martin  
 Dr. and Mrs. William M. McDermott  
 Mr. Paul McGonigle  
 Dr. and Mrs. David McGrath  
 Mr. and Mrs. James McSherry  
 Dr. Martin Mendelson  
 Dr. Melanie and Mr. Klein Merriman  
 Dr. Nancy S. Milburn  
 Dr. and Mrs. Ricardo Miledi  
 Drs. David and Virginia Miller  
 Mr. and Mrs. Robert W. Morey, Jr.  
 Mr. and Mrs. Samuel Murphy  
 Dr. and Mrs. X. J. Musacchia  
 Dr. and Mrs. John E. Naugle  
 Messrs. William and David Newton

Mr. and Mrs. Brian Nickerson  
 Mr. and Mrs. Michael O'Rand  
 Dr. and Mrs. Rudolf Oldenbourg  
 Dr. Janice and Mr. Albert Olszowka  
 Mr. James G. Ottos  
 Dr. and Mrs. Ray D. Owen  
 Mr. Malcolm A. Park  
 Ms. Marina H. Park  
 Dr. and Mrs. Roderic B. Park  
 Dr. and Mrs. John B. Pearce  
 Mr. and Mrs. David Pearson  
 Dr. and Mrs. Courtland D. Perkins  
 Dr. Bruce J. Peterson  
 Drs. David and Jeanette Pleasure  
 Dr. Jeanne S. Poindexter  
 Dr. and Mrs. Harvey B. Pollard  
 Drs. Mary Porter and Tom Hays  
 Dr. Dale Purves and Ms. Shannon Ravenel  
 Mr. and Mrs. George Putnam, III  
 Ms. Katherine E. Putnam  
 Dr. and Mrs. James P. Quigley  
 Dr. and Mrs. Robert F. Rakowski  
 Dr. Carol Reinisch and Mr. Robert Sutor  
 Dr. Judith Rhodes  
 Drs. Paul Ringel and Michele Lorand  
 Mr. and Mrs. John Ripple  
 Dr. Hope Ritter  
 Mr. Dana Rodin  
 Dr. and Mrs. Lawrence C. Rome  
 Dr. Joel L. Rosenbaum  
 Drs. William Ross and Nechama Lasser-Ross  
 Dr. Uldis Roze  
 Dr. William Devine Russell-Hunter  
 Mrs. Anne W. Sawyer  
 Mrs. Lilian M. Scherper  
 Dr. Herbert Schuel  
 Dr. and Mrs. Robert Seidler  
 Ms. Barbara Park Shapiro  
 Mr. and Mrs. John J. Sheridan  
 Drs. Roy Silverstein and Jacquelyn Joseph-Silverstein  
 Dr. Maxine F. Singer

Continued ..

Mr. and Mrs. Alain Singer  
 Mrs. Cynthia C. Smith  
 Dr. and Mrs. Paul F. Smith  
 Drs. Roxanna and Ronald S. Slowitz  
 Mr. David Space and Mrs. Judith Jarvis  
 Dr. and Mrs. Alan B. Steinhilber  
 Dr. and Mrs. William K. Stephenson  
 Mr. and Mrs. Thomas Stewart  
 Dr. Elijah Steiner and Ms. Jasmin Bihler  
 Drs. Albert Stunkard and Margaret Maurin  
 Dr. and Mrs. Mutsuyuki Sugimori  
 Mr. and Mrs. E. Kent Swift, Jr.  
 Dr. Margaret W. Taft  
 Drs. Bruce Telzer and Leah T. Haimo  
 Mr. and Mrs. W. Nicholas Thorndike  
 John F. Towle, DDS  
 Mr. and Mrs. William Traver  
 Dr. and Mrs. David M. Travis  
 Dr. and Mrs. Steven N. Treistman  
 Miss Ruth Tucker  
 Dr. and Mrs. Kenyon S. Tweedell  
 Mr. and Mrs. Volker Ulbrich  
 Dr. and Mrs. Ivan Valiela  
 Drs. Claude and Dorothy Villee  
 Mr. and Mrs. Samuel Vincent  
 Dr. Talbot H. Waterman  
 Dr. Annemarie Weber  
 Dr. and Mrs. George Weiffenbach  
 Dr. Gary Wessel  
 Mrs. Rose T. Wheeler  
 Dr. and Mrs. Martin Keister White  
 Dr. and Mrs. Roland L. Wigley  
 Drs. Jonathan and Beatrice Wittenberg  
 Drs. Joshua Zimmerberg and Teresa Jones

## Other

Mr. and Mrs. David C. Ahearn  
 Mr. and Mrs. Scott M. Allard  
 Mr. and Mrs. John J. Aziz  
 Dr. and Mrs. Richard H. Backus  
 Mr. and Mrs. Joe Barrington  
 Ms. Jane Berger and Mr. Roger Gittines  
 Ms. Pauline F. Blanchard  
 Ms. Casey Bliss  
 Mr. and Mrs. Anthony Briana  
 Mrs. Jennie P. Brown  
 Mr. and Mrs. Thomas A. Brown  
 Dr. Roberto Bruzzone  
 Mr. and Mrs. Arnold H. Burroughs  
 Mr. and Mrs. E. Brewster Buxton  
 Mr. and Mrs. George Cadwalader  
 Mr. Arthur D. Calfee  
 Dr. Peter Clark and Ms. Ellen Barol  
 Mr. and Mrs. James M. Cleary  
 Mrs. Elizabeth Ann Cohen  
 Mr. and Mrs. Peter Connolly  
 Mr. and Mrs. J. Sterling Crandall  
 Mrs. Marcia Donovan  
 Dr. Patricia L. Dudley  
 Dr. Quan-Yang Duh and Ms. Ann Comer  
 Mrs. Frances E. Eastman  
 Dr. Hugh Young Elder  
 Mrs. Helen M. Erickson  
 Dr. Alan Scott Fanning  
 Mrs. Ruth Alice Fitz  
 Mr. John H. Ford

Mr. and Mrs. Alvin Fossner  
 Dr. Krystyna Frenkel  
 Drs. Patricia Garrett and Oliver Woshinsky  
 Dr. Stephen E. Gellis  
 Mr. and Mrs. James E. Gifford  
 Mrs. Barbara B. Glade  
 Dr. Joel S. Gordon  
 Dr. Martin Gorovsky  
 Mrs. Erika A. Green  
 Dr. Nancy Carole Greep  
 Mr. and Mrs. Joseph Guttenplan  
 Mr. and Mrs. Peter A. Hall  
 Mr. and Mrs. Robert Hall  
 Drs. Clifford and Drusilla Harding  
 Dr. and Mrs. Richard Bennet Harvey  
 Dr. Audrey E. V. Haschemeyer  
 Ms. Elizabeth E. Hathaway  
 Mr. John Hay  
 Dr. Teru Hayashi  
 Dr. David S. Hays  
 Mrs. Jane M. Heald  
 Dr. Simone Helluy  
 Drs. Richard and Susan Hill  
 Dr. and Mrs. Robert B. Hill  
 Mr. and Mrs. Gerald J. Holtz  
 Dr. Linda A. Hufnagel-Zackroff  
 Mr. and Mrs. Felix Inigo  
 Mr. and Mrs. Charles A. Johnson  
 Dr. and Mrs. James E. Johnson  
 Dr. Harry S. Kahn  
 Dr. Edna S. Kaneshiro  
 Mr. and Mrs. Robert K. Karpus  
 Prof. Mark D. Kirk  
 Dr. Peter Kivy and Ms. Joan Pearlman  
 Mr. and Mrs. Paul W. Knaplund  
 Mrs. Phyllis Kuffler  
 Mr. and Mrs. Ted Kulesza  
 Mr. and Mrs. Ray La Ranger  
 Mr. and Mrs. Alan K. Lauria  
 Ms. Corinne Le Bovit  
 Dr. and Mrs. Stephen B. Leighton  
 Mr. and Mrs. Edwin M. Libbin  
 Dr. and Mrs. John H. Lochhead  
 Mr. and Mrs. Edward Loessel  
 Dr. Irene Loewenfeld  
 Dr. and Mrs. Frank J. Longo  
 Ms. Lena T. Lord  
 Mr. Fred E. Lux  
 Mrs. Priscilla M. Makay  
 Dr. Robert P. Malchow  
 Dr. Dawn Morin Manck  
 Mr. and Mrs. Joseph S. Maranchie  
 Dr. and Mrs. Joe L. Martinez, Jr.  
 Mr. and Mrs. Frank J. Mather, III  
 Dr. Rita W. Mathews  
 Mrs. Dorothea J. Mautner  
 Mrs. Polly Miles  
 Dr. and Mrs. Daniel G. Miller  
 Cdr. and Mrs. Lloyd C. Morris USN (RET.)  
 Mr. and Mrs. Dana S. Morse  
 Mr. Thomas A. Mulholland

RADM Paul J. Mulloy USN (Ret)  
 Ms. Iris Nelson  
 Ms. Kathryn Paine  
 Mr. and Mrs. Nicholas Pantazis  
 Mr. David Parker, Jr.  
 Dr. and Mrs. Charles Parmenter  
 Dr. Leonard M. Passano  
 Ms. Joan Pearlman and Dr. Peter Kivy  
 Ms. Joyce S. Pendery  
 Dr. and Mrs. Murray E. Pendleton  
 Dr. and Mrs. Ronald J. Pfohl  
 Mr. and Mrs. Harold Pilskaln  
 Mr. and Mrs. Kenneth Poehls  
 Dr. and Mrs. Richard A. Polin  
 Dr. and Mrs. Daniel A. Pollen  
 Mr. and Mrs. Abraham I. Pressman  
 Mr. and Mrs. Gerald B. Reynolds  
 Dr. Robert V. Rice  
 Dr. Morris Rockstein  
 Mr. and Mrs. Peter J. Romano  
 Mr. Dorothy C. Ryder  
 Mr. and Mrs. Herbert Shanker  
 Dr. and Mrs. Gaius R. Shaver  
 Ms. Kathleen Lake Shaw  
 Mr. Richard W. Shriner  
 Dr. Jeffrey D. Silberman  
 Mrs. Louise M. Specht  
 Rev. and Mrs. William A. Spurrier, III  
 Mrs. Eleanor Steinbach  
 Dr. Raymond G. Stross  
 Mrs. Belle K. Taylor  
 Dr. Leana and Mr. Joby Topper  
 Prof. and Mrs. Michael Tytell  
 Mrs. Alice H. van Buren  
 Mr. James Ware and Ms. Sharon McCarthy  
 Mr. Michael S. Weinstein  
 Dr. and Mrs. Charles R. Wytenbach  
 Mrs. Marilyn J. Young  
 Mr. and Mrs. Kenneth H. Zimble  
 Mrs. Margery P. Zinn  
 Dr. and Mrs. Steven J. Zottoli

## ALUMNI FUND 2002

*Gifts to the Alumni Fund are used to meet the basic needs of MBL courses, including tuition support for students.*

Anonymous  
 Dr. Joan Abbott  
 Prof. and Mrs. Laurence F. Abbott  
 Dr. William Agnew  
 Drs. Dianne and Thomas Allen  
 Dr. C. Ronald Anderson  
 Dr. William DeWitt Andrus, Jr.  
 Drs. Robert and Lynne Angerer  
 Dr. Carolina V. Arancibia  
 Drs. Carol Arnosti and Andreas Teste  
 Dr. Michael S. Ascher  
  
 Dr. and Mrs. Robert Barker, Jr.  
 Dr. Edward Joseph Behrman  
 Dr. William H. Bergstrom  
 Dr. Gerald Bergtrom  
 Dr. Ari Berkowitz  
 Dr. Emmanuel C. Besa  
 Mr. Edward M. Blumenthal  
 Dr. Mark Boothby  
 Dr. Richard T. Born  
 Dr. Elayne Bornslaeger-Bednar and  
 Mr. Michael Bednar  
 Dr. Emil Borysko  
 Dr. Peter Brodfuehrer  
 Dr. and Mrs. Donald D. Brown  
 Dr. Harley P. Brown  
 Dr. Richard R. Burgess  
  
 Mr. and Mrs. Patrick J. Calie  
 Dr. David Campbell  
 Dr. James R. Campi  
 T. Joiner Cartwright, Jr., Ph.D.  
 Dr. Clarissa M. Cheney  
 Dr. Jonathan Chernoff  
 Dr. Chi-Bin Chien  
 Dr. Carson C. Chow  
 Dr. Ka Hou Chu  
 Dr. Carl Cyrus Clark  
 Dr. William T. Clusin  
 Dr. and Mrs. R. John Collier  
 Dr. and Mrs. Marc D. Coltrera  
 Dr. Clark E. Corliss  
 Dr. Jeffrey T. Corwin  
 Mr. John Cromie and Dr. Gloria Gallo-Cromie  
 Dr. Alice M. Curry  
  
 Dr. Stephen C. Dahl  
 Dr. and Mrs. Harry W. Dickerson  
 Dr. William J. Dickinson  
 Dr. Bruce A. Diner  
 Mr. Jonathan S. and Dr. Thelma Dixon  
 Mr. and Mrs. Richard Drucker  
 Dr. Catherine Asleson Dundon  
 Dr. Kathleen Dunlap  
 Dr. and Mrs. David Durica

Ms. Joan Edstrom  
 Ms. Marcia Edwards  
 Dr. Marilynn E. Etzler  
 Dr. and Mrs. Arnold G. Eversole  
  
 Prof. Donald Faber  
 Dr. and Mrs. Richard R. Fay  
 Dr. Marta Feldmesser  
 Dr. Cyril V. Finnegan, Jr.  
 Dr. Thomas R. Flanagan  
 Dr. Karl W. Flessa  
 Ms. Christine M. Foreman  
 Dr. Elizabeth Fowler and Dr. James Parmentier  
 Dr. Kenneth I. Freedman  
 Drs. Hugo and Anita Freudenthal  
 Dr. Marvin J. Fritzler  
 Dr. Anne E. Fry  
  
 Dr. Theresa Gaasterland  
 Dr. Paul E. Gallant  
 Dr. Helen W. Gjessing  
 Prof. James A. Glazier  
 Dr. Joel S. Gordon  
 Dr. Joan Eiger Gottlieb  
 Dr. Esther M. Goudsmit  
 Dr. and Mrs. Eugene Grebner  
 Dr. Lewis J. Greene  
 Dr. Warren M. Grill  
 Dr. Jerome Gross

Dr. Marnie E. Halpern  
 Dr. Lisa M. Halvorson  
 Dr. Cadet Hammond Hand, Jr.  
 Dr. Susan M. Harding  
 Dr. Robert D. Harvey  
 Dr. Norman B. Hecht  
 Dr. Joseph Heitman  
 Drs. Joseph and Barbara Hichar  
 Dr. Raymond W. Holton  
 Dr. and Mrs. Seymour Holtzman  
 Mr. Timothy E. Holy  
 Dr. Xudong Huang  
 Drs. Deborah Hursh and Mark Mortin  
 Dr. Jerard Hurwitz

Dr. Richard Intres  
 Dr. Allen Isaacson  
 Dr. and Mrs. Stephen K. Itaya

Dr. Jon W. Jacklet  
 Dr. Nancy A. Johnson  
 Dr. Leslie and Mr. James Jolly

## ALUMNI RELATIONS ADVISORY BOARD

Dr. Robert B. Barlow, Jr. (Physiology, 1963)  
*SUNY Upstate Medical University*

Dr. Thomas L. Benjamin (Physiology, 1959/  
 Neurophysiology, 1966), *Harvard Medical School*

Dr. Richard T. Born (Neural Systems & Behavior, 1987)  
*Harvard Medical School*

Dr. Stephen C. Cannon (Neurobiology, 1988)  
*University of Texas Southwestern Medical Center*

Dr. Eloise E. Clark (Physiology, 1956)  
*Bowling Green State University*

Dr. Jeffrey T. Corwin (Neurobiology, 1975)  
*University of Virginia, School of Medicine*

Dr. Joseph T. Coyle (Neurobiology, 2001)  
*Harvard Medical School*

Dr. Joseph R. Fetcho (Neural Systems & Behavior,  
 1984), *State University of New York*

Dr. Elizabeth Fowler (Physiology, 1966)  
*Millennium Pharmaceuticals*

Dr. Leah T. Haimo (Physiology, 1974),  
*University of California, Riverside*

Dr. Marnie E. Halpern (Neurobiology, 1986)  
*Carnegie Institution of Washington*

Dr. Alexander Keynan (Physiology, 1961)  
*Israel Academy of Sciences and Humanities*

Dr. Daniel P. Kiehart (Physiology, 1975)  
*Duke University Medical Center*

Dr. George M. Langford (Physiology, 1972),  
*Dartmouth College*

Dr. William M. McDermott (Invertebrate Zoology,  
 1950), *U.S. Navy (retired)*

Dr. Melanie Pratt Merriman (Embryology, 1975/  
 Physiology, 1976), *Touchstone Consulting*

Dr. Thomas D. Pollard (Physiology, Director 1989-  
 1993), *Yale University*

Dr. Joshua R. Sanes (Neurobiology, 1971)  
*Washington University Medical Center*

Dr. Wise Young (Neurobiology, 1972)  
*Rutgers University*

### Ex-Officio

Dr. Peter B. Armstrong (Invertebrate Zoology, 1961)  
 Chairman, MBL Annual/Alumni Fund  
*University of California, Davis*

Dr. John E. Dowling (Neurobiology, 1970)  
 President, MBL Corporation  
*Harvard University*

Continued...



Students get  
dockside instruction  
from Marine  
Resources  
Center staff,  
Elizabeth Armstrong

Dr. and Mrs. James W. Kalat  
Dr. Marianna M. Kane  
Dr. Alvin M. Kaye  
Dr. Gordon I. Kaye  
Drs. Thomas and Laura Keller  
Dr. and Mrs. R. Emmett Kenney  
Dr. Richard G. Kessel  
Dr. Lynda A. Kiefer  
Dr. Elizabeth L. Kimberly  
Dr. Donald W. King  
Dr. Leonard B. Kirschner  
Dr. and Mrs. Paul M. Knopf  
Dr. Robert E. Knowlton  
Dr. Carol A. Koenigsberger  
Dr. Wieslaw J. Kozek  
Dr. Ajit Kumar

Dr. Michael J. Landzberg  
Dr. Holly A. Lavoie  
Dr. Matthew K. Lee  
Dr. William J. Lehman  
Dr. Ellen K. LeMosy  
Dr. Ethan Lerner  
Drs. Brian Link and Vivian Lee  
Ms. Anne M. Linton  
Drs. Joan and James Lisak  
Mr. and Mrs. Edward K. Lobenhofer  
Dr. and Mrs. Robert J. Loeffler  
Dr. Ann M. Lohof  
Dr. Jane Lubchenco

Dr. Stephen E. Malawista  
Dr. David E. Mann, Jr.  
Dr. and Mrs. Phillip B. Maples  
Dr. Junko Munakata Marr  
Dr. Michael Massarani  
Dr. Jon M. McCormick  
Dr. Duane P. McPherson  
Dr. Anne Messer  
Dr. Laurie Miller  
Dr. Maria I. Morasso  
Dr. Yasuhiro Morita  
Mr. Stephen H. Munroe

Dr. David P. Nagle, Jr.  
Drs. Angus Nairn and Marina Picciotto  
Dr. Lee Niswander

Dr. Dana T. Nojima  
Mrs. Phyllis Norris  
Drs. Victor and Ruth Nussenzweig

Dr. Michael D. Oberdorfer  
Dr. Catherine L. Olsen  
Dr. Ingrith Deyrup Olsen  
Prof. John M. Olson  
Dr. and Mrs. Brett A. Oxberry

Mrs. Mary G. Pacifici  
Drs. Kimberly Paul and Charles Thomas  
Mr. Matthew Person and Ms. Jill Erickson  
Dr. Norman J. Pieniazek  
Dr. Louis Pierro  
Dr. Carl B. Pilcher  
Dr. and Mrs. Anthony Pires  
Dr. Sabrina and Mr. Bradford Powell

Dr. Esther L. Racoosin  
Dr. Jennifer L. Raymond  
Dr. Jean and Mr. Ronald Regal  
Dr. and Mrs. Robert Alan Resnik  
Dr. Kristin Lester Revill  
Dr. Randall W. Reyer  
Ms. Marian C. Rice  
Dr. Austen F. Riggs  
Dr. Regina M. Robbins  
Drs. Duncan and Grace Saunders Rollason  
Brian K. Romias, MD, MS  
Dr. James T. Russell  
Ms. Carol Ann Ryder

Dr. David R. Samols  
Dr. Noriyuki Satoh  
Dr. Richard L. Saunders  
Dr. Charles H. Sawyer  
Dr. Rolf Schauder  
Dr. Paul R. Schloerb  
Dr. James H. Schwartz  
Dr. Carla Shatz  
Dr. and Mrs. Alan Sher  
Dr. David R. Sherwood  
Dr. Joyce M. Simpson  
Dr. Max Snodderly  
Dr. Sandra C. Souza  
Mr. Nelson Spruston

Dr. Joel P. Stafstrom  
Dr. Gary R. Strichartz  
Dr. David T. Sullivan  
Dr. Frank J. Swartz  
Ms. Hyla C. Sweet  
Dr. Ben G. Szaro

Ms. Penny A. Tavormina  
Mrs. Vera A. Taylor  
Dr. Saul Teichberg  
Dr. Wesley J. Thompson  
Dr. Barbara Holland Toomey

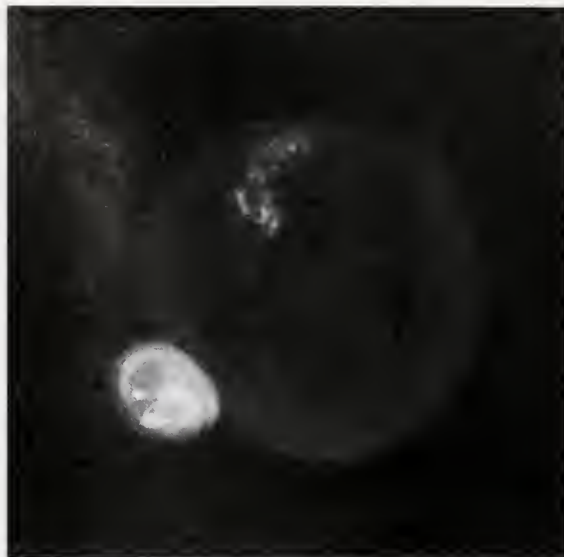
Dr. Jeanine A. Ursitti

Dr. Raghunath Virkar  
Ms. Melissa A. Vollrath  
Dr. Susan Volman

Dr. William G. Wadsworth  
Dr. Brant G. Wang  
Dr. Deborah Williams Ward  
Drs. Gary E. Ward and Zail Berry  
Mr. and Mrs. Herman Ward  
Dr. and Mrs. Samuel Ward  
Dr. Susanna H. Weerth  
Ms. Kay E. Wellik  
Dr. Harold Bancroft White  
Dr. Clayton Wiley  
Dr. Ulrike Wille  
Dr. Katherine Wilson  
Dr. Andrea G. Witlin  
Dr. Anne M. Wood  
Drs. Lawrence Wysocki and Judith Spiegel

Dr. Ayako Yamaguchi  
Dr. Naoyuki Yamamoto  
Ms. Judith L. Yanowitz  
Dr. Karen P. York  
Dr. Lin Yue

Dr. and Mrs. Cheng Zhu  
Dr. Richard E. Zigmund



## FELLOWSHIPS AND SCHOLARSHIPS

Endowed and expendable funds for scholarships and fellowships are an integral part of the MBL's successful research and education programs. In 2002, twenty-two scientists from the U.S. and abroad were awarded fellowship grants that allowed them to work in our uniquely collaborative research environment. The Laboratory also awarded scholarships to 97 highly qualified students, enabling them to participate in our total-immersion courses.

We gratefully acknowledge the donors listed below, who provided \$245,270 for research fellowships and \$726,558 for scholarships in 2002.

- |   |   |
|---|---|
| American Society of Cell Biology<br>Summer Research Awards<br>American Society of Cell Biology                          | Aline D. Gross Scholarship Fund<br>Dr. and Mrs Paul R Gross<br>Dr. and Mrs Benjamin Kaminer<br>Dr and Mrs Lewis P Rowland<br>Technic, Inc                               |
| Robert Day Allen Fellowship Fund<br>Drs. Joseph and Jean Sanger   | E. E. Just Endowed Research Fellowship Fund<br>The Cole Memorial Family Fund<br>William Townsend Porter Foundation<br>Georgia-Pacific Corporation                       |
| MBL Associates Endowed Scholarship Fund<br>MBL Associates<br>Mrs. Nawrie Meigs-Brown                                    | Fred Karush Endowed Library Readership<br>Dr and Mrs Laszlo Lorand<br>Dr and Mrs. Arthur M. Silverstein   |
| Frederik B. Bang Fellowship Fund<br>Dr. and Mrs Jack Levin  | H. Keffer Hartline Fellowship Fund<br>Dr Peter Hartline<br>Mr and Mrs Frederick F. Hartline<br>Dr and Mrs Thomas R. Hedges, Jr<br>Ms Rebecca Kucera<br>Dr. Earl Weidner |
| Charles R. Crane Fellowship Fund<br>Friendship Fund   | Kuffler Fellowship Fund<br>Dr and Mrs Edward A. Kravitz   |
| John O. Crane Fellowship Fund<br>Friendship Fund  | Frank R. Lillie Fellowship and Scholarship<br>Estate of Emily Ann Cramer  |
| Jean and Katsuma Dan Fellowship Fund<br>Mr. William A. Haskins<br>Mrs. Eleanor Steinbach<br>Drs. Joseph and Jean Sanger | Mountain Memorial Fund<br>Dr and Mrs Dean C. Allard, Jr<br>Ms Brenda J. Bodian<br>Mr and Mrs Amos L. Roberts<br>Mr and Mrs Thomas H. Roberts                            |
| Bernard Davis Fellowship Fund<br>Mrs Elizabeth M. Davis   |   |
| Daniel S. and Edith T. Grosch Scholarship Fund<br>Ms. Laura Grosch and Mr. Herb Jackson                                 |   |



- | James A. and Faith Miller Fellowship Fund  
Drs David and Virginia Miller
- | Frank Morrell Endowed Memorial Scholarship  
Dr Leyla de Toledo Morrell
- | Emily Hartshorne Mudd Scholarship Fund  
World Academy of Art and Science
- | Neural Systems and Behavior Scholarship Fund  
Dr and Mrs Alan Gelperin  
Dr. Warren M. Grill  
Drs William Kristan and Kathleen French  
Dr and Mrs Richard B. Levine  
Dr Mark W. Miller  
Drs. Janis C. Weeks and William M. Roberts  
Drs. Harold Zakon and M. Lynne McAnelly  
Ms M. Jade Zee
- | Nikon Fellowship  
Nikon Instruments Inc
- | The Plum Foundation John E. Dowling  
Fellowship Fund  
The Plum Foundation
- | William Townsend Porter Scholarship Fund  
for Minority Students  
William Townsend Porter Foundation
- | Florence C. Rose and S. Meryl Rose Endowed  
Scholarship Fund  
Dr. Gwynn Akin Bowers  
Dr. and Mrs. D. Eugene Copeland  
Mrs. Edna B. Hill  
Ms. Kaaren Janssen  
Dr. and Mrs. Benjamin Kaminer  
W. K. Kellogg Foundation  
Dr. Hans Laufer  
Dr. and Mrs. Anthony Liuzzi  
Dr. and Mrs. Roger D. Milkman  
Mrs. Eleanor M. Nace  
Drs. Keen A. and Nancy S. Rafferty  
Mrs. Florence C. Rose  
Dr. and Mrs. John W. Saunders, Jr.  
Dr. and Mrs. J. P. Trinkaus
- | The Catherine Filene Shouse SES Scholarship Fund  
The Catherine Filene Shouse Foundation
- | The Catherine Filene Shouse Scholarship Fund  
The Catherine Filene Shouse Foundation
- | The Catherine Filene Shouse Fellowship Fund  
The Catherine Filene Shouse Foundation
- | The Gruss Lipper Fund  
The Gruss Lipper Foundation
- | The Bill and Phoebe Speck Fund  
Dr William T. Speck
- | The Evelyn and Melvin Spiegel Fellowship Fund  
Dr. and Mrs. Jack Levin  
The Sprague Foundation  
Drs. Joseph and Jean Sanger
- | H. B. Steinbach Fellowship Fund  
Mrs. Eleanor Steinbach
- | Horace W. Stunkard Scholarship Fund  
Drs. Albert Stunkard and Margaret Maurin
- | Eva Szent-Györgyi Scholarship Fund  
Dr. and Mrs. Benjamin Kaminer  
Dr. and Mrs. Laszlo Lorand  
Drs. Joseph and Jean Sanger  
Dr. Andrew and Ms. Ursula Szent-Györgyi
- | Universal Imaging Fellowship Fund  
Universal Imaging Corporation
- | Walter L. Wilson Endowed Scholarship  
Dr. Paul N. Chervin  
Dr. Jean R. Wilson
- | Young Scholars/Fellows Program  
Drs. James and Helene Anderson  
Drs. Harry Conner and Carol Scott-Conner  
Dr. and Mrs. James L. German  
Dr. and Mrs. Anthony Liuzzi  
Drs. Luigi and Elaine Mastroianni  
Drs. David and Miriam Mauzerall  
Drs. Matthew and Jeanne Meselson  
Drs. Dorothy Skinner and John Cook  
Dr. and Mrs. Edward A. Spiegel  
Dr. Annemarie Weber  
Drs. Jonathan and Beatrice Wittenberg  
Mr. and Mrs. Kenneth H. Zimble

Mouse cell invasion pores  
and membrane, mouse  
blastosist, Umit Ali Kayish

## MEMORIAL AND TRIBUTE GIFTS

*The following donors have chosen to support the Marine Biological Laboratory as a special way to remember or honor a relative or friend.*



### Bequests

Estate of Emily Ann Cramer

Estate of Madelene E. Pierce

| In Honor of Drs. Clay and Clara Armstrong  
Ms Lynn Snyder Mackler

| In Memory of Dr. Kimball C. Atwood, III  
Mrs Eleanor Steinbach

| In Memory of Dr. Frank A. Brown, Jr.  
Mrs Jennie P. Brown

| In Memory of Dr. Francis D. Carlson  
Mrs. Carolyn S. Carlson

| In Honor of Mr. Richard D. Cutler  
Gilbane Building Company

| In Memory of Eugene Floyd DuBois  
Mrs James R. Glazebrook

| In Memory of Dr. and Mrs. James D. Ebert  
Dr and Mrs Charles R Wyttenbach

| In Memory of Morris Goldman  
Dr and Mrs Harris Ripps

| In Memory of Elizabeth K. Hartline  
Dr. and Mrs. Thomas R Hedges, Jr

| In Memory of John Helfrich  
Drs. Colleen Cavanaugh and Philip Gschwend  
Drs Bruce and Teresa Corliss  
Harken Foundation  
Ms. Keri Holland  
Dr Max Holmes  
Drs Knute Nadelhoffer and Barbara Billings  
Ms. Andrea Ricca  
Dr. and Mrs Gaius R Shaver  
Mr. Jeffrey Shelkey and Ms Joanne Willey  
Ms Jane Tucker  
Dr. and Mrs. Lawrence J Wangh  
Dr Xiangming Xiao

| In Memory of Mr. Robert Huettner  
Mrs Carmela J Huettner  
Mr and Mrs Richard A Huettner  
Ms Catherine N Norton

| In Memory of Dr. Arthur G. Humes  
Dr Patricia L Dudley

| In Honor of Macy Lawrence  
Dr and Mrs. Gerald Weissmann

| In Memory of Dr. Frank Morrell  
Dr Thomas P. Bleck

| In Honor of Cooper Neely  
Mr and Mrs Joe Barrington

| In Memory of Dr. Lionel I. Rebhun  
Drs Robert and Anne Goldman

| In Memory of Elizabeth Russell (Tibby)  
Dr and Mrs Ray D. Owen

| In Honor of Marjorie Salmon  
Drs. David Forkosh and Linda Hirshman

| In Honor of Mr. Arthur D. Traub  
Ms Natalie Miller

| In Memory of Dr. George E. Wheeler  
Dr. Khela Ransier  
Mrs Rose T Wheeler

| In Memory of Dr. Charles G. Wilber  
Mrs Clare M. Wilber

| In Honor of Alfred and Joyce Zeien  
Mr Michael C. Ruettgers

## OTHER GIFTS AND PROGRAMS

*The quality and success of the MBL educational program is maintained through the loan of research equipment, reagents, and computers by:*



Elizabeth Armstrong

### Equipment Lenders

### Matching Gifts

Aetna Inc  
BP Foundation, Inc  
The Commonwealth Fund  
ExxonMobil Foundation, Inc  
Johnson & Johnson  
The Henry J. Kaiser Family  
Foundation  
W. K. Kellogg Foundation  
McDonald's Corporation  
National Grid  
Oracle Corporation  
The David & Lucile Packard  
Foundation  
Saint-Gobain Corporation  
Foundation

Accelrys Inc  
Adams & List Associates  
Agilent Technologies, Inc.  
Amersham Pharmacia Biotech Inc  
A. M. P.I.  
Apogent Discoveries/ Robbins  
Scientific  
Applied Precision, Inc  
Aquatic Eco-Systems, Inc.  
Aquatic Habitats  
Arcturus Engineering, Inc  
Atto Bioscience  
AutoQua,™  
Imaging, Inc  
Axon Instruments, Inc

Barnstead/ThermoLyne  
Beckman Coulter Instruments, Inc  
Becton Dickinson IS  
Biocare Medical  
BD Biosciences  
Biophotonics International  
Bioptechs  
Bio-Rad Confocal  
Bio-Rad Laboratories  
Brinkmann Instruments  
Brownlee Precision Co  
Burleigh Instruments, Inc

Cairn Research LTD  
Cambridge Electronic Design  
Cambridge Research  
Instrumentation, Inc  
CBS Scientific Company, Inc  
Chroma Technology Corporation  
Coherent Inc  
COMPAC Computer Corporation  
Compix Inc., Imaging Systems  
Crest Technologies  
CyBio, Inc

Dagan Corporation  
Dako Corporation  
David Kopf Instruments  
Del Imaging Systems, LLC  
Diagnostic Instruments, Inc  
DNA Star, Inc.  
DVC Co. Inc.

Eastman Kodak  
Edinburgh Biocomputing Systems  
Eppendorf Scientific Inc.

FHC  
Fine Science Tools  
Fisher Scientific/Zylux Corp  
Fluke Corporation

General Valve Corporation  
Genetronics, Inc / BTX Instrument  
Division Genomic Solutions  
GlaxoSmithKline  
Grass Instrument Company/  
Astro-Med, Inc. GrassTelefactor

Hamamatsu Photonic Systems  
Harvard Apparatus, Inc

Improvison Inc  
Instrutech Corporation  
Intelligent Imaging Innovations, Inc  
Invitrogen

Jackson ImmunoResearch  
Laboratories, Inc

Kepeco Power Co  
Kinetic Systems, Inc  
Kipp & Zonen/Division of SCI-TEC  
Instruments, Inc

Lab Line  
Laser Science  
Leica Confocal  
Leica Microsystems Inc.  
Ludl Electronic Products, Ltd  
Ludlum Measurements, Inc

MatTek Corporation  
McCrone Microscopes  
Micro Video Instruments, Inc  
Microway  
Miltenyi Biotec, Inc  
MJ Research  
Molecular Dynamics  
Molecular Probes  
MWG Biotech

Nanodrop Technologies  
Narishige USA, Inc  
National Instruments  
Nikon Confocal  
Nikon, Inc

Olympus Confocal  
Olympus Corporation  
Omega Optical, Inc  
Ophthalmic Instrument Co  
Optiquip  
Optronics

PCB Assembly  
Peak Performance Technologies, Inc  
Perkin Elmer Applied Biosystems  
Perkin Elmer Life Sciences  
Photon Technology International  
Photonic Instruments  
Platform Computing Inc  
Promega Corporation

Quantitative Imaging Corporation

Research Precision Instruments, Co  
Roche Applied Science  
Roper Scientific

San Diego Instruments  
Santa Cruz Biotechnology  
Scanalytics  
Scion Corporation  
SD Instruments  
Sigma  
Sinauer Associates, Inc  
Soma Scientific Instruments  
SONY Medical Systems  
Stoelting  
Sutter Instrument Company  
Synaptosoft, Inc

Technical Manufacturing  
Corporation  
The Company of Biologists, Ltd  
ThermoElectron  
ThermoEC  
ThermoNeslab  
ThermoSavant  
ThermoShandon  
ThermoSpectronics

Universal Imaging Corporation

Vashaw Scientific  
Vibratome  
Vincent Associates

WWR  
Warner Instrument Corporation  
World Precision Instruments

Carl Zeiss, Inc  
Carl Zeiss Confocal  
Carl Zeiss Imaging

# governance & administration

---



## BOARD OF TRUSTEES

*Chairman of the Board of Trustees*  
Sheldon J. Segal, The Population Council

*Vice Chair of the Board of Trustees*  
George W. Logan, Pine Street Partners

*President of the Corporation*  
John E. Dowling, Harvard University

*Director and Chief Executive Officer*  
William T. Speck, Marine Biological Laboratory\*

*Treasurer of the Corporation*  
Mary B. Conrad, Fiduciary Trust International\*

*Clerk of the Corporation,*  
Thomas S. Crane, Mintz, Levin, Cohn, Ferris, Glovsky & Popeo, PC\*

*Chair of the Science Council*  
Robert E. Palazzo, Rensselaer Polytechnic Institute\*

### Class of 2003

Darcy Brisbane Kelley, Columbia University  
Laurie J. Landeau, Marinetics, Inc  
Burton J. Lee, III, Vero Beach, FL  
Ronald P. O'Hanley, Mellon Institutional Asset Mgt  
Jean Pierce, Boca Grande, FL  
Vincent J. Ryan, Schooner Capital LLC

### Class of 2004

M. Howard Jacobson, Bankers Trust  
George M. Langford, Dartmouth College  
G. William Miller, G. William Miller & Co., Inc  
Frank Press, The Washington Advisory Group  
Christopher M. Weld, Sullivan and Worcester, Boston  
Torsten N. Wiesel, The Rockefeller University

### Class of 2005

Porter W. Anderson, Key Largo, FL  
Claire M. Fraser, The Institute for Genomic Research  
George W. Logan, Salem, VA  
Robert Prendergast, Falmouth, MA  
John W. Rowe, Aetna U.S. Healthcare

### Class of 2006

Margaret C. Bowles, Woods Hole, MA  
Martha W. Cox, Hobe Sound, FL  
Walter E. Massey, Morehouse College  
Marcia C. Morris, Boston, MA  
Gerald Weissmann, New York University School of Medicine

### Ex Officio Trustees

William T. Speck, Director and Chief Executive Officer  
Robert E. Palazzo, Chair of the Science Council  
Mary B. Conrad, Fiduciary Trust International

### Executive Committee of the Board of Trustees

Margaret C. Bowles  
Mary B. Conrad\*  
George W. Logan  
Marcia Morris  
Ronald P. O'Hanley  
Robert E. Palazzo\*  
Sheldon J. Segal  
William T. Speck\*  
Christopher M. Weld

### Honorary Trustees

William T. Golden, New York, NY  
Robert E. Mainer, Wayland, MA

### Trustees Emeriti

Edward A. Adelberg, Yale University, New Haven, CT  
John B. Buck, Sykesville, MD  
Seymour S. Cohen, Woods Hole, MA  
Arthur L. Colwin, Key Biscayne, FL  
Laura Hunter Colwin, Key Biscayne, FL  
Donald Eugene Copeland, Woods Hole, MA  
Sears Crowell, Jr., Indiana University, Bloomington, IN  
Teru Hayashi, Woods Hole, MA  
Ruth Hubbard, Cambridge, MA  
C. Ladd Prosser, University of Illinois, Urbana, IL  
W. D. Russell-Hunter, Syracuse University, Syracuse, NY  
John W. Saunders, Waquoit, MA  
David Sheprow, Boston, MA  
D. Thomas Trigg Wellesley, MA  
Walter S. Vincent, Woods Hole, MA

### Directors Emeriti

Paul Gross, Falmouth, MA  
Harlyn O. Halvorson, Woods Hole, MA

---

\*Ex officio  
As of April 1, 2002

## STANDING COMMITTEES

### Development Committee

Christopher Weld, Chair  
Porter W. Anderson  
Peter Armstrong  
Robert Barlow  
Mardi Bowles  
Martha Cox  
John Dowling  
Claire Fraser  
M. Howard Jacobson  
Burton Lee  
G. William Miller  
Jean Pierce  
Robert Prendergast  
John W. Rowe  
Torsten Wiesel

### Facilities & Capital Equipment Committee

Mardi Bowles, Chair  
Porter Anderson  
George Langford  
Walter Massey  
Andrew McArthur  
Frank Press  
Christopher Weld

### Nominating Committee

John W. Rowe, Chair  
Martha Cox  
\*John E. Dowling, President of  
the Corporation  
Claire Fraser  
\*Robert Palazzo, Science Council  
Chair  
Jean Pierce  
Vincent J. Ryan  
\*William T. Speck, Director & CEO  
Gerry Weissmann

### Finance Committee

Ronald P. O'Hanley, Chair  
Mary B. Conrad  
Thomas S. Crane  
Maynard Goldman  
M. Howard Jacobson  
Darcy Kelley  
Laurie Landeau  
George W. Logan  
Robert Prendergast

### Investment Committee

Mary B. Conrad, Chair  
Thomas S. Crane  
George W. Logan  
G. William Miller  
Marcia Morris  
Ronald O'Hanley  
Vincent J. Ryan

## STRATEGIC PLANNING COMMITTEES

### Steering Committee

Fred Bay  
Kerry Bloom  
Mardi Bowles  
Ron Calabrese  
John Dowling, Co-Chair  
M. Howard Jacobson  
John Lakian  
George Langford  
George Logan  
Jerry Melillo  
Robert Palazzo  
Tom Pollard  
Joan Ruderman  
Vin Ryan  
Sheldon Segal  
Mitchell Sogin  
William T. Speck, Co-Chair  
Gerald Weissmann  
Al Zeien

### Phase II Task Forces

ENSURING DISTINCTIVENESS  
AND COLLABORATION IN  
RESIDENT RESEARCH  
Co-Chairs: John Dowling and  
George Logan  
Barbara Ehrlich  
Claire Fraser  
Rick Goetz  
Bob Goldman  
Nancy Hopkins  
Matthew Meselson  
Marcia Morris  
Dick Mullen  
Cathy Norton  
Ron O'Hanley  
Thoru Pederson  
Bruce Peterson  
Peter Smith  
Jennifer Wernegreen

### ENSURING CONTINUED EXCELLENCE IN EDUCATION

Co-Chairs: Kerry Bloom and  
Howard Jacobson  
Jelle Atema  
Bob Barlow  
Mary Beckwith  
Ron Calabrese  
Lenny Dawidowicz  
Susan Goux  
Lenny Guarante  
John Hobbie  
Laurinda Jaffe  
Bill Miller  
Kip Sluder  
Steve Zottoli

ATTRACTING THE NEXT  
GENERATION OF VISITING  
SCIENTISTS  
Co-Chairs: Joan Ruderman and  
Vin Ryan  
Clay Armstrong  
Barbara Furie  
Roger Hanlon  
Pam Clapp Hinkle  
Marc Kirschner  
Andy Mattox  
Jerry Melillo  
Orian Shirihai  
Mitch Sogin  
Gerry Weissmann

### Phase III Task Forces

AFFILIATION  
Co-Chairs: Gerry Weissmann  
and Al Zeien  
Dick Chappell  
Linda Deegan  
Claire Fraser  
Rick Goetz  
Harlyn Halvorson  
John Hobbie  
Marcia Morris  
Tom Pollard  
Frank Press  
Peter Smith  
Diana Blazis  
Dick Mullen  
Cathy Norton, staff chair

### GOVERNANCE/ADMINISTRATIVE STRUCTURE

Co-Chairs: Robert Palazzo and  
George Logan  
Tom Crane  
John Dowling  
Barbara Ehrlich  
Leah Haimo  
M. Howard Jacobson  
Jerry Melillo  
Shelly Segal  
Steve Zottoli  
Pamela Clapp Hinkle  
Susan Goux, staff chair  
Kate Shaw

### FACILITIES/HOUSING/SUPPORT SERVICES

Co-Chairs: George Langford and  
John Lakian  
Mardi Bowles  
Carole Browne  
Bob Goldman  
Steve Hajduk  
Roger Hanlon  
Andrew McArthur  
Joan Ruderman  
Orian Shirihai  
Harold Zakon  
Mary Beckwith  
Rich Cutler, staff chair  
Louis Kerr  
Bill Mebane  
Eleanor Uhlinger  
Rudi Rottenfusser

### FINANCE/FUNDING OPTIONS

Co-Chairs: Mitchell Sogin and  
Vin Ryan  
Peter Armstrong  
George Augustine  
David Burgess  
Bibi Conrad  
Barbara Furie  
Bob Mainer  
Ed Rastetter  
Jack Rowe  
Tony Cave  
Wendy Faxon  
Homer Lane, staff chair  
David McLean  
Becky Mountford

### SCIENCE COUNCIL 2002-2003

Palazzo, Robert E., Chair

Armstrong, Clay M.  
Armstrong, Peter  
Atema, Jelle  
De Weer, Paul  
Fraser, Scott  
Hadjuk, Steven  
Haimo, Leah  
Hopkinson, Charles  
Smith, Peter J.S.  
Sogin, Mitchell  
Weeks, Janis C.  
Dawidowicz, E.A.\*  
Speck, William T.\*

## CORPORATION

## | Life Members

- Dr Edward A. Adelberg, New Haven, CT  
 Dr Bjorn Afzelus, Stockholm University  
 Dr Ernest Amatniek, (address unknown)  
 Dr. John M. Arnold, Falmouth, MA
- Mrs Betsy G. Bang, Woods Hole, MA  
 Dr Alan W. Bernheimer, New York University  
 Medical Center  
 Dr Lloyd M. Bertholf, Bloomington, IL  
 Dr Herman F. Bosch, Falmouth, MA  
 Dr F. J. Brinley, Jr., National Institutes of Health  
 Dr John B. Buck, Sykesville, MD  
 Dr Madeline P. Burbanck, Atlanta, GA  
 Dr William D. Burbanck, Atlanta, GA
- Dr Alfred B. Chaet, Maitland, FL  
 Dr Arnold M. Clark, Woods Hole, MA  
 Mr James M. Clark, Palm Beach, FL  
 Dr Maynard M. Cohen, Rush Medical College  
 Dr Seymour S. Cohen, Woods Hole, MA  
 Dr Jack R. Collier, Effie, LA  
 Dr Marjorie McCann Collier, Effie, LA  
 Dr Arthur L. Colwin, Key Biscayne, FL  
 Dr Laura Hunter Colwin, Key Biscayne, FL  
 Dr Sherwin J. Cooperstein, University of  
 Connecticut  
 Dr D. Eugene Copeland, Woods Hole, MA  
 Dr John O. Corliss, Bala Cynwyd, PA  
 Dr Helen M. Costello, Chapel Hill, NC  
 Dr Helen Crouse, Hayesville, NC
- Dr Nigel W. Daw, Branford, CT  
 Dr Robert L. DeHaan, Emory University School  
 of Medicine  
 Dr Patricia L. Dudley, Seattle, WA
- Dr Charles Edwards, Longboat Key, FL  
 Dr. Gerald F. Elliott, The Open University  
 Research Unit
- Dr. Patricia M. Failla, Johns Island, SC  
 Dr. Donald T. Frazier, University of Kentucky  
 Medical Center
- Dr. Mordecai L. Gabriel, Brooklyn College  
 Dr. Murray Glusman, New York State  
 Psychiatric Institute  
 Dr. Herbert Graham, Woods Hole, MA
- Dr. Howard L. Hamilton, University of Virginia  
 Dr Clifford V. Harding, Jr., Falmouth, MA  
 Dr Audrey E. V. Haschemeyer, Woods Hole, MA  
 Dr Teru Hayashi, Woods Hole, MA  
 Dr Frederick L. Hisaw, McMinnville, OR  
 Dr Francis C. G. Hoskin, Canton, MA  
 Prof. Ruth Hubbard, Harvard University  
 Dr W. Bruce Hunter, Peterborough, NH  
 Dr Charles Hurwitz, Stratton VA Medical Center
- Dr George Katz, Sarasota, FL  
 Dr John M. Kingsbury, Cornell University  
 Dr Kiyoshi Kusano, National Institutes of Health
- Mr Ezra Laderman, Yale University  
 Dr Paul H. LaMarche, Eastern Maine Medical  
 Center  
 Dr Max A. Lauffer, Penn State University  
 Medical Center
- Dr Herbert Levitan, National Science Foundation  
 Dr John H. Lochhead, London, England  
 Dr Birgit Rose Loewenstein, Falmouth, MA  
 Dr Frank A. Loewus, Washington State University  
 Dr Robert B. Lofffield, University of New Mexico  
 Dr Laszlo Lorand, Northwestern University  
 Medical School
- Dr Robert E. Mainer, The Boston Company, Inc  
 Dr Julian B. Marsh, Chestnut Hill, MA  
 Mr Lowell V. Martin, Woods Hole, MA  
 Dr Rita W. Mathews, Southfield, MA  
 Dr. Janis Metzuzals, Ontario, Canada  
 Dr. John A. Moore, University of California  
 (deceased 2002)  
 Dr. John W. Moore, Duke University Medical  
 Center  
 Dr Aron A. Moscona, New York, NY  
 Dr X. J. Musacchia, Bella Vista, AR  
 Dr. Maimon Nasatir, Ojai, CA
- Dr Leonard M. Passano, University of Wisconsin  
 Dr. William T. W. Potts, University of Lancaster  
 Dr. Carl A. Price, Falmouth, MA  
 Dr Margaret McDonald Prytz (address unknown)
- Dr Charles E. Renn (address unknown)  
 Dr. George T. Reynolds, Princeton University  
 Dr. Robert V. Rice, Falmouth, MA  
 Dr. Morris Rockstein, Coral Gables, FL  
 Dr Raphael R. Ronkin, Washington, DC  
 Dr John D. Roslansky, Woods Hole, MA  
 (deceased 2003)  
 Dr Priscilla F. Roslansky, Associates of  
 Cape Cod, Inc.  
 Dr Jay S. Roth, Woods Hole, MA
- Dr Hidemi Sato, Nagoya University  
 Dr R. Walter Schlesinger, North Falmouth, MA  
 Dr Allan C. Scott, Colby College  
 Dr Arthur M. Silverstein, Johns Hopkins  
 University  
 Dr Raymond A. Sjodin, Baltimore, MD  
 Dr Paul F. Smith, Woods Hole, MA  
 Mr John W. Speer, Portsmouth, RI  
 Dr Nicholas Sperelakis, University of Cincinnati  
 Dr Evelyn Spiegel, Dartmouth College  
 Dr Melvin Spiegel, Dartmouth College  
 Dr Grover C. Stephens, University of California  
 Mrs Jane Lazarow Stetten, Chevy Chase, MD  
 Dr Bernard L. Strehler, Laguna Niguel, CA  
 Dr Maurice Sussman, Falmouth, MA  
 Dr Raquel B. Sussman, Manne Biological  
 Laboratory  
 Mrs Gwen P. Szent-Gyorgyi, Woods Hole, MA
- Mr W. Nicholas Thorndike, Wellington  
 Management Company  
 Dr William Trager, The Rockefeller University  
 Dr. J. P. Trinkaus, Yale University (deceased 2003)
- Dr Claude A. Villee, Jr., Harvard Medical School  
 Dr Walter S. Vincent, Woods Hole, MA
- Dr Talbot H. Waterman, Yale University  
 Dr Roland L. Wigley, Woods Hole, MA  
 Dr Lon A. Wilkens, University of Missouri  
 Dr Paul Witkovsky, NYU Medical Center

## Members

- Dr Donald A. Abt, University of Pennsylvania School of Veterinary Medicine
- Dr James A. Adams, Tallahassee, FL
- Dr William J. Auejman, Jr., Falmouth, MA
- Dr Daniel L. Alkon, Rockefeller Neuroscience Institute
- Dr Garland E. Allen, Washington University
- Dr Nina Stromgren Allen, North Carolina State University
- Dr Mark C. Allegro, Louisiana State University Medical Center
- Dr Everett Anderson, Harvard Medical School
- Dr John M. Anderson, Ithaca, NY
- Dr Porter W. Anderson, Jr., Key Largo, FL
- Dr Christine Armet-Kibel, University of Massachusetts, Boston
- Prof Clay M. Armstrong, University of Pennsylvania School of Medicine
- Mrs Ellen Prosser Armstrong, Woods Hole, MA
- Dr Peter B. Armstrong, University of California
- Mr Robert W. Ashton, Bay Foundation
- Dr Jelle Atema, Boston University Marine Program
- Dr Baccio Baccetti, University of Sienna, Italy
- Dr Robert G. Baker, New York University Medical Center
- Dr David Baltimore, California Institute of Technology
- Dr Robert B. Barlow, Jr., SUNY Upstate Medical University
- Dr Daniel T. Barry, South Hadley, MA
- Dr Susan R. Barry, Mount Holyoke College
- Dr Andrew H. Bass, Cornell University
- Dr Barbara-Anne Battelle, University of Florida
- Mr Frederick Bay, Bay Foundation
- Dr Elaine L. Bearer, Brown University
- Dr John M. Beatty, University of Minnesota
- Dr Luis Alberto Beauge, Instituto de Investigacion Medica, Argentina
- Dr Ted Begenisich, University of Rochester
- Dr David A. Begg, University of Alberta, Canada
- Dr Eugene Bell, TEI Biosciences Inc.
- Dr Thomas L. Benjamin, Harvard Medical School
- Dr Michael V. L. Bennett, Albert Einstein College of Medicine
- Dr Miriam F. Bennett, Colby College
- Dr R. Suzanne Bennett, Albert Einstein College of Medicine
- Dr Suzanne T. Berlin, York, ME
- Mr Norman Bernstein, Columbia Realty Venture
- Dr Francisco Bezanilla, Health Science Center
- Dr John D. Biggers, Harvard Medical School
- Dr Stephen H. Bishop, Ames, IA
- Dr Dieter Blennemann, Riverside, CT
- Dr George S. Bloom, University of Texas Southwestern Medical Center
- Dr Kerry S. Bloom, University of North Carolina
- Dr David A. Bodznick, Wesleyan University
- Dr Edward G. Boettger, Rochester, VT
- Dr Richard A. Boolootian, Sherman Oaks, CA
- Dr Thomas A. Borgese, Lehman College, CUNY
- Dr David W. Borst, Jr., Illinois State University
- Dr Francis P. Bowles, Marine Biological Laboratory
- Dr Barbara C. Boyer, Union College
- Dr Bruce P. Brandhorst, Simon Fraser University
- Dr Marianne Bronner-Fraser, California Institute of Technology
- Dr Stephen C. Brown, SUNY at Albany
- Mr William L. Brown, Weston, MA
- Dr Carole L. Browne, Wake Forest University School of Medicine
- Dr Robert A. Browne, Wake Forest University
- Dr Anne C. Bucklin, University of New Hampshire
- Dr Max M. Burger, Novartis International AG
- Dr David R. Burgess, Boston College
- Dr Mario H. Burgos, IHEM Medical School
- Dr John E. Burris, Beloit College
- Dr Harold L. Burstyn, Syracuse University
- Dr Sherry Bursztajn, Dartmouth Medical School
- Dr Ronald L. Calabrese, Emory University
- Dr R. Andrew Cameron, California Institute of Technology
- Mr Richard H. Campbell, Bang-Campbell Associates
- Dr Graciela C. Candelas, University of Puerto Rico
- Dr Lucio Cariello, Stazione Zoologica "A. Dohrn," Italy
- Dr Catherine Emily Carr, University of Maryland
- Prof James F. Case, University of California
- Father Joseph D. Cassidy, O.P., Ph.D., Providence College
- Dr Colleen M. Cavanaugh, Harvard University
- Dr Edward L. Chambers, University of Miami School of Medicine
- Dr Donald C. Chang, Hong Kong University of Science and Technology
- Dr Richard L. Chappell, Hunter College
- Dr Frank M. Child, Woods Hole, MA
- Dr Rex Leslie Chisholm, Northwestern University
- Dr Elena Citkowitz, Hospital of St. Raphael
- Dr David E. Clapham, Children's Hospital
- Dr Eloise E. Clark, Bowling Green State University
- Mr Hays Clark, Hobe Sound, FL
- Prof Wallis H. Clark, Jr., Madison, ME
- Dr John R. Clay, National Institutes of Health
- Dr Alexander W. Clowes, University of Washington
- Dr Jewel Plummer Cobb, California State University
- Dr Carolyn Cohen, Brandeis University
- Dr Lawrence B. Cohen, Yale University School of Medicine
- Dr William D. Cohen, Hunter College
- Dr Annette W. Coleman, Brown University
- Dr Paul Colinaux, Marine Biological Laboratory
- Dr R. John Collier, Harvard Medical School
- Dr James P. Collins, Arizona State University
- Dr D. Wesley Corson, Jr., Storm Eye Institute
- Dr Jeffrey T. Corwin, University of Virginia, School of Medicine
- Dr Ernest F. Couch, Texas Christian University
- Dr Rachel Llanelly Cox, Marine Biological Laboratory
- Thomas S. Crane, Esq., Mintz, Levin, Cohn, Ferris, Glovsky & Popeo, P.C.
- Dr Karen Crawford, St. Mary's College of Maryland
- Dr Gertrud Cremer-Bartels, Muenster, Germany
- Dr Terry J. Crow, University of Texas Medical School
- Mr Robert J. Crowther, Shriners Hospitals for Children
- Dr Michael P. Cummings, Marine Biological Laboratory
- Mr Richard D. Cutler, Marine Biological Laboratory
- Dr Eric H. Davidson, California Institute of Technology
- Dr Daniel B. Davison, Bristol-Myers Squibb PRI
- Dr Eliezar A. Dawidowicz, Marine Biological Laboratory
- Dr Paul J. De Weer, University of Pennsylvania
- Dr Linda A. Deegan, Marine Biological Laboratory
- Dr Robert C. DeGroof, Doylestown, PA
- Dr Martha Bridge Denckla, Johns Hopkins University
- Dr Henry A. DePhillips, Jr., Trinity College
- Dr Douglas W. DeSimone, University of Virginia
- Dr Wolf-Dietrich Dettbarn, Nashville, TN
- Dr Vincent E. Dionne, Boston University Marine Program
- Dr John E. Dowling, Harvard University
- Dr Arthur Brooks DuBois, John B. Pierce Foundation Laboratory
- Dr Thomas K. Duncan, Nichols College
- Dr Philip B. Dunham, Syracuse University
- Dr Paul V. Dunlap, University of Michigan
- Dr William R. Eckberg, Howard University
- Dr Kenneth T. Edds, Bayer Diagnostics
- Dr Howard A. Eder, Albert Einstein College of Medicine
- Ms. Joan Edstrom, Falmouth, MA
- Dr Barbara E. Ehrlich, Yale University
- Dr Arthur Z. Eisen, Washington University
- Dr Herman N. Eisen, Massachusetts Institute of Technology
- Dr Hugh Young Elder, University of Glasgow, Scotland
- Dr Paul T. Englund, Johns Hopkins Medical School
- Dr David Epel, Stanford University
- Dr Herman T. Epstein, Woods Hole, MA
- Mr Ray L. Epstein, Taunton, MA
- Prof Donald Faber, Albert Einstein College of Medicine
- Dr David H. Farb, Boston University School of Medicine
- Dr A. Verdi Farmanfarman, Rutgers University
- Dr Barry William Festoff, VA Medical Center
- Dr Rachel D. Fink, Mount Holyoke College
- Dr Alan Finkelstein, Albert Einstein College of Medicine
- Dr Gerald D. Fischbach, Columbia University
- Dr Harvey M. Fishman, University of Texas Medical Branch
- Mr Dennis Flanagan, New York, NY

- Dr Richard Allen Fluck, Franklin and Marshall College  
 Dr Kenneth H. Foreman, Marine Biological Laboratory  
 Dr. Thomas O. Fox, Harvard Medical School  
 Dr. Clara Franzini-Armstrong, University of Pennsylvania  
 Dr Scott Fraser, California Institute of Technology  
 Dr. Kathleen A. French, University of California, San Diego  
 Dr. Robert J. French, University of Calgary  
 Dr Chandler M. Fulton, Brandeis University  
 Dr Barbara C. Furie, Beth Israel Deaconess Medical Center  
 Dr Bruce Furue, Beth Israel Deaconess Medical Center  
 Dr Edwin J. Furshpan, Harvard Medical School  
 Dr Robert P. Futrelle, Northeastern University
- Dr. Howaida Gabr, Suez Canal University  
 Dr David C. Gadsby, The Rockefeller University  
 Dr Harold Gainer, National Institutes of Health  
 Dr. Robert M. Galatzer-Levy, Chicago, IL  
 Dr Joseph G. Gall, Carnegie Institution  
 Dr Michael A. Gallo, UMDNJ-Robert Wood Johnson Medical School  
 Dr. Alan Gelperin, Monell Chemical Senses Center  
 Dr James L. German, III, Weill Medical College of Cornell University  
 Dr Martin Gibbs, Brandeis University  
 Dr Anne E. Giblin, Marine Biological Laboratory  
 Dr A. Jane Gibson, Enta, NH  
 Dr Prosser Gifford, Library of Congress  
 Prof. Giovanni Giudice, Università di Palermo, Italy  
 Dr. Antonio Giuditta, Università di Napoli "Federico II," Italy  
 Dr Paul Glynn, Brunswick, ME  
 Mr William T. Golden, Chairman Emeritus, American Museum of Natural History  
 Dr. Robert D. Goldman, Northwestern University Medical School  
 Dr. Paul K. Goldsmith, National Institutes of Health  
 Dr Timothy H. Goldsmith, Yale University  
 Dr Moise H. Goldstein, Jr., The Johns Hopkins University  
 Dr. Robert Michael Gould, NYS Institute of Basic Research  
 Mr Dick Grace, Doreen Grace Fund  
 Dr Werner M. Graf, College of France, France  
 Dr Philip Grant, National Institutes of Health  
 Dr Judith P. Grassle, Rutgers University  
 Dr. Katherine G. Graubard, University of Washington  
 Dr E. Peter Greenberg, University of Iowa  
 Dr Michael J. Greenberg, University of Florida  
 Dr Mary J. Greer, New York, NY  
 Dr Donald R. Griffin, Harvard University  
 Dr Albert Grossman, New York University Medical Center  
 Prof. Lawrence Grossman, The Johns Hopkins University  
 Dr Yosef Gruenbaum, The Hebrew University of Jerusalem  
 Dr. John A. Gruner, Cephalon, Inc
- Mr A. Robert Gunning, Falmouth, MA  
 Dr G. Francis Gwilliam, Reed College
- Prof. Leah T. Haimo, University of California  
 Dr Stephen L. Hajduk, Marine Biological Laboratory  
 Dr Linda M. Hall, Functional Insect Genomics Institute  
 Dr. Tatsuji Haneji, The University of Tokushima, Japan  
 Dr Roger T. Hanlon, Marine Biological Laboratory  
 Dr. Ferenc Harosi, New College of the University of South Florida  
 June F. Harrigan, Ph.D., Honolulu, HI  
 Dr. John P. Harrington, SUNY - New Paltz  
 Dr Stephen C. Harrison, Harvard University  
 Dr Robert Haselkorn, University of Chicago  
 Dr J. Woodland Hastings, Harvard University  
 Dr. Raymond L. Hayes, Jr., Howard University  
 Dr Diane E. Heck, Rutgers University  
 Dr. Jonathan Joseph Henry, University of Illinois  
 Dr. Peter K. Hepler, University of Massachusetts  
 Dr Walter R. Herndon, University of Tennessee  
 Prof. Avram Hershko, Technion-Israel Institute of Technology, Israel  
 Dr Theodore T. Herskovits, Fordham University  
 Dr Howard H. Hiatt, Brigham and Women's Hospital  
 Dr Stephen M. Highstein, Washington University School of Medicine  
 Dr John G. Hildebrand, University of Arizona  
 Dr Richard W. Hill, Michigan State University  
 Dr. Robert B. Hill, University of Rhode Island  
 Dr Susan D. Hill, Michigan State University  
 Dr Llewellyn W. Hillis, Marine Biological Laboratory  
 Dr Edward H. Hinchcliffe, University of Massachusetts Medical School  
 Dr Michael Hines, Yale University School of Medicine  
 Dr Gregory J. Hinkle, Millennium Pharmaceuticals  
 Dr Gertrude W. Hirsch, University of South Florida  
 Dr. Jan Hirsch, Leica, Inc  
 Dr John E. Hobbie, Marine Biological Laboratory  
 Dr Alan J. Hodge, San Diego, CA (deceased 2002)  
 Dr Joseph F. Hoffman, Yale University School of Medicine  
 Dr George G. Holz, IV, New York University Medical Center  
 Dr Charles S. Hopkinson, Jr., Marine Biological Laboratory  
 Dr James C. Houk, Northwestern University Medical School  
 Dr Ronald R. Hoy, Cornell University  
 Dr Alice S. Huang, California Institute of Technology  
 Dr Linda A. Hufnagel-Zackroff, University of Rhode Island  
 Dr William D. Hummon, Ohio University  
 Dr. Susie H. Humphreys, Food and Drug Administration  
 Dr. Tom Humphreys, University of Hawaii  
 Dr Tim Hunt, ICRF Clare Hall Labs, England
- Dr Robert D. Hunter, Oakland University  
 Dr Hugh E. Huxley, Brandeis University
- Dr Joseph Ilan, Case Western Reserve University  
 Dr Nicholas A. Ingoglia, New Jersey Medical School  
 Dr Sadyki Inoue, McGill University, Canada  
 Dr Shinya Inoué, Marine Biological Laboratory  
 Dr Kurt J. Isselbacher, Massachusetts General Hospital Cancer Center  
 Dr. Marietta Radovic Issidorides, Theodor Theohari Cozzika Foundation  
 Dr Colin S. Izzard, SUNY - Albany
- Dr Laurinda A. Jaffe, University of Connecticut Health Center  
 Dr Lionel Jaffe, Marine Biological Laboratory  
 Dr William R. Jeffery, University of Maryland  
 Dr. Diana E. J. Jennings, Marine Biological Laboratory  
 Dr Daniel Johnston, Baylor College of Medicine  
 Dr Teresa L. Z. Jones, National Institutes of Health  
 Dr Robert K. Josephson, University of California  
 Dr Leonard K. Kaczmarek, Yale University School of Medicine  
 Dr Gabor Kaley, New York Medical College  
 Dr. Jane C. Kaltenbach, Mount Holyoke College  
 Dr Benjamin Kaminer, Boston University Medical School  
 Dr Edna S. Kaneshiro, University of Cincinnati  
 Dr Ehud Kaplan, Mount Sinai School of Medicine  
 Dr. Stephen J. Karakashian, Milwaukie, OR  
 Dr Arthur Karlin, Columbia University  
 Dr Morris John Karnovsky, Harvard Medical School  
 Mr H. Ernst Keller, Carl Zeiss, Inc.  
 Dr. Darcy B. Kelley, Columbia University  
 Dr Robert E. Kelly, Woods Hole, MA  
 Dr Norman E. Kemp, University of Michigan  
 Mr John P. Kendall, Faneuil Hall Associates  
 Mr Louis M. Kerr, Marine Biological Laboratory  
 Dr Alexander Keynan, Israel Academy of Sciences/Humanities, Israel  
 Dr Shahid M. M. Khan, SUNY Upstate Medical University  
 Dr Kamran Khodakhah, Albert Einstein College of Medicine  
 Dr Daniel P. Kiehart, Duke University Medical Center  
 Dr Irving M. Klotz, Northwestern University  
 Mr Robert A. Knudson, Marine Biological Laboratory  
 Dr Samuel S. Koide, The Rockefeller University  
 Sir Hans Kornberg, Boston University  
 Dr Edward M. Kosower, Tel-Aviv University, Israel  
 Dr Stephen M. Krane, Massachusetts General Hospital  
 Dr Robert Krauss, Denton, MD  
 Dr Edward A. Kravitz, Harvard Medical School  
 Dr William B. Kristan, Jr., University of California, San Diego  
 Dr Andrew M. Kropinski, Queen's University, Canada  
 Dr Damien P. Kuffler, Institute of Neurobiology  
 Dr William J. Kuhns, The Hospital for Sick Children, Canada

- Dr. Joseph G. Kunkel, University of Massachusetts  
 Dr. Alan M. Kuzirian, Marine Biological Laboratory
- Dr. Airmlee D. Laderman, Yale University  
 Dr. Laurie J. Landeau, Listowel, Inc.  
 Dr. Dennis M. D. Lands, University Hospital of Cleveland  
 Dr. Story C. Lanois, National Institutes of Health  
 Dr. David Landowne, University of Miami  
 Dr. George M. Langford, Dartmouth College  
 Dr. Jeffrey Laskin, University of Medicine and Dentistry of New Jersey  
 Dr. Nechama Lasser-Ross, New York Medical College  
 Dr. Leonard Laster, University of Massachusetts Medical School  
 Dr. Alan Laties, Scheie Eye Institute  
 Dr. Hans Laufer, University of Connecticut  
 Dr. Paul B. Lazarow, Mount Sinai - School of Medicine  
 Mr. Maurice Lazarus, Federated Department Stores  
 Dr. Edward R. Leadbetter, University of Connecticut  
 Dr. Joshua Lederberg, The Rockefeller University  
 Dr. John J. Lee, City College of CUNY  
 Mr. Donald B. Lehy, North Falmouth, MA  
 Dr. Stephen B. Leighton, Beecher Instruments  
 Dr. Aaron B. Lerner, Yale University School of Medicine  
 Dr. Jack Levin, University of California School of Medicine  
 Dr. Michael S. Levine, University of California  
 Dr. Richard B. Levine, University of Arizona  
 Dr. Francoise Levinthal, Columbia University  
 Prof. Irwin B. Levitan, University of Pennsylvania School of Medicine  
 Dr. Richard W. Linck, University of Minnesota School of Medicine  
 Dr. Raymond J. Lipicky, Food and Drug Administration  
 Dr. John E. Lisman, Brandeis University  
 Dr. Anthony Liuzzi, Boston, MA  
 Dr. Rodolfo R. Llinás, New York University Medical Center  
 Dr. Phillip S. Lobel, Boston University Marine Program, Marine Biological Laboratory  
 Dr. Werner R. Loewenstein, Falmouth, MA  
 Dr. Irving M. London, Harvard-MIT  
 Dr. Frank J. Longo, University of Iowa  
 Dr. Louise M. Luckenbill, Falmouth, MA
- Dr. Edward F. MacNichol, Jr., Boston University School of Medicine  
 Dr. Jane Ann Maienschein, Arizona State University  
 Dr. Craig C. Malbon, State University of New York  
 Dr. Robert P. Malchow, University of Illinois, Chicago  
 Dr. Richard S. Manalis, Indiana-Purdue University  
 Dr. Lynn Margulis, University of Massachusetts  
 Dr. Andrew C. Marinucci, Mercerville, NJ  
 Dr. Joe L. Martinez, Jr., University of Texas  
 Dr. Luigi Mastroianni, Jr., Hospital of University of Pennsylvania  
 Dr. David Mauzerall, Rockefeller University  
 Dr. M. Lynne McAnelly, University of Texas  
 Dr. Andrew G. McArthur, Marine Biological Laboratory
- Dr. Frances V. McCann Murray, Dartmouth Medical School  
 Ms. Jane A. McLaughlin, Marine Biological Laboratory  
 Dr. Robert F. McMahon, University of Texas  
 Dr. Thomas Meedel, Rhode Island College  
 Prof. Ian A. Meinertzhagen, Dalhousie University, Canada  
 Dr. Dennis E. Meiss, Immunodiagnostic Laboratories  
 Dr. Jerry M. Melillo, Marine Biological Laboratory  
 Dr. DeForest Mellon, Jr., University of Virginia  
 Mr. Richard P. Mellon, Laughlinton, PA  
 Dr. Michael E. Mendelsohn, New England Medical Center  
 Dr. Allen F. Mensinger, University of Minnesota  
 Dr. Melanie Pratt Merriman, Touchstone Consulting  
 Dr. Matthew Meselson, Harvard University  
 Dr. Ricardo Miledi, University of California, Irvine  
 Dr. Roger D. Milkman, University of Iowa  
 Dr. Andrew L. Miller, Hong Kong University of Science and Technology  
 Mr. Thomas J. Miller, Concord, MA  
 Dr. Gradimir Misevic, University Hospital of Basel, Switzerland  
 Dr. Ralph Mitchell, Harvard University  
 Dr. Timothy Mitchison, Harvard University Medical School  
 Dr. Hiroyoshi Miyakawa, Tokyo College of Pharmacy, Japan  
 Dr. David M. Miyamoto, Drew University  
 Dr. Merle Mizell, Tulane University  
 Dr. Jorge E. Moreira, National Institutes of Health  
 Dr. James G. Morin, Cornell University  
 Dr. Leyla de Toledo Morrell, Rush-Presbyterian-St. Lukes  
 Dr. Stephen S. Morse, Columbia University  
 Dr. Andrew W. Murray, Harvard University
- Dr. Samuel M. Nabrit, Atlanta, GA  
 Dr. Knute J. Nadelhoffer, National Science Foundation  
 Dr. Ronald L. Nagel, Albert Einstein College of Medicine  
 Dr. Yasuko Nakajima, University of Illinois, College of Medicine  
 Prof. Toshio Narahashi, Northwestern University Medical School  
 Dr. Enrico Nasi, Boston University School of Medicine  
 Dr. Christopher Neill, Marine Biological Laboratory  
 Margaret C. Nelson, Ph.D., Cornell University  
 Dr. Peter A. Nickerson, SUNY, Buffalo  
 Dr. Santo V. Nicosia, University of South Florida  
 Ms. Catherine N. Norton, Marine Biological Laboratory  
 Dr. Michael P. Nusbaum, University of Pennsylvania School of Medicine
- Mr. Jonathan O'Herron, Lazard Freres & Company  
 Dr. Ana Lia Obaid, University of Pennsylvania School of Medicine  
 Dr. Shinpei Ohki, SUNY at Buffalo  
 Dr. Rudolf Oldenbourg, Marine Biological Laboratory  
 Dr. James L. Olds, George Mason University
- Dr. Ada L. Olins, Foundation for Blood Research  
 Dr. Donald E. Olins, Foundation for Blood Research  
 Dr. James L. Oschman, Dover, NH
- Dr. Robert E. Palazzo, Rensselaer Polytechnic Institute  
 Dr. John D. Palmer, University of Massachusetts  
 Dr. Harish C. Pant, National Institutes of Health  
 Dr. George D. Pappas, University of Illinois  
 Dr. Arthur B. Pardee, Dana-Farber Cancer Institute  
 Dr. Rosevelt L. Pardy, University of Nebraska  
 Dr. James L. Parmentier, International Health Organization  
 Dr. Thoru Pederson, University of Massachusetts Medical Center  
 Dr. Courtland D. Perkins, Alexandria, VA  
 Dr. Philip Person, Flushing, NY  
 Dr. Bruce J. Peterson, Marine Biological Laboratory  
 Dr. Ronald Pethig, University College of North Wales, UK  
 Dr. Ronald J. Pfohl, Miami University  
 Dr. Sidney K. Pierce, Jr., University of South Florida  
 Dr. David E. Pleasure, Children's Hospital  
 Dr. Jeanne S. Poindexter, Barnard College  
 Dr. Harvey B. Pollard, U S U H S  
 Dr. Thomas D. Pollard, Yale University  
 Dr. Beverly H. Porter, Columbia, MD  
 Dr. Marie E. Porter, University of Minnesota  
 Dr. David D. Potter, Harvard Medical School  
 Dr. Maureen K. Powers, San Pablo, CA  
 Dr. Robert A. Prendergast, Johns Hopkins University  
 Dr. David J. Prior, Northern Arizona University  
 Dr. Robert D. Prusch, Gonzaga University  
 Dr. Dale Purves, Duke University Medical Center
- Dr. James P. Quigley, The Scripps Research Institute
- Mr. Irving W. Rabb, Cambridge, MA  
 Dr. Harvey Rabin, Rockville, MD  
 Dr. Michael B. Rabinowitz, Boston, MA  
 Dr. Nancy S. Rafferty, Marine Biological Laboratory  
 Dr. Robert F. Rakowski, Ohio University  
 Dr. Fidel Ramon, Universidad Nacional Autonoma de Mexico, Mexico  
 Dr. Edward B. Rastetter, Marine Biological Laboratory  
 Dr. Lionel I. Rebhun, University of Virginia (deceased 2002)  
 Dr. John R. Reddan, Oakland University  
 Dr. Thomas S. Reese, National Institutes of Health  
 Dr. Carol L. Reinisch, Marine Biological Laboratory
- Dr. Frederick R. Rickles, George Washington University  
 Dr. Conly L. Rieder, Wadsworth Center  
 Dr. Monica Riley, Marine Biological Laboratory  
 Dr. Harris Ripps, University of Illinois at Chicago  
 Dr. J. Murdoch Ritchie, Yale University School of Medicine  
 Dr. Lawrence C. Rome, University of Pennsylvania  
 Dr. Jack Rosenbluth, New York University School of Medicine  
 Dr. Raja Rosenbluth, Simon Fraser University  
 Dr. Allan Rosenfield, Columbia University School of Public Health  
 Dr. Herbert S. Rosenkranz, Florida Atlantic University

Dr William N. Ross, New York Medical College  
 Mr Rudi Rottenfusser, Carl Zeiss Inc  
 Dr Lewis P. Rowland, Neurological Institute  
 Dr Joan V. Ruderman, Harvard Medical School  
 Dr John D. Rummel, NASA Headquarters  
 Dr Norman B. Rushforth, Case Western  
 Reserve University  
 Dr William Devine Russell-Hunter, Easton, MD

Dr Mary Beth Saffo, Harvard University  
 Dr Guy Salama, University of Pittsburgh  
 Dr Edward D. Salmon, University of  
 North Carolina  
 Dr Abigail Salyers, University of Illinois  
 Prof. Brian M. Salzberg, University of  
 Pennsylvania School of Medicine  
 Dr Jean M. Sanger, University of Pennsylvania  
 School of Medicine  
 Dr Joseph W. Sanger, University of Pennsylvania  
 Medical Center  
 Dr John W. Saunders, Jr., Waquoit, MA  
 Prof. Howard K. Schachman, University of  
 California  
 Dr Gerald P. Schatten, University of Pittsburgh  
 Dr Arlene C. Schmeer, Merceene Cancer  
 Research Institute  
 Dr Herbert Schuel, SUNY at Buffalo  
 Dr Lawrence Schwartz, University of  
 Massachusetts  
 Dr A. Nicola Schweitzer, Brookline, MA  
 Dr Felix E. Schweizer, University of California,  
 Los Angeles  
 Dr Sheldon J. Segal, The Population Council  
 Dr Stephen Lamont Sentf, Woods Hole, MA  
 Dr Douglas R. Shanklin, University of Tennessee  
 Dr Nadav Shashar, The Interuniversity Institute  
 of Eilat, Israel  
 Dr Victor E. Shashoua, Harvard Medical School  
 Dr Gaius R. Shaver, Marine Biological  
 Laboratory  
 Dr John R. Shaver, Michigan State University  
 (deceased 2003)  
 Dr Michael P. Sheetz, Columbia University  
 Dr David Sheprow, Boston University  
 Dr Irwin W. Sherman, University of California  
 Dr Osamu Shimomura, Falmouth, MA  
 Mr. Alan M. Shipley, Forestdale, MA  
 Dr Robert B. Silver, Wayne State University  
 Dr Kathleen K. Siwicki, Swarthmore College  
 Dr Dorothy M. Skinner, Falmouth, MA  
 Dr Roger D. Sloboda, Dartmouth College  
 Dr Greenfield Sluder, University of  
 Massachusetts Medical Center  
 Dr Peter J. S. Smith, Marine Biological  
 Laboratory  
 Dr Stephen J. Smith, Stanford University School  
 of Medicine  
 Dr Roxanna S. Smolowitz, Marine Biological  
 Laboratory  
 Dr Mitchell L. Sogin, Marine Biological  
 Laboratory  
 Dr Martha M. Sorenson, Cidade Universitaria-  
 UFRJ, Brazil  
 Dr William T. Speck, Marine Biological  
 Laboratory

Dr Abraham Spector, Columbia University  
 Dr. Johanna E. Speksnijder, Odijk, The  
 Netherlands  
 Dr. David C. Spray, Albert Einstein College  
 of Medicine  
 Dr Kenneth R. Spring, National Institutes  
 of Health  
 Dr John H. Steele, Woods Hole Oceanographic  
 Institution  
 Dr Antoinette Steinacker, University of  
 Puerto Rico  
 Dr Malcolm S. Steinberg, Princeton University  
 Dr Andreas C. Stemmer, Institut fuer Robotik,  
 Switzerland  
 Prof. Johan Stenflo, M.D., Ph.D., University of  
 Lund, Sweden  
 Mr. Paul A. Stuedler, Marine Biological Laboratory  
 Dr Darrell R. Stokes, Emory University  
 Dr Elijah W. Stommel, Dartmouth Hitchcock  
 Medical Center  
 Dr Alfred Stracher, SUNY Health Science Center  
 at Brooklyn  
 Dr Felix Strumwasser, East Falmouth, MA  
 Dr Ann E. Stuart, University of North Carolina at  
 Chapel Hill  
 Dr. Mutsuyuki Sugimori, New York University  
 Medical Center  
 Dr William C. Summers, Western Washington  
 University  
 Dr. Kathy A. Suprenant, University of Kansas  
 Prof. Mary Anne Sydlík, Hope College  
 Dr. Andrew G. Szent-Gyorgyi, Brandeis University  
  
 Dr. Marvin L. Tanzer, University of Connecticut,  
 School of Dental Medicine  
 Dr Ichiji Tasaki, National Institutes of Health  
 Dr Edwin W. Taylor, University of Chicago  
 Dr William H. Telfer, University of Pennsylvania  
 Dr Bruce Telzer, Pomona College  
 Prof. Mark Terasaki, University of Connecticut  
 Health Center  
 Dr James G. Townsel, Meharry Medical College  
 Dr David M. Travis, Woods Hole, MA  
 Dr Steven N. Treisman, University of  
 Massachusetts Medical Center  
 Dr Walter Troll, NYU Medical Center  
 Dr Robert F. Troxler, Boston University School  
 of Medicine  
 Dr Kenyon S. Tweedell, University of Notre Dame  
 Dr Mark L. Tykocinski, Case Western Reserve  
 University  
 Prof. Michael Tytell, Wake Forest University  
 School of Medicine  
  
 Dr. Hiroshi Ueno, Kyoto University, Japan  
  
 Dr. Ivan Valiela, Boston University Marine Program  
 Dr Richard Vallee, University College of  
 Physicians & Surgeons  
 Mr John J. Valois, Woods Hole, MA  
 Dr. Cindy Lee Van Dover, The College of William  
 and Mary  
 Dr Kensal E. Van Holde, Oregon State University

Dr Patricia Wadsworth, University of  
 Massachusetts  
 Dr Norman R. Wainwright, Marine Biological  
 Laboratory  
 Dr Byron H. Waksman, New York University  
 Medical Center  
 Dr Betty Wall, Woods Hole, MA  
 Dr Lawrence J. Wanhg, Brandeis University  
 Dr Robert C. Warner, Laguna Beach, CA  
 Dr Leonard Warren, Wistar Institute  
 Dr John B. Waterbury, Woods Hole  
 Oceanographic Institution  
 Dr Stephen G. Waxman, Yale Medical School  
 Dr Annemarie Weber, University of Pennsylvania  
 School of Medicine  
 Dr Janis C. Weeks, University of Oregon  
 Dr Earl Weidner, Louisiana State University  
 Dr Alice Sara Weiss, Silver Spring, MD  
 Dr. Dieter G. Weiss, University of Rostock,  
 Germany  
 Dr Leon P. Weiss, University of Pennsylvania  
 School of Veterinary Medicine  
 Dr Marisa C. Weiss, Paoli Memorial Hospital  
 Dr Gerald Weissmann, New York University  
 Medical Center  
 Dr Jennifer J. Wernegreen, Marine Biological  
 Laboratory  
 Dr Monte Westerfield, University of Oregon  
 Dr J. Richard Whittaker, University of New  
 Brunswick  
 Dr Torsten N. Wiesel, The Rockefeller University  
 Dr Darcy B. Wilson, Torrey Pines Institute  
 Dr T. Hastings Wilson, Harvard Medical School  
 Dr Beatrice Wittenberg, Albert Einstein College  
 of Medicine  
 Dr Jonathan B. Wittenberg, Albert Einstein  
 College of Medicine  
 Dr William F. Wonderlin, West Virginia University  
 Dr Mary Kate Worden, University of Virginia  
 Dr Basil V. Worgul, Columbia University  
 Dr Chau Hsiung Wu, Northwestern University  
 Medical School  
 Dr Charles R. Wyttenbach, University of Kansas  
  
 Dr Harold H. Zakon, University of Texas  
 Dr Seymour Zigman, Falmouth, MA  
 Dr Michael J. Zigmund, University of Pittsburgh  
 Dr Joshua J. Zimmerberg, National Institutes  
 of Health  
 Dr Steven J. Zottoli, Williams College

## ASSOCIATES

### Patron

Mr and Mrs. Malcolm Campbell  
The Honorable and Mrs. John S. Langford  
Dr and Mrs. Edward F. MacNichol, Jr.  
Mrs. William O. Niles, II

### Sustaining Associate

Mr and Mrs. David Bakalar  
Mr and Mrs. Norman Bernstein  
Mr. Brian Braginton-Smith  
Bufftree Building Co., Inc.  
Mrs. Martha Saunders Ferguson  
Dr. David Forkosh and Dr. Linda Hirshman  
Dr. and Mrs. Leonard Laster  
Dr. and Mrs. John W. Rowe

### Supporting Associate

Mrs. Margaret Clowes  
Mrs. Sally Cross  
Ms. Anne R. DuBois  
Mr. Clifton H. Eaton  
Dr. and Mrs. Harold S. Ginsberg  
Mrs. Rebeckah DuBois Glazebrook  
Drs. Alfred and Joan Goldberg  
Ms. Penelope Hare  
Mr. and Mrs. Gary G. Hayward  
Mr. and Mrs. William K. Mackey, Esq.  
Dr. and Mrs. William M. McDermott  
Mr. and Mrs. Robert Parkinson  
Mr. and Mrs. William J. Pechilis  
Dr. and Mrs. Alan D. Perlmutter  
Mr. and Mrs. Walter J. Salmon  
Mrs. Anne W. Sawyer  
Dr. John Tochko and  
Mrs. Christina Myles-Tochko

### Family Membership

Dr. and Mrs. David E. Adelberg  
Dr. and Mrs. Dean C. Allard, Jr.  
Dr. Peggy Alsup  
Mr. and Mrs. Douglas Amon  
Drs. James and Helene Anderson  
Dr. and Mrs. Samuel C. Armstrong  
Mr. and Mrs. Duncan P. Aspinwall  
Mr. and Mrs. Donald R. Aukamp  
Mr. and Mrs. John M. Baitzell  
Dr. and Mrs. Robert B. Barlow, Jr.  
Mr. and Mrs. John E. Barnes  
Dr. and Mrs. Harriet P. Bemheimer  
Mr. and Mrs. Robert O. Bigelow  
Dr. and Mrs. Edward G. Boettiger  
Mr. and Mrs. Kendall B. Bohr  
Dr. and Mrs. Thomas A. Borgese  
Dr. and Mrs. Francis P. Bowles  
Mr. and Mrs. Peter Boyer  
Mr. and Mrs. Thomas A. Brown  
Dr. and Mrs. John B. Buck  
Mr. and Mrs. William O. Burwell  
Mr. and Mrs. Bruce E. Buxton  
Dr. and Mrs. Richard L. Chappell

Dr. and Mrs. Frank M. Child  
Dr. and Mrs. Arnold M. Clark  
Mr. and Mrs. James M. Cleary  
Dr. and Mrs. Laurence P. Cloud  
Drs. Harry Conner and Carol Scott-Conner  
Mr. and Mrs. Donald B. Cook  
Mr. and Mrs. Theron S. Curtis, Jr.  
Mr. and Mrs. Joel Davis  
Mr. and Mrs. Joseph L. Dixon  
Mr. and Mrs. F. Gerald Douglass  
Dr. and Mrs. John E. Dowling  
Mr. and Mrs. W. J. Doyle  
Dr. and Mrs. Arthur Brooks DuBois  
Mr. and Mrs. Robert Elias  
Mr. and Mrs. Jerome Fanger  
Dr. and Mrs. Michael J. Fishbein  
Mr. and Mrs. Howard G. Freeman  
Dr. and Mrs. Robert A. Frosch  
Dr. and Mrs. John J. Funkhouser  
Dr. and Mrs. Mordecai L. Gabriel  
Dr. and Mrs. David Garber  
Miss Eleanor Garfield  
Dr. and Mrs. James L. German, III  
Dr. and Mrs. Prosser Gifford  
Dr. and Mrs. Murray Glusman  
Dr. and Mrs. Moise H. Goldstein  
Mrs. Ann Goodman and Dr. Arthur Pardee  
Mr. and Mrs. Charles Goodwin, III  
Mr. and Mrs. Frederic Greenman  
Dr. and Mrs. Thomas C. Gregg  
Dr. and Mrs. Newton H. Gresser  
Ms. Kathryn Hackett  
Dr. and Mrs. Harlyn O. Halvorson  
Mr. and Mrs. Benjamin Handelman

Dr. and Mrs. Richard Bennet Harvey  
Dr. and Mrs. J. Woodland Hastings  
Dr. Robert R. Haubrich  
Mrs. Elizabeth Heald  
Mr. and Mrs. Edward S. Heard  
Dr. and Mrs. Howard H. Hiatt  
Mr. and Mrs. David Hibbitt  
Dr. Llewellyn Hillis and Dr. Paul Colinaux  
Dr. and Mrs. John E. Hobbie  
Dr. Peter A. Hoening  
Mr. and Mrs. Gerald J. Holtz  
Drs. Francis C. Hoskin and Elizabeth Farnham  
Mrs. Carmela J. Huettner  
Ms. Susan A. Huettner  
Dr. and Mrs. Shinya Inoué  
Dr. and Mrs. Kurt J. Isselbacher  
Mrs. Mary D. Janney  
Dr. and Mrs. James E. Johnson  
Mrs. Sally S. Joslin  
Dr. and Mrs. Benjamin Kaminer  
Dr. and Mrs. Morris John Karnovsky  
Dr. and Mrs. George Katz  
Mr. and Mrs. Arthur King  
Mr. and Mrs. Paul W. Knaplund  
Mr. and Mrs. A. Sidney Knowles, Jr.  
Mr. and Mrs. Walter E. Knox  
Sir Hans and Lady Kornberg  
Dr. and Mrs. S. Andrew Kulin  
Mr. Ezra Laderman  
Dr. and Mrs. George M. Langford  
Dr. Hans Laufer  
Dr. and Mrs. John J. Lee  
Mr. Russ Lemcke  
Mr. and Mrs. James E. Lloyd

### THE 2001-2002 FALMOUTH FORUM SERIES sponsored by the MBL Associates

October 5, 2001

"Why I Sing in the Shower"

Keith Lockhart, Conductor, The Boston Pops Orchestra

October 19, 2001

"Memoirs of a Geisha: The Making of a Novel"

Arthur Golden, Author, *Memoirs of a Geisha*

December 7, 2001

"An Evening with Norm Abram"

Norm Abram, Master Carpenter and host of *The New Yankee Workshop*

January 18, 2002

"The Great Powers and the East Mediterranean World"

Erik Goldstein, Chairman, Department of International Relations;  
Professor of International Relations, Boston University

February 1, 2002

"Around the Other Round Stone Barn: The History, Restoration,  
and Relevance of the Hancock Shaker Community"

Mary Rentz, Past-President, Board of Trustees, Hancock Shaker Village

Friday, March 1, 2002

"Osteoporosis: The Research Frontier - Hopes for a Cure"

Bjorn R. Olsen, Hersey Professor of Cell Biology;  
Harvard-Forsyth Professor of Oral Biology; Chairman,  
Harvard-Forsyth Department of Oral Biology, Harvard Medical School

## ASSOCIATES EXECUTIVE BOARD

Ruth Ann Laster, President  
Sallie Giffen, Vice-President  
Kitty Brown, Treasurer  
Ruth Shephard, Secretary

Tammy Amon  
Helen Barnes  
Peter Boyer  
Bruce Buxton  
Julie Child  
Martha Ferguson  
Thomas Gregg  
James Johnson  
Alice Knowles  
Hans Kornberg  
Rebecca Lash  
Susan Loucks  
Jack Pearce  
Alan Perlmutter  
Virginia Reynolds  
Marjorie Salmon  
Volker Ulbrich

*Ex-officio members*

William T. Speck, Director & CEO, MBL  
John E. Dowling, President of the  
Corporation, MBL  
Sheldon J. Segal, Chairman of the Board  
of Trustees, MBL

*Associates Administrator*  
Susan Joslin

*Associates, continued*

Dr. and Mrs. Laszlo Lorand  
Mr. Richard C. Lovering  
Mr. and Mrs. Francis C. Lowell, Jr.  
Mrs. Phyllis M. MacNeil  
Mr. and Mrs. Joseph Martyna  
Drs. Luigi and Elaine Mastroianni  
Dr. and Mrs. Robert T. McCluskey  
Mr. and Mrs. Derek J. McDonald  
Mr. and Mrs. James McSherry  
Mrs. Nawrie Meigs-Brown  
Dr. and Mrs. Jerry M. Melillo  
Dr. Martin Mendelson  
Mr. and Mrs. Richard Meyers  
Mr. and Mrs. Charles A. Mitchell  
Dr. and Mrs. Merle Mizell  
Dr. and Mrs. Charles H. Montgomery  
Mr. and Mrs. Stephen A. Moore  
Mr. James V. Moynihan  
Mr. and Mrs. Lewis Nassikas  
Dr. and Mrs. John E. Naugle  
Dr. Pamela Nelson and Mr. Christopher Olmsted  
Mr. and Mrs. Frank L. Nickerson  
Dr. and Mrs. Clifford T. O'Connell  
Mr. and Mrs. James J. O'Connor  
Mr. and Mrs. Daniel O'Grady  
Mr. and Ms. David R. Palmer  
Dr. and Mrs. Clement E. Papazian

Mr. and Mrs. Richard M. Paulson, Jr.  
Dr. and Mrs. John B. Pearce  
Mrs. Nancy Pendleton  
Mr. and Mrs. John B. Peri  
Dr. and Mrs. Courtland D. Perkins  
Dr. and Mrs. Philip Person  
Mr. Frederick S. Peters  
Mrs. Grace M. Peters  
Mr. and Mrs. E. Joel Peterson  
Mr. and Mrs. Harold Piskaln  
Mr. and Mrs. Andrew H. Plevin  
Mr. and Mrs. George H. Plough  
Dr. and Mrs. Aubrey Pothier, Jr.  
Mr. and Mrs. Allan Ray Putnam  
Mrs. Lionel I. Rebhun  
Dr. and Mrs. George T. Reynolds  
Dr. and Mrs. Harns Ripps  
Ms. Jean Roberts  
Rev. Michael Robertson and Dr. Emmy Robertson  
Drs. Priscilla and John Roslansky  
Mr. and Mrs. John D. Ross  
Dr. and Mrs. John W. Saunders, Jr.  
Mr. and Mrs. Savely Schuster  
Mr. and Mrs. Harold H. Sears  
Dr. and Mrs. Sheldon J. Segal  
Dr. and Mrs. Robert Seidler  
Mr. and Mrs. Daniel Shearer  
Dr. and Mrs. David Sheprow  
Dr. and Mrs. Irwin Sherman  
Mr. and Mrs. Bertram R. Silver  
Mr. and Mrs. Jonathan O. Simonds  
Mr. and Mrs. John A. Simourian  
Drs. Frederick and Marguente Smith  
Drs. William Speck and Evelyn Lipper  
Dr. and Mrs. Guy L. Steele, Sr.  
Dr. and Mrs. Alan B. Steinbach  
Dr. and Mrs. William K. Stephenson  
Dr. and Mrs. Thomas R. Stetson  
Mr. and Mrs. E. Kent Swift, Jr.  
Mr. and Mrs. Gerard L. Swope  
Mr. and Mrs. Emil D. Tietje, Jr.  
Mr. D. Thomas Tngg  
Dr. and Mrs. Walter Troll  
Prof. and Mrs. Michael Tytell  
Mr. and Mrs. Volker Ulbrich  
Mr. and Mrs. John J. Valois  
Drs. Claude and Dorothy Villee  
Dr. John Waterbury and Ms. Vicky Cullen  
Mr. and Mrs. John T. Weeks  
Dr. and Mrs. Gerald Weissmann  
Dr. and Mrs. Paul S. Wheeler  
Ms. Mabel Whelpley and Mr. George Rollins  
Mrs. Geoffrey Whitney  
Mr. and Mrs. Lynn H. Wilke  
Mr. and Mrs. Leslie J. Wilson  
Dr. and Mrs. T. Hastings Wilson  
Mr. and Mrs. Leonard M. Wilson  
Mr. and Mrs. Richard Yoder  
Mrs. Manlyn G. Zacks  
Mr. and Mrs. Bruce Zimmerli

*Individual Membership*

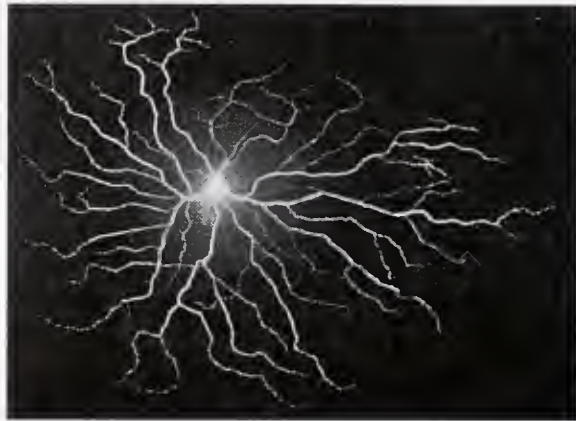
Mr. Richard A. Ahern  
Dr. Nina Stromgren Allen  
Mrs. Frederica Z. Alpert  
Mr. Dean N. Arden  
Mrs. Ellen Prosser Armstrong  
Mr. Garfield M. Arthur  
Mrs. Barbara Atwood  
Mrs. June Atwood  
Mr. Everett E. Bagley  
Ms. Megan E. Barrasso  
Ms. Patricia M. Barry  
Mr. Mike Barry  
Dr. Millicent Bell  
Mr. C. John Berg  
Ms. Olive C. Beverly  
Mr. George Billings  
Mrs. Ellen F. Binda  
Ms. Avis Blomberg  
Dr. Robert H. Broyles  
Mr. Joseph W. Burke  
Mrs. Barbara Gates Burwell  
J. G. Butch  
Dr. Graciela C. Candelas  
Mr. Frank C. Carotenuto  
Dr. Robert H. Carner  
Dr. Chia-Yen Chen  
Dr. Sallie Chisholm  
Ms. Paula Ciara  
Mrs. Octavia C. Clement  
Dr. Jewel Plummer Cobb  
Mrs. Margaret H. Coburn  
Dr. Seymour S. Cohen  
Ms. Genevieve Coleman  
Ms. Anne S. Concannon  
Ms. Margaret S. Cooper  
Dr. D. Eugene Copeland  
Mrs. Molly N. Cornell  
Dr. Vincent Cowling  
Mrs. Marilyn E. Crandall  
Ms. Cathleen Creedon  
Ms. Helen M. Crossley  
Ms. Dorothy Crossley  
Mrs. Villa B. Crowell  
Mrs. Doris M. Curran  
Mrs. Elizabeth M. Davis  
Ms. Maureen Davis  
Ms. Carol Reimann DeYoung  
Mrs. Virginia A. Dierker  
Mr. David L. Donovan  
Ms. Suzanne Drobán  
Ms. Maureen J. Dugan  
Ms. Deborah Dunn  
Mrs. Frances E. Eastman  
Dr. Frank Egloff  
Ms. Elizabeth Egloff  
Mrs. Eleanor B. Faithorn  
Ms. Helen C. Farrington  
Mrs. Ruth Alice Fitz  
Ms. Sylvia M. Flanagan  
Mr. John W. Folino, Jr.

## GIFT SHOP VOLUNTEERS

Marion Adelburg  
 Beth Berne  
 Avis Blomberg  
 Gloria Borgese  
 Julie Child  
 Janet Daniels  
 Carol De Young  
 Frances Eastman  
 Pat Ferguson  
 Barbara Grossman  
 Jean Halvorson  
 Hanna Hastings  
 Marcella Katz  
 Donna Kornberg  
 Barbara Little  
 Florence Mixer  
 Bertha Person  
 Julie Rankin  
 Arlene Rogers  
 Atholie Rosett  
 Cynthia Smith  
 Alice Todd  
 Natalie Trousof  
 Clare Wilber  
 Betty Wilson  
 Grace Witzell  
 Bunnie Zigman

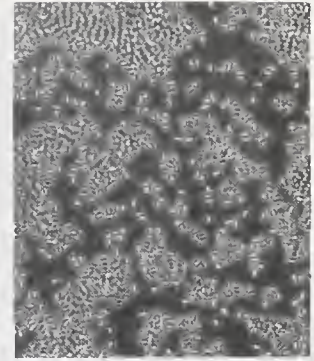
## TOUR GUIDES

Gloria Borgese  
 Frank Child  
 Nancy Fraser  
 Sallie Giffen  
 Ronald Glantz  
 Charles Mahoney  
 Haskell Maude  
 Andrew McArthur  
 Vivagean Merz  
 Carl Ollivier  
 William Phillips  
 Julie Rankin  
 Howard Redpath  
 Sheila Silverberg  
 Mary Ulbrich  
 John Valois



### Associates, continued

Mr Paul J. Freyheit  
 Mrs Ruth E. Fye  
 Mr Joseph C. Gallagher  
 Mrs Lois E. Galvin  
 Miss Lan Ge  
 Mrs Matilda L. Gellis  
 Mrs Doris D. Gerace  
 Ms Sallie Giffen  
 Mrs Janet F. Gillette  
 Mr Michael P. Goldring  
 Ms Muriel Gould  
 Mrs Winifred M. Green  
 Ms Janet M. Gregg  
 Mrs Jeanne B. Griffith  
 Mrs Barbara Grossman  
 Mrs Valerie A. Hall  
 Ms Mary Elizabeth Hamstrom  
 Mrs. Jane M. Heald  
 Mr Mark Hollander  
 Mrs Betsy Honey  
 Mr Roger W. Hubbell  
 Ms Alexandra Izzo  
 Dr. Diana E. Jennings  
 Mrs. Megan H. Jones  
 Ms Barbara W. Jones  
 Mrs. Joan T. Kanwisher  
 Mrs Sally Karush  
 Ms Patricia E. Keoughan  
 Dr. Peter N. Kivy  
 Ms Kathryn M. Kleekamp  
 Ms Margaret D. Lakis  
 Ms Meryl Langbort  
 Ms. Rebecca Lash  
 Mr William Lawrence  
 Dr Marian E. LeFevre  
 Mr Edwin M. Libbin  
 Mr Lennart Lindberg  
 Mrs Barbara C. Little  
 Mrs Sarah J. Loessel  
 Ms Susan Loucks  
 Mr. Jeremy Loyd  
 Dr Zella Luria  
 Ms Sallie G. Lyon  
 Mrs Margaret M. MacLeish  
 Mrs Annemarie E. Mahler  
 Mrs Nancy R. Malkiel  
 Mr Brett Mandel and  
     Ms. Laura Weinbaum  
 Mrs Diane B. Maranchie  
 Mrs Marjorie Marshall  
 Mrs. Mary Hartwell Mavor  
 Mr Bill McGoey  
 Mr Paul McGonigle  
 Dr Susan G. McIlwain  
 Ms Mary W. McKoan  
 Ms Jane A. McLaughlin  
 Ms Louise McManus  
 Ms Cornelia Hanna McMurtrie  
 Ms Paula A. Mealy  
 Dr Carmen Merryman  
 Ms Vivagean V. Merz  
 Mrs Marianne F. Milkman  
 Mrs Florence E. Mixer  
 Mr. Ken Moffitt  
 Mr Lawrence A. Monte  
 Ms Cynthia Moor  
 RADM. Paul J. Mulloy USN (Ret)  
 Mrs Carol Murray  
 Mrs Eleanor M. Nace  
 Mrs Anne Nelson  
 Dr Eliot H. Nerman  
 Mr. Edmund F. Nolan  
 Ms Peggy Schiffer Noland  
 Ms Catherine N. Norton  
 Dr Renee Bennett O'Sullivan  
 Dr Jack S. Parker  
 Mr. David Parker, Jr  
 Ms Carolyn L. Parmenter  
 Ms Joan Pearlman  
 Dr. Daniel A. Pollen  
 Mr. Barry Pratt  
 Ms Elizabeth T. Price  
 Ms Dianne Purves  
 Mrs Julia S. Rankin  
 Dr. Margaret M. Rappaport  
 Mrs Carol V. Rasic  
 Mr Fred J. Ravens, Jr  
 Ms Mary W. Rianhard  
 Ms Andrea Ricca  
 Dr Mary Elizabeth Rice  
 Ms Sandy L. Richardson  
 Dr Monica Riley  
 Mrs. Lola E. Robertson  
 Dr Steven R. Rodermel  
 Mrs Arlene Rogers  
 Mrs Wendy E. Rose  
 Mrs Atholie K. Rosett  
 Dr. Virginia F. Ross  
 Dr John D. Rummel  
 Mrs Rosalind Russell  
 Dr Albert Samuel  
 Mr Raymond A. Sanborn  
 Dr Thomas Sbarra  
 Ms Mary M. Scanlan  
 Mr. Claude Schoepf  
 Mr. Samuel C. Schon  
 Mrs Elsie M. Scott  
 Dr Cecily Cannan Selby  
 Mrs Deborah G. Senft  
 Ms Dorothy Sgarzi  
 Mrs Charlotte Shemin  
 Mrs Ruth Shepard  
 Mr Frank Shepard  
 Ms Dorothy Shiebler  
 Ms Enid K. Sichel  
 Dr Jeffrey D. Silberman  
 Mrs Phyllis J. Silver  
 Mrs. Cynthia C. Smith  
 Mrs Louise M. Specht  
 Dr Evelyn Spiegel  
 Mrs Helene E. Spurrier  
 Dr Robert E. Steele  
 Mrs Eleanor Steinbach  
 Dr Malcolm S. Steinberg  
 Ms Eleanor Sterling  
 Mrs. Jane Lazarow Stetten  
 Mr Edward Stimpson, III  
 Mrs Elizabeth Stommel  
 Ms Maren Studlien  
 Mr Albert H. Swain  
 Mr Dorman J. Swartz  
 Mr James K. Taylor  
 Mrs Alice Todd  
 Mr Arthur D. Traub  
 Ms Natalie Trousof  
 Mr Louis C. Turner  
 Ms Eleanor S. Uhlinger  
 Ms Ciona Ulbrich  
 Ms Sylvia Vatuk  
 Ms Dawn Vaughn  
 Ms Susan Veeder  
 Mr Lee D. Vincent  
 Mr Arthur D. Voorhis  
 Mrs Ann Wadsworth  
 Mrs Eve Warren  
 Mr. Michael S. Weinstein  
 Ms Lillian Wendorff  
 Dr Gary Wessel  
 Mr George R. Wezniak  
 Mr Gerry White  
 Mrs Barbara Whitehead  
 Mrs Clare M. Wilber  
 Mrs Helen Wilson  
 Mrs Grace Witzell  
 Ms Nancy Wotkoski  
 Mr Dale Wolfgram  
 Mrs Dorothy M. York  
 Dr Linda Amaral Zettler  
 Mrs Bunnie Rose Zigman  
 Mrs Margery P. Zinn



## COUNCIL OF VISITORS

*The purpose of the Council of Visitors is to increase awareness of the Marine Biological Laboratory and to inform members about the broad range of activities in research and educational programs. COV members serve as ambassadors of the Laboratory, and thus raise visibility of the MBL.*

Mr. Robert W Ashton  
Bay Foundation  
New York, New York

Mr Donald J. Bainton  
Continental Can Co  
Boca Raton, Florida

Mr. David Bakalar  
Chestnut Hill, Massachusetts

Dr. George P. Baker  
Massachusetts General Hospital  
Boston, Massachusetts

Dr. Sumner A. Barenberg  
Bernard Technologies  
Chicago, Illinois

Mr. Mel Barkan  
The Barkan Companies  
Boston, Massachusetts

Mr. Frederick Bay  
Josephine Bay Paul & C. Michael Paul  
Foundation, Inc  
New York, New York

Mr Robert P Beech  
Component Software International, Inc  
Mason, Ohio

Mr George Berkowitz  
Legal Sea Foods  
Allston, Massachusetts

Jewelle and Nathaniel Bickford  
New York, New York

Dr. Elkan R. Blout  
Harvard Medical School  
Boston, Massachusetts

Mr Malcolm K. Brachman  
Northwest Oil Company  
Dallas, Texas

Dr. Goodwin M. Breinin  
New York University Medical Center  
New York, New York

Mr Murray H. Bring  
New York, New York

Mr. John Callahan  
Carpenter, Sheperd & Warden  
New London, New Hampshire

Mrs. Elizabeth Campanella  
West Falmouth, Massachusetts

Dr. R. John Collier  
Harvard Medical School  
Boston, Massachusetts

Dr. Stephen D. Crocker  
Bethesda, Maryland

Mr. Michael J. Cronin  
Cognition Corporation  
Bedford, Massachusetts

Mrs. Lynn W. Piasecki Cunningham  
Film and Videomaker, Piasecki Productions  
New York, New York

Dr. Anthony J. Cutaià  
Anheuser-Busch, Inc  
St. Louis, Missouri

Dr. Lorenzo DiCarlo  
Mrs. Sally Stegeman DiCarlo  
Ann Arbor, Michigan

Dr. Charles Di Cecca  
Medford, Massachusetts

Mr. Diarmaid H. Douglas-Hamilton  
Hamilton Thorne Research  
Beverly, Massachusetts

Mr. Benjamin F. du Pont  
Du Pont Company  
Deepwater, New Jersey

Dr. Sylvia A. Earle  
Deep Ocean Engineering  
Oakland, California

Mr & Mrs Hoyt Ecker  
Vero Beach, Florida

Mr. Anthony B. Evnin  
Venrock Associates  
New York, New York

Mr. Michael Fenlon  
Nathan Sallop Insurance Agency, Inc  
Boston, Massachusetts

Judah Folkman, M.D.  
Children's Hospital  
Boston, Massachusetts

Mrs. Hadley Mack French  
Edsel & Eleanor Ford House  
Grosse Pointe Farms, Michigan

Mr and Mrs Huib Geerlings  
Boston, Massachusetts

Mr. Maynard Goldman  
Maynard Goldman & Associates  
Boston, Massachusetts

Ms. Charlotte I. Hall  
Edgartown, Massachusetts

Ms. Penelope S. Hare  
West Falmouth, Massachusetts

Mrs. Elizabeth Heald  
West Falmouth, Massachusetts

Dr. Thomas R. Hedges, Jr.  
Neurological Institute, Pennsylvania Hospital  
Philadelphia, Pennsylvania

Drs. Linda Hirshman and David Forkosh  
Brandeis University & FMH Foundation  
Waltham, Massachusetts

COUNCIL OF VISITORS MEETING  
JUNE 27, 28, 2002

*Modern Molecular Approaches to Global Infectious Diseases*  
John R. David, M.D., Moderator  
Harvard School of Public Health

*A 21st Century Challenge: Using Genomics, Proteomics, and Molecular Immunology to Develop Vaccines for Malaria and Lung Cancer*  
Stephen L. Hoffman, M.D.  
Senior Vice President, Biologics  
Celera Genomics

*AIDS in Africa: New Epidemics, New Viruses*  
Max Essex, D.V.M., Ph.D.  
Chairman, Department of Immunology and Infectious Diseases  
Harvard School of Public Health

*The Conundrum of Tuberculosis and HIV/AIDS*  
Jerold J. Ellner, M.D.  
Director, Center for Emerging and Re-Emerging Pathogens  
New Jersey School of Medicine

Mr Robert S. Shifman  
St. Simon's Island, Georgia

Mr and Mrs Gregory Skau  
Grosse Pointe Farms, Michigan

Mr John C. Stegeman  
Campus Rentals  
Ann Arbor, Michigan

Mr. Joseph T. Stewart, Jr  
Skillman, New Jersey

Mr. Richard H. Stowe  
Capital Counsel LLC  
New York, New York

Mr. Gerard L. Swope  
Washington, DC

Mr. John F. Swope  
Concord, New Hampshire

Mr. and Mrs. Stephen E. Taylor  
Milton Massachusetts

Mr. Samuel Thorne  
Thorne Trading Company, LLC  
Manchester, Massachusetts

Mrs Karen Tierney  
Wellesley, Massachusetts

Mrs Donna Vanden Bosch-Flynn  
Spring Lake, New Jersey

Mr. Benjamin S. Warren III  
Grosse Pointe Farms, Michigan

Nancy B. Weinstein, R.N  
The Hospice, Inc  
Glen Ridge, New Jersey

Stephen S. Weinstein, Esq  
Morristown, New Jersey

John C. West, M.D  
Danville, Pennsylvania

Mr Frederick J. Weyerhaeuser  
Beverly, Massachusetts

Mrs Robin Wheeler  
West Falmouth, Massachusetts

Ms Rosalind C. Whitehead  
New York, New York

Mrs. Annette Williamson  
Forth Worth, Texas

Mrs Barbara W. Hostetter  
Barr Foundation  
Boston, Massachusetts

Mr Charles Hunter  
Kessinger Hunter & Co  
Kansas City, Missouri

Mr Thomas J. Hynes, Jr  
Meredith & Grew, Inc.  
Boston, Massachusetts

Mrs Mary D. Janney  
Washington, D.C.

Dr. Morris J. Karnovsky  
Harvard Medical School  
Boston, Massachusetts

Ms Ellyn V. Korzun  
Goldman, Sachs & Co  
New York, New York

Mr. and Mrs. Robert Lambrecht  
Boca Grande, Florida

Mr. Rudy Landry  
Pocasset, Massachusetts

Catherine C. Lastavica, M.D.  
Tufts University School of Medicine  
Boston, Massachusetts

Dr. Anna Logan Lawson  
Daleville, Virginia

Mr. Joel A. Leavitt  
Boston, Massachusetts

Mrs. Margaret Lilly  
West Falmouth, Massachusetts

Mr. Richard Lipkin  
Shipan Capital  
New York, New York

Mr. Michael T. Martin  
SportsMark, Inc.  
New York, New York

Mrs. Christy Swift Maxwell  
Grosse Pointe Farms, Michigan

Mr. Ambrose Monell  
G. Unger Vetlesen Foundation  
Palm Beach, Florida

Dr. Mark Novitch  
Washington, DC

Mr David R. Palmer  
David Ross Palmer & Associates  
Waquoit, Massachusetts

Mr and Mrs. Joseph P. Pellegrino  
Boston, Massachusetts

Mr Robert Pierce, Jr.  
Pierce Aluminum Co  
Franklin, Massachusetts

Mr. Manus A. Robinson  
Fundamental Investors Ltd  
Key Biscayne, Florida

Mr Edward Rowland  
Tucker Anthony, Inc.  
Boston, Massachusetts

Mr Andrew E. Sabin  
Sabin Metal Corporation  
East Hampton, New York

Ms. Linda Sallop  
Nathan Sallop Insurance Agency, Inc.  
Boston, Massachusetts

Mr. Gregory A. Sandomirsky  
Mintz Levin Cohen Ferris Glovsky & Popeo, PC  
Boston, Massachusetts

Dr Cecily C. Selby  
New York, New York

## ADMINISTRATIVE SUPPORT STAFF<sup>1</sup>

### Biological Bulletin

Greenberg, Michael J.,  
Editor-in-Chief  
Hinkle, Pamela Clapp,  
Managing Editor  
Child, Wendy  
Gibson, Victoria R  
Schachinger, Carol H

### Financial Services Office

Lane, Jr., Homer W., Chief  
Financial Officer  
McLean, David, Controller  
Mullen, Richard J., Manager,  
Research Administration  
Adams, Taryn  
Aguiar, Deborah  
Bliss, Casey M  
Brady, Caroline  
Crosby, Kenneth  
Griffin, Bonnie Jean  
Lancaster, Cindy  
Newman, Melissa  
Nunes, Kenda  
Solchenberger, Carolyn  
Stellrecht, Lynette

### Director's Office

Speck, William T., Director  
and Chief Executive Officer  
Donovan, Marcia H.

### Equal Employment Opportunity

MacNeil, Jane L

### Veterinarian Services

Smolowitz, Roxanna, Campus  
Veterinarian  
Allen, Taylor<sup>2</sup>  
Bonacci, Lisa<sup>2</sup>  
Dalpe, Heather  
Ehlen, Jill<sup>2</sup>  
Hancock, Amy<sup>2</sup>  
Stukey, Jetley

### Stock Room

Schorer, Timothy M., Supervisor  
Galatzer-Levy, David<sup>2</sup>  
Olive, Jr., Charles W.

### Purchasing

Hall Jr, Lionel E., Supervisor  
Hunt, Lisa M.  
Widdiss, Brittany<sup>2</sup>

### Educational Programs

Dawidowicz, Eliezar A., Director  
Hamel, Carol C.  
Holzworth, Kelly

### Central Microscopy Facility and General Use Rooms

Kerr, Louis M., Supervisor  
Histen, Gavin<sup>2</sup>  
Inzina, Jessica<sup>2</sup>  
Luther, Herbert  
Ogomo, Christopher On<sup>2</sup>  
Parmenter, Marjorie<sup>2</sup>  
Peterson, Martha B  
Scanlon, John<sup>2</sup>

### Housing and Conferences

Beckwith, Mary M., Director  
Fuglister, Charles K  
Grasso, Deborah  
Kruger, Sally J  
Livingstone, Suzanne  
Oldham, Pamela  
Perito, Diana  
Stackhouse, Barbara  
Wagner, Carol

### Housekeeping

Bailey, Jeffrey Jr.<sup>2</sup>  
Barnes, Susan M.  
Barron, Laura<sup>2</sup>  
Bernos, Jessica  
Chen, Zhi Xin  
Doherty, Bryant<sup>2</sup>  
Johnston, David<sup>2</sup>  
Hannigan, Catherine  
MacDonald, Cynthia C  
McNamara, Noreen M  
Santiago, Crystal  
Shum, Mei Wah  
Waterbury, Matthew<sup>2</sup>

### External Affairs

Carotenuto, Frank C., Director  
Butcher, Valerie  
Faxon, Wendy P  
George, Mary  
Johnson, A Kristine  
Patch-Wing, Dolores  
Quigley, Barbara A  
Shaw, Kathleen L

### Associates Program

Joslin, Susan  
Sgarzi, Dorothy J.

### Communications Office

Hinkle, Pamela Clapp, Director  
Hemmerdinger, Catherine  
Hartmann, Kelley<sup>2</sup>  
Hlista, Laurel<sup>2</sup>  
Langill, Christine<sup>2</sup>  
Liles, Beth R  
Mansfield, Samantha  
Mock-Munoz De Luna, Dana<sup>2</sup>  
Rullo, Gina

### Human Resources

Goux, Susan P., Director  
Damery, Angela<sup>2</sup>  
Houser, Carmen  
Snow, Linda

### J. Erik Jonsson Center, NAS

Carlisle, Ann<sup>2</sup>  
Doherty, Joanne  
Elchalt, Donald  
Shurtleff, Joan<sup>2</sup>



Photo by Volker Steger

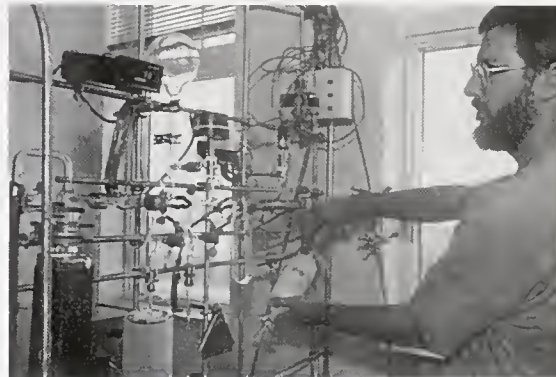


Photo by Elizabeth Armstrong

### Senior Staff

Mary Beckwith, Director of Housing and Conferences  
Frank Carotenuto, Director of External Affairs  
Richard Cutler, Director of Facilities and Services  
Lenny Dawidowicz, Director of Education  
Susan Goux, Director of Human Resources  
Roger Hanlon, Director of the Marine Resources Center  
Pamela Clapp Hinkle, Director of Communications  
Homer Lane, Chief Financial Officer  
Andrew Mattox, Environmental Health and Safety Manager  
Richard Mullen, Manager of Research Administration  
Cathy Norton, Director of the MBL/WHOI Library  
William T. Speck, Director and Chief Executive Officer

<sup>1</sup> Including persons who joined or left the staff during 2001

<sup>2</sup> Summer or temporary

## Support staff, continued

Josephine Bay Paul Center for  
Comparative Molecular  
Biology and Evolution

Lim, Pauline  
Nihill, Tara

## Marine Resources Center

Hanlon, Roger T., Director  
Maddux, Betty L S<sup>2</sup>  
Santore, Gabrielle

## Aquatic Resources Department

Enos, Jr., Edward G.,  
Superintendent  
Dimond, James L.<sup>2</sup>  
Grossman, William M.  
Klimm III, Henry W  
Sexton, Andrew W  
Sterling, Andrew<sup>2</sup>  
Sterling, Christian<sup>2</sup>  
Sullivan, Daniel A  
Tassinari, Eugene  
Whelan, Sean P

## MRC Life Support System

Mebane, William N., Systems  
Operator  
Carroll, James  
Hanley, Janice S  
Kuzirian, Alan  
Linnon, Beth

## MBL/WHOI LIBRARY

Norton, Catherine N., Director  
Uhlinger, Eleanor, Assistant  
Director, MBL Library  
Deveer, Joseph M  
Monahan, A Jean  
Nelson, Heidi  
Person, Matthew  
Reuter, Laura  
Riley, Jacqueline  
Stafford, Nancy  
Stout, Amy  
Walton, Jennifer

## Digital Processing Center

Clark, Sarah  
Hadway, Nancy  
Mannix, Jessica<sup>2</sup>  
Reuter, Laura  
Westburg, Joanne

## Information Technology Division

Inzina, Barbara, Network Manager  
Callahan, Michael<sup>2</sup>  
Cohen, Alex<sup>2</sup>  
Dematos, Christopher  
Fournier, Pamela  
Jones, Patricia L  
Leary, Patrick<sup>2</sup>  
Lowell, Gregory  
Mountford, Rebecca J  
Remsen, David P  
Renna, Denis J  
Space, David B  
Wagner, Paul<sup>2</sup>

NASA Center for Advanced  
Studies in the Space Life  
Sciences

Blazis, Diana, Administrator  
Farrell, Heather

## Safety Services

Mattox, Andrew H., Environmental,  
Health, and Safety Manager  
Elder, Kristopher<sup>2</sup>

## Research Space Administration

Kaufmann, Sandra J.

Satellite/Periwinkle Children's  
Programs

Robinson, Paulina H.<sup>2</sup>  
Butler, Meredith<sup>2</sup>  
Camire, Aaron<sup>2</sup>  
Guiffrida, Beth<sup>2</sup>  
Halter, Sarah<sup>2</sup>  
Karalekas, Nina<sup>2</sup>  
Langill, Susan<sup>2</sup>  
Leveque, Rachel<sup>2</sup>  
Noonan, Brendan<sup>2</sup>  
Noonan, Patrick<sup>2</sup>  
O'Connor, Caitlin<sup>2</sup>  
Orfila, Cecelia<sup>2</sup>  
Plourde, Anna<sup>2</sup>  
Sturbaum, Sonja<sup>2</sup>  
Swetish, Margaret<sup>2</sup>  
Swiniarski, Kathryn<sup>2</sup>  
Thamm, Jennifer<sup>2</sup>  
Urciuoli, Karen<sup>2</sup>  
Vachon, Julia<sup>2</sup>

## Services, Projects and Facilities

Cutler, Richard D., Director  
Enos, Joyce B  
Stackhouse, Aaron<sup>2</sup>

## Apparatus

Atwood, Paul  
Baptiste, Michael G  
Barnes, Franklin D  
Haskins, William A  
Pratt, Barry

## Transportation Services &amp; Grounds

Hayes, Joseph H., Supervisor  
Bailey, Jeffrey B  
Boucher, Richard L.  
Brereton, Richard S.<sup>2</sup>  
Clayton, Daniel  
Collins, Paul J  
Cutler, Matthew<sup>2</sup>  
Duane, James<sup>2</sup>  
Illgen, Robert F  
Malchow, Robert<sup>2</sup>  
McHugh, Clare<sup>2</sup>  
Mendoza, Guy<sup>2</sup>  
Rogers, William<sup>2</sup>  
Santoro, John<sup>2</sup>

## Plant Operations and Maintenance

Abbott, Thomas E., Supervisor  
Anderson, Lewis B  
Atwood, Paul R  
Auclair, Donald<sup>2</sup>  
Bailey, Jeffrey B  
Barnes, John S  
Bryant, Horace<sup>2</sup>  
Cadose, James W  
Callahan, John J  
Cormier, Garrett<sup>2</sup>  
Elias, Michael  
Ficher, Jason  
Goehl, George  
Gonsalves, Jr., Walter W  
Henderson, Jon R  
House, James  
Howell, Robert  
Langill, Richard  
Laurino, Frank  
Mancevice, Corinne<sup>2</sup>  
McAdams III, Herbert M  
McHugh, Michael O  
McQuillan, Jeffrey<sup>2</sup>

Mendoza, Duke  
Mills, Stephen A  
Pratt, Barry  
Rattacasa, Frank<sup>2</sup>  
Settlemyre, Donald  
Shepherd, Denise M  
Sullivan, Brendon  
Toner, Michael  
Ware, Lynn M.

## Security and Projects

Fleet, Barry M., Manager  
Blunt, Hugh F  
Fish Jr., David L.  
Hathaway, Peter J  
Kelley, Kevin  
Lochhead, William M.  
Rozum, John  
Scanlan, Melanie

## The Ecosystems Center

Cave, Anthony, Center Research  
Administrator  
Nunez, Guillermo, Center  
Research Administrator  
Berthel, Dorothy J.  
Donovan, Suzanne J.  
Seifert, Mary Ann

# MARINE RESOURCES CENTER

MARINE BIOLOGICAL LABORATORY • WOODS HOLE, MA 02543 • (508)289-7700

WWW.MBL.EDU/SERVICES/MRC/INDEX.HTML

## Animal and Tissue Supply for Education & Research

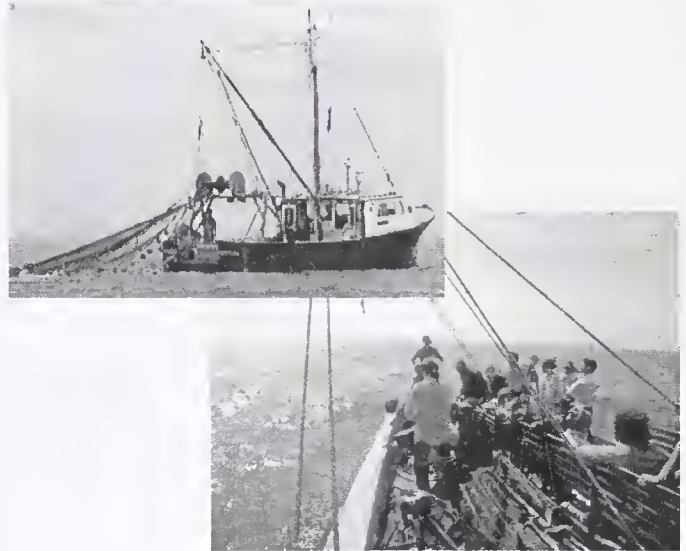
- 150 aquatic species available for shipment via online catalog: <<http://www.mbl.edu/animals/index.html>>; phone: (508)289-7375; or e-mail: [specimens@mbi.edu](mailto:specimens@mbi.edu)
- zebrafish colony containing limited mutant strains
- custom dissection and furnishing of specific organ and tissue samples



zebrafish facilities

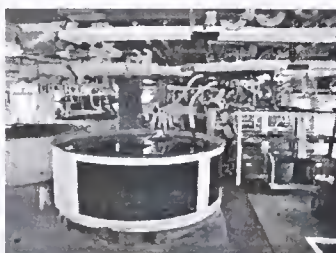
## MRC Services Available

- basic water quality analysis
- veterinary services (clinical, histopathologic, microbial services, health certificates, etc.)
- aquatic systems design (mechanical, biological, engineering, etc.)
- educational tours and collecting trips aboard the R/V Gemma

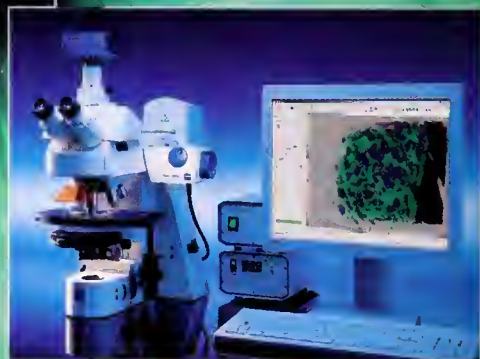
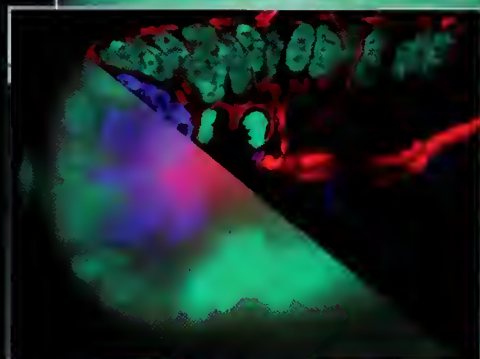


## Using the MRC for Your Research

- capability for advanced animal husbandry (temperature, light control, etc.)
- availability of year-round, developmental life stages
- adaptability of tank system design for live marine animal experimentation



# **New ApoTome** Suddenly everything looks different



**The evolution in fluorescence microscopy**

ApoTome. Nothing less than a minor revolution in fluorescence microscopy.

In z-direction, the ApoTome increases visible resolution by a factor of 2. Now you can display 2D & 3D images of optical sections

collected from the full sample with maximum contrast & optimal image quality. Even with the thick specimens of cell research.

For more information, call 800.233.2343.

Carl Zeiss MicroImaging, Inc. • Thornwood, NY 10594 • [micro@zeiss.com](mailto:micro@zeiss.com) • [zeiss.com/micro](http://zeiss.com/micro)



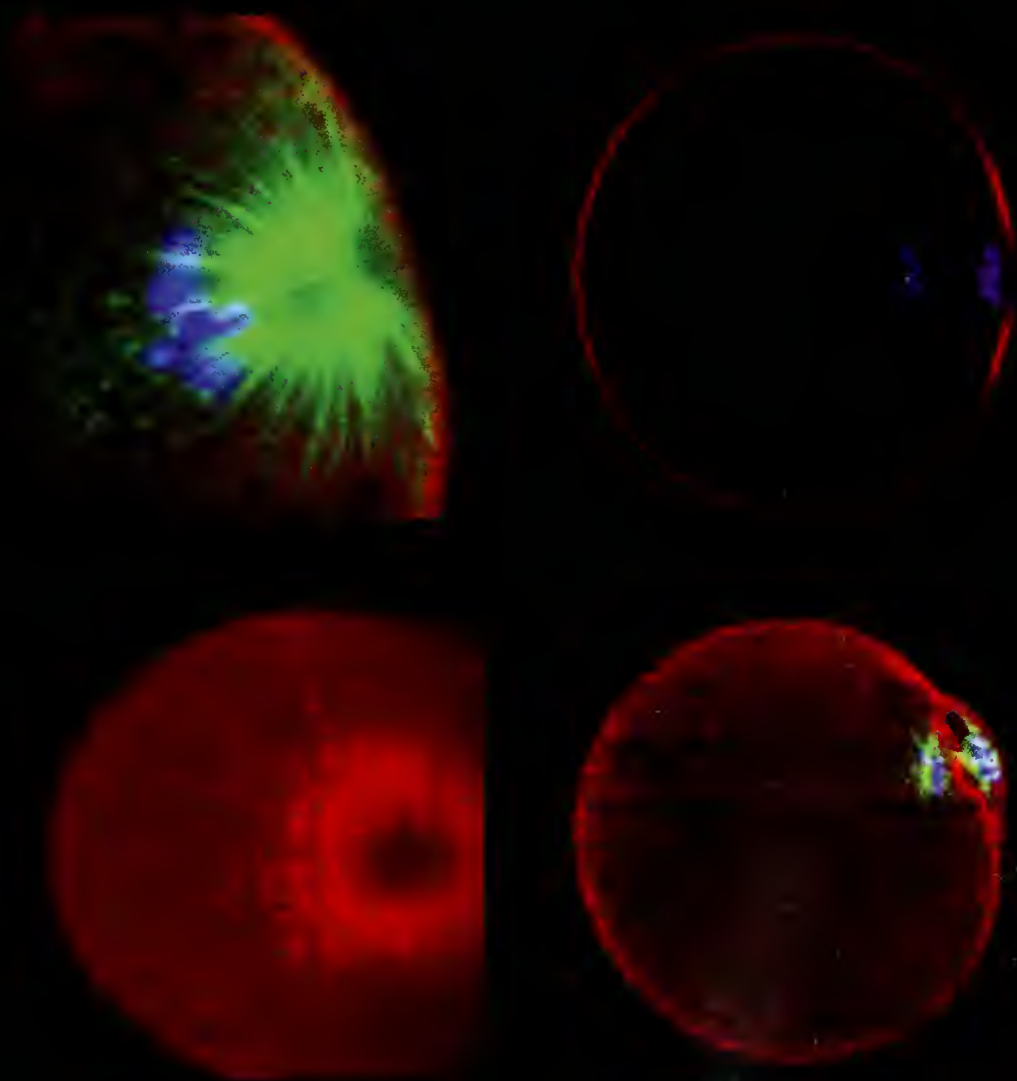
We make it visible.

October 2003

THE

Volume 205 • Number 2

# BIOLOGICAL BULLETIN



Published by the Marine Biological Laboratory

[www.biolbull.org](http://www.biolbull.org)



# THE BIOLOGICAL BULLETIN ONLINE

The Marine Biological Laboratory is pleased to announce that the full text of *The Biological Bulletin* is available online at

<http://www.biolbull.org>

*The Biological Bulletin* publishes outstanding experimental research on the full range of biological topics and organisms, from the fields of Neurobiology, Behavior, Physiology, Ecology, Evolution, Development and Reproduction, Cell Biology, Biomechanics, Symbiosis, and Systematics.

Published since 1897 by the Marine Biological Laboratory (MBL) in Woods Hole, Massachusetts, *The Biological Bulletin* is one of America's oldest peer-reviewed scientific journals.

The journal is aimed at a general readership, and especially invites articles about those novel phenomena and contexts characteristic of intersecting fields.

*The Biological Bulletin Online* contains the full content of each issue of the journal, including all figures and tables, beginning with the February 2001 issue (Volume 200, Number 1). The full text is searchable by keyword, and the cited references include hyperlinks to Medline. PDF files are available beginning in February 1990 (Volume 178, Number 1), some abstracts are available

beginning with the October 1976 issue (Volume 151, Number 2), and some Tables of Contents are online beginning with the October 1965 issue (Volume 129, Number 2).

Each issue will be placed online approximately on the date it is mailed to subscribers; therefore the online site will be available prior to receipt of your paper copy. Online readers may want to sign up for the eTOC (electronic Table of Contents) service, which will deliver each new issue's table of contents *via* e-mail. The web site also provides access to information about the journal (such as Instructions to Authors, the Editorial Board, and subscription information), as well as access to the Marine Biological Laboratory's web site and other *Biological Bulletin* electronic publications.

The free trial period for access to *The Biological Bulletin* online has ended. Individuals and institutions who are subscribers to the journal in print or are members of the Marine Biological Laboratory Corporation may now activate their online subscriptions. All other access (*e.g.*, to Abstracts, eTOCs, searching, Instructions to Authors) remains freely available. Online access is included in the print subscription price.

For more information about subscribing or activating your online subscription, visit [www.biolbull.org/subscriptions](http://www.biolbull.org/subscriptions).

---

<http://www.biolbull.org>

# SEEKERS IN THE SOCIETY OF CELLS.

At Dr. Simon Watkins' lab, they look at cells the way anthropologists look at human culture: as communities of good guys and bad guys, of traders and communicators, of connections and relationships. "We are the observers,"

Simon says. "We never jump to conclusions. We let the conclusions jump to us." His mantra? "Imaging is everything." Which is why the best and the brightest of tomorrow's seekers and solvers find their way to Pittsburgh and the Watkins Lab.

**OLYMPUS MICROSCOPES. ROCKET SCIENCE™**

Find out more about Olympus microscopes at [www.olympusamerica.com/microscopes](http://www.olympusamerica.com/microscopes) 800-455-8236

## OLYMPUS®

*(From L to R)*  
Ana Bursick - Research Specialist  
Stuart Shand - Research Specialist  
Simon C. Watkins, Ph.D. - Director  
Glenn Papwarth - Research Associate  
Ramesh Draviam - Graduate Student  
Center for Biologic Imaging,  
University of Pittsburgh Medical School,  
Pittsburgh, PA



## Cover

---

Mature eggs of the surf clam *Spisula solidissima* are arrested in prophase of the first meiotic division. When the eggs are activated by sperm or KCl, the first meiotic division is completed, the second meiotic division follows, and then (with sperm) embryonic development ensues. As in all meioses, the cleavages are very eccentric, and each produces a small polar body. Because very large numbers of *Spisula* eggs can be activated simultaneously, and thus form their polar bodies in near synchrony, these eggs are an excellent model with which to study, not only the usual embryonic cell division, but also polar body formation—an example of extremely asymmetrical cytokinesis.

In this issue of *The Biological Bulletin* (pp. 192–193), Rafal Pielak, Valeriya Gaysinskaya, and William D. Cohen report on the organization of F-actin and microtubules in meiotic stages that immediately precede the formation of polar bodies in *Spisula* eggs. The movements and locations of these structures were revealed by confocal fluorescence microscopy after appropriate staining (F-actin, red-orange; microtubules, green; chromosomes, blue-violet). Four images from the report—set upon a background of diagrammatic surf clams—appear on the cover (see scale bars in Fig. 1, p. 193).

At about 13 min after activation (23°C), the metaphase spindle of the first meiotic division is already fully formed and eccentrically positioned; it then moves toward the cell surface. In the upper left

image on the cover, microtubules of the peripheral aster curve outward along the F-actin-containing cortex, away from a microtubule-poor central region. At about 20 min post-activation, with the aster diminishing, the chromosomes are now arranged in anaphase (upper-right image), and a “bull’s-eye” F-actin ring—the cytokinetic ring—appears on the cortex (side view, upper right; computer-generated face view, lower left). Finally, at about 26 min post-activation, the peripheral nucleus and its remaining centrosomal material enter the F-actin-poor center of the ring to produce the first polar body (lower-right image).

These stages include critical activities—particularly, docking of the spindle with the cell cortex, and signaling to generate the cytokinetic contractile ring—that occur in all sexually reproducing animals by mechanisms yet unknown. But note that, at metaphase, the pattern and dimensions of the contact between the astral rays and the egg cortex approximate those of the F-actin ring at anaphase. This correspondence suggests that generation of the contractile ring is triggered by signals from the astral microtubule-cortex contact.

Rafal Pielak and Valeriya Gaysinskaya were summer 2003 research interns in Hunter College-Howard Hughes Medical Institute (HHMI) Undergraduate Biological Science Education Program at the Marine Biological Laboratory. The surf clam pattern on the cover was designed by William D. Cohen. The cover was designed by Beth Liles (Marine Biological Laboratory).

# THE BIOLOGICAL BULLETIN

## OCTOBER 2003

<b>Editor</b>	MICHAEL J. GREENBERG	The Whitney Laboratory, University of Florida
<b>Associate Editors</b>	LOUIS E. BURNETT R. ANDREW CAMERON CHARLES D. DERBY MICHAEL LABARBERA	Grice Marine Laboratory, College of Charleston California Institute of Technology Georgia State University University of Chicago
<b>Section Editor</b>	SHINYA INOUÉ, <i>Imaging and Microscopy</i>	Marine Biological Laboratory
<b>Online Editors</b>	JAMES A. BLAKE, <i>Keys to Marine Invertebrates of the Woods Hole Region</i> WILLIAM D. COHEN, <i>Marine Models Electronic Record and Compendia</i>	ENSR Marine & Coastal Center, Woods Hole Hunter College, City University of New York
<b>Editorial Board</b>	PETER B. ARMSTRONG JOAN CERDÁ ERNEST S. CHANG THOMAS H. DIETZ RICHARD B. EMLET DAVID EPEL KENNETH M. HALANYCH GREGORY HINKLE NANCY KNOWLTON MAKOTO KOBAYASHI ESTHER M. LEISE DONAL T. MANAHAN MARGARET MCFALL-NGAI MARK W. MILLER TATSUO MOTOKAWA YOSHITAKA NAGAHAMA SHERRY D. PAINTER J. HERBERT WAITE RICHARD K. ZIMMER	University of California, Davis Center of Aquaculture-IRTA, Spain Bodega Marine Lab., University of California, Davis Louisiana State University Oregon Institute of Marine Biology, Univ. of Oregon Hopkins Marine Station, Stanford University Auburn University, Alabama Millennium Pharmaceuticals, Cambridge, Massachusetts Scripps Inst. Oceanography & Smithsonian Tropical Res. Inst. Hiroshima University of Economics, Japan University of North Carolina Greensboro University of Southern California Kewalo Marine Laboratory, University of Hawaii Institute of Neurobiology, University of Puerto Rico Tokyo Institute of Technology, Japan National Institute for Basic Biology, Japan Marine Biomed. Inst., Univ. of Texas Medical Branch University of California, Santa Barbara University of California, Los Angeles
<b>Editorial Office</b>	PAMELA CLAPP HINKLE VICTORIA R. GIBSON CAROL SCHACHINGER WENDY CHILD	Managing Editor Staff Editor Editorial Associate Subscription & Advertising Administrator

Published by  
MARINE BIOLOGICAL LABORATORY  
WOODS HOLE, MASSACHUSETTS

<http://www.biolbull.org>

# 64-bit! Itanium<sup>®</sup> 2 and Opteron<sup>™</sup> Clusters

## Robust Solutions for Life Sciences Applications

### Itanium2, Opteron, Xeon, Athlon and Alpha Clusters

#### Expert Integration...

Microway offers innovative, competitively priced, custom designed clusters with NodeWatch<sup>™</sup> management and monitoring tools. Our solutions incorporate the latest processors, proprietary cooling and storage solutions, plus high-speed Myrinet and InfiniBand interconnects for both fine and coarse grain parallel applications.

#### Superior Service and Tech Support...

We understand that on-time delivery, out-of-the-box reliability and excellent ongoing technical support are critical to our users. Microway offers professional services from specialists with a wide range of expertise in HPC applications. On-site installations and training are also available.

#### Satisfied Customers...

ALTANA Research, EOS Biotechnology, GlaxoSmithKline, Johnson & Johnson, LION Bioscience, MBL, Millennium Pharmaceuticals, NIH, RIB-X Pharmaceuticals, Rockefeller University, US Air Force, Army, Navy, NASA, NOAA and hundreds of leading universities are among our satisfied customers since 1982.

"The Brain Imaging Research Center (a joint center of Carnegie Mellon University and University of Pittsburgh) decided to purchase our Linux cluster from Microway because of the proven performance of their clusters at Carnegie Mellon in the processing of high-volume brain imaging data. Microway was flexible and helpful at all stages, starting from the initial custom configuration and ending with timely delivery and full installation."

— Marcel Just, Co-Director, Brain Imaging Research Center

Call us first at **508-746-7341**

for quotations and benchmarking services.  
Find technical information, testimonials, and  
online newsletter at **www.microway.com**.

See us at **SC2003**, Booth 2227  
Phoenix — November 17-20



**CoolRak<sup>™</sup> Cabinet**  
Features 3 10" 535 CFM Fans, yielding 7 degrees cooler ambient per node. Available only on Microway 1U Opteron, Athlon and Xeon chassis.



**Microway 1U CoolRak<sup>™</sup>**  
features dual 2.8GHz Xeons with proprietary Across the Board<sup>™</sup> Cooling

### Innovative Technology and Services at Competitive Prices

- **Xeon XBlade<sup>™</sup> Technology by Microway**  
Incorporates two dual Xeon XBlades in our 1U chassis for 880 Gigaflops performance per 44U cabinet. Each Xeon XBlade provides two 133 MHz PCI-X sockets enabling next generation interconnects including InfiniBand.
- **NodeWatch<sup>™</sup>** provides automatic remote monitoring of vital cluster parameters and failsafe shutdown of the cluster. NodeWatch monitors temperatures, voltages, and chassis fans, runs as the master, and can be controlled by a secure web-based GUI. Available on Microway 1U Opteron, Xeon and Athlon chassis.
- **Integrated solutions powered by Platform Computing Workload Management and Grid Computing software solutions** to optimize computing resources. From Microway's Clusterware powered CW Series, to integration of LSF 5 on an Microway cluster, all Platform solutions are "gracefully ready" for future system enhancements.
- **Integrated professional MPI/Pro<sup>®</sup>** enhances cluster value with middleware for high performance, scalable and robust message passing.
- **Fully redundant, highly-available storage system** based on 2Gbit fiber channel technology for multi-terabyte storage requirements. State-of-the-art storage directors for full access to storage from any cluster node. Easily scales to address rapidly expanding storage requirements.
- **Consulting Services:** Microway offers expertise designing custom software for financial analysis, genomics, proteomics, plus data warehousing, project management tools, network/data center design, and lab integration/management systems

**Microway**  
Technology you can count on<sup>™</sup>



# CONTENTS

VOLUME 205, No. 2: OCTOBER 2003

## RESEARCH NOTE

- Seibel, Brad A., and Heidi M. Dierssen**  
Cascading trophic impacts of reduced biomass in the Ross Sea, Antarctica: Just the tip of the iceberg? . . . 93
- Lee, Raymond W.**  
Thermal tolerances of deep-sea hydrothermal vent animals from the Northeast Pacific . . . . . 98

## NEUROBIOLOGY AND BEHAVIOR

- Robison, Bruce H., Kim R. Reisenbichler, James C. Hunt, and Steven H. D. Haddock**  
Light production by the arm tips of the deep-sea cephalopod *Vampyroteuthis infernalis* . . . . . 102

## ECOLOGY OF PARASITES

- Fingerut, Jonathan T., Cheryl Ann Zimmer, and Richard K. Zimmer**  
Patterns and processes of larval emergence in an estuarine parasite system . . . . . 110

## DEVELOPMENT AND REPRODUCTION

- Gibson, Glenys D.**  
Larval development and metamorphosis in *Pleurobranchaea maculata*, with a review of development in the Notaspidea (Opisthobranchia) . . . . . 121

## ECOLOGY AND EVOLUTION

- Chadwick-Furman, Nanette E., and Irving L. Weissman**  
Effects of allogeneic contact on life-history traits of the colonial ascidian *Botryllus schlosseri* in Monterey Bay . . . . . 133
- Bell, J. J., and D. K. A. Barnes**  
Effect of disturbance on assemblages: an example using Porifera . . . . . 144

## PHYSIOLOGY AND BIOMECHANICS

- Hamdoun, Amro M., Daniel P. Cheney, and Gary N. Cherr**  
Phenotypic plasticity of HSP70 and HSP70 gene expression in the Pacific oyster (*Crassostrea gigas*): implications for thermal limits and induction of thermal tolerance . . . . . 160

## SHORT REPORTS FROM THE 2003 GENERAL SCIENTIFIC MEETINGS OF THE MARINE BIOLOGICAL LABORATORY

- The Editor**  
The MBL Awards for 2003 . . . . . 175

### DEVELOPMENTAL BIOLOGY

- Gilland, Edwin, Robert Baker, and Winfried Denk**  
Long duration three-dimensional imaging of calcium waves in zebrafish using multiphoton fluorescence microscopy . . . . . 176
- Gileadi, Opher, and Alon Sabban**  
Squid sperm to clam eggs: imaging wet samples in a scanning electron microscope . . . . . 177
- Wadeson, P. H., and K. Crawford**  
Formation of the blastoderm and yolk syncytial layer in early squid development . . . . . 179
- Crawford, K.**  
Lithium chloride inhibits development along the animal vegetal axis and anterior midline of the squid embryo . . . . . 181
- Hill, Susan D., and Barbara C. Boyer**  
HNK-1/N-CAM immunoreactivity correlates with ciliary patterns during development of the polychaete *Capitella* sp. 1 . . . . . 182

### CELL BIOLOGY

- Heck, D. E., and J. D. Laskin**  
Ryanodine-sensitive calcium flux regulates motility of *Arbacia punctulata* sperm . . . . . 185
- Gallant, P. E.**  
Axotomy inhibits the slow axonal transport of tubulin in the squid giant axon . . . . . 187

<b>Delacruz, John, Jeremiah R. Brown, and George M. Langford</b>	
Interactions between recombinant conventional squid kinesin and native myosin-V . . . . .	188
<b>DeSelm, Carl J., Jeremiah R. Brown, Renne Lu, and George M. Langford</b>	
Rab-GDI inhibits myosin V-dependent vesicle transport in squid giant axon . . . . .	190
<b>Pielak, R. M., V. A. Gaysinskaya, and W. D. Cohen</b>	
Cytoskeletal events preceding polar body formation in activated <i>Spisula</i> eggs. . . . .	192
<b>Shribak, Michael, and Rudolf Oldenburg</b>	
Three-dimensional birefringence distribution in reconstituted asters of <i>Spisula</i> oocytes revealed by scanned aperture polarized light microscopy . . . . .	194
<b>Wöllert, Torsten, Ana S. DePina, Carl J. DeSelm, and George M. Langford</b>	
Rho-kinase is required for myosin-II-mediated vesicle transport during M-phase in extracts of clam oocytes. . . . .	195
<b>Cusato, K., J. Zakevicius, and H. Ripps</b>	
An experimental approach to the study of gap-junction-mediated cell death . . . . .	197
<b>Tepsuporn, S., J. C. Kaltenbach, W. J. Kuhns, M. M. Burger, and X. Fernández-Busquets</b>	
Apoptosis in <i>Microciconia prolifera</i> allografts. . . . .	199
<b>Armstrong, Peter B., and Margaret T. Armstrong</b>	
The decorated clot: binding of agents of the innate immune system to the fibrils of the <i>Limulus</i> blood clot. . . . .	201
<b>Isakova, Victoria, and Peter B. Armstrong</b>	
Imprisonment in a death-row cell: the fates of microbes entrapped in the <i>Limulus</i> blood clot . . . . .	203
<b>Harrington, John M., and Peter B. Armstrong</b>	
A liposome-permeating activity from the surface of the carapace of the American horseshoe crab, <i>Limulus polyphemus</i> . . . . .	205

NEUROBIOLOGY AND BEHAVIOR

<b>Bogorff, Daniel J., Mark A. Messerli, Robert P. Malchow, and Peter J. S. Smith</b>	
Development and characterization of a self-referencing glutamate-selective micro-biosensor . . . . .	207
<b>Chappell, R. L., J. Zakevicius, and H. Ripps</b>	
Zinc modulation of hemichannel currents in <i>Xenopus</i> oocytes. . . . .	209
<b>Zottoli, S. J., O. T. Burton, J. A. Chambers, R. Eseh, L. M. Gutiérrez, and M. M. Kron</b>	
Transient use of tricaine to remove the telencephalon has no residual effects on physiological recordings of supramedullary/dorsal neurons of the cunner, <i>Tautoglabrus adspersus</i> . . . . .	211
<b>Redenti, S., and R. L. Chappell</b>	
Zinc chelation enhances the sensitivity of the ERG b-wave in dark-adapted skate retina . . . . .	213

<b>Molina, Anthony J. A., Katherine Hammar, Richard Sanger, Peter J. S. Smith, and Robert P. Malchow</b>	
Intracellular release of caged calcium in skate horizontal cells using fine optical fibers . . . . .	215
<b>Palmer, L. M., B. A. Giuffrida, and A. F. Mensinger</b>	
Neural recordings from the lateral line in free-swimming toadfish, <i>Opsanus tau</i> . . . . .	216
<b>Child, F. M., H. T. Epstein, A. M. Kuzirian, and D. L. Alkon</b>	
Memory reconsolidation in <i>Hermisenda</i> . . . . .	218
<b>Kuzirian, A. M., F. M. Child, H. T. Epstein, M. E. Motta, C. E. Oldenburg, and D. L. Alkon</b>	
Training alone, not the tripeptide RGD, modulates calcitonin in <i>Hermisenda</i> . . . . .	220
<b>Savage, Anna, and Jelle Atema</b>	
Neurochemical modulation of behavioral response to chemical stimuli in <i>Homarus americanus</i> . . . . .	222
<b>Mann, K. D., E. R. Turnell, J. Atema, and G. Gerlach</b>	
Kin recognition in juvenile zebrafish ( <i>Danio rerio</i> ) based on olfactory cues. . . . .	224
<b>Turnell, E. R., K. D. Mann, G. G. Rosenthal, and G. Gerlach</b>	
Mate choice in zebrafish ( <i>Danio rerio</i> ) analyzed with video-stimulus techniques . . . . .	225

MOLECULAR BIOLOGY, PATHOLOGY, AND MICROBIOLOGY

<b>Roberts, S. B., and F. W. Goetz</b>	
Expressed sequence tag analysis of genes expressed in the bay scallop, <i>Argopecten irradians</i> . . . . .	227
<b>Hsu, A. C., and R. M. Smolowitz</b>	
Scanning electron microscopy investigation of epizootic lobster shell disease in <i>Homarus americanus</i> . . . . .	228
<b>Orchard, Elizabeth, Eric Webb, and Sonya Dyhrman</b>	
Characterization of phosphorus-regulated genes in <i>Trichodesmium</i> spp. . . . .	230
<b>Galac, Madeline, Deana Erdner, Donald M. Anderson, and Sonya Dyhrman</b>	
Molecular quantification of toxic <i>Alexandrium fundyense</i> in the Gulf of Maine . . . . .	231
<b>Sangster, C. R., and R. M. Smolowitz</b>	
Description of <i>Vibrio alginolyticus</i> infection in cultured <i>Sepia officinalis</i> , <i>Sepia apama</i> , and <i>Sepia pharaonis</i> . . . . .	233
<b>Baird, Krystal D., Hemant M. Chikarmane, Roxanna Smolowitz, and Kevin R. Uhlinger</b>	
Detection of <i>Edwardsiella</i> infections in <i>Opsanus tau</i> by polymerase chain reaction. . . . .	235
<b>Weidner, Earl, and Ann Findley</b>	
Catalase in microsporidian spores before and during discharge . . . . .	236

ECOLOGY AND POPULATION BIOLOGY

<b>Agnew, A. M., D. H. Shull, and R. Buchsbaum</b>	
Growth of a salt marsh invertebrate on several species of marsh grass detritus . . . . .	238

<b>Cavatorta, Jason R., Morgan Johnston, Charles Hopkinson, and Vinton Valentine</b> Patterns of sedimentation in a salt marsh-dominated estuary . . . . .	239	<b>Morgan, J. A., A. B. Aguiar, S. Fox, M. Teichberg, and I. Valiela</b> Relative influence of grazing and nutrient supply on growth of the green macroalga <i>Ulva lactuca</i> in estuaries of Waquoit Bay, Massachusetts . . . . .	252
<b>Thoms, T., A. E. Giblin, K. H. Foreman</b> Multiple approaches to tracing nitrogen loss in the West Falmouth wastewater plume . . . . .	242	<b>O'Connell, C. W., S. P. Grady, A. S. Leschen, R. H. Carmichael, and I. Valiela</b> Stable isotopic assessment of site loyalty and relationships between size and trophic position of the Atlantic horseshoe crab, <i>Limulus polyphemus</i> , within Cape Cod estuaries . . . . .	254
<b>Talbot, J. M., K. D. Kroeger, A. Rago, M. C. Allen, and M. A. Charette</b> Nitrogen flux and speciation through the subterranean estuary of Waquoit Bay, Massachusetts . . . . .	244	<b>Walker, C., E. Davidson, W. Kinglerlee, and K. Savage</b> Incubation conditions of forest soil yielding maximum dissolved organic nitrogen concentrations and minimal residual nitrate . . . . .	256
<b>Abraham, D. M., M. A. Charette, M. C. Allen, A. Rago, and K. D. Kroeger</b> Radiochemical estimates of submarine groundwater discharge to Waquoit Bay, Massachusetts . . . . .	245	<b>Holden, M. T., C. Lippitt, R. G. Pontius, Jr., and C. Williams</b> Building a database of historic land cover to detect landscape change . . . . .	257
<b>Johnston, M. E., J. R. Cavatorta, C. S. Hopkinson, and V. Valentine</b> Importance of metabolism in the development of salt marsh ponds . . . . .	248		
<b>Aguiar, A. B., J. A. Morgan, M. Teichberg, S. Fox, and I. Valiela</b> Transplantation and isotopic evidence of the relative effects of ambient and internal nutrient supply on the growth of <i>Ulva lactuca</i> . . . . .	250		
		<i>ORAL PRESENTATIONS</i>	
		Published by title only . . . . .	259

#### Notice to Subscribers

2004 SUBSCRIPTION RATES FOR *THE BIOLOGICAL BULLETIN*  
Prices include print and electronic versions

	Libraries	Individuals
Per year (six issues, two volumes):	\$325.00	\$120.00
Per volume (three issues):	\$165.00	\$70.00
Back and single issues (subject to availability):	\$75.00	\$25.00

For additional information, please contact our subscription administrator at the Maine Biological Laboratory, 7 MBL Street, Woods Hole, MA 02543; tel: (508) 289-7402; e-mail: [wchild@mbl.edu](mailto:wchild@mbl.edu). Visit our website at [www.biolbull.org](http://www.biolbull.org)

## THE BIOLOGICAL BULLETIN

THE BIOLOGICAL BULLETIN is published six times a year by the Marine Biological Laboratory, 7 MBL Street, Woods Hole, Massachusetts 02543.

Corrections and similar matter should be addressed to Subscription Administrator, THE BIOLOGICAL BULLETIN, Marine Biological Laboratory, 7 MBL Street, Woods Hole, Massachusetts 02543. Subscription rates for both print and online journals. Subscription per year (six issues, two volumes): \$280 for libraries; \$105 for individuals. Subscription per volume (three issues): \$140 for libraries; \$52.50 for individuals. Back and single issues (subject to availability): \$50 for libraries; \$20 for individuals.

Communications relative to manuscripts should be sent to Michael J. Greenberg, Editor-in-Chief, or Pamela Clapp Hinkle, Managing Editor, at the Marine Biological Laboratory, 7 MBL Street, Woods Hole, Massachusetts 02543. Telephone: (508) 289-7149. FAX: 508-289-7922. E-mail: pclapp@mbl.edu.

---

<http://www.biolbull.org>

---

THE BIOLOGICAL BULLETIN is indexed in bibliographic services including *Index Medicus* and MEDLINE, *Chemical Abstracts*, *Current Contents*, *Elsevier BIOBASE/Current Awareness in Biological Sciences*, and *Geo Abstracts*.

Printed on acid free paper,  
effective with Volume 180, Issue 1, 1991.

---

POSTMASTER: Send address changes to THE BIOLOGICAL BULLETIN, Marine Biological Laboratory, 7 MBL Street, Woods Hole, MA 02543.

Copyright © 2003, by the Marine Biological Laboratory

Periodicals postage paid at Woods Hole, MA, and additional mailing offices.

ISSN 0006-3185

---

## INSTRUCTIONS TO AUTHORS

*The Biological Bulletin* accepts outstanding original research reports of general interest to biologists throughout the world. Papers are usually of intermediate length (10–40 manuscript pages). A limited number of solicited review papers may be accepted after formal review. A paper will usually appear within four months after its acceptance.

Very short, especially topical papers (less than 9 manuscript pages including tables, figures, and bibliography) will be published in a separate section entitled "Research Notes." A Research Note in *The Biological Bulletin* follows the format of similar notes in *Nature*. It should open with a summary paragraph of 150 to 200 words comprising the introduction and the conclusions. The rest of the text should continue on without subheadings, and there should be no more than 30 references. References should be referred to in the text by number, and listed in the Literature Cited section in the order that they appear in the text. Unlike references in *Nature*, references in the Research Notes section should conform in punctuation and arrangement to the style of recent issues of *The Biological Bulletin*. Materials and Methods should be incorporated into appropriate figure legends. See the article by Lohmann *et al.* (October 1990, Vol. 179: 214–218) for sample style. A Research Note will usually appear within two months after its acceptance.

The Editorial Board requests that regular manuscripts conform to the requirements set below; those manuscripts that do not conform will be returned to authors for correction before review.

**1. Manuscripts.** Manuscripts, including figures, should be submitted in quadruplicate, with the originals clearly marked. (Xerox copies of photographs are not acceptable for review purposes.) If possible, please include an electronic copy of the text of the manuscript. Label the disk with the name of the first author and the name and version of the wordprocessing software used to create the file. If the file was not created in some version of Microsoft Word, save the text in rich text format (rtf). The submission letter accompanying the manuscript should include a telephone number, a FAX number, and (if possible) an E-mail address for the corresponding author. The original manuscript must be typed in no smaller than 12 pitch or 10 point, using double spacing (including figure legends, footnotes, bibliography, etc.) on one side of 16- or 20-lb. bond paper, 8 by 11 inches. Please, no right justification. Manuscripts should be proofread carefully and errors corrected legibly in black ink. Pages should be numbered consecutively. Margins on all sides should be at least 1 inch (2.5 cm). Manuscripts should conform to the *Council of Biology Editors Style Manual*, 5th Edition (Council of Biology Editors, 1983) and to American spelling. Unusual abbreviations should be kept to a minimum and should be spelled out on first reference as well as defined in a footnote on the title page. Manuscripts should be divided into the following components: Title page. Abstract (of no more than 200 words). Introduction, Materials and Methods, Results, Discussion, Acknowledgments, Literature Cited, Tables, and Figure Legends. In addition, authors should supply a list of words and phrases under which the article should be indexed.

2. **Title page.** The title page consists of a condensed title or running head of no more than 35 letters and spaces, the manuscript title, authors' names and appropriate addresses, and footnotes listing present addresses, acknowledgments or contribution numbers, and explanation of unusual abbreviations.

3. **Figures.** The dimensions of the printed page, 7 by 9 inches, should be kept in mind in preparing figures for publication. We recommend that figures be about 1 times the linear dimensions of the final printing desired, and that the ratio of the largest to the smallest letter or number and of the thickest to the thinnest line not exceed 1:1.5. Explanatory matter generally should be included in legends, although axes should always be identified on the illustration itself. Figures should be prepared for reproduction as either line cuts or halftones. Figures to be reproduced as line cuts should be unmounted glossy photographic reproductions or drawn in black ink on white paper, good-quality tracing cloth or plastic, or blue-lined coordinate paper. Those to be reproduced as halftones should be mounted on board, with both designating numbers or letters and scale bars affixed directly to the figures. All figures should be numbered in consecutive order, with no distinction between text and plate figures and cited, in order, in the text. The author's name and an arrow indicating orientation should appear on the reverse side of all figures.

**Digital art:** *The Biological Bulletin* will accept figures submitted in electronic form; however, digital art must conform to the following guidelines. Authors who create digital images are wholly responsible for the quality of their material, including color and halftone accuracy.

**Format.** Acceptable graphic formats are TIFF and EPS. Color submissions must be in EPS format, saved in CMYK mode.

**Software.** Preferred software is Adobe Illustrator or Adobe Photoshop for the Mac and Adobe Photoshop for Windows. Specific instructions for artwork created with various software programs are available on the Web at the Digital Art Information Site maintained by Cadmus Professional Communications at <http://cpc.cadmus.com/da/>

**Resolution.** The minimum requirements for resolution are 1200 DPI for line art and 300 for halftones.

**Size.** All digital artwork must be submitted at its actual printed size so that no scaling is necessary.

**Multipanel figures.** Figures consisting of individual parts (e.g., panels A, B, C) must be assembled into final format and submitted as one file.

**Hard copy.** Files must be accompanied by hard copy for use in case the electronic version is unusable.

**Disk identification.** Disks must be clearly labeled with the following information: author name and manuscript number; format (PC or Macintosh); name and version of software used.

**Color:** *The Biological Bulletin* will publish color figures and plates, but must bill authors for the actual additional cost of printing in color. The process is expensive, so authors with more than one color image should—consistent with editorial concerns, especially citation of figures in order—combine them into a single plate to reduce the expense. On request, when supplied with a copy of a color illustration, the editorial staff will provide a pre-publication estimate of the printing cost.

4. **Tables, footnotes, figure legends, etc.** Authors should follow the style in a recent issue of *The Biological Bulletin* in

preparing table headings, figure legends, and the like. Because of the high cost of setting tabular material in type, authors are asked to limit such material as much as possible. Tables, with their headings and footnotes, should be typed on separate sheets, numbered with consecutive Arabic numerals, and placed after the Literature Cited. Figure legends should contain enough information to make the figure intelligible separate from the text. Legends should be typed double spaced, with consecutive Arabic numbers, on a separate sheet at the end of the paper. Footnotes should be limited to authors' current addresses, acknowledgments or contribution numbers, and explanation of unusual abbreviations. All such footnotes should appear on the title page. Footnotes are not normally permitted in the body of the text.

5. **Literature cited.** In the text, literature should be cited by the Harvard system, with papers by more than two authors cited as Jones *et al.*, 1980. Personal communications and material in preparation or in press should be cited in the text only, with author's initials and institutions, unless the material has been formally accepted and a volume number can be supplied. The list of references following the text should be headed Literature Cited, and must be typed double spaced on separate pages, conforming in punctuation and arrangement to the style of recent issues of *The Biological Bulletin*. Citations should include complete titles and inclusive pagination. Journal abbreviations should normally follow those of the U. S. A. Standards Institute (USASI), as adopted by BIOLOGICAL ABSTRACTS and CHEMICAL ABSTRACTS, with the minor differences set out below. The most generally useful list of biological journal titles is that published each year by BIOLOGICAL ABSTRACTS (BIOSIS List of Serials; the most recent issue). Foreign authors, and others who are accustomed to using THE WORLD LIST OF SCIENTIFIC PERIODICALS, may find a booklet published by the Biological Council of the U.K. (obtainable from the Institute of Biology, 41 Queen's Gate, London, S.W.7, England, U.K.) useful, since it sets out the WORLD LIST abbreviations for most biological journals with notes of the USASI abbreviations where these differ. CHEMICAL ABSTRACTS publishes quarterly supplements of additional abbreviations. The following points of reference style for THE BIOLOGICAL BULLETIN differ from USASI (or modified WORLD LIST) usage:

A. Journal abbreviations, and book titles, all underlined (for italics)

B. All components of abbreviations with initial capitals (not as European usage in WORLD LIST e.g., *J. Cell. Comp. Physiol.* NOT *J. cell. comp. Physiol.*)

C. All abbreviated components must be followed by a period, whole word components *must not* (i.e., *J. Cancer Res.*)

D. Space between all components (e.g., *J. Cell. Comp. Physiol.*, not *J.Cell.Comp.Physiol.*)

E. Unusual words in journal titles should be spelled out in full, rather than employing new abbreviations invented by the author. For example, use *Rit Vísindafjélag Íslendinga* without abbreviation.

F. All single word journal titles in full (e.g., *Veliger*, *Ecology*, *Brain*).

G. The order of abbreviated components should be the same as the word order of the complete title (*i.e.*, *Proc.* and *Trans.* placed where they appear, not transposed as in some BIOLOGICAL ABSTRACTS listing).

H. A few well-known international journals in their preferred forms rather than WORLD LIST or USASI usage (*e.g.*, *Nature*, *Science*, *Evolution* NOT *Nature, Lond.*, *Science, N.Y.*; *Evolution, Lancaster, Pa.*)

6. *Sequences.* By the time a paper is sent to the press, all nucleotide or amino acid sequences and associated alignments should have been deposited in a generally accessible database

(*e.g.*, GenBank, EMBL, SwissProt), and the sequence accession number should be provided.

7. *Reprints, page proofs, and charges.* Authors may purchase reprints in lots of 100. Forms for placing reprint orders are sent with page proofs. Reprints normally will be delivered about 2 to 3 months after the issue date. Authors will receive page proofs of articles shortly before publication. They will be charged the current cost of printers' time for corrections to these (other than corrections of printers' or editors' errors). Other than these charges for authors' alterations, *The Biological Bulletin* does not have page charges.

## Cascading Trophic Impacts of Reduced Biomass in the Ross Sea, Antarctica: Just the Tip of the Iceberg?

BRAD A. SEIBEL\* AND HEIDI M. DIERSSEN†

*Monterey Bay Aquarium Research Institute, Moss Landing, California 95039*

*A significant reduction in phytoplankton biomass in the Ross Sea was reported in the austral summer of 2000–2001, a possible consequence of a disruption in sea-ice retreat due to the presence of an immense iceberg, B15 (1) (Fig. 1). Our observations in McMurdo Sound suggest temporally and trophically cascading impacts of that depression in productivity. Reduced phytoplankton stocks clearly affected the pteropod *Limacina helicina* (Phipps, 1774) (Gastropoda: Mollusca), an abundant primary consumer in the region (2, 3), as indicated by depressed metabolic rates in 2000–2001. The following season, for the first time on record, *L. helicina* was absent from McMurdo Sound. Many important predators, including whales and fishes, rely heavily on *L. helicina* for food (3, 4). However, most obviously impacted by its absence was *Clione antarctica* (Smith, 1902), an abundant pteropod mollusc (Gastropoda) that feeds exclusively on *L. helicina* (5). Metabolic rates of *C. antarctica* were depressed by 50% in 2001–2002. Both *L. helicina* and *C. antarctica* are important components of polar ecosystems and may be good indicators of overall ecosystem “health” in McMurdo Sound and perhaps in the Ross Sea. In this last austral summer, 2002–2003, sea-ice extent was much higher and phytoplankton stocks were dramatically lower than any reported previously, effects possibly associated with El Niño conditions, and we hypothesize that pteropods and their consumers may be further impacted.*

In the Southern Ocean, phytoplankton production is linked strongly to the seasonal oscillations in the extent of the sea ice (6, 7) and survival of higher trophic levels is

dependent on reproductive cycles that are synchronous with phytoplankton blooms. This is especially true of the direct food link between *L. helicina* and *C. antarctica*. *L. helicina* lives and feeds in the water column by extending a web of mucus that traps phytoplankton and, to a lesser extent, small zooplankton (3). *L. helicina* is the exclusive food source of *C. antarctica* throughout the life cycle, and the two species have parallel life histories. They grow in concert, with the preferred prey size increasing with predator size (3). Such specificity within the context of a highly seasonal environment requires precise timing to ensure that predator and prey coexist. The coevolved predator-prey relationship between *L. helicina* and *C. antarctica* provides a unique opportunity to study the ecological and trophic consequences of a depression in primary productivity in the Ross Sea.

A 50% to 75% reduction in phytoplankton biomass, estimated as chlorophyll *a* (Chl) concentrations, and high sea-ice cover was observed in December 2000–2001 relative to previous years (Table 1; Fig. 2; 8). A limited bloom did form by February, but annual primary production was still only 60% of the previous year (1). We believe that the reduced phytoplankton stocks in 2000–2001 had pronounced impacts on the condition of primary consumers in the region, causing cascading effects through higher trophic levels in the following year. This assertion is supported here by a series of metabolic measurements made on *L. helicina* and *C. antarctica* between 1999 and 2002.

Nutritional state is known to be among the primary determinants of metabolism in all organisms, including pteropods (3), and is especially important in the highly seasonal Antarctic environment (9, 10). Food availability will influence, among other things, the rates of protein synthesis, oxygen consumption, growth, and reproduction (9–11). We collected *L. helicina* and *C. antarctica* at four sampling stations along Ross Island (Fig. 1) and measured the oxygen

Received 20 November 2002; accepted 21 July 2003.

\* To whom correspondence should be addressed. Current address: 100 Flagg Road, Biological Sciences Center, Biological Sciences Department, University of Rhode Island, Kingston, RI 02881. E-mail: seibel@uri.edu

† Current address: Department of Marine Sciences, University of Connecticut at Avery Point, 1080 Shennecosset Road, Groton, CT 06340.

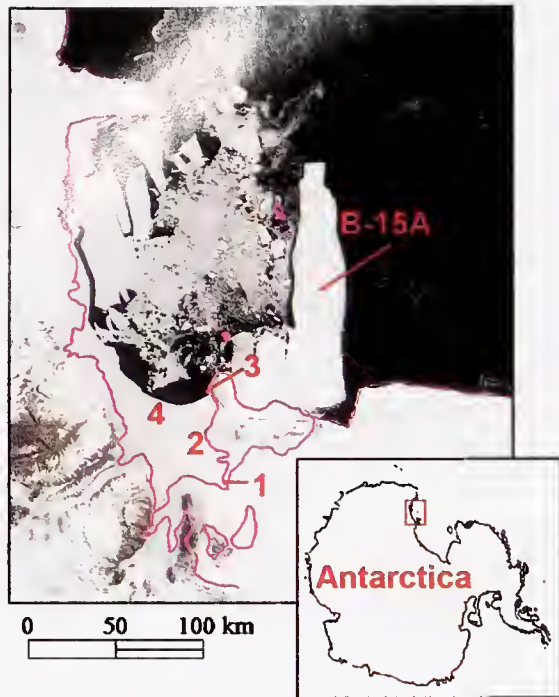


**Figure 1.** True-color imagery of McMurdo Sound and the iceberg B15A in the Ross Sea, Antarctica, on 26 December 2001. Imagery is from the Moderate Resolution Imaging Spectroradiometer (MODIS) (33) at 250-m resolution. Sites on Ross Island where pteropod specimens were collected are marked 1, McMurdo Station; 2, Cape Royds; 3, Cape Bird; and 4, ice edge.

consumption rates of both species in January of 1999, 2001, and 2002, using end-point analysis as described previously (12, 13). The measurement temperature in all analyses was

–1.86 °C, which is the year-round ambient temperature in McMurdo Sound. The oxygen consumption rates of *L. helicina* in 2001 were reduced by more than 30% relative to those measured in 1999 (Table 1). This reduction was presumably a result of food deprivation due to reduced phytoplankton stocks, although we cannot rule out a possible additional influence of changes in food quality (*i.e.*, species composition may also have changed from 1999 to 2001). The following season, phytoplankton stocks were elevated; but for the first time on record (see below), *L. helicina* was not found at any station sampled.

As a monophagous predator, *C. antarctica* was heavily impacted by the absence of its prey in McMurdo Sound. The oxygen consumption rates measured for this species in 2002 are only 50% of those measured in previous years (Table 1; Fig. 3). We also conducted laboratory experiments in 2001 in which specimens of *C. antarctica* were deprived of food for 3 weeks. Over the first 14 days, metabolic rates declined gradually to about 50% of control (wild-caught and laboratory-fed animals) levels. The 2002 rates correspond closely to those of individuals deprived of food in 2001, strongly supporting the suggestion that the depressed rates resulted from the extended absence of *L. helicina* in the region.

*C. antarctica*, like many polar zooplankton (14, 15), accumulates large lipid stores (5% wet mass) during the productive spring and summer months, presumably for survival through the winter and production of eggs that are released the following spring (16). With a depressed metabolic rate of  $0.99 \mu\text{mol} (0.022 \text{ ml}) \text{ O}_2 \text{ g}^{-1} \text{ h}^{-1}$  (Table 1), an oxy-calorific conversion of  $4.7 \text{ kcal l}^{-1} \text{ O}_2$ , and an energy content of  $9.4 \text{ kcal g}^{-1}$  lipid, a 100-mg animal could survive nearly 6 months on lipid alone, but at the expense of

**Table 1**

*Impacts of reduced biomass on trophic dynamics*

	1997–1998	1998–1999	1999–2000	2000–2001	2001–2002	2002–2003
Mean chlorophyll <i>a</i> ( $\text{mg m}^{-3}$ ) in the Western Ross Sea (See Fig. 2 for details)						
December	2.1	3.9	3.4	1.0	5.4	0.56
January	1.6	1.5	3.1	2.2	3.4	0.56
Fraction of the Western Ross Sea covered with sea ice (See Fig. 2 for details) <sup>1</sup>						
December	0.72	0.50	0.31	0.66	0.30	0.88
January	0.52	0.29	0.16	0.57	0.20	0.78
Oxygen consumption rate ( $\mu\text{mol O}_2 \text{ g}^{-1} \text{ h}^{-1}$ ), mean $\pm$ SE( <i>n</i> ): data pooled from all collection sites (Fig. 1) <sup>2</sup>						
<i>Limacina</i>	n.d.	$5.51 \pm 0.4$ (12)	n.d.	$3.78 \pm 0.20$ (22)*	absent	present
<i>Clione</i>	n.d.	$1.93 \pm 0.21$ (10)	n.d.	$2.04 \pm 0.12$ (31)	$0.99 \pm 0.05$ (30)*	present
<i>Clione</i> starved				$0.96 \pm 0.10$ (7)*		

<sup>1</sup> Sea ice cover determined as the fraction of Western Ross Sea not covered by open water, as shown in Fig. 2.

<sup>2</sup> n.d., no data; \*indicates that oxygen consumption rates were significantly different from those in 1998–1999 ( $P < 0.01$ ).

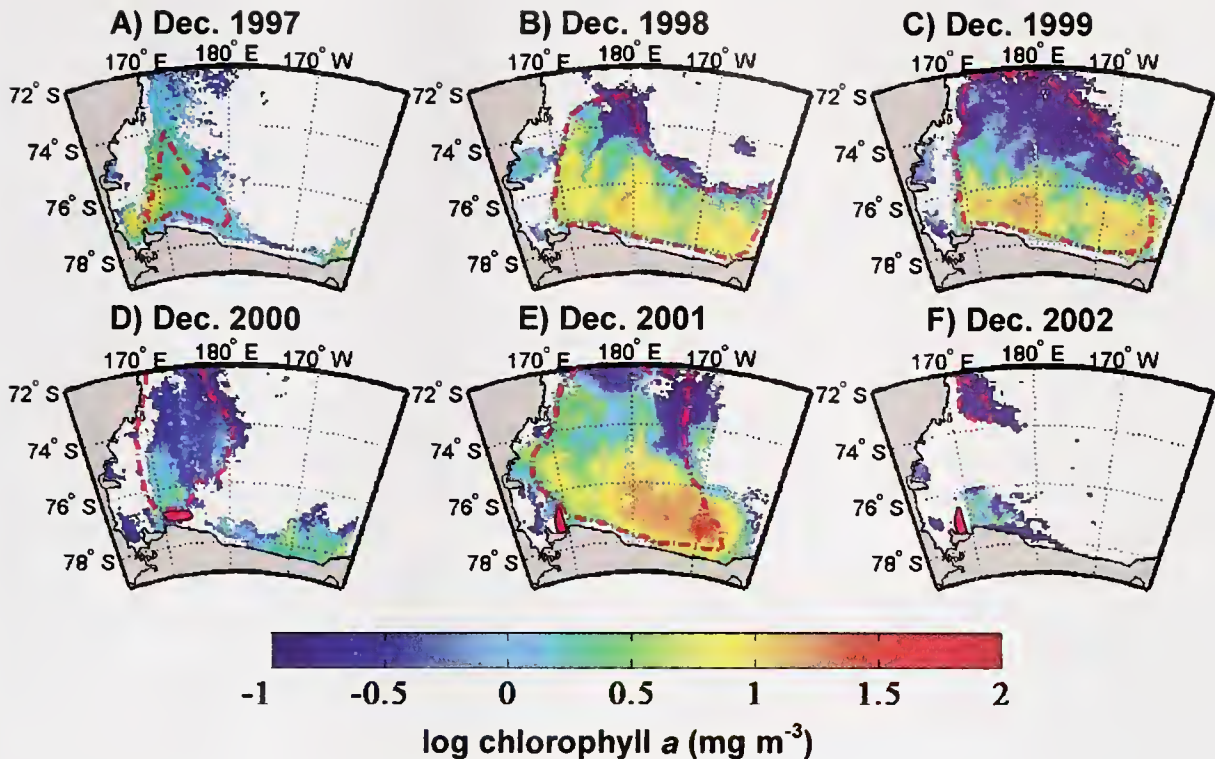


**Figure 2.** Ross Sea chlorophyll *a* (Chl) concentrations, representing the monthly mean of sea-ice-free pixels at 9-km resolution, derived from satellite ocean color imagery obtained from Sea-viewing Wide Field-of-view Sensor (SeaWiFS; Level 3 Standard Mapped Image, Reprocessing #4) (33) for December 1997 (A)–2002 (F). Gray areas designate land and white areas indicate the presence of sea ice. The dashed magenta line represents the average extent of sea ice determined from passive microwave satellite data (SSM/I NASA Team Algorithm). The sea ice extent and Chl data reported in Table 1 were determined from the area within this line. The location of the B15A iceberg is shown as a solid magenta shape.

reproduction. A positive correlation between egg production and availability of food (*i.e.*, *Limacina*) has been demonstrated in the laboratory for *C. limacina* (3).

*L. helicina* is typically abundant throughout the Southern Ocean, sometimes displacing krill as the dominant zooplankton (17). In McMurdo Sound, *L. helicina* may constitute more than 20% of the zooplankton biomass and reach concentrations exceeding 300 individuals per cubic meter along the ice edge (18, 19). *L. helicina* is also an important prey item for a number of other species in the Antarctic, including whales and myctophid and notothenioid fishes (4, 20), themselves important components in the diet of penguins and mammals (21, 22). Although *Clione limacina*, the northern hemisphere congener of *C. antarctica*, has also been reported in the diet of fishes and whales (3), *C. antarctica* may have limited importance for higher trophic levels in McMurdo Sound because it produces a novel “anti-feedant” compound (19). However, both *L. helicina* and *C. antarctica* are functionally important components of the ecosystem with the potential to influence phytoplankton stocks (18), carbon flux (23), and dimethyl sulfide (DMS) levels (24) that, in turn, influence global climate through

ocean-atmosphere feedback loops. The state of pteropod populations is almost certainly indicative of overall ecosystem “health” in McMurdo Sound, and perhaps throughout the Ross Sea.

Large aggregations of both pteropod species were found at all four sampling stations (Fig. 1) in January of 1999 and 2001. Equally large aggregations of both species have been reported in McMurdo Sound in every systematic zooplankton sampling study to date (2, 5, 18, 19, 25, 26). The Antarctic Biology Training Course sponsored by the U.S. National Science Foundation also confirmed an abundance of *L. helicina* in McMurdo Sound every year of its operation (1994–1996, 1999–2001; D. Karentz, University of San Francisco, California, pers. comm.). Thus, the absence of *L. helicina* in 2001–2002 appears to be unprecedented in McMurdo Sound, although we cannot rule out the possibility that *L. helicina* was recruited from other parts of the Ross Sea later in the year.

The absence of *L. helicina* in 2001–2002 may have resulted from food limitation. In the Arctic, *L. helicina* has a life cycle of 1.5 to 2 years, and veliger larvae are most abundant in late summer to early fall (27). Assuming a

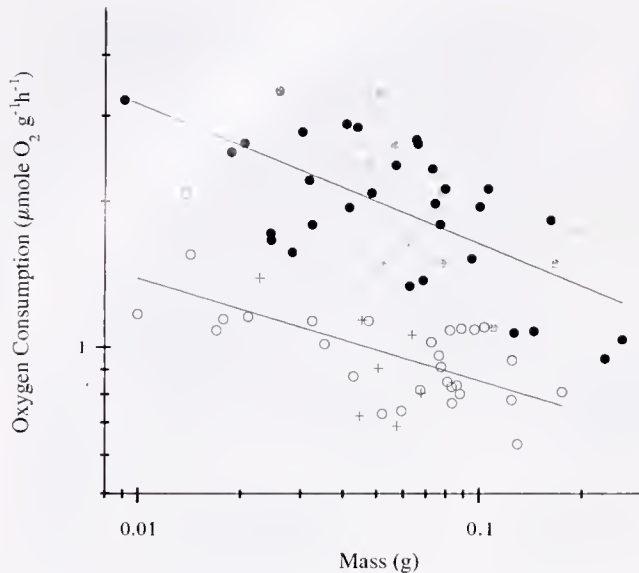


**Figure 3.** Oxygen consumption rates of *Clione antarctica* plotted as a function of wet body mass. All rates were measured at  $-1.86^{\circ}\text{C}$ , the year-round ambient temperature in McMurdo Sound. The rates from animals captured in 2002 (open circles,  $y = 0.43x^{-0.28}$ ) were significantly lower than those measured in 2001 (black circles,  $y = 0.93x^{-0.25}$ ) or 1999 (grey circles) (ANCOVA;  $P < 0.01$ ). Consumption rates of animals deprived of food in the laboratory in 2001 (+) are similar to those measured in 2002, supporting the suggestion that animals captured in 2002 were suffering food deprivation due to the apparent absence of *Limacina helicina* in the region.

similar life history for *L. helicina* in the Ross Sea, veligers there may not have metamorphosed and grown to adult sizes by summer 2001–2002. Relatively short delays in food availability are known to lead to failed metamorphosis of larval zooplankton (28). Unfortunately, we have no data outside of McMurdo Sound in 2002. An alternative hypothesis is that *L. helicina* was simply excluded from McMurdo Sound by changes in the local currents due to an immense iceberg, B15, a large fragment of which ran aground along the eastern edge of Ross Island in austral spring 2000–2001 (Fig. 1). The iceberg and associated ice cover in 2001–2002 may have prevented the typical flow of water from the Ross Sea gyre around Cape Bird and southward into McMurdo Sound (29), and this may have caused a more localized absence of *L. helicina*. This current typically carries the phytoplankton bloom, and presumably, pteropod populations into McMurdo Sound. This explanation is consistent with the change in the position of the iceberg between 2000–2001 and 2001–2002, but it is not supported by more recent observations. Substantial populations of both *C. antarctica* and *L. helicina* were found in McMurdo Sound in 2002–2003 (Luke Hunt, Hopkins Marine Station, pers. comm.) even, though the iceberg continues to block the mouth of McMurdo Sound.

A number of factors may have influenced the sea-ice

conditions and thus contributed to the low biomass observed in 2000–2001. Among the most compelling is that the immense iceberg B15 prevented the retreat of pack ice out of the Ross Sea, causing a reduction in open water and a shortened growing season that delayed and stunted the phytoplankton bloom (1). However, substantial interannual variability exists in both sea-ice extent and phytoplankton production. For example, both 1997 and 2002 had high ice cover (Fig. 2; Table 1) even though the iceberg was no longer preventing the retreat of pack ice in those years. Phytoplankton biomass was reduced somewhat in 1997, but was dramatically reduced in 2002 (mean chlorophyll concentration of  $0.56 \text{ mg m}^{-3}$ ). Interestingly, both 1997 and 2002 experienced El Niño events that are known to influence Antarctic waters (30).

Continued monitoring is required to assess the causes of variability in Ross Sea phytoplankton stocks, the role of sea ice in the Southern Ocean ecosystem, and the resulting impacts on trophic interactions. Climate variations may further disrupt the timing of sea-ice formation and retreat (31, 32), and thus primary productivity, with consequences for entire food webs, as observed here.

### Acknowledgments

We thank J. Rosenthal, F. Bezanilla, R. Dudley, J. Barry, B. Robison, J. Drazen, A. DeVries, L. Hunt, D. Karentz, W. Smith, and S. Kim for helpful discussions, comments on the manuscript, assistance in the field and laboratory, or both. The constructive comments of two anonymous reviewers greatly improved this manuscript. We thank Raytheon Polar Services and the National Science Foundation—Office of Polar Programs for facilitating and funding this work. This work was additionally supported by the Monterey Bay Aquarium Research Institute and the NSF-sponsored Antarctic Biology Training Course and its instructors, including A. Marsh, D. Karentz, G. Somero, G. Hoffman, C. Marshall, L. Goff, and D. Manahan.

### Literature Cited

1. Arrigo, K. R., G. L. van Dijken, D. G. Ainley, M. A. Fahnestock, and R. Markus. 2002. Ecological impact of a large Antarctic iceberg. *Geophys. Res. Lett.* **29**: 1–4.
2. Foster, B. A. 1989. Time and depth comparisons of sub-ice zooplankton in McMurdo Sound, Antarctica. *Polar Biol.* **9**: 431–435.
3. Lalli, C. M., and R. W. Gilmer. 1989. *Pelagic Snails: The Biology of Holoplanktonic Gastropod Mollusks*, Stanford University Press, Stanford, CA.
4. Foster, B. A., and J. C. Montgomery. 1993. Planktivory in benthic nototheniid fish in McMurdo Sound, Antarctica. *Environ. Biol. Fishes* **36**: 313–318.
5. Gilmer, R. W., and C. M. Lalli. 1990. Bipolar variation in *Clione*, a gymnosomatous pteropod. *Am. Malacol. Bull.* **81**: 67–75.
6. Brierley, A. S., and D. N. Thomas. 2002. Ecology of southern ocean pack ice. *Adv. Mar. Biol.* **43**: 171–277.
7. Smith, R. C., K. S. Baker, H. M. Dierssen, S. E. Stammerjohn, and

- M. Vernet. 2001. Variability of primary production in an Antarctic marine ecosystem as estimated using a multi-scale sampling strategy. *Am. Zool.* **41**: 40–56.
8. Gow, A. J., S. F. Ackley, J. W. Govoni, and W. F. Weeks. 1998. Physical and structural properties of land-fast sea ice in McMurdo Sound, Antarctica. Pp. 355–374 in *Antarctic Sea Ice: Physical Processes, Interactions and Variability*, Vol. 74, M.O. Jeffries, ed. American Geophysical Union, Washington D.C.
9. Brockington, S., and A. Clarke. 2001. The relative influence of temperature and food on the metabolism of a marine invertebrate. *J. Exp. Mar. Biol. Ecol.* **258**: 87–99.
10. Peck, L. S. 1998. Feeding, metabolism and metabolic scope in Antarctic marine ectotherms. Pp. 365–390 in *Cold Ocean Physiology*, H. O. Pörtner, and R. C. Playle, eds. Cambridge University Press, Cambridge.
11. Ross, R. M., L. B. Quetin, K. S. Baker, M. Vernet, and R. C. Smith. 2000. Growth limitation in young *Euphausia superba* under field conditions. *Limnol. Oceanogr.* **45**: 31–43.
12. Marsh, A. G., and D. T. Manahan. 1999. A method for accurate measurements of the respiration rates of marine invertebrate embryos and larvae. *Mar. Ecol. Prog. Ser.* **184**: 1–10.
13. Seibel, B. A., E. V. Thuesen, J. J. Childress, and L. A. Gorodezky. 1997. Decline in pelagic cephalopod metabolism with habitat depth reflects differences in locomotory efficiency. *Biol. Bull.* **192**: 262–278.
14. Geiger, S. P., H. G. Kawall, and J. J. Torres. 2001. The effect of the receding ice edge on the condition of copepods in the northwestern Weddell Sea: results from biochemical assays. *Hydrobiologia* **453–454**: 79–90.
15. Hagen, W., E. S. Van Vleet, and G. Kattner. 1996. Seasonal lipid storage as overwintering strategy of Antarctic krill. *Mar. Ecol. Prog. Ser.* **134**: 85–89.
16. Phleger, C. F., P. D. Nichols, and P. Virtue. 1997. Lipids and buoyancy in Southern Ocean pteropods. *Lipids* **32**: 1093–1100.
17. Cabal, J. A., F. Alvarez-Marqués, J. L. Acuña, M. Quevedo, R. Gonzalez-Quirós, I. Huskin, D. Fernández, C. R. Del Valle, and R. Anadón. 2002. Mesozooplankton distribution and grazing during the productive season in the Northwest Antarctic Peninsula (FRUELA cruises). *Deep-sea Res. II* **49**: 869–882.
18. Hopkins, T. L. 1987. Midwater food web in McMurdo Sound, Ross Sea, Antarctica. *Mar. Biol.* **96**: 93–106.
19. Bryan, P. J., W. Y. Yoshida, J. B. McClintock, and B. J. Baker. 1995. Ecological role for pteroenone, a novel antifeedant from the conspicuous antarctic pteropod *Clione antarctica* (Gymnosomata: Gastropoda). *Mar. Biol.* **122**: 271–277.
20. Pakhomov, E. A., R. Perissinotti, and C. D. McQuaid. 1996. Prey composition and daily rations of myctophid fishes in the Southern Ocean. *Mar. Ecol. Prog. Ser.* **134**: 1–14.
21. Davis, R. W., L. A. Fuiman, T. M. Williams, S. O. Collier, W. P. Hagey, S. B. Kanatous, S. Kobin, and M. Horning. 1999. Hunting behavior of a marine mammal beneath the Antarctic fast ice. *Science* **283**: 993–996.
22. Eastman, J. T. 1993. *Antarctic Fish Biology: Evolution in a Unique Environment*. Academic Press, San Diego, CA.
23. Noji, T. T., U. V. Bathmann, B. von Bodungen, M. Voss, A. Antia, M. Krumbholz, B. Klein, I. Peeken, C. I.-M. Noji, and F. Rey. 1997. Clearance of picoplankton-sized particles and formation of rapidly sinking aggregates by the pteropod, *Limacina retroversa*. *J. Plankton Res.* **19**: 863–875.
24. Levasseur, M., M. D. Keller, E. Bonneau, D. D'Amours, and W. K. Bellows. 1994. Oceanographic basis of a DMS-related Atlantic cod (*Gadus morhua*) fishery problem: blackberry feed. *Can. J. Fish. Aquat. Sci.* **51**: 881–889.
25. Whitehead, K., D. Karentz, and J. I. Hedges. 2001. Mycosporine-like amino acids (MAAs) in phytoplankton, a herbivorous pteropod (*Limacina helicina*) and its pteropod predator (*Clione antarctica*) in McMurdo Bay, Antarctica. *Mar. Biol.* **139**: 1013–1019.
26. Knox, G. A., E. J. Waghorn, and P. H. Ensor. 1996. Summer plankton beneath the McMurdo ice shelf at White Island, McMurdo Sound, Antarctica. *Polar Biol.* **16**: 87–94.
27. Kobayashi, H. A. 1974. Growth cycle and related vertical distribution of the thecosomatous pteropod *Spiratella* ("*Limacina*") *helicina* in the central Arctic Ocean. *Mar. Biol.* **26**: 295–301.
28. Ross, R. M., and L. B. Quetin. 1989. Energetic cost to develop to the first feeding stage of *Euphausia superba* Dana and the effect of delays in food availability. *J. Exp. Mar. Biol. Ecol.* **133**: 103–127.
29. Barry, J. P., and P. K. Dayton. 1988. Current patterns in McMurdo Sound, Antarctica and their relationship to local biotic communities. *Polar Biol.* **8**: 367–376.
30. Comiso, J. C., C. R. McClain, C. W. Sullivan, J. P. Ryan, and C. L. Leonard. 1993. Coastal Zone Color Scanner pigment concentrations in the Southern Ocean and relationships to geophysical surface features. *J. Geophys. Res.* **98**(C2):2419–2451.
31. Scambos, T. A., C. Hulbe, M. Fahnestock, and J. Bohlander. 2000. The link between climate warming and break-up of ice shelves in the Antarctic Peninsula. *J. Glaciol.* **46**: 516–530.
32. Dierssen, H. M., R. C. Smith, and M. Vernet. 2002. Glacial meltwater dynamics in coastal waters west of the Antarctic Peninsula. *Proc. Natl. Acad. Sci. USA* **99**: 1790–1795.
33. Yoder, J. A. 2000. Terra's view of the sea. *Science* **288**: 1978–1980.

# Thermal Tolerances of Deep-Sea Hydrothermal Vent Animals From the Northeast Pacific

RAYMOND W. LEE

*School of Biological Sciences, Washington State University, Pullman, Washington 99164*

*Dense biological communities on sulfide structures at deep-sea hydrothermal vents survive in one of Earth's most extreme environments. The thermotolerance of vent animals dwelling on sulfide chimneys in the Northeast Pacific was determined by maintaining them in pressurized chambers under controlled temperature and chemical conditions. Observations indicated that lethal temperature correlates strongly with distributions observed in nature. One species studied, the alvinellid sulfide worm *Paralvinella sulfincola*, exhibited a thermal limit of 50–56 °C. Since observations of survival under controlled conditions are the only unambiguous means of demonstrating that an animal can tolerate a given environmental condition, the documented thermal limit for metazoan life at hydrothermal vents should be considered to be above 45 °C, but less than 60 °C.*

Although the biology of hydrothermal vents has been actively investigated over the past 20 years, delineating linkages between the physical environment and the biota has been difficult. Gradients and temporal changes are pronounced. Therefore, to know what conditions a vent organism routinely encounters, measurements would ideally be conducted with spatial resolution at the sub-centimeter level, with temporal resolution over the course of days to weeks, and without modifying fluid flow by the presence of the sensor or submersible. Consequently, investigators are generally cautious in inferring physiological tolerance from environmental measurements. A recent study presents environmental data suggesting that *Alvinella pompejana*, a vent-chimney alvinellid worm, lives under sustained temperatures of 60 °C, which could make it the Earth's most thermotolerant metazoan (1). However, steep thermal gradients and the difficulty of sampling fragile alvinellid tubes from a submersible have raised questions about the validity

of these conclusions (2). For animals inhabiting less remote environments, corroborative evidence has often come from laboratory investigations of live animals. Such an approach has not been extensively used in studies of vent animals due to the requirement that experiments be conducted at high pressure. However, this kind of evidence is necessary to determine actual physiological limits. Documented survival under controlled conditions provides unambiguous evidence for thermotolerance. In the present study, this type of direct approach was taken to investigate the thermal tolerance of several species of vent animals.

Some of the sulfide-chimney assemblages at the Juan de Fuca and Explorer ridges in the Northeast Pacific are ideal for investigation of environmental tolerance since the dominant invertebrates, unlike those from other vent systems, are small and can fit in relatively inexpensive pressure vessels. Pressures at these sites (depths 1500–1800 m) are moderate, making it easier to maintain *in situ* pressure in experiments, and most organisms are motile, allowing behavioral investigations. In the present study, thermal limits were investigated for four abundant species of chimney invertebrates: the paralvinellids *Paralvinella sulfincola* and *P. palmiformis*, the limpet *Lepetodrilus fucensis*, and the snail *Depressigyra globulus*.

The distributions of these organisms on vent chimneys were described by Sarrazin *et al.* (3) and exhibit a "zonation" pattern of distinct invertebrate assemblages (named I through V) that differ in temperature and flow characteristics (3). Assemblage I, closest to hot vent fluids, consists almost entirely of *P. sulfincola*, which suggests that this species may be the most thermotolerant metazoan at Northeast Pacific vents. The second warmest assemblage, assemblage II, is dominated by *P. sulfincola* and *P. palmiformis*. The gastropods *L. fucensis* and *D. globulus* are also found in assemblage II, but are more common, and dominant, where

the influence of venting is weaker (assemblages III–V). It is not clear what factors govern the distribution of organisms on sulfide structures. It has been postulated that tolerance to abiotic factors such as high temperature or hydrogen sulfide may be important regulators, but analysis of available environmental data and faunal distributions indicates that less than 30% of the variance in species distribution can be accounted for by abiotic factors that have been measured so far (4). If thermal tolerance is a factor governing distributions, then thermotolerance should be highest in *P. sulfincola*, followed by *P. palmiformis*, then *L. fucensis* and *D. globulus*. Specimens of *P. sulfincola* were collected from assemblage I, *P. palmiformis* from assemblage II and III, and gastropods from assemblage III. Differences in thermal tolerance among collections were not tested for. It is likely that further study could reveal acclimation to microhabitat conditions.

Observations of mixed assemblages of these species in pressurized chambers subjected to temperature increases are summarized in Figure 1. Each data point shown represents the outcome of a single experiment in one pressure chamber. The following endpoints were measured: (1) activity at experimental temperature by one or more individuals, with continued activity following return to low temperatures; (2) obvious reduction or cessation of activity, with restoration of activity following return to low temperatures; (3) activity at experimental temperature, but no activity at higher temperatures and no activity after return to low temperature in all individuals; or (4) no activity in all individuals, with no return of activity at lower temperatures. In some cases, category 2 was not readily observable; *i.e.*, *D. globulus* appeared to exhibit high activity or none at all. In some trials, the threshold temperature at which activity ceases was not monitored. In these cases, animals exhibited no activity at a given temperature, but the threshold may have been lower. These instances were designated as category 4. Experiments consisted of a temperature increase (10 °C per hour) followed by return of temperature to 10–15 °C. In some cases, multiple experiments (at sequentially higher maximum temperatures) were conducted on the same sets of individuals (for *D. globulus*, *L. fucensis*, and *P. palmiformis*, 9 of 23, 8 of 17, and 2 of 8 experiments were from individuals exposed to two or three experimental temperature increases; all other experiments and all *P. sulfincola* experiments consisted of a single elevated temperature exposure). It is possible that exposure of animals to more than one temperature increase could have resulted in lower thermal limits for activity in those experiments.

Thermal tolerance was correlated with distributions observed in nature. The temperature above which activity ceased (with no recovery at lower temperatures) was interpreted to be the thermal limit. *L. fucensis* was the least thermotolerant, with reduction or cessation of activity be-

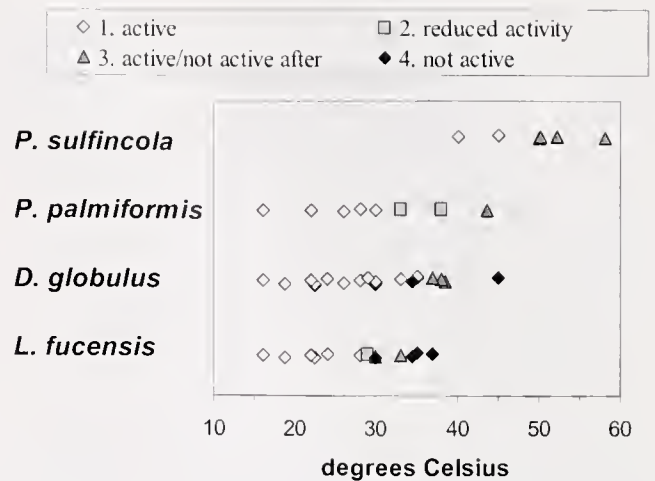


**Figure 1.** Effects of experimental temperature on activity of chimney invertebrates. The ROPOS submersible was used to collect animals from sulfide structures on the Explorer Ridge at a depth of 1800 m. Immediately upon arrival at the surface, animals were placed in 30-ml pressure chambers and returned to an *in situ* pressure of 2600 psi. Depressurization during recovery was unavoidable since pressurized recovery systems are only in the developmental stages. Within minutes after animals were placed in pressure chambers, activity was generally observed. Animals not pressurized and kept at 1 atm also exhibited activity, but appeared to be less active than pressurized animals. For experiments, high-pressure liquid chromatography pumps were used to continuously perfuse (0.3 ml/min) the chambers with filtered seawater equilibrated with 20% oxygen at pH 8. Sulfide was metered in to give concentrations of 100–200 micromoles liter<sup>-1</sup>. Chamber temperature was controlled using a programmable recirculating waterbath. Temperature was maintained initially at 10–15 °C for 2–3 h, then ramped at a rate of 10 °C/h to experimental temperatures. Chamber temperature was determined by monitoring an identical unpressurized control chamber, perfused at the same rate as experimental chambers, using a Yellow Springs Instruments temperature probe (calibrated against a NIST-traceable digital thermometer). Activity was monitored through 1.25-cm diameter viewports, either by using a video camera or by direct observation. Each data point represents the outcome of a single experiment in one pressure chamber. Behavior categories 1 to 4 are described in the text. Experiments consisted of a temperature increase followed by return of temperature to 10–15 °C.

tween 30 and 35 °C. *D. globulus* and *P. palmiformis* exhibited reduction or cessation of activity in the ranges of 35–40 °C and 40 °C respectively. The sulfide worm *P. sulfincola* was clearly highly thermotolerant. Activity did not cease until temperatures of 50–56 °C were achieved (Fig. 2; 7/20, 7/28 expts.). *P. sulfincola* survived sustained exposure to 45 °C on the order of 1 h or longer (Fig. 2; 8/2 expt.). This indicates that temperatures of 50 °C or above, rather than exposure to lower temperatures, accounted for cessation of activity at 50–56 °C (Fig. 2; 7/20, 7/28 expts.). Time-lapse video from experiments can be found at (<http://www.wsu.edu/~rlee/sulfideworm/psulf.html>).

These findings are consistent with, and may account for, the distributions observed in nature, and indicate that these organisms inhabit microenvironments close to their thermal

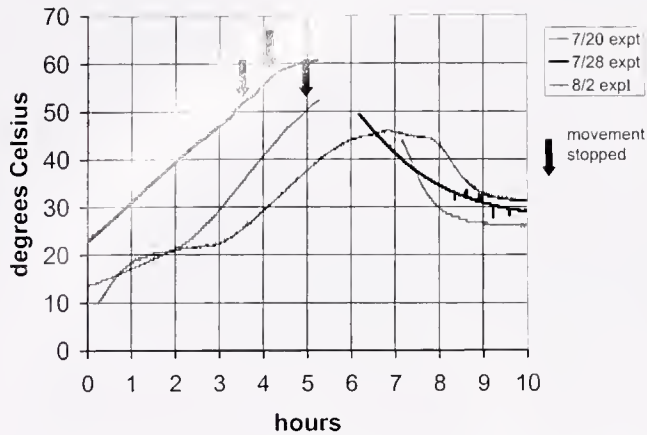


**Figure 2.** Temperature conditions from three experiments in pressure vessels containing *Paralvinella sulfincola*. Arrows denote time point at which cessation of activity was observed. 7/20 experiment—observation of two animals: both ceased activity when temperature was 51 °C. 7/28 experiment—observation of two animals: one stopped activity when temperature was 52 °C; the second when temperature was 58 °C. Gaps in temperature data indicate periods when temperature sensor was turned off. 8/2 experiment—observation of three animals: temperature increased to 45 °C, then held. Activity persisted for the duration of the experiment.

limits. The mean temperature of 42 °C (3) observed in the sulfide worm habitat is above or at the limit of temperatures tolerated by the other species and would explain why they are excluded from these areas. Average temperatures measured in assemblage II, where all four species are encountered, ranged from 17 to 37 °C (4), which is within the experimental range tolerated by palm worms and can be at the limits tolerated by gastropods. Habitat temperature may explain why gastropods are more dominant in cooler assemblages.

It is possible that experimentally determined temperature limits underestimate the tolerance shown *in situ*. This possibility is difficult to assess, but will be addressed in future tests of different conditions in pressure incubations (*e.g.*, low pH, elevated pCO<sub>2</sub>) and experiments with animals recovered under pressure in pressurized recovery devices. In addition, trials of paralvinellid worms were conducted with their mucus tubes removed. It is possible that these tubes, which also contain mineral deposits, may provide some thermoprotective benefit. When animals are brought to the surface and repressurized, survival appears to be indefinite. At 1 atm, survival was a few days to weeks depending on species, indicating that pressure is required for long-term maintenance. Experiments in my laboratory and elsewhere have shown that vent animals collected from these and other sites survive for months in pressure chambers, even with periodic depressurization and repressurization to clean chambers or remove specimens. Additional study is underway to determine how long animals can tolerate sustained (several days) and transient (several minutes) exposure to

experimental treatments as well as behaviorally preferred temperatures.

The limit of aquatic metazoan life is generally thought to be around 45 °C. The results presented here for *P. sulfincola* represent the first conclusive evidence that a vent animal tolerates temperatures that exceed 40 °C. The alvinellid *Alvinella pompejana* had previously been reported to be the Earth's "hottest" living metazoan, based on a finding of sustained temperatures of 60 °C in occupied *A. pompejana* tubes (1). In addition, a single individual of *A. pompejana* had been observed to survive brief exposure to 105 °C when it crawled onto a submersible's high-temperature probe (5). These findings are at odds with biochemical evidence indicating that the structure and function of enzymes and other macromolecules of *A. pompejana* are perturbed at temperatures of 50 °C or below (2, 6–10). The only previous study to directly investigate the thermal limits of live vent polychaetes shows that *Hesiolyra bergi*, which lives in the *A. pompejana* environment, does not tolerate temperatures above 40 °C (11). Thus the thermal limit of alvinellids remains a contentious issue. While extreme temperatures may be present in the alvinellid environment, alvinellids may inhabit cooler microenvironments or receive only transient pulses of extreme temperature, perhaps on the order of seconds. This disagreement may never be resolved. Unlike *P. sulfincola*, *A. pompejana* has not yet survived collection and recovery.

*P. sulfincola* may be as thermotolerant as *A. pompejana* since it exhibits properties of high enzyme thermostability (12) and inhabits a similar niche on sulfide structures. Temperatures at *P. sulfincola* tube openings range as high as 80–90 °C (S.K. Juniper, University of Quebec at Montreal, pers. comm.). Thus the data presented here are probably representative of tolerances exhibited by animals living at the limits for metazoan life at deep-sea vents. Pressurized experiments are the only unambiguous means of testing for survival under documented temperature. A combination of detailed environmental measurements, biochemical studies, and observation under controlled conditions is needed to reliably assess the thermal limits of vent fauna. The investigation of highly thermotolerant metazoans at deep-sea vents will remain an exciting area of investigation. The results shown here place the upper limit of aquatic animal life in the range of 45–55 °C.

#### Acknowledgments

This work benefited greatly from the captain and crew of the R.V. *Thompson*; ROPOS submersible group; Bob Embley (expedition chief scientist); Amanda Bates (at-sea help and discussions); Ray Romjue, George Henry, and John Rutherford (vessel design and machining). Funding was provided by the National Science Foundation and the West

Coast and Polar Regions National Undersea Research Center.

### Literature Cited

1. Cary, S. C., T. Shank, and J. Stein. 1998. Worms bask in extreme temperatures. *Nature* **391**: 545–546.
2. Chevaldonné, P., C. R. Fisher, J. J. Childress, D. Desbruyères, D. Jollivet, F. Zal, and A. Toulmond. 2000. Thermotolerance and the "Pompeii worms." *Mar. Ecol. Prog. Ser.* **208**: 293–295.
3. Sarrazin, J., V. Robigou, S. K. Juniper, and J. R. Delaney. 1997. Biological and geological dynamics over four years on a high-temperature sulfide structure at the Juan de Fuca Ridge hydrothermal observatory. *Mar. Ecol. Prog. Ser.* **153**: 5–24.
4. Sarrazin, J., S. K. Juniper, G. Massoth, and P. Legendre. 1999. Physical and chemical factors influencing species distributions on hydrothermal sulfide edifices of the Juan de Fuca Ridge, northeast Pacific. *Mar. Ecol. Prog. Ser.* **190**: 89–112.
5. Chevaldonné, P., D. Desbruyères, and J. J. Childress. 1992. . . and some even hotter. *Nature* **359**: 593–594.
6. Dahlhoff, E., J. O'Brien, G. N. Somero, and R. D. Vetter. 1991. Temperature effects on mitochondria from hydrothermal vent invertebrates: evidence for adaptation to elevated and variable habitat temperatures. *Phys. Zool.* **64**: 1490–1508.
7. Dahlhoff, E., and G. N. Somero. 1991. Pressure and temperature adaptation of cytosolic malate dehydrogenases of shallow- and deep-living marine invertebrates: evidence for high body temperatures in hydrothermal vent animals. *J. Exp. Biol.* **159**: 473–487.
8. Terwilliger, N. B., and R. C. Terwilliger. 1984. Hemoglobin from the "Pompeii worm," *Alvinella pompejana*, an annelid from a deep sea hot hydrothermal vent environment. *Mar. Biol. Lett.* **5**: 191–201.
9. Toulmond, A., F. El Idrissi Slitine, J. De Frescheville, and C. Jouin. 1990. Extracellular hemoglobins of hydrothermal vent annelids: structural and functional characteristics in three alvinellid species. *Biol. Bull.* **179**: 366–373.
10. Gaill, F., H. Wiedemann, K. Mann, K. Kühn, R. Timpl, and J. Engel. 1991. Molecular characterization of cuticle and interstitial collagens from worms collected at deep sea hydrothermal vents. *J. Mol. Biol.* **221**: 209–223.
11. Shillito, B., D. Jollivet, P. M. Sarradin, P. Rodier, F. Lallier, D. Desbruyères, and F. Gaill. 2001. Temperature resistance of *Hesiolepta bergi*, a polychaetous annelid living on deep-sea vent smoker walls. *Mar. Ecol. Prog. Ser.* **216**: 141–149.
12. Jollivet, D., D. Desbruyères, C. Ladrat, and L. Laubier. 1995. Evidence for differences in allozyme thermostability of deep-sea hydrothermal vent polychaetes (Alvinellidae): a possible selection by habitat. *Mar. Ecol. Prog. Ser.* **123**: 125–136.

# Light Production by the Arm Tips of the Deep-Sea Cephalopod *Vampyroteuthis infernalis*

BRUCE H. ROBISON\*, KIM R. REISENBICHLER, JAMES C. HUNT<sup>1</sup>,  
AND STEVEN H. D. HADDOCK

Monterey Bay Aquarium Research Institute, 7700 Sandholdt Rd., Moss Landing, California 95039

**Abstract.** The archaic, deep-sea cephalopod *Vampyroteuthis infernalis* occurs in dark, oxygen-poor waters below 600 m off Monterey Bay, California. Living specimens, collected gently with a remotely operated vehicle (ROV) and quickly transported to a laboratory ashore, have revealed two hitherto undescribed means of bioluminescent expression for the species. In the first, light is produced by a new type of organ located at the tips of all eight arms. In the second, a viscous fluid containing microscopic luminous particles is released from the arm tips to form a glowing cloud around the animal. Both modes of light production are apparently linked to anti-predation strategies. Use of the tip-lights is readily induced by contact stimuli, while fluid expulsion has a much higher triggering threshold. Coelenterazine and luciferase are the chemical precursors of light production. This paper presents observations on the structure and operation of the arm-tip light organs, the character of the luminous cloud, and how the light they produce is incorporated into behavioral patterns.

## Introduction

*Vampyroteuthis infernalis* Chun, 1903 (Fig. 1) is the lone occupant of the cephalopod order Vampyromorpha. Its unique morphological characteristics, combining features of both the octopodiformes and decapodiformes, suggest that it represents an evolutionary position intermediate between the two groups (Young, 1977; Healy, 1989); and it may be a relic from an ancestral cephalopod line (Pickford, 1946). This phylogenetic issue has not yet been clearly resolved,

which only adds to the enigmatic status of the species (Young *et al.*, 1998). *Vampyroteuthis* inhabits temperate and tropical waters of the Pacific, Atlantic, and Indian Oceans, typically between 600 and 1200 m. At these depths, sunlight is dim or absent altogether, oxygen content is low, and temperatures range from about 2° to 6°C (Pickford, 1946). In waters over the Monterey Submarine Canyon, we have found *Vampyroteuthis* throughout the year at depths between 600 and 900 m and at oxygen concentrations centered around 0.4 ml/l.

When observed in its natural habitat, *Vampyroteuthis* has the appearance of a robust and substantial animal, but this impression is somewhat misleading. Manipulation *in situ* and in the laboratory reveals that its body is very soft, with watery tissues and little dense musculature. It has a very low metabolic rate and lives at extremely low oxygen concentrations, yet it is capable of relatively high swimming speeds, relying on its fins rather than jet propulsion (Hunt, 1996; Seibel *et al.*, 1997, 1998, 1999).

*Vampyroteuthis* has been reported to feed upon copepods, prawns, and cnidarians (Young, 1977; Nixon, 1987), but dietary evidence is very scarce. In the laboratory, members of this species will take euphausiids and pieces of fish when the food is placed in contact with the oral surface of the arms, although this is hardly natural feeding. In turn, *Vampyroteuthis* beaks have been reported from the stomachs of large, deep-diving fishes, pinnipeds, and whales, and from benthopelagic fishes (*e.g.*, Percy and Ambler, 1974; Antonelis *et al.*, 1987; Fiscus *et al.*, 1989; Clarke *et al.*, 1996; Clarke and Young, 1998; Drazen *et al.*, 2001). All but the whales are visually cued predators with large eyes that function effectively in dim, monochromatic light.

Cephalopods, particularly deep-water squids, employ a diverse suite of light-producing organs that can occur on the mantle, fins, arms, tentacles, head, eyes, viscera, or else-

Received 10 February 2003; accepted 15 July 2003.

\*To whom correspondence should be addressed. E-mail: robr@mbari.org

<sup>1</sup>Current address: University of New England, 11 Hills Beach Rd., Biddeford, ME 04005.



**Figure 1.** *Vampyroteuthis infernalis*, frame grab from high-definition video footage shot at a depth of 717 m in Monterey Bay, California. Mantle length = 10.2 cm. The fin-base photophore is located behind the dark patch of skin, posterior to (to the right of) the fin. The composite organ is the small, elongate white patch dorsal to and on a line just behind the eye. Minute epidermal organs are scattered over the surface of the mantle and the arms, but not on the web. The new arm-tip light organs described here are located on the oral surface of the filamentous portion of each arm, beyond the margin of the web.

where, depending on the species (Herring, 1977). The light they produce is used for attracting prey, deterring predators, and presumably for intraspecific communication. Luminous secretions are found in a number of deep-living invertebrates but are rare among cephalopods and fishes (Herring, 1977, 1988).

Three types of light-emitting organs have been described in *Vampyroteuthis infernalis*: large, paired, complex photophores at the bases of the fins; small, simple, epidermal organs scattered over the surface of the animal; and composite organs—two clusters of small, pale nodules located dorsally on a line just behind the eyes (Pickford, 1949). Light production has been observed only from the fin-base photophores; emission spectra of these organs were measured at 460 nm by Herring (1983) and 461–466 nm by Widder *et al.* (1983). Herring *et al.* (1994) examined all three organ types and, based on detailed histological evidence, concluded that the composite organs are probably extraocular photoreceptors, while the epidermal organs are most likely light producers. They also found that the reflective surfaces in the light organs were collagen instead of the iridosomal platelets found in other modern cephalopods. To date, no one has observed light from the epidermal organs, nor has there been any behavioral evidence of light sensitivity by the composite organs. We have discovered two new forms of bioluminescent expression in *Vampyroteuthis*:

light produced by organs at the tips of all eight arms, and luminous fluid released by the arm tips.

### Materials and Methods

*In situ* behavioral observations and quantitative video surveys of meso- and bathypelagic cephalopods have been a component of MBARI's midwater research program since 1991 (Hunt, 1996). The program is based on the use of remotely operated vehicles, or ROVs. Over a 10-year time span we have carefully observed 57 individuals of *Vampyroteuthis in situ* and have collected 18 to establish in laboratory aquaria. Specimens in this study included adult males and females with mantle lengths ranging from 7.9 to 12.1 cm. All were gently collected with the ROV *Ventana* (Robison, 1993) at a time-series station 1600 m deep over the axis of the Monterey Submarine Canyon. Field observations and collections occurred under full illumination from the ROV's four 500-W, broad-spectrum lights. Once the ROV was recovered, the animals were placed in darkened containers and were quickly transferred to our laboratory ashore. In the shoreside facility they were maintained in the dark, at 4° to 6° C, in circular, 260-l kreisel tanks (Hamner, 1990) for as long as 2 months.

Most of the specimens appeared to be temporarily blinded by the vehicle's lights during capture. After several hours in the dark, they responded to point sources of white

light by moving away, and by contracting the iris-like sphincter muscle (Pickford, 1949) that surrounds the front of the eye. Laboratory observations were made both under red light and in the dark, often with an image intensifier classified as Gen 4+ according to the U.S. Army Night Vision Laboratory's criteria. Light production was recorded with a variety of low-light video cameras.

For chemical assays of arm-tip light organs, we removed the distal portions of arms from several specimens and used them either fresh or after they had been frozen in liquid nitrogen. Light output from each assay listed below was measured with a Hamamatsu HC-124 photomultiplier tube, in a custom-built integrating sphere, for at least 20 s.

Coelenterazine assay: To test for the presence of coelenterazine, we homogenized individual arm tips in 500  $\mu$ l of methanol (approximately 10:1 by volume). One milliliter of purified *Oplophorus* luciferase in a solution of 20 mM Tris and 100 mM NaCl was injected into 200  $\mu$ l of the sample solution. Mantle tissue with epidermal light organs and web tissue (which lacks the epidermal light organs) were also assayed for the presence of this luciferin.

Luciferase assay: Sample arm tips to be tested for luciferase activity were extracted in an aqueous solution of 100 mM Tris pH 8.1 and 50 mM EDTA. Calcium chloride addition caused no light output, indicating that a calcium-activated photoprotein was not involved. The test solution was added to 20  $\mu$ l of coelenterazine in 0.5  $\mu$ g/ $\mu$ l MeOH, and the light production was measured. For negative controls, tissue from the web was homogenized, and the extracts were added to methanol.

Bacterial luciferase assay: Assays for luminous bacteria

in the arm-tip light organs, the ejecta from the organs, and the surrounding water followed the reduced flavin assay described in Hastings *et al.* (1978), with the flavin reduced by bubbling with H<sub>2</sub> gas in the presence of platinized carbon. Cultured *Vibrio harveyi* were used as positive controls for this assay. We also tested for the presence of luminous bacteria in samples of arm-tip exudate that were streaked on seawater agar plates kept at 4°C for 2 weeks.

Fluorescence microscopy: Autofluorescence images of arm-tip light organs and ejecta were obtained with a Zeiss Axioplan microscope using 10 $\times$  and 40 $\times$  Neofluar objectives, under DAPI illumination.

Electron microscopy: Material was fixed in 2% glutaraldehyde with 0.1 M cacodylate buffer. Samples were post-fixed using osmium tetroxide and embedded in Epon. Thick (1–2  $\mu$ m) sections through the light-producing region of the arm tip were stained with toluidine blue. Thin sections from the same region were stained with uranyl acetate and lead citrate.

## Results

In the laboratory we observed that the tips of all eight arms often glowed when an animal was handled (Fig. 2). The bright blue lights usually appeared as a tight chain of 4 to 6 small discs, tapering in size distally along the oral surface of each arm tip. Occasionally there was a different pattern, in which the light appeared as two parallel lines separated by a dark gap. With a mild contact stimulus, the arms and web flared outward, with the arm tips glowing. With stronger prodding, the arms were curled, writhing up



**Figure 2.** Frame grab from a low-light video recording, showing the glowing arm tips of *Vampyroteuthis infernalis*. The animal is oriented such that its head and beak are directed toward the camera, with the arms and web beginning to flare outward.

over the head to the apex of the mantle, exposing the suckers and cirri and placing the glowing arm tips in a cluster at the top. When an animal rolled the arms and mantle back down to their normal position, it frequently tucked the arm tips within the web, where they were shielded from view. This behavior, which was observed both in the field and in the laboratory, is similar to a nonluminous pattern seen in octopuses attacked by moray eels (Hanlon and Messenger, 1996). The eight arm-tip light organs of *Vampyroteuthis* always glowed and dimmed simultaneously. They flashed 1 to 3 times per second, or glowed steadily, but rarely for longer than one minute. The pulsing could include complete extinction of the light, or just dimming, before returning to the previous level of intensity. There is a dark, densely pigmented layer of skin on the aboral surface and on the sides of each arm tip, but the oral surface is generally unpigmented.

The structure of the oral surface of the arm tips continues the basic pattern found along the entire length of the arm—a series of central plates alternating with paired lateral plates (Fig. 3). In the proximal and medial portions of the arm, the lateral plates support cirri, while the central plates are the bases for suckers (Pickford, 1949, plate VI, fig. 20). Plates, cirri, and suckers get smaller toward the distal end; near the tip, the plates bear mere rudiments. Proximally, the plates are pale and opaque, but as they approach the distal tip they become translucent. Within this window at the tip of the arm are subdermal clusters of particles that impart an iridescent green and yellow sheen to the plates. When the arm is viewed from the side, the central plates appear bulbous and extend outward beyond the lateral plates (Pickford, 1949, plate VI, fig. 19). Light expressed from the central plates alone may be the source of the pattern that appears as a chain of discs, while light coming from just the lateral plates would show as parallel lines. The light-producing area of the arm tip can be occluded by the edges of the dark skin along both sides, which close together along the midline of the oral surface. This means of controlling light output is similar to that described for the arm-tip photophores of *Taningia danae* by Herring *et al.* (1992).

Given a strong contact stimulus to the arms or body, the arm tips exuded a viscous fluid containing small glowing particles. As the arms swept up over the head and mantle, the particles dispersed, enveloping the animal in a luminous cloud (Fig. 4). To all observers, the light from the cloud was much dimmer than that of the fin lights and arm tips, but we were unable to measure its intensity. The number of particles released varied from a few dozen to several hundred, usually related to the strength of the stimulus. Cloud luminescence persisted for 2 to 3 min, and individual particles glowed for as long as 9 min (Hunt, 1996). Once the particles had gone dark, stirring the water did not re-initiate luminescence. After several such displays, production of the luminous fluid ceased, and while the arm tips could still be

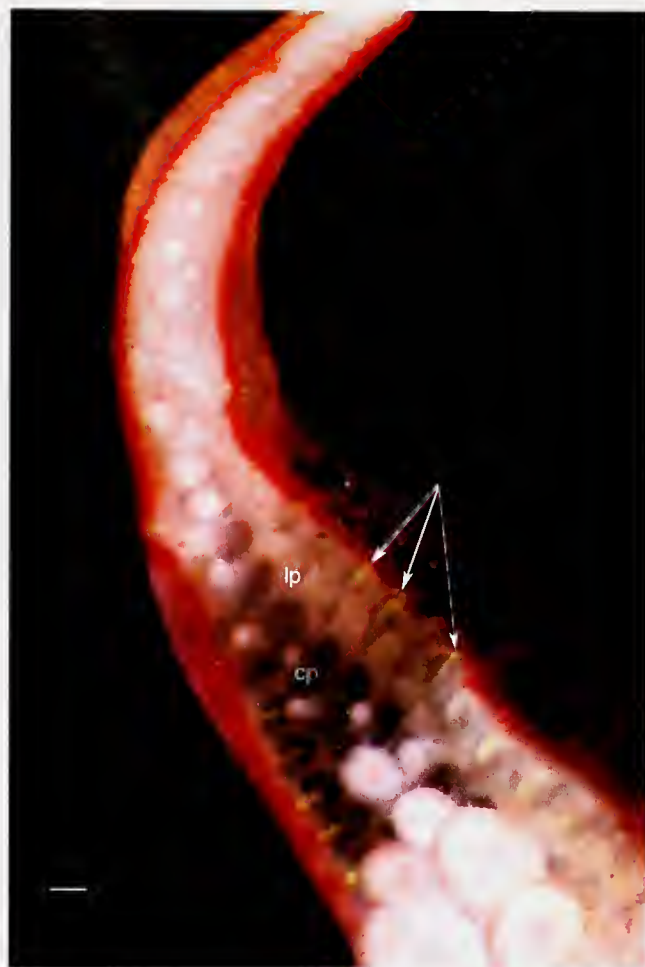


**Figure 3.** Arm tip of a living specimen of *Vampyroteuthis infernalis*, showing the distal light-producing region, and patches of small, green particles in the lateral plates that are associated with the luminous ejecta. cp = central plate; lp = lateral plate; scale bar = 1 mm; the arrows point to patches of iridescent particles that are not present after an extensive luminous cloud has been created.

stimulated to glow, the dense clusters of particles in the arm tips were gone. The fluid matrix that bears the luminous particles is viscous and somewhat sticky. Arm tips that brushed across the inner surface of a kreisel during a bioluminescent display usually left behind a lingering streak of light. The release of luminous particles often preceded an escape response by the animal.

The chemical assays provided clear evidence of the presence of coelenterazine (luciferin) and luciferase in the arm-tip light organs of *Vampyroteuthis* (Fig. 5), which indicates that these compounds are the basis for light production. No calcium-activated photoprotein activity was detected in any assay. Small amounts of coelenterazine were found in the mantle epidermal tissue. These results support the conclusion by Herring *et al.* (1994) that the epidermal organs produce light. Assays for luciferin and luciferase in the web tissue were negative. The assay for bacterial luciferase in



**Figure 4.** Frame grab from a low-light video recording showing the release of glowing particles from the arm tips of *Vampyroteuthis infernalis*. The head of the specimen is directed toward the camera. Particles in the cloud are swirled by movements of the arms and web, and by water jetting through the siphon. "Tails" on the glowing particles are caused by electronic lag in the camera's image intensifier.

the tip lights was negative, as were the culturing efforts to demonstrate the presence of luminous bacteria in the arm tips and their exudate.

Microscopic examination of the iridescent clusters in the arm tips of animals that had not yet secreted luminous material revealed extensive patches of rounded yellow particles that glowed blue-green under fluorescent illumination (Fig. 6). No pores that might release the fluid were evident on the arm tips, although the rudimentary suckers are likely sites. The particles matched, in size and configuration, particles culled from the arm-tip exudate and from the water in which a luminous cloud had been produced. Sections of the arm tips showed a low-density central core with prominent nuclei on the oral side and sparse muscle tissue on the aboral. We saw no evidence of an iridosomal reflective layer nor of layered collagen fibers like those found by Herring *et al.* (1994) in the fin-base photophores.

A comparison of our specimens with others collected by trawling in Monterey Bay and elsewhere in the North Pacific revealed that, in almost every case, the arm-tip light organs had broken off the trawl-caught specimens. This observation is similar to that made on *Octopoteuthis* (Herring *et al.*, 1992) and may explain why the arm-tip light organs of *Vampyroteuthis* were not discovered until we could collect the animals in perfect condition. On two of our ROV-caught specimens, we found a short, apparently regenerated arm, each with what appeared to be a small light source at its tip.

Over a gradient of stimuli, the fin lights were the most readily illuminated, and although this pair always worked

together, they could operate independently of the other two light sources. Light emission from the fin lights was regulated by chromatophores and by iris-like skin closures similar to those that shield the eyes. The arm-tip lights seldom glowed without the fin lights also being on, and all 10 could pulse in concert. The luminous ejecta was never observed without the tip lights glowing as well.

On one occasion, male and female specimens were collected on the same day and were then placed in separate kreisels less than a meter apart, in the darkened laboratory ashore. When the female was disturbed and began to flash her arm-tip lights, the undisturbed male quickly and vigorously responded with tip-light flashes. This reaction was repeated twice (Hunt, 1996). We saw no evidence of differential light production by females and males. In the Cranchiidae and Lycoteuthidae, arm-tip photophores develop as secondary sexual characters (Herring *et al.*, 1992). We detected no sexual dimorphism in the light organs of *Vampyroteuthis*. Luminous suckers on the deep-sea octopus *Stauroteuthis syrtensis* may be used for intraspecific communication (Johnsen *et al.*, 1999a, b), but the structure of the light organs in this species is not at all like the arm-tip lights of *Vampyroteuthis*. Although animals in kreisels reacted to point sources of artificial light by shading their eyes with their arms and web, or by moving away from the light, the response of *Vampyroteuthis* to artificial light never included luminescence.

Supplemental images (*in situ* video, laboratory low-light video, digital stills, and electron micrographs) are available online at <http://www.mbari.org/midwater/vamp>.

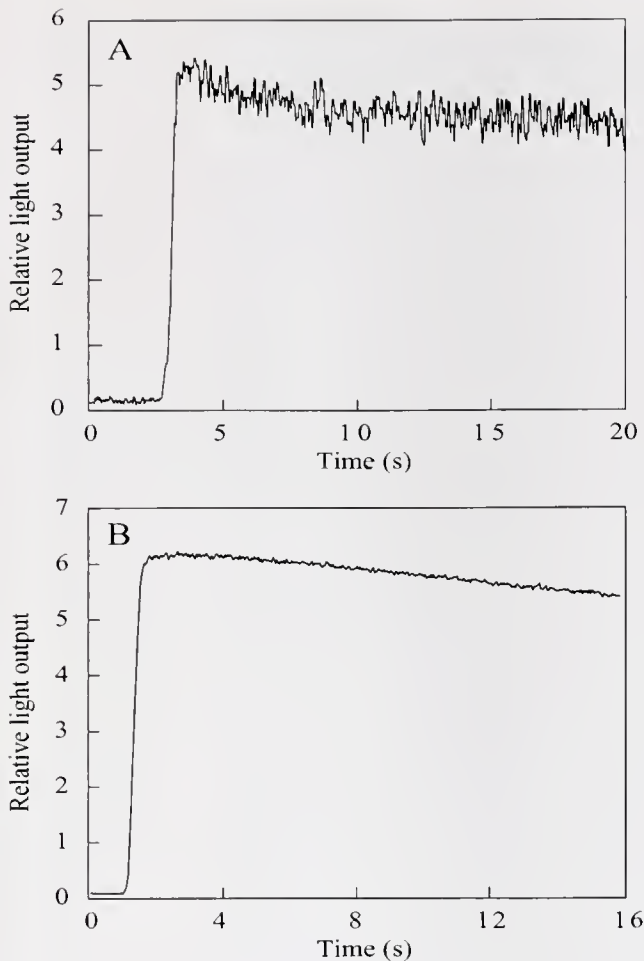


**Figure 5.** Luciferin and luciferase assays for arm-tip light organs of *Vampyroteuthis infernalis*. (A) Light produced by methanolic extracts upon the addition of *Oplophorus* luciferase indicates the presence of the luciferin coelenterazine. (B) Addition of coelenterazine to aqueous extracts shows high luciferase activity. Negative controls for both assays (omitted here for clarity) did not deviate measurably from the pre-injection baseline. The higher noise associated with the coelenterazine assay is due to the higher gain setting required to detect the presence of that molecule.

### Discussion

The effect of arm-tip luminescent displays on the dark-adapted human eye is striking; coupled with the bright blue light emitted by the two fin-base photophores, these displays produce a complex and dynamic visual field. The fundamental question they raise is, how does *Vampyroteuthis* use the light? Because these responses can be elicited by mechanical stimuli, we assume that production of light from the arm-tip organs and the cloud of luminous particles are elements of an anti-predation strategy based on startling or distracting a potential predator, thus allowing for escape (Young, 1983). The visual predators that we know about are all better swimmers than *Vampyroteuthis*, so its escape strategy must rely on more than speed. Deceptive, deimatic

behavior, such as chromatophore displays and unpredictable protean behavior, is often coupled with locomotion in cephalopod escape strategies (Hanlon and Messenger, 1996). In the darkness of its habitat, *Vampyroteuthis* may substitute luminescence for chromatophore displays in an otherwise familiar cephalopod behavior pattern of deception, diversion, and flight.

Arm-tip light organs, which can be bitten or broken off and then regenerated, may serve as sacrificial diversions for predators (Herring, 1977). Tip lights are found in several deep-living squids such as *Chroteuthis* and *Octopoteuthis*, where they may also serve as lures for prey, thus functioning like the escae of anglerfish and the barbels of stomiid fishes (Herring, 1977; Young, 1983). Our observations of apparently regenerated light organs at the ends of shortened arms in *Vampyroteuthis* may be evidence of their potential as sacrificial structures. The characteristics of the arm-tip displays indicate that there is direct neural control of their luminescence.

The production of luminous clouds is common among other deep-living pelagic invertebrates but rare in cephalopods. Anecdotal evidence for the production of luminous clouds by squids was summarized by Young *et al.* (1979), who suggested that renal fluid might be the luminous substrate. The only well-documented case is the sepiolid *Heteroteuthis*, which ejects a cloud of luminous particles when it is disturbed, presumably as a distraction to predators (Herring, 1977). The ejecta is produced by glands within the mantle that contain dense populations of light-producing bacteria, which are combined with ink and mucus during release through the siphon (Herring, 1988, 2002). The glands themselves emit light and have complex internal reflectors, which suggests that they have multiple uses (Herring, 1988). Structurally and operationally, the release of luminous fluids appears to be a completely different process in *Vampyroteuthis* than it is in *Heteroteuthis*.

Visual trickery is common within the depth range and light regime that *Vampyroteuthis* occupies (Robison, 1995, 1999; Herring, 2002), and our observations suggest some additional ways that its luminescence may be employed. Because the luminous fluid released by *Vampyroteuthis* is sticky, it would adhere to a potential predator and might initiate a "burglar alarm" consequence by painting it with bioluminescence that cannot be turned off or readily removed, thus making the attacker vulnerable to secondary predators. A similar behavior has been described for the bathypelagic holothurian *Enypsiastes eximia* (Robison, 1992). Glowing particles in the ejecta might be used to attract smaller prey such as copepods, which would then become trapped by the viscous matrix. This function has been proposed for the twinkling bioluminescent suckers and mucous glands of the cirrate octopus *Stauwoteuthis syrtensis* (Johnsen *et al.*, 1999b). It is tempting to correlate the size and abundance of light sources in the cloud with the epi-



**Figure 6.** Epifluorescence micrograph of the oral surface of an arm tip of *Vampyroteuthis infernalis*, showing patches of clustered particles. The dark areas along the midline are in the central plates, which bear suckers or their rudiments. Scale bar = 1 mm. Individual particles ranged from 10 to 15  $\mu\text{m}$  in greatest dimension.

dermal organs of *Vampyroteuthis*, but we have never seen the latter luminesce.

The luminous secretion from the arm tips of *Vampyroteuthis* is unique among the known cephalopod bioluminescent systems. Likewise, the arm-tip light organs are structurally distinct from all others. Predator avoidance seems the most likely function of the luminous behavior we have seen, but clearly, much is yet to be learned from observing these animals in their natural habitat.

#### Acknowledgments

R. E. Sherlock provided invaluable support both at sea and ashore. We gratefully acknowledge the skills and ded-

ication of the ROV *Ventana*'s pilots and the crew of the R/V *Point Lobos*. Coelenterazine, synthesized by S. Inoue, and *Oplophorus* luciferase, purified by Y. Haneda, were kindly provided by O. Shimomura. M. Haygood and J. W. Hastings gave us advice on the bacterial luciferase assays. We thank J. F. Case for a helpful review of the paper. Supported by the David and Lucile Packard Foundation.

#### Literature Cited

- Antonelis, G. A., M. S. Lowry, D. P. DeMaster, and C. H. Fiscus. 1987. Assessing northern elephant seal feeding by stomach lavage. *Mar. Mamm. Sci.* 3: 308-322.
- Clarke, M. R., and R. E. Young. 1998. Description and analysis of

- cephalopod beaks from stomachs of six species of odontocete cetaceans stranded on Hawaiian shores. *J. Mar. Biol. Assoc. UK* **78**: 623–641.
- Clarke, M. R., D. C. Clark, H. R. Martins, and H. M. Da Silva. 1996. The diet of the blue shark (*Prionace glauca* L.) in Azorean waters. *Arquipelago* **14**: 41–56.
- Drazen, J. C., T. W. Buckley, and G. R. Hoff. 2001. The feeding habits of slope dwelling macrourid fishes in the eastern North Pacific. *Deep-Sea Res. I* **48**: 909–935.
- Fiscus, C. H., D. W. Rice, and A. A. Wolman. 1989. Cephalopods from the stomachs of sperm whales taken off California. *NOAA Tech. Rep. Nat. Mar. Fish. Serv.* **83**: 1–12.
- Hammer, W. M. 1990. Design developments in the planktonkreisel, a plankton aquarium for ships at sea. *J. Plankton Res.* **12**: 397–402.
- Hanlon, R. T., and J. B. Messenger. 1996. *Cephalopod Behaviour*. Cambridge University Press, Cambridge.
- Hastings, J. W., T. O. Baldwin, and M. Z. Nicoli. 1978. Bacterial luciferase: assay, purification and properties. *Methods Enzymol.* **57**: 135–152.
- Healy, J. M. 1989. Spermatozoa of the deep-sea cephalopod *Vampyroteuthis infernalis* Chun: ultrastructure and possible phylogenetic significance. *Philos. Trans. R. Soc. Lond. B* **323**: 589–600.
- Herring, P. J. 1977. Luminescence in cephalopods and fish. *Symp. Zool. Soc. Lond.* **38**: 127–159.
- Herring, P. J. 1983. The spectral characteristics of luminous marine organisms. *Proc. R. Soc. Lond. B* **220**: 183–217.
- Herring, P. J. 1988. Luminescent organs. Pp. 449–489 in *The Mollusca. II. Form and Function*, E. R. Trueman and M. R. Clarke, eds. Academic Press, San Diego.
- Herring, P. J. 2002. *The Biology of the Deep Ocean*. Oxford University Press, Oxford.
- Herring, P. J., P. N. Dilly, and C. Cope. 1992. Different types of photophores in the oceanic squids *Octopoteuthis* and *Taningia* (Cephalopoda: Octopoteuthidae). *J. Zool. Lond.* **227**: 479–491.
- Herring, P. J., P. N. Dilly, and C. Cope. 1994. The bioluminescent organs of the deep-sea cephalopod *Vampyroteuthis infernalis* (Cephalopoda: Vampyromorpha). *J. Zool. Lond.* **233**: 45–55.
- Hunt, J. C. 1996. The behavior and ecology of midwater cephalopods from Monterey Bay: submersible and laboratory observations. Ph.D. dissertation, University of California, Los Angeles.
- Johnsen, S., E. J. Balsler, and E. A. Widder. 1999a. Light-emitting suckers in an octopus. *Nature* **398**: 113–114.
- Johnsen, S., E. J. Balsler, E. C. Fisher, and E. A. Widder. 1999b. Bioluminescence in the deep-sea cirrate octopod *Stauroteuthis syrtensis* Verrill (Mollusca: Cephalopoda). *Biol. Bull.* **197**: 26–39.
- Nixon, M. 1987. Cephalopod diets. Pp. 201–219 in *Cephalopod Life Cycles. II. Comparative Reviews*. P. R. Boyle, ed. Academic Press, Orlando, FL.
- Pearcy, W. G., and J. W. Ambler. 1974. Food habits of deep-sea macrourid fishes off the Oregon coast. *Deep-Sea Res.* **21**: 745–759.
- Pickford, G. E. 1946. *Vampyroteuthis infernalis* (Chun) an archaic dibranchiate cephalopod. I. Natural history and ecology. *Dana Rep.* **29**: 1–40.
- Pickford, G. E. 1949. *Vampyroteuthis infernalis* (Chun) an archaic dibranchiate cephalopod. II. External anatomy. *Dana Rep.* **32**: 1–132.
- Robison, B. H. 1992. Bioluminescence in the benthopelagic holothurian *Eupniastes eximia*. *J. Mar. Biol. Assoc. UK* **72**: 463–472.
- Robison, B. H. 1993. Midwater research methods with MBARI's ROV. *Mar. Technol. Soc. J.* **26**: 32–39.
- Robison, B. H. 1995. Light in the ocean's midwaters. *Sci. Am.* **273**: 60–64.
- Robison, B. H. 1999. Shape-change behavior by mesopelagic animals. *Mar. Freshw. Behav. Physiol.* **32**: 17–25.
- Seibel, B. A., E. V. Thuesen, J. J. Childress, and L. A. Gorodezky. 1997. Decline in pelagic cephalopod metabolism with habitat depth reflects differences in locomotory efficiency. *Biol. Bull.* **192**: 262–278.
- Seibel, B. A., E. V. Thuesen, and J. J. Childress. 1998. Flight of the vampire: ontogenetic gait-transition in *Vampyroteuthis infernalis* (Cephalopoda: Vampyromorpha). *J. Exp. Biol.* **201**: 2413–2424.
- Seibel, B. A., F. Chausson, F. H. Lallier, F. Zal, and J. J. Childress. 1999. Vampire blood: respiratory physiology of the vampire squid (Cephalopoda: Vampyromorpha) in relation to the oxygen minimum layer. *Exp. Biol. Online* **4**: 1–10.
- Widder, E. A., M. I. Latz, and J. F. Case. 1983. Marine bioluminescence spectra measured with an optical multichannel detection system. *Biol. Bull.* **165**: 791–810.
- Young, J. Z. 1977. Brain, behaviour and evolution of cephalopods. *Symp. Zool. Soc. Lond.* **38**: 377–434.
- Young, R. E. 1983. Oceanic bioluminescence: an overview of general functions. *Bull. Mar. Sci.* **33**: 829–845.
- Young, R. E., C. F. E. Roper, K. Mangold, G. Leisman, and F. G. Hochberg. 1979. Luminescence from non-bioluminescent tissues in oceanic cephalopods. *Mar. Biol.* **53**: 69–77.
- Young, R. E., M. Vecchione, and D. T. Donovan. 1998. The evolution of coleoid cephalopods and their present biodiversity and ecology. *S. Afr. J. Mar. Sci.* **20**: 393–420.

# Patterns and Processes of Larval Emergence in an Estuarine Parasite System

JONATHAN T. FINGERUT,<sup>1,\*</sup> CHERYL ANN ZIMMER,<sup>1,†</sup> AND RICHARD K. ZIMMER<sup>1,2,§</sup>

<sup>1</sup>*Department of Biology,* <sup>2</sup>*Neurosciences Program and Brain Research Institute, University of California, Los Angeles, California 90095-1606*

**Abstract.** Trematode parasites in intertidal estuaries experience constantly varying conditions, with the presence or absence of water potentially limiting larval transport between hosts. Given the short life spans ( $\leq 24$  h) of cercariae, emergence timing should be optimized to enhance the probability of successful transmission. In the present study, field measurements and laboratory experiments identified processes that regulate the emergence of cercariae from their first intermediate snail hosts in an intertidal marsh. Larvae emerged over species-specific temperature ranges, exclusively during daylight hours, and only when snails were submerged. The three factors operate over different temporal scales: temperature monthly, light diurnally (24-h period), and water depth tidally (12-h period). Each stimulus creates a necessary condition for the next, forming a hierarchy of environmental cues. Emergence as the tide floods would favor transport within the estuary, and light may trigger direct (downward or upward) swimming toward host habitats. Abbreviated dispersal would retain asexually reproduced cercariae within the marsh, and local mixing would diversify the gene pool of larvae encysting on subsequent hosts. In contrast to the timing of cercarial release, emergence duration was under endogenous control. Duration of emergence decreased from sunrise to sunset, perhaps in response to the diminishing lighted interval as the day progresses. Circadian rhythms that control cercarial emergence of freshwater species (including schistosomes) are often set by the activity patterns of subsequent hosts. In this estuary, however, the synchronizing agent is the tides. To-

gether, exogenous and endogenous factors control emergence of trematode cercariae, mitigating the vagaries of an intertidal environment.

## Introduction

Parasite larvae typically disperse prior to finding and infecting a host. As with propagules of free-living organisms, such as crabs (Forward *et al.*, 1986; Morgan, 1996), sponges (Amano, 1988), and plants (Horn *et al.*, 2001; Schaubert *et al.*, 2002), external cues may direct emergence of parasite larvae under favorable conditions. Because dispersal stages of digenetic trematodes have life spans of 24 h or less (McCarthy, 1999; Toledo *et al.*, 1999), timing emergence to correspond with host availability would be especially advantageous (Combes *et al.*, 1994; Pechenik and Fried, 1995). Moreover, the widespread distribution of trematodes in fresh water (Pages and Theron, 1990; Gerard, 2001) and saltwater (Martin, 1972; Bartoli and Combes, 1986; Jonsson and André, 1992; Curtis, 1997) environments allows for cross-habitat comparisons of emergence characteristics.

Trematode emergence has been studied largely in freshwater systems, with much of this research addressing medical and agricultural concerns (Bergquist, 2002; McKerrow and Salter, 2002). In common parasites, such as schistosomes, larval emergence from intermediate host snails varies on a circadian cycle and is synchronized with definitive host availability (Pages and Theron, 1990; N'Goran *et al.*, 1997). Circadian rhythms are usually entrained by photoperiod or thermoperiod (Theron, 1984; Mouchet *et al.*, 1992; Combes *et al.*, 1994). Freshwater parasite larvae moving from aquatic to terrestrial vertebrate hosts time their emergence to coincide with waterfront activities of the hosts, on scales of hours (Theron, 1989; Raymond and Probert, 1991).

Received 12 February 2003; accepted 16 June 2003.

\* Current address: Patrick Center for Environmental Research, Academy of Natural Sciences, 1900 Benjamin Franklin Parkway, Philadelphia, PA 19103-1195.

† Formerly Cheryl Ann Butman.

§ Corresponding author. E-mail: z@biology.ucla.edu

In southern California intertidal marshes, there is a guild of more than 18 digenetic trematode species (Martin, 1972). Sexual reproduction occurs in definitive shorebird hosts, which defecate parasite embryos into the marsh. Free-living miracidia hatch and infect the California horn snail, *Cerithiidea californica* (Haldeman), causing castration and other sublethal effects (Sousa, 1983; Sousa and Gleason, 1989). Asexual reproduction ensues, producing tens to thousands of cercariae per snail per day. The cercariae are produced in the area previously filled by the snail gonad, and the larvae then crawl within the snail hindgut to emerge from tissues in the rectum. Once released into the environment, cercariae encyst on second intermediate hosts, such as benthic snails (including *C. californica*), crabs, and fishes. Ingestion of these intermediate hosts by birds completes the parasite life cycle. Swimming cercariae are short-lived, so they must move toward or remain near host habitat for effective transmission. In marshes, tidally varying water depth and currents may limit transport.

The purpose of the present study was to identify factors controlling cercarial emergence in an intertidal estuary, as compared to freshwater systems. Two hypotheses were tested. (1) Timing of cercarial release varies over the day, as in freshwater trematodes. Light (24-h period) may impose a similar diel periodicity in both systems, but tidal (12-h period) effects (presence or absence of water, currents) would be unique to the estuary. (2) Exogenous factors control cercarial emergence in intertidal estuarine habitats, whereas in many freshwater species, larval release is controlled endogenously. Circadian rhythms in freshwater cercariae are often associated with innate activity patterns of intermediate or definitive hosts (Combes *et al.*, 1994). Such predictable host signals may not be important in an estuarine system, where submergence is limited by the tidal cycle.

Our research was conducted in two stages. Field studies measured emerging parasite larvae as a function of external variables (temperature, salinity, tidal height). Then, laboratory experiments identified the role of the specific factors in controlling the onset and duration of emergence. We herein define "emergence" as the shedding of cercariae from intermediate host snails. This study does not distinguish between the effects of larval behavior and rates of asexual reproduction on cercarial emergence patterns.

## Materials and Methods

### Field observations

In the field, we collected emerging cercariae of all species from snails (*Cerithiidea californica*) while simultaneously measuring environmental variables. Data were collected on 38 days from 1999 to 2002. Measurement intervals were selected to span all hours of the day and months of the year. Moreover, six night collections ( $\geq 1$  h after sundown) were

paired with a day collection on the preceding or proceeding tide to compare emergence within the same group of snails.

The field site (tidal channel) was located in Carpinteria Salt Marsh Reserve (CSMR), east of Santa Barbara, California (34°24'16" N, 119°31'30" W). Detailed physical characteristics are given in Fingerut *et al.* (2003). Biological measurements took place along the centerline of a channel 400 m long, 5 m wide, and 0.6 m deep (at high tide). A centrally located 3-m-wide mudflat was carpeted ( $460 \pm 16/\text{m}^2$ ) with *C. californica*, the first intermediate host for the trematodes studied here. The snail population extended hundreds of meters in the along-channel direction. The hydrodynamic regime in this and similar southern California marshes (*e.g.*, Mission Bay and Newport Bay) was dominated by slow flows ( $< 5$  cm/s), with shear velocities ( $u_*$ ) of 0.02 cm/s or less occurring more than 80% of the time (Fingerut *et al.*, 2003). Rarer, storm-driven currents ( $u_* \geq 0.8$  cm/s) occurred only about 1% of the time. Intertidal mudflats in channels were located 1.3 m above MLLW (mean lower low water) and were inundated twice a day by the semidiurnal tide. Water depth exceeded this height for an average of 4 h during each 12-h tidal cycle. Daily variations in salinity were 28–34 psu, consistent across seasons (Fingerut *et al.*, 2003). Salinity and temperature were relatively constant throughout the water column, indicating well-mixed conditions in the shallow channel.

*Collections of emerged cercariae.* A specially designed larval collector was used to measure (non-intrusively) cercarial emergence from a specified group of snail hosts. The main body of the collector was a flat, clear acrylic chamber (50 cm wide by 50 cm deep by 2.5 cm tall) with 34- $\mu\text{m}$ -mesh side panels and a solid bottom. Penetrating the top of the chamber was a 4 by 4 array of 8-cm-diameter holes (covering 32% of the surface area), each fitted with an inverted funnel (*i.e.*, small end pointing away from the chamber) intake. Contents of all funnels were united into a single 12.5-mm (ID) tube that fed into a peristaltic pump (Masterflex IP variable speed). The pump continuously filtered water from the chamber at a rate of about 5 liters/min over a 34- $\mu\text{m}$  mesh. The chamber volume was flushed 8 times during each 10-min sampling interval.

During each sampling event, 200 snails—from the largest ( $\approx 2.5$ -cm-long) size class in the marsh—were placed in the collector. Once on the mudflat, the chamber was gradually inundated by the incoming tide at the same time as the free-ranging snail population. There was no movement of cercariae into or out of the chamber. Captives were provided with oxygenated water at ambient temperature. Thus, cercariae collected on the filter could be ascribed solely to the enclosed host population. Size ranges of marsh cercariae are 50–100  $\mu\text{m}$  (width) and 200–1000  $\mu\text{m}$  (length) (Martin, 1950; Adams and Martin, 1963), so the mesh retained all species.

The system self-primed when the water level reached the

bottom of the funnels (5 cm water depth), usually 5–10 min after the tide first rose to the level of the mudflat. Every 10 min the filter was removed (and replaced), dipped in 90% ethyl alcohol, and placed in a sealed petri dish for later staining (0.5% Lugol's solution) and counting. Samples were also examined to identify numerically dominant species throughout the year and day. Each collection lasted 4 h, matching the average period of snail inundation. A cumulative frequency distribution was assembled from the total number of emerged cercariae during each 10-min collection. The time for 95% of all cercariae to emerge was compared between collections.

*Environmental measurements.* Properties of the physical environment during tidal inundation (4-h interval during flood or ebb) were measured on the 38 periods of quantified cercarial emergence. The mudflat was exposed to air for about 8 h between each tidal inundation. Maximal water depth was 60 cm during each tide. Using an ORION model 140 probe, seawater temperature and salinity were recorded 1 cm above the bed every 10 min. An underwater quantum sensor (LICOR model 190SA) was flush-mounted at the mudflat surface before tidal inundation to register light intensity at 1 Hz over the duration of the flood and ebb tides.

#### Laboratory experiments

Field measurements (see *Results*) indicated that the following factors may control cercarial emergence: temperature, host inundation (water depth), light, and time of day. Because we used only infected snails (rather than a random sample of the host population) in laboratory experiments, numbers of cercariae emerging were 10–100 times higher than those reported for field observations. With one exception, all laboratory experiments were conducted during summer months (June–September). Trials to evaluate cercarial emergence as a function of water temperature were performed during the spring (March–April).

*Effects of temperature.* Two time series were conducted in the laboratory, each using the same 53 snails (*C. californica*). The animals were placed individually in chambers (27 cm<sup>3</sup>) filled with seawater. In the first 7-day series, snails were held at a higher (+1 °C) water temperature on consecutive days, over the range 13–19 °C. Water was changed to the new temperature at 1000 h each day, and cercariae were collected 4 h later. (All times are reported as Pacific daylight time). Snails were kept dry at a constant 18 °C between runs (average spring air temperature for daylight hours). The second 7-day series followed the same protocol, except that exposure temperature was decreased 1°C per day, from 19 to 13 °C. At the end of a 4-h incubation period, contents of individual chambers were processed separately to determine species (Martin, 1972) and number of emerged cercariae.

*Effects of host inundation.* Two groups of 100 snails each

were randomly assigned to one of two treatments, and were placed in trays (21 cm long by 11 cm wide by 3 cm deep), at 20 snails per tray. Both groups were then situated in an environmental chamber at 21°C (average summer water temperature) with constant light (40  $\mu\text{mol}/\text{m}^2/\text{s}$ ). For one group, trays were kept dry for 4 h; for the other group, trays were filled with water from CSMR. At the end of 4 h the dry trays were briefly filled to suspend any emerged cercariae, and the water from both groups was filtered through a 34- $\mu\text{m}$  mesh. The number of emerged cercariae from each treatment was determined using the same processing methods as for the field samples. The following day, the treatments were reversed for the two snail groups. This 2-day experiment (one 4-h test period each day) was replicated three times, with a new batch of snails each time.

*Effects of light intensity.* Snails were exposed to a midday intensity ( $\sim 2000 \mu\text{mol}/\text{m}^2/\text{s}$ ) or to simulated dawn/dusk intensity ( $\sim 40 \mu\text{mol}/\text{m}^2/\text{s}$ ), created by reducing midday intensity with a neutral density filter. Snails (100 per group) placed in water-filled trays (see *Effects of host inundation*) were randomly assigned to one of the light conditions. Every 15 min, trays were overturned onto a 1-mm-mesh panel. Snails remained in the trays, but water and cercariae passed through. Trays were immediately refilled. Water and larvae were filtered over 34- $\mu\text{m}$  mesh and processed as in the field study. To control for the warming effect of the stronger sunlight, snail trays were held in a water bath maintained at 21°C (average for summer months). Trials lasted 2 d, with each group exposed to both conditions on consecutive days, and was replicated three times, each with different snails.

*Effects of time of day.* Two series of experiments were performed, one testing time of day (TOD) on emergence duration and the other testing for the existence of an endogenous rhythm. In the first series, 100 snails were placed in water-filled trays (see *Effects of host inundation*) at constant temperature (21°C) and light (40  $\mu\text{mol}/\text{m}^2/\text{s}$ ) for 4 h, starting at a different time each day (0900, 1200, 1500, and 1800). During each 4-h interval, emergence duration was determined as in the light experiments. Three replicate trials, each with new snails, were run at all four start times.

The goal of the second series of experiments was to determine if an endogenous rhythm, stimulated by light, might control emergence duration. This research is necessary but not sufficient to establish a circadian rhythm (Aschoff, 1960; Pittendrigh, 1993; Dunlap, 1999). The experiment held light:dark ratio constant while varying the onset of daylight. The prediction was that emergence duration would track with an internal clock set by incipient dawn, independent of the absolute time of day.

Two temperature- and light-controlled chambers were set at 21°C and 40  $\mu\text{mol}/\text{m}^2/\text{s}$ . The control chamber was set on a light:dark (14:10) cycle, with the natural (0600) sunrise. The experimental chamber used the same light:dark ratio

but with sunrise shifted either 8 h forward to 1400 or backward to 2200. In the first experiment, 100 snails were placed in the control and another 100 in the forward-shifted light chamber for 1 week before the trial began. After this acclimation period, emerging cercariae in both chambers were monitored over 4 h, beginning at 1800, as in the light experiments. In the second experiment, new snails were acclimated to the control and backward-shifted light regime for 1 week, and snails were monitored for 4 h beginning at 1000. In both experiments, the control and light-shifted snails were tested on sequential days. Moreover, as a check on the repeatability of the results, the same set of snails was monitored over an additional 4 d. Both experimental series were conducted once in 2000 and once in 2001.

**Results**

*Field observations*

The magnitude of cercarial emergence correlated significantly with water temperature, but not with salinity or total irradiance (Table 1 and Fig. 1). Snails (*Cerithidea californica*) first appeared in tidal channels in February, when temperatures rarely exceeded 13 °C (Fig. 2A). Emergence did not begin until March, however, when seawater warmed to 15 °C and above (Fig. 1). Despite continued warming during April and May, emergence was moderate until June. A relatively close correspondence between temperature and emergence is evident for the spring cercariae, which vacated their hosts at about the same temperature threshold (15 °C) during each tidal cycle (Fig. 2B). As cool ocean water flooded the marsh, the shallow water mass was warmed first from contact with the mudflat and then by the sun. Cercarial emergence following snail inundation was typically delayed up to 2 h, until water temperature exceeded 15 °C.

During the warm summer months, June to September, when water temperature was above 18 °C (average of 21 °C), the number of emerged cercariae increased substantially (Fig. 1). Larvae left snails as soon as they were inundated (Fig. 2C). Despite similarity in temperature (1–2 °C difference) between paired day/night collections, few or no cercariae were collected at night (Table 2). Seawater cooled by about 3 °C in October, but emergence remained

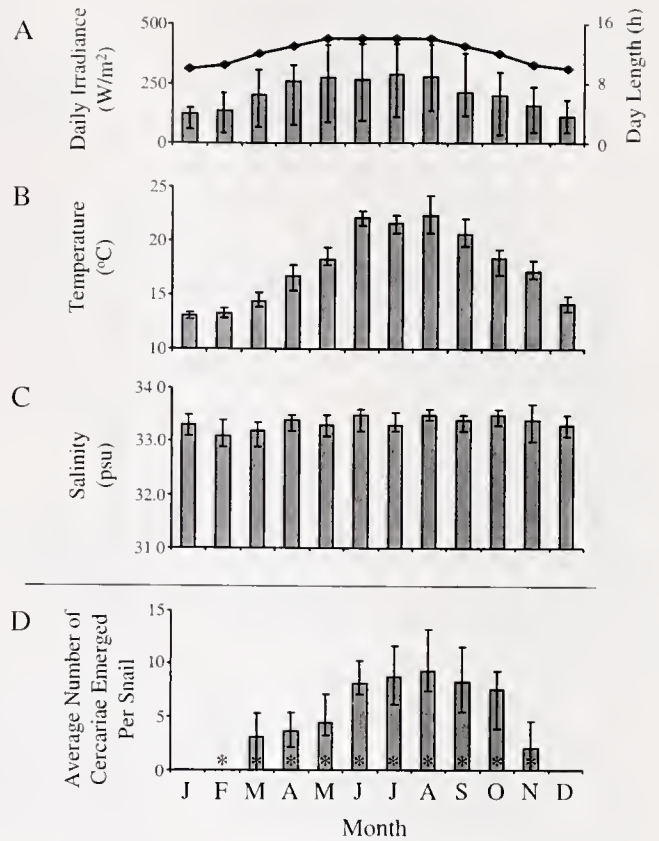


**Figure 1.** Variation throughout the year in average monthly (A) daily irradiance (histograms) and day length (diamonds), (B) water temperature, (C) salinity, (D) cercarial emergence and snail host presence on the mudflat (\*). Histograms represent monthly means, and vertical bars plot the ranges. For day length, ranges are smaller than the data points. Irradiance data were taken from the California Irrigation Management System website ([www.cimis.water.ca.gov](http://www.cimis.water.ca.gov)) and day length from the United States Naval Observatory website (<http://aa.usno.navy.mil>).

high until November. Once temperature dipped below 18 °C, only the cool-water species emerged.

Observations were made on the appearance of dominant species in the samples. *Himasthla rhigedana* (Dietz) and *Parorchis acanthus* (Nicoll) were the first species collected during the cool spring months (March to May), making up about 90% of the cercarial population. Other species, such as *Renicola buchanaani* (Cohn), *Euhaplorchis californensis* (Martin), and *Microphallid* sp. (Martin), first appeared in late May or early June. Due to its high prevalence (Kuris, 1990) and fecundity, *E. californensis* numerically dominated the June to September samples. Together, *H. rhigedana* and *E. californensis* composed more than 75% of all cercariae collected throughout the day during the warm summer months.

Whereas cercarial emergence was high and relatively constant from June through September, duration of emergence events varied considerably among the 21 summer daylight samples. A stepwise multiple regression analysis of

**Table 1**

*Stepwise multiple regression analysis of environmental cues as sources of variation in the number of emerged cercariae*

Source	F-value	df	P	% of variation explained
Temperature	37.14	1/31	<0.0001	68.3
Total irradiance	0.05	1/31	0.82	<1.0
Salinity	0.34	1/31	0.56	<1.0

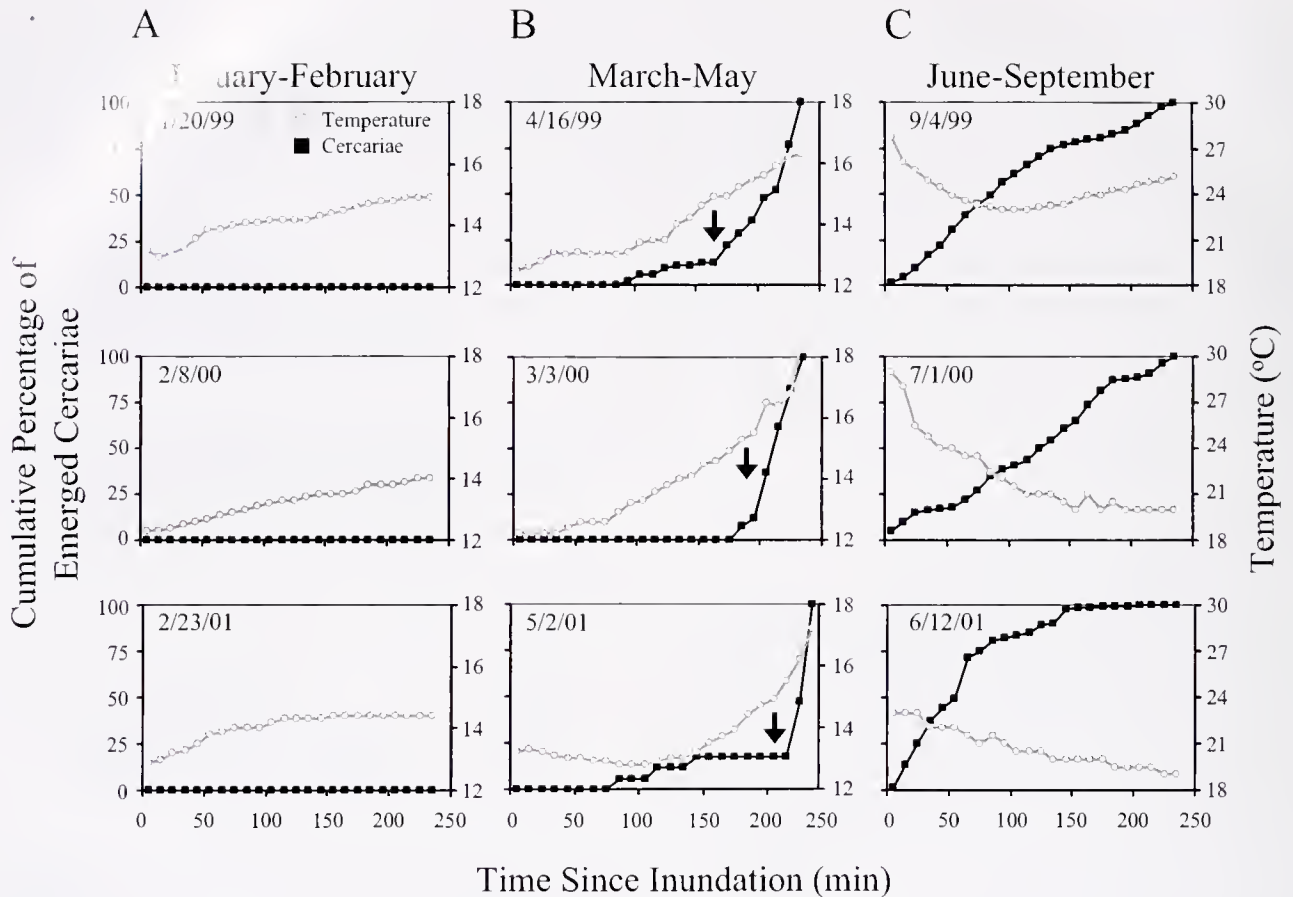


**Figure 2.** Three representative cercarial emergence patterns for each of three seasons of the year: (A) January–February (winter), (B) March–May (spring), and (C) June–September (summer). Water temperature (open circles) and cumulative percentages of emerged cercariae (closed squares) are from samples taken every 10 min. In (B), arrows correspond to the point in time when water temperature was first  $\geq 15$  °C.

emergence duration against temperature, salinity, time of year, and time of day yielded only one significant factor: time of day (Table 3). Duration of cercarial emergence decreased significantly throughout the day (Fig. 3A). Emergence intervals ranged from 4 h in the morning to 1 h or less by dusk (Figs. 3A and 4). This trend was present regardless of the numerical threshold for emergence duration (*i.e.*, 95%, as used here, *versus* 75% or 50%). Decreasing duration of cercarial emergence over the day resulted from an increase in the rate of emergence (number cercariae/h) (Fig. 3A, and least squares regression:  $F = 27.36$ ,  $df = 1/19$ ,  $P < 0.0001$ ;  $r^2 = 0.73$ ), not from a decrease in the total number of emerging cercariae (Fig. 3B, and  $P = 0.68$ ). Long (~4 h) emergence durations during the early morning resulted from a relatively small but constant larval delivery over the entire period of inundation. As the day progressed, more cercariae emerged per unit time, but over a contracted interval. Approaching dusk, large numbers of cercariae emerged in a quick burst as inundation commenced.

**Table 2**

*Number of cercariae shed during paired day/night collections*

Date	Day or night	Average temperature (°C)	Number emerged per 4 h collection
1 Aug 2000	Day	21.4	1043
	Night	20.1	22
18 Aug 2000	Day	20.9	1543
	Night	19.9	11
24 July 2001	Day	22.3	1684
	Night	20.5	28
12 Aug 2002	Day	19.3	537
	Night	18.2	3
22 Aug 2002	Day	22.1	832
	Night	21.7	1
6 Sept 2002	Day	19.3	349
	Night	17.9	0

Water temperature is averaged over the entire 4-h collection. Mean light intensity during nighttime collections, even under full moon conditions, was always  $< 0.01 \mu\text{mol}/\text{m}^2/\text{s}$ , compared to  $> 1035 \mu\text{mol}/\text{m}^2/\text{s}$  during daylight collections.

**Table 3**

Stepwise multiple regression analysis of abiotic factors as sources of variation in emergence duration

Source	F-value	df	P	% of variation explained
Time of day	47.96	1/19	<0.0001	72.8
Time of year (month)	0.03	1/19	0.86	<1.0
Temperature	<0.01	1/19	0.95	<1.0
Salinity	1.78	1/19	0.19	8.1

*Laboratory experiments*

*Host inundation.* Throughout all laboratory studies, cercariae emerged only if snails were totally submerged. The average number of cercariae to emerge in paired treatments with submerged ( $3861 \pm 599$  SEM) and dry ( $0 \pm 0$  SEM) snails showed unequivocally that cercariae would not leave the host unless it was underwater (Student's *t* test:  $t = 8.497$ ,  $df = 5$ ,  $P < 0.0001$ ). The muddy channel containing the highest snail densities was at a tidal height of about

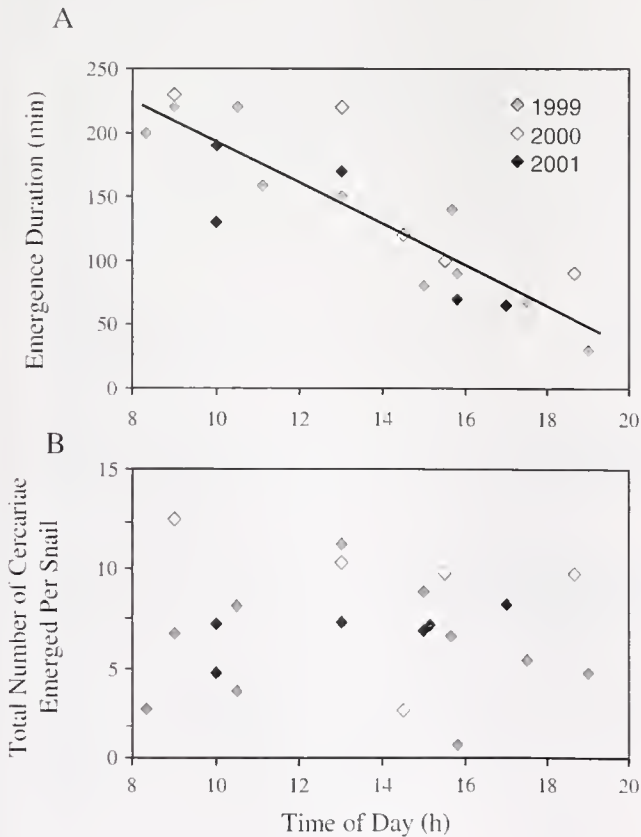


**Figure 3.** Effect of time of day (TOD) on cercarial emergence duration in the field. (A) The amount of time for 95% of all cercariae to emerge during a given event (4 h) as a function of TOD. (B) The total number of cercariae emerged per snail during a given event as a function of TOD.

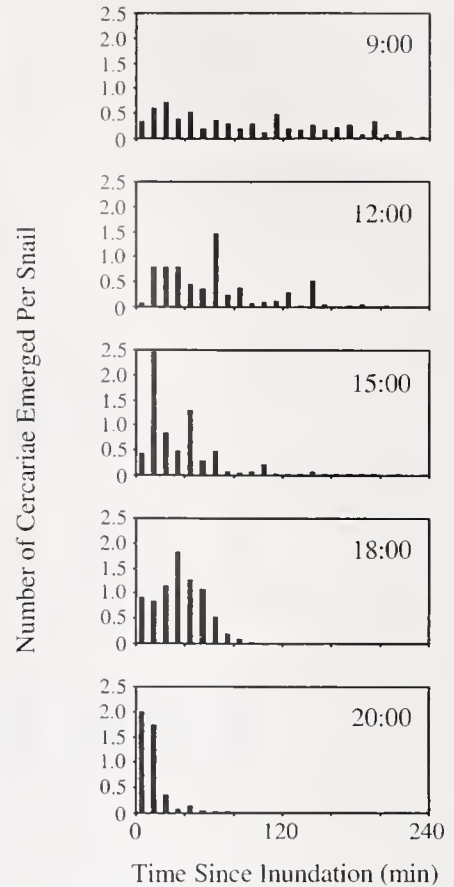


**Figure 4.** Representative series of histograms throughout the day, showing number of emerged cercariae per snail (10-min samples) as a function of time since tidal inundation. Times indicate when snail hosts were first submerged. Because snail inundation resulted from the natural high tide, each histogram was constructed on a different day.

1.3 m MLLW, so hosts spent 16 h/day out of water. Thus, inundation was a necessary condition for emergence.

*Temperature.* Cercariae of five trematode species emerged at three temperature thresholds (Fig. 5). Emergence of *H. rhigedana* and *P. acanthus* began in 15 °C water and continued for the maximal temperature (19 °C) tested. *Renicola buchmanii* emerged at an intermediate threshold of 17 °C through 19 °C. The two warm-water species, *E. californensis* and *Microphallid* sp., vacated their hosts only in the warmest waters tested (18–19 °C). Two-way nested ANOVAs were performed for each species separately. The numbers of emerged cercariae were significantly different among temperatures ( $P \leq 0.0001$  for all species) and individual snails ( $P \leq 0.04$ ) for all species except *R. buchmanii* ( $P = 0.17$ ). Because the order (ascending, descending) of temperature change had no significant ( $P \geq 0.11$ ) effect on the outcome, Schefflé *post hoc* comparisons were done for both series. Either way, there were two significantly ( $P \leq 0.005$ ) different temperature groupings for all species: one within their emergence range and

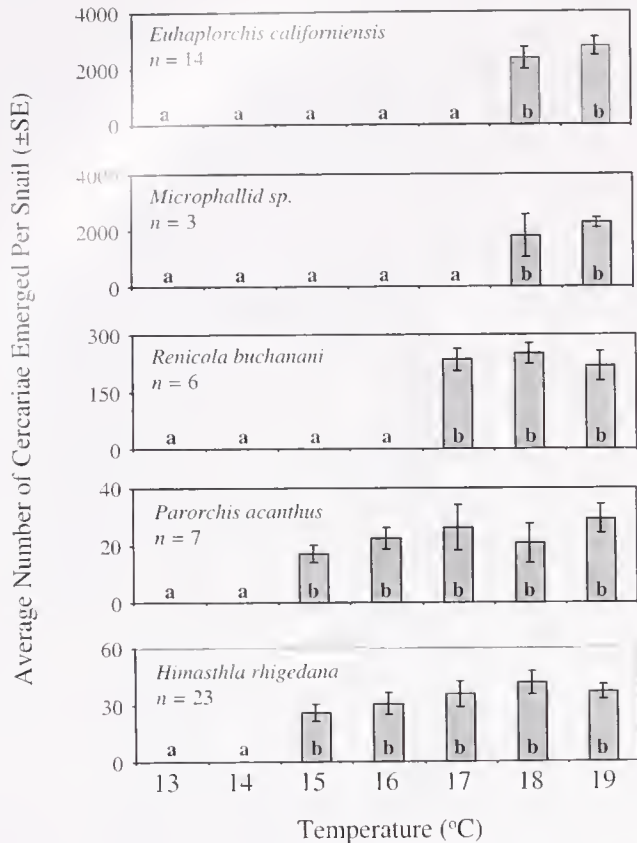


**Figure 5.** Number of cercariae emerged per snail over the temperature range 13–19 °C. Data are shown for five common trematode species. Histograms are means, and vertical bars are standard errors;  $n$  = number of snail hosts for a given trematode species. Means differ significantly when highlighted by a different letter (one-way ANOVA with *post hoc* Scheffé test;  $P < 0.001$ ).

the other for the lower temperatures that prohibited emergence (Fig. 5).

**Light.** Although daylight is required for cercarial emergence (Table 2), even low intensities approximating those at dawn and dusk ( $40 \mu\text{mol}/\text{m}^2/\text{s}$ ) were sufficient to trigger emergence under both field and laboratory settings. There was no significant difference, however, in the number of emerged cercariae or the duration of emergence at maximal midday intensity ( $2000 \mu\text{mol}/\text{m}^2/\text{s}$ ) relative to a minimal dawn/dusk intensity ( $40 \mu\text{mol}/\text{m}^2/\text{s}$ ) ( $t$  test;  $t = 1.021$ ,  $df = 10$ ,  $P = 0.36$  for duration;  $t = 0.475$ ,  $df = 10$ ,  $P = 0.65$  for number emerged).

**Time of day.** As in the field collections, the duration of cercarial emergence decreased over the course of the day (Fig. 6A), varying from a modest, protracted stream of cercariae at dawn to a contracted burst at dusk. There was a significant relationship between emergence duration and TOD (least squares regression:  $F = 199.78$ ,  $df = 1/10$ ,  $P < 0.0001$ ;  $r^2 = 0.93$ ), but not between number of emerged cercariae and TOD ( $P = 0.28$ ) (Fig. 6B). Moreover, there

was a noticeable change in the duration of emergence when the host light:dark cycle was shifted forward or back (Fig. 7). As predicted, emergence duration decreased when sunrise was shifted forward, implying that snails perceived a later time of day. Likewise, emergence duration increased when sunrise was shifted back. These changes agree qualitatively with the diel pattern observed in both the field and laboratory. Shifting the light:dark cycle had no apparent effect on the number of cercariae emerging (data not shown).

## Discussion

All digenetic trematodes have a free-swimming cercarial stage that transmits infection from the first intermediate host to the second intermediate or definitive host. Given the short life span of cercariae, emergence timing may be optimized to enhance the probability of successful transmission. In this study, larvae emerged from *Cerithidea californica* over species-specific temperature ranges, exclusively during day-

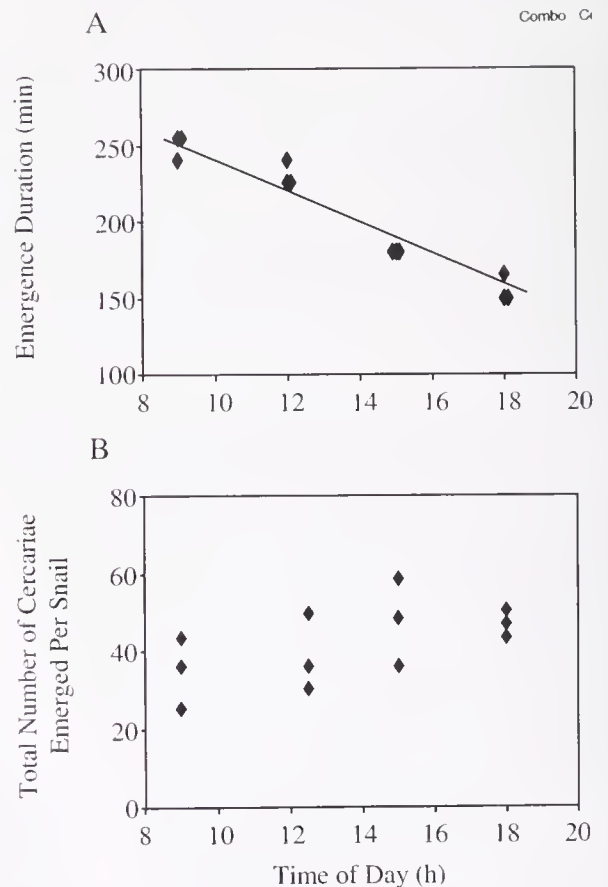


**Figure 6.** Effect of time of day (TOD) on emergence duration in the laboratory. (A) The amount of time for 95% of all cercariae to emerge during a given event (4 h) as a function of TOD. (B) The total number of cercariae emerged per snail during a given event as a function of TOD.

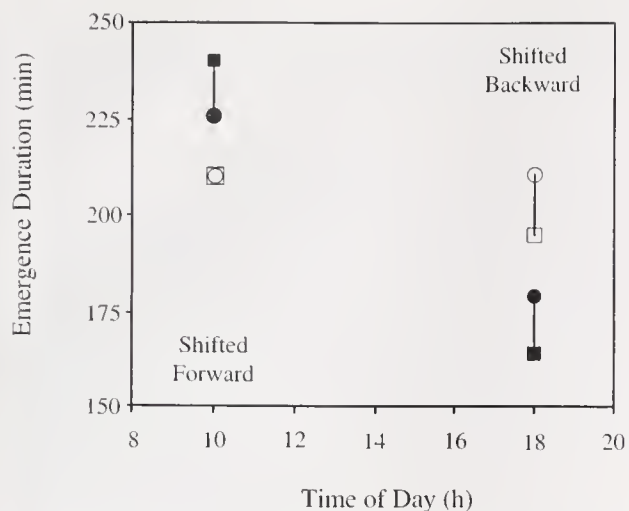


**Figure 7.** Effect on emergence duration of shifting sunrise forward or backward 8 h, compared to unshifted control groups. Filled symbols indicate control values by year (2000 ●, 2001 ■), and open symbols indicate shifted regimes (2000 □, 2001 □).

light hours, and only when snails were submerged (Fig. 8). The three determinants operated over different time scales: temperature monthly, light diurnally (24-h period), and water depth tidally (12-h period). Light/dark and tidal cycles also varied daily, according to the solar and lunar cycles, respectively. Each stimulus creates a necessary condition for the next, forming a hierarchy of environmental cues. Duration of cercarial emergence varied over the day and was under endogenous control. Although many studies have

identified two or more factors that affect propagule release, evidence for a cue hierarchy is relatively rare (some exceptions include Levy *et al.*, 2000; Watson *et al.*, 2000).

The timing and length of the transmission season was controlled, at least in part, by water temperature. Host snails (*C. californica*) occupied the muddy surface of the channel when water was 12 °C or above. Thus, the much narrower temperature ranges for emergence of the five trematode species may forecast the presence of second intermediate hosts. For example, cercariae of *Himasthla rhigedana* and *Parorchis acanthus* emerged over the broadest temperature range ( $\geq 15$  °C) and use the eurythermal *C. californica* as a second intermediate host. In contrast, *Euhaplorchis californiensis*, which emerged only in  $\geq 18$  °C water, infects several fish species that increase in abundance over the warming summer (Fritz, 1975; Brooks, 1999; Madon *et al.*, 2001).

Temperature thresholds for cercarial emergence occur in both estuarine and freshwater habitats (Lo and Lee, 1996; McCarthy, 1999). The number of emerged cercariae also varies with temperature in freshwater species (Shostak and Esch, 1990; Lyholt and Buchmann, 1996). Temperature-dependent emergence in freshwater species has been ascribed to a trade-off between the number emerged (positively related to temperature) and functional (infective), and the total life span (both negatively related to temperature) (McCarthy, 1999; Toledo *et al.*, 1999).

A characteristic common to estuarine and freshwater systems is diel variation in cercarial emergence, supporting our first hypothesis (see *Introduction*). In our study, cercariae

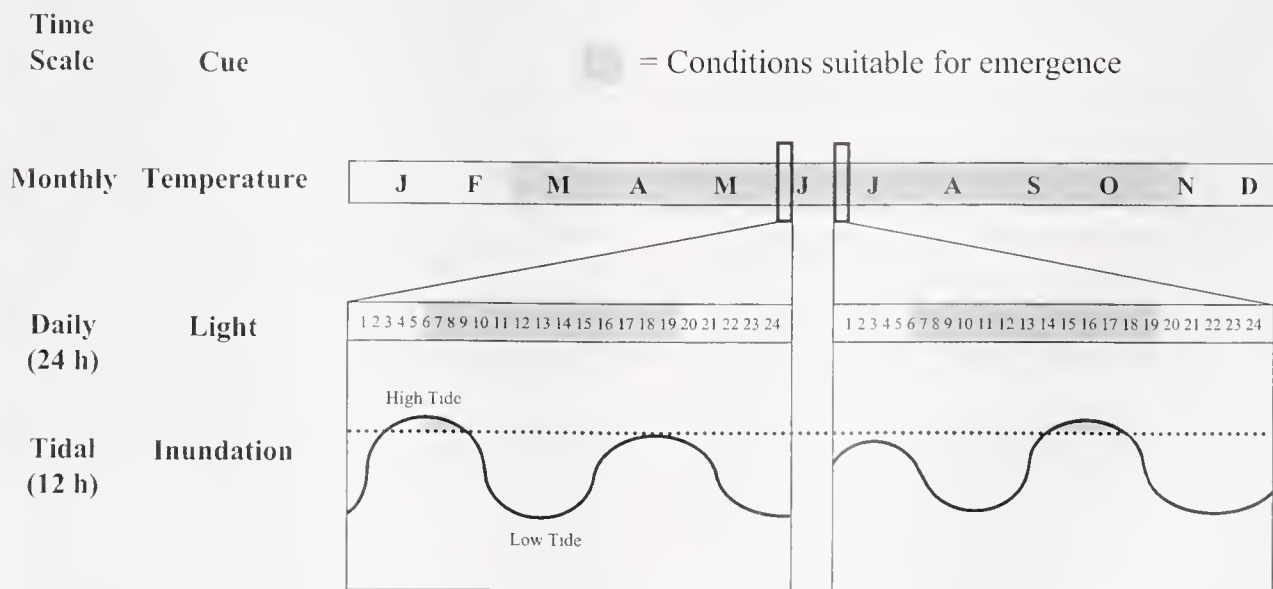


**Figure 8.** Diagram of the hierarchy of cues controlling cercarial emergence at monthly (temperature), daily (light), and tidal (host inundation) time scales. Dotted line represents tidal height (1.3 m above MLLW) of mudflat where sampling took place.

left submerged snails only during daylight hours. In intertidal estuaries, tidal currents are a predictable signal that determines both submersion time of the hosts and aquatic transport of the larvae. Thus, emergence of cercariae tracked with the daytime flood tide, which changes daily according to the lunar cycle. The daylight requirement may indicate that light is a critical cue. In laboratory flume studies, photo-triggered downward swimming of *H. rhigedana* was effective in slow flows typical of CSMR (Fingerut *et al.*, 2003). This activity quickly brings larvae to the bed for contact with benthic hosts. Moreover, we observed that *E. californiensis* cercariae swam upward in response to light (authors' unpubl. data). Such behavior could increase contact with host fish in the water column. Likewise, most freshwater cercariae are shed on the bottom, and light or gravity directs swimming up or down, depending on the location of the next host (Combes *et al.*, 1994). Within the CSMR estuary, cercarial emergence during flood tides would transport larvae 100–300 m/h (Fingerut, 2003). Yet, emerged *H. rhigedana* were dispersed only about 1–2 m before encystment (Fingerut, 2003). Directed swimming by larvae thus may have greatly shortened their transport distances.

Abbreviated dispersal would retain asexually reproduced larvae within the marsh, where local mixing could diversify the gene pool of cercariae encysting on subsequent hosts. All except 2 of 18 species within the southern California estuarine trematode guild have benthic second intermediate hosts (snails and crabs) that are interspersed within first intermediate host populations. In fact, some trematodes (*e.g.*, *H. rhigedana*, *P. acanthus*) use the same first and second host species. Turbulent mixing could commingle larval genotypes throughout the marsh, enhancing genetic diversity of the multiple cercariae that encyst each second host. Ensuing sexual reproduction between dissimilar genetic parasites within the definitive shorebird host may enhance fitness of the trematode population (*e.g.*, Scheltema, 1971; Jablonski, 1986; Pechenik, 1999, for marine invertebrates).

As in digenetic trematodes, larval release in free-living estuarine invertebrates is contingent on tidal flows. For example, estuarine mud-dwelling isopods (*e.g.*, *Paragnathia formica* [Hess]) release larvae only when high tides reach their burrows, facilitating transport (Tinsley and Reilly, 2002). Shore crabs living in high-intertidal refuges limit larval release to nighttime spring tides (Morgan and Christy, 1995; Hovel and Morgan, 1997). Darkness reduces predation on spawners, whereas large-amplitude tides flush larvae away from diurnal predators. Similarly, in tidally influenced riverine habitats, adult terrestrial crabs, such as *Sesarma haematocheir* (de Haan), release larvae on a nighttime semilunar cycle that minimizes predation on adults while providing optimal conditions for survival and dispersal of larvae (Saigusa, 1982).

Endogenously regulated emergence differs between the estuarine intertidal trematodes studied here and many freshwater species. This result was not predicted by our second hypothesis (see *Introduction*), and may be explained by the major synchronizing agents in these systems. In freshwater, emergence timing is often under endogenous control and is directly linked to presence of the subsequent host. For freshwater schistosomes, definitive vertebrate hosts frequent the waterfront on a predictable innate cycle. Circadian rhythms of cercarial emergence are tuned to the biological clocks and activity patterns of these vertebrates (Combes, 1991; Combes *et al.*, 1994). For example, maximal emergence of some schistosome cercariae corresponds with the proximity of their bovine hosts. Cercariae emerge and swim to the surface in the morning, thus infecting the animals while they drink at the waterfront (Mouahid *et al.*, 1991; Raymond and Probert, 1991). Likewise, afternoon emergence peaks occur in trematode species infecting human hosts that wash, play, or drink at midday (Theron, 1984; Pages and Theron, 1990). Emergence in non-schistosome species, such as *Proterometra edneyi* (Uglen) also occurs on a circadian cycle timed to the presence of fish that are their second intermediate hosts (Lewis *et al.*, 1989). There is no emergence rhythm in cercariae of *Fasciola hepatica* (Linnaeus), however, because second intermediate host plants are always available (Bouix-Busson *et al.*, 1985), making synchronization unnecessary.

In the CSMR intertidal estuary, duration rather than timing of emergence was apparently under endogenous control, and the tide was the synchronizing agent. There is a finite, tidally determined period of sufficient immersion for larval transport in lighted hours. Emergence duration decreased throughout the day in response to dwindling daylight. An endogenous rhythm associated with the light:dark cycle may be responsible for the changing emergence rate over the course of a suitable flood tide. Apportioning larvae over the entire lighted submerged interval maximizes the dispersal envelope. Contraction of emergence duration throughout the day may optimize use of remaining daylight hours. As the day progresses, larger pulses of larvae must emerge over a shorter interval to take advantage of the vestigial light. Such diel adjustments to the emergence period are unnecessary in freshwater systems, where water depth is relatively stable. Thus driven by the submergence constraints of their natal habitat, the emergence strategies of estuarine cercariae involve both exogenous and endogenous factors that optimize transport to tidally accessible hosts.

#### Acknowledgments

This study was supported by awards from the National Science Foundation (OCE 97-22972 and OCE 02-47834) and the UCLA Council on Research. We thank M. Grattan and E. Maldonado for their tireless help in the field. A.

Kuris contributed valuable insights on trematode parasites and comments that substantially improved earlier drafts of this manuscript.

### Literature Cited

- Adams, J. E., and W. E. Martin. 1963. Life cycle of *Himasthla rhigedana* Dietz 1909 (Trematoda: Echinostomatidae). *Trans. Am. Microsc. Soc.* **82**: 1–6.
- Amano, S. 1988. Morning release of larvae controlled by the light in an intertidal sponge, *Callyspongia ramosa*. *Biol. Bull.* **175**: 181–184.
- Aschoff, J. 1960. Exogenous and endogenous components in circadian rhythms. *Cold Spring Harbor Symp. Quant. Biol.* **25**: 11–28.
- Bartoli, P., and C. Combes. 1986. Dissemination strategies of trematode cercariae in a coastal marine ecosystem. *Acta Oecol. Oecol. Gen.* **7**: 101–114.
- Bergquist, N. R. 2002. Schistosomiasis: from risk assessment to control. *Trends Parasitol.* **18**: 309–314.
- Bonix-Busson, D., D. Rondelaud, and C. Combes. 1985. L'infestation de *Lymnaea glabra* Müller par *Fasciola hepatica* L: les caractéristiques des émissions cercariennes. *Ann. Parasitol. Hum. Comp.* **60**: 11–21.
- Brooks, A. J. 1999. Factors influencing the structure of an estuarine fish community: the role of interspecific competition (*Gillichthys mirabilis*, *Leptocottus armatus*). Ph.D. dissertation, University of California, Santa Barbara.
- Combes, C. 1991. Ethological aspects of parasite transmission. *Am. Nat.* **138**: 866–880.
- Combes, C., A. Fournier, H. Mone, and A. Theron. 1994. Behaviors in trematode cercariae that enhance parasite transmission: patterns and processes. *Parasitology* **109**: S3–S13.
- Curtis, L. A. 1997. *Ilyanassa obsoleta* (Gastropoda) as a host for trematodes in Delaware estuaries. *J. Parasitol.* **83**: 793–803.
- Dunlap, J. C. 1999. Molecular basis for circadian clocks. *Cell* **96**: 271–290.
- Fingerut, J. T. 2003. From host to host: interaction of environmental conditions and larval behavior in transmission of an estuarine parasite. Ph.D. dissertation, University of California, Los Angeles.
- Fingerut, J. T., C. A. Zimmer, and R. K. Zimmer. 2003. Larval swimming overpowers turbulent mixing and facilitates transmission of a marine parasite. *Ecology* **84**: 2502–2515.
- Forward, R. B. Jr., J. K. Douglass, and B. E. Kenney. 1986. Entrainment of the larval release rhythm of the crab *Rhithropanopeus harrissi* (Brachyura: Xanthidae) by cycles in salinity change. *Mar. Biol.* **90**: 537–544.
- Fritz, E. S. 1975. The life history of the California killifish *Fundulus parvipinnis* in Anaheim Bay, California, USA. *Fish. Bull.* **165**: 91–106.
- Gerard, C. 2001. Structure and temporal variation of trematode and gastropod communities in a freshwater ecosystem. *Parasite* **8**: 275–287.
- Horn, H. S., R. Nathan, and S. R. Kaplan. 2001. Long-distance dispersal of tree seeds by wind. *Ecol. Res.* **16**: 877–885.
- Hovel, K. A., and S. G. Morgan. 1997. Planktivory as a selective force for reproductive synchrony and larval migration. *Mar. Ecol. Prog. Ser.* **157**: 79–95.
- Jablonski, D. 1986. Larval ecology and macroevolution in marine invertebrates. *Bull. Mar. Sci.* **39**: 565–587.
- Jonsson, P. R., and C. Andre. 1992. Mass mortality of the bivalve *Cerastoderma edule* on the Swedish west coast caused by infestation with the digenian trematode *Cercaria cerastodermae* I. *Ophelia* **36**: 151–157.
- Kuris, A. 1990. Guild structure of larval trematodes in molluscan hosts: prevalences, dominance and significance of competition. Pp. 69–100 in *Parasite Communities: Patterns and Processes*, G.W. Esch, ed. Chapman and Hall, London.
- Levy, O., I. Mizrahi, N. E. Chadwick-Furman, and Y. Achituv. 2001. Factors controlling the expansion behavior of *Favia fava* (Cnideria: Scleractinia): effects of light, flow, and planktonic prey. *Biol. Bull.* **200**: 118–126.
- Lewis, M. C., I. G. Welsford, and G. L. Uglem. 1989. Cercarial emergence of *Proterometra macrostoma* and *P. edneyi* (Digenea: Azygiidae): contrasting responses to light:dark cycling. *Parasitology* **41**: 201–208.
- Lo, C. T., and K. M. Lee. 1996. Pattern of emergence and the effects of temperature and light on the emergence and survival of heterophyid cercariae (*Centrocestus formosanus* and *Haplorchis pumilio*). *J. Parasitol.* **82**: 347–350.
- Lyholt, H. C. K., and K. Buchmann. 1996. *Diplostomum spathaceum*: effects of temperature and light on cercarial shedding and infection of rainbow trout. *Dis. Aquat. Org.* **25**: 169–173.
- Madon, S. P., G. D. Williams, J. M. West, and J. B. Zedler. 2001. The importance of marsh access to growth of the California killifish, *Fundulus parvipinnis*, evaluated through bioenergetics modeling. *Ecol. Model.* **136**: 149–165.
- Martin, W. E. 1950. *Euhaplorchis californiensis* N.G., N. Sp., Heterophyidae, Trematoda, with notes on its life cycle. *Trans. Am. Microsc. Soc.* **69**: 194–209.
- Martin, W. E. 1972. An annotated key to the cercariae that develop in the snail *Cerithidea californica*. *Bull. S. C. Acad. Sci.* **79**: 39–43.
- McCarthy, A. M. 1999. The influence of temperature on the survival and infectivity of the cercariae of *Echinoparyphium recurvatum* (Digenea: Echinostomatidae). *Parasitology* **118**: 383–388.
- McKerrow, J. H., and J. Salter. 2002. Invasion of skin by *Schistosoma* cercariae. *Trends Parasitol.* **18**: 193–195.
- Morgan, S. G. 1996. Influence of tidal variation on reproductive timing. *J. Exp. Mar. Biol. Ecol.* **206**: 237–251.
- Morgan, S. G., and J. H. Christy. 1995. Adaptive significance of the timing of larval release by crabs. *Am. Nat.* **145**: 457–479.
- Mouahid, A., H. Mone, A. Chaib, and A. Theron. 1991. Cercarial shedding patterns of *Schistosoma bovis* and *Schistosoma haematobium* from single and mixed infections of *Bulinus truncates*. *J. Helminthol.* **65**: 8–14.
- Mouchet, F., A. Theron, P. Bremond, E. Sellin, and B. Sellin. 1992. Pattern of cercarial emergence of *Schistosoma curassoni* from Niger and comparison with three sympatric species of schistosomes. *J. Parasitol.* **78**: 61–63.
- N'Goran, E., P. Bremond, and E. Sellin. 1997. Intraspecific diversity of *Schistosoma haematobium* in West Africa: chronobiology of cercarial emergence. *Acta Trop.* **66**: 35–44.
- Pages, J. R., and A. Theron. 1990. Analysis and comparison of cercarial emergence rhythms of *Schistosoma haematobium*, *Schistosoma intercalatum*, *Schistosoma bovis*, and their hybrid progeny. *Int. J. Parasitol.* **20**: 193–198.
- Pechenik, J. 1999. On the advantages and disadvantages of larval stages in benthic marine invertebrate life cycles. *Mar. Ecol. Prog. Ser.* **177**: 269–297.
- Pechenik, J. A., and B. Fried. 1995. Effect of temperature on survival and infectivity of *Echinostoma trivolvis* cercariae: a test of the energy limitation hypothesis. *Parasitology* **111**: 373–378.
- Pittendrigh, C. S. 1993. Temporal organization: reflections of a darwinian clock-watcher. *Annu. Rev. Physiol.* **55**: 16–54.
- Raymond, K., and A. J. Probert. 1991. The daily cercarial emission rhythm of *Schistosoma margrebowiei* with particular reference to dark period stimuli. *J. Helminthol.* **65**: 159–168.
- Saigusa, M. 1982. Larval release rhythm coinciding with solar day and tidal cycles in the terrestrial crab *Sesarma*—harmony with the semi-lunar timing and its adaptive significance. *Biol. Bull.* **162**: 371–386.
- Schauber, E. M., D. Kelly, P. Turchin, C. Simon, W. G. Lee, R. B. Allen, I. J. Payton, P. R. Wilson, P. E. Cowan, and R. E. Brockie.

2002. Masting by eight New Zealand plant species: the role of temperature as a synchronizing cue. *Ecology* **83**: 1214–1225.
- Scheltema, R. S. 1973. Larval dispersal as a means of genetic exchange between geographically separated populations of shallow-water benthic marine gastropods. *Biol. Bull.* **140**: 284–322.
- Shostak, A. W., and G. W. Esch. 1990. Photocycle-dependent emergence by cercariae of *Halipegus occidualis* from *Helisoma anceps*, with special reference to cercarial emergence patterns as adaptations for transmission. *J. Parasitol.* **76**: 790–795.
- Sousa, W. P. 1983. Host life history and effect of parasitic castration on growth: a field study of *Cerithidea californica* Haldeman (Gastropoda: Prosobranchia) and its trematode parasites. *J. Exp. Mar. Biol. Ecol.* **73**: 273–296.
- Sousa, W. P., and M. Gleason. 1989. Does parasitic infection compromise host survival under extreme environmental conditions? The case for *Cerithidea californica* (Gastropoda: Prosobranchia). *Oecologia* **80**: 456–464.
- Theron, A. 1984. Early and late shedding patterns of *Schistosoma mansoni* cercaria: ecological significance in transmission to human and murine hosts. *J. Parasitol.* **70**: 652–665.
- Theron, A. 1989. Hybrids between *Schistosoma mansoni* and *Schistosoma rodhaini*: characterization by cercarial emergence rhythms. *Parasitology* **99**: 225–228.
- Tinsley, M. C., and S. D. Reilly. 2002. Reproductive ecology of the saltmarsh-dwelling marine ectoparasite *Paragnathia formica* (Crustacea: Isopoda). *J. Mar. Biol. Assoc. UK* **82**: 79–84.
- Toledo, R., C. Munoz-Antoli, and J. G. Esteban. 1999. Production and chronobiology of emergence of the cercariae of *Euparyphium albufeirensis* (Trematoda: Echinostomatidae). *J. Parasitol.* **85**: 263–267.
- Watson, G. J., M. E. Williams, and M. G. Bentley. 2000. Can synchronous spawning be predicted from environmental parameters? A case study of the lugworm *Arenicola marina*. *Mar. Biol.* **136**: 1003–1017.

# Larval Development and Metamorphosis in *Pleurobranchaea maculata*, With a Review of Development in the Notaspidea (Opisthobranchia)

GLENYS D. GIBSON

*Department of Biology, Acadia University, Wolfville, Nova Scotia, Canada B4P 2R6*

**Abstract.** *Pleurobranchaea maculata* is a carnivorous notaspidean that is common in New Zealand. This species produces small eggs (diameter 100  $\mu\text{m}$ ) and planktotrophic veligers that hatch in 8 d and are planktonic for 3 weeks before settling on biofilmed surfaces (14 °C). Larval development is known in detail for only two other notaspidean species, *P. japonica* and *Berthellina citrina*. In all three species of pleurobranchids, mantle and shell growth show striking differences from veligers of other opisthobranch taxa. In young veligers of pleurobranchids, the shell is overgrown by the mantle, new shell is added by cells other than those of the mantle fold, and an operculum does not form. Thus some "adult" traits (*e.g.*, notum differentiation, mechanism of shell growth, lack of operculum) are expressed early in larval development. This suggests that apomorphies characteristic of adult pleurobranchids evolved through heterochrony, with expression in larvae of traits typical of adults of other clades. The protoconch is dissolved post-settlement and not cast off as occurs in other opisthobranch orders, indicating that shell loss is apomorphic. *P. maculata* veligers are atypical of opisthobranchs in having a field of highly folded cells on the lower velar surface, a mouth that is posterior to the metatroch, and a richly glandular, possibly chemodefensive mantle. These data indicate that notaspidean larvae are highly derived in terms of the novel traits and the timing of morphogenic events. Phylogenetic analysis must consider embryological origins before assuming homology, as morphological similarities (*e.g.*, shell loss) may have developed through distinct mechanisms.

## Introduction

The Notaspidea is a small, specialized order of opisthobranchs that are considered to be phylogenetically intermediate between the highly derived Nudibranchia and the more basal Cephalaspidea (Schmekel, 1985; Willan, 1987; Mikkelsen, 1998) or monophyletic with the Nudibranchia to form the Nudipleura (Wägele and Willan, 2000). Comparative embryological studies of the Notaspidea are therefore significant for phylogenetic analyses but also for understanding morphological evolution in the Opisthobranchia, a clade rich in homoplastic similarities (Gosliner, 1991, 1994; Mikkelsen, 1998). Unfortunately, little is known about notaspidean development. My goal is to describe larval development in *Pleurobranchaea maculata* (Quoy and Gaimard, 1832) and to provide a preliminary analysis of development in Notaspidea.

Adult notaspideans are carnivores and opportunistic scavengers. They are characterized by a single, external ctenidium on the right side, rolled rhinophores, and a flattened shell (Willan, 1983; Schmekel, 1985; Willan, 1987). The order traditionally includes the Umbraculomorpha (families Tylodinidae and Umbraculidae) with large limpet-like external shells and a small mantle, and the Pleurobranchomorpha (Pleurobranchidae) with a prominent mantle and shells that are internal and reduced or lost in adults (Thompson, 1976; Willan, 1983, 1987). Mantle secretions provide chemical defense in many species, both shelled and shell-less, through the release of acid (Thompson and Slinn, 1959; Thompson, 1988), secondary metabolites (Ciavatta *et al.*, 1993, 1995; Spinella *et al.*, 1997), or dietary alkaloids (Ebel *et al.*, 1999). On the basis of adult anatomy, some investigators suggest that the Notaspidea are polyphyletic (Schmekel, 1985), while others argue that they are

paraphyletic and require inclusion of the Nudibranchia (Wägele and Willis 2000).

Phylogenetic analysis promotes an understanding of the relatedness among taxa, and of morphological evolution, for which comparative developmental data are essential. Although there is no reason to assume that larval and adult traits have coevolved, inclusion of larval traits strengthens analyses by increasing the data set, but more importantly, by revealing homologies in traits with similar embryological origins. While we have an abundance of data on nudibranchs, development is poorly known for some of the less speciose orders. For the Notaspidea in particular, detailed descriptions of larval development are limited to two species of Pleurobranchidae: *Berthellina citrina* Rueppell and Leuckart, 1828 (Gohar and Abul-Ela, 1957; Usuki, 1969), and *Pleurobranchaea japonica* Thiele, 1925 (Tsubokawa and Okutani, 1991). Partial information on larvae is available for less than a half-dozen additional species. Even these limited data suggest that larval pleurobranchids are diverse and can be planktotrophic, lecithotrophic, or direct developing (Gohar and Abul-Ela, 1957; Usuki, 1969; Thompson, 1976; Tsubokawa and Okutani, 1991; Wägele, 1996; Goddard, 2001b). We lack descriptions of development for all species of the Tylodinidae and Umbraculidae.

My objectives are to describe development of *Pleurobranchaea maculata*, and to compare development of notaspideans with other opisthobranchs. *P. maculata* is an opportunistic carnivore found in New Zealand, southeastern Australia, China, Sri Lanka, and Japan (Willan, 1983; Marcus and Gosliner, 1984). Notes by Willan (1983) indicate that *P. maculata* produces long, cylindrical egg masses that release planktotrophic veligers. The present study extends this record to include embryology, larval structure, and metamorphosis using bright field and scanning electron microscopy (SEM).

### Materials and Methods

Specimens of *Pleurobranchaea maculata* were collected from intertidal sandflats at the Tahuna Torea Reserve, Tamaki Estuary, Auckland, New Zealand, in August 2001. Adults were maintained at ambient conditions (seawater temperature 14 °C) and were fed cockles (*Austrovenus stutchburyi* Wood, 1828) or oysters (*Osireia lutaria* Hutton, 1873) daily. Egg masses were cultured in flowing seawater (14 °C), and small sections were removed for observation. Larvae were cultured in 1-l jars of 1- $\mu$ m-filtered seawater at 17–19 °C. Larvae were fed a 1:1:1 mixture of *Dunaliella salina* Teodoresco, 1905, *Isochrysis galbana* Parke, 1949, and *Pavlova lutheri* Green, 1975 three times weekly. Settlement occurred in pediveligers that were cultured in a 1-l jar (17–19 °C) with a 1-week growth of biofilm on the glass surface.

Live embryos, larvae, and juveniles were observed, sketched, and photographed with a Nikon AFX photomicroscope. Measurements were taken to the nearest 5  $\mu$ m. Pediveligers and early juveniles were fixed for SEM in 2.5% glutaraldehyde followed by post-fixation in 1% osmium tetroxide, both in filtered seawater. After fixation, specimens were dehydrated in ethanol, critical-point-dried with a Polaron B3000 Series II critical-point drier, and coated with gold-palladium with a Polaron SC7640 sputter coater. Specimens were observed with a Phillips XL 30S SEM at 5 kV. Plates were composed in Corel Photo Paint 9.0 and Corel Draw 9.0, using both scanned negatives (light micrographs) and digital images (electron micrographs).

### Results

The cylindrical egg masses were  $171.60 \pm 59.61$  mm in length ( $X \pm SD$ ;  $n = 5$ ; range 88–240 mm) and about 8–12 mm in width, as produced by two adults 110 and 145 mm in length. *P. maculata* spawned frequently, and these two individuals produced 15 egg masses in about 5 weeks of laboratory culture. Usually adults deposited the loosely coiled egg strings on the side walls of the tank near the air-water interface. The eggs were white,  $100.91 \pm 2.18$   $\mu$ m in diameter ( $n = 45$ ), and deposited in egg capsules housed within long strings that formed a double spiral at the periphery of the jelly mass. Capsules were  $259.50 \pm 10.92$  by  $250.00 \pm 10.54$   $\mu$ m in size ( $n = 20$ ), and contained an average of  $3.97 \pm 1.02$  eggs per capsule (range 2–6;  $n = 30$  capsules in each of 7 egg masses). Small globules of yolk (filled with lipid droplets and several times larger than polar bodies) detached from developing young in about 18% of the egg capsules observed ( $n = 244$  capsules, from a total of 8 egg masses). Early veligers ingested this extra-embryonic yolk before hatching. Fecundity was estimated to be  $318,417 \pm 110,602$  embryos per egg mass ( $n = 5$ ). Egg masses were as figured by Willan (1983).

Spawning generally occurred over a period of 2–3 h in the early and mid-morning. A chronology of early embryological events is summarized in Table 1. Elongate trochophores, with a flat velar field and small pedal rudiment, developed by 4 d. The shell was visible by 4.5 d and had grown to cover the visceropallial mass by 5 d. Also at 5 d, the statocysts, each with a single statolith, were visible, and embryos were capable of ingesting extra-embryonic yolk. By 5.5 d, the dark red pigmented mantle organ was visible and the internal organs, although still yolky, were better defined. The elongate foot lacked an operculum, and velar cilia were capable of metachronic beating and reversals. By 6 d, the internal organs, including the pigmented mantle organ, were sharply defined. The larval retractor muscles, visible at 6 d, were functional by 7 d although the embryos were capable of incomplete retraction only, leaving the velar lobes and foot partially exposed.

Table 1

Summary of the major events in embryonic development of *Pleurobranchaea maculata* at 14 °C

Time (d, h)	Event
0 h	Spawning
2.5 h	1 <sup>st</sup> polar body
4.5 h	2 <sup>nd</sup> polar body
8.5 h	1 <sup>st</sup> cleavage
9.15 h	2 <sup>nd</sup> cleavage
9.45 h	3 <sup>rd</sup> cleavage
22 h	Morula
24–48 h	Blastula formation
48–72 h	Gastrulation
4 d	Trochophores: pedal rudiment and velar field present, embryo elongate
4.5 d	Cap-like shell visible
5 d	Early veligers: larval shell complete, pigmented mantle organ, statocysts, right and left digestive gland present, foot visible but lacks an operculum
6 d	Pigmented mantle organ well developed, retractor muscle present but not functional, digestive glands becoming more distinct
7 d	Retractor muscle functional, velar lobes large, digestive glands still yolky but yolk depleted from stomach, mantle fold well developed
8 d	Hatching: subvelar ridge prominent, kidney rudiment present, pigmented mantle organ, mantle edge rounded, shell surface granulated. Eyes and operculum lacking

Spawning occurred over a 2–3-h period. Timing of early events is relative to the onset of oviposition.

Veligers hatched at 8 d, with a shell length of  $135 \pm 5.5 \mu\text{m}$  ( $n = 20$ ), and began feeding on phytoplankton immediately (Table 1, Fig. 1A). The digestive glands were still yolky and the ciliated stomach had hyaline rods in the posterior wall, as described in nudibranchs (Thompson, 1959). Just above the pigmented mantle organ was a small, transparent organ, presumably the rudiment of the definitive kidney (Gohar and Abul-Ela, 1957). The kidney rudiment remained in close association with the pigmented mantle organ and anus throughout larval development. Larvae lacked eyes at hatching, and the finely ciliated foot lacked an operculum throughout development. The Type 1 shell (types by Thompson, 1961) lacked pigment and was finely granulated on the surface; ridges, as occur in *P. japonica* (Tsubokawa and Okutani, 1991), were not observed.

One week after hatching, the larval shell was about  $190 \pm 15 \mu\text{m}$  ( $n = 20$ ) in length, and the velar lobes had increased substantially in size (Fig. 1B, C, D). New sensory structures had formed, including a pair of black eyes and the pedal tuft, a prominent cluster of elongate cilia on the tip of the foot. The stomach was greatly enlarged relative to shell size, and the hyaline rods were more numerous in the posterior stomach wall. The larval heart was also present and beating. The pigmented mantle organ, now black, was larger (Fig.

1B, D), and the kidney rudiment was much larger, slightly bilobed, and lacking any visible contents. Buds of the rhinophores were present on the anterior velar field (Fig. 1D).

Also in the first week of larval life, the mantle began to envelope the larval shell by growing up and over the dorsal shell aperture (Fig. 1B). The larval shell continued to grow, concurrent with overgrowth by the mantle, during larval development. The veliger was unable to completely retract into the shell, possibly because of the size of the velar lobes and also because the growth of the mantle reduced the effective shell aperture.

About 3 weeks after hatching, the first pediveligers settled on the biofilmed surface of the culture container. The shell,  $480 \pm 23 \mu\text{m}$  in length ( $n = 20$ ), was almost completely covered by the thick, glandular mantle (Fig. 2A–F). The growth zone of the mantle was thin as it extended over the shell, while older mantle tissue became thickened as the mantle glands developed (Fig. 2C). The mantle glands invaginated from the epidermis to the shell margin, forming elongate, simple tubular glands (Fig. 2D, E). Small tufts of cilia were scattered over the mantle surface, between the openings of the mantle glands (Fig. 2E). A lateral ciliary tract was present externally from the opening of the pre-branchial aperture on the right side of the “neck” and along the upper right side of the foot (Fig. 2F). The densely ciliated mouth was located ventral and posterior to the subvelar ridge (Fig. 2F). The foot was well developed and covered with fine cilia ventrally and with tufts of cilia on the lateral and upper surfaces (Fig. 2F). The pedal tuft, as described for veligers 1 week after hatching, was absent.

In late-stage larvae and pediveligers, the velum showed additional structures on both the upper and lower surfaces. The rhinophores extended from the upper velar surface as two curved ridges of tissue that were covered with fine cilia (Fig. 2A, F). As the rhinophores developed, they grew anteriorly, then laterally; but they remained open on the lateral surface, thus giving rise to the scroll-like morphology that is typical of adults (Willan, 1983). The oral veil was also visible as a broad, ciliated ridge on the upper surface of the velum, located immediately ventral to the rhinophores but not connected to them (Fig. 2F). The lower velar surface was covered by large ( $\sim 15 \mu\text{m}$  in diameter) rounded cells with a highly folded, microvillar surface (Fig. 2F, G). These post-velar cells were tightly packed together and covered the lower surface of each velar lobe from the subvelar ridge to the body wall.

Some internal organs were difficult to observe in live pediveligers because of the thick mantle. The eyes and statocysts were well developed, and the buccal mass was prominent in the anterior digestive tract (Fig. 2A). The pigmented mantle organ was darker, and the enlarged, transparent kidney was easily observed though the thick mantle tissue (Fig. 2B, D).

Acquisition of a juvenile morphology occurred gradually

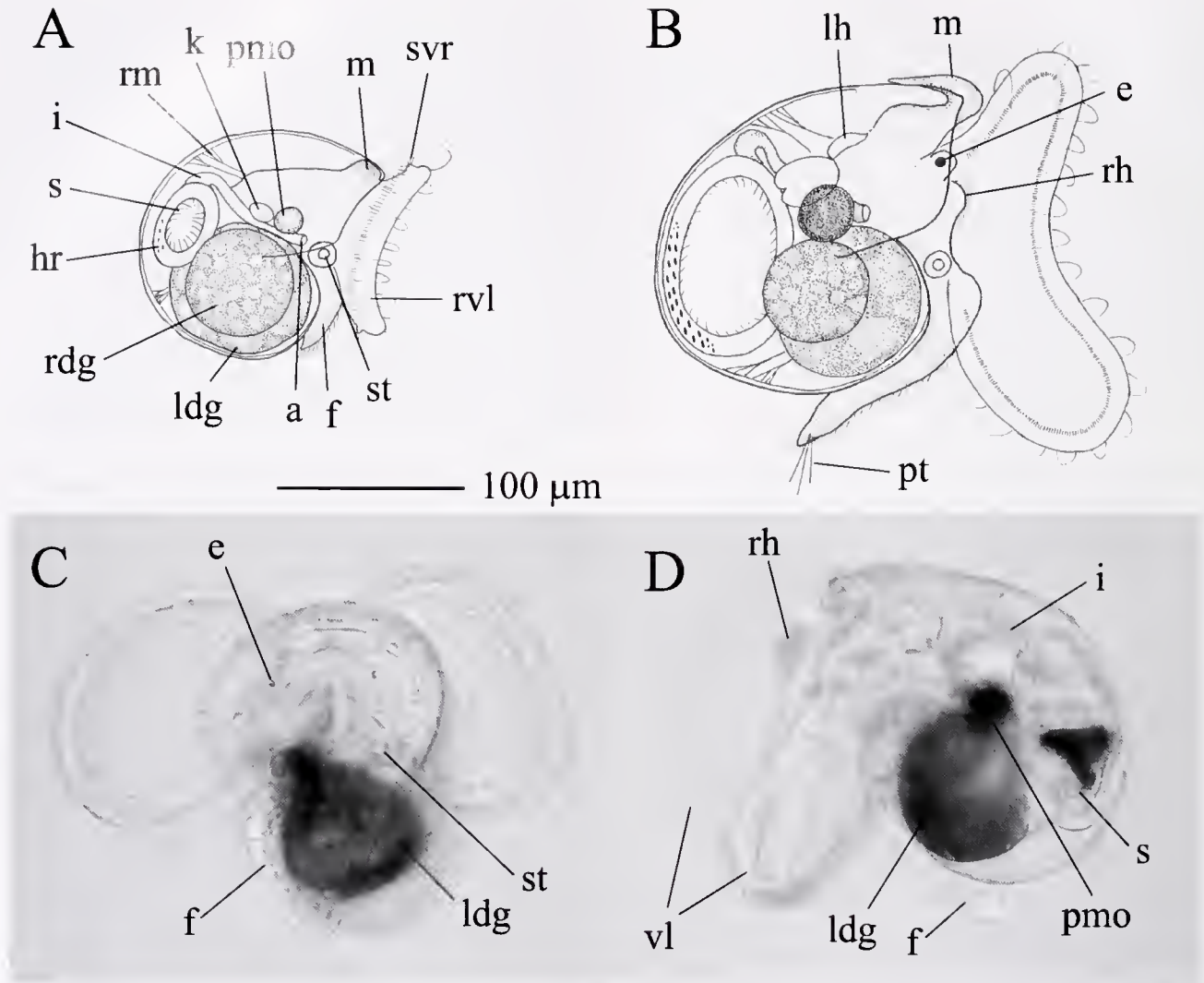
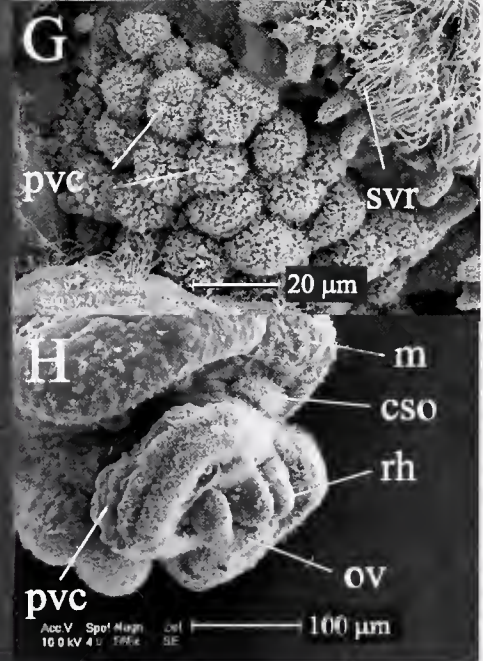
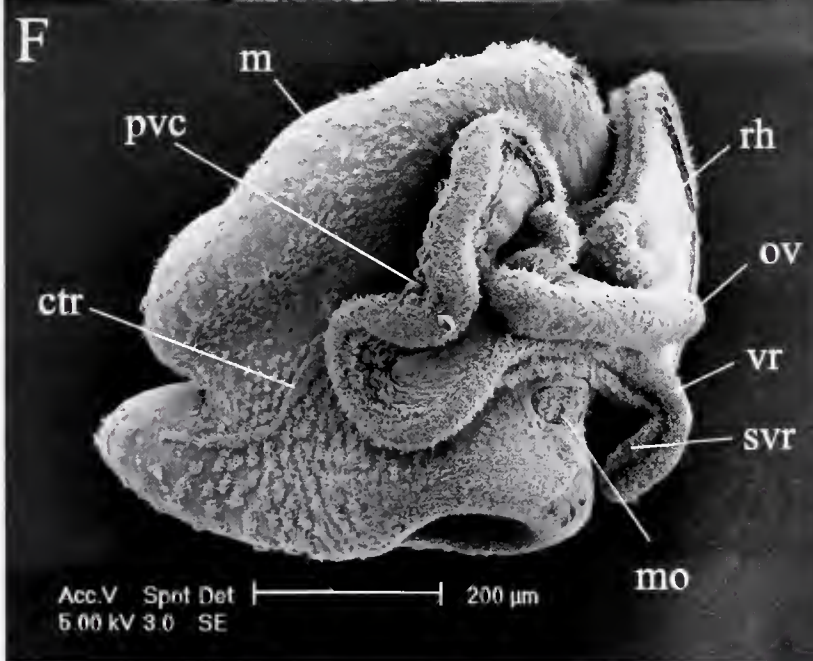
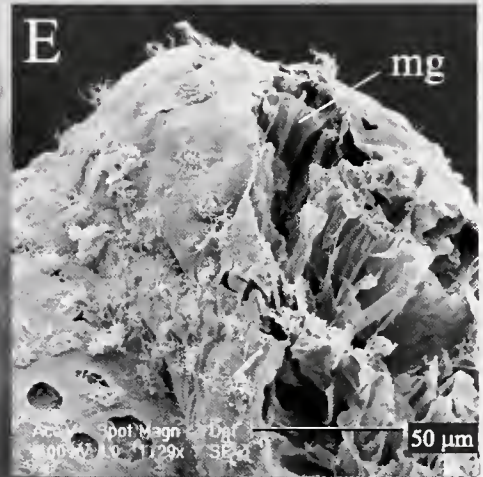
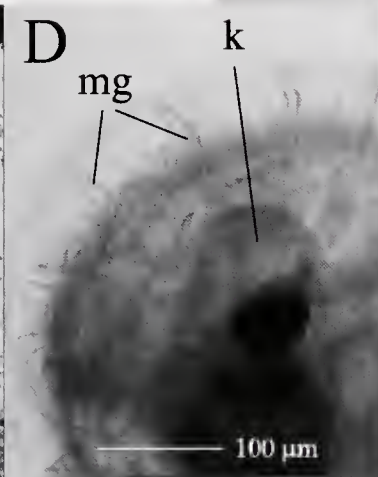
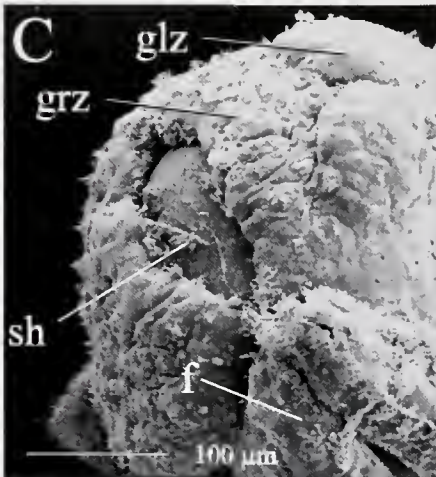
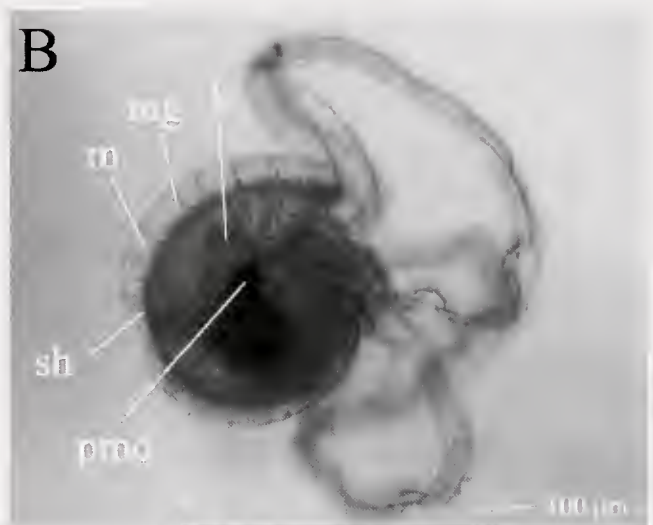
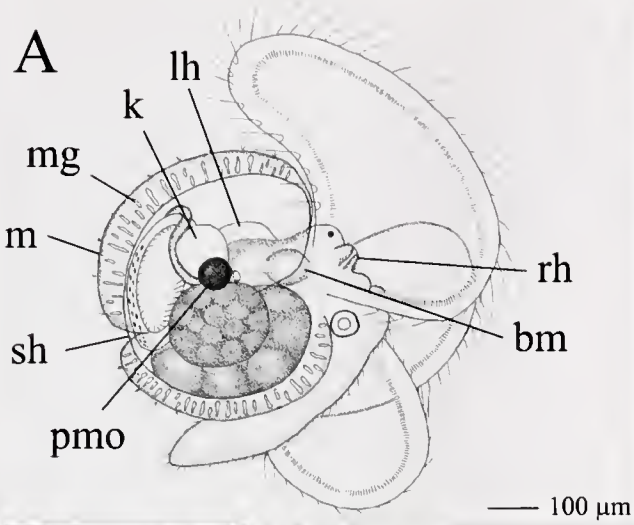


**Figure 1.** Early veligers of *Pleurobranchaea maculata*. (A) Veliger on the first day of hatching, drawn from life. (B) Veliger 7 d after hatching, drawn from life. (C, D) Bright field micrographs of veligers 7 d after hatching. Scale bar is the same for all four illustrations. a, anus; e, eye; f, foot; hr, hyaline rods; i, intestine; k, kidney rudiment; ldg, left digestive gland; lh, larval heart; m, mantle; pmo, pigmented mantle organ; pt, pedal tuft; rdg, right digestive gland; rh, rhinophore bud; rm, retractor muscle; rvl, right velar lobe; s, stomach; st, statocyst; svr, subvelar ridge; vl, velar lobes.

and involved development of the mantle throughout most of larval life. The final stage of metamorphosis primarily involved loss of the velum. As the velar and subvelar cilia

were shed, the highly folded surface of post-velar cells became smooth and the cells were gradually resorbed into the lower velar surface, followed by resorption of the velar

**Figure 2.** Pediveligers of *Pleurobranchaea maculata*, 3 weeks after hatching. (A, B) Drawing and bright field micrograph of live pediveligers. (C) Scanning electron micrograph of the overgrowth of the larval shell by the mantle. (D, E) Mantle glands in bright field and scanning electron micrographs. (F) Scanning electron micrographs of a pediveliger. (G) Scanning electron micrograph of the post-velar cells on the lower velar surface; the subvelar ridge is shown in the upper right. (H) Scanning electron micrograph of the partially resorbed velar lobes during metamorphosis. bm, buccal mass; eso, cephalic sensory organ; ctr, lateral ciliary tract; f, foot; glz, glandular zone; grz, growth zone; k, kidney rudiment; lh, larval heart; m, mantle; mg, mantle gland; mo, mouth; ov, oral veil; pmo, pigmented mantle organ; pvc, post-velar cells; rh, rhinophore; sh, shell; svr, subvelar ridge; vr, velar ridge.



lobes into the head (Fig. 2H). Early juveniles retained lateral remnants of the velar lobes for several days (Fig. 3A–D). Loss of the velar lobes revealed the cephalic sensory organ, a prominent ciliated organ located dorsally between the two velar lobes (Fig. 2H). The rhinophores extended anteriorly from the remnant of the velar field (Fig. 3A, C), and the oral veil projected as a broad ridge to cover the mouth and anterior foot (Fig. 3A–C). The prebranchial aperture, open on the right side, led to the lateral ciliary tract. The gill had not yet formed (Fig. 3D). The opaque mantle, both glandular and also with a scattering of red pigment, made it difficult to determine when the shell was dissolved, although the buccal mass and digestive glands were easily observed through the ventral body wall (Fig. 3B). The pigmented mantle organ appeared to be lost during late metamorphosis. The kidney remained next to the prebranchial aperture.

## Discussion

### *Morphogenesis of Pleurobranchaea maculata*

Development of *Pleurobranchaea maculata* is similar to that of *P. japonica* (Tsubokawa and Okutani, 1991) in terms of egg mass characteristics and overall larval morphology. However, the present study revealed several additional traits that warrant discussion, including the mantle glands, post-velar cells, sensory organs, and the position of the mouth.

The mantle of *P. maculata* becomes richly glandular as it grows back over the larval shell. These simple, tubular glands project through the entire thickness of the mantle, appear fairly early in ontogeny, and persist through metamorphosis. Thompson and Slinn (1959) and Thompson (1988) reported the secretion of sulfuric acid from the mantle of adult Pleurobranchidae from both simple columnar cells and flask-shaped glands. Adults of *Pleuro-*

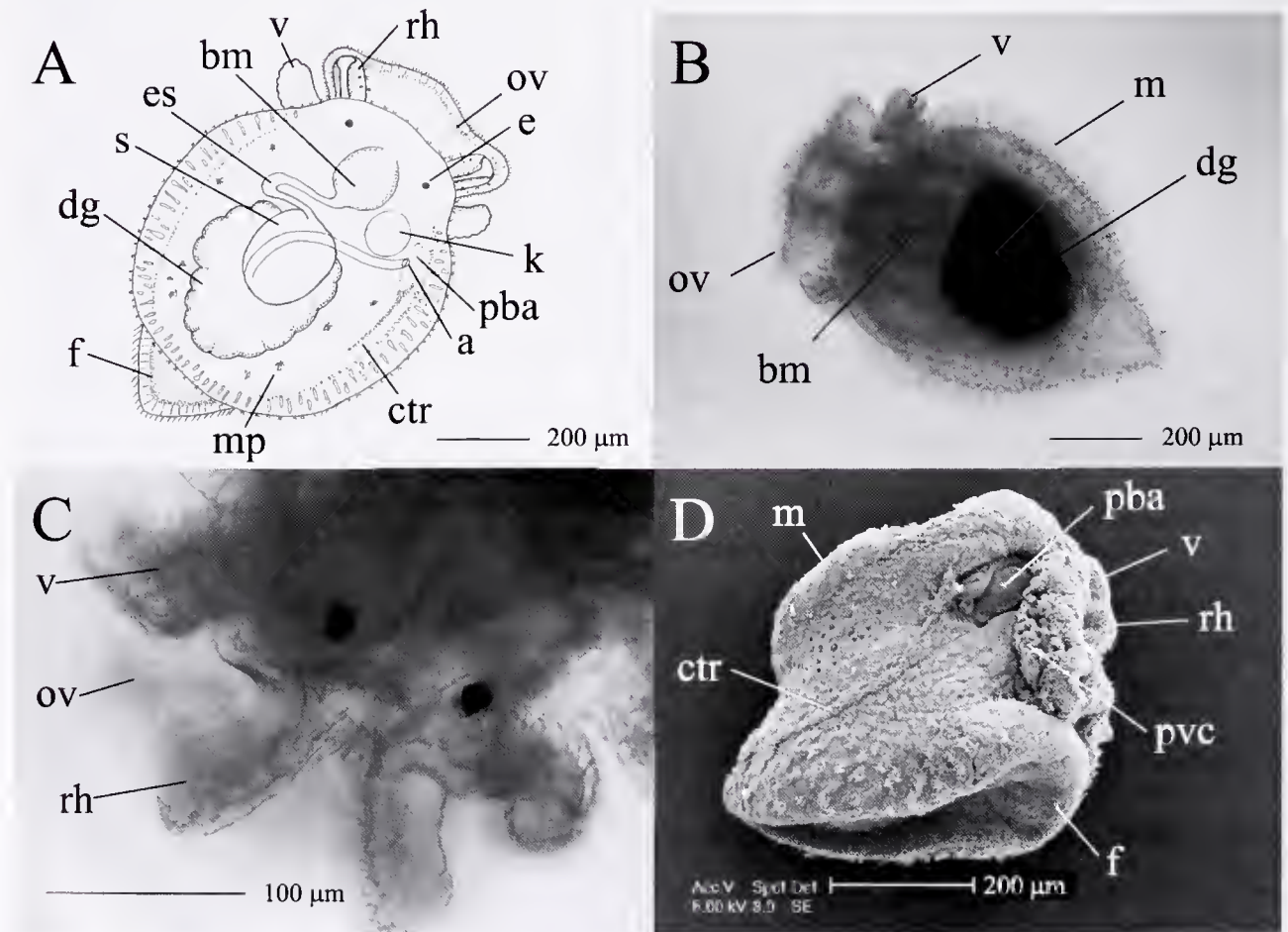


**Figure 3.** Early juveniles of *Pleurobranchaea maculata*. (A) Newly settled juvenile, dorsal aspect, drawn from life. (B) Bright field micrograph of a newly settled juvenile, ventral aspect. (C) Bright field micrograph of the head. (D) Scanning electron micrograph of a newly settled juvenile. a, anus; bm, buccal mass; ctr, lateral ciliary tract; dg, digestive gland; e, eye; es, esophagus; f, foot; k, kidney; m, mantle; mp, mantle pigment; ov, oral veil; pba, prebranchial aperture; pvc, post-velar cells; rh, rhinophore; s, stomach; v, remnant of velar lobe.

*branchaea* and *Pleurobranchus* also synthesize a variety of defensive compounds (Ciavatta *et al.*, 1995; Spinella *et al.*, 1997). The abundance and differentiation of mantle glands in *P. maculata* pediveligers suggest that they function in late-stage larvae and likely confer chemical protection to planktonic pediveligers and newly settled juveniles. The capacity of larvae to synthesize their own chemical defense is unusual. Chemical defense occurs in eggs or egg masses of some opisthobranchs; however, in these other taxa, the defensive compounds are maternally derived, as occurs in the Anaspidea (Pennings, 1994), Ascoglossa (Paul and Van Alstyne, 1988), Nudibranchia (Pawlik *et al.*, 1988), and tyloidinid Notaspidea (Ebel *et al.*, 1999).

The post-velar cells are also unusual and, to my knowledge, have not been reported elsewhere. These cells develop in larvae, persist through early metamorphosis, and are resorbed with the rest of the velum. The post-velar cells greatly increase the surface area of the lower velar surface through their abundance and highly folded apical surface. While the function of these cells is unknown, it seems reasonable to suggest that they are secretory because of their size, number, and morphology. If secretory, they may protect the head and velum by neutralizing secretions of the mantle glands.

The rhinophores of *P. maculata* originate from the center of the upper velar surface; appear fairly early in larval development; and grow anteriorly as curved, ciliated ridges of tissue. In contrast, the rhinophores of *P. japonica* arise from a pair of depressions at the lateral edges of the oral veil (Tsubokawa and Okutani, 1991). The intravelar location of the rhinophores in *P. maculata* is similar to that of the nudibranch *Rostanga pulchra* MacFarland, 1905 (Chia and Koss, 1982, 1991), although the definitive morphology differs in that the rhinophores of nudibranchs are solid and lack a lateral groove. A cephalic organ, as observed in *P. maculata*, was not reported in *P. japonica* (Tsubokawa and Okutani, 1991) but would be difficult to observe without SEM. However, a cephalic organ is present in some cephalaspids (Schaeffer and Ruthensteiner, 2001) and nudibranchs (Chia and Koss, 1984).

Also of interest is the position of the mouth posterior to the subvelar ridge in pediveligers. Veligers typically have a mouth positioned between the velar cilia (*i.e.*, the pre-oral cilia, or prototroch) and the subvelar ridge (*i.e.*, the post-oral cilia, or metatroch). Whether this is the original embryological location of the mouth (*e.g.*, protostomal) or represents a secondary mouth opening is not known. Comparative work is needed to clarify the embryological origins and potential migration of the definitive mouth from the protostome.

The ciliary tract on the right lateral foot has not been reported elsewhere in notaspideans, but is reported for nudibranchs (*e.g.*, Bonar and Hadfield, 1974; Goddard, 1996). The ciliary tract in *P. maculata*, not present in adults, occupies the position of the adult gill (Willan, 1983). The

tract may serve to generate water currents directed away from the prebranchial aperture, which houses the anus and nephroproct; this function is likely taken over by the gill cilia once the gill has formed. Gill formation was not observed in the present study, although Tsubokawa and Okutani (1991) describe the gill in *P. japonica* in early juveniles.

#### *Pattern and process in notaspidean development*

*Egg mass structure.* Egg masses have been described for several species of Notaspidea (Table 2). As is typical of opisthobranchs, eggs are located in capsules within an elongate string that runs in a double spiral around the periphery of a jelly mass, although in some notaspideans the string is poorly defined (Millen, unpubl. obs. cited in Strathmann, 1987) or highly modified (Bandel, 1976). In some species, capsules contain a single egg; in others, as many as 37 eggs per capsule are common (Table 2). Egg size is variable among species and, although the sample size is small, appears correlated with developmental mode (Table 2), as expected for opisthobranchs (Hadfield and Miller, 1987). However, in some Notaspidea, egg size can vary considerably within one species; in the lecithotrophic *Berthellina citrina*, for example, variation in egg size is reported to span 140  $\mu\text{m}$ , ranging from 270 to 410  $\mu\text{m}$  over 15 egg masses (Usuki, 1969).

*Larval morphology.* Morphogenesis in notaspidean veligers is modified from the pattern—characteristic of benthic opisthobranchs—that is observed in the Cephalaspidea, Ascoglossa, Anaspidea, and Nudibranchia (*e.g.*, Thompson, 1976). Major differences include shell growth and loss, notum formation, and lack of an operculum. Otherwise, morphogenesis appears similar to that of other opisthobranchs.

In most notaspideans (Table 2), larval shells are Type 1 (whorled; typical of most classes of opisthobranchs) or less commonly, Type 2 (inflated and cuplike; occurs in some nudibranchs). However, once the protoconch has formed, growth of the larval shell in pleurobranchids is atypical of other opisthobranchs in mechanism and timing. In other opisthobranchs, the larval shell grows *via* secretions by the mantle fold, a ridge of tissue next to the shell aperture (Tardy, 1991). In pleurobranchids, the mantle fold is lost in early veligers at the same time as the mantle extends past the aperture to ultimately cover the entire larval shell. This occurs after hatching for planktotrophic species of *Pleurobranchaea* (Tsubokawa and Okutani, 1991; this study) or within the egg capsule for lecithotrophic species of *Berthellina* (Usuki, 1969) and direct-developing *Bathyberthella* (Wägele, 1996). Thus larval shell growth is concurrent with mantle overgrowth and occurs despite the migration of the mantle edge away from the aperture; presumably, the region of mantle adjacent to the aperture retains shell-secretion

Table 2

Summary of reproductive data for the Notaspidea

Species	Development Mode*	Egg Size	Egg Mass Shape†	No. Eggs/Mass	No. Eggs/Capsule	Veliger Shell Type‡	Time to Hatching (d. °C)	Hatching Size¶	Length of Planktonic Period (d)	Ref.
Umbraclulidae										
<i>Unbraculum sinicum</i> (Gmelin, 1791)	P	80 µm	A	10,206,000	30	1	10	—	—	Ostergaard, 1950
Tylodimidae										
<i>Tylodina corticalis</i> Tate, 1889	—	88 µm	A	4,500,000	37	—	—	—	—	Thompson, 1970
Pleurobranchidae										
<i>Bathyerthella antarctica</i> Willan and Bertsch, 1987	D	—	B	—	1	2	100 <sup>+</sup> d, 0 °C	(1.6 mm)	0	Wägele, 1996
<i>Berthella agassizii</i> (MacFarland, 1909)	—	—	A	70,000	1	—	7 d, —	—	—	Bandel, 1976
<i>Berthella californica</i> (Dall, 1900)	—	—	A	—	—	—	—	—	—	Behrens, 1980
<i>Berthella plumula</i> (Montagu, 1803)	P	93 µm	A	—	1-2	1	18 d, 12 °C	153 µm	—	Goddard 1984, 2001b
<i>Berthella strongi</i> (MacFarland, 1966)	L	200 µm	A	—	—	1	—	—	—	Thompson, 1976
<i>Berthellina citrina</i> (Rueppell and Leuckart, 1828)	P	—	B	—	1	1	8 d, 18 °C	131 µm	—	J. Goddard, pers. comm.
<i>Berthellina engeli</i> Gardiner, 1936	—	—	A	50,000	1	—	15 d, —	—	—	Bandel, 1976
<i>Berthellina quadridens</i> (Moersch, 1863)	P	—	—	—	—	1	—	—	—	Goddard, 2001b
<i>Pleurobranchaea californica</i> MacFarland, 1966	P	—	—	—	—	1	—	180	—	—
<i>Pleurobranchaea japonica</i> Thiele, 1925	P	100 µm	B	530,000	7	1	6 d, 21 °C	152 µm	15 d	Tsubokawa and Okutani, 1991
<i>Pleurobranchaea maculata</i> (Quoy and Gaimard, 1832)	P	—	B	—	—	—	10 d, —	180 µm	6 d	Willan, 1983
<i>Pleurobranchus membranaceus</i> Montagu, 1811	P	100 µm	B	318,400	4	1	8 d, 20 °C	135 µm	21 d	present study
<i>Pleurobranchus testudinarius</i> Cantraine, 1835	P	88 µm	A	1,795,500	1	1	—	—	—	Tchang Si, 1931
	—	—	A	300,000	1	—	10 d, —	—	—	Bandel, 1976

\* Modes of larval development include planktotrophy (P), lecithotrophy (L) or direct development (D).

† Classification of egg masses follows that of Hurst (1967) and includes ribbons (A) and cylindrical cords (B).

‡ Larval shell type follows Thompson (1961) as whorled (1) or inflated (2).

¶ Hatching size refers to shell length unless given in parentheses, when it refers to body length.

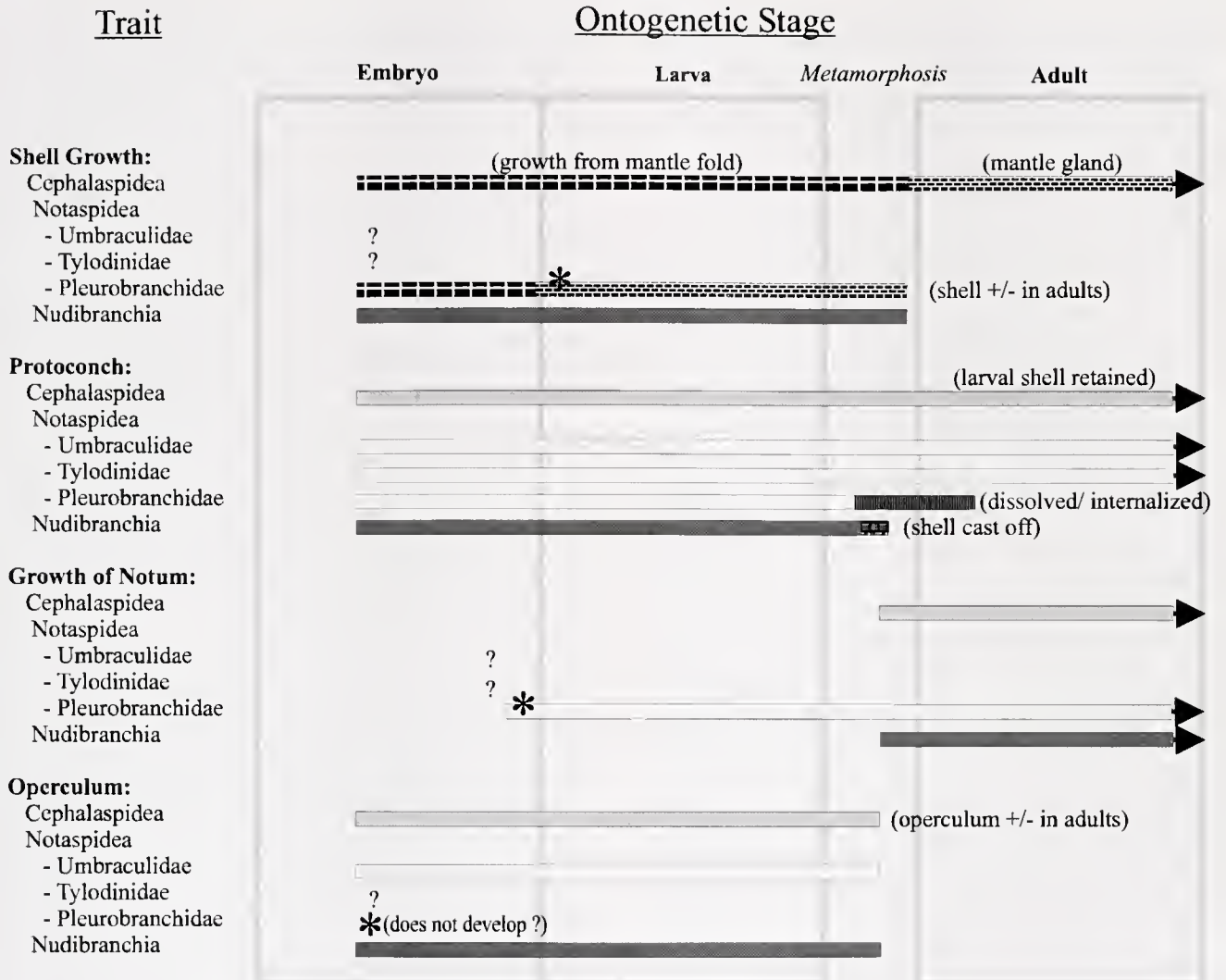


**Figure 4.** Heterochrony and pleurobranchid development. Data summarize the time of onset and offset of shell growth, protoconch (formation/loss), notum growth, and operculum (formation/loss). Timing is generalized to ontogenetic stage (embryo, larva, and adult) for Cephalaspidea (light gray bars), Notaspidea (white bars), and Nudibranchia (dark gray bars). Different patterns within a bar indicate differences in the developmental process underlying a particular trait; for example, shell growth occurs at the mantle fold in early stages and the mantle gland in later stages, and shell loss occurs through dissolution (some pleurobranchids) or being cast off (Nudibranchia). \* Denotes a change in time of onset in pleurobranchids, relative to other indicated groups. +/- Indicates that the trait is present in the adults of only some species in each family or order. ? Indicates that time of onset is not known. References are provided in the text and in Table 2.

activity in larvae. Migration of the mantle edge away from the aperture suggests that shell growth in pleurobranchids is modified in several ways. First, shell growth in larvae occurs by means of the early onset of an ontogenetic process found in juveniles and adults of species that retain their shells (Fig. 4). Second, morphogenesis of the shell and mantle are decoupled from other morphological changes that occur during metamorphosis. Third, shell-less notaspideans have retained the plesiomorphic mechanism of adult shell overgrowth found in shelled notaspideans. This mechanism of shell overgrowth is also distinct from the

growth of epipodial (*e.g.*, Anaspidea) or parapodial (*e.g.*, Cephalaspidea) lobes in juveniles of other shelled opisthobranchs (Tardy, 1991).

In shell-less notaspideans, the mechanism of loss of the larval shell is also atypical of opisthobranchs (Fig. 4). In other opisthobranch orders, the retractor muscles are severed and the shell cast off at metamorphosis (*e.g.*, AscoGLOSSA, Nudibranchia, Gymnosomata). In contrast, the shell-less Pleurobranchidae lose the larval shell through overgrowth and dissolution by the mantle during or shortly after metamorphosis (Tsubokawa and Okutani, 1991). This

distinctive mechanism of shell loss supports the hypothesis that in the Notaspidea—as has been suggested throughout the opisthobranchs (Gosliner, 1994)—shell loss is apomorphic. It additionally suggests that similarities among adults in shell loss and notum morphology have evolved through homoplasy in Notaspidea and Nudibranchia.

Mantle growth in notaspideans is also atypical. In most opisthobranchs the mantle remains small until after metamorphosis. In contrast, the mantle in Notaspidea begins to take on adult characteristics at an early larval stage. This early development includes formation of the notum (Gohar and Abul-Ela, 1957; Thompson, 1976; Tardy, 1991; Tsubokawa and Okutani, 1991; Wägele, 1996) and also the differentiation of cilia and glands (present study). Early onset of notum differentiation may provide the larva and newly settled juvenile with an effective means of defense (e.g., potential acid cells), increased sensory perception (e.g., mantle ciliary tufts), and a larger size, with the associated advantages of predator deterrence and increased buoyancy.

Larvae of pleurobranchid notaspideans lack an operculum. The single recorded exception is Willan's (1983) note of an operculum in *P. maculata*; however, an operculum was not observed in the present study of this species. Lack of an operculum may be characteristic only of pleurobranchids, however, as larvae of the tyloidinid *Umbraculum sinicum* (Gmelin, 1791) is described as having an operculum (Ostergaard, 1950). Larvae of all other opisthobranch orders have an operculum, with individual exceptions such as the nudibranch *Aegires albopunctatus* MacFarland, 1905 (Goddard, 2001a). The operculum is lost at metamorphosis in most opisthobranchs, except for a few species of Cephalaspidea (Thompson, 1976). This suggests that loss of an operculum in pleurobranchid larvae is an apomorphic trait that represents an earlier (i.e., embryonic) onset of a condition common to the adults of other orders (Fig. 4).

As with other opisthobranchs, the mantle cavity of notaspidean veligers contains several cell clusters that have been referred to as "larval kidneys" and "anal cells" (Gohar and Abul-Ela, 1957; Usuki, 1969; Tsubokawa and Okutani, 1991). The function and ultrastructure of these organs are unknown, and the terms are used inconsistently across gastropod taxa. Thus, it is more appropriate to use the descriptor "pigmented mantle organ" to refer to the darkly pigmented structure associated with the anus. A pigmented mantle organ is found in the planktotrophic veligers of several notaspideans, including *P. californica* MacFarland, 1966 (Goddard, 2001a), *P. japonica* (Tsubokawa and Okutani, 1991), *P. maculata* (present study), *Berthella californica* (Dall, 1900) (Goddard, 1984), *B. strongi* (MacFarland, 1966) (Goddard, pers. comm.), *Berthellina engeli* Gardiner, 1936 (Goddard, pers. comm.) and *Umbraculum sinicum* (Ostergaard, 1950). A similar organ is found in planktotrophic species of Cephalaspidea. A pigmented mantle organ is

lacking in non-planktotrophic notaspideans, including *Berthellina citrina* (Usuki, 1969), the probably lecithotrophic *Berthella plumula* (Montagu, 1803) (Thompson, 1976) and the direct-developing *Bathyberthella antarctica* Willan and Bertsch, 1987 (Wägele, 1996). Although the pigmented mantle organ appears similar in the Notaspidea and Cephalaspidea, ultrastructural and detailed embryological studies are needed to determine if they are homologous. All three studied species of *Pleurobranchaea* (*P. japonica*, *P. californica*, and *P. maculata*; Tsubokawa and Okutani, 1991; Goddard, 2001b; present study) also have a large, transparent organ positioned adjacent and dorsal to the pigmented mantle organ, which is here considered to be the rudiment of the kidney (following Gohar and Abul-Ela, 1957).

*Settlement and metamorphosis.* Pediveligers of *Berthellina citrina*, *Pleurobranchaea japonica*, and *P. maculata* all settle on biofilmed culture dishes (Gohar and Abul-Ela, 1957; Usuki, 1969; Tsubokawa and Okutani, 1991; present study). Preferences for specific substrates were not tested, but a nonspecific cue is probable as all three species are opportunistic carnivores.

Settlement and metamorphosis are also decoupled events in pleurobranchids. Whereas settlement (acquisition of a benthic lifestyle) occurs over a relatively short time span, metamorphosis (the acquisition of an adult morphology) begins early in larval life with an accelerated onset of some processes of differentiation typical of adults (e.g., shell and notum growth), while differentiation of other organ systems (e.g., velum, foot) appears similar to that of other opisthobranch orders. For example, the larval shell is produced by a mantle region other than the mantle fold; thus we see an early onset of a shell-growth mechanism common in juveniles and adults of shelled species (Fig. 4). Also, in the mantle of early larvae, "adult" structures such as glands and external cilia undergo rapid growth and differentiation processes that also are associated with juvenile development in other orders. Absence of an operculum in pleurobranchid larvae is also a trait typical of adult opisthobranchs. Collectively, these observations suggest that in the Pleurobranchidae, aspects of the specialized morphology of the adult have evolved through heterochronic changes in specific morphogenetic events associated with metamorphosis.

#### *Phylogenetic implications*

Development in the Notaspidea is relatively poorly known, and the data we have primarily includes the Pleurobranchidae, while details are lacking for the Umbraculidae and Tyloidinidae. The descriptions of development that are available for the Pleurobranchidae support the current hypothesis that the Notaspidea are phylogenetically closely linked with the Nudibranchia (Schmekel, 1985; Gosliner, 1994; Wägele and Willan, 2000) yet share some, possibly plesiomorphic, traits with the Cephalaspidea. Potentially

plesiomorphic larval traits include the pigmented mantle organ (common to planktotrophic species of the Cephalaspidea and Notaspidea), the cephalic sensory organ (found in Cephalaspidea and Nudibranchia), and a type I larval shell (common to all orders).

Synapomorphies with the Nudibranchia include the shape of the egg mass and the presence of rhinophores that arise from the upper velar field. This agrees with Wägele and Willan (2000), who suggest that similarities in innervation of the rhinophores support homology in the Pleurobranchoidea and Nudibranchia, despite differences in morphology (rolled *versus* solid structure, respectively). Apomorphies in the Pleurobranchidae include lack of the larval operculum, the mechanism of shell loss or internalization, and the pattern of notum formation. These apomorphies have evolved through heterochrony, manifest as an early (*i.e.*, embryonic or larval) onset of developmental processes that typically occur in juveniles of other orders (Fig. 4). Understanding the phylogenetic relevance of novel traits shown by *P. maculata* (*e.g.*, post-velar cells, position of the mouth) awaits further, comparative embryological and ultrastructural work.

### Acknowledgments

This research was conducted at the Leigh Marine Laboratory, University of Auckland, New Zealand. I thank the Leigh staff, particularly B. Dobson, for their support. Specimens were examined with SEM at the Research Centre for Surface and Materials Science at the University of Auckland. I especially thank C. Hobson (School of Engineering), A. Turner (School of Biological Sciences), and B. James (School of Engineering) for their kind assistance and providing access to their lab facilities. J. Goddard generously provided unpublished observations and insight into opisthobranchs, which have considerably added to the manuscript. This manuscript benefited from the comments of an anonymous reviewer and of M. Gibson and I. Paterson. J. Havenhand and L. Page provided insight on veliger structure and physiology. This research was supported by the Natural Science and Engineering Research Council of Canada (NSERC).

### Literature Cited

- Bandel, K. 1976.** Egg masses of 27 Caribbean opisthobranchs from Santa Maria, Columbia. *Stud. Neotrop. Fauna Environ.* **11**: 87–118.
- Behrens, D. 1980.** *Pacific Coast Nudibranchs: A Guide to the Opisthobranchs of the Northeast Pacific*. Sea Challengers, Los Osos, CA.
- Bonar, D., and M. Hadfield. 1974.** Metamorphosis of the marine gastropod *Phestilla sibogae* Bergh (Nudibranchia: Aeolidacea): I. Light and electron microscopic analysis of larval and metamorphic stages. *J. Exp. Mar. Biol. Ecol.* **16**: 227–255.
- Chia, F.-S., and R. Koss. 1982.** Fine structure of the larval rhinophores of the nudibranch, *Rostanga pulchra*, with emphasis on the sensory receptor cells. *Cell Tissue Res.* **225**: 235–248.
- Chia, F.-S., and R. Koss. 1984.** Fine structure of the cephalic sensory organ in the larva of the nudibranch *Rostanga pulchra* (Mollusca, Opisthobranchia, Nudibranchia). *Zoomorphology* **104**: 131–139.
- Chia, F.-S., and R. Koss. 1991.** Sensory structures and behaviour in opisthobranch veliger larvae. *Bull. Inst. Zool. Acad. Sin. Monograph* **16**: 455–484.
- Ciavatta, M., E. Trivellone, G. Villani, and G. Cimino. 1993.** Membranes: New polypropionates from the skin of the mediterranean mollusc *Pleurobranchus membranaceus*. *Tetrahedron Lett.* **34**: 6791–6794.
- Ciavatta, M., G. Villani, E. Trivellone, and G. Cimino. 1995.** Two new labdane aldehydes from the skin of the notaspidean *Pleurobranchaea meckelii*. *Tetrahedron Lett.* **36**: 8673–8676.
- Ebel, R., A. Marin, and P. Proksch. 1999.** Organ-specific distribution of dietary alkaloids in the marine opisthobranch *Tyrodina perversa*. *Biochem. Syst. Ecol.* **27**: 769–777.
- Goddard, J. 1984.** The opisthobranchs of Cape Arago, Oregon, with notes on their biology and a summary of benthic opisthobranchs known from Oregon. *Veliger* **27**: 143–163.
- Goddard, J. 1996.** Lecithotrophic development in *Doto amyra* (Nudibranchia: Dendronotacea), with a review of developmental mode in the genus. *Veliger* **39**: 43–54.
- Goddard, J. 2001a.** The early veliger larvae of *Aegires albopunctatus* (Nudibranchia: Aegiridae), with morphological comparisons to members of the Notaspidea. *Veliger* **44**: 398–406.
- Goddard, J. 2001b.** Mollusca: Gastropoda. P. 314 in *An Identification Guide to the Larval Marine Invertebrates of the Pacific Northwest*, A. Shanks, ed. Oregon State University Press, Corvallis, OR.
- Gohar, H., and I. Abul-Ela. 1957.** The development of *Berthellina citrina* (Mollusca: Opisthobranchiata). *Publ. Mar. Biol. Sm., Al Ghardaqa, Egypt* **9**: 69–84.
- Gosliner, T., 1991.** Morphological parallelism in opisthobranch gastropods. *Malacologia* **32**: 313–327.
- Gosliner, T., 1994.** Gastropoda: Opisthobranchia. Pp. 253–355 in *Microscopic Anatomy of the Invertebrates*, F. Harrison and A. Kohn, eds. Wiley-Liss, New York.
- Hadfield, M., and S. Miller. 1987.** On developmental patterns of opisthobranchs. *Am. Malacol. Bull.* **5**: 197–214.
- Hurst, A., 1967.** The egg masses and veligers of thirty northeast Pacific opisthobranchs. *Veliger* **9**: 255–287.
- Marcus, E., and T. Gosliner. 1984.** Review of the family Pleurobranchaeidae (Mollusca, Opisthobranchia). *Ann. S. Afr. Mus.* **93**: 1–52.
- Mikkelsen, P. 1998.** Review of shell reduction and loss in traditional and phylogenetic molluscan systematics, with experimental manipulation of a negative gain character. *Am. Malacol. Bull.* **14**: 201–218.
- Ostergaard, J. 1950.** Spawning and development of some Hawaiian marine gastropods. *Pac. Sci.* **4**: 75–115.
- Paul, V., and K. Van Alstyne. 1988.** The use of ingested algal diterpenoids by *Elysia halimeda* MacNae (Opisthobranchia: Ascoglossa) as antipredator defences. *J. Exp. Mar. Biol. Ecol.* **119**: 15–29.
- Pawlik, J., M. Kernan, T. Molinski, M. Harper, and D. Faulkner. 1988.** Defensive chemicals of the Spanish dancer nudibranch *Hexabranchius sanguineus* and its egg ribbons: macrolides derived from a sponge diet. *J. Exp. Mar. Biol. Ecol.* **119**: 99–109.
- Pennings, S. 1994.** Interspecific variation in chemical defences in the sea hares (Opisthobranchia: Anaspidea). *J. Exp. Mar. Biol. Ecol.* **180**: 203–219.
- Schaeffer, K., and B. Ruthensteiner. 2001.** The cephalic sensory organ in pelagic and intracapsular larvae of the primitive opisthobranch genus *Haminocoe* (Mollusca: Gastropoda). *Zool. Anz.* **240**: 69–82.
- Schmckel, L. 1985.** Aspects of evolution within the opisthobranchs. Pp. 221–268 in *The Mollusca*, K. Wilbur, E. Trueman, and M. Clarke, eds. Academic Press, Orlando, FL.
- Spinella, A., E. Mollo, E. Trivellone, and G. Cimino. 1997.** Testudi-

- nariol A and B, two unusual triterpenoids from the skin and the mucus of the marine mollusc *Pleurobranchus testudinarius*. *Tetrahedron* **53**: 16891–16896.
- Strathmann, M. 1987.** *Reproduction and Development of Marine Invertebrates of the Northern Pacific Coast*. University of Washington Press, Seattle, WA. 670 pp.
- Tardy, J. 1991.** Types of opisthobranch veligers: their notum formation and torsion. *J. Molluscan Stud.* **57**: 103–112.
- Tchang, Si. 1931.** *Contribution a l'étude des mollusques opisthobranchs de la Côte Provençale*. Thèse Université de Lyon. 211 pp.
- Thompson, T. 1959.** Feeding in nudibranch larvae. *J. Mar. Biol. Assoc. UK* **38**: 329–248.
- Thompson, T. 1961.** The importance of the larval shell in the classification of the Sacoglossa and the Acoela. *Proc. Malacol. Soc. Lond.* **34**: 333–338.
- Thompson, T. 1970.** Eastern Australian Pleurobranchomorpha (Gastropoda, Opisthobranchia). *J. Zool. Lond.* **160**: 173–198.
- Thompson, T. 1976.** *Biology of Opisthobranch Molluscs*, Vol. 1. The Ray Society, London. 207 pp.
- Thompson, T. 1988.** Acidic allomones in marine organisms. *J. Mar. Biol. Assoc. UK* **68**: 499–517.
- Thompson, T., and D. Slinn. 1959.** On the biology of the opisthobranch *Pleurobranchus membranaceus*. *J. Mar. Biol. Assoc. UK* **38**: 507–524.
- Tsuhokawa, R., and T. Okutani. 1991.** Early life history of *Pleurobranchaea japonica* Thiele, 1925 (Opisthobranchia: Notaspidea). *Veliger* **34**: 1–13.
- Usuki, I. 1969.** The reproduction, development and life history of *Berthellina citrina* (Ruppell et Leuckart) (Gastropoda, Opisthobranchia). *Sci. Rep. Niigata Univ. Ser. D Biol.* **6**: 107–127.
- Wägele, H. 1996.** On egg clutches of some Antarctic Opisthobranchia. *Malacol. Rev. Suppl.* **0**: 21–30.
- Wägele, H., and R. Willan. 2000.** Phylogeny of the Nudibranchia. *Zool. J. Linn. Soc.* **130**: 83–181.
- Willan, R. 1983.** New Zealand side-gilled sea slugs (Opisthobranchia: Notaspidea: Pleurobranchidae). *Malacologia* **23**: 221–270.
- Willan, R. 1987.** Phylogenetic systematics of the Notaspidea (Opisthobranchia) with a reappraisal of families and genera. *Am. Malacol. Bull.* **5**: 215–241.

# Effects of Allogeneic Contact on Life-History Traits of the Colonial Ascidian *Botryllus schlosseri* in Monterey Bay

NANETTE E. CHADWICK-FURMAN<sup>1,\*</sup> AND IRVING L. WEISSMAN<sup>2</sup>

<sup>1</sup>*Life Science Department, Bar-Ilan University, Ramat Gan, Israel, and Interuniversity Institute for Marine Science, P.O. Box 469, Eilat, Israel; and* <sup>2</sup>*Department of Pathology, Stanford Medical School, Stanford University, Stanford, California 94305-5323*

**Abstract.** The formation of chimeric colonies following allogeneic contact between benthic invertebrates may strongly affect colony fitness. Here we show that, in a field population of the colonial ascidian *Botryllus schlosseri* in Monterey Bay, California, more than 20% of all colonies occur in allogeneic contact with conspecifics. We experimentally assessed the effects of allogeneic contact on the following life-history traits under natural field conditions: growth, age and size at first reproduction, and egg production (fecundity). When compared with isolated colonies, and in some cohorts also with colonies that rejected allogeneic neighbors, colonies that fused with neighbors incurred reduced fitness in terms of most life-history traits measured. We propose that one of the benefits of precise allorecognition is that, in fused colonies, it limits the unit of selection to chimeric individuals composed of closely related kin.

## Introduction

Tissue fusion and chimera formation between allogeneic individuals occurs in sessile invertebrates such as sponges (Ilan and Loya, 1990), corals (Chadwick-Furman and Rinkevich, 1994; Hidaka *et al.*, 1997; Frank *et al.*, 1997), and protochordate ascidians (Chadwick-Furman and Weissman, 1995a; Rinkevich, 1996). The formation of chimeras between kin may confer benefits on colonial invertebrates due to increased body size, early onset of sexual reproduction, and increased survival following partial predation (Buss, 1982; Grosberg and Quinn, 1986; Sabbadin, 1994).

However, fusion of different genotypes also may come at a cost to individuals, in terms of germ and somatic cell parasitism (Stoner and Weissman, 1996; Rinkevich, 1996; Stoner *et al.*, 1999).

Studies of fused allogeneic colonies of the protochordate *Botryllus schlosseri* have shown that the eggs of one partner may be retained and brooded by the other partner over several reproductive cycles (Sabbadin and Zaniolo, 1979). In laboratory studies, fusion between allogeneic colonies of *B. schlosseri* leads to costs rather than benefits in terms of several fitness parameters (Rinkevich and Weissman, 1987, 1992a, b); indeed an inevitable result of such fusion is the death and resorption of all zooids (colonial units) of one colony, and the survival of the zooids of the other colony for up to many weeks after fusion (Rinkevich and Weissman, 1992a, b). In nature, however, resorption is not the inevitable conclusion of fusion prior to the onset of reproductive competence (Chadwick-Furman and Weissman, 1995a). Further, the resorbed partner also may parasitize the germ cell line of the resorbing partner in chimeras under both laboratory and field conditions (Pancer *et al.*, 1995; Stoner and Weissman, 1996; Stoner *et al.*, 1999). Thus, the genetic composition of chimeric colonies in nature may be more complex than previously observed in the laboratory.

Previously we reported on seasonal variation in life history traits of *B. schlosseri* colonies in a field population in Monterey Bay, California (Chadwick-Furman and Weissman, 1995b). Here we determine natural frequencies of allogeneic contact in the same field population, and assess the resulting impacts on life-history traits in this colonial ascidian. We also describe the morphology and stability of chimeric colonies under natural field conditions.

Received 3 July 2002; accepted 8 July 2003.

\*To whom correspondence should be addressed. E-mail: furman@mail.biu.ac.il

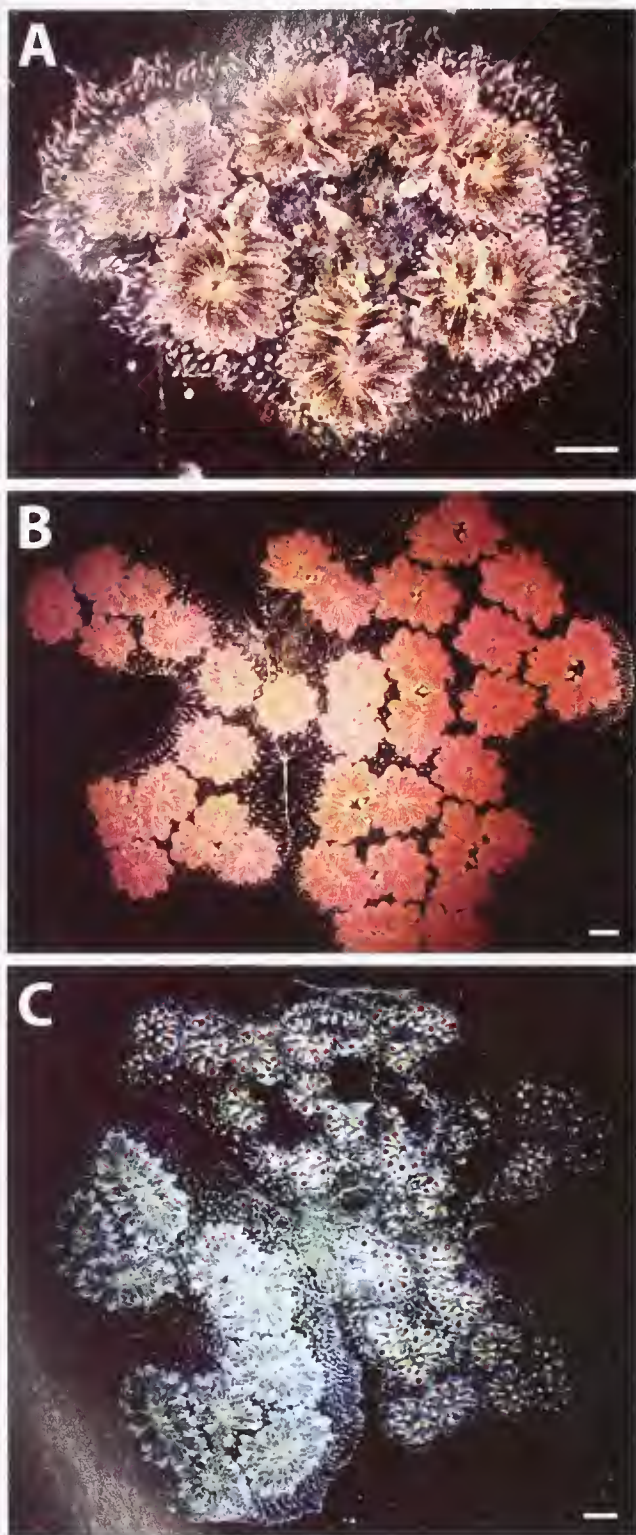


**Figure 1.** Colonies of the ascidian *Botryllus schlosseri* that were grown under three types of allogeneic contact conditions in Monterey Bay, California. Scale bars = 5 mm. (A) An isolated colony at 49 days old, consisting of 70 clonal units, termed zooids, that are arranged into six circular groups (systems) of 10–14 zooids each. The zooids are embedded in a clear gelatinous tunic and connected by a closed circulatory system.

## Materials and Methods

Under field conditions, individuals of the cosmopolitan ascidian *Botryllus schlosseri* pallas form compact, disc-shaped colonies (Fig. 1a), which occur in protected shallow marine environments, such as bays, harbors, and marinas, in temperate areas of both the northern and southern hemispheres (Chadwick-Furman and Weissman, 1995b, and references therein). Our experimental studies were conducted in the Monterey Municipal Marina, Monterey County, California (36°37.4'N;121°54'W), where colonies of *B. schlosseri* are a dominant component of the fouling community on hard submerged surfaces (Chadwick-Furman and Weissman, 1995b).

We observed colonies of *B. schlosseri* on submerged columns and docks in the Monterey Marina at depths from the surface to 1 m and determined the frequencies of natural contacts between these colonies and other encrusting macroorganisms. This survey was conducted during November 1990, in the season of low abundance of fouling organisms in the marina (Boyd *et al.*, 1986; Carwile, 1989); thus our estimates represent minimal contact rates. Three hundred and nine colonies of *B. schlosseri* were observed in the marina for determination of their contact status.

To test the effects of allogeneic contact on life-history traits in *B. schlosseri*, we set up three treatments using each of four cohorts of newly settled offspring from field-collected colonies. The four cohorts settled on 19 May 1990, 3 July 1990, 15 October 1990, and 25 January 1991 (after Chadwick-Furman and Weissman, 1995b). In each cohort, newly settled, one-system colonies of 1–7 zooids each (= one circular system of zooids, Fig. 1a), were either (1) isolated on plates, (2) placed in incompatible pairs that rejected each other, or (3) placed in compatible pairs that fused. We distinguished between fusible and incompatible pairs by placing the small, one-system colonies into contact and observing the outcome. We used only colony pairs that established contact during the one-system stage of develop-

---

Bulbous ampullae, or sacs of the circulatory system, are visible around the perimeter of the colony. This colony settled in May 1990, began sexually producing eggs in August, and produced a total of 683 eggs in four clutches before it died in September. (B) Fused chimeric colony at 142 days old. The left genotype, according to developmental characters (see text), consists of 151 zooids; the right genotype, which is slightly darker, consists of 215 zooids. The line of fusion of their tunics is visible at center. Both members of this chimera settled in October 1990, came into contact and fused in January 1991, and died simultaneously in March 1991 at 149 days old, without having produced any eggs. (C) Pair of rejecting colonies at 68 days old. Both colonies settled in May 1990, and came into contact and rejected during June 1990. Along their interacting borders at center, 25 pairs of blood-system ampullae are in allogeneic tissue contact. The right colony, which consists of 129 decaying zooids, is in the process of senescing and dying. The left colony, which consists of 89 zooids, died one week later at 75 days old. Neither colony produced eggs.

ment. In each cohort, offspring from 10 field-collected colonies were assigned randomly to each of the three treatments ( $n = 8\text{--}36$  newly settled colonies per treatment). A total of 274 colonies from all cohorts were monitored.

Each experimental colony or pair of colonies was placed on a glass plate measuring  $5.0 \times 7.5$  cm and allowed to attach firmly for 1 week in the laboratory (after Rinkevich and Weissman, 1992a; Chadwick-Furman and Weissman, 1995b). Colonies that did not firmly attach to the plates, or that appeared damaged, were removed from the study at this point. All well-attached colonies were then transferred to the marina field site, in an area where abundant colonies of *B. schlosseri* grow naturally on fouling surfaces. About every 7 days, depending on the time of year, all the zooids in each colony passed through an asexual growth cycle (hereafter termed "cycle"). During each cycle, the zooids produced buds, then shrank and were replaced by their buds; thus a new asexual generation of zooids was formed in each colony. To examine cycle-related life-history traits, every 4–7 days we collected all the experimental colonies, observed them under a dissecting microscope in the laboratory, and returned them to the field within a few hours (after Chadwick-Furman and Weissman, 1995a, b).

We examined the following life-history parameters for each colony: (1) growth rate of somatic tissues, as measured by the number of clonal units (zooids, Fig. 1) produced per cycle; (2) age and size at sexual maturity, defined as the beginning of egg production; and (3) sexual reproductive output, as measured by the number of eggs produced by each zooid during each cycle, the number of cycles in which eggs were produced (# clutches), and the total number of eggs produced by each colony throughout its lifespan (fecundity) (after Sabbadin and Zaniolo, 1979; Sabbadin and Astorri, 1988; Chadwick-Furman and Weissman, 1995b). We assigned zooids in chimeric colonies to genotype on the basis of morphological and developmental characters, such as their relative positions in the chimera, the number of buds produced, and in some cases, color patterns (after Chadwick-Furman and Weissman, 1995a; Yund *et al.*, 1997). Since colonies were observed every 4–7 days, we counted directly the number of buds produced by each zooid at each cycle, and thus accurately assigned each new budded zooid to original colony genotypes in chimeras.

All statistical analyses were performed using STATA, version 7.0 (Statacorp, 2001). Effects of allogeneic contact treatment on life-history traits were examined only within each cohort, since between-cohort comparison of life-history traits were made previously (Chadwick-Furman and Weissman, 1995b). For life-history traits that were examined on a per-cycle basis (*i.e.*, number of zooids produced per cycle and number of eggs per zooid per cycle, see above), we measured the value for each cycle within a colony, but we present only the mean of these values for each colony. Thus, a one-way model was used in analyzing

these traits. Log-transformed values of all life-history traits had approximately equal variances between treatment groups within each cohort, so ANOVA tests were applied to the data.

## Results

### *Frequencies of natural contacts*

We observed high frequencies of natural contact between colonies of *Botryllus schlosseri* and other encrusting macroorganisms. About one-third of all colonies (28.2%,  $n = 309$ ) contacted encrusting bryozoans. Many colonies of *B. schlosseri* contacted the other colonial ascidians *Botrylloides violaceus* (23.6%) or *Diplosoma macdonaldi* (4.8%), or individuals of solitary ascidians (5.5%). In addition, 21.4% of *Botryllus schlosseri* colonies occurred in allogeneic contact with conspecifics. Only one colony was observed to contact macroalgae (0.3%), and some colonies were isolated from contact with other sessile macroorganisms (16.2%).

### *Morphology and growth*

Colony morphology was similar in all cohorts and experimental treatments. All colonies were flat and disc-shaped when small, with closely spaced groups of zooids (Fig. 1a). As they grew, some of the colonies developed irregular outlines, but the zooid systems remained compact and close together (Fig. 1b, c). In fused chimeric colonies, the area of fusion became barely visible over time, and some zooid systems straddled the area of initial fusion (Fig. 1b). The zooids of all genotypes in fused colonies appeared to grow constantly and to coexist in chimeras during their entire lifespan (Fig. 1b). We did not observe any shrinkage or somatic resorption of one genotype by another in chimeras. Until the time of chimeric colony senescence and death, robust blastozooids from all partners appeared to coexist within a single fused colony (Fig. 1b).

Colonies that contacted noncompatible partners underwent rejection reactions that persisted along an extensive border of contacting tissues (Fig. 1c). As colonies grew, the contact area expanded along this border, and the number of points of rejection increased. Up to 15 points of rejection were observed during each sampling period throughout the lifespan of rejecting colonies. All rejecting colonies maintained a long, continuous border throughout their lifespans, until one of them senesced and died (Fig. 1c). Pairs of rejecting colonies were compact, grew actively, and neither retreated nor grew away from each other.

Colonies grew until they reached the edges of the glass culture plate, then grew around the plate edges, and continued to spread over the back sides of the plate. None of the colonies filled all of the space available on both sides of the plate (Fig. 1).

Juvenile colonies grew exponentially, regardless of treatment (Fig. 2). During January and October, exponential growth began after a lag time of 3–5 cycles (= 32 to 64 days, Fig. 2). In other cohorts, colonies in the isolated treatment reached the largest maximum size (Fig. 2). This pattern persisted even in the October cohort, in which some isolated colonies experienced partial predation during cycle 9 that reduced their size to almost zero, after which they recovered and became the largest colonies in the cohort (Fig. 2). Growth rate slowed upon commencement of sexual reproduction in all cohorts (Fig. 2).

In most cohorts, there was a significant effect of treatment on colony growth rate (Tables 1 and 2, Fig. 3a). Isolated colonies grew faster than did both rejected and fused colonies in the cohorts born during January and May (Table 2).

In two of the cohorts, rejected colonies also grew faster than did colonies that fused to become chimeras (Table 2). In the October cohort, none of the fused colonies grew past the juvenile stage, and so were not included in statistical analyses of life-history differences among colonies that reached sexual maturity (Fig. 3, Tables 1 and 2).

### Sexual reproduction

There was no effect of allogeneic contact treatment on the age at which colonies reached first reproduction, except in the May cohort, where rejected colonies reached sexual maturity at a significantly later age than did both isolated and fused colonies (Tables 1 and 2, Fig. 3b). The age at which colonies began to reproduce sexually appeared to be

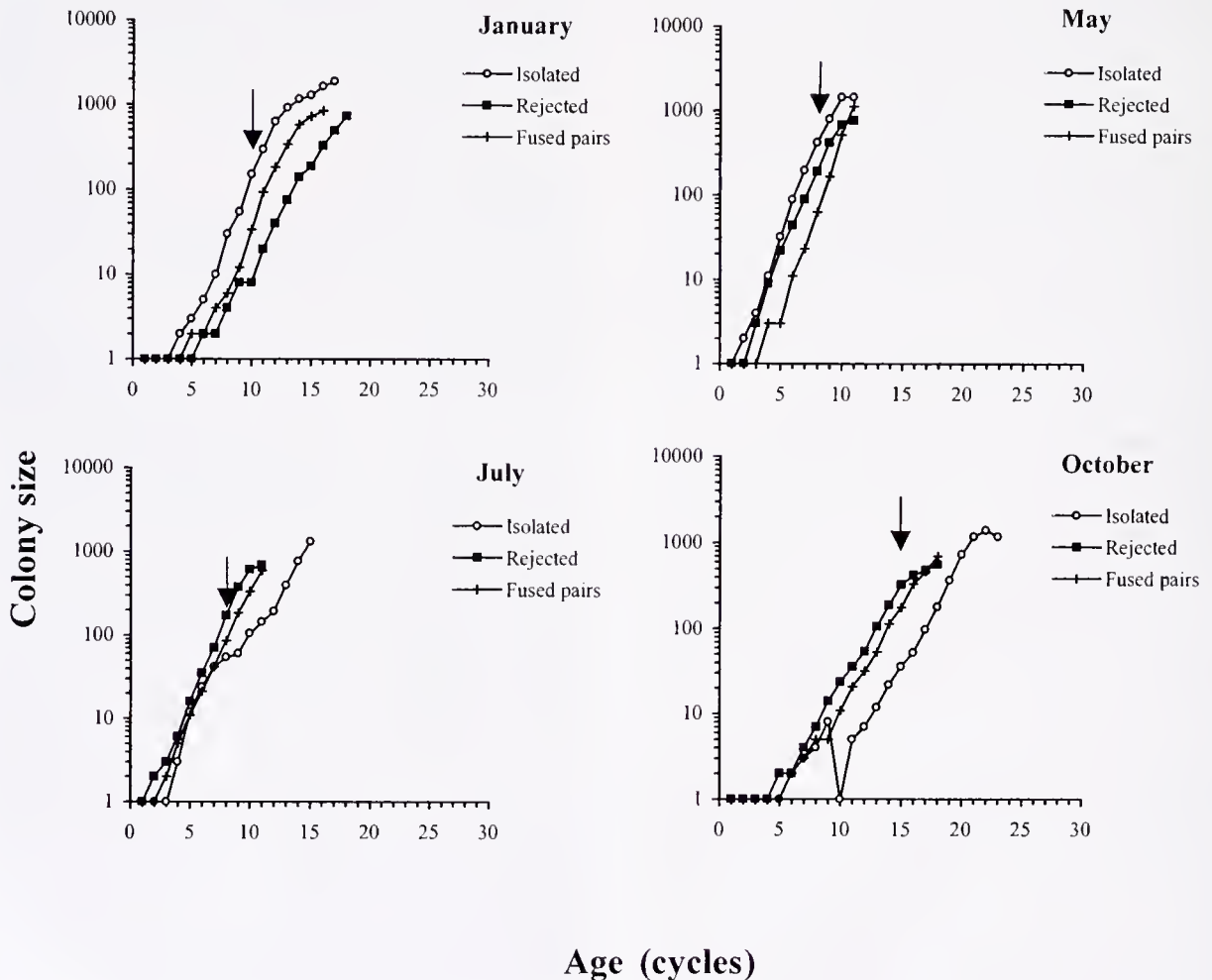


**Figure 2.** Typical growth curves of colonies of the ascidian *Botryllus schlosseri* for three allogeneic contact treatments and four cohorts in Monterey Bay, California. The shape of growth curves varied widely within each treatment, so mean and error values cannot be shown clearly here. Thus, only the largest colony in each treatment is shown for each cohort (for mean growth rates, see Fig. 3a). Note that colony size is plotted on a logarithmic scale. Arrows mark the commencement of sexual reproduction (egg production) for the first colonies to reach maturity in each cohort. Data on isolated colonies were published previously as Figure 1 in Chadwick-Furman and Weissman (1995b).

Table 1

One-way ANOVAs of life-history traits between allogenic contact treatments within each of four cohorts of the colonial ascidian *Botryllus schlosseri* grown in Monterey Bay, California

Life-history trait	Cohort	Source of variation	DF	Mean square	F	P
Growth rate	January	Treatment	2	0.105	10.44	***
		Error	33	0.010		
	May	Treatment	2	0.521	41.20	***
		Error	53	0.013		
	July	Treatment	2	0.200	4.71	*
		Error	47	0.049		
	October	Treatment	1	0.030	1.62	ns
		Error	8	0.019		
Age at first reproduction	January	Treatment	2	0.356	3.02	ns
		Error	33	0.118		
	May	Treatment	2	0.073	9.90	***
		Error	53	0.007		
	July	Treatment	2	0.016	1.03	ns
		Error	47	0.016		
	October	Treatment	1	0.107	4.61	ns
		Error	8	0.023		
Size at first reproduction	January	Treatment	2	1.953	3.72	*
		Error	33	0.525		
	May	Treatment	2	14.400	41.66	***
		Error	53	0.346		
	July	Treatment	2	3.036	3.35	*
		Error	47	0.907		
	October	Treatment	1	2.142	4.56	ns
		Error	8	0.470		
Number of eggs/zooid/cycle	January	Treatment	2	0.641	3.25	ns
		Error	33	0.197		
	May	Treatment	2	1.008	5.00	*
		Error	53	0.202		
	July	Treatment	2	0.343	2.31	ns
		Error	47	0.148		
	October	Treatment	1	0.305	4.10	ns
		Error	8	0.074		
Clutch number	January	Treatment	2	2.696	9.83	***
		Error	33	0.274		
	May	Treatment	2	0.179	1.34	ns
		Error	53	0.133		
	July	Treatment	2	0.795	2.35	ns
		Error	47	0.339		
	October	Treatment	1	1.692	12.04	**
		Error	8	0.140		
Fecundity	January	Treatment	2	12.844	15.79	***
		Error	33	0.813		
	May	Treatment	2	19.587	25.71	***
		Error	53	0.762		
	July	Treatment	2	4.695	3.17	*
		Error	47	1.480		
	October	Treatment	1	16.656	23.43	**
		Error	8	0.711		

\*  $P < 0.05$ ; \*\*  $P < 0.01$ ;  $P < 0.001$ ; ns = not significant.

controlled mainly by environmental factors, such as temperature, that varied with season of birth (see Chadwick-Furman and Weissman, 1995b).

Variation in the size of colonies at first reproduction followed the same pattern as did colony growth rate (Table

2), but the differences between groups were magnified (compare Figs. 3a and c). In both the January and May cohorts, isolated colonies, which grew relatively rapidly as juveniles (Fig. 3a), were significantly larger at maturity than were fused and rejected colonies (Fig. 3c, Table 2). Where

Table 2

Tukey-Kramer multiple comparisons tests for differences in life-history traits between allogeneic contact treatments within each of 4 cohorts of the colonial ascidian *Botryllus schlosseri* grown in Monterey Bay, California

Life-history trait	Cohort	Treatment*
Growth rate (# buds/zooid/cycle)	January	I > R F
	May	I > R > F
	July	I R > F
	October	I R
Age at first reproduction (# cycles)	January	I R F
	May	I F > R
	July	I R F
	October	I R
Size at first reproduction (# zooids)	January	I > R F
	May	I > R > F
	July	I R > F
	October	I R
Number of eggs/zooid/cycle	January	I R F
	May	I > R F
	July	I R F
	October	I R
Clutch number	January	I > R F
	May	I R F
	July	I R F
	October	I > R
Fecundity (total # eggs/colony)	January	I > R F
	May	I > R F
	July	I R F
	October	I > R

\* Symbols for treatments: I = isolated, R = rejected, F = fused. Treatments that did not differ significantly ( $P > 0.05$ ) are conjointly underlined. > signs indicate which treatments had significantly larger values of each life-history trait within each cohort. In the October cohort, none of the fused colonies survived to reproduce, and so they were not included in analysis of variation in life-history traits among colonies that survived to maturity.

there were significant differences, isolated colonies were, on average, 1.5–2.5 times larger at sexual maturity than rejected colonies, and 2–3 times larger than colonies that fused to form chimeras (Fig. 3c).

The number of eggs produced per zooid per cycle (= reproductive effort) varied widely between colonies within each treatment, and did not vary between treatments, except in the May cohort (Table 1, Fig. 3d). For colonies born during May, isolated individuals produced significantly more eggs per zooid per cycle than did colonies in either of the allogeneic contact treatments (Table 2).

The total number of egg clutches produced by each colony was affected by treatment in only the two cohorts that overwintered, those born during October and January (Table 1, Fig. 3d). In both cases, colonies that were isolated from contact produced significantly more egg clutches than did those in either of the two allogeneic contact treatments (on average, 2–3 times more clutches, Fig. 3e, Table 2).

The lifetime fecundity of colonies varied significantly

with treatment in all cohorts (Table 1). The combined effects of relatively rapid somatic growth, large size at maturity, and a large number of egg clutches in the isolated colony treatment (Fig. 3a–e) resulted in much higher lifetime fecundity in isolated than in either the fused or rejected treatments (Fig. 3f, Table 2). The mean fecundity of isolated colonies ranged from 1.8 to 2.5 times that of fused or rejected colonies in summer cohorts (May and July). In the winter cohorts (January and October), the mean fecundity of isolated colonies was more than 5–10 times that of fused or rejected colonies. Fused colonies that were born in October did not produce eggs at all (Fig. 3f).

#### Colony longevity and survivorship

Colonies in all treatments and cohorts had short, subannual lifespans (Fig. 4). Within each cohort, colonies in all treatments reached sexual maturity at about the same age (Fig. 3b), reproduced sexually for a few cycles, and then all died within a few cycles of each other (Fig. 4). The percentage of colonies that survived to reproduce was high and did not vary significantly among treatments in the January and May cohorts (chi-square tests,  $\chi^2_{0.05(2)} = 5.99$ ,  $G = 0.68$  and  $3.78$  respectively, Fig. 5). In the July cohort, survivorship also was high, but did vary with treatment; rejected colonies had the lowest survivorship to maturity ( $G = 13.16$ ). Colonies born in October had low survivorship that did not vary significantly with treatment, even though all colonies in the fused treatment died as juveniles ( $G = 5.04$ , Fig. 5).

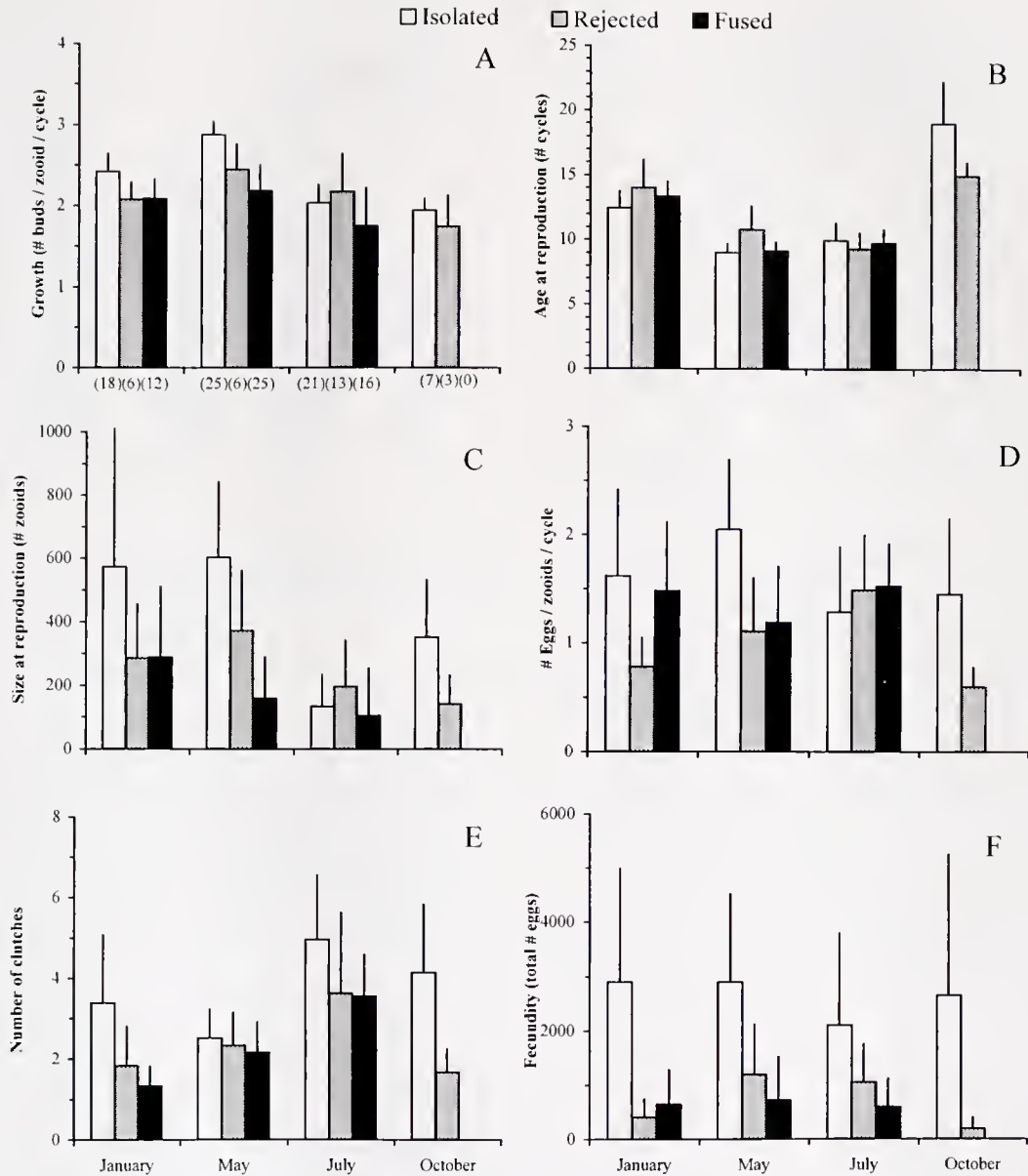
Colony longevity in all treatments and cohorts was controlled mainly by the timing of colony senescence (Fig. 1c). Senescence occurred in four distinct stages that began 1–2 weeks before death (details in Chadwick-Furman and Weissman, 1995b). The stages of senescence did not vary with treatment or cohort.

When senescence began in the zooids of one genotype, it spread to the zooids of fused, but not rejected, partners (Fig. 1b, c). After one of the partners in a rejecting pair died, the other colony continued to live for a few cycles (Fig. 1c).

#### Discussion

We document here that allogeneic contacts, whether they lead to fusion or rejection, result in significantly reduced fitness in field-grown colonies of the colonial ascidian *Botryllus schlosseri*. This is the first demonstration in a protochordate that, under natural field conditions, allogeneic contacts leading to both fusion and rejection come at a cost to life-history processes such as growth and reproduction.

We also show that colonies of *Botryllus schlosseri* in the wild frequently contact those of conspecifics and of other species of sessile invertebrates, so associated fitness costs may be a ubiquitous and important phenomenon in nature. Contact rates with the colonial ascidian *Botrylloides viola-*



### Cohort

**Figure 3.** Variation in life-history traits among three allogeneic contact treatments and four cohorts in the colonial ascidian *Botryllus schlosseri*, grown in Monterey Bay, California. Note that for fused colonies, traits are presented for each genotype within the colony. Means plus one standard deviation are shown. Sample sizes for all life-history traits are given in parentheses in graph A. Sample sizes are low in some groups due to mortality of some colonies before reaching sexual maturity (compare sample sizes with those in Fig. 5). Data on isolated colonies were published previously as Figure 2 in Chadwick-Furman and Weissman (1995b).

*ceous* were especially high at our site (see Results). Yet, because our survey of contact frequencies was based on a one-time observation, which inherently underestimates contacts throughout the life of a colony, lifetime contact rates between colonies of *Botryllus schlosseri* and other sessile

organisms at Monterey are even higher than those presented here (see Results). Our limited manipulation of colonies in one of the cohorts of *Botryllus schlosseri* (born on 15 October 1990) indicates that xenogeneic interaction with *Botrylloides violaceous* results in a level of fecundity inter-

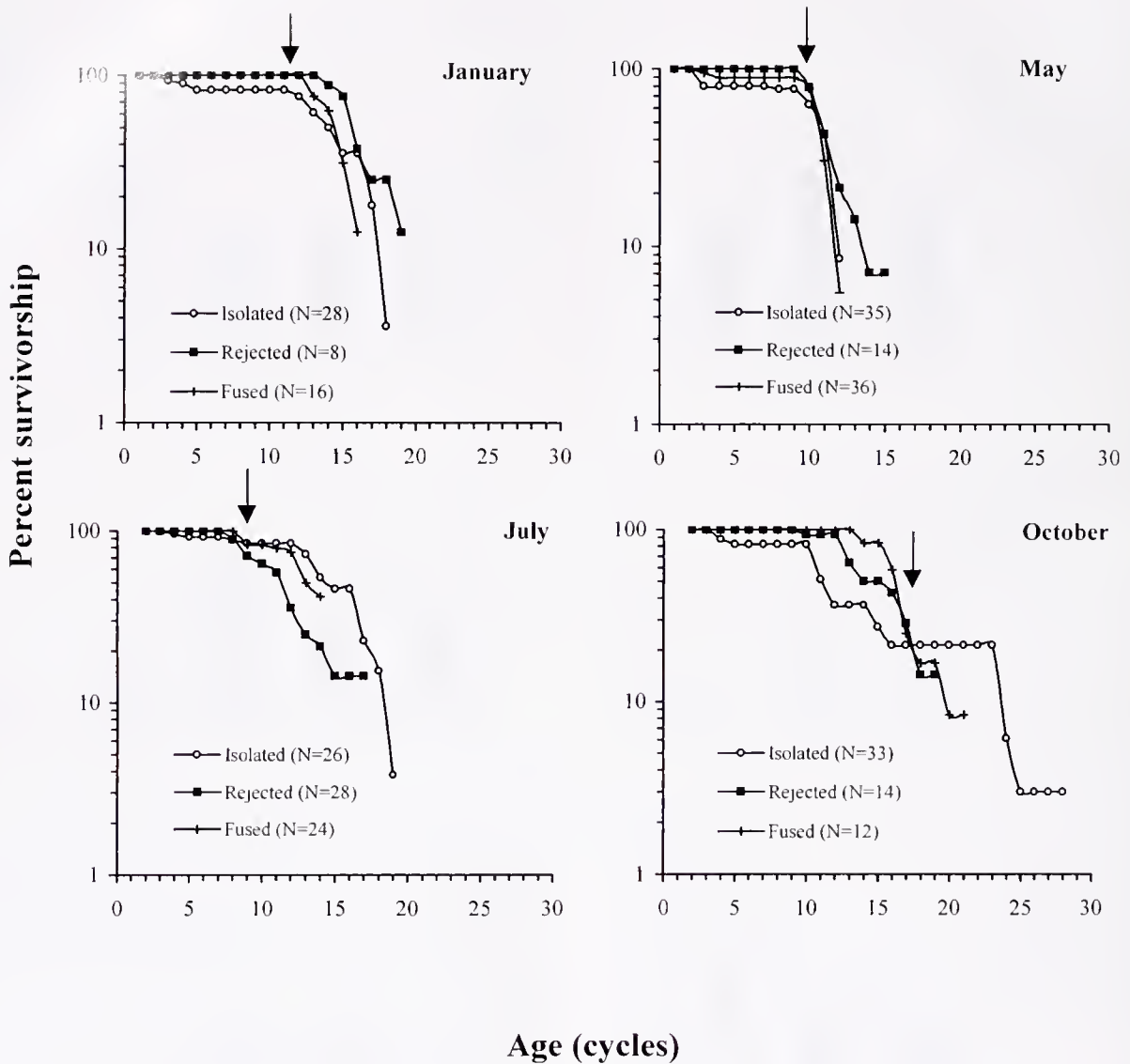


**Figure 4.** Survivorship curves for colonies of the ascidian *Botryllus schlosseri* grown in Monterey Bay, California, in four cohorts and three allogeneic contact treatments. Arrows indicate the commencement of sexual reproduction in each cohort. The last point in each line represents the last surviving colony of each group. Note that survivorship is plotted on a logarithmic scale. Data on isolated colonies were published previously as Figure 3 in Chadwick-Furman and Weissman (1995b).

mediate between those of isolated and allocontacted colonies [total number of eggs produced =  $1383 + 769$  ( $\bar{x} + SD$ ),  $n = 9$  xenocontacted colonies of *Botryllus schlosseri* that survived to maturity, N. E. Chadwick-Furman, pers. obs.; compare with October cohort in Fig. 3f]. Thus, xenogeneic contact appears to affect colony fecundity, but not as severely as allogeneic contact.

The reduced fitness of colonies following fusion or rejection may result from energetic or physiological costs associated with recognizing and reacting to non-self tissue. The process of interaction along the borders of rejecting colonies involves extensive tissue damage and resource

demand on both colonies (Scofield and Nagashima, 1983; reviewed in Rinkevich, 1992). In addition, competition between somatic and germ cell lines within fused chimeras also may draw heavily on the physiological resources of the partners involved (Buss, 1982). Colonies that are isolated from allogeneic contact do not face these costs.

The lack of resorption observed here in field-raised chimeras of *Botryllus schlosseri* is in striking contrast to previous results from laboratory studies (Rinkevich and Weissman, 1987, 1992a, b; Pancer *et al.*, 1995). The reduced chimeric stability of laboratory colonies has been demonstrated by growing genetically identical replicates of chime-

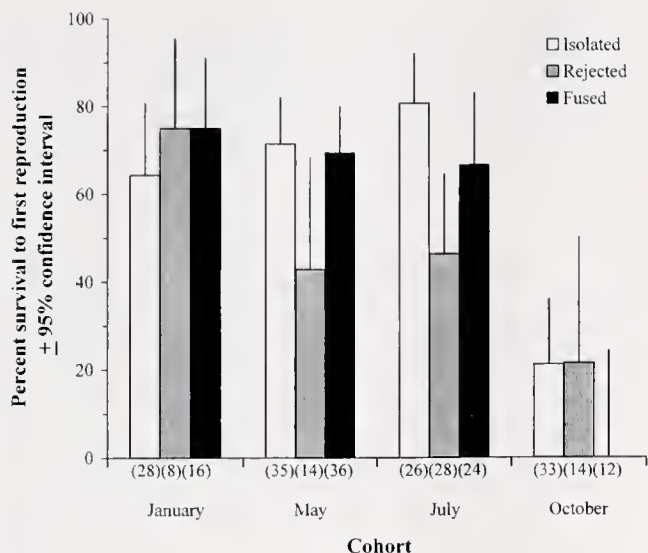


**Figure 5.** Variation in percent survivorship to first reproduction among four cohorts and three allogeneic contact treatments of colonies of the ascidian *Botryllus schlosseri* grown in Monterey Bay, California. Sample sizes for each treatment are given in parentheses.

ras under field *versus* laboratory conditions (Chadwick-Furman and Weissman, 1995a). The present results show that, under field conditions in Monterey, the partners of a chimera appear to grow in a stable manner and do not undergo somatic resorption. Previous field studies indicate a high level of environmentally dependent plasticity in fitness-related life-history traits of *B. schlosseri* (Chadwick-Furman and Weissman, 1995a; Yund *et al.*, 1997).

The reduced reproductive success of interacting *versus* isolated colonies (Fig. 3 and Table 1) reveals effects of allogeneic contacts on sexual reproduction as well as on somatic tissue production. Recruitment of larvae at Monterey in the springtime may be derived from a small number of parent colonies that overwinter (Carwile, 1989; Chadwick-Furman and Weissman, 1995b). Thus, the costs of interactions in this experiment would have resulted in reduced representation of the offspring of winter allo-contacting colonies in the summer bloom.

Allogeneic interactions do not alter the survivorship of colonies in most cohorts (Fig. 5). The longer lifespans (Figs. 3b and 4) and lower survivorship (Fig. 5) of colonies during winter, as compared to summer, appear to be due to a slowing of colony growth and development during low temperatures in the winter in Monterey Bay (Boyd *et al.*, 1986; Chadwick-Furman and Weissman, 1995b). As found in past studies, whole-colony senescence causes the death of most colonies (Chadwick-Furman and Weissman, 1995a, b) and is genetically controlled (Rinkevich *et al.*, 1992).

At the time of our experiments, we did not have markers to identify the genotypes of blood cells, bud cells, or gametes in the fused colonies, and so we did not test for

somatic or germ cell parasitism as a result of colony fusion. However, germ cell parasitism has been reported in this species (Rinkevich and Weissman, 1987; Sabbadin and Astorri, 1988; Pancer *et al.*, 1995), and recent work has verified that it occurs in both male and female gametes capable of fertilization (Stoner and Weissman, 1996; Stoner *et al.*, 1999). The process of germ cell parasitism, in which one partner in a chimera uses the somatic resources of the other to produce its own germ cells, may alter the relative fitness of fused genotypes in chimeras (Buss, 1982; Stoner and Weissman, 1996; Stoner *et al.*, 1999; Weissman, 2000). However, because the fitness of fused pairs of genotypes was less than half that of isolated colonies in all cohorts (Fig. 3f), the reproductive output of all the genotypes combined in chimeric colonies was less than that of genotypes in isolated colonies. Thus, germ cell parasitism may alter the relative amount of fitness lost due to fusion in chimeric colonies, but cannot prevent an overall reduction in fitness due to fusion. Even if germ cell parasitism were extensive in the chimeras tested here, chimera formation causes reduced fecundity, regardless of which genotype dominates (Fig. 3f). In 30% of the field chimeras examined by Stoner and Weissman (1996) at the same Monterey marina site, little or no germ or somatic cell parasitism was found. Thus, the values presented here for genotype-specific measures of fitness (Fig. 3) may represent realistic estimates for at least some chimeras that retain a stable genetic composition in the wild.

A drawback of the present study is that we could not set up, as controls, undissected pairs of isogenic colonies, to determine whether isogenic contact affects fitness. Thus, an evaluation of the actual costs of allogeneic contact *per se* is problematic. However, set-up of this control group would have required dissecting apart and re-uniting systems from multi-system colonies, thus introducing further manipulation of all colonies in this experiment. As the colonies grew, they produced lobes of tissue that contacted along their edges and fused along the undulating margins of the colony in all treatments (Fig. 1b, c). Thus, if isogenic contact affected fitness, it did so equally in all treatments here.

We show here that egg production in fused colonies is greatly reduced (Fig. 3f), possibly due to competition between the genetically different individuals that fused to make up that colony. Thus, one benefit of precise allorecognition in this species may be that it limits the unit of selection to chimeras composed of closely related kin (Grosberg and Quinn, 1986; Rinkevich and Weissman, 1987; Stoner and Weissman, 1996; Stoner *et al.*, 1999). Because of the high polymorphism of the *Fu/HC* gene locus (that permits fusion rather than rejection to occur; Scofield *et al.*, 1982), fused individuals in the wild most likely represent kin rather than a random assortment of genotypes (Grosberg and Quinn, 1986). In *Botryllus schlosseri*, the proportion of fusions occurring between siblings is higher

than between nonsiblings (Scofield *et al.*, 1982; Magor *et al.*, 1999). Thus, the unit of genetic inheritance for chimeric colonies of fused siblings would be the outcome of germline competition between the mother colony and the diverse sperm that fertilized her. In addition to kin fusion, regulated by *Fu/HC* matching, kin cosettlement is encouraged by the limited dispersal of tadpole larvae from the maternal colony and nonrandom cosettlement according to shared *Fu/HC* genotype (Grosberg and Quinn, 1986). A common selected trait in these chimeras is allele-sharing at the *Fu/HC* locus (Weissman *et al.*, 1990). Kin selection would act also on shared genes other than the selected *Fu/HC* types that are common to these siblings. Reproductive outcomes in these chimeras could be as simple as the direct gametic representation of the diverse blastozoid units in the chimera; or could be as complex as the outcomes of selective resorption or germ cell parasitism that generate skewing from that simple representation (Pancer *et al.*, 1995; Stoner and Weissman, 1996; Stoner *et al.*, 1999; Weissman, 2000).

No matter whether allogeneic colony contact results in fusion or rejection, if it leads to reduced fitness, as measured by growth and fecundity, with no increase in survivorship, why have these organisms developed and maintained an elaborate system of allorecognition? Perhaps, in this species, genetically based allorecognition is nonadaptive. It may be linked to other processes that are adaptive, and thus have evolved as a by-product of processes such as disease recognition (Buss and Green, 1985; Magor *et al.*, 1999) or gametic compatibility (Scofield *et al.*, 1982). However, the ability to recognize and reject nonrelated colonies, and to fuse only with closely related kin that share alleles at the *Fu/HC* locus, may be directly beneficial in that it reduces the costs of germ cell parasitism in colonies (Stoner *et al.*, 1999).

The phenomena of cosettlement, fusion, and development of reproductive competence in chimeras are not limited to protochordates, and may be important selective factors in other sessile organisms as diverse as fungi, sponges, and cnidarians (reviewed in Buss, 1982; Rinkevich and Weissman, 1987; Pancer *et al.*, 1995). Our findings that allogeneic contact, and especially chimera formation, reduce individual fitness under natural field conditions may have broad implications for the evolution of allorecognition systems.

### Acknowledgments

We thank Buki Rinkevich for discussions and collaborations that led to and resulted from these studies. We also thank Kathi Ishizuki and Karla Palmeri for assistance in data collection, Simona Bartl and Robert Lauzon for discussions, and Uri Frank and Buki Rinkevich for comments that improved the manuscript. Karen Tarnaruder assisted with the graphics. Prof. Maureen Lahiff of the School of Public Health at the University of California at Berkeley is

gratefully acknowledged for advice on statistical analysis. Funding was provided by a Frederick B. Bang Scholarship from the American Association of Immunologists, and PHS Grant CA09302 awarded by the National Cancer Institute, DHHS, to N.E.C.-F., and by PHS Grant CA42551 to I.L.W.

### Literature Cited

- Boyd H. C., S. K. Brown, J. A. Harp, and I. L. Weissman. 1986. Growth and sexual maturation of laboratory-cultured Monterey *Botryllus schlosseri*. *Biol. Bull.* **170**: 91–109.
- Buss, L. W. 1982. Somatic cell parasitism and the evolution of somatic tissue compatibility. *Proc. Natl. Acad. Sci. USA* **79**: 5337–5341.
- Buss, L. W., and D. R. Green. 1985. Histoincompatibility in vertebrates: the relict hypothesis. *Dev. Comp. Immunol.* **9**: 191–201.
- Carwile, A. H. 1989. Settlement of larvae, colony growth and longevity in three species of ascidians and the effect on the species composition of a marine fouling community. Ph.D. dissertation, University of California, Los Angeles.
- Chadwick-Furman, N., and B. Rinkevich. 1994. A complex allorecognition system in a reef-building coral: delayed responses, reversals and nontransitive hierarchies. *Coral Reefs* **13**: 57–63.
- Chadwick-Furman, N. E., and I. L. Weissman. 1995a. Life history plasticity in chimeras of the colonial ascidian *Botryllus schlosseri*. *Proc. R. Soc. Lond. B* **262**: 157–162.
- Chadwick-Furman, N. E., and I. L. Weissman. 1995b. Life histories and senescence of *Botryllus schlosseri* (Chordata, Ascidiacea) in Monterey Bay. *Biol. Bull.* **189**: 36–41.
- Frank, U., U. Oren, Y. Loya, and B. Rinkevich. 1997. Alloimmune maturation in the coral *Stylophora pistillata* is achieved through three distinctive stages, 4 months post-metamorphosis. *Proc. R. Soc. Lond. B* **264**: 99–104.
- Grosberg, R. K., and J. F. Quinn. 1986. The genetic control and consequences of kin recognition by the larvae of a colonial marine invertebrate. *Nature* **322**: 456–459.
- Hidaka, M., K. Yurugi, S. Sunagawa, and R. A. Kinzie III. 1997. Contact reactions between young colonies of the coral *Pocillopora damicornis*. *Coral Reefs* **16**: 13–20.
- Ilan, M., and Y. Loya. 1990. Ontogenetic variation in sponge histocompatibility responses. *Biol. Bull.* **179**: 279–286.
- Magor, B. G., A. De Tomaso, B. Rinkevich, and I. L. Weissman. 1999. Allorecognition in colonial tunicates: protection against predatory cell lineages? *Immunol. Rev.* **167**: 69–79.
- Pancer, Z., H. Gershon, and B. Rinkevich. 1995. Coexistence and possible parasitism of somatic and germ cell lines in chimeras of the colonial urochordate *Botryllus schlosseri*. *Biol. Bull.* **189**: 106–112.
- Rinkevich, B. 1992. Aspects of the incompatibility nature in botryllid ascidians. *Anim. Biol.* **1**: 17–28.
- Rinkevich, B. 1996. Bi- versus multichimerism in colonial urochordates: a hypothesis for links between natural tissue transplantation, allogeny and evolutionary ecology. *Exp. Clin. Immunogenet.* **13**: 61–69.
- Rinkevich, B., and I. L. Weissman. 1987. Chimeras in colonial invertebrates: a synergistic symbiosis or somatic- and germ-cell parasitism? *Symbiosis* **4**: 117–134.
- Rinkevich, B., and I. L. Weissman. 1992a. Chimeras vs. genetically homogeneous individuals: potential fitness costs and benefits. *Oikos* **63**: 119–124.
- Rinkevich, B., and I. L. Weissman. 1992b. Allogeneic resorption in colonial protochordates: consequences of nonself recognition. *Dev. Comp. Immunol.* **16**: 275–286.
- Rinkevich, B., R. J. Lauzon, B. W. M. Brown, and I. L. Weissman. 1992. Evidence for a programmed life span in a colonial protochordate. *Proc. Natl. Acad. Sci. USA* **89**: 3546–3550.

- Sabbadin, A. 1994.** Coloniality in ascidians and its adaptive value, with special reference to *Botryllus schlosseri*. *Ann. Biol.* **3**: 157–163.
- Sabbadin, A., and C. Astorri. 1988.** Chimeras and histocompatibility in the colonial ascidian *Botryllus schlosseri*. *Dev. Comp. Immunol.* **12**: 737–747.
- Sabbadin, A., and G. Zaniolo. 1979.** Sexual differentiation and germ cell transfer in the colonial ascidian *Botryllus schlosseri*. *J. Exp. Zool.* **207**: 289–304.
- Scofield, V. L., and L. S. Nagashima. 1983.** Morphology and genetics of rejection reactions between oozoids from the tunicate *Botryllus schlosseri*. *Biol. Bull.* **165**: 733–744.
- Scofield, V. L., J. M. Schlumpberger, L. A. West, and I. L. Weissman. 1982.** Protochordate allorecognition is controlled by an MHC-like gene system. *Nature* **295**: 499–502.
- Statacorp. 2001.** Stata Statistical Software: Release 7.0. Stata Corporation, College Station, Texas.
- Stoner, D., and I. L. Weissman. 1996.** Somatic and germ cell parasitism in a colonial ascidian: possible role for a highly polymorphic allorecognition system. *Proc. Natl. Acad. Sci. USA* **93**: 15254–15259.
- Stoner, D., B. Rinkevich, and I. L. Weissman. 1999.** Heritable germ and somatic cell lineage competitions in chimeric colonial protochordates. *Proc. Natl. Acad. Sci. USA* **96**: 9148–9153.
- Weissman, I. L. 2000.** Stem cells: units of development, units of regeneration, and units in evolution. *Cell* **100**: 157–168.
- Weissman, I. L., Y. Saito, and B. Rinkevich. 1990.** Allorecognition histocompatibility in a protochordate species: Is the relationship to MHC semantic or structural? *Immunol. Rev.* **113**: 227–241.
- Yund, P. O., Y. Marcum, and J. Stewart-Savage. 1997.** Life-history variation in a colonial ascidian: broad-sense heritabilities and tradeoffs in allocation to asexual growth and male and female reproduction. *Biol. Bull.* **192**: 290–299.

## Effect of Disturbance on Assemblages: an Example Using Porifera

J. J. BELL<sup>1,\*</sup> AND D. K. A. BARNES<sup>2</sup>

<sup>1</sup>*Department of Zoology and Animal Ecology, University College Cork, Lee Maltings, Co. Cork, Ireland;*  
*and* <sup>2</sup>*British Antarctic Survey, N.E.R.C., High Cross, Madingley Road, Cambridge CB3 0ET, United Kingdom*

**Abstract.** Extensive sponge assemblages are found in a number of habitats at Lough Hyne Marine Nature Reserve. These habitats are unusual in experiencing a range of environmental conditions, even though they are only separated by small geographic distances (1–500 m), reducing the possibility of confounding effects between study sites (*e.g.*, silica concentrations and temperature). Sponge assemblages were examined on ephemeral (rocks), stable (cliffs), and artificial (slate panels) hard substrata from high- and low-energy environments that were used to represent two measures of disturbance (flow rate and habitat stability). Sponge assemblages varied considerably between habitat types such that only 26% (25 species) of species reported were common to both rock and cliff habitats. Seven species (of a total of 96 species) were found in the least-developed assemblages (slate panels) and were common to all habitats. Sponge assemblages on rocks and panels varied little between high- and low-energy environments, whereas assemblages inhabiting cliffs varied considerably. Assemblage composition was visualized using Bray-Curtis similarity analysis and Multi-Dimensional Scaling, which enabled differences and similarities between sponge assemblages to be visualized. Cliffs from high- and low-energy sites had different assemblage compositions compared to large rocks, small rocks, and panels, all of which had similar assemblages irrespective of environmental conditions. Differences in assemblages were partially attributed to sponge morphology (shape), as certain morphologies (*e.g.*, arborescent species) were excluded from 2-D rock habitats. Other mechanisms were also considered responsible for the sponge assemblages associated with different habitats.

### Introduction

The development of any community (*e.g.*, mature or young) is controlled by a suite of biological and physical factors that may be closely related and interlinked (Buss and Jackson, 1979). In some marine environments, such as caves, communities (all species) are well developed (mature); in others, such as ice-scoured polar shores, all communities tend to be poorly developed (young). Yet there are other localities that contain communities in various stages of development in proximity to one another. Lough Hyne is such an example, where adjacent communities may experience some similar conditions (*e.g.*, flow rate, temperature, food concentration) but are at different stages of development. For example, rocks in areas with fast currents, where disturbance is high, may have less well-developed communities than rocks in areas experiencing slight current flow, where disturbance is reduced (Maughan and Barnes, 2000a), even though they are separated by less than 300 m. The same may be true for sublittoral cliff habitats where climax community states may be achieved only under certain environmental conditions. In the case of rocks, size may also be important to community development because smaller rocks are more likely to be moved than larger rocks, causing differences in community (all species) and assemblage (component phyla) composition (Barnes *et al.*, 1996). Unstable or highly disturbed (*e.g.*, small rocks) habitats are often colonized by fast-growing, opportunistic, and *r*-strategic species that are able to quickly take advantage of newly created habitats or space (Lilly *et al.*, 1953; Osman, 1977; Sousa, 1979; Barnes *et al.*, 1996; McCook and Chapman, 1997).

Sponges are an important component of hard-substratum communities throughout most polar (*e.g.*, Dayton, 1978), temperate (*e.g.*, Hiscock *et al.*, 1983; Bell and Barnes, 2000a), and tropical regions (*e.g.*, Alcolado, 1990). There is a wide body of literature that considers the influence of

Received 27 August 2001; accepted 23 May 2003.

\* To whom correspondence should be addressed. Current address: Institute of Biological Sciences, Edward Llwyd Building, The University of Wales, Aberystwyth, Ceredigion SY23 3DA.

environmental parameters on the composition of sponge assemblages (e.g., Wilkinson and Cheshire, 1989; Alcolad, 1990; Alvarez *et al.*, 1990; Diaz *et al.*, 1990; Schmahl, 1990; Witman and Sebens, 1990). There are also examples of studies comparing sponge assemblages on large (100–1000 km) spatial scales (Maldonado and Uriz, 1995; Hooper *et al.*, 2002) and on smaller scales (2–20 km) between sponges inhabiting mangrove pools (Rützler *et al.*, 2000). However, comparisons between different habitat types (e.g., between loose rock and cliffs) under fixed environmental conditions or on local scales (hundreds of meters) where confounding effects are reduced are less common.

Studies of sponge assemblages suggest that a number of physical factors control species distributions; these factors include water flow rate (Bell and Barnes, 2000a), sedimentation (Könnecker, 1973), nutrient levels (Storr, 1976), depth (Alvarez *et al.*, 1990; Witman and Sebens, 1990), light (Sarà *et al.*, 1978; Cheshire and Wilkinson, 1991), and habitat availability (Könnecker, 1973; Barthel and Tendal, 1993). Habitats classified within these physical parameters (e.g., fast water flow at a depth of 20 m) often contain many smaller or cryptic habitats with their own predefined physical characteristics. For example, at a site of slight water flow, where sedimentation is high, the amount of sediment falling on inclined, vertical, or overhanging cliff surfaces varies considerably, resulting in different assemblages on each surface type (see Bell and Barnes, 2000b, c). Although not as well studied, biological factors are also known to influence the composition of sponge assemblages (see Paine, 1974; Wulff, 1995, 2000), and predation may also limit the local distribution of sponge species (Dunlap and Pawlik, 1996; Wulff, 2000; Bell, 2001). Rich sponge assemblages on sublittoral cliffs at Lough Hyne have been the focus of recent studies, but abundant and diverse sponge populations also occur on the undersides of loose rocks (Lilly *et al.*, 1953; van Soest and Weinberg, 1980; van Soest *et al.*, 1981). At many sites within Lough Hyne, these two habitats can be separated by less than 1 m, providing the opportunity to investigate differences between sponge assemblages occurring in habitats experiencing different levels of stability, without the confounding effects created by larger spatial scales.

The high overall diversity and richness found on hard substrata within Lough Hyne, coupled with the large range of local habitat stability, results in assemblages at various stages of development existing in proximity. Such environmental characteristics provide opportunities to examine the contribution of certain taxa (in this case sponges) to the overall community. This study investigates assemblages inhabiting three substratum types—artificial panels (the most ephemeral), rocks, and cliffs (the most stable)—which represent a qualitative series in terms of habitat stability (*i.e.*, amount of disturbance). The degree of development of sponge assemblages at different levels of habitat stability can be investigated within a particular environmental re-

gime (e.g., fast flow rates). Also, the use of a common substratum (*i.e.*, panel, rock, and cliff) between sites with different environmental conditions (flow regime) gives a second environmental gradient based on flow-rate-generated disturbance (rather than habitat stability). This study attempts to answer four questions: (1) How do sponge assemblages vary with environmental conditions and habitat stability? (2) How does the composition of sponge assemblages vary with water flow rate compared with different rock sizes; both are surrogate measures of disturbance, so do they have similar consequences? (3) Are there discriminating species for (local) habitats of differing stability and flow rates? (4) Are there consistent similarities or differences in assemblage composition in extremes of flow rate and habitat stability?

## Materials and Methods

### Study site

Lough Hyne Marine Nature Reserve (Fig. 1) is a small (0.5 km<sup>2</sup>) temperate sea lough on the southwest coast of Ireland (51°29'N, 9°18'W). It is characterized by a large number of habitats within a small area (Kitehing, 1987). Habitats range from current-swept cliff faces to soft-sediment basins where water currents are slight. The lough is connected to the adjacent Atlantic coast by a shallow and narrow channel (The Rapids). This constriction results in an unusual tidal regime whereby water flows into Lough Hyne for about 4 h and out for 8 h. The squeeze causes fast current velocities (>250 cm s<sup>-1</sup>) in the eastern parts of the lough during inflow, but only slight surface currents in the vicinity of the rapids during outflow (Bassindale *et al.*, 1957). As water moves from east to west across the lough, there is a quick reduction in current flow rate with a corresponding increase in sedimentation.

The small size of Lough Hyne means that communities are only separated on small spatial scales (hundreds of meters). Nevertheless, these communities are discrete because cliff and rock habitats in different parts of the lough are separated by soft sediments. Sponge assemblages are thus isolated and predictable, rather than occurring along a continuous gradient. Different substratum types (*i.e.*, rocks, cliffs, and panels) within a specific environment were separated by less than several meters and therefore not discrete. Panels were sited at Labhra Cliff and Whirlpool Cliff, and rock habitats were sampled at West Cliff and Whirlpool Cliff (Fig. 1). West Cliff and Labhra Cliff have similar sedimentation and rates of water flow, and the sponge assemblages are also similar. Both sites are characterized by slight current flow rates (<5 cm s<sup>-1</sup>) and heavy sediment accumulation, which increases with depth. Hard substratum extends more than 30 m at both of these sites. Rocks were not sufficiently abundant at Labhra Cliff to sample. Whirlpool Cliff experiences a very fast (>200 cm s<sup>-1</sup>), unidirectional flow regime, resulting in high disturbance. This site

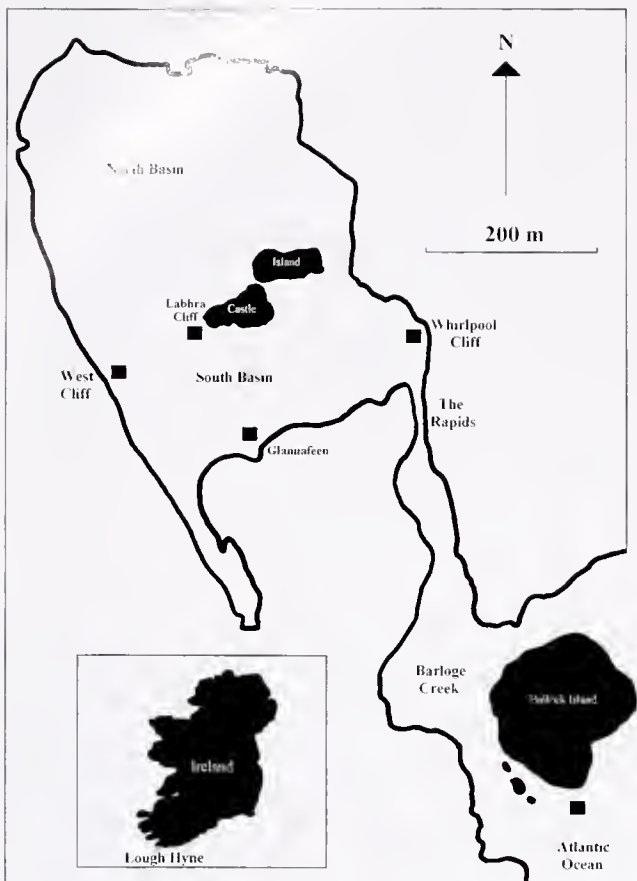


**Figure 1.** Sites where sponge rock and cliff assemblages were sampled in Lough Hyne Marine Nature Reserve.

extends to about 18 m, and current flow rates decrease with depth, falling to  $100 \text{ cm s}^{-1}$  at 18 m (Fig. 2). Some data were taken from the literature (Bell and Barnes, 2000a) to enable greater comparison between sponge assemblages from different habitats within Lough Hyne. These data, which were included in the analysis, concerned sponge assemblages inhabiting vertical and inclined surfaces on sublittoral cliffs at Labhra Cliff, West Cliff, Whirlpool Cliff, and Bullock Island (an adjacent Atlantic coastal site with a turbulent flow regime). The tidal range within Lough Hyne is about 1.5 m.

#### Sampling and observation methods

The artificial substrata (panels) used were square machined slate panels ( $15 \times 15 \text{ cm}$ ), prepared and assembled as for Turner and Todd (1994). They were used to investigate an early pioneer stage in community succession. A blue square ( $10 \text{ cm} \times 10 \text{ cm}$ ) was drawn in the center of each panel with a permanent blue marker pen. Panels were placed in running water for 24 h and then dried; this process was repeated twice more prior to deployment. The blue background makes it easier to identify recruits that are small or

translucent. Three panels (forming one panel array) were attached by cable ties to welded steel bars. The panel array was positioned with the blue surfaces facing down (to simulate the undersides of a boulder). Bolts at the corner of each steel frame allowed the panels to be adjusted so they were 20 mm above the substratum. Panel arrays were deployed at depths of 0 m, 6 m, and 12 m at Labhra Cliff and Whirlpool Cliff. The first panels were deployed at the start of October 1997 and were replaced bimonthly until March 2001. Before panels were replaced, they were cleaned using a razor blade. Each panel was examined under a binocular microscope, and the number of sponge recruits was recorded. Spicule preparations of sponge recruits were made to confirm identification. Additional panel arrays were placed at the same depths, but were not replaced bimonthly. Each panel was photographed 1, 2, 6, and 12 months after the date of deployment. Photographs were then projected onto a grid composed of 400 random dots, and the percentage cover of sponges on each panel was estimated. The mean percent cover was calculated for panels submerged at each time interval.

Twenty-five rocks were randomly selected within three size classes—small ( $10\text{--}150 \text{ cm}^2$ ), medium ( $151\text{--}500 \text{ cm}^2$ ), large ( $501\text{--}1000 \text{ cm}^2$ ), and very large ( $1001\text{--}2000 \text{ cm}^2$ ) such that equal numbers of boulders of each size were examined (*i.e.*, this does not represent the true boulder size distribution). The surface areas of both upper and lower rock surfaces were measured using a transparent cloth marked in square centimeters. The number of sponges (number of patches) for each species on each rock was recorded. Each species was photographed, and samples were taken for spicule analysis to confirm identification. Sponge samples were dissolved in concentrated nitric acid, or bleach as required, and were examined through a compound microscope at high power ( $\times 400$ ). All observations were made between October 1999 and February 2000, which eliminated faunistic inter-site differences caused by seasonal growth or tissue retraction over the study period.

The morphologies of all sponges observed on rocks were classified within the following groups (after Boury-Esnault and Rützler, 1997; Bell and Barnes, 2000d): encrusting (EN), flabellate (FL), clathrate (CL), massive (MA), arborescent (AR), repent (RE), tubular (TU), ficiform (FI), massive globulose (MG), and papillate (PA).

#### Data visualization and statistical procedures

Data were subjected to Bray-Curtis similarity analysis using hierarchical agglomerative group-average clustering for all habitats and depths (including data from Bell and Barnes, 2000a). This analysis was performed using the unweighted pair group method using arithmetic averages (UPGMA) with the PRIMER program (ver. 5.2.8, Plymouth Marine Laboratory, Plymouth, England). Data were  $\log(x + 1)$  transformed to reduce the importance of extreme

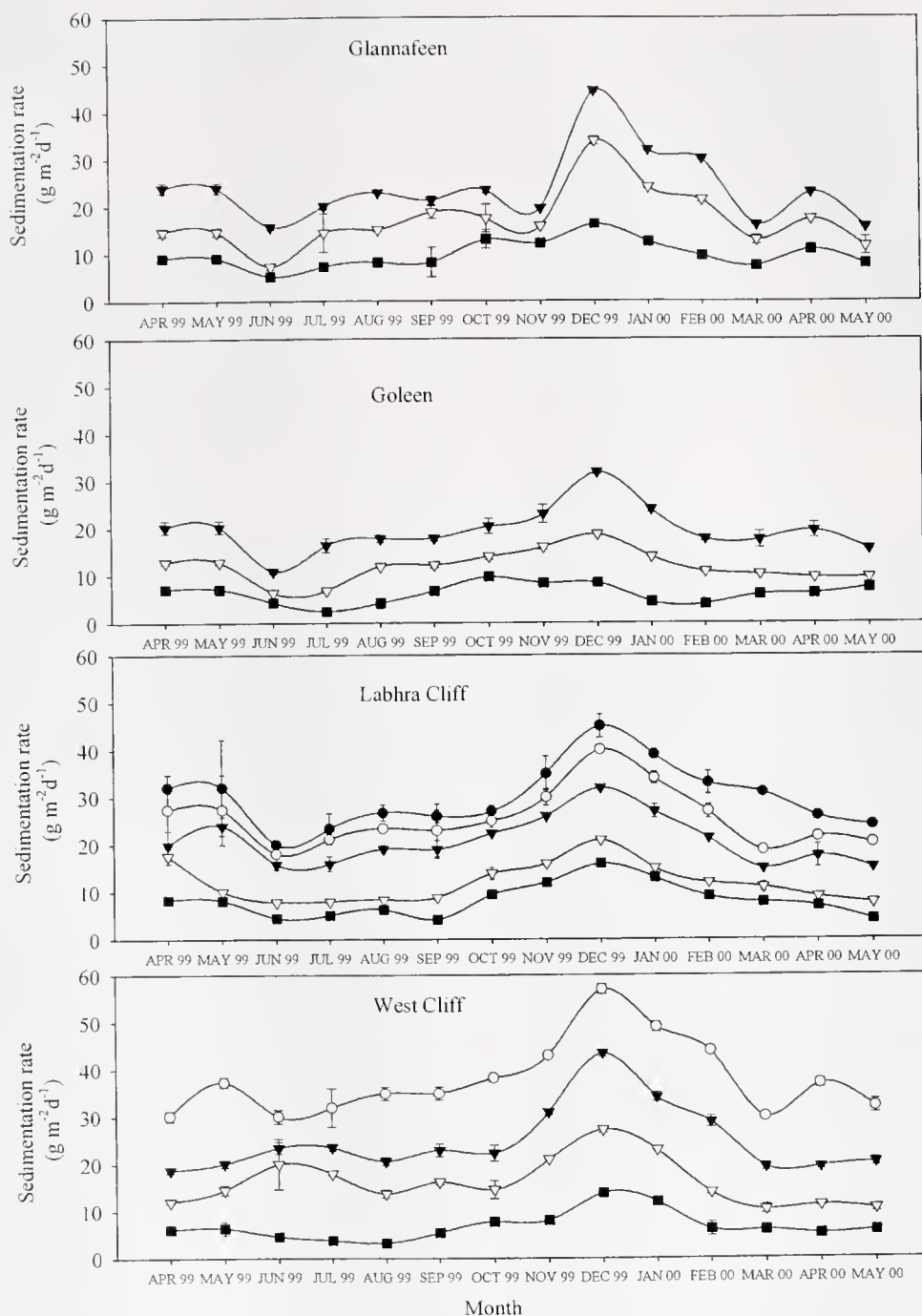


**Figure 2.** Annual variation in sedimentation rates ( $\text{g sediment m}^{-2} \text{d}^{-1}$ ) at 6-m depth intervals at four sublittoral cliff sites within Lough Hyne. 6 m (■) 12 m (□) 18 m (▼) 24 m (○) 30 m (●). Standard error bars are shown. [After Bell (2001).]

values (rare species). Ordination by non-metric Multi-Dimensional Scaling (MDS in PRIMER) was undertaken on a dissimilarity matrix created from Bray-Curtis similarity analysis. SIMPER analysis (in PRIMER) was used to determine the contribution of each species to the average Bray-Curtis dissimilarity between habitats and sites. This method of analysis determines which species are responsi-

ble for any differences that occur. Data were transformed as for Bray-Curtis analysis. Because sampling areas differed between habitat types, the area of each habitat and the abundance of each species were scaled up or down to standardize sampling areas between sites, depths, and habitats ( $\text{sponges m}^{-2}$ ).

Patterns of species diversity for sponge assemblages on

rocks were described with the Shannon and Weiner (Krebs, 1989) information function  $H' = -\sum p_i \ln p_i$ . Paired Student's *t* tests were used to examine differences between rock surface types. A general linear model analysis of variance (GLM ANOVA) was used to compare logarithmically (Log10) transformed sponge species diversity, richness, and rock surface area relationships between West Cliff and Whirlpool Cliff. The same method was used to compare the untransformed relationship between sponge density and rock surface area. This method compares the average linear relationship to an average linear relationship fitted to all the data. Kruskal-Wallis tests were used to compare the differences between percentage cover on submerged panels after 1, 2, 6, and 12 months.

## Results

### *Assemblage composition*

A total of 96 species were reported during this study, 44 of which were found on rocks and 76 from cliff habitats (Table 1). Twenty-five sponge species were shared between rock and cliff habitats. All but two of the species (*Hymeniacidon perlevis* and *Halichondria bowerbanki*) of sponge found on rocks occurred on the undersides. These two species were often found growing on the fronds of algae as well as on rock surfaces. Although sponge assemblages varied considerably between habitat types, there was little variation between rock sponge assemblages inhabiting the different sites (extremes of water flow rate) (Table 2). Of the 44 species inhabiting rocks, only 7 (16%) differed between West Cliff and Whirlpool Cliff, with only 1 of these species (*Mycale rotalis*) being found exclusively at Whirlpool Cliff. The remaining 6 species were only found at West Cliff. Nineteen of the 44 species found on rocks were exclusive to rock habitats, illustrating the high degree of species exclusivity within this habitat type. The panels at Labhra Cliff and Whirlpool Cliff showed no exclusive species, and only 7 species of sponge were reported (Table 1). Therefore, no juvenile settlement was recorded for the majority of sponge species reported during this study despite the nearly 4-year duration of panel deployment. All species found on panels occurred in both rock and cliff habitats. Because panels can be considered a similar habitat to rocks (but younger in terms of community development), community age was the most likely determinant of the composition of the sponge assemblage. Of the total 76 species of sponge reported from cliff habitats, 31 species (data included from Bell and Barnes, 2000a) were found at Bullock Island, compared to 40 species at Whirlpool Cliff and 52 from both Labhra Cliff and West Cliff (Table 3). Although many of these species were shared between cliff habitats, only 10 of the total 76 species were shared between all cliff habitats. Environmental parameters, therefore, proved important in determining the sponge assemblage in cliff habitats. A much higher proportion of species were shared within the same habitat

than between different habitat types (Table 3). However, the proportion of species shared between sites was higher for rock and panel habitats (>85%) than for cliff habitats (<50%).

### *Sponge morphology*

On rocks, encrusting morphologies were the most abundant form (20 of 44 species), followed by massive (15 of 44 species) and repent forms (7 of 44 species) (all pooled rock data). The remaining species exhibited cylindrical (*Scypha ciliatum*) and clathrate forms (*Clathrina coriacea*). On cliff surfaces, 30 species were encrusting, 19 were massive, and 6 exhibited repent forms (pooling cliff data). Sponge species on panels had a wide range of morphologies (given the small number of species), including tubular, repent, encrusting, massive, and clathrate forms. Differences were observed between the proportions of sponge morphologies between certain habitats and sites (Table 4). There was a considerable difference between the proportion of morphologies between cliff sites (Table 3). Encrusting forms were more abundant at the high-energy cliff sites (Bullock Island and Whirlpool Cliff) than at low-energy sites (Labhra Cliff and West Cliff), where they were replaced by arborescent and papillate forms. In rock habitats, high proportions of encrusting and massive forms were found, with no differences between sites. Panel assemblages were also very similar in the proportions of morphologies between sites.

### *Identification of different sponge assemblages*

Small sponges were difficult to identify, (particularly on panels) and potentially represent an error in the analysis. However, this problem was reduced by the transformation of the data prior to analysis, which decreased the importance of extreme values or apparent rare species.

Bray-Curtis similarity analysis and Multi-Dimensional Scaling (MDS) (Fig. 4) were used to distinguish between sponge assemblages within different habitats and sites. The Bray-Curtis analysis identified five major assemblage groups that showed increasing similarity, as follows: rocks (all sites and sizes), panels (all sites), Whirlpool Cliff, Bullock Island, and Labhra Cliff/West Cliff. However, each major assemblage group had a very low similarity (<25%) with the others. MDS distinguished two additional, smaller assemblages, which were not obvious from the Bray-Curtis analysis. The first of these assemblages was at 30 m at Labhra Cliff; it showed the greatest affinity with the other cluster at Labhra Cliff and West Cliff (cliff habitat). The second assemblage was composed of 0-m sponges at Labhra Cliff and West Cliff (cliff habitat). These assemblages were most similar to those at Whirlpool Cliff. The subtidal (6 and 12 m) panels had high levels of correspondence ( $\approx 65\%$ ) between sites, but differed considerably from those in the intertidal zone (0 m) ( $\approx 30\%$  similarity). To account for morphological differences created by the nature of the dif-

Table 1

Sponge species found within Lough Hyne on sublittoral cliff and rocks and on the adjacent Atlantic coast

	B U	W H	L A	W C		B U	W H	L A	W C
<i>Antho involvens</i> (EN)	*			*	<i>Hymeraphia stellifera</i> (EN)	*	*	*	*
<i>Antho inconstans</i> # (EN)					<i>Iophon hyndmani</i> (EN)		*		
<i>Aplysilla rosea</i> (EN)					<i>Iophon ingalli</i> (EN)	*	*		
<i>Aplysilla sulfurea</i> (EN)	*	*	*	*	<i>Iophonopsis nigricans</i> (EN)	*			
<i>Axinella damicornis</i> (FL)			*	*	<i>Laxosuberites incrustans</i> (EN)		*		
<i>Axinella dissimilis</i> (AR)		*	*	*	<b><i>Leucosolenia complicata</i></b> (RE)	*	*		
<i>Biemna variantia</i> (MA)			*	*	<i>Leuconia nivea</i> (EN)	*	*		
<b><i>Clathrina coriacea</i></b> (CL)		*	*	*	<i>Microciona fallax</i> # (EN)				
<i>Ciona celata</i> (MA)	*	*	*	*	<i>Microciona strepsitoxa</i> # (EN)				
<i>Dercitus bucklandi</i> # (MA)					<i>Mycale contarenii</i> (MA)		*	*	*
<i>Dysidea fragilis</i> (MA)	*	*	*	*	<i>Mycale macilentia</i> (MA)				*
<i>Dysidea pallascens</i> (MA)			*	*	<i>Mycale rotalis</i> (MA)		*		*
<b><i>Eспериopsis fucorum</i></b> (RE)	*	*			<i>Myxilla rosacea</i> (MA)	*			*
<i>Eurypon</i> sp. 1 (EN)			*	*	<i>Myxilla incrustans</i> (EN)				
<i>Eurypon</i> sp. 2 (EN)			*	*	<i>Myxilla fimbriata</i> (MA)		*		
<i>Eurypon</i> sp. 3 (EN)			*	*	<i>Pachymatisma johnstonia</i> (MA)	*	*		
<i>Eurypon</i> sp. 4 (EN)			*	*	<i>Parotimea constellata</i> (EN)	*	*	*	*
<i>Eurypon</i> sp. 5 (EN)			*	*	<i>Phakellia</i> sp. (PA)			*	*
<i>Eurypon</i> sp. 6 (EN)			*	*	<i>Phorbas fictitius</i> (EN)	*	*		
<i>Eurypon</i> sp. 7 (EN)			*	*	<i>Plakortis simplex</i> (EN)		*	*	
<i>Eurypon</i> sp. 8 (EN)			*	*	<i>Plocamilla coriacea</i> # (EN)				
<i>Halichondria bowerbanki</i> (RE)		*	*	*	<i>Polymastia</i> sp. 1 (PA)			*	*
<b><i>Halichondria panicea</i></b> (EN)	*	*			<i>Polymastia</i> sp. 2 (PA)			*	*
<i>Haliclona cinerea</i> (MA)		*			<i>Polymastia</i> sp. 3 (PA)			*	*
<i>Haliclona fistulosa</i> (RE)	*	*	*	*	<i>Polymastia</i> sp. 4 (PA)	*		*	*
<i>Haliclona simulans</i> (RE)		*			<i>Polymastia</i> sp. 5 (PA)	*		*	*
<i>Haliclona</i> sp. 1 (MA)	*		*	*	<i>Polymastia</i> sp. 6 (PA)			*	*
<i>Haliclona</i> sp. 2 (MA)	*		*	*	<i>Polymastia</i> sp. 7 (PA)		*	*	*
<i>Haliclona</i> sp. 3 (RE)	*		*	*	<i>Polymastia</i> sp. 8 (PA)		*	*	*
<i>Haliclona</i> sp. 4 (MA)		*	*	*	<i>Pseudosuberites sulphureus</i> (EN)	*	*		
<i>Haliclona</i> sp. 5 (MA)	*	*			<i>Rhaphidostyla kitchingi</i> (AR)	*	*		
<i>Haliclona</i> sp. 6 # (MA)					<i>Raspailia hispida</i> (AR)		*	*	*
<i>Haliclona</i> sp. 7 # (RE)					<i>Raspailia ramosa</i> (AR)		*	*	*
<i>Haliclona</i> sp. 8 # (RE)					<b><i>Scypha cilatum</i></b> (TU)	*	*	*	*
<i>Haliclona</i> sp. 9 # (RE)					<i>Spanioplion armaturum</i> # (EN)				
<i>Haliclona</i> sp. 10 # (MA)					<i>Stelligera rigida</i> (FL)		*	*	*
<i>Haliclona</i> sp. 11 # (MA)					<i>Stelligera stuposa</i> (AR)*	*	*	*	
<i>Haliclona</i> sp. 12 # (RE)					<i>Stylostichon dives</i> (EN)		*		
<i>Haliclona urceolus</i> (TU)			*	*	<i>Stylostichon plumosum</i> # (MA)				
<i>Haliclona viscosa</i> (MA)			*	*	<i>Suberites carnosus</i> (FI)			*	*
<i>Halicnemia patera</i> (EN)			*	*	<i>Suberites ficus</i> (FI)			*	*
<i>Halisarca</i> sp. (MA)			*		<i>Suberites</i> sp. 1 (EN)			*	*
<i>Hemimycale columella</i> (EN)	*	*			<i>Suberites</i> sp. 2 (EN)	*	*	*	
<i>Hymedesmia brondstedii</i> # (EN)					<i>Suberites</i> sp. 3 (EN)	*	*		
<i>Hymedesmia jecusculum</i> # (EN)					<i>Suberites</i> sp. 4 (EN)	*			
<i>Hymedesmia pansa</i> # (EN)					<i>Terpias fugax</i> # (EN)				
<i>Hymedesmia paupertus</i> (EN)			*	*	<i>Tethya aurantium</i> (MG)	*	*	*	*
<i>Hymeniacidon perlevis</i> (MA)	*	*	*	*	<b>Unidentified sponges</b>				

An asterisk indicates species found at a particular site (BU, Bullock Island; WH, Whirlpool Cliff; LA, Labhra Cliff; WC, West Cliff). Underlining denotes species found on rocks, and the symbol # indicates that the species was exclusive to rocks; boldface type denotes species found on panels (none were exclusive). Uppercase letters in parentheses after the species name are macro-morphological descriptions: AR, arborescent; CL, clathrate; EN, encrusting; FI, ficiform; FL, flabellate; MA, massive; MG, massive globulose; PA, papillate; RE, repent; TU, tubular.

ferent habitats, the same MDS and Bray-Curtis analysis was repeated using only species that exhibited encrusting or massive morphologies. However, no differences were ob-

served between the original dendrogram and the 2-D scaling plot produced (output not shown).

SIMPER analysis was used to determine which species

Table 2

*Sponge species that were reported from the under (\*) and upper (+) sides of rocks found at two sites at Lough Hyne*

Species (Morphology)#	West Cliff†				Whirlpool Cliff†			
	S	M	L	VL	S	M	L	VL
<i>Antho inconstans</i> (EN)			*	*	*	*	*	*
<i>Antho involvens</i> (EN)			*	*			*	*
<i>Aplysilla sulfurea</i> (EN)	*	*	*	*	*	*	*	*
<i>Aplysilla rosea</i> (EN)	*	*	*	*	*	*	*	*
<i>Clathrina coriacea</i> (CL)	*	*	*	*	*	*	*	*
<i>Cliona celata</i> (MA)			*	*			*	*
<i>Dercitus bucklandi</i> (MA)		*	*	*		*	*	*
<i>Dysidea fragilis</i> (MA)	*	*	*	*	*	*	*	*
<i>Dysidea pallescens</i> (MA)			*	*			*	*
<i>Esperiopsis fucorum</i> (RE)		*	*	*		*	*	*
<i>Haliclona</i> sp. 1 (MA)	*	*	*	*			*	*
<i>Haliclona</i> sp. 2 (RE)	*	*	*	*	*	*	*	*
<i>Haliclona</i> sp. 3 (RE)		*	*	*	*	*	*	*
<i>Haliclona</i> sp. 4 (RE)	*	*	*	*	*	*	*	*
<i>Haliclona</i> sp. 5 (MA)	*	*	*	*	*	*	*	*
<i>Haliclona</i> sp. 6 (MA)	*	*	*	*	*	*	*	*
<i>Haliclona</i> sp. 7 (MA)		*	*	*		*	*	*
<i>Haliclona</i> sp. 8 (MA)	*	*	*	*		*	*	*
<i>Halichondria bowerbanki</i> (RE)+			*+	*+			*+	*+
<i>Hymedesmia brondstedti</i> (EN)	*	*	*	*	*	*	*	*
<i>Hymedesmia jecusculum?</i> (EN)				*			*	*
<i>Hymedesmia pansa</i> (EN)				*		*	*	*
<i>Hymedesmia paupertas</i> (EN)		*	*	*		*	*	*
<i>Hymeniacion perlevis</i> (MA)+	*+	*+	*+	*+	*+	*+	*+	*+
<i>Iophon ingalli</i> (EN)				*				*
<i>Leuconia nivea</i> (EN)		*	*	*				*
<i>Leucosolenia complicata</i> (RE)	*	*	*	*	*	*	*	*
<i>Microciona fallax</i> (EN)		*	*	*				*
<i>Microciona strepsitoxa</i> (EN)				*			*	*
<i>Mycale contarenii</i> (MA)			*	*				*
<i>Mycale macilema</i> (MA)			*	*				*
<i>Mycale rotalis</i> (MA)							*	*
<i>Myxilla rosacea</i> (MA)	*	*	*	*		*	*	*
<i>Myxilla incrustans</i> (EN)				*				*
<i>Pachymatisma johnstonia</i> (MA)		*	*	*	*	*	*	*
<i>Phorbas fictitius</i> (EN)			*	*				*
<i>Plakortis simplex</i> (EN)	*	*	*	*	*	*	*	*
<i>Plocamilla coriacea?</i> (EN)				*				*
<i>Scypha ciliatum</i> (TU)		*	*	*			*	*
<i>Spanioplion armaturum</i> (EN)			*	*		*	*	*
<i>Stylostichon dives</i> (EN)	*	*	*	*	*	*	*	*
<i>Stylostichon plumosum</i> (MA)	*	*	*	*	*	*	*	*
<i>Suberites</i> sp. (EN)	*	*	*	*		*	*	*
<i>Terpios fugax</i> (EN)			*	*		*	*	*
Total number of species	18	27	37	43	17	25	30	30

# The morphological group of each species is given in parentheses: CL, clathrate; EN, encrusting; MA, massive; RE, repent; TU, tubular.

† Four sizes of rock were distinguished: S, small; M, medium; L, large; VL, very large.

were most responsible for the differences seen between sites and habitats with the Bray-Curtis analysis. Only the top five of these indicator, or "discriminating" species (those with the least similarity between different habitats) are illustrated (Table 5). The discriminating species between rock habitats (irrespective of site) and all other habitats were very similar. *Plakortis simplex*, *Clathrina coriacea*, *Aplysilla rosacea*,

*H. brondstedti*, and *L. complicata* can all be considered indicative of rock habitats. When the rock assemblages from West Cliff and Whirlpool Cliff were compared, the discriminating species were, however, not those found at only one of the sites. The most important discriminating species from the cliffs at Bullock Island was *Hemimycale columella*. In most cases, Whirlpool Cliff could be characterized by the

Table 3

The number of sponge species shared between sites

Site	WC (B) (43) ↓	WH (B) (38) ↓	BI (C) (31) ↓	WH (C) (40) ↓	LC (C) (52) ↓	WC (C) (52) ↓	WH (P) (7) ↓
WH (B) (38)	37 (84%)						
BI (C) (31)	14 (23%)	13 (23%)					
WH (C) (40)	16 (23%)	17 (28%)	22 (45%)				
LC (C) (52)	13 (16%)	13 (17%)	15 (22%)	22 (31%)			
WC (C) (52)	15 (19%)	16 (22%)	16 (24%)	20 (28%)	48 (86%)		
WH (P) (7)	6 (14%)	6 (15%)	5 (15%)	6 (15%)	3 (5%)	3 (5%)	
WC (P) (7)	6 (14%)	6 (15%)	5 (15%)	6 (15%)	3 (5%)	3 (5%)	7 (100%)

Numbers in parentheses indicate total number of species at each site and habitat. C, cliff; B, rock; P, panel; WC, West Cliff; WH, Whirlpool Cliff; BI, Bullock Island; LC, Labhra Cliff. % indicates the proportion of all species shared for each pair of habitats: % = number of shared species ÷ (number of species at habitat A × number of species at habitat B) – number of shared species.

presence of *Esperiopsis fucorum* and *Scypha ciliatum*. For panel habitats, it was not possible to identify true discriminating species because only seven species were reported from panels. Therefore, the technique of using individual species as discriminating, or indicator, species was not applicable in these very young (panel) sponge assemblages.

#### Development of assemblages on panels

The contribution of sponges to early community development (panels) varied considerably between Whirlpool Cliff and Labhra Cliff (Fig. 5). The percentage cover of sponges on subtidal panels at Whirlpool Cliff and Labhra

Cliff increased significantly (from about 0% to between 4% and 10% cover) over the 12-month period (Kruskal-Wallis,  $H < 11.12$ ,  $P < 0.01$ ,  $df = 4$ ). In contrast, sponges did not constitute any part of the community on intertidal panels at either site (irrespective of time interval). At Labhra Cliff, the panels did not have a significantly higher percentage cover of sponges than at Whirlpool Cliff after 1, 2, or 6 months (at either 6 or 12 m). However, a significantly higher percentage cover (twice as high) of sponges was found on panels at Labhra Cliff than at Whirlpool Cliff after 12-month deployments at both 6 and 12 m (Mann-Whitney,  $W = 144$ ,  $P < 0.01$ ,  $df = 5$ ).

Table 4

The number of sponge species showing different morphological types at different sites and habitats at Lough Hyne and the percentage of each morphology as a proportion of the total number of species

Site*	Morphological Group†									
	EN	MA	RE	PA	FL	CL	AR	TU	FI	MG
Bullock Island (C)	14 45%	8 26%	4 13%	2 6%	0 0%	0 0%	1 3%	1 3%	0 0%	1 3%
Whirlpool Cliff (C)	16 40%	10 25%	5 13%	2 5%	0 0%	1 3%	4 10%	1 3%	0 0%	1 3%
Labhra Cliff (C)	17 33%	12 23%	2 4%	9 17%	2 4%	1 2%	5 10%	2 4%	1 2%	1 2%
West Cliff (C)	16 31%	13 25%	2 4%	9 17%	2 4%	1 2%	5 10%	2 4%	1 2%	1 2%
Whirlpool Cliff (B)	16 42%	14 37%	6 16%	0 0%	0 0%	1 3%	0 0%	1 3%	0 0%	0 0%
West Cliff (B)	20 47%	15 35%	6 14%	0 0%	0 0%	1 2%	0 0%	1 2%	0 0%	0 0%
Whirlpool Cliff (P)	1 17%	1 17%	1 17%	0 0%	0 0%	1 17%	0 0%	1 17%	0 0%	0 0%
Labhra Cliff (P)	1 17%	1 17%	2 33%	0 0%	0 0%	1 17%	0 0%	1 17%	0 0%	0 0%

\* C, cliff; B, rocks; P, panels.

† EN, encrusting; MA, massive; RE, repent; PA, papillate; FL, flabellate; CL, clathrate; AR, arborescent; TU, tubular; FI ficiform; MG, massive globulose.

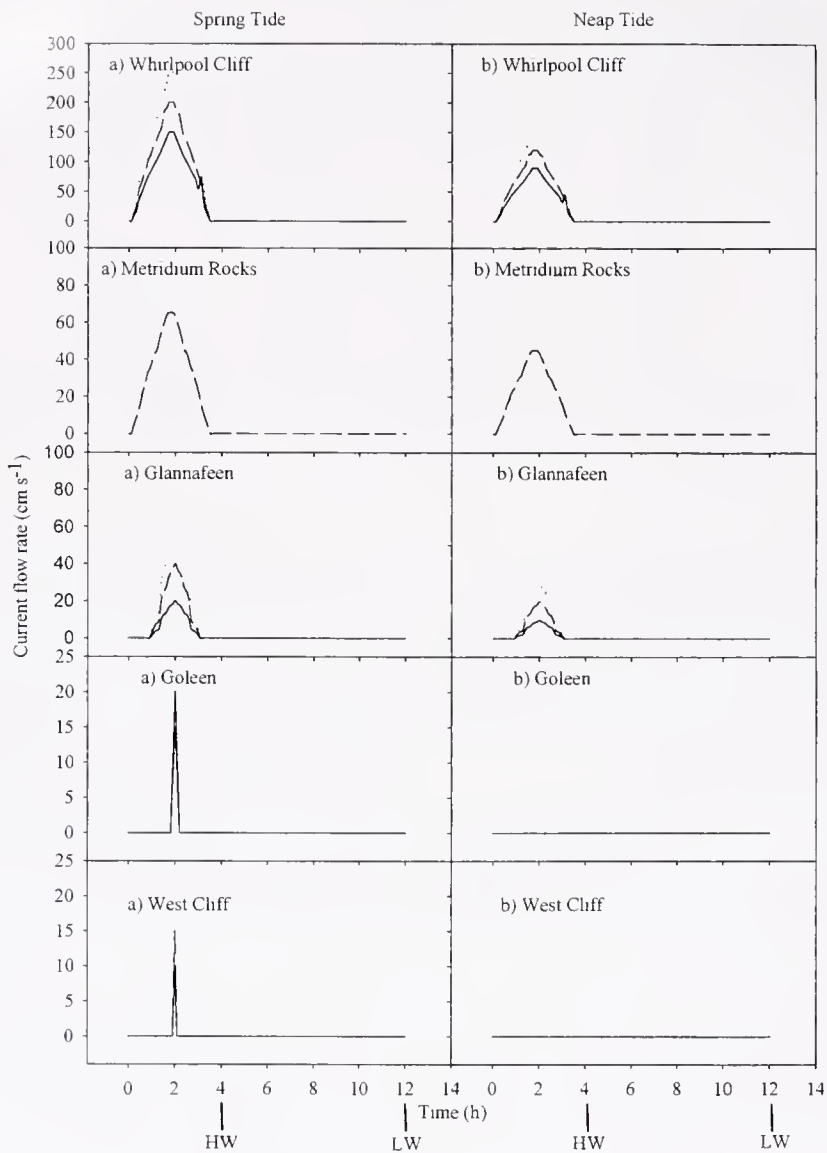


**Figure 3.** Spring (a) and neap (b) tide flow rates over one tidal period at four sites within Lough Hyne. Note that graphs have different y axes. [After Bell (2001).]

### Assemblages on rocks

Bray-Curtis analysis and MDS showed that sponge assemblages on rock had a very high level of similarity (65%) between sites and different rock sizes (Fig. 4). But, when the cluster composed of assemblages from various sized rocks was considered alone, assemblages inhabiting medium, large, and very large rocks had a greater similarity between different sites than the assemblages on small rocks had with other rock sizes within the same site. At both sites, assemblages on medium, large, and very large boulders gave rise to clusters that then formed a larger cluster with the small rock assemblages. Rock size had important influences on sponge assemblages (Table 2). A higher number of species was reported from larger rather than smaller rocks at both

sites (as expected given the area effect). Yet few differences were observed between the sponge assemblages on the small and medium-sized rocks at West Cliff and Labhra Cliff.

There was a logarithmic relationship between substratum area and sponge species diversity on rocks from both West Cliff and Whirlpool Cliff. Data were Log10 transformed, resulting in linear relationships (Fig. 6). The relationship between the number of sponges (per rock) and the area of rock surface at both sites was linear (Fig. 7). General linear model (GLM) ANOVA was used to compare the linear relationships between substratum area, number of sponges, and diversity. In the relationships between species diversity and area, no significant difference was observed in slope or

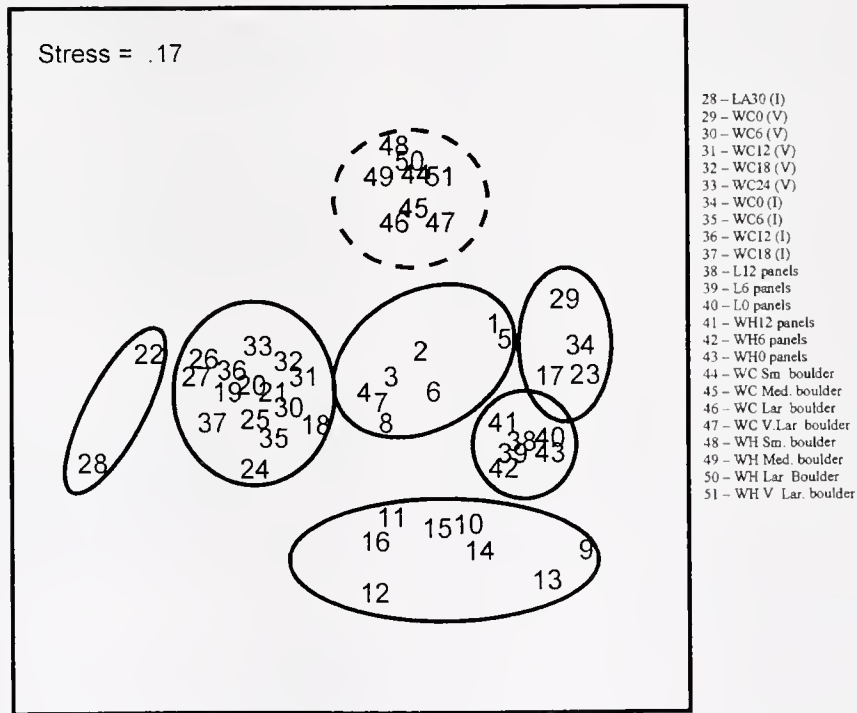
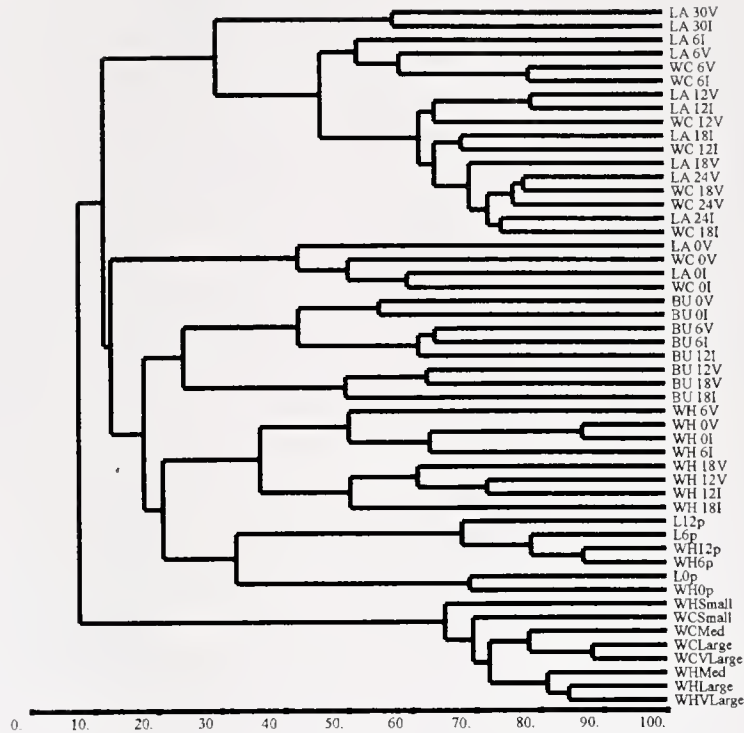


**Figure 4.** Bray-Curtis similarity and Multi-Dimensional Scaling (MDS) analysis to compare the sponge assemblages inhabiting panels, rocks, and cliff at a number of sites, depths, and surface inclinations from Lough Hyne. The dashed circle indicates the grouping that MDS produced for loose rock assemblages.

intercept between West Cliff and Whirlpool Cliff (GLM ANOVA;  $F$  ratio = 0.07,  $P$  = 0.78, denominator  $df$  = 1, numerator  $df$  = 278). This was also true for the transformed

relationships between species richness and rock surface area at West Cliff and Whirlpool Cliff (graph not shown) (GLM ANOVA;  $F$ -ratio = 1.1,  $P$  = 0.25, denominator  $df$  = 1,

**Table 5**  
*Simplex analysis (Primer) to determine the five most dissimilar species in terms of percentage abundance for each pair of habitats/sites*

Site	West Cliff (cliff) ↓	Whirlpool Cliff (rocks) ↓	West Cliff (rocks) ↓	Whirlpool Cliff (cliff) ↓	Bullock Island (cliff) ↓	Labhra Cliff (panels) ↓	Labhra Cliff (cliff) ↓
Whirlpool Cliff (rocks)	<i>Plakortis simplex</i> * <i>Clathrina coriacea</i> * <i>Aplysilla rosacea</i> * <i>H. brondstedti</i> * <i>L. complicata</i> *	<i>Haliclona</i> sp. 6 <i>Hymedesmia pansa</i> <i>Hymeniacidon perlevis</i> * <i>Scypha ciliatum</i> * <i>Leuconia nivea</i> *	<i>Plakortis simplex</i> <i>Clathrina coriacea</i> <i>Aplysilla rosacea</i> <i>H. brondstedti</i> <i>L. complicata</i>	<i>Plakortis simplex</i> <i>Aplysilla rosacea</i> <i>Haliclona</i> sp. 7 <i>H. brondstedti</i> <i>Clathrina coriacea</i>			
West Cliff (rocks)	<i>Esperopsis fucorum</i> * <i>Scypha ciliatum</i> * <i>Suberites carnosus</i> <i>Eurypon orange</i> <i>Stelligera rigida</i>	<i>Plakortis simplex</i> <i>Clathrina coriacea</i> <i>Aplysilla rosacea</i> <i>H. brondstedti</i> <i>L. complicata</i>	<i>Plakortis simplex</i> <i>Aplysilla rosacea</i> <i>Clathrina coriacea</i> <i>Haliclona</i> sp. 7				
Whirlpool Cliff (cliff)	<i>Haliclondria panacea</i> * <i>Suberites carnosus</i> <i>Stelligera rigida</i> <i>Raspailia ramosa</i> <i>Hemimysale columella</i> *	<i>Plakortis simplex</i> <i>Clathrina coriacea</i> <i>H. brondstedti</i> <i>L. complicata</i> <i>S. plumosum</i>	<i>Plakortis simplex</i> <i>Aplysilla rosacea</i> <i>Clathrina coriacea</i> <i>Haliclona</i> sp. 7 <i>H. brondstedti</i>	<i>Haliclondria panacea</i> * <i>Suberites carnosus</i> <i>Stelligera rigida</i> <i>Raspailia ramosa</i> <i>Hemimysale columella</i> *			
Bullock Island (cliff)	<i>Scypha ciliatum</i> * <i>Stelligera rigida</i> <i>Suberites carnosus</i> <i>Raspailia ramosa</i> <i>Eurypon orange</i>	<i>Plakortis simplex</i> <i>Clathrina coriacea</i> <i>Aplysilla rosacea</i> <i>H. brondstedti</i> <i>L. complicata</i>	<i>Plakortis simplex</i> <i>A. rosacea</i> <i>Haliclona</i> sp. 7 <i>H. brondstedti</i> <i>Clathrina coriacea</i>	<i>Esperopsis fucorum</i> <i>Scypha ciliatum</i> <i>Tethya aurantium</i> <i>Dysidea fragilis</i> <i>Haliclona</i> sp. 4	<i>Scypha ciliatum</i> * <i>Haliclondria panacea</i> * <i>Dysidea fragilis</i> * <i>Hemimysale columella</i> <i>Cliona celata</i>		
Labhra Cliff (panels)	<i>Suberites carnosus</i> * <i>Haliclona</i> sp. 4* <i>Eurypon orange</i> <i>Raspailia ramosa</i> * <i>Paratinea constellata</i> *	<i>Plakortis simplex</i> <i>Clathrina coriacea</i> <i>Aplysilla rosacea</i> <i>H. brondstedti</i> <i>L. complicata</i>	<i>Plakortis simplex</i> <i>A. rosacea</i> <i>Clathrina coriacea</i> <i>Haliclona</i> sp. 7 <i>H. brondstedti</i>	<i>Esperopsis fucorum</i> <i>Scypha ciliatum</i> <i>Haliclona</i> sp. 4 <i>Eurypon major</i> * <i>Stelligera rigida</i> *	<i>Scypha ciliatum</i> <i>Stelligera rigida</i> * <i>Hemimysale columella</i> <i>Haliclona</i> sp. 4* <i>Cliona celata</i> *	<i>Scypha ciliatum</i> <i>Dysidea fragilis</i> * <i>Stelligera rigida</i> * <i>Haliclona</i> sp. 4* <i>Eurypon major</i> *	
Labhra Cliff (cliff)	<i>Suberites carnosus</i> * <i>Haliclona</i> sp. 4* <i>Eurypon orange</i> <i>Raspailia ramosa</i> * <i>Paratinea constellata</i> *	<i>Plakortis simplex</i> <i>Clathrina coriacea</i> <i>Aplysilla rosacea</i> <i>H. brondstedti</i> <i>L. complicata</i>	<i>Plakortis simplex</i> <i>A. rosacea</i> <i>Clathrina coriacea</i> <i>Haliclona</i> sp. 7 <i>H. brondstedti</i>	<i>Esperopsis fucorum</i> <i>Scypha ciliatum</i> <i>Haliclona</i> sp. 4 <i>Eurypon major</i> * <i>Stelligera rigida</i> *	<i>Haliclondria panacea</i> * <i>Stelligera rigida</i> * <i>Hemimysale columella</i> <i>Haliclona</i> sp. 4* <i>Cliona celata</i> *	<i>Scypha ciliatum</i> <i>Dysidea fragilis</i> * <i>Stelligera rigida</i> * <i>Haliclona</i> sp. 4* <i>Eurypon major</i> *	
Whirlpool Cliff (panels)	<i>Haliclondria panacea</i> * <i>Scypha ciliatum</i> * <i>Esperopsis fucorum</i> * <i>Stelligera rigida</i> <i>Suberites carnosus</i>	<i>Plakortis simplex</i> <i>Clathrina coriacea</i> <i>Aplysilla rosacea</i> <i>H. brondstedti</i> <i>L. complicata</i>	<i>Plakortis simplex</i> <i>A. rosacea</i> <i>Clathrina coriacea</i> <i>Haliclona</i> sp. 7 <i>H. brondstedti</i>	<i>Haliclondria panacea</i> * <i>Scypha ciliatum</i> <i>Esperopsis fucorum</i> <i>Tethya aurantium</i> <i>Dysidea fragilis</i>	<i>Haliclondria panacea</i> * <i>Scypha ciliatum</i> <i>Dysidea fragilis</i> <i>Hemimysale columella</i> <i>Esperopsis fucorum</i>	<i>Scypha ciliatum</i> <i>Haliclondria panacea</i> <i>Esperopsis fucorum</i> <i>Dysidea fragilis</i> <i>L. complicata</i>	<i>Haliclondria panacea</i> * <i>Scypha ciliatum</i> * <i>Dysidea fragilis</i> <i>Stelligera rigida</i> <i>Haliclona</i> sp. 4

An asterisk indicates that the species is characteristic of the site or habitat to its left; an unasterisked species is characteristic of the site or habitat at the top of the column.

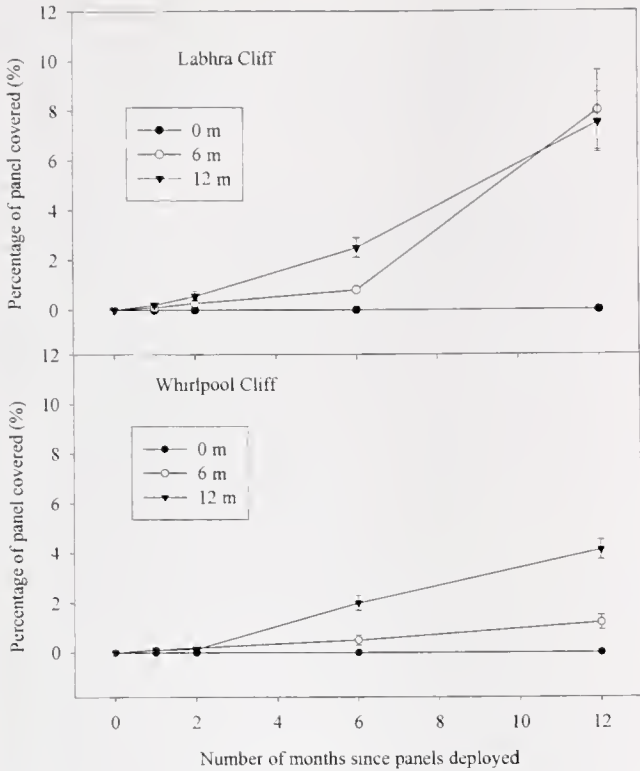


Figure 5. The proportion of artificial settlement panels covered in sponges after 1, 2, 6, and 12 months of deployment at high-energy (Whirlpool Cliff) and low-energy (West Cliff) sites at Lough Hyne.

numerator  $df = 278$ ). However, when GLM ANOVA was used to compare the linear relationship between sponge numbers and rock surface area, a significant difference was found between the slopes of the relationships at West Cliff

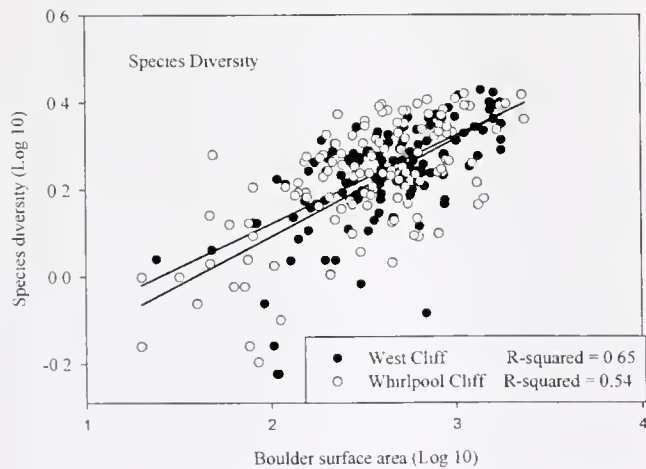


Figure 6. The relationships between sponge species diversity and richness vs. rock surface area at high-energy (Whirlpool Cliff) and low-energy (West Cliff) sites on the undersides of rocks at Lough Hyne. Species diversity (antilog 10) =  $2.09 (\pm 0.15) + 2.09 (\pm 0.04) \times$  surface area.

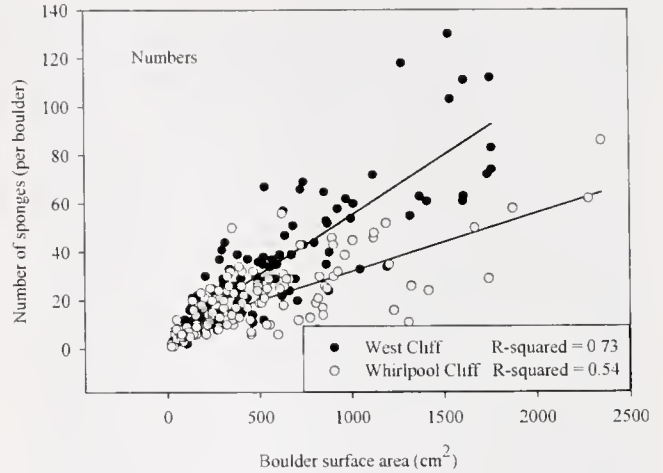


Figure 7. The linear relationship between sponge densities and rock surface area at high-energy (Whirlpool Cliff) and low-energy (West Cliff) sites on the undersides of rocks at Lough Hyne. Number of sponges (West Cliff) =  $60.3 (\pm 35.84) + 14.8 (\pm 0.85) \times$  surface area. Number of sponges (Whirlpool Cliff) =  $47.3 (\pm 46.54) + 22.6 (\pm 1.87) \times$  surface area.

and Whirlpool Cliff (GLM ANOVA;  $F$  ratio = 16.16,  $P < 0.001$ , denominator  $df = 1$ , numerator  $df = 278$ ). Any unit increase in surface area resulted in a greater increase in sponge density at West Cliff than at Whirlpool Cliff. Also, any given rock size harbored a greater number of sponges at West Cliff than at Whirlpool Cliff.

### Discussion

Animal communities are known to vary between large geographic areas (scale of kilometers), but the variability between localized habitats (1 to 100 m) under similar environmental conditions is far less well known. This is true for sponge assemblages: broad distributions have been described by habitat at Lough Hyne (Picton, 1991; van Soest and Weinberg, 1980; van Soest *et al.*, 1981), and recently more detailed studies have added environmental variables to such distributions (Bell and Barnes, 2000b, c). As with most, if not all organisms, environmental factors are critical to the distribution of sponge species. To date, little quantitative information has been provided on localized (where confounding factors are minimized) habitat-associated differences between sponge assemblages in temperate localities.

#### *Morphological variability with habitat stability and environmental characteristics*

The studied sponge assemblages (within Lough Hyne) varied considerably between habitats of differing stability (*i.e.*, cliff and boulders) and environmental conditions (*i.e.*, high and low flow), even when habitats were separated by only several meters or less. Sponges inhabiting hard sub-

stratum have been shown to exhibit considerable morphological adaptation in response to a variety of factors, including flow regime, sedimentation, and substratum type, at both assemblage (Bell and Barnes, 2000d) and individual levels (Manconi and Pronzato, 1991; Bell *et al.*, 2002). It seems, therefore, that morphology alone may account for some of these differences in assemblage composition between sites and habitats. The two-dimensional nature of rock (under-surface) habitats undoubtedly accounts for the high proportion of encrusting forms because the overt three-dimensional nature of many other sponge species common to cliff habitats is inhibited (*e.g.*, arborescent forms). High-energy cliff sites were dominated by encrusting and massive forms and showed greater levels of similarity (in assemblage composition) to rock habitat assemblages than to those of low-energy cliffs. However, high proportions of encrusting and massive morphologies were found in both cliff and rock habitats, although the species compositions were very different. Morphology alone cannot account for all the differences found. Organisms living on the undersides of rocks have a number of advantages, including reduced competition from fast-growing algae found on upper rock surfaces, since many sponges are considered slow-growing (Ayling, 1983), and protection against potentially harmful UV radiation. Underside rock communities also experience reduced sediment settlement in areas of low current flow, reduced effects of desiccation (in the intertidal), and reduced predation from fish and other large invertebrates (Dunlap and Pawlik, 1996; Wulff, 2000). A combination of these factors may account for the presence or absence of any single species on the undersides of loose rocks. Therefore, the distribution and habitat of each species should be considered individually.

Morphology alone has already proved valuable in separating sponge assemblages inhabiting sublittoral cliffs (Bell and Barnes, 2000a). Increased numbers of delicate morphologies, exhibited by a number of species exclusive to low-energy sites, have been associated with decreasing flow rate and as a mechanism to reduce sediment settlement (Bell, 2001). However, the rate of water flow had little effect on the sponge assemblages found on rocks and apparently was not a regulatory factor of such assemblages (in the present study). One aspect of morphology that was not considered within this study is the potential importance of the surface texture of encrusting sponges in response to habitat disturbance or stability. For example, sponges with smooth surfaces may be suited to areas of high current flow since they experience reduced drag. Also, the actual flow (in terms of speed and direction) experienced by sponges may be significantly influenced by seabed characteristics (Hiscock, 1983), such that their morphology and species distribution may be influenced by microscale environmental characteristics, which are themselves difficult to characterize. For example, the overlying nature of loose rocks may lead to

localized areas of negligible current flow, even in high-current areas.

#### *Assemblage composition variability with flow rate and rock size*

Negligible (between-site) differences in sponge diversity or species richness attributable to flow rate were found on the under-surfaces of rocks. This suggests that in rock habitats unlike cliff habitats (Bell and Barnes, 2000a), water flow rate is not directly important in determining the composition of sponge assemblages. Sponge diversity and richness did, as with most organisms, increase with area (rock size), which is usually termed an area effect. The density of sponges for any given rock size was greater at West Cliff than at Whirlpool Cliff, most likely due to reduced competition in low-energy environments from superior spatial competitors such as colonial ascidians and anthozoans (Maughan and Barnes, 2000b; Bell, 2001a; Bell and Barnes, 2003). Increased sedimentation, to which sponges may show morphological and physiological adaptation, has been credited for the shift in competitive ability (Bell, 2001a). However, since the organisms inhabiting the undersides of rocks experience little direct sedimentation, other factors must be responsible for the lack of superior competitors, such as increased sediment loading (rather than direct settlement) in the water, a condition that sponges appear to tolerate (Lilly *et al.*, 1953). Also important is the difference between upper and lower rock surfaces. The domination of sponges on lower surfaces relates to the absence of macroalgae, which has been considered to control both large- and small-scale sponge distributions (Witman and Sebens, 1990). Sponge proliferation on upper surfaces may also be prevented by interference competition from the sweeping action of algal fronds, as suggested for other invertebrates (Jenkins *et al.*, 1999). The linear increase in the number of sponges with increasing surface area of rock may appear unusual. One might expect that the dominant sponge species would occupy most of the primary substratum (Russ, 1982; Maughan and Barnes, 2000b). However, competitive encounters and interactions between sponges may be non-hierarchical and resemble a network (Buss and Jackson, 1979; Bell and Barnes, 2003), thereby preventing monospecies dominance. Even if certain sponge species inhabiting rocks are dominant over others, these species may show seasonal growth and retraction of tissue that prevents them from monopolizing rock surfaces (Sarà, 1970; Stone, 1970; Elvin, 1976; Barthel, 1989). The distribution of sponges may also be limited by other biological factors, in particular predation (*e.g.*, Wulff, 1995); but in the observations of sponge assemblages at Lough Hyne, predation of sponges was rarely observed. Fish feeding on algae sometimes broke branches from arborescent species on cliffs, but extensive predation was not seen. Sponge population heterogeneity is also affected by competitive processes (Becerro *et al.*,

1994), because interactions between spatial competitors influence the direction of growth (in encrusting species) and lead to the patchiness observed within habitats.

Disturbance has been considered an important factor structuring marine epifaunal communities, and rock size has been considered a surrogate of such disturbance (Dayton, 1971; Osman, 1977). This theory is based upon the principle that smaller rocks are more likely to be moved than larger rocks. However, all but the smallest rocks at Lough Hyne showed very similar sponge assemblages across sites experiencing differential flow rates. Sponge assemblages do vary between some surrogate measures of disturbance (flow rate), but not between actual extremes of habitat stability. This suggests that treatment of rock surface area as a surrogate measure of disturbance is unsatisfactory and shows no correlation between extremes of surrogate (*i.e.*, small and large rocks) and true (*i.e.*, high- and low-energy sites) measures of disturbance. At Lough Hyne, small rocks are often held in place by overlying larger rocks, as a result, the probability of motion can be lower (rather than higher) for small rocks than for larger rocks, because the movement of smaller rocks is dependent on the movement of larger rocks *a priori*. Thus, lack of space rather than level of community development (and age) can explain why impoverished sponge assemblages are seen more frequently on small rocks. For organisms (including sponges) that inhabit disturbed habitats (such as loose rocks), succession will be important in structuring the community. Occasional disturbance will prevent the development of a climax community and permit colonization by weaker competitors that might have been excluded from a habitat that had reached a state of climax.

Sponge assemblages on panels had little similarity with other habitats examined and, in contrast to findings with other taxa (Maughan and Barnes, 2000a; Barnes and Maughan, 2001), showed negligible inter-site differences. However, the space occupation (percentage cover) of sponges during the development of the (pioneer succession) panel assemblage varied significantly over the 12-month deployment period (continuous immersion for 12 months). The greater area occupied by sponges on the undersides of panels at Labhra Cliff than Whirlpool Cliff is consistent with the results of other studies of sponge assemblage differences between cliff environments at these two sites (Bell and Barnes, 2000a, d). Sponges are more abundant on panels, rocks, and cliffs at low-energy sites in Lough Hyne than at high-energy sites. Again, this is most likely due to reduced competition in low-energy environments from superior spatial competitors, such as colonial ascidians and anthozoans (Maughan and Barnes, 2000b; Bell, 2001; Bell and Barnes, 2003). All species found on panels submerged for 2-month periods were also found on rocks and cliffs. These early colonizers were important to both mature and immature communities, even though sponges are widely regarded as late colonizers (Dayton, 1971; Maughan, 2000).

Since all species found on panels, which simulated early development of rock communities, were also found in cliff and rock habitats, we suggest that habitat is not as critical in determining species composition at this early stage in development as it is in more mature communities. However, sponge assemblages (rather than species) found on panels did show greater affinities with rock assemblages than with cliffs, which is to be expected given that the panels were used as a surrogate for young rock habitats. Even though a number of sponges were reported from the panels, it is also true that most of the species found in this study did not settle on the panels and thus can still be considered late colonizers of benthic communities. For a complete evaluation of the contribution of sponges to communities of different ages (since panels represent a pioneer succession stage, while cliff communities may be many years old), monitoring must extend over many more time intervals than in the present study. Small rock assemblages had a much greater affinity with the species found to inhabit panels, with two species (*Leucosolenia complicata* and *Scypha ciliatum*) being of particular interest. The presence of these two calcareous species is consistent with other studies of panels (Maughan and Barnes, 2000b) and of the early development of hard-substratum communities (Osman, 1977). These were two of only three calcareous sponges reported during the study, and they appear to be *r*-strategic, or opportunistic, in the use of newly available space. It is unclear if the calcareous nature of these sponges provides them with some adaptive advantage over siliceous sponges.

*Are there discriminating species for (local) habitats of differing stability and experiencing different flow rates?*

Most habitats and sites could be characterized by several abundant sponge species. Different cliff sites were easily distinguishable from each other and from other habitats on the basis of many species. In rock habitats seven species differed between the high- and low-energy sites, though they were too rare to be between-site discriminating species (as determined by SIMPER analysis). Given the similarities in assemblage composition, it is not surprising that the five most important discriminating species between rock and other habitats did not differ between sites. The low number and ubiquitous nature of species on artificial substrata made the identification of true inter-site discriminating species in this habitat irrelevant.

*Are there consistent similarities or differences in assemblage composition from extremes of flow rate and habitat stability?*

Although certain environmental characteristics have been found to influence sponge communities, patterns of sponge assemblages on rocks are not consistent with those described from other hard-substratum environments (Storr, 1976; Alvarez *et al.*, 1990; Witman and Sebens, 1990; Bell

and Barnes, 2000a). From our results, the abundance of sponges on rocks, but not the composition of the assemblage, seemed to be manifestly affected by rate of water flow.

Despite the late-colonizer "tag" applied to sponges in marine communities (Dayton, 1971; Maughan 2000), the present study found a number of species contributing to lithophilic communities on panels that had been deployed for only a few months. Rock habitats did not display a consistent trend of decreasing similarity in assemblage composition from extremes of environmental stability, and rock size was judged to be more important than current flow rate in determining sponge assemblage composition. Disturbance seemed to be more important in determining sponge assemblage composition on cliffs than in loose rock habitats. This study has shown that habitat stability is an important factor to be taken into account along with other measures of disturbance such as flow rate, when considering the distribution of sponge species.

### Acknowledgments

The authors thank Claire Shaw for assisting in data collection and manuscript revision, Declan O'Donnell (Irish Wildlife Service) for granting permits for research at Lough Hyne, and Chris Todd for provision of artificial substrata. We also thank Enterprise Ireland for financial assistance. Thanks also to the anonymous referees for significantly improving this manuscript.

### Literature Cited

- Alcolado, P. M. 1990. General features of Cuban sponge communities. Pp. 351–357 in *New Perspectives in Sponge Biology*, K. Rützler, ed. Smithsonian Institution Press, Washington, DC.
- Alvarez, B., M. C. Diaz, and R. A. Laughlin. 1990. The sponge fauna on a fringing coral reef in Venezuela. I. Composition, distribution, and abundance. Pp. 358–366 in *New Perspectives in Sponge Biology*, K. Rützler, ed. Smithsonian Institution Press, Washington, DC.
- Ayling, A. L. 1983. Growth and regeneration rates in thinly encrusting demospongiae from temperate waters. *Biol. Bull.* **165**: 343–352.
- Barnes, D. K. A., and B. C. Maughan. 2001. Seasonality and inter-annual variability in recruitment patterns of temperate encrusting bryozoans. Pp. 19–27 in *Bryozoan Studies 2001*, P. Wyse Jackson, C. Buttler and M. Spencer Jones, eds., Balkema, Rotterdam.
- Barnes, D. K. A., P. Rothery, and A. Clarke. 1996. Colonisation and development in encrusting communities from the Antarctic intertidal and sublittoral. *J. Exp. Mar. Biol. Ecol.* **196**: 248–265.
- Barthel, D. 1989. Growth of the sponge *Halichondria panicea* in the North Sea habitat. Pp. 23–30 in *Proceedings of the 21<sup>st</sup> European Marine Biology Symposium*, R. Z. Klekowski, E. Styczynska-Jurewicz, and L. Falkowski, eds. Gdańsk, 14–19 September 1986.
- Barthel, D., and O. S. Tendal. 1993. The sponge association of the abyssal Norwegian Greenland Sea: species composition, substrate relationships and distributions. *Sarsia* **78**: 83–96.
- Bassindale, R., E. Davenport, F. J. Ebling, J. A. Kitching, M. A. Sleight, and J. F. Sloane. 1957. The ecology of Lough Hyne Rapids with special reference to water currents. VI. Effects of the rapids on the hydrography of the South Basin. *Ecology* **45**: 879–900.
- Becerro, M. A., M. J. Riu, and X. Turon. 1994. Trends in space occupation by the encrusting sponge *Crambe crambe*: variation in shape as a function of size and environment. *Mar. Biol.* **121**: 301–307.
- Bell, J. J. 2001. The ecology of sponges at Lough Hyne Marine Nature Reserve, Co. Cork, Ireland. Ph.D. thesis, University College Cork.
- Bell, J. J., and D. K. A. Barnes. 2000a. A sponge diversity centre within a marine island. *Hydrobiologia* **440**: 55–64.
- Bell, J. J., and D. K. A. Barnes. 2000b. The distribution and prevalence of sponges in relation to environmental gradients within a temperate sea lough: vertical cliff surfaces. *Divers. Distrib.* **6**: 283–303.
- Bell, J. J., and D. K. A. Barnes. 2000c. The distribution and prevalence of sponges in relation to environmental gradient within a temperate sea lough: inclined cliff surfaces. *Divers. Distrib.* **6**: 305–323.
- Bell, J. J., and D. K. A. Barnes. 2000d. The influence of bathymetry and flow regime on the morphology of sublittoral sponge populations at Lough Hyne MNR. *J. Mar. Biol. Assoc. UK* **80**: 707–718.
- Bell, J. J., and D. K. A. Barnes. 2003. The importance of competitor identity, morphology and ranking methodology to outcomes in interference competition: an example of sponges. *Mar. Biol.* (In Press).
- Bell, J. J., D. K. A. Barnes, and J. R. Turner. 2002. The importance of micro and macro morphological variation in adaptation of a sublittoral demosponge to current extremes. *Mar. Biol.* **140**: 75–81.
- Boury-Esnault, N., and K. Rützler, eds. 1997. *Thesaurus of Sponge Morphology*. *Smithson. Contrib. Zool.* **596**. Smithsonian Institution Press, Washington DC.
- Buss, L. W., and J. B. C. Jackson. 1979. Competitive networks: nontransitive competitive relationships in cryptic coral reef environments. *Am. Nat.* **113**: 223–234.
- Cheshire, A. C., and C. R. Wilkinson. 1991. Modelling the photosynthetic by sponges on Davies Reef, Great Barrier Reef. *Mar. Biol.* **109**: 13–18.
- Dayton, P. K. 1971. Competition, disturbance and community organization: the provision and subsequent utilization of space in a rocky intertidal community. *Ecol. Monogr.* **41**: 351–389.
- Dayton, P. K. 1978. Observations of growth, dispersal and population dynamics of some sponges in McMurdo Sound, Antarctica. Pp. 271–282 in *Sponge Biology*, C. Levi, and N. Boury-Esnault, eds. Colloques internationaux du C.N.R.S. 291.
- Diaz, M. C., B. Alvarez, and R. A. Laughlin. 1990. General features of Cuban sponge communities. Pp. 367–375 in *New Perspectives in Sponge Biology*, K. Rützler, ed. Smithsonian Institution Press, Washington, DC.
- Dunlap, M., and J. R. Pawlik. 1996. Video-monitored predation by Caribbean reef fishes on an array of mangrove and reef sponges. *Mar. Biol.* **126**: 117–123.
- Elvin, D. W. 1976. Seasonal growth and reproduction of an intertidal sponge, *Haliclona pernellis* (Bowerbank). *Biol. Bull.* **151**: 108–125.
- Hiscock, K. 1983. Water movement. Pp. 58–96 in *The Ecology of the Shallow Sublittoral Benthos*, R. Earll, and D. G. Erwin, eds. Clarendon Press, Oxford.
- Hiscock, K., S. Stone, and D. George. 1983. The marine fauna of Lundy. Porifera (sponges): A preliminary study. *Rep. Lundy Field Soc.* **34**: 16–35.
- Hooper, J. N. A., J. A. Kennedy, and R. J. Quinn. 2002. Biodiversity 'hotspots,' patterns of richness and endemism, and taxonomic affinities of tropical Australian sponges (Porifera). *Biodivers. Conserv.* **11**: 851–885.
- Jenkins, S. R., T. A. Norton, and S. J. Hawkins. 1999. Settlement and post-settlement interactions between *Senibalanus balanoides* (L.) (Crustacea: Cirripedia) and three species of fucoid canopy algae. *J. Exp. Mar. Biol. Ecol.* **236**: 49–67.
- Kitching, J. A. 1987. Ecological studies at Lough Hyne. *Adv. Ecol. Res.* **17**: 115–186.
- Könnecker, G. 1973. Littoral and benthic investigations on the West Coast of Ireland. I. The sponge fauna of Kilkieran Bay and adjacent

- areas. Section A: Faunistic and Ecological Studies. *Proc. R. Ir. Acad.* **73B** (26): 450–472.
- Krebs, C. J. 1989. *Ecological Methodology*. Harper Collins, London.
- Lilly, S. J., J. F. Sloane, R. Bassindale, F. J. Ebling, and J. A. Kitching. 1953. The ecology of the Lough Hyne rapids with special reference to water currents. IV. The sedentary fauna of sublittoral rocks. *J. Anim. Ecol.* **22**: 87–122.
- Maldonado, M., and M. J. Uriz. 1995. Biotic affinities in a transitional zone between the Atlantic and the Mediterranean: a biogeographical approach based on sponges. *J. Biogeogr.* **22**: 89–110.
- Manconi, R., and R. Pronzato. 1991. Life cycle of *Spongilla lacustris* (Porifera, Spongillidae): a cue for environment-dependent phenotype. *Hydrobiologia* **220**: 155–160.
- Maughan, B. C. 2000. The ecology of encrusting epifauna in Lough Hyne Marine Nature Reserve. Ph.D. thesis, University College Cork.
- Maughan, B. C., and D. K. A. Barnes. 2000a. Epilithic boulder communities of Lough Hyne: the influences of water movement and sediment. *J. Mar. Biol. Assoc. UK* **80**: 767–776.
- Maughan, B. C., and D. K. A. Barnes. 2000b. A 'minimum stress inflexion' in relation to environmental and biotic influences on the dynamics of subtidal encrusting communities. *Hydrobiologia* **440**: 101–109.
- McCook, L. J., and A. R. O. Chapman. 1997. Patterns and variations in natural succession following massive ice-scour of a rocky intertidal seashore. *J. Exp. Mar. Biol. Ecol.* **214**: 121–147.
- Osman, R. W. 1977. The establishment and development of a marine epifaunal community. *Ecol. Monogr.* **47**: 37–63.
- Paine, R. T. 1974. Intertidal community structure: experimental studies on the relationship between a dominant competitor and its principal predator. *Oecologia* **15**: 93–120.
- Picton, B. E. 1991. The sessile fauna of sublittoral cliffs. Pp. 139–142 in *The Ecology of Lough Hyne: Proceedings of a Conference 4–5 Sept. 1990*, A. A. Myers, C. Little, M. J. Costello, and J. C. Partridge, eds. Royal Irish Academy, Dublin.
- Russ, G. R. 1982. Overgrowth in a marine epifaunal community: competitive hierarchies and competitive networks. *Oecologia* **53**: 12–19.
- Rützler, K., M. C. Diaz, R. W. M. Van Soest, S. Zea, K. P. Smith, B. Alvarez, and J. Wulff. 2000. Diversity of sponge fauna in mangrove ponds, Pelican Cays, Belize. Pp. 232–248 in *Natural History of the Pelican Cays, Belize*. Atoll Research Bulletin, National Museum of Natural History, Smithsonian Institution Press, Washington DC.
- Sarà, M. 1970. Competition and cooperation in sponge population. *Symp. Zool. Soc. Lond.* **25**: 273–284.
- Sarà, M., M. Pansini, and R. Pronzato. 1978. Zonation of photophilous sponges related to water movement in reef biotopes of Ohhor Creek (Red Sea). Pp. 283–295 in *Sponge Biology*. C. Levi, N. Boury-Esnault, eds. Colloques internationaux du C.N.R.S 291.
- Schmahl, G. P. 1990. General features of Cuban sponge communities. Pp. 376–383 in *New Perspectives in Sponge Biology*. K. Rützler, ed. Smithsonian Institution Press, Washington, DC.
- Sousa, W. P. 1979. Disturbance in marine intertidal boulder fields: the non-equilibrium maintenance of species diversity. *Ecology* **60**: 1225–1239.
- Stone, A. R. 1970. Growth and reproduction of *Hymeniacidon perleve* (Montagu) (Porifera) in Langstone Harbour, Hampshire. *J. Zool. Lond.* **161**: 443–459.
- Storr, J. F. 1976. Ecological factors controlling sponge distributions in the Gulf of Mexico and the resulting zonation. Pp. 261–276 in *Aspects of Sponge Biology*. F.W. Harrison, and R.R. Cowden, eds. New York Academic Press, New York.
- Turner, S. J., and C. D. Todd. 1994. Competition for space in encrusting bryozoan assemblages: the influence of encounter angle, site and year on outcome variability. *J. Mar. Biol. Assoc. UK* **74**: 603–622.
- van Soest, R. W. M., and S. Weinberg. 1980. A note on the sponges and octocorals from Sherkin Island and Lough Ine. *Co. Cork. Ir. Nat. J.* **20**: 1–15.
- van Soest, R. W. M., J. D. Guiterman, and M. S. Sayer. 1981. Sponges from Roaringwater Bay and Lough Ine. *J. Sherkin Island* **12**: 35–49.
- Wilkinson, C. R., and A. C. Cheshire. 1989. Patterns in the distribution of sponge populations across the central Great Barrier Reef. *Coral Reefs* **8**: 127–143.
- Witman, J. D., and K. P. Sebens. 1990. Distribution and ecology of sponges at a subtidal rock ledge in the central Gulf of Maine. Pp. 391–396 in *New Perspectives in Sponge Biology*. K. Rützler, ed. Smithsonian Institution Press, Washington, DC.
- Wulff, J. I. 1995. Sponge-feeding by the Caribbean starfish *Oreaster reticulatus*. *Mar. Biol.* **123**: 313–325.
- Wulff, J. 2000. Sponge predators may determine differences in sponge fauna between two sets of mangrove cays, Belize barrier reef. Pp. 249–263 in *Natural History of the Pelican Cays, Belize*. Atoll Research Bulletin, National Museum of Natural History, Smithsonian Institution Press, Washington DC.

# Phenotypic Plasticity of HSP70 and HSP70 Gene Expression in the Pacific Oyster (*Crassostrea gigas*): Implications for Thermal Limits and Induction of Thermal Tolerance

AMRO M. HAMDOUN<sup>1,\*</sup>, DANIEL P. CHENEY<sup>2</sup>, AND GARY N. CHERR<sup>1,3,†</sup>

<sup>1</sup>Bodega Marine Laboratory, PO Box 247, Bodega Bay, California 94923; <sup>2</sup>Pacific Shellfish Institute, 120 State Ave. NE #142, Olympia, Washington; and <sup>3</sup>Departments of Environmental Toxicology and Nutrition, University of California Davis, Davis, California 95616

**Abstract** Pacific oysters, *Crassostrea gigas*, living at a range of tidal heights, routinely encounter large seasonal fluctuations in temperature. We demonstrate that the thermal limits of oysters are relatively plastic, and that these limits are correlated with changes in the expression of one family of heat-shock proteins (HSP70). Oysters were cultured in the intertidal zone, at two tidal heights, and monitored for changes in expression of cognate (HSC) and inducible (HSP) heat-shock proteins during the progression from spring through winter. We found that the “control” levels (*i.e.*, prior to laboratory heat shock) of HSC77 and HSC72 are positively correlated with increases in ambient temperature and were significantly higher in August than in January. The elevated level of HSCs during the summer was associated with moderate, 2–3 °C, increases in the upper thermal limits for survival. We measured concomitant increases in the threshold temperatures ( $T_{on}$ ) required for induction of HSP70. Total *hsp70* mRNA expression reflected the seasonal changes in the expression of inducible but not cognate members of the HSP70 family of proteins. A potential cost of increased  $T_{on}$  in the summer is that there was no extension of the upper thermal limits for survival (*i.e.*, induction of thermotolerance) after sublethal heat shock at temperatures that were sufficient to induce thermotolerance during the winter months.

## Introduction

Marine invertebrates tolerate a remarkable array of natural and anthropogenic stresses. Although the nearshore environment supports great invertebrate diversity, it is physiologically challenging. Littoral invertebrates routinely encounter anoxia, osmotic stress, and wide thermal fluctuations. Withstanding these conditions usually requires the initiation of coordinated cellular responses to stress. These responses are particularly important in the adaptive response of sessile intertidal invertebrates such as mussels and oysters.

Many of these natural stresses can directly alter protein conformation and stability. Because proteins must be sufficiently labile to interact with their substrates, they are often highly susceptible to protein-denaturing stresses such as reduced intracellular pH or elevated temperature (Somero, 1995). Protein-denaturing stressors such as heat can result in the revealing of hydrophobic domains of proteins and cause nonspecific protein interactions. Under these conditions, several families of proteins known as heat-shock proteins (HSP), or molecular chaperones, perform critical protein-stabilizing functions (Lindquist, 1986; Gething and Sambrook, 1992; Morimoto *et al.*, 1994). Under “non-stress” conditions, molecular chaperones are required to stabilize hydrophobic protein domains exposed to aqueous cellular environments during protein synthesis and translocation (for review, see Hartl and Hayer-Hartl, 2002). Stress-induced expression of HSPs contributes dramatically to tolerance of otherwise lethal conditions (Parsell and Lindquist, 1994), known as “induced thermotolerance.”

Received 12 April 2002; accepted 24 June 2003.

Bodega Marine Laboratory Contribution Number: 2175

\* Present Address: Hopkins Marine Station, Stanford University, Pacific Grove, California 93950.

† To whom correspondence should be addressed. E-mail: gncherr@ucdavis.edu

Natural variation in the heat-shock response appears to be correlated with distribution along environmental gradients of stress (Hofmann and Somero, 1996; Tomanek and Somero, 1999). Threshold induction temperatures for HSPs are positively correlated with ambient environmental temperatures (Dietz and Somero, 1992; Buckley *et al.*, 2001). In the marine mussel *Mytilus*, threshold temperatures can be higher in animals living at higher tidal heights (Roberts *et al.*, 1997). In congeneric species of the marine snail *Tegula*, threshold temperatures are positively correlated with the maximal tidal height at which each species is found. In *Tegula*, these differences are maintained even after laboratory acclimation, suggesting a role for gene regulatory factors that establish set points for HSP induction or interspecific variation in the stability of cellular proteins (Tomanek and Somero, 1999).

The basic features of the heat-shock response in the Pacific oyster, *Crassostrea gigas*, have been well characterized (Clegg *et al.*, 1998). HSP70 has been shown to be the primary family of HSP that is responsive to thermal stress. Three isoforms of HSP70 family protein are resolved after one-dimensional electrophoresis and western blotting. Two proteins, HSC77 and HSC72, are constitutively expressed, and their level of expression and accumulation increases after acute thermal stress. In contrast to other bivalve species such as *Mytilus*, *C. gigas* can express a third protein, HSP69, but it is typically only detectable after acute thermal stress. Several days after heat shock, the levels of HSP69 account for roughly one-third of total HSP70. In the absence of additional stress, HSP69 completely disappears within 7–10 days of heat shock. Two genes encoding mRNAs that correspond to the constitutively expressed (cognate) and inducible forms of oyster HSP70 family have been sequenced and characterized. Distinct gene products encode a cognate protein of about 72 kDa (Gourdon *et al.*, 2000) and an inducible protein of about 68–70 kDa (Boutet *et al.*, 2003). In Pacific oysters, a single sublethal heat shock sufficient to cause significant HSP69 expression also results in induced thermotolerance for a remarkably prolonged period of up to 2 weeks (Clegg *et al.*, 1998).

In this study, we attempted to determine the extent and the mechanism of adaptive plasticity of the heat-shock response in a group of sibling Pacific oysters planted at two tidal heights (+0.3 m and +1.2 m) at Totten Inlet, Southern Puget Sound, Washington State. We measured the seasonal changes in HSP70 and *hsp70* gene expression in these oysters, and we examined these findings in the context of the observed, concomitant changes in control and inducible upper thermal limits for survival. Our findings suggest that phenotypic plasticity of the heat-shock response is a significant component of adaptation to natural thermal stress.

## Materials and Methods

### *Animals and study site*

A commercial oyster bed in Totten Inlet, south Puget Sound, Washington, was selected as an experimental study site. The juvenile "seed" (about 5–10 cm in length) oysters for this experiment, 1999 age class, were obtained in late June 1999 and planted at two tidal elevations: a low-intertidal plot at 0.3 m mean lower low water (MLLW) and a high-intertidal plot at 1.2 m MLLW. The seed were initially placed in rectangular, 0.5-cm mesh, plastic grow-out bags set on top of metal racks at each tidal height. The oysters were later transplanted to larger, 2–4-cm mesh, grow-out bags. Oysters were sampled monthly during low tide events starting in April 2000 and continuing until January 2001.

External site temperature data were recorded every 15 min using Hobo temperature sensors. Internal temperature data were recorded using Hobo 4-channel external data loggers and TMC6-HA temperature sensors. Temperature data were recorded at each tidal height from three oysters with internally mounted sensors and one externally mounted sensor (TMC6-HA sensor), which was placed next to the oysters either in a grow-out bag or on the ground. The internal temperature sensors were placed inside the shell of live oysters through a 6mm opening. The sensors were secured and sealed by using marine epoxy.

### *Heat shock*

Immediately after collection oysters were shipped overnight in chilled (12–15 °C) coolers to Bodega Marine Laboratory, Bodega Bay, California, for use in experiments. After 24 h of recovery in flow-through tanks with raw Bodega Bay seawater (RSW; 13°C,  $\pm$  2°C), animals were placed in fine mesh bags and heat-shocked at a variety of temperatures (see Results) by being submerged in pre-heated, aerated filtered seawater baths for 65 min. Animals were returned to the flow-through seawater tanks immediately after heat shock. Five to six oysters were heat-shocked at each temperature for sampling of gills for northern and western blots. After heat shock, oysters were returned to the RSW tanks for 48 h before gills were sampled for protein and mRNA analysis; 48 h has previously been shown to be the point at which accumulation of HSP70 protein is maximal, and *de novo* synthesis of HSP70 is still elevated relative to control specimens of *C. gigas* (Clegg *et al.*, 1998). This protocol allowed us to compare the level of HSP70 protein and mRNA from identical gill sections. It is important to note that HSP70 levels remain elevated in oysters for at least one week following heat shock. Thermal limits were determined by heat-shocking three groups of seven animals (in fine-mesh bags) at each temperature. Survival was determined after 10 d of recovery at 13°C ( $\pm$  2°C) in RSW tanks.

To ensure that shipping and brief holding did not alter the profile of HSP70 expression, we compared samples of gill from freshly collected oysters (prior to shipping), from oysters that had just arrived at the laboratory, and from oysters that had been held for 2 days in ambient RSW. No difference in HSP70 protein levels was observed between any of these groups (data not shown).

#### *Tissue sampling and sample preparation*

Oysters were opened and gills were dissected and divided into two sections for protein and RNA isolation. Gill samples for western blots were prepared according to Clegg *et al.* (1998). Briefly, they were rinsed in double-distilled H<sub>2</sub>O, blotted dry, weighed, and flash-frozen in liquid nitrogen. These samples were stored at  $-70^{\circ}\text{C}$  and later homogenized on ice in glass tissue grinders containing potassium gluconate buffer (5 mM MgSO<sub>4</sub>, 5 mM NaH<sub>2</sub>PO<sub>4</sub>, 40 mM HEPES, 70 mM gluconic acid, 150 mM sorbitol; pH 7.5) at a concentration of 100 milligrams of tissue per milliliter of buffer. Homogenates were prepared for electrophoresis by mixing 1:1 in 2 $\times$  sample buffer and boiling for 5 min.

Gill sections for RNA isolation were immediately preserved in 5 volumes of RNAlater (Ambion) solution, frozen in liquid nitrogen, and stored at  $-70^{\circ}\text{C}$ . Gills were later homogenized in 3 ml guanidine thiocyanate denaturing solution: 900  $\mu\text{l}$  of this homogenate was mixed with 100  $\mu\text{l}$  of 2 M sodium acetate and incubated on ice for 5 min. Samples were next mixed 1:1 with ice-cold phenol/chloroform (pH 4.3; Sigma) and incubated on ice for 20 min. After centrifugation for 25 min at 10,000  $\times g$ , the aqueous layer was removed, and RNA was precipitated overnight in an equal volume of isopropyl alcohol. The next day the RNA was pelleted, washed, and resuspended in DEPC H<sub>2</sub>O. Purity and concentration were checked using a spectrophotometer.

#### *cDNA cloning and probe synthesis*

Total RNA was isolated from heat-shocked oysters and used to synthesize cDNA with Superscript Reverse Transcriptase (Gibco-BRL) according to manufacturer's instructions. A 660-bp fragment of oyster HSC72 cDNA was amplified from this template using degenerate HSP70 primers (Cochrane *et al.*, 1994). PCR products were checked for size and yield on 1% agarose gel prior to TA cloning using the dual promoter pCRII-TOPO vector (Invitrogen) and cloning kit. Aliquots of plasmid minipreps (Qiagen) of positive clones were sent to Davis Sequencing (Davis, California) for sequencing. Results were analyzed by using the BLAST program at the National Center for Biotechnology Information to compare existing sequences. A 660-bp fragment was cloned that was identical to a portion of a previously submitted sequence of Pacific oyster HSC72 mRNA (Gourdon *et al.*, 2000).

An antisense RNA probe for total HSP70 probe was

synthesized from minipreps (confirmed to be positive for the *hsc72* gene product by sequencing). Briefly, a digoxigenin-labeled UTP (Roche) probe was synthesized by *in vitro* transcription (Maxiscript; Ambion) of the antisense strand. Because of the high homology in this region of the known oyster HSP70 genes, we expected this probe to hybridize with all of the known gene products of the HSP70 family. The yield of resulting probe was determined by using a dot blot of the probe *versus* a digoxigenin-RNA probe standard (Roche) according to manufacturer's instructions.

#### *Western blotting*

Western blots of oyster HSP70 family were prepared according to Clegg *et al.* (1998) and 10  $\mu\text{l}$  of each solubilized sample was resolved on a 10% SDS-polyacrylamide gel. To normalize between blots, multiple aliquots of a single sample of heat-shocked oyster gill were made. Each time gels were run, an aliquot of this sample was loaded on the center lane of each gel. The internal control sample was arbitrarily chosen from a previous experiment and was known to have all three isoforms of HSP70 family protein. Therefore, levels of each HSP70 family member were normalized relative to the level of the corresponding band from the internal standard (the maximal variation in standard level between gels was less than 10-fold). To ensure that the large differences in HSP70 protein levels between summer and winter controls were not attributable to blot variation, the summer and winter samples were run on a single blot and their values relative to heat-shocked oysters were adjusted according to the level of the corresponding standard sample run on that blot. Control levels of HSP70 mRNA were compared from samples run on a single northern blot.

Proteins were transferred onto nitrocellulose and probed using a monoclonal rat anti-HSP70 antibody (Affinity Bioreagents, MA3-001), and an HRP-conjugated goat secondary antibody (Sigma). Signal was detected by chemiluminescence using enhanced detection reagents (Supersignal, Pierce) on a Bioimaging Systems digital gel scanner or by exposing blots to photographic film (Kodak, Biomax MR). Relative levels of band were intensified using gel plotting macros available on Scion Image (ver. 1.61) software.

#### *Northern blotting*

For each northern blot, 4  $\mu\text{g}$  of denatured total RNA was loaded onto each lane of 1% agarose (in 1 $\times$  MOPS), 6.66% formaldehyde gels and run for 3–5 h at 50 V. RNAs were transferred overnight onto nylon membranes (Hybond) using standard capillary methods in 10 $\times$  SSC buffer. After transfer, RNA was cross-linked to the blots (Stratalinker), and blots were stored at  $-20^{\circ}\text{C}$  until probed. DIG-labeled RNA probes were prepared at a final concentration of 50

ng/ml in high SDS buffer (all buffers in RNA detection were prepared according to instructions from DIG applications manual, Roche). Blots were incubated overnight at 50°C in probe solution with gentle rotation. The next day, nonspecific hybridization was removed using four 15-min stringency washes at 60°C in decreasing concentration of SSC solution (2×–0.5×). Blots were then washed twice in maleic acid buffer containing 0.3% Tween 20, and blocked for 30 min using 1× blocking buffer (Roche). Blocked blots were incubated for 1 h with gentle rotation at room temperature in a 1:10,000 solution of anti-DIG AP Fab fragments (Roche) in blocking buffer. CSPD solution (Roche) was used 1:100 in detection buffer to detect hybridized probe. Chemiluminescence was enhanced by 15-min incubation of the blot at 37°C, followed by detection using a Bioimaging Systems digital gel scanner.

### Statistics

Differences in protein and mRNA level were analyzed for statistical significance using one-way ANOVA, and multiple pairwise comparisons were performed according to Dunn's method; all tested data conformed to equal variance and normality assumptions. All analyses were conducted using Sigmastat software ver. 2.03.

## Results

### Animals and study site

Temperatures recorded in living oysters generally matched those recorded by external data temperature loggers placed alongside the oysters in the culture bags (Fig. 1). This suggests that despite its thickness, oyster shell is a relatively poor insulator against thermal stress. Oysters at 1.2 m MLLW generally experienced higher temperatures and longer durations of exposure to elevated temperature than oysters at 0.3 m. To estimate the duration of exposure to elevated (>20°C) temperatures, measurements from data loggers were sorted into 5°C intervals, and measurements in each class were summed together. Each data point was assumed to represent about 15 min of exposure to the recorded temperature. In nearly all cases the approximate duration of exposure to warm temperatures was longer at the high tidal height (Fig. 2) for the 2 weeks preceding the summer sampling. During the summer 2000 period, the total exposure to temperatures in excess of 20°C was about 67 h at the high tidal height compared to 44 h at the lower tidal height. The thermal regime based on mean emersion is summarized in Figure 3. The majority (>70%) of the time (not shown), oysters at both tidal heights were submerged and encountered temperatures in the 15–20°C range. Oysters encountered elevated (>20°C) and reduced (<15°C) temperatures at or above the point of emersion.

No significant difference in mortality was recorded in

animals at either site during the experiment. Total mortality at both sites was less than 20% annually. Animals at the high tidal height (1.2 m) showed a cumulative mortality of 16.5% (62 out of 375 animals); those at the low tidal height (0.3 m) experienced an 18.4% (69 out of 375 animals) mortality. Most of the mortalities occurred during the warmest months (June–September).

### HSP70 protein and hsp70 mRNA levels

The levels of HSC70 (HSC77 and HSC72) in control (non-heat-shocked) Pacific oysters were associated with the level of environmental thermal stress (Fig. 4). At both study sites the control levels of HSC77 and HSC72 were as much as 100-fold greater in summer than in winter ( $P < 0.001$ ). These differences were not attributed to differences in total protein levels, as mean control protein levels were 41.5 mg/g wet weight and 46.2 mg/g wet weight in winter and summer, respectively (Bradford protein assay, BioRad), and these differences were not significantly different ( $P > 0.07$ ). During the winter months there was no statistically significant difference in the control levels of HSC70 between the high and low tidal height sites ( $P = 0.917$ ).

The threshold temperature for induction of HSP69 appeared to be associated with the level of environmental thermal stress (Figs. 1–4). In January, HSP69 accumulation was induced in oysters from both sites after heat shock at 37°C. In contrast, limited or no induction of HSP69 and HSC72 was observed following heat shock at 37°C in August oysters living at high or low tidal height (Fig. 4; see also Fig. 6A). Full induction (*i.e.*, HSP69 expression at levels approximating those of HSC77 or HSC72) of HSP69 was not observed in August until after heat shock at 40–43°C. Thus, both the threshold temperature for HSP69 induction and the control levels of HSC70 exhibited significant seasonal plasticity.

The level of *hsp70* mRNA in summertime high tidal height oysters increased dramatically relative to control after heat shock at 40 and 43°C, but not after heat shock at 33 and 37°C (Fig. 5). This result reflected the observed increases in HSP69 protein after heat shock at these temperatures in the same animals.

A subset of oysters from each site was sampled and heat-shocked at 37°C monthly during the summer, beginning in April and ending in September (not shown). Based on the results of these observations, the greatest change in threshold temperature for HSP69 induction and control level of HSC77/HSC72 temperature occurred between our June and July sampling dates and winter (January) (Fig. 6A, B; Fig. 7). In June, oysters at the high tidal height completely induced HSP69 after a 37°C heat shock. In contrast, by July, induction of HSP69 was much more limited in these oysters. Control levels of HSC70 also increased markedly during this period. Although there were slight increases

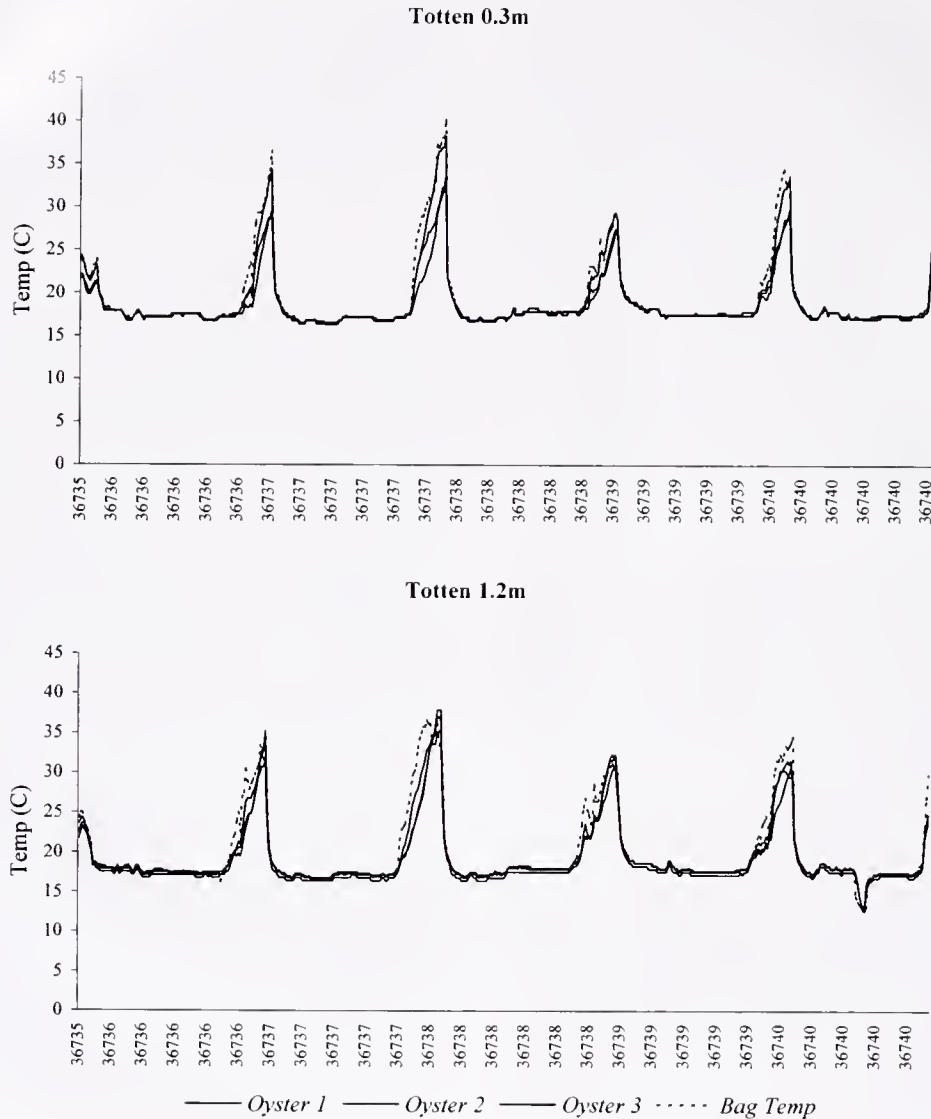


**Figure 1.** Internal temperatures of three living oysters (solid lines) at two tidal heights (1.2 m and 0.3 m at Totten Inlet, Washington) and external temperatures from a temperature probe placed alongside the oysters (dotted lines). Internal temperatures closely track external temperatures.

in mean levels of control *hsp70* mRNA in summer relative to winter oysters, the differences were not significant ( $P = 0.13$ ; Fig. 7).

#### *Thermal limits and induction of thermal tolerance*

Laboratory heat shock of oysters at both tidal heights suggested both seasonal and tidal height influences on the upper thermal limits for survival (Fig. 8). In January there was no significant difference in lethal temperatures between oysters at the two tidal heights. However, by August there were significant increases in the baseline thermal limits of oysters at both study sites. Moreover, oysters at the high tidal height appeared to exhibit elevated thermal limits

compared to their low tidal height counterparts during the summer. August survival of high tidal height oysters after 44°C heat shock was significantly higher than that of the low tidal height oysters ( $P = 0.03$ ). These differences occurred in the absence of HSP69 expression, suggesting that control thermal limits in Pacific oysters are likely to be more closely associated with cognate HSC70 expression than to inducible HSP70 expression. In contrast, induced thermal tolerance appeared to be associated with inducible HSP70 expression (Fig. 9). Oysters at the high tidal height that were heat-shocked at 37°C during the winter were able to completely withstand a subsequent lethal treatment of 44°C. Heat shock at 37°C did not induce thermotolerance

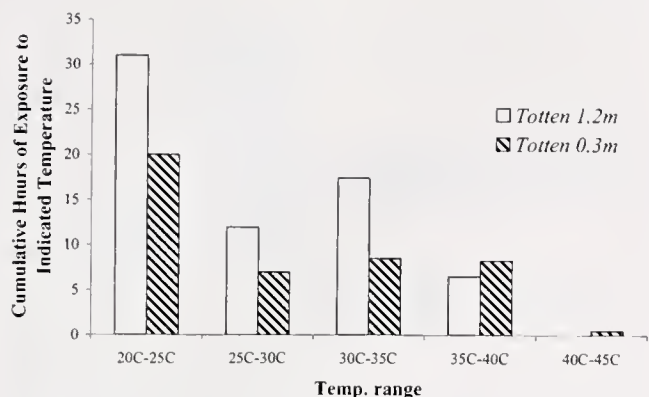


**Figure 2.** The approximate hours of exposure to elevated (>20°C) air temperatures in oysters at high and low tidal heights for the 2 weeks prior to the summer sampling. The vast majority of the time, oysters experienced temperatures (15–20°C) below the range shown.

(to 46°C) during the summer. However, when August oysters were heat-shocked at 40°C, they were able to withstand heat shock at 46°C. These results suggest that induction of thermal tolerance is more closely associated with inducible HSP70 family expression.

**Discussion**

Our results demonstrate significant phenotypic plasticity in the heat-shock response of Pacific oysters. Massive changes (10- to 100-fold increases) in the amounts of constitutively expressed HSP70 proteins were measured in summer as compared to winter. These changes are associated with concomitant increases in thermal limits and set point for HSP69 induction. In oysters at both high and low tidal height, the threshold for complete (*i.e.*, equivalent to levels of HSC77 and HSC72) induction of HSP69 increased

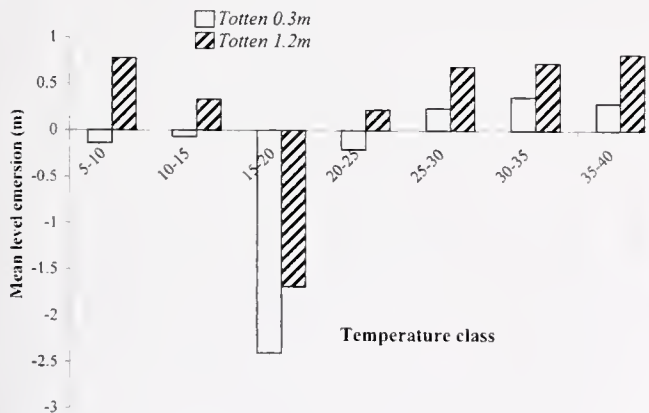


**Figure 3.** Mean level of emersion for 5°C temperature intervals encountered during the month of August. For the vast majority of time (> 70%), temperatures were in the range of 15–20°C. At this temperature range, oysters were completely submerged. At temperatures outside of this range, oysters were at or above the point of emersion.

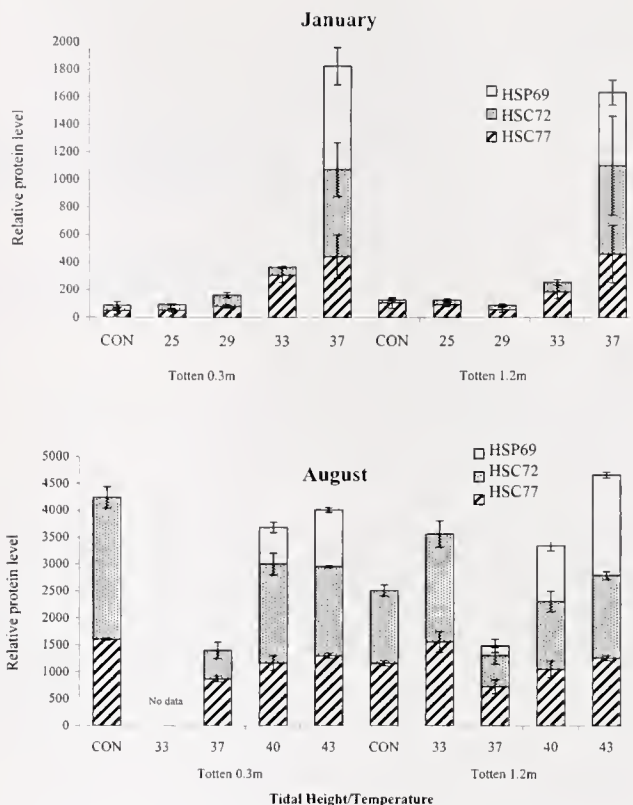


**Figure 4.** Relative levels of HSP70 as determined from western blots for animals sampled in August and later in January. Bars represent the mean values of total HSP70 for 5–6 animals ( $\pm$  s.e.m. for each isoform). The relative amount of each isoform is indicated within the total amount. Three isoforms were resolved by one-dimensional electrophoresis: two cognate forms (HSC77 and HSC72) and one inducible isoform (HSP69). The x-axis of each graph indicates the heat-shock temperature series for the low tidal height (0.3-m) group, followed by the temperature series for the high tidal height (1.2-m) group.

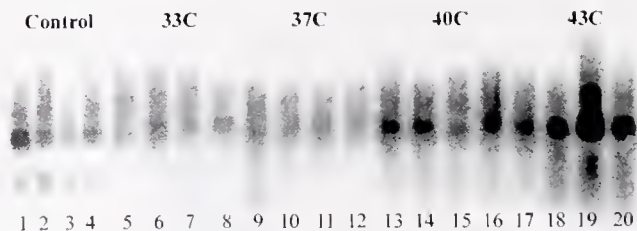
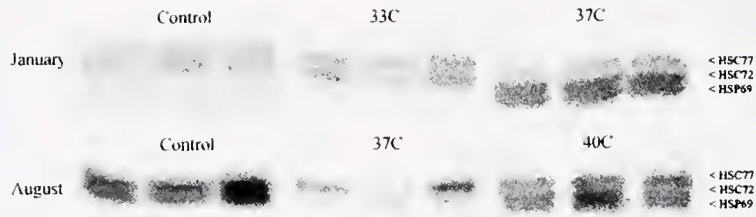


**Figure 5.** Northern blots of *hsp70* mRNA in high tidal height (1.2-m) oysters 48 h after heat shock (HS) in August. Lanes are loaded with equivalent amounts (4  $\mu$ g) of total mRNA. HSP70 was analyzed with an antisense digoxigenin-labeled UTP probe corresponding to a 660-bp portion of oyster HSC72. Each lane represents mRNA from one oyster. Four oysters were subjected to each treatment (1–4 are Controls, 5–8 are 33°C heat shock (HS), 9–12 are 37°C HS, 13–16 are 40°C HS, 17–20 are 43°C HS).

A.



B.



**Figure 6.** (A) Western blots, captured on digital scanner, of HSP70 family expression in high tidal height (1.2-m) oysters (3 individuals per treatment) in August and in January. HSC77 and HSC72 are dramatically elevated in control oysters sampled in August. (B) Western blots, exposed to film, of HSP70 protein family in oysters (5 individuals per treatment) living at high tidal height (1.2-m). In June, a single 1-h heat shock (37°C) completely induces HSP69 expression. In July, HSP69 expression is absent in most animals sampled, but the control levels of HSC77 and HSC 72 are elevated relative to June.

from about 33–37°C in winter to 37–40°C in summer. In high tidal height oysters, the temperature required for induction of thermal tolerance also increased from 37°C in winter to 40°C in summer.

Although we did not determine the changes to the absolute limits for control and inducible thermal tolerance, the observed changes suggest potential costs for plasticity of the heat-shock response. It is clear that seasonal increases in thermal limits are associated with concomitant increases in the temperatures required for induction of tolerance to oth-

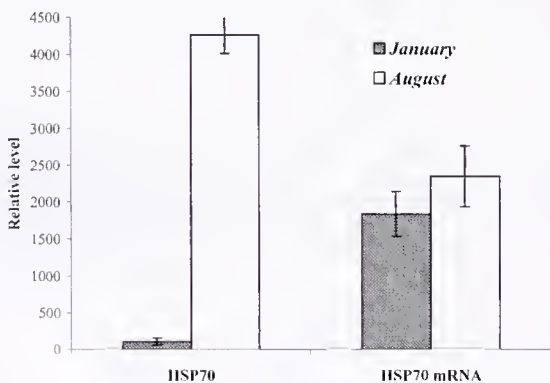


**Figure 7.** Control levels of total *hsp70* mRNA ( $n = 4$ ) and total HSP70 ( $n = 5$ ) prior to heat shock in summer and winter from oysters from the high tidal height (1.2 m). Summer and winter protein samples were run on the same blot, as were mRNA samples, and relative levels were measured in arbitrary units using Scion Image software.

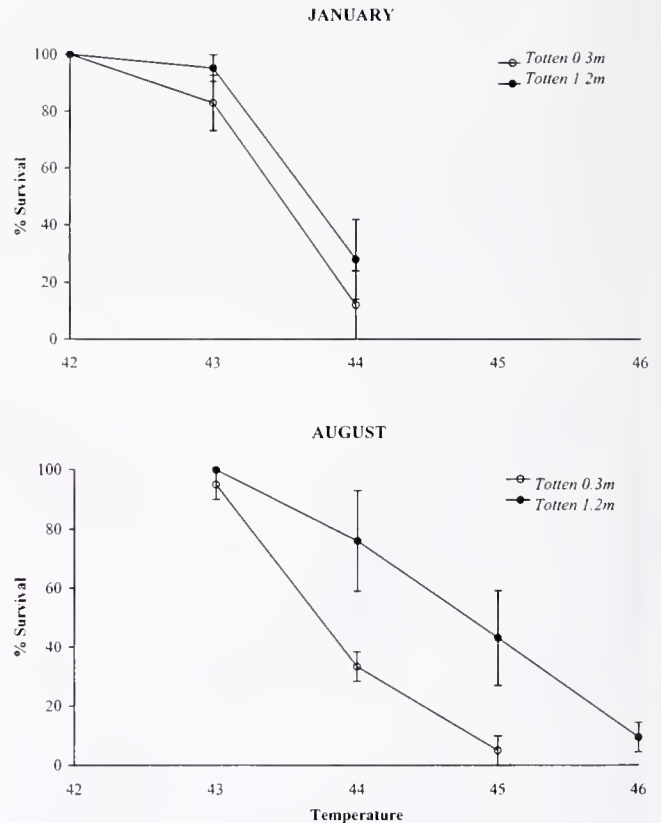


**Figure 8.** Survival of oysters after 1 h of submerged heat shock in summer and winter. Points are the means of three groups of seven oysters each ( $\pm$  s.e.m.).

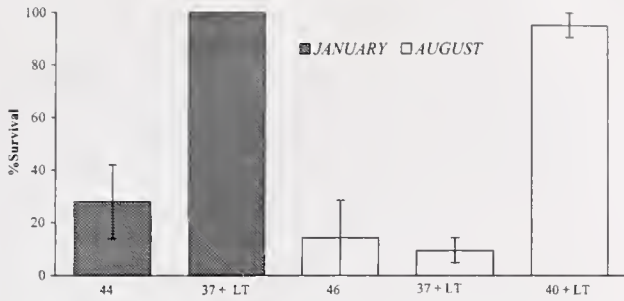


**Figure 9.** Induced thermal tolerance in oysters from the high tidal height (1.2 m). Oysters were either heat-shocked directly at lethal temperature or shocked for 1 h at a sublethal temperature and then allowed to recover for 2 days before lethal temperature treatment. Numbers below bars indicate the initial treatment temperature, followed by the temperature of the subsequent treatment (LT = lethal temperature as determined for each group of oysters 1 week prior to the start of the experiments). LT was 44°C in the winter and 46°C in the summer. Bars represent means of three groups of seven oysters each ( $\pm$  s.e.m.).

erwise lethal temperatures. However, induction of thermal tolerance is a laboratory phenomenon and may not directly relate to changes in thermal limits in nature. Clearly most of the temperatures encountered in nature are far below those required to measure changes in thermal limits. Thus the consequences of changes in inducible thermal tolerance may be most significant during periods when elevated temperatures are extreme or when they occur in concert with other stresses.

Over-expression of HSPs is known to have deleterious consequences. Initiation of heat-shock responses usually results in a concomitant reduction in the synthesis of all other proteins (Parsell and Lindquist, 1994). During stress, HSPs can account for a large fraction of cellular protein; thus it is hypothesized that their synthesis represents a significant energetic cost. In *Drosophila*, artificially high levels of HSP70 can reduce thermotolerance and slow the development of larvae (Krebs and Feder, 1998). Thus it is possible that the observed plasticity of the heat-shock response in Pacific oysters represents a trade-off between the costs of maintaining elevated control thermal tolerance and the cost of the resting state in which the heat shock proteins are maintained at lower levels.

In the laboratory, other bivalve species such as *Mytilus* exhibit significant plasticity in various features of the heat-shock response (Buckley *et al.*, 2001). However, two factors confound the interpretation of results from experiments with adult bivalves collected from the field. First, significant selection occurs at settlement (Launey and Hedgecock, 2001), and it is likely to correspond with distribution along gradients of stress (Michener and Kenny, 1991). Second, large-scale mortality may occur within adult bivalve beds during warm seasons (Cheney *et al.*, 2000). Because there was no significant differential mortality during our experiments, we can downgrade the likelihood of a strong site-

specific effect due to selection. Moreover, by planting sibling juvenile oysters at each site, we limited any confounding effect of selection for thermal tolerance at settlement. Thus, we conclude that our results and perhaps those previously observed in *Mytilus* (Roberts *et al.*, 1997; Buckley *et al.*, 2001) are probably the consequence of significant phenotypic plasticity in the heat-shock response rather than of fixed genotypic differences between bivalves living along gradients of stress.

Further experiments using genetically characterized families of bivalves, and other model organisms, may be the most useful in differentiating components of the heat response that are genetically fixed from those that exhibit adaptive plasticity or intra-specific variability. Oysters may be an ideal system for these studies. Because oysters are a commercially valuable species, recent studies (*e.g.*, Launey and Hedgecock, 2001) have focused on characterizing the genetics of Pacific oysters from known lineages. The possibility of producing oysters with characterized genotypes and improved culture performance under a wide range of environmental conditions is being explored (Langdon *et al.*, 2003). A major challenge facing oyster growers is reducing mortality during the warmest summer months (Cheney *et al.*, 2000). It is not yet known if the improved performance of these characterized families of oysters is related, at least in part, to genetically fixed differences in their ability to mount functional heat-shock responses and withstand thermal stress.

Our results suggest that both accumulation of HSP and rates of gene expression are responsive to environmental stress, but that changes in gene expression alone are not sufficient to account for the differences in protein accumulation. Remarkably, *hsp70* mRNA levels were elevated 2 days after heat shock in high tidal height oysters that were heat-shocked at 40 and 43°C. It is possible that elevated mRNA levels would have also been measured at lower temperatures if tissues were sampled sooner than 48 h after heat shock. Our results suggest that cognate HSP70 protein expression in oysters is not directly controlled at the transcriptional level. It is possible that changes in the rate of HSP70 protein synthesis and degradation may be important regulatory components of the long-term modulation in control HSP70 level. Consistent with this hypothesis, Clegg *et al.* (1998) demonstrated that levels of HSC77 and HSC72 remain elevated long after total HSP70 synthesis has returned to control levels.

Other authors (Tomanek and Somero, 2002) have proposed that level of cognate HSP70 isoforms may be an index of protein synthesis capacity, whereas the levels of inducible isoforms may be more accurate indices of adaptation to heat stress. In our study it was the threshold for HSP69 expression that reflected adaptation to thermal stress associated with seasonal changes. The seasonal plasticity of the heat-shock response was reflected most dramatically in

the large seasonal changes in the control levels of HSC77 and HSC72, suggesting that these isoforms may also play important roles in mediating the effects of thermal stress.

In laboratory selection experiments using *Drosophila* (Lerman and Feder, 2001), there is evidence that the heat-shock response may be regulated by genetic factors that are fixed during evolution in a particular environment. However, in sessile intertidal species, several key features of the heat-shock response (e.g., control levels of HSP and threshold temperatures of HSP induction) appear to be sensitive to acclimation to laboratory and natural seasonal conditions (Roberts *et al.*, 1997; Buckley *et al.*, 2001). In sessile species such as oysters or mussels, behavioral adaptation plays a more limited role in regulating exposure to environmental stress. Thus, we hypothesize that the heat-shock response, and particularly the levels of HSC70 in Pacific oysters, must exhibit sufficient phenotypic plasticity to allow organisms to cope with a wide array of environmental conditions.

Most studies of the ecological physiology of stress proteins have two key limitations (Feder and Block, 1991; Feder and Hofmann, 1999). First, most relevant stressors initiate responses from a variety of cellular and systemic stress-response systems. Second, single stresses are rarely encountered in the environment. More typically, organisms encounter multiple stresses that interact with a variety of stress-responsive systems. In the case of sessile bivalves, a critical stressor that has been overlooked is the simultaneous exposure to anoxia or hypoxia during periods of thermal stress. Since most periods of elevated ambient temperatures occur during emersion (Fig. 3), it will be important to address the question of whether anoxic and hypoxic conditions interact with heat-shock responses in intertidal bivalves.

Plasticity of the heat-shock response is apparently a common feature in sessile intertidal invertebrates but not in other marine invertebrates (Tomanek and Somero, 1999; Spees *et al.*, 2002). This suggests that the potential costs of adaptive plasticity of the heat-shock response outweigh the benefits in species and life-history stages for which behavioral regulation of thermal environment is possible. Perhaps more significantly, these results could indicate that although heat-shock proteins and the genes that encode them are highly conserved, the composition and expression of the regulatory components that collectively constitute the cellular thermostat may exhibit significant interspecific variability. Thus oysters, mussels, and other species that exhibit significant adaptive plasticity of the heat-shock response may have evolved the most complex and robust regulatory mechanisms. An unresolved question is the mechanism by which control or resting levels of HSP70 are regulated during chronic stress exposure. It is not yet clear if these mechanisms provide distinct regulatory pathways that might

be adaptive in specific tolerance of acute *versus* chronic stress.

This study has shown that a change in the threshold temperature for HSP70 induction, in response to chronic stress, is associated with a concomitant change in the threshold temperature required to induce thermotolerance. We have shown that the changes in threshold temperature for induction of thermal tolerance match the seasonal changes in threshold temperature for HSP70 induction and expression. Of particular ecological significance is the finding that an increase in threshold temperature narrows the range of temperatures at which HSP induction can contribute to the acquisition of thermotolerance in oysters. Although this suggests a cost for adaptive plasticity of the heat-shock response, the impact of this cost on survival in the field is not clear.

### Acknowledgments

The authors thank Brian McDonald, Andrew Suhrbier and Sheila Walsh for their technical assistance. The authors thank Drs. Jim Clegg, Fred Griffin, and Lars Tomanek for their many helpful comments and thought-provoking discussions about this work. We greatly thank Drs. Jeff Spees and Ernie Chang for their generous help during the analysis of *hsp70* mRNA. The work was supported by a grant from the National Sea Grant College Oyster Disease Research Program (ODRP) Grant No. NA96RG0488 and the UC Toxic Substances Research and Teaching Program.

### Literature Cited

- Buckley, B. A., M. Owen, and G. E. Hoffman. 2001. Adjusting the thermostat: the threshold induction temperature for the heat shock response in intertidal mussels (genus *Mytilus*) changes as a function of thermal history. *J. Exp. Biol.* **204**: 3571–3579.
- Cheney, D. P., B. F. MacDonald, and R. A. Elston. 2000. Summer mortality of Pacific oysters, *Crassostrea gigas* (Thunberg): initial findings on multiple environmental stressors in Puget Sound, Washington, 1998. *J. Shellfish Res.* **19**: 353–359.
- Clegg, J. S., K. R. Uhlinger, S. A. Jackson, G. N. Cherr, E. Rifkin, and C. S. Friedman. 1998. Induced thermotolerance and the heat-shock protein-70 family in the Pacific oyster *Crassostrea gigas*. *Mol. Mar. Biol. Biotechnol.* **7**: 21–30.
- Cochrane, B. J., Y. Mattley, and T. W. Snell. 1994. Polymerase chain reaction as a tool for developing stress protein probes. *Environ. Toxicol. Chem.* **13**: 1221–1229.
- Dietz, T. J., and G. N. Somero. 1992. The threshold induction temperature of the 90-kDa heat shock protein is subject to acclimatization in eurythermal goby fishes (genus *Gillichthys*). *Proc. Natl. Acad. Sci. USA* **89**: 3389–3393.
- Feder, M. E., and B. A. Block. 1991. On the future of animal physiological ecology. *Funct. Ecol.* **5**: 136–144.
- Feder, M. E., and G. E. Hoffman. 1999. Heat shock proteins, molecular chaperones and the stress response: evolutionary and ecological physiology. *Annu. Rev. Physiol.* **61**: 243–282.
- Gething, M. J., and J. Sambrook. 1992. Protein folding in the cell. *Nature* **355**: 33–45.
- Gourdon, I., L. Gricourt, K. Kellener, P. Roch, and J. M. Escoubas.

- 2000.** Characterization of a cDNA encoding a 72kDa heat shock cognate protein (HSC72) from the Pacific oyster, *Crassostrea gigas*. *DNA Seq.* **11**: 265–270.
- Hartl, F. U., and M. Hayer-Hartl. 2002.** Molecular chaperones in the cytosol: from nascent chain to folded protein. *Science* **295**: 1852–1858.
- Hofmann, G. E., and G. N. Somero. 1996.** Interspecific variation in thermal denaturation of proteins in the congeneric mussels *M. trossulus* and *M. galloprovincialis*: evidence from the heat shock response and protein ubiquitination. *Mar. Biol.* **126**: 65–75.
- Krebs, R. A., and M. E. Feder. 1998.** Hsp70 and larval thermotolerance in *Drosophila melanogaster*: How much is enough, and when is more, too much? *J. Insect Physiol.* **44**: 1091–1101.
- Langdon, C., F. Evans, D. Jacobson, and M. Blouin. 2003.** Improved family yields of Pacific oysters *Crassostrea gigas* (Thunberg) derived from selected parents. *Aquaculture* **220**: 227–244.
- Launey, S., and D. Hedgecock. 2001.** High genetic load in the Pacific oyster *Crassostrea gigas*. *Genetics* **159**: 255–265.
- Lerman, D. N., and M. E. Feder. 2001.** Laboratory selection at different temperatures modifies heat-shock transcription factor (HSF) activation in *Drosophila melanogaster*. *J. Exp. Biol.* **204**: 315–323.
- Lindquist, S. 1986.** The heat shock response. *Annu. Rev. Biochem.* **55**: 1151–1191.
- Michener, W. K., and P. D. Kenny. 1991.** Spatial and temporal patterns of *Crassostrea virginica* (Gmelin) recruitment: relationship to scale and substratum. *J. Exp. Mar. Biol. Ecol.* **154**: 97–122.
- Morimoto, R. I., A. Tissieres, and C. Georgopoulos, eds. 1994.** *The Biology of Heat Shock Proteins and Molecular Chaperones*. Cold Spring Harbor Laboratory Press, Plainview, NY.
- Parsell, D. A., and S. Lindquist. 1994.** Heat shock proteins and stress tolerance. Pp. 457–494 in *The Biology of Heat Shock Proteins and Molecular Chaperones*, R.I. Morimoto, A. Tissieres, and C. Georgopoulos, eds. Cold Spring Harbor Laboratory Press, Plainview, NY.
- Roberts, D. A., G. E. Hofman, and G. N. Somero. 1997.** Heat-shock protein expression in *Mytilus californianus*: Acclimatization (seasonal and tidal-height comparisons) and acclimation effects. *Biol. Bull.* **192**: 309–320.
- Somero, G. N. 1995.** Proteins and temperature. *Annu. Rev. Physiol.* **57**: 43–68.
- Spees, J. L., S. A. Chang, M. J. Snyder, and E. S. Chang. 2002.** Thermal acclimation and stress in the American lobster, *Homarus americanus*: equivalent temperature shifts elicit unique gene expression patterns for molecular chaperones and polyubiquitin. *Cell Stress Chaperones* **7**: 97–106.
- Tomanek, L., and G. N. Somero. 1999.** Evolutionary and acclimation-induced variation in the heat-shock responses of congeneric marine snails (Genus *Tegula*) from different thermal habitats: implications for limits of thermotolerance and biogeography. *J. Exp. Biol.* **202**: 2925–2936.
- Tomanek, L., and G. Somero. 2002.** Interspecific- and acclimation-induced variation in levels of heat-shock proteins 70 (hsp 70) and 90 (hsp 90) and heat-shock transcription factor-1 (HSF 1) in congeneric marine snails (genus *Tegula*): implications for regulation of hsp gene expression. *J. Exp. Biol.* **205**: 677–685.



*Reports of Papers Presented at*  
THE GENERAL SCIENTIFIC MEETINGS  
OF THE MARINE BIOLOGICAL LABORATORY,  
Woods Hole, Massachusetts  
11 to 13 August 2003

*Program Chairs:*

KAREN CRAWFORD, St. Mary's College of Maryland  
ROBERT GOULD, New York State Institute for Basic Research  
ROBERT PAUL MALCHOW, University of Illinois at Chicago  
JOSEPH VALLINO, The Ecosystems Center, MBL

---

Each of these reports was reviewed by two members of a special editorial board  
drawn from the research community of Woods Hole, Massachusetts.

Reviewers included scientists from  
THE MARINE BIOLOGICAL LABORATORY  
AND THE WOODS HOLE OCEANOGRAPHIC INSTITUTION



## SHORT REPORTS FROM THE 2003 GENERAL SCIENTIFIC MEETINGS OF THE MARINE BIOLOGICAL LABORATORY

<b>The Editor</b>	
The MBL Awards for 2003 . . . . .	175
<i>DEVELOPMENTAL BIOLOGY</i>	
<b>Gilland, Edwin, Robert Baker, and Winfried Denk</b>	
Long duration three-dimensional imaging of calcium waves in zebrafish using multiphoton fluorescence microscopy. . . . .	176
<b>Gileadi, Opher, and Alon Sabban</b>	
Squid sperm to clam eggs: imaging wet samples in a scanning electron microscope. . . . .	177
<b>Wadeson, P. H., and K. Crawford</b>	
Formation of the blastoderm and yolk syncytial layer in early squid development. . . . .	179
<b>Crawford, K.</b>	
Lithium chloride inhibits development along the animal vegetal axis and anterior midline of the squid embryo . . . . .	181
<b>Hill, Susan D., and Barbara C. Boyer</b>	
HNK-1/N-CAM immunoreactivity correlates with ciliary patterns during development of the polychaete <i>Capitella</i> sp. 1 . . . . .	182
<i>CELL BIOLOGY</i>	
<b>Heck, D. E., and J. D. Laskin</b>	
Ryanodine-sensitive calcium flux regulates motility of <i>Arbacia punctulata</i> sperm . . . . .	185
<b>Gallant, P. E.</b>	
Axotomy inhibits the slow axonal transport of tubulin in the squid giant axon. . . . .	187
<b>Delacruz, John, Jeremiah R. Brown, and George M. Langford</b>	
Interactions between recombinant conventional squid kinesin and native myosin-V . . . . .	188
<b>DeSelm, Carl J., Jeremiah R. Brown, Renne Lu, and George M. Langford</b>	
Rab-GDI inhibits myosin V-dependent vesicle transport in squid giant axon . . . . .	190
<b>Pielak, R. M., V. A. Gaysinskaya, and W. D. Cohen</b>	
Cytoskeletal events preceding polar body formation in activated <i>Spisula</i> eggs. . . . .	192
<b>Shribak, Michael, and Rudolf Oldenbourg</b>	
Three-dimensional birefringence distribution in reconstituted asters of <i>Spisula</i> oocytes revealed by scanned aperture polarized light microscopy . . . . .	194
<b>Wöllert, Torsten, Ana S. DePina, Carl J. DeSelm, and George M. Langford</b>	
Rho-kinase is required for myosin-II-mediated vesicle transport during M-phase in extracts of clam oocytes. . . . .	195
<b>Cusato, K., J. Zakevicius, and H. Ripps</b>	
An experimental approach to the study of gap-junction-mediated cell death . . . . .	197
<b>Tepsuporn, S., J. C. Kaltenbach, W. J. Kuhns, M. M. Burger, and X. Fernández-Busquets</b>	
Apoptosis in <i>Microciona prolifera</i> allografts . . . . .	199
<b>Armstrong, Peter B., and Margaret T. Armstrong</b>	
The decorated clot: binding of agents of the innate immune system to the fibrils of the <i>Limulus</i> blood clot. . . . .	201
<b>Isakova, Victoria, and Peter B. Armstrong</b>	
Imprisonment in a death-row cell: the fates of microbes entrapped in the <i>Limulus</i> blood clot . . . . .	203
<b>Harrington, John M., and Peter B. Armstrong</b>	
A liposome-permeating activity from the surface of the carapace of the American horseshoe crab, <i>Limulus polyphemus</i> . . . . .	205
<i>NEUROBIOLOGY AND BEHAVIOR</i>	
<b>Bogorff, Daniel J., Mark A. Messerli, Robert P. Malchow, and Peter J. S. Smith</b>	
Development and characterization of a self-referencing glutamate-selective micro-biosensor . . . . .	207
<b>Chappell, R. L., J. Zakevicius, and H. Ripps</b>	
Zinc modulation of hemichannel currents in <i>Xenopus</i> oocytes. . . . .	209
<b>Zottoli, S. J., O. T. Burton, J. A. Chambers, R. Eseh, L. M. Gutiérrez, and M. M. Kron</b>	
Transient use of tricaine to remove the telencephalon has no residual effects on physiological recordings of supramedullary/dorsal neurons of the cunner, <i>Tautoglabrus adspersus</i> . . . . .	211
<b>Redenti, S., and R. L. Chappell</b>	
Zinc chelation enhances the sensitivity of the ERG b-wave in dark-adapted skate retina . . . . .	213
<b>Molina, Anthony J. A., Katherine Hammar, Richard Sanger, Peter J. S. Smith, and Robert P. Malchow</b>	
Intracellular release of caged calcium in skate horizontal cells using fine optical fibers . . . . .	215
<b>Palmer, L. M., B. A. Giuffrida, and A. F. Mensinger</b>	
Neural recordings from the lateral line in free-swimming toadfish, <i>Opsanus tau</i> . . . . .	216

**Child, F. M., H. T. Epstein, A. M. Kuzirian, and D. L. Alkon**  
 Memory reconsolidation in *Hermisenda* . . . . . 218

**Kuzirian, A. M., F. M. Child, H. T. Epstein, M. E. Motta, C. E. Oldenberg, and D. L. Alkon**  
 Training alone, not the tripeptide RGD, modulates calcitonin in *Hermisenda* . . . . . 220

**Savage, Anna, and Jelle Atema**  
 Neurochemical modulation of behavioral response to chemical stimuli in *Homarus americanus* . . . . . 222

**Mann, K. D., E. R. Turnell, J. Atema, and G. Gerlach**  
 Kin recognition in juvenile zebrafish (*Danio rerio*) based on olfactory cues . . . . . 224

**Turnell, E. R., K. D. Mann, G. G. Rosenthal, and G. Gerlach**  
 Mate choice in zebrafish (*Danio rerio*) analyzed with video-stimulus techniques . . . . . 225

MOLECULAR BIOLOGY, PATHOLOGY, AND MICROBIOLOGY

**Roberts, S. B., and F. W. Goetz**  
 Expressed sequence tag analysis of genes expressed in the bay scallop, *Argopecten irradians*. . . . . 227

**Hsu, A. C., and R. M. Smolowitz**  
 Scanning electron microscopy investigation of epizootic lobster shell disease in *Homarus americanus* . . . . . 228

**Orchard, Elizabeth, Eric Webb, and Sonya Dyhrman**  
 Characterization of phosphorus-regulated genes in *Trichodesmium* spp. . . . . 230

**Galac, Madeline, Deana Erdner, Donald M. Anderson, and Sonya Dyhrman**  
 Molecular quantification of toxic *Alexandrium fundyense* in the Gulf of Maine . . . . . 231

**Sangster, C. R., and R. M. Smolowitz**  
 Description of *Vibrio alginolyticus* infection in cultured *Sepia officinalis*, *Sepia apama*, and *Sepia pharaonis*. . . . . 233

**Baird, Krystal D., Hemant M. Chikarmane, Roxanna Smolowitz, and Kevin R. Uhlinger**  
 Detection of *Edwardsiella* infections in *Opsanus tau* by polymerase chain reaction. . . . . 235

**Weidner, Earl, and Ann Findley**  
 Catalase in microsporidian spores before and during discharge . . . . . 236

ECOLOGY AND POPULATION BIOLOGY

**Agnew, A. M., D. H. Shull, and R. Buchsbaum**  
 Growth of a salt marsh invertebrate on several species of marsh grass detritus . . . . . 238

**Cavatorta, Jason R., Morgan Johnston, Charles Hopkinson, and Vinton Valentine**  
 Patterns of sedimentation in a salt marsh-dominated estuary . . . . . 239

**Thoms, T., A. E. Giblin, K. H. Foreman**  
 Multiple approaches to tracing nitrogen loss in the West Falmouth wastewater plume . . . . . 242

**Talbot, J. M., K. D. Kroeger, A. Rago, M. C. Allen, and M. A. Charette**  
 Nitrogen flux and speciation through the subterranean estuary of Waquoit Bay, Massachusetts. . . . . 244

**Abraham, D. M., M. A. Charette, M. C. Allen, A. Rago, and K. D. Kroeger**  
 Radiochemical estimates of submarine groundwater discharge to Waquoit Bay, Massachusetts . . . . . 246

**Johnston, M. E., J. R. Cavatorta, C. S. Hopkinson, and V. Valentine**  
 Importance of metabolism in the development of salt marsh ponds . . . . . 248

**Aguiar, A. B., J. A. Morgan, M. Teichberg, S. Fox, and I. Valiela**  
 Transplantation and isotopic evidence of the relative effects of ambient and internal nutrient supply on the growth of *Ulva lactuca*. . . . . 250

**Morgan, J. A., A. B. Aguiar, S. Fox, M. Teichberg, and I. Valiela**  
 Relative influence of grazing and nutrient supply on growth of the green macroalga *Ulva lactuca* in estuaries of Waquoit Bay, Massachusetts . . . . . 252

**O'Connell, C. W., S. P. Grady, A. S. Leschen, R. H. Carmichael, and I. Valiela**  
 Stable isotopic assessment of site loyalty and relationships between size and trophic position of the Atlantic horseshoe crab, *Limulus polyphemus*, within Cape Cod estuaries. . . . . 254

**Walker, C., E. Davidson, W. Kingerlee, and K. Savage**  
 Incubation conditions of forest soil yielding maximum dissolved organic nitrogen concentrations and minimal residual nitrate . . . . . 256

**Holden, M. T., C. Lippitt, R. G. Pontius, Jr., and C. Williams**  
 Building a database of historic land cover to detect landscape change . . . . . 257

ORAL PRESENTATIONS

Published by title only. . . . . 259

## The MBL Awards for 2003

MBL Awards are given for the best paper presented at the General Scientific Meetings by a senior investigator, a junior investigator, a graduate student, and an undergraduate. The awards are based on both the oral presentation and the short report, and additional papers are selected for Honorable Mention.

The four presentations selected for MBL Awards this year reflect the broad scope of science at the Laboratory. Among these reports, we find a classic vegetalizing agent used to study morphogenesis in squids, multiphoton fluorescence microscopy revealing complex, 3-D signaling events in zebrafish embryos, a dermal exudate that may keep the horseshoe crab's exoskeleton clean, and serotonin prolonging the response of lobsters to food odors. This year's awardees are listed below with the title of their presentation and the page on which their short report appears.

—The Editor  
August 2003

---

### Senior Investigator

- WINNER . . . . . Paul Gallant  
Axotomy inhibits the slow axonal transport of tubulin in the squid giant axon (p. 187)
- HONORABLE MENTION . . . . . Karen Crawford  
Lithium chloride inhibits development along the animal vegetal axis and anterior midline of the squid embryo (p. 181)

### Graduate Student

- WINNER . . . . . John M. Harrington  
with Peter B. Armstrong  
A liposome-permeating activity from the surface of the carapace of the American horseshoe crab, *Limulus polyphemus* (p. 205)
- HONORABLE MENTION . . . . . Anthony Molina  
with Katherine Hammar, Richard Sanger, Peter J. S. Smith, and Robert P. Malchow  
Intracellular release of caged calcium in skate horizontal cells using fine optical fibers (p. 215)
- HONORABLE MENTION . . . . . Cheryl Sangster  
with Roxanna Smolowitz  
Description of *Vibrio alginolyticus* infection in cultured *Sepia officinalis*, *Sepia apama*, and *Sepia pharaonis* (p. 233)

### Junior Investigator

- WINNER . . . . . Edwin Gilland  
with Robert Baker and Winfried Denk  
Long duration three-dimensional imaging of calcium waves in zebrafish using multiphoton fluorescence microscopy (p. 176)
- HONORABLE MENTION . . . . . Karen Cusato  
with Jane Zakevicius and Harris Ripps  
An experimental approach to the study of gap-junction-mediated cell death (p. 197)

### Undergraduate

- WINNER . . . . . Anna Savage  
with Jelle Atema  
Neurochemical modulation of behavioral response to chemical stimuli in *Homarus americanus* (p. 222)
  - HONORABLE MENTION . . . . . Danial Abraham  
with Matthew Charette, Matthew Allen, Adam Rago, and Kevin Kroeger  
Radiochemical estimates of submarine groundwater discharge to Waquoit Bay, Massachusetts (p. 246)
  - HONORABLE MENTION . . . . . Rafal Pielak  
with Valeriya Gaysinskaya and William Cohen  
Cytoskeletal events preceding polar body formation in activated *Spisula* eggs (p. 192)
-

Reference: *Biol. Bull.* 205: 176–177. (October 2003)  
© 2003 Marine Biological Laboratory

## Long Duration Three-Dimensional Imaging of Calcium Waves in Zebrafish Using Multiphoton Fluorescence Microscopy

Edwin Gilland<sup>1,\*</sup>, Robert Baker<sup>1</sup>, and Winfried Denk<sup>2</sup>

<sup>1</sup> NYU School of Medicine, New York, NY

<sup>2</sup> Max Plank Institute, Heidelberg, Germany

Both luminescent (1, 2) and fluorescent (2) reporters have been used to image periodic large-scale intercellular calcium waves that begin during zebrafish gastrulation, at about 65% epiboly, and continue for at least 12 hours. These waves arise every 5 to 10 min from a variety of locations and traverse the blastoderm margin and main body axis (1). During somitogenesis they appear as a series of pulses of elevated calcium levels centered on the tailbud region. The waves travel at approximately 5–10  $\mu\text{m}$  per s and thus fall into the category of fast calcium waves that likely propagate by a positive feedback mechanism involving calcium-induced calcium release from intracellular stores, possibly including diffusion of calcium or IP<sub>3</sub> through gap junctions (3). Likely targets of the waves include calcium-sensitive proteins involved in epiboly (3) and convergent extension (4), and others such as calreticulin that may play a role in the temporal regulation of nuclear receptor activity (5). Long-distance signaling by rhythmic calcium waves is an appealing mechanism for synchronizing calcium-triggered events throughout the embryo with high temporal precision. Since the zebrafish embryo is a roughly spherical body approximately 600  $\mu\text{m}$  in diameter, imaging these waves in a single optical plane, as in previous studies, can only approximate their three-dimensional trajectories. Moreover, other calcium signals that may be occurring at the same time, but in different optical planes within the embryo, cannot be documented. Ideally, free calcium levels should be imaged for many hours throughout the entire volume of the embryo at intervals shorter than the lifetimes of individual signaling events. Luminescent techniques require considerable temporal integration to achieve adequate spatial resolution and thus cannot approach this goal. Conversely, scanning laser microscopy using visible light has the necessary spatial and temporal resolution, but cannot be used for prolonged imaging at high sampling rates due to phototoxic damage to the embryo (E. Gilland, pers. obs.). The present study demonstrates that multiphoton fluorescence microscopy has the potential to achieve the goal of sampling calcium dynamics throughout the entire zebrafish embryo for long durations with sufficient spatial and temporal resolution to reveal complex three-dimensional signaling events.

Glass micropipettes with outside tip diameters of 7 to 10  $\mu\text{m}$  were used to pierce the chorion and inject zebrafish embryos (2- to 4-cell stages) with 1 to 2 nl of a 2% solution of Fluo-4 dextran (calcium K<sub>d</sub> = 3  $\mu\text{M}$ ; MW = 10 kDa; Molecular Probes) dissolved in 0.2 M KCl. The injections were made by a vegetal approach and placed into the dorsal half of the yolk mass. Dye was carried into the cytoplasm by diffusion and cytoplasmic streaming.

Embryos were injected while in 30% Danieau's solution (1) and then transferred to 10% Danieau's solution, placed into 1 mm diameter grooves in agarose-coated dishes, and maintained at 28 °C on a thermoelectric heating stage. Imaging was performed with a custom-built multiphoton fluorescence microscope using 890 nm excitation light from a 5-W Mira titanium-sapphire pulsed laser (Coherent) and a 20 $\times$ , wide aperture, infrared objective, N.A. 0.8 (Olympus). Embryos were imaged in a series of optical planes, either parasagittal, frontal, or horizontal, starting just below the surface of the embryo, with successive planes separated along the z axis by distances from 5 to 20  $\mu\text{m}$ , for total imaging depths of up to approximately 300  $\mu\text{m}$ . Scanning each image plane in a 256  $\times$  256 pixel pattern required 0.4 to 0.8 s, depending on the beam dwell time. In a typical experiment, a sequence of 15 optical slices was repeated every 14 s over 8 h. Collected image sequences were analyzed using the IDL (SRI) and ImageJ (NIH) software packages.

The experiments showed that the periodic increases in calcium levels seen in previous studies (1, 2) pass through all cellular regions of the embryo and, at later stages, through most or all of the yolk cell. Figure 1 shows data from an experiment in which 45 calcium waves were imaged over 4 h. Time lapse movies of the imaging sequences can be viewed on the *Biological Bulletin's* web site ([www.mbl.edu/BiologicalBulletin/VIDEO/BB.video.html](http://www.mbl.edu/BiologicalBulletin/VIDEO/BB.video.html)). Single images (X-Y) from different parasagittal optical planes during one imaging cycle (15 planes in 14.3 s) are shown in Figure 1, a–e. A plot of pixel values through time, for an area dorsal to the tailbud, shows calcium levels oscillating with a mean period of 315 s over many hours (Fig. 1f). As found in previous studies (1, 2), the strongest modulation of calcium levels was seen in the caudal half of the embryo centered around the region of the tail bud, with the brightest signals in the mesoderm, endoderm, and subjacent yolk syncytial layer. Since cellular densities and dye distribution (not shown) vary in different tissue layers, ratio imaging will be required to determine whether the greater intensities of signal in specific locations represent genuinely higher calcium levels. The movement of calcium waves through the embryo can be roughly assessed by eye in the time lapse movies, and more precisely, either by comparing the time coordinates of peaks at different X-Y-Z locations (not shown), or by reslicing an X-Y time series along a line in the X-Y plane (Fig. 1g). The calcium oscillations appear as light and dark bands in the resliced image, and the slopes of the bands indicate the direction of wave movement. In the case shown, most of the oscillations appeared earliest at dorsal and ventral locations, and latest at a region dorso-anterior to the tail bud, indicating that the waves were sweeping caudally

\* Corresponding author: [egilland@mbledu](mailto:egilland@mbledu)

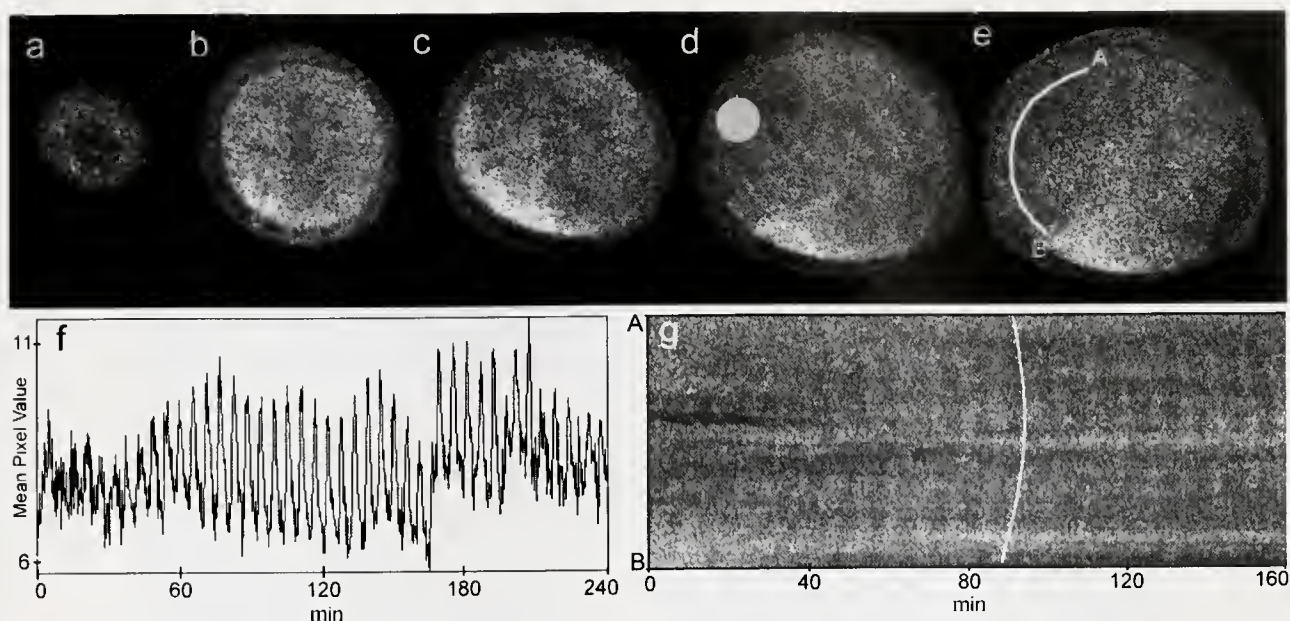


**Figure 1.** Lateral views of a 5-somite zebrafish embryo showing 5 parasagittal imaging planes (a–e). The planes are separated by 40  $\mu\text{m}$  and span a total of 200  $\mu\text{m}$  in depth. Plane (a) is nearest the surface of the embryo while plane (e) is nearest the midline. The time interval represented by (a–e) is near 200 min in (f). The circle in (d) shows a sampling area whose pixel intensity profile is shown in (f). The curved line in (e) indicates the path in the X-Y plane along which the data stack was re-sliced, as shown in (g). The white line in (g) shows the approximate time profile of one wave.

through the embryo towards the tail bud. Other waves showed the inverse pattern, *i.e.*, they started near the tail bud and traveled rostrally. The three-dimensional structure of the calcium waves hinted at by these initial experiments are far more complex than could be inferred from sequences imaged at single optical planes. To completely reconstruct the waves through space and time, the temporal phase of wave peak values must be quantified for all X-Y positions in all optical planes through the time series. Such analyses may provide further clues to the developmental role of the panembryonic calcium signaling system.

#### Literature Cited

- Gilland, E., A. Miller, E. Karplus, R. Baker, and S. Webb. 1999. *Proc. Natl. Acad. Sci. USA* **96**: 157–161.
- Webb, S., and A. Miller. 2003. *Zygote* **11**: 175–182.
- Webb, S., and A. Miller. 2003. *Nat. Rev. Mol. Cell. Biol.* **4**: 539–551.
- Wallingford, J., A. Ewald, R. Harland, and S. Fraser. 2001. *Curr. Biol.* **11**: 652–661.
- Holaska, J., B. Black, F. Rastinejad, and B. Paschal. 2002. *Mol. Cell. Biol.* **22**: 6286–6297.

**Reference:** *Biol. Bull.* **205**: 177–179, (October 2003)  
© 2003 Marine Biological Laboratory

## Squid Sperm to Clam Eggs: Imaging Wet Samples in a Scanning Electron Microscope

Opher Gileadi\* and Alon Sabban  
Quantomix Ltd., Rehovot, Israel

We introduce Wet SEM, a new imaging technology that allows electron microscopy of wet samples. The samples are placed in sealed specimen capsules and are separated from the vacuum in the microscope chamber by an impermeable, electron-transparent membrane. Imaging is performed in a standard scanning electron microscope (SEM) using a backscattered electron detector (BSE) (Fig. 1A). The technique is described in a pending patent application (1).

The Wet SEM technique presents, in many respects, a new imaging modality. First, the complete separation of the sample from the vacuum allows direct imaging of fully hydrated, whole-mount samples in an electron microscope operating at moderate beam energies. Such samples include primary or cultured animal cells, micro-organisms, plants, animal and human tissues, and a variety of fluid samples. Second, the use of backscattered electron detection and the elimination of charging allow the internal structure of cells to be visualized by scanning electron microscopy. This is in contrast with customary SEM imaging (using secondary electron detection), which is restricted to the surface. The depth of

\* Corresponding author: opher@quantomix.com

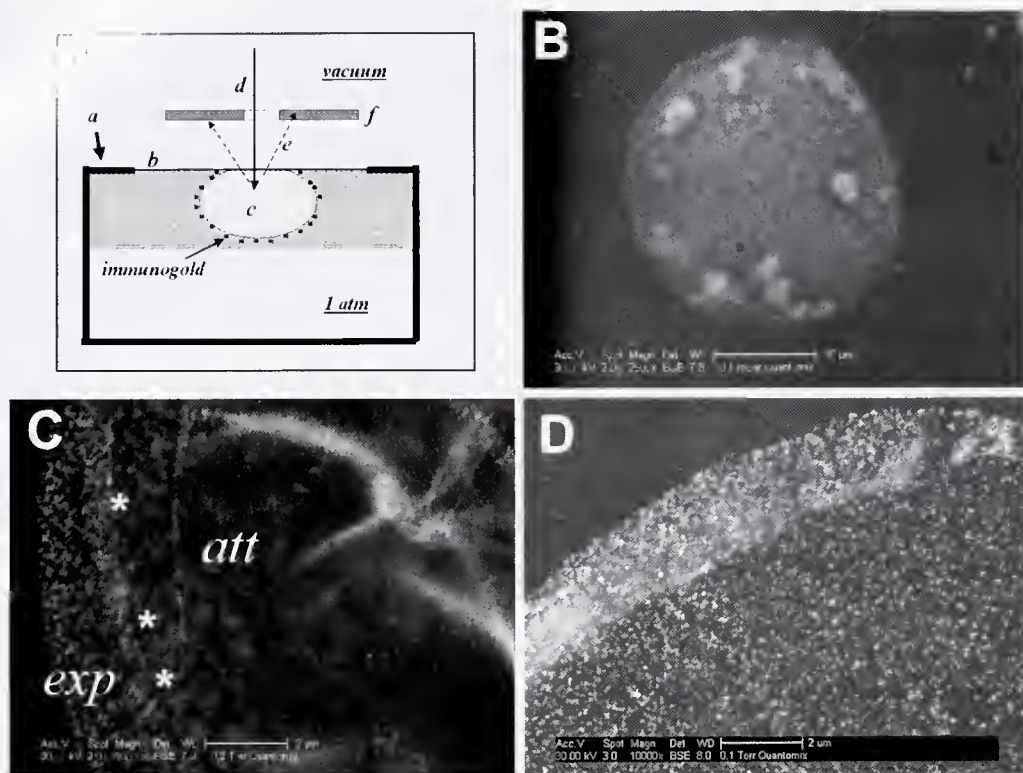


**Figure 1.** Wet SEM imaging of clam egg nuclei. (A) Schematic cross-sectional view of the capsule enclosing a sample. The generally rigid capsule (a) is topped by a window, covered by an electron-transparent partition membrane (b). The sample (c) is in close contact with the partition membrane. When placed in the evacuated chamber of a SEM, the sample is maintained in a wet state at atmospheric pressure. The microscopic image is obtained when the scanning electron beam (d) penetrates the partition membrane and interacts with the sample, and backscattered electrons (BSE) (e) are detected by a BSE detector (f). (B) Clam egg nucleus, adhering to the capsule's partition membrane, was stained with uranyl acetate and imaged in a wet state in a scanning electron microscope (FEI XL-30 ESEM-FEG). Bar = 10  $\mu\text{m}$ . (C) Clam egg nucleus, adhering to the capsule's partition membrane, labeled with anti-nuclear pore complex antibodies and 0.8-nm gold secondary antibodies, followed by silver enhancement. Bar = 2  $\mu\text{m}$ . (D) Clam egg nucleus, labeled as in (C) but with anti-lamin antibodies. Bar = 2  $\mu\text{m}$ .

the imaged layer is limited by the penetration of the beam electrons, and is estimated to be 2–3  $\mu\text{m}$ . Furthermore, the depth can be varied by changing the acceleration voltage of the electron beam (typically within the range of 10–30 keV), yielding three-dimensional information.

The method presents some additional beneficial features, some of which were not wholly anticipated. We obtain resolutions between 10–100 nm, an order of magnitude smaller than could be predicted from the volume of interaction of the electron beam with an aqueous sample. Contrast between materials of low atomic number, such as carbon and oxygen, can be readily detected. Thick samples, such as tissue biopsies, can be imaged without thin sectioning: only the top layer of up to 3  $\mu\text{m}$  is seen. Both the global and high-resolution distribution of colloidal gold labels on cells can be readily determined.

The Wet SEM is uniquely suitable for samples, including lipid-rich structures and hydrated gels, which are adversely affected by standard processes of dehydration that use organic solvents. The method has several practical advantages over standard EM techniques that derive from the simplicity of sample preparation; these advantages include the ability to process and image numerous samples, the ability to look at whole cells, the imaging of tissue

specimens (especially of epithelial tissues), and the imaging of myelin sheaths in neural tissue.

During our 2-month stay at the Marine Biological Laboratory, we have explored several applications of the technology with scientists and visitors. One example is shown in Figure 1. Clam egg nuclei were fixed in formaldehyde, then placed in the imaging capsule. A brief centrifugation (500  $\times$  g, 5 min) caused the nuclei to adhere stably to the poly-L-lysine-coated partition membrane, and all subsequent treatments were performed in the capsule.

Figure 1B shows a nucleus stained with uranyl acetate; the condensed chromosomes are clearly visible, as are the outline of the nucleus and diffusely stained nuclear proteins. The chromosomes seem to be surrounded by a dark "halo," the significance of which is not yet clear.

Figure 1C shows a portion of a nucleus stained with antibodies to the nuclear pore complex, followed by secondary antibodies that are conjugated to 0.8-nm colloidal gold particles. The silver-enhanced gold particles are visible as bright dots. Note the edge (asterisk) between the region of the nuclear membrane that is attached to the partition membrane of the capsule (*att*) and the region that is exposed to the solution (*exp*); the immunolabel, which recognizes the outer aspect of the nuclear pore, has bound

only the exposed region (as depicted in the schematic distribution of gold labels in Fig. 1A).

Figure 1D shows a portion of a nucleus stained with antibodies to lamin. Note that, in contrast to Figure 1C, the immunolabeling extends through the entire visible region of the nucleus. We attribute the difference to the location of lamin inside the nucleus, so access by labeling antibodies is not blocked by adhesion to the capsule's partition membrane.

These results show that the Wet SEM technique can derive meaningful information at high resolution from samples that were subjected to treatments comparable to those used to prepare for light microscopy.

This work was performed in collaboration with Yosef Gruenbaum of the Hebrew University and Robert Goldman of Northwestern University. The XL-30 scanning electron microscope was a generous loan from FEI Company, Peabody, MA.

### Literature Cited

1. Moses, E., O. Zik, and S. Thiberge. 2002. Device and method for the examination of samples in a non-vacuum environment using a scanning electron microscope. International patent application PCT/IL01/01108 published as WO02/45125. [Online] Available: <http://ep.espacenet.com/> [2003, August 25].

Reference: *Biol. Bull.* 205: 179–180. (October 2003)  
© 2003 Marine Biological Laboratory

## Formation of the Blastoderm and Yolk Syncytial Layer in Early Squid Development

P. H. Wadeson<sup>1,3</sup> and K. Crawford<sup>2,3,\*</sup>

<sup>1</sup> Rochester Institute of Technology, Rochester, NY

<sup>2</sup> St. Mary's College of Maryland, St. Mary's City, MD

<sup>3</sup> Marine Biological Laboratory, Woods Hole, MA

*You can observe a lot by watching.*

—Yogi Berra

Nearly all of what we know of cephalopod development has been drawn from live or fixed embryos collected from naturally laid jelly capsules (1, 2, 3). Many aspects of development—including pronuclear migration and cleavage (4), cytoplasmic and cellular movements (5), differentiation and organogenesis—would be better understood and more effectively compared to other embryos if examined in the living state. To begin this work, we have used time-lapse video microscopy to record the development of *in vitro*-fertilized squid embryos, *Loligo pealeii*, from early cleavage through the formation of the external yolk syncytial layer (YSL) and the early phase of epiboly. Adding the dimension of time to our analysis revealed new and intriguing elements in the development of this organism.

*In vitro*-fertilized squid embryos were prepared (6) and oriented for imaging in depressions made in 0.2% agarose (Sigma)-lined plastic petri dishes (Falcon) filled with Millipore (0.22  $\mu$ m) filtered seawater. Dishes of embryos were placed on a universal transmitted light illuminator with an adjustable reflector that allowed for bright field or oblique illumination, or a combination of the two. To minimize heat transfer, a KL 1500 constant-color-temperature fiber-optic source with an infrared filter was used to illuminate the specimen. A Zeiss Stemi SV 11 stereomicroscope with a 1.6 $\times$  Planapochromat lens was used for time-lapse imaging. An intermediate mount was placed between the lens and microscope body to align the light path with the center of the front lens, right

eyepiece, and camera. A computer-controlled Axiovision software program was used for image acquisition from an MRc5 Zeiss digital camera set to optimal resolution (2584  $\times$  1936). Digital images were collected at 5- or 7-min intervals at 21  $^{\circ}$ C for 2–12.5 h. Throughout these periods, embryos appeared to cleave and develop normally.

Ten separate time-lapse sessions were carried out and images from two are presented. In the first session, images were collected at 5-min intervals, from first cleavage through blastoderm formation; three of these images are presented in Fig. 1a–c. The first image was taken 8 h post-fertilization (hpf) after the fourth cleavage (Fig. 1a). Each cleavage furrow is numbered in the order of its occurrence, and the polar bodies (pb and arrow) are visible resting in the first cleavage furrow. The larger blastomeres, formed by the unequal third cleavage furrow characteristic of cephalopod embryos (1), identify the future anterior midline of the embryo. The second image (Fig. 1b) was taken 9.6 hpf at sixth cleavage (arrowhead). This cleavage separates the central blastomeres from the outer syncytial layer of the embryo, which is continuous with the yolk cell. The final image (Fig. 1c) was taken 16.25 hpf and reveals a well-defined blastoderm surrounded by radiating clusters of cells, the outermost of which are continuous with the yolk cell. The boundary created at sixth cleavage (arrowhead) remains well preserved.

In the second session, images were collected at 7-min intervals, from blastoderm formation to the onset of epiboly, 26–27.5 hpf; three of these images are presented in Fig. 1d–f. At 26 hpf, the boundary formed at sixth cleavage has become more distinct, as cells have moved into the blastoderm; and pairs or small clusters of sister blastomeres formed during earlier cleavages radiate

\* Corresponding author: [kcrawford@smcm.edu](mailto:kcrawford@smcm.edu)

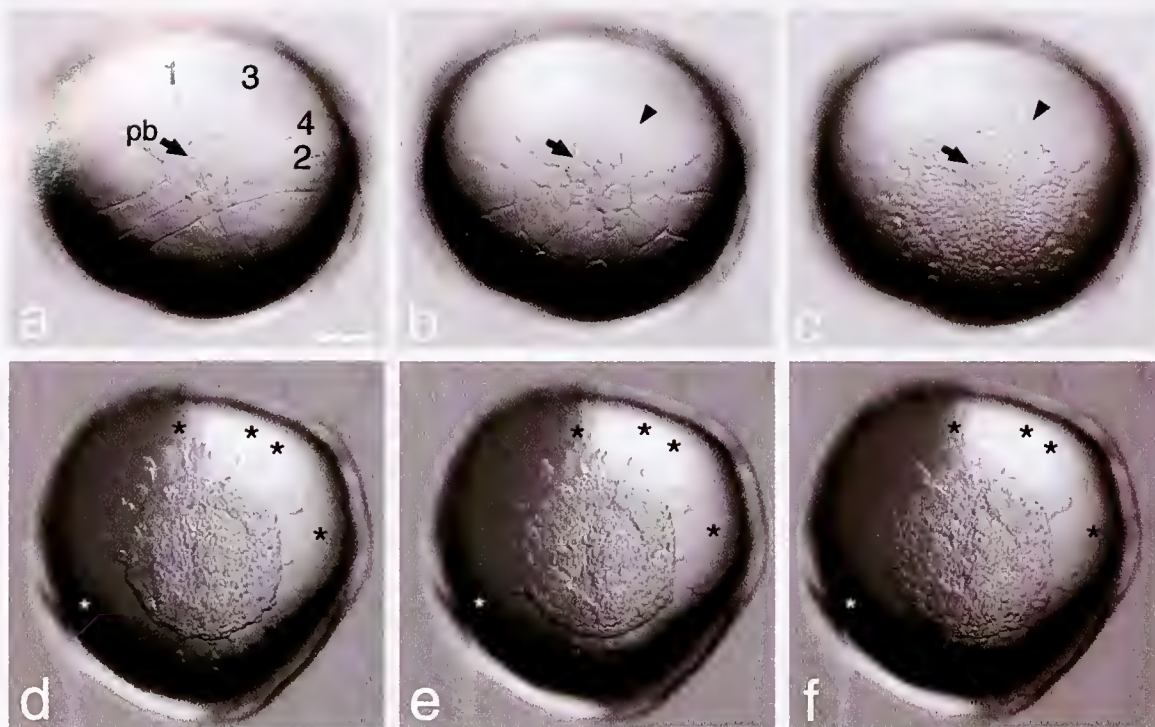


**Figure 1.** Images of developing squid embryos selected from two time-lapse sessions. (a, b, c) Early cleavage through blastoderm formation, 4–16.5 h post-fertilization (hpf); an arrow indicates the polar bodies (pb) in each panel in this session. (a) Fourth cleavage, 8 hpf. (b) Sixth cleavage (arrowhead), 9.6 hpf. (c) Blastoderm formation, 16.25 hpf. The boundary created at sixth cleavage (arrowhead) is well preserved at this stage of development. (d, e, f) Blastoderm formation to the onset of epiboly, 26–27.5 hpf. (d) A distinct blastoderm with radiating pairs or clusters (\*) of outer blastomeres, 26 hpf. (e) Blastoderm, 26.7 hpf; the inner blastomeres from each marked pair have migrated toward the developing blastoderm while their outer sister cells and the one lone cell simultaneously collapse into the cytoplasmic cortex of the yolk cell. (f) Blastoderm, 27.5 hpf; the migrating inner blastomeres have reached the blastoderm while their outer sister cells are no longer visible. Scale bar = 200  $\mu$ m. For further description, see text.

**Video Note.** Supplementary video clips are available for viewing on The Biological Bulletin web site at [<http://www.mbl.edu/BiologicalBulletin/VIDEO/BB.video.html>].

around the blastoderm. An asterisk (\*) has been placed by each of four pairs of these radiating sister blastomeres, in addition to one lone cell (Fig. 1d). By 26.7 hpf, the inner blastomeres from each marked pair have migrated toward the developing blastoderm, while their outer sister cells simultaneously collapse, a cell behavior first described by J. P. Trinkaus in fish (7), into the cortex of the yolk cell (Fig. 1e). One hour later, the migrating inner blastomeres have reached the blastoderm, while the nuclei of their outer sister cells have entered the yolk cell, contributing to the yolk syncytium (Fig. 1f).

In teleosts, the YSL is critical to patterning and development (7, 8), and time-lapse video analysis has played an important role in our understanding of this model system (9). As in squid, the YSL separates the yolk from the embryo and regulates the transfer of all nutrients and factors present within the yolk to the developing embryo. Formation of this important layer involves the collapse of blastomeres at the boundary between the developing blastoderm and the yolk cell cytoplasm. That cephalopods form their YSL through similar developmental mechanisms to those of teleosts exemplifies the fundamental similarities that exist between embryos faced with similar structural constraints and highlights the importance and need for further comparative study.

This work was made possible by support from a Faculty Development Grant and the Aldom-Plansoen Distinguished Endowed Professorship in Contemporary Studies to K.C. from St. Mary's College of Maryland. K.C. is most grateful to Bill Eckberg, Howard University, who graciously provided laboratory space, collaborative guidance, and digital imaging assistance. We thank Rudi Rottenfusser, MBL Zeiss representative, for allowing his summer intern (P.H.W.) to participate in this work. Finally, K.C. wishes to thank J.P. Trinkaus and his many students for reminding us to "watch."

### Literature Cited

1. Brooks, W. K. 1880. *Anniv. Mem. Boston Soc. N.H.* 1–22.
2. Arnold, J. M. 1965. *Biol. Bull.* 128: 24–32.
3. Segawa, S., W. T. Yang, H.-J. Marthy, and R. T. Hanlon. 1988. *Veliger* 30: 230–243.
4. Crawford, K. 2000. *Biol. Bull.* 199: 207–208.
5. Crawford, K. 2001. *Biol. Bull.* 201: 251–252.
6. Crawford, K. 2002. *Biol. Bull.* 203: 216–217.
7. Trinkaus, J. P. 1993. *J. Exp. Zool.* 265: 258–284.
8. Trinkaus, J. P. 1996. *Dev. Biol.* 177: 356–370.
9. Concha, M. L., and R. J. Adams. 1998. *Development* 125: 983–994.

Reference: *Biol. Bull.* **205**: 181–182, (October 2003)  
 © 2003 Marine Biological Laboratory

## Lithium Chloride Inhibits Development Along the Animal Vegetal Axis and Anterior Midline of the Squid Embryo

K. Crawford

*St. Mary's College of Maryland, MD  
 Marine Biological Laboratory, Woods Hole, MA*

When squid embryos, *Loligo pealeii*, are cultured *in vitro* (1) they may be individually manipulated with classic and molecular techniques, providing insights into the conservation of developmental pathways. Dorsoventral polarity in many embryos is associated with precise gene transduction cascades involving the Wnt signaling pathway (2). Results from experiments with frog (3), fish (4), and mouse (5) embryos suggest that a component of this cascade,  $\beta$ -catenin, plays a major role in axis formation. Additional support for the role of  $\beta$ -catenin in the early development of many embryos comes from studies using lithium chloride (LiCl). LiCl is a known vegetalizing agent for sea urchins (6), and in echinoderms generally, it enhances and expands levels and regions of nuclear  $\beta$ -catenin localization coincident with increases in endoderm and mesoderm (7, 8). In contrast, its effect on amphibian embryos is species- and stage-specific. For example, when gastrulating embryos are treated with LiCl, they develop reduced notochords and enhanced vegetal structures, but when treatments are given at earlier or later cleavage stages, dorsalizing and anteriorizing effects, respectively, are observed (3, 9). In this study, embryos cultured *in vitro* were treated with lithium chloride to determine its effect on development; this is the first step towards understanding the molecular mechanisms of patterning in squid.

Embryos were fertilized *in vitro* (1) and cultured at 17 °C in 60-mm plastic petri dishes (Falcon) that were lined with 0.2% agarose (Type II-A, Sigma), filled with Millipore (0.22  $\mu$ M) filtered seawater (MFSW), and supplemented with bovine serum albumin (BSA) (0.5%). Each LiCl treatment dish also contained 20, 40, or 60 mM LiCl (Sigma). Three trials of 15 embryos per treatment were performed. Dishes and solutions were changed every other day. Embryos were treated with LiCl for the first 6 d of development, by which time epiboly of the outer yolk cell was complete. Development was observed until the control embryos began to hatch from their chorions, at 19–20 d after fertilization. The classical stages of J. M. Arnold (10) were used to describe embryonic development. Embryos cultured in the presence of LiCl exhibited a dosage-dependent inhibition of development that was evident by 6 d in culture (Fig. 1a, b, 6 d post-fertilization (dpf), stage 18), but it was more easily detected later, during organogenesis (Fig. 1d, e, f, 17 dpf, stage 27). Development was inhibited in many structures normally associated with ectodermal tissues, such as tentacles, eyes, mantle, fins, and funnel. Moreover, convergence and inhibition of anterior midline structures was observed in embryos treated with 40 and 60 mM LiCl. In one trial, for example,

8 of 16 embryos cultured in the presence of 60 mM LiCl had anterior midline structures that were inhibited. As a result, the eyes were abnormally placed: either converged (5/16, Fig. 1f), fused (2/16), or cyclopic (1/16). In contrast, structures that normally form on the posterior body wall such as the funnel or paired statocysts, although reduced, were always present in these embryos. These observations suggest that various regions in the embryo are differentially sensitive to LiCl treatment.

Lithium chloride treatment inhibits development along the animal-vegetal axis in the squid embryo and causes convergence and fusion of anterior cephalic structures. This result is consistent with the notion that LiCl treatment induces vegetalization of the squid embryo and thereby enhances mesodermal and endodermal structures at the expense of ectodermal derivatives, as it does in other invertebrate and vertebrate embryos (3, 6, 7, 8, 9). That LiCl treatment may induce convergence, fusion, and cyclopia in squid embryos strengthens this interpretation (see 11 for a survey of the early literature on cyclopia produced by experimental means) and provides insights into the possible conservation of developmental mechanisms in cephalopods.

This work was made possible by support from a Faculty Development Grant and the Aldom-Plansoen Distinguished Endowed Professorship in Contemporary Studies to K.C. from St. Mary's College of Maryland. K.C. is most grateful to Bill Eckberg, Howard University, who graciously provided laboratory space, collaborative guidance, and digital imaging assistance.

### Literature Cited

1. Crawford, K. 2002. *Biol. Bull.* **203**: 216–217.
2. Sokol, S., J. L. Christian, R. T. Moon, and D. A. Melton. 1991. *Cell* **67**: 741–752.
3. Schneider, S., H. Steinbeisser, R. M. Warga, and P. Hausen. 1996. *Mech. Dev.* **57**: 191–198.
4. Haegel, H., L. Larue, M. Ohsugi, L. Fedorov, K. Herrenknecht, and R. Kemler. 1995. *Development* **121**: 3529–3537.
5. Kelly, G. M., D. F. Erezylimaz, and R. T. Moon. 1995. *Mech. Dev.* **53**: 261–273.
6. Lallier, R. 1975. Pp. 473–507 in *The Sea Urchin Embryo: Biochemistry and Morphogenesis*, G. Czihak, ed. Springer, New York.
7. Logan, C. Y., J. R. Miller, M. J. Ferdowicz, and D. R. McClay. 1999. *Development* **126**: 345–357.
8. Kitazawa, C., and S. Amemiya. 2001. *Dev. Growth Differ.* **43**: 73–82.
9. Kao, K. R., and R. P. Elinson. 1989. *Dev. Biol.* **132**: 81–90.
10. Arnold, J. M. 1965. *Biol. Bull.* **128**: 24–32.
11. Rogers, K. T. 1963. *Dev. Biol.* **8**: 129–150.

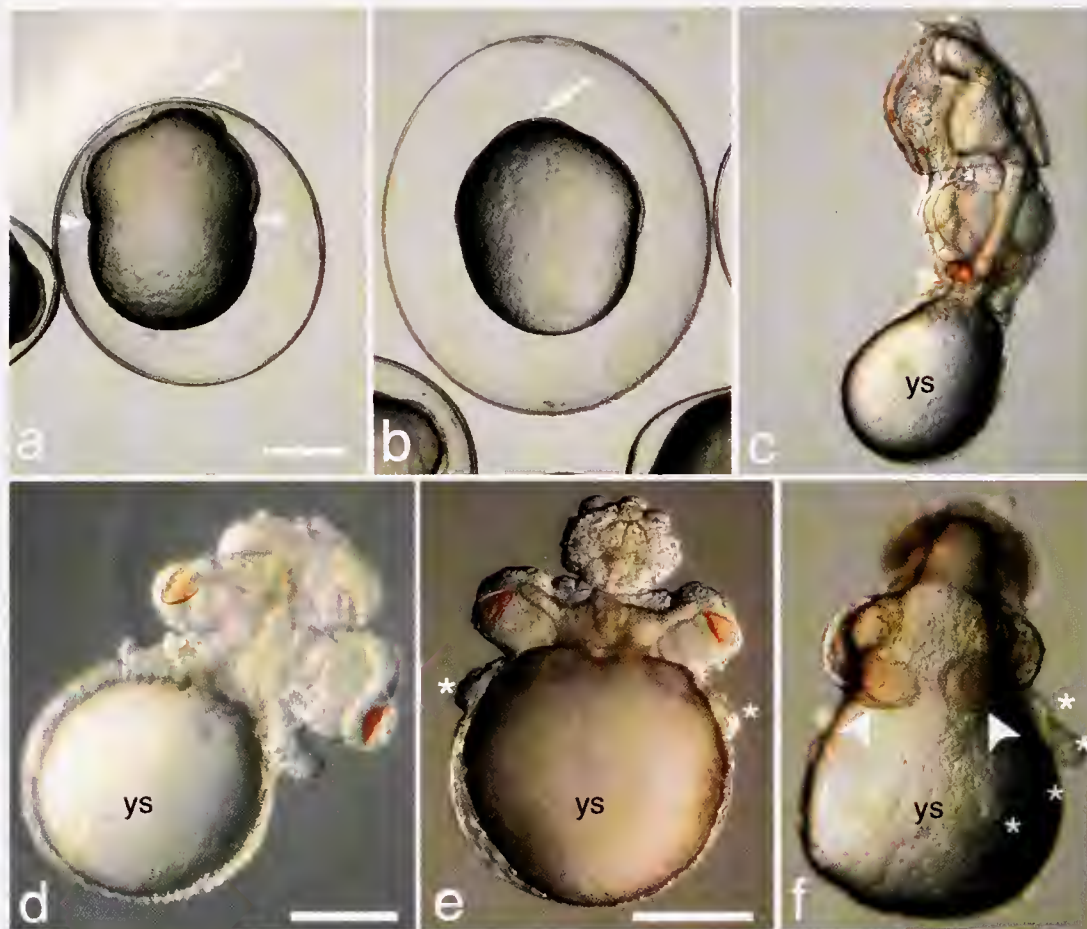


**Figure 1.** Lithium chloride inhibits the animal-vegetal body axis and normal organogenesis in squid embryos. (a) Control embryo, 6 days post-fertilization (dpf) stage 18; an arrow marks the developing tail bud. Note the well-defined indentation that indicates the boundary between the embryo and yolk sac (arrowheads). (b) Embryo treated with 20 mM LiCl, 6 dpf. The arrow indicates the developing tail bud. When compared to the control, this embryo is rounder and less well developed. (c and d) Embryos from control (side view), 17 dpf, stage 27, and 20 mM LiCl (anterior view) cultures, respectively. The mantle and body have failed to develop properly in the LiCl-treated embryo, although differentiation has occurred in the eyes and tentacles. (e) Anterior view of an embryo treated with 40 mM LiCl, 17 dpf. The mantle and organs within it are inhibited; eyes and tentacle primordia (\*) are present but poorly differentiated. (f) Embryo treated with 60 mM LiCl, 17 dpf. Large arrowheads indicate lightly pigmented eyes with lenses visible in their centers that have converged toward the anterior mid-line. An \* indicates each of the four tentacle primordia on the left side of the embryo. ys = yolk sac. a, b and c, and e and f are the same magnification. Scale bars = 500  $\mu$ m in each view.

Reference: *Biol. Bull.* **205**: 182–184. (October 2003)  
 © 2003 Marine Biological Laboratory

## HNK-1/N-CAM Immunoreactivity Correlates with Ciliary Patterns During Development of the Polychaete *Capitella* sp. I

Susan D. Hill<sup>1,\*</sup> and Barbara C. Boyer<sup>2</sup>

<sup>1</sup> Michigan State University, East Lansing, MI

<sup>2</sup> Union College, Schenectady, NY

*Capitella* sp. I is an opportunistic polychaete that is widespread and is among the early colonizers of disturbed areas that are high

in organic content. Larvae are lecithotrophic and are competent to settle within a few moments of emerging from the brood tube, although they can remain viable in the water column without feeding for two or three days if environmental cues for settling are not present. Under experimental conditions larvae demonstrate a

\* Corresponding author: hillss@msu.edu

notable ability to select the appropriate environment for settlement and metamorphosis (1, 2).

Fertilized eggs develop in a brood tube, emerging after eight or nine days as segmented, motile metatrochophores. The muscular framework that will be used by the juvenile worm after metamorphosis is already in place (3), but swimming is powered by two bands of cilia, an anterior prototroch, and a posterior telotroch. A large cluster of cilia, the neurotroch, is apparent on the ventral surface in scanning electron micrographs (4). These ciliary bands are not only important in locomotion, but may also have a chemosensory role in settlement and metamorphosis (5).

This study is part of an ongoing investigation of the interaction between nerves and muscles during development and its role in locomotion. We used a monoclonal antibody against HNK-1/N-CAM, which is expressed on neuroepithelial cells in early embryos (6), as a tool to follow neural development; we have found that it is also a marker of ciliary pattern formation in capitellid larvae. In the present study, HNK-1 antibody is used to visualize the sequence of ciliary development in *Capitella* sp. 1.

Capitellids were cultured in filtered seawater and mud in finger bowls (J. P. Grassle, pers. comm.), and brood tubes were collected. Larvae at different developmental stages were removed from the brood tubes and fixed in 4% formaldehyde in PBS. They were then permeabilized in acetone, treated with blocking serum, and incubated in anti-HNK-1/N-CAM (Molecular Probes). This was followed by incubation in a Texas red-labeled secondary antibody. Whole mount preparations were made and observed with an Olympus BX60 fluorescence microscope and imaged with an Olympus Magnifier digital camera (model S99860).

There is no evidence of HNK-1 reactivity during cleavage or gastrulation. If larvae are removed from the brood tube immediately after gastrulation, no locomotion or distinct morphological characteristics are visible. For a brief period before they begin to swim, the larvae are able to glide slowly over the substrate. Most of the changes in patterns of fluorescence occur as the larvae acquire swimming ability.

A positive reaction is first observed in nonmotile, postgastrula larvae several days prior to emergence from the brood tube. The label is seen in the developing prototrochal region in the form of a row of sparse fluorescent dots. This is followed by a small amount of punctate fluorescence in the perianal region and in the episphere, the region anterior to the prototroch, which will become the prostomium (Fig. 1a).

The fluorescent dots then become more numerous, delineating the prototrochal region and forming a slightly thickened band around the larva. Concurrently the punctate fluorescence, which at first seems to be randomly arranged, continues to appear in the episphere. In the pygidial region, posterior to the telotroch, scattered fluorescence is seen.

The width of the prototrochal band of fluorescence next increases significantly, although the posterior edge remains less defined than the anterior. The amount of label in the episphere

continues to increase. Antibody labeling reveals a distinct perianal ring and beginning organization of the pygidial region. In contrast to the labeled prototroch, there is not yet a distinct band of telotrochal label (Fig. 1b). At this stage the larvae are able to glide on the substrate.

After reaching its maximum width, the prototrochal fluorescence begins to recede towards the initial band, which is now prominently labeled. Concurrently the neurotroch becomes evident as a midventral mass of punctate fluorescence, with the densest reactivity just posterior to the stomodeum. Label in the pygidium is becoming dense and organized except in the dorsal region where there is no fluorescence. This reflects the ciliary patterns seen in scanning electron micrographs in which the dorsal area of the pygidium in the hatched larva is devoid of cilia (4). The telotroch is now prominently labeled, forming a band of fluorescence several dots wide (Fig. 1c). Although they have not yet emerged from the brood tube, the larvae are now capable of swimming.

Next, the anterior boundary of the prototroch remains lightly labeled, and some scattered fluorescence persists in the episphere. The neurotrochal labeling is greatly diminished, while the pygidial region and telotroch are heavily labeled (Fig. 1d). By this stage, the ciliary patterning appears to be complete.

The patterns of cilia in newly emerged metatrochophores of *Capitella* sp. 1 have been described by Eckelbarger and Grassle (4). These include well-developed prototrochal and telotrochal bands, and a distinct neurotroch—a midventral cluster of cilia beginning posterior to the prototroch and terminating a short distance anterior to the telotroch. There is no apical tuft, although there are scattered cilia and mucous glands in the episphere. Discrete rays of cilia radiate from the perianal ring toward the telotroch except in the dorsal area, which is free of cilia. Our labeling, which proceeds from anterior to posterior and corresponds to these patterns, indicates that the HNK-1/N-CAM protein is being expressed sequentially as the ciliary organization is laid down. We suggest that anti-HNK-1/N-CAM labeling may prove to be an important tool for studying the development of cilia.

This work was supported in part by Michigan State University and the Union College Faculty Research Fund. The authors gratefully acknowledge the generous assistance of Dr. William Eckberg in creating the figure.

### Literature Cited

1. Butman, C. A., J. P. Grassle, and C. M. Webb. 1988. *Nature* 333: 771–773.
2. Butman, C. A., and J. P. Grassle. 1992. *J. Mar. Res.* 50: 669–675.
3. Hill, S. D., and B. C. Boyer. 2001. *Biol. Bull.* 201: 257–258.
4. Eckelbarger, K. J., and J. P. Grassle. 1987. *Biol. Soc. Wash. Bull.* 7: 62–67.
5. Biggers, W. J., and H. Lanfer. 1999. *Biol. Bull.* 196: 187–198.
6. Kruse, J., R. Mailhammer, H. Wernecke, A. Faissner, I. Sommer, C. Goriadis, and M. Schachner. 1984. *Nature* 311: 153–155.

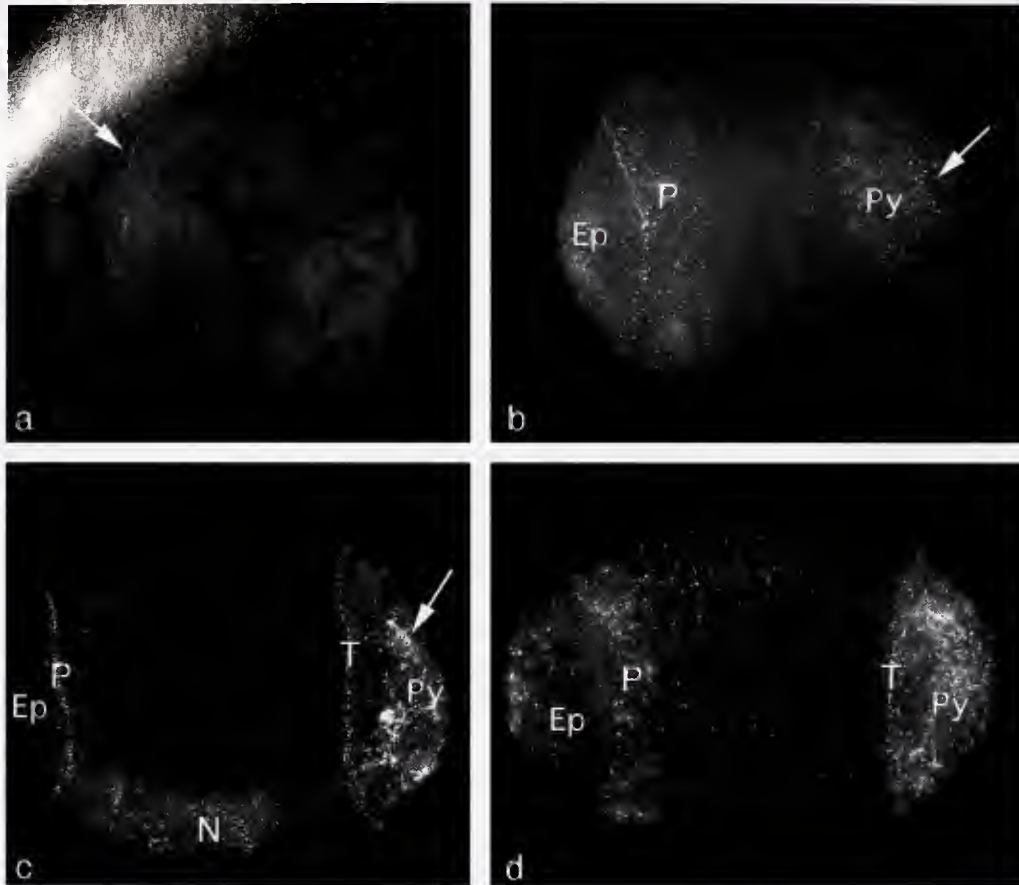


**Figure 1.** Whole mounts of developing *Capitella sp. 1* larvae showing labeling of developing ciliary bands. Anterior is to the left. Early embryos measure approximately  $240 \times 175 \mu\text{m}$ . As development proceeds they become more elongated without increasing in size. (a) The first HNK-1 expression is seen in the developing prototroch (arrow). (b) The wide prototrochal band is apparent. Note scattered fluorescence in the episphere. In the pygidial region a distinct perianal ring is labeled (arrow). (c) Labeling of the prototroch has narrowed and the ventral neurotroch and the telotroch are visible. Rays of fluorescence (arrow) extend from the perianal ring toward the telotroch except on the dorsal surface of the pygidium, which remains cilia-free. (d) Labeling is most prominent in the telotroch and pygidium. The prototroch continues to be lightly labeled. Ep, episphere; N, neurotroch; P, prototroch; Py, pygidial region; T, telotroch.

Reference: *Biol. Bull.* 205: 185–186. (October 2003)  
 © 2003 Marine Biological Laboratory

## Ryanodine-Sensitive Calcium Flux Regulates Motility of *Arbacia punctulata* Sperm

D. E. Heck<sup>1,\*</sup> and J. D. Laskin<sup>2</sup>

<sup>1</sup> Rutgers University, Piscataway, NJ

<sup>2</sup> UMDNJ-Robert Wood Johnson Medical School, Piscataway, NJ

The motility of sea urchin spermatozoa and the direction of their movement are due to the beat of the flagellum, which is controlled by an ion flux across the plasma membrane. When sea urchin sperm contact egg jelly, channels are activated that rapidly (<5 s) and transiently elevate intracellular calcium, initiating a cascade of events that lead to the sperm acrosome reaction (1–3). This process, in turn, induces a complex sequence of events that include protein phosphorylation and elevation of calcium levels thought to be dependent on intracellular calcium mobilization (4). Recent reports have identified ryanodine-gated intracellular calcium stores as critical for controlling the motility of mammalian sperm (5). In the present studies, we determined whether increases in intracellular calcium and motility in the sperm of the sea urchin *Arbacia punctulata* that are mediated by egg-derived products are also mediated by ryanodine-gated intracellular calcium stores.

In initial studies, we found that *Arbacia punctulata* egg-derived products (egg water) that stimulate sperm motility also increase sperm intracellular free calcium (Fig. 1, panel A). The increase was about 10-fold, occurred within 2 min, and persisted for at least 10 min. These experiments and all further experiments were repeated three times with similar results. The increase in intracellular calcium did not require calcium in the seawater, indicating that the ion was likely released from internal stores (data not shown). In further experiments, therefore, we used calcium-free seawater. Sperm motility and increases in intracellular free calcium were also found to be stimulated 2- to 3-fold by ryanodine (0.3–1  $\mu$ M) or caffeine (1–3  $\mu$ M), both agonists of ryanodine-gated ion channels (for reviews see refs. 5 and 6) (data not shown). We next examined the effects on sea urchin sperm of ruthenium red, a potent inhibitor of ryanodine-sensitive channel activity (6–8). We found that 1  $\mu$ M ruthenium red would inhibit the calcium mobilization and sperm motility initiated by egg water, or by ryanodine and caffeine (Fig. 1, panel C and not shown). Taken together, these data indicate that a ryanodine-sensitive calcium flux regulates the motility of *Arbacia punctulata* sperm.

Recent studies indicate that ryanodine receptors are regulated by nitric oxide-induced oxidation and reduction of critical sulfhydryl residues (9, 10). In previous studies, we and others have demonstrated that nitric oxide is also important in regulating motility in sea urchin sperm, and we have found further that this process is likely to be dependent on the activity of GTP-binding proteins (11–13). In these reports, sperm motility and nitric oxide production were inhibited by cholera toxin, and motility was recovered by

the addition of the nitric oxide/peroxynitrite-releasing drug 3-morpholinosydnonimine (SIN-1). We found that SIN-1 (1  $\mu$ M) also stimulated sperm calcium mobilization (Fig. 1, panel B). Increases in intracellular calcium were approximately 3- to 4-fold, persisted for at least 10 min, and were also independent of extracellular calcium. Motility and calcium mobilization induced by SIN-1 in *Arbacia punctulata* sperm were also found to be inhibited by ruthenium red (Fig. 1, panel D, and not shown). These data indicate that nitric oxide, like egg water, is effective at mobilizing intracellular calcium. Moreover, nitric oxide appears to function in sea urchin sperm upstream of ryanodine-sensitive calcium channels.

The lower panel in Figure 1 shows a schematic representation of events leading to the activation of *Arbacia punctulata* sperm. In this model, the interaction of the egg-derived mediator with sperm receptors activates the guanylate cyclase activity of the receptor, resulting in the formation of cGMP. The resulting cascade of events, including an intermediate calcium-induced release of sequestered intracellular calcium (“gray box”) that provokes the activity of high capacity sodium channels in the plasmalemma, ultimately culminates in motility. We hypothesize that nitric oxide, produced in response to enzymatic binding of calcium/calmodulin made available by the initial brief rise in intracellular calcium, interacts with ryanodine-gated ion channels to mediate the release of calcium from internal stores. We speculate that, in a manner similar to that of ryanodine-gated release of calcium from stores in mammalian skeletal muscles (7, 14), nitric oxide-mediated alterations to channel proteins are central to the prolonged and hyperactive motility of egg mediator-activated sperm.

### Literature Cited

1. Ward, G. E., D. L. Garbers, and V. D. Vacquier. 1985. *Science* 227: 768–770.
2. Schackmann, R. W., and P. B. Chock. 1986. *J. Biol. Chem.* 261: 8719–8728.
3. Su, Y. H., and V. D. Vacquier. 2002. *Proc. Natl. Acad. Sci. USA* 99: 6743–6748.
4. Schackmann, R. 1986. *Methods Cell Biol.* 27: 57–71.
5. Walensky, L. D., T. M. Dawson, J. P. Steiner, D. M. Sabatini, J. D. Suarez, G. R. Klinefelter, and S. H. Snyder. 1998. *Mol. Med.* 4: 502–514.
6. Ehrlich, B. E., E. Kaftan, S. Bezprozvannaya, and I. Bezprozvanny. 1994. *Trends Pharmacol. Sci.* 15: 145–149.
7. Salama, G., E. V. Menshikova, and J. J. Abramson. 2000. *Antioxid. Redox Signal.* 2: 5–16.
8. Ozawa, T. 2001. *Int. J. Mol. Med.* 7: 21–25.
9. Galione, A., and G. C. Churchill. 2002. *Cell Calcium* 32: 343–354.
10. Heck, D. E. 2001. *Antioxid. Redox Signal.* 3: 249–260.

\* Corresponding author: heck@cohsi.rutgers.edu

11. Heck, D. E., W. Tröll, and J. D. Laskin. 1996. *Biol. Bull.* **191**: 275–276.
12. Heck, D. E., W. Tröll, and J. D. Laskin. 1996. Pp. 16–17 in *The Biology of Nematodes*, V. S. Moncada, S. Gross, J. Stamler, and A. Higgs, eds. Academic Press, Portland, ME.
13. Herrero, J. B., E. de Lamirande, and C. Gagnon. 2003. *Curr. Pharm. T.* **9**: 419–425.
14. Sun, J., L. Xu, J. P. Eu, J. S. Stamler, and G. Meissner. 2003. *J. Biol. Chem.* **278**: 8184–8189.

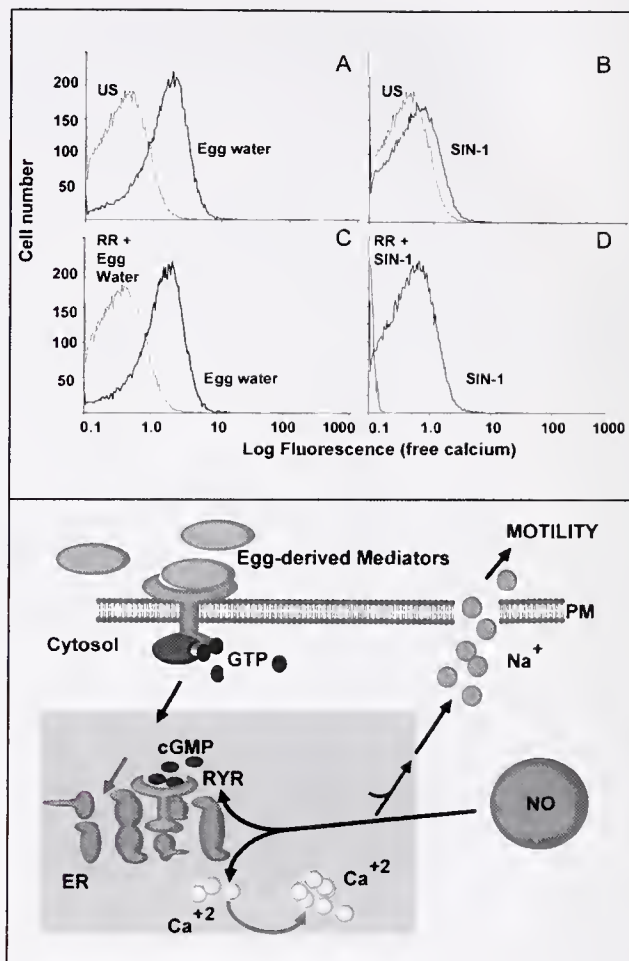


**Figure 1.** Effects of egg water and SIN-1 on calcium mobilization in sperm from the sea urchin *Arbacia punctulata*. Freshly isolated sea urchin sperm were incubated with the cell permeant calcium-sensitive fluorescent indicator fluo-4AM (Molecular Probes, Eugene, OR, 5  $\mu$ M, 10 min) and then stimulated with egg water (panels A and C) or SIN-1 (Molecular Probes, 1  $\mu$ M, panels B and D). After 3 min, intracellular levels of free calcium were analyzed using a Coulter EPICS flow cytometer (excitation wavelength 488 nm, emission wavelength 525 nm). Data are presented on a 4-decade log scale. US, unstimulated sperm. In experiments where cells were treated with ruthenium red, the sperm were first transiently permeabilized using a Live Cell Permeabilization Kit (Gibco, Grand Island, NY) to allow uptake of the compound (panels C and D). Note that sperm treated with ruthenium red failed to mobilize calcium in response to egg water or SIN-1 (panels C and D). (Lower panel): Schematic representation of events leading to activation of *Arbacia punctulata* sperm. Events originate with the binding of egg-derived mediators to their receptors on the surface of the sperm and progress through signaling to stimulate the release of calcium from internal stores. This release potentially involves protein interaction with intracellularly produced nitric oxide and presumably occurs within the endoplasmic reticulum, which mediates the opening of high-capacity sodium channels in the plasmalemma and ultimately leads to motility. PM, plasma membrane; RYR, ryanodine receptor; ER, endoplasmic reticulum; NO, nitric oxide.

Reference: *Biol. Bull.* 205: 187–188. (October 2003)  
© 2003 Marine Biological Laboratory

## Axotomy Inhibits the Slow Axonal Transport of Tubulin in the Squid Giant Axon

P. E. Gallant

National Institutes of Health, Bethesda, MD  
Marine Biological Laboratory, Woods Hole, MA

Slow axonal transport is essential to axonal growth and survival. In our previous work we demonstrated that many macromolecules, including fluorescently labeled tubulin, move slowly down the squid giant axon (1, 2). We (1, 2) and others (3) have proposed that the slow transport of tubulin might be due to the intermittent associations of axonal tubulin with a fast motor or motor-carrier complex. Since most rapidly moving axonal proteins, including this presumed rapidly moving tubulin carrier, should be continuously synthesized in neuronal cell bodies and transported down the axons (4), separating the axon from its cell bodies by axotomy should eventually reduce the amount of this hypothetical tubulin carrier, and thus inhibit tubulin transport.

To test this possibility, the lateral giant axon was transected, and tubulin transport was then assayed. For each experiment a squid (*Loliguncula brevis*, obtained most months of the year from the National Resource Center for Cephalopods, Galveston TX, or *Loligo pealeii*, obtained during May or October from the Marine Resource Center, Marine Biological Laboratory, Woods Hole, MA) was first anesthetized with 1% ethanol in seawater for about 5 min. The stellate ganglia were then located by eye through the mantle opening. A pair of Vannas micro-dissection scissors angled on the flat was inserted through the mantle opening, and one of the first lateral giant axons was transected (axotomized). The squid was then returned to a fresh seawater tank for 2 days. Squid were usually fed once a day for 2 days after return to the seawater tanks. After 2 days the squid was sacrificed, and the distal end of the transected lateral axon as well as the uncut control axon from the other side were removed, cleaned, and prepared for the slow transport assays. The air pressure system described previously (2) was used to inject both fluorescently labeled tubulin (Cytoskeleton, Inc.) and a marker oil drop into the control and transected axons. Axons were injected in the middle of the 2–4 cm isolated axons. Transport was visualized by recording the fluorescent image over time with a Zeiss microscope equipped with a Photometrics Cool Snap HQ camera driven by Openlab software (Improvision).

In the control axons ( $n = 6$ ), tubulin diffused while simultaneously being transported anterogradely (to the right in Fig. 1A). The injection site is marked by an arrowhead. As illustrated in Figure 1B, this anterograde tubulin transport was arrested 2 days after axotomy. The tubulin diffused in both directions away from the injection site (arrowhead) but was not transported anterogradely ( $n = 6$ ).

To determine whether the inhibition of tubulin transport after axotomy might be due to some nonspecific damage or degeneration of the isolated axon, a number of structural and biochemical tests of axonal health were performed. We have previously demonstrated that when a squid axon is damaged or becomes leaky, its light scattering increases, mitochondria become swollen, and its

cytoplasm becomes disorganized (5). Though most of these signs of damage could be seen at distances closer than 1 mm from the transection site (not shown), the rest of the 1–4 cm axons showed no signs of axonal damage. As illustrated in Figure 1 (compare C with D), no change in darkfield light scattering was detected in these or other transected axons ( $n = 12$ ); and as illustrated in Figure 1 (compare E with F), the cytoskeletal elements appeared normal in the transected axon, and the mitochondria were not swollen ( $n = 10$ ).

Since protein loss in general, and neurofilament proteolysis in particular (6), are sensitive indicators of axonal damage in squid as well as in other axons, we compared the levels of neurofilament and other axonal proteins in transected and control axons. Total protein was measured as follows: Equal lengths (from 1–4 cm in different squids) of an axotomized axon and its paired control were excised in calcium-free seawater. The isolated axon was then dissolved in solubilization buffer (2% SDS, 2% BME, 8 M urea, Tris pH 6.8), and the solubilized proteins were separated by 7.5% PAGE. To measure changes in total axonal proteins, the separated proteins were stained with Ruby protein stain (Molecular Probes). A dilution series of control axons was run with each experiment to verify that optical density was linearly related to protein concentration in each run (not shown). As illustrated in Figure 1G, axotomy produced no changes in neurofilament (NF200 and NF60), tubulin, or any other major axonal protein. Equal lengths of control (1c) and transected (1t) axons from the same squid (squid 1) had virtually identical protein-staining profiles. Smaller paired axons from a smaller squid (squid 2) had proportionately less protein (2c and 2t), but there was no visible difference in protein levels between the control axon (2c) and the previously transected axon (2t) in this or other squids tested ( $n = 6$ ).

To determine if the loss of conventional kinesin might be responsible for the loss of slow tubulin transport (3), we measured kinesin levels in the control and transected axons. Since conventional kinesin and other potential motors are minor constituents of axoplasm, Ruby protein stain would not detect these protein. To measure the kinesin levels, axons were cut, cleaned, dissolved, and run on PAGE as above. The PAGE-separated proteins were then transferred onto PVDF paper by western blotting in Tris-glycine buffer, and exposed to an anti-kinesin antibody (3) (Chemicon MAB 1614). The amount of antibody was detected with chemiluminescence. As with the protein measurements, axoplasm standards were run to insure that the recorded optical densities varied linearly with kinesin concentration. As illustrated in Figure 1H (Kinesin), there was no significant difference in kinesin levels between the control and the transected axon in either squid 1 (compare 1c with 1t) or squid 2 (compare 2c with 2t) or with any other animals tested ( $n = 9$ ).

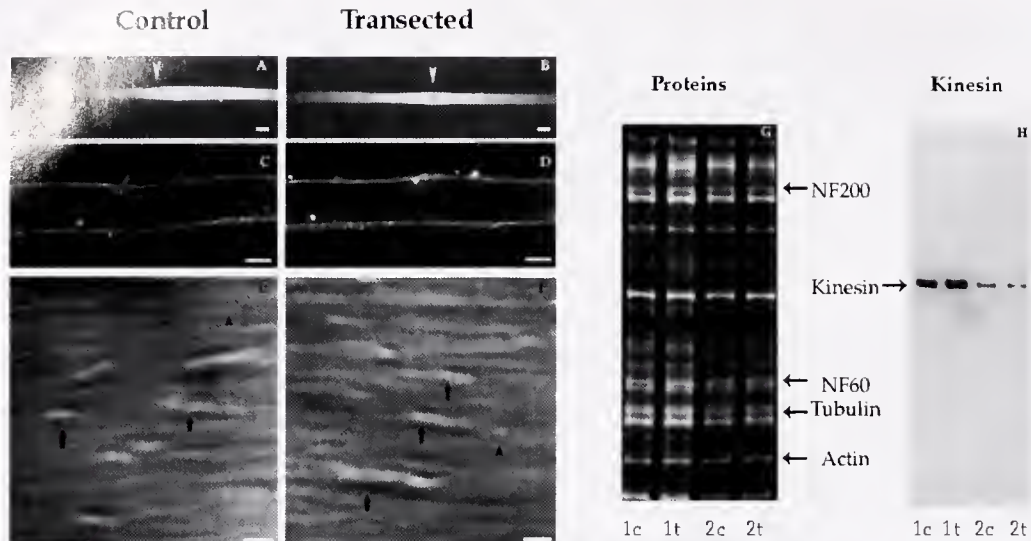


**Figure 1.** Effects of axotomy on axonal transport, structure and proteins. Fluorescent tubulin injected into an axon moved anterogradely (to the right) away from the injection site (arrowhead in A). Tubulin injected into an axon that had been separated from its cell bodies 2 d prior showed no anterograde transport (B). This tubulin just diffused in both directions around the injection site (arrowhead in B). Darkfield light scattering was unaffected by axotomy. Light scattering was the same in control (C) as it was in transected axons (D). Higher resolution video enhanced differential interference microscopy also showed no difference between control (E) and paired transected (F) axons. Mitochondria (arrows in E and F) and smaller organelles (arrowheads) were present in control and transected axons. Scale bars: 100  $\mu\text{m}$  for A and B, 50  $\mu\text{m}$  for C and D, and 1  $\mu\text{m}$  for E and F. Solubilized axonal proteins (G) from equal lengths of axon from the control (1c) and the transected side (1t) of a squid that had been axotomized 2 d earlier showed no change in protein-staining intensity. Paired axons from a smaller squid (2) with shorter axons had proportionately less protein than the larger squid (1), but there was no significant difference in protein levels between the control side (2c) and the transected side (2t). Similarly, axotomy had no effect on total immunochemically measured kinesin levels (H) in the paired axons from these same two squids. (1c vs. 1t and 2c vs. 2t).

The present experiment suggests that some unidentified factor essential to axonal tubulin transport is lost or inhibited 2 days after axotomy. This inhibition is not due to the depletion of conventional kinesin. It could be due to the inactivation of conventional kinesin or to the inactivation or depletion of some other motor or factor essential to axonal tubulin transport. This model of protein transport in the squid giant axon may facilitate the identification of some of the factors essential to the control and maintenance of slow axonal transport.

The author thanks James Galbraith and Thomas Reese for helpful discussions and comments.

### Literature Cited

1. Terasaki, M., A. Schmeidek, J. A. Galbraith, P. E. Gallant, and T. S. Reese. 1995. *Proc. Natl. Acad. Sci. USA* 92: 11,500–11,503.
2. Galbraith, J. A., T. S. Reese, M. L. Schlieff, and P. E. Gallant. 1999. *Proc. Natl. Acad. Sci. USA* 96: 11,589–11,594.
3. Terada, S., M. Kinjo, and N. Hirokawa. 2000. *Cell* 103: 141–155.
4. Gallant, P. E. 2000. *J. Neurocytol.* 29: 779–782.
5. Gallant, P. E., and J. A. Galbraith. 1997. *J. Neurotrauma* 14: 811–822.
6. Gallant, P. E., H. C. Pant, R. M. Pruss, and H. Gainer. 1986. *J. Neurochem.* 46: 1573–1581.

Reference: *Biol. Bull.* 205: 188–190. (October 2003)  
© 2003 Marine Biological Laboratory

## Interactions Between Recombinant Conventional Squid Kinesin and Native Myosin-V

John Delacruz, Jeremiah R. Brown, and George M. Langford  
Dartmouth College, Hanover, NH

Axoplasm from the squid giant axon is one of a small number of cell-free extracts within which axonal transport can be studied *in vitro* (1). In squid axoplasm, one can observe both microtubule-based and actin-based vesicle transport and the seamless transition of vesicles from microtubules to actin filaments (2). Based on studies of vesicle transport in this cell-free preparation, a new

model of axonal transport has emerged called “dual transport” in which long-range vesicle transport is microtubule-based while short-range transport is actin-based (3).

An exciting recent discovery is the finding that the cargo-binding domains of myosin-V, an actin-based motor, and kinesin, a microtubule-based motor, interact to form a hetero-motor com-

plex (4, 5, 6, 7). The interaction of myosin-V with kinesin has been established through yeast 2-hybrid assay, co-immunoprecipitation, co-affinity isolation, and co-purification with myosin-V (4, 5, 6, 7). The distal/globular tail domain of myosin-V binds to the rod-tail domain of kinesin in the "hetero-motor" complex. The members of the kinesin super family that have been shown to bind to myosin-V include conventional or ubiquitous kinesin (kinI) and Smy1p (4, 5, 6, 7). Evidence that myosin-V and kinesin interact on the membrane surface has not yet been demonstrated.

In this report, we performed experiments to determine the functional significance of the interactions between kinesin and myosin-V. Our working hypothesis is that tail-tail interactions between these motors provide feedback and thereby allow coordination of motor activity during the transition of vesicles from microtubules to actin filaments. For example, one motor may become inactive when its partner is actively transporting a vesicle along a filament (3). Several studies have shown that the ATPase activity of kinesin is inhibited when the head and tail domains of the molecule interact (8, 9). Auto-inhibition may be the mechanism by which one motor becomes inactive when its partner motor binds to a filament. Therefore, only one motor is actively engaged in movement and a tug-of-war between motors is prevented. Such feedback between motors could explain the seamless transition of vesicles from microtubules to actin filaments observed in the squid giant axon.

In this study we used a histidine-tag bound to the tail fragment of squid conventional kinesin (His-tagged) to study the interactions between kinesin and myosin-V. A cDNA construct coding for the rod-tail domain of conventional squid kinesin (SK KheU; gift of K. Kosik) was engineered into a vector containing a His-tag. The 1.5 kb SK KheU contained most of the rod II domain and the entire tail domain including the stop codon. The sequence of the insert was confirmed by PCR. The His-kinesin vector was expressed in *E. coli*, and the recombinant protein was then purified on a nickel-column. A gel of the fraction eluted from the column with 40 mM imidazole showed a prominent band at 45 kDa, the expected molecular weight of the fragment (Fig. 1A, lane 1). This band was identified as the His-labeled kinesin fragment on nitrocellulose membranes that were probed with the His-antibody (Fig. 1A, lane 2).

Next, we applied a clarified extract of His-kinesin tail fragment to a Ni-column to make a kinesin tail affinity column. Nonspecific proteins were removed by several buffer washes; and a clarified squid optic lobe extract was then passed over the column, followed by buffer washes. The proteins that bound specifically to the tail domain of kinesin were eluted with imidazole and analyzed by SDS-PAGE. Multiple protein bands were visible on the gel of the eluted fraction (Fig. 1B, lane 1). The proteins were transferred to membrane and probed with an antibody to myosin-V, a known binding partner of kinesin. A prominent band was observed on the blot (Fig. 1B, lane 2). These data showed that the recombinant His-kinesin fragment interacted with myosin-V and several other proteins in the squid brain extract. Finally, we asked whether the His-kinesin fragment blocked microtubule-based vesicle movement in motility assays. Preliminary experiments were performed in which the His-kinesin tail fragment was added to extruded axoplasm from the squid giant axon (Fig. 1C). Vesicle transport was measured by counting the number of vesicles moving/micro-

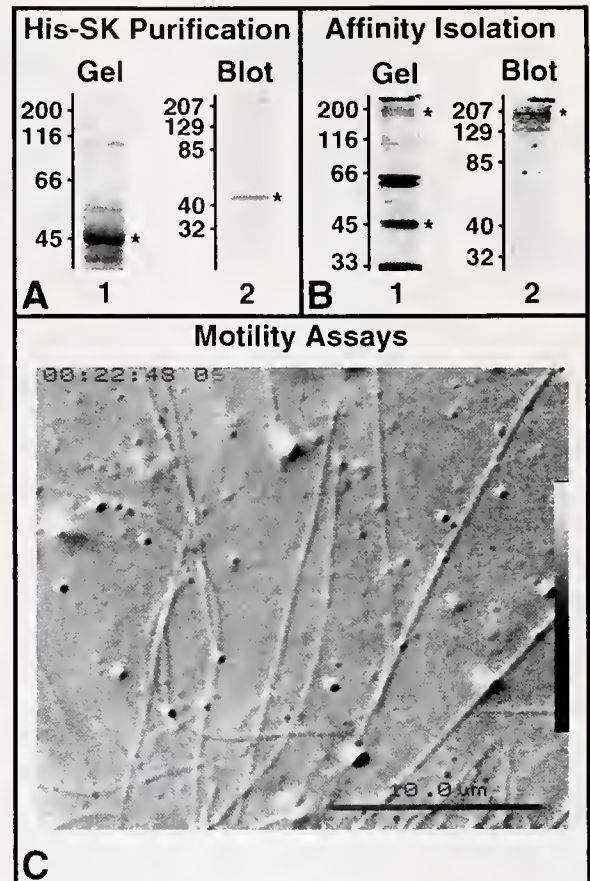


**Figure 1.** (A) The presence of the His-tagged recombinant squid kinesin tail construct was verified using SDS-PAGE and western blots, and sequencing data. Lane 1 shows an SDS-PAGE gel confirming the presence of a protein with a molecular weight of 45 kDa, which matches the expected weight of the kinesin construct. Lane 2 shows a western blot probed with anti-His antibody; the blot confirms that the 45 kDa protein contains a His-tag. (B) The squid kinesin tail fragment is shown to interact with native squid myosin-V obtained from homogenized optic lobes. The homogenized extract was run through a His-kinesin affinity column. Lane 1 shows an SDS-PAGE gel of the elution fraction and shows that the 45 kDa kinesin tail and the 196 kDa native myosin-V are present. The elution fraction was blotted and probed with myosin-V antibody  $\alpha$ -QLLQ (lane 2) and confirms myosin-V. (C) Allen Video Enhanced Contrast-Digital Interference Contrast (VEC-DIC) microscopy is used to image microtubules and vesicle motility in extruded squid axoplasm. Experiments are being performed to determine whether the recombinant kinesin tail fragment conclusively inhibits vesicle motility along microtubules.

tubule/min (v/mt/m; motile activity) at 15-min intervals. A reduction of motile activity occurred but the number of replicates was not sufficient to provide conclusive evidence.

In summary, recombinant, His-labeled, squid kinesin tail fragment binds to squid brain myosin-V, as demonstrated by affinity column isolation. The recombinant tail fragment is thus an excellent tool for identifying specific binding partners of kinesin and potentially for studies of kinesin-mediated vesicle transport.

This work was supported by NSF Grant IBN-0131470, and the Leadership Alliance Grant and MBL-Shifman Award to JMD.

## Literature Cited

- Allen, R. D., D. G. Langford, J. R. Hayden, D. T. Brown, H. Fujiwaka, and M. Simpson. 2002. *Cell Motil. Cytoskelet.* **1**: 291–302.
- Kuznetsov, S., G. M. Langford, and D. G. Weiss. 1992. *Nature* **356**: 722.
- Langford, G. M. 2002. *Traffic* **3**: 859–865.
- Brown, J. R., K. R. Simonetta, L. A. Sandberg, P. Stafford, and G. M. Langford. 2001. *Biol. Bull.* **201**: 240–241.
- Brown, J. R., E. M. Peacock-Villada, and G. M. Langford. 2002. *Biol. Bull.* **203**: 210–211.
- Huang, J. D., S. T. Brady, B. W. Richards, D. Stenolen, J. H. Resau, N. G. Copeland, and N. A. Jenkins. 1999. *Nature* **397**: 267–270.
- Lillie, S. H., and S. S. Brown. 1998. *J. Cell Biol.* **140**: 873–883.
- Freidman, D. C., and R. D. Vale. 1999. *Nat. Cell Biol.* **1**: 288–292.
- Coy, D. L., W. O. Hancuck, M. Wagenbach, and J. Howard. 1999. *Nat. Cell Biol.* **1**: 288–297.

Reference: *Biol. Bull.* **205**: 190–191. (October 2003)  
 © 2003 Marine Biological Laboratory

## Rab-GDI Inhibits Myosin V-Dependent Vesicle Transport in Squid Giant Axon

Carl J. DeSelm, Jeremiah R. Brown, Renne Lu<sup>1</sup>, and George M. Langford

Dartmouth College, Hanover, NH

<sup>1</sup>Boston Biomedical Research Institute, Watertown, MA

Myosin-V, an actin-based motor, and kinesin, a microtubule-based motor, interact to form a "hetero-motor" complex (1). Axoplasmic vesicles containing these hetero-motor complexes move on microtubules in the axon and on actin filaments at the cell cortex (2). Negative feedback between these two motors is thought to facilitate the transition of vesicles from microtubules to actin filaments (3). Proteins that couple the hetero-motor complex to vesicles have not been identified. Recent studies have shown that the Rab family of GTPases is involved in the recruitment of myosin-V to vesicles. In melanocytes, myosin Va is recruited to melanosomes by Rab 27a (4, 5, 6). Melanophilin, an activator of Rab 27a, has been shown to be required for the binding of myosin-V to Rab 27a (7). Therefore, Rab 27a and melanophilin have been identified as the receptor complex for myosin Va on melanosomes. The Rab GTPase responsible for myosin-V recruitment to axoplasmic vesicles in the squid giant axon has not been determined, although Rab 3a is known to be associated with synaptic vesicles in squid brain (8). In this study we show that Rab-GDI pulled down myosin-V by affinity isolation and blocked vesicle transport in motility assays. We also show that the tail domain of myosin-V binds to tubulin dimers, presumably through kinesin or another linker protein.

To identify the Rab GTPase involved in myosin-V/kinesin binding to axoplasmic vesicles, and to identify all binding partners of the hetero-motor complex, we used a recombinant glutathione S-transferase (GST)-labeled globular tail domain of myosin-V (GST-GTD) and a GST-labeled Rab GDP dissociation inhibitor (GST-GDI) in motility and affinity isolation experiments. In a previous study, we showed that GST-GTD binds to squid brain vesicles and displaces the native myosin-V. The displacement of native myosin-V blocked transport of axoplasmic vesicles on actin filaments in assays using the squid giant axon (9, 10). In this study, the GST-GTD and GST-GDI were used to pull down binding partners of myosin-V for analysis by 2-D gel electrophoresis and protein sequencing.

A plasmid containing a cDNA insert for GST-mouse myosin-V AF6/Cno tail-globular-domain (gift from Dr. Huang) was expressed in *E. coli* (9). The bacterially expressed 84 kDa GST-myosin-V globular tail fragment was bound to a GST-column to

generate an affinity column for isolation of binding partners of the myosin-V tail. Clarified squid brain extract was applied to the column and, after extensive washes, GST-GTD was eluted with glutathione. As a control, clarified brain extract was also applied to and eluted from a column without GST-GTD. GST-GTD was present in the eluted fraction from the GST-GTD column, as revealed by SDS-PAGE (Fig. 1A, lane 1). There were no proteins in the fraction eluted from the column in the absence of GST-GTD (Fig. 1A, lane 2). The presence of GST-GTD in the eluted fraction was confirmed by probing blots of this fraction with GST antibody (Fig. 1A, lane 3). Kinesin, a known binding partner of myosin-V, was identified in the fraction eluted from the GST-GTD column (Fig. 1A, lane 4). This fraction was analyzed further by 2-D gel electrophoresis. A pH range of 3–10 was used in the first dimension and an 8.5% SDS-PAGE gel for the second dimension. The 2-D gel was electroblotted to PDVF membrane (ProBlott, Applied Biosystems), and the protein spots were stained with Coomassie Blue R-250. Approximately 35 spots were clearly visible on the membranes (Fig. 1B). The major spots were excised and the N-terminal sequences were determined using an Applied Biosystem Procise sequencer. The identification of the proteins was based on sequence homology using BLAST.

Sequence information has been obtained for eight proteins excised from the 2-D gel. The two most interesting proteins thus far identified are  $\alpha$ - and  $\beta$ -tubulin. These data show that tubulin dimers are retained on the column, suggesting that the tail domain of myosin-V binds directly or indirectly to microtubules. An indirect link between myosin-V and tubulin may be through kinesin, which binds directly to the tail of myosin-V (Fig. 1A, lane 4). Several studies have shown interactions between myosin-V tail and other proteins that bind to microtubules. Therefore, we conclude that tubulin binds to myosin-V indirectly, either through kinesin or another microtubule-associated protein.

A plasmid containing the full-length cDNA for *Drosophila* GST-Rab-GDI (gift from Dr. C. Cheney) was expressed in *E. coli*. The 75 kDa GST-tagged protein was purified on a GST affinity column (Fig. 1C, lane 1) and used in pull-down experiments with squid brain extracts. Myosin-V was identified as one of the proteins in the fraction eluted from the GST affinity column (Fig. 1C,

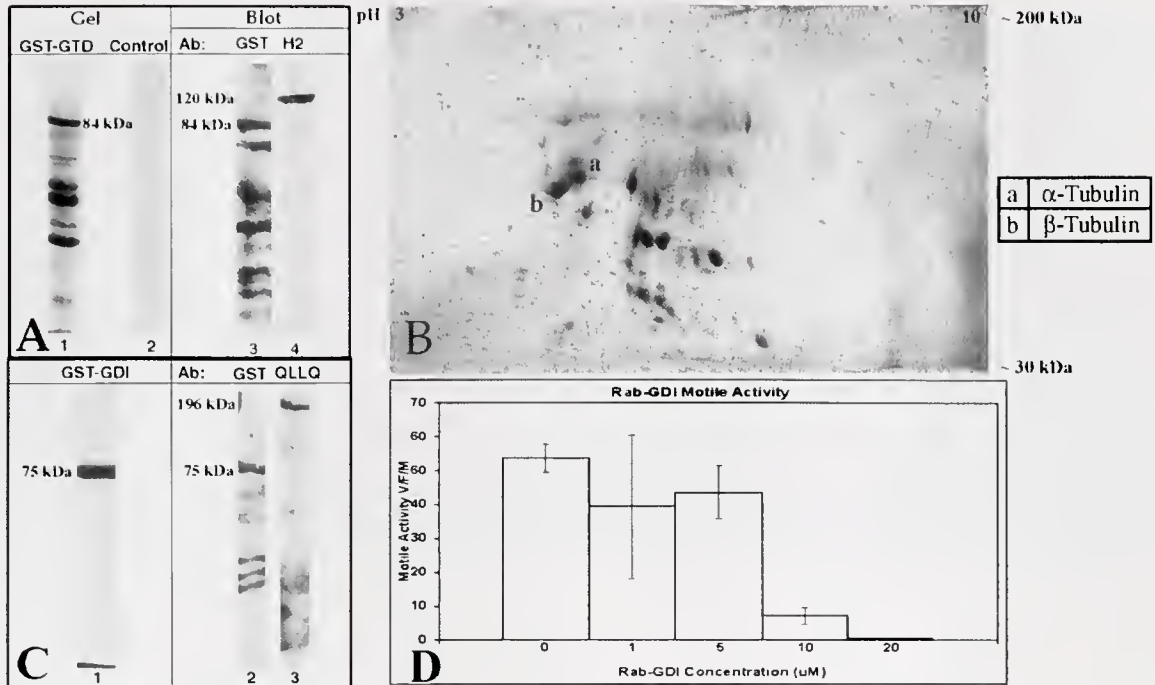


**Figure 1.** A plasmid containing GST-myosin-V tail (GST-GTD) was expressed in *E. coli*. The 84 kDa fusion protein was bound to a GST-affinity column, then clarified squid brain extract was applied to the column, washed, and eluted with glutathione to identify binding partners of the myosin-V tail. (A) SDS-PAGE gel of the fraction containing GST-GTD is shown in lane 1. A band at 84 kDa indicates the presence of GST-GTD. The lower molecular weight proteins are putative myosin-V tail-binding partners. An SDS-PAGE gel of the fraction eluted with glutathione from the control column (no GST-GTD) is shown in lane 2. There were no proteins in this fraction. A blot of the GST-GTD fraction probed with GST antibody (lane 3) confirmed the presence of the myosin-V tail fragment (84 kDa). The lower molecular weight bands represent breakdown products of the GST-GTD fusion protein. A blot of the GST-GTD fraction probed with H2 (lane 4) shows the presence of kinesin (120 kDa), indicating interaction between myosin-V and kinesin. (B) A 2-D gel of the GST-GTD fraction shows approximately 35 spots. Two identified spots, a and b, are  $\alpha$ -tubulin and  $\beta$ -tubulin, respectively. (C) A plasmid containing GST-Rab-GDI (GST-GDI) was expressed in *E. coli*, applied to a GST affinity column, and eluted with glutathione. An SDS-PAGE gel of the fraction containing GST-GDI (75 kDa) is shown in lane 1. A blot of the GST-GDI fraction probed with GST antibody indicates the presence of GST-GDI at 75 kDa (lane 2). A blot of GST-GDI probed with QLLQ indicates interaction between native myosin-V (196 kDa) and Rab-GDI (lane 3). (D) Motility assays in extruded squid axoplasm were used to determine the effect of Rab-GDI on actin-based vesicle transport. The number of vesicles moving per field per min (V/F/M) was measured at concentrations of 0–20  $\mu\text{M}$  GST-GDI. Vesicle transport was inhibited by 99% at 20  $\mu\text{M}$  GST-GDI.

lane 3). Therefore, these data show that myosin-V interacts with a Rab-G protein.

Motility assays were performed with GST-Rab-GDI to determine whether Rab GTPases are involved in vesicle transport in the squid giant axon. Rab-GDI blocks the exchange of GTP for GDP and thereby inactivates Rab proteins. Motile activity at 20  $\mu\text{M}$  GST-Rab-GDI decreased from  $54 \pm 4$  vesicles/field/min (V/F/M) in the control assay to  $0.5 \pm 0.2$  V/F/M (Fig. 1D). Therefore, the GST-Rab-GDI inhibited vesicle transport by 99% at this concentration. At 10  $\mu\text{M}$  GST-Rab-GDI, motile activity decreased by 86%. These data show that Rab activity is required for myosin-V-mediated vesicle transport in the axon. These data are consistent with published results showing that myosin-V is recruited to melanosomes and endosomes by Rabs 27a and 11a respectively. Our studies support the hypothesis that Rab GTPases are required for the recruitment of myosin-V to vesicles for transport.

This work was supported by NSF Grant IBN-0131470 and MBL-Shifman Award to CJD.

## Literature Cited

- Huang, J. D., S. T. Brady, B. W. Richards, D. Stenoién, J. H. Resau, N. G. Copeland, and N. A. Jenkins. 1999. *Nature* 397: 267–270.
- Kuznetsov, S. A., G. M. Langford, and D. M. Weiss. 1992. *Nature* 356: 722–725.
- Langford, G. M. 2002. *Traffic* 3: 859–865.
- Hammer, J. A., III, and X. S. Wu. 2002. *Curr. Opin. Cell Biol.* 14: 69–75.
- Wu, X., F. Wang, R. Kang, J. R. Sellers, and J. A. Hammer, III. 2002. *Mol. Cell Biol.* 13: 1735–1749.
- Bahadoran, P., E. Aberdam, F. Mantoux, R. Busca, K. Bille, N. Yalman, G. de Saint Basile, R. Casaroli-Marano, J-P. Ortonne, and R. Ballotti. 2001. *J. Cell Biol.* 152: 843–849.
- Wu, X., K. Rao, H. Zhang, F. Wang, J. Seller, L. Matesic, N. Copeland, N. Jenkins, and J. Hammer, III. 2002. *Nat. Cell Biol.* 4: 271–278.
- Chin, G., and S. Goldman. 1992. *Brain Res.* 571: 89–96.
- Brown, J. R., E. M. Peacock-Villada, and G. M. Langford. 2002. *Biol. Bull.* 203: 210–211.
- Brown, J. R., P. Stafford, and G. M. Langford. 2003. *J. Neurobiol.* (In Press).

Reference: *Biol. Bull.* 205: 192–193. (October 2003)  
 © 2003 Marine Biological Laboratory

## Cytoskeletal Events Preceding Polar Body Formation in Activated *Spisula* Eggs

R. M. Pielak, V. A. Gaysinskaya, and W. D. Cohen\*

Hunter College, New York, NY

Marine Biological Laboratory, Woods Hole, MA

Polar body formation is of interest both as a fundamental process in sexual reproduction and as an extreme example of unequal cytokinesis in cell biology. Eggs of the surf clam *Spisula solidissima*, released in the germinal vesicle stage, are readily induced to form polar bodies by activation with KCl or by fertilization. However, although *Spisula* eggs are utilized in current studies of centrosomes and the cell cycle (e.g., 1), polar body formation in this model system is described only in older literature (2, 3). We have examined changes occurring in major cytoskeletal elements—microtubules and F-actin—in the stages immediately preceding formation of the first polar body. These stages are thought to be critical for docking of the meiotic spindle with the cell cortex, and for meiotic apparatus-cortex signaling that mediates the positioning and generation of the contractile ring. These processes occur by as yet unknown mechanisms.

In this study, confocal fluorescence microscopy was used to localize actin and tubulin relative to meiotic chromosomal stage. Ripe *Spisula* were obtained from the Aquatic Resources Division of the Marine Biological Laboratory (MBL) and maintained at 11–13 °C until used. Clams were opened by dissection, the gonad was removed, and the eggs were filtered through cheesecloth. Before use, the eggs were washed 3 times in 0.2- $\mu$ m filtered seawater (FSW), and resuspended to a concentration of 1:10 ( $V_{\text{eggs}}/V_{\text{FSW}}$ ). The eggs were activated, either by adding excess KCl to the seawater or by fertilization with freshly obtained sperm, according to standard methods for this species (4, 5). Time of KCl or sperm addition was recorded as  $t = 0$ . After germinal vesicle breakdown (GVBD), the eggs were resuspended to a concentration of 1:100 ( $V_{\text{eggs}}/V_{\text{FSW}}$ ). Time-course samples, taken approximately every 2 min after GVBD, were prepared by simultaneous lysis and fixation of eggs in a medium consisting of 0.6% Brij-58, 4% formaldehyde in PEM (100 mM PIPES, 5 mM EGTA, 1 mM  $\text{MgCl}_2$ , pH 6.8 using NaOH). After incubation for 1 h, the samples were washed in PEM and then stained. For F-actin, the eggs were stained with rhodamine or Alexa Fluor 568-phalloidin. Microtubules were stained with a 1:1 mass mixture of mouse monoclonal anti- $\alpha$  and anti- $\beta$  tubulins (Sigma T9026, T-4026) pre-labeled with Alexa fluor 488-labeled anti-mouse  $F_{ab}$  fragments (Zenon™, Molecular Probes), and chromosomes and nuclei were stained with DAPI. These procedures followed protocols developed in previous work on microtubule localization in a variety of cell types (6), and our measurements showed that normal *Spisula* egg diameters (~50–55  $\mu$ m) were retained after such treatment. Confocal fluorescence microscopy of stained samples was performed using the

Zeiss Laser Scanning System LSM 5 PASCAL, and images were processed with Zeiss LSM Image Examiner software.

Using the KCl-activation method at 23 °C, GVBD occurred in about 7 min, and was followed at approximately 13 min post-activation by the appearance of the first metaphase meiotic spindle. At first, the metaphase spindle was slightly eccentric (Fig. 1a). Subsequently, it moved toward the cell surface and approached the cortex while remaining in metaphase (Fig. 1b; ~18 min). Microtubules of the peripheral aster, initially straight, were now observed to curve outward along the cell cortex, symmetrically away from a central microtubule-poor region (Fig. 1b, b' arrow). At ~20 min the spindle entered anaphase (Fig. 1c), and a ring of thickened F-actin, ~17–20  $\mu$ m in diameter, then appeared in the cortex (Fig. 1d, d'). This ring surrounded a small circular cortical area, ~7–9  $\mu$ m in diameter, in which the F-actin was considerably thinner, creating a "bull's-eye" appearance in 3-D computer-generated rotated images (Fig. 1d', and online supplemental animation at [www.mbl.edu/BiologicalBulletin/VIDEO/BB.video.html](http://www.mbl.edu/BiologicalBulletin/VIDEO/BB.video.html)). The peripheral aster was now greatly diminished in size, and no longer visible along the cortex. Subsequently, it became apparent that the bull's-eye center of the F-actin ring (Fig. 1d, d') was the region through which the polar body nucleus and associated remaining centrosomal material passed (~22–24 min post-activation; Fig. 1e). The first polar body appeared fully formed at about 26 min; it was enclosed by an actin-containing cortex that followed an outwardly and inwardly bulging contour (Fig. 1f). Results similar to those shown in Figure 1 were obtained with KCl-activated eggs from several different clams, and also with sperm-activated eggs. These observations are consistent with, and extend, older electron microscopic work on polar body formation in eggs of *Spisula* and *Tubifex* (2, 7) and are of value for comparison with current findings on unequal cell division in *Saccharomyces cerevisiae* and *Caenorhabditis elegans* (8, 9).

The sequence of cytoskeletal events observed in *Spisula* eggs prior to polar body formation, as illustrated in the Figure 1 diagram, is suggestive of mechanisms. The initially eccentric metaphase meiotic apparatus moves toward the cortex, and the peripheral aster contacts the surface (diagram b). Curvature of the astral microtubules and spreading outward along the cortex at the metaphase-to-anaphase transition follows (diagram c, d), rather than shortening of straight astral microtubules on contact. Such behavior is consistent with models in which spindle movement toward the surface is brought about by the capture of plus ends of microtubules and microtubule transport, either by cortical dynein, or by a formin-based mechanism (10, 11). The thickened ring of cortical F-actin—the inner layer of which (at least) is presumed to represent formation of the contractile ring—is not established until late

\* Corresponding author: [cohen@genectr.hunter.cuny.edu](mailto:cohen@genectr.hunter.cuny.edu).

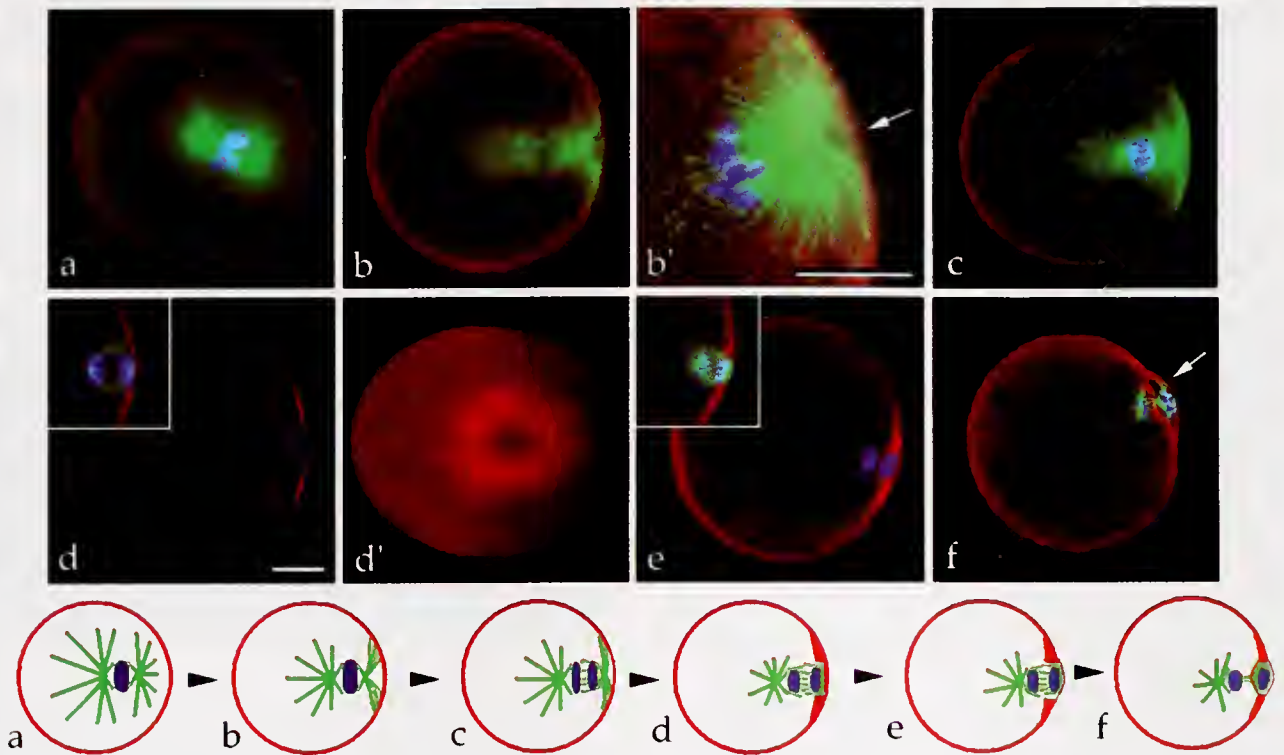


**Figure 1.** Stages in KCl-activated eggs at 23 °C, with triple staining for F-actin, microtubules, and chromosomes (white letters) and a diagrammatic summary (black letters). (a) First metaphase meiotic spindle, eccentrically positioned;  $t \approx 16$  min post-activation. (b) Metaphase spindle at cell cortex with astral microtubules curving outward from central microtubule-poor region;  $\sim 18$  min post-activation. (b') Higher magnification view of stage (b); arrow: microtubule-poor central region. (c) Early anaphase with microtubules spread along cortex. (d) Edge view of thickened cortical F-actin ring, only chromosomes and actin stained;  $\sim 20$  min post-activation. Inset: same stage, with microtubules also stained. (d') Computer-generated, rotated image of the F-actin ring shown in (d). (e) Telophase chromosome set within F-actin ring; only chromosomes and actin stained;  $\sim 24$  min post-activation. Inset: same cell, microtubules also stained. (f) First polar body, enclosed by an actin-containing cortex;  $\sim 26$  min post-activation. Magnification bars = 10  $\mu\text{m}$ ; bar for all figures (other than b') as shown in d.

anaphase (diagram d). This suggests the involvement of anaphase signaling following a metaphase checkpoint.

It is evident that the sequence involves a mechanism for peripheral aster disassembly (Fig. 1d, inset), but such disassembly is delayed until after astral spreading along the cortex. In addition, the earlier pattern of contact between peripheral aster microtubules and the cortex, with its central microtubule-poor area (diagram b), is a close match to the "bull's-eye" pattern of thickened F-actin, with its central thinner area, which appears later (diagram d). The dimensions of the later pattern also correspond to those of the earlier aster ( $\sim 16$ – $20$ - $\mu\text{m}$  outer diameter,  $\sim 7$ – $9$ - $\mu\text{m}$  inner diameter). Taken together, these observations strongly suggest that the signaling mechanism for contractile ring generation involves the astral microtubules.

We thank Kyeng-Gea Lee, Dr. David Burgess, Dr. Robert Palazzo, Dr. Shirley Raps, Ruben Pinkhasov, and Alex Braun, for assistance and helpful discussion. Support by the Howard Hughes Medical Institute Undergraduate Science Education Program in Biology (grant 52002679), and by PSC-CUNY64249 and NSF9726771, is gratefully acknowledged.

## Literature Cited

- Palazzo, R. E., E. A. Veisberg, D. G. Weiss, S. A. Kuznetsov, and W. Steffen. 1999. *J. Cell Sci.* 112: 1291–1302.
- Longo, F. J., and E. Anderson. 1970. *J. Ultrastruct. Res.* 33: 495–514.
- Kuriyama, R., G. G. Borisy, and Y. Masui. 1986. *Dev. Biol.* 114: 151–160.
- Allen, R. D. 1953. *Biol. Bull.* 105: 213–239.
- Costello, D. P., and C. Henley. 1971. *Methods for Obtaining and Handling Marine Eggs and Embryos*, 2<sup>nd</sup> ed. Marine Biological Laboratory, Woods Hole, MA.
- Lee, K.-G., A. Braun, I. Chaikhouidinov, J. DeNobile, M. Conrad, and W. Cohen. 2002. *Biol. Bull.* 203: 204–206.
- Shimizu, T. 1983. *Eur. J. Cell Biol.* 30: 74–82.
- Knoblich, J. A. 2001. *Nat. Rev. Mol. Cell Biol.* 2: 11–20.
- Guertin, D. A., S. Trautmann, and D. McCollum. 2002. *Microbiol. Mol. Biol. Rev.* 66: 155–178.
- Busson, S., D. Dujardin, A. Moreau, J. Dompierre, and J. R. De Mey. 1998. *Curr. Biol.* 8: 541–544.
- Gundersen, G. G., and A. Bretscher. 2003. *Science* 300: 2040–2041.

Reference: *Biol. Bull.* 205: 194–195. (October 2003)  
 © 2003 Marine Biological Laboratory

### Three-Dimensional Birefringence Distribution in Reconstituted Asters of *Spisula* Oocytes Revealed by Scanned Aperture Polarized Light Microscopy

Michael Shribak and Rudolf Oldenbourg

Marine Biological Laboratory, Woods Hole, MA 02543

Ten years ago we reported the first measurement of the distribution of birefringence in asters dispersed in lysates of *Spisula* oocytes; the observations were made with a new type of polarized light microscope, the Pol-Scope (1). Since then, the Pol-Scope and its commercial version, the LC-PolScope (CRI, Inc., Woburn, MA ([www.cri-inc.com](http://www.cri-inc.com))), have become a mature microscopical technique used in many laboratories around the world for studying living cells and other specimens (2).

Asters consist of microtubules radiating in all directions from centrosomes—microtubule-organizing centers found in almost all animal cells. Nevertheless, both the structure of centrosomes and the mechanism by which they nucleate microtubules are still poorly understood. The Pol-Scope reveals the birefringence retardation, also called retardance, of astral microtubules irrespective of their orientation within the plane of focus. But when microtubules are inclined away from the plane of focus, the measured retardance is reduced, and the angle of inclination cannot be discerned.

Now we are introducing a new technique called scanned aperture polarized light microscopy (Fig. 1). The Scanned Aperture Pol-Scope not only measures the microtubule orientation within the plane of focus, but it also measures the angle of inclination away from the focal plane. In addition, the Scanned Aperture Pol-Scope measures the retardance of all microtubules equally, irrespective of their orientation and inclination angle.

Figure 2 shows images of an aster reconstituted by polymerizing tubulin off a centrosome purified from *Spisula* oocytes (3). The images were recorded with the LC-PolScope (panel B) and with the Scanned Aperture Pol-Scope (panel C and D). As illustrated in the schematic of panel A, the focal plane was offset by 5  $\mu\text{m}$  relative to the center of the aster (focal depth approximately 0.3  $\mu\text{m}$ ). While the LC-PolScope image lacks retardance in the center of the structure, the image recorded with the Scanned Aperture Pol-Scope reveals the retardance of the dense microtubule arrays that are located near the center and are oriented almost parallel to the microscope axis. In addition, panels C and D also indicate the measured inclination and orientation angle of the birefringence axis, which also indicates the orientation of the astral microtubules.

We also recorded images after adjusting the focal plane to include the centrosome in the center of the aster (images not shown). In this configuration, the retardance values in images recorded with the Scanned Aperture Pol-Scope were below 0.3 nm near the center of the aster, increased rapidly at a radius of 3  $\mu\text{m}$ , and peaked at a radius of 7.4  $\mu\text{m}$  (peak retardance  $\sim$  3 nm). In addition, the inclination angle was close to zero for all retardance values measured in the focal plane that included the center of the aster. This latter result conforms to the expectation that all astral microtubules are oriented parallel to the focal plane at this focal

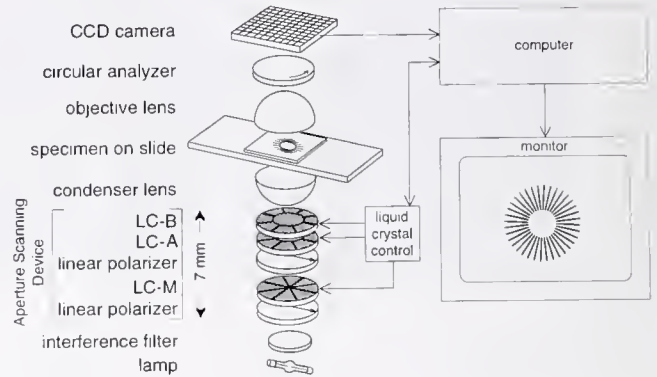


**Figure 1.** Schematic of optical (left) and electronic components of the Scanned Aperture Pol-Scope. The optical set-up is based on a traditional light microscope enhanced by an aperture scanning device and an analyzer for circular polarized light. The scanning device includes the liquid crystal devices LC-A, LC-B, and LC-M. LC-M is sandwiched between two linear polarizers. All liquid crystal devices are linear retarder plates with 8 or 9 individually controlled sectors. LC-M and the two linear polarizers are used to block or transmit light passing through 8 pie-shaped sectors. A pair of sectors in LC-A and LC-B, arranged in series, function as a universal compensator, controlling the polarization state of the passing light [4]. All components of the scanning device are bonded together and form a 7 mm-thick optical flat with electrical connections and an approximate diameter of 25 mm. The computer-controlled scanning device is placed in the front aperture plane of the condenser lens and is used to sequentially illuminate the specimen with a polarized, converging light beam whose central ray is typically tilted to the microscope axis. Tilt angles are controlled by blocking or passing the light in the 8 pie sectors. By passing the light in all 8 sectors, the tilt angle is zero, and recorded images are equivalent to LC-PolScope images. Currently, images are recorded at 5 different tilt angles and are combined using specially developed algorithms for measuring the 3-dimensional birefringence distribution in every resolved specimen point (see Fig. 2; for a more detailed description of the instrument see [5]).

position. All results reported here are typical of our observations of at least 3 asters and repeated measurements at different focus positions.

Our findings indicate that the centrosome essentially lacks aligned microtubule arrays. However, the density of astral microtubules increases sharply at the surface of the centrosome. We propose to interpret the radius at which the measured retardance has the steepest gradient as the location of the centrosome surface (radius = 3.1  $\mu\text{m}$ ). In the future we plan to measure the density of microtubule arrays as a function of radius from the center of asters that are exposed to various physiological conditions to determine their potential for microtubule nucleation.

In conclusion, we have demonstrated that the Scanned Aperture

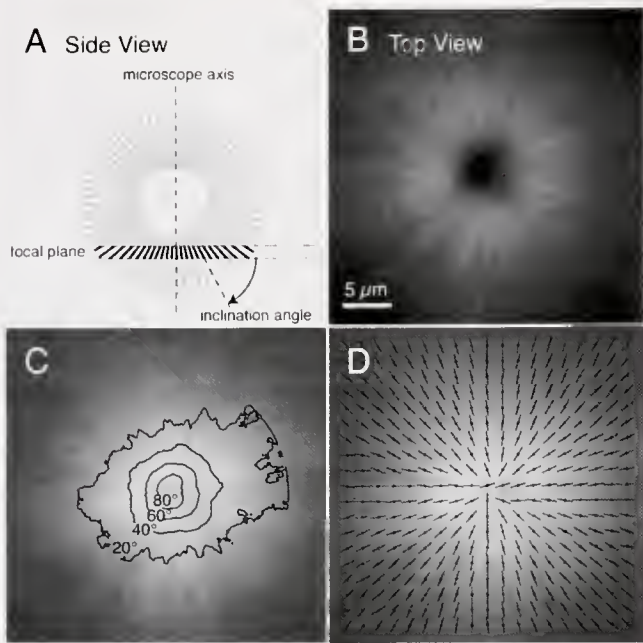


**Figure 2.** An aster reconstituted from purified centrosome and tubulin was imaged with the LC-PolScope and the Scanned Aperture Pol-Scope using an oil immersion condenser and objective lens (Zeiss Neofluar 100 $\times$ /1.3 NA Pol). (A) Schematic side view of the aster indicating the position of the plane of focus in panels B, C, and D and the definition of the inclination angle. (B) LC-PolScope image of microtubule retardance in the focal plane. The measured retardance in the center of the image is close to zero because the microtubule arrays are oriented nearly perpendicular to the focal plane (parallel to the microscope axis). (C) Microtubule retardance measured with the Scanned Aperture Pol-Scope. Gray scale image shows retardance of all microtubule arrays, regardless of inclination angle. Overlay indicates lines of equal inclination angle in steps of 20°. (D) Same microtubule retardance image as in panel C; the image is overlaid with lines indicating the orientation of measured birefringence axis in the plane of focus. For clarity, both overlays show only a subset of orientation and inclination angles, which are measured in every resolved image point. In images of panels B, C, and D, black is zero retardance, and white is 3 nm retardance.

Pol-Scope can be used to measure the orientation and inclination angle of the birefringence axis of objects exhibiting low birefringence, such as asters. In addition, the technique measures the retardance of all birefringent objects equally, regardless of their orientation and inclination angle. The measurements are performed at all resolved specimen points simultaneously, at high spatial resolution ( $\sim 0.3 \mu\text{m}$ ), and high sensitivity (0.1 nm retardance). This seems to be the first reported technique that can measure the 3-dimensional distribution of birefringence in microscopic specimens. We expect this technique to impact many application areas of the traditional polarized light microscope, including the imaging of living cells, tissues, and functional model systems in biology and medicine.

Purified components for reconstituting asters *in-vitro* were kindly provided by Robert E. Palazzo of Rensselaer Polytechnic Institute and the Marine Biological Laboratory. The research is supported by NIH grants GM49210 and EB002045.

### Literature Cited

1. Oldenbourg, R., G. Mei, and R. E. Palazzo. 1993. *Biol. Bull.* **185**: 288.
2. Oldenbourg, R. In *Live Cell Imaging: A Laboratory Manual*, D. L. Spector and R. D. Goldman, eds. Cold Spring Harbor Laboratory Press, Cold Spring Harbor, NY. (In press).
3. Schnackenberg, B. J., and R. E. Palazzo. 2001. *Methods Cell Biol.* **67**: 149–165.
4. Shribak, M., and R. Oldenbourg. 2003. *Appl. Opt.* **42**: 3009–3017.
5. Shribak, M. I., and R. Oldenbourg. 2002. Pp. 104–109 In *Three-Dimensional and Multidimensional Microscopy: Image Acquisition and Processing IX*. Proceedings of SPIE 4621, San Jose, CA.

Reference: *Biol. Bull.* **205**: 195–197. (October 2003)

© 2003 Marine Biological Laboratory

## Rho-kinase Is Required for Myosin-II-Mediated Vesicle Transport During M-Phase in Extracts of Clam Oocytes

Torsten Wöllert<sup>1</sup>, Ana S. DePina<sup>2</sup>, Carl J. DeSelm<sup>2</sup>, and George M. Langford<sup>2</sup>

<sup>1</sup> Rostock University, Rostock, Germany

<sup>2</sup> Dartmouth College, Hanover, NH

In mammalian cells, Rho proteins Rho/Rac/Cdc42 regulate the formation of the actin cytoskeleton in stress fibers, lamellipodia, and filopodia (1). One of the ways in which Rho proteins mediate effects on the actin cytoskeleton is *via* the Rho-ROK/Rho kinase-myosin phosphatase pathway. In this pathway, myosin light chain phosphatase (MyoP) is phosphorylated by ROK/Rho kinase and is thereby inhibited (2). The net result is the activation of myosin-

II-mediated activities. In addition, Rho-family proteins have also been shown to regulate the actin cytoskeleton during cell division (3).

To study the role of Rho proteins in myosin-II mediated vesicle transport during the M-phase of the cell cycle, we used Y27632 to inhibit Rho kinase activity in extracts of clam oocytes. We have shown previously that actin filaments assemble spontaneously in

such extracts and organize into a three-dimensional network of interconnected filaments (4). This self-organized network of actin filaments resembles the cytokinetic ring of dividing cells in the following ways: (i) it exhibits myosin-II-mediated, anti-parallel sliding of actin filaments (4, 5), and (ii) it assembles during the M-phase of the cell cycle. Fortuitously, actin filaments in the extracts co-align to form bundles (10–20 parallel filaments) that are visible by AVEC-DIC microscopy. We have also shown that vesicles are moved along the actin filaments by a class II myosin motor (4). In this report, we show that a specific inhibitor of Rho kinase, Y27632, blocks vesicle transport in these extracts, thereby

providing additional evidence that vesicle movement on actin in these extracts is mediated by myosin-II.

Extracts prepared from mature oocytes arrested at the G2/M phase of the cell cycle were snap frozen and stored at  $-80^{\circ}\text{C}$ . To begin an experiment, the pH of the cytoplasmic extracts was shifted from 6.8 to 7.2 by diluting 2-fold with pH-8 buffer to initiate progression through M-phase. Nocodazole ( $30\ \mu\text{M}$ ) was added to the extracts to block microtubule assembly; an ATP regenerating system was added to maintain ATP levels; and the preparation was incubated at  $18^{\circ}\text{C}$  to assemble actin filaments and reconstitute motor activity. Rhodamine-phalloidin ( $0.5\ \mu\text{M}$ ) was

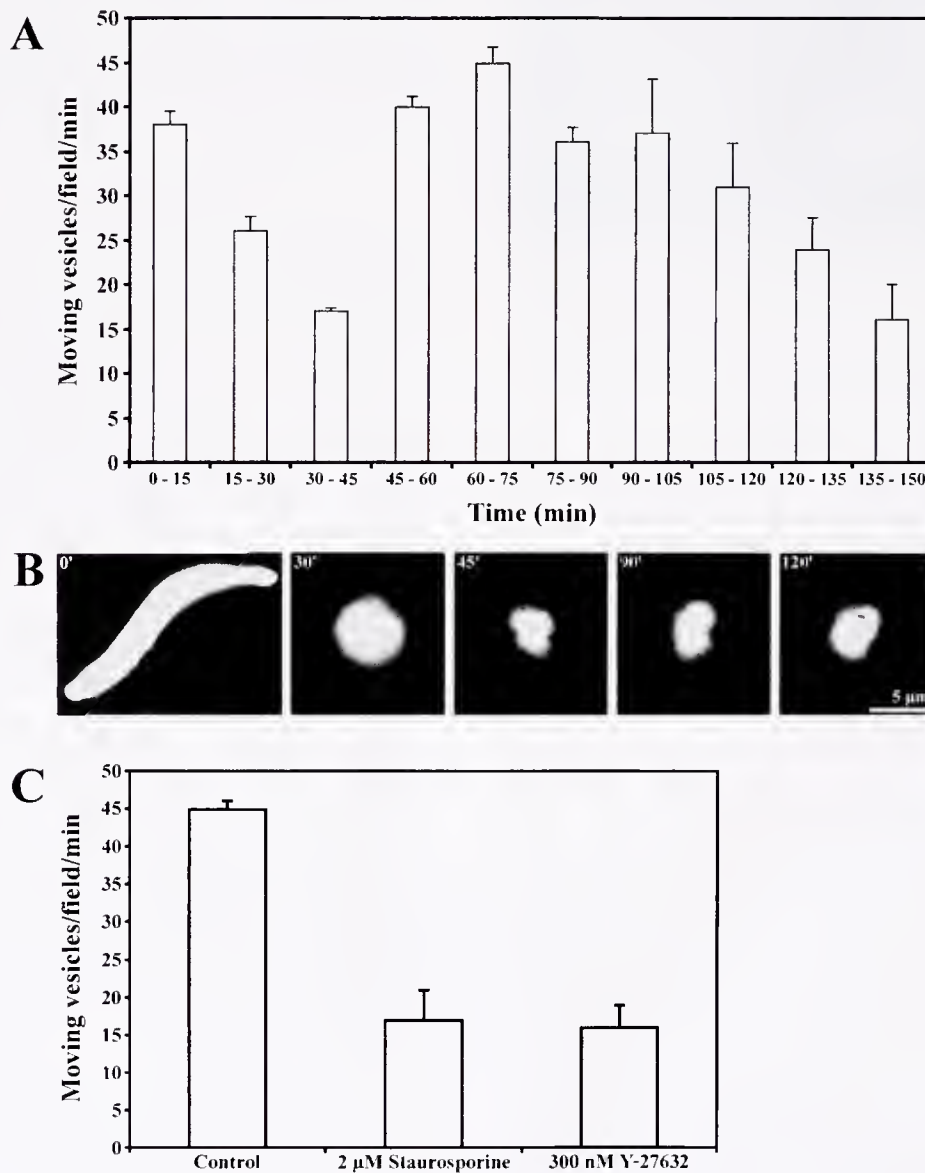


**Figure 1.** (A) Vesicle transport was measured at regular intervals. Motile activity is defined as the number of vesicles moving/video field/min. Motile activity is high initially but declines at 15–30 min. Motile activity returns to high levels between 45 and 120 min. (B) *Xenopus* sperm nuclei were added to the extract at time zero to determine the phase of the cell cycle. The initial elongated shape changed to a round shape at 30 min, and the chromosomes condensed at 45 min, diagnostic of M-phase. The nucleus remained condensed at 90 min but then began to expand at 120 min. (C) Inhibition of motile activity in the presence of Y27632 and staurosporine. A reduction of the motile activity was observed.

added to stain the actin filaments, and the myosin-II motor activity was monitored by AVEC-DIC and fluorescence microscopy.

In control extracts, vesicle transport was measured at regular time points to determine whether motile activity varied upon entry into M-phase of the cell cycle. Vesicle transport was measured by counting the number of vesicles moving per video field per min ( $v/f/m$ ; motile activity) at 15-min time intervals. We found that the motile activity was high during the first 15 min of incubation at 18 °C, then declined during the 15–30-min interval but rose again and remained stably high between 45 and 60 min (Fig. 1A). Motile activity declined again after 120 min at 18 °C. The actin network, as revealed by rhodamine-phalloidin staining, did not change during the 2-h period of incubation. To determine when the extracts were in the M-phase of the cell cycle, a *Xenopus* sperm-nucleus shape-change assay was performed. *Xenopus* sperm nuclei were added to the extract, stained with DAPI, and observed by fluorescence microscopy at regular intervals during incubation. In the initial period, the *Xenopus* sperm nuclei remained elongated, but they began to expand and appear uniformly bright at 30 min (Fig. 1B). At 45 min, the nuclei assumed an irregular shape as the chromosomes condensed. Chromosome condensation is diagnostic of M-phase. The nuclei remained irregular in shape with condensed chromosomes from 45–120 min, the period when motile activity was high (Fig. 1A). Based on this assay, extracts incubated for 45 to 60 min were judged to be in M-phase.

To determine whether Rho kinase is required for vesicle transport, extracts were incubated at 18 °C for 45 min, and then the inhibitor Y27632 was added at a concentration of 300 nM. We found that Y27632 inhibited vesicle transport by 65% compared to the control (Fig. 1C). The inhibitor had no effect on the actin cytoskeleton. The fact that vesicle transport was strongly inhibited

at low concentrations of the inhibitor suggested that the specific target of the inhibitor was Rho kinase, the most sensitive target of this inhibitor. Inhibition was also achieved with 2 mM staurosporine (Fig. 1C), a general kinase inhibitor. Based on the results with the Y27632 inhibitor, we conclude that Rho kinase is required for movement of vesicles on actin filaments.

In summary, these data show that Rho kinase is directly involved in vesicle transport. Because there was no effect on the actin cytoskeleton in this case, the downstream target of Rho kinase is mostly likely myosin II. This is the only myosin-mediated pathway known to be regulated by Rho GTPases. The downstream effector of the Rho proteins is most likely myosin light chain phosphatase (1). Therefore, we can conclude that the Rho-ROK/Rho kinase-myosin phosphatase pathway regulates vesicle transport during M-phase in clam oocytes.

This work was supported by NSF Grant IBN-0131470 and MBL Shifman award to CJD.

### Literature Cited

1. Bishop, A. L., and A. Hall. 2000. *Biochem. J.* 348: 241–255.
2. Kimura, K., M. Ito, M. Amano, K. Chihara, Y. Fukata, M. Nakafuku, B. Yamamori, J. Feng, T. Nakano, K. Okawa, A. Iwamatsu, and K. Kaihuchi. 1996. *Science* 273: 245–248.
3. Yoshizaki, H., Y. Ohba, K. Kurokawa, R. E. Itoh, T. Nakamura, N. Mochizuki, K. Nagashima, and M. Matsuda. 2003. *J. Cell Biol.* 162: 223–232.
4. Wöllert, T., A. S. DePina, R. F. Reid, and G. M. Langford. 2002. *Biol. Bull.* 203: 208–210.
5. Wöllert, T., A. S. DePina, L. A. Sandberg, and G. M. Langford. 2001. *Biol. Bull.* 201: 241–243.

Reference: *Biol. Bull.* 205: 197–199. (October 2003)  
© 2003 Marine Biological Laboratory

## An Experimental Approach to the Study of Gap-Junction-Mediated Cell Death

K. Cusato<sup>1</sup>, J. Zakevicius<sup>2</sup>, and H. Ripps<sup>2,\*</sup>

<sup>1</sup> Albert Einstein College of Medicine, Bronx, NY

<sup>2</sup> University of Illinois College of Medicine, Chicago, IL

The vertebrate retina is a highly specialized sheet of neural tissue derived from an undifferentiated population of neural progenitor cells, which, upon completion of their final division, migrate to their laminar positions and differentiate (1). In the adult retina, almost every class of neuron and glial cell is linked to its neighbors by gap junctions—aqueous channels that allow the intercellular exchange of ions, second messengers, and other small molecules ( $\leq 1$  kDa). Thus, this communication pathway aids in the synchronization of cellular activity, and plays a significant role in maintaining cellular homeostasis (2). During development, however, many retinal cells undergo programmed cell death, or apoptosis, and both intracellular and intercellular communication are known to regulate the process (3). Indeed, we recently reported

that gap junctions mediate a form of “bystander” cell death in the developing retina (4). Although this process is largely arrested in the mature retina, differentiated neurons and glia undergo apoptosis in neurodegenerative diseases (5), as well as in ischemia and trauma. In all of these cases, the spread of cell death from one dying cell to its otherwise unaffected neighbors (bystanders) may increase the total number of cells that enter the apoptotic pathway.

Because the retina is a complex tissue, some studies of bystander cell death are technically unfeasible at this time. We have developed a model system for the study of gap junction-mediated cell death using *Xenopus* oocytes which express an endogenous gap-junctional protein (connexin38, [Cx38]). Oocytes are paired at their vegetal poles following removal of their vitelline membranes and become electrically coupled *via* gap junctions. Because the *Xenopus* oocyte can serve to express many different connexins, the system should enable us to identify which gap junctional channels

\* Corresponding author: harrripp@uic.edu

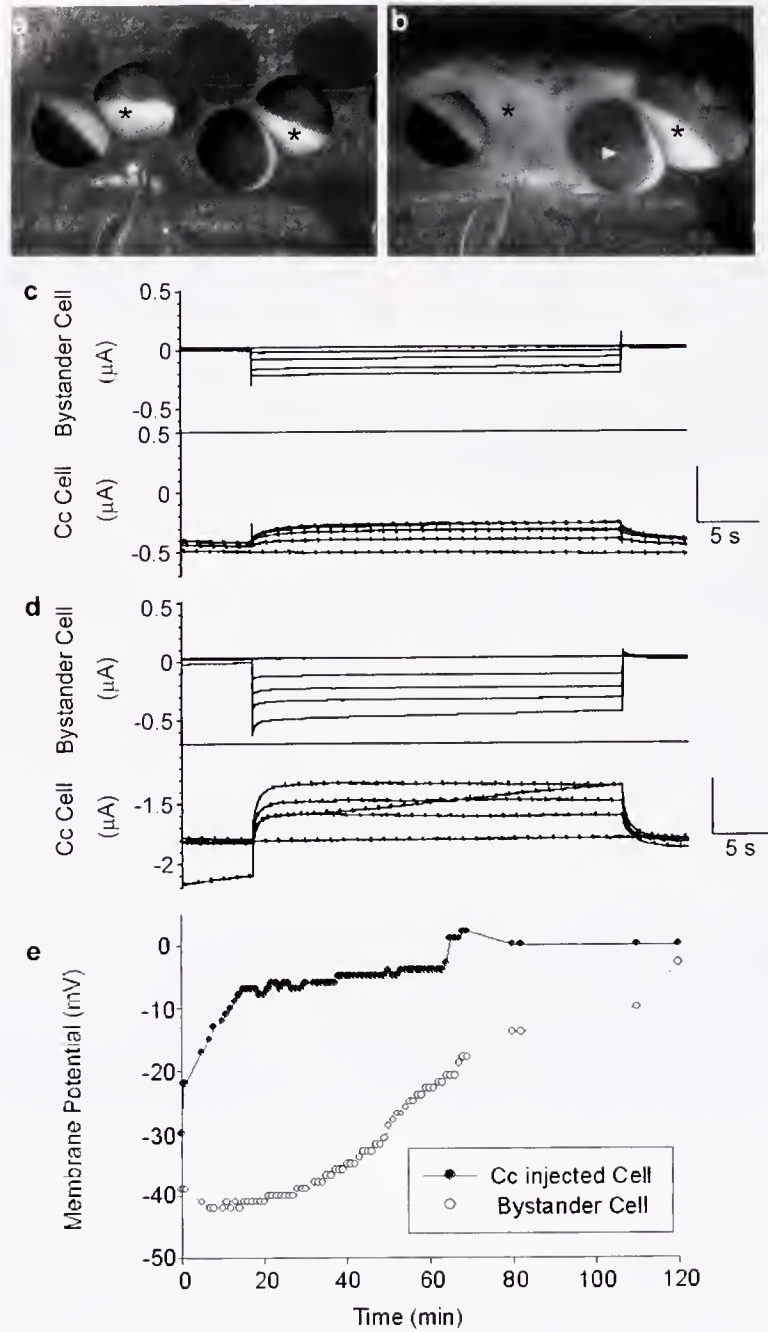


**Figure 1.** (a,b) Photographic images of two pairs of *Xenopus* oocytes that have been juxtaposed at their vegetal poles. The oocytes express an endogenous connexin (Cx38) and one member of each pair (asterisks) was injected with cytochrome *c*. Images were collected at 20 min (a) and 3 h (b) following cytochrome-*c* injection. Both cytochrome-*c*-injected cells have undergone cell death (evidenced by lysis or cell swelling). Note that the noninjected cell in b (arrowhead in right pair) also showed clear signs of cell death, whereas the noninjected cell paired to an injected cell that had deteriorated completely in less than 40 min did not. (c) Currents recorded from paired oocytes under dual electrode voltage clamp, shortly after cytochrome *c* injection, illustrate that the cells are electrically coupled. The upper trace shows currents from a cell in which hyperpolarizing voltage steps ( $-100$  to  $-20$  mV) were applied, while the bottom trace shows currents from the coupled cell. (d) Same cell pair and same protocol 30 min later. Traces indicate that cells remain coupled despite loss of membrane integrity; note the greater currents required to maintain the cells in voltage clamp. (e) The time course of membrane potential changes recorded from a pair of oocytes expressing Cx38 following cytochrome *c* injection into one cell. Note the rapid loss of membrane potential in the injected cell and the slower changes associated with death of the bystander cell. See text for details.

remain open under apoptotic conditions, to study the dynamics of gap junctional coupling during cell death, and to determine which molecules may pass from a dying cell to its neighbors to trigger the apoptotic process. Conversely, it is important to recognize that gap-junction-mediated cell death may result from the depletion of essential molecules (e.g., ATP) passing from the healthy cell to its dying neighbor.

Previous studies of single *Xenopus* oocytes have shown that microinjection of cytochrome c induces apoptotic cell death, accompanied by a progressive loss of membrane potential, activation of caspase 3, and DNA fragmentation (6). In the present study we have shown that injection of cytochrome c into one oocyte of a Cx38-coupled pair causes death in both the injected and noninjected cells over a period of 2–3 h (Fig. 1a,b). Pairs of oocytes preinjected with an antisense oligonucleotide to Cx38 did not exhibit bystander cell killing following cytochrome c injection; although the cell into which cytochrome c had been injected did die, its paired neighbor did not. Similarly, in cases where the cells were electrically coupled, but where the cytochrome c injected cell lysed in less than 40 min, the noninjected cell did not die (Fig. 1a,b, left pair). This result suggests that the intercellular channels joining the cytoplasm of the coupled cells must remain intact for longer than 40 min for bystander cell death to occur. It also indicates that bystander killing is not mediated by contact or by extracellular toxins, since the surviving cell continued to be in close apposition to the dying cell but remained intact. Vehicle injections failed to induce cell death in either injected or noninjected cells of electrically coupled pairs.

Dual electrode voltage-clamp using GeneClamp 500 amplifiers controlled by pClamp 8 software (Axon Instruments, Foster City, CA) was used to monitor gap junctional coupling between cell pairs after injecting one of the cells with cytochrome c. The two cells were voltage-clamped to the same potential (–40 mV), voltage steps were applied to the noninjected cell, and the current responses of both cells were recorded (7). As shown in Figure 1 (c,d), cells remained electrically coupled despite the gradual death of the injected cell. In addition, we found that the loss of membrane potential resulting from cytochrome c injection reported by Bhuyan *et al.* (6) in single oocytes could be seen also in cell pairs. After injecting one cell with cytochrome c, both cells underwent

membrane depolarization, with the injected cell losing membrane potential more rapidly following injection (Fig. 1e).

Although we have induced cell death by intracellular injection of cytochrome c, it is evident that the molecular mass of this apoptotic agent (13 kDa) is too great to pass through gap junctions (8). Clearly, cytochrome c itself cannot be the toxic substance carrying the death signal to bystander cells. Likewise, bystander killing is unlikely to be mediated by contact or diffusible substances, since antisense to Cx38 prevented bystander cell death, but not primary cell death. Of particular interest is the fact that gap junctional coupling persists during the apoptotic process, encouraging us to use the *Xenopus* oocyte and other expression systems in future experiments to identify the intercellular signals that pass between a dying cell and its coupled partners to induce bystander cell death.

These studies were conducted at the Marine Biological Laboratory, Woods Hole, Massachusetts, and were supported by grants from the NIH (HR: EY-06516 and EY-01792; KC: HL-07675); a Grass Foundation Fellowship (KC); an unrestricted award to the UIC Department of Ophthalmology and Visual Sciences from Research to Prevent Blindness, Inc.; a Senior Research Investigator Award from the RPB (HR); and an Award of Merit from the Alcon Research Institute (HR).

### Literature Cited

1. **Robinson, S. R. 1991.** Pp. 69–128 in *Vision and Visual Dysfunction, Vol 3: Neuroanatomy of the Visual Pathways and their Development*, B. Dreher and S. R. Robinson, eds. Macmillan, London.
2. **Andrade-Rozental, A. F., R. Rozental, M. G. Hopperstad, J. K. Wu, F. D. Vrionis, and D. C. Spray. 2000.** *Brain Res. Rev.* 32: 308–315.
3. **Linden, R. 2000.** *Brain Res. Rev.* 32: 146–158.
4. **Cusato, K., A. Bosco, R. Rozental, C. A. Guimarães, B. E. Reese, R. Linden, and D. C. Spray. 2003.** *J. Neurosci.* 23: 6413–6422.
5. **Ripps, H. 2002.** *Exp. Eye Res.* 74: 327–336.
6. **Bhuyan, A. K., A. Varshney, and M. K. Mathew. 2001.** *Cell Death Differ.* 8: 63–69.
7. **Dahl, G., T. Miller, D. L. Paul, R. Voellmy, and R. Werner. 1987.** *Science* 236: 11,290–11,293.
8. **Bennett, M. V. L., V. K. Verselis, R. L. White, and D. C. Spray. 1988.** Pp. 287–304 in *Gap Junctions*, E. L. Hertzberg, and R. G. Johnson, eds. Liss, New York.

Reference: *Biol. Bull.* 205: 199–201. (October 2003)

© 2003 Marine Biological Laboratory

### Apoptosis in *Microciconia prolifera* Allografts

S. Tepsuporn<sup>1,\*</sup>, J. C. Kaltenbach<sup>1</sup>, W. J. Kuhns<sup>2</sup>, M. M. Burger<sup>3</sup>, and X. Fernández-Busquets<sup>4</sup>

<sup>1</sup> Mount Holyoke College, South Hadley, MA

<sup>2</sup> Hospital for Sick Children, Toronto, Canada

<sup>3</sup> Friedrich Miescher Institute, Basel, Switzerland

<sup>4</sup> University of Barcelona, Barcelona, Spain

When two sponge tissue fragments from the same individual are adjoined, isogenic recognition occurs, and the fragments fuse. On

the other hand, if the two pieces are from different individuals, allogeneic recognition occurs, followed by failure of fusion and, presumably, death of cells at the graft contact zone (1, 2). It has been proposed that two cell types, archaeocytes and gray cells, are involved in sponge allogeneic recognition. Archaeocytes are large

\* Corresponding author: stepsupo@mholyoke.edu

phagocytic cells with large nucleoli; they are commonly found in wound healing and regenerating areas of the sponge (1). Gray cells are motile cells that contain many dense cytoplasmic granules (1); they do not have well-defined pseudopodia and are commonly found in gray cell regions of the sponge but are rare in the marginal region (2).

Apoptosis (programmed cell death) in sponges was first demonstrated by TUNEL nick-end labeling assay in hibernating sponges that had undergone tissue regression as a naturally occurring winter event (4). The development of an alternate method for detecting apoptosis was the finding that a series of caspases (proteases) delineated sequential enzymes leading to cell death (5). Of these, caspase-3 enzyme was the final and most important protease. From this have emerged antibodies for the detection of caspase-3 (6). Biochemical methods were used by Wiens *et al.* (7) to study apoptotic events in extracts of the marine sponge *Geodia cydonium*, where caspase-3 activity was found to be greatly increased in allograft extracts when compared with isografts. The objectives of the present research are (a) to determine by immunohistochemistry whether cell death at the allograft contact zone is a result of apoptosis rather than necrosis (death by injury that may result from mechanical damage to the cells) and (b) to identify the cell type or types, if any, that undergo apoptosis at the contact zone.

To examine whether the death of cells at the contact zone is a result of apoptosis, we used an indirect labeling technique that provides precise tissue localization of active caspase-3 as a marker for cells undergoing apoptosis. Processed cells that were reactive were visualized by the presence of a dark brown precipitate when color was developed with diaminobenzidine (DAB).

Individuals of *Microciona prolifera* were collected by the Marine Resources Center of the Marine Biological Laboratory (Woods Hole, MA) and were maintained until use in a tank with running cold seawater. The two sponge pieces for isografts and allografts were held together with number zero stainless steel pins attached to a Styrofoam board floating in a tank of running cold seawater. The grafts were fixed at 6-h intervals from 0 to 24 h in 3.7% formaldehyde in MBL artificial seawater (MBLASW) overnight, then washed and dehydrated in a series of ethyl alcohol concentrations from 30% to 70% in MBLASW. Spicules were dissolved by overnight treatment of grafts with 4% hydrofluoric acid in 70% ethanol. The grafts were then embedded in paraffin and sectioned at 7  $\mu\text{m}$ .

The slides of sectioned isografts and allografts were deparaffinized, hydrated, and treated with 3% hydrogen peroxide to remove endogenous peroxidase activity. Tissue presumed to possess caspase-3 activity was incubated using purified rabbit IgG anti-active human caspase-3, which had been generated by affinity purification from a caspase-3 enzyme fragment (PharMingen #559565); the antibody was used at a concentration of 0.25  $\mu\text{g}/\text{ml}$  for 2 h at room temperature. The slides were then washed with phosphate-buffered saline (PBS, pH 7.5) (Sigma), followed by treatment with appropriate biotinylated secondary antibody (Vector Laboratories). After another wash in PBS, the slides were treated with avidin-biotinylated enzyme complex (VectaStain Elite ABC Kit, Vector Laboratories) before the peroxidase substrate DAB (Sigma) was applied. The slides were washed, dehydrated,

mounted, and photographed with a digital camera on a Zeiss microscope.

Isograft sections treated with anti-active caspase-3 primary antibody did not stain, indicating that apoptosis did not occur in either the line of contact or any of the cells in the grafts during a 24-h period (Fig. 1A). On the contrary, treatment of allograft sections with the same primary antibody showed that cell death at the contact zone was indeed a result of apoptosis. Cells near the contact zone started to undergo apoptosis 6 h after grafting (data not shown). The line of contact became most apparent at 24 h (Fig. 1B). The longer the period of allogeneic contact, the higher the number of large, elongated apoptotic cells accumulated at the contact zone. The morphology of these cells was consistent with their identity as archaeocytes.

However, the existence of archaeocytes and gray cells in the contact area (1) prompted the use of a gray cell identity marker in

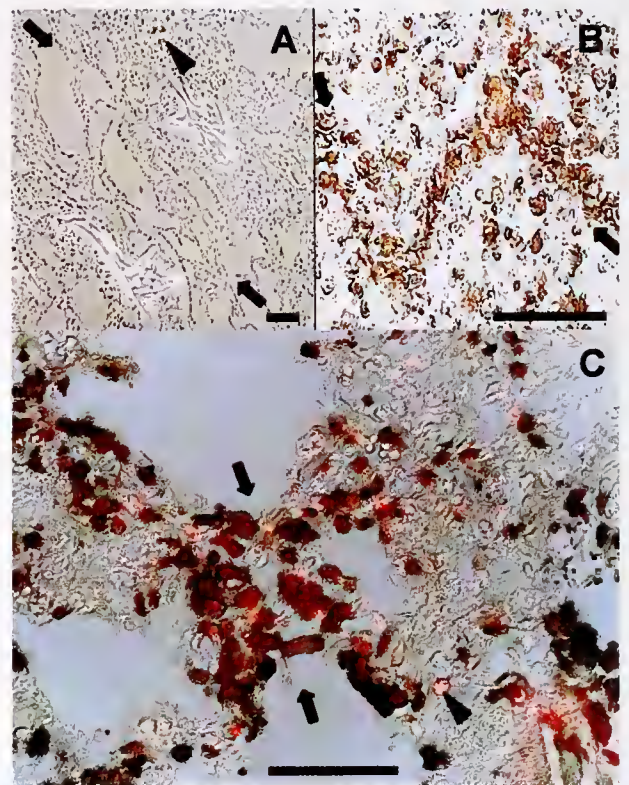


**Figure 1.** Apoptotic response of allografts prepared from the marine sponge *Microciona prolifera*. (A) Control isograft: fixed tissue stained with anti-active caspase-3 antibody. Arrows indicate the zone of contact. No reaction occurs in this zone or in cells in the area. Only occasionally do a few cells within the tissue show positive staining (arrowhead). Viewed under phase contrast. (B) Allograft fixed at 24 h, stained with anti-active caspase-3 antibody. A marked reaction is seen at the zone of contact (arrows), and in cells in the neighborhood of the contact area. (C) Allograft fixed at 6 h double stained with anti-active caspase-3 antibody, visualized as a brown precipitate with DAB- $\text{H}_2\text{O}_2$ , and with anti-CD44 antibody, visualized as pink fluorescence. Brown apoptotic cells designated as archaeocytes surround the contact line (arrows), and appear to be distinct from the pink fluorescent (i.e., CD44 positive) gray cells (arrowhead). Colocalization of caspase-3 and of CD44 was not observed. Bar represents 50  $\mu\text{m}$ .

addition to identification by morphology. CD44 has previously been demonstrated in gray cells, but not in archaeocytes (1), and therefore anti-CD44 antibodies were used in combination with anti-active caspase-3 antibodies in double labeling experiments. CD44 staining was done using a rat anti-mouse CD44 (Pharmin-gen) at 1  $\mu\text{g}/\text{ml}$  for 12 h at 4 °C, followed by wash and biotin-labeled secondary antibody (Vector Laboratories). Fluorescence was developed using Texas red-avidin (Vector Laboratories). The slides were treated as described above (microscope setting for single field imaging in fluorescent double staining: 647 nm filter, mercury and halogen lamp as light sources). Colocalization of anti-active caspase-3 and anti-CD44 was not observed (Fig. 1C).

We conclude that cell death at the allograft contact zone is a result of apoptosis rather than tissue necrosis, and that the apoptotic cells are most likely archaeocytes, not gray cells.

The ability to recognize self from non-self has been conserved throughout evolution. A better knowledge of this process in the sponge model should enhance our understanding of allogeneic recognition and its regulation in more complex species, including humans. The knowledge gained from such basic mechanisms should be of use in developing effective specific drugs that can abrogate the pathological effects of allogeneic responses (8).

Acknowledgments: Mount Holyoke College HHMI Cascade Mentoring Program; Research Experience for Undergraduates of

the Boston University Marine Program; Friedrich Miescher Institute of the Novartis Research Foundation. X. F.-B. holds a Ramón y Cajal tenure-track position from the Ministerio de Ciencia y Tecnología (MCyT), Spain, and acknowledges the support of grant BIO2002-00128 from the MCyT.

### Literature Cited

1. Fernández-Busquets, X., W. J. Kuhns, T. L. Simpson, M. Ho, D. Gerosa, M. Grob, and M. M. Burger. 2002. *Dev. Comp. Immunol.* **26**: 313–323.
2. Yin, C., and T. Humphreys. 1996. *Biol. Bull.* **191**: 159–167.
3. Simpson, T. L. 1968. P. 23 in *The Structure and Function of Sponge Cells: New Criteria for the Taxonomy of Poecilosclerid Sponges*. Peabody Museum of Natural History, New Haven, CT.
4. Kuhns, W. J., M. Ho, M. M. Burger, and R. Smolowitz. 1997. *Biol. Bull.* **193**: 239–241.
5. Kaufmann, S. H., and M. O. Hengartner. 2001. *Trends Cell Biol.* **11**: 526–534.
6. Voim, M., J. Mattern, and R. Koomaegi. 1999. *Anticancer Res.* **19**: 1669–1672.
7. Wiens, M., A. Krasko, S. Perovic, and W. E. Müller. 2003. *Biochim. Biophys. Acta* **1593**: 179–189.
8. Kuhns, W. J., M. M. Burger, M. Sarkar, X. Fernández-Busquets, and T. L. Simpson. 2000. *Biol. Bull.* **199**: 192–194.

Reference: *Biol. Bull.* **205**: 201–203. (October 2003)  
© 2003 Marine Biological Laboratory

## The Decorated Clot: Binding of Agents of the Innate Immune System to the Fibrils of the *Limulus* Blood Clot

Peter B. Armstrong<sup>1,2,\*</sup>, and Margaret T. Armstrong<sup>1,2</sup>

<sup>1</sup> Marine Biological Laboratory, Woods Hole, MA

<sup>2</sup> University of California, Davis, CA

The fibrillar blood clot functions as an important element of the innate immune system by its ability to entrap and immobilize bacteria that have entered the body *via* wounds, thereby preventing their systemic dissemination throughout the body of the injured host (1, 2). The coagulin clot of the horseshoe crab appears to play a similar role in protecting that animal from pathogenic attack. Bacteria entrapped in the coagulin clot are held so tightly as to abolish even thermal (Brownian) motion, and the clot synergizes with plasma in the killing of entrapped microbes (3). The present study investigates the proteins of the innate immune system of *Limulus* that bind to the fibrils of the coagulin clot, potentially supplementing the entrapment actions of the clot in two ways: first, by the lethality of clot-bound proteins for the entrapped microbes and second, by the ability of these proteins that decorate the clot fibrils to bind and inactivate the toxic products of entrapped microbes.

To establish the clot, the blood cells contained in 1 drop of blood collected under sterile conditions were dispersed in 2 ml of sterile 3% NaCl (Baxter Healthcare Corp., Deerfield, IL) in a 35-mm

plastic petri dish (Falcon Cat # 35-1008). After 5 min to allow attachment of the cells to the dish surface, the saline was replaced with 50% or 100% sterile *Limulus* plasma. Under these conditions, the blood cells rapidly degranulated, releasing the coagulin blood-clotting system. A dense coagulin clot then formed above the monolayer of attached blood cells. After 0.5–2 h of washing with several changes of wash buffer, this was either fixed directly in 4% paraformaldehyde dissolved in 3% NaCl, 10 mM CaCl<sub>2</sub> or was extracted with 0.5% Triton X-100 in the same buffer and then fixed in paraformaldehyde. All of the antibodies used for this report showed identical staining patterns for the two preparations. The various proteins used to prepare antibodies were purified as follows: coagulogen, the structural protein of the blood clot, as described by Srimal *et al.* (4); *Limulus*  $\alpha_2$ -macroglobulin, as described by Armstrong *et al.* (5); the *Limulus* pentraxins, as described by Armstrong *et al.* (6); and hemocyanin, purified by ultracentrifugation (285,000  $\times$  g, 8 h) followed by gel filtration chromatography (Sephacryl S-300). Antibody production in rabbits and immunocytochemical staining utilized standard methods (7). The polyclonal antibodies were checked for specificity by Western blotting (8) and in some cases were affinity-purified on antigen-Sepharose affinity columns (7).

\* Corresponding author: pbarmstrong@ucdavis.edu

The fibrillar structure of the coagulin clot showed to advantage both by phase contrast microscopy and by immunocytochemical staining with specific antigen antibodies (data not shown). The same fibrils were immunostained with antibodies prepared against highly purified preparations of *Limulus*  $\alpha_2$ -macroglobulin (data not shown), *Limulus* pentraxins (Fig. 1), and hemocyanin (data not shown). *Limulus*  $\alpha_2$ -macroglobulin functions in the binding and clearance of proteases, including, presumably, the proteases of pathogenic microbes (9). The *Limulus* pentraxins show a potent cytolytic activity against foreign cells and may operate to assist in the cytolytic destruction of microbial invaders (6, 10). Hemocyanin is the respiratory protein in solution in the blood but additionally shows a phenoloxidase activity that potentially functions to kill microorganisms by the generation of oxygen radicals (11).

The binding of  $\alpha_2$ -macroglobulin may be covalent because it was not removed by treatment prior to fixation with boiling SDS-polyacrylamide gel sample buffer containing 2-mercaptoethanol. Most of the known ligand-recognition properties of the *Limulus* pentraxins are  $\text{Ca}^{+2}$ -dependent (6). In contrast, binding to the coagulin clot is  $\text{Ca}^{+2}$ -independent, because immunostaining is not diminished by treatment of the clot with a  $\text{Ca}^{+2}$ -chelating agent, ethylenediaminetetraacetic acid (EDTA—0.1 M EDTA, 0.5 M NaCl, 10 mM Tris, pH 7.3). Most of the bound hemocyanin is removed by treatment of the clot with EDTA, but it is not certain whether this is simply a reflection of the dependence of the

oligomeric structure of the hemocyanin molecule on  $\text{Ca}^{+2}$  (12) or a true  $\text{Ca}^{+2}$ -dependent binding of hemocyanin to the coagulin fibrils. There are two potential sources for the clot-bound  $\alpha_2$ -macroglobulin: the plasma (13) and the  $\alpha_2$ -macroglobulin released from the secretory granules of the blood cells (14). We have not ruled out binding of plasma  $\alpha_2$ -macroglobulin, but secretory-granule-derived  $\alpha_2$ -macroglobulin does contribute to the clot-bound protein, because the clot fibrils produced by cells that degranulate in saline (0.5 M NaCl, 10 mM  $\text{CaCl}_2$ ) in the absence of plasma are decorated with  $\alpha_2$ -macroglobulin.

The fibrin fibers of the mammalian blood clot are known to bind a suite of proteins that assist in the functions of the clot. The blood clot of mammals binds fibronectin, which potentiates the immigration of wound-repair fibroblasts (15); FGF-2, which promotes proliferation of clot-associated endothelium (16, 17); and the serpins, plasmin activator inhibitor-2 (PAI-2) and  $\alpha_2$ -antiplasmin, which are presumed to protect the clot from proteolysis (18). However, we are not aware of any reports of agents of the immune system binding to the fibrin clot of mammals. Thus the observation that immune effector proteins bind to the *Limulus* clot suggests the novel idea that the clot is more than a passive entrapment device for invading microbes; it is potentially a delivery vehicle for proteins that are lethal to the entrapped microbes and proteins that inactivate toxic products of those microbes. Indeed, the clot syn-

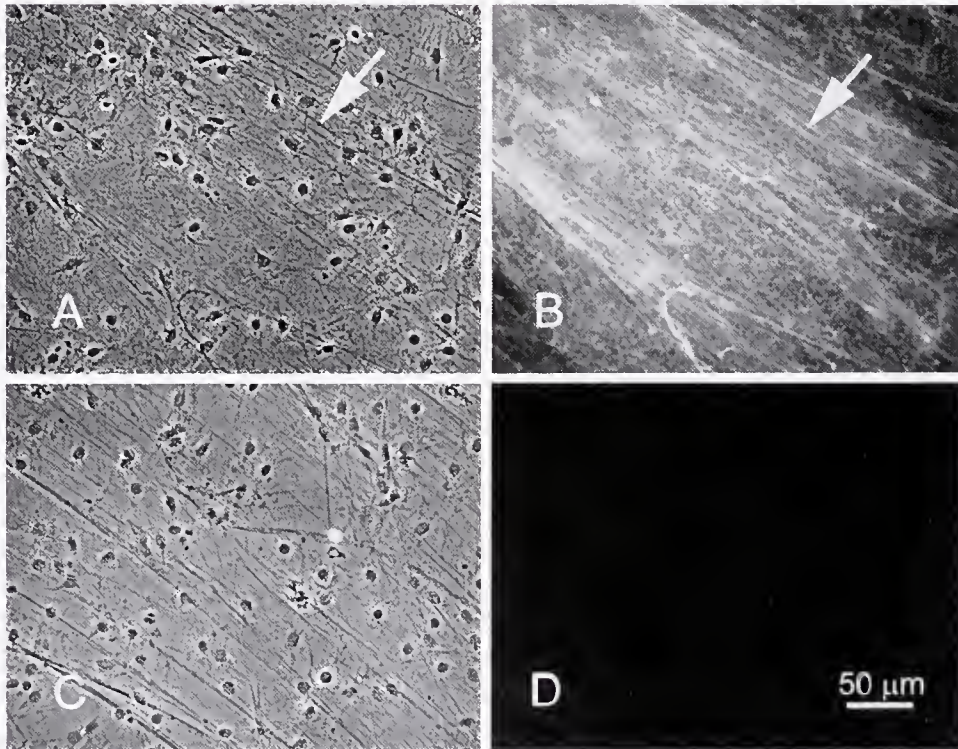


**Figure 1.** Binding of the *Limulus* pentraxins to fibrils of the *Limulus* blood clot in specimens not extracted with Triton X-100. The fibrils of the clot produced by monolayers of *Limulus* blood cells are visible by phase contrast microscopy (A, C) and immunostain with an antibody against the *Limulus* pentraxin (B). The arrows in A and B indicate the same fibril visible by phase contrast microscopy (A) and immunofluorescence (B). The darkish bodies seen by phase contrast microscopy (A, C) are the nuclei of the blood cells attached to the culture surface. When normal rabbit serum replaces specific antibody, the fibrils that are clearly visible by phase contrast microscopy (C) fail to stain (D). B and D were photographed under identical conditions and were manipulated identically in Photoshop, so are directly comparable.

ergizes with factors in the plasma in effecting the active killing of clot-entrapped microbes (3).

This research was supported by Grant No MCB-26771 from the National Science Foundation.

### Literature Cited

1. Dunn, D. L., and R. L. Simmons. 1982. *Surgery* **92**: 513–519.
2. Rotstein, O. D. 1992. *Eur. J. Clin. Microbiol. Infect. Dis.* **11**: 1064–1068.
3. Isakova, V., and P. B. Armstrong. 2003. *Biol. Bull.* **205**: 203–204.
4. Srimal, S., T. Miyata, S. Kawabata, and S. Iwanaga. 1985. *J. Biochem. Tokyo* **98**: 305–318.
5. Armstrong, P. B., R. Melchior, and J. P. Quigley. 1996. *J. Insect Physiol.* **42**: 53–64.
6. Armstrong, P. B., S. Swarnakar, S. Srimal, S. Misquith, E. A. Hahn, R. T. Aimes, and J. P. Quigley. 1996. *J. Biol. Chem.* **271**: 14,717–14,721.
7. Hartow, E., and D. Lane, eds. 1988. *Antibodies, a Laboratory Manual*. Cold Spring Harbor Laboratory, Cold Spring Harbor, NY.
8. Towbin, H., T. Stachelin, and J. Gordon. 1979. *Proc. Natl. Acad. Sci. USA* **76**: 4350–4354.
9. Melchior, R., J. P. Quigley, and P. B. Armstrong. 1995. *J. Biol. Chem.* **270**: 13,496–13,502.
10. Swarnakar, S., R. Asokan, J. P. Quigley, and P. B. Armstrong. 2000. *Biochem. J.* **347**: 679–685.
11. Nagai, T., and S. Kawabata. 2000. *J. Biol. Chem.* **275**: 29,264–29,267.
12. Van Holde, K. E., and K. I. Miller. 1982. *Q. Rev. Biophys.* **15**: 1–129.
13. Quigley, J. P., and P. B. Armstrong. 1983. *J. Biol. Chem.* **258**: 7903–7906.
14. Armstrong, P. B., J. P. Quigley, and F. R. Rickles. 1990. *Biol. Bull.* **178**: 137–143.
15. Mosher, D. F. 1975. *J. Biol. Chem.* **250**: 6614–6621.
16. Sahni, A., and C. W. Francis. 2000. *Blood* **96**: 3772–3778.
17. Sabni, A., T. Odrliin, and C. W. Francis. 1998. *J. Biol. Chem.* **273**: 7554–7559.
18. Ritchie, H., L. C. Lawrie, P. W. Crombie, M. W. Mosesson, and N. A. Booth. 2000. *J. Biol. Chem.* **275**: 24,915–24,920.

Reference: *Biol. Bull.* **205**: 203–204. (October 2003)

© 2003 Marine Biological Laboratory

## Imprisonment in a Death-Row Cell: The Fates of Microbes Entrapped in the *Limulus* Blood Clot

Victoria Isakova<sup>1,2</sup> and Peter B. Armstrong<sup>1,3,\*</sup>

<sup>1</sup> Marine Biological Laboratory, Woods Hole, MA

<sup>2</sup> Hunter College of the City University of New York, New York, NY

<sup>3</sup> University of California, Davis, CA

The fibrillar blood clot is an extracellular matrix established at sites of damage to the walls of the blood-vascular system. In humans, the clot is a polymer of the protein, fibrin. In the horseshoe crab, *Limulus polyphemus*, the clot is a meshwork of fibrillar polymers of the protein, coagulin (1). The blood clot functions to seal the wound to staunch bleeding, operates as a transient extracellular matrix for the migration of wound-healing epithelial and connective tissue cells, and serves as a barrier to entry of microbes into the interior of the animal *via* the wound. This study concerns the characterization of this last function for the coagulin blood clot of *Limulus*. We investigated the extent of immobilization of bacteria by the coagulin blood clot and the viability of the clot-entrapped bacteria.

Plasma was collected from adult horseshoe crabs under sterile, lipopolysaccharide-free conditions by cardiac puncture. Blood cells were removed immediately after collection and the plasma was sterile-filtered through a filter with a pore size of 0.22  $\mu\text{m}$  (Corning, Inc., Cat # 430769). The marine bacterium *Vibrio alginolyticus* was grown in liquid culture on Marine Broth 2216 (Difco). Log-phase growing populations were established by culture for 12 h at room temperature. Blood clots were established by plating the cells contained in 1 drop of *Limulus* blood collected by cardiac puncture under sterile conditions in 2 ml of sterile 3% NaCl (Baxter Healthcare Corp., Deerfield, IL) in a 35-mm plastic petri dish (Falcon, Cat # 35-1008). Bacteria suspended in 0.1 M

sucrose, 3% NaCl, equivalent to the bacteria contained in 250  $\mu\text{l}$  of the original culture medium, were introduced into the culture dish before the blood cells were added to facilitate direct presentation of bacteria to the blood cells while the latter were attaching to the culture surface of the dish. Under these conditions, the blood cells degranulate to release coagulogen and the proteases that process it into coagulin, the form that polymerizes into the fibrillar clot (2). The result is the entrapment of numbers of bacterial cells in the meshwork of fibers of the coagulin clot. The fate of the entrapped bacteria was investigated by direct light microscopic observation. The two parameters of greatest interest were the immobilization of bacteria by the clot and the killing of clot-entrapped bacteria by components of the plasma operating in synergy with the clot.

In suspension, *V. alginolyticus* shows rapid flagellar-driven swimming locomotion. Bacteria entrapped in the coagulin clot are immotile, and are held so tightly as to lack even thermal (Brownian) motion. When bacteria were killed to eliminate swimming motility, more than 90% of the killed bacteria in suspension showed thermal (Brownian) motion; in contrast, all bacteria enmeshed in the clot were absolutely stationary, without thermal motion.

Entrapped bacteria survive and proliferate in clots maintained in artificial seawater, which is isotonic to *Limulus* blood. In a typical trial, 87% of the bacterial clusters enmeshed in the clot contained only one cell immediately after capture, but 54% of the bacterial clusters contained two or more cells by 4 h of incubation.

\* Corresponding author: pbarmstrong@ucdavis.edu

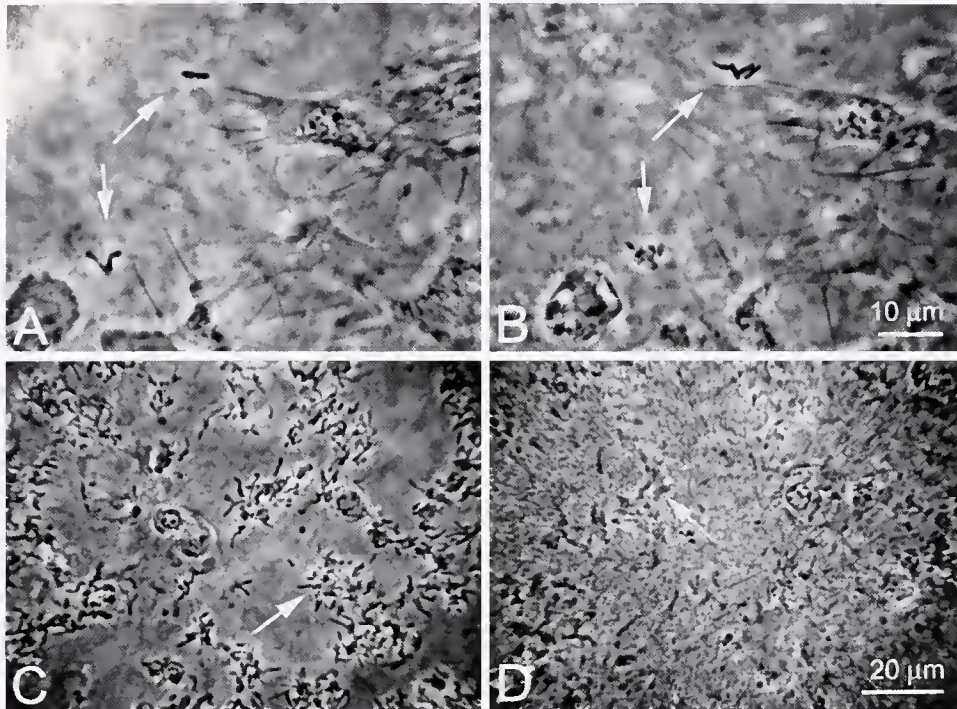


**Figure 1.** Proliferation and killing of *Vibrio alginolyticus* entrapped in the *Limulus* blood clot. Sequential views of the same microscopic field showing individual bacteria entrapped in the clot (A,  $t = 0$  h) survive and proliferate to establish clumps of two or more cells (B,  $t = 2$  h) when the clot with contained bacteria is incubated in bacteriologic culture medium. Bacteria entrapped in the clot are efficiently killed when the preparation is exposed to plasma. After 4 h incubation in marine broth culture medium, the clot-entrapped bacteria show as dense phase-bright bodies when viewed by phase contrast microscopy (C). Clot-entrapped bacteria become nonrefractile ghost cells when incubated for 4 h in plasma (D).

Proliferation is rapid if the clot, with its cargo of entrapped bacteria, is transferred to bacterial culture medium (Fig. 1A, B). After 4 h of incubation of the clot with entrapped bacteria in culture medium, 84% of bacterial clusters contained two or more cells. However, bacteria were killed when the preparation of clot with entrapped bacteria was transferred to sterile *Limulus* plasma. Killing was monitored by loss of refractility of the bacterial cells under phase-contrast microscope examination (Plan 100/1.3 NA objective) (Fig. 1C, D). The non-refractile cells ("ghost cells") are presumed to be dead or seriously damaged. Loss of bacterial refractility shows a lag period of 1.5 h, after which killing is rapid. In a typical trial, cells appeared normal and strongly refractile at 1.5 h, but about 80% of the cells had become transparent at 2 h. We did not observe bacterial proliferation in the plasma-treated clot even after 8 h of incubation; whereas, as noted above, the seawater-treated clot did support bacterial growth. The LD<sub>50</sub> was at a 25% dilution of plasma. Interestingly, plasma-based cytotoxicity was dependent on entrapment in the coagulin clot because free bacterial cells diluted into plasma remained phase-dense and presumably alive. These cells did lose the capacity for flagellar-generated motility, but showed the same capacity for proliferation when transferred to nutrient agar as did cells treated under equivalent conditions in plain seawater.

Hemocyanin-free plasma produced by ultracentrifugation ( $285,000 \times g$ , 8 h) retained the bacteriolytic activity of whole plasma; and purified hemocyanin was not bacteriolytic at 40 mg/ml, its concentration in plasma, indicating that hemocyanin is not

involved in killing. The cytotoxic agent of plasma appears to be a protein, because heat-treated plasma (100 °C, 0.5 h) lost bacteriolytic activity. Dialyzed plasma, which lacked all components smaller than 10–12 kDa, was fully active, indicating that small molecules are not necessary for cytotoxicity.

In summary, we have defined two important contributions of the coagulin blood clot to immunity in *Limulus*. The clot immobilizes microbes, which presumably impedes their dissemination throughout the animal after gaining access *via* a wound. Plasma also shows an immobilizing action by its inhibition of flagellar swimming motility. Neither clot nor plasma alone kill the bacteria but the two synergize to effect the cytotoxic destruction of clot-entrapped microbes.

This research was supported by a grant MCB 26771 from the National Science Foundation (PBA) and a fellowship from the Howard Hughes Medical Institute Undergraduate Science Education Program in Biology, grant 52002679 (V1). We thank Ms. Alice Child, Mr. Joseph Lee, and Drs. William Cohen and Norman Wainwright for help with the research.

#### Literature Cited

- Iwanaga, S., T. Miyata, F. Tokunaga, and T. Muta. 1992. *Thromb. Res.* 68: 1–32.
- Armstrong, P. B., and F. R. Rickles. 1982. *Exp. Cell Res.* 140: 15–24.

Reference: *Biol. Bull.* 205: 205–206, (October 2003)  
© 2003 Marine Biological Laboratory

## A Liposome-Permeating Activity From the Surface of the Carapace of the American Horseshoe Crab, *Limulus polyphemus*

John M. Harrington<sup>1,2</sup> and Peter B. Armstrong<sup>1,2,\*</sup>

<sup>1</sup> Marine Biological Laboratory, Woods Hole, MA

<sup>2</sup> University of California, Davis, CA

Colonization by sessile fouling organisms (epibionts) is the usual fate for solid surfaces in the marine environment. The American horseshoe crab, *Limulus polyphemus*, ceases molting upon reaching maturity and lives several years as an adult in an epibiont-rich milieu, yet it typically maintains a cuticle that is largely free of macroscopic flora and fauna. Indeed, it is in the interest of the animal to maintain its carapace free from such organisms, as colonization of the cuticle by green and blue-green algae can be fatal (1). The mechanisms by which *Limulus* maintains a clean carapace are not well understood. We have investigated the antibiological properties of a potential anti-fouling system of *Limulus*, a viscous secretion of a system of dermal glands that discharge their product onto the surface of the carapace (2). We propose that this substance, dermal exudate (DE), contributes to maintaining the cleanliness, and thus the integrity, of the cuticle. In the past we have identified and partially characterized a hemolytic activity present in DE (3, 4). It was shown that the presence of macromolecular osmolites in the hemolysis assay medium, dextran-8 and to a lesser extent dextran-4, prevented lysis of the red blood cells. This effect is attributed to the ability of these macromolecular osmolites to establish an osmotic balance between the interior and exterior of the cell so that no net water flow into the cell occurs, protecting the cell from cytolysis. The inhibitory effect of dextrans suggests that DE-induced lysis results from hydrophilic pore formation in the lipid bilayer of the red blood cell rather than from a detergent-like disruption of lipid packing or from phospholipase activity. To investigate the potential interactions of DE directly with lipid bilayers, we have utilized a model system in which a self-quenching fluorescent dye has been trapped inside liposomes; an increase in the fluorescence of the dye is a marker for membrane permeation. Here we report the ability of an acid-precipitable constituent of DE to permeabilize liposomes. The agent or agents responsible for these hemolytic and liposome-permeating activities may function as deterrents against potential colonizers of the *Limulus* cuticle.

The secretion of DE can be stimulated by housing *Limulus* in stressful conditions such as a cage stocked with decaying fish material. Dermal exudate was collected by scraping the dorsal carapace. The exudate was stored at  $-20^{\circ}\text{C}$  or with 0.02%  $\text{NaN}_3$  to prevent bacterial growth. Liposomes were prepared with soybean type II phosphatidylcholine from Sigma. Lyophilized lipid was dissolved in chloroform and dried under a nitrogen stream to a thin film. The film was placed under vacuum overnight to remove any traces of solvent. The lipids were hydrated in 20 mM Tris pH 7.4, 100 mM carboxyfluores-

cein (CF), a self-quenching fluorescent dye. The resulting multilamellar liposomes were made unilamellar through five successive freeze-thaw cycles. Untrapped CF was removed from the liposome suspension by passage over a Sephadex G-50 column. The release of CF from the interior of liposomes was monitored as an indicator of lipid bilayer permeation. Assays were performed with a 1:1000 dilution of liposomes in 20 mM Tris, pH 7.2. Fluorescence intensity was observed with a Photon technologies fluorometer. Excitation and emission wavelengths were 460 nm and 550 nm respectively. The slit widths were adjusted such that the Raman scatter peak of distilled, deionized water at 397 nm gave an intensity of approximately 350,000 counts/s when excited at 350 nm. Release of entrapped CF from liposomes was seen as an increase in fluorescence intensity. A unit of activity is arbitrarily defined as an initial increase in fluorescent intensity of 5% per minute. Intensity values corresponding to 100% lysis were obtained with the addition of Triton X-100.

Crude dermal exudate showed potent liposome-permeating activity at a 1:100 dilution. Addition of 10 mM  $\text{CaCl}_2$  markedly reduced activity, as did acidic pH. The membrane-permeating activity of crude DE was retained by a 10-kDa cutoff filter (Amicon P-10) and was precipitated by 1 M HCl, suggesting that the responsible agent is a large molecule. When, however, the material that precipitated during the acid extraction was resuspended in an equivalent volume of 20 mM Tris, pH 7.2, a 71-fold increase in liposome-permeating activity was seen. Presumably, acid treatment removes an inhibitor. The activity of the resuspended material was, like that of crude DE, inactive at low pH. The active agent present in the acid-induced precipitate also failed to pass through a 10,000 molecular weight cutoff filter. Addition of NaCl or  $\text{CaCl}_2$  attenuated the activity in a concentration-dependant fashion. This suggests that the lytic agent might initially bind the lipid bilayer through ionic interactions.

The secretion is most likely the product of transdermal glands whose ducts open onto the surface of the carapace (2, 5). The viscosity of DE may provide for a matrix that slows the diffusion of cytolytic effector molecules into the surrounding aqueous environment. Direct cytolytic attack is a method of defense from potential pathogens that is used by many animal phyla. A voluminous literature exists documenting the diversity and mechanisms of proteins and peptides capable of permeabilizing lipid bilayers (6). We propose that the ancient arthropod *Limulus polyphemus* may employ just such a method for maintaining a carapace free from colonizing organisms. We have, in past publications, documented the ability of DE to lyse red blood cells and presented evidence for a mechanism of pore formation in the lipid bilayer of

\* Corresponding author: pbarmstrong@ucdavis.edu

the target cell. Here we present further evidence for direct interaction of a lytic agent in DE with lipid bilayers in such a manner as to make them permeable. We propose that these lytic activities are components of a defensive system that operates at the surface of the carapace of *Limulus* to maintain the cleanliness and integrity of the animal's cuticle.

This research was supported by Grant No. MCB-26771 from the National Science Foundation. We thank Mr. Louis Kerr for important assistance with use of the fluorometer and Dr. David Gadsby for donation of striped bass heads for the stimulation of DE production by caged horseshoe crabs.

### Literature Cited

1. Liebovitz, L., and G. A. Lewbart. 1987. *Biol. Bull.* **173**: 430.
2. Fahrenbach, W. H. 1999. Pp. 21-115 In *Chelicerate Arthropoda*, F. W. Harrison and R. R. Foelix, eds. Wiley-Liss, New York.
3. Harrington, J. M., and P. B. Armstrong. 1999. *Biol. Bull.* **197**: 274-275.
4. Harrington, J. M., and P. B. Armstrong. 2000. *Biol. Bull.* **199**: 189-190.
5. Stagner, J. L., and J. R. Redmond. 1975. *Mar. Fish. Rev.* **37**: 11-19.
6. van't Hof, W., E. C. Veerman, E. J. Helmhorst, and A. V. Amerongen. 2001. *Biol. Chem.* **382**: 597-619.

Reference: *Biol. Bull.* **205**: 207–208. (October 2003)  
© 2003 Marine Biological Laboratory

## Development and Characterization of a Self-Referencing Glutamate-Selective Micro-biosensor

Daniel J. Bogorff<sup>1</sup>, Mark A. Messerli<sup>1</sup>, Robert P. Malchow<sup>2</sup>, and Peter J. S. Smith<sup>1</sup>

<sup>1</sup> Marine Biological Laboratory, Woods Hole, MA

<sup>2</sup> University of Illinois at Chicago, Chicago, IL

Glutamate is the primary excitatory neurotransmitter in the CNS of vertebrates, activating both ionotropic and metabotropic receptors (1). Glutamate, along with other amino acids, has also been identified as an osmoticum used to regulate the water potential across the plasma membrane of animal cells (2). The molecular mechanisms regulating the release and uptake of glutamate are consequently of considerable physiological interest. The release of glutamate from single cells can be detected with outside-out patches of glutamate receptors pulled from nerve cells (3), but these sensors lack consistency, are technically arduous to construct, and lose sensitivity over time. Fluorescent detection methods have also been used, but are also difficult to make and quantitate (4). Our specific aim is to avoid the difficulties inherent in these other techniques, by developing a noninvasive, real-time micro-biosensor that will quantitatively measure glutamate release and uptake by single cells.

High-sensitivity, real-time detection of glutamate can be achieved using electrochemical detection of  $H_2O_2$ , a byproduct of the enzymatic conversion of L-glutamate to  $\alpha$ -ketoglutarate catalyzed by glutamate oxidase (5). Glutamate oxidase itself has approximately 61- and 325-fold selectivity for glutamate over aspartate and glutamine when immobilized on macroelectrodes (5).  $H_2O_2$  can be directly detected with a platinum wire electrode polarized to +0.6 V (6). However, this method can be problematic due to (a) electrical drift of the electrode response, which reduces the useful sensitivity and reliability of the measurement, and (b) oxidation of other compounds released by cells, most notably ascorbate. Electrical drift can be eliminated if the electrode is used in a self-referencing format (7). In this mode, measurements are made alternately, near the source of glutamate influx or efflux, and then at a second location a set distance away; the difference in the readings at the two locations is the measurement of the flux. Electrical drift is subtracted out by this process, provided that the signal generated by the electrode occurs more quickly than the rate of electrical drift; if it is too slow, the signal itself will also be subtracted. The oxidation of interfering compounds can be eliminated by using enzyme-coupled detection of  $H_2O_2$  at a lower electrical potential. This is accomplished by coating the electrode with a redox polymer containing horseradish peroxidase (HRP) and osmium. HRP catalyzes the reduction of  $H_2O_2$  to water and is itself reduced by osmium(II), which is converted to osmium(III). The electrode then donates electrons to osmium(III), regenerating osmium(II) and, in the process, producing a measurable electrical current (8, 9). Our goal in the present work is to determine if such a hydrogel-based glutamate-selective electrode could be miniaturized for use in a self-referencing mode.

Microelectrodes were fabricated in a manner similar to oxygen sensors (10), except that 8- $\mu$ m carbon fiber, 12- $\mu$ m gold wire, and 10- and 25- $\mu$ m platinum wire were used at the reactive surface. Electrodes were dip-coated with Os-gel-HRP redox polymer

(BAS, W. Lafayette, IN) and allowed to dry for 10 min. Electrodes were then dip-coated in 50 units/ml glutamate oxidase (Sigma) and allowed to dry for 10–30 min. Glutamate electrodes were polarized to either 0 or +100 mV against a Ag/AgCl reference in physiological saline. The average response of platinum-based electrodes was  $0.45 \text{ pA} \pm 0.15 \text{ pA}/\mu\text{M}$  of glutamate, whereas gold-based electrodes produced a weaker signal of  $0.21 \pm 0 \text{ pA}/\mu\text{M}$ , and carbon gave the weakest signal,  $0.1 \pm 0.01 \text{ pA}/\mu\text{M}$ . Figure 1A shows the electrical current detected from a platinum gel electrode; it was placed 20  $\mu$ m from a source pipette containing 25  $\mu\text{M}$  glutamate and moved alternately to a position 50  $\mu$ m away. The initial period of oscillation was 0.1 Hz, and the electrode completed its translation to each location in 1.5 s. At the arrow, the period of oscillation of the electrode was slowed to approximately 30 s. The record clearly shows that the electrical current induced by glutamate had reached more than 90% of its maximal response within the 10-s time frame of oscillation. While this sensor could be used in a static configuration to detect glutamate, the electrical drift inherent in the electrode, which can limit detection at low concentrations of glutamate, can also be plainly seen as the slow rise in the baseline current (Fig. 1A). Figure 1B shows the differential responses obtained when the electrode was employed in a self-referencing mode to reduce the impact of this drift. The electrode was initially placed 20  $\mu$ m from a 25  $\mu\text{M}$  glutamate source pipette, and differential recordings were made by subtracting responses obtained at a point 50  $\mu$ m distant; the rate of oscillation was 0.1 Hz. In this condition, a steady differential signal of approximately 650 fA could be detected. The electrode was then progressively moved to positions more distant from the glutamate source, and differential recordings were obtained in the same fashion. The decline in the differential signal as a function of distance is apparent. Note also the clear, steady, small signal of approximately 50 fA that can be detected with the electrode 100  $\mu$ m away from the source pipette—a signal that is significantly smaller than the electrical drift and noise depicted in the raw recordings presented in Figure 1A.

Our work demonstrates that glutamate-selective electrodes based on a redox polymer hydrogel system can be miniaturized sufficiently to permit detection of glutamate. It also shows that the response time of these electrodes is short enough that they can be used in a self-referencing mode, which is useful for enhancing the signal-to-noise ratio for measuring slowly changing glutamate gradients. The sensitivity of these electrodes is suitable for measurements of glutamate release from living cells (5, 11).

This work was supported by grants from the National Center for Research Resources (P41 RR01395) and National Science Foundation (009-1240). Special thanks to Robert Lewis, Richard H. Sanger, and Kasia Hammar for their efforts and assistance.

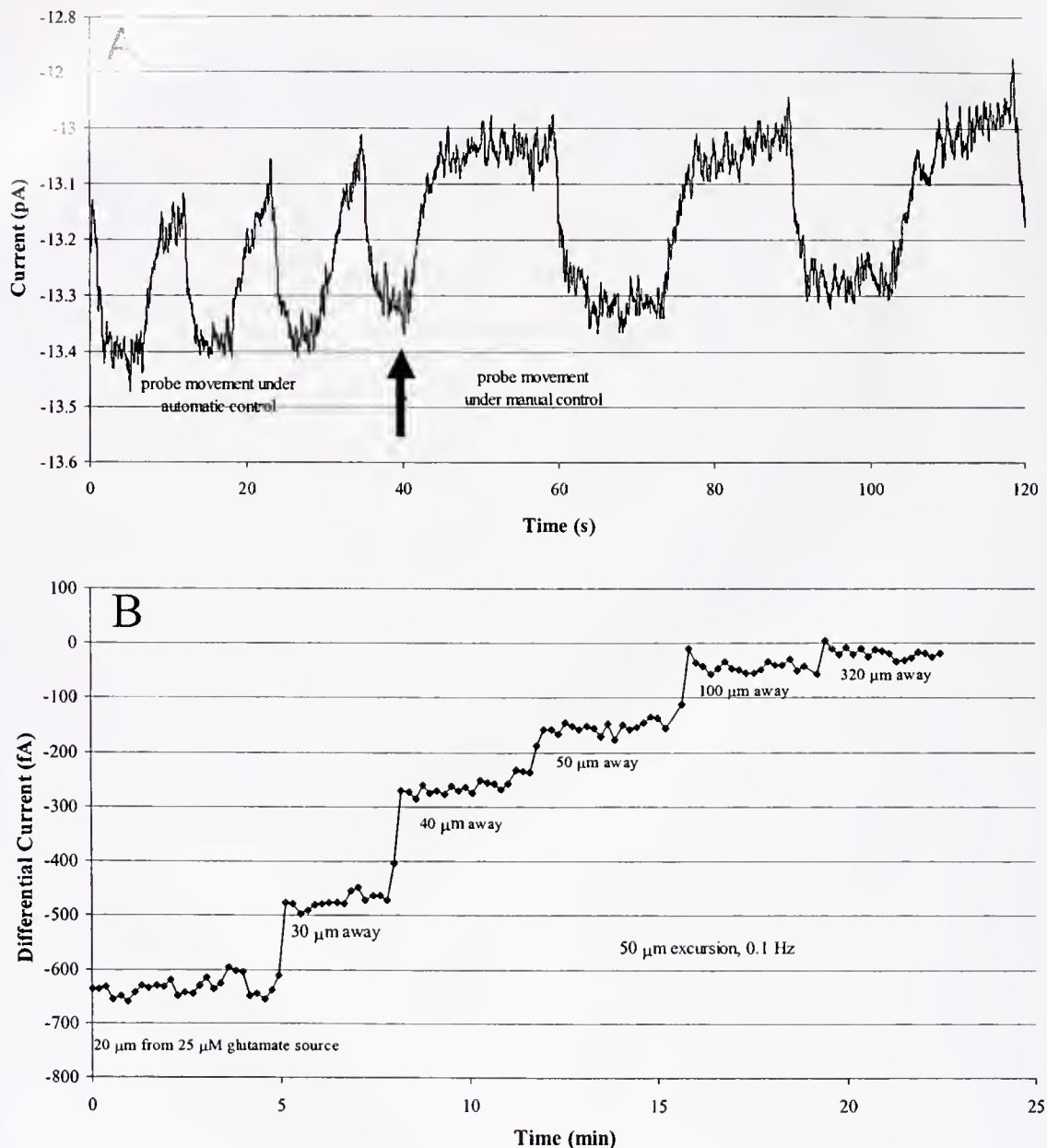


**Figure 1.** (A) Electrical current from a glutamate-selective micro-biosensor placed 20  $\mu\text{m}$  from a 25  $\mu\text{M}$  glutamate source pipette. The electrode was moved alternately to a position 50  $\mu\text{m}$  distant, first at a rate of 0.1 Hz, then at 0.03 Hz. (B) Recording of differential currents obtained when the electrode is used in a self-referencing made at increasing distances from the source.

### Literature Cited

- Jahr, C. E., and R. A. Lester. 1992. *Curr. Opin. Neurobiol.* 2: 270-274.
- Pasantes-Morales, H., R. Franco, L. Ochoa, and B. Ordaz. 2002. *Neurochem Res.* 27: 59-65.
- Copenhagen, D. R., and C. E. Jahr. 1989. *Nature* 341: 536-539.
- Ayoub, G. S., and D. R. Copenhagen. 1991. *J. Neurosci. Methods* 37: 7-14.
- Hu, Y., K. M. Mitchell, F. N. Albadidy, E. K. Michaelis, and G. S. Wilson. 1994. *Brain Res.* 659: 117-125.
- Twig, G., S.-K. Jung, M. A. Messerli, P. J. S. Smith, and O. S. Shirihai. 2001. *Biol. Bull.* 201: 261-262.
- Smith, P. J. S., K. Hammar, D. M. Porterfield, R. H. Sanger, and J. R. Trimarchi. *Microsc. Res. Tech.* 46: 398-417.
- Kulagina, N. V., L. Shankar, and A. C. Michael. 1999. *Anal. Chem.* 71: 5093-5100.
- Yigzaw, Y., L. Gordon, and T. Solomon. 2002. *Curr. Separations* 19: 119-125.
- Land, S. C., D. M. Porterfield, and P. J. S. Smith. 1999. *J. Exp. Biol.* 202: 211-218.
- Takahashi, M., B. Billups, D. Rossi, M. Sarantis, M. Hamann, and D. Attwell. 1997. *J. Exp. Biol.* 200: 401-409.

Reference: *Biol. Bull.* 205: 209–211. (October 2003)  
© 2003 Marine Biological Laboratory

## Zinc Modulation of Hemichannel Currents in *Xenopus* Oocytes

R. L. Chappell,<sup>1</sup> J. Zakevicius,<sup>2</sup> and H. Ripps<sup>2,\*</sup>

<sup>1</sup> Hunter College and The Graduate Center, CUNY, New York, NY

<sup>2</sup> University of Illinois College of Medicine, Chicago, IL

Connexins are a multigene family of structural proteins comprising gap-junctional channels, the aqueous pores that link electrically coupled cells in tissues throughout the body. These narrow passages ( $d \approx 16 \text{ \AA}$ ) allow the intercellular exchange of ions, second messengers, and other small molecules having a molecular mass  $\leq 1 \text{ kDa}$ . In the course of forming gap junctions, the connexins oligomerize into hexameric arrays known as "connexons" or "hemichannels" that assemble in the plasma membrane before docking with the connexons of adjacent cells (1). There is now abundant evidence that, at this penultimate stage of gap-junction formation, hemichannels can be activated both chemically and electrically (2, 3), that their properties often reflect those of fully formed gap junctions (4), and that the modulation of hemichannel activity may be of physiological significance (5).

Light-induced changes in the chemical environment of the vertebrate retina have profound effects on both neurotransmitter-gated and electrical synapses; and these effects can, in turn, alter the sensitivity, receptive field organization, and signalling pathways that transmit the visual message to the CNS. One putative neuro-modulator that has aroused a great deal of interest in recent years is zinc, which has been found in the synaptic vesicles of glutamatergic neurons in brain and retina (6). In the retinas of amphibia (7), fish (8), and mammals (6), zinc is present in photoreceptors, which signal second-order cells by regulating glutamate release in response to photic stimulation. Although the co-release of zinc with glutamate remains conjectural (9), the effects it exerts on retinal neurons have not been explored extensively (8, 10); and no studies have addressed the question of its effect on connexins or the channels they form.

In the present study, we used the two-electrode voltage-clamp recording technique to examine the effects of zinc on the currents mediated by the connexons formed by the endogenous connexin (Cx38) of stage V-VI *Xenopus* oocytes, and those formed by perch Cx35, a connexin expressed in neurons of the vertebrate retina (11, 12). To study the behavior of Cx35, cells were tested 48 to 72 h after they were injected with 46 nl of a mixture of 10 ng/cell Cx35 cRNA and 10 ng/cell of an antisense oligonucleotide to Cx38. The recordings were made with the cells bathed in a  $\text{Na}^+$ -free medium to eliminate the large  $\text{Na}^+$ -dependent currents that are similar in time course to the hemichannel currents, but of opposite polarity (13); zinc chloride was added without substitution. Responses were elicited with a series of 10-s pulses from a holding potential of  $-40 \text{ mV}$  to  $+60 \text{ mV}$  (see protocol, Fig. 1B inset), and were recorded with low resistance electrodes ( $0.7\text{--}1.5 \text{ M}\Omega$ ) connected to a GeneClamp 500 amplifier (Axon Instruments, Foster City, CA) and controlled by protocols generated in pClamp 8 (Axon).

Data were analyzed in ClampFit (Axon) and plotted with software programs in Origin (Microcal Inc., Northampton, MA).

Membrane currents recorded in a sodium-free modified Barth's (MB) solution from *Xenopus* oocytes expressing Cx35 are shown in Figure 1A. The slowly developing outward currents characteristic of hemichannel activity are seen with depolarizing voltage steps  $\geq +20 \text{ mV}$ . After changing the bath solution to one containing  $10 \mu\text{M}$  zinc, substantially greater hemichannel currents were elicited at these voltages (Fig. 1B). When the bathing medium was switched to one containing  $1 \text{ mM}$  zinc, the hemichannel currents were suppressed below those recorded in MB (Fig. 1C). The I-V data obtained with an oocyte expressing Cx35 for the range of zinc concentrations tested are illustrated in Figure 1D. It is evident that relatively low concentrations of zinc ( $1 \mu\text{M}$  and  $10 \mu\text{M}$ ) produce enhanced current responses at depolarizing voltages  $\geq 40 \text{ mV}$ , and the effect is reversed when the Zn concentration is increased to  $\geq 100 \mu\text{M}$ . It should be noted that hemichannel currents recorded during experimental runs in which the solutions were delivered in reverse order (*i.e.*, decreasing zinc concentrations from  $1 \text{ mM}$  zinc through  $1 \mu\text{M}$  zinc to Na-free MB) gave rise to the same biphasic behavior. Comparable results were obtained with Cx38 (Fig. 1E), where we show, in addition, that the blocking effect of  $1 \text{ mM}$  zinc could be completely reversed by coapplication of  $1 \text{ mM}$  histidine, a zinc chelator. Hemichannel currents elicited by depolarizing voltage steps from  $-40 \text{ mV}$  to  $+40 \text{ mV}$  from all oocytes tested were normalized to their control current in Na-free MB solution and averaged according to connexin type for each concentration of zinc applied. The results from 5 Cx35 oocytes (Fig. 1F) and 11 Cx38 oocytes (Fig. 1G) were similar. Currents recorded in  $1$  and  $10 \mu\text{M}$  zinc were greater than in the control (MB) solution, but decreased when the cells were bathed in  $100 \mu\text{M}$  and  $1 \text{ mM}$  zinc. A return to MB (Fig. 1F) following a zinc series returned the hemichannel currents to their control values. Cells injected with the antisense to Cx38 alone (controls) did not exhibit significant hemichannel activity (results not shown).

The biphasic effect of zinc on membrane currents is not unique. As shown in an earlier study (8), the addition of  $10 \mu\text{M}$  zinc greatly enhanced GABA-induced currents mediated by GABA<sub>A</sub> receptors (GABA<sub>A</sub>R) of skate bipolar cells; in contrast, the currents were markedly reduced when the cells were exposed to  $1 \text{ mM}$  zinc. Moreover, the zinc enhancement of hemichannel currents appears to be insensitive to voltage; currents in  $1 \mu\text{M}$  and  $10 \mu\text{M}$  zinc recorded at  $+40$  and  $+60 \text{ mV}$  were approximately 1.7 times greater than in MB, a finding consistent with that obtained for GABA<sub>A</sub>R-mediated currents of bipolar cells. These observations suggest that zinc may interact with connexins at two external membrane binding sites, with very different affinities for zinc. The high affinity site, activated at low concentrations of zinc, gives rise

\* Corresponding author: harrripp@uic.edu

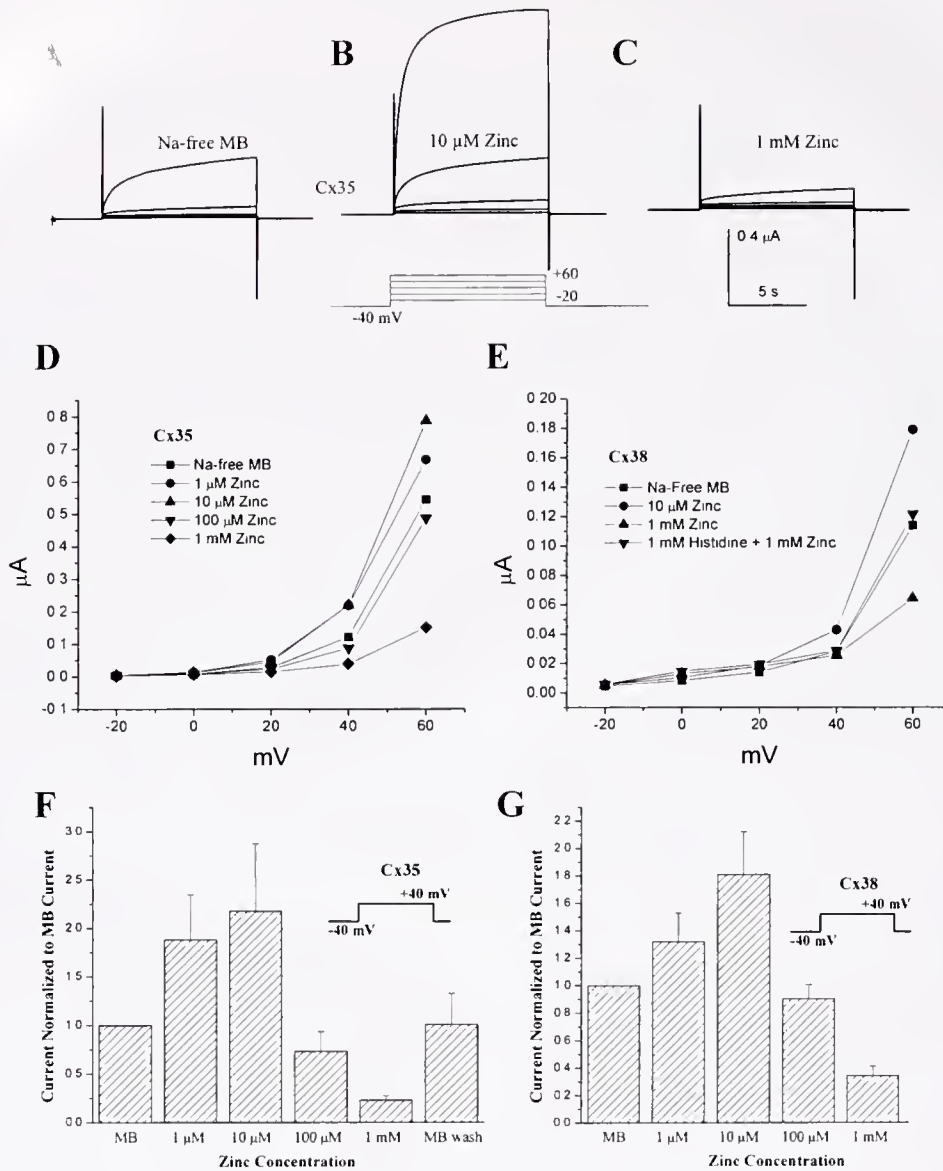


**Figure 1.** (A) Depolarizing voltage steps from  $-40$  mV to  $+60$  mV in  $20$  mV increments (inset) elicit hemichannel currents in a *Xenopus* oocyte expressing Cx35. With the cell bathed in a sodium-free modified Barth's (MB) solution, in which most of the sodium is replaced by choline ( $\text{Na}^+$  reduced to  $<3$  mM), a slowly developing outward current, attributable to the opening of membrane hemichannels, is evident at voltages  $> +20$  mV. The "Na-free" MB solution contained [in mM]  $\text{C}_5\text{H}_{14}\text{NOCl}$  [88],  $\text{KCl}$  [1],  $\text{NaHCO}_3$  [2.4], *N*-2-hydroxyethylpiperazine-*N'*-2-ethanesulfonic acid (HEPES) [15],  $\text{Ca}(\text{NO}_3)_2$  [0.33],  $\text{CaCl}_2$  [0.41], and  $\text{MgSO}_4$  [0.82];  $10$  mg/l gentamycin was added, and the solution titrated with NaOH to pH 7.6. (B) With the addition of  $10$   $\mu\text{M}$  zinc chloride, the hemichannel currents are greatly enhanced. (C) Increasing the zinc concentration to  $1$  mM suppresses the hemichannel currents to levels below those obtained in MB. (D) The effects of zinc concentration on the current-voltage relation (corrected for leakage currents) obtained for an oocyte expressing Cx35. (E) The I-V relation for the endogenous connexin (Cx38) displays a similar response to zinc; i.e., a large enhancement of hemichannels in  $10$   $\mu\text{M}$  zinc and suppression in  $1$  mM zinc. With the addition of  $1$  mM histidine, a zinc chelator, the suppressive effect of  $1$  mM zinc is reversed. (F-G) Bar graphs show averaged data obtained with Cx35 and Cx38 at different concentrations of zinc. In each data set, the currents recorded in response to a voltage step from the holding potential ( $-40$  mV) to  $+40$  mV have been normalized to the value obtained initially in Na-free MB. Error bars =  $\pm$  SEM ( $n = 5$  for Cx35; with Cx38,  $n = 6$  for  $1$   $\mu\text{M}$  Zn, and  $n = 12$  for the higher concentrations).

to an enhancement of hemichannel currents, whereas the low affinity site requires high concentrations of zinc to produce its inhibitory effect.

The present findings, and evidence that zinc is located within the synaptic terminals of vertebrate photoreceptors (7, 8), raise the

possibility that zinc modulation of hemichannel activity contributes to the processing of visual information in the distal retina.

These studies were conducted at the Marine Biological Laboratory, Woods Hole, Massachusetts, and supported by grants from the National Eye Institute (EY-06516 and EY-01792), a PSC/

CUNY grant (65711-0034) to RC, an unrestricted award to the UIC Department of Ophthalmology and Visual Sciences from Research to Prevent Blindness, Inc., a Senior Research Investigator Award from the RPB (HR), and an Award of Merit from the Alcon Research Institute (HR).

### Literature Cited

- Musil, L. S., and D. A. Goodenough. 1991. *J. Cell Biol.* **115**: 1357–1374.
- DeVries, S. H., and E. A. Schwartz. 1992. *J. Physiol.* **445**: 201–230.
- Malchow, R. P., H. Qian, and H. Ripps. 1994. *J. Gen. Physiol.* **104**: 1039–1055.
- Ebihara, L., V. M. Berthoud, and E. C. Beyer. 1995. *Biophys. J.* **68**: 1796–1803.
- Kamerlans, M., I. Fahrenfort, K. Schultz, U. Janssen-Bienhold, T. Sjoerdsma, and R. Weiler. 2001. *Science* **292**: 1178–1180.
- Ugarte, M., and N. N. Osborne. 2001. *Prog. Neurobiol.* **64**: 219–249.
- Wu, S. M., X. Qiao, J. L. Noebels, and X. L. Yang. 1993. *Vision Res.* **33**: 2611–2616.
- Qian, H., L. Li, R. L. Chappell, and H. Ripps. 1997. *J. Neurophysiol.* **78**: 2402–2412.
- Kay, A. R. 2003. *J. Neurosci.* **23**: 6847–6855.
- Rosenstein, F. J., and R. L. Chappell. 2003. *Neurosci. Lett.* **345**: 81–84.
- O'Brien, J., M. R. Al-Ubaidi, and H. Ripps. 1996. *Mol. Biol. Cell* **7**: 233–243.
- White, T. W., M. R. Deans, J. O'Brien, M. R. Al-Ubaidi, D. A. Goodenough, H. Ripps, and R. Bruzzone. 1999. *Eur. J. Neurosci.* **11**: 1883–1890.
- Ripps, H., H. Qian, and J. Zakevicius. 2002. *J. Neurosci. Meth.* **121**: 81–92.

Reference: *Biol. Bull.* **205**: 211–212. (October 2003)  
© 2003 Marine Biological Laboratory

## Transient Use of Tricaine to Remove the Telencephalon Has No Residual Effects on Physiological Recordings of Supramedullary/Dorsal Neurons of the Cunner, *Tautoglabrus adspersus*

S. J. Zottoli, O. T. Burton, J. A. Chambers, R. Eseh, L. M. Gutiérrez, and M. M. Kron  
Williams College, Williamstown, MA

When used as a general anesthetic, tricaine significantly alters physiological parameters recorded from supramedullary/dorsal cells of the cunner, *Tautoglabrus adspersus*. Specifically, tricaine reduces spike height, increases the current needed to elicit an action potential, and blocks afferent input (1). In contrast, equivalent recordings from locally anesthetized fish are not altered in this way. However, although the use of local anesthetic is a better alternative to tricaine general anesthesia for physiological recordings (1), there are limitations. Local anesthetics have a limited lifetime, are difficult to reapply while recording, and can enter the bloodstream.

As in other vertebrates, the telencephalic hemispheres of fish are considered to be the "highest" brain centers. For example, the telencephalon of goldfish has been implicated in spatial and avoidance learning (e.g., 2, 3). The removal of the telencephalon under transient tricaine anesthesia is used in lieu of general anesthesia in many laboratories (e.g., 4, 5). However, no studies have been conducted to determine whether tricaine—after its removal—affects physiological parameters of neurons whose somata lie within the central nervous system. We have therefore studied whether either the transient use of tricaine or telencephalon removal have any residual effects on resting potential, spike height, and current needed to elicit a spike.

Responses of supramedullary/dorsal cells to depolarizing current pulses and to electrical stimulation of the skin on the right operculum were recorded from cunner, 10.5 ± 1.2 cm (mean ± SD;  $n = 22$ ) in body length. The fish were either transiently anesthetized with tricaine during the removal of the telencephalic hemispheres, or were not anesthetized.

In the first condition, the fish were initially anesthetized in tricaine (ethyl-*m*-aminobenzoate: 300 mg/l, Sigma-Aldrich) in sea-

water adjusted to pH 8. When respiration ceased, the fish were transferred to an operating chamber where tricaine (100 mg/l) in chilled seawater adjusted to pH 8 was recirculated through the mouth and over the gills. Ice packs were placed in the operating chamber on either side of the fish. The skull was removed to expose the telencephalic hemispheres, and these structures were removed. The fish were injected with tubocurarine chloride (0.1 mg/kg) to block neuromuscular transmission, and then the seawater with anesthetic was replaced with anesthetic-free, chilled seawater. Finally, the rostral spinal cord was exposed. In the second condition no anesthetic was used. Fish were injected with tubocurarine chloride and placed in an operating chamber. Their telencephalic hemispheres and the rostral spinal cord were exposed. In seven experiments, the telencephalon was stimulated to determine whether any input to the dorsal cells could be elicited.

Single microelectrode recordings (3 M KCl-filled, 5–20 M $\Omega$  initial resistance) were made from somata of supramedullary/dorsal cell neurons in both anesthetic and anesthetic-free conditions. The recordings were all made within 78 ± 43.4  $\mu$ m (mean ± SD;  $n = 26$ ) of the surface of the brain.

After tricaine was used transiently to remove the telencephalic hemispheres, action potentials 102.1 ± 9.4 mV (mean + SD,  $n = 16$ ) in amplitude could be evoked by 4.5 ± 2.9 nA current (initial recordings were started 68 ± 55 min after removal of tricaine). In anesthetic-free experiments neither the spike height (103.3 ± 12.5 mV,  $n = 11$ ) nor the current needed to evoke the spike (2.4 ± 1.7 nA) was significantly different ( $P > 0.05$ ; Bonferroni's Multiple Comparison Test). In addition, there were no significant differences in resting membrane potential (transient use of tricaine = -74.1 ± 5.8 mV; anesthetic free = -72 ± 7.1 mV). Post-synaptic potentials (PSPs) were readily evoked by stimulation of the skin of

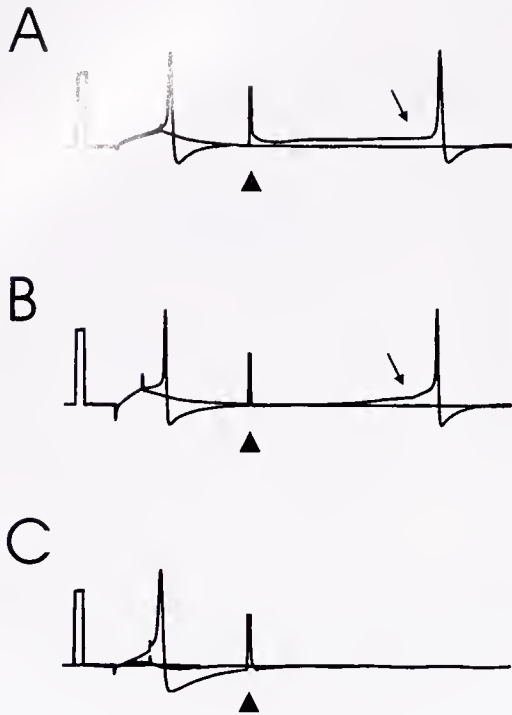


**Figure 1.** Comparison of PSPs evoked by electrical stimulation of the skin in supramedullary/dorsal cells. (A, B, C) A calibration pulse of 80 mV, 2 ms is present at the beginning of each recording. Cells fired action potentials in response to a short intracellular depolarizing pulse in one of the two superimposed traces. This pulse was followed by electrical stimulation of the skin of the right operculum (to provide a baseline, in one of the two superimposed traces this stimulus was not given; stimulus artifacts are designated with arrowheads). (A) Recordings from a fish in which tricaine was used transiently to remove the telencephalon. A PSP (arrow) gives rise to an action potential. (B) Recordings from an unanesthetized fish. A PSP (arrow) gives rise to an action potential. (C) Recordings from a fish under general tricaine anesthesia. No PSPs could be evoked to electrical stimulation of the right operculum.

the right operculum in both conditions. This was not the case in animals under general anesthesia (1; Fig. 1).

In anesthetic-free experiments, stimulation of the telencephalic hemispheres at only the high voltages (80–100 V) activated the dorsal cells. To test whether this activation was the result of direct or indirect telencephalic input to the supramedullary/dorsal cells and not current spread to adjacent nervous tissue, in three experiments the telencephalic hemispheres were removed and then replaced in their original positions. The disconnected telencephalic

hemispheres were stimulated again at roughly the same location and the same voltages. The response to stimulation persisted. These results indicate that activation was through current spread to adjacent structures such as the trigeminal nerve, which is known to contain processes of dorsal cells.

General anesthetics, such as tricaine, are known to reduce sodium currents, and their effects are reversible (6). The transient use of tricaine and the removal of the telencephalic hemispheres in this study appear to have had no residual effect on spike height, on the current needed to elicit an action potential, or on the ability to elicit PSPs from the supramedullary/dorsal cells.

Although Rose (7) provides a compelling argument that it is implausible for fish to experience pain, implausible is not conclusive. Nociceptors have been identified in the trout (8, 9). Endogenous opioid peptides (10) and opioid receptors in fish (e.g., 11, 12) may serve an anti-nociceptive function as in mammals (11). If there is no telencephalic influence on the system being studied, then the transient use of tricaine followed by removal of the telencephalon serves as a reasonable precaution against the possibility that fish experience pain.

This work was supported in part by Howard Hughes Medical Institute and Essel Foundation grants to Williams College. All experimental procedures were approved by the MBL IACUC.

#### Literature Cited

1. Arnolds, D. E. W., S. J. Zottoli, C. E. Adams, S. M. Dineen, S. Fevrier, U. Guo, and A. J. Pascal. 2002. *Biol. Bull.* 203: 188–189.
2. Overmier, J. B., and M. R. Papini. 1986. *Behav. Neurosci.* 100: 190–199.
3. Portavella, M., J. P. Vargas, B. Torres, and C. Salas. 2002. *Brain Res. Bull.* 57: 397–399.
4. Duman, C. H., and D. Bodznick. 1996. *J. Comp. Physiol. A* 179: 797–807.
5. Rohregger, M., and N. Dieringer. 2002. *J. Neurophys.* 87: 385–398.
6. Frazier, D. T., and T. Narahashi. 1975. *Eur. J. Pharmacol.* 33: 313–317.
7. Rose, J. D. 2002. *Rev. Fish. Sci.* 10: 1–38.
8. Sneddon, L. U. 2003. *Brain Res.* 972: 44–52.
9. Sneddon, L. U., V. A. Braithwaite, and M. J. Gentle. 2003. *Proc. R. Soc. Lond. B* 270: 1115–1121.
10. Gonzalez-Nunez, V., R. Gonzalez-Sarmiento, and R. E. Rodriguez. 2003. *Mol. Brain Res.* 114: 31–39.
11. Darlison, M. G., F. R. Greten, R. J. Harvey, H.-J. Kreienkamp, T. Stühmer, H. Zwierns, K. Lederis, and D. Richter. 1997. *Proc. Natl. Acad. Sci.* 94: 8214–8219.
12. Rodriguez, R. E., A. Barrallo, F. Garcia-Malvar, I. J. McFadyen, R. Gonzalez-Sarmiento, and J. R. Traynor. 2000. *Neurosci. Lett.* 288: 207–210.

Reference: *Biol. Bull.* 205: 213–214. (October 2003)  
© 2003 Marine Biological Laboratory

## Zinc Chelation Enhances the Sensitivity of the ERG b-Wave in Dark-Adapted Skate Retina

S. Redenti<sup>1</sup> and R. L. Chappell<sup>1,2,\*</sup>

<sup>1</sup>The Graduate Center, CUNY, New York, NY

<sup>2</sup>Hunter College, CUNY, New York, NY

A decade ago, Wu *et al.* reported evidence of a dense band of ionic zinc in the region of the photoreceptor terminals of the salamander retina (1). They speculated that zinc may play a neuromodulatory role in the outer retina, including possible feedback onto photoreceptors to down-regulate transmitter release, as well as feed-forward onto second order cells. Subsequently, a high ionic zinc concentration was identified in a similar region near the base of the photoreceptors in the all-rod retina of the skate (2). In addition, Ugarte and Osborne (3) have reported recently that a dense band of ionic zinc, located in the photoreceptor region of the light-adapted rat retina, is redistributed under dark-adapted conditions.

Zinc has been known to affect the response of receptors on a number of retinal cell types to various neurotransmitters (4). In the skate, zinc regulates both GABA (2) and glutamate (5) receptors of isolated cells. Furthermore, the zinc chelator histidine (an amino acid endogenous in the retina, where it may play various roles in cell metabolism and disease (6, 7, 8, 9, 10)) has been shown to enhance the size of the b-wave of the electroretinogram (ERG) of the skate (5) and zebrafish (11). Histidine can also increase the membrane currents recorded postsynaptically from horizontal cells during voltage-clamp in the skate retinal slice preparation (12). The effects of histidine support the notion that endogenous zinc may be playing a role in the physiological response of the retina to light.

Recent studies of the effects of histidine on the zebrafish ERG have demonstrated an increase in sensitivity of its mixed rod-cone retina in the presence of a zinc chelator (11). Here, we report studies of the effect of histidine on the retina of the skate, *Raja erinacea*, indicating that application of this zinc chelator enhances the sensitivity of the b-wave of the ERG in an all-rod retina.

Skates were obtained through the Marine Resources Center of the Marine Biological Laboratory (Woods Hole, MA). The animals were allowed to dark-adapt for at least one hour prior to an experiment. After approved euthanasia, the eyes were enucleated and dissected under dim red light. The anterior portion of the eye, including cornea and lens, was removed; and the remaining retinal eyecup preparation was used for ERG recordings. Eyecups were placed into a chamber over a silver chloride reference electrode within a Faraday cage. The active silver chloride electrode was connected to superfusion solutions in the eyecup via a glass capillary containing Ringer/agar. ERG responses to increasing intensities of illumination were recorded while the preparation was superfused (~0.5 ml/min) with skate-modified Ringer's solution (2) alone, or to which 200  $\mu$ M picrotoxin (to block GABAergic receptors in the retina known to be zinc-sensitive (2)), and then 100  $\mu$ M histidine plus 200  $\mu$ M picrotoxin had been added. We had found that responses in picrotoxin did not increase after the first 10

min, but that ERG responses in histidine could continue to increase for up to 30 min. Therefore, the preparation was kept in the dark for 30 min in Ringer, at least 10 min in picrotoxin, and at least 30 min in histidine plus picrotoxin prior to recording an intensity-response series. One-second flashes were used to elicit ERG responses from which b-wave amplitudes were measured. The intensity of the unattenuated beam ( $\text{Log } I = 0$ ) was 260  $\mu\text{W}/\text{cm}^2$ .

Individual ERG responses recorded from one skate eyecup preparation in response to stimulation at an intensity of  $\text{Log } I = -3.0$  are shown in Figure 1A. Note that in addition to increased b-wave amplitude observed when picrotoxin, or histidine plus picrotoxin, were applied, an increased a-wave as well as a more prominent OFF component were often observed, as described previously by Chappell and Rosenstein (13) using picrotoxin alone.

Similar data at all intensities were obtained from five preparations. Intensity-response data from one such preparation are plotted in Figure 1B. A  $V_{\text{max}}$  under normal Ringer conditions for each eye was determined by obtaining the best fit of a Naka-Rushton curve (14) to the intensity-response data obtained in the control Ringer solution. The value of  $V_{\text{max}}$  obtained was used to normalize the data before averaging it and plotting the results, which are shown in Figure 1C and 1D. Figure 1C is a bar graph of the averaged data from five preparations at the intensity  $\text{Log } I = -4$ , an intensity near the half amplitude intensity ( $\sigma$ ) for the intensity-response curve obtained in Ringer. The curves plotted with the intensity-response data in Figure 1D are the best fit of the data in Ringer, picrotoxin, and histidine plus picrotoxin, respectively, to the Naka-Rushton relation, using the least-squares approximation in Origin. Using this approach, we could obtain the value of the intensity corresponding to the half amplitude ( $\sigma$ ) of the Naka-Rushton curves, as well as the  $V_{\text{max}}$  for each of these curves. The values of  $V_{\text{max}}$  obtained increased from 0.95 in Ringer, to 1.09 in 200  $\mu$ M picrotoxin, and 1.4 in 100  $\mu$ M histidine plus 200  $\mu$ M picrotoxin, while the values of  $\sigma$  shifted from a  $\text{Log } I$  of  $-4.3$  to  $-4.52$  to  $-5.13$ , respectively.

The shift of  $\sigma$  toward dimmer intensities represents an increase in sensitivity of 0.8 log units (roughly a factor of 6) in the presence of histidine. Such an increase in sensitivity is consistent with the feedback model proposed by Wu *et al.* (1), in which they suggest that  $\text{Zn}^{2+}$  may feed back onto photoreceptor terminals to reduce  $\text{Ca}^{2+}$  entry and thereby reduce vesicular transmitter release from the photoreceptor terminals. It would also be consistent with a reduced inhibition of glutamate receptors on second-order retinal neurons (5), or possibly even an action of zinc on hemichannels (15), since hemichannels have been suggested as a means of feedback from horizontal cells onto cones in the carp retina, where the hemichannel blocker cambenoxolone has been shown to alter feedback-mediated responses (16). Whatever mechanism is in-

\* Corresponding author: rchappell@gc.cuny.edu

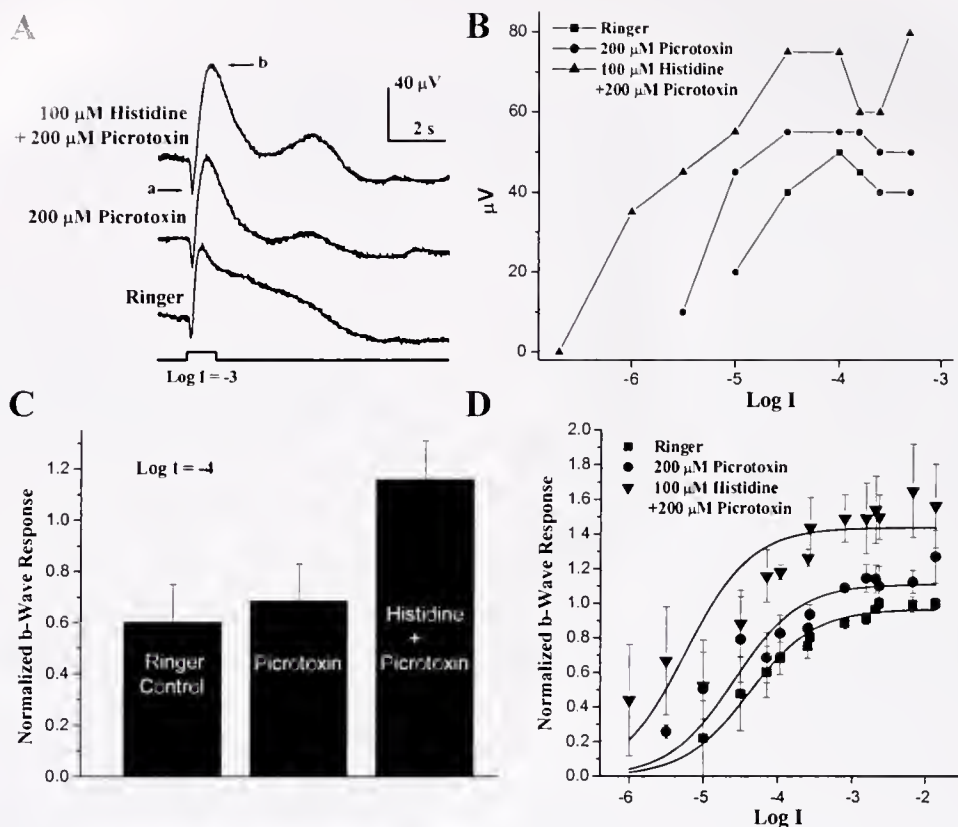


**Figure 1.** The zinc chelator histidine increases sensitivity of the skate electroretinogram (ERG) b-wave response. (A) ERG responses recorded from a dark-adapted skate eyecup preparation in response to a 1-s flash of white light at an intensity of  $\text{Log } I = -3$  (Unattenuated beam intensity,  $\text{Log } I = 0$ , was  $260 \mu\text{W}/\text{cm}^2$ ). The amplitude of the b-wave ("b", upper trace) of the ERG recorded from a dark-adapted skate eyecup preparation increased when  $100 \mu\text{M}$  histidine (in the presence of  $200 \mu\text{M}$  picrotoxin to block zinc-sensitive GABA receptors) was added to the superfusate. A small increase in the a-wave ("a", upper trace) was sometimes seen as well. (B) Intensity-response data from one eyecup preparation in Ringer,  $200 \mu\text{M}$  picrotoxin, and  $100 \mu\text{M}$  histidine plus  $200 \mu\text{M}$  picrotoxin. (C) Normalized data at  $\text{Log } I = -4$  from 5 preparations. (D) Intensity-response data, averaged and plotted (mean  $\pm$  SEM), with curves representing the best fit to the Naka-Rushton equation for each condition. The  $\text{Log } I$  of the half-amplitude intensity ( $\sigma$ ) of these curves determined in Ringer,  $200 \mu\text{M}$  picrotoxin, and in  $100 \mu\text{M}$  histidine plus  $200 \mu\text{M}$  picrotoxin were  $-4.3$ ,  $-4.5$ , and  $-5.1$ , respectively. Thus, in addition to a 50% increase in  $V_{\text{max}}$ ,  $\sigma$  for the histidine intensity-response curve was shifted 0.8 log units to the left, representing a 6-fold increase in sensitivity in the presence of histidine.

involved, the evidence that removal of extracellular zinc by chelation alters the sensitivity of the physiological response to light in an all-rod retina suggests that zinc may be playing an important role as a neuromodulator of rod afferent pathways in the vertebrate retina. Supported by PSC/CUNY grant 65711-0034.

### Literature Cited

- Wu, S. M., X. Qiao, J. L. Noebels, and X. L. Yang. 1993. *Vision Res.* 33: 2611-2616.
- Qian, H., L. Li, R. L. Chappell, and H. Ripps. 1997. *J. Neurophysiol.* 78: 2402-2412.
- Ugarte, M., and N. N. Osborne. 1999. *Exp. Eye Res.* 69: 459-461.
- Ugarte, M., and N. N. Osborne. 2001. *Prog. Neurobiol.* 64: 219-249.
- Rosenstein, F. J., and R. L. Chappell. 2003. *Neurosci. Lett.* 345: 81-84.
- Jiang, Y., V. C. Yu, F. Buchholz, S. O'Connell, S. J. Rhodes, C. Candeloro, Y. R. Xia, A. J. Lusis, and M. G. J. Rosenfeld. 1996. *Biol. Chem.* 271: 10,723-10,730.
- Kusakari, S., S. Nishikawa, S. Ishiguro, and M. Tamai. 1997. *Curr. Eye Res.* 16: 600-604.
- Lewin, A. S., K. A. Drenser, W. W. Hauswirth, S. Nishikawa, D. Yasumura, J. G. Flannery, and M. M. LaVail. 1998. *Nat. Med.* 4: 967-971.
- Mondal, M. S., A. Ruiz, J. Hu, D. Bok, and R. R. Rando. 2001. *FEBS Lett.* 489: 14-18.
- Wistow, G., S. L. Bernstein, M. K. Wyatt, R. N. Fariss, A. Behal, J. W. Touchman, G. Bouffard, D. Smith, and K. Peterson. 2002. *Mol. Vis.* 8: 205-220.
- Redenti, S., and R. L. Chappell. 2002. *Biol. Bull.* 203: 200-202.
- Chappell, R. L., and S. Redenti. 2001. *Biol. Bull.* 201: 265-267.
- Chappell, R. L., and F. J. Rosenstein. 1996. *J. Gen. Physiol.* 107: 535-544.
- Naka, K. I., and W. A. II, Rushton. 1966. *J. Physiol. (Lond.)* 185: 587-599.
- Chappell, R. L., J. Zakevicius, and H. Ripps. 2003. *Biol. Bull.* 205: 209-211.
- Kamermans, M., I. Fahrenfort, K. Schultz, U. Janssen-Bienhold, T. Sjoerdsma, and R. Weiler. 2001. *Science* 292: 1178-1180.

Reference: *Biol. Bull.* 205: 215–216. (October 2003)  
© 2003 Marine Biological Laboratory

## Intracellular Release of Caged Calcium in Skate Horizontal Cells Using Fine Optical Fibers

Anthony J. A. Molina<sup>1</sup>, Katherine Hammar<sup>2</sup>, Richard Sanger<sup>2</sup>, Peter J. S. Smith<sup>2</sup>, and Robert P. Malchow<sup>1</sup>

<sup>1</sup> University of Illinois at Chicago, Chicago, IL

<sup>2</sup> Marine Biological Laboratory, Woods Hole, MA

Horizontal cells are second order retinal neurons that receive direct input from photoreceptors and are involved in establishing a number of key features of visual perception. These cells mediate the formation of the inhibitory surround portion of the classic center-surround receptive fields of retinal neurons (1). The center-surround receptive fields are important for enhancing the contrast of visual objects and are also involved in color perception. The molecular mechanisms by which horizontal cells send lateral inhibitory signals to photoreceptors and bipolar cells are still under debate, but protons released from horizontal cells have been hypothesized to alter the flow of visual information within the outer retina (2). Indeed, small changes in extracellular pH can dramatically alter neural signals within the retina, in part because photoreceptor calcium channels are highly sensitive to protons. When protons bind to photoreceptor calcium channels, the voltage activation range of the channels shifts to more depolarized potentials and the overall conductance of the cell to calcium is reduced, which significantly reduces neurotransmitter release (3). Our previous work has shown that glutamate, the neurotransmitter released by photoreceptors onto horizontal cells, modulates the flux of hydrogen ions from skate retinal horizontal cells (4). Glutamate-induced changes in H<sup>+</sup> flux depend on the presence of extracellular calcium and likely reflect the activation of plasma membrane calcium/H<sup>+</sup> ATPases. These transporters extrude intracellular calcium in exchange for extracellular hydrogen ions, decreasing the concentration of protons at the extracellular face of the horizontal cells (5).

We would like to know whether local changes in calcium cause localized alterations in proton flux from horizontal cells. In the experiments reported here, we sought to develop methods to locally raise intracellular calcium levels in horizontal cells. We explored the use of small optical fibers that can apply focal ultraviolet stimuli to cells loaded with the caged calcium buffer NP-EGTA. This compound contains a UV-sensitive calcium binding site that releases its bound calcium upon absorption of ultraviolet light (6).

Horizontal cells were isolated from skate retinas by enzymatic dissociation, as described by Malchow *et al.* (7). The dissociated horizontal cells were placed in primary culture, where they were readily identified due to their distinct morphology and large size, about 150  $\mu\text{m}$ . Cells plated on Falcon 3001 35-mm culture dishes were loaded with the cell membrane permeable AM ester forms of NP-EGTA and the calcium-sensitive dye Oregon Green, prepared as follows. NP-EGTA (50  $\mu\text{g}$ ) and Oregon Green (50  $\mu\text{g}$ ) were dissolved in DMSO with 20% pluronic acid and added to 8 ml of skate Ringer's solution, yielding final concentrations of 5  $\mu\text{M}$  Oregon Green-AM and 8  $\mu\text{M}$  NP-EGTA-AM. The cultured horizontal

cells were then incubated with this solution for 30 min at 14 °C, washed twice with skate Ringer's solution, and allowed to stand for a minimum of 1 h. During this time, endogenous esterases cleave off the AM portion of the dye and the caged calcium compound, thereby trapping them inside the cell. Because NP-EGTA enters the cell unbound to calcium, it is important to pre-expose the preparation to a brief rise in intracellular calcium. Application of 100  $\mu\text{M}$  glutamate for 20 s permits calcium entry and loading of NP-EGTA compounds trapped within the cell. The cells were then thoroughly washed with fresh Ringer's solution, and experiments were typically conducted 10–30 min after calcium loading. Imaging of intracellular calcium concentration was performed with a Zeiss Attofluor imaging system.

Multi-mode optical fibers, F-MCB-T, were obtained from the Newport Corp.; they have a core diameter of 100  $\mu\text{m}$ , a cladding diameter of 100  $\mu\text{m}$ , a coating diameter of 140  $\mu\text{m}$ , and a numerical aperture (NA) of 0.22, which gives them a high coupling efficiency. We prepared these fibers as follows. First, the coating and cladding were burned off the fibers with a heated tungsten coil, leaving a 5-cm portion bare. This portion of the fiber was then pulled to a final tip diameter of 1–2  $\mu\text{m}$  with a Sutter P-2000 laser puller. The fiber was inserted into a borosilicate capillary tube previously pulled to a 5- $\mu\text{m}$  tip diameter and placed so that the tip of the optical fiber protruded about 5  $\mu\text{m}$  from the tip of the glass. The fiber was then glued in place with cyanoacrylate glue. Fibers were coupled to another multi-mode fiber, which was coupled to an ultraviolet laser.

Figure 1A shows the ultraviolet light output from one such pulled fiber. In this experiment, the dish was filled with a fluorescein solution, and the fluorescence of the solution, caused by ultraviolet light stimulation, was examined. The fluorescence was cone-shaped, with the region of highest intensity localized at the aperture of the optical fiber. A Narashige hydraulic manipulator was then used to place the fiber in a dish with the tip positioned 5  $\mu\text{m}$  away from the membrane of a horizontal cell. Figure 1B shows the change in Oregon Green fluorescence measured from a single horizontal cell upon the photolytic release of calcium from NP-EGTA-loaded cells. When the cell is stimulated for 5 s with ultraviolet light from the pulled optical fiber, a significant increase in fluorescence is detected, indicative of a rise in intracellular calcium concentration. The stimulus was then repeated two more times, which induced calcium increases that were smaller with each subsequent stimulation. In control experiments, with cells loaded only with Oregon Green, application of ultraviolet stimuli led to increases in measured fluorescence. Note that these increases were about 85% smaller ( $n = 2$ ) than those on cells containing NP-EGTA. Moreover, the control fluorescence disappeared imme-

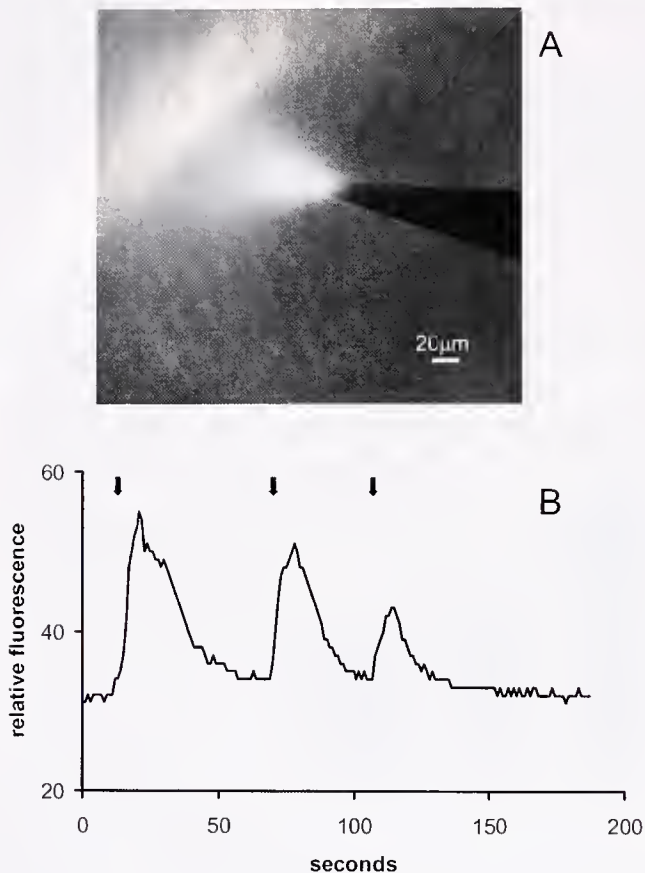


**Figure 1.** (A) A pulled optical fiber, which has been inserted into a capillary tube with a 5- $\mu\text{m}$  opening and placed in a dish containing fluorescein. Laser-generated ultraviolet light has been coupled to the fiber that is inducing fluorescence of the fluorescein solution. Fluorescence was detected through a 520-nm emission filter. (B) Oregon Green fluorescence from a retinal horizontal cell loaded with NP-EGTA and stimulated with ultraviolet light from a nearby optical fiber. Arrows indicate 5-s ultraviolet light pulses delivered via the pulled fiber optic.

Reference: *Biol. Bull.* **205**: 216–218. (October 2003)  
 © 2003 Marine Biological Laboratory

## Neural Recordings From the Lateral Line in Free-Swimming Toadfish, *Opsanus tau*

L. M. Palmer<sup>1,2</sup>, B. A. Guffrida<sup>2</sup>, and A. F. Mensinger<sup>1,2</sup>

<sup>1</sup> University of Minnesota, Duluth, MN

<sup>2</sup> Marine Biological Laboratory, Woods Hole, MA

Fish and aquatic amphibians have evolved a unique lateral line system that detects local water displacements. The lateral line functions in surface feeding, rheotaxis, localization of underwater objects, and subsurface prey detection (1). The detection of biologically relevant stimuli must often be accomplished during re-afferent stimulation from self-generated motion (swimming, ventilation). However, due to the constraints of conventional recording techniques, the activity of the lateral line during movement is difficult to quantify.

diately after the ultraviolet stimulus was removed. In contrast, changes in fluorescence with NP-EGTA-loaded cells persisted for many seconds after the UV stimulus was turned off. Additionally, the size of the fluorescent signal did not decay with subsequent UV stimuli.

Our work demonstrates that local stimulation of caged calcium trapped within horizontal cells by ultraviolet light delivered by small optic fibers can be used to increase intracellular levels of calcium in isolated horizontal cells. For future studies, this approach must be modified to achieve the proper spatial resolution of calcium uncaging. Currently, we are examining various methods to decrease the UV light output of the pulled optical fiber by adding neutral density filters and optimal alignment of the laser source. We hope to use this technique, in conjunction with self-referencing recordings of  $\text{H}^+$  flux from horizontal cells, to examine the spatial dependence of proton flux from these cells.

This work was supported by grants from the National Center for Research Resources (P41 RR01395), the National Science Foundation (009-1240), and a Grass Foundation Summer Fellowship.

### Literature Cited

1. Baylor, D. A., M. G. Fuortes, and P. M. O'Bryan. 1971. *J. Physiol.* **214**: 265–294.
2. Kamermans, M., and H. Spekrijse. 1999. *Vision Res.* **39**: 2449–2468.
3. Barnes, S., V. Merchant, and F. Mahmud. 1993. *Proc. Natl. Acad. Sci. USA* **90**: 10,081–10,085.
4. Molina, A. J. A., P. J. S. Smith, and R. P. Malchow. 2000. *Biol. Bull.* **199**: 168–170.
5. Schwiening, C., H. J. Kennedy, and R. C. Thomas. 1993. *Proc. R. Soc. Lond. B* **253**: 285–289.
6. Nerbonne, J. M. 1996. *Curr. Opin. Neurobiol.* **6**: 379–386.
7. Malchow, R. P., H. Qian, H. Ripps, and J. E. Dowling. 1990. *J. Gen. Physiol.* **95**: 177–198.

The development of an inductive telemetry system (2) enables neural activity to be recorded from free-swimming fish. The system utilizes inductive telemetry to transmit biological information from the fish to an external recording device. Consequently, fish are free from constraints and are able to behave in a quasi-natural environment. Using this technique, we investigated the activity of primary afferent fibers of the anterior lateral line nerve during self-induced motion in the oyster toadfish, *Opsanus tau*. Adult toadfish ( $28 \pm 1.4$  SE cm standard length,  $675 \pm 46$  SE g) of either

sex were lightly anesthetized in 0.001% tricaine (Sigma) and lightly paralyzed with pancuronium bromide (Sigma) ( $600 \mu\text{g}/\text{kg}$ ). A microwire electrode was inserted into the dorsal ramus of the anterior lateral line nerve, which innervates the supraorbital and infraorbital lateral line (3). Once spontaneous or evoked activity of 1 to 3 afferent fibers was obtained, the electrode was attached to a cylindrical telemetry tag (15 mm diameter  $\times$  38 mm length) and mounted externally on the dorsal surface of the fish. The rechargeable telemetry tag was inductively coupled to a bimodal recording stage (45 cm diameter). The stage acts passively to receive the inductive telemetry signal and actively to produce the magnetic field necessary to recharge the capacitors on the tag. The fish is free to move throughout the aquarium; however, data acquisition and tag charging are only possible when the fish remains on or near the stage. Fish were placed on the stage in an experimental tank (1.6 m diameter, 20 cm water depth), and allowed to recover from the surgical procedure for at least 3 h before experiments were conducted.

Fish movement was monitored with a digital camera (30 frames/s) and correlated with nerve firing offline (ADInstruments, Chart4; Cambridge Electronic Designs, Spike2). Spontaneous neural activity was recorded in each fiber and correlated with ventilation cycles. Nerve firing was also recorded when the fish moved independently or was provoked into swimming by gently prodding its caudal fin with a rod. All swimming events consisted of short swimming bursts that displaced the fish up to a body length forward. Swimming speeds (range: 3.6–15.1 cm/s) were determined by videotape analysis.

The primary afferents of the anterior lateral line in the toadfish

increased firing in response to swimming and ventilatory movements. During forward swimming, the firing rate of the anterior lateral line increased above spontaneous rates (Fig. 1A), and neural activity returned to spontaneous rate within 2 s. There was no correlation ( $r^2 \leq 0.07$ ) between swimming speed and firing rate, suggesting that firing was saturated at all swimming events. This contrasted with previous work that indicates lateral line afferent activity is reduced during vigorous body movement (4). Anterior lateral line afferents were also stimulated by ventilatory movements (Fig. 1B). The responses of 15 (6 silent and 9 spontaneously active) fibers to the ventilatory cycle were monitored. Three silent fibers and three spontaneously active fibers fired in correlation with the exhalation phase of the ventilation cycle. The other nine fibers were not modulated by ventilation; however, we were unable to determine whether this was due to the distant location of the neuromast from the operculum or to efferent inhibitory activity.

Efferent stimulation has been shown to reduce the activity of afferent fibers of the lateral line (5). Other studies also illustrated efferent inhibition of the lateral line in response to visual octavolateralis stimuli (6). However, in this study, all fibers were activated by swimming and 40% were activated by ventilatory activity. Thus reafferent noise does not appear to be inhibited by efferent activity at the primary afferent level. Consequently, self-generated noise is possibly filtered from the signal in higher order neurons. Bodznick and Montgomery (7) indicate that the lateral line medullary nuclei contain an adaptive filter capability that cancels inputs consistently associated with an animal's own movements. Fish are generally mobile animals; however, the ability of the lateral line to function

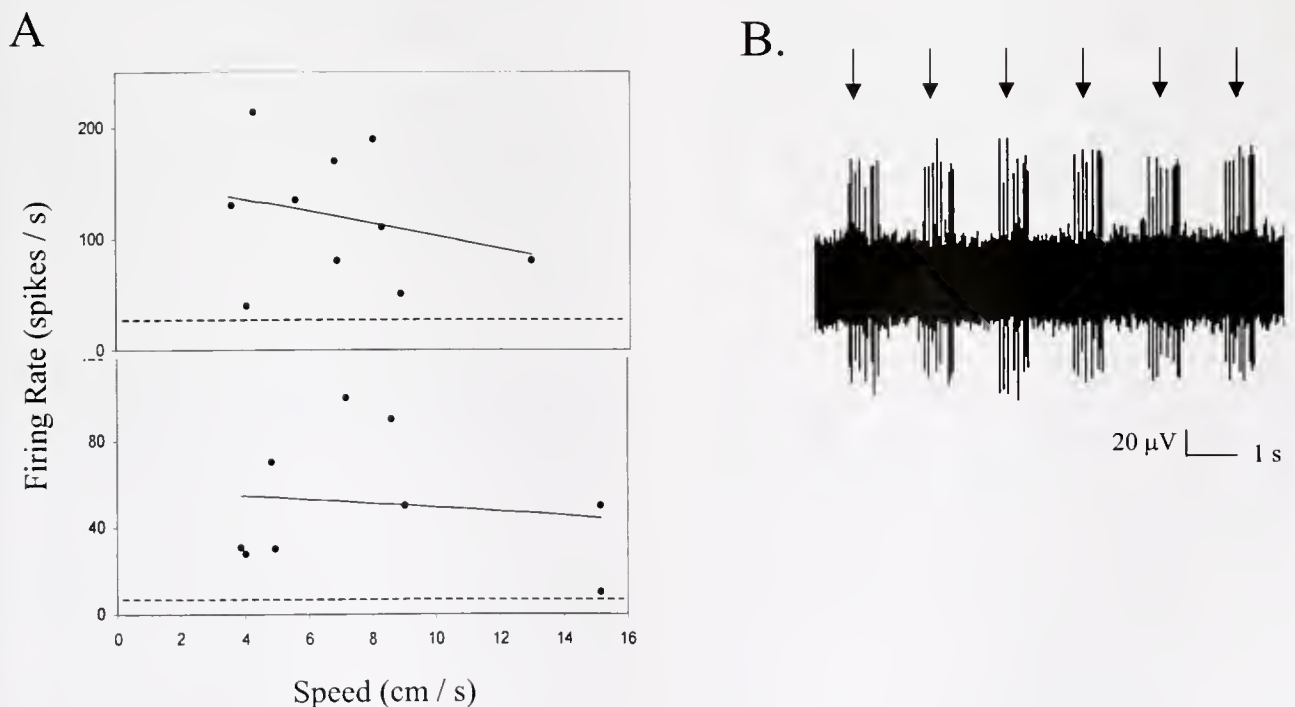


**Figure 1.** Neural activity of the anterior lateral line in *Opsanus tau* in response to reafferent self-generated motion. (A) The response of two fibers to short-range swimming events. The dashed black line represents the spontaneous activity of each fiber. The solid black line represents a linear regression through all data points (upper:  $y = -5.5x + 158.4$ ,  $r^2 = 0.07$ ; lower:  $y = -0.9x + 58.3$ ,  $r^2 = 0.02$ ). (B) Neural trace of a silent fiber (i.e., fiber with no spontaneous activity) that was responsive to the ventilation cycle. The fiber innervated a neuromast located on the infraorbital canal line. Arrows indicate the period of maximum operculum abduction during the ventilation cycle (measured by video analysis).

during self movement is largely unknown. This study reports preliminary findings of enhanced nerve activity of the anterior lateral line during self-generated motion, indicating that perhaps mechanosensory noise is not inhibited in afferent activity.

This work was supported by the Minnesota Sea Grant College Program supported by the NOAA Office of Sea Grant, United States Department of Commerce, under grant No. NOAA-NA16-RG1046 (AFM). The U.S. Government is authorized to reproduce and distribute reprints for government purposes, not withstanding any copyright notation that may appear hereon. This paper is journal reprint No. JR-494 of the Minnesota Sea Grant College Program. This work was also supported by Sigma Xi Grants in Aid of Research (LMP).

Reference: *Biol. Bull.* **205**: 218–219. (October 2003)  
© 2003 Marine Biological Laboratory

### Memory Reconsolidation in *Hermisenda*

F. M. Child<sup>1,\*</sup>, H. T. Epstein<sup>1</sup>, A. M. Kuzirian<sup>1</sup>, and D. L. Alkon<sup>2</sup>

<sup>1</sup> Marine Biological Laboratory, Woods Hole, MA 02543

<sup>2</sup> Blanchette Rockefeller Neuroscience Institute, Rockville, MD 20850

Remembering seems *a priori* to be composed of three main processes: acquisition (or input), storage (or consolidation), and retrieval (or recall) (1). In this study the acquisition of memory is the form of Pavlovian conditioning elaborated by Lederhendler *et al.* (2).

The consolidation of this conditioning in *Hermisenda* was studied by Epstein *et al.* (3). Consolidation of memories has been known experimentally at least since Müller and Pilzecker (4) demonstrated it in humans in 1900. It is defined as the process by which memory reaches a state in which interferences (or interferences) no longer inhibit recall of what was presented to be remembered. This does not mean, as initially inferred (5, 6), that the installed memory cannot be altered; it is just that it is stable with respect to the said interferences. Examples of such interferences include the four treatments (chemicals, sensory input) used in this study.

Reconsolidation (a much newer finding) is defined as the ending of the interference-insensitive state brought about by the recall of what was memorized. That is, after a memory has been consolidated, if it is recalled it becomes sensitive to agents such as inhibitors of mRNA synthesis and protein synthesis that did not affect it just before the recall. Since the consolidated memory is regenerated after recall, it will become important to determine whether the fact of reconsolidation has more to do with temporary memory degradation or with a weakening of the retrieval process.

Consolidation and reconsolidation are being studied in many organisms from molluscs to humans (5, 6, 7, 8). The existence of reconsolidation may allow more detailed study of many proposed aspects of consolidation. We therefore undertook a preliminary study of reconsolidation in *Hermisenda*. This nudibranch has proven to be a high-connectivity model for the more complex

### Literature Cited

1. Montgomery, J., S. Coombs, and M. Halstead. 1995. *Rev. Fish. Biol. Fish.* **5**: 399–416.
2. Mensinger, A. F., and M. Deffenbaugh. 1998. *Biol. Bull.* **195**: 194–195.
3. De Rosa, F., and M. L. Fine. 1988. *Brain Behav. Evol.* **31**: 312–317.
4. Russell, I. J., and B. L. Roberts. 1974. *J. Comp. Physiol.* **94**: 7–15.
5. Flock, A., and I. J. Russell. 1976. *J. Physiol.* **257**: 45–62.
6. Tricas, T. C., and S. M. Highstein. 1991. *J. Comp. Physiol. A.* **169**: 25–37.
7. Montgomery, J. C., and D. Bodznick. 1994. *Neurosci. Lett.* **174**: 145–148.

vertebrate nervous system, especially in the area of learning and memory (3, 9, 10).

Our training procedure with *Hermisenda* was a Pavlovian conditioning regime (2). Animals were placed in transparent acrylic plastic trays (with 16 fluid-filled lanes about 0.9 cm wide and deep and 15 cm long) in a closed 11 °C incubator for 10 min of dark adaptation before training or testing. Training consists of exposing the animals to a bright white light (650–700 lux) for 6 s (the conditioned stimulus, CS), paired, after a 2-s delay, with a 4-s vigorous orbital shaking of the tray containing the animals (the unconditioned stimulus, US). The animals respond to the shaking by contracting lengthwise. This combination of the two stimuli is called a paired training event (TE) and is repeated at 1-min intervals.

Testing of recall was done by four presentations of the CS at 1-min intervals, and was recorded using a videocassette recorder whose input was registered by a camera placed below the transparent trays. Animal length was measured on the video monitor. The measure used was the percentage by which the animal's length changed between light-on and light-off times. From those percentage changes we compute a mean and the standard error of the mean.

We used four interventions after training to probe the acquisition and consolidation of memory in *Hermisenda*. The first intervention is the sensory input used by Epstein *et al.* (3). The other three are drugs dissolved in seawater, pH 8, and administered by replacement of the seawater bathing the animal.

1. Sensory input: the tray containing the animals is quickly rotated by hand 180° around its long axis and, after 5 s, quickly rotated back to its original position. This produces a vestibular input (in addition to the TE) and is termed a sensory block (SB).
2. Anisomycin (ANI) interferes with protein synthesis by in-

\* Corresponding author: fchild@mbledu

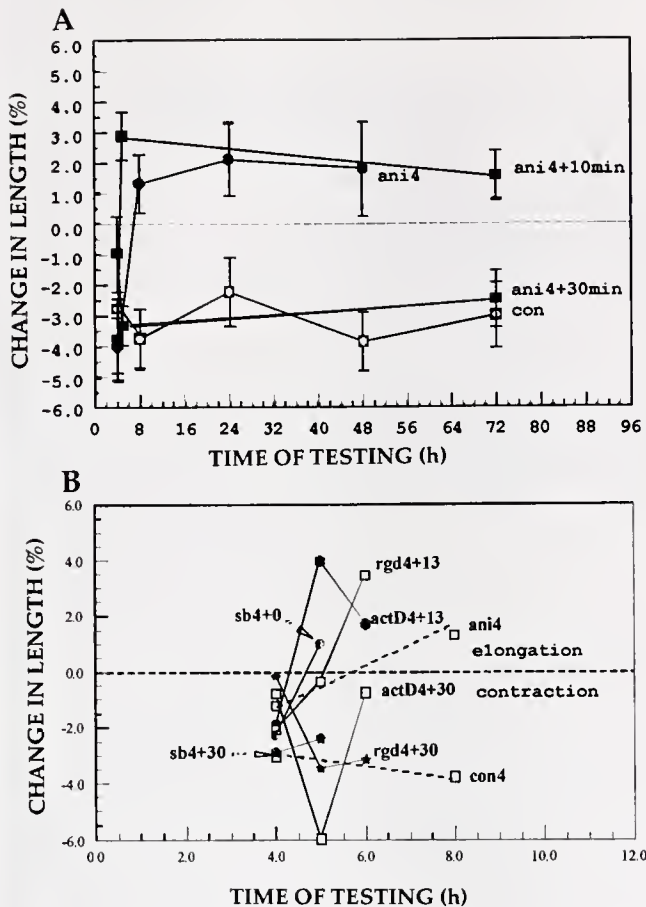


**Figure 1.** Effects of inhibitors on the behavior and memory recall (as measured by change in body length) of *Hermissenda*. (A) Effects of anisomycin (ANI). Animals were trained with nine training events and then tested for recall at 4 h post-training. For three groups of animals, ANI was added either immediately after (curve *ani4*), or at 10 min later (curve *ani4+10*) or 30 min after the testing at 4 h (curve *ani4+30*). Animals were then retested at 8, 24, 48, and for some, 72 h for recall or retention of the training. Controls (*con*) were not treated with ANI. Data points below the zero line indicate foot contraction and positive recall of the training; positive numbers indicate body elongation as in normal locomotion with recall inhibition and blocked memory. (B) Combined results of the four inhibitors, actinomycin-D (*act-D*), anisomycin (*ani*), the tripeptide CAM inhibitor (*rgd*), and the sensory block (*sb*). Animals were treated as described in A, with the inhibitors added at the times indicated (on the graph) after the initial testing at 4 h. The animals were tested again for recall at 5, 6, or 8 h post-training.

- hibiting translation. It was administered at 1  $\mu\text{g}/\text{ml}$ . The translation-inhibition was not checked.
- Actinomycin-D (Act-D) interferes with mRNA synthesis by inhibiting transcription. It was administered at 0.1  $\mu\text{g}/\text{ml}$ . The transcription-inhibition was not checked.
  - RGD (arginyl-glycyl-aspartate) inhibits bond formation between cell adhesion molecules (CAMs). It was administered at 10  $\mu\text{g}/\text{ml}$ . The bond formation inhibition was not checked.

In the first experiment, specimens of *Hermissenda* were given nine TEs and tested at 4 h; this is the time at which our previous studies have shown recall to become insensitive to all four inhibitors we are using, thereby showing that the stored memory is consolidated long-term memory (CLTM). After testing to verify arrival at CLTM, ANI was added either immediately, 10 min later, or 30 min later. The data in Figure 1A show that adding anisomycin immediately or 10 min after testing for recall resulted in the loss of recall; adding the anisomycin after 30 min showed that recall has been re-established.

We next studied whether the other three inhibitors had similar effects (Fig. 1B). All three inhibitors wiped out recall if added immediately after testing at 4 h, whereas waiting for 30 min before using the inhibitors revealed that recall had been re-established, as had been found for ANI (Fig. 1A).

Thus, these results demonstrate the existence of reconsolidation in *Hermissenda*. Reconsolidation was triggered by testing for recall after 4 h and then probing with each of the four inhibitors. The reconsolidation was found to be reached by about 30 min after recall; thus it is a much more rapid process than the initial acquisition and consolidation phase, which has been shown to take nearly 4 h.

The sensory block (SB) was previously shown by Epstein *et al.* (3) to inhibit short-term memory (STM) as well as long-term (LTM) and consolidated long-term memory (CLTM). The fact that it works on both consolidation and reconsolidation raises again the question of what steps it is affecting. Molecular and physiological studies will be needed to get at this question.

Finally, both consolidation and reconsolidation deserve study in that there may be ramifications for learning and schooling. If the first consolidation study by Müller and Pilzecker (3) is correct, teaching additional novel material within 6 to 10 min after having taught a primary point that is meant to be remembered could well weaken retention of that point. Similarly, if recalling something weakens the memory, then new information might prevent reconsolidation and thus should be avoided. These aspects need serious study by researchers in the field of education.

## Literature Cited

- Abel, T., and K. M. Lattal. 2001. *Curr. Opin. Neurobiol.* **11**: 180–187.
- Lederhendler, I. I., S. Gart, and D. L. Alkon. 1986. *J. Neurosci.* **6**: 1325–1331.
- Epstein, D. A., H. T. Epstein, F. M. Child, A. M. Kuzirian, and D. L. Alkon. 2000. *Biol. Bull.* **199**: 182–183.
- Müller, G. E., and A. Pilzecker. 1900. *Z. Psychol. Ergänzungsband* **1**: 1–300.
- Riccio, D. C., E. W. Moody, and P. M. Millin. 2002. *Integr. Physiol. Behav. Sci.* **37**: 245–253.
- Sara, S. J. 2000. *Learn. Mem.* **7**: 73–84.
- Nader, K. 2003. *Trends Neurosci.* **26**: 65–72.
- Pedreira, M. E., and H. M. Maldonado. 2003. *Neuron* **38**: 863–869.
- Kuzirian, A. M., H. T. Epstein, D. Buck, F. M. Child, T. Nelson, and D. L. Alkon. 2001. *J. Neurocytol.* **30**: 993–1008.
- Epstein, H. T., F. M. Child, A. M. Kuzirian, and D. L. Alkon. 2003. *Neurobiol. Learn. Mem.* **79**: 127–131.

Reference: *Biol. Bull.* 205: 220–222, (October 2003)  
 © 2003 Marine Biological Laboratory

### Training Alone, Not the Tripeptide RGD, Modulates Calnexin in *Hermisenda*

A. M. Kuzirian,<sup>1,\*</sup> F. M. Child,<sup>1</sup> H. T. Epstein,<sup>1</sup> M. E. Motta,<sup>2</sup> C. E. Oldenburg,<sup>3</sup> and D. L. Alkon<sup>4</sup>

<sup>1</sup> Marine Biological Laboratory, Woods Hole, MA

<sup>2</sup> University of New Hampshire, Durham, NH

<sup>3</sup> Carnegie Mellon University, Pittsburgh, PA

<sup>4</sup> Blanchette Rockefeller Neuroscience Institute, Johns Hopkins University, Rockville, MD

In the nudibranch mollusc *Hermisenda crassicornis*, the intensity of immunostaining for the Ca<sup>2+</sup>/GTP-binding protein calnexin (1) correlates positively with the degree of learning obtained and the level of memory expressed after Pavlovian conditioning (2, 3). When inhibitors of transcription (actinomycin-D; Act-D) and translation (anisomycin; ANI) are applied after training, they affect the animal's ability to recall the learned behavior. Epstein *et al.* (4) have recently described the time windows for these effects. They noted that there are two phases of sensitivity to the inhibitors: an early phase, immediately after training (0–13 min), and a later phase (70–160 min for Act-D, and 70–220 min for ANI). Subsequently, Epstein *et al.* (5) reported that long-term memory also has two distinct biological configurations: long-term memory (LTM), which lasts about 24 h, and consolidated long-term memory (CLTM), which persists up to 6 days. The amount of memory retained by conditioned animals appears to depend, in part, on how much consolidation has been completed; and the transition from LTM to CLTM is sensitive to a cell adhesion molecule (CAM) inhibitor, the tripeptide arginyl-glycyl-aspartate (RGD). One working hypothesis predicts that increased calnexin levels are needed to establish LTM, and that RGD-sensitive CAMs are subsequently involved in the transition from LTM to CLTM. What was unknown was the possible relationship between calnexin levels and the effects of RGD during this critical transition period. Thus, as part of a continuing study to describe and define the memory stages demonstrated in *Hermisenda* (6, 4, 5), we undertook an immunocytochemical study to investigate possible correlations between calnexin levels and the observed effects of RGD during the transition from LTM to CLTM.

*Hermisenda* were purchased from Sea Life Supply (Sand City, California), and the tripeptide CAM inhibitor, arginyl-glycyl-aspartate (RGD), was obtained from Calbiochem (San Diego, CA). Animals were acclimated to laboratory conditions for a minimum of 3 days. The training procedure used was adapted from a Pavlovian conditioning regime developed by Crow and Alkon (7), elaborated later by Lederhendler, Gart, and Alkon (8), and modified by Kuzirian *et al.* (9) and Epstein (10). Before training or testing, animals were dark-adapted for 10 min in a transparent acrylic plastic tray with 16 lanes (15 cm long and 0.9 cm by 0.9 cm in cross section) in an 11 °C incubator. In paired training, animals were exposed to a bright, white light (650–700 lux) for 6 s (the conditioned stimulus, CS) coincident with, after a 2-s delay, 4 s of vigorous agitation (the unconditioned stimulus, US). Animals respond to the agitation by contracting lengthwise (unconditioned

response, UR). The two stimuli are designated a paired training event (TE), which was repeated at 1-min intervals for nine repetitions. Recall of training was tested by four presentations of the CS alone at 1-min intervals. Behavioral recall was assessed by calculating the percentage by which the animal's length changed between light-on and light-off. Untrained (naive) animals show no recall and typically lengthen as a normal response to light, as do animals given light and agitation in an unpaired or random fashion (10).

Experimental conditions shown by Epstein *et al.* (5) to demonstrate the RGD-sensitive transition between LTM and CLTM were repeated to test for possible correlations between different times of RGD application after training and changes in calnexin intensities. RGD was diluted to an effective working dosage of 10 µg/ml (29 µM) with Tris-buffered (20 mM) natural seawater (NSW-Tris) (pH 8.0). All solutions were administered post-training, at designated times, by bath application using a training tray with a modified injection-port cover (4). After training, the RGD-exposed animals were tested for retention of recall at 4 and 24 h, then rapidly decapitated. The central nervous systems (CNS) were immediately fixed in 4% paraformaldehyde/NSW-Tris to preserve, as accurately as possible, the expressed calnexin levels.

To discern the temporal effects of training alone on the immunostaining intensities of calnexin, and to test for possible effects from testing with the CS alone, animals were similarly conditioned with 9 TEs in natural seawater, but they were not exposed to RGD or tested for recall. They were decapitated and fixed at time points similar to those for the RGD-exposed animals. Naive, untrained animals were used as overall experimental controls and were tested after 24 h.

All fixed CNSs were then processed for embedding in polyethylene glycol-400-distearate and were sectioned (6 µm). Calnexin was immunolabeled with a primary polyclonal antibody (25U2; cloned from squid optic lobe and raised in rabbit; 1:1000 dil) (2, 3); subsequently, color was developed with a biotinylated secondary antibody, and avidin-bound microperoxidase reacted with the chromogen 3-amino-9-ethylcarbazole (AEC). Gray-scale intensity was measured (using NIH Image software) from digital photomicrographs of serial sections of the B-photoreceptors in the eyes of each animal. Intensity differences between conditions were statistically analyzed using ANOVA and Student's *t* tests.

The data indicate that the levels of calnexin remained steady from 40 to 200 min post-training, whether the animals were exposed to RGD or not (Fig. 1). Levels then fell to a baseline about 240 min after training. ANOVA and pairwise Student's *t* tests among and between intensities measured during the first phase (40–200 min post-training) indicated no significant differences between all intensity values ( $F = 0.67$ ,  $ts < 2.0$ ;  $P = >0.7$ ;

\* Corresponding author: akuziria@mbi.edu

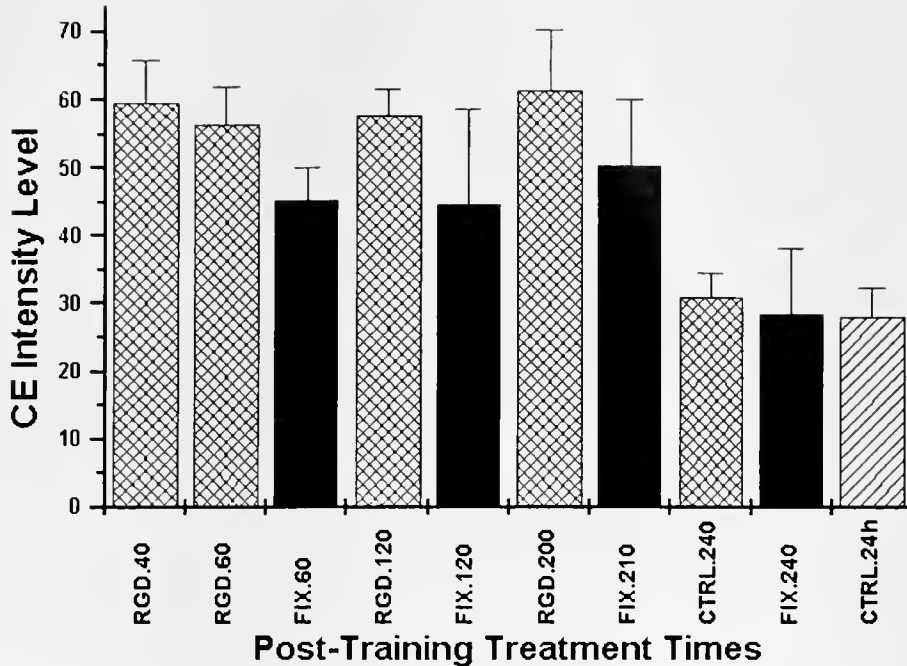


**Figure 1.** Immunostaining intensity levels for calcectin under two experimental conditions. First, specimens of *Hermisenda* were exposed to 10  $\mu\text{g/ml}$  of RGD, a tripeptide, cell adhesion molecule inhibitor, at the designated post-training (nine training events) application times through to 240 min (designated RGD. $\lambda$  (min); double-hatched columns). At 240 min, the animals were tested, the RGD removed, and the animals transferred in the training tray to a tub with running seawater being siphoned through each lane until they were tested again at 24-h post-training. Second, replicate sets of animals (solid black columns) were similarly trained but not exposed to RGD or tested, and then decapitated and fixed at time points similar to those for the RGD-exposed animals. An overall control group (single-hatched column) consisted of naive, untrained animals held under similar conditions until they were also decapitated and fixed. All central nervous systems were processed collectively for immunocytochemistry. Calcectin immunostaining intensity was measured from digital photomicrographs using NIH image software. Results were statistically compared using ANOVA and pairwise Student's *t* tests (see text).

$n = 4-10$  eyes measured), whether animals were treated with RGD and tested at 4 and 24 h, or simply trained and fixed at similar time points. The same was true for the second phase (240 min to 24 h post-training). Again, the intensities were statistically identical, whether animals were tested or not, at 240 min or at 24 h ( $F = 0.07$ ,  $t_s < 2.0$ ;  $P = >0.9$ ;  $n = 4-10$  eyes measured). However, the overall ANOVA between all conditions did show significant differences between the first and second phases ( $F = 7.49$ ;  $P = <0.001$ ).

The principal results obtained from this study indicate that the working hypothesis must be redefined to indicate that, to preserve a memory, calcectin levels must remain elevated through the transition of LTM to CLTM. Also, the previously demonstrated RGD inhibition of this LTM/CLTM transition does not appear to operate by affecting calcectin levels, but rather, as predicted by Epstein *et al.* (5), through the competitive inhibition and functioning of CAMs. Calcectin itself may contribute to the LTM/CLTM transition through the initiation of early gene transcription and translation of CAMs.

The calcectin immunostaining intensities observed during this study were similar to levels reported previously for LTM (3). The initial study by Kuzirian *et al.* (3) showed that the rise in calcectin intensity occurred by 90 min post-training, the earliest time point sampled. However, this study indicates that the intensity rise begins earlier, by 40 min or even sooner. The results of this study

further demonstrated that the treatment of *Hermisenda* with the CAM inhibitor RGD is independent of the expressed levels of calcectin. Therefore, the behavioral effects related to RGD exposure reported by Epstein *et al.* (5) were not mediated directly through changes in calcectin levels. The similarity of intensity levels in tested and nontested animals also suggests that calcectin levels may be insensitive to the immediate perturbation of recall caused solely by testing; a phenomenon known as reconsolidation (11) (also described as extinction). Memory generated by an associative conditioning regime can be weakened by testing with the conditioned stimulus (CS) alone and must be reconsolidated to remain fixed. The data indicated quite clearly that there were no differences in calcectin intensity related to testing alone.

Previous reports (3, 12) show that calcectin is involved in establishing LTM. This was accomplished by exposing *Hermisenda* to a sensory block (an additional vestibular input) at time points before LTM is established (at 60 min post-training) (5) and afterward. The sensory block suppressed this rise in calcectin levels until LTM was fixed. However, the current data indicate that calcectin levels remain high through to the period coinciding with the establishment of CLTM (4, 5), and thus calcectin may also be involved in some way with the consolidation of LTM to CLTM. Calcectin was also elevated during the time period designated by Epstein *et al.* (4) as potentially being an intermediate-term memory phase, a phenomenon known to occur in *Hermisenda* and *Aplysia*.

among other animals (13–14). Since calyculin, once activated by PKC, is known to regulate the release of internal calcium stores by binding to ryanodine receptors on the ER, and is responsible for early gene activation, all of which are involved in memory acquisition, storage, and recall (15), it would be logical to broaden this study by measuring the effects of transcription and translation inhibitors on the immuno-expression levels of calyculin under experimental conditions similar to those just described. Indeed, such studies are underway.

Drs. Daniel Alkon and Thomas Nelson provided *Hermisenda* and calyculin antibodies for this study. MEM and CEO acknowledge the assistance of Beth Linnon, program coordinator, and the student internship program sponsored by the Marine Resources Center, Marine Biological Laboratory.

### Literature Cited

- Nelson, T. J., S. Cavallaro, C. L. Yi, D. McPhie, B. G. Schreurs, P. A. Gusev, A. Favit, O. Zhar, J. Kim, S. Beushausen, G. Ascoli, J. Olds, R. Neve, and D. L. Alkon. 1996. *Proc. Natl. Acad. Sci. USA* **93**: 13808–13813.
- Kuzirian, A. M., H. T. Epstein, T. J. Nelson, N. S. Rafferty, and D. L. Alkon. 1998. *Biol. Bull.* **195**: 198–201.
- Kuzirian, A. M., H. T. Epstein, D. Buck, F. M. Child, T. Nelson, and D. L. Alkon. 2001. *J. Neurocytol.* **30**: 993–1008.
- Epstein, H. T., F. M. Child, A. M. Kuzirian, and D. L. Alkon. 2003. *Neurobiol. Learn. Mem.* **79**: 127–131.
- Epstein, H. T., A. M. Kuzirian, F. M. Child, and D. L. Alkon. 2003. *Neurobiol. Learn. Mem.* (In press).
- Epstein, D. A., H. T. Epstein, F. M. Child, A. M. Kuzirian, and D. L. Alkon. 2000. *Biol. Bull.* **199**: 182–183.
- Crow, T., and D. L. Alkon. 1974. *Science* **201**: 1239–1241.
- Lederhendler, I. I., H. S. Gart, and D. L. Alkon. 1986. *J. Neurosci.* **6**: 1325–1331.
- Kuzirian, A. M., F. M. Child, H. T. Epstein, P. J. S. Smith, and C. T. Tamse. 1996. *Biol. Bull.* **191**: 260–261.
- Epstein, H. T. 1997. *Biol. Bull.* **193**: 255–257.
- Sara, S. J. 2000. *Learn. Mem.* **7**: 73–84.
- Borley, K. A., H. T. Epstein, and A. M. Kuzirian. 2002. *Biol. Bull.* **203**: 197–198.
- Crow, T., J. J. Xue-Bian, and V. Siddiqi. 1999. *J. Neurophysiol.* **82**: 495–500.
- Sutton, M. A., S. E. Masters, M. W. Bagnall, and T. J. Carew. 2001. *Neuron* **31**: 143–154.
- Alkon, D. L., T. J. Nelson, W. Zhao, and S. Cavallaro. 1998. *Trends Neurosci.* **21**: 529–537.

Reference: *Biol. Bull.* **205**: 222–223. (October 2003)  
© 2003 Marine Biological Laboratory

## Neurochemical Modulation of Behavioral Response to Chemical Stimuli in *Homarus americanus*

Anna Savage<sup>1,2</sup> and Jelle Atema<sup>2,\*</sup>

<sup>1</sup> Amherst College, Amherst, MA

<sup>2</sup> Boston University Marine Program, Woods Hole, MA

Serotonin (5-HT) and octopamine have been implicated in regulating the behavioral phenotype of lobsters by altering levels of aggression in agonistic interactions (1). High-dosage injections of these amines consistently evoke extension (5-HT) and flexion (octopamine) postures in both lobsters and crayfish. These postures have been likened—probably erroneously—to aggressive and submissive postures, suggesting a specific role for these neuromodulators in social behavior (2). Dopamine injections into freely moving lobsters have also induced motor activity, including extension of claws, legs, and tail, originally interpreted as an agonistic posture (3). However, the relationship between neuromodulator treatment and overall crustacean behavior is not simple, with responses varying with the stimuli presented and the aminergic manipulations performed (4, 5). Serotonin is known to regulate feeding behavior in other animal species (6), but its effects on lobster feeding behavior and responses to odors have not yet been investigated. As lobsters are known to rely heavily on chemical signals for food and social information (7), we examined the reaction of *H. americanus* to food and social odors after the animals had been injected with serotonin and two other biological amines common to the lobster central nervous system (CNS).

Seven adult intermolt male lobsters (81–93 mm carapace length)

were injected with serotonin, octopamine, dopamine (Sigma Chemicals), or lobster saline. Each injection of amine was administered in random order over 4 consecutive days of testing, and consisted of 0.3 mg of neuromodulator per kg of animal dissolved in 1 ml lobster saline. Injections were made intramuscularly into the first abdominal segment to the right of the ventral nerve cord, following Peeke *et al.* (4). After injection, each lobster was placed in an observation tank (36 × 46 × 72 cm) with a constant flow of unfiltered seawater. Each tank had a plastic, two-entrance shelter in front of the window and a constantly flowing air-lift water circulation system with funnel interruption (7). Food odor and body odor were injected into the funnel, which delivered an irregular flow of tank water into the shelter at a mean rate of 4.8 ml/s. Lobsters were not fed for the 4-d duration of the experiment. Tanks were kept dark during observations except for a 25-watt bulb covered in black plastic with a small hole cut through that allowed a narrow beam of light to illuminate the shelter interior.

Body odor stimuli were prepared by collecting water samples from one male and one female lobster isolated in 10 l of aerated standing seawater for at least 3 h. Food odor consisted of store-bought clam juice. Fifteen minutes after drug injection, lobsters were presented with 0.5 ml of each stimulus at 5-min intervals, and the resulting behaviors and their durations were recorded to the nearest second. The order of stimulus introduction was held constant over the four days of injections but varied randomly among the animals. We selected behaviors from Atema and Cowan (7) based on frequency and quanti-

\* Corresponding author: atema@bu.edu

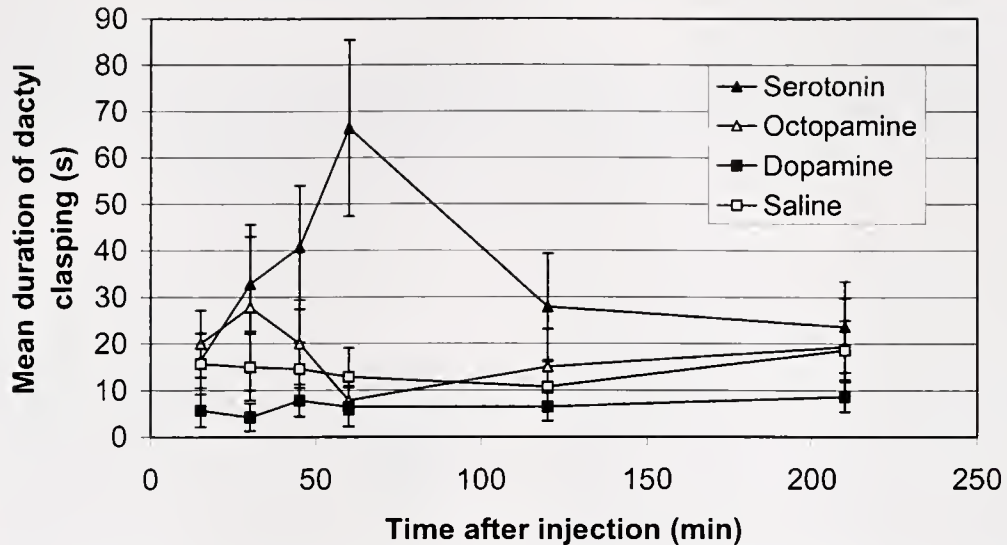


**Figure 1.** The effect of injections with 0.3 mg/kg of serotonin, octopamine, dopamine, or saline on the duration of lobster dactyl clamping behavior in response to clam juice. Mean duration  $\pm$  SE shown for 7 lobsters at 6 time points post-injection. The serotonin-affected response was significantly higher, and the dopamine-affected response was significantly lower, than the saline control (see text).

fiability. They included "locate source," turning toward the glass at the front of the shelter and probing the stimulus inflow tube; "check entrance," walking over to, and standing still at, one of the two entrances; and "dactyl clamping," a typical feeding response marked by opening and closing the dactyls of the first two pairs of walking legs. Stimulus introductions were repeated every 15 min for the first hour, and then again 120 and 210 min post-injection to test for a time delay in response. The study was conducted blind for six of the eight animals tested, with the observer unaware of the amine injected from day to day.

Lobsters injected with serotonin and presented with clam juice displayed a mean duration of dactyl clamping that was twice that observed after saline injections. Statistical analysis showed that this difference in duration was significant (ANOVA post-hoc  $t$  test,  $t = 6.69$ ,  $P = 7e^{-11}$ ). The serotonin effect peaked at 60 min post-injection, when the duration of clamping was over 5 times that of the saline control; the effect then returned to initial levels by  $t = 120$  min (Fig. 1). The  $t = 60$  min response was also significantly longer than the initial response at  $t = 15$  min ( $t = -2.69$ ,  $P = .0082$ ). In contrast to serotonin, dopamine induced a shorter duration of clamping in response to clam juice at all times examined; the mean response was less than 50% that of saline. This difference was statistically significant ( $t = -2.68$ ,  $P = .0078$ ). Octopamine-induced clamping in response to clam juice varied widely between animals, and the overall difference in duration for octopamine injections compared to saline was not significant ( $t = 1.254$ ,  $P = 0.21$ ). Dactyl clamping was not observed in response to body odor. The occurrence of "locate source" and "check entrance" behaviors, infrequent for all three chemical stimuli, appeared unrelated to treatment condition.

The significant increase in length of dactyl clamping after injection with serotonin and the decrease after injection with dopamine suggest that these neuromodulators are priming lobsters toward certain behaviors, making them more (5-HT) or less (dopamine) motivated to feed when given the opportunity. This serotonin-induced persistence

has been demonstrated in agonistic encounters, where 5-HT-treated subordinate lobsters are less willing to retreat (8). However, serotonin's effects are not limited to aggression. Rather, it appears to act as a general motivator of lobster behaviors, including both agonistic encounters and feeding responses. Additionally, prolonged dactyl clamping requires sequences of rapid flexion and extension; thus the behaviors induced by serotonin cannot be attributed to simple extensor effects. The observed inconsistency of dactyl clamping following octopamine injection reflects the complex relationship between neuromodulator action and lobster behavior (4). Dopamine-induced depression of response is a novel result and merits further behavioral and neurochemical investigation.

Financial support is acknowledged from NSF-REU (OCE-0097498 site awarded to Boston University Marine Program). We thank Sean Sapcarciu for overseeing blind injection schedules, Molly Steinbach for design advice, and Gabi Gerlach for her aid in statistical analysis.

### Literature Cited

1. Huber, R., and E. A. Kravitz. 1995. *Brain Behav. Evol.* **46**: 72–83.
2. Livingstone, M. S., R. M. Harris-Warrick, and E. A. Kravitz. 1980. *Science* **208**: 76–79.
3. Barthe, J. Y., N. Mons, D. Cattaert, M. Geffard, and F. Clarac. 1989. *Brain Res.* **497**: 368–373.
4. Peeke, H. V. S., G. S. Blank, M. H. Figler, and E. S. Chang. 2000. *J. Comp. Physiol.* **186**: 575–582.
5. Doernberg, S. B., S. I. Cromarty, R. Heinrich, B. S. Beltz, and E. A. Kravitz. 2001. *J. Comp. Physiol.* **187**: 91–103.
6. Mancilla-Díaz, J. M., R. E. Escartín-Pérez, V. E. López-Alonso, and S. E. Cruz-Morales. 2002. *Eur. Neuropsychopharmacol.* **12**: 445–451.
7. Atema, J., and D. F. Cowan. 1986. *J. Chem. Ecol.* **12**: 2065–2080.
8. Huber, R., K. Smith, A. Delago, K. Isaksson, and E. A. Kravitz. 1997. *Proc. Natl. Acad. Sci.* **94**: 5939–5942.

Reference: *Biol. Bull.* 205: 224–225. (October 2003)  
 © 2003 Marine Biological Laboratory

## Recognition in Juvenile Zebrafish (*Danio rerio*) Based on Olfactory Cues

K. D. Mann<sup>1</sup>, E. R. Turnell<sup>1</sup>, J. Atema<sup>2</sup>, and G. Gerlach<sup>1,\*</sup>

<sup>1</sup> Marine Biological Laboratory, Woods Hole, MA

<sup>2</sup> Boston University Marine Program, Woods Hole, MA

Genetic analyses of numerous fish species have shown that shoals formed by larvae often consist of closely related kin (1). Aggregating with kin may be an altruistic trait that evolved through kin selection (2). Individuals would increase their inclusive fitness by sharing the benefits of shoaling among related individuals (3). Laboratory experiments on recognition of kin vs. non-kin groups of Atlantic Salmon (*Salmo salar*) (4) demonstrated possible advantages: kin groups had fewer aggressive interactions, used a greater proportion of "threat" behavior as opposed to fighting, and subordinates especially had improved growth.

The mechanisms by which these kin groups develop and stay separate from each other are not known. The genes of the major histocompatibility complex (MHC) are a source of individual odors released into the water via urine (5). Such pheromones might be involved in olfactory kin recognition. Here, we tested the hypothesis that zebrafish can recognize kin based on olfactory cues.

Zebrafish (*Danio rerio*) live in freshwater streams and rice paddies in the Ganges River of East India, Bangladesh, and Burma. Although this species is widely used as a model in genetic and developmental research, little is known about its natural behavior. Zebrafish spawn up to several hundred eggs at a time, and these develop in the substrate without any parental care. Larvae (G.G. pers. obs.), and sometimes adults, can be observed in shoals (6, 7), but their genetic relatedness is unknown.

We observed wild-type juvenile zebrafish, aged 6–8 weeks; the fish were kept in 2.5-l aquaria under a day/night cycle of 14/10 h and fed on a standard diet of brine shrimp nauplii and dry fish food. Twenty-four hours before an experiment started, 2 separate kin groups consisting of 12 full siblings each were placed into two 9-l aquaria with standing water. From each kin group, 3 fish were tested in the flume, one at a time, for a total of 6 fish. This procedure was repeated 3 times for a total of 6 kin groups and 18 test animals. Water from each of the two aquaria was used as the two stimuli in an olfactory preference test. Single individuals of either group were used as test fish and were placed into a choice flume (20 cm long × 4 cm wide, water level 2.5 cm) that maintained two separate water columns (Fig. 1) (8). Uniform and unidirectional water flow was maintained at a constant rate of 40 ml/min (= 3.5 mm/s). Periodic dye tests showed that the two water columns remained well separated. Prior to each trial, formulated fresh water was run through both channels of the flume for 5 min to allow the subject to acclimate. Each trial consisted of four 3-min periods, during which water from kin and non-kin aquaria was presented on alternate sides of the flume to correct for the possibility of unidirectional side bias. Every 10 s, we recorded which side of

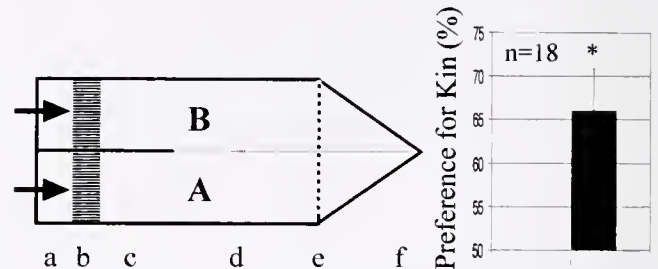


**Figure 1.** Diagram of the choice flume, and a graph of test result. (a) Water inflow area; (b) collimator to homogenize turbulent flow; (c) barrier-separated channels; (d) area of flume where water columns remain separated without the barrier (fine dotted center line); (e) screen to contain test subjects; (f) outflow channel. Black bar in graph indicates preference [% ± SEM] for kin over non-kin by test subjects (\* =  $P < 0.05$ ).

the flume (A or B, Fig. 1) the fish was swimming on. The number of times each animal was recorded on the side with kin stimulus was expressed as a percentage of the total number of recorded observations (i.e., kin plus non-kin). A score greater than 50% (random distribution) indicated a preference for the kin stimulus; and when the percentages of all the fish were compared using a Wilcoxon matched-pairs signed-ranks (WSR) test, the preference for kin was significant (WSR = 45.0,  $P = 0.050$ ) (Fig. 1). Our study is the first to show that juvenile zebrafish can recognize and prefer their siblings to unrelated conspecifics based on olfactory cues.

There are two general categories of kin recognition mechanisms, both based on learning processes as Tang-Martinez (9) emphasized. The first ("indirect") mechanism is based on familiarity, where individuals behave nepotistically to conspecifics with whom they grow up. The second ("direct") kin recognition mechanism allows individuals to identify even unfamiliar kin. Direct recognition is thought to be based on 'phenotype matching', in which an individual must learn cues, either from the phenotypes of close relatives (familial imprinting) (10), or from itself, to form a template for comparison with the phenotype of other individuals. Our results cannot distinguish between these recognition mechanisms.

### Literature Cited

1. Krause, J., D. J. Hoare, D. Croft, J. Lawrence, A. Ward, G. D. Ruxton, J. G. J. Godin, and R. James. 2000. *Proc. R. Soc. Lond. B Biol. Sci.* 267: 2011–2017.
2. Pitcher, T. J. 1986. *The Behaviour of Teleost Fishes*. Croom Helm, London.
3. Hamilton, W. D. 1964. *J. Theor. Biol.* 7: 1–16.
4. Brown, G. E., and J. A. Brown. 1993. *Behav. Ecol. Sociobiol.* 33: 225–231.

\* Corresponding author: ggerlach@mbl.edu

5. Apanius, V., D. Penn, P. R. Slev, L. R. Ruff, and W. Potts. 1997. *Crit. Rev. Immunol.* **17**: 179–224.
6. Pritchard, V. L., J. Lawrence, R. K. Butlin, and J. Krause. 2001. *Anim. Behav.* **62**: 1085–1088.
7. Delaney, M., C. Follet, N. Ryan, N. Hanney, J. Lusk-Yablick, and G. Gerlach. 2002. *Biol. Bull.* **203**: 240–241.
8. Atema, J., M. Kingsford, and G. Gerlach. 2002. *Mar. Ecol. Prog. Ser.* **241**: 151–160.
9. Tang-Martinez, Z. 2001. *Behav. Process.* **53**: 21–40.
10. Sherman, P. W., H. K. Reeve, and D. W. Pfennig. 1997. Pp. 69–96 in *Behavioral Ecology: An Evolutionary Approach*, J. R. Krebs and N. B. Davies, eds. Blackwell Scientific, Oxford, UK.

Reference: *Biol. Bull.* **205**: 225–226. (October 2003)  
 © 2003 Marine Biological Laboratory

## Mate Choice in Zebrafish (*Danio rerio*) Analyzed With Video-Stimulus Techniques

E. R. Turnell<sup>1</sup>, K. D. Mann<sup>1</sup>, G. G. Rosenthal<sup>2</sup>, and G. Gerlach<sup>1,\*</sup>

<sup>1</sup> Marine Biological Laboratory, Woods Hole, MA

<sup>2</sup> Boston University Marine Program, Woods Hole, MA

In many species, individuals of both sexes have developed a variety of visual signals and behavioral patterns with which to broadcast their quality as mating partners (1). The complexity of these signals makes it difficult to distinguish those that are most important in mate selection. Animated models offer a solution to this problem by allowing for the alteration of single parameters in the complex stimulus presented. In this study, we have tested the use of computer animated three-dimensional models to analyze mate choice criteria in zebrafish; we applied this tool to examine the roles played by two visual characteristics in mate selection.

Sexually mature wild-type zebrafish, aged at least 8 months, were kept in 9-l aquaria under a day/night cycle of 14/10 h. Subjects were tested in a 50 cm × 32 cm tank: a vertical line drawn on the wall of the tank divided it into two equal sections, A and B. The tank was placed between two 17-inch Dell computer monitors on which animated models of swimming zebrafish were displayed. The models were created using 3D Studio Max 1.0 (Kinetic) on a Dell Optiplex GXPro computer and a Targa 1000 board for digital/analog conversion of video signals, as described by Rosenthal (2, 3).

Before each trial, an individual fish was placed in the tank and allowed to acclimate for 5 min. During each trial, the subject was simultaneously shown two different animated stimuli. Each trial consisted of four 5-min viewing periods separated by 1-min intervals during which black covers were gently slid in front of the monitors. Three pairs of stimuli were shown to the subjects: [1] male *versus* female body shape (both with natural horizontal stripes), [2] vertical *versus* horizontal stripes (both with female shape), and [3] vertical *versus* horizontal stripes (both with male shape). The vertical and horizontal stripe patterns had equal amounts of blue coloration. Female-shaped images differed from male-shaped images only in that their bellies were 10% larger in side view. Stimulus pairs [1] and [2] were presented to both male and female subjects, while stimulus pair [3] was presented to female subjects only. In addition, stimulus pair [1] was shown to females who had spawned on the day of the trial. (The females

used in all other trials did not spawn on the day of the trial.) The two animated stimuli were alternated between the monitors to balance for side effects. During each viewing period, the location of the fish was recorded every 10 s. The percentage of time the subject spent in proximity to each stimulus (presence on side A or B) was calculated and compared using a Wilcoxon matched-pairs signed-ranks (WSR) test.

The results and statistical evaluations are shown in Figure 1. Males did not differentiate between the male and female-shaped images but showed a significant preference (19.6%) for the horizontal stripe pattern over the vertical stripe pattern when the images were female-shaped. Female zebrafish preferred a male-shaped stimulus over a female-shaped stimulus by 20.3%. However, females that had just spawned eggs on the morning of the trial did not show a preference for either the male or the female shape. Females also showed a significant preference (10.7%) for the horizontal stripe pattern over the vertical stripe pattern when the images were male-shaped, but did not differentiate between stripe patterns when the images were female-shaped.

The preference of females for the male-shaped stimulus over the female-shaped stimulus indicates that belly size alone allows female zebrafish to distinguish between sexes. The indifference of the females who had recently laid eggs suggests that females' interest in males correlates with their reproductive stage. The significant bias of males and females against vertical stripe pattern in the opposite-sex animation may result from selection against mating with heterospecifics.

The failure of males to distinguish between the male- and female-shaped images has at least two possible explanations: (a) the belly of the female image may not have been large enough to realistically simulate a fecund female zebrafish; or (b) male zebrafish may rely less on visual cues than on olfactory cues to select mates. Prior studies have shown that male zebrafish are attracted to the pheromones released by females (4–6).

This study shows that video-stimulus techniques can be used to further study mate choice and visual preferences in zebrafish.

\* Corresponding author: ggerlach@mbl.edu

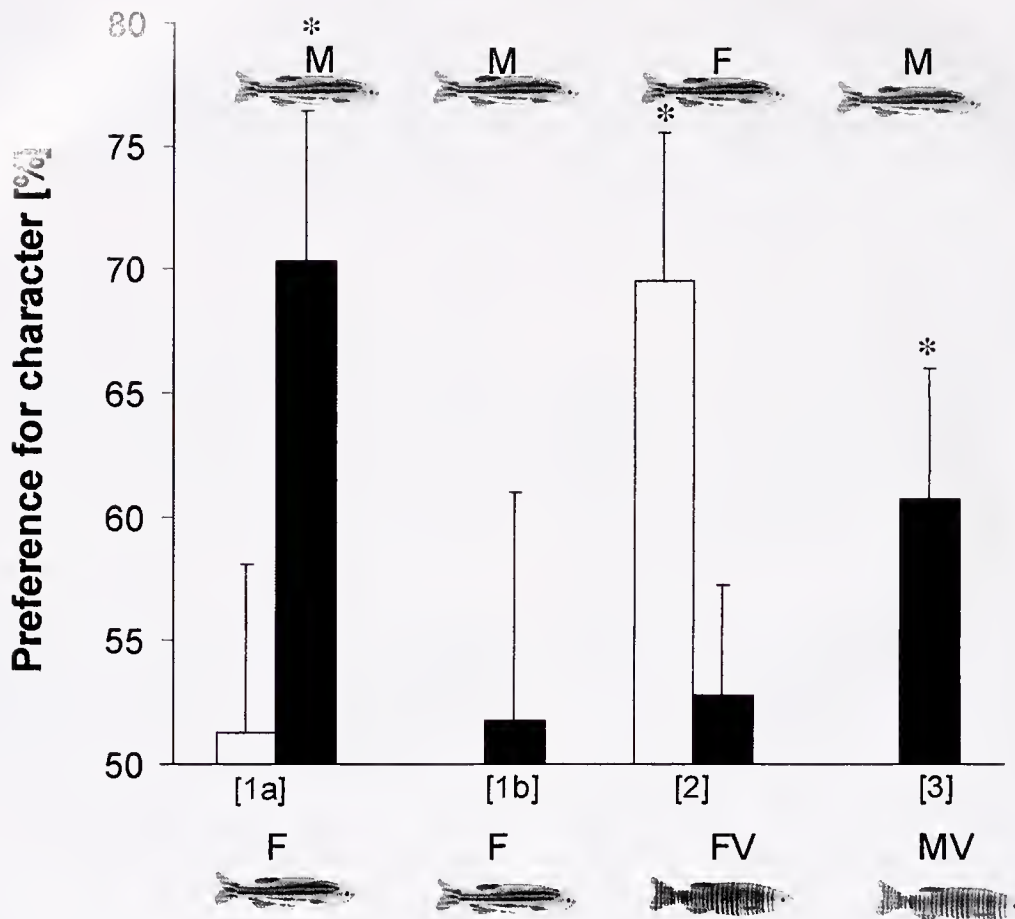


**Figure 1.** Preference (%  $\pm$  SEM) of males (white bars) and females (black bars) for each stimulus image, as measured by time spent in proximity to each one. [1a] Females significantly preferred the male-shaped stimulus (M) over the female-shaped stimulus (F) (WSR = 27.0,  $n = 12$ ,  $P = 0.034$ ); males showed no preference (WSR = 3.0,  $n = 15$ ,  $P = 0.868$ ). [1b] Females who had spawned the day of the trial also showed no preference between images M and F (WSR = 17.5,  $n = 15$ ,  $P = 0.288$ ). [2] Males significantly preferred the horizontal to the vertical stripe pattern when both images were female (F, FV) (WSR = 37.0,  $n = 15$ ,  $P = 0.017$ ); females showed no preference (WSR = 2.0,  $n = 15$ ,  $P = 0.923$ ). [3] Females significantly preferred the horizontal to the vertical stripe pattern when both images were male (M, MV) (WSR = 38.0,  $n = 16$ ,  $P = 0.049$ ). \* =  $P < 0.05$ .

### Literature Cited

- Dugatkin, L. A., and G. J. FitzGerald. 1997. Pp. 266–291 in *Behavioral Ecology of Teleost Fishes*, J.-G. J. Godin, ed. Oxford University Press, Oxford.
- Rosenthal, G. G. 1999. *Environ. Biol. Fishes* 56: 307–316.
- Rosenthal, G. G., W. E. Wagner, and M. J. Ryan. 2002. *Anim. Behav.* 63: 37–45.
- van den Hurk, R., and J. G. D. Lambert. 1983. *Can. J. Zool.* 61: 2381–2387.
- Bloom, H. D., and A. Perlmutter. 1977. *J. Exp. Zool.* 199: 215–226.
- Delaney, M., C. Follet, N. Ryan, N. Hanney, J. Lusk-Yablick, and G. Gerlach. 2002. *Biol. Bull.* 203: 240–241.

Reference: *Biol. Bull.* 205: 227–228. (October 2003)  
 © 2003 Marine Biological Laboratory

## Expressed Sequence Tag Analysis of Genes Expressed in the Bay Scallop, *Argopecten irradians*

S. B. Roberts and F. W. Goetz

Marine Biological Laboratory, Woods Hole, MA

The bay scallop (*Argopecten irradians*) is a marine bivalve found along the eastern United States. As in other pectinids, the bay scallop has a single, large adductor muscle which acts to open and close the shell with great force. This muscle is a prominent feature observed when the shell is removed, and is a favorite of both scientists and consumers, as it offers an excellent model for understanding muscle physiology and provides a healthy, high-protein food source. Consumer demand has caused the increase in aquaculture of bay scallops for direct marketing or to seed local waters.

The objective of the present study was to better understand the factors that contribute to the growth and development of the scallop adductor muscle. Because little is known about these processes in scallops, we have started by isolating and identifying genes from adductor muscle tissue. The results from this work could help facilitate future research. One example is in aquaculture, where these genes could be used as markers for a selective breeding programs. The use of such techniques could result in increasing the yield of adductor muscle or altering the size and density of the muscle fibers.

To identify the factors or genes involved in scallop muscle structure and function, a cDNA library was constructed from bay scallop adductor muscle, and expressed sequence tags (ESTs) were sequenced. ESTs are small pieces of DNA sequence (usually 100 to 800 nucleotides long) generated by sequencing randomly selected cDNA clones from a library. In this paper, the sequences of genes expressed in the bay scallop adductor muscle are reported.

To construct the cDNA library, adductor muscle tissue was dissected from four adult bay scallops obtained from Woods Hole, Massachusetts. Total RNA was extracted with Tri-Reagent (Molecular Research Center Inc.), and mRNA was isolated using the Poly-A-Tract mRNA Isolation System (Promega). The cDNA library was constructed using the  $\lambda$  Zap Express cDNA/Gigapack

cloning kit (Stratagene), starting with 5  $\mu$ g of mRNA as previously described (1).

To obtain ESTs, the library was mass excised to pBK-CMV phagemids and plated. From these plates, 454 randomly chosen cDNA clones were picked and sequenced from the 5' region by using the dideoxy chain termination method, with Big Dye Terminator (Applied Biosystems) and a vector-specific primer. The reactions were precipitated and resuspended in Hi-Di Formamide with EDTA (Applied Biosystems) and run on an ABI Prism 3730 automated sequencer (Applied Biosystems). Gene identification analysis was performed using Phred (base-calling) and Cross\_match (vector removal) software (<http://www.phrap.org/>); then EST sequences were compared with those in the NCBI database (nr) using the Blast-X and Blast-N programs (<http://www.ncbi.nlm.nih.gov/BLAST>) (2).

Of the 454 cDNA clones, 20 yielded no sequence and an additional 9 produced sequences of less than 150 bp; these were not used for sequence analysis. The average length of the remaining 425 sequences was 792 bp. Based on top Blast hits, 137 distinct sequences were observed and 90 of these genes were putatively identified; 47 lacked similarity with known genes and could not be identified. Of the latter 47 distinct sequences, 38 were most similar to unidentified products (*e.g.*, hypothetical protein, unnamed protein product) and 9 produced no hits in the database. Only 16 of the distinct sequences had previously been sequenced from the genus *Argopecten* and were either myosins, ribosomal proteins, or mitochondrial sequence. The mitochondrial sequence appeared 54 times (13%) in the ESTs and does not necessarily code for a protein; the presence of a poly-A region in the sequence leads to its isolation along with mRNA.

Of the genes identified based on sequence similarity, 33% are involved in cell structure (Fig. 1). The two genes most prevalent in the cDNA library were actin and myosin because they are the

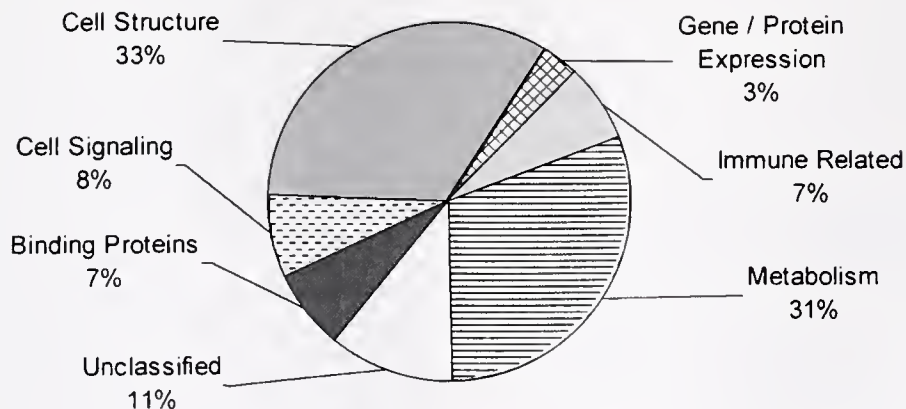


Figure 1. Percentages of identifiable ESTs sequenced that could be grouped together based on gene function or that could not be classified.

major components of muscle tissue. Of the 425 cDNA clones, actin (2 forms) occurred 80 times (19%) and myosin (11 forms) was found 68 times (16%). The remaining ESTs could be classified as being involved in gene/protein expression (3%), immunity (7%), metabolism (34%), protein binding (7%), or cell signaling (8%) (Fig. 1). Some identified genes (11%) could not be classified into any of these groups.

The sequences of all the ESTs generated from the bay scallop cDNA library and the putative identifications determined to date are available on a Bay Scallop EST project website (<http://www.mbl.edu/goetz/EST.html>) as well as in NCBI's GenBank database (<http://www.ncbi.nlm.nih.gov/>) [GenBank Accession numbers

CF197421-CF197787]. The ESTs generated offer a valuable resource to scientists in a wide range of disciplines including muscle physiology, growth and development, immunity, genetic identification, and aquaculture.

Funding for this research was provided by USDA grant #2002-03633—Program in Growth and Nutrient Utilization.

### Literature Cited

1. Garczynski, M. A., and F. W. Goetz. 1997. *Biol. Reprod.* **57**: 856–864.
2. Altschul, S. F., W. Gish, W. Miller, E. W. Myers, and D. J. Lipman. 1990. *J. Mol. Biol.* **215**: 403–410.

Reference: *Biol. Bull.* **205**: 228–230. (October 2003)  
© 2003 Marine Biological Laboratory

## Scanning Electron Microscopy Investigation of Epizootic Lobster Shell Disease in *Homarus americanus*

A. C. Hsu<sup>1</sup> and R. M. Smolowitz<sup>2,\*</sup>

<sup>1</sup> Boston University Marine Program, Woods Hole, MA

<sup>2</sup> Marine Biological Laboratory, Woods Hole, MA

The American lobster, *Homarus americanus*, represents an important fishery for much of the New England coast as well as several coastal provinces in Canada. Yet during the past decade, New England has reported dramatic decreases in the catch value in this lucrative industry (1). Shell disease is the deterioration of the crustacean exoskeleton by chitinoclastic organisms occurring in both marine and freshwater environments (2). In the past 6 years, the prevalence and severity of shell disease has markedly increased (K. Castro, Rhode Island Sea Grant, pers. comm). Predominately occurring in areas from Buzzard's Bay (Massachusetts) to eastern Long Island Sound (New York), it has been termed epizootic lobster shell disease (ELSD). Recently ELSD lobsters have been observed in Cape Cod Bay (Massachusetts), Kittery (Maine), and in offshore waters of New England (1).

For the present study, carapace lesions from wild-caught specimens of *H. americanus* were examined for the etiological agent responsible for ELSD. Although previous studies on lobster shell disease have used histology and molecular techniques to define the organisms involved in lesions (3, 4) no study has used scanning electron microscopy (SEM) to observe the progression of lesion development. For this study, SEM was used to produce three-dimensional views of ELSD development from geographically distinct areas along the New England coast for site comparisons.

During 2002–2003, lobsters with lesions ( $n = 22$ ) and without lesions ( $n = 14$ ) were collected. The sites sampled were the inshore waters of eastern Long Island Sound ( $n = 4$ ), Rhode Island ( $n = 13$ ), Buzzards Bay ( $n = 7$ ), Cape Cod Bay ( $n = 3$ ), and Maine ( $n = 4$ ), and the offshore waters of New Hampshire ( $n = 5$ ). Animals were defined as "healthy" or "infected" depending on the presence of noticeable lesions on the cephalothorax.

Carapace pieces were collected, fixed in 10% formalin in sterile seawater (5), and dehydrated in increasing concentrations of ethanol on ice. Samples were trimmed, critical-point-dried, and sputter-coated with gold palladium (6). The surface of cuticle lesions in early disease phases and the deeper interface between lesions and normal cuticle (leading edge of lesions) were compared and analyzed. To compare the presence of morphologically distinct bacteria identified in lesions, images were analyzed using Sigma-Scan 4.0 (Jandel Scientific).

Gross examination of carapace pieces showed that the carapaces of healthy animals showed no degradation, while samples from infected animals were severely eroded. Microscopic analysis of healthy carapace revealed minimal bacterial buildup (Fig. 1A). In contrast, carapace lesions of infected lobsters were covered with bacterial cells. Setal cores and natural abrasions were consistently filled with bacteria embedded in the cuticle at the lesion surface (Fig. 1B). Additionally, bacteria were abundant at the leading edge of the lesions (Fig. 1C). Overall, healthy carapace samples had substantially fewer bacteria on the carapace surface. These observations were consistent for all sampling sites.

The role of bacteria in the progression of lesion development was indicated by bacteria found embedded in shallow pits along the epicuticle (Fig. 1D). In other areas on the surface, halo-like holes surrounded several bacterial types that were associated with shallow erosions. These holes were not observed at the deep leading edges of the lesions. Bore holes appeared to match the length/width ratio of associated bacteria and, therefore, were believed to be caused by bacteria secreting chitinase, lipase, or protease (7). Diatoms, algae, and fungi/actinomycetes were noted typically in low abundance within the cuticle filaments, but bacteria were consistently the dominant organisms on both the carapace surface and the leading edge of lesions.

\* Corresponding author: [rsmol@mbi.edu](mailto:rsmol@mbi.edu)

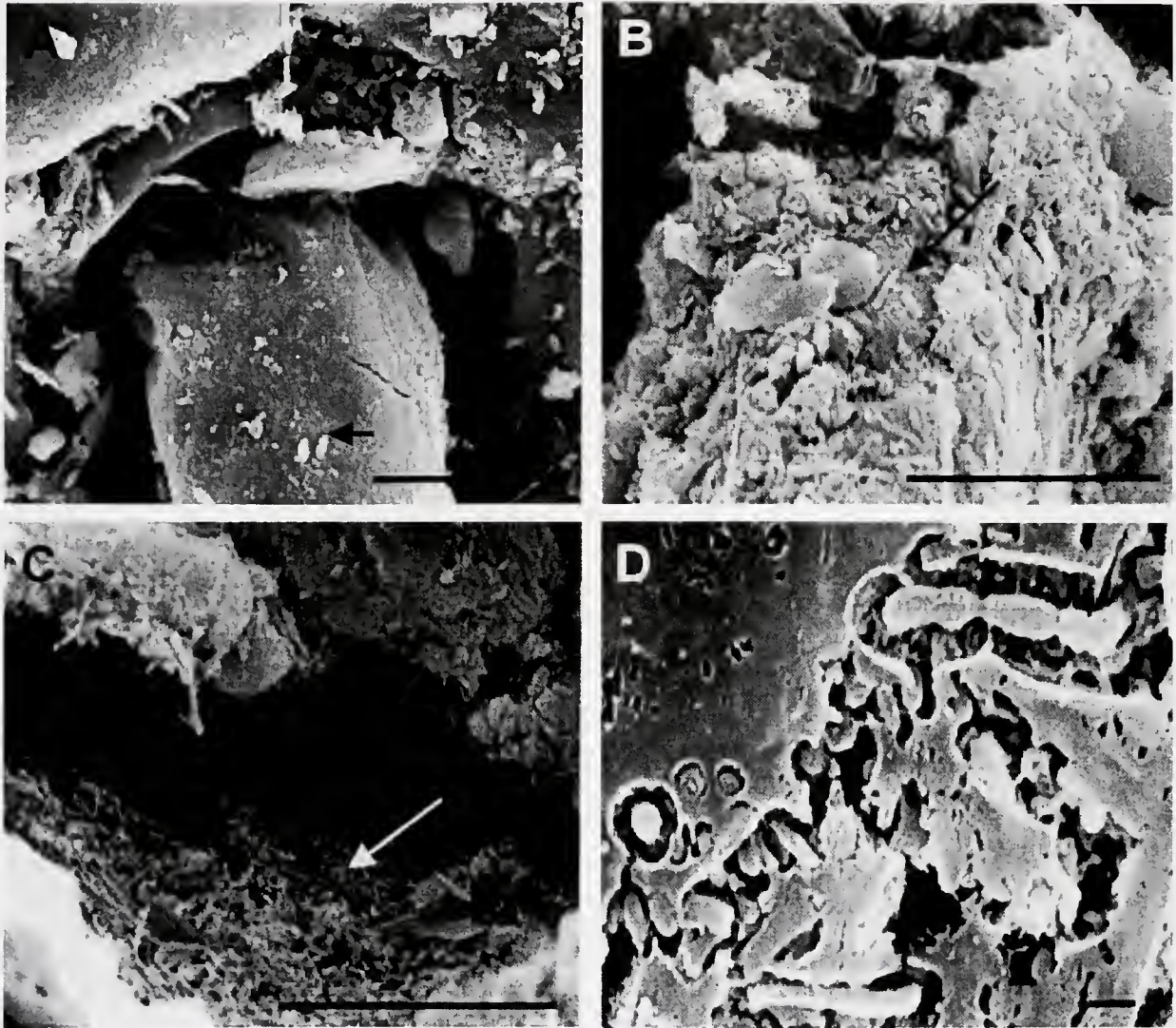


**Figure 1.** SEM images from infected and healthy lobsters collected from various sampling sites. (A) Healthy setae with minimal bacterial cells at base of core (arrow) from a non-diseased Maine lobster. (B) Infected setae with a high abundance of bacteria (arrow) from a diseased New Hampshire lobster. (C) Bacterial buildup (arrow) in the leading edge of a lesion from an infected Buzzard's Bay lobster. (D) Enzymatic digest by coccoid, rod, and rod linked bacteria from an infected Buzzard's Bay lobster. Bars represent 10  $\mu\text{m}$  in A, B, and C, and 1  $\mu\text{m}$  in D.

Five morphologically distinct bacterial types were observed on both healthy and infected animals. The majority of cells were either rods ( $1 \times 0.4 \mu\text{m}$ ), coccoid rods ( $0.8 \times 0.5 \mu\text{m}$ ), or cocci ( $0.5 \times 0.45 \mu\text{m}$ ). Segmented rod links (each piece  $1.5 \times 0.5 \mu\text{m}$ ) and coccoid links (each piece  $1.5 \times 1.0 \mu\text{m}$ ) were less abundant and found on infected animals only. Most bacterial types were found on animals from all geographical areas, but coccoid links were observed only on infected Rhode Island and Cape Cod Bay samples, indicating that they may be secondary invaders.

Bacteria are ubiquitous in the marine environment, so identifying the causative agents in a disease can be difficult. Examination of the interface between healthy and necrotic tissue provided the evidence necessary to identify bacteria as the disease-initiating organisms. Scanning electron microscopic imagery cannot speciate bacteria, so additional techniques such as those used in molecular biology are needed to identify the bacteria responsible for ELSD.

Findings from the present study revealed the complexity of this disease in its progression and development and demonstrated the necessity for further molecular strides, including bacterial speciation and infection studies, in ELSD research.

#### Literature Cited

1. Dean, M. J., K. A. Lundy, and T. B. Hoopes. 2002. *Massachusetts Division of Marine Fisheries, Technical Report TR-13* (Online). Available: <http://www.state.ma.us/dfwele/dmf/index.html> [accessed August 2003].
2. Stewart, J. E. 1980. Pp. 321–329 in *The Biology and Management of Lobsters*, Vol. 1. J. S. Cobb and B. F. Phillips, eds. Academic Press, New York.
3. Chistoserdov, A., R. Smolowitz, and A. Hsu. 2003. Pp. 61–64 in *Connecticut Sea Grant Extension, Third Long Island Sound Lobster Health Symposium*. University of Connecticut, Storrs.

4. Smolowitz, R. M., R. A. Bullis, and D. A. Abt. 1992. *Biol. Bull.* 183: 99–112.
5. Luna, L. G. 1992. p. 107 in *Histopathologic Methods and Color Atlas of Special Stains and Tissue Artifacts*. Johnson Printers, Downers Grove, IL.
6. Flegler, S. L., J. W. Heckman Jr., and K. L. Klomparens. 1993. Pp. 151–167 in *Scanning and Transmission Electron Microscopy: An Introduction*. Oxford University Press, New York.
7. Baross, J. A., P. A. Tester, and R. Y. Morita. 1978. *J. Fish. Res. Board Canada* 35: 1141–1149.

Reference: *Biol. Bull.* 205: 230–231. (October 2003)  
 © 2003 Marine Biological Laboratory

## Characterization of Phosphorus-Regulated Genes in *Trichodesmium* spp.

Elizabeth Orchard<sup>1</sup>, Eric Webb<sup>2</sup>, and Sonya Dyrhman<sup>2,\*</sup>

<sup>1</sup> Cornell University, Ithaca, NY

<sup>2</sup> Woods Hole Oceanographic Institution, Woods Hole, MA

Cyanobacteria of the genus *Trichodesmium* are abundant in tropical and subtropical regions and significantly contribute to carbon and nitrogen fixation in these environments (1). Recent studies suggest that phosphorus (P) supply may influence carbon and nitrogen fixation by *Trichodesmium* in the Atlantic (2, 3). However, evidence of phosphorus deficiency in field populations differs among *Trichodesmium* species (2, 3), suggesting that the individual species may have unique scavenging mechanisms. Here we examine several genes involved in phosphorus physiology within four species, *T. erythraeum*, *T. tenue*, *T. thiebautii*, and the related species *Katagnymene spiralis*.

Three genes thought to be related to phosphorus physiology were examined in this study: *phoA* and two copies of *pstS*, designated *pstS1* and *pstS2*. These genes are common components of P-regulated scavenging mechanisms in other cyanobacteria and heterotrophic bacteria (4, 5). The *phoA* gene codes for a predicted alkaline phosphatase, an enzyme that hydrolyzes inorganic phosphorus from organic phosphorus, which can then be used by the organism for growth. The activity of this enzyme has been used as an indicator of phosphorus stress in field populations (2). PstS is a high-affinity binding protein for inorganic phosphorus and is part of a phosphate-induced high-affinity scavenging system.

The sequenced genome of *T. erythraeum* ([http://genome.jgi-psf.org/draft\\_microbes/trier/trier.home.html](http://genome.jgi-psf.org/draft_microbes/trier/trier.home.html)) was used to identify *phoA* and two copies of *pstS* (*pstS1* and *pstS2*) on the basis of their similarity to characterized genes in GenBank as part of the ongoing

*Trichodesmium* annotation effort (unpubl. data). Multiple primer pairs were designed to amplify internal fragments (referred to as internal) or the complete *phoA*, *pstS1*, or *pstS2* gene (referred to as external) (Table 1). DNA was extracted following the method described by Orcutt *et al.* (6). PCR amplification conditions were performed with PfuTurbo DNA polymerase (Stratagene, La Jolla, CA) using conditions optimized for each gene and species (Table 1). To optimize amplification, the annealing temperature was varied for each gene and species over a range of at least 25 °C. Other variables included magnesium and enzyme concentration.

We were able to amplify the complete *phoA* and *pstS1* gene from *T. erythraeum* and *T. tenue*, and the complete *pstS2* gene from *T. erythraeum*. We amplified gene fragments from *pstS1* in *T. thiebautii* and *K. spiralis*, and from *pstS2* in *T. tenue* and *K. spiralis* (Table 2). With the entire 3.5 kb of the *phoA* gene amplified from *T. erythraeum*, we were able to clone it into the pBluescript II SK (+) plasmid in *Escherichia coli* DH5 $\alpha$ , in order to identify the activity associated with the putative gene. However, activity and expression work is still ongoing.

All PCR products were sequenced at the Josephine Bay Paul Center of the Marine Biological Laboratory (Woods Hole, MA) using the facility's protocols. With the *T. erythraeum* genome as a guide, internal primers were designed to obtain full coverage of the entire gene on both strands. Genes were aligned between species to compare their sequence divergence using Sequencher 4.1 software (Gene Codes Inc. Ann Arbor, MI).

Preliminary sequencing data for the genes and gene fragments indicate that *pstS1*, *pstS2*, and *phoA* in *T. tenue* as well as *pstS2* in

Table 1

Primer sequences and annealing temperatures for PCR reactions

Gene	External 5'–3'	Annealing temp.	Internal 5'–3'	Annealing temp.
<i>PhoA</i>	ATGCGTGGGGACTTAACAGTAA TCTAATCACAAAATCATCTGTGTGAGAG	61.2	TTCGCTATCATCATACACCATAATTCCACC AGAACCTAATGATGACTATACTAACGACCC	60
<i>PstS1</i>	ACAGCACAAACTAAAACCAG GACGAATCAGCAGTGACAAG	58.5	TTCCATCACCTATATATCAAC CATAACCATACTCAACATATCC	51.2
<i>PstS2</i>	AAATTAGTATCGTTGCCTAAAT TTGTGCTTATACATTTATTATC	59	ATCTTTCCAGCTCCACTATAC CTCCTACTTCTTTTCCACTC	50.2

\* Corresponding author: sdyhrman@whoi.edu

Table 2

Amplified genes from *Trichodesmium* and *Katagnymene spiralis*

	<i>PhoA</i>	<i>PstS1</i>	<i>PstS2</i>
<i>T. erythraeum</i>	XXX	XXX	XXX
<i>T. tenue</i>	XXX	XXX	X
<i>K. spiralis</i>	XXX	X	X
<i>T. thiebautii</i>		X	

XXX—entire gene

X—gene fragment

*Katagnymene* are approximately 98% identical to the corresponding genes in *T. erythraeum*. Given the morphological distinction of the *Trichodesmium* species, this high degree of similarity was surprising. However, coverage of the entire gene in each species may reveal regions within the genes that are less highly conserved. This hypothesis is consistent with the results for the only other functional gene to be sequenced from multiple *Trichodesmium* species, *hetR*, which shows a lower degree of similarity, 91%–95% (7).

Despite extensive efforts to amplify all the genes by varying annealing temperature, primers, and concentrations of magnesium, enzyme, and template, we were unable to amplify *pstS2* or *phoA* from *T. thiebautii*. This is particularly interesting because *T. thiebautii* has been shown to have alkaline phosphatase activity (2), and because of the degree of similarity of *phoA* among the other species. Additionally, *T. thiebautii*'s evolutionary relationship, in-

ferred from *Trichodesmium* ITS sequences (6), indicates *T. tenue* and *K. spiralis* are more closely related to each other than to *T. thiebautii*. It may be that *phoA* in *T. thiebautii* is very different compared to the other species or that a different gene and gene product are used in the hydrolysis of dissolved organic phosphorus for this species.

Future work is needed to determine whether *pstS2* and *phoA* are present in *T. thiebautii*. Although other species and isolates of *Trichodesmium* should be analyzed, our initial identification of putative P-regulated genes in these *Trichodesmium* species has improved our knowledge of phosphorus scavenging mechanisms in this important genus.

This work was funded by NSF grant OCE-0220945, and by NSF Research Experience for Undergraduates grant OCE-0097498.

### Literature Cited

1. Capone, D., J. Zehr, H. Paerl, B. Bergman, and E. Carpenter. 1997. *Science* 276: 1221–1229.
2. Dyhrman, S., E. Webb, and D. Anderson. 2002. *Limnol. Oceanogr.* 47: 1832–1836.
3. Sanudo-Wilhelmy, S. A., C. Gobler, D. Hutchins, M. Yang, K. Lwiza, J. Burns, D. Capone, J. Raven, and E. Carpenter. 2001. *Nature* 411: 66–69.
4. Scanlan, D., and N. West. 2002. *FEMS Microbiol. Ecol.* 40: 1–12.
5. Scanlan, D., and W. H. Wilson. 1999. *Hydrobiologia* 401: 149–175.
6. Orcutt, K. M., U. Rasmussen, E. A. Webb, J. B. Waterbury, K. Gundersen, and B. Bergman. 2002. *Appl. Environ. Microbiol.* 68: 2236–2245.
7. Janson, S., B. Bergman, E. Carpenter, S. Giovannoni, and K. Vergin. 1999. *FEMS Microbiol. Ecol.* 30: 57–65.

Reference: *Biol. Bull.* 205: 231–232. (October 2003)  
© 2003 Marine Biological Laboratory

## Molecular Quantification of Toxic *Alexandrium fundyense* in the Gulf of Maine

Madeline Galac<sup>1</sup>, Deana Erdner<sup>2</sup>, Donald M. Anderson<sup>2</sup>, and Sonya Dyhrman<sup>2,\*</sup>

<sup>1</sup> State University of New York at Stony Brook, Stony Brook, NY

<sup>2</sup> Woods Hole Oceanographic Institution, Woods Hole, MA

The toxic dinoflagellate *Alexandrium fundyense* is widespread in the northeastern part of North America, including the Gulf of Maine, and is responsible for seasonal harmful algal blooms in these regions. Even at low cell densities, *A. fundyense* produces toxin that can accumulate in shellfish and cause paralytic shellfish poisoning (PSP). PSP can be debilitating or lethal to humans and other shellfish consumers and is a public health concern (1). Accurate measurements of *A. fundyense* distributions, at a low cell density, are critical to continued PSP monitoring and mitigation efforts.

Traditional assessments of *A. fundyense* cell number rely on microscopic counts of species abundance. However, it is difficult to visually distinguish *A. fundyense* from other dinoflagellates and other species of *Alexandrium*, as there are often only subtle morphological differences between taxa. Oligonucleotide probe-based

methods (2) help to distinguish between *Alexandrium* and other genera and are commonly employed in the Gulf of Maine to map cell distribution. Although these approaches are useful, we developed and applied an assay that does not require microscopy. Various studies have used quantitative PCR (qPCR) to assay cell numbers of dinoflagellates such as *Pfiesteria piscicida* (3). In this study we mapped *A. fundyense* distribution using a qPCR assay that appears to be specific and sensitive.

Primers were designed to amplify a 174 base pair region of the large ribosomal subunit (LSU) gene (4). This gene was chosen because it has been sequenced from many species of *Alexandrium*, is commonly used for phylogenetic analyses (5), and is present in high copy number.

Building on previous work (4), the specificity of the LSU primers was tested against DNA extracted from phytoplankton cultures with Qiagen's DNEasy Kit, according to the manufacturer's instructions, using standard hot start amplification conditions

\* Corresponding author: sdyhrman@whoi.edu

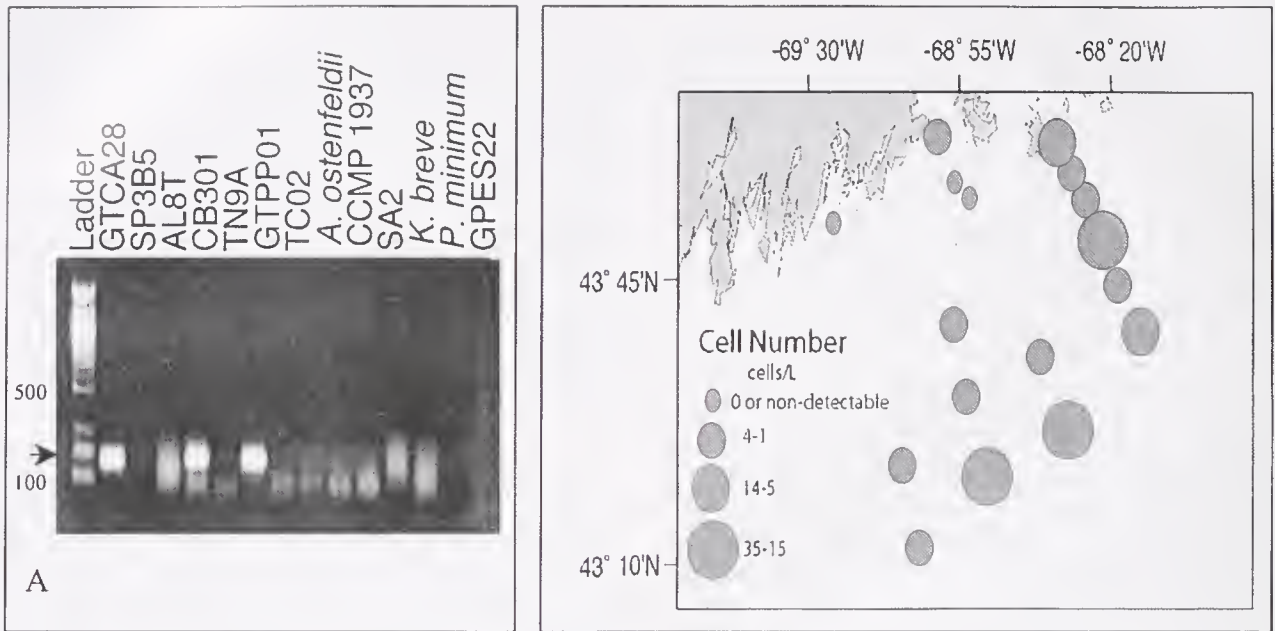


**Figure 1.** Specificity of large ribosomal subunit (LSU) gene primers and a map of *Alexandrium fundyense* distribution. (A) The arrow indicates a 174-bp fragment of the LSU gene, as shown by the 100-bp ladder. Amplification occurred only in strains of *A. fundyense* that are present in the Gulf of Maine (GTCA28, CB301, GTPP01). Amplification did not occur in *Alexandrium* strains from other parts of the world (SP3B5, AL8T, TN9A); nor did amplification occur in other *Alexandrium* species such as *A. ostenfeldii* and *A. andersoni* that could occur with *A. fundyense* in the Gulf of Maine (*A. ostenfeldii*, TC02). Other dinoflagellate species also did not amplify (CCMP1937, SA2, *Karenia breve*, *Prorocentrum minimum*, GPES22). (B) A map of *A. fundyense* distribution in surface water of the Gulf of Maine during a cruise from 29 May to 6 June 2003.

and a 60 °C annealing temperature. Under these conditions amplification occurred only with *A. fundyense* isolated from the Gulf of Maine (Fig. 1A).

Field samples were collected from surface water along transects in the Gulf of Maine from 29 May through 6 June 2003. At each station, 4 l of surface water was collected, prescreened through a 64- $\mu$ m sieve, and collected on a 15- $\mu$ m filter. The samples were each extracted with Qiagen DNEasy kit.

Using qPCR, the number of cells in a field sample was determined. In this study, qPCR was performed using Stratagene Brilliant SYBR Green QPCR Master Mix, and a fluorescence threshold was set by the analytical software for the BioRad iCycler. The PCR cycle during which this threshold was crossed for each sample designated the  $C_T$ . Sample  $C_T$  can be compared to the  $C_T$  of standards with a known cell count to specify the number of cells present in the sample (4).

To ensure that different strains of *A. fundyense* have the same copy number of the LSU gene, standard curves were built from two Gulf of Maine strains in culture (GTCA28 and CB301). Both strains resulted in similar standard curves ( $y = -2.5281x + 30.664$ ,  $R^2 = 0.9514$  for the first strain and  $y = -2.0291x + 27.61$ ,  $R^2 = 1$  for the second strain). A dilution series of a known number of cells was also analyzed with a field sample matrix. No significant PCR inhibition of the target was detected from extraneous DNA in the field samples.

The number of cells detected in the Gulf of Maine ranged from 1 to 35 cells per liter (Fig. 1B). This range is similar to the range of cell numbers calculated from other methods (live counts done

during the cruise and oligonucleotide probe counts [Anderson, unpubl. data]), which we did not expect to be exactly the same since the samples were taken from different Niskin bottles and processed differently. Of the stations tested, station 86 and off-shore stations 104 and 105 had the highest concentrations of cells. To confirm amplification of *A. fundyense* from the field samples, PCR products generated from samples 89 and 128 were sequenced at the Marine Biological Laboratory, Woods Hole, Massachusetts, using the facility's protocols and were shown to be *A. fundyense*.

In summary, qPCR appears to be a specific and sensitive approach to monitoring the abundance of *A. fundyense*. This method shows great promise for mapping the *A. fundyense* populations in the Gulf of Maine.

This research was supported by an EPA Star Award through the ECOHAB Program (R-83041501-0) and a NSF-REU site grant (OCE-0097498) to the Boston University Marine Program.

### Literature Cited

1. Anderson, D. M. 1997. *Limnol. Oceanogr.* **42**: 1009–1022.
2. Anderson, D. M., D. M. Kulis, B. A. Keafer, and E. Berdalet. 1999. *J. Phycol.* **35**: 870–883.
3. Bowers, H. A., T. Tengs, H. B. Glasgow, J. M. Burkholder, P. A. Rutlee, and D. W. Oldach. 2000. *Appl. Environ. Microbiol.* **66**: 4641–4648.
4. La Du, J., D. Erdner, S. Dyhrman, and D. Anderson. 2002. *Biol. Bull.* **203**: 244–245.
5. Scholin, C. A., M. Herzog, M. Sogin, and D. M. Anderson. 1994. *J. Phycol.* **30**: 999–1011.

Reference: *Biol. Bull.* **205**: 233–234. (October 2003)  
© 2003 Marine Biological Laboratory

## Description of *Vibrio alginolyticus* Infection in Cultured *Sepia officinalis*, *Sepia apama*, and *Sepia pharaonis*

C. R. Sangster<sup>1</sup> and R. M. Smolowitz<sup>2,\*</sup>

<sup>1</sup> Western College of Veterinary Medicine, Saskatoon, Canada

<sup>2</sup> Marine Biological Laboratory, Woods Hole, MA

Cuttlefish of the genus *Sepia* (*S. officinalis*, *S. apama*, and *S. pharaonis*) have been cultured at the Marine Resources Center (MRC) of the Marine Biological Laboratory since 1992. The objectives of this retrospective study were to identify common causes of morbidity and mortality in the cuttlefish populations maintained at the MRC, and to describe the histological appearance of those lesions. Such information can be used in developing more effective methods of diagnosis, prevention, and treatment.

Necropsy cases were selected for inclusion in this study if bacterial cultures had been obtained at necropsy. Bacterial cultures had been obtained from 53 necropsies performed between March 1999 and June 2003. Those culture samples were taken from the digestive gland, kidney sac, or gonad and were plated on marine brain heart infusion medium (1).

Retrospective examination of archived necropsy cases of *Sepia* spp. showed that mortality was commonly associated with bacterial cultures positive for *Vibrio alginolyticus*, a marine bacterium routinely found in coastal waters, sediment, and culture systems (2, 3). Of the 53 cases in which bacterial cultures were taken, 33 were positive for *V. alginolyticus*.

Of the 33 animals with cultures positive for the bacterium, archived histological sections were available in 19 cases. The sections were paraffin-embedded fixed tissues, sectioned at 6  $\mu\text{m}$  and stained with hematoxylin and eosin (4). Examination of these sections showed that the most commonly affected tissues were the kidney, branchial heart appendage, branchial heart, and gill (42%). A high incidence of infection (47%) was noted in the reproductive organs (nidamental gland, accessory nidamental gland, and gonads). All animals with reproductive lesions were older than 9 months. Of the 19 included cases, 16 (84%) had some form of epidermal ulceration, with 7 classified as moderate to severe, and 9 as mild. No reaction was detected in the digestive gland of any animal. Examination of Gram-stained tissue sections (3) confirmed the presence of gram-negative bacteria in the infected foci.

Histopathological examination of sections showed that, based on the appearance of the response as identified in the tissues, the sepioid inflammatory reaction to *V. alginolyticus* occurred in one of three distinct forms. The first was multifocal, necrotizing, granuloma-like lesions (0.95–1.4 mm diameter), most often seen in reproductive tissues such as the testicular ducts and accessory nidamental glands (Fig. 1A, B). The second form consisted of multifocal, necrotizing, granulomatous-like inflammation that resulted in subtle lesions (0.1–0.25 mm diameter) containing small numbers of hemocytes and bacteria, and was predominately found in the gills of affected animals. Finally, multifocal, necrotizing,

granulomatous-like inflammation of intermediate size was commonly found in branchial heart and its appendage (0.2–0.7 mm diameter) (Fig. 1C).

Severe, necrotizing hemocytic inflammation also occurred in the serosa of various organs including the branchial heart and stomach, which are anatomically suspended in large vascular sinuses. Similar hemocytic inflammation of the kidney fronds was unique in that the bacteria and associated necrosis occurred primarily at the periphery of the fronds (suspended in the renal sac), while the hemocytic response was located in the vascular/connective tissue core (Fig. 1D).

Bacteria causing the observed lesions may have accessed the circulation *via* epidermal ulcerations, but ulceration was not recognized in all animals and was only mild in others, so the potential for other routes should not be ignored. In the circulation, the bacteria lodged in the branchial heart, resulting in foci of moderate inflammation and necrosis. Most other lesions appear to have been spread by bacterial seeding of organs that receive circulation from the branchial heart. Thus, bacteria-laden hemolymph that passed from the heart directly to the gill and branchial heart appendage resulted in foci of inflammation. The branchial heart appendage forms an ultrafiltrate that is discharged into the kidney sac and bathes the kidney fronds; the epithelium of the kidney fronds modifies the filtrate before it exits the body through a renal pore. Bacteria can proliferate in the filtrate and attack the suspended kidney fronds. Hemocytes, which mount the inflammatory response, migrate from vessels within the connective core of the kidney fronds to the site of infection.

These results show that *V. alginolyticus* is a pathogen of significance in sepioids cultured at the MRC. *V. alginolyticus* is common in coastal waters and is therefore likely to be present in the facility's seawater supply (2). This pathogen has been associated with tank surfaces in culture systems (5). Comparisons between bacterial populations on wild-caught and laboratory-reared squid, *Lolliguncula brevis*, showed that animals reared in the laboratory had higher total numbers of bacteria. The increase was primarily due to *Vibrio* spp., including *V. alginolyticus* (6). In that study, the increase in bacteria was not linked to the ulceration of the epidermis. Similarly, *V. alginolyticus* has caused disease in juvenile red abalone, *Haliotis rufescens*, but large numbers can be found on the foot of otherwise healthy individuals (5). Such findings suggest that direct infection of the epidermis is an unlikely pathogenesis for *V. alginolyticus* in cuttlefish. Routes of infection probably include infection secondary to ulceration, especially if the injury is caused by jetting into tank walls colonized by the bacteria. *V. alginolyticus* has also been found on the carapace of copepods (7).

\* Corresponding author: rsmol@mbledu

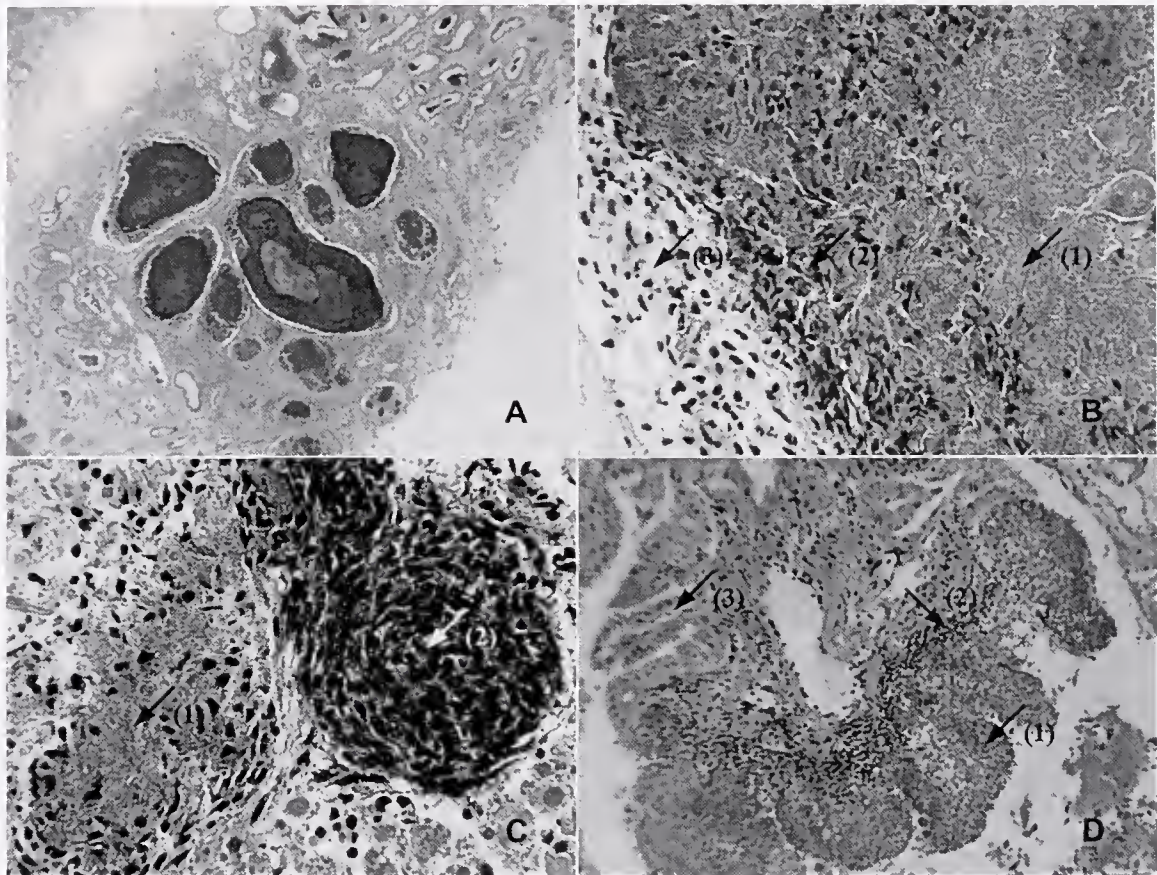


**Figure 1.** Histological reaction of *Sepia* spp. to *Vibrio alginolyticus*. (A) Granuloma-like formation in the accessory nidamental gland. (B) Coagulative necrosis and bacteria in the center of the granuloma (1) are surrounded by a layer of dying hemocytes (2), which is in turn surrounded by a fibrotic hemocytic reaction (3). (C) Moderate inflammation in the branchial heart is typified by large numbers of bacteria and cellular necrosis (1), and hemocytic infiltration (2). (D) The periphery of the kidney fronds are necrotic and bacteria-laden (1), while a front of hemocytes infiltrates the tissue from vessels in the core (2). A normal tissue frond is also present (3).

Crustaceans, including amphipods, are the primary food fed to cuttlefish cultured at the MRC, and thus may be an important source of infection. Finally, over half of the studied cuttlefish with reproductive-associated lesions were at or near the upper limit of their life span (8), suggesting that senescent tissues are more susceptible to this pathogen and are a potential point of initiation for a systemic infection.

This retrospective study shows that systemic *V. alginolyticus* is a common pathogen in *Sepia* spp. cultured at the MRC. A number of potential routes of infection exist but, as in most aquatic animal diseases, stress and husbandry likely play an important role in the occurrence of disease. Better sepoid husbandry methods may help reduce or prevent this disease from occurring. Additionally, the data collected in this study indicate that, when systemic bacterial disease is suspected in *Sepia* spp., the branchial heart and branchial heart appendage should be examined histologically, and bacterial cultures should be obtained from the renal sac.

### Literature Cited

1. Wenuganen, S., R. Bullis, and R. Smolowitz. 1997. *Biol. Bull.* **193**: 269–270.
2. Balows, A., H. G. Truper, M. Dworkin, W. Hardner, and K. Schleifer. 1992. Pp. 2995–2996 in *The Prokaryotes*, 2nd ed., Springer-Verlag, New York.
3. Hormansdorfer, S., H. Wentges, K. Nengebauer-Buchler, and J. Bauer. 2000. *Int. J. Hyg. Environ. Health* **203**: 169–175.
4. Humanson, G. L. 1962. Pp. 3–126 in *Animal Tissue Techniques*. W. H. Freeman, San Francisco.
5. Elston, R., and G. S. Lockwood. 1983. *J. Fish Dis.* **6**: 111–128.
6. Ford, L. A., S. K. Alexander, K. M. Cooper, and R. T. Hanlon. 1986. *J. Invertebr. Pathol.* **48**: 13–26.
7. Dumontet, S., K. Krovacek, S. B. Svenson, V. Pasquale, S. B. Baloda, and G. Figliuolo. 2000. *Comp. Immunol. Microbiol. Infect. Dis.* **23**: 53–72.
8. Forsythe, J. W., R. H. De Rusha, and R. T. Hanlon. 1994. *J. Zool. Lond.* **233**: 175–192.

Reference: *Biol. Bull.* 205: 235–236. (October 2003)  
© 2003 Marine Biological Laboratory

### Detection of *Edwardsiella* Infections in *Opsanus tau* by Polymerase Chain Reaction

Krystal D. Baird<sup>1,2</sup>, Hemant M. Chikarmane<sup>1,3</sup>, Roxanna Smolowitz<sup>1,\*</sup>, and Kevin R. Uhlinger<sup>1</sup>

<sup>1</sup> Marine Biological Laboratory, Woods Hole, MA

<sup>2</sup> Barnstable County AmeriCorps Cape Cod, Barnstable, MA

<sup>3</sup> Cape Cod Community College, W. Barnstable, MA

*Opsanus tau*, the oyster toadfish, is an important laboratory animal used in hearing and balance research at the Marine Biological Laboratory (MBL) (1). Wild-caught and cultured fish are maintained year-round in both recirculation and flow-through tanks in the Marine Resources Center (MRC) at the MBL. A major cause of disease in toadfish held at the MRC is *Edwardsiella tarda* (1, 2). A member of the Enterobacteriaceae, *E. tarda* is a natural inhabitant of fresh and marine water and causes gastrointestinal and extraintestinal disease in humans (3). Published reports of fish disease caused by *E. tarda* involve cultured warm-water fish, but the disease can also affect cold-water salmon (4). Poor water quality, high water temperatures, feces, and decaying organic matter likely contribute to the onset and severity of the disease and probably allow for occurrence and proliferation of the bacteria in the fish's environment. These factors, combined with capture and holding-induced stresses, may account for the high levels of disease caused by *E. tarda* in the toadfish in our facility.

Currently, the only diagnostic test available for identification of *E. tarda* in diseased fish is bacterial culture and identification using traditional biochemical tests. At the MRC, these tests are sent to an outside laboratory, and the process takes about three weeks. Treatment is often attempted before verification that the lesions identified at necropsy were caused by *E. tarda*. Using the PCR methods described here, we can specifically and rapidly identify *E. tarda*, resulting in timely and appropriate management procedures and treatments for infected fish.

The polymerase chain reaction (PCR) is a DNA-based method that can be used for the quick and sensitive detection of microorganisms in both antemortem and necropsied tissues. PCR primers specific for *E. tarda* isolates from Japanese eels have been derived from an anonymous species-specific sequence (5) or from the hemolysin gene (6). Here we describe PCR primers based on *Edwardsiella* small subunit (ssu) RNA genes for direct identification of *E. tarda*. Primer development will be described in detail elsewhere.

The type strains *E. tarda* ATCC 15947 and *E. ictaluri* ATCC 33202 were obtained from the American Type Culture Collection. *E. ictaluri* is an important pathogen of cultured catfish and produces very similar lesions to those caused by *E. tarda* in toadfish. In addition, *E. tarda* has been shown to cause disease in catfish (7). Cultures were grown in Difco marine brain heart infusion broth. One milliliter of the liquid broth culture was transferred aseptically to 1.5-ml microfuge tubes, which were then centrifuged at 2790 × g for 4 min to pellet cells. Pellets were resuspended in 0.6 ml of lysis buffer (10 mM Tris-Cl pH 8.0, 5 mM EDTA, and 1% SDS).

Proteinase K (50 µg) was added, and tubes were incubated overnight at 50°C. Genomic DNA was precipitated by the addition of 0.55 ml of isopropanol; the liquid portion was removed completely. The DNA pellet was rinsed twice with 0.8 ml of 70% ethanol. After the ethanol was evaporated, the DNA was dissolved in 0.8 ml of TE (Tris-EDTA; 8).

Forward primer Eta1-363f (5'-GTG TRC GTG TTA ATA GCA-3') was designed to amplify *E. tarda* from human sources (biotype 1), represented by the type strain ATCC 15947. Forward primer Eta2-351 (5'-TAG GGA GGA AGG TGT GAA-3') was designed to amplify *E. tarda* strains isolated from fish (biotype 2). An *Edwardsiella* genus-specific reverse primer Edwsp-780r (5'-CTC TAG CTT GCC AGT CTT-3') was used with the forward primers.

PCR amplification was performed with an Applied Biosystems GeneAmp 9700. The reaction mixture (10 µl) contained 1× Taq polymerase buffer (Promega), 1.5 mM MgCl<sub>2</sub>, 1 mM dNTP mix, 100 nM each of forward and reverse primer, 0.5 units Taq polymerase (Promega) and template DNA. The thermal cycle profile commenced with an initial denaturation for 1 min at 94°C; 30 cycles of denaturation (1 min at 94°C), annealing (1 min at 58°C), and extension (1 min at 72°C); and a final extension at 72°C for 7 min. Amplification products were electrophoresed in a 1.5% agarose gel (Fisher Scientific) in 0.5 × Tris-Borate-EDTA (TBE) buffer (8). Gels were stained with 1 µg/ml ethidium bromide and digitally photographed. Images were manipulated in Adobe Photoshop. Some amplifications were carried out directly from bacterial colonies, in which case the initial denaturation time in the PCR profile was increased to 5 min at 94°C.

The results, as determined by electrophoresis, showed that DNA of *E. tarda* and *E. ictaluri* could be distinctly amplified by the appropriate primers (Fig. 1). The Eta1-363f-Edwsp-780r primers amplified *E. tarda* ATCC 15947, yielding a product of 216 bp, and did not amplify *E. ictaluri* ATCC 33202 (Fig. 1A, lanes 1–4) or MRC fish isolates biochemically identified as *E. tarda* (not shown). As would be expected, Eta2-351f-Edwsp-780r failed to amplify both type strains (Fig. 1A, lanes 5–8). However, Eta2-351f-Edwsp-780r primers amplified the *E. tarda* fish isolates (Fig. 1B, lanes 1–6), demonstrating that the strains isolated at the MRC were clearly of fish origin, and biotype 2. The biotype 2 amplifications were performed directly from bacterial colonies, showing that direct identifications were indeed possible.

Future work will involve development of a direct assay method for *E. tarda* from both postmortem toadfish tissues and, more importantly, antemortem tissues. The ability to amplify *E. tarda* strains from toadfish is the first step to being able to understand, isolate, and control future outbreaks of *E. tarda*.

\* Corresponding author: rsmol@mbl.edu.

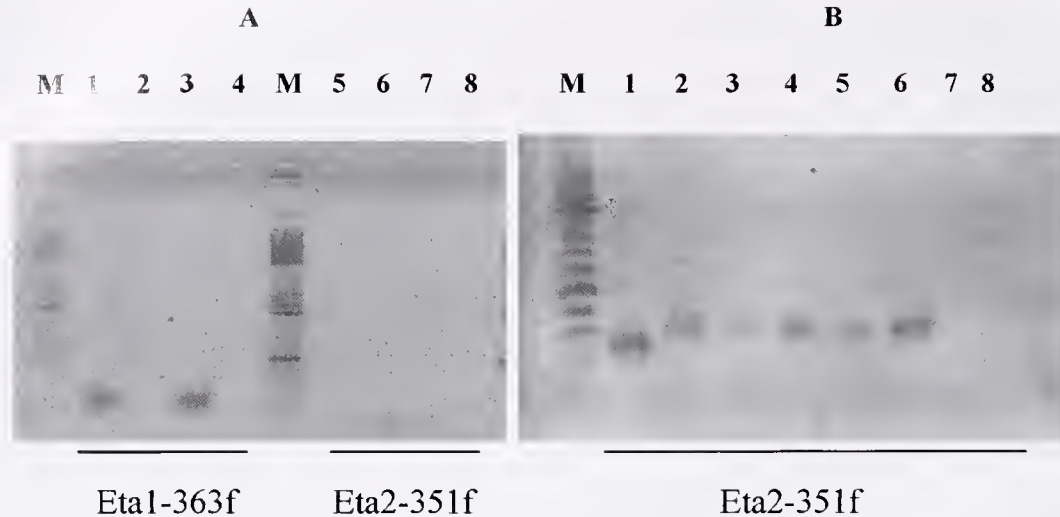


**Figure 1.** Gel electrophoresis of PCR amplification products from *Edwardsiella*. (Panel A) Amplifications from purified genomic DNA. Lanes 1, 3, 5, 7 are *E. tarda* ATCC 15947. Lanes 2, 4, 6, 8 are *E. ictaluri* ATCC 33202. (Panel B) Amplifications from bacterial colonies. Lanes 1–6, *E. tarda* fish isolates. Lane 7, *Vibrio* sp. negative control. Lane 8, no template control. *Edwsp-780r* was used as the reverse primer in all cases. Forward primers are indicated.

R. Smolowitz acknowledges support from NIH/NIDCD grant 5P01 DC001837-09. H. Chikarmane acknowledges support from the Wilkens Foundation and the Cape Cod Community College Educational Foundation.

#### Literature Cited

1. Smolowitz, R., and R. Bullis. 1997. *Biol. Bull.* **193**: 270–271.
2. Wenuganen, S., R. Bullis, R. Smolowitz, and E. Barbieri. 1997. *Biol. Bull.* **193**: 269–270.
3. Janda, J. M., and S. L. Abbott. 1993. *Clin. Infect. Dis.* **17**: 742–748.
4. Plumb, J. A. 1999. Pp. 479–490 in *Fish Diseases and Disorders Vol. 3. Viral, Bacterial, and Fungal Infections*, P. T. K. Woo and D. W. Bruno, eds. CABI Publishing, New York.
5. Aoki, T., and I. Hirano. 1995. *Asian Fisheries Society Special Publication*. **10**: 135–146.
6. Chen, J. D., and S. Y. Lai. 1998. *Zool. Stud.* **37**: 169–176.
7. Darwish, A., J. A. Plumb, and J. C. Newton. 2000. *J. Aquat. Anim. Health* **12**: 255–266.
8. Sambrook, J., and D. Russell. 2001. *Molecular Cloning: A Laboratory Manual*, 3<sup>rd</sup> ed. Cold Spring Harbor Laboratory Press, New York.

Reference: *Biol. Bull.* **205**: 236–237. (October 2003)  
© 2003 Marine Biological Laboratory

## Catalase in Microsporidian Spores Before and During Discharge

Earl Weidner<sup>1</sup> and Ann Findley<sup>2</sup>

<sup>1</sup> Louisiana State University, Baton Rouge, LA

<sup>2</sup> University of Louisiana at Monroe, Monroe, LA

The noted parasitologist Horace W. Stunkard characterized microsporidians as among the most widespread of parasites, possessing significant survival adaptations, a consequence of their long-term host associations (1). One of the more obvious adaptations within this group is the extrusion apparatus of the infective spore stage. This apparatus consists of an aperture, a polaroplast membrane, a polar filament, and a posterior vacuole, or swelling organelle. The energy source for the firing of this apparatus is thought to reside in the posterior vacuole (2). In an earlier report (3), we indicated that the posterior vacuole had properties of peroxisomes, which function primarily to process very long chain fatty acids (VLCFA) with the assistance of key enzymes, acyl-CoA oxidase (ACOX) and catalase. Although peroxisomes are

characteristically found in aerobic cells with mitochondria, there is evidence that peroxisomal enzymes occur in the amitochondriate microsporidian *Spraguea lophii*. In particular, biochemical assays and western blot analyses indicate that ACOX and catalase are discharged from the spores of *S. lophii* (Findley, unpubl. data). Here, we report the localization of catalase within the spore cell.

We used a cytochemical protocol described by Angermuller and Fahimi (4). In brief, spores were prefixed in 2.5% glutaraldehyde (to eliminate resident peroxiase activity) and were subsequently incubated in Tris buffer (pH 10.5) in the presence of diaminobenzidine (DAB) and hydrogen peroxide. The cells were then post-fixed in 2% osmium tetroxide and processed for transmission electron microscopy.

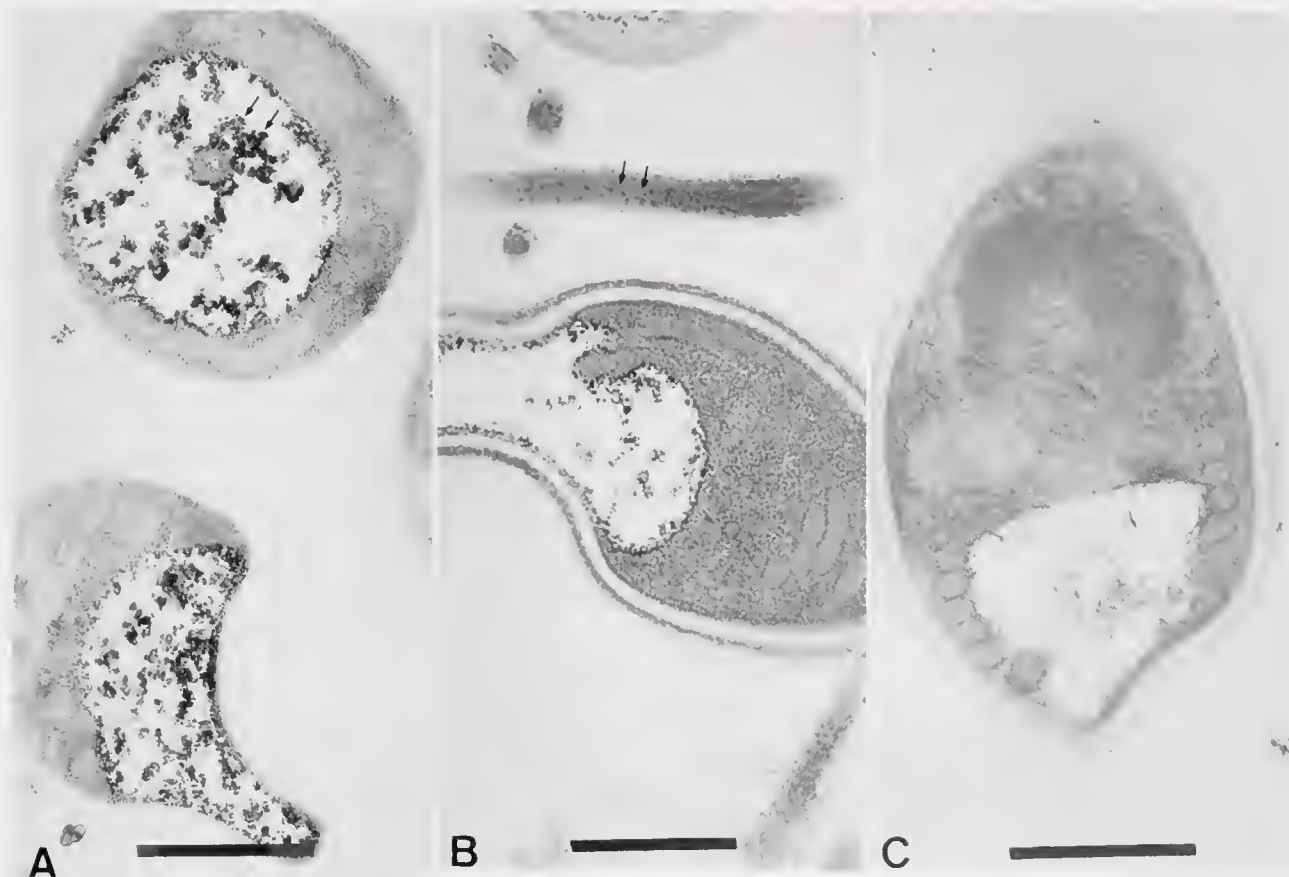


**Figure 1.** Localization of *Spraguea lophii* catalase activity. (A) Electron micrograph of alkaline-DAB reaction confined to the posterior vacuole. Arrows show reaction product in vacuole. (B) Similar image of DAB reaction extended to discharged spore tube (arrows). Discharged tube at lower right portion of image has DAB reaction on outside. (C) Control preparation without DAB or hydrogen peroxide shows no reaction in the spore posterior vacuole. Bar scales represent 0.5  $\mu\text{m}$ .

Electron micrographs revealed DAB reaction product in the posterior vacuole of the spores before and during its discharge (Fig. 1A). As the invasion tube emerges from the firing spore, the DAB reaction is associated with the inner surface of the tube (Fig. 1B) and also along the outer surface of the discharged tube. In the control preparations without DAB and hydrogen peroxide, there was no catalase-induced reaction product in the spore posterior vacuole (Fig. 1C). In addition to the peroxisomal enzymes, spores of *S. lophii* extrude the VLCFA nervonic acid into the external medium. Nervonic acid is a characteristic peroxisomal component, and the data indicate that it is discharged from the spores along with the catalase and ACOX enzymes. Of particular interest is the sizeable drop in nervonic acid levels that occurs during and after discharge of *S. lophii* spores (Findley, unpubl. data).

These data indicate that DAB-labeled catalase is initially restricted to the posterior vacuole, subsequently moves to the extruding polar tube during spore firing, appears on the outside of the discharged tube, and finally diffuses to the extracellular medium that bathes the discharged sporoplasms (not shown). The results

reported here also support the Lom and Vavra model of spore discharge (2). In this model, the posterior vacuole swells significantly after the spore is activated, the extrusion apparatus everts, and a membraneous sac forms at the end of the discharged tube to accommodate the exiting spore cell, or sporoplasm.

If the Lom and Vavra model is correct, the membrane of the extruded sporoplasm may be derived from the extrusion apparatus and may therefore be reversed. Indeed, studies with cytoplasmic protein probes indicate that in discharged sporoplasms, the membrane orientation is reversed as proposed (DeGiorgis and Weidner, unpubl. obs.).

#### Literature Cited

1. Stunkard, J. W., and F. E. Lux. 1965. *Biol. Bull.* **129**: 371-385.
2. Lom, J., and J. Vavra. 1963. *Acta Protozool.* **1**: 81-92.
3. Weidner, E., and A. Findley. 2002. *Biol. Bull.* **203**: 212.
4. Angermuller, S., and H. D. Fahimi. 1981. *Histochem.* **71**: 33-44.

Reference: *Biol. Bull.* 205: 238–239. (October 2003)  
© 2003 Marine Biological Laboratory

## Growth of a Salt Marsh Invertebrate on Several Species of Marsh Grass Detritus

A. M. Agnew<sup>1</sup>, D. H. Shull<sup>1,\*</sup>, and R. Buchsbaum<sup>2</sup>

<sup>1</sup> Gordon College, Wenham, MA

<sup>2</sup> Massachusetts Audubon Society, Wenham, MA

Salt marshes are important and productive ecosystems. Marsh grasses fuel coastal ecosystem production, and marsh invertebrates convert abundant decomposing marsh grasses into biomass available to higher trophic levels. Changes in climate, land use, nutrient input, and introduced species potentially threaten this ecosystem, however. An accelerated rate of sea-level rise has allowed cord grass (*Spartina alterniflora*) to migrate shoreward (1). Meanwhile, the high-marsh invasive reed *Phragmites australis* has expanded seaward, reducing the extent of indigenous high-marsh grasses such as *Spartina patens* and *Distichlis spicata* (2). Although changes in invertebrate community structure have been observed following *Phragmites* invasion (3), less is known about its effect on ecosystem function. How would changes in the species composition of marsh grasses affect food supply for higher trophic levels? Are all species of marsh grass equally nutritious for the invertebrates that feed on them? These questions are closely related to some of the primary goals of the Plum Island Ecosystem Long Term Ecological Research (PIE-LTER) program, which is concerned with the processing of organic matter within the salt marsh.

To address some of the above questions, our study investigated the growth rates of the salt marsh amphipod *Orchestia grillus*, one of the most abundant and best-studied detritivores at our study site (4), feeding on four species of marsh grass. Two sites were studied, Clubhead Creek and Greenwood Creek; the latter is nutrient enriched due to its proximity to a sewage outfall. The purpose of our research was to examine the nutritional quality of the detritus in terms of *O. grillus* growth rates and nitrogen and carbon content.

The four plant species studied were *Spartina alterniflora* (cord grass), *Spartina patens* (marsh hay), *Distichlis spicata* (spike grass), and *Phragmites australis* (common reed). *S. alterniflora* is the dominant low-marsh species, *S. patens* and *D. spicata* are native high-marsh species, and *P. australis* is a high-marsh invasive.

Samples of one-year-old standing dead grasses and young new-growth grasses were collected from each site from 2 to 6 June 2003. We sampled two differently aged grasses to assess how the quality of detritus changes over time. Old samples were sorted, cut, and frozen at  $-20^{\circ}\text{C}$ . Young grass samples were dried at  $70^{\circ}\text{C}$  for 24 h, soaked in seawater for 63 h, and then dried again at  $70^{\circ}\text{C}$  for 24 h before freezing, to simulate the formation of fresh detritus. Organisms collected from the marshes were allowed to acclimate to laboratory conditions in a large tank containing marsh wrack for 3 days. At the start of the experiment on 22 June 2003, single organisms were weighed and placed into petri dishes containing a single type of grass from each site. Ten replicates were designated

for each grass-species/age/site treatment. These were placed at random over a numbered grid on a laboratory bench. Grasses were changed about once a week, and dishes were kept wet by the addition of filtered seawater from the marsh every few days. Growth data for *O. grillus* were collected weekly by removing, patting dry, and weighing individuals, and then returning them to their petri dish. These data were normalized by dividing measurements by the initial size of each individual. Mortality data were collected daily, but all organisms that died before the end of the experiment were eliminated from growth data sets. The experiment was allowed to run for 38 days.

Within a few weeks, nearly 80% of the organisms feeding on fresh grass were dead, and it became clear that those individuals remaining alive in these treatments were not growing. This pattern may have been due to the presence of high phenolic concentrations in the fresh marsh grass detritus. Phenolic concentrations (determined by absorbance of methanol extracts at 320 nm) were significantly higher in the fresh detritus, as demonstrated by two-factor ANOVA with grass species and age as fixed factors ( $F_{11,241} = 331$ ,  $P < 0.0001$ ), and *Orchestia* mortality rates were significantly correlated with phenolic concentrations ( $R^2 = 0.56$ ,  $P = 0.01$ ). For these reasons, we focused our analysis of growth rates on the year-old detritus.

The mean growth rates for *O. grillus* consuming year-old detritus varied with marsh grass species. Rates were highest for amphipods consuming *D. spicata* (*O. grillus* increased in size by 40% to 50%) and decreased in the order of *S. alterniflora*, *S. patens*, and *P. australis* (Fig. 1A). Growth rates were determined from the slope of organism size versus time plots by linear regression, and rates among sites and species were compared by two-factor analysis of variance, with collection site and marsh grass species as fixed factors. Data were log-transformed prior to analysis to correct for heteroscedasticity. No differences in growth rates between the two sites were found ( $F_{11,491} = 0.088$ ,  $P = 0.77$ ). Variation in the growth rates of *O. grillus* on different marsh grass species was highly significant ( $F_{13,491} = 5.7$ ,  $P = 0.002$ ), with no significant interaction ( $F_{13,491} = 0.12$ ,  $P = 0.95$ ). *Post hoc* comparisons indicated that the growth rates of *O. grillus* on *P. australis* were significantly lower than those on *S. alterniflora* and *D. spicata* (Scheffé *F*-test,  $P < 0.01$ ).

Variation in *O. grillus* growth rate was not correlated with the percent carbon content of the detritus ( $R^2 = 0.052$ ,  $P = 0.59$ ). However, linear regression analysis indicated that nitrogen content in year-old detritus accounted for approximately 70% of the variation in growth rates (Fig. 1B,  $F_{11,61} = 13.7$ ,  $P = 0.01$ ).

Our results indicate that, when compared to the three native marsh plant species studied, the invasive species, *P. australis*, is a relatively poor food source for *O. grillus*. A diet of salt marsh

\* Corresponding author: dshull@gordon.edu

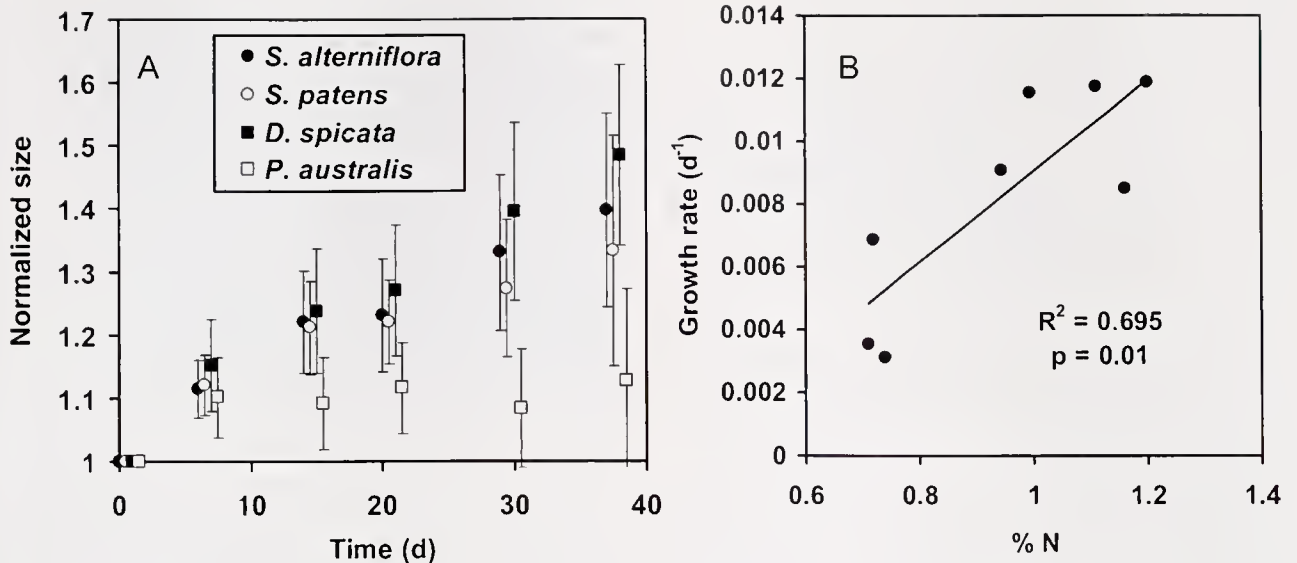


**Figure 1.** (A) Changes in size of *Orchestia grillus* feeding on year-old detritus over the course of the growth experiment. Data from the two sampling sites were pooled. Locations of points along the x-axis were staggered to improve readability. Error bars represent 95% confidence limits. (B) Averaged growth rates for *O. grillus* consuming year-old detritus species from both sites versus nitrogen content of the detritus.

species with higher nitrogen content, such as *D. spicata*, resulted in significantly higher growth rates for this organism. Furthermore, the observed seaward encroachment of *P. australis* is slowly pushing out *D. spicata*, the species that we found to have the highest nutritional quality (2). Given a continued shoreward migration of *S. alterniflora* due to sea-level rise and the seaward spread of *P. australis*, the overall food quality of marsh detritus for this invertebrate could decline. This suggests that changes in marsh grass species composition could affect higher trophic levels in this salt-marsh ecosystem.

This research was supported by an NSF-REU fellowship through the Plum Island Ecosystem LTER to AMA.

**Literature Cited**

1. Donnelly, J., and M. Bertness. 2001. *Proc. Natl. Acad. Sci. USA* 98: 14218–14223.
2. Windham, L., and R. Lathrop. 1999. *Estuaries* 22: 927–935.
3. Talley, T. S., and L. A. Levin. 2001. *Biol. Invasions* 3: 51–68.
4. Lopez, G., J. S. Levinton, and L. B. Stohodkin. 1977. *Oecologia* 30: 111–127.

Reference: *Biol. Bull.* 205: 239–241. (October 2003)  
 © 2003 Marine Biological Laboratory

**Patterns of Sedimentation in a Salt Marsh-Dominated Estuary**

Jason R. Cavatorta<sup>1,\*</sup>, Morgan Johnston<sup>2</sup>, Charles Hopkinson<sup>3</sup>, and Vinton Valentine<sup>3</sup>

<sup>1</sup> Amherst College, Amherst, MA

<sup>2</sup> The Pennsylvania State University, University Park, PA

<sup>3</sup> Marine Biological Laboratory, Woods Hole, MA

Salt marshes survive sea-level rise by an accompanied increase in elevation. This increase in elevation results from the accumulation of organic matter produced by marsh plants and of sediment transported to the marsh platform by tidal activity, storm events, and rafts of ice (1). Sea level is currently rising and is predicted to continue doing so (2); if marshes cannot increase in elevation at an equal or greater rate, inundation may eventually occur (3). Marsh inundation initially occurs by an increase in internal marsh ponds

(4). We traced changes in internal marsh ponds and identified the spatial distribution of suspended solids in tidal waters and marsh sedimentation in the Parker River estuary in northeastern Massachusetts.

Changes in marsh ponds were qualitatively assessed by comparing a 1953 topographic map of the area, compiled from early 1950s aerial photography, with 2001 color orthophotography. The topographic map was obtained from the National Oceanic and Atmospheric Administration (NOAA) and georeferenced (*i.e.*,

\* Corresponding author: JRCavatorta@amherst.edu

given a geographic location) using ArcGIS (version 8.3.0) software.

We determined the distribution of total suspended solids (TSS) along the main axis of the estuary as well as along three third-order tidal creeks within marshes of the lower estuary. We collected known volumes of water at high water on a spring tide adjacent to where sedimentation was examined and filtered it through pre-weighed 0.7- $\mu\text{m}$  glass fiber filters. We deployed 94 sediment traps along the estuary; these consisted of pre-weighed 9-cm glass fiber filters secured with rubber bands to upside-down plastic petri dish covers (5). Marsh grass was cut away, and a galvanized nail was inserted through the petri dish covers to secure the structures to the marsh. At West Creek, Club Head Creek, and Nelson Island Creek, we set up transects of sediment traps perpendicular to a mosquito ditch and a first-, second-, and third-order stream (Fig. 1, inset). Each transect consisted of three sites: 4, 20, and 50 m in from the creek edge to investigate the amount of sediment reaching the marsh interior. Eleven sites were also selected along the Parker River (Fig. 1). We deployed two replicate sediment traps at each site. We recovered two sets of sediment traps on 2 and 23 July 2003, after they were exposed to several spring tidal cycles. Several samples ( $n = 5$ ) with anomalously high weight increases were moderated by rinsing with distilled water to reduce high salt concentrations.

Comparisons were made using a single factor analysis of variance (6). Post-ANOVA pairs were analyzed using Student's  $t$  test with a Bonferroni adjusted alpha value to account for multiple comparisons.

Internal marsh ponds have increased in number and area since the early 1950s. Many areas that are largely ponded today (several of which cover thousands of square meters) were not ponded on the 1953 topographic map. Few ponds appear (during either year) in the upper 10 km of the estuary. Broad marshes adjacent to the lower third of the estuary are densely ponded. Pond drainage and vegetative recovery seem to have occurred only rarely.

TSS along the main axis clearly show the influence of Parker River runoff; solids in the water column are most concentrated in the upper estuary and decrease towards the sound ( $P = 0.003$ ), which receives regular exchange with the ocean (Fig. 2B). TSS were also low at the mouths of tidal creeks adjacent to the sound and increased in the second- and third-order reaches, where TSS is about double the amount in the sound (Fig. 2A).

Nelson Island Creek received 0.050 g of sedimentation per 9-cm filter, significantly more than West Creek, which is located farther upstream ( $P = 0.009$ ). Club Head Creek, which is located between them, received an intermediate amount of sediment (Fig. 2E). We did not observe a strong relationship between TSS and sediment accumulation; their maximum values, however, overlap somewhat in the creeks (Fig. 2A, C). The slight overlap is not surprising since TSS measurements were taken only once. More TSS measurements would perhaps yield mean values more strongly correlated with sedimentation. We did not observe a significant difference between sediment accumulation 4 m and 50 m from the creek.

The three creeks considered in this study are fed from water with relatively low TSS. Our data indicate that sediment accreting

on the marsh platform may be generated within the creeks themselves, presumably from eroded riverbanks. Slumping banks deliver large amounts of sediment to stream channels, where it may become suspended and deposited on the marsh surface during flood tides. Examination of 1953 and 2001 imagery supports this conclusion, as creek bank erosion is pronounced near the mouths of these creeks, especially at Nelson Island Creek where the most sedimentation was observed.

The spatial distributions of sedimentation and TSS along the main axis of the estuary are complex, but generally decrease with distance down the estuary. Parker River sediments seem to originate at the headwaters of the river and to remain in its system. This sediment source may explain why internal ponds are rare along the river's upper reaches (although a higher concentration of mosquito ditches, dug to drain the marsh, also prevent pond formation). Greater sedimentation may not have been observed along the Parker because of the brevity of the study and the fact that summer is typically the season with the lowest sediment transport (5). Generally low sedimentation may also explain why decreasing sedimentation was not measured farther from the creek bank. Sediment sources from other nearby creeks may also have inflated interior marsh accretion.

Because of limited sediment source in the creeks, belowground plant production may be more important than sedimentation in marsh accretion, even though softer organic sediments may be greatly compacted. This supposition is corroborated by the fact that the Parker River marsh sediments consist of 55% organic matter or more. Because plant productivity is higher on creek banks (7), depressed internal areas may develop because subterranean accretion rates are slower away from the creek bank.

The increase in size and number of internal ponds, which coincides with observed patterns of sedimentation, may be a useful indicator that marshes are not maintaining elevation relative to a rising sea level. Because the marshes studied are typical of New England macro-tidal marshes, similar marsh degradation is likely occurring in other areas.

This study received support from The Woods Hole Marine Sciences Consortium, the Plum Island Sound LTER NSF #OCE-9726921, and the Atlantic Coast Environmental Indicators Consortium EPA grant number R828677. Special thanks to Hap Garritt and W. McDonald Lee for their assistance.

### Literature Cited

1. Gleason, M. L., D. A. Elmer, N. C. Pien, and J. S. Fisher. 1979. *Estuaries* 2(4): 271-273.
2. Houghton, J. T., Y. Ding, D. J. Griggs, and M. Noguera. 2001. *Climate Change 2001: The Scientific Basis*. Cambridge University Press, Cambridge, England.
3. Orson, R., W. Panagiotou, and S. Leatherman. 1985. *J. Coastal Res.* 1: 29-37.
4. Kearney, M. S., R. E. Grace, and J. Stevenson. 1988. *Geogr. Rev.* 78: 205-220.
5. Reed, D. J. 1989. *Estuaries* 12(4): 222-227.
6. Rooth, J., J. Cornwell, and J. Stevenson. 2003. *Estuaries* 26: 475-483.
7. Frey, R., and P. Basan. 1985. Pp. 222-301 in *Coastal Sedimentary Environments*, R. Davis, Jr., ed. Springer-Verlag, New York.

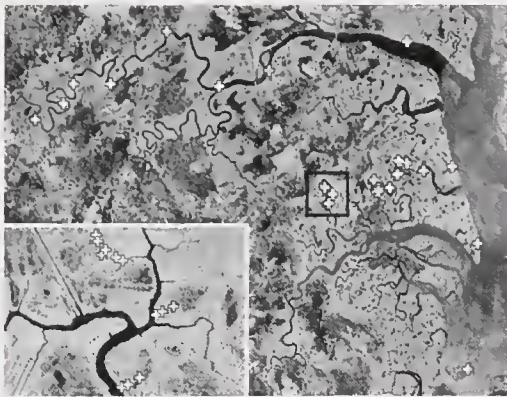


Figure 1

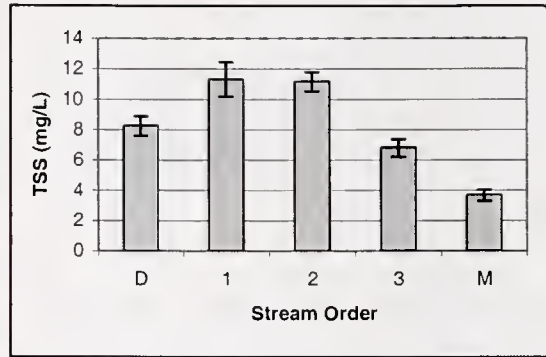


Figure 2A

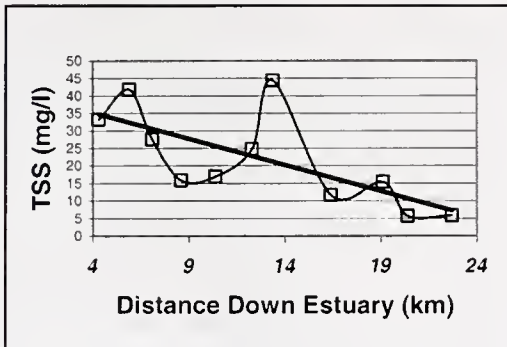


Figure 2B

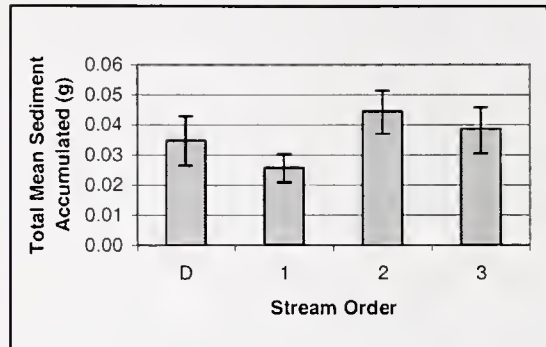


Figure 2C

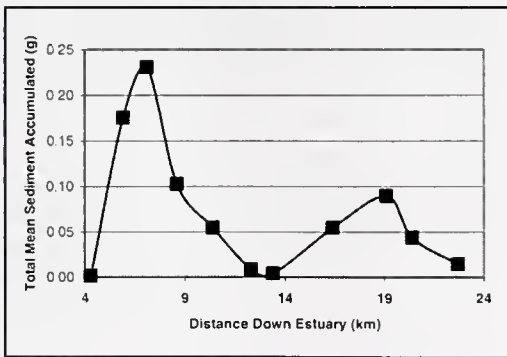


Figure 2D

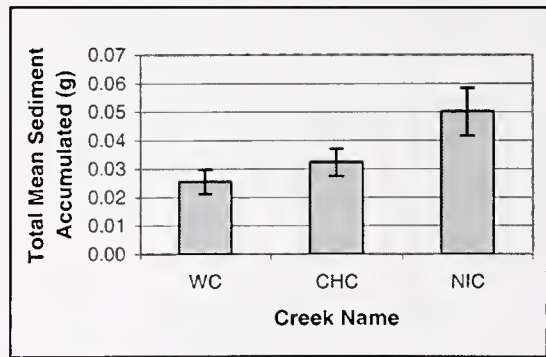


Figure 2E

Figure 1. Map with white crosses showing locations of sedimentation traps. Inset is a close-up of West Creek.

Figure 2. Total mean sediment accumulated on sediment traps, and total suspended solids (TSS) of selected locations along the estuary. "D" as an axis title refers to mosquito ditch, "M" refers to creek mouth. (A) TSS of creek order, averaged from three creeks adjacent to estuary. (B) TSS down estuary starting at the dam on Central Street in Byfield. Mean total of nonorganic sediment accumulated plotted against individual creek, by (C) order of creek and (D) distance down Parker River Estuary. (E) Mean total of nonorganic sediment accumulated in each of the three creeks adjacent to estuary. Error bars represent standard error.

Reference: *Biol. Bull.* 205: 242–243 (October 2003)  
 © 2003 Marine Biological Laboratory

## Multiple Approaches to Tracing Nitrogen Loss in the West Falmouth Wastewater Plume

T. Thoms<sup>1</sup>, A. E. Giblin<sup>2</sup>, and K. H. Foreman<sup>2</sup>

<sup>1</sup> Colorado College, Colorado Springs, CO

<sup>2</sup> Marine Biological Laboratory, Woods Hole, MA

Wastewater transported through groundwater to receiving estuaries is a major contributor of nitrogen (N) in densely settled watersheds, and contributes to coastal eutrophication (1–3). Although nitrate removal by microbial denitrification, adsorption, and uptake by plants is well documented, little is known about the nitrogen loss in the vadose zone and aquifer (1, 4).

This project focused on the fate of nitrogen leaving the Falmouth Wastewater Treatment Plant (FWTP) in Falmouth, Massachusetts. The plant lies on the Snug Harbor sub-watershed of West Falmouth Harbor (WFH), and the wastewater it discharges percolates through 25–30 m of vadose zone before meeting the aquifer and traveling in groundwater to WFH (3). This site provides a good model for a study of N loss due to the well-documented history of wastewater discharge and previous research involving N loading and removal.

The two principal objectives of this study were (1) to assess the efficiency of N removal as wastewater travels from FWTP to WFH, and (2) to determine where N loss is occurring. To satisfy our first objective, we quantified N loss using two independent methods: a mass balance calculation, and a conservative tracer technique. We then compared these results to a previous study conducted in 1999 (3). The site of N removal was examined using the same conservative tracer technique applied to samples within the path of the plume in the aquifer. We further investigated whether denitrification was the primary mechanism responsible for N loss in the aquifer by using dissolved N<sub>2</sub> and Ar gas analysis (5). With the development of the membrane inlet mass spectrometer, it has recently become possible to measure dissolved N<sub>2</sub>/Ar ratios with sufficient precision and accuracy to estimate denitrification (6).

We measured dissolved inorganic nitrogen (DIN; nitrate + ammonium), and boron (B) in wastewater effluent at FWTP and in monitoring wells located within and outside of the treatment plant. Boron, a component of laundry detergent, can be used as a conservative tracer for wastewater (7). We also sampled groundwater about to enter WFH within the boundaries of the Snug Harbor watershed. Samples were taken from 0.5 to 1.5 m below the sediment surface, using well-points. These shoreline samples were analyzed for DIN, B, and dissolved N<sub>2</sub> and Ar gas concentrations. Samples with elevated salinity, indicating seawater intrusion, were rejected. Nitrate, ammonium, and B concentrations were measured using standard colorimetric techniques.

We compiled discharge data for the FWTP from its establishment in 1987 to the present, and observed that loading increased during the first 7 years of operation (Fig. 1A). Based upon an estimated 1<sup>1/2</sup>-year groundwater travel time from the center of the plant to WFH (3), we used the 1993 discharge value of 13,177 kg N/y to compare with the loading now reaching the harbor. To

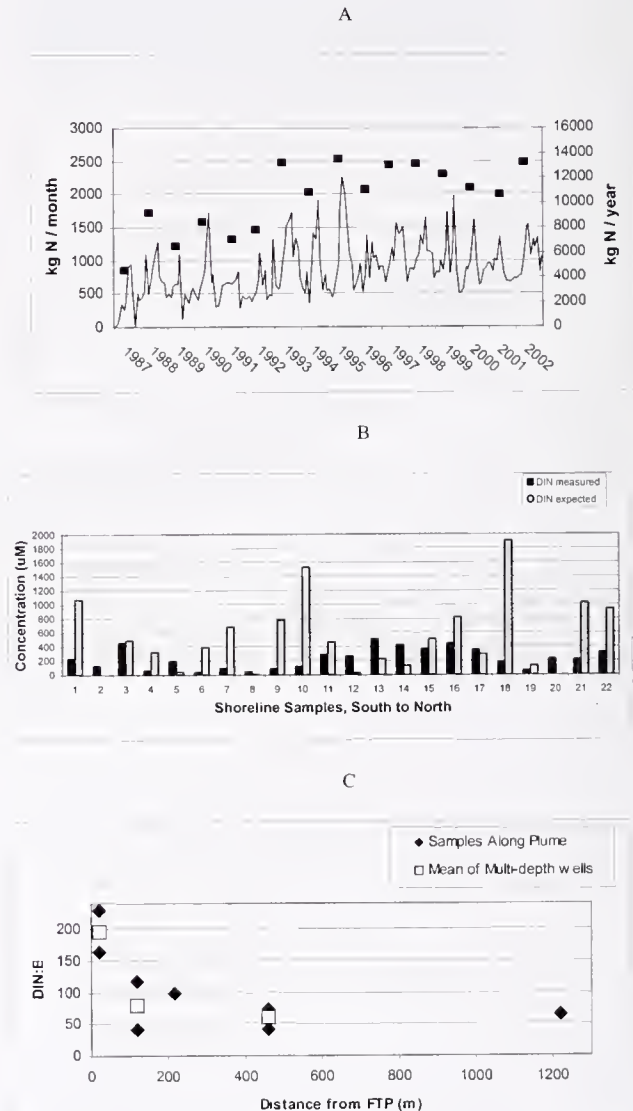


**Figure 1.** Loading data from the Falmouth Wastewater Treatment Plant (FWTP), and data from the wells and shoreline well points down gradient of the plant. (A) Monthly (line) and annual (filled squares) discharge (DIN concentration in effluent \* flow), in kg N, from FWTP, 1987–2002. (B) Comparison of measured DIN to expected DIN at each shore well-point based on dilution correction estimated from the DIN/B ratio. (C) DIN/B ratios from the effluent in the last holding pond from FWTP, from monitoring wells located 100 to 460 m down gradient, and from average of shoreline samples. Squares represent the average value for replicate samples of the effluent in the last holding pond and multi-depth wells.

calculate the DIN entering WFH, we used the average DIN concentration of shoreline groundwater, 208.5  $\mu\text{M}$  ( $n = 28$ ,  $se = 27.8$ ), multiplied by a literature value for the groundwater flux ( $1737 * 10^3 \text{m}^3/\text{y}$ ) (3). Thus, 5070 kg/y of DIN is currently discharging from the Snug Harbor sub-watershed. To isolate DIN originating at FWTP, we subtracted 554 kg of DIN reaching the shore derived from fertilizer, atmospheric deposition, and septic wastewater (3). Thus, we calculate that 66% of the DIN discharged from the FWTP in 1993 was lost en route to the harbor.

The conservative tracer method produced similar results. Changes in the DIN/B were used to calculate N loss based on the following formulas:

DIN expected (at each wellpoint)

$$= (\text{DIN effluent} * \text{B measured}) / \text{B effluent}$$

%DIN loss =  $(1 - (\text{Average (DIN measured)}/$

$$\text{Average (DIN expected)})) * 100$$

Expected and measured concentrations refer to shoreline samples (Fig. 1B), and DIN and B effluent concentrations (2017  $\mu\text{M}$  and 13.3  $\mu\text{M}$  respectively) were measured from the last holding pond at FWTP. This method estimates that 56% of DIN is lost. The method corrects for dilution, but it does not account for N input from fertilizers or atmospheric deposition and thus may slightly underestimate DIN loss.

Using the DIN shoreline load measured in 1999 (3) compared with 1989 effluent data, we calculated an 81% DIN loss. The lower percent removal that we found in 2003, in addition to the two-fold increase in DIN concentration in shoreline samples over 4 years (109  $\mu\text{M}$  in 1999, 208  $\mu\text{M}$  in 2003), suggests that the efficiency of N removal may be declining over time. Alternatively, we may have underestimated groundwater travel time, thus underestimating losses (Fig. 1A).

To ascertain where the loss occurred, we used DIN/B ratios from the monitoring wells in the wastewater plume (Fig. 1C). The DIN/B data show that about 60% of the DIN is lost between the point of effluent discharge and the first monitoring well. Thereafter, DIN/B ratios decrease little with distance traveled in groundwater, suggesting that the primary loss due to denitrification and retention occurs either in the vadose zone, at the interface of the aquifer and vadose zone, or during the initial 100 m of travel in the aquifer.

A second approach to examining the loss of DIN within the

aquifer was to use  $\text{N}_2/\text{Ar}$  ratios to calculate the excess  $\text{N}_2$  gas present in the shoreline samples. The Ar content of the water was used to calculate the temperature of the water entering the aquifer. We assumed that when the water entered the aquifer, both gases were in atmospheric equilibrium at that temperature. The amount by which the  $\text{N}_2$  measured in the water exceeded the amount expected with atmospheric equilibration was used to estimate denitrification within the aquifer. Values of excess  $\text{N}_2$  along the shore averaged 46.8  $\mu\text{M N}$  ( $n = 18$ ,  $se = 3.9$ ), indicating that only 8% of the DIN in the effluent leaving the FWTP was denitrified within the aquifer. Because high rates of denitrification within the aquifer should have been detected as  $\text{N}_2$ , we believe that denitrification is not a major process in the initial 100 m of the aquifer. However, we cannot ignore the interface, where  $\text{N}_2$  gas can escape, as a possible site of N removal.

These results, coupled with the DIN/B data from within the plume, suggest that denitrification within this aquifer is small and most of the removal may occur in the vadose zone, as has been reported previously (1). This is consistent with the idea that dissolved organic carbon, a component of the denitrification process, is largely consumed in vadose zones thicker than 5 m, therefore allowing for little denitrification activity in the aquifer (8).

This research was supported by a grant from the NSF Research Experience for Undergraduates (OCE-0097498).

### Literature Cited

1. Valiela, I., G. Collins, J. Kremer, K. Lajtha, M. Geist, B. Seely, J. Brawley, and C. H. Sham. 1997. *Ecol. Appl.* 7(2): 358-380.
2. Kroeger, K. D., J. Bowen, D. Corenran, J. Moorman, J. Michalowski, and I. Valiela. 1999. *Environ. Cape Cod* 2: 15-26.
3. Kroeger, K. D. 2003. Controls on Magnitude and Species Composition of Groundwater-Transported Nitrogen Exports From Glacial Outwash Plain Watersheds. Ph.D. Dissertation. Boston Marine University Program. Boston.
4. Jordan, M. J., K. J. Nadelhoffer, and B. Fry. 1997. *Ecol. Appl.* 7(3): 864-881.
5. Vogel, J. C., A. S. Talma, and T. H. E. Heaton. 1981. *J. Hydrol.* 50: 191-200.
6. Kana, T. M., C. Darkangelo, M. D. Hunt, J. B. Oldham, G. E. Bennett, and J. C. Cornwell. 1994. *Anal. Chem.* 66: 4166-4170.
7. Westgate, E. J., K. Kroeger, W. J. Pabich, and I. Valiela. 2000. *Biol. Bull.* 199: 221-223.
8. Pabich, J. W., I. Valiela, and H. F. Hemond. 2001. *Biogeochemistry* 55: 247-268.

Reference: *Biol. Bull.* 205: 244–245. (October 2003)  
© 2003 Marine Biological Laboratory

## Nitrogen Flux and Speciation Through the Subterranean Estuary of Waquoit Bay, Massachusetts

J. M. Talbot<sup>1</sup>, K. D. Kroeger<sup>2</sup>, A. Rago<sup>2</sup>, M. C. Allen<sup>2</sup>, and M. A. Charette<sup>2,\*</sup>

<sup>1</sup> Boston University, Boston, MA

<sup>2</sup> Woods Hole Oceanographic Institution, Woods Hole, MA

Fresh groundwater discharge is an important vehicle for nitrogen transport to coastal waters (1). In near-shore aquifers, mixing of fresh groundwater with saline pore waters produces groundwater of intermediate salinity that fluxes to sea as submarine groundwater discharge (2). Discharge of this mixed water, known as a subterranean estuary (3), may affect the rate of delivery of nitrogen to the water column. In this study we estimated the flux of dissolved inorganic nitrogen ( $\text{NO}_3^-$  and  $\text{NH}_4^+$ ) to the head of Waquoit Bay through both the fresh and intermediate-salinity portions of the near-shore aquifer and investigated the behavior of N during transport through the subterranean estuary.

To quantify nitrogen concentrations in the aquifer, we collected groundwater samples from four locations on the shore of Waquoit Bay along a 12-m transect that was perpendicular to shore and extended 6 m above and below the mean tide line on the beach. At each location we collected groundwater samples at depth intervals of 0.15 to 0.6 m to a depth of 7 to 8.5 m below the land surface. Samples were collected using an AMS Retract-a-Tip piezometer with a peristaltic pump and filtered through an in-line 0.45- $\mu\text{m}$  polyethersulphone filter. About 20 groundwater samples from each profile were obtained and stored frozen until analysis. Salinity was measured by salinometer (4); pH, temperature, dissolved oxygen, and redox potential were measured on-site with a YSI 600 multi-probe. Samples were analyzed colorimetrically for dissolved ammonium and nitrate concentration with a QuickChem FIA+ Lachat nutrient auto-analyzer (Zellweger Analytics, QuickChem 8000 Series) within 3 weeks of collection.

In each profile, salinity (Fig. 1A) increased with depth beneath an area of fresh groundwater. This follows the Ghyben-Hertzberg model of high-density seawater intrusion beneath the lower density fresh groundwater (5). Nitrate was the most abundant DIN species present in the relatively oxidizing fresh groundwater (Fig. 1B). This N traveled as a plume and apparently discharged to the bay within the intertidal zone. DIN was present almost exclusively as ammonium in the reducing intermediate-salinity portion of the aquifer (Fig. 1C). Low concentrations were found near the salt-fresh groundwater interface and approached a uniform concentration with depth. These results are consistent with collections from across the head of the bay (Kroeger and Charette, unpubl.).

Low concentrations of  $\text{NH}_4^+$  in Waquoit Bay surface water and in fresh groundwater (Fig. 1D) suggested that ammonium is transported into the subterranean estuary by advection through marine sediments where organic N is mineralized. Our data show that ammonium moved conservatively through the intermediate-salinity zone (Fig. 1D). High concentrations of  $\text{NH}_4^+$  in saline groundwater may be explained by cation exchange and ion pairing, but

considering the linear relationship with salinity, such activity is negligible. This conservative transport suggests that the  $\text{NH}_4^+$  must travel with intermediate-salinity groundwater discharging to sea.

Absence of  $\text{NO}_3^-$  within the subterranean estuary, low concentrations in bay surface water, and high concentrations in fresh groundwater (Fig. 1E) suggest loss of  $\text{NO}_3^-$  by denitrification within the reducing conditions of the saline groundwater. However, it may be that much of the fresh groundwater containing high  $\text{NO}_3^-$  discharges without mixing with the subterranean estuary. Assessing the amount of  $\text{NO}_3^-$  that is mixing with the saline groundwater is difficult since nitrate tends to travel as a plume and concentration in the freshwater endmember is not clear.

To estimate relative groundwater flux of N to estuarine surface waters, we multiplied the average DIN concentration in each portion of the aquifer by estimated rates of groundwater advection through each zone. We calculated average DIN concentrations using our collections plus previously collected samples from an along-shore transect across the head of the bay (Kroeger and Charette, unpubl.). Freshwater flux of N was calculated using a freshwater discharge rate of 6500  $\text{m}^3/\text{day}$ , determined from hydrological measurements of head gradient and hydraulic conductivity at our sampling sites (Mulligan and Hutchinson, unpubl.). A rate of intermediate-salinity groundwater discharge of 3400  $\text{m}^3/\text{day}$  was calculated as the difference between an estimated total (fresh + saline) groundwater discharge rate of 9900  $\text{m}^3/\text{day}$  and the fresh groundwater discharge rate. Total groundwater discharge to the head of the bay was based on mass-balance-derived estimates of submarine groundwater discharge using measurements of radon activity in groundwater and bay surface waters (6). Total DIN flux to the bay was calculated as the sum of the DIN flux through each portion of the aquifer.

On the basis of these calculations, the freshwater portion of the aquifer discharged 6.2 kg N/day to the head of the bay. DIN flux through the intermediate-salinity zone was 1.5 kg N/day, which accounts for 20% of the total DIN flux to the head of the bay of 7.7 kg N/day.

These results suggest that DIN flux through the subterranean estuary of Waquoit Bay may be significant relative to DIN flux due to freshwater discharge. The DIN transported is composed entirely of regenerated ammonium, as opposed to the terrestrially derived (7) nitrate transported by fresh groundwater. Despite mixing of fresh and saline groundwater masses (Fig. 1A), the subterranean estuary is not a site of net biogeochemical transformations of ammonium.

This research was funded by a National Science Foundation Research Experience for Undergraduates site Grant (OCE-0097498) to J. Valiela, NSF grant (OCE-0095384) to M.A.C., and Woods Hole Oceanographic Institution Coastal Ocean Institute Postdoctoral Fellowship to K.D.K. We thank the Waquoit Bay National Estuarine Research Reserve staff for use of their facilities. Special thanks to Dan Abraham, Rachel Hutchinson, Ann Mulligan, and Craig Herbold for their assistance with this project.

\* Corresponding author: mcharette@whoi.edu

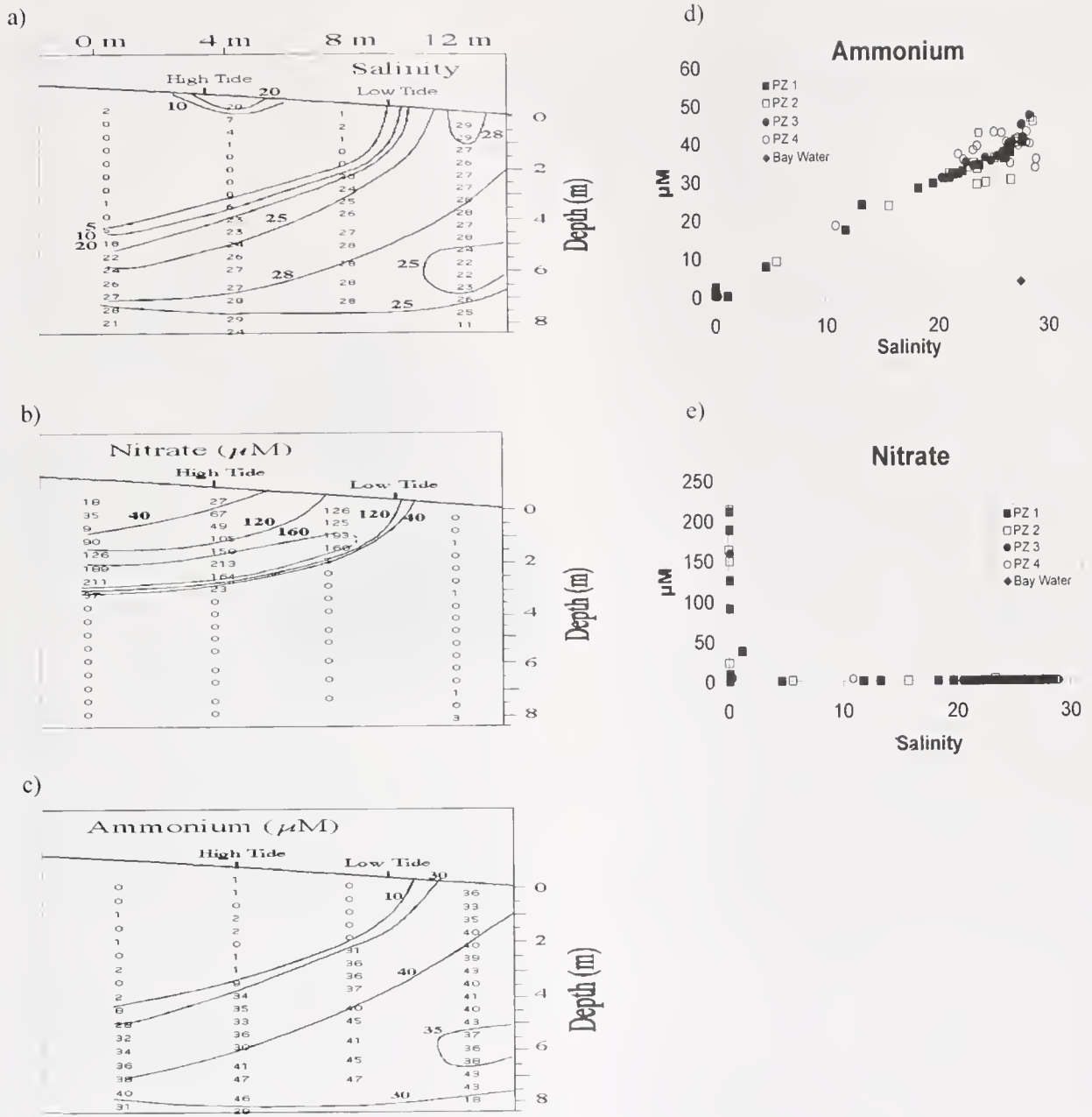


**Figure 1.** Behavior of nitrate and ammonium in near-shore aquifer. Cross-sectional contour plots based on depth profiles collected in a transect beginning 6 m above mean tide line for (A) salinity, (B)  $\text{NO}_3^-$  concentration, and (C)  $\text{NH}_4^+$  concentration. Concentrations of (D) ammonium and (E) nitrate versus salinity for each profile. Different symbols indicate samples collected at piezometer locations 1, 2, 3, and 4 from 0–12 m, depicted in panels A, B, and C of this figure. Filled diamond symbols indicate average ammonium ( $3.3 \mu\text{M}$ ) and nitrate ( $1.2 \mu\text{M}$ ) concentrations in Waquoit Bay surface water.

**Literature Cited**

1. Valiela, I., K. Foreman, M. LaMontagne, D. Hersh, J. Costa, C. D'Avanzo, M. Babione, P. Peckol, B. DeMeo-Anderson, C. Sham *et al.* 1992. *Estuaries* 15: 443–457.
2. Li, L., D. A. Barry, F. Stagnitti, and J.-Y. Parlange. 1999. *Water Resour. Res.* 35: 3253–3259.
3. Moore, W. S. 1999. *Mar. Chem.* 65: 111–125.
4. Knapp, G. P., M. C. Stalcup, and R. J. Stanley. 1990. *Technical Report WHOI-90-35*, Woods Hole Oceanographic Institution, Woods Hole, MA. 25 pp.
5. Freeze, R. A., and J. A. Cherry. 1979. *Groundwater*. Prentice Hall, Edgewood Cliffs, NJ. Pp. 375–378.
6. Abraham, D. M., M. A. Charette, M. C. Allen, A. Rago, and K. D. Kroeger. 2003. Radiochemical estimates of submarine groundwater discharge to Waquoit Bay, Massachusetts. *Biol. Bull.* 205: 246–247.
7. Valiela, I., G. Collins, J. Kremer, K. Lajtha, J. Geist, B. Seely, J. Brawley, and C. H. Sham. 1997. *Ecol. Appl.* 7: 358–380.

Reference: *Biol. Bull.* 205: 246–247. (October 2003)  
 © 2003 Marine Biological Laboratory

## Radiochemical Estimates of Submarine Groundwater Discharge to Waquoit Bay, Massachusetts

D. M. Abraham<sup>1</sup>, M. A. Charette<sup>2,\*</sup>, M. C. Allen<sup>2</sup>, A. Rago<sup>2</sup>, and K. D. Kroeger<sup>2</sup>

<sup>1</sup> Bowdoin College, Brunswick, ME

<sup>2</sup> Woods Hole Oceanographic Institution, Woods Hole, MA

Submarine groundwater discharge (SGD) is the flux of fresh and brackish groundwater to the ocean through a coastal aquifer (1). Groundwater often transports large amounts of anthropogenic nitrogen and phosphorus to the ocean, and understanding the magnitude of groundwater flux is important to the environmental protection and management of coastal waters (2, 3). Recent studies have employed radium isotopes (4) and radon-222 (5), both naturally enriched in groundwater relative to surface water due to a high uranium content in aquifer sediments, to quantify SGD in coastal systems. However, these studies have been limited by a poor understanding of the distribution of these isotopes in coastal groundwater, the processes controlling these distributions, and a lack of high-resolution time-series sampling of tracer activities in surface waters. Here, we attempt to overcome these earlier limitations by mapping the distribution of  $^{222}\text{Rn}$  ( $t_{1/2} = 3.83$  days) and  $^{226}\text{Ra}$  ( $t_{1/2} = 1600$  years) across a groundwater salinity gradient, and by deploying a new *in situ*  $^{222}\text{Rn}$  analyzer to study the time dependence of SGD in Waquoit Bay.

Using a drive-point piezometer, four depth profiles of groundwater  $^{226}\text{Ra}$  and  $^{222}\text{Rn}$  were collected along a transect perpendicular to the shore at the head of Waquoit Bay, creating a vertical cross section of each isotope at the groundwater-seawater interface (Fig. 1). At each sampling depth,  $^{226}\text{Ra}$  was extracted from ~15 l of groundwater on a column of Mn-impregnated fiber. In the laboratory, the fiber was ashed and  $^{226}\text{Ra}$  quantified via gamma ray spectroscopy (6). For  $^{222}\text{Rn}$ , 250 ml of groundwater was collected in a glass bottle and directly analyzed on a DurrIDGE RAD7 electronic radon monitor; activities were decay-corrected to the time of collection. To quantify tracer concentrations in surface water, discrete bay water samples for  $^{226}\text{Ra}$  were collected at four locations at the head of the bay. Continuous measurements of  $^{222}\text{Rn}$  at a single station at the head of Waquoit Bay were obtained using the RAD7 coupled to an air-water equilibrator as described in Burnett and Dulajova (5). The instrument recorded the  $^{222}\text{Rn}$  activity of surface water every 30 min for 3 days. Tidal height, measured as water column depth to the sea floor at the sampling location, was monitored with a YSI 600 series CTD, and local atmospheric conditions were obtained from a nearby NOAA weather tower (# BUZM3, Buzzards Bay, MA).

$^{226}\text{Ra}$  activity in the groundwater increased with increasing salinity: the highest activities occurred above a salinity of 25 (Fig. 2a). The low activities ( $<3$  dpm  $l^{-1}$ ) observed at salinities of 25 or greater are from the landward portion of the transect. This is in contrast to the typical distribution of radium in estuarine surface waters, where activities are elevated at all salinities  $>0$  and often peak at intermediate salinity (15–20) due to a desorption reaction

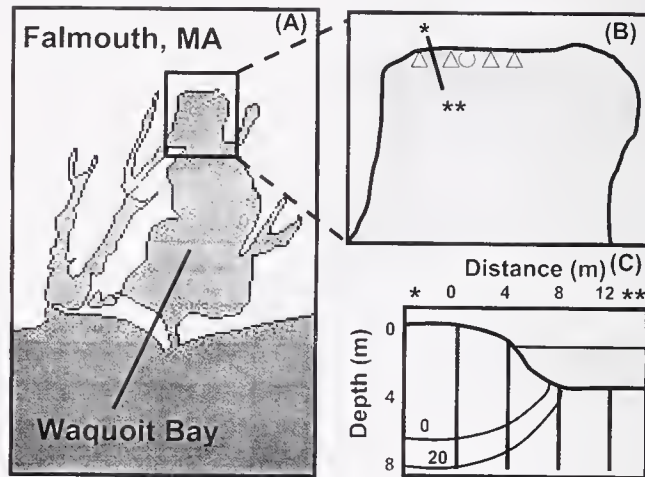


**Figure 1.** Location of Waquoit Bay, Massachusetts, and our sampling site during the summer of 2003. Waquoit Bay is located on the eastern border of the town of Falmouth, Massachusetts, on Cape Cod (A). Our sampling site was situated along the beach at the head of the bay (B). Surface measurements of radium-226 activity, a continuous measurement of radon-222, and a transect of four depth profiles oriented perpendicular to the beach were used to quantify SGD (B,  $\Delta = ^{226}\text{Ra}$ ,  $O = ^{222}\text{Rn}$ , \* - \*\* = transect of 4 depth profiles). A vertical cross section of groundwater revealed a sharp increase in salinity at the freshwater-saltwater interface (C, contour plot from \* to \*\*).

related to ion exchange (7). The pattern we observed could be explained by an increased  $^{226}\text{Ra}$  source with increasing depth and distance from shore, a function of either higher sediment content of thorium-230 (radiogenic parent of  $^{226}\text{Ra}$ ) or a decrease in the grain size of aquifer sediments. This latter scenario would result in greater sediment surface area, thereby increasing the availability of radium for desorption. However, sediment sampling at the head of Waquoit Bay is necessary to determine which of these two possibilities is the most likely explanation for the observed pattern.

The pattern of groundwater  $^{222}\text{Rn}$  with salinity was similar to that of  $^{226}\text{Ra}$ , with ~3-fold increases in activity at salinities higher than 20 (Fig. 2a).  $^{222}\text{Rn}$  also displayed an increase in activity with increasing depth and distance from the berm (Fig. 2b). Because Rn is a noble gas, its distribution throughout the aquifer should be uniform, and not affected by changes in salinity. Also, because the residence time of fresh groundwater beneath the bay is several years (8), the activities of  $^{222}\text{Rn}$  in this zone are likely to be in equilibrium with the sediment activity of its parent isotope  $^{226}\text{Ra}$ . Therefore, the higher observed activities of  $^{222}\text{Rn}$  in the saline portion of the aquifer must be a function of a greater  $^{226}\text{Ra}$  source, which is consistent with the observed  $^{226}\text{Ra}$  distribution.

\* Corresponding author. mcharette@whoi.edu

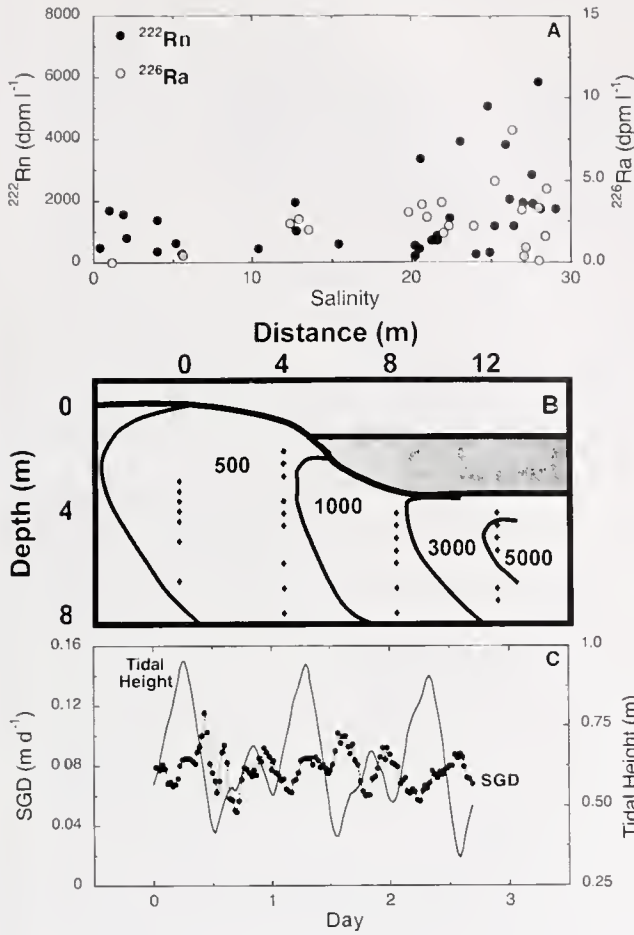


**Figure 2.** The distributions of radium-226 and radon-222 in groundwater displayed a pattern of increasing activity with increasing salinity, depth, and distance from the beach berm. The non-conservative distribution of  $^{226}\text{Ra}$  and  $^{222}\text{Rn}$  is displayed in a plot of isotope activities, measured as disintegrations per minute per liter of water ( $\text{dpm l}^{-1}$ ), as a function of increasing salinity (A). A vertical cross section of  $^{222}\text{Rn}$  activities through the fresh, intermediate, and saline portions of the aquifer (B, contour plot, individual samples represented by diamonds ( $\blacklozenge$ )) reveals increasing activity from the surface to 8 m, and distance from the berm to 12 m. A 5-point running average of the time-series record of groundwater velocities is plotted alongside tidal height above sea floor (C).

To quantify SGD to Waquoit Bay, we applied a non-steady-state mass balance model to our time-series  $^{222}\text{Rn}$  record collected over 3 days at the head of the bay. Corrections for atmospheric evasion, loss due to advection to the lower bay, and changes in inventory due to water column depth were all applied to the time-series data using the approach of Burnett and Dulaiova (5) to calculate the excess  $^{222}\text{Rn}$  flux ( $\text{dpm m}^{-2} \text{d}^{-1}$ ) during each 30-min interval. Dividing by the average groundwater  $^{222}\text{Rn}$  activity ( $\text{dpm m}^{-3}$ ), we estimated SGD rates ranging from 0 to  $0.16 \text{ m d}^{-1}$ , with a mean of  $0.08 \pm 0.02 \text{ m d}^{-1}$  ( $n = 132, 1-\sigma$ ). In general, SGD was related to tidal stage (Fig. 2c), whereby SGD was highest at low tide and lowest at high tide, a result consistent with other time-

series estimates of SGD in coastal systems (6, 9). We suggest that both a change in hydraulic head gradient, modulated by the rise and fall of the tide, and the effects of subsurface recirculation due to tidal pumping are the likely explanation for this observation.

To calculate a volumetric flux of SGD ( $\text{m}^3 \text{d}^{-1}$ ), we must first estimate the area of the seepage face at the head of Waquoit Bay. The length of the seepage face (1760 m) was obtained from a false-color aerial infrared image (1-m resolution) taken at low tide in the fall of 2002 (Charette, unpubl. data). A seepage meter study by Michael *et al.* (10) found the width of the seepage face to be 70 m. Based on this effective seepage surface area of  $123,200 \text{ m}^2$ , we estimated a volume discharge of  $9900 \text{ m}^3 \text{d}^{-1}$ . Following the mass balance model of Charette *et al.* (4) and using the same effective seepage area, we estimated a  $^{226}\text{Ra}$ -derived volumetric flux of SGD of  $\sim 1200 \text{ m}^3 \text{d}^{-1}$  ( $n = 4$ ). Since high levels of  $^{226}\text{Ra}$  are present only in the saline portion of the aquifer and  $^{222}\text{Rn}$  is high in both fresh and saline groundwater (relative to surface waters), it is possible that the difference between these two estimates represents the fresh component of SGD. However, an alternative explanation is greater uncertainty in the  $^{226}\text{Ra}$  estimate due to the limited data compared to the  $^{222}\text{Rn}$  record.

Recent applications of  $^{222}\text{Rn}$  and  $^{226}\text{Ra}$  to estimate SGD have assumed that groundwater discharge is static over time and space. The flux estimate derived from the continuous  $^{222}\text{Rn}$  record, however, suggests substantial temporal variability in groundwater discharge across a tidal cycle. This method would be useful for longer-term studies, where variability in SGD may be driven by the spring/neap tidal cycle and seasonal to interannual changes in aquifer recharge. Also, high-resolution sampling (cm scale) of  $^{222}\text{Rn}$  and  $^{226}\text{Ra}$  in groundwater revealed that these isotopes do not behave as predicted across a salinity gradient, probably because of an increased source term across the freshwater-saltwater interface.

We thank the Waquoit Bay National Estuarine Research Reserve (WBNERR) for the use of their field site and research facilities during the summer of 2003. This study was funded by a NSF-Research Experience for Undergraduates (REU) site grant (OCE-0097498) and a NSF grant (OCE-0095384) to M.A.C.

**Literature Cited**

1. Zektzer, I. S., V. A. Ivanov, and A. V. Meskheteli. 1973. *J. Hydrol.* **20**: 1–36.
2. Johannes, R. E. 1980. *Mar. Ecol. Prog. Ser.* **3**: 365–373.
3. Moore, W. S. 1999. *Mar. Chem.* **65**: 111–125.
4. Charette, M. A., K. O. Buesseler, and J. E. Andrews. 2001. *Limnol. Oceanogr.* **46**(2): 465–470.
5. Burnett, W. C., and H. Dulaiova. 2003. *J. Environ. Radioact.* **69**: 21–35.
6. Moore, W. S. 1984. *Nucl. Instrum. Methods* **222**: 407–411.
7. Moore, W. S., H. Astwood, and C. Lindstrom. 1995. *Geochim. Cosmochim. Acta* **59**(20): 4285–4298.
8. Cambareri, T. C., and E. M. Eichner. 1998. *Ground Water* **36**(4): 626–634.
9. Sholkovitz, E. R., C. W. Herbold, and M. A. Charette. 2003. *Limnol. Oceanogr. Methods* **1**: 16–28.
10. Michael, H. A., J. S. Lubestky, and C. F. Harvey. 2003. *Geophys. Res. Lett.* **30**(6): 1–4.

Reference: *Biol. Bull.* 205: 248–249. (October 2003)  
© 2003 Marine Biological Laboratory

## Importance of Metabolism in the Development of Salt Marsh Ponds

M. E. Johnston<sup>1,\*</sup>, J. R. Cavatorta<sup>2</sup>, C. S. Hopkinson<sup>3</sup>, and V. Valentine<sup>3</sup>

<sup>1</sup>The Pennsylvania State University, University Park, PA

<sup>2</sup>Amherst College, Amherst, MA

<sup>3</sup>Marine Biological Laboratory, Woods Hole, MA

Ponds are a common feature on the salt marsh surface and are typically found in depressed regions of the high-marsh platform (1). They are widely held to be valuable habitat for larval and juvenile fish as well as for avifauna. Pools of standing water develop in areas that do not receive a regular supply of sediment with flooding. This standing water often becomes hypersaline and anoxic, thus inhibiting marsh grass production and further exacerbating marsh accretion (2). In areas where the rate of marsh accretion is less than the rate of sea-level rise, the formation of interior marsh ponds is expected to increase, thus contributing to marsh degradation (3).

This study focuses on pond metabolism, measured by dissolved oxygen changes, as a possible mechanism of marsh pond expansion, as well as an indication of habitat quality. A network of ponds that formed in the past 50 years in about a 1-hectare (ha) area of intertidal salt marsh was examined along the Rowley River of the Plum Island Sound estuary in northeastern Massachusetts (4).

Pond metabolism was investigated using two techniques: free-water diurnal changes in dissolved oxygen, and oxygen consumption of sediment cores. In the free-water technique, dissolved oxygen (DO) was measured in three ponds at ½-h intervals for durations of 3 to 5 days during June and July of 2003. DO was measured using a pulsed, polarographic O<sub>2</sub> electrode, which is corrected for temperature and conductivity (YSI, Inc.). Rates of change in DO attributable to gross primary production and respiration were corrected for diffusion across the air-sea interface using a gas transfer velocity proportional to wind speed (5). Net ecosystem production was calculated as the balance between gross primary production and respiration over 24-h intervals.

Sediment cores (15.5 × 50 cm) were taken in the field from the edge and the center of a pond and returned to the laboratory to measure the respective benthic respiration rates. Another set of cores (10 × 50 cm) was used to determine the average carbon content of the peat in the pond environment by drying and combusting peat samples of known depth and volume and assuming a ratio of carbon to organic matter of 0.5:1. To investigate the relative lability of organic matter from varying depths, root and rhizome material (5 g wet weight) from depths corresponding to the sediment cores was placed in BOD bottles with seawater (297 ml) and a bacterial/sediment inoculum (3 ml), and respiration was measured.

Dissolved oxygen levels in all the ponds fluctuated greatly over a 24-h period, with values ranging from 0% to 200% of saturation (Fig. 1a). Along with high temperatures and salinity, this range of

dissolved oxygen emphasizes the extreme conditions of these ponds as habitat. These conditions seem paradoxical in view of the assumed value of these habitats to juvenile and larval organisms.

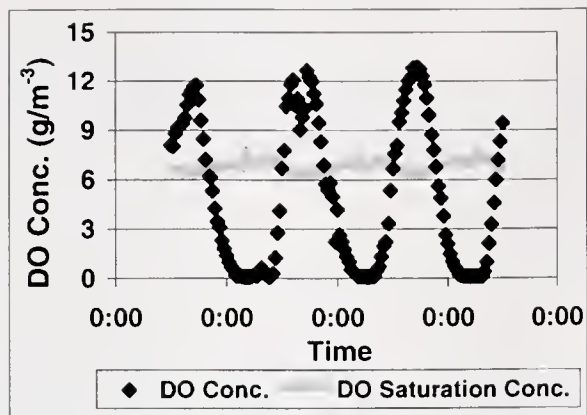
The rates of gross primary production ranged from 2.75 to 6.98 g O<sub>2</sub> m<sup>-2</sup> d<sup>-1</sup> in the ponds, and the rates of respiration from 3.61 to 6.91 g O<sub>2</sub> m<sup>-2</sup> d<sup>-1</sup>. These rates are similar to those found in the Plum Island Sound estuary (J. Vallino, Marine Biological Laboratory, pers. comm.) and eutrophic estuaries in general (6). On average, rates of respiration exceeded gross primary production in the ponds such that net ecosystem production was negative 8 out of 12 days (Fig. 1b). A negative value for net ecosystem production indicates that more organic matter is consumed than produced internally (7). The most likely source of this organic matter is the highly organic marsh sediment. Our estimates of metabolism are likely to be conservative during this time of year to the extent that anaerobic products of sulfate reduction are stored temporarily in anoxic sediments (8).

Decomposition rates of root and rhizome material decreased with depth, indicating that peat lability decreases with depth (Fig. 1c). Respiration rates in benthic cores were higher in the deep center of the pond than along the shallow edge (Fig. 1d). On the basis of root and rhizome decomposition, however, we expected to see lower respiration rates in the benthic cores taken from the center of the pond than in those taken from the edge where the remains of recently dead macrophytes were evident. Higher respiration rates in the pond center can be attributed to the presence of *Enteromorpha*. This alga grows around the periphery of the ponds, and its remains tend to collect in the deeper, more central portions of the ponds. Benthic respiration decreased following removal of this highly labile, detrital *Enteromorpha* layer from the second center core (Fig. 1d—labeled Center 2\*).

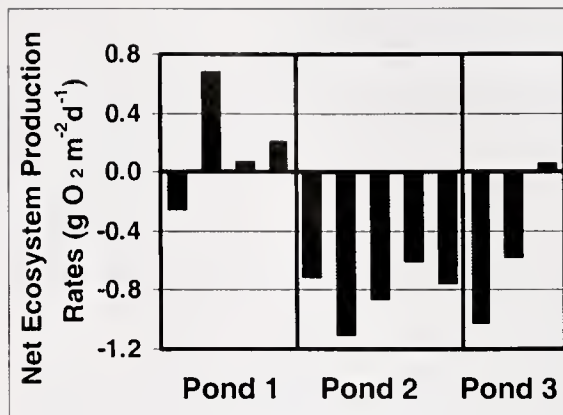
The importance of excess respiration as a mechanism contributing to pond enlargement over time can be seen by comparing our measurements of net ecosystem production with our independent estimates of the rate of pond formation. Average depth-integrated carbon content of marsh peat surrounding ponds is approximately 38,446 g m<sup>-3</sup>. Assuming a maximum pond age of 50 y and an average pond depth of 20 cm (data not shown), we estimate a peat decomposition rate of 154 g C m<sup>-2</sup> y<sup>-1</sup>.

However, two mechanisms are responsible for the increase in pond depth: peat decomposition and accretion of organic and inorganic material in the marsh adjacent to the ponds. Because the areas of marsh surrounding the ponds are not yet inundated, we can assume that the surrounding marsh has been accreting sediment at a rate comparable to that of sea-level rise, which is 2.65 mm y<sup>-1</sup> locally (9). Accordingly, the adjacent marsh has accreted by at

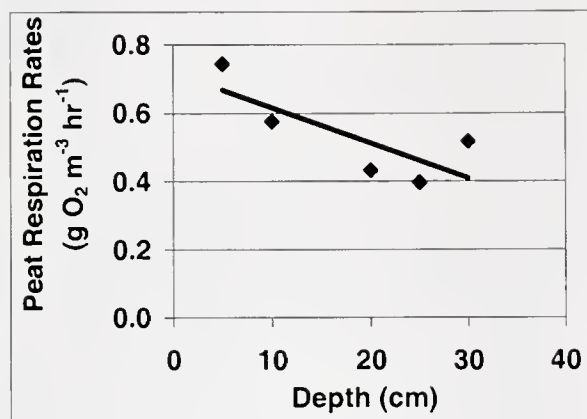
\* Corresponding author: mejl36@psu.edu



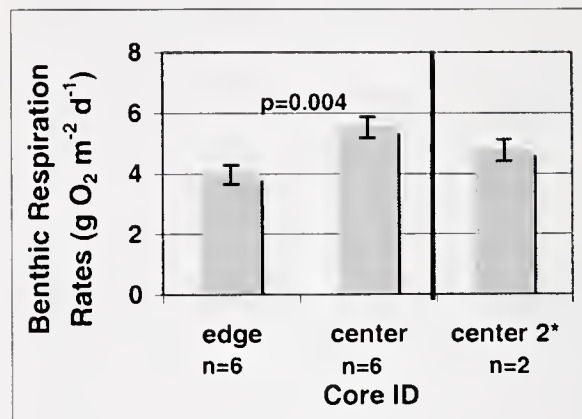
a



b



c



d

**Figure 1.** Patterns of metabolism in three salt marsh ponds. (a) Diurnal patterns of dissolved oxygen in Pond 3 over a 3-day period. (b) Net ecosystem production rates in three ponds. (c) Peat respiration rates by depth. (d) Benthic respiration rates in the edge and center of a pond. Center 2\* indicates that the respiration rates were measured after the removal of the detrital *Enteromorpha* layer. P-value refers to the left two columns of the graph only.

least 8 cm over the past 50 years. Therefore, accretion of surrounding marsh areas accounts for 40% of the depth of the ponds.

The remaining 12 cm of depth increase can then be attributed to decomposition of the inundated peat. Decomposition of 12 cm of peat over 50 years is equivalent to  $92 \text{ g C m}^{-2} \text{ yr}^{-1}$  or an oxygen consumption of  $0.67 \text{ g O}_2 \text{ m}^{-2} \text{ d}^{-1}$  (assuming a production-to-respiration ratio of 1) (7). The average rate of net ecosystem production in the ponds is  $-0.38 \text{ g O}_2 \text{ m}^{-2} \text{ d}^{-1}$ . Thus, on average, respiration can account for over half the required rate of decomposition; in fact, for the majority of the observations, it can account for nearly 100% of the required carbon loss (Fig. 1b). Although our study was conducted only during the summer season, our results do suggest that respiration is an important and actively functioning process in the development of marsh ponds.

This work was supported by NSF-REU Site Grant (OCE-0097498), the Boston University Marine Program, NSF Grant OCE 9726921, and EPA STAR Grant R828677.

**Literature Cited**

1. Redfield, A. 1972. *Ecol. Monogr.* 42: 201–237.
2. Friedrichs, C., and J. Perry. 2001. *J. Coastal Res.* 27: 7–37.
3. Kearney, M., R. Grace, and J. Stevenson. 1988. *Geogr. Rev.* 78(2): 205–220.
4. NOAA Coast & Geodetic Survey. 1953. Topographic Sheet, scale: 1:10,000. National Oceanic and Atmospheric Administration.
5. Emerson, S. 1975. *Limnol. Oceanogr.* 20(5): 754–761.
6. Day, J., C. Hall, W. Kemp, and A. Yanez-Arancibia. 1989. *Estuarine Ecology*. John Wiley and Sons, New York. 558 pp.
7. Odum, H. 1956. *Limnol. Oceanogr.* 1: 102–117.
8. Howarth, R., and J. Teal. 1979. *Limnol. Oceanogr.* 24(6): 999–1013.
9. Zervas, C. 2001. NOAA Technical Report, NOS CO-OPS 36. National Oceanic and Atmospheric Administration, Silver Spring, MD.

Reference: *Biol. Bull.* 205: 250–251. (October 2003)  
© 2003 Marine Biological Laboratory

## Transplantation and Isotopic Evidence of the Relative Effects of Ambient and Internal Nutrient Supply on the Growth of *Ulva lactuca*

A. B. Aguiar<sup>1</sup>, J. A. Morgan<sup>2</sup>, M. Teichberg<sup>3,\*</sup>, S. Fox<sup>3</sup>, and I. Valiela<sup>3</sup>

<sup>1</sup> Lafayette College, Easton, PA

<sup>2</sup> Yale University, New Haven, CT

<sup>3</sup> Boston University Marine Program, Woods Hole, MA

Growth of macroalgae in coastal environments is, to a large extent, limited by the available supply of nitrogen (1, 2). Macroalgal growth rates may be influenced by their internal pool of nitrogen, and also by the supply of new nitrogen provided by ambient water (3). Few studies have investigated the relative role of internal and external nitrogen supply on growth of macroalgae. In this study we investigate the net growth of *Ulva lactuca*, a widespread opportunistic species of macroalga found in the estuaries of Waquoit Bay, Cape Cod, Massachusetts, in response to internal and external nitrogen supply by using a field transplantation experiment and isotopic measurements (4).

FronDS of *U. lactuca* were collected from Sage Lot Pond, Quashnet River, and Childs River, subestuaries in the Waquoit Bay estuarine system. The land-use patterns on the watershed of these estuaries differ enough to lead to substantially different nitrogen loads of 14, 350, and 601 kg N ha<sup>-1</sup> y<sup>-1</sup>, respectively (2). FronDS collected from these three estuaries will therefore have grown under different nitrogen regimes and have entered the experiment with different internal nitrogen contents. Two fronds from the same originating estuary were weighed (blotted wet weight) and placed inside cages constructed out of transparent disposable containers (GladWare) with two sides covered by mesh, allowing for water flow.

To assess the effect of ambient nitrogen supply on growth of *U. lactuca*, the algae collected from each estuary and placed in the cages were then transplanted into either Sage Lot Pond, which has the lowest nitrogen load (and hence the lowest nitrogen supply for fronds (5)), or Childs River, which has the highest nitrogen load (and highest supply of nitrogen), with 30 cages per estuary. The cages were randomly set 1 m apart within the existing macroalgal canopy, and 0.2 m above the bottom in locations with salinities between 25 and 30 ppt. This experimental design was deployed from 18 to 27 June 2003 and was repeated from 17 to 24 July 2003.

We measured the net growth response of *U. lactuca* by determining the initial and final wet weights of each algal frond within each cage. Growth data from both runs of the experiment were pooled to span possible differences across the months. FronDS were dried at 60 °C, ground, and sent to the Stable Isotope Facility, University of California, Davis, for analysis of carbon and nitrogen content and stable isotope signatures.

Net growth rate of *U. lactuca* depended on both the nitrogen pool within the fronds, obtained from the estuary from which the fronds were collected, and the nitrogen supply provided by the estuary to which the fronds were transplanted (Fig. 1A). Growth

rates of *U. lactuca* collected from Sage Lot Pond were significantly lower than those achieved by fronds collected from Childs and Quashnet rivers when transplanted into the Childs River (ANOVA,  $F = 13.66$ ,  $P = 0.000017$ ). An *ad hoc* Duncan's test showed no differences between growth rates of algae collected from the Childs and Quashnet rivers when transplanted into Childs River (ANOVA,  $F = 2.64$ ,  $P = 0.11$ ). Growth rates of fronds from all three estuaries transplanted into Sage Lot Pond were not significantly different (ANOVA,  $F = 0.71$ ,  $P = 0.40$ ). These results suggest that, first, fronds of *U. lactuca* grown in an estuary with nutrient-poor water grew slowly if at all, even when transplanted in nutrient-rich estuaries. Second, *U. lactuca* fronds from nutrient-rich estuaries grew faster, and more so when transplanted in nutrient-rich estuaries. Third, fronds from nutrient-poor estuaries lag considerably, even when transplanted into nutrient-rich water; this is evidence of some other impairment of growth.

To further examine the effects of internal and external nitrogen, we plotted net percent growth of *U. lactuca* in Childs River and Sage Lot Pond versus initial percent nitrogen in the fronds (Fig. 1B). Some growth took place in all three estuaries (Fig. 1B), which is not surprising because initial percent nitrogen in the fronds was above 0.71, the minimum % nitrogen content in the tissue of *U. lactuca* required for growth (3). The initial nitrogen content of fronds from the nutrient-rich estuary was 3-fold larger than that of fronds from the nutrient-poor estuary (Fig. 1B). The steeper slope of the growth rate for fronds transplanted into Childs River (black points in the figure) suggests that net growth rates of *U. lactuca* were more affected by external nitrogen supply than by internal nitrogen content, as found in studies on other macroalgae (1, 6).

The relative importance of external nitrogen supply and internal nitrogen content were corroborated by the isotopic signatures (Fig. 1C). FronDS initially differed markedly in carbon and nitrogen isotopic signatures; signatures in fronds from Childs River and transplanted into Childs River were notably different from those of Sage Lot Pond fronds transplanted into Sage Lot Pond (Fig. 1C). Transplanted fronds soon reflected the signature of the nitrogen in the estuaries in which they were incubated, and showed less influence from the estuary of origin. Although the initial percent nitrogen may have slowed growth of Sage Lot Pond fronds (Fig. 1A, 1B), the nitrogen pools of the fronds from Childs River and from Quashnet River showed fast responses to the ambient nitrogen supply (Fig. 1C). Some factor other than internal pool size must be responsible for the lag in growth of Sage Lot Pond fronds.

The range of  $\delta^{15}\text{N}$  between Childs River and Sage Lot Pond has been reported (7), and is associated with different land-derived nitrogen loads, bearing different  $\delta^{15}\text{N}$  signatures, arriving from the

\* Corresponding author: mirta@bu.edu

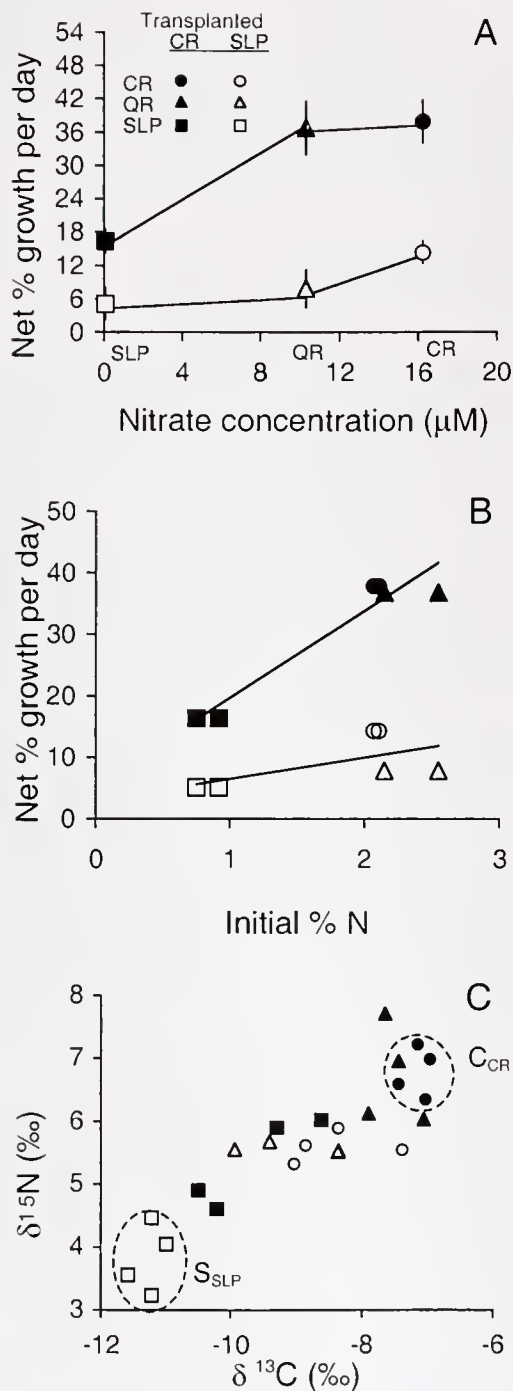


**Figure 1.** Growth rates and isotopic evidence for algal fronds collected from Chिल्ds River (CR), Quashnet River (QR), and Sage Lot Pond (SLP) and transplanted into CR and SLP. (A) Net % growth per day (mean ± s.e.) of *U. lactuca* transplanted into SLP and CR versus the average nitrate concentration (in µM) for June 2002 (data from G. Tomasky, Boston University Marine Program) in the estuaries of origin of the fronds, SLP, QR, and CR. (B) Mean net % growth per day of algae transplanted into CR, QR, and SLP in relation to initial N content (%) in fronds of algae collected from each estuary. Symbols as in A. (C) Comparison of δ<sup>15</sup>N and δ<sup>13</sup>C isotopic values (in ‰) of *U. lactuca* fronds transplanted to CR and SLP from the three estuaries of origin, CR, QR, and SLP. Symbols as in A. Dotted outlines encompass isotopic values of algae from SLP and incubated in SLP (S<sub>SLP</sub>) and from CR and incubated in CR (C<sub>CR</sub>).

watershed to Chिल्ds River and Sage Lot Pond. The range of δ<sup>13</sup>C values measured for *U. lactuca* in our study (-12‰ to -7‰) fall within the heavier part of the range (-35‰ to -5‰) reported in a compilation of such values for macroalgae (8). Various mechanisms, such as the use of HCO<sub>3</sub><sup>-</sup> in photosynthesis (8, 9), have been proposed to explain the range of values, but further work is needed to understand the processes that control the values found in *U. lactuca*.

The isotopic conversion evident in Figure 1C suggests that there is relatively rapid turnover of the internal N pools of *U. lactuca*. For the 8-day duration of the transplant, and assuming linear growth, we roughly calculate that the nitrogen pool turns over completely every 12–15 d. This relatively rapid turnover seems consistent with our conclusion that external nitrogen supply plays a larger role than initial nitrogen content in the growth of this macroalgal species.

This research was supported by internships to A.B.A. from the Woods Hole Marine Science Consortium and to J.A.M. from a grant from the National Science Foundation's Research Experience for Undergraduates (# OCE-0097498). This work was also supported by a grant from the National Oceanic and Atmospheric Association/NOS (ECOHAB award # NA16OP2728), and is ECOHAB publication #76.

**Literature Cited**

- Duarte, C. M. 1995. *Ophelia* 41: 87–112.
- Valiela, I., J. McClelland, J. Hauxwell, P. J. Behr, D. Hersh, and K. Foreman. 1997. *Limnol. Oceanogr.* 42: 1105–1118.
- Pederson, M. F., and J. Borum. 1997. *Mar. Ecol. Prog. Ser.* 161: 155–163.
- McClelland, J. W., and I. Valiela. 1998. *Limnol. Oceanogr.* 43: 577–585.
- Valiela, I., K. Foreman, M. LaMontagne, D. Hersh, J. Costa, P. Peckol, B. DeMeo-Anderson, C. D'Avanzo, M. Babinne, C. Sham, J. Brawley, and K. Lajtha. 1992. *Estuaries* 15: 443–457.
- Peckol, P., B. DeMeo-Anderson, J. Rivers, I. Valiela, M. Maldonado, and J. Yates. 1994. *Mar. Biol.* 121: 175–185.
- McClelland, J. W., I. Valiela, and R. H. Michener. 1997. *Limnol. Oceanogr.* 42: 930–937.
- Fry, B., and E. B. Sherr. 1984. *Mar. Sci.* 27: 13–47.
- Raven, J. A., A. M. Johnston, J. E. Knebler, R. Korb, S. G. McInroy, L. L. Handley, C. M. Scrimgeour, D. I. Walker, J. Beardall, M. Vanderklift, S. Fredriksen, and K. H. Dunton. 2002. *Funct. Plant Biol.* 29: 355–378.

Reference: *Biol. Bull.* 205: 252–253, (October 2003)  
© 2003 Marine Biological Laboratory

## Relative Influence of Grazing and Nutrient Supply on Growth of the Green Macroalga *Ulva lactuca* in Estuaries of Waquoit Bay, Massachusetts

J. A. Morgan<sup>1</sup>, A. B. Aguiar<sup>2</sup>, S. Fox<sup>3</sup>, M. Teichberg<sup>3</sup>, and I. Valiela<sup>3</sup>

<sup>1</sup>Yale University, New Haven, CT

<sup>2</sup>Lafayette College, Easton, PA

<sup>3</sup>Boston University Marine Program, Woods Hole, MA

Nitrogen supply is a major control on growth of coastal macroalgae (1, 2, 3). Top-down effects in which grazing significantly affects macroalgae (4, 5), and nutrient-grazer interactions (3) have also been described. In this paper we describe an experiment in which we measured net growth of a common macroalga, *Ulva lactuca*, in treatments that allowed different numbers of grazers to access fronds as well as incubation of fronds in estuaries with demonstrably different nutrient supplies. These treatments were intended to assess the relative influence of grazer and nitrogen supply on net growth rates of a coastal producer.

To examine the effect of grazing on growth of *U. lactuca*, we constructed acrylic plastic cages with sides of 1-mm, 4-mm, or 18-mm mesh. The different mesh openings were intended to allow entry to different numbers of grazers, which we took as a proxy for grazing pressure. The cage design also allowed for light penetration and horizontal water flow. The 18-mm mesh permitted larger size classes and a greater number of grazers to enter the cages, while the 1-mm mesh excluded larger size classes and allowed fewer grazers. The 4-mm mesh was intended to furnish an intermediate grazer treatment.

To evaluate the effect of nitrogen supply and grazing on algal growth, cages with the three mesh sides were placed in three estuaries in Waquoit Bay, Massachusetts. These three estuaries experience different nitrogen loads—Sage Lot Pond, 14 kg ha<sup>-1</sup>y<sup>-1</sup>; Quashnet River, 350 kg ha<sup>-1</sup>y<sup>-1</sup>; and Childs River, 601 kg ha<sup>-1</sup>y<sup>-1</sup>—from their watershed (6). These nitrogen loads led to different mean nitrate concentrations measured in the estuaries during July 2002, one year prior to the time of our experiments: 0.04, 6.1, and 11.75 μM for Sage Lot Pond, Quashnet River, and Childs River, respectively (G. Tomasky, Boston University Marine Program, unpubl. data). To minimize effects of differences between estuaries other than our treatments, we chose sites similar in salinity, depth, and algal composition. In each estuary we placed four replicates of each of the three grazing pressure treatments, for a total of 36 cages.

Three fronds of *U. lactuca*, each approximately 300 mg (blotted wet weight), were suspended inside each cage. To measure the effect of top-down versus bottom-up factors, we measured net growth as the dependent variable. Net growth was the growth achieved by the fronds minus the biomass consumed by grazers. To determine net growth, the *U. lactuca* fronds were weighed initially (blotted wet weight) and again after 10 days of field incubation.

First, we assess the success of the treatments. To roughly measure the grazing pressure, we sorted and counted the potential grazers found in the cages for two replicates of each treatment at

the end of the incubation. The grazers were sorted into four groups, amphipods, shrimp, crabs, and isopods. The total number of grazers in the 1-mm mesh cages was significantly lower in all three estuaries than the number in the 4-mm cages (Fig. 1a; ANOVA  $F = 31.0$ ,  $P = 0.0014$ ). The number of grazers found in the 18-mm mesh cages was also significantly different, although they contained lower grazer abundances than the 1-mm and 4-mm mesh cages (Fig. 1a). Predatory fish and large shrimp entered the cages with 18 mm mesh and likely fed on the smaller grazers, thus decreasing grazer abundances. This possible effect of predators on grazers suggests that there might be important top-down cascade effects in this system waiting to be studied.

The difference in nitrogen load in the three estuaries provided quantitatively different nutrient supplies, as evident in the nitrate concentrations cited above. Bottom-up effects from these different nitrogen supplies on net growth of *U. lactuca* were dominant factors. Rates of net growth were higher in estuaries receiving larger external nitrogen loads (Fig. 1b; ANOVA  $F = 61.8$ ,  $P < 0.001$ ). Percent net growth of *U. lactuca* in Childs River was almost three times that in Sage Lot Pond (Fig. 1b). This response of macroalgae to nitrogen supply is similar to that reported by others (2).

Top-down effects caused by grazers were small compared to the effects of nutrients (Fig. 1b). Across all estuaries, net growth in the 1-mm (fewer grazers) cages was higher than growth in 4-mm (more grazers) cages, but these differences were statistically insignificant. In contrast, there was more than a 200% increase in percent net growth caused by the nutrient effects. Taken together, these results suggest that the direct and indirect bottom-up effects associated with nitrogen loading were much larger than the top-down effects of grazing on the net growth of *U. lactuca*.

Increased nutrient inputs might affect the composition of the grazers found in the three estuaries (Fig. 1c). Shrimp (*Palaemonetes* sp.) and amphipods (Gammaridea) accounted for over 85% of grazers in all cages. Shrimp were far more abundant in high nitrogen load conditions (Childs River), while amphipods were more plentiful in lower nitrogen load conditions (Sage Lot Pond; Fig. 1c). Shrimp are predators as well as grazers (7), so they could have fed upon amphipods. Similar shifts in species composition have been reported elsewhere (3, 8). Increased anthropogenic supplies of nitrogen might therefore not only change the growth rates of *U. lactuca* directly, but also alter the relative abundances of consumers and lower abundances of grazers. This effect is possibly linked to more frequent anoxic and hypoxic conditions in the more nitrogen-loaded estuaries such as Childs River (9).

To further assess possible grazer effects, we plotted percent net

Mesh opening (mm)	No. of grazers/ cage		
	SLP	QR	CR
1	24±0.0	78.0±30.0	38.5±10.5
4	177.5±14.5	112.5±2.5	59.5±13.5
18	80.5±25.5	61.5±25.5	17.5±9.5
Mean	94.0±44.8	84.0±15.0	38.5±12.1

Mesh opening (mm)	% net growth		
	SLP	QR	CR
1	69.8±10.0	118.1±12.8	247.1±7.5
4	61.3±5.8	104.2±19.2	223.0±36.3
18	76.6±15.3	92.1±14.7	285.5±31.6
Mean	69.2±4.4	104.8±7.5	251.9±18.2

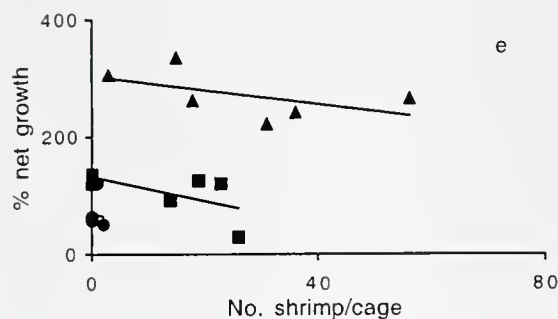
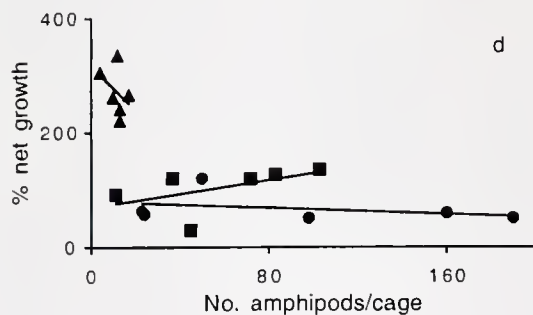
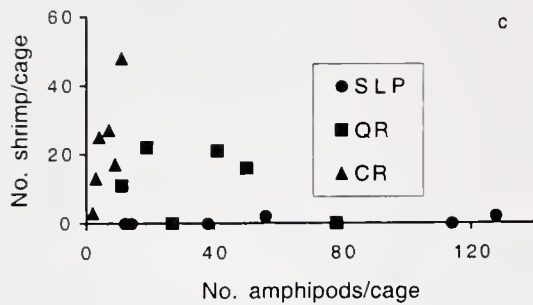


**Figure 1.** The effects of grazing and nitrogen load on the net growth of *Ulva lactuca* in cages with mesh sides of 1, 4, or 18 mm in three estuaries with different land-derived nitrogen loads—Sage Lot Pond (SLP), 14 kg N ha<sup>-1</sup>y<sup>-1</sup>; Quashnet River (QR), 350 kg N ha<sup>-1</sup>y<sup>-1</sup>; and Childs River (CR), 601 kg N ha<sup>-1</sup>y<sup>-1</sup>. (a) Number (mean ± s.e.) of potential grazers (shrimp, amphipods, isopods, and crabs) in the cages after incubation. (b) Percent net growth (mean ± s.e.) of *U. lactuca* fronds. Vertical lines show values for which the differences in mesh opening were found to be not significant by an ad hoc Duncan's test. (c) Number of shrimp found in each cage vs. amphipods per cage. (d) Percent net growth vs. the number of amphipods found in each cage (SLP: F = 0.66, QR: F = 1.41, CR: F = .75; all F values not significant). (e) Percent net growth vs. the number of shrimp found in each cage (SLP: F = 0.04, QR: F = 2.14, CR: F = 1.69; all F values not significant).

growth separately versus the abundance of amphipods and shrimp. The difference in abundances of these two groups is evident in Figure 1c, d, and e. Despite the shift in grazer composition among the estuaries, there was no significant effect of either amphipod or shrimp number on percent net growth of *U. lactuca* (Fig. 1d, e). Even though the treatments significantly varied the abundance of grazers, we could find no compelling evidence of significant top-down control of *U. lactuca* net growth by grazers in Waquoit Bay estuaries. This differs from the results of other studies, which show that under eutrophic conditions, top-down effects play a significant role in controlling macroalgal biomass (10). Our results corroborate the conclusions of previous studies that bottom-up effects may overwhelm top-down forces in nutrient-enriched estuaries (3, 4).

This research was supported by internships to J.M. from a grant from the National Science Foundation's Research Experience for Undergraduates #OCE-0097498, and to A.A. from the Woods Hole Marine Consortium. This work was also supported by a grant from the National Oceanic and Atmospheric Association/NOS, ECOHAB #NA16OP2728, and is ECOHAB publication #77. Special thanks to Paulina Martinetto for help with statistical analysis.

**Literature Cited**

- Duarte, C. 1995. *Ophelia* 41: 87–112.
- Valiela, I., J. McClelland, J. Hauxwell, P. Behr, D. Hersh, and K. Foreman. 1997. *Limnol. Oceanogr.* 42: 1105–1118.
- Hauxwell, J., J. McClelland, P. Behr, and I. Valiela. 1998. *Estuaries* 21: 347–360.
- Geertz-Hansen, O., K. Sand-Jensen, D. F. Hansen, and A. Christiansen. 1993. *Aquat. Biol.* 46: 101–109.
- Balducci, C., A. Sfriso, and B. Pavoni. 2001. *Mar. Environ. Res.* 52: 27–49.
- Valiela, I., G. Collins, J. Kremer, K. Lajtha, B. Seely, J. Brawley, and C. Sham. 1997. *Ecol. Appl.* 7: 358–380.
- McClelland, J. W., and I. Valiela. 1998. *Mar. Ecol. Progr. Ser.* 168: 259–271.
- Millman, M., M. Teichberg, P. Martinetto, and I. Valiela. 2002. *Biol. Bull.* 203: 263–264.
- D'Avanzo, C., and J. N. Kremer. 1994. *Estuaries* 17: 131–139.
- Menge, B. A., B. A. Daley, P. A. Wheeler, E. Dahlhoff, E. Sanford, and P. T. Strub. 1997. *Proc. Natl. Acad. Sci. USA* 94: 14530–14535.

Reference: *Biol. Bull.* 205: 254–255. (October 2003)  
© 2003 Marine Biological Laboratory

## Stable Isotope Assessment of Site Loyalty and Relationships Between Size and Trophic Position of the Atlantic Horseshoe Crab, *Limulus polyphemus*, within Cape Cod Estuaries

C. W. O'Connell,<sup>1</sup> S. P. Grady,<sup>2</sup> A. S. Leschen,<sup>2</sup> R. H. Carmichael,<sup>2</sup> and I. Valiela<sup>2</sup>

<sup>1</sup> Bucknell University, Lewisburg, PA

<sup>2</sup> Boston University Marine Program, Woods Hole, MA

Carmichael *et al.* (1) used stable isotope analysis to define the food webs of horseshoe crabs, *Limulus polyphemus*, in Pleasant Bay, Cape Cod, Massachusetts, and also found that these animals forage within relatively small areas of estuaries. In this study, we used field measurements and stable isotope analysis (2) to determine whether the trophic position and site loyalty described by Carmichael *et al.* (1) in Pleasant Bay were also found in two additional Cape estuaries, Stage Harbor and Barnstable Harbor, and to determine how the trophic position of horseshoe crabs might change as adult crabs grow.

Increased population densities and the resulting anthropogenic wastes within watersheds increase nitrogen loads to estuaries (2). Pleasant Bay is part of the Cape Cod National Seashore Reserve and has a low nitrogen load due to the lack of developed land in its watershed (1). Stage Harbor and Barnstable Harbor have relatively greater population densities in their watersheds, and as reported elsewhere in Cape Cod (2), should have greater relative nitrogen loads. The land-derived nitrogen loading rates to the three estuaries are likely to rank in the order of Stage Harbor > Barnstable Harbor > Pleasant Bay (3, 4). Since increased urban development results in heavier nitrogen signatures of estuarine water and biota (2), we opted to study these estuaries with different land use in their watersheds to take advantage of potential resulting differences in  $\delta^{15}\text{N}$  and  $\delta^{13}\text{C}$  signatures (5, 6).

We collected samples during July 2003 at a site in Barnstable Harbor and three sites in Stage Harbor in Cape Cod. We measured the size of horseshoe crabs as the width at the widest region of the prosoma (7). To obtain samples for isotope analysis, we sampled tissue from the last two segments of the second or third walking leg of adult horseshoe crabs (1). To identify some potential foods of horseshoe crabs, we also sampled quahogs (*Mercenaria mercenaria*), polychaetes (*Nereis* sp., *Nephtys* sp., and *Glycera* sp.), seston filtered from 1-l water samples, and sediment from two 10-ml sediment cores taken 3 cm deep, which were pooled into a single sample. All samples were dried at 60°C, ground, and sent to the Stable Isotope Facility, University of California, Davis, for mass spectrometry.

The  $\delta^{13}\text{C}$  signatures of the horseshoe crabs suggest that their diet may have included a mix of polychaetes and quahogs (Fig. 1a). Quahogs, in turn, assimilated carbon from a mixture of seston and sediment, judging from their position relative to values on the  $\delta^{13}\text{C}$  axis. The carbon in seston and sediment was likely initially derived from phytoplankton and macroalgal organic particulates (gray lines in Fig. 1a) (8). Polychaetes seemed to belong to a separate branch of the food web, since they had relatively heavier signatures, and most likely incorporated a mix of carbon from

macroalgae and *Spartina* grass (Fig. 1a). These  $\delta^{13}\text{C}$  values are consistent with carbon signatures found in Pleasant Bay (1).

$\delta^{15}\text{N}$  signatures suggested that the horseshoe crabs consumed a combination of quahogs, polychaetes, and particulate organic matter, given the expected fractionation from food source to consumer of 2‰–4‰ (Fig. 1a) (2).  $\delta^{15}\text{N}$  values for bivalves and polychaetes were 2‰–5‰ heavier than those of particulate matter. In all cases, the  $\delta^{15}\text{N}$  values for each taxon (shown by points within dashed ovals, Fig. 1a) seem to be heavier in Stage Harbor than in Barnstable Harbor, suggesting, as suspected from the different land-use patterns, heavier land-derived nitrogen sources from freshwater inputs into Stage Harbor (5, 6).

Isotopic signatures of individual crabs varied considerably. Part of the variation was associated with different crab size: larger crabs tended to have significantly heavier  $\delta^{15}\text{N}$  signatures ( $F = 9.5$ ,  $P = 0.004$ ) and lighter  $\delta^{13}\text{C}$  values ( $F = 13.94$ ,  $P = 0.0005$ ) (Fig. 1b, c). The increased  $\delta^{15}\text{N}$  signatures may be related to increased prey size among larger crabs (9). The slopes of the regression lines in Figure 1b did not differ, but the intercepts were significantly different (ANOVA:  $F = 9.26$ ,  $P = 0.004$ ). The offset between the regressions shows that Stage Harbor crabs had a heavier  $\delta^{15}\text{N}$  signature than Barnstable Harbor crabs. In Figure 1c, we added a gray reference area that represents the prosomal width and  $\delta^{15}\text{N}$  values for crabs from Pleasant Bay (1), the most pristine of the three estuaries. The Pleasant Bay values were appreciably lighter than those of either Stage Harbor or Barnstable Harbor (Fig. 1b). These isotopic comparisons suggested that the watershed-derived nitrogen loads (and contribution by wastewater) were greater in Stage Harbor than in Barnstable Harbor and that both these estuaries received greater anthropogenic nitrogen loads than Pleasant Bay.

The significant difference in the isotopic signature of horseshoe crabs collected in the three estuaries can also be interpreted to mean that crabs tend to remain foraging in an estuary long enough to acquire  $\delta^{15}\text{N}$  values characteristic of the estuary in which they were found. These results corroborate earlier observations (1) that in spite of the evident mobility of horseshoe crabs, they do tend to remain within relatively circumscribed areas for considerable periods of time.

The  $\delta^{13}\text{C}$  values provided additional information about the foraging and feeding behavior of horseshoe crabs (Fig. 1c).  $\delta^{13}\text{C}$  became lighter as size of crabs increased ( $F = 13.93$ ,  $P = 0.0005$ ) (Fig. 1c). As adult horseshoe crabs grew, signatures shifted from values near the  $\delta^{13}\text{C}$  for the *Spartina*-based side of the food web to values more closely associated with phytoplankton (dashed boxes in Fig. 1c, and Fig. 1a). This transition suggests that as adult crabs grew, a larger percentage of their diet consisted of

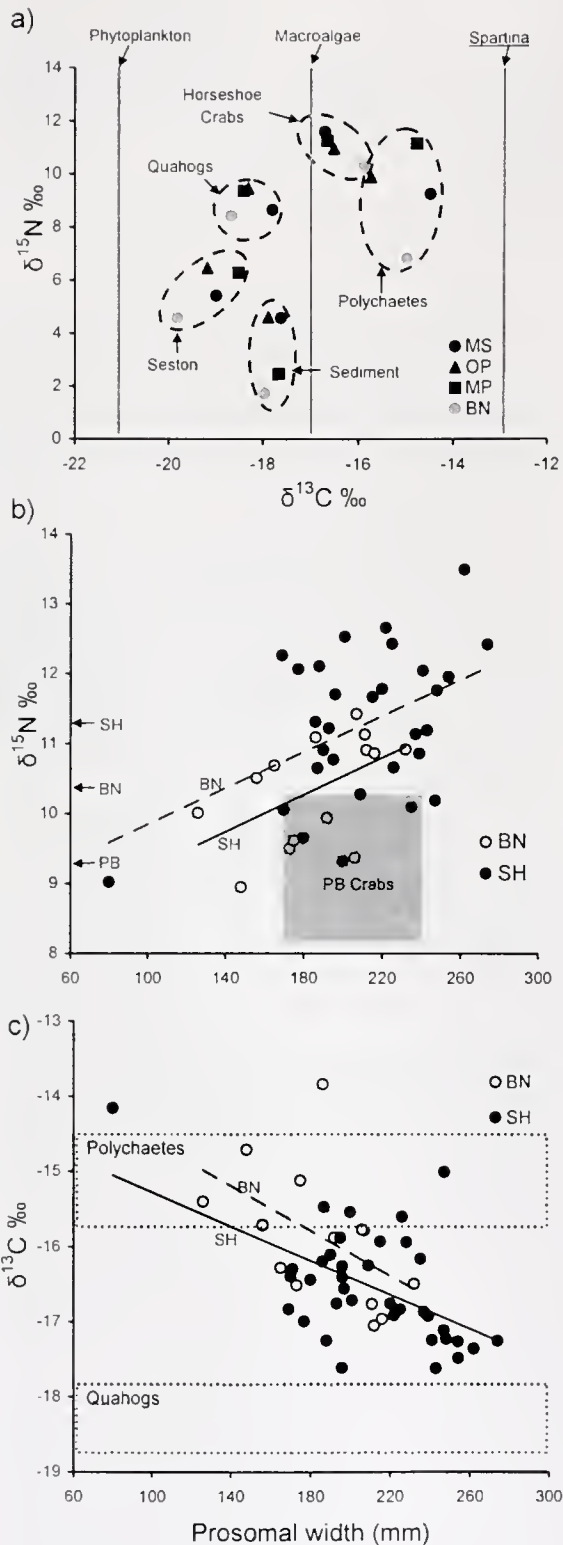


**Figure 1.** Isotopic measurements of samples collected in Barnstable Harbor (BN), Stage Harbor (SH), and Pleasant Bay (PB), Cape Cod, Massachusetts. (a)  $\delta^{15}\text{N}$  and  $\delta^{13}\text{C}$  signatures of horseshoe crab and other components of the estuary system of BN and SH. The dashed ovals include measurements taken in BN and the three other sites within SH (Main Bay,

sources supported by the phytoplankton-based portion of the food web.

The results of this work lend support to earlier findings about the position of horseshoe crabs as generalist predators in the estuarine food webs of Cape Cod; demonstrate that horseshoe crabs are clearly linked to land-derived nitrogen sources; suggest a possible diet shift from *Spartina*-based food sources to more phytoplankton-based sources as adult crabs grow; and show that the crabs exhibit considerable within-estuary loyalty in their foraging habits.

This study was supported by an internship to C.W.O. from the Woods Hole Marine Sciences Consortium and funding from MIT Sea Grant. We are grateful to Ed Eichner of the Cape Cod Commission for sharing information on land use, and to Mirta Teichberg, Allyson Papa, and Rachel Allen for assistance in many ways.

**Literature Cited**

1. Carmichael, R. H., D. Rutecki, B. Annett, E. Gaines, and I. Valiela. *J. Exp. Mar. Biol. Ecol.* (In press).
2. Peterson, B. J., and B. Fry. 1987. *Annu. Rev. Ecol. Syst.* 18: 293–320.
3. Eichner, E. M., S. C. Michaud, T. C. Cambareri, B. Smith, G. Prahm, and M. Fenn. 2002. *Cape Cod Surface Water Nutrient Management Study*. Unpublished report. Water Resource Office, Cape Cod Commission, Barnstable, MA.
4. Eichner, E. M., K. Livingston, B. Smith, V. Morill, and A. Carbonell. 1998. *Pleasant Bay Nitrogen Loading Analysis*. Unpublished report. Water Resource Office, Cape Cod Commission, Barnstable, MA.
5. McClelland, J. W., I. Valiela, and R. H. Michener. 1997. *Limnol. Oceanogr.* 42: 930–937.
6. McClelland, J. W., and I. Valiela. 1998. *Limnol. Oceanogr.* 43: 577–585.
7. Shuster, C. N. 1955. On morphometric and serological relationships within the Limulidae, with particular reference to *Limulus polyphemus* (L.). Ph.D. thesis, New York University.
8. McClelland, J. W., and I. Valiela. 1998. *Mar. Ecol. Prog. Ser.* 168: 259–271.
9. Valiela, I. 1995. *Marine Ecological Processes*. Springer-Verlag, New York.

MS; Oyster Pond, OP; and Mill Pond, MP). The vertical lines show approximate mean value of  $\delta^{13}\text{C}$  for phytoplankton, macroalgae, and *Spartina* as found in similar Cape Cod estuaries (2, 8). (b)  $\delta^{15}\text{N}$  value vs. prosomal width of horseshoe crabs collected in BN and SH. Regression information for BN:  $y = 0.0137x + 8.9$ ,  $F = 10.81$ ,  $P = 0.002$ ; for SH:  $y = 0.014x + 8.41$ ,  $F = 4.48$ ,  $P = 0.05$ . Mean of horseshoe crab  $\delta^{15}\text{N}$  from SH, BN, and PB [data from (1)] are shown on y-axis. The shaded reference area covers range of PB from (1). (c)  $\delta^{13}\text{C}$  values vs. prosomal width of horseshoe crabs collected in BN and SH. Symbols as in Fig. 1b. Dashed boxes include range of values for polychaetes and for quahogs for Fig. 1a.

Reference: *Biol. Bull.* 205: 256–257. (October 2003)  
© 2003 Marine Biological Laboratory

## Incubation Conditions of Forest Soil Yielding Maximum Dissolved Organic Nitrogen Concentrations and Minimal Residual Nitrate

C. Walker, E. Davidson,\* W. Kinglerlee, and K. Savage  
Woods Hole Research Center, Woods Hole, MA

Soil is a dominant long-term sink for N in forest ecosystems (1). With increasing atmospheric N deposition in forests caused by combustion of fossil fuels (2, 3), concern over effects of N loading on ecosystem sustainability is substantial. Net primary productivity is thought to be limited by N in most temperate forests (4), but much of the N from deposition appears to be immobilized in the organic matter of the soil rather than being taken up by plants (1). However, the mechanisms of N immobilization as well as the bioavailability and ultimate fate of organic N remain poorly understood. One hypothesized pathway of immobilization is abiotic reduction of nitrate to nitrite and reaction of nitrite with dissolved organic matter to produce dissolved organic nitrogen (DON) (5). Studying the fate of DON would be facilitated by the development of a  $^{15}\text{N}$  label in a realistic soil DON product. In the present study, we tested incubation conditions that would permit nitrate immobilization to DON during 24 h, followed by conditions that would minimize the remaining nitrate. Water content and N concentrations were varied in 1–8-day incubations of organic horizon to study the dynamic of nitrate reduction and DON formation.

Soil for these incubations was collected from the humus ( $\text{O}_d$ ) layer of a forest stand dominated by oak at the Harvard Forest, Massachusetts. The stand developed after agricultural abandonment at the end of the 19th century and after a devastating hurricane in 1938 (6). The soil samples were passed through a 2-mm sieve to remove large roots. Subsamples of 10 g ( $n = 64$ ) were placed in 60-ml serum bottles, which then received a combination of two treatments in a factorial design. First, 3.33 ml of either deionized water or nitrate solution ( $50 \mu\text{g N/g}$  dry soil as  $\text{KNO}_3$ ) was added. Second, 30 ml of deionized water was added to half of the samples to create saturated conditions, whereas those not receiving additional water were considered unsaturated. The bottles were sealed using rubber stoppers and tear-away metal crimping seals. Each treatment combination was replicated 16 times so that four replicates could be destructively sampled by extraction in water at 0, 1, 4, and 8 days after the start of the incubation. The "day zero" extraction was done immediately after sample treatment (addition of nitrogen or water) to measure background nitrate and DON and to measure initial recovery of added nitrate. Ambient aerobic conditions prevailed during the first day of incubation to allow for aerobic immobilization processes. After the first day, air was flushed from the serum bottles with dinitrogen gas to create anaerobic conditions in an effort to increase denitrification, thus reducing

residual nitrate. At the end of each incubation period, 60 ml of water was added to the saturated samples and 30 ml to the unsaturated. All samples were shaken and immediately filtered through No. 1 Whatman filter paper. Filtrate from each incubation was analyzed for nitrate, ammonium, and total N using a Lachat 8000 flow-injection autoanalyzer with in-line persulfate digestion (7, 8). DON was calculated by subtracting the sum of nitrate and ammonium from total N.

Nitrate concentrations in soil extracts remained at low values throughout the experiment in incubations under saturated and unsaturated conditions with no added nitrate (Fig. 1). In incubations with added nitrate, concentrations increased slightly and similarly under saturated and unsaturated conditions during the first day, after which they declined for the remainder of the experiment. Incubation time, addition of nitrate, and the interaction of time by nitrate were significant ( $P < 0.01$ ) in an analysis of variance. Saturation was also found to be significant ( $P < 0.05$ ), as nitrate concentrations were lower in saturated incubations compared to those remaining unsaturated.

Ammonium concentrations in soil extracts increased in a linear fashion, with day 8 values higher (close to  $74 \mu\text{g N/g}$  dry soil with or without added nitrate) in incubations under saturated conditions than those remaining unsaturated ( $53 \mu\text{g N/g}$  dry soil with and  $46 \mu\text{g N/g}$  dry soil without added nitrate). In summary, water saturation apparently enhanced denitrification and either stimulated mineralization or inhibited nitrification, thus yielding lower nitrate and higher ammonium than did unsaturated conditions.

DON concentrations in soil extracts increased over time in incubations with and without nitrate addition under saturated and unsaturated conditions. An analysis of variance shows incubation time to be the only significant ( $P < 0.01$ ) factor. Also, there was not a stoichiometric conversion of nitrate to DON, suggesting that DON was produced primarily from sources other than nitrate immobilization. However, only a small amount of nitrate immobilization to DON would be necessary to create a labeled DON pool when  $^{15}\text{N}$ -labeled nitrate is used.

This experiment will be repeated with a  $^{15}\text{N}$  label in the added nitrate to determine the recovery of labeled N in the extracted DON, ammonium, and in the small remaining nitrate pool. These preliminary results using unlabeled N demonstrate that it may be possible to create a series of incubation conditions that would permit nitrate immobilization into DON while minimizing remaining nitrate. Hence, it may be possible to obtain an extract with labeled DON that is created naturally within the soil and that can be used to study DON bioavailability in subsequent experiments.

This research was funded by the NSF Research Experience for Undergraduates site Grant (OCE-0097498).

\*Corresponding author: edavidson@whrc.org

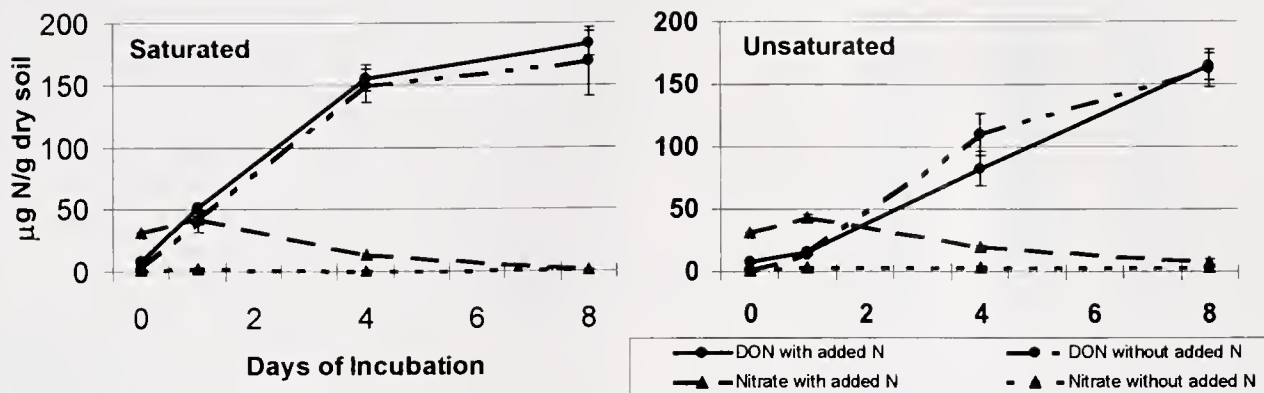


**Figure 1.** Mean concentrations ( $n = 4$ ) of N in saturated (left) and unsaturated (right) soil incubations. Solid lines represent DON concentrations of soil extract with added N, and dashed dotted lines represent concentrations without added N. Long dashed lines represent nitrate concentrations of soil extract with added N, and short dashed lines represent concentrations without added N.

**Literature Cited**

1. Nadelhoffer, K. J., M. R. Downs, and B. Fry. 1999a. *Ecol. Appl.* **9**: 72–86.  
 2. Gunderson, P., B. A. Emmet, and O. J. Kjonaas. 1998. *Forest Ecol. Manage.* **101**: 37–55.  
 3. Galloway, J. N., W. H. Schlesinger, and H. Levy II. 1995. *Global Biogeochem Cycles* **9**: 235–252.

4. Vitousek, P. M., and R. W. Howarth. 1991. *Biogeochemistry* **13**: 87–115.  
 5. Davidson, E. A., J. Chorover, and D. B. Dail. 2003. *Global Change Biol.* **9**: 228–236.  
 6. Foster, D. 1992. *J. Ecol.* **80**: 753–772.  
 7. Ranger, C. B. 1981. *Anal. Chem.* **20a**: 53–59.  
 8. Ruzica, J. 1983. *Anal. Chem.* **55**(11): 1040a–1053a.

Reference: *Biol. Bull.* **205**: 257–258. (October 2003)  
 © 2003 Marine Biological Laboratory

**Building a Database of Historic Land Cover to Detect Landscape Change**

M. T. Holden,\* C. Lippitt, R. G. Pontius, Jr., and C. Williams  
 Clark University, Worcester, MA

Since 1999, researchers at Clark University have collaborated with scientists at the Marine Biological Laboratory in Woods Hole, Massachusetts, to examine the relationship between land cover and nutrient concentrations in the Ipswich River watershed. The watershed covers 404 km<sup>2</sup>, involves 22 towns, and drains into the Plum Island Ecosystem—Long Term Ecological Research site of the National Science Foundation. Previous research has associated increases in nitrogen concentrations with conversion from forest in 1971 to built land in 1999 (1). Land-cover before 1971 is also important in understanding nutrient cycling; however, maps of the pre-1971 landscape exist only in paper form. The first part of this paper describes the transformation of 1951 paper maps to digital land-cover maps (2). The second part describes a novel technique for comparing maps from two points in time and attributing the differences to either map error or true landscape change.

To begin the digitizing process, the 14¼ in. × 19 in. 1951 paper maps (1:31,680) were scanned in grayscale at 300 dpi using a large-format scanner. We used the GIS software ERDAS Imagine 8.5 to georeference (spatially orient) the scanned images. In order to do this, a digital data layer that matches features on the paper

maps is needed. We used the Massachusetts 2000 Census roads layer (3) because roads are the only abundant features on the 1951 maps. We then imported the georeferenced images into the software R2V, which automatically vectorized (traced) the various land-cover areas. We manually edited this vector file for quality control and labeled each land category in the ESRI software ArcMap. Finally, we imported the vector land-cover data into the GIS software Idrisi at a resolution of 30-m pixels in order to make it compatible with the digital land-cover map for 1999 and to perform analyses. We reclassified the land of the 1951 and 1999 maps into the seven categories of the Anderson Level I classification system (4): Built, Agriculture, Range, Forest, Water, Wetland, and Barren.

The most common technique for assessing landscape change is to compare maps of two times, T1 and T2. A naïve interpretation of this map comparison would lead to the conclusion that the differences between the maps of T1 and T2 indicate landscape change. However, even if there were no landscape changes between T1 and T2, possible errors in both maps would result in differences between the two maps.

To overcome this problem, we created a method to distinguish between the difference due to map error and difference due to true

\*Corresponding author: mholden@clarku.edu

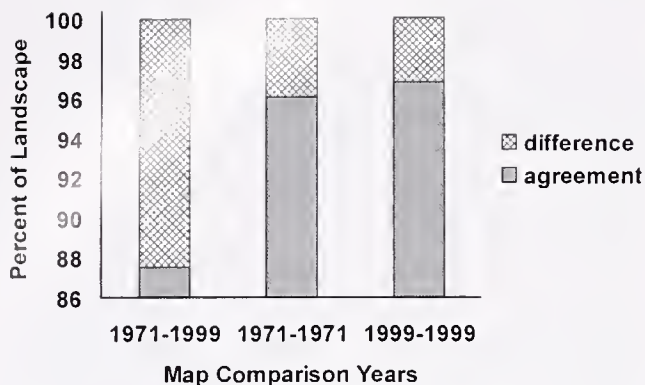


Figure 1. Method to estimate change from 1971 to 1999 among seven land categories for 22 towns of the Ipswich River watershed.

change. The method estimates the expected difference between the maps assuming no change on the landscape between T1 and T2, based on accuracy assessments of the original maps. The true landscape change is thus calculated as the observed difference minus the expected difference. We have applied this technique using existing digital maps, where T1 = 1971 and T2 = 1999. We will also apply this technique to the 1951 maps when we are finished digitizing.

Systematic accuracy assessment does not exist for the maps of 1971 and 1999. The map producer estimates the combined accuracy of both maps to be approximately 98% because the categories seemed obvious from the high-quality photography used in the map-making process; the quality of the 1999 photographs was higher than those from 1971 (David Goodwin, University of Massachusetts, Amherst, pers. comm.). Check plots were done on the 1971 and 1999 data to compare the final digitized land-cover map to the photo-created base map.

In our analytic technique, the producer of the 1971 map is called A, and the producer of the 1999 map is called B. Based on the accuracies reported above, we assume that producer A makes maps with an accuracy of 97% for each category, and that producer B makes maps with an accuracy of 99% for each category.

The left bar of Figure 1 shows that the observed agreement is

88% in the direct comparison between the map of 1971 and 1999. The middle bar of Figure 1 shows that if producers A and B were each to make a map of the 1971 landscape, then the expected agreement between their two maps would be 96%. Since the observed agreement is 88%, the computed true landscape change is 8%. The right bar of Figure 1 shows that if producers A and B were each to make a map of the 1999 landscape, then the expected agreement between their two maps would be 97%, thus the computed true landscape change is 9%. Consequently, the technique estimates the true change to be between 8% and 9%.

Our technique may underestimate the amount of true change because we assume that some of the observed differences are due to map error. Therefore, we should interpret the calculation of the true change as a lower bound on the estimate of landscape change. Our method is conservative because it recognizes that differences in maps do not always indicate true landscape change.

The National Science Foundation (NSF) supported this work through the Research Experience for Undergraduates Summer Fellowship Program via the Marine Biological Laboratory (Award OCE-9726921). Research was conducted at Clark University's Human Environment Regional Observatory, which is also supported by NSF (Award SES-0243772, SubAward 2500-CU-NSF-3772). David Goodwin of the University of Massachusetts Amherst provided scanning equipment and expertise. Joseph Spencer and Louis Paladino provided their georeferencing knowledge. We thank reviewers for helpful comments.

#### Literature Cited

1. Pontius, R. G., Jr., L. Claessens, C. Hopkins, Jr., A. Marzouk, E. Rastetter, L. Schneider, and J. Vallino. 2000. Proceedings of the 4th International Conference on Integrating GIS and Environmental Modeling. CIRES, University of Colorado, Boulder. Online. Available: <http://www.colorado.edu/research/cires/banf/pubpapers/165/> (accessed June 2003).
2. MacConnell, W. 1951. Massachusetts Land-Use, 1: 31680. University of Massachusetts, Amherst: U.S. Geol. Survey.
3. Massachusetts Geographic Information System. 2000. Online. Available: [http://www.state.ma.us/mgis/cen2000\\_tiger.htm](http://www.state.ma.us/mgis/cen2000_tiger.htm) (accessed June 2003).
4. Anderson, J. R., E. E. Hardy, J. T. Roach, and R. E. Witmer. 1976. U.S. Geol. Survey Prof. Paper 964.

## Published by Title Only

**Chung, Clare, and John Dowling**

Anatomical analysis of retinal ganglion cells in larval zebrafish

**Davison, Ian, and Kerry Delaney**

GABA(B)-mediated inhibition of receptor neuron inputs to the olfactory bulb

**Freeman, Chris, Heather Haas, Linda Deegan, and John Logan**

Comparison of invertebrate populations between the platform and aquatic border along a salinity gradient in a New England salt marsh

**Gherardi, Francesca, and Jelle Atema**

Individual recognition and memory in hermit crabs

**Henderson, Kristin, and Rebecca Gast**

Comparison of *Acanthamoeba* distribution between environmental samples and enrichment cultures

**Hernandez, Ruben, Randy Elizando, Nelly Garcia, Myra Guzman, Ileana Juarez, Joe Martinez, Jr., and Richard LeBaron**

Evidence that FAK is differentially expressed in naive and theta-burst stimulated hippocampal slice

**Hopp, Joshua, Bonnie Keeler, Richard Garritt, and Linda Deegan**

Distribution of benthic chlorophyll among habitats in salt marsh tidal creeks

**Kuhlman, Sandra, Hiro Higashiyama, and Z. Josh Huang**

Role of inhibition in timing onset of ocular dominance plasticity in visual cortex

**Lyons, M. M., K. R. Uhlinger, J. E. Ward, and R. Smolowitz**

Role of marine aggregates in the transmission of bivalve parasites

**Miller-Sims, Vanessa, and Jelle Atema**

Tuning of mechanoreceptors in the lobster antennule

**Mrizek, Michael D., Nelly I. Garcia, Myra Guzman, Ruben Hernandez, Joe L. Martinez, Jr., and Richard G. LeBaron**

Indication that theta-burst stimulation influences an alpha5 immune-related protein in hippocampus CA

**Murphy, Gabe**

Mechanisms of feedback inhibition in the retina: reciprocal synaptic signaling between bipolar and amacrine cells

**Smolowitz, R., J. Hanley, and M. Tubbs**

Nutritional myopathy in cultured toadfish

**Watanabe, Shigeo, Matthew Larkum, Paul Rhodes, Nechama Lasser-Ross, and William Ross**

Dendritic properties of turtle cortical pyramidal neurons

# 2004 SUMMER RESEARCH FELLOWSHIPS

## FUNDING AVAILABLE FOR SUMMER RESEARCH IN NEUROSCIENCE AT THE MARINE BIOLOGICAL LABORATORY IN WOODS HOLE

---

The Marine Biological Laboratory is pleased to announce the availability of funding for the following summer research programs in Neuroscience in 2004. These programs will provide up to \$50,000/year/award with a possibility for renewal for 3 years. Scholars in these programs will benefit from the rich intellectual and interactive environment of the scientific community at the MBL.

**APPLICATION DEADLINE:  
JANUARY 30, 2004  
FOR  
NEUROSCIENCE  
FELLOWSHIPS**

*Applications are encouraged from women and members of underrepresented minorities.*

### **Albert and Ellen Grass Faculty Grants Program**

Proposals must describe collaborative research in any area of neuroscience by teams of two or more investigators, with a minimum stay of six weeks at the Marine Biological Laboratory in Woods Hole. Collaborative teams must consist of a minimum of two Assistant/Associate Professor level neuroscientists. Collaborative units may be formed with senior investigators but only the more junior neuroscientists will receive direct funding. Awards provide costs for research and laboratory rental, plus housing and travel costs for the PIs.

### **Dart Foundation Scholars Program in Learning & Memory**

Proposals must be devoted to the study of learning and memory with a minimum stay of six weeks at the Marine Biological Laboratory in Woods Hole. Applications are encouraged from junior or senior level neuroscientists holding a Ph.D., M.D. or equivalent degree. Awards provide costs for research and laboratory rental, plus housing and travel costs.

---

## FUNDING AVAILABLE FOR SUMMER RESEARCH

The Marine Biological Laboratory is pleased to announce the availability of funding for the following summer research programs in 2004 for junior or senior investigators holding a Ph.D., M.D., or equivalent degree. These prestigious awards provide costs for research and housing. Proposals for Fellowship support will be considered in, but are not limited to, the following fields of investigation:

**APPLICATION DEADLINE:  
JANUARY 15, 2004  
FOR  
SUMMER RESEARCH  
FELLOWSHIPS**

*Applications are encouraged from women and members of underrepresented minorities.*

**Cellular & Molecular Physiology  
Developmental Biology  
Ecology  
Microbiology**

**Molecular Biology  
Neurobiology  
Parasitology**



---

FOR APPLICATION FORMS AND ADDITIONAL INFORMATION, PLEASE CONTACT:

Sandra Kaufmann, Fellowship Coordinator  
508-289-7441; [skaufman@mbl.edu](mailto:skaufman@mbl.edu)

Visit our web site at

**<http://www.mbl.edu/fellowships>**

*The MBL is an Equal Opportunity/  
Affirmative Action Employer.*

**Marine Biological Laboratory~7 MBL Street~Woods Hole~Massachusetts~02543**

# THE BIOLOGICAL BULLETIN

## 2004 Subscription Rates Volumes 206-207

\*Paid Subscriptions include both print and electronic subscriptions at: [www.biolbull.org](http://www.biolbull.org)

	Institutional*	Individual*
One year subscription (6 issues - 2 volumes)	\$325.00	\$120.00
Single volume (3 issues)	\$165.00	\$70.00
Single Issues	\$ 75.00	\$25.00

\*Surface delivery included in above prices.

For prompt delivery, we encourage subscribers outside the U.S. to request airmail service.

### Airmail Delivery Charge

U.S. and Canada:	\$ 45.00
Mexico:	\$ 60.00
All other locations:	\$100.00

**Orders Must Be Prepaid in U.S. Dollars, Check Payable to The Marine Biological Laboratory**

### About *The Biological Bulletin*

ISSN: 0006-3185

Frequency: Bimonthly

Number of issues per year: 6

Months of Publication: February, April, June, August, October, December

Subscriptions entered for calendar year

Volume indexes contained in June and December issues

Annual report of the Marine Biological Laboratory contained in August issue

Most back issues available

Claims handled upon receipt

No agency discounts

Internet:

[www.biolbull.org](http://www.biolbull.org)

### Please address orders to:

Wendy Child

Subscriptions

The Biological Bulletin

Marine Biological Laboratory

7 MBL Street

Woods Hole, MA 02543-1015 U.S.A.

Fax: 508-289-7922 Tel: 508-289-7402 Email: [wchild@mbl.edu](mailto:wchild@mbl.edu)

Published by the Marine Biological Laboratory

Woods Hole, Massachusetts, 02543 U.S.A.

THE BIOLOGICAL BULLETIN  
(www.biolbull.org)  
2004 SUBSCRIPTION FORM  
(VOLUMES 206-207, 6 ISSUES)

(please print)

NAME: \_\_\_\_\_

INSTITUTION: \_\_\_\_\_

ADDRESS: \_\_\_\_\_

CITY: \_\_\_\_\_ STATE: \_\_\_\_\_

POSTAL CODE: \_\_\_\_\_ COUNTRY: \_\_\_\_\_

TELEPHONE: \_\_\_\_\_ FAX: \_\_\_\_\_

E-MAIL ADDRESS \_\_\_\_\_

All subscriptions run on the calendar year; price includes both print and online journals

Please send me a 2004 subscription to *The Biological Bulletin* at the rate indicated below:

Individual: \$120.00 (6 ISSUES)

Institutional : \$325.00 (6 ISSUES)

Individual: \$70.00 (3 ISSUES)

Institutional : \$165.00 (3 ISSUES)

Check one:  February April June or  August October December

Please send me the following back issue(s): \_\_\_\_\_

Individual: at \$25.00 (PER ISSUE)  Institutional : at \$75.00 (PER ISSUE)

### Delivery Options

\_\_\_\_\_ Surface Delivery (Surface delivery is included in the subscription price.)

\_\_\_\_\_ Air delivery (Please add the correct amount to your payment.)

U.S. and Canada: \$46.00  Mexico: \$60.00  All other locations: \$100.00

### Payment Options

\_\_\_\_\_ Enclosed is my check or U.S. money order for \$ \_\_\_\_\_ payable to The Marine Biological Laboratory

\_\_\_\_\_ Please charge my  VISA,  MasterCard  Discover Card \$ \_\_\_\_\_

\_\_\_\_\_ Please send me an invoice. (Note: Payment must be received before subscription commences.)

Account No.: \_\_\_\_\_ Exp. Date: \_\_\_\_\_

Signature: \_\_\_\_\_ Date: \_\_\_\_\_

**Return this form with your check or credit information to:**

Marine Biological Laboratory

Subscription Office ♦ The Biological Bulletin ♦ 7 MBL Street ♦ Woods Hole, MA 02543-1015

# MARINE RESOURCES CENTER

MARINE BIOLOGICAL LABORATORY • WOODS HOLE, MA 02543 • (508)289-7700

[WWW.MBL.EDU/SERVICES/MRC/INDEX.HTML](http://WWW.MBL.EDU/SERVICES/MRC/INDEX.HTML)



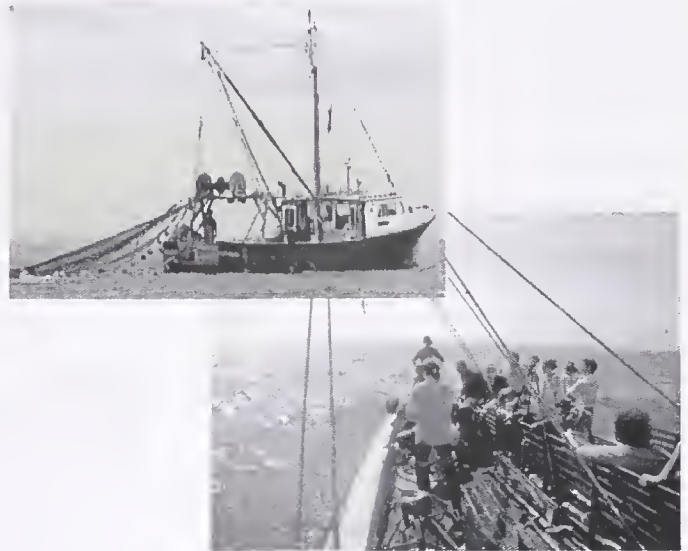
zebrafish facilities

## Animal and Tissue Supply for Education & Research

- 150 aquatic species available for shipment via online catalog: <<http://www.mbl.edu/animals/index.html>>; phone: (508)289-7375; or e-mail: [specimens@mbi.edu](mailto:specimens@mbi.edu)
- zebrafish colony containing limited mutant strains
- custom dissection and furnishing of specific organ and tissue samples

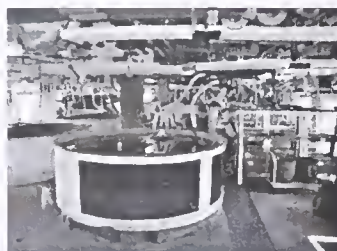
## MRC Services Available

- basic water quality analysis
- veterinary services (clinical, histopathologic, microbial services, health certificates, etc.)
- aquatic systems design (mechanical, biological, engineering, etc.)
- educational tours and collecting trips aboard the R/V Gemma



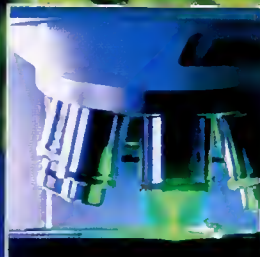
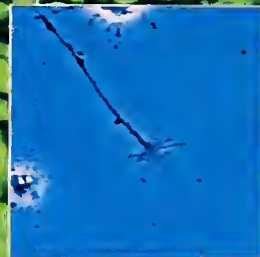
## Using the MRC for Your Research

- capability for advanced animal husbandry (temperature, light control, etc.)
- availability of year-round, developmental life stages
- adaptability of tank system design for live marine animal experimentation



# (R)EVOLUTION

## Live Cell Imaging with Carl Zeiss



You need more than brilliant optics to uncover life's secrets. You need a revolutionary new system for live cell research: The Cell Observer™ from Carl Zeiss. This innovative system was developed specifically for the observation & digital documentation of living processes. It provides a powerful combination of perfectly

matched high-performance components: microscopes, digital cameras, software & incubation peripherals. Carl Zeiss systems: so forward-thinking, we revolutionized the field.

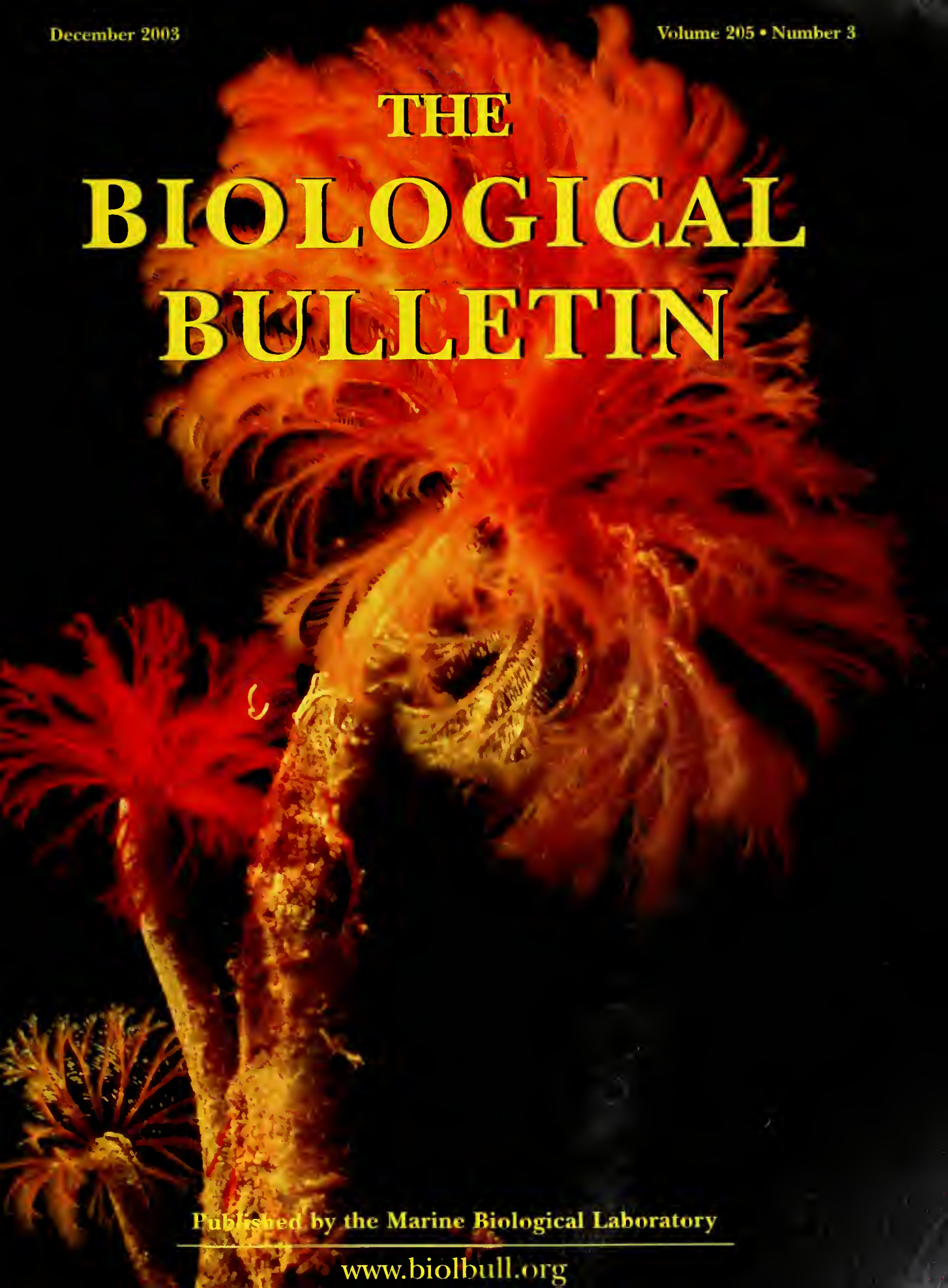
For information about Zeiss products please call 800-233-2343 or visit us online: [zeiss.com/micro](http://zeiss.com/micro).



We make it visible.

December 2003

Volume 205 • Number 3



# THE BIOLOGICAL BULLETIN

Published by the Marine Biological Laboratory

---

[www.biolbull.org](http://www.biolbull.org)



# THE BIOLOGICAL BULLETIN ONLINE

The Marine Biological Laboratory is pleased to announce that the full text of *The Biological Bulletin* is available online at

<http://www.biolbull.org>

*The Biological Bulletin* publishes outstanding experimental research on the full range of biological topics and organisms, from the fields of Neurobiology, Behavior, Physiology, Ecology, Evolution, Development and Reproduction, Cell Biology, Biomechanics, Symbiosis, and Systematics.

Published since 1897 by the Marine Biological Laboratory (MBL) in Woods Hole, Massachusetts, *The Biological Bulletin* is one of America's oldest peer-reviewed scientific journals.

The journal is aimed at a general readership, and especially invites articles about those novel phenomena and contexts characteristic of intersecting fields.

*The Biological Bulletin Online* contains the full content of each issue of the journal, including all figures and tables, beginning with the February 2001 issue (Volume 200, Number 1). The full text is searchable by keyword, and the cited references include hyperlinks to Medline. PDF files are available beginning in February 1990 (Volume 178, Number 1), some abstracts are available

beginning with the October 1976 issue (Volume 151, Number 2), and some Tables of Contents are online beginning with the October 1965 issue (Volume 129, Number 2).

Each issue will be placed online approximately on the date it is mailed to subscribers; therefore the online site will be available prior to receipt of your paper copy. Online readers may want to sign up for the eTOC (electronic Table of Contents) service, which will deliver each new issue's table of contents *via* e-mail. The web site also provides access to information about the journal (such as Instructions to Authors, the Editorial Board, and subscription information), as well as access to the Marine Biological Laboratory's web site and other *Biological Bulletin* electronic publications.

The free trial period for access to *The Biological Bulletin* online has ended. Individuals and institutions who are subscribers to the journal in print or are members of the Marine Biological Laboratory Corporation may now activate their online subscriptions. All other access (*e.g.*, to Abstracts, eTOCs, searching, Instructions to Authors) remains freely available. Online access is included in the print subscription price.

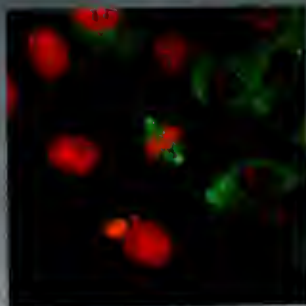
For more information about subscribing or activating your online subscription, visit [www.biolbull.org/subscriptions](http://www.biolbull.org/subscriptions).

---

<http://www.biolbull.org>

WHEN IT COMES TO INPUT/OUTPUT FLEXIBILITY, NOTHING WILL GET YOU TO AN IMAGE FASTER.

# SCIENCE UTILITY VEHICLE.



## IX81 MOTORIZED INVERTED MICROSCOPE.

Olympus' most advanced motorized inverted microscope will position your research lab at the very vanguard of multi-wavelength advanced fluorescence, DIC and deconvolution techniques.

It is totally motorized from the built-in Z-Drive, 6-position nosepiece, 6-position condenser, 6-position fluorescence filter turret, and transmitted and epifluorescence shutters.

Nine access ports allow you to keep dedicated cameras and lasers in place and still have plenty of ports available for new devices.

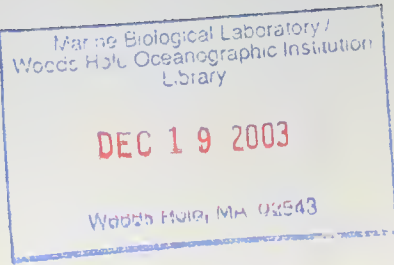
The IX81 demonstrates Olympus' leadership in Total Internal Reflection Fluorescence Microscopy (TIRFM) with exceptional ease of operation and features such as the fully integrated TIRFM illuminator, a 1.45 NA TIRFM objective and the exclusive 1.65 NA objective.

The Olympus IX81 provides extraordinary system flexibility that will satisfy the most demanding research applications.



## THE OLYMPUS IX81. ROCKET SCIENCE™

[olympusamerica.com/microscopes](http://olympusamerica.com/microscopes) 800-455-8236



### Cover

---

Sabellids, or feather-duster worms, are a diverse group of polychaete annelids common in many benthic marine habitats. Each adult sabellid secretes and inhabits an organic tube, from which it extends a crown of tentacles used for both suspension feeding and respiration. The image on the cover shows three individuals of a sabellid common in shallow waters of the northeastern Pacific, *Schizobranchia insignis*; its generic name reflects its distinctive, dichotomously branching tentacles (which, because of their respiratory function, are sometimes called branchiae). In life, the crown of the largest individual shown here is about 4 cm in diameter.

Like the planktonic larvae of other sabellids, those of *Schizobranchia insignis* do not ingest particulate food; instead, development to metamorphosis is fueled by lipids, proteins, and carbohydrates stored in the eggs. Phylogenetic evidence suggests that the nonfeeding mode of development common to sabellids is a specific example of a frequent evolutionary transition among marine invertebrates—the loss of the requirement for particulate food during the larval stage. In most known cases, this transition in larval nutrition is soon followed by dramatic reduction or outright loss of the larval structures involved in feeding. But as reported by Bruno Per-

net in this issue of *The Biological Bulletin* (p. 295), the nonfeeding larvae of *S. insignis* (and some other sabellids) possess ciliary bands that resemble, in form and behavior, bands that are used by the feeding larvae of closely related annelids to capture food particles (see Figures 3 and 4, pp. 300 and 301). In fact, larvae of *S. insignis* can use these vestigial feeding structures to capture food particles and transport them to the mouth; but because the mouth is not connected to the midgut, these particles cannot be ingested. A functional digestive system does not develop in these larvae until well after metamorphosis.

Why the larvae of some sabellids retain functional particle capture systems despite loss of both the need for food and the ability to ingest it is an interesting puzzle that remains unresolved. More generally, however, these observations suggest new, testable hypotheses about the developmental processes underlying the evolutionary loss of larval feeding in annelids and other animals with embryos that undergo spiral cleavage.

The image on the cover was photographed by Bruno Pernet (Friday Harbor Laboratories, University of Washington). The cover was designed by Beth Liles (Marine Biological Laboratory, Woods Hole, Massachusetts).

# THE BIOLOGICAL BULLETIN

## DECEMBER 2003

<b>Editor</b>	MICHAEL J. GREENBERG	The Whitney Laboratory, University of Florida
<b>Associate Editors</b>	LOUIS E. BURNETT R. ANDREW CAMERON CHARLES D. DERBY MICHAEL LABARBERA	Grice Marine Laboratory, College of Charleston California Institute of Technology Georgia State University University of Chicago
<b>Section Editor</b>	SHINYA INOUÉ, <i>Imaging and Microscopy</i>	Marine Biological Laboratory
<b>Online Editors</b>	JAMES A. BLAKE, <i>Keys to Marine Invertebrates of the Woods Hole Region</i> WILLIAM D. COHEN, <i>Marine Models Electronic Record and Compendia</i>	ENSR Marine & Coastal Center, Woods Hole Hunter College, City University of New York
<b>Editorial Board</b>	PETER B. ARMSTRONG JOAN CERDÁ ERNEST S. CHANG THOMAS H. DIETZ RICHARD B. EMLET DAVID EPEL KENNETH M. HALANYCH GREGORY HINKLE NANCY KNOWLTON MAKOTO KOBAYASHI ESTHER M. LEISE DONAL T. MANAHAN MARGARET MCFALL-NGAI MARK W. MILLER TATSUO MOTOKAWA YOSHITAKA NAGAHAMA SHERRY D. PAINTER J. HERBERT WAITE RICHARD K. ZIMMER	University of California, Davis Center of Aquaculture-IRTA, Spain Bodega Marine Lab., University of California, Davis Louisiana State University Oregon Institute of Marine Biology, Univ. of Oregon Hopkins Marine Station, Stanford University Auburn University, Alabama Dana Farber Cancer Institute, Boston Scripps Inst. Oceanography & Smithsonian Tropical Res. Inst. Hiroshima University of Economics, Japan University of North Carolina Greensboro University of Southern California Kewalo Marine Laboratory, University of Hawaii Institute of Neurobiology, University of Puerto Rico Tokyo Institute of Technology, Japan National Institute for Basic Biology, Japan Marine Biomed. Inst., Univ. of Texas Medical Branch University of California, Santa Barbara University of California, Los Angeles
<b>Editorial Office</b>	PAMELA CLAPP HINKLE VICTORIA R. GIBSON CAROL SCHACHINGER WENDY CHILD	Managing Editor Staff Editor Editorial Associate Subscription & Advertising Administrator

Published by  
MARINE BIOLOGICAL LABORATORY  
WOODS HOLE, MASSACHUSETTS

<http://www.biolbull.org>

# 2004 SUMMER RESEARCH FELLOWSHIPS

## FUNDING AVAILABLE FOR SUMMER RESEARCH IN NEUROSCIENCE AT THE MARINE BIOLOGICAL LABORATORY IN WOODS HOLE

---

The Marine Biological Laboratory is pleased to announce the availability of funding for the following summer research programs in Neuroscience in 2004. These programs will provide up to \$50,000/year/award with a possibility for renewal for 3 years. Scholars in these programs will benefit from the rich intellectual and interactive environment of the scientific community at the MBL.

**APPLICATION DEADLINE:  
JANUARY 30, 2004  
FOR  
NEUROSCIENCE  
FELLOWSHIPS**

*Applications are encouraged from women and members of underrepresented minorities.*

### **Albert and Ellen Grass Faculty Grants Program**

Proposals must describe collaborative research in any area of neuroscience by teams of two or more investigators, with a minimum stay of six weeks at the Marine Biological Laboratory in Woods Hole. Collaborative teams must consist of a minimum of two Assistant/Associate Professor level neuroscientists. Collaborative units may be formed with senior investigators but only the more junior neuroscientists will receive direct funding. Awards provide costs for research and laboratory rental, plus housing and travel costs for the PIs.

### **Dart Foundation Scholars Program in Learning & Memory**

Proposals must be devoted to the study of learning and memory with a minimum stay of six weeks at the Marine Biological Laboratory in Woods Hole. Applications are encouraged from junior or senior level neuroscientists holding a Ph.D., M.D. or equivalent degree. Awards provide costs for research and laboratory rental, plus housing and travel costs.

---

## FUNDING AVAILABLE FOR SUMMER RESEARCH

The Marine Biological Laboratory is pleased to announce the availability of funding for the following summer research programs in 2004 for junior or senior investigators holding a Ph.D., M.D., or equivalent degree. These prestigious awards provide costs for research and housing. Proposals for Fellowship support will be considered in, but are not limited to, the following fields of investigation:

**APPLICATION DEADLINE:  
JANUARY 15, 2004  
FOR  
SUMMER RESEARCH  
FELLOWSHIPS**

*Applications are encouraged from women and members of underrepresented minorities.*

**Cellular & Molecular Physiology  
Developmental Biology  
Ecology  
Microbiology**

**Molecular Biology  
Neurobiology  
Parasitology**



---

FOR APPLICATION FORMS AND ADDITIONAL INFORMATION, PLEASE CONTACT:

Sandra Kaufmann, Fellowship Coordinator  
508-289-7441; skaufman@mbl.edu

Visit our web site at

**<http://www.mbl.edu/fellowships>**

*The MBL is an Equal Opportunity/  
Affirmative Action Employer.*

**Marine Biological Laboratory~7 MBL Street~Woods Hole~Massachusetts~02543**

# CONTENTS

VOLUME 205, No. 3: DECEMBER 2003

## PHYSIOLOGY AND BIOMECHANICS

- Motokawa, Tatsuo, and Akifumi Tsuchi**  
Dynamic mechanical properties of body-wall dermis in various mechanical states and their implications for the behavior of sea cucumbers . . . . . 261
- Tomanek, Lars, and Eric Sanford**  
Heat-shock protein 70 (Hsp70) as a biochemical stress indicator: an experimental field test in two congeneric intertidal gastropods (Genus: *Tegula*) . . . 276

## DEVELOPMENT AND REPRODUCTION

- Byrne, Maria, Michael W. Hart, Anna Cerra, and Paula Cisternas**  
Reproduction and larval morphology of broadcasting and viviparous species in the *Cryptasterina* species complex . . . . . 285
- Pernet, Bruno**  
Persistent ancestral feeding structures in nonfeeding annelid larvae . . . . . 295
- Ruddell, Carolyn J., Geoffrey Wainwright, Audrey Gefen, Michael R. H. White, Simon G. Webster, and Huw H. Rees**  
Cloning, characterization, and developmental expression of a putative farnesoic acid O-methyl transferase in the female edible crab *Cancer pagurus* . . . . 308

- Lasker, Howard R., Michael L. Boller, John Castanaro, and Juan Armando Sánchez**  
Determinate growth and modularity in a gorgonian octocoral . . . . . 319

## SYMBIOSIS AND PARASITOLOGY

- Joyner, Joanna L., Suzanne M. Peyer, and Raymond W. Lee**  
Possible roles of sulfur-containing amino acids in a chemotrophic bacterium–mollusc symbiosis . . . 331
- Schwarz, J. A., and V. M. Weis**  
Localization of a symbiosis-related protein, Sym32, in the *Anthopleura elegantissima*–*Symbiodinium muscatinei* association . . . . . 339

## ECOLOGY AND EVOLUTION

- Price, Rebecca M.**  
Columellar muscle of neogastropods: muscle attachment and the function of columellar folds . . . . . 351
- Frick, Kinsey**  
Response in nematocyst uptake by the nudibranch *Flabellina verrucosa* to the presence of various predators in the southern Gulf of Maine . . . . . 367
- \* \* \*
- Index for Volume 205** . . . . . 377

# ERRATUM

On page 175 of the October issue (Volume 205, Number 2), we erred in listing the winner of the Senior Investigator category of the awards for a Short Report presented at the 2003 General Scientific Meetings of the Marine Biological Laboratory. Karen Crawford, who was listed as receiving honorable mention, should have been named as the winner of the award; Paul Gallant received honorable mention.

## THE BIOLOGICAL BULLETIN

THE BIOLOGICAL BULLETIN is published six times a year by the Marine Biological Laboratory, 7 MBL Street, Woods Hole, Massachusetts 02543.

Subscriptions and similar matter should be addressed to Subscription Administrator, THE BIOLOGICAL BULLETIN, Marine Biological Laboratory, 7 MBL Street, Woods Hole, Massachusetts 02543. Subscription includes both print and online journals. Subscription per year (six issues, two volumes): \$280 for libraries; \$105 for individuals. Subscription per volume (three issues): \$140 for libraries; \$52.50 for individuals. Back and single issues (subject to availability): \$50 for libraries; \$20 for individuals.

Communications relative to manuscripts should be sent to Michael J. Greenberg, Editor-in-Chief, or Pamela Clapp Hinkle, Managing Editor, at the Marine Biological Laboratory, 7 MBL Street, Woods Hole, Massachusetts 02543. Telephone: (508) 289-7149. FAX: 508-289-7922. E-mail: pclapp@mbl.edu.

---

<http://www.biolbull.org>

---

THE BIOLOGICAL BULLETIN is indexed in bibliographic services including *Index Medicus* and MEDLINE, *Chemical Abstracts*, *Current Contents*, *Elsevier BIOBASE/Current Awareness in Biological Sciences*, and *Geo Abstracts*.

Printed on acid free paper,  
effective with Volume 180, Issue 1, 1991.

---

POSTMASTER: Send address changes to THE BIOLOGICAL BULLETIN, Marine Biological Laboratory, 7 MBL Street, Woods Hole, MA 02543.

Copyright © 2003, by the Marine Biological Laboratory

Periodicals postage paid at Woods Hole, MA, and additional mailing offices.

ISSN 0006-3185

---

## INSTRUCTIONS TO AUTHORS

*The Biological Bulletin* accepts outstanding original research reports of general interest to biologists throughout the world. Papers are usually of intermediate length (10–40 manuscript pages). A limited number of solicited review papers may be accepted after formal review. A paper will usually appear within four months after its acceptance.

Very short, especially topical papers (less than 9 manuscript pages including tables, figures, and bibliography) will be published in a separate section entitled "Research Notes." A Research Note in *The Biological Bulletin* follows the format of similar notes in *Nature*. It should open with a summary paragraph of 150 to 200 words comprising the introduction and the conclusions. The rest of the text should continue on without subheadings, and there should be no more than 30 references. References should be referred to in the text by number, and listed in the Literature Cited section in the order that they appear in the text. Unlike references in *Nature*, references in the Research Notes section should conform in punctuation and arrangement to the style of recent issues of *The Biological Bulletin*. Materials and Methods should be incorporated into appropriate figure legends. See the article by Lohmann *et al.* (October 1990, Vol. 179: 214–218) for sample style. A Research Note will usually appear within two months after its acceptance.

The Editorial Board requests that regular manuscripts conform to the requirements set below; those manuscripts that do not conform will be returned to authors for correction before review.

1. **Manuscripts.** Manuscripts, including figures, should be submitted in quadruplicate, with the originals clearly marked. (Xerox copies of photographs are not acceptable for review purposes.) If possible, please include an electronic copy of the text of the manuscript. Label the disk with the name of the first author and the name and version of the wordprocessing software used to create the file. If the file was not created in some version of Microsoft Word, save the text in rich text format (rtf). The submission letter accompanying the manuscript should include a telephone number, a FAX number, and (if possible) an E-mail address for the corresponding author. The original manuscript must be typed in no smaller than 12 pitch or 10 point, using double spacing (including figure legends, footnotes, bibliography, etc.) on one side of 16- or 20-lb. bond paper, 8 by 11 inches. Please, no right justification. Manuscripts should be proofread carefully and errors corrected legibly in black ink. Pages should be numbered consecutively. Margins on all sides should be at least 1 inch (2.5 cm). Manuscripts should conform to the *Council of Biology Editors Style Manual*, 5th Edition (Council of Biology Editors, 1983) and to American spelling. Unusual abbreviations should be kept to a minimum and should be spelled out on first reference as well as defined in a footnote on the title page. Manuscripts should be divided into the following components: Title page, Abstract (of no more than 200 words), Introduction, Materials and Methods, Results, Discussion, Acknowledgments, Literature Cited, Tables, and Figure Legends. In addition, authors should supply a list of words and phrases under which the article should be indexed.

2. **Title page.** The title page consists of a condensed title or running head of no more than 35 letters and spaces, the manuscript title, authors' names and appropriate addresses, and footnotes listing present addresses, acknowledgments or contribution numbers, and explanation of unusual abbreviations.

3. **Figures.** The dimensions of the printed page, 7 by 9 inches, should be kept in mind in preparing figures for publication. We recommend that figures be about 1 times the linear dimensions of the final printing desired, and that the ratio of the largest to the smallest letter or number and of the thickest to the thinnest line not exceed 1:1.5. Explanatory matter generally should be included in legends, although axes should always be identified on the illustration itself. Figures should be prepared for reproduction as either line cuts or halftones. Figures to be reproduced as line cuts should be unmounted glossy photographic reproductions or drawn in black ink on white paper, good-quality tracing cloth or plastic, or blue-lined coordinate paper. Those to be reproduced as halftones should be mounted on board, with both designating numbers or letters and scale bars affixed directly to the figures. All figures should be numbered in consecutive order, with no distinction between text and plate figures and cited, in order, in the text. The author's name and an arrow indicating orientation should appear on the reverse side of all figures.

**Digital art:** *The Biological Bulletin* will accept figures submitted in electronic form; however, digital art must conform to the following guidelines. Authors who create digital images are wholly responsible for the quality of their material, including color and halftone accuracy.

**Format.** Acceptable graphic formats are TIFF and EPS. Color submissions must be in EPS format, saved in CMYK mode.

**Software.** Preferred software is Adobe Illustrator or Adobe Photoshop for the Mac and Adobe Photoshop for Windows. Specific instructions for artwork created with various software programs are available on the Web at the Digital Art Information Site maintained by Cadmus Professional Communications at <http://cpc.cadmus.com/da/>

**Resolution.** The minimum requirements for resolution are 1200 DPI for line art and 300 for halftones.

**Size.** All digital artwork must be submitted at its actual printed size so that no scaling is necessary.

**Multipanel figures.** Figures consisting of individual parts (e.g., panels A, B, C) must be assembled into final format and submitted as one file.

**Hard copy.** Files must be accompanied by hard copy for use in case the electronic version is unusable.

**Disk identification.** Disks must be clearly labeled with the following information: author name and manuscript number; format (PC or Macintosh); name and version of software used.

**Color:** *The Biological Bulletin* will publish color figures and plates, but must bill authors for the actual additional cost of printing in color. The process is expensive, so authors with more than one color image should—consistent with editorial concerns, especially citation of figures in order—combine them into a single plate to reduce the expense. On request, when supplied with a copy of a color illustration, the editorial staff will provide a pre-publication estimate of the printing cost.

4. **Tables, footnotes, figure legends, etc.** Authors should follow the style in a recent issue of *The Biological Bulletin* in

preparing table headings, figure legends, and the like. Because of the high cost of setting tabular material in type, authors are asked to limit such material as much as possible. Tables, with their headings and footnotes, should be typed on separate sheets, numbered with consecutive Arabic numerals, and placed after the Literature Cited. Figure legends should contain enough information to make the figure intelligible separate from the text. Legends should be typed double spaced, with consecutive Arabic numbers, on a separate sheet at the end of the paper. Footnotes should be limited to authors' current addresses, acknowledgments or contribution numbers, and explanation of unusual abbreviations. All such footnotes should appear on the title page. Footnotes are not normally permitted in the body of the text.

5. **Literature cited.** In the text, literature should be cited by the Harvard system, with papers by more than two authors cited as Jones *et al.*, 1980. Personal communications and material in preparation or in press should be cited in the text only, with author's initials and institutions, unless the material has been formally accepted and a volume number can be supplied. The list of references following the text should be headed Literature Cited, and must be typed double spaced on separate pages, conforming in punctuation and arrangement to the style of recent issues of *The Biological Bulletin*. Citations should include complete titles and inclusive pagination. Journal abbreviations should normally follow those of the U. S. A. Standards Institute (USASI), as adopted by BIOLOGICAL ABSTRACTS and CHEMICAL ABSTRACTS, with the minor differences set out below. The most generally useful list of biological journal titles is that published each year by BIOLOGICAL ABSTRACTS (BIOSIS List of Serials; the most recent issue). Foreign authors, and others who are accustomed to using THE WORLD LIST OF SCIENTIFIC PERIODICALS, may find a booklet published by the Biological Council of the U.K. (obtainable from the Institute of Biology, 41 Queen's Gate, London, S.W.7, England, U.K.) useful, since it sets out the WORLD LIST abbreviations for most biological journals with notes of the USASI abbreviations where these differ. CHEMICAL ABSTRACTS publishes quarterly supplements of additional abbreviations. The following points of reference style for THE BIOLOGICAL BULLETIN differ from USASI (or modified WORLD LIST) usage:

A. Journal abbreviations, and book titles, all underlined (for italics)

B. All components of abbreviations with initial capitals (not as European usage in WORLD LIST e.g., *J. Cell. Comp. Physiol.* NOT *J. cell. comp. Physiol.*)

C. All abbreviated components must be followed by a period, whole word components *must not* (i.e., *J. Cancer Res.*)

D. Space between all components (e.g., *J. Cell. Comp. Physiol.*, not *J.Cell.Comp.Physiol.*)

E. Unusual words in journal titles should be spelled out in full, rather than employing new abbreviations invented by the author. For example, use *Rit Vísindafjélagss Íslendinga* without abbreviation.

F. All single word journal titles in full (e.g., *Veliger, Ecology, Brain*).

G. The order of abbreviated components should be the same as the word order of the complete title (*i.e.*, *Proc.* and *Trans.* placed where they appear, not transposed as in some BIOLOGICAL ABSTRACTS li

H. Use well-known international journals in their preferred forms rather than WORLD LIST or USASI usage (*e.g.*, *Nature*, *Science*, *Evolution* NOT *Nature, Lond.*, *Science, N.Y.*; *Evolution, Lancaster, Pa.*)

6. **Sequences.** By the time a paper is sent to the press, all nucleotide or amino acid sequences and associated alignments should have been deposited in a generally accessible database

(*e.g.*, GenBank, EMBL, SwissProt), and the sequence accession number should be provided.

7. **Reprints, page proofs, and charges.** Authors may purchase reprints in lots of 100. Forms for placing reprint orders are sent with page proofs. Reprints normally will be delivered about 2 to 3 months after the issue date. Authors will receive page proofs of articles shortly before publication. They will be charged the current cost of printers' time for corrections to these (other than corrections of printers' or editors' errors). Other than these charges for authors' alterations, *The Biological Bulletin* does not have page charges.

#### Notice to Subscribers

2004 SUBSCRIPTION RATES FOR *THE BIOLOGICAL BULLETIN*  
Prices include print and electronic versions

	<b>Libraries</b>	<b>Individuals</b>
Per year (six issues, two volumes):	\$325.00	\$120.00
Per volume (three issues):	\$165.00	\$70.00
Back and single issues (subject to availability):	\$75.00	\$25.00

For additional information, please contact our subscription administrator at the Maine Biological Laboratory, 7 MBL Street, Woods Hole, MA 02543; tel: (508) 289-7402; e-mail: [wchild@mbledu](mailto:wchild@mbledu). Visit our website at [www.biolbull.org](http://www.biolbull.org)

# CONTENTS

## for Volume 205

No. 1: AUGUST 2003

### RESEARCH NOTE

**Drazen, Jeffrey C., Shana K. Goffredi, Brian Schlining, and Debra S. Stakes**

Aggregations of egg-brooding deep-sea fish and cephalopods on the Gorda Escarpment: a reproductive hot spot ..... 1

### EVOLUTION

**Zigler, Kirk S., and H. A. Lessios**

250 million years of bindin evolution ..... 8

### NEUROBIOLOGY AND BEHAVIOR

**Painter, Sherry D., Bret Clough, Sara Black, and Gregg T. Nagle**

Behavioral characterization of attractin, a water-borne peptide pheromone in the genus *Aphysia* ... 16

**Bergman, Daniel A., and Paul A. Moore**

Field observations of intraspecific agonistic behavior of two crayfish species, *Orconectes rusticus* and *Orconectes virilis*, in different habitats ..... 26

### PHYSIOLOGY AND BIOMECHANICS

**Etmier, Shelley A.**

Twisting and bending of biological beams: distribution of biological beams in a stiffness mechano-space ..... 36

**Eyster, L. S., and L. M. van Camp**

Extracellular lipid droplets in *Idiosepius notoides*, the Southern pygmy squid ..... 47

**Christensen, Ana Beardsley, James M. Colacino, and Celia Bonaventura**

Functional and biochemical properties of the hemoglobins of the burrowing brittle star *Hemipholis elongata* Say (Echinodermata, Ophiuroidea) ..... 54

### SYMBIOSIS AND PARASITOLOGY

**Davy, Simon K., and John R. Turner**

Early development and acquisition of zooxanthellae in the temperate symbiotic sea anemone *Anthopleura ballii* (Cocks) ..... 66

### DEVELOPMENT AND REPRODUCTION

**Neumann, Dietrich, and Heike Kappes**

On the growth of bivalve gills initiated from a lobule-producing budding zone ..... 73

**Beninger, Peter G., Gaël Le Penneec, and Marcel Le Penneec**

Demonstration of nutrient pathway from the digestive system to oocytes in the gonad intestinal loop of the scallop *Pecten maximus* L. .... 83

\* \* \*

**Annual Report of the Marine Biological Laboratory ... R1**

No. 2: OCTOBER 2003

### RESEARCH NOTE

**Seibel, Brad A., and Heidi M. Dierssen**

Cascading trophic impacts of reduced biomass in the Ross Sea, Antarctica: just the tip of the iceberg? ... 93

**Lee, Raymond W.**

Thermal tolerances of deep-sea hydrothermal vent animals from the Northeast Pacific. .... 98

### NEUROBIOLOGY AND BEHAVIOR

**Robison, Bruce H., Kim R. Reisenbichler, James C. Hunt, and Steven H. D. Haddock**

Light production by the arm tips of the deep-sea cephalopod *Vampyroteuthis infernalis* ..... 102

### ECOLOGY OF PARASITES

**Fingerut, Jonathan T., Cheryl Ann Zimmer, and Richard K. Zimmer**

Patterns and processes of larval emergence in an estuarine parasite system ..... 110

### DEVELOPMENT AND REPRODUCTION

**Gibson, Glenys D.**

Larval development and metamorphosis in *Pleurobranchaca maculata*, with a review of development in the Notaspidea (Opisthobranchia) ..... 121

## ECOLOGY AND EVOLUTION

- Chadwick-Furns, Nanette E., and Irving L. Weissman**  
Effects of allopatric genetic contact on life-history traits of the colonial ascidian *Botryllus schlosseri* in Monterey Bay . . . . . 133
- Bell, J. J., and D. K. A. Barnes**  
Effect of disturbance on assemblages: an example using Porifera . . . . . 144

## PHYSIOLOGY AND BIOMECHANICS

- Hamdoun, Amro M., Daniel P. Cheney, and Gary N. Cherr**  
Phenotypic plasticity of HSP70 and HSP70 gene expression in the Pacific oyster (*Crassostrea gigas*): implications for thermal limits and induction of thermal tolerance . . . . . 160

## SHORT REPORTS FROM THE 2003 GENERAL SCIENTIFIC MEETINGS OF THE MARINE BIOLOGICAL LABORATORY

- The Editor**  
The MBL Awards for 2003 . . . . . 175

## DEVELOPMENTAL BIOLOGY

- Gilland, Edwin, Robert Baker, and Winfried Denk**  
Long duration three-dimensional imaging of calcium waves in zebrafish using multiphoton fluorescence microscopy . . . . . 176
- Gileadi, Opher, and Alon Sabban**  
Squid sperm to clam eggs: imaging wet samples in a scanning electron microscope . . . . . 177
- Wadeson, P. H., and K. Crawford**  
Formation of the blastoderm and yolk syncytial layer in early squid development . . . . . 179
- Crawford, K.**  
Lithium chloride inhibits development along the animal vegetal axis and anterior midline of the squid embryo . . . . . 181
- Hill, Susan D., and Barbara C. Boyer**  
HNK-1/N-CAM immunoreactivity correlates with ciliary patterns during development of the polychaete *Capitella* sp. 1 . . . . . 182

## CELL BIOLOGY

- Heck, D. E., and J. D. Laskin**  
Ryanodine sensitive calcium flux regulates motility of *Arbacia punctulata* sperm . . . . . 185
- Gallant, P. E.**  
Axotomy inhibits the slow axonal transport of tubulin in the squid giant axon . . . . . 187

- Delacruz, John, Jeremiah R. Brown, and George M. Langford**  
Interactions between recombinant conventional squid kinesin and native myosin-V . . . . . 188
- DeSelm, Carl J., Jeremiah R. Brown, Renne Lu, and George M. Langford**  
Rab-GDI inhibits myosin V-dependent vesicle transport in squid giant axon . . . . . 190
- Pielak, R. M., V. A. Gaysinskaya, and W. D. Cohen**  
Cytoskeletal events preceding polar body formation in activated *Spisula* eggs . . . . . 192
- Shribak, Michael, and Rudolf Oldenbourg**  
Three-dimensional birefringence distribution in reconstituted asters of *Spisula* oocytes revealed by scanned aperture polarized light microscopy . . . . . 194
- Wöllert, Torsten, Ana S. DePina, Carl J. DeSelm, and George M. Langford**  
Rho-kinase is required for myosin-II-mediated vesicle transport during M-phase in extracts of clam oocytes . . . . . 195
- Cusato, K., J. Zakevicius, and H. Ripps**  
An experimental approach to the study of gap-junction-mediated cell death . . . . . 197
- Tepsuporn, S., J. C. Kaltenbach, W. J. Kuhns, M. M. Burger, and X. Fernández-Busquets**  
Apoptosis in *Microciona prolifera* allografts . . . . . 199
- Armstrong, Peter B., and Margaret T. Armstrong**  
The decorated clot: binding of agents of the innate immune system to the fibrils of the *Limulus* blood clot . . . . . 201
- Isakova, Victoria, and Peter B. Armstrong**  
Imprisonment in a death-row cell: the fates of microbes entrapped in the *Limulus* blood clot . . . . . 203
- Harrington, John M., and Peter B. Armstrong**  
A liposome-permeating activity from the surface of the carapace of the American horseshoe crab, *Limulus polyphemus* . . . . . 205

## NEUROBIOLOGY AND BEHAVIOR

- Bogorff, Daniel J., Mark A. Messerli, Robert P. Malchow, and Peter J. S. Smith**  
Development and characterization of a self-referencing glutamate-selective micro-biosensor . . . . . 207
- Chappell, R. L., J. Zakevicius, and H. Ripps**  
Zinc modulation of hemichannel currents in *Xenopus* oocytes . . . . . 209
- Zottoli, S. J., O. T. Burton, J. A. Chambers, R. Eseh, L. M. Gutiérrez, and M. M. Kron**  
Transient use of tricaine to remove the telencephalon has no residual effects on physiological recordings of supramedullary/dorsal neurons of the cunner, *Tautoglabrus adspersus* . . . . . 211
- Redenti, S., and R. L. Chappell**  
Zinc chelation enhances the sensitivity of the ERG b-wave in dark-adapted skate retina . . . . . 213

**Molina, Anthony J. A., Katherine Hammar, Richard Sanger, Peter J. S. Smith, and Robert P. Malchow**  
 Intracellular release of caged calcium in skate horizontal cells using fine optical fibers . . . . . 215

**Palmer, L. M., B. A. Giuffrida, and A. F. Mensinger**  
 Neural recordings from the lateral line in free-swimming toadfish, *Opsanus tau* . . . . . 216

**Child, F. M., H. T. Epstein, A. M. Kuzirian, and D. L. Alkon**  
 Memory reconsolidation in *Hemissenda* . . . . . 218

**Kuzirian, A. M., F. M. Child, H. T. Epstein, M. E. Motta, C. E. Oldenburg, and D. L. Alkon**  
 Training alone, not the tripeptide RGD, modulates calcitonin in *Hemissenda* . . . . . 220

**Savage, Anna, and Jelle Atema**  
 Neurochemical modulation of behavioral response to chemical stimuli in *Homarus americanus* . . . . . 222

**Mann, K. D., E. R. Turnell, J. Atema, and G. Gerlach**  
 Kin recognition in juvenile zebrafish (*Danio rerio*) based on olfactory cues . . . . . 224

**Turnell, E. R., K. D. Mann, G. G. Rosenthal, and G. Gerlach**  
 Mate choice in zebrafish (*Danio rerio*) analyzed with video-stimulus techniques . . . . . 225

MOLECULAR BIOLOGY, PATHOLOGY, AND MICROBIOLOGY

**Roberts, S. B., and F. W. Goetz**  
 Expressed sequence tag analysis of genes expressed in the bay scallop, *Argopecten irradians*. . . . . 227

**Hsu, A. C., and R. M. Smolowitz**  
 Scanning electron microscopy investigation of epizootic lobster shell disease in *Homarus americanus* . . . . . 228

**Orchard, Elizabeth, Erie Webb, and Sonya Dyhrman**  
 Characterization of phosphorus-regulated genes in *Trichodesmium* spp. . . . . 230

**Galac, Madeline, Deana Erdner, Donald M. Anderson, and Sonya Dyhrman**  
 Molecular quantification of toxic *Alexandrium fundyense* in the Gulf of Maine . . . . . 231

**Sangster, C. R., and R. M. Smolowitz**  
 Description of *Vibrio alginolyticus* infection in cultured *Sepia officinalis*, *Sepia apama*, and *Sepia pharaonis*. . . . . 233

**Baird, Krystal D., Hemant M. Chikarmane, Roxanna Smolowitz, and Kevin R. Uhlinger**  
 Detection of *Edwardsiella* infections in *Opsanus tau* by polymerase chain reaction. . . . . 235

**Weidner, Earl, and Ann Findley**  
 Catalase in microsporidian spores before and during discharge . . . . . 236

ECOLOGY AND POPULATION BIOLOGY

**Agnew, A. M., D. H. Shull, and R. Buchsbaum**  
 Growth of a salt marsh invertebrate on several species of marsh grass detritus . . . . . 238

**Cavatorta, Jason R., Morgan Johnston, Charles Hopkinson, and Vinton Valentine**  
 Patterns of sedimentation in a salt marsh-dominated estuary . . . . . 239

**Thoms, T., A. E. Giblin, K. H. Foreman**  
 Multiple approaches to tracing nitrogen loss in the West Falmouth wastewater plume . . . . . 242

**Talbot, J. M., K. D. Kroeger, A. Rago, M. C. Allen, and M. A. Charette**  
 Nitrogen flux and speciation through the subterranean estuary of Waquoit Bay, Massachusetts. . . . . 244

**Abraham, D. M., M. A. Charette, M. C. Allen, A. Rago, and K. D. Kroeger**  
 Radiochemical estimates of submarine groundwater discharge to Waquoit Bay, Massachusetts . . . . . 245

**Johnston, M. E., J. R. Cavatorta, C. S. Hopkinson, and V. Valentine**  
 Importance of metabolism in the development of salt marsh ponds . . . . . 248

**Aguiar, A. B., J. A. Morgan, M. Teichberg, S. Fox, and I. Valiela**  
 Transplantation and isotopic evidence of the relative effects of ambient and internal nutrient supply on the growth of *Ulva lactuca*. . . . . 250

**Morgan, J. A., A. B. Aguiar, S. Fox, M. Teichberg, and I. Valiela**  
 Relative influence of grazing and nutrient supply on growth of the green macroalga *Ulva lactuca* in estuaries of Waquoit Bay, Massachusetts . . . . . 252

**O'Connell, C. W., S. P. Grady, A. S. Leschen, R. H. Carmichael, and I. Valiela**  
 Stable isotopic assessment of site loyalty and relationships between size and trophic position of the Atlantic horseshoe crab, *Limulus polyphemus*, within Cape Cod estuaries. . . . . 254

**Walker, C., E. Davidson, W. Kinglerlee, and K. Savage**  
 Incubation conditions of forest soil yielding maximum dissolved organic nitrogen concentrations and minimal residual nitrate . . . . . 256

**Holden, M. T., C. Lippitt, R. G. Pontius, Jr., and C. Williams**  
 Building a database of historic land cover to detect landscape change . . . . . 257

ORAL PRESENTATIONS

Published by title only . . . . . 259

**PHYSIOLOGY AND BIOMECHANICS**

**Motokawa, Tatsuo, and Akifumi Tsuchi**  
 Dynamic mechanical properties of body-wall dermis in various mechanical states and their implications for the behavior of sea cucumbers . . . . . 261

**Tomanek, Lars, and Eric Sanford**  
 Heat-shock protein 70 (Hsp70) as a biochemical stress indicator: an experimental field test in two congeneric intertidal gastropods (Genus: *Tegula*) . . . 276

**DEVELOPMENT AND REPRODUCTION**

**Byrne, Maria, Michael Hart, Anna Cerra, and Paula Cisternas**  
 Reproduction and larval morphology of broadcasting and viviparous species in the *Cryptasterina* species complex . . . . . 285

**Pernet, Bruno**  
 Persistent ancestral feeding structures in nonfeeding annelid larvae . . . . . 295

**Ruddell, Carolyn J., Geoffrey Wainwright, Andrey Gef-fen, Michael R. H. White, Simon G. Webster, and Huw H. Rees**  
 Cloning, characterization, and developmental ex-pression of a putative farnesoic acid *O*-methyl trans-ferase in the female edible crab *Cancer pagurus* . . . . 308

**Lasker, Howard R., Michael L. Boller, John Castanaro, and Juan Armando Sánchez**  
 Determinate growth and modularity in a gorgonian octocoral . . . . . 319

**SYMBIOSIS AND PARASITOLOGY**

**Joyner, Joanna L., Suzanne M. Peyer, and Raymond W. Lee**  
 Possible roles of sulfur-containing amino acids in a chemoautotrophic bacterium–mollusc symbiosis . . . 331

**Schwarz, J. A., and V. M. Weis**  
 Localization of a symbiosis-related protein, Sym32, in the *Anthopleura elegantissima*–*Symbiodinium muscatinei* association . . . . . 339

**ECOLOGY AND EVOLUTION**

**Price, Rebecca M.**  
 Columellar muscle of neogastropods: muscle attach-ment and the function of columellar folds . . . . . 351

**Frick, Kinsey**  
 Response in nematocyst uptake by the nudibranch *Elabellina verrucosa* to the presence of various preda-tors in the southern Gulf of Maine . . . . . 367

\* \* \*

**Index for Volume 205** . . . . . 377

# Dynamic Mechanical Properties of Body-Wall Dermis in Various Mechanical States and Their Implications for the Behavior of Sea Cucumbers

TATSUO MOTOKAWA\* AND AKIFUMI TSUCHI

*Department of Biological Sciences, Graduate School of Bioscience and Biotechnology, Tokyo Institute of Technology, Meguro, Tokyo, 152-8551 Japan*

**Abstract.** The dermis of the sea cucumber body wall is a typical catch connective tissue that rapidly changes its mechanical properties in response to various stimuli. Dynamic mechanical properties were measured in stiff, standard, and soft states of the sea cucumber *Actinopyga mauritiana*. Sinusoidal deformations were applied, either at a constant frequency of 0.1 Hz with varying maximum strain of 2%–20% or at a fixed maximum strain of 1.8% with varying frequency of 0.0005–50 Hz. The dermis showed viscoelasticity with both strain and strain-rate dependence. The dermis in the standard state showed a J-shaped stress-strain curve with a stiffness of 1 MPa and a dissipation ratio of 60%; the curve of the stiff dermis was linear with high stiffness (3 MPa) and a low dissipation ratio (30%). Soft dermis showed a J-shaped curve with low stiffness (0.3 MPa) and a high dissipation ratio (80%). The strain-induced softening was observed in the soft state. Stiff samples had a higher storage modulus and a lower tangent  $\delta$  than soft ones, implying a larger contribution of the elastic component in the stiff state. A simple molecular model was proposed that accounted for the mechanical behavior of the dermis. The model suggested that stiffening stimulation increased intermolecular bonds, whereas softening stimulation affected intra-molecular bonds. The adaptive significance of each mechanical state in the behavior of sea cucumbers is discussed.

## Introduction

Echinoderms have collagenous connective tissues that can alter their mechanical properties rapidly under nervous

control (Motokawa, 1984a; Wilkie, 1996). Connective tissue with such mutability is called catch connective tissue or mutable connective tissue. The mutability has been attributed to the changes in the mechanical properties of the extracellular materials in the tissue (Motokawa, 1984a; Wilkie, 2002; Tipper *et al.*, 2003). The dermis in the body wall of sea cucumbers is a favored material for studies of connective tissue catch because of its large size. The mechanical properties of the dermis have been described by various mechanical methods such as creep tests (Motokawa, 1981; Eylers, 1982), stress-strain tests (Motokawa, 1982), stress-relaxation tests (Motokawa, 1984b; Greenberg and Eylers, 1984), tensile tests (Motokawa, 1982), and dynamic tests (Shibayama *et al.*, 1994; Szulgit and Shadwick, 2000). These studies revealed the viscoelastic nature of the dermis. They drew, however, contradictory conclusions about which component, elastic or viscous, changed during alterations in mechanical properties. Motokawa (1984b) concluded from the results of creep tests and stress-relaxation tests that the changes in the mechanical properties mainly occurred in the viscous component, whereas Szulgit and Shadwick (2000) concluded that it was the elastic component that changed. The former used a fixed strain and the latter a fixed strain and strain rate. The apparently contradictory conclusions of these two studies are not surprising, because viscoelastic materials exhibit different properties when tested under different conditions of strain and strain rate (Wainwright *et al.*, 1976). Therefore, description of the mechanical properties of viscoelastic materials is not satisfactory in a limited range of strain and strain rate. The present study was undertaken to describe the dynamic mechanical properties of the holothurian dermis under wide ranges of both strain and strain rate. The information obtained establishes a basis for understanding the mechanism of connective tissue catch and how sea cucumbers adapt to

Received 12 May 2003; accepted 5 September 2003.

\* To whom correspondence should be addressed. E-mail: tmotokaw@bio.titech.ac.jp

various mechanical environments by changing the mechanical properties of the dermis.

## Materials and Methods

### Tissue samples

Specimens of the aspidochirotid sea cucumber *Actinopyga mauritiana* (Quay and Gaimard) were collected from the lagoon in front of Sesoko Marine Science Center, University of the Ryukyus, Okinawa. They were shipped to Tokyo Institute of Technology and kept in an aquarium in our laboratory. This sea cucumber has a thick body wall (about 1–1.5 cm). The connective tissue dermis occupies most of the thickness. The outer side of the dermis is covered with a thin epidermis, and the inner side is lined with body wall muscles. Unlike some dendrochirotid species such as *Cucumaria frondosa*, the dermis of this aspidochirotid sea cucumber looks uniform, showing no differentiation into layers. A dermis sample was dissected from the lateral interambulacrum of the body wall. Both the epidermis and muscles were removed and the middle portion of the dermis was cut out for experiments. The dimensions of the samples were measured with a caliper to a precision of 0.05 mm. The mean length of the samples from oral to aboral end was 2.3 mm ( $\pm 0.89$  mm SD;  $n = 79$ ), and the mean cross-sectional area was 5.4 mm<sup>2</sup> ( $\pm 1.9$  mm<sup>2</sup> SD;  $n = 79$ ). The samples were rested in artificial seawater of normal composition (ASW) for 17–24 h before being subjected to mechanical tests. The temperature of the seawater was 18–25 °C, which roughly corresponded to the temperature of the water from which the sea cucumbers were collected. Mechanical tests were performed at a constant temperature of 20 °C.

Samples that were rested in ASW for 17–24 h and tested in ASW are described here as being in a standard state. Soft-state samples were prepared by removal of calcium ions (Hayashi and Motokawa, 1986); they were rested in calcium-free artificial seawater (CaFASW) and tested in CaFASW. Stiff-state samples are those that were tested in ASW without a resting period. Rough physical handling makes the dermis stiffen reversibly (Motokawa, 1984c). Soon after the dissection, the dermis experienced quite rough physical handling, so these are termed the physically stimulated samples. This state probably corresponds to the state the sea cucumbers are in after being stimulated physically. Two other kinds of stimulation were employed to invoke the stiff state (possibly through stimulating the stiffening mechanism *in vivo*)—chemical stimulation by the neurotransmitter acetylcholine (ACh) (Motokawa, 1987) and chemical stimulation using artificial seawater with an elevated potassium concentration (KASW). The latter likely stimulates a cellular mechanism that controls stiffness, such as nerves, through depolarization (Motokawa, 1981).

The samples for chemical stimulation were rested for 17–24 h in ASW, and chemicals were applied 20 min before

the mechanical testing. The composition of ASW was as follows (in mmol/l): NaCl, 433.7; KCl, 10.0; CaCl<sub>2</sub>, 10.1; MgCl<sub>2</sub>, 52.5; NaHCO<sub>3</sub>, 2.5. In KASW, the concentration of potassium was raised to 100 mmol/l, and CaFASW contained 5 mmol/l EGTA (ethylene glycol bis( $\beta$ -aminoethyl-ether)-*N*, *N*, *N'*, *N'*-tetraacetic acid). In both cases, the sodium concentration was adjusted to keep the osmotic concentration constant. ACh concentration was 10<sup>-4</sup> mol/l in ASW. The pH of all the solutions was adjusted to 8.2.

### Experimental apparatus

A dermis sample was subject to forced vibrations using sinusoidal displacements. The sample was stretched and compressed cyclically, and the resulting forces were recorded. The experimental apparatus (Fig. 1) included a vibrator (511-A, EMIC, Japan) driven by sinusoidal currents that were generated by a function generator (SG-4101, Iwatsu, Japan). The force developed in the dermis was measured by a micro load cell (LTS-200GA, Kyowa, Japan). The compliance of the load cell was 0.3  $\mu$ m/g, which contributed at most 4% to the measured value of strain in the present experiments. The deformation of the dermis was monitored by an eddy-current displacement sensor (502-F, EMIC, Japan). Force signals were amplified by a strain amplifier (DPM-602A, Kyowa, Japan). Both force and displacement signals were displayed on an oscilloscope and simultaneously recorded by a computer through a data-acquisition unit (Lab Stack, Keisoku Giken, Japan). The dermis sample was glued with cyanoacrylate glue to the holders, one attached to the vibrator and the other to the load

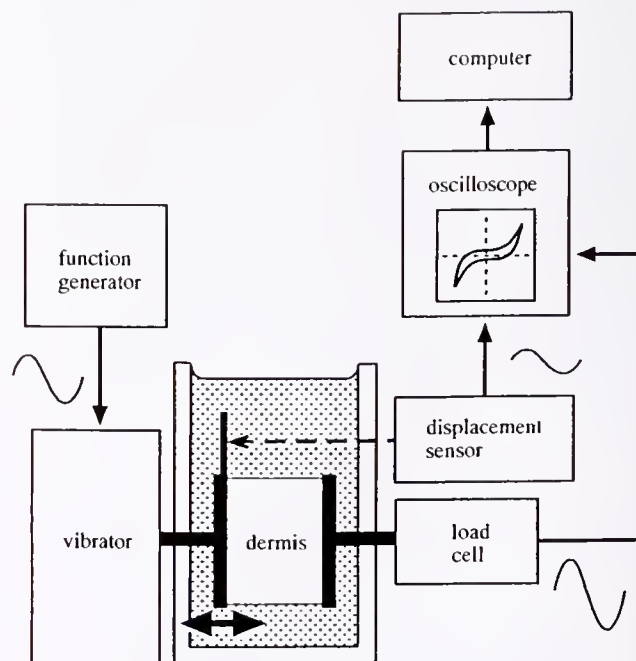


Figure 1. Schematic of the experimental apparatus for dynamic tests.

cell, and an experimental solution was introduced to the trough. The sample was usually rested for 20 min in the trough; however, the physically stimulated sample was tested immediately. The trough was water-jacketed to keep the temperature constant at 20 °C.

We performed two series of experiments. In the constant-frequency experiments, the frequency of vibration was kept constant at 0.1 Hz and the maximum strain in a cycle was varied between 2% and 20%. A frequency of 0.1 Hz was chosen because the differences in the mechanical properties of the three states were most prominent at this frequency (see Results). In the constant-maximum-strain experiments, the maximum strain in a cycle was kept at 1.8% and the frequency was varied between 0.0005 and 50 Hz. A maximum strain of 1.8% was chosen because the dermis behaved as a linear viscoelastic material at this strain (see Results).

The samples were preconditioned by applying oscillations for 10 min prior to the test; the amplitude and frequency were the same as those in the test. A steady-state response was reached by the preconditioning.

#### Constant-frequency experiment

In experiments that examined the effects of strain, a dermis sample was subjected to successive oscillatory tests with different levels of maximum strain. The hysteresis loop of the stress-strain relationship showed almost point symmetry. The point of symmetry was brought to the origin of the coordinates by adjusting the length of the sample. Data were then collected, and a typical hysteresis loop was generated for that maximum strain. When the data acquisition was finished at a certain maximum strain, the maximum strain in an oscillatory cycle was increased by about 4% (range 2%–7%), the sample was preconditioned, and data were collected with the new maximum strain.

Strain ( $\epsilon$ ) was defined as the length change divided by the original length of the sample, and stress ( $\sigma$ ) as the force divided by the cross-sectional area at the original length. When stress was plotted against strain, a closed hysteresis loop was obtained (Fig. 2). Because the dermis behaved quite similarly in tension and in compression, the values given in this paper are the averages of the absolute values at equal strains in tension and in compression. The maximum strain imposed in a loop was denoted as the maximum strain ( $\epsilon_{\max}$ ), and the maximum stress observed in a loop was denoted as the maximum stress ( $\sigma_{\max}$ ). A quarter of the loop had the shape of the letter “J” with a flat “toe” region and a more vertical “pole” region. We introduced an index (the  $J$  index) to quantify the degree of concavity of the stress-strain curves in the loading and unloading phases in tensile strain. We defined the  $J$  index as the area enclosed by the stress-strain curve and the line connecting the peak point with the intersecting point at 0 strain in the curve, divided by the area of a right triangle whose hypotenuse was the same line as before, one side was a horizontal extending

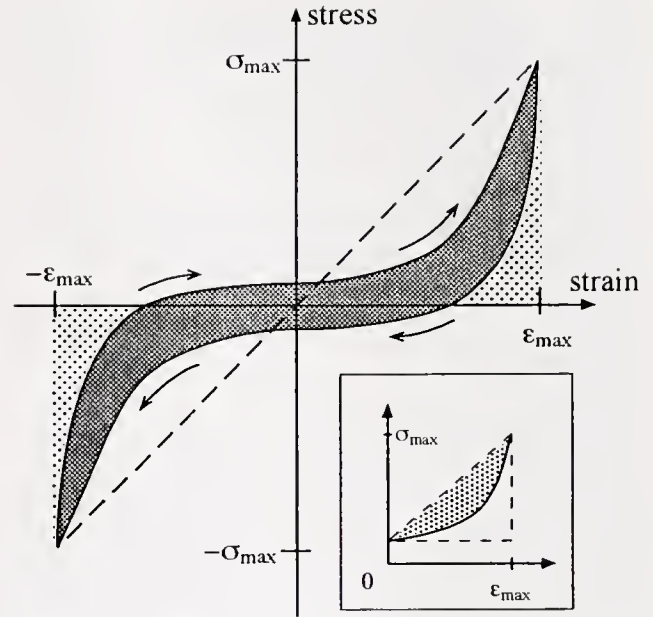


**Figure 2.** Schematic of a hysteresis loop of the dermis in standard state under a sinusoidal deformation of 10% maximum strain at 0.1 Hz. The loop showed clockwise rotation (arrows). The stiffness was defined as the slope of the dotted line. The darker hatched area represents the dissipated energy, the lighter hatched areas the conserved energy, and the total hatched area the deformation energy. The inset shows how the  $J$  index was measured: it was the percent ratio of the hatched area to the area of the triangle shown by dotted lines.

from the intersecting point, and the other side was a vertical extending from the peak point (Fig. 2 inset). The  $J$  index was equivalent to the difference between the energy fed into the specimen and the deformation energy of an elastic body with a linear stress-strain curve; the  $J$  index is thus a measure of how concave the stress-strain curve was. The  $J$  index was defined as 0 when the curve was convex. The stiffness was defined as the slope between the two peaks of a hysteresis loop. The deformation energy ( $E_t$ ) was defined as the hatched area in Figure 2. It corresponds to the energy required to deform the dermis of a unit volume for one cycle. In each cycle of deformation, the deformation energy is partly conserved and reused as elastic recoil to restore the geometry of the sample; the rest is dissipated and lost, primarily as thermal energy. The energy dissipated ( $E_d$ ) corresponds to the area enclosed by the hysteresis loop. The dissipation ratio  $D$  was defined as  $D = E_d/E_t$  and was expressed as a percentage.

The limit strain was estimated as the average of the smallest maximum strain that caused the strain-induced softening and a maximum strain one step smaller (where strain-induced softening was not observed).

Reversibility of the response was determined by successive mechanical tests using the same sample. The sample in the stiff state caused by physical stimulation was tested, then rested for 22 h and tested again. In the chemically

stimulated stiff samples, the preparations were first tested in ASW and then treated with stimulation media for 20 min before the second mechanical tests. Samples were washed thoroughly in ASW for 24 h, and the third mechanical test was performed.

We also determined whether softening induced by stretching the samples in CaFASW beyond the limit strain was recoverable when the maximum strain was reduced to less than the limit strain. The sample was tested at  $\epsilon_{\max} = 2\%$  in CaFASW. Then oscillations of  $\epsilon_{\max}$  of about 30% were given for 10 min, and the sample was tested again at  $\epsilon_{\max} = 2\%$ .

#### Constant-maximum-strain experiment

In this experiment, the maximum strain was kept constant at 1.8% and the frequency was varied in a dermis sample. A sample was tested first at 0.1 Hz. Then the test frequency was either increased stepwise to 0.5, 1, 5, 10, and 50 Hz or decreased to 0.05, 0.01, 0.005, 0.001, and 0.0005 Hz. The data from 10 cycles at each frequency were averaged in all experiments except at the lowest two frequencies, where data for two cycles were averaged.

In a viscoelastic material, stress and strain are not in phase—rather, strain lags behind stress by a phase angle  $\delta$ . For a linear viscoelastic material, the complex modulus  $E^*$ , the storage modulus  $E'$ , and the loss modulus  $E''$  are defined as follows (Oka, 1974).

$$E^* = \sigma/\epsilon = E' + iE''$$

$$E' = |E^*| \cos \delta$$

$$E'' = |E^*| \sin \delta$$

$$\tan \delta = E''/E'$$

The complex modulus represents the conventional "stiffness." The storage modulus is equivalent to the elastic modulus in phase with the stress and is a measure of the energy elastically stored in each cycle. The loss modulus is the out-of-phase component and is a measure of the energy dissipated. Tangent  $\delta$  is the ratio of the energy lost to the energy stored.

The soft state was induced by a vibration of 0.1 Hz with  $\pm 20\%$  maximum strain applied for 30 min in CaFASW. Such a treatment caused strain-induced softening (see Results). The softened sample was subsequently tested in CaFASW.

## Results

#### Constant-frequency experiments

*Hysteresis loop at maximum strain = 10% and frequency = 0.1 Hz.* When stress was plotted against strain, a closed hysteresis loop of clockwise rotation was generated. The loop could be divided into four phases: a tensile phase

in which the dermis was gradually stretched, a tension-unloading phase in which the tensile strain decreased, a compressing phase in which the dermis was gradually compressed, and a compression-unloading phase in which the compressive strain decreased.

The hysteresis loop of a sample in the standard state at 10% maximum strain is shown in Figure 3a. When stretched from zero strain, the dermis could be deformed quite easily; thus the slope of the curve was flat at first, corresponding to the toe region of the J. When strain exceeded about 5%, the slope became progressively steeper; thus the tensile stress-strain relation followed a typical J-shaped curve (Wainwright *et al.*, 1976). The *J* index averaged 43% ( $\pm 9.1\%$  SD,  $n = 17$ ). After the tensile stress peaked, the unloading phase started and stress decreased rapidly. The slope was steeper than that in the loading phase at each strain. As the strain progressively decreased, the slope declined and the curve became almost flat. The *J* index of the unloading phase averaged 71% ( $\pm 13\%$  SD,  $n = 17$ ), much greater than that of the loading phase (significant difference by paired *t* test,  $P < 0.01$ ). In the loading and unloading phases of the compression half of the cycle, the curve followed almost the same course as that of the tensile half with the sign of stress and strain reversed. Thus the dermis behaved similarly in tension and compression. The four phases of the hysteresis loop all exhibited a J shape, and the whole loop showed approximate point symmetry.

The loops of stiff samples differed from those of samples in the standard state both in shape and in the stress developed (Fig. 3b, c, d). The J shape became less prominent: the toe region became short (restricted to strains under 2%–4%) and was not flat but had a steep slope so that there was only a small kink between toe and pole. Thus each phase of the hysteresis loop in stiff samples was rather straight, which made the *J* index small. The *J* indices of the loading phase in samples stiffened by physical stimulation, KASW stimulation, and ACh stimulation were  $9.0\% \pm 8.2\%$  ( $n = 4$ ),  $19\% \pm 11\%$  ( $n = 4$ ), and  $26 \pm 6.0$  ( $n = 5$ ), respectively (average  $\pm$  SD). The average *J* indices were significantly smaller than that of the standard state (Scheffé test,  $P < 0.01$ ). In stiff samples, the shape of the stress-strain curve during the unloading phase showed no great difference from that of the loading phase. The *J* indices during the unloading phase in samples stiffened by physical stimulation, KASW stimulation, and ACh stimulation were  $14\% \pm 8.6\%$  ( $n = 4$ ),  $23\% \pm 12\%$  ( $n = 4$ ), and  $33 \pm 8.9$  ( $n = 5$ ), respectively (average  $\pm$  SD). The *J* index of the unloading phase in a hysteresis curve was slightly larger than that of the loading phase, but the statistical comparison of the averages showed no significant difference. In stiff samples, the maximum stress was much larger and the area enclosed by a loop was much smaller than in samples in standard state. These features implied that the stiffened dermis behaved like a stiff, resilient spring.

The hysteresis loop of soft samples was rather flat in

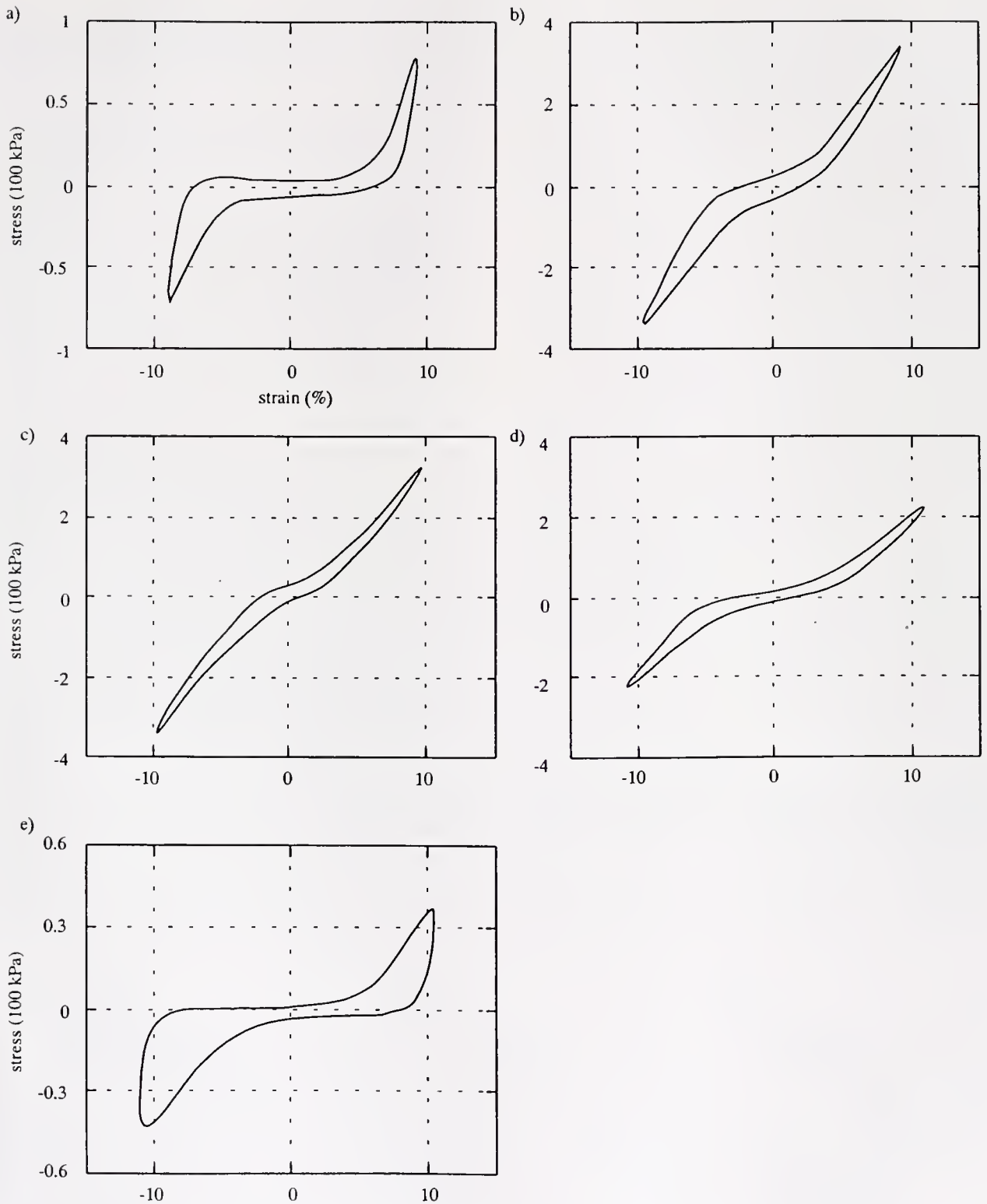


**Figure 3.** Typical hysteresis loops at 10% maximum strain and 0.1 Hz frequency. (a) Standard state. (b–d) Stiff state induced by physical stimulation (b), by KASW (c), and by  $10^{-4}$  mol/l acetylcholine (d). (e) Soft state.

loading (Fig. 3e). This is because the toe region was similar, both in length (strain) and in height (stress) to that of the standard, but the pole was shorter; for example, the maxi-

mum stress was much smaller in the soft state than in the standard state. The  $J$  index in loading phase averaged  $27\% \pm 8.9\%$  (average  $\pm$  SD,  $n = 9$ ) which was significantly

smaller than that of the standard state (Scheffé test,  $P < 0.01$ ). The shape of the stress-strain curve during the unloading phase showed marked differences from that of the loading phase: in the unloading phase, stress sharply decreased from the peak to give a  $J$  index as high as  $86\% \pm 7.1\%$  (average  $\pm$  SD,  $n = 9$ ), which was statistically different from that of the loading phase (paired  $t$  test,  $P < 0.01$ ). This made the area enclosed by the hysteresis loop larger. These features implied that the dermis in the softened state became more compliant and less resilient.

*Influence of maximum strain on the hysteresis loop.* At  $\epsilon_{\max} = 0.5\%–3\%$ , the hysteresis loop followed a skewed ellipse regardless of the state of the samples, showing no signs of the J-shaped curve seen at larger strains. Both  $E^*$  and  $\tan \delta$  were constant in this strain range. Thus the dermis behaved as a linear viscoelastic material.

The maximum strain was increased stepwise by increments of 2%–4% starting from  $\epsilon_{\max} = 2\%–3\%$ . In standard samples, the hysteresis loops of  $\epsilon_{\max} = 5\%–25\%$  were composed of prominent J curves. The peak stress became higher as  $\epsilon_{\max}$  increased (Fig. 4a). The  $J$  index increased as  $\epsilon_{\max}$  increased from 5% to 15%, and thus the stress-strain curve showed a more pronounced J shape as  $\epsilon_{\max}$  increased up to 15%. In stiff samples, the shape of the loop was quite similar for  $\epsilon_{\max}$  between 5% and 15% (Fig. 4b) with a constant  $J$  index. The maximum stress ( $\sigma_{\max}$ ) increased as  $\epsilon_{\max}$  increased. The samples detached from the holders when  $\epsilon_{\max}$  exceeded about 15%.

In soft samples, the shape of the hysteresis loop and the maximum stress both showed a marked dependence on  $\epsilon_{\max}$  (Fig. 4c). When  $\epsilon_{\max}$  was increased above 5%,  $\sigma_{\max}$  also increased at first, but once  $\epsilon_{\max}$  exceeded a certain value (the limit strain)  $\sigma_{\max}$  decreased as  $\epsilon_{\max}$  increased. The limit strain was 8.0%–18.2% (average = 11.2%, SD = 3.9%,

$n = 6$ ). The hysteresis loop above the limit strain had a long toe region, which was expected from the larger  $J$  index with smaller  $\sigma_{\max}$ . The dermis ruptured when  $\epsilon_{\max}$  exceeded 18%–26%.

The sample that experienced strain-induced softening was softer than before, even when measured at strains smaller than the limit strain. The stiffness of soft samples was measured first at  $\epsilon_{\max} = 2\%$  in CaFASW; values averaged 0.24 MPa ( $\pm 0.12$  SD,  $n = 11$ ). The samples were then subjected to vibrations beyond the limit strain for 10 min and tested again at 2%  $\epsilon_{\max}$ . The stiffness in the second series of tests averaged 0.010 MPa ( $\pm 0.005$  SD,  $n = 10$ ), which was significantly smaller (paired  $t$  test,  $P < 0.01$ ) than the initial values. Once strain-induced softening occurred, the decreased stiffness was apparent not only at strains over the limit strain but also for strains under the limit strain.

*Stiffness, deformation energy, and dissipation ratio.* Table 1 summarizes the mechanical properties of the samples in each of the three states, and Figure 5 shows the dependence of mechanical properties on the maximum strain. In standard samples, the stiffness increased 2- to 3-fold as  $\epsilon_{\max}$  increased from 2% to 5%; it remained almost constant at a value of about 1 MPa above 5% (Fig. 5a). In stiff samples, the stiffness was almost independent of  $\epsilon_{\max}$  at a value of about 3 MPa, 2.5–3.5 times greater than that of standard samples. The average stiffness values of stiff samples (regardless of the stimulation used to stiffen the sample) were significantly greater than those of standard samples ( $P < 0.01$ ) at a maximum strain of both 3% and 5% (Table 1). There were no significant differences in stiffness among stiff samples produced by different stimuli.

The stiffness was low in the soft samples. At strains less

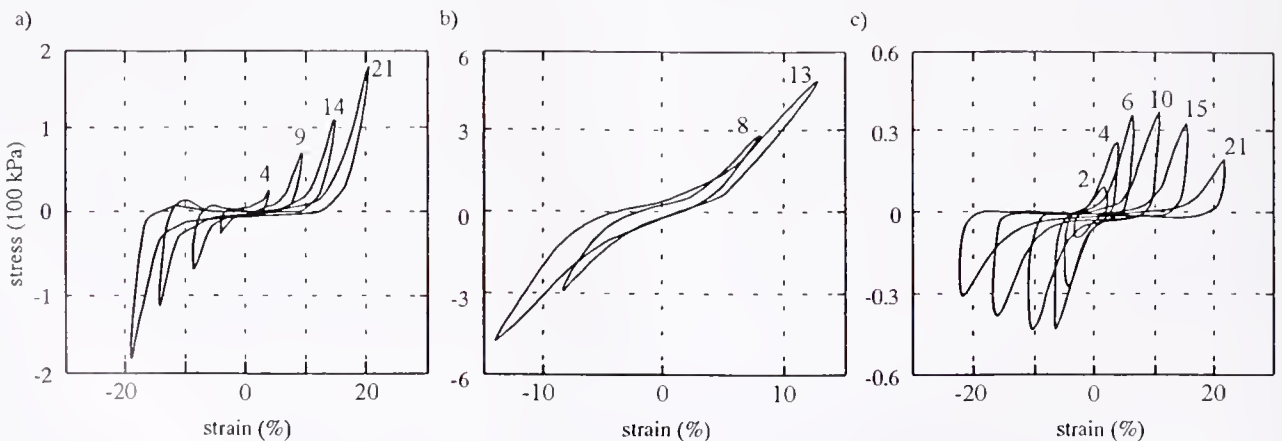


Figure 4. Typical examples of effects of maximum strain on hysteresis loops measured at 0.1 Hz: (a) standard state; (b) stiff state induced by physical stimulation; (c) soft state. The maximum strain was increased stepwise in a single sample in each state. The number above each loop is the maximum strain rounded to the nearest integer. The curves of some steps were not shown except in c. Note that in the soft state, strain-induced softening was observed; the maximum stress decreased as maximum strain increased from 10% to 21%. The limit strain was estimated as 11.2% (see text).

Table 1

Mechanical properties of sea cucumber dermis

Mechanical properties	Maximum strain		
	3%	10%	18%
<b>Stiffness (MPa)</b>			
Stiff			
physical	3.1 ± 0.37 (5)**	3.4 ± 0.61 (4)**	—
KASW	3.1 ± 0.95 (5)**	2.7 ± 0.53 (4)**	—
ACh	2.3 ± 0.60 (6)**	2.4 ± 0.85 (5)**	—
Standard	0.77 ± 0.30 (14)	1.0 ± 0.34 (17)	1.1 ± 0.32 (9)
Soft	0.28 ± 0.11 (4)	0.29 ± 0.25 (9)**	0.12 ± 0.070 (5)**
<b>Deformation energy (kPa)</b>			
Stiff			
physical	5.0 ± 0.85 (5)**	38 ± 6.9 (4)**	—
KASW	5.1 ± 1.1 (5)**	28 ± 9.1 (4)**	—
ACh	3.7 ± 0.61 (6)**	22 ± 7.6 (5)**	—
Standard	1.4 ± 0.53 (14)	9.4 ± 3.9 (17)	25 ± 9.8 (9)
Soft	0.48 ± 0.31 (4)	3.0 ± 2.8 (9)	3.1 ± 2.3 (5)**
<b>Dissipation ratio (%)</b>			
Stiff			
physical	19 ± 11 (5)**	29 ± 7.0 (4)*	—
KASW	20 ± 11 (5)**	31 ± 5.1 (4)*	—
ACh	32 ± 8.3 (6)	32 ± 11 (5)*	—
Standard	48 ± 10 (14)	59 ± 18 (17)	54 ± 12 (9)
Soft	61 ± 14 (4)	78 ± 11 (9)*	77 ± 16 (5)*

A series of data at different maximum strain were obtained from the same sample. Values are averages ± SD (*n*). The average is that of samples that were taken from different individuals. For 3% and 10% maximum strains, the Scheffé test was used for *post hoc* statistical analysis after the analysis of variance. An unpaired *t* test was used for 18% maximum strain.

\* The mean is significantly different from that of the standard (*P* < 0.05).

\*\* The mean is significantly different from that of the standard (*P* < 0.01).

— No data were obtained because the samples detached from the holders when maximum strain exceeded about 15%.

than 10%, the stiffness of soft samples was one-tenth that of the stiff state and one-third of the standard state. Because the peak stress (and thus the stiffness) decreased above the limit strain, the differences in the stiffness were more marked at  $\epsilon_{max} = 18\%$ , where stiffness was one-tenth of the standard (Table 1).

Deformation energy increased with  $\epsilon_{max}$  in all three states except for the region above the limit strain in soft samples (Fig. 5b). When compared with standard samples, stiff samples required 2–4 times more energy to deform, whereas soft samples required less energy, especially when  $\epsilon_{max}$  exceeded the limit strain (Table 1).

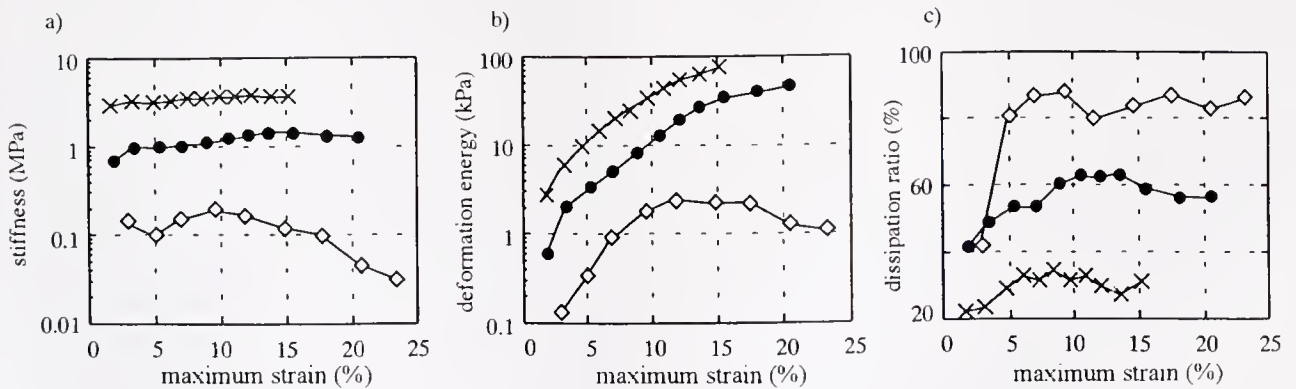


Figure 5. Effects of maximum strain on mechanical properties measured at 0.1 Hz. A typical example was chosen for each state from 5 to 6 dermis samples from different individuals: (a) stiffness; (b) deformation energy; (c) dissipation ratio. Curves with the same symbol are from the same preparation. The stiff sample (cross) was produced by physical stimulation. Filled circle, standard sample; diamond, soft sample.

The dissipation ratio increased as  $\varepsilon_{\max}$  increased from 2% to 5%, but it remained almost constant for larger  $\varepsilon_{\max}$  (Fig. 5c). About 60% of the deformation energy was dissipated in standard samples at  $\varepsilon_{\max} = 10\%$  (Table 1). The dissipation ratio was halved in stiff samples but increased to as much as 80% in soft samples. The average values at a maximum strain of 10% in the stiff and soft states were significantly different from that of the standard state ( $P < 0.05$ ).

**Reversibility of responses.** Whether the stiffened dermis, which was stimulated from the standard state, resumed the standard state after removal of the stimuli was examined by successive measurements on the same sample. The stiffening response was reversible—stiffened samples resumed the standard state after resting in ASW for 1 day (Fig. 6). Although it took 2 days from the time of preparation to the completion of measurements in the chemically stimulated samples, the samples did not show any sign of decay, and the mechanical parameters in ASW after stimulation were similar to those in ASW before stimulation.

#### Constant-maximum-strain experiments

No increase in stress was observed during the preconditioning period, which implied that the imposed vibration of 1.8% strain did not act as a mechanical stimulus for the dermis. Stiffening of the dermis by forced vibration has been reported in other sea cucumbers but at much larger strains (Shibayama *et al.*, 1994).

The frequency dependence of  $E^*$ ,  $E'$ ,  $E''$ , and  $\tan \delta$  in the standard state is given in Figure 7. The complex modulus  $E^*$  gave a sigmoid curve (Fig. 7a).  $E^*$  took a low and rather constant value of about 20 kPa at frequencies lower than 0.005 Hz. At 1 Hz and higher it showed a rather constant value of about 3 MPa.  $\tan \delta$  was more or less constant in the lower frequencies with a maximum value of about 1, and for frequencies exceeding 0.01 Hz it decreased with frequency to 0.06 at 50 Hz (Fig. 7b).  $E'$  exhibited a curve similar to that of  $E^*$ , with the value for each frequency a

little smaller than that of  $E^*$  (Fig. 7c).  $E''$  also showed a sigmoid curve (Fig. 7d) with values similar to that of  $E'$  for frequencies lower than 0.01 Hz. However,  $E''$  was about one-tenth of  $E'$  in the high-frequency range, reflecting the fact that  $\tan \delta$  was less than 1 at higher frequencies.

The frequency dependence of stiff and soft states is given in Figure 8. All curves of stiff states induced by different stimuli coincided well, suggesting that the three stimuli invoked an identical mechanical state.

The curve of  $E^*$  in the stiff state was different in shape and position from that in the standard state (Fig. 8a). The curve was not sigmoid. It sharply increased with frequency in the low frequency range ( $5 \times 10^{-4}$ – $1 \times 10^{-3}$  Hz); the rate of increase diminished as frequency increased, reaching a constant value of around 3 MPa. In the stiff state,  $E^*$  was higher than  $E^*$  of the standard at every frequency—by as much as two orders of magnitude at the lower frequencies. At frequencies higher than 0.5 Hz, however, the difference decreased by a factor of 2. In the soft state,  $E^*$  was different in shape and value from both those in the standard state and those in the stiff state (Fig. 8a).  $E^*$  was rather constant at a low value (about 10 kPa) for frequencies lower than 0.5 Hz but sharply increased at higher frequencies to about 1 MPa.  $E^*$  was 1/100–1/10 the value of  $E^*$  of the standard state seen in the middle frequency region (0.05–5 Hz).

$\tan \delta$  in the stiff states decreased with frequency to reach rather a constant value at 5 Hz and higher. The values were similar to those in the standard state at low frequencies (less than 0.005 Hz), but at higher frequencies  $\tan \delta$  was much less. In the soft state,  $\tan \delta$  was about 1, with a little decrease with increasing frequency in the range higher than 0.005 Hz, but a sharp drop between 0.0005 and 0.005 Hz. The values of  $\tan \delta$  were similar to those of the standard in the frequency range 0.005–0.05 Hz, but at in other frequencies—higher or lower—the values were much higher than those in either the standard or stiff states.

The curve of  $E'$  in the stiff state appeared on the top, that

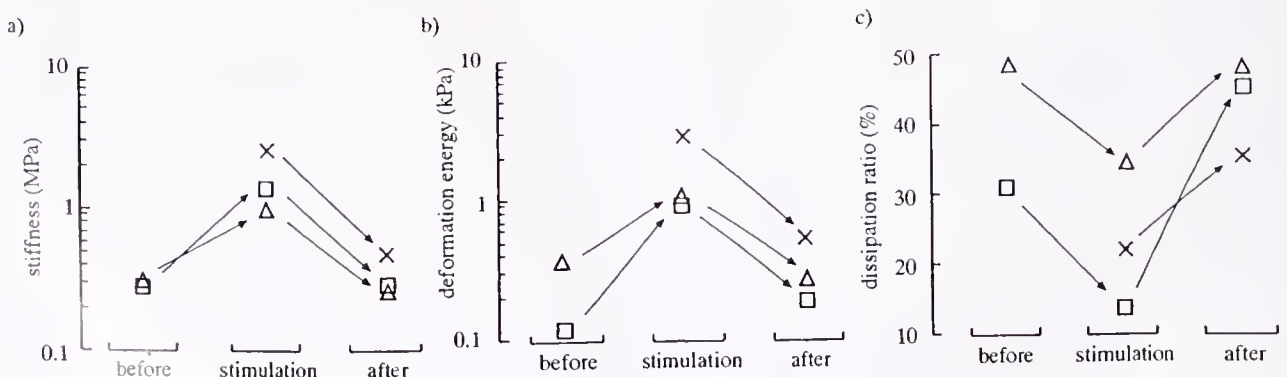
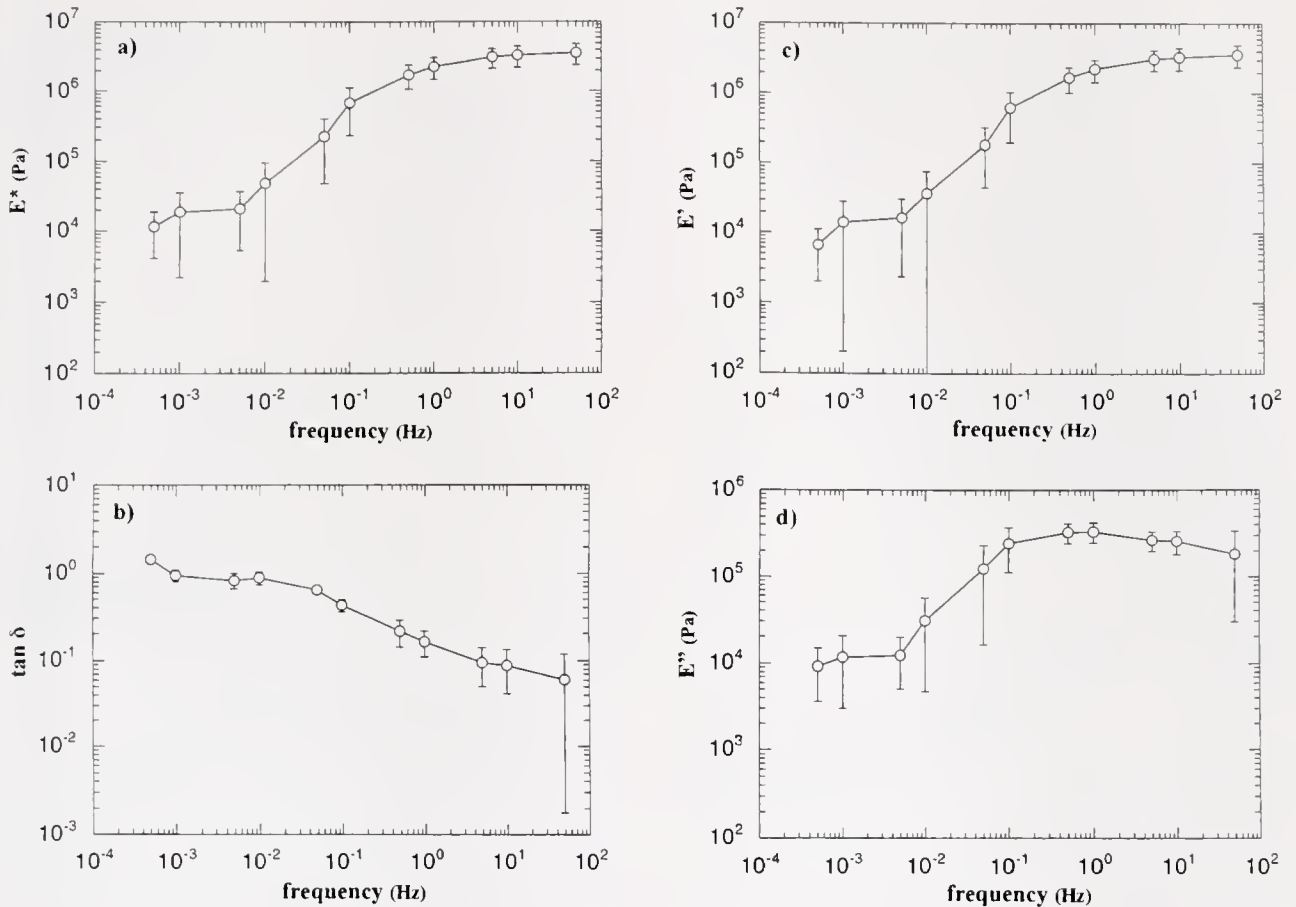


Figure 6. Reversibility of stiffening responses induced by ACh (triangle), KASW (square), and physical stimulation (cross). For chemical stimulation, measurements in ASW were made both before and after the stimulation. (a) Stiffness; (b) deformation energy; (c) dissipation ratio. Identical symbols are from the same sample.



**Figure 7.** Frequency dependence of mechanical properties of samples in the standard state at 1.8% strain. Circles give the average of 8 samples from 4 different individuals; bars are  $\pm$  SD. (a) Complex modulus  $E^*$ ; (b) tangent  $\delta$ ; (c) storage modulus  $E'$ ; (d) loss modulus  $E''$ .

in the soft state on the bottom, and that in the standard in-between (Fig. 8c). As for  $E^*$ , the difference in the values of  $E'$  became smaller with increasing frequency in the frequency range higher than 1 Hz, especially the difference between standard and stiff states.  $E'$  for the stiff state gave a curve similar to that of  $E^*$ . The curve of  $E'$  in the soft state was similar to that of  $E^*$  except at low frequencies (less than 0.005 Hz), where  $E'$  showed a sharp increase with frequency, reflecting the sharp decrease of  $\tan \delta$  in this frequency range.

The curve of  $E''$  in the stiff state was rather flat with a value on the order of 100 kPa. The curve of  $E''$  in the soft state was sigmoid, as was that in the standard.  $E''$  increased with frequency, but plateaued above 0.1 Hz in standard state, whereas in the soft state it plateaued at a higher frequency (5 Hz). The saturated  $E''$  value of about 200 kPa was the same in all three states (frequency range 5–50 Hz).

Comparison of curves in different states (Fig. 8) showed that both the viscous component and the elastic component changed with tissue states; the relative contributions of the two components to the changes in  $E^*$  appeared to be dif-

ferent at different frequencies. For example, a fairly large increase in  $E^*$  occurred at 0.005 Hz without a change in  $\tan \delta$  when the dermis stiffened from standard state. At this frequency, both increases in the elastic component ( $E'$ ) and increases in the viscous component ( $E''$ ) contributed equally to the increase in  $E^*$ . At 5–50 Hz, however, a decrease in  $E'$  without changes in  $E''$  caused a decrease in  $E^*$  when the dermis softened from the standard state.

## Discussion

### Strain and strain-rate dependence

The present work studied the mechanical properties of the catch connective tissue in the holothurian dermis and their changes upon stimulation. Dynamic sinusoidal strain of 0.5%–25% over a frequency range covering 5 logarithmic decades was applied and mechanical parameters were examined. This is the first description of the dynamic viscoelasticity of mutable connective tissues that systematically varied both strain and strain-rate over wide ranges. The study revealed that the viscoelastic properties of the holothurian dermis is both strain and strain-rate dependent.

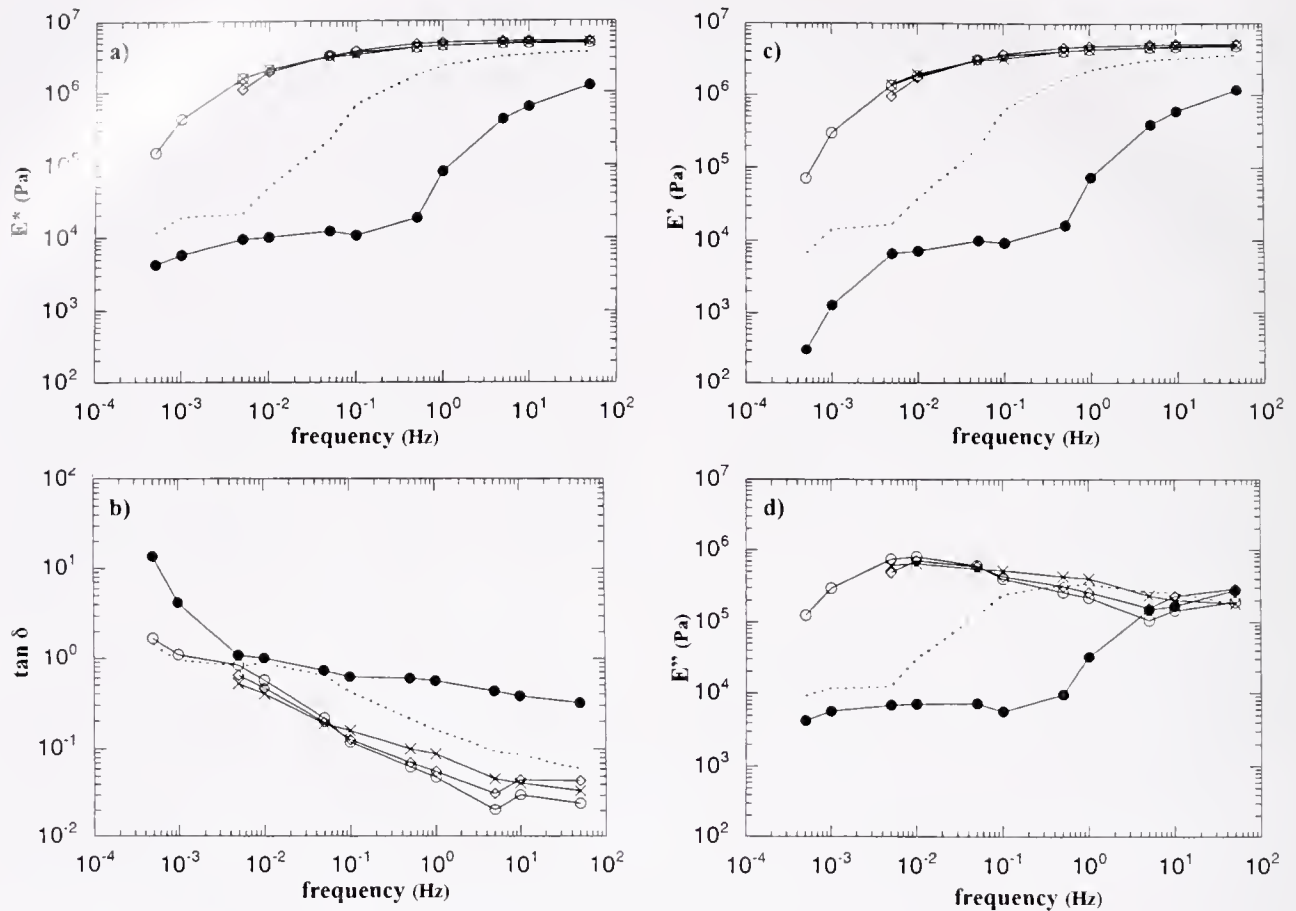


**Figure 8.** Frequency dependence of mechanical properties of the stiff state and of the soft state (strain 1.8%). (a) Complex modulus  $E^*$ ; (b) tangent  $\delta$ ; (c) storage modulus  $E'$ ; (d) loss modulus  $E''$ . Values are averages of 6 samples from 3 individuals. Hollow circle, stiff state (dissection); hollow diamond, stiff state (KASW); cross, stiff state (ACh); filled circle, soft state. Broken lines are the curves of the standard state.

We observed several kinds of strain dependence. The dermis behaved as a linear viscoelastic material at small strains (less than 3%), whereas it showed nonlinearity at larger strains. Two kinds of notable nonlinear strain dependence were observed. One was the J-shaped stress-strain relationship, which is a common feature of soft biological materials (Wainwright *et al.*, 1976). The J-shaped curve was apparent in the standard and soft states but not in the stiff state. The introduction of the  $J$  index enabled us to quantitatively describe the difference in the shape of the curves. The other nonlinearity, which was observed only in the soft state, was strain-induced softening—the stiffness decreased when strain exceeded the limit strain of about 10%. These nonlinear strain dependences were thus tissue-state dependent.

We obtained a modulus-frequency curve by varying the frequency. The curves of  $E^*$ ,  $E'$ , and  $E''$  in the standard state were sigmoid, which clearly showed that the mechanical properties of the dermis were strain-rate dependent. The curves and thus the dependence were quite

different in different tissue states. The curves of  $E'$  in stiff, standard, and soft states were different from each other, which implied that changes in elasticity accompanied the alteration in tissue states. The curves of  $E''$  in the three states were also different, which implied that the changes in viscosity also occurred at tissue-state changes. Thus, both elasticity and viscosity changed with the changes in tissue states. The curves of  $\tan \delta$  for the three states gave different values at most frequencies. This clearly showed that the ratio of the contribution of the viscous component to the contribution of the elastic component changed with tissue states. The change in elasticity and the change in viscosity appeared either simultaneously or independently at a given frequency. Previous studies based on experiments with a fixed, arbitrarily selected strain rate drew contradictory conclusions on which components (elastic or viscous) mainly changed at alteration in tissue states (Motokawa, 1984b; Szulgit and Shadwick, 2000). The present study clearly showed that both components change.

### Stiff state

The present study employed three different stimuli that possibly acted through stimulating the stiffening mechanism active in the intact dermis. Although the stiff state was induced by different methods, all produced almost identical parameter-frequency curves. Therefore we concluded that the same mechanical state was induced by these methods. Acetylcholine is a ubiquitous neurotransmitter that functions in the control of dermal stiffness in sea cucumbers (Motokawa, 1987; Birenheide *et al.*, 1998). The potassium-rich media very likely worked through stimulating cellular elements controlling the dermal stiffness by membrane depolarization (Motokawa, 1994). The stiffening caused by the handling at preparation likely corresponds to the dermal stiffening that occurs when the organism is mechanically disturbed in nature. We thus regard the stiff state seen in the present study as representative of the stiff state occurring naturally in the intact dermis. The stiff state was characterized, in the constant-frequency experiments, by high stiffness, high deformation energy, low dissipation ratio, and low  $J$  index. In the constant-maximum-strain experiments, this state was characterized by high moduli and low  $\tan \delta$ . The low values in  $\tan \delta$  and dissipation ratio implied that elasticity prevailed over viscosity.  $\tan \delta$  was less than 0.1 when the frequency exceeded 0.1 Hz, which implies that the contribution of the viscous component was quite small. This and the low  $J$  index imply that the tissue behaved rather like a linear elastic solid at frequencies higher than 0.1 Hz. The high values of stiffness, moduli, and deformation energy are the features associated with the increase in the elastic modulus. Thus, in short, the dermis in the stiff state behaved like a stiff spring. This state has been believed to function in posture maintenance and mechanical defense (Motokawa, 1985). The stiff, spring-like properties seem to be adaptive features for such functions. The high stiffness is helpful in defense and body support, and the springy feature helps restore the original posture after the imposed force is removed. The dominance of elasticity over viscosity also helps by minimizing plastic flow.

### Soft state

The soft state is characterized in the constant-frequency experiments by low stiffness, low deformation energy, high dissipation ratio, high  $J$  index in unloading, and strain-induced softening. In the constant-maximum-strain experiments, the soft state was characterized by low moduli and high  $\tan \delta$ .  $\tan \delta$  was about 1 over a wide frequency range, which implies that the contribution of the viscous component was as large as that of the elastic component. At the lowest frequency,  $\tan \delta$  exceeded 1, indicating the dominance of the viscous component. A significant contribution of the viscous component was also found in the constant-frequency experiments that showed a high dissipation ratio in the soft state.

When the maximum strain exceeded a limit strain of about 10%, stiffness decreased as the maximum strain increased. This phenomenon was never observed in other states. Although strain-induced softening has not been reported previously, we could explain the rather contradictory results reported for other sea cucumbers by this strain-induced softening phenomenon. The soft state in the present study was induced by calcium chelation. This procedure was found to cause drastic softening in creep tests (Hayashi and Motokawa, 1986), whereas in dynamic tests it caused much less softening (Szulgit and Shadwick, 2000) or no detectable changes (Shibayama *et al.*, 1994). Although Szulgit and Shadwick (2000) measured shear modulus, not elastic modulus, and thus strict comparison is not possible, the difference in the extent of softening seems to be interpretable, at least in part, by the difference in the strain used. In creep tests, the dermis was usually subjected to fairly large strain, while in dynamic tests, the strain imposed was much smaller than the limit strain of the present sea cucumber. In creep tests, the dermis is very likely in the strain-induced soft state, but in the previous dynamic tests it probably was not in that state.

Strain-induced softening of the dermis was observed in an intact sea cucumber that was subjected to large repetitive deformations (Motokawa, 1988), and thus it seems very likely that the state in CaFASW mimicked the soft state of intact animals. The dermis in CaFASW showed a drastic decrease in stiffness when the deformation exceeded the limit strain. This unique behavior, together with the quite high energy dissipation ratio in the soft state, seems to have adaptive significance in autotomy and fission. Sea cucumbers show evisceration, a kind of autotomy. They contract the body to increase the pressure in the coelomic cavity, causing a rupture in the body wall; they eject their viscera through that hole. Because the dermis in the ruptured portion is very soft to the touch, that part is no doubt in a soft state. The scenario for how the strain-induced softening works in the evisceration process is as follows. The animal would first make a small portion of the dermis—that to be ruptured—soft. At this stage, the softened part still contributes to the integrity of the body wall because the stiffness of the soft state at low strain is not as low as that after having exceeded the limit strain. The animal would then increase the coelomic pressure, causing larger deformations in the softened part. Once the deformation exceeds the limit strain, the stiffness drastically decreases and so the dissipation ratio increases, which allows the dermis to continue deforming at the same pressure (or even under lower pressure) until rupture. This is positive feedback: the more deformed the dermis, the more easily the dermis is deformed. Such mechanical properties allow the animal to eviscerate with only a transient increase in the coelomic pressure, and thus to confine the rupture to the small portion initially softened, leaving the rest of the dermis intact.

### *Standard state*

We employ the convention used in previous studies that the dermis, rested in ASW, was taken as the standard state (Motokawa, 1984a). We tested the dermis after a resting period of 1 day in ASW. Such a lengthy resting period was chosen because the dermis, when rested for less than 15 h, showed stiffness values that were between those of the stiff state and the standard state. Thus, recovery from the effects of handling at preparation took quite a long time in this species. The long resting period seems not to adversely affect the dermis, because the sample rested for 1 day showed clear responses both to KASW and to ACh. Previous studies did not employ such a long resting period, which may be one reason for the notoriously large variations in the reported mechanical properties of non-stimulated dermis in ASW (Motokawa, 1984c; Hayashi and Motokawa, 1986; Szulgit and Shadwick, 2000).

By touching the living sea cucumber, we can feel the stiffening of the body wall. If such a stiffened body wall is then vigorously squeezed, it becomes very soft—soft enough to show a viscous flow (Motokawa, 1988). The isolated dermis in the standard state also showed both stiffening and softening responses. Thus it seems reasonable to suppose that the dermis of the intact animal at rest is in a state that corresponds to the present standard state; in this state, the animal is likely to change its body shape for movement. The standard state showed a J-shaped stress-strain relationship with a prominent flat toe region followed by a steep pole region. The toe region allows animals to change their posture easily, with little energy expenditure, by using their body wall muscles. In contrast, to protect the animal from damage, the steep region resists large, externally imposed forces. Thus the standard state with its J-shaped stress-strain curve seems to have adaptive significance.

The standard state showed mechanical properties intermediate between the stiff and soft states, and thus the standard state appears to be just an intermediate between two extremes. Close inspection of the stress-strain relationship, however, suggests that the mechanisms of stiffening and of softening from the standard state are probably different (see next section), and thus we conclude that the dermis of the sea cucumber can assume three distinct mechanical states—stiff, standard, and soft.

### *Simple polymer model and implications for mechanism of catch*

The dermis of the sea cucumber is composed mainly of extracellular materials whose mechanical properties have been thought to determine those of the whole dermis. The main components of the extracellular materials are macromolecules such as collagen and proteoglycans (Matsumura, 1974; Kariya *et al.*, 1990). The dermis shows continuous creep to final breakage under even a small load. This be-

havior is observed not only in the standard state (Motokawa, 1981) but also in soft and stiff states (unpubl. obs.), which suggests that the main components of the dermis do not make covalent cross-links with each other. It seems to be possible to regard dermis as a blend of non-cross-linked polymers, and thus it is tempting to interpret the present results in terms of polymer science.

Let us suppose that the force-bearing structure in the dermis is a meshwork of polymers. In the meshwork, polymer molecules make a noncovalent bond with adjacent molecules at each crossing point of the molecular mesh. The polymer chain between adjacent crossing points is here called a segment. Two kinds of bonds are postulated in the meshwork. One is the intermolecular bond that forms the crossing point of the meshwork, and the other is the segmental bond found within the molecular chain that comprises the segment (Fig. 9). A part of the molecule in the segment is presumed to take a folded structure in which the folds were maintained by intra-molecular or segmental bonds. Such bonds make the segment less flexible and resistant to stretch. The introduction of inter-molecular bonds implies that more molecules in the dermis are recruited into the force-bearing meshwork.

When the dermis in the standard state is stretched, each molecular segment freely rotates around the crossing points of the mesh until all the segments become parallel to the direction of stretch. Further stretch directly stretches the segment and thus stretches the segmental bonds (central column of Fig. 9). The free rotation of segments corresponds to the toe region of the J curve, and the direct stretching of segments corresponds to the pole region. The unloading curve shows a higher *J* index than that of the loading curve. This implies that stretching segments induces some plastic deformation. Such plastic deformation must be temporary rather than permanent, because the next hysteresis loop exhibited exactly the same shape. To explain this behavior, we postulate that some segmental bonds are stretched plastically, but they recover their original state in the unloading and compressing phases that follow. Temporarily plastic behavior explains the rather high dissipation ratio seen in the standard state.

Stiffening stimulation induces inter-molecular bonds, which reduces the segment length of the mesh (upper right of Fig. 9). A reduced segment length accounts for the short toe region. It also increases the resistance to rotation around crossing points because a smaller mesh size increases the resistance to displacement of water from the mesh, and thus increases the slope of the toe region. An increase in inter-molecular bonds recruits more molecules into the meshwork, and thus increases the resistance to stretch of the meshwork. This explains the higher stiffness of the pole region. The newly recruited molecules are presumed not to contain plastic segmental bonds given the small difference between loading and unloading curves and the low dissipation ratio in the stiff state.

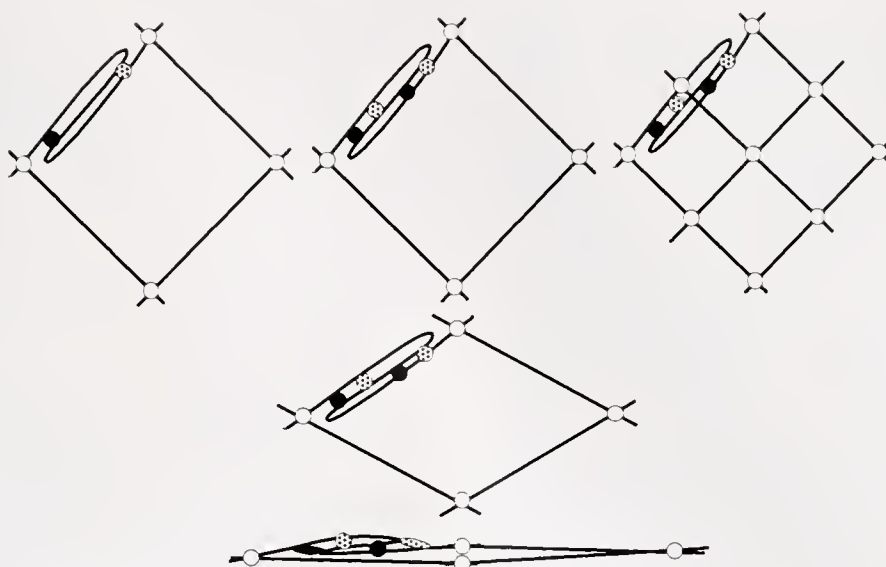


**Figure 9.** Schematic of a simple polymer model for the dermis. A single mesh is drawn. Top row portrays, from left to right, the soft state, the standard state, and the stiff state. Hollow circle, intermolecular bond; filled circle, segmental bond that deforms elastically when stretched; stippled circle, segmental bond that deforms plastically when stretched. The folded structure of the segment is drawn only for one side of a mesh. Central column is the mesh of the standard state under increasing strain from top to bottom when stretched horizontally. The mesh is free to deform (middle); the segmental bonds experience deformation after the segments become oriented parallel to the direction of stretch (bottom).

In the soft state, the length of the toe region remained the same as that in the standard state. From this result we postulate that the segment length remains the same, and thus the number of inter-molecular bonds remained unchanged at the transition from standard to soft states (upper left of Fig. 9). The segmental bonds are, however, postulated to decrease in number. Removal of segmental bonds makes the segment more flexible and stretchy, which accounts for the low stiffness of the pole region in the soft state. A fair proportion of the remaining segmental bonds show plastic deformation on stretch, producing a fairly large  $J$  index at unloading and a large dissipation ratio in the soft state. In the soft state, segmental bonds break when the strain exceeds some limit. This endows the model with strain-softening behavior. The loss of segmental bonds that had held the folded structure of the chain results in elongation of the segment. This explains the longer toe region in samples that experienced strain-induced softening. The breakage of bonds also accounts for the decrease in the maximum stress.

This meshwork model simulates well the mechanical behavior of the dermis with only a small number of assumptions. The model suggests that the molecular mechanism involved in stiffening is different from that involved in softening. Inter-molecular bonds are associated with changes between the standard state and the stiff state, whereas segmental bonds or intra-molecular bonds are associated with changes between the standard state and the soft state. An increase in  $E'$  associated with the formation of bonds between molecules has been reported in the colla-

nous mesogloea of a sea anemone (Gosline, 1971). The stiffening mechanism and the softening mechanism seem to have their own cross-bridging molecules. Tensilin, a protein that stiffens the dermis by binding to collagen (Tipper *et al.*, 2003), is a candidate for the inter-molecular bonding agent. The presence of a softening molecule has also been shown (Koob *et al.*, 1999; Szulgit and Shadwick, 2000). The stiffening mechanism and the softening mechanism also seem to have their own neural pathways (Motokawa, 1987; Birenheide *et al.*, 1998). In the present model, calcium ions are involved in segmental bonds. Calcium ions have a number of possible sites that they affect in both polymer systems and in biological systems. They seem to have some roles in a "polymer system" of the dermis because detergent-treated dermis is quite sensitive to calcium ions (Motokawa, 1994). They are also probably involved in the "biological system" of the dermis, affecting neuronal activities, secretion processes, or both (Motokawa and Hayashi, 1987; Trotter and Koob, 1995). Calcium translocation in the holothurian dermis has been suggested (Matsuno and Motokawa, 1992). Thus calcium ions no doubt play one or more important roles in the mechanism of connective tissue catch.

A meshwork of noncovalently cross-linked polymers gives an  $E'$ -frequency curve with four characteristic regions (Ferry, 1980). They are, from the high-frequency end to the low-frequency end, the glass region with a high value of  $E'$ , the transition region with decreasing  $E'$  as frequency decreases, the rubbery or plateau region of constant  $E'$ , and the flow region of decreasing  $E'$  as the frequency decreases.

These four regions are all apparent only when measurements are performed over a very wide range of frequencies, which is often not practicable. In the present study, the dermis in the soft state showed an  $E'$ -frequency curve with decreasing  $E'$  as frequency decreases in the lowest frequency region. It is reasonable to regard this region as the flow region because a  $\tan \delta$  value of 10 implies that the dermis behaves like a liquid, and because the softened intact dermis does exhibit flow (Motokawa, 1988). The stiff state showed an increase in  $E'$  with increasing frequency to reach a constant value of  $E'$  of about 5 MPa. Because  $E'$  in the glass state is 2 orders of magnitude higher than this (Fukahori, 2000), the high-frequency region of the stiff state is very probably the plateau region, not the glass region.

In polymer science, it is possible to construct a single  $E'$ -frequency curve from experimental data of limited frequency ranges by using the time-temperature superposition principle. For linear viscoelastic materials such as amorphous polymers, the effects of time and temperature on mechanical properties are equivalent; thus the curve at one temperature can be superimposed upon those at different temperatures by shifting the curves from lower temperatures to the left and those from higher temperatures to the right along the frequency axis to generate a smooth master curve (Ferry, 1980). This method is convenient because it generates a single curve that gives an overview of the frequency dependence of mechanical properties. A master curve is usually made by varying the temperature. It is, however, sometimes composed from curves derived from different concentrations of polymers or in solutions of different ionic strength (Gibbs *et al.*, 1968). We attempted to generate an "apparent master curve" in order to get a single curve that gives an overview of the frequency dependence of mechanical properties of the holothurian dermis. Temperature manipulation was not practicable because temperature greatly affected the mechanical properties, acting not only directly on the polymer meshwork but also indirectly through affecting the activities of nerves and secretory cells controlling mechanical properties. Instead we shifted the curve in the stiff state to the right and that in the soft state to the left, leaving that of the standard state as a reference. We could construct a smooth curve of  $E'$  with four different phases quite similar to the usual master curve of polymers (Fig. 10), although there is no physicochemical theory at hand that supports the present procedure. Therefore, the similarity is just an apparent one. A smooth curve could also be generated on  $E''$  by lateral shifting (data not shown). The fact that we could construct a smooth curve suggests that some physicochemical processes corresponding to frequency shifts occurred at state changes.

### Acknowledgments

We thank Drs. Makoto Kaihara and Akio Sakanishi for discussion, and the staff of Sesoko Station, Tropical Bio-

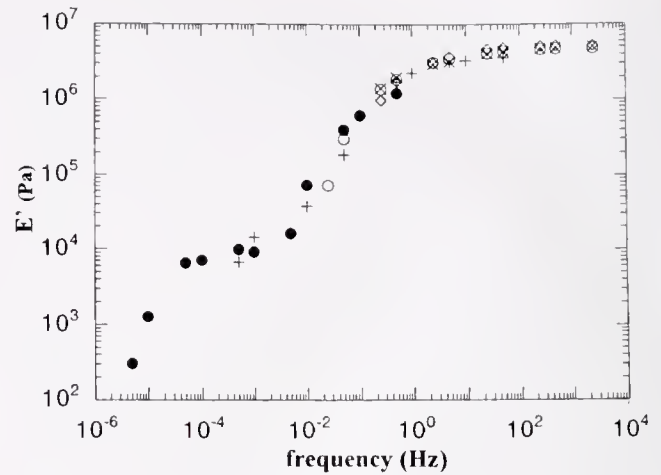


**Figure 10.** "Apparent master curve" of storage modulus  $E'$ . Hollow circle, the stiff state (dissection); hollow diamond, the stiff state (KASW);  $\times$ , the stiff state (ACh); +, the standard state; filled circle, the soft state. The logarithm of the shift factor was 1.7 for the stiff states; for the soft state it was  $-2$ , meaning that the curve shifted to the left by 2 orders of magnitude in frequency.

sphere Research Center, University of the Ryukyus, for the supply of sea cucumbers. Supported by Grant-in-aid for scientific research on priority area (A) "Molecular synchronization for design of new materials system."

### Literature Cited

- Birenheide, R., M. Tamori, T. Motokawa, M. Ohtani, E. Iwakoshi, Y. Muneoka, T. Fujita, H. Minakata, and K. Nomoto. 1998. Peptides controlling stiffness of connective tissue in sea cucumbers. *Biol. Bull.* **194**: 253–259.
- Eylers, J. P. 1982. Ion-dependent viscosity of holothurian body wall and its implications for the functional morphology of echinoderms. *J. Exp. Biol.* **99**: 1–8.
- Ferry, J. D. 1980. *Viscoelastic Properties of Polymers*, 3rd ed. Wiley, New York, 641 pp.
- Fukahori, Y. 2000. *Kobunshi no Rikigaku* (Mechanics of Polymers, in Japanese). Gihodo, Tokyo, 384 pp.
- Gibbs, D. A., E. W. Merrill, and K. A. Smith. 1968. Rheology of hyaluronic acid. *Biopolymers* **6**: 777–791.
- Gosline, J. M. 1971. Connective tissue mechanics of *Metridium senile*. II. Visco-elastic properties and macromolecular model. *J. Exp. Biol.* **55**: 775–795.
- Greenberg, A. R., and J. P. Eylers. 1984. Influence of ionic environment on the stress relaxation behavior of an invertebrate connective tissue. *J. Biomechanics* **17**: 161–166.
- Hayashi, Y., and T. Motokawa. 1986. Effects of ionic environment on viscosity of catch connective tissue in holothurian body wall. *J. Exp. Biol.* **125**: 71–84.
- Kariya, Y., S. Watabe, K. Hashimoto, and K. Yoshida. 1990. Occurrence of chondroitin sulfate E in glycosaminoglycans isolated from the body wall of sea cucumber *Stichopus japonicus*. *J. Biol. Chem.* **265**: 5081–5085.
- Koob, T. J., M. M. Koob-Edmunds, and J. A. Trotter. 1999. Cell-derived stiffening and plasticizing factors in sea cucumber (*Cucumaria frondosa*). *J. Exp. Biol.* **202**: 2291–2301.
- Matsumura, T. 1974. Collagen fibrils of the sea cucumber, *Stichopus*

- japonicus*: purification and morphological study. *Connective Tissue Res.* **2**: 117–125.
- Matsuno, A., and T. Motokawa. 1992.** Evidence for calcium translocation in catch connective tissue of the sea cucumber *Stichopus chloronotus*. *Cell Tissue Res.* **267**: 307–312.
- Motokawa, T. 1981.** The stiffness change of the holothurian dermis caused by chemical and electrical stimulation. *Comp. Biochem. Physiol.* **70C**: 41–48.
- Motokawa, T. 1982.** Factors regulating the mechanical properties of holothurian dermis. *J. Exp. Biol.* **99**: 29–41.
- Motokawa, T. 1984a.** Connective tissue catch in echinoderms. *Biol. Rev.* **59**: 255–270.
- Motokawa, T. 1984b.** Viscoelasticity of holothurian body wall. *J. Exp. Biol.* **109**: 63–75.
- Motokawa, T. 1984c.** The viscosity change of the body-wall dermis of the sea cucumber *Stichopus japonicus* caused by mechanical and chemical stimulation. *Comp. Biochem. Physiol.* **77A**: 419–423.
- Motokawa, T. 1985.** Catch connective tissue: the connective tissue with adjustable mechanical properties. Pp. 69–73 in *Echinodermata*, B. F. Keegan and B. D. S. O'Connor, eds. A. A. Balkema, Rotterdam.
- Motokawa, T. 1987.** Cholinergic control of the mechanical properties of the catch connective tissue in the holothurian body wall. *Comp. Biochem. Physiol.* **86C**: 333–337.
- Motokawa, T. 1988.** Catch connective tissue: a key character for echinoderms' success. Pp. 39–54 in *Echinoderm Biology*, R. D. Burke, P. V. Mladenov, P. Lambert, and R. L. Parsley, eds. A. A. Balkema, Rotterdam.
- Motokawa, T. 1994.** Effects of ionic environment on viscosity of Triton-extracted catch connective tissue of a sea cucumber body wall. *Comp. Biochem. Physiol.* **109B**: 613–622.
- Motokawa, T., and Y. Hayashi. 1987.** Calcium dependence of viscosity change caused by cations in holothurian catch connective tissue. *Comp. Biochem. Physiol.* **87A**: 579–582.
- Oka, S. 1974.** *Reorji (Rheology)*, in Japanese. Shokabo, Tokyo. 481 pp.
- Shihayama, R., T. Kobayashi, H. Wada, H. Ushitani, J. Inoue, T. Kawakami, and H. Sugi. 1994.** Stiffness changes of holothurian dermis induced by mechanical vibration. *Zool. Sci.* **11**: 511–515.
- Szulgit, G. K., and R. E. Shadwick. 2000.** Dynamic mechanical characterization of a mutable collagenous tissue: response of sea cucumber dermis to cell lysis and dermal extracts. *J. Exp. Biol.* **203**: 1539–1550.
- Tipper, J. P., G. Lyons-Levy, M. A. L. Atkinson, and A. Trotter. 2003.** Purification, characterization and cloning of tensilin, the collagen-fibril binding and tissue-stiffening factor from *Cucumaria frondosa* dermis. *Matrix Biol.* **21**: 625–635.
- Trotter, A., and T. J. Knob. 1995.** Evidence that calcium-dependent cellular processes are involved in the stiffening response of holothurian dermis and that dermal cells contain an organic stiffening factor. *J. Exp. Biol.* **198**: 1951–1961.
- Wainwright, S. A., W. D. Biggs, J. D. Currey, and J. M. Gosline. 1976.** *Mechanical Design in Organisms*. Princeton University Press, Princeton. 423 pp.
- Wilkie, I. C. 1996.** Mutable collagenous tissue: extracellular matrix as mechano-effector. Pp. 61–102 in *Echinoderm Studies*, vol. 5, M. Jangoux and J. M. Lawrence, eds. A. A. Balkema, Rotterdam.
- Wilkie, I. C. 2002.** Is muscle involved in the mechanical adaptability of echinoderm mutable collagenous tissue? *J. Exp. Biol.* **205**: 159–165.

# Heat-Shock Protein 70 (Hsp70) as a Biochemical Stress Indicator: an Experimental Field Test in Two Congeneric Intertidal Gastropods (Genus: *Tegula*)

LARS TOMANEK<sup>1</sup> AND ERIC SANFORD<sup>2</sup>

*Hopkins Marine Station, Stanford University, Pacific Grove, California 93950-3094*

**Abstract.** Although previous studies have demonstrated that heat-shock protein 70 (Hsp70) can be induced by environmental stress, little is known about natural variation in this response over short time scales. We examined how Hsp70 levels varied over days to weeks in two intertidal snail species of the genus *Tegula*. Sampling was conducted both under naturally changing environmental conditions and in different vertical zones on a rocky shore. The subtidal to low-intertidal *T. brunnea* was transplanted into shaded and unshaded mid-intertidal cages to assess temporal variation in Hsps under conditions of increased stress. For comparison, the low to mid-intertidal *T. funebris* was transplanted into mid-intertidal cages, within this species' natural zone of occurrence. Snails were sampled every 3 to 4 days for one month, and endogenous levels of two Hsp70-kDa family members (Hsp72 and Hsp74) were quantified using solid-phase immunochemistry. Following periods of midday low tides, levels of Hsps increased greatly in transplanted *T. brunnea* but not in *T. funebris*. Levels of Hsps increased less in *T. brunnea* transplanted to shaded cages than to unshaded cages, suggesting that prolonged emersion and reduction in feeding time *per se* are factors that are only mildly stressful. Upregulated levels of Hsps returned to base levels within days. In unmanipulated snails collected from their natural zones, Hsp levels showed little change with thermal variation, indicating that these species did not experience thermally stressful conditions during this study. However, under common conditions in the mid-intertidal

zone, Hsp70 levels reflected the different thermal sensitivities of the physiological systems of these two species.

## Introduction

The synthesis of heat-shock proteins (Hsps) is induced when environmental variation perturbs an organism's physiological system to the extent that its proteins denature. Under such environmental conditions Hsps and other molecular chaperones stabilize denaturing proteins, refold reversibly denatured proteins, and facilitate the degradation of irreversibly denatured proteins (Lindquist, 1986; Lindquist and Craig, 1988; Parsell and Lindquist, 1994; Feige *et al.*, 1996; Frydman, 2001; Hartl and Hayer-Hartl, 2002). Numerous studies have investigated the relationship between Hsp synthesis and various potential stress factors; however, very few studies have investigated the variation of Hsp levels under varying natural conditions (for review see Feder and Hofmann, 1999). Even fewer studies have investigated short-term variation in Hsp levels (*e.g.*, hours, days to weeks) in response to variable physical conditions in the field (Hofmann and Somero, 1995; Nakano and Iwama, 2002). A comprehensive understanding of such a time course of variation in Hsp levels under natural conditions is needed to interpret Hsp levels from field-collected organisms and therefore to evaluate stress under natural conditions. Furthermore, predictions about the ecological role of the heat-shock response that are made from laboratory comparisons of species that occupy widely varying thermal environments have not been tested under natural conditions.

Our study focuses on Hsp variation in response to physical stress in intertidal organisms. Physical factors, in particular temperature, play an important role in setting the upper limits to the vertical distribution range of intertidal organisms and confine them to distinct bands on the shore

Received 28 May 2003; accepted 24 September 2003.

<sup>1</sup>To whom correspondence should be addressed. Present address: Dept. of Animal Science, University of California, One Shields Avenue, Davis, CA 95616. E-mail: ltomanek@ucdavis.edu

<sup>2</sup>Present address: Eric Sanford, Dept. of Ecology and Evolutionary Biology, Brown University, Providence, RI 02912.

with species-specific upper and lower vertical limits (see reviews in Benson, 2002; Tomanek and Helmuth, 2002). This view is supported by numerous laboratory studies demonstrating that physiological resistance to physical conditions is greater in species that live at higher tidal heights (Newell, 1979; Somero, 2002).

Intraspecific variation in the expression of Hsps has been found in intertidal species in association with seasonal acclimatization (Dietz and Somero, 1992; Hofmann and Somero, 1995; Roberts *et al.*, 1997; Chapple *et al.*, 1998; Buckley *et al.*, 2001), laboratory acclimation (Hofmann and Somero, 1996a; Roberts *et al.*, 1997; Tomanek and Somero, 1999, 2000, 2002), competition for space (Rossi and Snyder, 2001), food availability and wave exposure (Dahlhoff *et al.*, 2001), and microhabitat (Helmuth and Hofmann, 2001). Interspecific differences in the heat-shock response, especially among congeneric species, often correlate positively with thermal extremes in the environment (Sanders *et al.*, 1991; Dietz and Somero, 1993; Hofmann and Somero, 1996a; Tomanek and Somero, 1999, 2000, 2002; Nakano and Iwama, 2002; Tomanek, 2002). Some of these studies have shown how Hsp levels vary over hours in response to thermal stress under natural (Hofmann and Somero, 1995, 1996b; Nakano and Iwama, 2002) as well as laboratory conditions (Tomanek and Somero, 2000). To our best knowledge, nothing is known about the variation of Hsp levels in response to changing natural conditions over days to weeks. Furthermore, whether interspecific differences in the heat-shock response limit a species' thermal niche and contribute to setting its vertical distribution range within the intertidal zone has not been tested under natural conditions.

This study focuses on two herbivorous gastropod species of the genus *Tegula* that occupy distinct vertical zones on the shore: *T. brunnea* (Philippi, 1848), common in the subtidal to low-intertidal zone, and *T. funebris* (Adams, 1855), common in the low- to mid-intertidal zone (Riedman *et al.*, 1981; Watanabe, 1984). Our previous laboratory work suggested that heat stress might prevent the low-intertidal *T. brunnea* from occupying the mid-intertidal zone (Tomanek and Somero, 1999, 2000, 2002). Thus, we predicted that *T. brunnea* transplanted upward into the mid-intertidal zone would express increased levels of Hsp70 in its new thermal environment. Laboratory results (Tomanek and Somero, 1999) also suggested that the mid-intertidal *T. funebris* would activate the heat-shock response frequently in its natural zone of occurrence due to the temperature extremes and fluctuations that characterize the mid-intertidal zone. In this study we test these predictions by following the time course of expression of two Hsp70 isoforms (Hsp72 and Hsp74) over a month-long sampling period in specimens transplanted from the low-intertidal into the mid-intertidal zone, and in control individuals collected from their natural vertical zones.

This combination of ecological and molecular approaches

thus attempts to comprehensively test how Hsp levels vary over time in response to the changing physical conditions within and beyond a species' natural thermal zone.

## Materials and Methods

### *Study organisms and distribution patterns*

The two *Tegula* congeners used in this study differ in their biogeographic and vertical distributions. *Tegula brunnea* inhabits the subtidal to low-intertidal zones of the eastern Pacific Ocean from Cape Arago, Oregon (43° 25'N) to the Channel Islands, California (34° 00'N) (Abbott and Haderlie, 1980; Riedman *et al.*, 1981; Watanabe, 1984). *Tegula funebris* is found in the low- to mid-intertidal zone and has a wider latitudinal range, from Vancouver Island, British Columbia, Canada (48° 25'N), to central Baja California, Mexico (28° 00'N) (Abbott and Haderlie, 1980; Riedman *et al.*, 1981).

### *Experimental design*

Field experiments were conducted at Hopkins Marine Station of Stanford University in Pacific Grove, California (36° 36'N, 121° 54'W). To test the role of temperature in setting the upper vertical limit of the subtidal to low-intertidal *T. brunnea*, we transplanted this species above its natural zone of occurrence. Snails (shell diameter = 20–25 mm, marked with yellow nail polish) were placed into stainless steel cages (20 × 20 cm wide and 5 cm high; 316 stainless steel wire cloth with a 3-mm opening size) that were positioned at similar heights in the mid-intertidal zone (+0.64 ± 0.12 m above mean lower low water). These enclosures had no bottom and thus allowed snails to move over the rock surface and feed on the algal species present naturally. Cages were either unshaded (sun-exposed treatment) or shaded by covering them with plastic mesh (two layers of a black polyethylene mesh with a 3.8-mm opening size). Each treatment included seven cages, with 10 snails per cage.

In addition, we transplanted *T. funebris* from the mid-intertidal zone into unshaded mid-intertidal cages ( $n = 7$ ) positioned at the same tidal height. This treatment served two purposes. First, it allowed us to compare the thermal stress of *T. brunnea* transplanted into the mid-intertidal zone (above its natural upper limit) to that of similarly caged *T. funebris*, the natural inhabitant of the mid-intertidal zone. Secondly, it allowed us to test for caging artifacts by comparing caged mid-intertidal *T. funebris* to unmanipulated snails found naturally in that zone.

Single snails were collected from each cage and replaced with an unmarked specimen (to avoid changes in snail density during the experiment) every 3rd or 4th day over a month-long sampling period (31 March to 1 May 2000; see Figs. 1 and 2). To evaluate the response of snails in their

native thermal environment, we also collected unrestricted snails from the mid-intertidal (*T. funebris*) and the shallow subtidal zone (*T. brunnea*; specimens were always submerged before and during collection). All collections were made within 45 min of low tide to minimize any physiological variation that might be related to endogenous tidal rhythms. Snails were frozen immediately on dry ice following collection and kept at  $-70^{\circ}\text{C}$  until further processing. To obtain a record of *Tegula* body temperature, temperatures in gelatin-filled snail shells were recorded inside mid-intertidal cages and outside (on adjacent rocks) by a StowAway XTI temperature data logger (Onset Computer Corp, Pocasset, MA). For further details on this method, see Tomanek and Somero (1999). Because of equipment failure, only one complete record, from a *T. funebris* shell attached to open rock adjacent to a mid-intertidal cage, was obtained from the six data loggers installed. Temperatures shown (Figs. 1 and 2) therefore represent the thermal variation of field-acclimatized *T. funebris* from the mid-intertidal zone. Immediately following the experiment (and discovery of the equipment failure), additional data loggers were deployed to characterize the difference among our treatments. During midday low tides, temperatures within unshaded cages were typically  $3\text{--}6^{\circ}\text{C}$  cooler than on the open rock outside the cage, whereas temperatures in shaded cages were an additional  $2\text{--}5^{\circ}\text{C}$  cooler than in cages without shades.

#### Tissue preparation

Gill tissue was dissected from whole snails that were thawed under conditions that do not induce heat shock ( $13^{\circ}\text{C}$ ) and immediately placed in  $200\ \mu\text{l}$  (*T. funebris*, 15.0 to 25.0 mg wet weight) or  $300\ \mu\text{l}$  (*T. brunnea*, 30.0 to 45.0 mg wet weight) of homogenization buffer ( $32\ \text{mmol l}^{-1}$  Tris-HCl, pH 7.5 at  $4^{\circ}\text{C}$ , 2% (w/v) SDS,  $1\ \text{mmol l}^{-1}$  EDTA,  $1\ \text{mmol l}^{-1}$  Pefabloc (Boehringer Mannheim),  $10\ \mu\text{g ml}^{-1}$  pepstatin, and  $10\ \mu\text{g ml}^{-1}$  leupeptin). Tissues were incubated for 5 min at  $100^{\circ}\text{C}$  and homogenized. The procedure was repeated and homogenates were centrifuged at  $15,800 \times g$  for 15 min. The supernatant was removed and stored at  $-70^{\circ}\text{C}$ . Protein concentrations were determined using the Micro-BCA assay (Pierce) according to the manufacturer's instructions.

#### Gel electrophoresis and immunodetection (Western) protocol

In general, we followed the procedure described in Tomanek and Somero (2002). Briefly, proteins were separated electrophoretically and subsequently transferred onto nitrocellulose membranes (Nitrobind, Schleicher and Schuell) in transfer buffer ( $25\ \text{mmol l}^{-1}$  Tris-base,  $0.193\ \text{mol l}^{-1}$  glycine, 20% methanol (v/v), pH 8.3 at  $20^{\circ}\text{C}$ ). After membranes were dried overnight they were treated with blocking

buffer ( $25\ \text{mmol l}^{-1}$  Tris-HCl, pH 7.5 at  $20^{\circ}\text{C}$ ,  $150\ \text{mmol l}^{-1}$  NaCl, 0.1% (v/v) Tween, 0.02% (w/v) Thimerosol, 5% (w/v) nonfat dried milk) for 1 h, subsequently washed with Tris-buffered saline (TBS;  $25\ \text{mmol l}^{-1}$  Tris-HCl, pH 7.5 at  $20^{\circ}\text{C}$ ,  $150\ \text{mmol l}^{-1}$  NaCl), and then incubated with a solution of a monoclonal rat antibody (IgG) against Hsp70 (clone 7.10; Affinity BioReagent, MA3-001; 1:2500 dilution of Hsp70 antibody in buffer A (BA): TBS, 2.5% (w/v) bovine serum albumin in TBS) for 1 h. After washing the membranes, we incubated them for 30 min with a rabbit-anti-rat bridging antibody (IgG) solution (1:2000 dilution in BA; Vector, AI-4000), followed again by several washing steps. Finally, we incubated membranes with a horseradish-peroxidase protein A solution (1:5000 dilution in BA; Bio-Rad) for 30 min. Membranes were washed and overlaid with a solution of enhanced chemiluminescent (ECL) reagent (Amersham Pharmacia) according to the manufacturer's instructions for 1 min. Under dark room conditions, we exposed membranes onto pre-flashed Hyperfilm (Amersham Pharmacia) for 5, 10, 20, 30, and 50 min after ECL treatment to obtain various exposures that were in the linear range of detection. All samples were run at least twice.

#### Image analysis and quantification of expression of heat-shock proteins

Film images were scanned on a densitometer (Sharp JX-330) and the digitized images were analyzed with image analysis software (ImageMaster 1D, ver. 2.01, Pharmacia) to quantify band intensities of the two Hsp70 isoforms, one with a molecular mass of about 72 kDa (Hsp72), the other of about 74 kDa (Hsp74). We express band intensities relative to a known amount of a bovine heat-shock cognate 70 (80 ng; StressGen, SPP-750) to account for variation among Western blots.

#### Statistical analysis

Variation in Hsp72 and Hsp74 was compared using a two-factor analysis of variance (ANOVA) with experimental treatments and sampling days as the main effects. We conducted *post hoc* comparisons of all five treatment groups (Student-Newman-Keuls test) within each sampling day separately. To calculate the critical value, we used the appropriate Studentized range statistic ( $\alpha = 0.95$ ;  $m =$  number of means;  $df =$  degrees of freedom of the error term from the ANOVA) and an adjusted  $n$  value ( $n_0$ ) to account for unequal sample sizes among the means using the following equation:

$$n_0 = \frac{1}{a-1} \left( \sum_i^a n_i - \frac{\sum_i^a n_i^2}{a} \right)$$

with “ $a$ ” the total number of means compared ( $a = 50$ ) and “ $n_i$ ” the sample size for each mean. Variances were not heterogeneous (Cochrane’s test,  $P > 0.05$ ), and therefore there was no need to transform the data.

A cross-correlation analysis (MatLab Software) compared average, minimum, maximum daily temperatures as well as daily temperature range with endogenous levels of Hsp72 and Hsp74 over the entire sampling time for field-acclimatized mid-intertidal *T. funebris* only.

## Results

Data logger records indicate that the body temperature of mid-intertidal *Tegula* varied dramatically with tidal cycle and date over the course of this experiment (Figs. 1A and 2A). The three panels B, C, and D (Figs. 1 and 2) show the endogenous levels of Hsp72 and Hsp74 over the month of sampling.

### *Variation of Hsp70 in Tegula brunnea transplanted above its natural limit*

Specimens of *T. brunnea* transplanted into unshaded cages in the mid-zone often showed dramatically elevated levels of both Hsp72 and Hsp74 relative to control individuals collected from the shallow subtidal zone (for statistical results, see Figs. 1B and 2B). The overall response of both Hsps was very similar. Moreover, these elevated levels of Hsps seen in transplanted individuals were correlated with environmental factors: 3 days on which Hsp72 and Hsp74 levels were 2 to 4 times higher in sun-exposed mid-intertidal snails than in control snails from the shallow subtidal were preceded by periods of 2 or more days of midday low tides that greatly raised body temperatures for 1–4 h (3 and 13 April and 1 May 01). However, on 21 April, sun-exposed specimens of *T. brunnea* showed 6 times higher endogenous levels of Hsp72 and Hsp74 than control animals, but maximal daily temperatures during the preceding 4 days were relatively low compared to other time periods.

In addition, individuals of *T. brunnea* that were transplanted into shaded mid-zone cages showed elevated levels of Hsps only slightly more often than control snails from the shallow subtidal, and to a greater degree in the case of Hsp74 (e.g., 10 April and 24 April) than in Hsp72. In contrast, sun-exposed individuals often showed greater Hsp levels relative to their shaded conspecifics that were transplanted into the mid-zone, with Hsp72 levels almost always being higher in the sun-exposed *T. brunnea* (Fig. 1B).

### *Time course of Hsps in transplanted and field-acclimatized Tegula funebris*

We quantified the time course of Hsp levels in specimens of *T. funebris* from the mid-intertidal zone that were either

experimentally caged (sun-exposed) or unrestricted (field-acclimatized) to address three issues. First, we tested for caging artifacts by comparing caged and uncaged snails within the same zone. Second, we tested the prediction that the mid-intertidal *Tegula* congener would activate the heat-shock response more frequently than the shallow subtidal congener due to their differing thermal environments and heat-shock responses (Tomanek and Somero, 1999, 2000). Third, we compared the response to thermal stress in the two temperate *Tegula* congeners that occupy different tidal heights under “common garden” conditions (see below).

Unrestricted individuals of *T. funebris* were collected in crevices next to the unshaded cages. The two groups did not differ until the last week in April, when Hsp72 levels were higher in sun-exposed caged snails than in field-acclimatized snails (Fig. 1C). Preceding this time period, peak temperatures from data loggers were relatively low, but they increased greatly with the onset of a 10-day period of early to midday low tides. Hsp74 levels showed a similar pattern, but in addition, field-acclimatized individuals showed higher levels than caged snails from 10 to 13 April (Fig. 2C). Thus, caged specimens of *T. funebris* were apparently more thermally stressed than their unrestricted conspecifics during the last week of the study, perhaps because caging limited the access of snails to shaded and moist microhabitats.

With time and changing temperatures, Hsp72 levels varied little until they increased in caged but not in unrestricted individuals (Fig. 1C). Although Hsp74 levels showed greater temporal variability, the resulting changes were still within the range of variation observed for shallow subtidal *T. brunnea* (Fig. 2B, C—field samples). Neither Hsp72 nor Hsp74 showed any correlations with any of the temperature variables (cross-correlation analysis,  $P > 0.05$ ). These results suggest that mid-intertidal *T. funebris* does not elevate levels of Hsps more often than *T. brunnea* does under the less thermally variable conditions of the shallow subtidal.

### *Interspecific comparisons of Tegula in the mid-zone*

Transplanting both species to unshaded cages in the mid-intertidal zone allowed us to compare their responses to thermal stress under common garden conditions. Whereas transplanted specimens of *T. brunnea* responded to thermal stress, specimens of *T. funebris* caged in the mid-zone (their natural zone of occurrence) changed little (Figs. 1D and 2D). Elevated levels of both Hsps indicate a response to thermal variation during time periods of midday low tides in *T. brunnea* (see above for details). Although base levels of Hsp72 in sun-exposed *T. brunnea* were close to levels found for *T. funebris*, Hsp74 levels were, regardless of the tidal

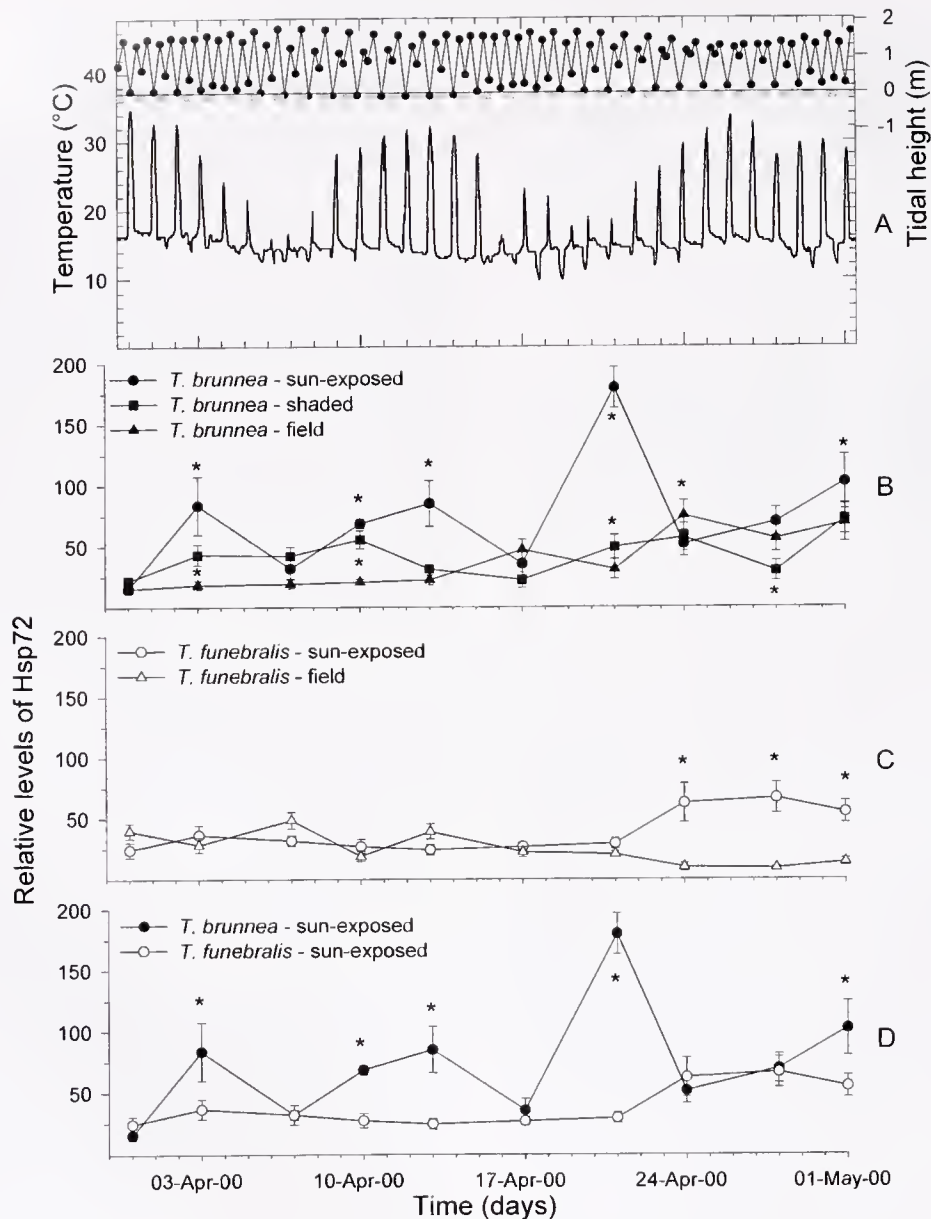


**Figure 1.** Environmental variation and time course of heat-shock protein expression (Hsp72) in experimental and control snails. (A) Tidal heights (m above mean lower low water) for Monterey Bay, day and night (gray) cycles, and temperatures recorded in a gelatin-filled snail shell (*Tegula funebris* attached in the mid-intertidal zone). Snails within unshaded (sun-exposed) and shaded cages experienced lower temperatures. (B) Time course of endogenous levels of Hsp72 for specimens of *Tegula brunnea* transplanted to unshaded and shaded mid-intertidal cages versus field-acclimatized conspecifics (shallow subtidal zone). (C) Hsp72 levels for restricted (caged) and unrestricted (field-acclimatized) individuals of *T. funebris* (mid-intertidal zone) and (D) for *T. funebris* and *T. brunnea* individuals transplanted into unshaded mid-intertidal cages. Levels are expressed relative to an internal control (a bovine heat-shock cognate 70). Values are mean  $\pm$  1 SEM; \* indicates significant differences ( $P \leq 0.05$ ) among treatments;  $n = 5-7$  snails for all data points (except  $n = 4$  for sun-exposed *T. brunnea* on 21 April).

regime, consistently elevated in *T. brunnea* (with one exception on 7 April), supporting our previous results from laboratory acclimation experiments (Tomanek and Somero, 2002).

## Discussion

Although temporal variation in levels of heat-shock protein (Hsp) has been suggested to closely track sublethal

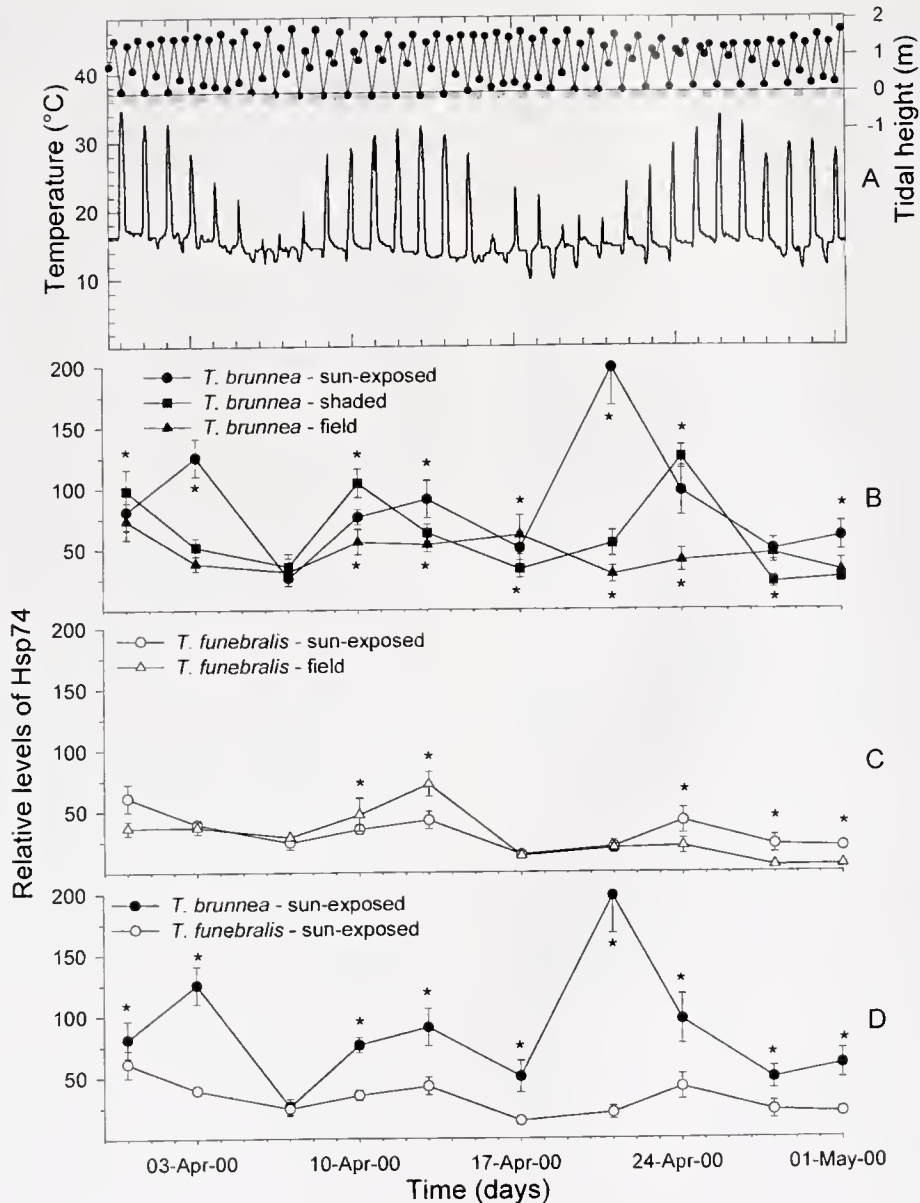


**Figure 2.** Environmental variation and time course of heat-shock protein expression (Hsp74) in experimental and control snails. (A) Tide heights, day and night cycles, and mid-intertidal temperatures (see Fig. 1 legend for details). (B) Time course of endogenous levels of Hsp74 for specimens of *Tegula brunnea* transplanted to unshaded (sun-exposed) and shaded mid-intertidal cages versus field-acclimatized conspecifics (shallow subtidal zone). (C) Hsp74 levels for restricted (caged) and unrestricted (field-acclimatized) individuals of *Tegula funebris* (mid-intertidal zone) and (D) for *T. funebris* and *T. brunnea* transplanted into unshaded mid-intertidal cages (see Fig. 1 legend for details).

stress, there have been few tests of this hypothesis under natural conditions. Furthermore, the ecological importance of interspecific variation in the heat-shock response deduced from laboratory studies has not been tested in the field. In this study we show that the subtidal to low-intertidal *Tegula brunnea* transplanted above its natural zone of occurrence experienced sublethal thermal stress, as reflected by elevated levels of two isoforms of the 70-kDa family of heat-

shock proteins (Hsp72 and Hsp74). In contrast, levels of Hsp72 and Hsp74 varied little in control specimens of *Tegula brunnea* collected from the shallow subtidal zone, and less in *T. brunnea* individuals transplanted to shaded mid-intertidal cages. In addition, *T. funebris* transplanted within its natural zone of occurrence, to mid-intertidal cages, but not field-acclimatized individuals, showed slightly elevated Hsp levels during a prolonged midday

low-tide period only. Here we discuss (1) how the time course of Hsp expression correlates with an organism's thermal history, and (2) how interspecific variation in the heat-shock response may limit the vertical distribution range of intertidal invertebrates.

#### *Time course of Hsp levels*

One of the objectives of this study was to examine the correlation between thermal events and the organism's response through time to better interpret the role of Hsps as biochemical indicators of sublethal thermal stress. The time course of levels of Hsp70 shows that periods of extreme thermal conditions upregulate endogenous levels of Hsp70 isoforms in transplanted *T. brunnea*, but not in individuals of both species that were collected from their natural thermal environment (Figs. 1B–C and 2B–C). One exception to the association between increased Hsp levels in transplanted *T. brunnea* and peak temperatures occurred on 21 April. However, changes in the daily temperature range (Tomanek, 2002) during the preceding days, from 16 to 17 April, were of similar magnitude as at the onset of a midday low-tide series (e.g., 8 to 9 April), even if maximal temperatures were relatively low. Hsp levels were upregulated in response to physiological stress for not more than 3 to 4 days.

It is still unclear what thermal signals elicit an increase in Hsp levels. Levels in field-acclimatized mid-intertidal *T. funebris* did not correlate with any of the thermal variables tested. Hsp levels will respond differently to chronic and acute thermal stress (Helmuth and Hofmann, 2001), but further studies are needed to test the response of Hsps to more complex thermal signals.

We predicted increased Hsp levels in transplanted *T. brunnea* on the basis of its long recovery (> 50 h) in the laboratory from a heat-shock-inducing thermal exposure typical of the mid-intertidal zone (30 °C; Tomanek and Somero, 2000). These studies also indicated that *T. funebris* would activate Hsp synthesis for at least several hours ( $\leq$  6 h for Hsp70) in response to temperatures of 30 °C or above—exposures that were reached at least several times during this month-long field experiment (Fig. 1A). In addition, the activation temperature of Hsp synthesis is 27 °C in laboratory-acclimated (constant temperature) specimens of *T. funebris* that were exposed to a wide range of incubation temperatures following rapid heating in seawater (Tomanek and Somero, 1999). Although these laboratory conditions do not match field conditions completely, the activation temperature should be within a few degrees of 27 °C, certainly below 35 °C—one of the highest temperatures that field-acclimatized specimens of *T. funebris* experienced during our month-long sampling period. Additionally, Hsp synthesis is upregulated for several hours in response to an acute thermal stress in mussels collected from

the field after low tide, presumably in response to protein denaturation due to thermal stress (Hofmann and Somero, 1996b).

This discrepancy between our field results and our laboratory-based predictions could be due to several factors: first, most of our laboratory incubations were done in water, leading to a high rate of heating. However, heat stress in the intertidal zone is typically experienced under aerial conditions, when heating is slower (Tomanek and Somero, 2000). Second, our collection interval of 3 to 4 days may have missed an increase in levels of Hsp70 isoforms in response to thermal stress on some collecting days that followed several midday low tides after which individuals may show an attenuated response. Yet some of those collecting days were preceded by the "first" extreme low tide following several days of minor tides (e.g., 10 and 24 April). Although the recovery time of elevated Hsp synthesis in response to heat stress in *T. funebris* is short (6 h; Tomanek and Somero, 2000), we should have detected elevated endogenous Hsp levels over a much longer time period. Other studies have observed elevated Hsp levels in response to short-term acute severe heat stress (elevation lasting up to 2 weeks; Clegg *et al.*, 1998) and to long-term chronic mild heat stress (elevation as long as 4 days; Nakano and Iwama, 2002). Alternatively, Hsp70 is closely regulated and quickly eliminated in granules following heat shock (Morimoto, 1998), and we may have therefore missed briefly elevated levels of Hsp70. A final factor may be that the moderation of temperatures generated by the cages themselves (even those cages without additional shading), may have kept the temperatures of caged snails below 30 °C.

#### *Interspecific variation in the heat-shock response and vertical distribution limits in intertidal invertebrates*

By transplanting *T. brunnea* above its natural zone of occurrence and by following the time course of changes in endogenous levels of Hsps over a month of thermal variation, we were able to directly evaluate the importance of interspecific variation in the heat-shock response in relation to vertical distribution limits.

Transplanted specimens of *T. brunnea* increased their endogenous levels of both Hsp72 and Hsp74 in response to midday low-tide periods and therefore reached, as predicted, temperatures above the activation threshold for their stress response (Tomanek and Somero, 1999, 2000). Mortality in transplanted *T. brunnea* is also indicative of severe stress (8.5% mortality in sun-exposed individuals over the entire month; no individuals of *T. funebris* died). Endogenous levels of Hsp72 and Hsp74 changed little in *T. funebris* in comparison to *T. brunnea*, and this could be mainly due to this species' higher activation temperature. In the laboratory, *T. funebris* activates the heat-shock response at 27 °C versus 24 °C in *T. brunnea* (following

acclimation to 13 °C and after rapid heating in seawater to a wide range of incubation temperatures). Thus the relative differences between activation temperatures of the stress response are good predictors of the relative levels of sublethal thermal stress and therefore the relative increases in endogenous levels of Hsps under common garden conditions, although the actual activation of the stress response depends on the heating rate and the medium (air *versus* water; Tomanek and Somero, 2000).

An increase in endogenous levels of Hsps in *T. brunnea* could also have been caused by the reduction in feeding time that accompanied the transplantation from the low- to the mid-intertidal zone. A reduction in feeding time is likely to lower metabolic rates (Shick, 1981; Branch *et al.*, 1988) and cellular energy levels (*e.g.*, ATP), which may disrupt protein homeostasis. Individuals of *T. brunnea* transplanted to shaded mid-intertidal cages differed from unmanipulated snails collected from the shallow subtidal zone in experiencing slightly higher body temperatures and much longer emersion times. Yet levels of Hsp72 and Hsp74 did not differ consistently between shaded mid-intertidal transplants and shallow subtidal controls, suggesting that longer emersion times *per se* were not activating increased Hsp levels. Other stress factors, *e.g.*, osmotic and desiccation stress, may also contribute to changes in Hsp70 levels, but these were not addressed in this study.

These results suggest that thermal conditions in the mid-intertidal zone are stressful for the subtidal to low-intertidal *T. brunnea*, but not for the low- to mid-intertidal *T. funebris*, and thus may contribute to preventing *T. brunnea* from inhabiting the mid-intertidal zone. This is in large part due to the lower activation temperature ( $T_{on}$ ) of the stress response, the 6 °C lower temperature of maximal Hsp synthesis ( $T_{peak}$ ), and the lower temperature at which the synthesis of proteins (including Hsps) ceases in *T. brunnea* ( $T_{off}$ ; Tomanek and Somero, 1999). In addition, levels of the heat-shock transcription factor1 (HSF1) are lower in *T. brunnea* than in *T. funebris* (Tomanek and Somero, 2002).

*T. funebris* is therefore better adapted to the physical conditions of the mid-intertidal zone, but such adaptations in the heat-shock response may be costly. For example, higher Hsp70 levels due to experimentally higher gene copy numbers of Hsp70 can impact life-history traits (*e.g.*, mortality and developmental time) that determine fecundity in *Drosophila* (Krebs and Feder, 1997a, b), and yeast strains with lower levels of Hsp104 grow faster (Sanchez *et al.*, 1992). Furthermore, Hsps can interact in detrimental ways with native proteins under nonstressful conditions and are therefore rapidly sequestered from the cytoplasm (Feder *et al.*, 1992). Thus, higher costs due to adaptations in the stress response to the mid-intertidal environment may in part explain why *T. funebris* shows slower growth rates than its low-intertidal to subtidal congeners *T. brunnea* and *T. montereyi* (Frank, 1965; Paine, 1969; Watanabe, 1982).

However costly elevated levels of Hsps are, the transient upregulation of endogenous levels in subtidal to low-intertidal gastropods in the mid-intertidal zone shows that Hsps are good indicators of the thermal sensitivities of physiological systems under common field conditions. Our results also confirm our prediction that interspecific variation in the heat-shock response of *Tegula* congeners is adaptive to life in the thermally variable mid-intertidal zone (Tomanek, 2002).

### Acknowledgments

The study was supported by the David and Lucile Packard Foundation and a National Science Foundation grant (IBN-0113184 to Dr. George Somero). We thank Michelle Phillips and Shanshan Bao for their help with the immunochemical analysis; Josh Troll for his help collecting animals in the field; and Drs. Jim Watanabe, Mark Denny, and Chris Harley for their comments and advice on the manuscript and statistical analyses. Dr. George Somero generously supported our work with advice, laboratory space, and funding. This is contribution number 137 of the Partnership for Interdisciplinary Studies of Coastal Oceans (PISCO): A Long-Term Ecological Consortium funded by the David and Lucile Packard Foundation.

### Literature Cited

- Abbott, D. P., and E. C. Haderlie. 1980. Prosobranchia: marine snails. Pp. 230–307 in *Intertidal Invertebrates of California*, R. H. Morris, D. P. Abbott, and E. C. Haderlie, eds. Stanford University Press, Stanford, CA.
- Benson, K. R. 2002. The study of vertical zonation on rocky intertidal shores—a historical perspective. *Integr. Comp. Biol.* **42**: 776–779.
- Branch, G. M., P. Borchers, C. R. Brown, and D. Donnelly. 1988. Temperature and food as factors influencing oxygen consumption of intertidal organisms, particularly limpets. *Am. Zool.* **28**: 137–146.
- Buckley, B. A., M.-E. Owen, and G. E. Hofmann. 2001. Adjusting the thermostat: the threshold induction temperature for the heat-shock response in intertidal mussels (genus *Mytilus*) changes as a function of thermal history. *J. Exp. Biol.* **204**: 2816–2829.
- Chapple, J. P., G. R. Smerdon, R. J. Berry, and A. J. S. Hawkins. 1998. Seasonal changes in stress-70 protein levels reflect thermal tolerance in the marine bivalve *Mytilus edulis* L. *J. Exp. Mar. Biol. Ecol.* **229**: 53–68.
- Clegg, J. S., K. R. Uhlinger, S. A. Jackson, G. N. Cherr, E. Rifkin, and C. S. Friedman. 1998. Induced thermotolerance and the heat shock protein-70 family in the Pacific oyster *Crassostrea gigas*. *Mol. Mar. Biol. Biotechnol.* **7**: 21–30.
- Dahlhoff, E. P., B. A. Buckley, and B. A. Menge. 2001. Physiology of the rocky intertidal predator *Nucella ostrina* along an environmental stress gradient. *Ecology* **82**: 2816–2829.
- Dietz, T. J., and G. N. Somero. 1992. The threshold induction temperature of the 90-kDa heat shock protein is subject to acclimatization in eurythermal goby fishes (genus *Gillichthys*). *Proc. Natl. Acad. Sci. USA* **89**: 3389–3393.
- Dietz, T. J., and G. N. Somero. 1993. Species and tissue-specific synthesis patterns for heat-shock proteins HSP70 and HSP90 in several marine teleost fishes. *Physiol. Zool.* **66**: 863–880.
- Feder, J. H., J. M. Rossi, J. Solomon, N. Solomon, and S. Lindquist.

1992. The consequences of expressing Hsp70 in *Drosophila* cells at normal temperatures. *Genes Dev.* **6**: 1402–1413.
- Feder, M. E., and G. E. Hofmann. 1999. Heat-shock proteins, molecular chaperones, and the stress response: evolutionary and ecological physiology. *Annu. Rev. Physiol.* **6**: 243–282.
- Feige, U., R. I. Morimoto, I. Yahara, and B. S. Polla. 1996. *Stress Inducible Cellular Responses*. Birkhäuser Verlag, Basel.
- Frank, P. W. 1965. Shell growth in a natural population of the turban snail, *Tegula funebralis*. *Growth* **29**: 395–403.
- Frydman, J. 2001. Folding of newly translated proteins *in vivo*: the role of molecular chaperones. *Annu. Rev. Biochem.* **70**: 603–649.
- Hartl, F. U., and M. Hayer-Hartl. 2002. Molecular chaperones in the cytosol: from nascent chain to folded protein. *Science* **295**: 1852–1858.
- Helmuth, B. S. T., and G. E. Hofmann. 2001. Microhabitats, thermal heterogeneity, and patterns of physiological stress in the rocky intertidal zone. *Biol. Bull.* **201**: 374–384.
- Hofmann, G. E., and G. N. Somero. 1995. Evidence for protein damage at environmental temperatures: seasonal changes in levels of ubiquitin conjugates and hsp70 in the intertidal mussel *Mytilus trossulus*. *J. Exp. Biol.* **198**: 1509–1518.
- Hofmann, G. E., and G. N. Somero. 1996a. Interspecific variation in thermal denaturation of proteins in the congeneric mussels *Mytilus trossulus* and *M. galloprovincialis*: evidence from the heat-shock response and protein ubiquitination. *Mar. Biol.* **126**: 65–75.
- Hofmann, G. E., and G. N. Somero. 1996b. Protein ubiquitination and stress protein synthesis in *Mytilus trossulus* occurs during recovery from tidal emersion. *Mol. Mar. Biol. Biotechnol.* **5**: 175–184.
- Krebs, R. A., and M. E. Feder. 1997a. Deleterious consequences of Hsp70 overexpression in *Drosophila melanogaster* larvae. *Cell Stress Chaperones* **2**: 60–71.
- Krebs, R. A., and M. E. Feder. 1997b. Natural variation in the expression of the heat-shock protein HSP70 in a population of *Drosophila melanogaster* and its correlation with tolerance of ecologically relevant thermal stress. *Evolution* **51**: 173–179.
- Lindquist, S. 1986. The heat-shock response. *Annu. Rev. Biochem.* **55**: 1151–1192.
- Lindquist, S., and E. A. Craig. 1988. The heat-shock proteins. *Annu. Rev. Genet.* **22**: 631–678.
- Morimoto, R. I. 1998. Regulation of the heat shock transcriptional response: cross talk between a family of heat shock factors, molecular chaperones, and negative regulators. *Genes Dev.* **12**: 3788–3796.
- Nakano, K., and G. K. Iwama. 2002. The 70-kDa heat shock protein response in two intertidal sculpins, *Oligocottus maculosus* and *O. snyderi*: relationship of hsp70 and thermal tolerance. *Comp. Biochem. Physiol. A* **133**: 79–94.
- Newell, R. C. 1979. *Biology of Intertidal Animals*. Marine Ecological Surveys, Faversham, Kent, UK.
- Paine, R. T. 1969. The *Pisaster-Tegula* interaction: prey patches, predator food preference, and intertidal community structure. *Ecology* **50**: 950–961.
- Parsell, D. A., and S. Lindquist. 1994. Heat shock proteins and stress tolerance. Pp. 457–494 in *The Biology of Heat Shock Proteins and Molecular Chaperones*, Vol. 26, R. I. Morimoto, A. Tissieres, and C. Georgopoulos, eds. Cold Spring Harbor Laboratory Press, Cold Spring Harbor, NY.
- Riedman, M. L., A. H. Hines, and J. S. Pearse. 1981. Spatial segregation of four species of turban snails (genus *Tegula*) in central California. *Veliger* **24**: 97–102.
- Roberts, D. A., G. E. Hofmann, and G. N. Somero. 1997. Heat-shock protein expression in *Mytilus californianus*: acclimation (seasonal and tidal-height comparisons) and acclimation effects. *Biol. Bull.* **192**: 309–320.
- Rossi, S., and M. J. Snyder. 2001. Competition for space among sessile marine invertebrates: changes in HSP70 expression in two Pacific cnidarians. *Biol. Bull.* **201**: 385–393.
- Sanchez, Y., J. Taulien, K. A. Borkovich, and S. Lindquist. 1992. Hsp104 is required for tolerance to many forms of stress. *EMBO J.* **11**: 2357–2364.
- Sanders, B. M., C. Hope, V. M. Pascoe, and L. S. Martin. 1991. Characterization of stress protein response in two species of *Collisella* limpets with different temperature tolerances. *Physiol. Zool.* **64**: 1471–1489.
- Shick, J. M. 1981. Heat production and oxygen uptake in intertidal sea anemones from different shore heights during exposure to air. *Mar. Biol. Lett.* **2**: 225–236.
- Somero, G. N. 2002. Thermal physiology and vertical zonation of intertidal animals: optima, limits, and costs of living. *Integr. Comp. Biol.* **42**: 780–789.
- Tomanek, L. 2002. The heat-shock response: its variation, regulation and ecological importance in intertidal gastropods (genus *Tegula*). *Integr. Comp. Biol.* **42**: 797–807.
- Tomanek, L., and B. Helmuth. 2002. Physiological ecology of rocky intertidal organisms: a synergy of concepts. *Integr. Comp. Biol.* **42**: 771–775.
- Tomanek, L., and G. N. Somero. 1999. Evolutionary and acclimation-induced variation in the heat-shock responses of congeneric marine snails (genus *Tegula*) from different thermal habitats: implications for limits of thermotolerance and biogeography. *J. Exp. Biol.* **202**: 2925–2936.
- Tomanek, L., and G. N. Somero. 2000. Time course and magnitude of synthesis of heat-shock proteins in congeneric marine snails (genus *Tegula*) from different tidal heights. *Physiol. Biochem. Zool.* **73**: 249–256.
- Tomanek, L., and G. N. Somero. 2002. Interspecific- and acclimation-induced variation in levels of heat-shock proteins 70 (hsp70) and 90 (hsp90) and heat-shock transcription factor-1 (HSF1) in congeneric marine snails (genus *Tegula*): implications for regulation of hsp gene expression. *J. Exp. Biol.* **205**: 677–685.
- Watanabe, J. M. 1982. Aspects of community organization in a kelp forest habitat: factors influencing the bathymetric segregation of three species of herbivorous gastropods. Ph.D. dissertation, University of California, Berkeley.
- Watanabe, J. M. 1984. The influence of recruitment, competition, and benthic predation on spatial distributions of three species of kelp forest gastropods (Trochidae: *Tegula*). *Ecology* **65**: 920–936.

# Reproduction and Larval Morphology of Broadcasting and Viviparous Species in the *Cryptasterina* Species Complex

MARIA BYRNE<sup>1\*</sup>, MICHAEL W. HART<sup>2</sup>, ANNA CERRA<sup>1</sup>, AND PAULA CISTERNAS<sup>1</sup>

<sup>1</sup> *Department of Anatomy and Histology, F13, University of Sydney, NSW 2006, Australia; and*

<sup>2</sup> *Department of Biology, Dalhousie University, Halifax, Nova Scotia B3H 4J1, Canada*

**Abstract.** The *Cryptasterina* group of asterinid sea stars in Australasia comprises cryptic species with derived life histories. *C. pentagona* and *C. hystera* have planktonic and intragonadal larvae, respectively. *C. pentagona* has the gonochoric, free-spawning mode of reproduction with a planktonic lecithotrophic brachiolaria larva. *C. hystera* is hermaphroditic with an intragonadal lecithotrophic brachiolaria, and the juveniles emerge through the gonopore. Both species have large lipid-rich buoyant eggs and well-developed brachiolariae. Early juveniles are sustained by maternal nutrients for several weeks while the digestive tract develops. *C. hystera* was reared *in vitro* through metamorphosis. Its brachiolariae exhibited the benthic exploration and settlement behavior typical of planktonic larvae, and they attached to the substratum with their brachiolar complex. These behaviors are unlikely to be used in the intragonadal environment. The presence of a buoyant egg and functional brachiolaria larva would not be expected in an intragonadal brooder and indicate the potential for life-history reversal to a planktonic existence. Life-history traits of species in the *Cryptasterina* group are compared with those of other asterinids in the genus *Patiriella* with viviparous development. Modifications of life-history traits and pathways associated with evolution of viviparity in the Asterinidae are assessed, and the presence of convergent adaptations and clade-specific features associated with this unusual mode of parental care are examined.

## Introduction

Speciation in marine invertebrate taxa is strongly influenced by the evolution of life-history traits. Evolutionary changes that influence speciation include modifications to gamete-binding proteins, oogenesis, larval nutrition (planktotrophic, lecithotrophic), and location (planktonic, benthic) of development (Strathmann, 1985; Reid, 1990; Palumbi, 1992; Vacquier *et al.*, 1995; Byrne *et al.*, 1999, 2003; Duda and Palumbi, 1999; ÓFoighil and Taylor, 2000; Villinski *et al.*, 2002). In a large number of these cases, the combination of rapid and diverse evolution of larval forms and stasis in adult stages has resulted in congeneric species with markedly different larval phenotypes and habitats but similar adult phenotypes and ecologies. This decoupling of larval and adult morphological evolution suggests that critical examination of suspected morphospecies will reveal undiscovered marine biodiversity. Molecular and developmental studies have shown that many problematic taxa include a suite of cryptic species (Reid, 1990; Knowlton, 1993; Degnan and Lavin, 1995; ÓFoighil and Smith, 1995; Arndt *et al.*, 1996; Huber *et al.*, 2000). Application of the comparative approach has made many of these taxa important models for the investigation of processes underlying evolution and development, and speciation in the sea (Hart *et al.*, 1997; Degnan and Lavin, 1995; Huber *et al.*, 2000).

The potential for species divergence through life-history evolution is common in some marine invertebrate taxa but rare in other, even closely related, taxa. Genera in which speciation is associated with evolution of development are found among gastropods (*Littorina*, *Comus*), clams (*Lasaea*), soft corals (*Alcyonium*), asteroids (*Asterina*, *Patiriella*), echinoids (*Helicoidaris*) and ascidians (*Molgula*) (Reid, 1990; ÓFoighil and Smith, 1995; Raff, 1996; Hart *et*

Received 28 March 2003; accepted 23 July 2003.

\* To whom correspondence should be addressed. E-mail: mbyrne@anatomy.usyd.edu.au

al., 1997; Duda and Palumbi, 1999; Huber *et al.*, 2000; McFadden *et al.*, 2001). Why some taxa are prone to developmental evolution and not others is not known. In the Asteroidea, the Asterinidae is a species-rich family comprising species that share derived forms of reproduction, larval morphology, and brood protection (Byrne and Cerra, 1996; Byrne *et al.*, 1999b). Molecular phylogenetic analyses of these sea stars revealed many examples of convergence in which derived life-history traits have evolved through independent pathways (Hart *et al.*, 1997, 2003).

In temperate Australia, the *Patiriella exigua* species group includes three species: one benthic egg layer and two viviparous lineages (Dartnall, 1969, 1971; Keough and Dartnall, 1978). Until the observation of live birth, the viviparous species were considered to be morphs of *P. exigua*. Detailed analysis of mtDNA sequences revealed the presence of a second cryptic group of asterinids in the genus *Cryptasterina*, which occurs throughout Australasia (Hart *et al.*, 2003; Dartnall *et al.*, 2003). These sea stars, formerly in the *Patiriella pseudoexigua* species complex (Dartnall, 1971; Rowe and Gates, 1995), have been reassigned to *Cryptasterina* in a recent taxonomic review (Dartnall *et al.*, 2003). One lineage, *C. pentagona*, (formerly *P. pseudoexigua*) occurs in Queensland. A second lineage, *Cryptasterina* n. sp. (also formerly known as *P. pseudoexigua*) occurs in Wanlitung, Taiwan, and its planktonic lecithotrophic life history is well-documented (Chen and Chen, 1992). The viviparous species described by Hayashi (1977), *Patiriella pseudoexigua pacifica*, has been reassigned to *C. pacifica* (Dartnall *et al.*, 2003).

On the basis of the position of *C. pentagona* in the phylogenetic tree, nested between broadcasting and brooding species (Hart *et al.*, 1997), and in light of the very broad geographic range of this nominal species, it appeared likely that Australian morphs of *C. pentagona* would have interesting modes of development. A recent molecular study revealed the relationships among four lineages of this taxon recently called *P. pseudoexigua* (Hart *et al.*, 2003). In Queensland these lineages comprise two species with different life histories (Hart *et al.*, 2003). One of these species, *C. hystera*, is a recently described intragonadal brooder (Dartnall *et al.*, 2003). In this study we examined populations of *Cryptasterina* from the original type locality in Queensland and elsewhere along the coast to document details of their reproduction and development. We compared the life history traits of *C. hystera* to those of other viviparous asterinids in the genus *Patiriella* and closely related broadcasting species to assess the changes associated with the evolution of viviparity. This life history is at the extreme end of the broadcast-brooding modes of propagation in the Asteroidea. The pathways in the evolution of viviparity in the Asterinidae are assessed, and the potential for convergent adaptations in species with this unusual mode of parental care is examined.

## Materials and Methods

*Cryptasterina pentagona* was collected from five locations along the Queensland coast (Fig. 1) at irregular intervals between 1996 and 2002. This included several sites in North Queensland (10/00; 11/00; 10/02), including Airlie Beach (20°30'S; 148°45'E); Rowes Bay, Townsville (19°15'S; 146°50'E); and Bingil Bay, Mission Beach (17°50'S; 146°06'E). *C. hystera* was collected from Statue Bay (23°15'S; 150°45'E) in central Queensland (8/96; 2/96; 9/97; 10/99). The samples were used to assess the condition of the gonads and preserve samples for histology. The type locality for *P. pseudoexigua* is Airlie Beach (Dartnall, 1971). In October 2002, the gonads of specimens from Airlie Beach and several sites in Bowen (20°1'S; 148°16'E)—Dalrymple Point, Rose Bay, and Murrays Bay (Fig. 1)—were examined and processed for histology. Isolated ovaries of females from these sites and from Rowes Bay, Townsville, were induced to spawn through the use of

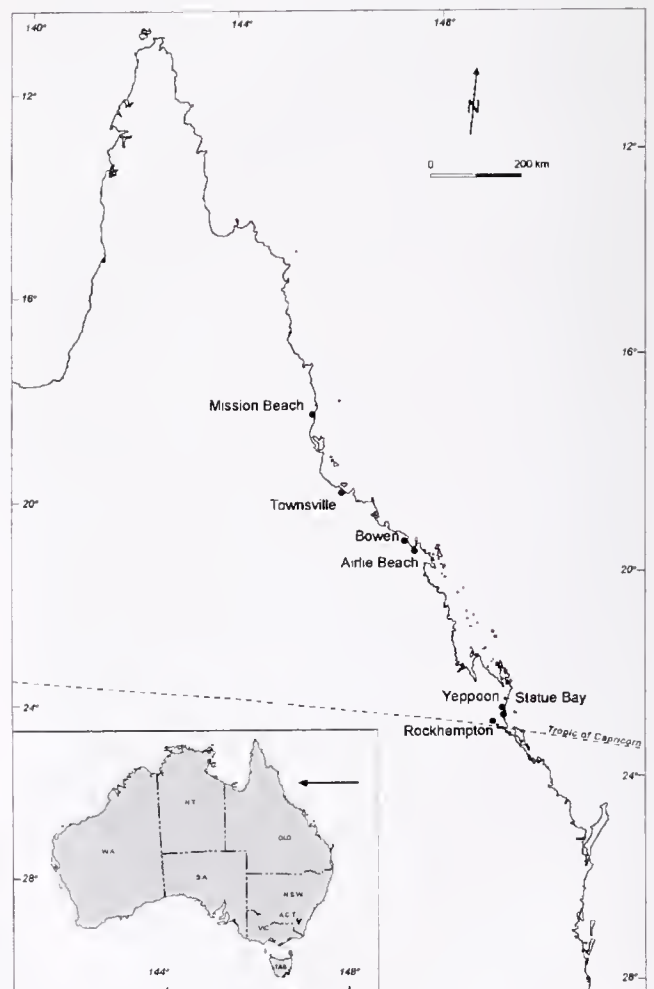


Figure 1. Map of Queensland showing sample locations and current known distributions of *Cryptasterina pentagona* and *C. hystera*.

the ovulatory hormone 1-methyladenine in filtered seawater ( $10^{-5}$  M in filtered seawater [FSW]). The eggs were fertilized with sperm removed from the testes, and the larvae were reared in FSW at 23–25 °C. Settlement substrata including glass slides aged in seawater and pieces of coralline algae were introduced into some culture dishes containing competent larvae. The gonads of the Statue Bay sea stars contained embryos. These were removed and reared *in vitro* in FSW (1.0  $\mu$ m) at 22 °C through metamorphosis.

For histology, the gonads were fixed in Bouin's fluid for 24 h, rinsed in distilled water, dehydrated in graded ethanols, and embedded in paraffin. Serial sections were stained with hematoxylin and eosin. For scanning electron microscopy, larvae and juveniles were fixed for 1 h in 2.5% glutaraldehyde in 0.45  $\mu$ m FSW. Use of a secondary fixative was found to be unnecessary (Byrne, pers. obs.). After fixation, the specimens were dehydrated, critical-point-dried, and viewed with a JEOL JSM-35C scanning electron microscope.

## Results

Our field survey of life-history traits in six populations of *Cryptasterina* provided data on the distribution of two lineages, one broadcasting species and one intragonadal brooder. *C. pentagona* from the type locality Airlie Beach (Fig. 1) was found to be a free-spawner with a short-lived planktonic larva. This species was found from Airlie Beach to Mission Beach in north Queensland (Fig. 1). Mission Beach is near the northern limit of the distribution of *C. pentagona* in Queensland (A.J. Dartnall, James Cook University, pers. comm.). This species was located under rocks high in the intertidal zone which dry out at low tide. Reports of *C. pentagona* south of Airlie Beach will have to be checked in light of the discovery of *C. hystera* in Statue Bay, Central Queensland (Fig. 1). *C. hystera* is an intragonadal brooder. Molecular data indicate that this new species also occurs in Yeppoon (Hart *et al.*, 1997). It occurs high in the intertidal under small rocks in mangrove habitats. The distribution of the two species may overlap south of Airlie Beach. A thorough search of the sites used in this study indicated that the two species do not co-occur in north Queensland.

### Planktonic developer

*C. pentagona* is a dioecious free-spawner with a planktonic lecithotrophic brachiolaria larva (Figs. 2A, B, D; 3A–C). Ovaries of specimens collected in October and November 2000 and October 2002 were gravid (Fig. 2A). They contained large eggs dominated by large lipid droplets. Spawned eggs (413  $\mu$ m diameter; SE = 6.4  $\mu$ m,  $n$  = 20) were an amber-gold color. They were positively buoyant and floated to the surface as they emerged from the gonopore. Mature testes were typical of asteroids, having a layer

of spermatogenic columns along the germinal epithelium and a lumen filled with sperm (Fig. 2B).

Development of *C. pentagona* through the stages of holoblastic radial cleavage, early blastula, wrinkled blastula, and gastrula was typical of development in lecithotrophic sea stars (Byrne, 1995). At 23 °C the early larvae (2 days) had a large preoral lobe and developing larval arms (brachia) (Fig. 3A). The central brachium developed as a bulge that emerged from the preoral lobe, flanked posteriorly on either side by two lateral brachia (Figs. 2D, 3B). Advanced brachiolariae (5 days) had a prominent brachiolar complex comprising three brachia and a central adhesive disc (Fig. 3C). Early larvae swam at the surface propelled by their cover of cilia (Fig. 3A, B, F); but as the juvenile rudiment developed in the posterior region, they swam at the bottom of the culture dishes, anterior end up. An extracellular matrix with meshlike holes covered the surface of the larvae and juveniles (Fig. 3F). This feature was most evident over the brachia of the larvae and on the oral surface and tube feet of the juveniles. Advanced larvae adhered to surfaces using their brachia. As they explored the substratum, they flexed dorsally to bring the adhesive disc to the surface. Once they were committed to metamorphose, permanent benthic attachment was achieved by the adhesive disc assisted by the brachia. The larvae attached to a range of substrata including the walls of the culture dishes, although they appeared to favor coralline algae (Fig. 2F). Most larvae metamorphosed regardless of whether a specific settlement substratum was introduced into the culture dishes. Many of them settled on the walls of their containers. Newly metamorphosed juveniles (620  $\mu$ m diameter; SE = 11.8,  $n$  = 15) had two pairs of tube feet in each radius (Fig. 3D, E). They were a dark amber color, indicating the presence of extensive maternal nutritive reserves. The mouth did not open for 3 weeks after settlement (Fig. 3D). Development to the settled juvenile stage took 9 days at 23 °C, while at ambient temperatures (30 °C) in Queensland, development was completed in 6 days (Dartnall, pers. comm.).

### Intragonadal developer

*C. hystera* had ovotestes that were a mosaic of oogenic and spermatogenic areas (Fig. 2C). Gravid specimens were present in all the samples obtained from September to November, indicating that the reproductive period lasts at least 3 months. In December 1999, the gonads contained juveniles and few gametes. The amount of spermatogenic tissue in the gonads varied among individuals ( $n$  = 20). In some specimens, sperm was only detectable histologically; in others, white testicular regions of the gonad were evident by direct examination. Like those of *C. pentagona*, the eggs were large (440  $\mu$ m diameter; SE = 6.0  $\mu$ m,  $n$  = 8) and contained abundant lipid droplets. They floated to the sur-

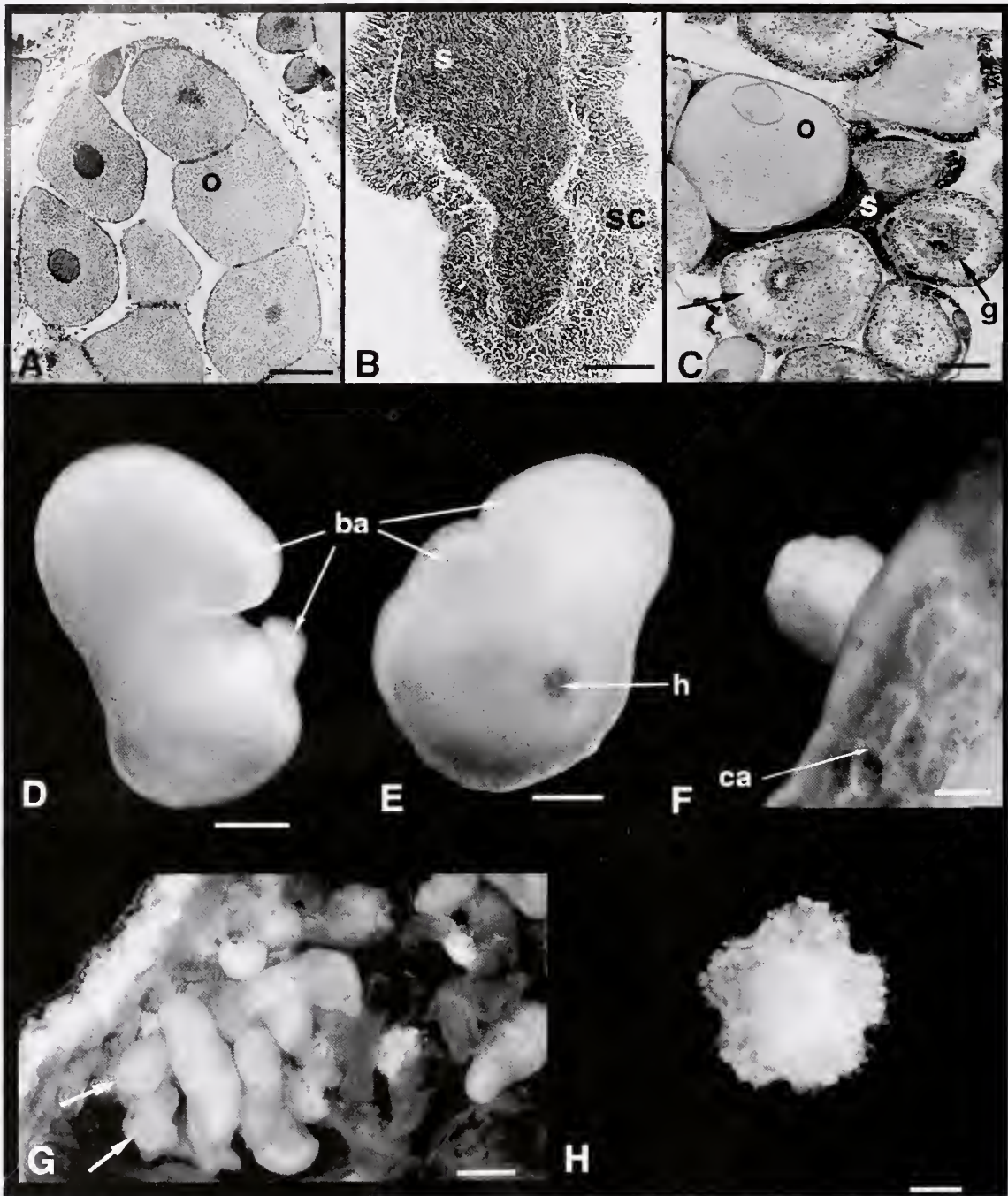


**Figure 2.** Histology and light microscopy. (A, B) *Cryptasterina pentagona* ovaries and testes. o, oocyte; s, spermatozoa; sc, spermatocyte columns. (C) *C. hystera*. The ovotestis contains lipid-rich eggs (o), sperm (s), and developing embryos (arrows); g, gastrula. (D, E) Brachiolaria larvae of *C. pentagona* and *C. hystera* respectively. ba, brachia; h, hydopore. (F) Metamorphosing juvenile *C. pentagona* on coralline algae (ca). (G) Dissected *C. hystera* showing juveniles (arrows) in gonad. (H) Newly released *C. hystera*. Scales: A–E = 100  $\mu\text{m}$ ; F, H = 200  $\mu\text{m}$ ; G = 500  $\mu\text{m}$ .

face when removed from the gonad and were gold-orange, with a dark vegetal pole.

Developing embryos and larvae were interspersed with gametes in the gonad (Fig. 2C, G). Embryos removed from

the gonad at the early blastula stage developed independently of the parent through the wrinkled blastula and gastrula stages into a planktonic highly buoyant brachiolaria. The developing brachia appeared as three bulges (Fig.

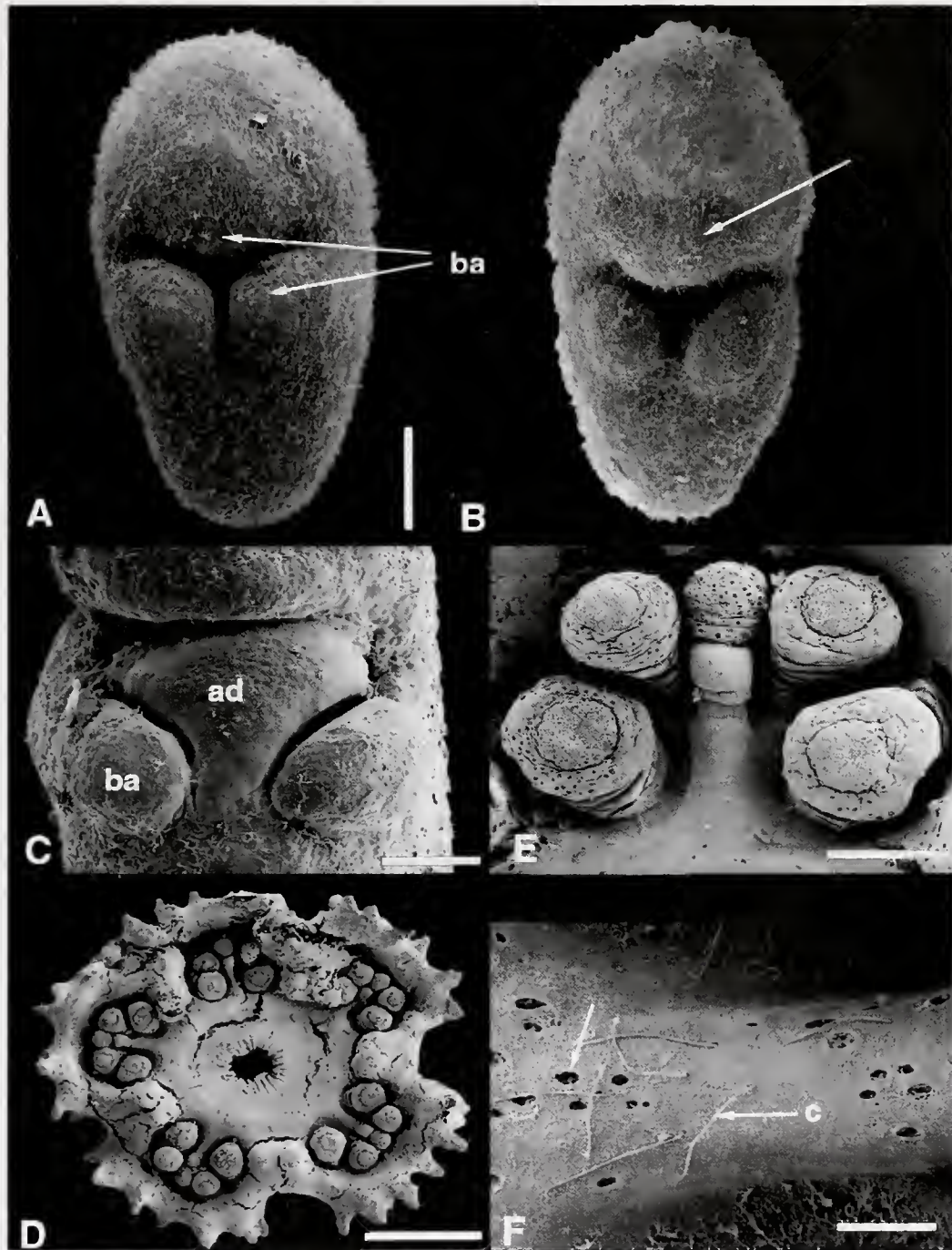


**Figure 3.** Scanning electron microscopy, *Cryptasterina pentagona*. (A, B) Brachiolaria larvae have a uniform cover of cilia. The central brachium (arrow) develops as a protrusion of the preoral lobe. (C) Advanced larva with a well-developed adhesive disc (ad) at the base of the brachia (ba). (D, E) Recently metamorphosed juvenile with two pairs of tube feet in each radius and with a mouth opening. (F) Detail of cilia (c) and meshlike matrix on larval surface. Scales: A, B = 100  $\mu\text{m}$ ; C, E = 50  $\mu\text{m}$ ; F = 4  $\mu\text{m}$ .

4A), and the adhesive disc developed between the arms (not illustrated). As in *C. pentagona*, advanced larvae had a well-developed preoral lobe from which the central brachium emerged as a bulge-like protrusion (Fig. 4B, C). They

swam anterior end up with their ciliary cover (Fig. 4F). Advanced larvae (10 days) had a well-developed brachiolar complex which was used for benthic attachment. They exhibited typical settlement behavior while exploring the

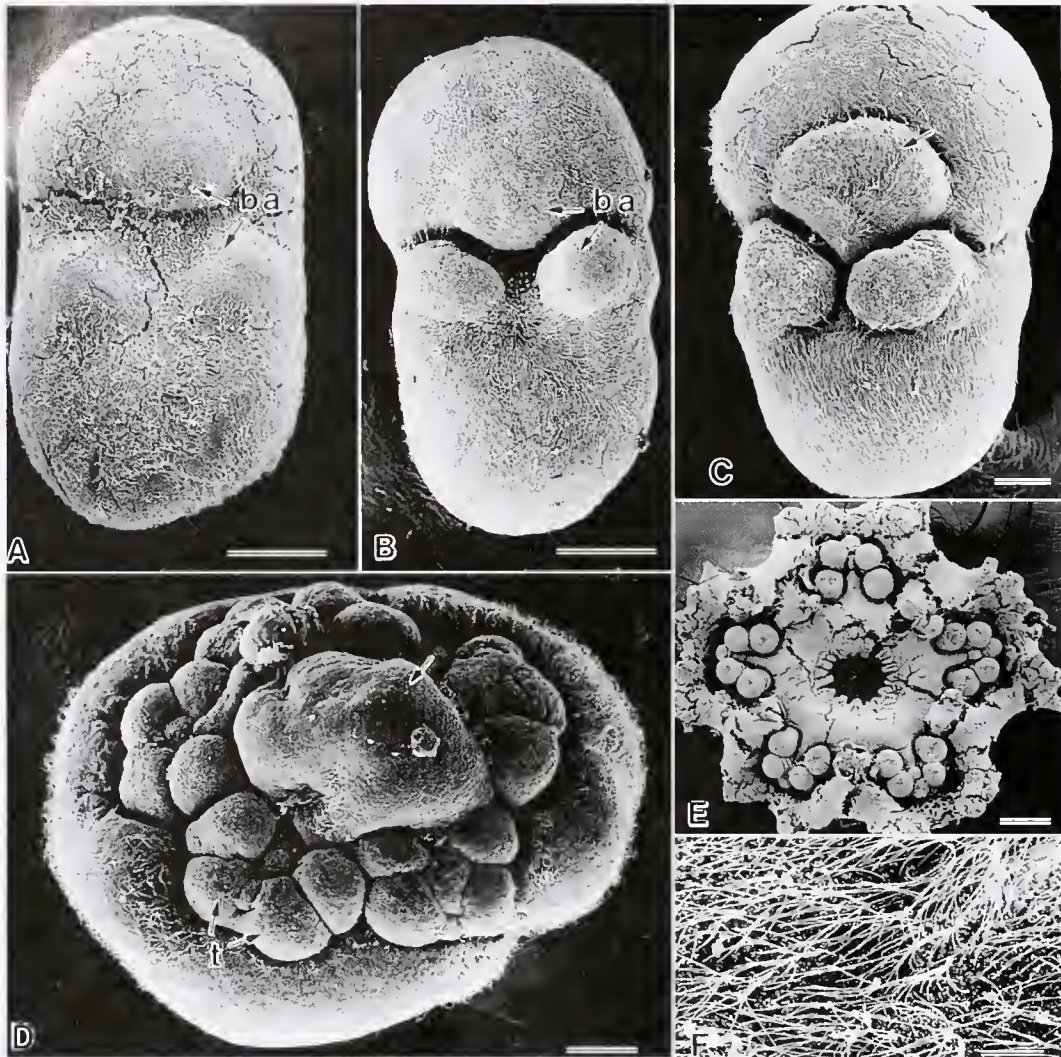


**Figure 4.** Scanning electron microscopy, *Cryptasterina hystera*. (A, B) Early larvae with developing brachia (ba). (C) Advanced larva. The central brachium (arrow) develops as a posterior protrusion of the preoral lobe. (D) Metamorphosing larva with resorbing larval body (arrow) and developing tube feet (t). (E) Recently metamorphosed juvenile with two pairs of podia in each radius and with a mouth opening. (F) Detail of cilia on larval surface. Scales: A, B, E = 100  $\mu\text{m}$ ; C, D = 50  $\mu\text{m}$ ; F = 12  $\mu\text{m}$ .

substratum and adhered to the surface of the culture dishes either with the tips of the brachia or by flexing the body to attach the adhesive disc. The juvenile rudiment developed in the posterior region as the larval body was resorbed (Fig. 4D). Development *in vitro* to the juvenile stage took 16 days. Newly settled juveniles had a dark amber pigment due to the presence of maternal nutritive reserves. It took 3 weeks for the mouth opening to develop, and by this time maternal reserves were no longer evident (Fig. 4E). Three-week-old juveniles had a well-developed skeleton.

In aquaria, juveniles (800  $\mu\text{m}$  diameter, SE = 6.3,  $n = 10$ ) with two pairs of tube feet in each radius emerged from the gonopore on the aboral surface of the adults (Fig. 2H). These juveniles had a mouth opening, a functional digestive

tract, and a well-developed skeleton. Newly released juveniles were white due to the color of the skeleton, and they appeared to lack residual maternal nutrients.

### Discussion

Recent discoveries of cryptic species in a range of taxa have been facilitated by investigation of developmental evolution and molecular phylogeny (Reid, 1990; Degnan and Lavin, 1995; ÓFoighil and Smith, 1995; Williams, 2000; Flowers and Foltz, 2001; McFadden *et al.*, 2001). Observations of juvenile birth resulted in the description of new viviparous *Patiriella* in the *P. exigua* group (Dartnall, 1969, 1971; Keough and Dartnall, 1978), and our investi-

gation of cryptic biodiversity in *Cryptasterina* was prompted by the results of molecular phylogeny (Hart *et al.*, 1997). The Asterinidae are a taxonomically difficult group and detection of the cryptic species investigated here would have been difficult with traditional taxonomy because adult forms appear very similar even to taxonomic experts (Dartnall, 1971; Rowe and Gates, 1995). Once specific status has been determined, however, close examination of cryptic species may reveal the presence of diagnostic morphological traits (Dartnall, pers. comm.). Indeed, life-history and molecular data have guided taxonomic effort in the discovery and description of several cryptic *Patriella* species in New Zealand and Australia (O'Loughlin *et al.*, 2002; Dartnall, pers. comm.). Molecular data revealed that *C. pentagona*, the broadcasting species, occurs from the type locality Airlie Beach north to Townsville (Fig. 5; Hart *et al.*, 2003). *C. hystera* is known only from two locations, about 10 km apart. An extremely limited distribution is also characteristic of the viviparous *Patriella* (Byrne *et al.*, 1999b). A survey of mangrove habitats along the central Queensland coast will be required to determine the distribution of *C. hystera*. The nominal taxon *C. pentagona* occurs through Asia (Marsh, 1977; VandenSpiegel *et al.*, 1998), and it is likely that other divergent lineages will be found (Dartnall *et al.*, 2003). Other widely distributed asterinids such as *Patriella exigua*, which occurs from South Africa to Australia, also appear to be a suite of cryptic species (Dartnall, pers. comm.).

The life-history traits and phylogenetic relationships of species in the *Cryptasterina pentagona* group and the *Patriella exigua* group are shown in Table 1 and Figure 5. The gonochoric, free-spawning mode of reproduction seen in *C. pentagona* and *Cryptasterina* n. sp. is ancestral for the Echinodermata, while acquisition of hermaphroditism, a derived character, is exhibited by most echinoderms that brood their young (Strathmann *et al.*, 1984; Byrne, 1991, 1999; Hendler, 1991). Like those of the other viviparous

species (Table 1), the gonads of *C. hystera* were ovotestes. This indicates the potential for self-fertilization, as appears to be the case for *P. vivipara* (Byrne, 1996). The amount of sperm in the gonads of *C. hystera* is more than sufficient to fertilize all the eggs produced, and so it is likely that some individuals release sperm. For out-crossing to occur, the sperm would have to gain access to eggs by swimming through the gonopore. A genetic study is required to determine if progeny in the gonads of the viviparous *Cryptasterina* and *Patriella* are full siblings or half siblings. The diversity of the fertilization biology in these asterinids with complete out-crossing in the free-spawners, partial self-fertilization in the benthic egg layers, and potential for selfing in viviparous forms provides a useful model in which to investigate the relationships between the evolution of mating systems and the genetic structure of sea star populations (Byrne, 1995, 1996).

As characteristic of echinoderms, the evolution of lecithotrophy in *Cryptasterina* species involved acquisition of a large egg (Table 1). The increase in egg size from what would have been an ancestral form with a small egg and planktotrophic development is considered to have been necessary to sustain development without feeding (Mortensen, 1921; Strathmann, 1978; Emler *et al.*, 1987). The presence of extensive nutritive reserves in newly metamorphosed juveniles, however, shows that a considerable portion of maternal reserves in the eggs of the two *Cryptasterina* species investigated here is allocated to the perimetamorphic postlarval period. A substantial proportion of the maternal provisions in their large eggs is stored through larval development to support development of the postlarval stages, a feature seen in other lecithotrophic echinoderms (Emler and Hoegh-Guldberg, 1997; Hoegh-Guldberg and Emler, 1997; Byrne *et al.*, 1999a, 2003; Villinski *et al.*, 2002). In contrast, the small eggs (135–150  $\mu\text{m}$  diameter) of *P. vivipara* and *P. parvivipara* are similar in size to those (150  $\mu\text{m}$  diameter) of their planktotrophic congener *P.*

Table 1

Life-history traits of the *Cryptasterina pentagona* and *Patriella exigua* species groups

Species*	Location†	Gonad structure	Egg size (diam in $\mu\text{m}$ )	Larval habitat
<i>C. pentagona</i> group				
<i>C. pentagona</i>	Qld	Dioecious	413	Planktonic
<i>C. hystera</i>	Qld	Hermaphrodite	440	Intragonadal
<i>C. pacifica</i> (1)	Japan	Hermaphrodite	450	Intragonadal
<i>C. n. sp.</i> (2)	Taiwan	Dioecious	320	Planktonic
<i>P. exigua</i> group				
<i>P. exigua</i> (3)	NSW, Tas, SA	Dioecious	360	Benthic
<i>P. vivipara</i> (4)	Tas	Hermaphrodite	150	Intragonadal
<i>P. parvivipara</i> (4)	SA	Hermaphrodite	135	Intragonadal

\* (1) Komatsu *et al.* (1990); (2) Chen and Chen (1992); (3) Byrne (1995); (4) Byrne (1996).

† NSW, New South Wales; Qld, Queensland; SA, South Australia; Tas, Tasmania.

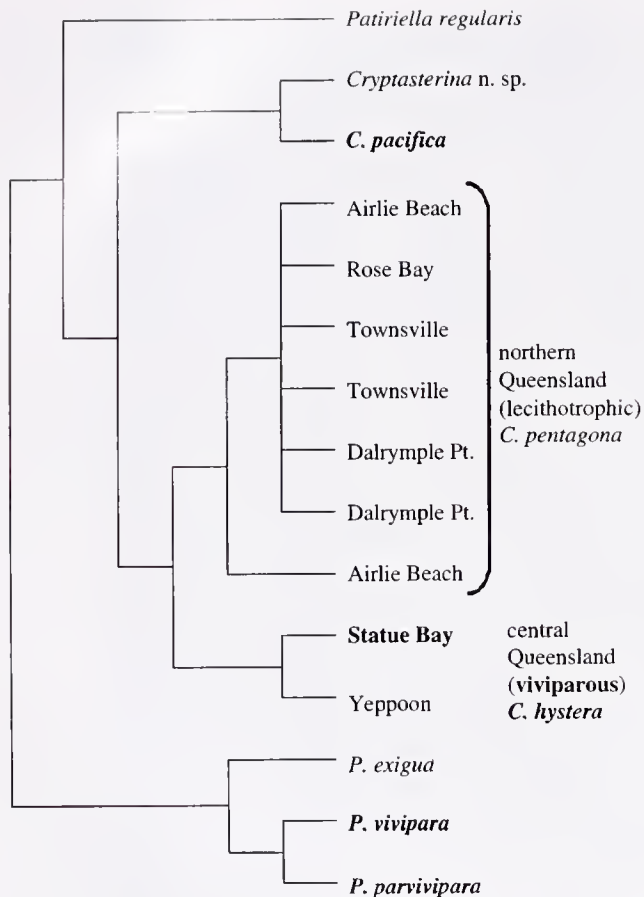


**Figure 5.** Phylogenetic tree based on branch-and-branch searching of mtDNA sequences (COI and 5 tRNA genes) from the *Cryptasterina pentagona* and *Patriella exigua* groups (after Hart *et al.*, 1997, 2003). Species in bold are known to be viviparous. Bootstrapping produced strong support ( $\geq 92\%$ ) for monophyly of the six northern Queensland lineages, for two southern Queensland lineages, and for all these lineages as a clade separate from *P. regularis*. The Yeppoon specimen was from a museum collection and the presence of intragonadal embryos could not be confirmed.

*regularis* and represent a secondary reduction in size (Byrne and Cerra, 1996; Hart *et al.*, 1997). The eggs of *P. vivipara* and *P. parvivipara* support intragonadal lecithotrophic development to a very small postlarva (200–300  $\mu\text{m}$  diameter), indicating that the maternal reserves in these eggs may be near the limit required to support development through metamorphosis in the absence of feeding (Byrne, 1996).

The larvae and juveniles of *C. pentagona* have a meshlike extracellular matrix covering regions of the body, similar to that described for *P. regularis* (Byrne and Barker, 1991). Preservation of this matrix depends on fixation method, suggesting it may be an artifact (Byrne, pers. obs.). Alternatively, its presence in some regions of larvae and juveniles such as the brachiolar arms and oral surface indicates that the extracellular matrix may have regional differences.

Newly settled juveniles of *C. pentagona* (612  $\mu\text{m}$  diam-

eter) and *C. hystera* (600  $\mu\text{m}$  diameter) reared *in vitro* were supported by maternal nutrients for several weeks until the digestive tract became functional and juveniles could feed. Juveniles of *C. hystera* (2–3 weeks old, 800  $\mu\text{m}$  diameter) left the parent with a functional gut. Similarly, newly metamorphosed juveniles of *C. pacifica* (650  $\mu\text{m}$  diameter) emerge from the gonopore (900  $\mu\text{m}$  diameter) with a functional gut (Komatsu *et al.*, 1990). The juveniles of *P. vivipara* and *P. parvivipara* continue their growth in the gonads to become the largest recruiting juveniles (1.0–5.0 mm diameter) known for the Asteroidea (Byrne, 1996). They spend up to a year in the gonads preying on their siblings, an unconventional source of maternal nutrients. There may be selection for extended brood care in the viviparous species. Intragonadal brooding of progeny through the vulnerable early postlarval stages and their release at a large size undoubtedly conveys a survival advantage for the juveniles. Mortality of the early settlement stages of marine invertebrates is usually high (Gosselin and Qian, 1997). Interestingly, the gonads of *C. hystera* contained a few large juveniles (1–2 mm diameter), indicating that brood cannibalism occasionally occurs in this species (Byrne, pers. obs.).

The eggs of species in the *Cryptasterina* group have conspicuous lipid reserves, a feature characteristic of echinoderms with planktonic lecithotrophy (Emlet *et al.*, 1987; Emlet and Hoegh-Guldberg, 1997; Hoegh-Guldberg and Emlet, 1997; Byrne *et al.*, 1999a, 2003; Villinski *et al.*, 2002). Their brachiolariae are also similar in appearance, with a prominent preoral lobe and a central brachium that develops as a bulge-like protrusion (Komatsu *et al.*, 1990). Possession of a buoyant egg and a functional larva in *C. hystera* and *C. pacifica* would not be expected in viviparous asterooids. These features and the morphological similarity of their larvae to those of congeners with planktonic development suggest that viviparity in these sea stars evolved through retention and fertilization of a large egg by a *C. pentagona*-like ancestor. This suggestion is supported by molecular phylogenetic data (Fig. 5; Hart *et al.*, 2003).

The intragonadal brachiolariae of *P. vivipara* and *P. parvivipara* are vestigial, unlike those of *C. hystera*. Their minute larvae have a reduced brachiolar complex comprising three small nonsticky protrusions that cannot function in attachment, and some embryos do not develop brachia at all. Intragonadal development in *P. vivipara* and *P. parvivipara* is thought to have evolved through a *P. exigua*-like ancestor that laid benthic egg masses and had highly modified benthic nondispersive larvae (Fig. 5; Byrne, 1995; Hart *et al.*, 1997). Evolution of viviparity through retention of eggs by an ancestor with benthic egg masses is suggested to have been a likely pathway for the acquisition of this form of brooding in asterinids (Strathmann *et al.*, 1984; Byrne, 1996).

Despite their intragonadal location, the larvae of *C. hys-*

*tera* exhibited exploratory settlement behavior and attached to the substratum with their brachia and adhesive disc prior to metamorphosis, in a manner typical of planktonic asteroid larvae. This behavior is unlikely to serve any function in the intragonadal environment. A reversal to a planktonic larva is readily envisaged for *C. hystera* and *C. pacifica*, a suggestion also made for *Pteraster tessellatus* (McEdward, 1992). These species could potentially use two modes of development, releasing some progeny as dispersive larvae and others as juveniles. By contrast, *P. vivipara* and *P. parvivipara* are committed to intragonadal development. A reversal to reacquire a large egg and functional larva appears unlikely for *P. vivipara* and *P. parvivipara*.

Intragonadal development is rare in the Echinodermata. Among asteroids, intragonadal development and live birth is known for only three genera, *Cryptasterina*, *Patriella* (Table 1), and the aberrant *Xyloplax medusiformis* from the deep sea (Rowe *et al.*, 1987). Morphological and molecular evidence supports the conclusion that viviparity evolved independently three times in *Patriella* and *Cryptasterina* (Fig. 5; Hart *et al.*, 1997, 2003). Parallel evolution of derived lecithotrophic life histories is common in echinoderms and is often associated with a suite of convergent phenotypes (Strathmann, 1985; Emler *et al.*, 1987; Wray, 1996; Hart *et al.*, 1997). For asterinids, some convergent adaptations associated with viviparity are evident in all brooding species, while other features follow phylogenetic lines (Table 1, Fig. 5). With respect to adult traits, convergence is seen in possession of ovotestes and the potential for self-fertilization in both *Cryptasterina* and *Patriella*. Egg type and composition, however, is similar within these genera, but not between them. With respect to developmental phenotype, *Cryptasterina* and *Patriella* differ in the presence of functional or nonfunctional larvae. Regardless of the pathways involved in evolution of viviparity, however, the probability of making the evolutionary switch to intragonadal development appears high in the Asterinidae. Selection for viviparity may be associated with colonization of marginal habitats along the upper fringe of the intertidal, a habitat not generally utilized by sea stars. Why this unusual form of parental care evolved in *Cryptasterina* and *Patriella* and not in other asteroid taxa is not known.

### Acknowledgments

Special thanks to Drs. S. McKillup and J. Collins for providing specimens. The research was supported by a grant from the ARC (MB) and a grant from NSERC (MH).

### Literature Cited

- Arndt, A., C. Marquez, P. Lambert, and M. J. Smith. 1996. Molecular phylogeny of eastern Pacific sea cucumbers (Echinodermata: Holotheroidea) based on mitochondrial DNA sequence. *Mol. Phylogenet. Evol.* 6: 425–437.
- Byrne, M. 1991. Reproduction, development and population biology of the Caribbean ophiuroid *Ophioneis olivacea*, a protandric hermaphrodite that broods its young. *Mar. Biol.* 111: 387–399.
- Byrne, M. 1995. Changes in larval morphology in the evolution of benthic development by *Patriella exigua* (Asteroidea: Asterinidae), a comparison with the larvae of *Patriella* species with planktonic development. *Biol. Bull.* 188: 293–305.
- Byrne, M. 1996. Viviparity and intragonadal cannibalism in the diminutive asterinid sea stars *Patriella vivipara* and *P. parvivipara*. *Mar. Biol.* 125: 551–567.
- Byrne, M. 1999. Echinodermata. Pp. 940–954 in *Encyclopedia of Reproduction*. E. Knobil and J. Neill, eds. Academic Press, New York.
- Byrne, M., and M. F. Barker. 1991. Embryogenesis and larval development of the asteroid *Patriella regularis* viewed by light and scanning electron microscopy. *Biol. Bull.* 180: 332–345.
- Byrne, M., and A. Cerra. 1996. Evolution of intragonadal development in the diminutive asterinid sea stars *Patriella vivipara* and *P. parvivipara* with an overview of development in the Asterinidae. *Biol. Bull.* 191: 17–26.
- Byrne, M., A. Cerra, and J. T. Villinski. 1999a. Oogenic strategies in the evolution of development in *Patriella* (Asteroidea). *Invertebr. Reprod. Dev.* 36: 195–202.
- Byrne, M., A. Cerra, M. W. Hart, and M. J. Smith. 1999b. Life history diversity and molecular phylogeny in the Australian sea star genus *Patriella*. Pp. 186–196 in *The Other 99%: The Conservation and Biodiversity of Invertebrates*, W. Ponder and D. Lunney, eds. Transactions of the Royal Society of New South Wales, Sydney.
- Byrne, M., P. Cisternas, P. Selvakumaraswamy, J. T. Villinski, and R. R. Ralf. 2003. Evolution of maternal provisioning in ophiuroids, asteroids and echinoids. Pp. 171–175 in *Echinoderm Research 2001*. J. P. Feral and B. David, eds. Balkema, Lisse, The Netherlands.
- Chen, B. Y., and C.-P. Chen. 1992. Reproductive cycle, larval development, juvenile growth and population dynamics of *Patriella pseudoexigua* (Echinodermata, Asteroidea) in Taiwan. *Mar. Biol.* 113: 271–280.
- Clark, A. M. 1993. An index of names of Recent Asteroidea. Part 2: Valvatida. Pp. 187–366 in *Echinoderm Studies*. M. J. Jangoux and J. M. Lawrence, eds. Balkema, Rotterdam.
- Dartnall, A. J. 1969. A viviparous species of *Patriella* (Asteroidea, Asterinidae) from Tasmania. *Proc. Linn. Soc. N.S.W.* 93: 294–296.
- Dartnall, A. J. 1971. Australian sea stars of the genus *Patriella* (Asteroidea, Asterinidae). *Proc. Linn. Soc. N.S.W.* 96: 39–51.
- Dartnall, A. J., M. Byrne, J. Collins, and M. W. Hart. 2003. A new viviparous species of asterinid (Echinodermata, Asteroidea, Asterinidae) and a new genus to accommodate the species of pan-tropical exiguoid sea stars. *Zootaxa* 359: 1–14.
- Degnan, B. M., and M. F. Lavin. 1995. Highly repetitive DNA sequences provide evidence for a lack of gene flow between two morphological forms of *Herdmania momus* (Ascidiacea: Stolidobranchia). *Mar. Biol.* 124: 293–299.
- Duda, T. F., and S. R. Palumbi. 1999. Developmental shifts and species selection in gastropods. *Proc. Natl. Acad. Sci. USA* 96: 10272–10277.
- Emler, R. B., and O. Hoegh-Guldberg. 1997. The effects of egg size on post-larval performance: experimental evidence from a sea urchin. *Evolution* 51: 141–152.
- Emler, R. B., L. R. McEdward, and R. R. Strathmann. 1987. Echinoderm larval ecology viewed from the egg. Pp. 55–136 in *Echinoderm Studies*, M. J. Jangoux and J. M. Lawrence, eds. Balkema, Rotterdam.
- Flowers, J. M., and D. W. Foltz. 2001. Reconciling molecular systematics and traditional taxonomy in a species-rich clade of sea stars (*Leptasterias* subgenus *Hexasterias*). *Mar. Biol.* 139: 475–483.
- Gosselin, L. A., and P. Y. Qian. 1997. Juvenile mortality in benthic marine invertebrates. *Mar. Ecol. Prog. Ser.* 146: 265–282.
- Hart, M. W., M. Byrne, and M. J. Smith. 1997. Molecular phyloge-

- netic analysis of life-history evolution in asterinid starfish. *Evolution* **51**: 1846–1859.
- Hart, M. W., M. Byrne, and S. L. Johnson. 2003. Cryptic species and modes of development in *Patiriella pseudoexigua*. *J. Mar. Biol. Assoc. UK* **83**: 1107–1116.
- Hayashi, R. 1977. A new sea-star of *Asterina* from Japan, *Asterina pseudoexigua pacifica* n. sp. *Proc. Jpn. Soc. Syst. Zool.* **13**: 88–91.
- Hendler, G. 1991. Echinodermata: Ophiuroidea. Pp. 356–511 in *Reproduction of Marine Invertebrates. Vol. VI: Echinoderms and Lophophorates*. A. C. Giese, J. S. Pearse, and V. B. Pearse, eds. Boxwood Press, Pacific Grove, CA.
- Hoegh-Guldberg, O., and R. B. Emlet. 1997. Energy use during the development of a lecithotrophic and planktotrophic echinoid. *Biol. Bull.* **192**: 27–40.
- Huber, J. L., K. Burke da Silva, W. R. Bates, and B. J. Swalla. 2000. The evolution of anural larvae in molgulid ascidians. *Semin. Cell Dev. Biol.* **11**: 419–426.
- Keough, M. J., and A. J. Dartnall. 1978. A new species of viviparous asterinid asteroid from Eyre Peninsula, South Australia. *Rec. S. Aust. Mus.* **17**: 407–416.
- Knowlton, N. 1993. Sibling species in the sea. *Annu. Rev. Ecol. Syst.* **24**: 189–216.
- Komatsu, M., Y. T. Kano, and C. Oguro. 1990. Development of a true ovoviviparous sea star, *Asterina pseudoexigua pacifica* Hayashi. *Biol. Bull.* **179**: 254–263.
- Marsh, L. M. 1977. Coral reef asteroids of Palau, Caroline Islands. *Micronesica* **13**: 251–281.
- McEdward, L. R. 1992. Morphology and development of a unique type of pelagic larva in the starfish *Pteraster tessellatus* (Echinodermata: Asteroidea). *Biol. Bull.* **182**: 177–187.
- McFadden, C. S., R. Donahue, B. K. Hadland, and R. Weston. 2001. A molecular phylogenetic analysis of reproductive trait evolution in the soft coral genus *Alcyonium*. *Evolution* **55**: 54–67.
- Mortensen, T. 1921. *Studies of the Development and Larval Forms of Echinoderms*. G.E.C. Gad, Copenhagen. 261 pp.
- ÓFoighil, D., and M. J. Smith. 1995. Evolution of asexuality in the cosmopolitan marine clam *Lasaea*. *Evolution* **49**: 140–150.
- ÓFoighil, D., and D. J. Taylor. 2000. Evolution of parental care and ovulation behavior in oysters. *Mol. Phylogenet. Evol.* **15**: 301–313.
- O'Loughlin, P. M., J. M. Waters, and M. S. Roy. 2002. Description of a new species of *Patiriella* from New Zealand and review of *Patiriella regularis* (Echinodermata, Asteroidea) based on morphological and molecular data. *J. R. Soc. NZ* **32**: 697–711.
- Palumbi, S. R. 1992. Marine speciation on a small planet. *Trends Ecol. Evol.* **7**: 114–118.
- Raff, R. A. 1996. *The Shape of Life*. University of Chicago Press, Chicago.
- Reid, D. G. 1990. A cladistic phylogeny of the genus *Littorina* (Gastropoda): implications for evolution or reproductive strategies and for classification. *Hydrobiologia* **193**: 1–19.
- Rowe, F. W. E., and J. Gates. 1995. Echinodermata. In *Zoological Catalogue of Australia*, Vol. 33, A. Wells, ed. CSIRO, Melbourne.
- Rowe, F. W. E., A. N. Baker, and H. E. S. Clark. 1987. The morphology, development and taxonomic status of *Xyloplax* Baker, Rowe and Clark (1986) (Echinodermata: Concentricycloidea), with the description of a new species. *Proc. R. Soc. Lond. B.* **233**: 431–459.
- Strathmann, R. R. 1978. The evolution and loss of feeding larval stages of marine invertebrates. *Evolution* **32**: 894–906.
- Strathmann, R. R. 1985. Feeding and nonfeeding larval development and life history evolution in marine invertebrates. *Annu. Rev. Ecol. Syst.* **16**: 339–361.
- Strathmann, R. R., M. F. Strathmann, and R. H. Emson. 1984. Does limited brood capacity link adult size, brooding and simultaneous hermaphroditism? A test with the starfish *Asterina phylactica*. *Am. Nat.* **123**: 796–818.
- Vacquier, V. D., W. J. Swanson, and M. E. Hellberg. 1995. What have we learned about sea urchin bindin? *Develop. Growth Differ.* **37**: 1–10.
- VandenSpiegel, D., D. J. W. Lane, S. Stapanato, and M. Jangoux. 1998. The asteroid fauna (Echinodermata) of Singapore with a distribution table and an illustrated identification to the species. *Raffles Bull. Zool.* **46**: 431–470.
- Villinski, J. T., J. L. Villinski, M. Byrne, and R. R. Raff. 2002. Convergent maternal provisioning and life history evolution in echinoderms. *Evolution* **56**: 1764–1775.
- Williams, S. T. 2000. Species boundaries in the starfish genus *Linckia*. *Mar. Biol.* **136**: 137–148.
- Wray, G. A. 1996. Parallel evolution of nonfeeding larvae in echinoids. *Syst. Biol.* **45**: 308–322.

# Persistent Ancestral Feeding Structures in Nonfeeding Annelid Larvae

BRUNO PERNET

*Friday Harbor Laboratories, 620 University Road, Friday Harbor, Washington 98250*

**Abstract.** Evolutionary loss of the requirement for feeding in larvae of marine invertebrates is often followed by loss of structures involved in capturing and digesting food. Studies of echinoderms suggest that larval form evolves rapidly in response to loss of the requirement for feeding, but a lack of data from other taxa makes it difficult to assess the generality of this result. I show that many members of a large clade of annelids, the Sabellidae, retain ancestral systems for particle capture despite loss of the need and ability to feed. In at least one species, *Schizobranchia insignis*, an opposed-band system of prototrochal, food-groove, and metatrochal ciliary bands can concentrate suspended particles and transport them to the mouth, but captured particles are invariably rejected because larvae lack a functional gut. The persistence of particle capture systems in larvae of sabellids suggests that they have lost larval feeding very recently, that opposed bands are inexpensive to construct and operate, or that opposed bands have some alternative function. These observations also suggest a hypothesis on how the ability to feed is lost in larvae of annelids and other spiralian following increases in egg size.

## Introduction

Larvae of some marine invertebrates require particulate food to complete development to the juvenile stage, but others cannot feed and instead rely on materials stored in the egg. These alternative nutritional modes are associated with differences in many other traits, including embryonic development (Wray and Bely, 1994), dispersal and population genetic structure (Palumbi, 1995), species duration (Jablonski, 1986), and perhaps most obviously, larval form. Feeding larvae bear structures that function in particle capture, ingestion, and assimilation, while nonfeeding larvae tend to lack such structures and are relatively simple in external

form (Emlet, 1991). Many species with nonfeeding larval development evolved independently from ancestors that had feeding larvae (Strathmann, 1978). This suggests a strong evolutionary association between the loss of the requirement for feeding and the loss of larval feeding structures (Wray, 1996).

How does this association arise? One model suggests that the first step in the evolution of nonfeeding development is an increase in the energy content of the egg (Jagersten, 1972; Strathmann, 1975; Raff, 1987; Kempf and Todd, 1989; Hart, 1996; Wray, 1996; McEdward and Janies, 1997). Increased egg energy content permits larvae to complete development without particulate food. These derived larvae may feed facultatively. However, once larvae have lost the requirement for food, stabilizing selection on feeding performance is weakened, and mutations that affect the form or function of feeding structures may accumulate (Strathmann, 1975). Selection on other larval functions like swimming or developing rapidly and efficiently may also lead to changes in larval form (Wray and Raff, 1991; Emlet, 1994). Under these conditions, feeding structures eventually become nonfunctional, and the resulting larvae are obligately nonfeeding. Loss of the ability to feed may occur by any of many different changes in morphology, physiology, or behavior, but details of this process are mostly unknown (Kempf and Todd, 1989; Wray, 1996). Further reduction of ancestral feeding structures, which may occur rapidly after loss of the requirement for particulate food (Wray and Raff, 1991; Hart, 1996; Wray, 1996), then leads to simplification of external form in nonfeeding larvae (Emlet, 1991; Byrne *et al.*, 2001). This scenario is a specific example of a more general model of the reduction and loss of nonfunctional characters (Fong *et al.*, 1995).

Though larval feeding has been lost in many lineages of marine invertebrates (Strathmann, 1978), subsequent patterns of change in larval form have been studied primarily in members of only one phylum, the Echinodermata.

Examples from other phyla would be useful in assessing the generality of these results. Here I provide such an example from a phylum only distantly related to the echinoderms, the Annelida. Sabellid annelids are sessile, tube-dwelling worms often known as "feather-duster worms" because of the crown of tentacles they extend from their organic, unmineralized tubes for suspension feeding. The family includes about 490 species that fall into two clades, the subfamilies Fabriciinae and Sabellinae (Rouse and Pleijel, 2001). All fabriciinae whose reproduction has been studied (about 15 of 75 species) brood embryos that undergo direct development. Sabellinae are more variable in reproductive biology, with some species brooding embryos and larvae through the juvenile stage; others brooding embryos and larvae for most of their development, releasing larvae for a brief planktonic phase before settlement; and still others releasing gametes directly into the sea where they are fertilized and develop into planktonic larvae. Though reproduction and development has been studied in few sabellinae (about 30 of 415 species), these are broadly distributed in phylogenies of the family (Rouse and Fitzhugh, 1994). No sabellid larvae are known to feed (Rouse and Fitzhugh, 1994).

A look at the relationships of annelid worms suggests that nonfeeding development in sabellids represents a loss of larval feeding (Fig. 1). Sister clade to the Sabellidae is the Serpulidae, which includes both species with feeding larvae and species with nonfeeding larval development. Sister to the clade [Serpulidae, Sabellidae] is the Sabellariidae. All sabellariids whose development has been described have feeding larvae. These character states are shown in Figure 1, with inferences on larval nutritional mode in ancestral forms. As no extant sabellid is known to have feeding

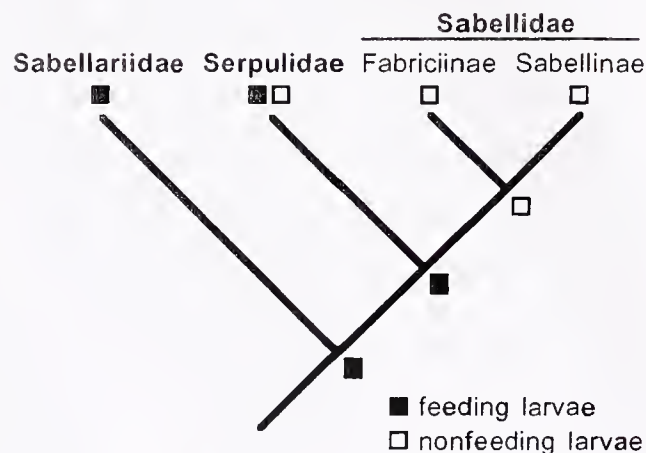


**Figure 1.** Relationships of sabellariid, serpulid, and sabellid annelids, as indicated by cladistic analyses of morphological and reproductive characters by Fitzhugh (1989) and Rouse and Fitzhugh (1994). This topology is also supported by analyses of DNA sequence data from the nuclear gene elongation factor-1alpha (D. McHugh, Colgate University, pers. comm.). Inferences on ancestral character states are discussed in the text.

larvae, nonfeeding development is likely plesiomorphic in the family (Rouse and Fitzhugh, 1994). The inference that the common ancestor of serpulids and sabellids had a feeding larval stage relies primarily on the observation that feeding larvae of sabellariids and serpulids capture particles using similar systems of three parallel ciliary bands, the prototroch, food groove, and metatroch (Fig. 2; Strathmann *et al.*, 1972; Strathmann, 1987; Strathmann and Pernet, unpubl. data). The cilia of the prototroch, which form a transverse band anterior to the mouth, beat from anterior to posterior. These cilia create a swimming current as well as being involved in feeding. Suspended particles passing near them are overtaken and moved towards the surface of the larval body. Cilia of the metatroch, located posterior to the mouth, beat from posterior to anterior. Particles caught between these two ciliary bands are transported towards the mouth by cilia of the food groove. This is usually referred to as "opposed band" feeding. (Note that Rouse [1999, 2000a] argues that sabellariid larvae do not feed with opposed bands of cilia. However, larvae of the only sabellariids in which larval feeding has been studied, *Sabellaria alveolata* and *S. cementarium*, do feed in this way [Strathmann, 1987; Strathmann and Pernet, unpubl. data].) The presence of similar feeding structures in sabellariids and serpulids suggests that ancestors of the clades [Sabellariidae [Serpulidae, Sabellidae]] and [Serpulidae, Sabellidae] had larvae that fed with opposed bands of cilia. Nonfeeding development in the sabellids thus represents a loss of larval feeding. Rouse (2000a) also concluded that sabellids were derived from ancestors that had feeding larvae.

Here I show that despite loss of the requirement and ability to feed as larvae, members of at least eight genera of sabellids retain opposed bands of cilia. In larvae of at least one species, *Schizobranchia insignis*, these structures can concentrate particles from suspension and transport them to the mouth, where they are invariably rejected because the larvae lack functional digestive systems. The persistence of ancestral systems for particle capture in nonfeeding sabellid larvae is unexpected in light of data from echinoderms, which suggest that once the requirement for larval feeding is lost, feeding structures are rapidly reduced or lost. These observations suggest that sabellids lost larval feeding very recently, that opposed bands are inexpensive to construct and operate, or that opposed bands have alternative functions in these larvae. These observations also suggest a hypothesis on how development mediates the loss of feeding ability in larvae of annelids and related phyla after increases in egg size.

## Materials and Methods

### Collection, spawning, and larval culture

I studied larvae of the sabellin sabellid *Schizobranchia insignis* Bush, 1905, intensively, and made additional observations on larvae of three other sabellins, *Demonax me-*

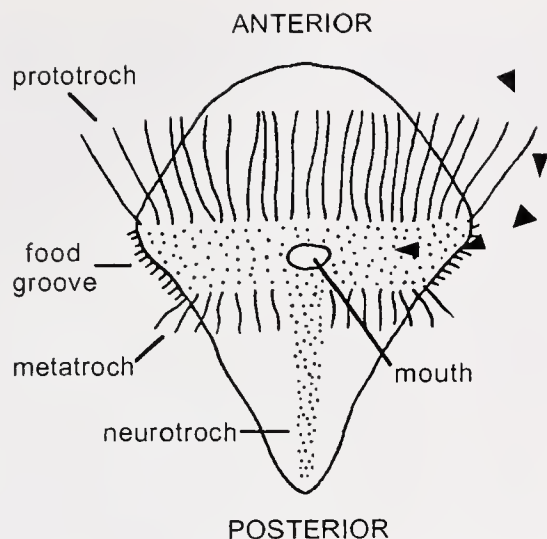


**Figure 2.** Diagrammatic ventral view of a larva of a serpulid annelid, showing structures used in the opposed-band feeding system and the path of a particle (arrowhead) captured from suspension. Cilia of a preoral band, the prototroch, beat from anterior to posterior. As they beat, particles that pass within their reach may be moved into a perioral band of cilia, the food groove. Metatrochal cilia beat from posterior to anterior and may help trap particles in the food groove. Once in the food groove, particles are transported ventrally to the mouth. Rejected particles are moved posteriorly by cilia of the neurotroch.

*dius* (Bush, 1905), *Myxicola aesthetica* (Claparède, 1870), and *Pseudopotamilla ocellata* (Moore, 1905). All of these species except *D. medius* are broadcast spawners; adults of *D. medius* brood embryos and larvae in a gelatinous mass around the opening of the adult tube, and larvae emerge from masses for a brief (~1 day) planktonic period (McEuen *et al.*, 1983). Adult *S. insignis* and *P. ocellata* were collected from floating docks on San Juan Island, Washington, from January to April in 2002 and 2003. The tube of each animal was cleaned of fouling organisms and trimmed to the length of the worm it contained. To induce spawning, 10–20 conspecific individuals were placed in a large container through which fresh seawater flowed. About half of the worms so treated spawned within 48 h, usually at night. I collected fertilized eggs from the bottom of the container the following morning, rinsed them several times in coarsely filtered seawater (FSW, mesh size ~5  $\mu\text{m}$ ), and cultured them in 1-liter beakers of FSW at densities of ~5 per milliliter. Beakers were partially submerged in flowing seawater at temperatures of 8–10 °C (near field temperatures) and stirred with paddles (M. Strathmann, 1987). Water in larval cultures was changed every 3–6 days. No food was added, but cultures certainly contained bacteria and unicellular protists. Larvae of *S. insignis* were followed through metamorphosis. These larvae settled on small pieces of adult tube that were scored with a razor blade to provide crevices. Juveniles were fed the unicellular algae *Isochrysis* sp. and *Rhodomonas* sp. at high concentrations.

I collected adult *Myxicola aesthetica* from floating docks in Anacortes, Washington, in July 2002. Adults spawned when removed from their tubes and subjected to gradual warming (to room temperature) and rapid cooling of the seawater they were incubated in. Embryos and larvae were raised as described above.

I obtained two egg masses of *Demonax medius* from the intertidal zone on the west side of San Juan Island in February and April 2002, and incubated them in FSW at 8–10 °C in the laboratory. I examined larvae that had been removed from masses, as well as planktonic larvae that had emerged from masses naturally. Planktonic larvae were raised as described above.

#### Larval morphology

Developmental stages were examined with a light microscope equipped with differential interference contrast (DIC) optics. Larvae were relaxed in a 1:1 solution of 7.5%  $\text{MgCl}_2$  and seawater before examination. Body dimensions were estimated with a calibrated ocular micrometer. For scanning electron microscopy, relaxed larvae were killed by gradual addition of dilute formalin. They were then rinsed in Millipore-filtered seawater (MPFSW, mesh size 0.45  $\mu\text{m}$ ) and fixed for 2 h in 2%  $\text{OsO}_4$  in 1.25% sodium bicarbonate buffer (pH 7.2). Fixed larvae were rinsed in distilled water, then dehydrated in ascending concentrations of ethanol. They were critical-point-dried, mounted on stubs with carbon adhesive disks, and sputter-coated with gold-palladium before being examined and photographed with a JEOL JSM-35 scanning electron microscope. Larvae of *Schizobranchia insignis* were also sectioned for study of internal anatomy. Relaxed larvae were fixed in 2.5% glutaraldehyde in 0.2 M Millonig's phosphate buffer for 1–3 h, rinsed in buffer, then post-fixed in 1%  $\text{OsO}_4$  in buffer for 1 h. After dehydration in ethanol, larvae were embedded in EMBED-812 (Electron Microscopy Sciences, Inc.) with propylene oxide as an infiltration solvent. Sections ~1  $\mu\text{m}$  thick were cut with glass knives and stained with Richardson's stain for light microscopy (Richardson *et al.*, 1960).

#### Functional morphology of ciliary bands

Beat patterns of cilia were recorded with a high-speed video camera (Motionscope 1000-S, RedLake Imaging Inc.) mounted on a compound microscope with DIC optics. Larvae were restrained under a coverslip supported with plasticene modeling clay. Images were collected at 250 frames per second and replayed at 10 frames per second. Sequences were routed from the camera through a Sony DVMC-DA2 analog-digital converter to a Macintosh iBook and saved as iMovie files (Apple Computer, Inc.).

Capture and transport of particles by larvae of *Schizobranchia insignis* were visualized by videotaping larvae in a suspension of particles. Larvae were mounted on a slide under a coverslip supported with plasticene modeling clay.

The coverslip was pressed down just enough to prevent larvae from swimming rapidly. High concentrations of polystyrene divinylbenzene beads (3- $\mu\text{m}$  diameter, blue-dyed, Polysciences, Inc.) were added and larvae were observed with a compound microscope. Beads had previously been incubated in a 2.5% solution of bovine serum albumin (BSA) in distilled water for 1–2 h, then rinsed and resuspended in MPFSW. Such beads are readily captured and ingested by free-swimming or restrained feeding larvae of sabellariids and serpulids (Strathmann and Pernet, unpubl. data). Images were collected with a video camera (Sony CCD SSC-S20) and recorded on VHS tape, with a date-time generator providing a time signal. Tapes were played frame by frame for analysis.

#### *Possible functions of opposed ciliary bands in sabellid larvae*

I tested two hypotheses on functions of opposed ciliary bands in larvae of sabellids.

*Opposed ciliary bands are used for capturing particulate food during the planktonic larval stage.* I verified that larvae of *Schizobranchia insignis* and *Demonax medius* are non-feeding by offering them particulate "food" through development and later examining their guts for ingested particles. For each assay, 20 larvae were placed in 20 ml MPFSW in a vial. Two types of particles were added to each vial: blue-dyed polystyrene divinylbenzene beads 3 and 6  $\mu\text{m}$  in diameter, previously incubated in 2.5% BSA as described above, and single-celled algae (*Dumaliella* sp.). Final concentrations of beads were 5–10 per microliter of each diameter; I did not measure algal concentrations. I included several feeding larvae of the echinoid echinoderm *Strongylocentrotus droebachiensis* or the serpulid annelid *Serpula columbiana* in each vial as positive controls. Vials were slowly rotated on a plankton wheel in the dark at 10 °C for 1–2 h. Larvae of sabellariids and serpulids feed at high rates under these conditions (Pernet, unpubl. data). Larvae were preserved at the end of feeding assays by addition of buffered formalin. They were later cleared and mounted in glycerin, and examined with a compound microscope to determine whether they had ingested particles. Through processing, beads retained blue dye, and algae retained pigment; both types of particles were easily visible when present in larval guts. Ten sabellid larvae, as well as several larvae known to feed, were examined in each assay. For *S. insignis*, assays were conducted every 5 days, from the 5th day after fertilization until larvae were 30 days old. For *D. medius*, feeding assays were carried out with swimming larvae that had left egg masses on their own.

*Opposed ciliary bands are sites of uptake of dissolved proteins.* Moran (1999) found that encapsulated larvae of several marine gastropods use velar cells to take up dissolved proteins from the capsular fluid. In related species with planktonic feeding larvae, these cells bear cilia that

function in an opposed-band feeding system. Using the methods of Rivest (1981) and Moran (1999), I tested the hypothesis that larvae of *Schizobranchia insignis* or *Demonax medius* take up proteins with the cells that bear the opposed ciliary bands. Ten larvae were placed in 1 ml of fluorescein isothiocyanate-conjugated bovine serum albumin (FITC-BSA) dissolved in MPFSW (1 mg/ml). Negative controls were incubated in MPFSW only. Larvae of species known to take up large proteins (veligers of *Littorina sitkana* [Moran, 1999] or *Crepidula adunca* [Rivest, 1981]) were included in all vials as positive controls. Larvae were incubated in test solutions for 6 h at 10 °C in the dark. After incubation, they were rinsed in MPFSW and observed by epifluorescence microscopy. At least five sabellid larvae, as well as several positive controls, were examined from each treatment. For *S. insignis*, assays were conducted every 5 days, from the 5th day after fertilization until larvae were 30 days old. For *D. medius*, assays were carried out with larvae that had hatched from their individual capsules but had not yet left egg masses on their own (these larvae were about 5–15 days old, and were removed from egg masses by agitation).

## Results

### *Larval development and form*

*Schizobranchia insignis.* Except for notes on egg size and developmental mode (Lee, 1970, 1975; McEuen *et al.*, 1983), development of this species has not previously been described. A summary of its development can be found in Table 1.

In the spawning events I observed, males always spawned before females. Fertilized eggs were spherical, opaque, negatively buoyant, gray in reflected light, and surrounded by an elevated envelope (Fig. 3A). Mean diameters ( $\pm$  one standard deviation) of 20 eggs from each of three separate females were 154 (3.4), 156 (2.8), and 157 (2.8)  $\mu\text{m}$ ; the fertilization envelope brought the total diameter to 180–190  $\mu\text{m}$  (Fig. 3A). First and second cleavages were both markedly unequal (without the formation of polar lobes), leading to a four-cell stage with one cell that was much larger than the others (Fig. 3B).

Two days after fertilization, embryos had become pear-shaped trochophore larvae (Fig. 3C). The widest part of the body bore a transverse, preoral band of cilia, the prototroch. The prototroch was composed of three parallel tiers of cilia—an anterior tier of short cilia, a middle tier of long compound cilia, and a posterior tier of short compound cilia. Cilia of all three tiers protruded through the fertilization envelope. They could be identified as preoral because a slight depression had appeared just behind them, midventrally at the site of the developing mouth.

By the 3rd day after fertilization, two additional bands of transverse cilia had appeared (Fig. 3D). Immediately posterior to the prototroch, at the level of the larval mouth, was

Table 1

Schedule of development in *Schizobranchia insignis* raised at temperatures of 8–10 °C

Time	Stage or event
<i>Planktonic larval development</i>	
0	Fertilization
1 d	Prototrochal cilia protrude through egg envelope; weakly swimming
2 d	Pear-shaped trochophores; prototroch well developed; ocelli, head and anal vesicles present
3 d	Metatroch and food-groove cilia present; neurotroch present; competent to settle
4 d	Notochaetae in chaetiger 1
5 d	Notochaetae in chaetiger 2
11 d	Notochaetae in chaetiger 3; neurochaetae (uncini) in chaetigers 2 and 3
12–15 d	Neurochaetae (uncini) in chaetiger 4
<i>Post-settlement development</i>	
0	Settlement; mucus tube formed around body
1 d	Neurotroch between peristomium and pygidium lost in some individuals; collar lobes present on peristomium
2 d	Neurotroch between peristomium and pygidium lost in all individuals; prototroch lost middorsally; radiole buds present on prostomium
3 d	Prostomial snout present; radiole buds each divided into 2 lobes; anus present
4 d	Radiole buds each divided into 3 lobes, ciliated; all long cilia of larval prototroch gone; ingestion of snout begins?
5 d	Radiole buds each divided into 4 lobes
6–7 d	Juvenile feeding begins

Timing data are summarized from observations of cohorts of offspring from six separate females. Though competent to settle 3 days after fertilization, larvae, if not offered a suitable settlement substrate, continue swimming and remain competent to settle until at least 30 days post-fertilization. For the schedule of post-settlement development, larvae were allowed to settle after a 15-d planktonic period. The timing of events in post-settlement development was similar in larvae that had 9-d and 30-d planktonic periods.

a narrow band of short, simple cilia. The width of this perioral band was about 4–5  $\mu\text{m}$  in five 10-day-old larvae. Just behind this perioral band was a postoral band of simple cilia. These ciliary bands are shown in greater detail in an illustration of an older larva (Fig. 3E). Positionally, these bands of cilia are identical to the perioral food groove and postoral metatroch known from annelid larvae that feed with opposed bands of cilia, and I will refer to them as food groove and metatroch in the rest of this paper. Both food groove and metatroch were incomplete dorsally; the dorsal gap in the food groove was substantially wider than that in the metatroch. Three-day-old larvae had also developed a midventral band of short cilia, the neurotroch, which stretched from the metatroch to the posterior end of the body.

Three-day-old larvae were competent to settle and metamorphose. However, if larvae were not offered settlement

substrates and were maintained in stirred cultures in clean glass beakers, most remained planktonic until at least 30 days after fertilization. Changes in form in larvae from 3–30 days of age—mostly involving the appearance of chaetae in developing segments (e.g., Fig. 3F)—are summarized in Table 1. Between the 25th and 30th day of development, many larvae began to show signs of metamorphosis while still in the plankton. In particular, they developed a pair of dorsolateral bulges on the prostomium. In normally metamorphosing worms, these bulges go on to form the adult feeding tentacles, or radioles. Mortality of larvae appeared to increase greatly at around 30 days.

Sections of larvae fixed at various ages allowed description of changes in gut morphology during development. Transverse sections of 8-day-old larvae showed that the mouth was represented only by a shallow, ciliated midventral depression (Fig. 3G). This depression was not connected to the midgut. The midgut wall was composed of endodermal cells that were so large that they completely occluded its lumen. Eight-day-old larvae had neither an intestine nor an anus. In 20-day-old larvae, the mouth had increased in depth and led to a very narrow ciliated stomodaeum (Fig. 3H). In serial sections of five 20-day-old larvae, I was unable to find a connection between the stomodaeum and midgut. The cells lining the midgut had shrunk slightly, and it now had a narrow central lumen at the level of the stomodaeum. This lumen disappeared posteriorly. I observed no intestine or anus in these larvae.

Larvae of *Schizobranchia insignis* were competent to settle from 3 to at least 30 days after fertilization. When offered pieces of adult tube in still water, 20%–50% of larvae settled within 24 h. Larvae usually settled in crevices in the tubes, or on the glass bowl beneath pieces of tube. The events following settlement of 15-day-old larvae are summarized in Table 1. Note that prototrochal cilia had been resorbed or shed by 4 days after settlement, before juveniles began feeding.

*Demonax medius*. All larvae of *D. medius* that I examined—larvae extracted from gelatinous brood masses, and larvae that had escaped from masses for a brief planktonic period—had prototroch, food groove, and metatroch cilia similar to those seen in *Schizobranchia insignis* (Fig. 4A). The width of the food groove ranged from about 6–8  $\mu\text{m}$  in five larvae that had left egg masses on their own. The metatrochal band was slightly broader than that of *S. insignis*. In most other respects my observations of development of two broods of *D. medius* are in accord with those of McEuen *et al.* (1983). One addition to their description is that embryos and early larval stages in gelatinous egg masses were individually encapsulated in spherical capsules only slightly larger in diameter than the developing worms themselves. Capsules are present in addition to fertilization envelopes like those described above for *S. insignis*. In the broods I observed, larvae hatched from capsules about 5–7

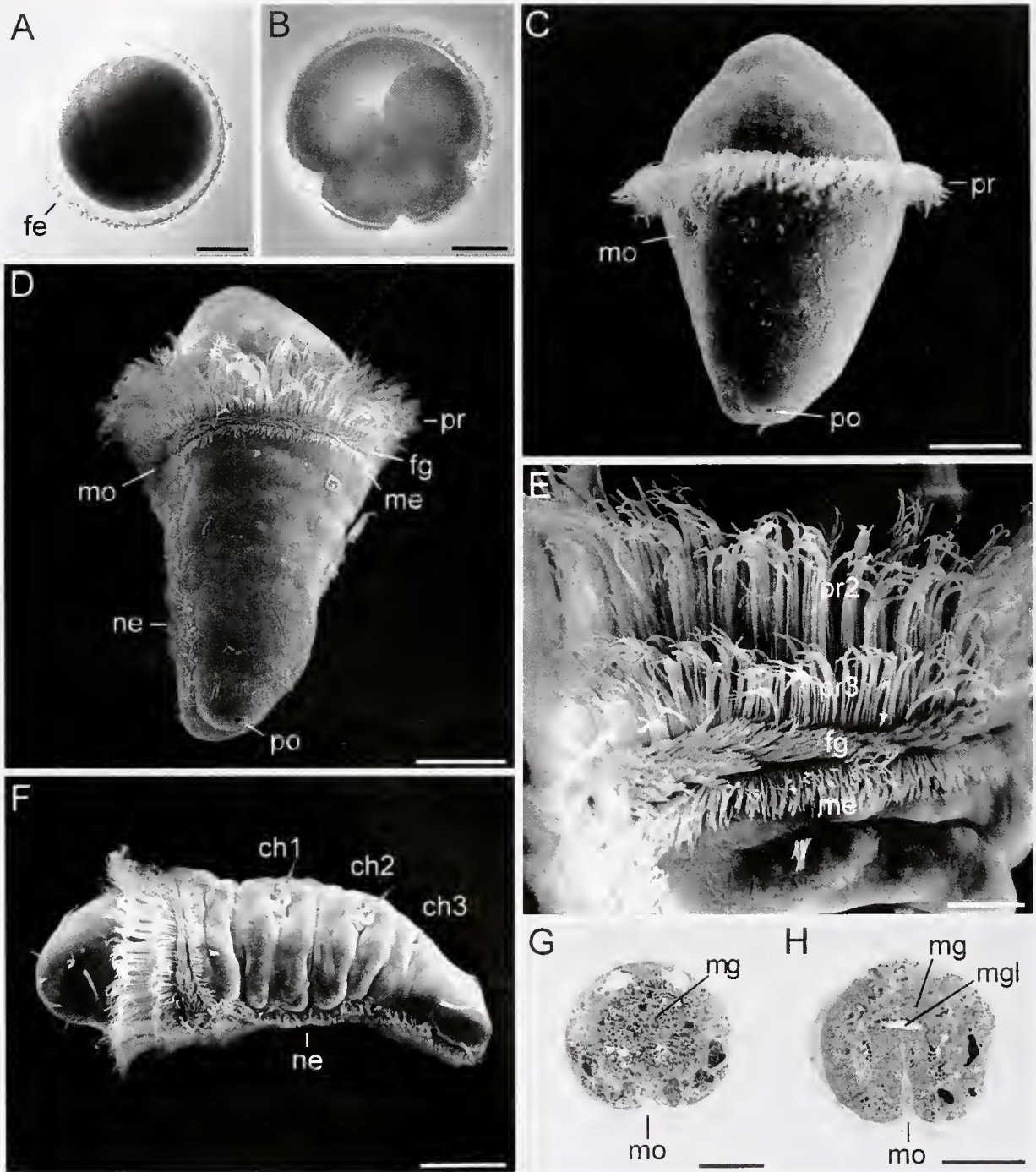


**Figure 3.** Embryonic and larval stages of *Schizobranchia insignis*. (A) Fertilized egg. (B) Four-cell embryo. (C) Two-day-old larva. (D) Three-day-old larva. (E) Detail of opposed ciliary bands of fourteen-day-old larva. (F) Fourteen-day-old larva. (G) Transverse section of eight-day-old larva at the level of the mouth. (H) Transverse section of twenty-day-old larva at the level of the mouth. Scale bars = 50  $\mu\text{m}$ , except for (E) where the scale bar = 15  $\mu\text{m}$ . ch1 = first chaetiger, ch2 = second chaetiger, ch3 = third chaetiger, fe = fertilization envelope, fg = food groove, me = metatroch, mg = midgut wall, mgl = midgut lumen, mo = mouth, ne = neurotroch, po = pore of one of the paired anal vesicles, pr = prototroch, pr2 = second tier of prototrochal cilia, pr3 = third tier of prototrochal cilia.

days after egg deposition, and they emerged from egg masses about 7–15 days after deposition.

*Myxicola aesthetica*. Fertilized eggs of *M. aesthetica*

were spherical, opaque, negatively buoyant, rose-colored in reflected light, and surrounded by an elevated envelope. The mean diameter ( $\pm$  one standard deviation) of 10 eggs from

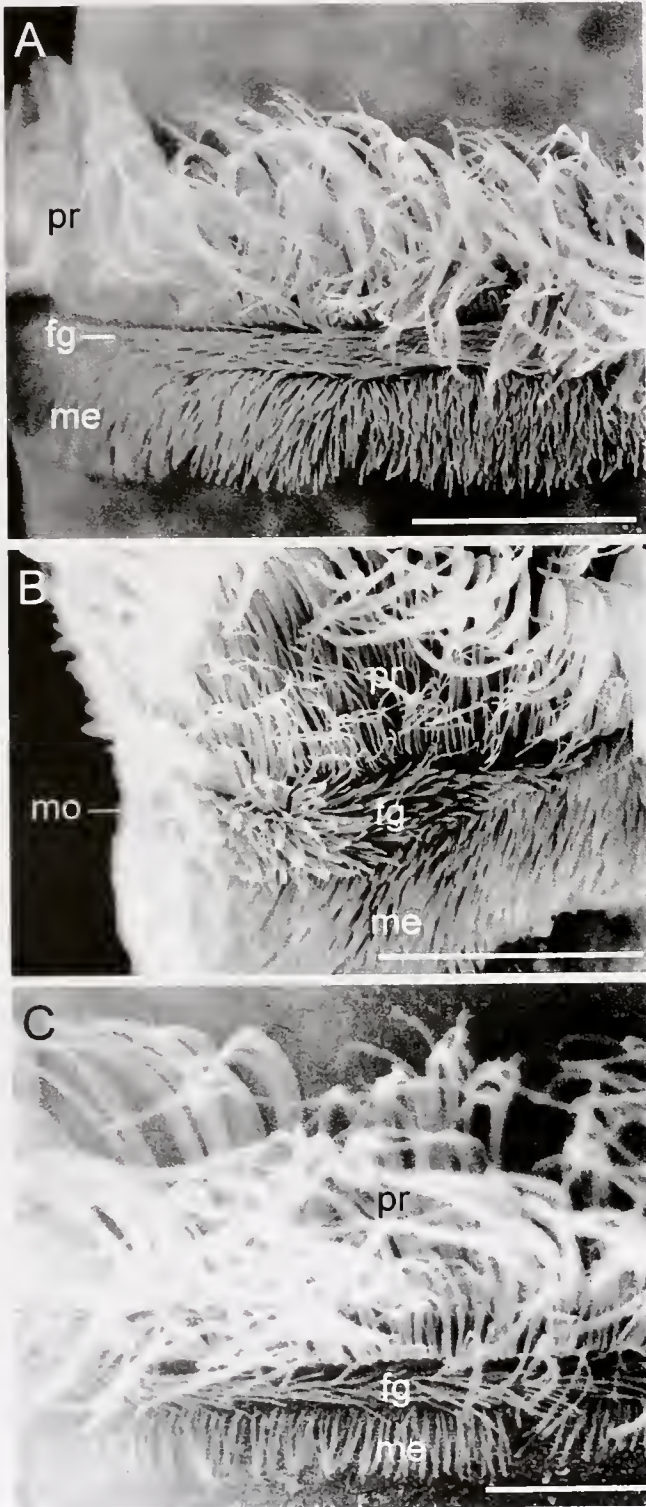


**Figure 4.** Opposed ciliary bands of *Demonax medius*, *Myxicola aesthetica*, and *Pseudopotamilla ocellata*. (A) Ciliary bands in the right ventral region of larva of *D. medius*. (B) Left lateral view of ciliary bands of 11-day-old larva of *M. aesthetica*. (C) Left dorsal view of ciliary bands of 3-day-old larva of *P. ocellata*. Scale bars = 25  $\mu\text{m}$ . fg, food groove; me, metatroch; mo, mouth; pr, prototroch.

a single female was 130 (4.9)  $\mu\text{m}$ . First and second cleavages were distinctly unequal. At incubation temperatures of 12–13  $^{\circ}\text{C}$ , larvae began swimming by about 18 h after fertilization. By 2 days after fertilization, larvae bore prototrochal, food-groove, and metatrochal cilia similar to those seen in *Schizobranchia insignis* (Fig. 4B). The width of the food groove was about 6  $\mu\text{m}$  in five larvae. As in *Demonax medius*, the metatrochal band of *M. aesthetica* was broader than that of *S. insignis*.

*Pseudopotamilla ocellata*. Fertilized eggs of *P. ocellata* were spherical, opaque, negatively buoyant, gray in reflected light, and surrounded by an elevated envelope. The mean diameter ( $\pm$  one standard deviation) of 15 eggs from a single female was 142 (2.9)  $\mu\text{m}$ . First and second cleavages were distinctly unequal. By 3 days after fertilization, larvae bore prototroch, food-groove, and metatroch cilia similar to those seen in *Schizobranchia insignis* (Fig. 4C). The width of the food groove was about 6  $\mu\text{m}$  in five larvae.

#### *Functional morphology of ciliary bands*

Food-groove and metatrochal ciliary bands in larvae of all four species behaved like similar ciliary bands in larvae that feed with opposed bands of cilia (e.g., Strathmann *et al.*, 1972). The directions of effective strokes of cilia were anterior to posterior (prototroch), posterior to anterior (metatroch), and laterally towards the mouth (food groove). All three bands of cilia could arrest their beat, apparently independently of the others. When metatrochal cilia were not beating, they lay flat along the larval body, pointed posteriorly. These ciliary beat patterns were confirmed by analyses of high-speed video footage, but were also clearly visible by inspection of living larvae at 400 $\times$  final magnification.

I examined the ability of larvae of *Schizobranchia insignis* to concentrate particles from suspension and transport them to the mouth using opposed bands of cilia. I videotaped four 9-day-old larvae in suspensions of 3- $\mu\text{m}$  beads for a total of 22 min. This footage included at least 30 particle captures. Analysis of these video sequences indicated that beads were caught in the current generated by the prototrochal cilia and moved into the food groove. Resolution of images was not sufficient to determine if metatrochal cilia were actively beating during captures. Captured beads were transported in the food groove around the body towards the larval mouth (Fig. 5). Once at the mouth, beads were moved along the neurotroch until they fell off the posterior end of the body.

#### *Possible functions of opposed ciliary bands in sabellid larvae*

I tested the hypothesis that planktonic larvae of *Schizobranchia insignis* or *Demonax medius* feed on particulate food by offering larvae particles that are readily ingested by

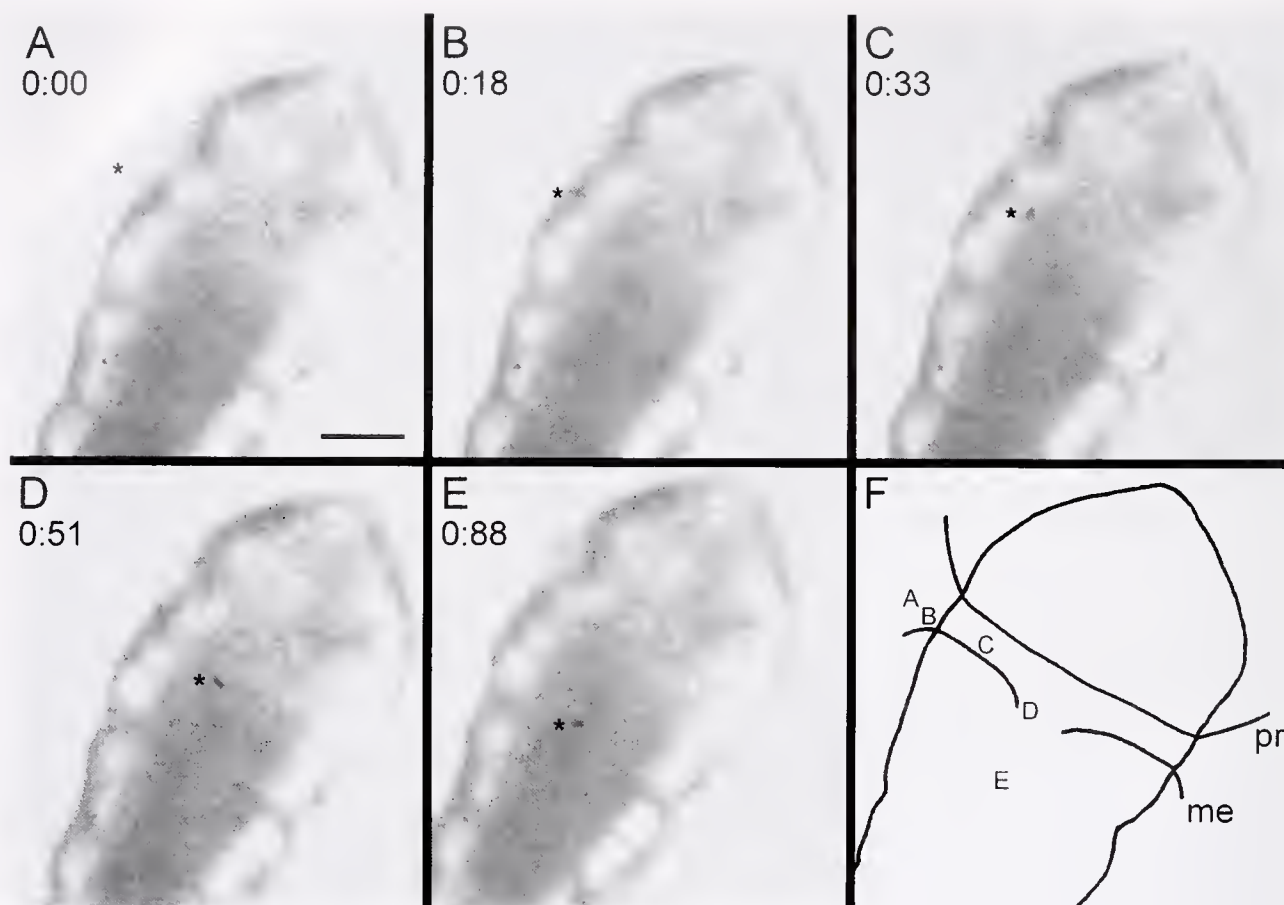


**Figure 5.** Capture and transport of a particle by a 9-day-old larva of *Schizobranchia insignis*, in ventral view. (A, B) Capture of a particle. (C, D) Transport to the mouth in the food groove. (E) Transport posteriorly on the neurotroch. Time (s) is marked on each frame. Scale bar = 50  $\mu\text{m}$ ; the asterisk is adjacent to the particle. (F) Composite diagram of particle positions in (A–E); me = metatroch, pr = prototroch. For clarity, only positions of the prototroch and metatroch are shown. Food-groove cilia lie between them, and the neurotrochal cilia run from the gap in the metatroch to the posterior tip of the body. The mouth is slightly anterior to the position of the particle shown in (D).

related feeding larvae. Particulate food was never observed in the guts of larvae of *S. insignis* ranging from 5 to 30 days old, or in the guts of larvae of *D. medius* that had hatched naturally from egg masses. Feeding larvae of echinoid echinoderms or serpulid annelids included as positive controls always ingested many of both types of particles.

I also tested the hypothesis that ciliated cells of the prototroch, food groove, or metatroch are involved in the uptake of dissolved proteins by endocytosis. Larvae of *Schizobranchia insignis* and *Demonax medius* exposed to FITC-BSA never showed any differences in fluorescence relative to larvae incubated only in MPFSW. In both treatments, larval chaetae autofluoresced when excited with ultraviolet light. Larvae known to be able to take up large dissolved proteins always showed fluorescence indicating uptake of FITC-BSA in velar cells (*Littorina sitkana*; Moran, 1999) or cells of the “larval kidney” (*Crepidula adunca*; Rivest, 1981) when incubated in FITC-BSA, but not when incubated in MPFSW.

## Discussion

Evolutionary loss of the requirement for larval feeding has occurred repeatedly in many phyla, and is typically followed by the loss of structures formerly involved in feeding (Strathmann, 1978; Emlet, 1991; Wray, 1996). Detailed hypotheses on how this association arises, however, have been tested mainly in the context of comparative data on members of only one phylum, the Echinodermata (Hart, 1996; Wray, 1996). The observations reported here on larvae of annelids permit an initial assessment of their generality. These data are also useful in generating hypotheses on other topics, including the specific sequence of events that lead to loss of feeding ability after increases in egg size and energy content in animals that develop *via* spiral cleavage.

### *Ancestral feeding structures in nonfeeding annelid larvae*

I interpret the transverse ciliary bands of the sabellid larvae described here as homologs of the prototroch, food

groove, and metatroch of closely related feeding larvae (*i.e.*, those of serpulids and sabelliids). Almost all annelid larvae bear a prototroch, and in all cases where detailed observations have been made, these are homologous by developmental criteria (Rouse, 1999). The lineages of the cells that bear food-groove and metatrochal cilia are not known in any detail, so other criteria must be used to infer homology of these ciliary bands. Two criteria that support my interpretation are those of position and behavior. The perioral and postoral cilia of larvae of *Schizobranchia insignis*, *Demonax medius*, *Myxicola aesthetica*, and *Pseudopotamilla ocellata* are located in the same positions as the food-groove and metatrochal cilia, respectively, of feeding sabelliid and serpulid larvae, and they show similar beat patterns (perioral cilia beat laterally towards the mouth, and postoral cilia beat from posterior to anterior). Together, the preoral, perioral, and postoral ciliary bands of *S. insignis* are capable of capturing particles from suspension and transporting them to the mouth, like the opposed bands of related feeding larvae. Given current hypotheses on the relationships of sabelliids, serpulids, and sabelliids, phylogenetic criteria for homology are also met (Fig. 1; Lauder, 1994). Under this interpretation, the food-groove and metatrochal ciliary bands of sabelliid larvae can be identified as ancestral structures retained after loss of larval feeding in the family.

The hypothesis that the opposed ciliary bands of these sabelliid larvae are homologous to those of related feeding larvae might be falsified with new phylogenetic, developmental, anatomical, or physiological data, but given current knowledge it appears likely that it is correct. An alternative hypothesis is that the opposed ciliary bands of sabelliids evolved in parallel with those of sabelliids and serpulids. This seems unlikely on grounds of parsimony. Further, the opposed ciliary bands of larvae of *Schizobranchia insignis* lack obvious functions, which makes it difficult to understand how they might have evolved independently.

Opposed ciliary bands may be widely distributed among the nonfeeding larvae of sabellin sabelliids. My observations show that food-groove and metatrochal ciliary bands are present in larvae of members of at least four genera of sabellins. I examined published descriptions of nonfeeding larvae of sabelliids for further evidence on the distribution of opposed bands of cilia in the family. This survey revealed probable opposed bands in nonfeeding larvae of four more genera of sabellins. Scanning electron micrographs provide evidence for the presence of food groove and metatroch in members of *Amphicorina* (Rouse and Fitzhugh, 1994) and *Laonome* (Hsieh, cited in Fig. 12.5D of Pernet *et al.*, 2002). A text description of the "prototrochal" cilia of *Megalomma* (as *Branchiomma*) *vesiculosum* (Wilson, 1936) is also suggestive of opposed bands. Early larvae of *M. vesiculosum* have three tiers of prototrochal cilia, but slightly later in development two more rows of cilia appear posterior to the prototroch. The most posterior row, when arrested, points posteriorly. This is precisely the pattern seen in *Schizo-*

*branchia insignis*, where the two new rows of cilia form the food groove and metatroch, and where the metatroch, when arrested, points posteriorly. Finally, a text description and drawings of larvae of *Chone teres* also suggest the presence of opposed bands. Okuda (1946) states that the "prototroch" of larvae of *C. teres* is composed of one band of long cilia followed posteriorly by two adjacent bands of short cilia. Unfortunately, he does not specify the spatial relationships of these cilia to the larval mouth. His drawings show ciliary bands similar to those observed here in four genera of sabellin sabelliids. Published illustrations of larvae of several other sabellins (*e.g.*, *Amphiglena nathae* [Rouse and Gambi, 1998] and *Perkinsiana riwo* [Rouse, 1996]) may indicate the presence of only a single band of cilia behind the prototroch, but more observations of these larvae are needed. I found no descriptions of sabellin larvae that unequivocally indicate the absence of food groove and metatroch.

Thus, members of at least eight genera of sabellins likely possess opposed bands of cilia. According to recent phylogenies (Rouse and Fitzhugh, 1994; Fitzhugh and Rouse, 1999), these genera are not clustered in any particular subclade of the Sabellinae: some (*e.g.*, *Amphicorina*, *Myxicola*) arise from deep nodes in the tree, and others (*e.g.*, *Laonome*, *Schizobranchia*) from shallow nodes. All known sabellin reproductive strategies (brooding to the juvenile stage, brooding with release of a planktonic larva, and freespawning; Rouse and Fitzhugh, 1994) are represented in the species for which there is evidence of opposed ciliary bands. I conclude that opposed ciliary bands are probably widespread in the sabellins, a clade that includes over 400 species. In contrast, opposed ciliary bands do not appear in the direct-developing embryos of fabriciian sabelliids (Rouse and Fitzhugh, 1994).

Though metatrochal cilia have previously been identified by position in larvae of several species of sabellins (*e.g.*, Rouse and Fitzhugh, 1994), their presence has more usually gone unnoticed. That metatrochal cilia may act with prototrochal and food-groove cilia as opposed-band systems in these larvae has not previously been described. It is possible that opposed ciliary bands are more widely distributed in nonfeeding annelid larvae. Indeed, the nonfeeding larvae of some serpulids also have opposed ciliary bands, at least by the criterion of position (Kupriyanova *et al.*, 2001; Nishi and Yamasu, 1992). Other annelid clades that should be examined for the presence of opposed bands in nonfeeding larvae include those that contain both species whose larvae feed with opposed bands and species that have nonfeeding larval development. Phylogenetic hypotheses delimiting some of these clades (*e.g.*, those including the families Amphinomidae, Opheliidae, and Polygordiidae, all of which include species that feed with opposed bands of cilia; Pernet *et al.*, 2002) are illustrated by Rouse (2000b). In some of these clades, nonfeeding larvae probably evolved from ancestors that possessed opposed bands of cilia.

Knowledge of the distribution of opposed bands in larvae of these groups will provide additional insight into the evolution of larval form in annelids.

*Why have ancestral feeding structures been retained by nonfeeding sabellid larvae?*

One possible explanation for the retention of feeding structures is that sabellids lost the need and requirement for larval feeding only very recently. If nonfeeding development is plesiomorphic for the sabellids, a minimal estimate of the age of their loss of larval feeding is the time of the clade's origin. Unfortunately, scarce fossil and molecular data make it difficult to estimate the age of this clade. Sabellid tubes are usually unmineralized, so are not expected to be easily preserved. Though putative sabellid fossils have been described from strata ranging from the lower Miocene to the Devonian (*e.g.*, Howell, 1962; Plicka, 1968; Termier *et al.*, 1973; Hayward, 1977; Schweigert *et al.*, 1998), these identifications are quite tentative. Sabellids are as speciose and widely distributed as their sister taxon, the serpulids, which are known from the Devonian (Glasby, 2000; Rouse and Pleijel, 2001). Assuming that patterns of diversification were similar in the two clades, this can be interpreted as weak evidence that sabellids are also Paleozoic in origin. Accurate determination of the age of the Sabellidae clearly requires more fossil and molecular data.

A second possibility is that food groove and metatrochal cilia might be very inexpensive to construct and operate. If there is little cost to maintaining these structures, they may be relatively invisible to selection for economy during development. Reduction of these ciliary bands might still occur, but only as a result of the slow accumulation of mutations in genes specifying their development. Indeed, degeneration of the opposed-band system may well be occurring in sabellids, as indicated by their unusually narrow food grooves. In annelid and mollusc larvae that feed with opposed bands, the food groove is typically 20–30  $\mu\text{m}$  wide (Phillips and Pernet, 1996; Pernet, unpubl. data), but in the sabellid larvae examined here, food grooves ranged in width from 5–8  $\mu\text{m}$ . Width of the food groove may constrain the sizes of particles transported to the mouth (R. Strathmann, 1987; Hansen, 1993). Thus the opposed bands of sabellid larvae, though "functional" in the sense that they can capture and transport particles, likely cannot capture particles of as wide a size range as those of related feeding larvae.

Finally, one might expect ancestral feeding structures to be retained in nonfeeding larvae if they have functions other than feeding. Prototrochal cilia clearly function in swimming in both feeding and nonfeeding annelid larvae. However, functions other than particle capture have rarely been considered for food groove and metatrochal ciliary bands in free-swimming larvae. Opposed ciliary bands have been retained in the encapsulated, "non-feeding" larvae of numerous species of gastropods, but in these cases the opposed

bands continue to have clear functions (*e.g.*, feeding on maternally provided particles within the capsule: Chaparro *et al.*, 2002). A variety of alternative functions of opposed ciliary bands in free-swimming sabellid larvae are possible. For example, opposed bands might serve as the site of uptake of dissolved organic material; might play a role in assessing potential settlement sites; might be involved in forming the initial juvenile tube; or might be used in feeding by recently settled juveniles while the definitive adult feeding structures develop. It is also possible that food groove and metatrochal ciliary bands play some role in development. Several of these hypotheses (uptake of dissolved organic material, feeding in juveniles) are likely false, as suggested by data reported in this paper. There is currently little evidence available with which to assess other hypotheses.

Retention of functional ancestral particle capture systems in nonfeeding larvae of sabellids contrasts sharply with data from echinoderms, where larval feeding structures appear to be lost very rapidly after loss of the requirement for particulate food during larval development (Wray and Raff, 1991; Hart, 1996; Wray, 1996). To make a more general assessment of how rapidly larval form responds to changes in larval nutritional mode, studies of more independent evolutionary events are clearly required. Since evolutionary losses of the requirement for larval feeding have been common in the history of marine invertebrates (Strathmann, 1978), as well-supported phylogenies become available for more taxa it should be possible to identify many more specific examples of the evolutionary loss of larval feeding, to estimate the timing of these events, and to assess how they are related to the evolution of larval form.

*Events in the evolutionary loss of larval feeding ability*

The observations reported here are generally consistent with the model discussed above to account for the association between loss of the requirement for food in the larval stage and loss of larval feeding structures. I argued above that sabellids are derived from an ancestor that had a feeding larval stage. For purposes of comparison, I assume that this ancestor shared characteristics of extant sabellariid and serpulid species that have feeding larvae. The evolution of increased energy content in the egg is thought to be the first step in the evolution of nonfeeding development. Compared to the eggs of sabellariids and serpulids with feeding larvae, which range in diameter from about 45–90  $\mu\text{m}$  (Giangrande, 1997 [her reference to 150- $\mu\text{m}$  eggs in *Sabellaria spinulosa* is incorrect, according to Wilson (1929)]; Kupriyanova *et al.*, 2001), the eggs of sabellids are relatively large (>110  $\mu\text{m}$ ; Rouse and Fitzhugh, 1994) and energy-rich (Pernet and Jaekle, unpubl. data). The second step in this sequence is loss of the ability to feed. All known sabellid larvae are obligately nonfeeding. However, they retain some ancestral feeding structures (in particular, cilia of the food

groove and metatroch). These larvae can thus be interpreted as intermediates in the evolutionary sequence discussed above. Such intermediates have previously been considered rare (Hart, 1996; Wray, 1996), but my observations suggest that they may be common in this clade of annelids.

These data may be useful in answering a question that has previously been poorly understood—that is, what specific events lead to the loss of larval feeding ability after an evolutionary increase in egg provisioning? Wray (1996) noted that loss of the ability to feed might be the result of any of many changes, such as loss of a particular digestive enzyme, loss of some aspect of ciliary coordination, or failure to complete morphogenesis of the larval mouth. He also noted that the rarity of nonfeeding larvae with only slightly derived morphology makes it difficult to identify the specific changes in morphology or behavior that render larvae unable to feed. Most putative intermediates (e.g., the sea urchin *Phyllacanthus imperialis*; Olson *et al.*, 1993) have undergone changes in multiple feeding-related traits (e.g., number and shape of arms, structure of the larval gut) since divergence from a feeding ancestor, and it is thus difficult to identify any one key change that resulted in a loss of feeding ability.

As putative intermediates, larvae of sabellins may provide insight into how larval feeding ability is lost after evolutionary increases in egg size. Larvae of *Schizobranchia insignis*, and probably many other sabellins, possess the ciliary bands needed to capture food particles from suspension. These ciliary bands remain capable of capturing particles and moving them to the mouth. The mouth, however, does not connect to the midgut, which in any case has no (or, later in development, a very small) lumen because the cells that make up its wall are swollen with energy reserves. Loss of feeding in larvae of *S. insignis* may thus be related primarily to a change in the digestive system.

This observation, along with a consideration of annelid development, suggests a specific hypothesis on the link between increased maternal provisioning of the egg and the loss of larval feeding ability. Embryos of annelids (and those of members of several other phyla, together known as spiralians) undergo spiral cleavage, a process in which the fates of some blastomeres are specified early in development. In spiralian embryos, the descendants of four cells—3A, 3B, 3C, and 4D—form the endoderm, the embryonic tissue that becomes the larval midgut. As a result of unequal cleavages from the third through the fifth cleavage cycles, these cells, known as macromeres, are usually far larger than the remaining embryonic cells, the micromeres. At gastrulation, the macromeres and their descendants are internalized, where they form the larval midgut (Kume and Dan, 1968; Anderson, 1973).

Annelids that have feeding larval stages typically have small eggs (Schroeder and Hermans, 1975). In these species, the descendants of 3A–C and 4D form the wall of a larval midgut that has a substantial lumen. In annelids with

nonfeeding larvae, however, eggs are larger. Increased egg volume is presumably due mainly to the addition of material used to fuel development of the larvae or juveniles. During early development most of this additional material is shunted to the macromeres for storage and gradual mobilization. In annelid embryos that develop from large eggs, then, macromeres are proportionally larger (relative to the micromeres) than those of embryos that develop from small eggs (Schneider *et al.*, 1992). Construction of a functional midgut may be difficult when a large volume of endodermal cells must fit in the relatively small volume delimited by the remaining cells of the embryo. In this case, it may be impossible to assemble the endoderm into a midgut that has a substantial lumen, or any lumen at all. Indeed, nonfeeding larvae of annelids typically lack midgut lumens (Wilson, 1936; Anderson, 1973; Heimler, 1988). In addition to simple size constraints, in annelid species with large eggs, division of endodermal cells (and subsequent gut morphogenesis) may be delayed relative to species with small eggs (e.g., Schneider *et al.*, 1992).

Thus, in annelids, a quantitative increase in egg volume, typically thought to be the initial step in the loss of larval feeding, may lead directly to a loss of larval digestive ability because of spatial constraints or delays in gut morphogenesis. These effects may persist through larval development, resulting in nonfeeding larval development; alternatively, they may last only through part of larval development, delaying the onset of larval feeding until cells of the midgut wall shrink as energy stores are consumed.

This hypothesis is attractive because of its simplicity and its vulnerability to test. One approach is the experimental reduction of endoderm volume by removal of one or more presumptive endodermal cells (e.g., Boring, 1989; Clement, 1962; Martindale, 1986). Carrying out this manipulation in annelid embryos that normally develop into nonfeeding larvae with occluded midguts might yield larvae with open midguts. It is not clear how morphogenesis of the rest of the gut (e.g., mouth and stomodaeum) might be affected by macromere ablation, but it is possible that a simple reduction of endodermal cell volume might permit the development of a complete larval gut. In species that retain ancestral particle capture systems, like the sabellids described here, this manipulation might result in conversion of a nonfeeding larva to a feeding larva.

Another approach is to use intraspecific variation in egg size and larval nutritional mode to examine the effects of egg size on midgut development. For example, some individuals of the annelid *Streblospio benedicti* (family Spionidae) produce small eggs (56–70  $\mu\text{m}$  diameter) that develop into feeding larvae, while others produce large eggs (115–152  $\mu\text{m}$ ) that develop into nonfeeding larvae (Levin, 1984; Schulze *et al.*, 2000). If the hypothesis proposed above is correct, nonfeeding development in *S. benedicti* should be a result of reduction in size of the midgut lumen or delayed development of the midgut in larvae that develop

from large eggs. This prediction can be tested with comparative developmental data.

This idea might also apply to other spiralian taxa such as molluscs and entoprocts. As their development is similar, they should be subject to similar effects of endodermal volume on midgut morphogenesis. Both approaches to testing the hypothesis—deletions of endodermal blastomeres and comparative studies within species with variable egg size and developmental mode (e.g., the ascoglossan *Alderia modesta*; Krug, 1998)—may be fruitful.

This hypothesis links changes in development (in this case, egg size and allocation to endodermal lineages) to changes in the form and function of later stages (loss of larval feeding ability *via* delayed midgut morphogenesis). Such connections have long been sought by developmental biologists (e.g., Lillie, 1899; Freeman and Lundelius, 1992). In addition, it may be useful in explaining a peculiar observation—that correlated intraspecific variation in egg size and larval nutritional mode (a form of “poecilogony”) appears to be limited in distribution to spiralians, in particular annelids and molluscs (Chia *et al.*, 1996). I propose that annelid and mollusc species with great intraspecific variation in egg size may show correlated variation in larval nutritional mode because of spatial constraints or heterochronic effects on midgut morphogenesis imposed by their conserved pattern of development.

### Acknowledgments

I thank A.H. Whiteley for reminding me of Lee's studies of *Schizobranchia insignis* eggs, and B. Bingham and C. Mills for helping locate populations of *Myxicola aesthetica*. R.R. Strathmann generously provided access to a culture-stirring apparatus and high-speed video camera system (purchased under NSF OCE-9633193 to RRS), and A. Moran advised on studies of protein uptake. G. Freeman, C. Hermans, K. Zigler, several anonymous reviewers, and participants in the 2002 Friday Harbor Laboratories Evolution Discussion Group provided many useful ideas and criticisms after reading earlier drafts of the manuscript. I gratefully acknowledge the director and staff of the Friday Harbor Laboratories for providing space and support.

### Literature Cited

- Anderson, D. T. 1973. *Embryology and Phylogeny in Annelids and Arthropods*. Pergamon Press, Oxford.
- Boring, L. 1989. Cell-cell interactions determine the dorsoventral axis in embryos of an equally cleaving opisthobranch mollusc. *Dev. Biol.* **136**: 239–253.
- Byrne, M., R. B. Emler, and A. Cerra. 2001. Ciliated band structure in planktotrophic and lecithotrophic larvae of *Heliocidaris* species: a demonstration of conservation and change. *Acta Zool.* **82**: 189–199.
- Chaparro, O. R., J. L. Charpentier, and R. Collin. 2002. Embryonic velar structure and function of two sibling species of *Crepidula* with different modes of development. *Biol. Bull.* **203**: 80–86.
- Chia, F.-S., G. Gibson, and P.-Y. Qian. 1996. Poecilogony as a reproductive strategy of marine invertebrates. *Oceanol. Acta* **19**: 203–208.
- Clement, A. C. 1962. Development of *Ilyanassa* following removal of the D macromere at successive cleavage stages. *J. Exp. Zool.* **166**: 77–88.
- Emler, R. B. 1991. Functional constraints on the evolution of larval forms of marine invertebrates: experimental and comparative evidence. *Am. Zool.* **31**: 707–725.
- Emler, R. B. 1994. Body form and patterns of ciliation in nonfeeding larvae of echinoderms: functional solutions to swimming in the plankton? *Am. Zool.* **34**: 570–585.
- Fitzhugh, K. 1989. A systematic revision of the Sabellidae-Caobangiidae-Sabellongidae complex (Annelida: Polychaeta). *Bull. Am. Mus. Nat. Hist.* **192**: 1–104.
- Fitzhugh, K., and G. W. Rouse. 1999. A remarkable new genus and species of fan worm (Polychaeta: Sabellidae: Sabellinae) associated with marine gastropods. *Invertebr. Biol.* **118**: 357–390.
- Fong, D. W., T. C. Kane, and D. C. Culver. 1995. Vestigialization and loss of nonfunctional characters. *Annu. Rev. Ecol. Syst.* **26**: 249–268.
- Freeman, G., and J. W. Lundelius. 1992. Evolutionary implications of the mode of D quadrant specification in coelomates with spiral cleavage. *J. Evol. Biol.* **5**: 205–247.
- Giangrande, A. 1997. Polychaete reproductive patterns, life cycles, and life histories: an overview. *Oceanogr. Mar. Biol. Annu. Rev.* **35**: 323–386.
- Glasby, C. J. 2000. Fossil record. Pp. 43–45 in *Polychaetes and Allies: The Southern Synthesis*, P. L. Beesley, G. J. B. Ross, and C. J. Glasby, eds. CSIRO Publishing, Melbourne.
- Hansen, B. 1993. Aspects of feeding, growth and stage development by trochophora larvae of the boreal polychaete *Mediomastus fragilis*. *J. Exp. Mar. Biol. Ecol.* **166**: 273–288.
- Hart, M. W. 1996. Evolutionary loss of larval feeding: development, form and function in a facultatively feeding larva, *Brisaster latifrons*. *Evolution* **50**: 174–187.
- Hayward, B. W. 1977. Lower Miocene polychaetes from the Waitakere Ranges, North Auckland, New Zealand. *J. R. Soc. N. Z.* **7**: 5–16.
- Heimler, W. 1988. Larvae. Pp. 352–271 in *The Ultrastructure of Polychaeta*, W. Westheide and C. O. Hermans, eds. Gustav Fischer Verlag, Stuttgart.
- Howell, B. F. 1962. Worms. Pp. 144–177 in *Treatise on Invertebrate Paleontology, Part W, Miscellaneous*, R. C. Moore, ed. University of Kansas Press, Lawrence, KS.
- Jablonski, D. 1986. Larval ecology and macroevolution in marine invertebrates. *Bull. Mar. Sci.* **39**: 565–587.
- Jagersten, G. 1972. *Evolution of the Metazoan Life Cycle*. Academic Press, London.
- Kempf, S. C., and C. D. Todd. 1989. Feeding potential in the lecithotrophic larvae of *Adalaria proxima* and *Tritonia hombergi*: an evolutionary perspective. *J. Mar. Biol. Assoc. UK* **69**: 659–682.
- Krug, P. J. 1998. Poecilogony in an estuarine opisthobranch: planktotrophy, lecithotrophy, and mixed clutches in a population of the ascoglossan *Alderia modesta*. *Mar. Biol.* **132**: 483–494.
- Kume, M., and K. Dan. 1968. *Invertebrate Embryology*. National Technical Information Services, Springfield, VA.
- Kupriyanova, E. K., E. Nishi, H. A. ten Hove, and A. V. Rzhavsky. 2001. Life-history patterns in serpulimorph polychaetes: ecological and evolutionary perspectives. *Oceanogr. Mar. Biol. Annu. Rev.* **39**: 1–101.
- Lauder, G. V. 1994. Homology, form, and function. Pp. 152–197 in *Homology: The Hierarchical Basis of Comparative Biology*, B. K. Hall, ed. Academic Press, London.
- Lee, Y. R. 1970. Biochemical studies on RNA synthesis during oogenesis of *Schizobranchia insignis*. M.S. thesis, University of Washington, Seattle.
- Lee, Y. R. 1975. Transcription of repeated and unique genes during oogenesis of *Schizobranchia insignis*. Ph.D. dissertation, University of Washington, Seattle.

- Levin, L. A. 1984. Multiple patterns of development in *Streblospio benedicti* Webster (Spionidae) from three coasts of North America. *Biol. Bull.* **166**: 494–508.
- Lillie, F. R. 1899. Adaptation in cleavage. Pp. 43–67 in *Biological Lectures from the Marine Biological Laboratory, Woods Hole, Mass., 1898*. Ginn, Boston.
- Martindale, M. Q. 1986. The “organizing” role of the D quadrant in an equal-cleaving spiralian, *Lynnaca stagnalis*, as studied by UV laser deletion of macromeres at intervals between third and fourth quartet formation. *Int. J. Invertebr. Reprod. Dev.* **9**: 229–242.
- McEdward, L. R., and D. A. Janies. 1997. Relationships among development, ecology, and morphology in the evolution of echinoderm larvae and life cycles. *Biol. J. Linn. Soc.* **60**: 381–400.
- McEuen, F. S., B. L. Wu, and F.-S. Chia. 1983. Reproduction and development of *Sabella media*, a sabellid polychaete with extratubular brooding. *Mar. Biol.* **76**: 301–309.
- Moran, A. L. 1999. Intracapsular feeding by embryos of the gastropod genus *Littorina*. *Biol. Bull.* **196**: 229–244.
- Nishi, E., and T. Yasasu. 1992. Brooding and development of a serpulid tube worm *Salmacina dysteri*. *Bull. Coll. Sci. Univ. Ryukyus* **54**: 107–121.
- Okuda, S. 1946. Studies on the development of Annelida Polychaeta I. *J. Fac. Sci. Hokkaido Univ. Ser. VI* **9**: 115–219.
- Olson, R. R., J. L. Cameron, and C. M. Young. 1993. Larval development (with observations on spawning) of the pencil urchin *Phyllacanthus imperialis*: a new intermediate larval form? *Biol. Bull.* **185**: 77–85.
- Palumbi, S. R. 1995. Using genetics as an indirect estimator of larval dispersal. Pp. 369–388 in *Ecology of Marine Invertebrate Larvae*, L. R. McEdward, ed. CRC Press, Boca Raton, FL.
- Pernet, B., P.-Y. Qian, G. Rouse, C. M. Young, and K. J. Eckelbarger. 2002. Phylum Annelida. Pp. 209–243 in *Atlas of Marine Invertebrate Larvae*, C. M. Young, M. A. Sewell, and M. E. Rice, eds. Academic Press, San Diego, CA.
- Phillips, N. E., and B. Pernet. 1996. Capture of large particles by suspension-feeding scaleworm larvae (Polychaeta: Polynoidae). *Biol. Bull.* **191**: 199–208.
- Plicka, M. 1968. Zoophycos, and a proposed classification of sabellid worms. *J. Paleontol.* **42**: 836–849.
- Raff, R. A. 1987. Constraint, flexibility, and phylogenetic history in the evolution of direct development in sea urchins. *Dev. Biol.* **119**: 6–19.
- Richardson, K. C., L. Jarett, and E. H. Finke. 1960. Embedding in epoxy resins for ultrathin sectioning in electron microscopy. *Stain Technol.* **35**: 313–323.
- Rivest, B. R. 1981. Nurse egg consumption and the uptake of albumen in the embryonic nutrition of marine snails. Ph.D. dissertation, University of Washington, Seattle.
- Rouse, G. W. 1996. A new species of *Perkinsiana* from Papua New Guinea, with a description of larval development. *Ophelia* **45**: 101–114.
- Rouse, G. W. 1999. Trochophore concepts: ciliary bands and the evolution of larvae in spiralian metazoa. *Biol. J. Linn. Soc.* **66**: 411–464.
- Rouse, G. W. 2000a. Bias? What bias? The evolution of downstream larval-feeding in animals. *Zool. Scripta* **29**: 213–236.
- Rouse, G. W. 2000b. The epitome of hand waving? Larval feeding and hypotheses of metazoan phylogeny. *Evol. Dev.* **2**: 222–233.
- Rouse, G. W., and K. Fitzhugh. 1994. Broadcasting fables: is external fertilization really primitive? Sex, size and larvae in sabellid polychaetes. *Zool. Scripta* **23**: 271–312.
- Rouse, G. W., and M. C. Gambi. 1998. Evolution of reproductive features and larval development in the genus *Amphiglena*. *Mar. Biol.* **131**: 743–753.
- Rouse, G. W., and F. Pleijel. 2001. *Polychaetes*. Oxford University Press, New York.
- Schneider, S., A. Fischer, and A. W. C. Dorresteijn. 1992. A morphometric comparison of dissimilar early development in sibling species of *Platynereis*. *Roux's Arch. Dev. Biol.* **201**: 243–256.
- Schroeder, P. C., and C. O. Hermans. 1975. Annelida: Polychaeta. Pp. 1–213 in *Reproduction of Marine Invertebrates*, Vol. III, A. C. Giese and J. S. Pearse, eds. Academic Press, New York.
- Schulze, S. R., S. A. Rice, J. L. Simon, and S. A. Karl. 2000. Evolution of poecilogony and the biogeography of North American populations of the polychaete *Streblospio*. *Evolution* **54**: 1247–1259.
- Schweigert, G., G. Dietl, and M. Röper. 1998. *Muensteria vermicularis* (Vermes, Sabellidae) aus oberjurassischen Plattenkalken Süddeutschlands. *Mitt. Bayer. Staatssamml. Palaentol. Hist. Geol.* **38**: 25–37.
- Strathmann, M. F. 1987. *Reproduction and Development of Marine Invertebrates of the Northern Pacific Coast*. University of Washington Press, Seattle.
- Strathmann, R. R. 1975. Larval feeding in echinoderms. *Am. Zool.* **15**: 717–730.
- Strathmann, R. R. 1978. The evolution and loss of feeding larval stages of marine invertebrates. *Evolution* **32**: 894–906.
- Strathmann, R. R. 1987. Larval feeding. Pp. 465–550 in *Reproduction of Marine Invertebrates*, Vol. IX, A. C. Giese, J. S. Pearse, and V. B. Pearse, eds. Blackwell Scientific, Palo Alto, CA.
- Strathmann, R. R., T. L. Jahn, and J. R. C. Fonseca. 1972. Suspension feeding by marine invertebrate larvae: clearance of particles by ciliated bands of a rotifer, pluteus, and trochophore. *Biol. Bull.* **142**: 505–519.
- Termier, G., H. Termier, and A. F. de Lapparent. 1973. Un sabellide du Devonien supérieur du Hoggar. Essai sur quelques *Spirophyton* du Sahara. *Doc. Lab. Geol. Fac. Sci. Lyon* **57**: 119–129.
- Wilson, D. P. 1929. The larvae of the British sabellarians. *J. Mar. Biol. Assoc. UK* **16**: 221–268.
- Wilson, D. P. 1936. The development of the sabellid *Branchiomma vesticulosum*. *Q. J. Microsc. Sci.* **78**: 543–603.
- Wray, G. A. 1996. Parallel evolution of nonfeeding larvae in echinoids. *Syst. Biol.* **45**: 308–322.
- Wray, G. A., and A. E. Bely. 1994. The evolution of echinoderm development is driven by several distinct factors. *Development (suppl.)* **97**: 106.
- Wray, G. A., and R. A. Raff. 1991. The evolution of developmental strategy in marine invertebrates. *Trends Ecol. Evol.* **6**: 45–50.

# Cloning, Characterization, and Developmental Expression of a Putative Farnesoic Acid *O*-Methyl Transferase in the Female Edible Crab *Cancer pagurus*

CAROLYN J. RUDELL<sup>1</sup>, GEOFFREY WAINWRIGHT<sup>1</sup>, AUDREY GEFFEN<sup>1</sup>,  
MICHAEL R. H. WHITE<sup>1</sup>, SIMON G. WEBSTER<sup>2</sup>, AND HUW H. REES<sup>1,\*</sup>

<sup>1</sup> *School of Biological Sciences, University of Liverpool, Liverpool L69 7ZB, United Kingdom; and*

<sup>2</sup> *School of Biological Sciences, University of Wales, Bangor, LL57 2UW, United Kingdom*

**Abstract.** Farnesoic acid methyl transferase (FAMTase) catalyzes methylation of farnesoic acid to yield the crustacean juvenoid, methyl farnesoate (MF). A full-length cDNA encoding a 275 amino acid putative FAMTase has been isolated from the mandibular organ of the female edible crab (*Cancer pagurus*) by reverse transcriptase-polymerase chain reaction in conjunction with cDNA library screening. A high degree of sequence identity was found between this and other putative crustacean FAMTases. Conceptual translation and protein sequence analysis suggested that phosphorylation could occur at multiple sites in the FAMTase. This finding is consistent with the recent observation that endogenous FAMTase activity in mandibular organ extracts can be regulated by phosphorylation *in vitro*. We demonstrated that the recombinant FAMTase could be expressed as a LacZ-fusion protein in *Escherichia coli* and have undertaken its partial purification from inclusion bodies. In an established assay system, the recombinant FAMTase lacked activity.

Northern blotting demonstrated widespread expression of an approximately 1250-nucleotide FAMTase transcript in female *C. pagurus* tissues. Levels of FAMTase transcripts in mandibular organs of female *C. pagurus* were found to fluctuate during vitellogenesis and embryonic development. Throughout the spring of 2002, an HPLC-based method was used to measure hemolymph MF titers in more than 70

female specimens of *C. pagurus*, which segregated into “high MF” and “low MF” groups. The high MF titers, which occurred before or during early vitellogenesis, coincided with, or were preceded by, elevated levels of putative FAMTase mRNA in the mandibular organs.

## Introduction

Methyl farnesoate (MF), a sesquiterpenoid structurally similar to insect juvenile hormone III, is produced and secreted by the mandibular organs of crustaceans (Laufer *et al.*, 1987a, b; Borst *et al.*, 1987; Wainwright *et al.*, 1996a, b, 1998). Just as the juvenile hormones maintain larval characteristics between successive molts in insects (for a review, see Riddiford, 1994), a recent report confirms that MF regulates larval metamorphosis in barnacles (Smith *et al.*, 2000). In adult insects, juvenile hormone has been implicated in the regulation of ovarian development (Davey, 1996; Belles, 1998), and a growing body of evidence suggests an analogous role for MF in crustaceans. In the spider crab *Libinia emarginata* and the edible crab *Cancer pagurus*, increased levels of MF synthesis in the mandibular organs (Laufer *et al.*, 1987a) and elevated levels of MF in the hemolymph (Wainwright *et al.*, 1996a) have been found to occur during vitellogenesis. In experiments where a variety of crustaceans were exposed to artificially enhanced levels of MF, either by the effects of eyestalk ablation (Jo *et al.*, 1999), by direct injection of MF (Reddy and Ramamurthi, 1998; Rodriguez *et al.*, 2002), or by administration of MF through the diet (Laufer *et al.*, 1998), oocyte growth and ovarian development were stimulated. Similarly, a significant increase in mean oocyte diameter was reported when ovary explants from shrimp, *Penaeus van-*

Received 25 April 2002; accepted 5 September 2003.

\* To whom correspondence should be addressed. E-mail: reeshh@liv.ac.uk

**Abbreviations:** FAMTase, S-adenosyl-L-methionine farnesoic acid *O*-methyl transferase; MF, methyl farnesoate; MO-IH, mandibular organ-inhibiting hormone.

*namei* (Tsukimura and Kamemoto, 1991) and red swamp crayfish, *Procambarus clarkii* (Rodriguez *et al.*, 2002) were incubated *in vitro* with physiologically relevant concentrations of MF. This combined evidence strongly supports a role for MF in the reproductive development of female crustaceans.

In crustaceans, ovarian development is broadly separated into two distinct phases, a pre-vitellogenic phase and a vitellogenic phase. During the pre-vitellogenic phase, primary oocytes begin to accumulate rough endoplasmic reticulum, and endogenous glycoprotein content increases. At the end of this phase, oocyte development arrests at prophase-I of meiosis, which synchronizes the oocytes at the same stage of development (for a review, see Charniaux-Cotton and Payen, 1988). Synchronization is critical because crustaceans fertilize and spawn all of their oocytes simultaneously. In locusts and shrimp, the meiotic block is released by physiological doses of ecdysteroids (Clédon, 1985; Lanot and Clédon, 1989). After meiosis resumes, germinal vesicle breakdown occurs, and vitellogenesis follows. The vitellogenic phase is characterized by a significant increase in the size of the ovary and an accumulation of yolk protein within the oocytes of the developing ovary tissue. In *C. pagurus*, oocytes are fertilized as they are laid, by sperm that has been stored in the spermathecae since copulation, when the female was soft-bodied after molting. Eggs are brooded under the abdomen attached to ovigerous pleopod hairs until embryogenesis is complete, and the hatched larvae are released as free-swimming zoeae. Egg-laying is believed to occur during the winter, and the larvae hatch 6 months later (Warner, 1977). The precise timing of vitellogenic events in *C. pagurus* has not been fully determined, although vitellogenesis appears to begin during the spring, presumably in response to environmental cues, such as photoperiod and temperature. The exact role of MF in crustacean ovarian development is still unclear, but in *C. pagurus* the hemolymph MF concentration is reported to peak during the earliest stage of vitellogenesis, suggesting its involvement in the control of this process (Wainwright *et al.*, 1996a).

Previously, we investigated the regulation of MF production in the mandibular organs of *C. pagurus*, isolating and characterizing two 78-residue peptides—mandibular organ-inhibiting hormones (MO-IHs)—that down-regulate the production of MF by the mandibular organs (Wainwright *et al.*, 1996b). Furthermore, we demonstrated that the action of MO-IH on mandibular organs ultimately regulates an *S*-adenosyl-L-methionine farnesoic acid *O*-methyl transferase (FAMTase), an enzyme that catalyses the final step of MF biosynthesis (Wainwright *et al.*, 1998). To date, putative FAMTase sequences from three decapod crustaceans have been published in on-line databases. Of these sequences, there is no evidence that the cloned gene products from the spiny lobster *Panulirus interruptus* (GenBank accession

number AF249871) or from the clawed lobster *Homarus americanus* (U25846) have FAMTase activity. However, the recombinant FAMTase from the shrimp *Metapenaeus ensis* (AF333042) has recently been reported to catalyze, *in vitro*, the conversion of farnesoic acid to methyl farnesoate (Silva Gunawardene *et al.*, 2002). No brachyuran decapod has been studied to date, but these findings with shrimp suggest that a homologous putative FAMTase from the crab *Cancer pagurus* might also have enzyme activity.

In this report, we describe the isolation and characterization of a full-length cDNA encoding a 275-residue putative FAMTase from mandibular organs of female specimens of *C. pagurus* (GenBank accession number AY337487). The recombinant FAMTase was heterologously expressed, and enzyme activity was investigated in an established assay system (Wainwright *et al.*, 1998). The distribution of putative FAMTase expression is presented for a range of *C. pagurus* tissues, throughout the course of ovarian development and during embryogenesis. We also present further details regarding the previously reported peak of hemolymph MF (Wainwright *et al.*, 1996a), which occurs prior to or during the earliest stage of vitellogenesis.

## Materials and Methods

### Animals

Adult females of *Cancer pagurus* (Linnaeus), the edible crab, were obtained weekly from local fishermen and maintained in a recirculating seawater system at ambient light and temperature. These wild-caught animals constituted a non-synchronized population; therefore, crabs at different stages of ovarian development could be encountered at any given time. Crabs were dissected after cold-anesthesia, and the stage of ovarian development was determined according to established criteria (Wainwright, 1995; Wainwright *et al.*, 1996a). In brief, crabs were assigned a stage of ovarian development from 0 to 4. Stage 1 to 4 ovaries are vitellogenic, with steadily increasing organ size, oocyte diameter, and quantity of accumulated yolk protein (orange color). Stage 0 crabs, with cream-colored undeveloped ovarian tissue, are classed as either "pre-vitellogenic," if the hemolymph color is gray, or "vitellogenic," if the hemolymph color is orange; the orange color indicates the presence of circulating yolk protein.

Two egg-carrying females were caught during the winter and maintained in individual tanks at the Marine Biological Laboratories at Port Erin, Isle of Man. Embryonic offspring were collected from the egg-bearing pleopod hairs in the abdominal brooding pouch using flat-ended forceps. Hatched larvae were collected by filtration of the tank water. Embryos, larvae, and dissected adult tissues were stored in Trizol reagent (Life Technologies, Inc.) at  $-80^{\circ}\text{C}$  prior to analysis.

### Isolation of a cDNA fragment of FAMTase using a nested PCR approach

The mandibular organs were dissected from three female *C. pagurus* specimens (ovary stage 0, hemolymph orange), and total RNA was isolated using Trizol reagent. Nested degenerate PCR primers were designed based on conserved regions within the crustacean FAMTase sequences published online.

First-strand cDNA synthesis was performed using 1  $\mu$ g total RNA, as described in the SMART cDNA Library Construction Kit User Manual (version #PR92334) (Clontech Laboratories, Inc.). Most of this material was used to synthesize a mandibular organ cDNA library (see below). One-tenth of the first-strand synthesis reaction was used as cDNA template for PCR, with DMTS1 sense (5'-GCNCAYGAYGCNCAYG TNGC) and DMTAS1 anti-

sense (5'-GGYTCNGGRTCTNGTCCAAYTC) primers (Fig. 1), and with the following temperature profile: 94 °C for 2 min, followed by 25 cycles of 94 °C for 1 min, 53 °C for 2 min, 72 °C for 1 min, and a final extension step of 7 min. PCR was carried out in a 20- $\mu$ l reaction volume containing 0.5 units Taq DNA polymerase (Roche) in the manufacturer's reaction buffer (with 1.5 mM MgCl<sub>2</sub>) in the presence of 0.5  $\mu$ M PCR primers (MWG Biotech) and 0.25 mM each dNTP (Promega). Nested PCR was performed with DMTS2 sense (5'-CNCCNGAYATHYTNWSNGARGAR) and DMTAS2 antisense (5'-YTTNCKYTCYTCYTCRCARC) primers (Fig. 1), using 5  $\mu$ l of the first PCR reaction as a template. The following thermal cycle was employed: 94 °C for 1 min, 54 °C for 1 min, 72 °C for 1 min for 25 cycles. Other PCR conditions and reaction mixture constituents were as described above. Agarose gel electrophoresis of the

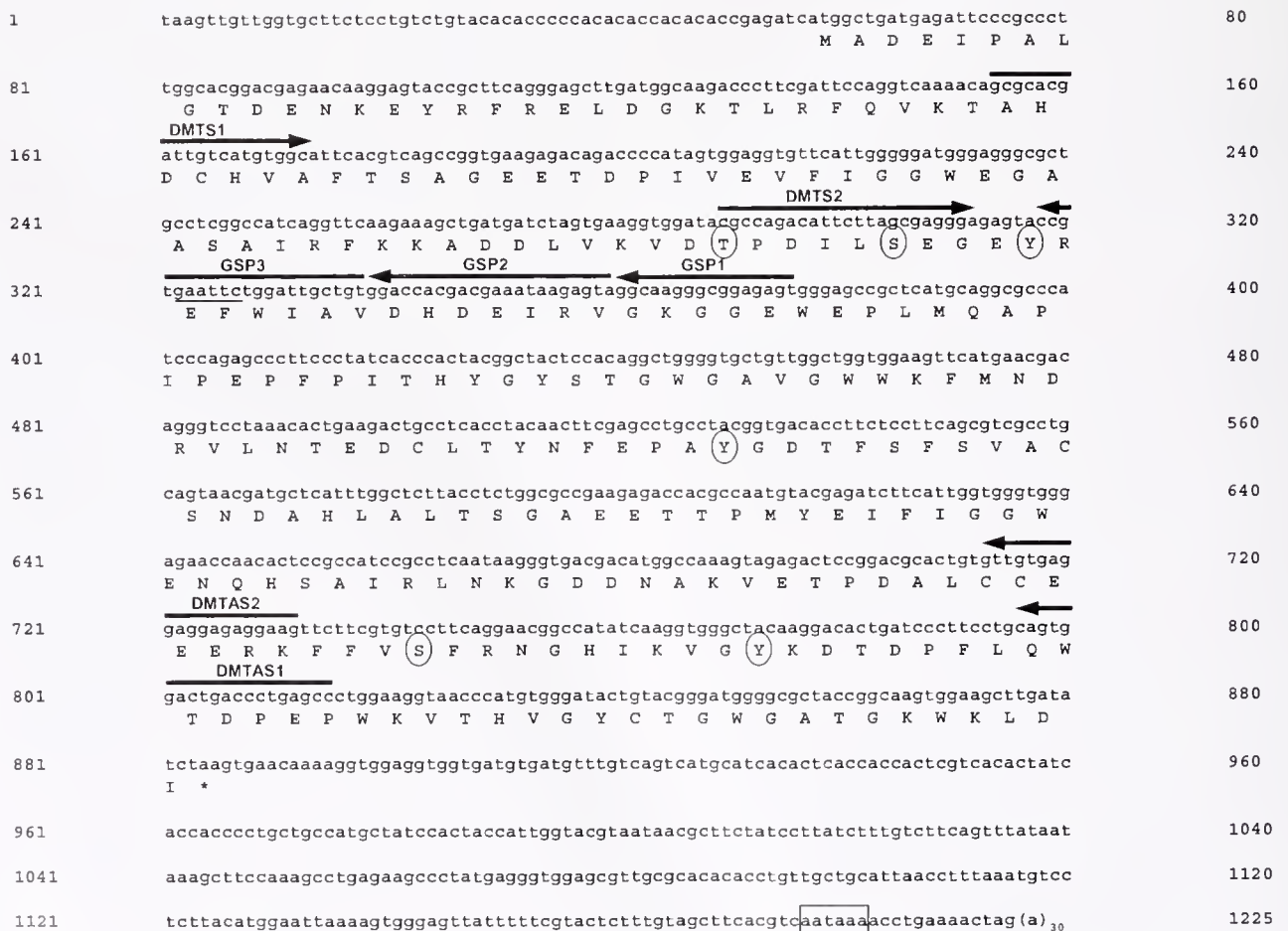


**Figure 1.** Sequence of cDNA from the mandibular organ encoding the putative FAMTase. The full-length cDNA was isolated by PCR and nucleotide sequence determined (see Methods). The cDNA sequence shows an 825-bp open reading frame, which encodes a 275 amino acid protein. The stop codon is indicated by an asterisk, and a polyadenylation signal (AATAAA) is enclosed in a box. Circles indicate potential phosphorylation sites in the mature protein. Arrows indicate positions of primers, which are identified (see Methods). A single *Eco* RI site at 322 bp is underlined.

nested PCR products revealed a band of about 450 bp, which was cloned into the pGEM T-easy TA cloning vector according to the manufacturer's instructions (Promega). Sequencing of the 450-bp cloned insert showed it to be very similar to the existing crustacean FAMTase sequences in databases. This cDNA fragment was used as a probe to isolate a full-length cDNA encoding *C. pagurus* FAMTase.

#### *Isolation of full-length FAMTase cDNA from a mandibular organ cDNA library*

From the remainder of the first-strand synthesis reaction (see above), a unidirectional, mandibular organ cDNA library was constructed in bacteriophage  $\lambda$ TriplEx2. The titer of the primary, unamplified library was  $0.97 \times 10^6$  pfu/ml with >95% positive recombinants.

To isolate clones containing full-length cDNAs encoding *C. pagurus* FAMTase, plaque hybridization screening was carried out using the 450-bp FAMTase fragment end-labeled with [ $\alpha$ - $^{32}$ P]-dCTP using the Ready-To-Go DNA Labeling Kit (Amersham Pharmacia) as a probe. Plaque lifts were carried out with BioTrace NT nitrocellulose blotting membrane (Gelman Sciences), and hybridizations and washes were carried out according to manufacturer's guidelines. A feature of the  $\lambda$ TriplEx2 vector is that it contains an embedded bacterial plasmid DNA, pTriplEx2. Excision and circularization of the plasmid DNA from the linear bacteriophage DNA is readily achieved by a process involving *in vivo* excision using Cre recombinase-mediated site-specific recombination at two *loxP* sites flanking the embedded plasmid. This is carried out by incubating  $\lambda$ TriplEx2 at 31 °C in the presence of *E. coli* BM25.8 (Clontech Laboratories, Inc.). The resultant plasmid can be used to express LacZ fusion protein variants of the encoded proteins under the regulation of a LacZ promoter. Positive clones from the library screening were converted into plasmid clones and analyzed by restriction enzyme digestion with *EcoRI* and *Sall*.

#### *5'-Rapid amplification of cDNA ends (5'-RACE)*

To obtain the 5'-end of the FAMTase cDNA clone, 5'-RACE was carried out using total RNA from mandibular organs. A 5'-RACE system version 2.0 (Life Technologies) was used to amplify the 5' terminus of the message for sequencing. Briefly, a gene-specific primer (GSP1, 5'-ACTCTCCGCCCTTGCC) was hybridized to the mRNA, and cDNA was synthesized using Superscript II reverse transcriptase. The RNA was then degraded with RNase mix (RNase H and RNase T1), and the cDNA was purified using a GlassMax spin cartridge supplied with the kit. A poly(dC) tail was added to the 3'-terminus of the purified cDNA using dCTP and terminal deoxynucleotidyl transferase, and the cDNA region corresponding to the 5'-end of the mRNA was amplified by two successive rounds of PCR using

additional gene-specific primers (GSP2, 5'-TACTCT-TATTCGTCGTGGTCC; GSP3, 5'-ACAGCAATCCA-GAATCACGG), together with anchor primers supplied by the manufacturer. The second-round PCR product of about 380 bp was cloned into pGEM-T Easy Vector, and the nucleotide sequences of several clones were determined.

#### *Expression of FAMTase protein*

Expression of protein encoded by cDNA within pTriplEx2 plasmid was carried out, as follows, in *E. coli* TOP10 F'. Bacteria containing the pTriplEx2 plasmid were grown to a density of OD<sub>600</sub> 0.5 to 0.6, at 37 °C, in LB medium supplemented with 50  $\mu$ g/ml of ampicillin. Expression of LacZ fusion protein was achieved by addition of isopropyl  $\beta$ -D-thiogalactopyranoside (IPTG) to a final concentration of 0.4 mM (Brent, 1994).

#### *SDS PAGE analysis of proteins*

Extracts of proteins from *E. coli* were prepared to yield both soluble protein fractions and insoluble inclusion-body fractions, according to a published method (Brent, 1994). In both cases, *E. coli* cells were harvested by centrifugation (3000  $\times$  g, 10 min, 4 °C), washed in PBS buffer, and centrifuged (3000  $\times$  g, 10 min, 4 °C). The pellet was resuspended in HEMGN buffer (100 mM KCl, 25 mM HEPES [pH 7.6], 0.1 mM EDTA [pH 8.0], 10% [v/v] glycerol, 0.1% [v/v] Triton X-100) containing protease inhibitors (1 mM dithiothreitol, 0.1 mM phenylmethylsulfonyl fluoride, 0.1 mM sodium metabisulfite and protease inhibitor cocktail [Sigma, #P8340] added at 10  $\mu$ l per 100 ml of original culture volume) and lysozyme (0.5 mg/ml), and lysed by sonication. After centrifugation (27,000  $\times$  g, 15 min, 4 °C) to separate soluble (supernatant) and insoluble fractions (pellet), the pellet was extracted into HEMGN buffer containing 8 M guanidinium-HCl, and centrifuged (87,000  $\times$  g, 30 min, 4 °C). The supernatant was dialyzed once against HEMGN buffer containing 1 M guanidinium-HCl and protease inhibitors (see above), then twice against HEMGN buffer containing protease inhibitors. The dialysate was centrifuged (12,000  $\times$  g, 5 min, 4 °C) to yield 8 M guanidinium-HCl soluble (supernatant) and insoluble (pellet) protein extracts (see Fig. 3). Portions of all extracts were analyzed by electrophoresis on a 10% polyacrylamide gel. Protein bands were visualized by staining with colloidal Coomassie blue G250.

#### *FAMTase assays*

Broken-cell extracts of *E. coli* were assayed for FAMTase activity using assay conditions previously published (Wainwright *et al.*, 1998). Briefly, extracts (200  $\mu$ l) were dialyzed against a hypotonic HEPES buffer (0.037 M HEPES, 0.3 M sucrose, 0.01 M KF, pH 7.4) before the

addition of 2.4  $\mu\text{M}$  [ $12\text{-}^3\text{H}$ ] farnesoic acid and 250  $\mu\text{M}$  S-adenosyl-L-methionine, in a final reaction volume of 50  $\mu\text{l}$ . Incubations were carried out at 37 °C for 1 h and were terminated by the addition of 150  $\mu\text{l}$  of acetonitrile. The reaction products were analyzed by reversed-phase HPLC with on-line radioactivity monitoring, as described previously (Wainwright *et al.*, 1998).

#### *Expression of FAMTase in C. pagurus tissues*

Total RNA from a variety of tissues (see Results) was isolated using Trizol reagent (Life Technologies). For Northern blotting, about 10  $\mu\text{g}$  of total RNA from individual tissues was electrophoresed on a formaldehyde/1% agarose gel for 3 h at 75 V. The RNA was blotted onto Eelectran nylon membrane (BDH) with  $20 \times \text{SSC}$  (SSC is 0.15 M NaCl/0.15 M sodium citrate) and RNA cross-linked to the membrane by UV radiation. The FAMTase probe was prepared, as described above, and hybridization was carried out in QuickHyb solution (Stratagene) for 1.5 h at 68 °C. After hybridization, the blot was washed three times, at room temperature, for 10 min each, in  $2 \times \text{SSC}$  containing 0.1% SDS, and twice, at 45 °C, for 10 min in  $0.1 \times \text{SSC}$  containing 0.1% SDS. Autoradiographs were exposed at  $-70$  °C.

To compare relative levels of expression of FAMTase in samples, a mouse 18S rRNA probe (Takeuchi *et al.*, 2000) was co-hybridized under the same conditions. This procedure provided an internal calibration for each sample and allowed for differences among lanes in the loading of RNA. In preliminary control experiments, when Northern blotting was carried out with individual probes alone, using identical hybridization and wash conditions, the hybridization patterns showed single bands of appropriate sizes for each probe (18S rRNA, 2000 nt; FAMTase mRNA, 1250 nt). Under the conditions used, therefore, the 18S rRNA and FAMTase mRNA probes did not cross-hybridize with their respective target transcripts. So we co-hybridized the blots in subsequent experiments. Densitometric analyses were carried out using Quantity One software (Bio-Rad) and amounts of FAMTase mRNA normalized against those of 18S rRNA.

#### *Preparation of hemolymph methyl farnesoate extracts for HPLC*

Hemolymph samples were taken from adult female specimens of *C. pagurus* with a hypodermic syringe; the arthrodistal membrane at the base of a walking leg was punctured, and 2 ml of hemolymph was extracted. Methyl farnesoate isomers were extracted into hexane using a triphasic procedure (Borst and Tsukimura, 1991) incorporating modifications according to Wainwright *et al.* (1996a). Briefly, hemolymph samples (2 ml) were added to tubes containing 2 ml NaCl 4% (w/v) in  $\text{H}_2\text{O}$ , 5 ml acetonitrile (Merck, far UV

HiPerSolv grade), and 100 ng *cis, trans*-MF isomer as an internal standard. The mixture was partitioned against 2 ml *n*-hexane (Merck, HiPerSolv grade), achieving phase separation by centrifugation at  $500 \times g$  for 10 min at 20 °C. The hexane layer (top) was removed and 300  $\mu\text{l}$  subjected directly to HPLC analysis.

#### *HPLC quantification of methyl farnesoate*

Levels of *all-trans*-MF contained in hemolymph hexane extracts were determined by adsorption HPLC on a Varian Pro Star chromatography workstation, with a modification of the method previously described by Borst *et al.* (2002). Separation of MF isomers contained in hexane extracts (300  $\mu\text{l}$ ) from hemolymph was achieved on a Rainin MicroSorb MV silica adsorption column (5  $\mu\text{m}$ ,  $250 \times 4.6$  mm internal diameter) using isocratic elution at 2 ml/min for 45 min in 0.4% diethyl ether in *n*-hexane (Merck, HiPerSolv grade) that had been dried overnight after the addition of 50 g of molecular sieve 4 Å (bead), 8–12 mesh (Sigma, #M1760), per 2.5 l of solvent. Eluted compounds were detected by UV absorbance at 229 nm. Peak areas were calculated using Star workstation software (Varian). *All-trans*-MF content of hemolymph samples was calculated by comparison of the *all-trans*-MF peak area to the *cis, trans*-MF peak area (internal standard 100 ng).

## Results

#### *Isolation, characterization, and expression of FAMTase from C. pagurus mandibular organ*

*Isolation and characterization of FAMTase.* To obtain full-length cDNA encoding FAMTase, nested PCR was followed by isolation of full-length cDNA from a mandibular organ cDNA library. Previously published putative FAMTase sequences provided information for the design of degenerate oligonucleotide primers for the isolation of a *ca.* 450-bp fragment of cDNA that encoded a putative FAMTase. Subsequent sequence analysis suggested that this was, in fact, a putative FAMTase cDNA fragment of 442 bp. This partial cDNA was used to screen a mandibular organ cDNA library. Initially, approximately  $8 \times 10^4$  recombinant bacteriophage were grown in two 15-cm petri dishes and screened. This initial screen identified four positive clones that were subsequently isolated and purified. All four phage clones were converted to their corresponding plasmid clones as described, and the inserts were analyzed by restriction enzyme digestion with *SalI* and *EcoRI*; the products were then separated electrophoretically on a 1% agarose gel. Of the clones analyzed, two distinct types were apparent: one type, on digestion, produced two products (900 and 300 bp) originating from the cloned insert cDNA, while the other type produced only a 900-bp insert. Sequencing and BLAST searching revealed the former type,

Group 1, to be putative FAMTase sequence clones. The complete sequence of the putative FAMTase clone was obtained (see Fig. 1). The clone was 1216 bp in length, and conceptual translation indicated an open reading frame of 825 bp encoding a 275 amino acid protein with a predicted molecular weight of 31114. The 5'-UTR was 48 bp long. The 3'-UTR was 336 bp long and contained a polyadenylation signal, AATAAA, 13 bp upstream of the poly(A) tail. 5'-RACE demonstrated that the isolated and sequenced clone was 9 bp shorter than the full length of the 5'-UTR. A single *EcoRI* restriction enzyme cutting site occurs at 322 bp.

ClustalW alignment of the isolated putative FAMTase from *C. pagurus*, with sequences identified in other crustacean species, demonstrated a high degree of sequence identity (Fig. 2). Analysis of the protein sequence with SignalP

ver. 1.1 software (<http://www.cbs.dtu.dk/services/SignalP/>) suggested that the protein does not contain a signal peptide cleavage site. Further analysis of the protein sequence, with NetPhos 2.0 (<http://www.cbs.dtu.dk/services/NetPhos/>) and ScanProsite (<http://ca.expasy.org/tools/scanprosite/>), for potential posttranslational modifications shows multiple high-scoring (score > 0.8) sites for possible phosphorylation at serine, threonine, and tyrosine side chains within the molecule (Fig. 2).

#### Expression and activity of FAMTase protein

To determine whether the protein encoded by the isolated FAMTase cDNA clone was indeed an active FAMTase, expression of the protein in *E. coli* was carried out as described (Methods). Just prior to the addition of IPTG to



**Figure 2.** Amino acid sequence alignment of putative FAMTases from four crustaceans. ClustalW alignment of FAMTases from *Cancer pagurus* (this report, GenBank accession number AY337487), *Homarus americanus* (U25846), *Metapenaeus ensis* (Silva Gunawardene *et al.*, 2001, AF333042), and *Panulirus interruptus* (AF249871). Identical amino acids at a particular position, in all sequences, are denoted by an asterisk. Colons denote alignment of amino acids with strong similarities; periods indicate aligned residues with weaker similarities, according to their physicochemical properties. Hyphens denote gaps introduced to maximize the sequence alignment. Circles indicate potential phosphorylation sites in the mature protein. EMBL ClustalW default alignment settings were used ([www.ebi.ac.uk/clustalw/](http://www.ebi.ac.uk/clustalw/)).

the cultures, a 1-ml sample (time = 0 h) was taken and protein extracts prepared as described (see Methods). Samples (1 ml) of bacterial culture were taken at 1, 2 and 5 h post-IPTG addition. Both soluble and insoluble extracts of the bacteria were prepared and analyzed by SDS-PAGE. Analysis of the samples taken 5 h after the addition of IPTG clearly shows that recombinant protein expression is induced by IPTG, and that the recombinant protein is produced predominantly in the insoluble inclusion body fraction (Fig. 3). Molecular weight analysis demonstrated the induction of a protein of approximately 40 kDa. This size is entirely consistent with the expected size of the FAMTase-LacZ fusion protein.

To determine whether the recombinant fusion protein exhibited any FAMTase activity, the protein extracts were assayed for their ability to convert farnesoic acid into methyl farnesoate using conditions previously described (see above; Wainwright *et al.*, 1998). The broken cell extracts exhibited no detectable FAMTase activity (results not shown).

#### *Expression of FAMTase during ovarian development and embryogenesis*

*Expression of FAMTase in tissues and developmental stages.* To determine the tissue distribution and developmental expression of the putative FAMTase, Northern blotting was carried out using the 450-bp clone as a probe. The probe detected a single band of approximately 1250 nt in a number of tissues, including muscle, eyes, mandibular organs, epidermis, gills, heart, ovary, hepatopancreas and gut (Fig. 4). The extremely low signals detected by Northern blotting in Y-organs and sub-epidermal adipose tissue pre-

cluded estimation of relative FAMTase expression levels in these tissues; and in hemolymph RNA, the FAMTase transcript was undetectable by Northern blotting.

To determine the developmental profile of expression of FAMTase in mandibular organs, RNA was extracted from the mandibular organs of female crabs at different stages of ovarian development, and Northern blotting was carried out as described. A representative blot (Fig. 5a) demonstrates a distinct variation in the level of expression of FAMTase in the mandibular organ during ovarian development. Following densitometric analysis of the Northern blot autoradiograms, the ratio of FAMTase to 18S rRNA was determined, and the results were displayed graphically (Fig. 5b). Expression of FAMTase from the mandibular organ is significantly higher before the onset of vitellogenesis than after vitellogenesis has begun (unpaired *t* test,  $P = 0.03$ ). During the mid and late stages of ovarian development, the levels of mandibular organ FAMTase expression appeared to fluctuate, but definitive trends could not be identified at these stages.

*Female methyl farnesoate hemolymph titers.* As part of an investigation aimed at further characterizing events that occur during the transition from the pre-vitellogenic to vitellogenic phases of ovarian development, we measured the hemolymph methyl farnesoate (MF) titers of over 100 female specimens of *C. pagurus* throughout the spring of 2002. In stage 0 crabs ( $n = 70$ ), hemolymph MF titers segregated into two groups: "low" (93%) and "high" (7%) MF, with a cut-off titer of about 150 ng/ml between the groups (Fig. 6). It was noted that although one high MF crab was at an early stage of vitellogenesis (stage 0, orange hemolymph), four of the five high MF crabs fell into the stage 0 pre-vitellogenic category (stage 0, gray hemolymph).

*FAMTase expression during embryonic and larval development.* As an extension of our investigations, samples of developing embryos, up to hatching, were collected and analyzed for expression of FAMTase transcripts. The results (Fig. 7) show that, in both groups of embryos sampled from each of the individual brooding females, levels of FAMTase transcript increased noticeably during development, and fell to near the basal level just before hatching.

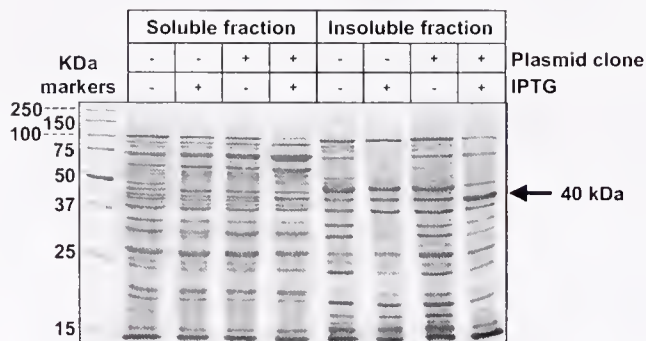


**Figure 3.** Expression of recombinant putative FAMTase. pTriplEx2 plasmids containing cDNA inserts encoding full-length FAMTase were grown in *E. coli* TOP10 F'. Protein expression was induced by addition of IPTG (see Methods). Extracts of *E. coli* prepared 5 h after induction with IPTG were analyzed for expression of recombinant protein by SDS-PAGE analysis (see Methods). Soluble and insoluble post-dialysis fractions are shown. The absence (-) or presence (+) of either IPTG (to induce recombinant protein expression when plasmid is present) or plasmid clone in the original *E. coli* culture conditions is indicated in the table above the gel image.

## Discussion

Here we report the isolation and characterization of a putative farnesoic acid methyl transferase cDNA from mandibular organs of the edible crab *Cancer pagurus*. Using a combination of a nested PCR-based approach and screening of a mandibular organ cDNA library, a 1216-bp cDNA was isolated that encodes an approximately 31-kDa protein molecule (Fig. 1). The putative FAMTase of *C. pagurus* exhibits a high degree of sequence similarity with those

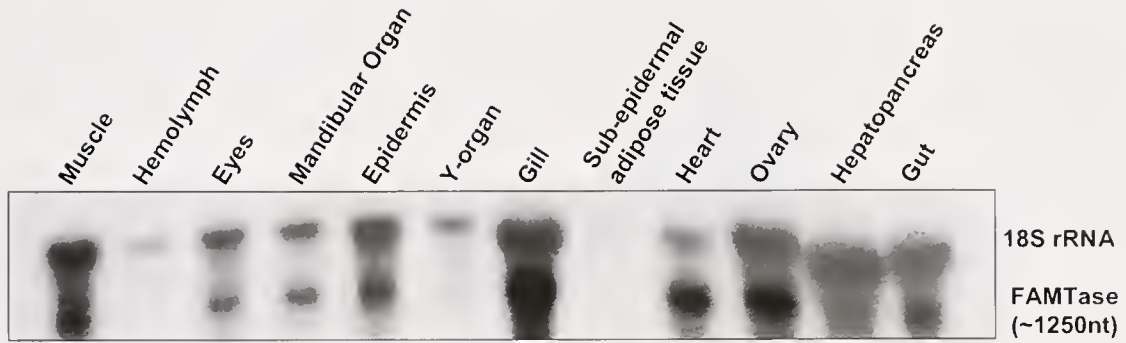


**Figure 4.** Northern blot analysis. Approximately 10  $\mu\text{g}$  of total RNA from a variety of *Cancer pagurus* tissues and two organ equivalents of Y-organ RNA was electrophoresed, blotted onto a nylon membrane, co-hybridized at 68 °C with a  $^{32}\text{P}$ -labeled-FAMTase probe and a mouse 18S rRNA probe, and washed at 45 °C (see Methods). The Northern blot shows the tissue distribution and size of the *C. pagurus* FAMTase transcript.

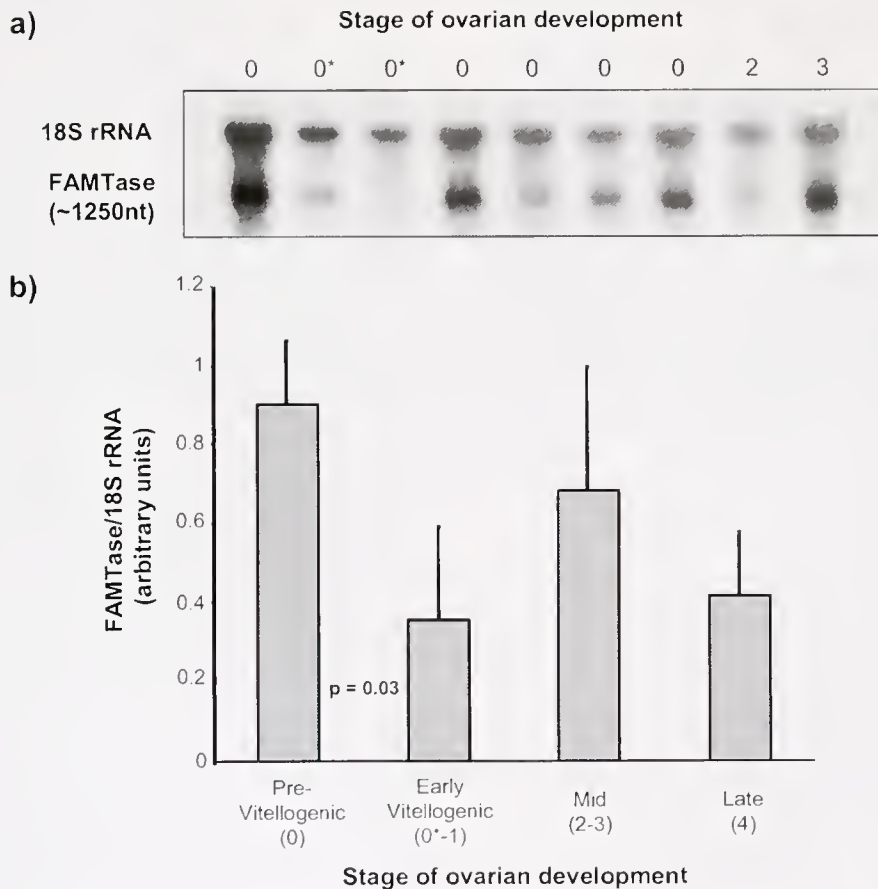


**Figure 5.** Profile of expression of putative FAMTase mRNA in mandibular organ throughout ovarian development in *Cancer pagurus*. (a) A typical Northern blot analysis of RNA isolated from mandibular organs from female crabs at different stages of ovarian development (0\* indicates stage 0 vitellogenic animals). Stage 4 (late vitellogenic stage) not shown. (b) Autoradiograms developed from Northern blotting experiments were analyzed by computerized densitometry. Images were acquired with a GS710 scanning densitometer (Bio-Rad) and analyzed with Quantity One software (Bio-Rad). The relative expression of FAMTase was normalized to the 18S rRNA signal to take account of unequal loading between samples in different lanes. Results are grouped as follows: pre-vitellogenic (stage 0), early vitellogenic (stage 0\* vitellogenic and stage 1), mid-stage vitellogenic (stages 2 and 3), and late vitellogenic (stage 4) animals. All values are mean  $\pm$  standard error of the mean for  $n = 3-6$  samples.

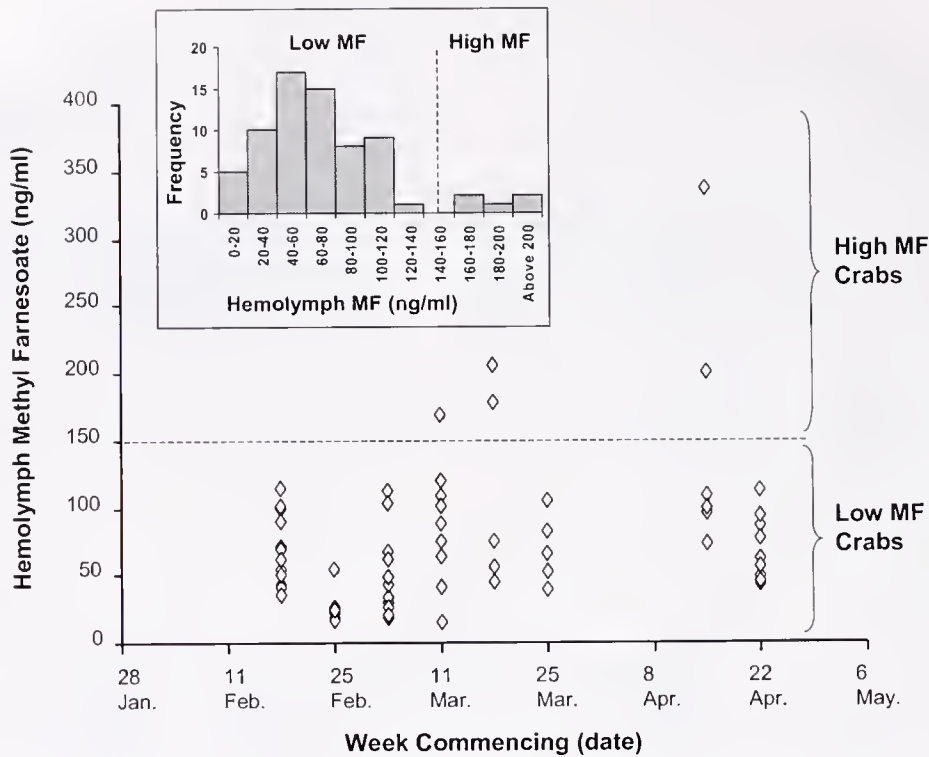


**Figure 6.** Titer of methyl farnesoate (MF) in the hemolymph of female specimens of *Cancer pagurus* measured during the spring of 2002. The hemolymph samples were processed and the hexane extracts were analyzed by adsorption HPLC, as described. The quantity of *all-trans*-MF was calculated by comparison of peak areas to those of 100-ng *cis, trans*-MF internal standard. *All-trans*-MF titers were plotted against date of sampling for each crab ( $n = 70$ ). The inset figure shows the frequency distribution of hemolymph MF titer. A threshold value of 150 ng/ml MF is indicated, between the groups of "low MF" or "high MF" crabs. Note: These crabs were a wild-caught non-synchronized population.

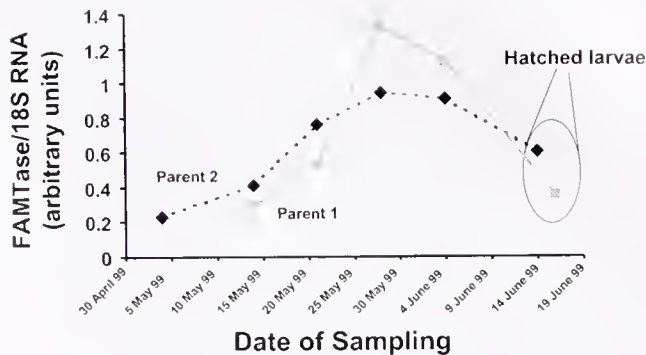


**Figure 7.** Expression of putative FAMTase in developing embryos and larvae of *Cancer pagurus*. Approximately 10  $\mu$ g of total RNA from whole embryos and larvae was electrophoresed, blotted onto a nylon membrane, co-hybridized at 68  $^{\circ}$ C with a  $^{32}$ P-labeled-FAMTase probe and a mouse 18S rRNA probe, and washed at 45  $^{\circ}$ C (see Methods). After densitometric analysis and normalization of the signal relative to that of rRNA, the expression levels were plotted against the time of year (date of sampling).

previously reported in other species of decapod crustaceans (lobster and shrimp sequences; Fig. 2). However, BLAST, PSI-BLAST, and MOTIF searches based on the putative farnesoic acid methyl transferases of *C. pagurus* or other crustaceans show no significant sequence similarity to any other *O*-methyl transferase enzymes, although, in common with most other members of the methyl transferase family, *S*-adenosyl-L-methionine is used as a cofactor. Analysis of the conceptually translated amino acid sequence of the FAMTase cDNA indicates that the native protein lacks a signal peptide. Further analysis suggests that a number of serine, threonine, and tyrosine side chains are potential substrates for phosphorylation. No other significant consensus sequences for other types of posttranslational modifications were found.

The apparent lack of signal peptide indicates that the putative FAMTase expressed in mandibular organ tissue is not secreted into the circulating hemolymph and may well be regulated by reversible phosphorylation of specific serine, threonine, or tyrosine residue side chains. In previous work, we have demonstrated that FAMTase activity in cytosolic extracts from *C. pagurus* mandibular organs can

be regulated by phosphorylation/dephosphorylation *in vitro*, suggesting that it may be a mechanism of regulation of enzyme activity *in vivo* (Wainwright and Rees, 2001). Indeed, other work has shown that treatment of mandibular organs with the peptide hormone MO-IH (mandibular organ-inhibiting hormone) leads to an increase in cAMP (Wainwright *et al.*, 1999). In turn, this may lead to changes in the phosphorylation state of FAMTase, thereby modulating the production of methyl farnesoate (MF).

To determine whether the protein characterized from the mandibular organ possesses FAMTase activity, the recombinant protein was expressed in *E. coli* as a LacZ fusion protein of approximately 40 kDa. On analysis, an approximately 40-kDa protein appeared in the inclusion body subcellular fractions; however, the inclusion body fractions had no detectable FAMTase activity. This observation has three possible explanations. First, the presence of the LacZ tag and linker sequence may interfere with the folding of the nascent protein and, thus, with the biological activity of the enzyme. Second, it may have been impossible to resolubilize the inclusion bodies *in vitro*. In this event, the activity of the FAMTase may have been disrupted. Third, previous attempts to stabilize FAMTase activity in extracts of cytosol during storage—and, thus, to facilitate traditional methods of enzyme purification and characterization—have resulted in almost complete loss of activity (G. Wainwright, unpubl. obs.). This sensitivity of FAMTase activity to its environment may also explain the lack of observed activity in the recombinantly expressed protein, under the experimental conditions described here. Similar difficulties have been encountered in expressing a functional recombinant FAMTase from the shrimp *Metapenaeus ensis*, when procedures largely equivalent to those described here were followed. In the *M. ensis* study, biological activity was eventually detected in a partially purified bacterial extract when a high-level expression system was employed (Silva Gunawardene *et al.*, 2002). It was surmised that only a tiny proportion of recombinant FAMTase may have been expressed in a correctly folded, active conformation in bacteria.

The distribution of the putative FAMTase among a variety of tissues was demonstrated by Northern blotting, which revealed a single transcript prevalent in muscle, eyes, mandibular organs, epidermis, gills, heart, ovary, hepatopancreas, and gut. Hemolymph did not exhibit a signal detectable by this method. Expression of the putative FAMTase transcript in a range of non-mandibular organ tissues in *C. pagurus*, described here, resembles that in *M. ensis* (Silva Gunawardene *et al.*, 2001, 2002), suggesting that FAMTase is quite broadly distributed in crustacean tissues. Perhaps the substrate specificity of the enzyme is not strict.

HPLC analysis of MF levels in the hemolymph of pre-vitellogenic and early vitellogenic crabs revealed a small number of individuals possessing “high MF” titers (Fig. 6).

These crabs were predominantly at a pre-vitellogenic stage of development. Interestingly, a hemolymph MF peak was previously reported to occur in early vitellogenic specimens (Wainwright *et al.*, 1996a) and, in agreement with this, we also observed a “high MF” titer in an early vitellogenic crab. These data suggest that, in contrast to what has previously been observed, elevated hemolymph MF may occur at different times during pre-vitellogenesis and early vitellogenesis in *C. pagurus*. As only 7% of pre- and early vitellogenic specimens were found to have high MF, we believe that the MF peak may be relatively short-lived. The transience of this peak (or peaks) would reduce the likelihood of it being observed in a wild-caught, non-synchronized population, and has presumably hindered its characterization to date.

We investigated, experimentally, whether the FAMTase also changes in expression in relation to ovarian development and the circulating levels of MF. Northern blot analysis of the expression of the putative FAMTase in mandibular organs from crabs at different stages of ovarian development showed that the relative expression of FAMTase, normalized using an 18S rRNA probe, was significantly higher in pre-vitellogenic crabs than in animals in the early stages of vitellogenesis (Fig. 5b). Since the peak in hemolymph MF appears to occur at some time during pre- or early vitellogenesis, it is apparent that FAMTase transcripts are elevated within the mandibular organ before, or during, the stages of development when the peaks in hemolymph MF titer occur. Consequently, the observed temporal pattern of peaks in FAMTase mRNA expression and hemolymph MF titer supports the view that our cloned gene product is indeed a FAMTase, although additional evidence is needed to confirm this.

The presence of FAMTase transcripts has also been demonstrated in the juvenile shrimp *M. ensis* (Silva Gunawardene *et al.*, 2001). Similarly, we detected the expression of a putative FAMTase in embryos of *C. pagurus*. The results showed that during embryonic development of *C. pagurus*, a peak in expression is observed during late embryogenesis, prior to hatching (Fig. 7). The significance of the role of FAMTase in biochemical and developmental processes in embryonic and juvenile crustaceans is as yet unclear, but it seems likely that, through regulation of production of MF, this enzyme will affect growth and developmental processes.

### Acknowledgments

We thank NERC (DEMA initiative) for financial support. We are grateful to Mr. N. Fullerton (Port Erin Marine Laboratory, University of Liverpool) for supplying samples of embryos and larval *C. pagurus* used in this work. We also thank Mr. A. Tweedale (University of Wales, Bangor, U.K.) and Mr. S. Corrigan (University of Liverpool, U.K.) for supply and maintenance of crabs, respectively.

## Literature Cited

- Belles, X. 1998.** Endocrine effectors in insect vitellogenesis. Pp. 71–90 in *Recent Advances in Arthropod Endocrinology*, G. M. Coast and S. G. Webster, eds. Cambridge University Press, Cambridge.
- Borst, D. W., and B. Tsukimura. 1991.** Quantification of methyl farnesoate levels in hemolymph by high-performance liquid chromatography. *J. Chromatogr.* **545**: 71–78.
- Borst, D. W., H. Laufer, M. Landau, E. S. Chang, W. A. Hertz, F. C. Baker, and D. A. Schooley. 1987.** Methyl farnesoate (MF) and its role in crustacean reproduction and development. *Insect Biochem.* **17**: 1123–1127.
- Borst, D. W., G. Wainwright, and H. H. Rees. 2002.** In vivo regulation of the mandibular organ in the edible crab, *Cancer pagurus*. *Proc. R. Soc. Lond. B* **269**: 483–490.
- Brent, R. 1994.** Protein expression. In *Current Protocols in Molecular Biology*, Vol. 12, Unit 16.5, V. B. Chanda, ed. John Wiley, New York.
- Charniaux-Cotton, H., and G. Payen. 1988.** Crustacean reproduction. Pp. 279–303 in *Endocrinology of Selected Invertebrate Types*, H. Laufer and R. G. H. Downer, eds. Alan R. Liss, New York.
- Clédon, P. 1985.** Cytological and experimental analysis of oocyte maturation and activation in the prawn, *Palaemon serratus* (Crustacé Decapodé Natantia). *C. R. Hebd. Seances Acad. Sci. Ser. D* **301**: 317–322.
- Davey, K. G. 1996.** Hormonal control of the follicular epithelium during vitellogenin uptake. *Invertebr. Reprod. Dev.* **30**: 249–254.
- Jo, Q.-T., H. Laufer, W. J. Biggers, and H. S. Kang. 1999.** Methyl farnesoate induced maturation in the spider crab, *Libinia emarginata*. *Invertebr. Reprod. Dev.* **36**: 79–85.
- Lanot, R., and P. Clédon. 1989.** Ecdysteroids and meiotic reinitiation in *Palaemon serratus* (Crustacea Decapoda Natantia) and in *Locusta migratoria* (Insecta Orthoptera): A comparative study. *Invertebr. Reprod. Dev.* **16**: 169–175.
- Laufer, H., D. W. Borst, F. C. Baker, C. Carrasco, M. Sinkus, C. C. Reuter, L. W. Tsai, and D. A. Schooley. 1987a.** Identification of a juvenile hormone-like compound in a crustacean. *Science* **235**: 202–205.
- Laufer, H., M. Landau, E. Homola, and D. W. Borst. 1987b.** Methyl farnesoate: its site of synthesis and regulation of secretion in a juvenile crustacean. *Insect Biochem.* **17**: 1129–1131.
- Laufer, H., W. J. Biggers, and J. S. B. Ahl. 1998.** Stimulation of ovarian maturation in the crayfish *Procambarus clarkii* by methyl farnesoate. *Gen. Comp. Endocrinol.* **111**: 113–118.
- Reddy, P. S., and R. Ramamurthi. 1998.** Methyl farnesoate stimulates ovarian maturation in the freshwater crab *Oziotelphusa senex senex* Fabricius. *Curr. Sci.* **74**: 68–70.
- Riddiford, L. M. 1994.** Cellular and molecular actions of juvenile hormone. I. General considerations and premetamorphic actions. *Adv. Insect Physiol.* **24**: 213–274.
- Rodriguez, E. M., L. S. Lopez Greco, D. A. Medesani, H. Laufer, and M. Fingerman. 2002.** Effect of methyl farnesoate, alone and in combination with other hormones, on ovarian growth of the red swamp crayfish, *Procambarus clarkii*, during vitellogenesis. *Gen. Comp. Endocrinol.* **125**: 34–40.
- Silva Gunawardene, Y. I. N., B. K. C. Chow, J.-G. He, and S.-M. Chan. 2001.** The shrimp FAMEt cDNA is encoded for a putative enzyme involved in the methylfarnesoate (MF) biosynthetic pathway and is temporarily expressed in the eyestalk of different sexes. *Insect Biochem. Mol. Biol.* **31**: 1115–1124.
- Silva Gunawardene, Y. I. N., S. S. Tobe, W. G. Bendena, B. K. C. Chow, K. J. Yagi, and S.-M. Chan. 2002.** Function and cellular localization of farnesoic acid O-methyltransferase (FAMTase) in the shrimp, *Metapenaeus ensis*. *Eur. J. Biochem.* **269**: 3587–3595.
- Smith, P. A., A. S. Clare, H. H. Rees, M. C. Prescott, G. Wainwright, and M. C. Thorndyke. 2000.** Identification of methyl farnesoate in the cypris larvae of the barnacle, *Balanus amphitrite*, and its role as a juvenile hormone. *Insect Biochem. Mol. Biol.* **30**: 885–890.
- Takeuchi, H., J.-H. Chen, D. R. O'Reilly, H. H. Rees, and P. C. Turner. 2000.** Regulation of ecdysteroid signalling: molecular cloning, characterization and expression of 3-dehydroecdysone 3 $\alpha$ -reductase, a novel eukaryotic member of the short-chain dehydrogenases/reductases superfamily from the cotton leafworm, *Spodoptera littoralis*. *Biochem. J.* **349**: 239–245.
- Tsukimura, B., and F. I. Kamemoto. 1991.** In vitro stimulation of oocytes by presumptive mandibular organ secretions in the shrimp, *Penaeus vannamei*. *Aquaculture* **92**: 59–66.
- Wainwright, G. 1995.** Hormonal control of ovarian development in the edible crab, *Cancer pagurus*. Ph.D. Thesis, University of Liverpool, UK.
- Wainwright, G., and H. H. Rees. 2001.** Hormonal control of reproductive development in crustaceans. Pp. 71–84 in *Environment and Animal Development: Genes, Life Histories and Plasticity*, D. Atkinson and M. C. Thorndyke, eds. BIOS Scientific, Oxford.
- Wainwright, G., M. C. Prescott, S. G. Webster, and H. H. Rees. 1996a.** Mass spectrometric determination of methyl farnesoate profiles and correlation with ovarian development in the edible crab, *Cancer pagurus*. *J. Mass Spectrom.* **31**: 1338–1344.
- Wainwright, G., S. G. Webster, M. C. Wilkinson, J. S. Chung, and H. H. Rees. 1996b.** Structure and significance of mandibular organ-inhibiting hormone in the crab, *Cancer pagurus*: involvement in multi-hormonal regulation of growth and reproduction. *J. Biol. Chem.* **271**: 12749–12754.
- Wainwright, G., S. G. Webster, and H. H. Rees. 1998.** Neuropeptide regulation of biosynthesis of the juvenoid, methyl farnesoate, in the edible crab, *Cancer pagurus*. *Biochem. J.* **334**: 651–657.
- Wainwright, G., S. G. Webster, and H. H. Rees. 1999.** Involvement of second messenger systems in mandibular organ-inhibiting hormone-mediated inhibition of methyl farnesoate biosynthesis in mandibular organs of the edible crab, *Cancer pagurus*. *Mol. Cell. Endocrinol.* **154**: 55–62.
- Warner, G. F. 1977.** *The Biology of Crabs*. Elek Science, London.

## Determinate Growth and Modularity in a Gorgonian Octocoral

HOWARD R. LASKER\*, MICHAEL L. BOLLER<sup>1</sup>, JOHN CASTANARO,  
AND JUAN ARMANDO SÁNCHEZ<sup>2</sup>

*Department of Biological Sciences, 109 Cooke Hall, University at Buffalo  
(The State University of New York), Buffalo, New York 14260*

**Abstract.** Growth rates of branches of colonies of the gorgonian *Pseudopterogorgia elisabethae* were monitored for 2 years on a reef at San Salvador Island, Bahamas. Images of 261 colonies were made at 6-month intervals and colony and branch growth analyzed. Branch growth rates differed between colonies and between the time intervals in which the measurements were made. Colonies developed a plumelike morphology through a pattern of branch origination and determinate growth in which branch growth rates were greatest at the time the branch originated and branches seldom grew beyond a length of 8 cm. A small number of branches had greater growth rates, did not stop growing, and were sites for the origination of subsequent “generations” of branches. The rate of branch origination decreased with each generation of branching, and branch growth rates were lower on larger colonies, leading to determinate colony growth. Although colonial invertebrates like *P. elisabethae* grow through the addition of polyps, branches behave as modules with determinate growth. Colony form and size is generated by the iterative addition of branches.

### Introduction

Taxa ranging from algae to higher plants, and from cnidarians to protochordates, grow through the iterated replication of individual modules to form large, integrated individuals or colonies (Jackson *et al.*, 1985). Such modular organisms are ubiquitous and are often dominant members

of a wide variety of animal and plant communities (Jackson, 1977; Hughes, 1989). Although the concept of modularity is applicable to many groups, the basic unit of replication, the module, is sometimes difficult to identify. This is perhaps best illustrated in plants where meristems, leaves, branches, and leaf-branch systems can each be characterized as the module from which the individual is constructed (Harper and White, 1974). Many of the same difficulties exist in the study of colonial invertebrates that grow through the iterative replication of polyps and zooids. The polyps of a coral—or the zooids of a tunicate—are undoubtedly “modules,” but in many taxa these modules are then organized into structures that are themselves iteratively replicated, such as the branches of gorgonians or the inhalant-exhalant systems of colonial tunicates. Colony growth and development, known as astogeny, can be characterized by the replication of these larger units as readily as by the demography of polyps and zooids (Lasker and Sánchez, 2002; Rinkevich, 2002). Although the history of colony growth can be portrayed using either polyps or branches, it is unclear which level of organization should be studied to understand the processes controlling colony size and form.

The construction of colonies from modules is closely associated with indeterminate growth, that is, continuous growth throughout an organism’s lifetime. Indeed, modular organisms are known to live for centuries and to attain sizes of tens of meters. The continuous production and addition of individuals leads to colonies that are remarkably variable in size and form. This mode of growth is central to a colony’s ability to survive and recover from both natural and anthropogenic disturbances (Done, 1987, 1988). However, modular growth does not necessarily lead to indeterminate growth. Many species can be characterized by a distinct colony form and a maximum colony size. The attribution of

Received 30 September 2002; accepted 3 September 2003.

\* To whom correspondence should be addressed. E-mail: hlasker@buffalo.edu

<sup>1</sup> Current address: Department of Biological Sciences, University of Rhode Island, Kingston, RI 02881.

<sup>2</sup> Current address: Department of Systematic Biology, National Museum of Natural History, Smithsonian Institution, Washington, DC 20013-7012.

a definable colony form and maximum size suggests that growth of the modules is in some fashion constrained, which suggests determinate growth.

The focus of the current study is to identify the pattern of colony and branch growth among colonies of the Caribbean gorgonian octocoral *Pseudopterogorgia elisabethae*. We show that branches on these colonies behave as modules, with a developmental sequence that leads to side branches of similar length throughout the colony. We show how both branches and entire colonies of *Pseudopterogorgia elisabethae* exhibit determinate growth.

### Materials and Methods

A colony of *Pseudopterogorgia elisabethae* starts developing when a planula larva settles and metamorphoses into a polyp. A single, vertical branch is produced as polyps are added alternately on both sides of the tip, thereby extending the branch (Fig. 1A). Formation of new branches occurs several centimeters below the branch tip (Figs. 1B and 2A). This pattern is apparent in Figure 2A, in which branches 32 through 35 developed on branch 1 between December 1998 and July 1999. Each new branch then grows in the same fashion as the original branch, and some give rise to additional branches (Fig. 1). This pattern of side branches themselves becoming sources of new side branches is illustrated by the growth of branches 2 and 5 in Figure 2A.

This mode of branching and growth in *P. elisabethae*

leads, eventually, to plume-like colonies that characteristically have a maximum height of less than 1 m (Fig. 2B). The pattern of branching creates a hierarchy among the branches, and we characterize branch order using an ordering system that we term generational ordering (Lasker and Sánchez, 2002; Sánchez, 2002; Sánchez *et al.*, 2003), in which branches are ranked on the basis of the number of branching events away from the original, primary branch (Fig. 1; Lasker and Sánchez, 2002). The original branch has a rank of 1; each branch that it produces is assigned a rank of 2; branches that grow off of the secondary branches are assigned a rank of 3; and so on. Each branch tip is assigned a rank, and the rank of any single branch remains constant. While having some similarities to ordering systems previously adapted to colonies (*i.e.*, Brazeau and Lasker, 1988), generational ordering has very different properties (Sánchez *et al.*, 2003). We also make a distinction between branches that give rise to additional branches, termed mother branches, and those from which no additional branches originate, termed daughter branches. Since there are no other morphological differences between mother and daughter branches, the distinction is based solely on the presence of side branches. The terminology is homologous to "sources and tributaries" used previously (Brazeau and Lasker, 1988; Lasker and Sánchez, 2002), but has the advantage of portraying the temporal relationships among the branches (Sánchez, 2002).

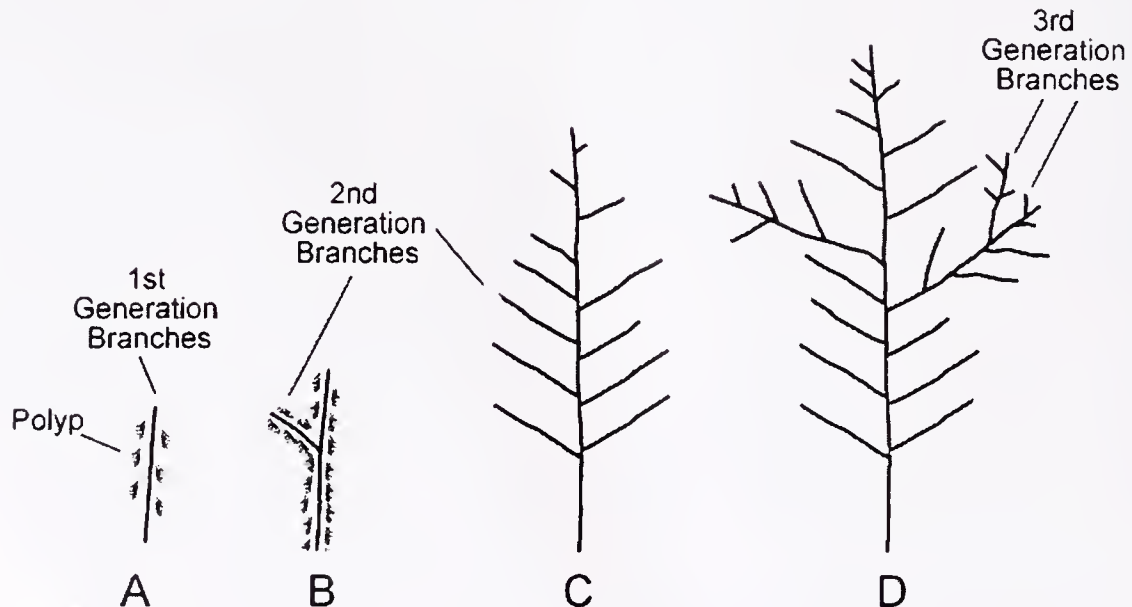


**Figure 1.** Colony development of *Pseudopterogorgia elisabethae*. (A) Initial development and subsequent branch elongation occurs through the addition of polyps at the branch tip. (B) The primary, "first generation" branch generates a side branch subapically (the second generation). (C) The colony continues to add a second generation of branches as the primary branch grows. (D) Two of the second-generation branches give rise to a third generation of branches. Polyps are no longer depicted in C and D. (After fig. 5, Lasker and Sánchez, 2002).

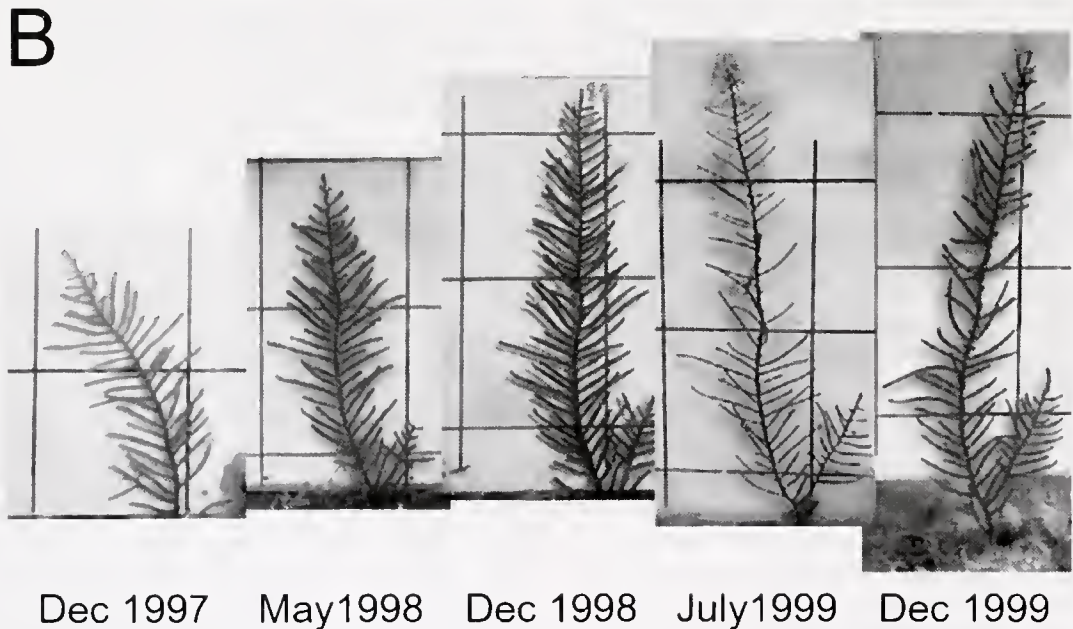
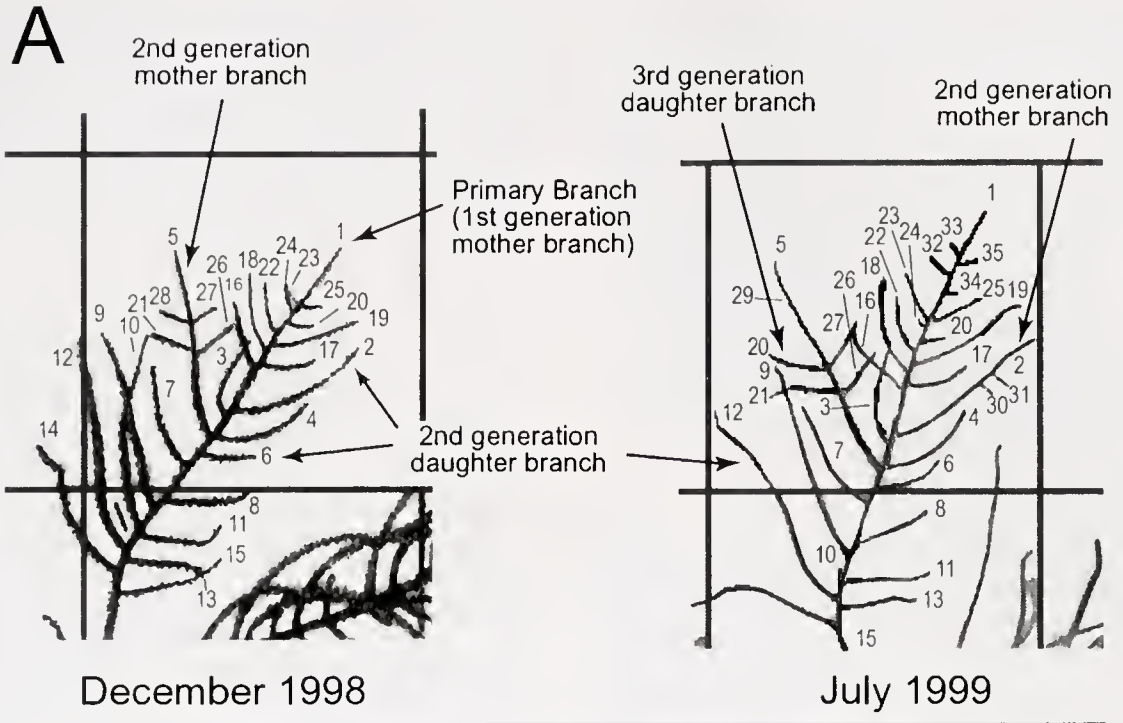


**Figure 2.** (A) Close-up photographs of a *Pseudopterogorgia elisabethae* branch in December 1998 and July 1999 showing branch growth and the system for numbering branches, which enabled successive measurements. Representative branches are labeled on the basis of type (mother, daughter) and order. Note that only the most distal (*i.e.*, youngest) daughter branches grew during the interval between photos, and that mother branches continued to extend and to branch regardless of position. Branches 30–35 originated, and 10 and 15 died, during the interval between photographs. Grid lines in the photos are 10 cm apart. See text for explanation of branch order. (B) Photographs of a *P. elisabethae* colony from San Salvador, Bahamas, taken over a 2-year period. All of the photographs have been normalized to the same scale, and the grid is 10 × 10 cm.

To follow the growth of individual colonies and branches, we found and tagged 261 colonies of *P. elisabethae* along three transects totaling 70 m<sup>2</sup> of substratum located at depths of 12–15 m on San Salvador, Bahamas. The colonies were photographed in place at roughly 6-month intervals between December 1997 and December 1999; and the growth of individual branches was determined by measuring changes in branch lengths through sequences of images, as in Figure 2. Branch generation and type (*i.e.*, mother vs. daughter) were assessed from the images, and the number of branches that originated in each time interval was recorded as well as the branches they developed from. Colony height was determined from either the images or from direct measurements in the field.

#### *Image analysis and branch measurements*

*Pseudopterogorgia elisabethae* forms colonies with most side branches oriented in a single plane. Therefore, readily measured images could be obtained by positioning colonies between a grid 10 cm × 10 cm and a clear acrylic plastic cover, which held the branches against the grid (Fig. 2). If a colony was small (<20 cm height), the entire structure was photographed; if it was large, an arbitrarily selected branch containing 15–25 branches was followed. In December 1997, photographs were taken with a Nikonos V underwater camera and Kodachrome 200 film. Those images were later digitized and converted to TIFF. In subsequent observations, photographs were taken at a resolution of 640 × 480 bits with a Sony Mavica digital camera (either MVC-7 or MVC-83) in an underwater housing. Distortion created when photographs were shot at a slight angle from the perpendicular was corrected in Photoshop (Version 4.0, Adobe). A 250 × 250 pixel grid was overlaid on the image, and the shape of the original image was adjusted with the free transform function of the program until the 10-cm grid in the photograph matched the 250-pixel grid.

The length of each branch in the photograph was measured with the program SCION (Scion Corporation, Frederick, MD). Although the program measures distance with high accuracy, variation is introduced into the measurements by several steps in the measurement process. First, although the tip of a branch is easily discerned in the images, it was also necessary to define its point of origin. We chose, as the point, the intersection of the branch with the line running along the middle of its mother branch, and that point had to be identified in each image. Second, the branches are curvilinear structures and were measured as segmented lines. Small differences in measurements are created by variation in the number and placement of those line segments. To assess the magnitude of measurement variation, three different observers measured each of 130 branches. The between-measurement standard deviation was 0.3 cm.

When an entire colony was included in the image, height was measured as the length of the longest branch. If the entire colony was not included in the image, height (length of the longest branch) was measured in the field with a flexible tape measure, to the nearest 0.1 cm. For purposes of analysis, colony heights were categorized into six size classes: 0.1–10.0 cm, 10.1–20.0 cm, 20.1–30.0 cm, 30.1–40.0 cm, 40.1–50.0 cm, >50.1 cm.

#### *Growth rates*

Over the 2 years, 261 colonies with 5870 branches were monitored, and 23,478 individual length measurements were made. Growth rate—the difference between successive measurements—was then determined, and those values were extrapolated to annual rates based on the number of months between the measurements. Measurement error for growth rates was 1.2 cm y<sup>-1</sup>, which combines the effects of extrapolation of the 6-month intervals to 1 year and the additive effect of variance in each of the two measurements of colony length. The individual growth measurements were categorized by the time interval in which the measurement was made and by branch age, based on when the branch originated. Branch ages were categorized into one of five classes: <6, 6–12, 13–18, 19–24 months, or present at the start of monitoring. In some analyses, we also designated branches that originated during the study as “new” branches. This latter category distinguished branches that were less than 2 years old from those branches present at the start of the study. Each of the growth rates was also classified according to the branch’s generation order and branch type (mother or daughter).

#### *Negative growth rates*

To reduce the effects of grazing on the analyses, cases in which growth was <0.0 were dropped from the data set. By rejecting these cases of negative growth, the most severe effects of grazing were eliminated. Grazing also may have reduced the observed growth of some branches with positive growth rates, but since scars from grazing heal rapidly, such branches could not be identified. Rejecting the negative values may have inflated the calculated growth rates of branches that were otherwise not growing. Since the measurement error was 1.2 cm y<sup>-1</sup>, some branches that had not grown would, through measurement error alone, have small negative growth rates, and some would have small positive growth rates. Exclusion of branches with growth less than 0.0 cm y<sup>-1</sup> would have eliminated the underestimates of the zero growth branches but not the overestimates.

#### *Statistical analyses*

Growth rates were compared by analysis of variance (ANOVA, functions UNIANOVA and MANOVA, SPSS

version 10.1). In those analyses, branches were classified using the five independent variables: branch order, branch type (mother or daughter), branch age, time interval in which the measurement was made, and colony height. Branch length was also included as a covariate in some of the analyses. Due to the size and complexity of the data set, it was impossible to examine all of the effects in a single analysis. Our strategy was to conduct multiple tests, each including the greatest number of variables possible, and to use Bonferroni corrections to significance testing when multiple tests were conducted on the same data.

*Between-colony variation and time interval effects.* The same branches were measured multiple times, so a repeated-measures ANOVA was the most appropriate design. However, because of the large number of branches nested within colonies, an ANOVA that included all five categorical variables could not be computed within a single repeated-measures design. We therefore conducted a repeated-measures ANOVA that tested for the random effects of branches within colonies and time interval (the 6-month interval in which the measurement was made). The effects of inter-colony variation were again examined in an ANOVA of the growth of branches that were less than 6 months old (*i.e.*, growth during the time interval in which the branch had originated). Growth rates in this analysis were compared with respect to colony and time interval (Table 1A). A simple two-way ANOVA was used for this analysis, as data from no single branch was included in more than one observation in this analysis.

*Between-colony variation and branch age.* Next, a series of analyses that simultaneously considered colony and age of the branch were conducted (Table 1B through 1E). The analysis was repeated for each of the four time intervals, which again led to a single branch being used only once in each of the analyses.

*Multi-way ANOVA.* Finally, a multi-way ANOVA that included all of the positive growth rates was conducted using branch type, branch order, branch age, and colony height as the independent variables (Table 2).

All of the ANOVA results are reported for untransformed data. Growth rates were heteroscedastic even after a variety of transforms (Levene's, Bartlett's or  $F_{\max}$  tests of homogeneity of variances, depending on the structure of the data set). ANOVA results were almost always concordant with a parallel ANOVA using the rank transformed data and with nonparametric analyses, which could only consider a single factor at a time.

## Results

### General observations

Growth of *Pseudopterogorgia elisabethae* colonies was not indeterminate. Branches exhibited a distinct developmental cycle in which they arose, grew rapidly, and then

grew at dramatically slower rates. This is evident in Figure 2A, where the rapid extension of daughter branches (*e.g.*, branches 22, 23, and 24) near the tip of the primary branch is in marked contrast to that of branches closer to the base, many of which exhibited no apparent growth (11, 13, 14). A simplified characterization of the results is that mother branches grew faster than daughters, new branches grew faster than those that were more than 6 months old (Fig. 3), and branches on small colonies had higher growth rates than those on large colonies (Fig. 4A).

The measured rates of branch growth were highly variable, ranging from negative values to  $17.8 \text{ cm y}^{-1}$ . Large negative values were often associated with almost total branch loss, as in the case of branch 10 in Figure 2A; this colony, for instance, lost two branches between December 1998 and July 1999. The presence of some uncharacteristically short daughter branches that did not grow during the study suggested that severely damaged branches did not grow further. When cases of negative growth rates were eliminated, the data set was reduced to 8341 individual growth rate measurements.

### Statistical analyses of branch growth

*Between-colony variation and time-interval effects.* The repeated-measures analysis of variance was restricted to the 608 branches for which measurements were available from

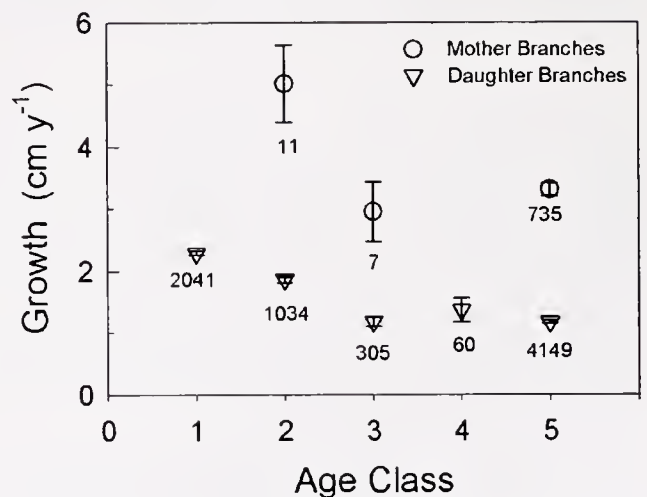


**Figure 3.** Branch growth rates for *Pseudopterogorgia elisabethae* colonies from San Salvador, Bahamas (mean  $\pm$  standard error) plotted as a function of branch age class. Branches in age classes 1 through 4 originated during the course of the monitoring: class 1, 6 months; 2, 6–12 months; 3, 12–18 months; 4, 18–24 months. Branches in class 5 were present at the start of the 2-year monitoring program. Since mother and daughter branches cannot be distinguished when they originate, there are no age-class 1 (<6 months old) mother branches. The data set also did not include any age-class 4 (18–24 months old) mother branches. Only non-negative growth rates were used in the analysis, and the number of measurements for each class is indicated above or below the error bar.

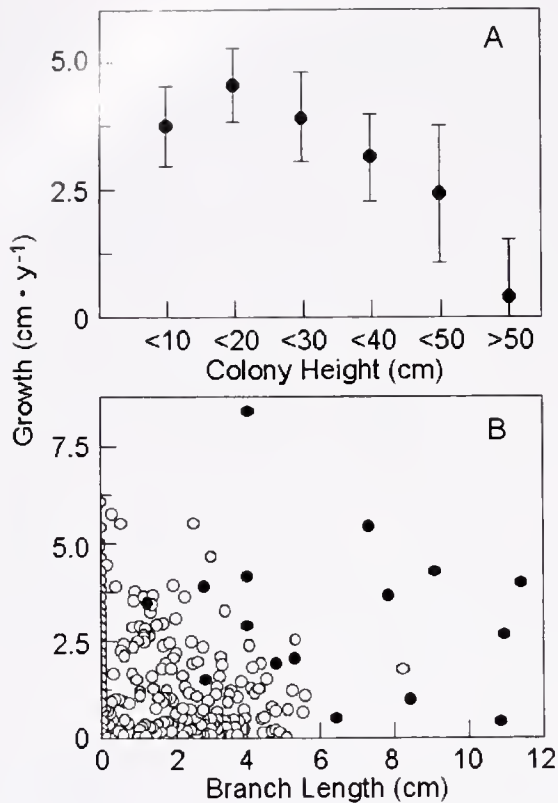


**Figure 4.** Growth rates of *Pseudopterogorgia elisabethae* branches from San Salvador, Bahamas, as a function of colony height (A) and branch length (B). Values in (A) are means  $\pm$  standard error. (B)  $\circ$  denotes daughter branches, and  $\bullet$  denotes mother branches. The figure presents a random subset of the over 10,000 points.

all four time intervals. (Branches were excluded from this analysis if they did not originate until later in the experiment, were lost during the experiment, or had a single interval in which the measurement could not be made due to poor photo quality.) The analysis identified significant effects of both time interval and colony, as well as an interaction of time interval by colony (all effects,  $P < 0.001$ ). The same result was obtained when the analysis was restricted to the middle two time intervals, thereby allowing the inclusion of a total of 2496 branches.

When the growth rates of newly originated branches were analyzed separately, growth rates differed among colonies, and there was also an interaction between colony and time interval, but no significant effect of time interval alone (Table 1A). These analyses indicate that the growth rates differed between colonies, and that the magnitude of differences between colonies varied between time intervals, but there was no simple additive difference in variance based on time interval alone. For instance, one colony may have had its highest growth rates in one time interval, while a different colony had its lowest growth in the same time interval.

*Between-colony variation and branch age.* Despite the

effects of colony and time interval on growth, significant fixed effects were detected when the data were partitioned into subsets based on branch type. Separate analyses of the growth of daughter branches during each of the time intervals (Table 1, B–E) identified a significant effect of branch age in three of the four time periods (C–E). There were significant interactions between colony and branch age in all four intervals, and significant colony effects in two of the time intervals (Table 1, D and E).

*Multi-way ANOVA.* The effects of branch type, generation, age, and colony height were compared in this large analysis (Table 2). Branch growth rates were significantly affected by branch type (growth rates of mother branches  $>$  daughter branches, Fig. 3), branch age (younger  $>$  older, Fig. 3), and colony height (short  $>$  tall, Fig. 4A). In addition, there were significant interactions between branch type and age, branch type and colony height, and in the three-way interaction between branch type, order, and colony height. The significant interactions reflect the nonlinearity of the patterns seen in Figures 3 and 4; that is, the effects of the different factors were not additive.

Variation between colonies was differentiated in these analyses due to the computational limits of incorporating colonies as a fourth independent variable with 260 degrees of freedom (*i.e.*, 261 colonies). Branches from the different colonies were represented in almost all of the combinations of branch type and age, which should have reduced the confounding effects of not incorporating colony identity as an independent variable. Time interval was not tested in these analyses because it is confounded with the age of the branches (*i.e.*, the later intervals for a given branch also record the growth of an older branch). Generation, which was marginally not significant, was confounded with branch type because first-generation branches are by definition mother branches. When daughter and mother branches were analyzed separately in an analysis that was otherwise identical to that in Table 2, generation was not a significant factor ( $P = 0.52$  and  $0.40$ , respectively).

The effect of branch age on growth rates of the new branches is underestimated in Figure 3 because it assumes that new branches grew over a 6-month period. If we assume that branches originated continuously over the 6-month interval, then the average age of a new branch would be 3 months, and the mean growth rate would be twice that reported in Figure 3. Furthermore, as noted in Materials and Methods, excluding negative values from the analysis has the effect of slightly inflating growth estimates when the true value is near zero. When cases of negative growth were included, older ( $>12$  mo) daughter branches had growth rates close to zero.

With branch length as a covariate, growth rates of daughter branches were analyzed separately for the effects of branch age. Both increasing age and increasing branch length (Fig. 4B) had significant negative effects on branch

Table 1

Analysis of variance tables testing colony and temporal variation in growth rates of *Pseudopterogorgia elisabethae* at San Salvador, Bahamas

Source of variation		df	Mean square	F	P <sup>1</sup>
A. Growth of newly originated branches during their first 6 months over four successive time intervals					
<b>COLONY</b>		166.0	5.27	1.52	<b>0.002</b>
	Error	207.4	3.46		
TIME INTERVAL		3.0	6.25	2.11	0.099
	Error	343.3	2.96		
<b>COLONY × TIME INTERVAL</b>		159.0	3.87	1.93	<b>0.000</b>
	Error	1702.0	2.00		
B. Growth of daughter branches as a function of branch age Dec 1997–June 1998					
COLONY		62.0	7.76	1.59	0.075
	Error	33.0	4.88		
AGE <sup>2</sup>		1.0	7.55	2.29	0.135
	Error	68.9	3.30		
<b>COLONY × AGE</b>		39.0	4.34	2.27	<b>&lt;0.001</b>
	Error	790.0	1.91		
C. Growth of daughter branches as a function of branch age June 1998–Dec 1998					
COLONY		125.0	5.49	1.48	0.015
	Error	120.3	3.71		
AGE		2.0	34.82	14.16	<b>&lt;0.001</b>
	Error	193.0	2.46		
<b>COLONY × AGE</b>		121.0	3.68	3.36	<b>&lt;0.001</b>
	Error	2131.0	1.10		
D. Growth of daughter branches as a function of branch age Dec 1998–July 1999					
<b>COLONY</b>		153.0	5.48	2.12	<b>&lt;0.001</b>
	Error	231.7	2.58		
AGE		3.0	85.86	40.23	<b>&lt;0.001</b>
	Error	435.8	2.13		
<b>COLONY × AGE</b>		199.0	2.75	1.87	<b>&lt;0.001</b>
	Error	2248.0	1.47		
E. Growth of daughter branches as a function of branch age July 1999–Dec 2000					
<b>COLONY</b>		122.0	6.08	2.13	<b>&lt;0.001</b>
	Error	258.6	2.86		
AGE		4.0	26.77	10.73	<b>&lt;0.001</b>
	Error	373.9	2.49		
<b>COLONY × AGE</b>		195.0	3.28	2.10	<b>&lt;0.001</b>
	Error	1303.0	1.56		

<sup>1</sup> Significant *P* values listed in bold. Since some of the same branches are tested in each of the time intervals (B–E), Bonferroni correction of significance levels would suggest that *P* = 0.0125 be used as the highest significant *P* value, *F* = Mean square/Error mean square.

<sup>2</sup> Age classes were 0–6, 7–12, 13–18, 19–24, and >24 months. The number of classes present increased as the experiment progressed, those branches aged, and new branches originated.

growth rates. However, the two variables are confounded, and cases of long, young branches do not exist, so determining whether age or branch size is the functional factor is difficult.

#### Patterns of branch and colony growth

*Mother-daughter comparisons.* Mother branches were not identified until they had produced a side branch, but their growth rates suggest that their growth behavior changes before their daughter branches are produced. A

retrospective analysis of branches that eventually became mother branches indicates that they had higher growth rates than daughter branches 1 year prior to the start of branching (Fig. 5). During the 6 months in which branching was first observed, these branches had the greatest growth rates of any of the groups of branches that we distinguished. In contrast to the mother branches, daughter branches exhibited decreasing growth rates as they aged and elongated (Fig. 5). After a year of growth, rates were near 1 cm y<sup>-1</sup>, and when negative growth is incorporated into the analysis, the rates were not significantly different from zero. The

Table 2

Analysis of variance of branch growth rates as a function of branch and colony characteristics

Source of variation	df	Mean square	F	P
<b>Branch age</b>	<b>4</b>	<b>11.95</b>	<b>5.06</b>	<b>0.000</b>
Generation	3	6.05	2.56	0.053
<b>Branch type</b>	<b>1</b>	<b>68.44</b>	<b>29.00</b>	<b>0.000</b>
<b>Colony height</b>	<b>5</b>	<b>13.14</b>	<b>5.57</b>	<b>0.000</b>
Branch age × Generation	7	2.26	0.96	0.459
<b>Branch age × Branch type</b>	<b>4</b>	<b>16.14</b>	<b>6.84</b>	<b>0.000</b>
Order × Branch type	2	7.01	2.97	0.051
Branch age × Generation × Branch type	3	2.59	1.10	0.349
Branch age × Colony height	18	1.42	0.60	0.902
<b>Generation × Colony height</b>	<b>15</b>	<b>5.96</b>	<b>2.52</b>	<b>0.001</b>
Branch age × Generation × Colony height	21	3.25	1.38	0.117
<b>Branch type × Colony height</b>	<b>5</b>	<b>6.16</b>	<b>2.61</b>	<b>0.023</b>
Branch age × Branch type × Colony height	5	2.43	1.03	0.399
<b>Generation × Branch type × Colony height</b>	<b>5</b>	<b>7.45</b>	<b>3.16</b>	<b>0.008</b>
Error	8236	2.36		
Total	8335			

Significant *P* values listed in hold. *F* = Mean square/Error Mean Square.

different growth trajectories for the two branch types, perhaps from their origination, also suggests that the estimated growth rates of daughter branches may have been inflated by the behavior of mother branches that had not started branching and were thus misidentified.

The existence of a determinate developmental sequence in the growth of daughter branches is again suggested by the distribution of branch sizes observed at San Salvador. If branch growth were indeterminate, then continuing growth of branches on a colony would have led to a steady accumulation of ever-larger branches, as well as to the presence of many branches with intermediate branch length. Most branches ceased growing when they reached a length of 5–8 cm (Figs. 4B and 6B). With time, colonies added height and new branches at their distal end (Fig. 2B), but colonies did not widen continuously at their base. The development of a plumelike morphology requires that the side elements of the plume show determinate growth. The few branches that became larger (Fig. 6B) were mother branches.

*Colony size.* Branch formation and extension control both the form and size of the colony, and colony size was also subject to determinate growth. Branching did not occur indefinitely among *P. elisabethae* branches. Colonies almost never had more than fourth-order branches (we have observed only one colony with fifth-order branches), and the number of branches produced by mother branches decreased with branch order. Branch origination rates were 4.7 (standard error = 0.2) new branches for each 6-month

monitoring period on first-order branches, and 3.2 (0.2) and 2.4 (0.5) on second- and third-order branches, respectively. Origination rates were significantly different between branch generations (two-way analysis of variance of natural-log-transformed data,  $F_{2,8,9} = 15.9$ ,  $P = 0.001$ ). Neither the time interval nor interaction effects were significant ( $P = 0.1$  and  $0.29$ , respectively). Branch growth also declined as a function of colony height independent of branch generation (Fig. 4A). The net effect of these processes was that, on San Salvador, colonies seldom exceeded 50 cm in height (Fig. 6A), and all of the monitored colonies were less than 70 cm in height.

## Discussion

The results lead to conclusions in three interrelated areas, all of which suggest that *Pseudopterogorgia elisabethae*, and by extension other gorgonians, have body plans that are under greater developmental control than generally considered in discussions of modularity. First, although colonies are built through the iterative generation of polyps, both the branch and the whole colony behave as integrated units. Second, the tempo and mode of branch origination and growth generate branches and colonies of finite size, as well as predictable form. Third, branches on *P. elisabethae* colonies appear to fall into two distinct developmental categories.

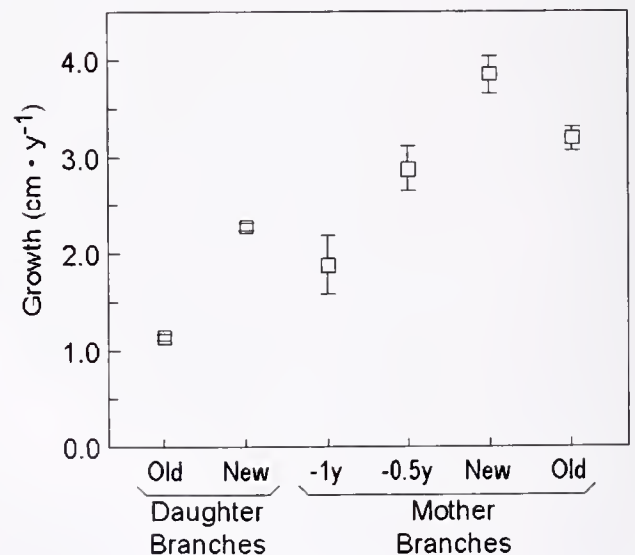
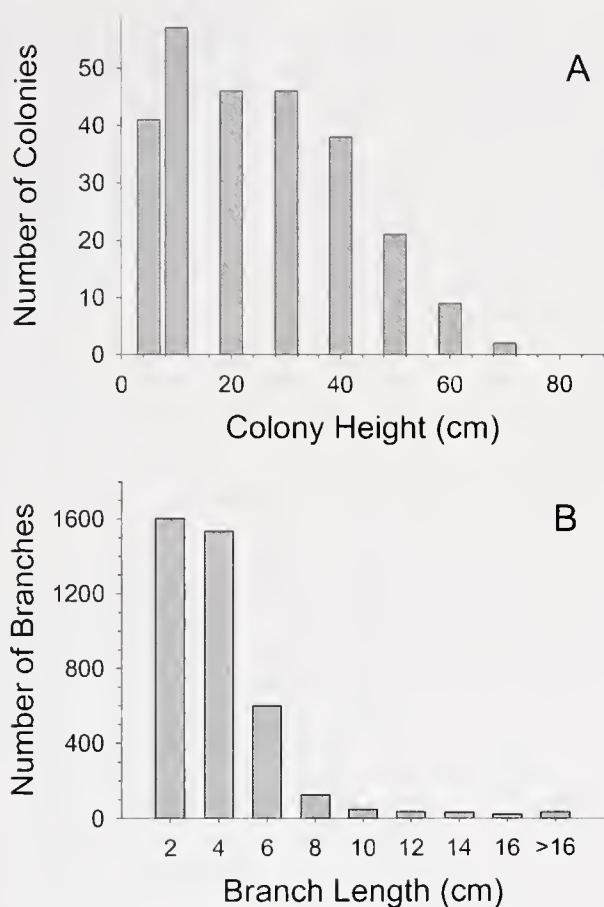


Figure 5. Growth of *Pseudopterogorgia elisabethae* branches from San Salvador, Bahamas. Daughter branches were divided into those present at the start of observations (old daughter) and those that were <0.5 y (new daughter). Branches that transformed from daughter to mother branches are included as mother branches, and their growth rates at 1 y and 0.5 y before they started branching, are denoted as -1 and -0.5 y, respectively. "New" mother branches started branching during the 6 months in which the growth rate was determined. Branches that were already mother branches at the start of the observations are labeled "Old." All values are means  $\pm$  standard error.



**Figure 6.** Size-frequency distribution of colonies (A) and branches (B) from 261 *Pseudopterogorgia elisabethae* found within 70 m<sup>2</sup> of belt transects at 12–16 m depth at San Salvador, Bahamas. Heights were measured as the length of the tallest branch, and the measurement was made either from photos or in the field with a tape measure. Height classes are centered on the upper limit of the size class; 0–5 cm and >50 cm classes were lumped with adjacent size classes in the statistical analyses. Branch lengths were determined from digital images either of entire colonies or, in the case of large colonies, from digital images of an arbitrarily selected subset of branches. Branch measurements are from December 1999. Branches include both daughter and mother branches.

ries, mothers and daughters, which exhibit different growth characteristics from the time they first originate. In addition to those findings, the results also have implications for colony regeneration following disturbance, and in a final section, we discuss the implications of the study for the harvest of *P. elisabethae*, which is already being conducted in the Bahamas.

#### *Branches as modules*

Growth of *P. elisabethae* colonies is best described in terms of branches, and each branch behaves as an integrated unit, or module. Daughter branches follow a predictable developmental sequence in which they first grow rapidly,

then slow as they age, and eventually stop growing. Mother branches follow a sequence in which they grow and generate both daughter and mother branches, but their growth and the rate at which they generate new branches also slow as the colony grows.

Concepts of integration and modularity have been used in describing the development and evolution of suites of morphologic features among solitary organisms (Pagliucci, 2002). This approach emphasizes the developmental relationships of traits. While not all groups of integrated traits need be “modules” as used in the invertebrate and plant literature, the modules that make up invertebrate colonies should exhibit the statistical correlations indicative of integrated development and evolution (*i.e.*, Magwene, 2001). Our analysis of branch growth rates suggests that both branches and colonies develop as integrated units. Similarly, correlations among five traits in 21 gorgonian species also differentiated polyp-level traits from those at the branch or colony level (Sánchez and Lasker, 2003). In the context of this broader definition of modularity, three levels of modularity or integration can be recognized in *P. elisabethae*: polyps, branches, and the colony. The polyp has always been recognized as a distinct unit with a well-defined ontogeny and determinate growth. Our data on branch growth suggest that the branches of *P. elisabethae* also exhibit a well-defined ontogeny. The colony must also be considered as a level of organization, because growth of the branches is also dependent on colony-level traits, that is, on colony height and generational order.

#### *Determinate growth among modular organisms*

Daughter branches on *P. elisabethae* stop growing as they age, and the growth rates decrease as the colony increases in height. Furthermore, origination rates of branches decrease with branch generation. In concert, these changes in developmental rates conserve a colony’s size and form, a pattern that is functionally equivalent to determinate growth. The pattern of determinate growth observed in *P. elisabethae* colonies could be generated by set developmental programs or through predictable responses to microenvironmental variation around the colony. Both are, at some level, growth in response to cues and are not mutually exclusive. We argue that a developmental program is the principal factor controlling the determinate growth of branches, while the size of whole colonies probably reflects a mix of both developmental effects and environmental and historical factors (Rinkevich, 2000).

Branches have a clear developmental cycle which, among the daughter branches, leads them to stop growing long before they reach 10 cm in length. Kim and Lasker (1997) report that interior branches of the gorgonian *Plexaura homomalla* have lower growth rates than those on the perimeter of the colony, a pattern they attributed to nutrient

supply and self-interference. A number of realistic models of form in modular organisms have been developed, in which growth is controlled by the local responses of the individual modules to their local environment (Braverman, 1974; Graus and MacIntyre, 1976; Colasanti and Hunt, 1997; Kaandorp and Kübler, 2001; Oborny *et al.*, 2001). However, the decrease in branch growth among *P. elisabethae* colonies is best described as an age-dependent decrease. Thus, although the smallest branches had the greatest growth rates, many small branches also exhibited low growth (Fig. 5). Furthermore, daughter branches stop growing while adjacent mother branches continue to grow, which indicates that position alone does not control branch growth.

Colony size in *P. elisabethae* also appears to be determinate, and observations of determinate growth have been reported among a wide range of colonial taxa. As noted, octocoral descriptions often include maximum colony sizes (*i.e.*, Bayer, 1961), and decreasing growth with increasing colony size has been reported for a number of gorgonians (Grigg, 1974; Velimirov, 1975; Mitchell *et al.*, 1993; Coma *et al.*, 1998; Cordes *et al.*, 2001). Among scleractinian corals, determinate growth of independently growing branches generates colonies with determinate form and size (Rinkevich, 2002). Among botryllid tunicates, groups of zooids, referred to as systems, undergo synchronous senescence (Sabbadin, 1969), and whole colonies, including isolated explants from a common source, undergo simultaneous senescence (Milkman, 1967; Rinkevich *et al.*, 1992). In addition, graptolite colonies are believed to have had determinate growth leading to distinct species-specific forms and sizes (Mitchell, 1988).

Maximum size alone does not demonstrate determinate growth. In a manner functionally equivalent to determinate growth, modular organisms may also stop growing, not according to a genetically determined developmental plan, but due to size-dependent interactions between the colony and environment, such as the balance between nutrient uptake and metabolic rates. Size-dependent change in colony growth that is mediated by metabolic rate and resource capture has been modeled by Sebens (1982, 1987) and by Kim and Lasker (1998). Taxa that exhibit growth patterns consistent with these simple models have been reported in octocorals (McFadden, 1986; Kim and Lasker, 1997) and tunicates (Holyoak, 1997).

Ecological processes such as size-dependent mortality also could generate a maximum colony size and the appearance of determinate growth. Colonies are susceptible to being knocked over because drag forces increase with colony size and bioerosion weakens the substratum around the holdfast (Birkeland, 1974). During most of this study, however, mortality decreased with colony height (mortality per 6 months: 0–10 cm, 0.146; 11–20 cm, 0.108; 21–30 cm, 0.071; 31–40 cm, 0.048; >40 cm, 0.000). That pattern of mortality would have led to the accumulation of large

colonies within the population. Mortality of colonies taller than 40 cm increased from 0.0% to 40.2% when Hurricane Floyd, a Category 4 hurricane, struck San Salvador on 13 September 1999. Although mortality events generated by such storms reduce the number of large colonies, the distribution of colony sizes observed in the San Salvador population would require that the mortality of large colonies be high almost every year, not only in those occasional years with severe hurricanes. Decreased growth rates among the larger colonies appears to be a more parsimonious explanation of the size-frequency distribution. Because aging and size are often correlated and the ages of most of the colonies were not known, the causative variable is difficult to distinguish.

#### *Mothers and daughters—two developmental classes of branches*

Age, generation, and colony height all affect rates of branch growth and origination, but the most striking differences in the growth of branches are those between mother and daughter branches. The data indicate that the two branch types are fundamentally different. First, mother branches continue growing while adjacent branches stop growing; for instance, compare branch 2 to branches 4 or 17 in Figure 2A. The self-shading effects hypothesized for *Plexaura homomalla* (Kim and Lasker, 1997) do not account for the continued growth of mother branches, which were otherwise indistinguishable from daughter branches. Second, mother branches exhibit high growth rates as soon as they originate, well before they have produced their first daughter. However, the two branch types are not immutable. When colonies are damaged, branches that were previously daughter branches begin to extend and generate new branches (Castanaro and Lasker, 2003). Understanding whether and how branches “become” mother branches will be essential to our understanding of developmental processes among these colonial organisms.

#### *Applications*

Modular growth is an especially advantageous growth strategy, when transplants are used to remediate populations (Rinkevich, 2000), when explants are used as stock in mariculture, and for the sustained harvest of wild populations where colonies are cropped at regular time intervals (Castanaro and Lasker, 2003). Understanding the pattern of growth of *P. elisabethae* colonies is particularly important because this species is harvested and extracted for a class of natural products called pseudopterosins (Mayer *et al.*, 1998). Material for extraction is collected by cropping branches from colonies. If growth is inversely related to the size of the colony, then reductions in colony size will enhance growth and productivity. Among harvested populations, this suggests that colonies can be maintained at an

optimal size, and that naturally occurring populations might recover from disturbance at rates greater than the growth rates observed before the disturbance. Alternatively, if there is also an age-based component to growth regulation (*i.e.*, Hughes and Connell, 1987), then recovery from either anthropogenic or natural disturbance may not be as great as suggested by colony size alone. Detailed understanding of colony growth patterns is essential to determining whether a species is suitable for sustained harvesting and whether remediation following anthropogenic disturbance is likely to succeed.

### Conclusions

Knowlton and Jackson (1994) have argued that—far more often than generally acknowledged—the apparent plasticity of coral reef cnidarians reflects genetic differentiation. Indeed, the literature provides numerous hints of genetic controls on size and form: genetically based, species-level differences in colony form within the *Montastraea annularis* complex (Weil and Knowlton, 1994); differences in regeneration among clones of the reef coral *Stylophora pistillata* (Rinkevich, 2000); age effects on the survival of stony corals (Hughes and Connell, 1987); graptolites with highly determinate patterns of colony size (Mitchell, 1986); and botryllid tunicates that exhibit zooid and colony senescence (Rinkevich *et al.*, 1992). Those studies, together with our observations of *P. elisabethae*, underscore the conclusion that the body plans of modular organisms are constrained by developmental programs as well as by the environment. If the potential for indeterminate growth that modularity seemingly confers is not realized, then, “Why not?” becomes a valuable question. How does constraining the size of branches affect the array of forms that can be realized by the whole colony? Since reproductive output is a function of colony size (Beiring and Lasker, 2000), can determinate colony growth be explained by trade-offs between current and future reproduction? Are there hydrodynamic or feeding advantages to the plumelike form of *P. elisabethae*, and are the advantages dependent on branch size, on colony size? Although colonial organisms are far more plastic than unitary forms, their growth should be studied as an internally regulated process that generates colony form. Both the form and the processes by which it is realized affect fitness and are subject to natural selection.

### Acknowledgments

We thank C. Gutiérrez-Rodríguez, T. Swain, and the staff of the Bahamian Field Station for assistance in the field. L. Bright, J. Nowak, and T. Swain assisted with the photo analyses. M. A. Coffroth, C. E. Mitchell, D. J. Taylor, and two anonymous reviewers made many useful comments on earlier drafts of the manuscript. This research was supported by the New York State Sea Grant Institute (Project R/XG-

2), the National Undersea Research Center at the Caribbean Marine Research Center (grants 99-301 and CMRC-99-NRHL-01-01C), and the National Geographic Society (#5968-97). Equipment for scuba diving was provided by a grant from Sherwood Scuba to the University at Buffalo. We also thank K. Buchan and the staff of the Gerace Research Centre for their assistance in the Bahamas.

### Literature Cited

- Bayer, F. M. 1961. *The Shallow Water Octocorallia of the West Indian Region*. Martinus Nijhoff, The Hague.
- Beiring, E. A., and H. R. Lasker. 2000. Egg production by colonies of a gorgonian coral. *Mar. Ecol. Prog. Ser.* **196**: 169–177.
- Birkeland, C. 1974. The effects of wave action on the population dynamics of *Gorgonia ventalina* Linnaeus. *Stud. Trop. Oceanogr.* **12**: 115–126.
- Braverman, M. 1974. The cellular basis of morphogenesis and morphostasis in hydroids. *Oceanogr. Mar. Biol. Annu. Rev.* **12**: 129–221.
- Brazeau, D. A., and H. R. Lasker. 1988. Inter- and intraspecific variation in gorgonian colony morphology: quantifying branching patterns in arborescent animals. *Coral Reefs* **7**: 139–143.
- Castanaro, J., and H. R. Lasker. 2003. Effects of clipping on growth of colonies of the Caribbean gorgonian *Pseudopterogorgia elisabethae*. *Invertebr. Biol.* **122**: 299–307.
- Colasanti, R. L., and R. Hunt. 1997. Resource dynamics and plant growth: A self-assembling model for individuals, populations and communities. *Funct. Ecol.* **11**: 133–145.
- Coma, R., M. Ribes, M. Zabala, and J.-M. Gili. 1998. Growth in a modular colonial marine invertebrate. *Estuar. Coast. Shelf Sci.* **47**: 459–470.
- Cordes, E. E., J. W. Nybakken, and G. Van Dykhuizen. 2001. Reproduction and growth of *Anthomastus ritteri* (Octocorallia: Alcyonacea) from Monterey Bay, California, USA. *Mar. Biol.* **138**: 491–501.
- Done, T. J. 1987. Simulation of the effects of *Acanthaster planci* on the population structure of massive corals in the genus *Porites*: evidence of population resilience? *Coral Reefs* **6**: 75–90.
- Done, T. J. 1988. Simulations of the recovery of pre-disturbance size structure in populations of *Porites* spp. damaged by crown-of-thorns starfish. *Mar. Biol.* **100**: 51–61.
- Graus, R. R., and I. G. MacIntyre. 1976. Light control of growth form in colonial reef corals: computer simulation. *Science* **193**: 895–898.
- Grigg, R. W. 1974. Growth rings: annual periodicity in two gorgonian corals. *Ecology* **55**: 876–881.
- Harper, J. L., and J. White. 1974. The demography of plants. *Annu. Rev. Ecol. Syst.* **5**: 419–463.
- Holyoak, A. R. 1997. Patterns and consequences of whole colony growth in the compound ascidian *Polyclinum planum*. *Biol. Bull.* **192**: 87–97.
- Hughes, R. N. 1989. *A Functional Biology of Clonal Animals*. Chapman and Hall, London.
- Hughes, T. P., and J. H. Connell. 1987. Population dynamics based on size or age? A reef-coral analysis. *Am. Nat.* **129**: 818–829.
- Jackson, J. B. C. 1977. Competition on marine hard substrata: the adaptive significance of solitary and colonial strategies. *Am. Nat.* **111**: 743–767.
- Jackson, J. B. C., L. W. Buss, and R. E. Cook, Eds. 1985. *Population Biology and Evolution of Clonal Organisms*. Yale University Press, New Haven.
- Kaandorp, J. A., and J. E. Kübler. 2001. *The Algorithmic Beauty of Seaweeds, Sponges and Corals*. Springer-Verlag, Heidelberg.
- Kim, K., and H. R. Lasker. 1997. Flow-mediated resource competition

- in the suspension feeding gorgonian *Plexaura homomalla* (Esper). *J. Exp. Mar. Biol. Ecol.* **215**: 49–64.
- Kim, K., and H. R. Lasker. 1998. Allometry of resource capture in colonial invertebrates and constraints on modular growth. *Funct. Ecol.* **12**: 646–654.
- Knowlton, N., and J. B. C. Jackson. 1994. New taxonomy and niche partitioning on coral reefs—jack of all trades or master of some? *Trends Ecol. Evol.* **9**: 7–9.
- Lasker, H. R., and J. A. Sánchez. 2002. Allometry and astogeny of modular organisms. Pp. 207–253 in *Reproductive Biology of Invertebrates. Vol. XI. Progress in Asexual Reproduction*, R. N. Hughes, ed. John Wiley & Sons, New York.
- Magwene, P. M. 2001. New tools for studying integration and modularity. *Evolution* **55**: 1734–1745.
- Mayer, A. M. S., P. B. Jacobson, W. Fenical, R. S. Jacobs, and K. B. Glaser. 1998. Pharmacological characterization of the pseudopterousins: Novel anti-inflammatory natural products isolated from the Caribbean soft coral, *Pseudopterogorgia elisabethae*. *Life Sci.* **62**: 401–407.
- McFadden, C. S. 1986. Colony fission increases particle capture rates of a soft coral—advantages of being a small colony. *J. Exp. Mar. Biol. Ecol.* **103**: 1–20.
- Milkman, R. 1967. Genetic and developmental studies on *Botryllus schlosseri*. *Biol. Bull.* **132**: 229–243.
- Mitchell, C. E. 1986. Morphometric studies of *Climacograptus* (Hall) and the phylogenetic significance of astogeny. Pp. 119–129 in *Palaeoecology and Biostratigraphy of Graptolites*, C. P. Hughes and R. B. Rickards, eds. Geological Society Special Publication 20, Geological Society of America, Boulder, CO.
- Mitchell, C. E. 1988. The morphology and ultrastructure of *Brevigraptus quadrithecatus* n. gen., n. sp. (Diplograptacea), and its convergence upon *Dicaulograptus hystrix* (Bulman). *J. Paleont.* **62**: 448–463.
- Mitchell, N. D., M. R. Dardeau, and W. W. Schroeder. 1993. Colony morphology, age structure, and relative growth of two gorgonian corals, *Leptogorgia hebes* (Verrill) and *Leptogorgia virgulata* (Lamarck), from the northern Gulf of México. *Coral Reefs* **12**: 65–70.
- Oborny, B., T. Czaran, and A. Kun. 2001. Exploration and exploitation of resource patches by clonal growth: a spatial model on the effect of transport between modules. *Ecol. Model.* **141**: 151–169.
- Pagliucci, M. 2002. Touchy and bushy: phenotypic plasticity and integration in response to wind stimulation in *Arabidopsis thaliana*. *Int. J. Plant Sci.* **163**: 399–408.
- Rinkevich, B. 2000. Steps towards the evaluation of coral reef restoration by using small branch fragments. *Mar. Biol.* **136**: 807–812.
- Rinkevich, B. 2002. The branching coral *Stylophora pistillata*: contribution of genetics in shaping colony landscape. *Isr. J. Zool.* **48**: 71–82.
- Rinkevich, B., R. J. Lauzon, B. W. M. Brown, and I. L. Weissman. 1992. Evidence for a programmed life-span in a colonial protochordate. *Proc. Natl. Acad. Sci. USA* **89**: 3546–3550.
- Sabbadin, A. 1969. The compound ascidian *Botryllus schlosseri* in the field and laboratory. *Publ. Stn. Zool. Napoli* **37**(suppl.): 67–72.
- Sánchez, J. A. 2002. Dynamics and evolution of colony form among branching modular organism. Ph.D. dissertation, University at Buffalo, State University of New York, Buffalo, NY. 137 pp.
- Sánchez, J. A., and H. R. Lasker. 2003. Patterns of morphologic integration in marine modular organisms: supra-module organization in branching octocoral colonies. *Proc. R. Soc. Lond.* DOI: 10.1098/rspb.2003.2471.
- Sánchez, J. A., W. Zeng, V. R. Coluci, C. Simpson, and H. R. Lasker. 2003. How similar are branching networks in nature? A view from the ocean: Caribbean gorgonian corals. *J. Theor. Biol.* **222**: 135–138.
- Sebens, K. P. 1982. The limits to indeterminate growth: an optimal size model applied to passive suspension feeders. *Ecology* **63**: 209–222.
- Sebens, K. P. 1987. The ecology of indeterminate growth in animals. *Annu. Rev. Ecol. Syst.* **18**: 371–407.
- Velimirov, B. 1975. Growth and age determination in the sea fan *Eunicella clavolinii*. *Oecologia* **19**: 259–272.
- Weil, E., and N. Knowlton. 1994. A multi-character analysis of the Caribbean coral *Montastraea annularis* (Ellis & Solander, 1786) and its two sibling species, *M. faveolata* (Ellis & Solander, 1786) and *M. franksi* (Gregory, 1895). *Bull. Mar. Sci.* **55**: 151–175.

# Possible Roles of Sulfur-Containing Amino Acids in a Chemoautotrophic Bacterium-Mollusc Symbiosis

JOANNA L. JOYNER<sup>1,\*</sup>, SUZANNE M. PEYER, AND RAYMOND W. LEE

*School of Biological Sciences, Washington State University, P.O. Box 644236, Pullman, Washington 99164-4236*

**Abstract.** Invertebrate hosts of chemoautotrophic symbionts face the unique challenge of supplying their symbionts with hydrogen sulfide while avoiding its toxic effects. The sulfur-containing free amino acids taurine and thiotaurine may function in sulfide detoxification by serving as sulfur storage compounds or as transport compounds between symbiont and host. After sulfide exposure, both taurine and thiotaurine levels increased in the gill tissues of the symbiotic coastal bivalve *Solemya velum*. Inhibition of prokaryotic metabolism with chloramphenicol, inhibition of eukaryotic metabolism with cycloheximide, and inhibition of ammonia assimilation with methionine sulfoximine reduced levels of sulfur-containing amino acids. Chloramphenicol treatment inhibited the removal of sulfide from the medium. In the absence of metabolic inhibitors, estimated rates of sulfide incorporation into taurine and thiotaurine accounted for nearly half of the sulfide removed from the medium. In contrast, amino acid levels in the nonsymbiotic, sulfide-tolerant molluscs *Geukensia demissa* and *Yoldia limatula* did not change after sulfide exposure. These findings suggest that sulfur-containing amino acids function in sulfide detoxification in symbiotic invertebrates, and that this process depends upon ammonia assimilation and symbiont metabolic capabilities.

## Introduction

Aquatic habitats such as deep-sea hydrothermal vents, mangrove swamps, eelgrass beds, and sewage outfall sites tend to be characterized by high levels of the metabolic

toxin hydrogen sulfide (Fenchel and Riedl, 1970; Felbeck *et al.*, 1981; Cavanaugh, 1983). Hydrogen sulfide diffuses freely across respiratory surfaces and therefore cannot be excluded from tissues (Denis and Reed, 1927; Julian and Arp, 1992). It also reversibly inhibits cytochrome *c* oxidase (Lovatt Evans, 1967; Nicholls, 1975) and decreases hemoglobin oxygen affinity (Carrico *et al.*, 1978). Consequently, animals living in these environments require physiological mechanisms to cope with hydrogen sulfide toxicity.

Invertebrates that harbor symbiotic chemoautotrophic bacteria also require sulfide, for their symbionts utilize the chemical energy generated by hydrogen sulfide oxidation to fix carbon dioxide into carbohydrates (Felbeck *et al.*, 1981; Ruby *et al.*, 1981; Cavanaugh, 1983). The invertebrate host delivers hydrogen sulfide and oxygen to its symbionts and relies upon the symbiont-produced carbohydrates as a source of nutrition (Rau, 1981; Southward *et al.*, 1981; Felbeck, 1985). This type of symbiotic relationship exists in over 100 species from at least five invertebrate phyla (Cavanaugh, 1994).

Sulfide detoxification and transport strategies have been well studied in the coastal protobranch bivalves of the genus *Solemya*, which harbor approximately  $1 \times 10^9$  intracellular chemoautotrophic symbionts per gram wet weight of gill tissue (Cavanaugh, 1983; Felbeck, 1983). These clams generally form U- or Y-shaped burrows in shallow-water reducing sediments and pump oxygenated water through their burrows (Frey, 1968), which enables them to simultaneously acquire the dissolved oxygen and sulfide needed for chemoautotrophy.

To detoxify sulfide, *Solemya velum* and *S. reidi*, two well-studied species, use several strategies apart from utilization by their symbionts. For example, *S. velum* has two types of cytoplasmic hemoglobins: one binds oxygen, and a second, which combines with sulfide to form ferric hemo-

Received 30 January 2003; accepted 12 September 2003.

<sup>1</sup> Current address: Department of Zoology, University of Florida, 223 Bartram Hall, Box 118525, Gainesville, Florida 32611-8525.

\* To whom correspondence should be addressed: jjoyner@zoo.ufl.edu

Abbreviations: MSX, methionine sulfoximine; ASW, artificial seawater; FIA, flow injection analysis; POS, polarographic oxygen sensor.

globin sulfide, may mediate sulfide transport to the symbionts (Doeller *et al.*, 1988). The sulfide-binding form of cytoplasmic hemoglobin is not present in *S. reidi* (Kraus *et al.*, 1992); rather, sulfide oxidation occurs in the mitochondria, hemein, and sulfide-oxidizing bodies (Powell and Somero, 1985, 1986; Powell and Arp, 1989).

Synthesis of sulfur-containing free amino acids may be an additional strategy for sulfide detoxification and transport in chemoautotrophic symbioses (Alberic and Boulegue, 1990; Conway and McDowell Capuzzo, 1992; Pranal *et al.*, 1995; Pruski *et al.*, 1997). In many marine organisms, including solemyid clams and some deep-sea symbiotic species, taurine (2-aminoethanesulfonic acid) is the dominant free amino acid (Alberic and Boulegue, 1990; Conway *et al.*, 1992; Conway and McDowell Capuzzo, 1992; Pranal *et al.*, 1995; Lee *et al.*, 1997; Pruski *et al.*, 1997). Intracellular free amino acid pools function in cell volume regulation (Pierce, 1982; Yancey *et al.*, 1982; Rice and Stephens, 1988), and the primary function of taurine may be as a compatible osmolyte, a function which is conserved throughout the animal kingdom (Allen and Garrett, 1971; Huxtable, 1992).

The exceptionally high levels of taurine and the related amino acid thiotaurine (2-aminoethanethiosulfonic acid) in several chemoautotrophic symbioses have prompted investigators to consider additional roles for these amino acids. For example, taurine appears to be an end product of ammonia assimilation in *S. reidi* (Lee *et al.*, 1997), and may be involved in sulfur cycling in *S. velum* (Conway and McDowell Capuzzo, 1992). Similarly, thiotaurine may function in sulfur cycling in deep-sea symbiotic bivalves (Alberic and Boulegue, 1990; Pruski *et al.*, 2000; Pruski, 2001). Taurine and thiotaurine may serve as important sulfide storage compounds, allowing *S. velum* to maintain low levels of intracellular sulfide. Under conditions where sulfide is low or absent, taurine and thiotaurine may provide sulfide to mitochondrial and symbiont sulfide oxidation pathways. Several species of aerobic gram-negative soil and enteric bacteria use taurine as a sulfur, carbon, and nitrogen source (Stapley and Starkey, 1970; Smiley and Wilkinson, 1983; Seitz *et al.*, 1993; King and Quinn, 1997; Chien *et al.*, 1999; Cook *et al.*, 1999; Reichenbecher and Murrell, 1999), and similar metabolic pathways may be present in the gram-negative chemoautotrophic symbionts. Additionally, taurine and thiotaurine production could facilitate sulfide detoxification under anaerobic conditions, thereby preventing deleterious effects such as the reaction of sulfide with metalloproteins. This strategy would be particularly beneficial in the burrow environment of solemyid clams, in which oxygen and sulfide levels vary.

In the present study, we tested the hypothesis that taurine and thiotaurine levels in intact gills of *S. velum* increase upon exposure to sulfide, which would occur if these amino acids are involved in sulfur storage or cycling. The effects

of sulfide exposure on levels of hypotaurine (2-aminoethanesulfonic acid), a possible precursor to taurine and thiotaurine, were also examined. Host- and symbiont-specific metabolic inhibitors were used to distinguish the roles of the *S. velum* host and its symbionts in ammonia assimilation and the maintenance of taurine, thiotaurine, and hypotaurine pools. Flow-through respirometry studies were conducted with *S. velum* to quantify rates of ammonia flux and to determine whether sulfide consumption is related to fluctuations in amino acid pools. In parallel studies, we tested for correlations between sulfide and free amino acid levels in two sulfide-tolerant, nonsymbiotic bivalve species: the estuarine mussel *Geukensia demissa* and the protobranch bivalve *Yoldia limatula*.

## Materials and Methods

### *Specimen collection and maintenance*

*Solemya velum* Say, 1822, *Geukensia demissa* (Dillwyn, 1817), and *Yoldia limatula* (Say, 1831) were collected by the Marine Resources Center of the Marine Biological Laboratory (Woods Hole, MA) and shipped on the day of collection. In our laboratory the clams were maintained for up to 5 days in a flow-through respirometry system (see <http://www.wsu.edu/~rlee/respirometer/respirometer.htm> and Fig. 1). In each experiment, the temperature of the respirometry system was regulated to match the ambient water temperature at which the clams were collected, which ranged seasonally from 5 to 15 °C over a nearly 2-year period. These temperature differences did not affect the free amino acid composition. Consumption of sulfide, oxygen, and ammonia was measured in a subset of experiments conducted in the late spring and at 15 °C. *Solemya velum* and *Y. limatula* were maintained in 0.45- $\mu\text{m}$  filtered, 35‰ artificial seawater (ASW; Instant Ocean, Aquarium Systems, Mentor, OH) supplemented with 50  $\mu\text{M}$  ammonia. *Geukensia demissa* was maintained in filtered, 30‰ ASW supplemented with 50  $\mu\text{M}$  ammonia. The ASW solution in the chambers was kept mixed with magnetic stir bars (60 to 100 rpm). ASW flow rates ranged from 0.18 to 0.19 ml  $\text{min}^{-1}$ .

Maintaining the clams in a flow-through respirometry system allowed for constant monitoring of experimental conditions. The oxygen concentrations in the chamber outflows were determined with a polarographic O<sub>2</sub> sensor (POS), whereas the concentrations of sulfide and, in some experiments, ammonia were measured by flow injection analysis (FIA). Throughout this paper, sulfide refers to  $\Sigma\text{H}_2\text{S}$  (primarily the sum of HS<sup>-</sup> and H<sub>2</sub>S), and ammonia refers to  $\Sigma\text{NH}_3$  (the sum of NH<sub>3</sub> and NH<sub>4</sub><sup>+</sup>). Outflows were pumped directly through a flow cell containing a sulfide-insensitive gold microcathode POS (Orbisphere 2120, Geneva) followed by a series of FIA injection sample loops

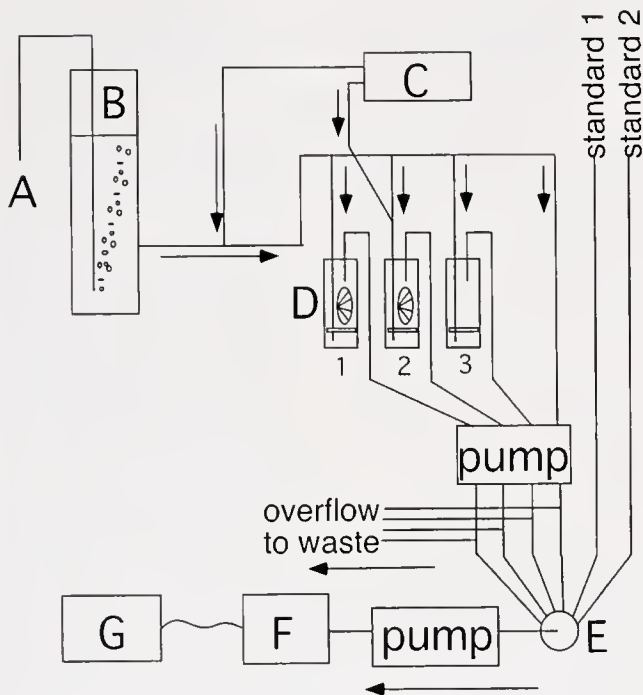


**Figure 1.** Schematic of flow-through respirometry system. (A)  $\text{CO}_2$ ,  $\text{N}_2$ , and  $\text{O}_2$  gas mixture. (B) Seawater-gas equilibration column with pH regulation. (C) Syringe pump for metering sodium sulfide stocks into seawater entering the chambers. The syringe pump is also used to meter inhibitor into chamber 2. (D) Water-jacketed chambers containing clams, with at least one empty chamber to function as a control. Outflows from the chambers are pumped to a pneumatically actuated six-way stream-selector valve (E). The position of this valve determines whether the outflow goes to waste or to the analysis system. The analysis system consists of a flow injection analyzer for sulfide and ammonia determination and an  $\text{O}_2$  sensor mounted in a flow cell (F). The analyzer and stream-selector valve are linked to a data acquisition and automated control system (G).

(Rheodyne Type 50 valves with Rheodyne 5701 pneumatic actuators, Rohnert Park, CA).

The FIA determination of sulfide involved derivitizing the sample stream with 1.5 mM 2,2'-dithiodipyridine, which forms a stable product with an absorbance maximum at 343 nm (Svenson, 1980). The derivitized sample was loaded into an injection loop and sent to a variable wavelength detector (Hyperquan VUV-20, Colorado Springs, CO). This method produces 343-nm absorbance peaks proportional to sulfide concentration (Svenson, 1980). Ammonia was determined by a modification of the FIA protocol of Willason *et al.* (1986). The sample was loaded into an injection loop and then treated with NaOH to raise the pH, converting ammonium to ammonia gas. Ammonia passes through a Teflon membrane into a carrier stream containing phenol red, raising the pH of the phenol red solution. The resulting color change (absorbance at 560 nm) is monitored with a detector fabricated from a green LED and a phototransistor. POS and FIA detector outputs were continuously recorded with a data acquisition system (Sable Systems, Datacan V,

Henderson, NV), which was also used to control FIA injection valve actuation.

Three respirometer chambers containing clams, one control chamber, and two standards were connected to a six-way stream-selector valve (Fig. 1). Every 0.13 h the valve was automatically switched, allowing sampling from all six channels every 0.8 h. Peak height (for FIA) or average output (for POS) was calculated to determine concentration differences between chambers containing clams and the control chamber. These data were continuously monitored to ensure, in the case of oxygen measurements, that the clams were not exposed to hypoxic conditions. Direct measurements of sulfide in samples taken from the respirometer outflow were used to standardize sulfide data obtained by FIA. Fluxes were calculated as follows:  $\mu\text{mol sulfide} \cdot \text{g}^{-1} \text{ wet weight} \cdot \text{h}^{-1} = (\text{concentration}_{\text{experimental chamber}} - \text{concentration}_{\text{control chamber}}) \times (\text{flow rate in l} \cdot \text{h}^{-1}) \times (\text{g}^{-1} \text{ wet weight})$ .

#### Experimental treatments

In all experiments, the clams were acclimated for 24 h in ASW prior to sulfide or inhibitor exposure. In experiments in which clams were exposed to sulfide, a syringe pump (Harvard Apparatus 944, South Natick, MA) was used to meter a 20 mM  $\text{Na}_2\text{S}$  solution (Fig. 1C) into the ASW solution before its entry into the respirometer chambers. Final sulfide concentration in the chambers was  $0.45 \pm 0.05$  mM. Clams assayed for amino acid levels were exposed to sulfide for 24 h. In some experiments, a metabolic inhibitor was added to the ASW solution after the 24-h acclimation period. The final concentrations of these inhibitors were 0.9 mM chloramphenicol (Sigma, St. Louis, MO), 0.02 mM cycloheximide (Sigma), and 0.25 mM methionine sulfoximine (MSX; Sigma). In experiments in which sulfide consumption was examined, the clams were acclimated for 24 h in ASW, then exposed to sulfide for up to 100 h. During the final 24 h of the sulfide exposure, metabolic inhibitors were added to the ASW solution. The clams were weighed before and after treatment.

#### Amino acid analyses

After experimental treatment, the bivalves were opened by severing their adductor muscles. The gills and foot of each clam were dissected free of other tissues, blotted briefly on a paper towel, then individually frozen in liquid nitrogen and stored at  $-80^\circ\text{C}$ . The gills and feet were individually homogenized in distilled water (1:25, tissue/ $\text{dH}_2\text{O}$ ) on ice. To precipitate proteins, the homogenates were treated with 5% sulfosalicylic acid (Sigma) in a 1:10 ratio of sulfosalicylic acid/homogenate (Lee and Slocum, 1988). The solutions were centrifuged for 5 min at  $16,000 \times \text{g}$ , and the supernatants were stored at  $-80^\circ\text{C}$ .

Total free amino acids were quantified in a Beckman

6300 amino acid analyzer following a protocol modified from Lee and Stocum (1988). The samples were diluted (1:30, by volume) with Li-S buffer (96.8% H<sub>2</sub>O, 1% LiCl, 1% thiourea, 0.7% HCl, 0.5% benzoic acid; pH 2.2; Beckman Coulter, Inc., Fullerton, CA). Of the 240–250  $\mu$ l of sample or standard loaded onto the sample loops, 50  $\mu$ l of each solution was analyzed. The amino acids were separated in Li-A buffer (98% H<sub>2</sub>O, 1% Li citrate, 0.5% LiCl, 0.5% HCl; pH 2.8; Beckman Coulter) on a 10-cm ion exchange column and reacted in-line with ninhydrin solution. Absorbances were monitored at 570 nm and 440 nm. After preliminary experiments, only taurine, hypotaurine, and thiotaurine were quantified. The standards were 200  $\mu$ M taurine (Sigma) and 20  $\mu$ M hypotaurine (Sigma) in Li-S buffer. The thiotaurine standard was prepared by dissolving 0.0011 g hypotaurine and 0.05 g Na<sub>2</sub>S · 9H<sub>2</sub>O (Fisher Scientific, Fair Lawn, NJ) in deionized water, heating to 100 °C, acidifying the solution with 1 M HCl, and evaporating the solution (Cavallini *et al.*, 1963). This standard was verified by mass spectrometry.

The temperature of the column affected the separation of thiotaurine from taurine and the reactivity of hypotaurine with ninhydrin. Thiotaurine could be detected only at 70 °C. The values of hypotaurine reported here are only from analyses run at 45 °C, because hypotaurine was not as reactive with ninhydrin at 70 °C. The temperature did not affect taurine levels. Reported values for taurine are averages between levels detected at 45 °C and 70 °C.

Results are presented as the mean  $\pm$  the standard error and as average rates of synthesis per gram wet weight over a 24-h period [(amino acid level in g<sup>-1</sup> wet weight in clams exposed to sulfide) – (amino acid level in clams not exposed to sulfide)/24 h] assuming the synthesis rate was linear over the 24-h period. Differences among means were detected using one-way ANOVA for each amino acid in *S. velum* samples (Statistica, Statsoft, Inc., Tulsa, OK). The appropriate comparisons were analyzed with Fisher's LSD procedure (Statistica). The *G. demissa* and *Y. limatula*

amino acid data were analyzed with two-sample *t* tests (Statistica).

## Results

### *Sulfide exposure increased taurine and thiotaurine levels in S. velum but not in two nonsymbiotic bivalves*

Specimens of *Solemya velum* exposed to sulfide had significantly more taurine ( $P = 0.0034$ ) and thiotaurine ( $P < 0.0001$ ) in their gill tissue than clams not so exposed (Table 1). These values equate to average rates of change in taurine and thiotaurine levels of 0.89  $\mu$ mol · g<sup>-1</sup> wet weight · h<sup>-1</sup> and 0.22  $\mu$ mol · g<sup>-1</sup> · h<sup>-1</sup> over the 24-h incubation period. Hypotaurine levels were not significantly affected ( $P = 0.064$ ). Cysteine and methionine, two other sulfur-containing amino acids, were below the limits of detection in all samples. Levels of the most abundant non-sulfur-containing free amino acids—alanine, glutamate, and aspartate—were unaffected by sulfide exposure (data not shown). In preliminary experiments with sulfide-exposed clams, free amino acid profiles of *S. velum* foot (symbiont-free) and gill tissues were similar (data not shown), as observed previously (Conway and McDowell Capuzzo, 1992). In subsequent experiments with metabolic inhibitors, only taurine, hypotaurine, and thiotaurine levels in the symbiont-containing gill tissues of *S. velum* were quantified.

Gill tissue from the nonsymbiotic bivalve species *Geukensia demissa* and *Yoldia limatula* contained less taurine ( $P < 0.0001$ , non-sulfide-exposed) than *S. velum* (Table 1), but comparable levels of hypotaurine ( $P = 0.068$ ) and thiotaurine ( $P = 0.648$ ). The concentrations of these amino acids were the same whether or not the bivalves were exposed to sulfide (all comparisons,  $P > 0.05$ ).

### *Metabolic inhibitors decreased taurine and thiotaurine levels in S. velum gills*

To investigate the role of the chemoautotrophic symbionts, clams were exposed to chloramphenicol, a specific

Table 1

Effects of sulfide exposure and inhibitors on taurine, hypotaurine, and thiotaurine levels in gills of three bivalve species

Species	Treatment (n)	Taurine		Hypotaurine		Thiotaurine	
		–Sulfide	+Sulfide	–Sulfide	+Sulfide	–Sulfide	+Sulfide
<i>Solemya velum</i>	No inhibitor (16)	100.3 $\pm$ 5.5 <sup>a</sup>	120 $\pm$ 5.4 <sup>a,b</sup>	13.7 $\pm$ 1.4	11.4 $\pm$ 1.3	0.35 $\pm$ 0.2 <sup>a</sup>	5.4 $\pm$ 0.6 <sup>a,b</sup>
	Chloramphenicol (9)	96.5 $\pm$ 6.5	102.2 $\pm$ 4.5 <sup>b</sup>	12 $\pm$ 0.8	12.9 $\pm$ 1.4	0.42 $\pm$ 0.2 <sup>a</sup>	3.6 $\pm$ 0.8 <sup>a,b</sup>
	Cycloheximide (5)	100.1 $\pm$ 6.6	109.5 $\pm$ 3.9	20.3 $\pm$ 2.6	15.1 $\pm$ 2.2	1.4 $\pm$ 0.2 <sup>a</sup>	5.5 $\pm$ 0.7 <sup>a</sup>
	MSX (7)	91.7 $\pm$ 10	96.1 $\pm$ 5.7 <sup>b</sup>	18.5 $\pm$ 3	12.7 $\pm$ 4	0.79 $\pm$ 0.3 <sup>a</sup>	6.5 $\pm$ 0.6 <sup>a</sup>
<i>Geukensia demissa</i>	No inhibitor (7)	37.9 $\pm$ 1.9	39.9 $\pm$ 1.2	4.7 $\pm$ 0.7	4.5 $\pm$ 0.6	0.65 $\pm$ 0.2	0.95 $\pm$ 0.4
<i>Yoldia limatula</i>	No inhibitor (3)	62 $\pm$ 5.5	56 $\pm$ 6.7	10.9 $\pm$ 1.5	9.9 $\pm$ 1.3	0.16 $\pm$ 0.16	0.24 $\pm$ 0.03

Data are mean  $\pm$  SEM in  $\mu$ mol amino acid/g wet weight of gill tissue. (n), Number of replicates; MSX, methionine sulfoximine.

<sup>a</sup> Significant differences ( $P < 0.05$ ) between clams exposed to sulfide (+Sulfide) and not exposed (–Sulfide).

<sup>b</sup> Significant differences ( $P < 0.05$ ) between clams treated with inhibitor and not treated.

inhibitor of bacterial protein synthesis (Burnap and Trench, 1989), at a concentration previously determined to disrupt symbiont metabolism but to be nontoxic to the host (R. W. Lee, unpubl.). To examine the role of the host, clams were exposed to cycloheximide, a specific inhibitor of eukaryotic protein synthesis (Burnap and Trench, 1989), at a concentration nontoxic to the host for the duration of the treatment. In additional experiments, the effects of the ammonia assimilation inhibitor, methionine sulfoximine (MSX; Rees, 1987) were examined; MSX inhibits glutamine synthetase, which has been detected in *S. velum* tissues (Lee *et al.*, 1999). To ensure complete inhibition of ammonia assimilation, the MSX level was 10-fold higher than that utilized by Rees (1987). Taurine, hypotaurine, and thiotaurine levels in clams not exposed to sulfide were not affected by exposure to any of the inhibitors (Table 1). Additionally, the wet weights of whole clams were not altered by treatment with sulfide or metabolic inhibitors.

When clams were treated with the three metabolic inhibitors, the usual sulfide-induced increase in taurine levels was not observed ( $P$  values for comparisons between  $-$ sulfide and  $+$ sulfide, in the presence of inhibitors: chloramphenicol,  $P = 0.552$ ; cycloheximide,  $P = 0.451$ ; MSX,  $P = 0.707$ ). Hypotaurine levels were not altered by sulfide exposure or treatment with inhibitors ( $P = 0.064$ ). Thiotaurine levels increased after sulfide exposure, even in the presence of metabolic inhibitors ( $P$  values for comparisons between  $-$ sulfide and  $+$ sulfide in the presence of inhibitors: chloramphenicol,  $P < 0.001$ ; cycloheximide,  $P < 0.001$ ; MSX,  $P < 0.0001$ ). This sulfide-stimulated increase, however, was reduced by treatment with chloramphenicol ( $P = 0.016$ , sulfide-exposed control clams *versus* chloramphenicol-treated sulfide-exposed clams).

#### *Chloramphenicol and MSX decreased S. velum sulfide and ammonia consumption*

The average rates of sulfide and oxygen consumption in the absence of inhibitors were  $2.57 \pm 0.06$  (5)  $\mu\text{mol} \cdot \text{g}^{-1}$  wet weight  $\cdot \text{h}^{-1}$  [mean  $\pm$  SE ( $n$  of experiments)] and  $3.98 \pm 0.01$  (5)  $\mu\text{mol} \cdot \text{g}^{-1} \cdot \text{h}^{-1}$ , respectively. Chloramphenicol exposure completely halted sulfide consumption after 10 h (Fig. 2A, hours 120–130). Cycloheximide treatment did not affect sulfide consumption rates. Treatment with MSX inhibited ammonia uptake (Fig. 2B, hours 10–30).

### Discussion

This study demonstrates that taurine and thiotaurine levels in *Solemya velum* gills increase after sulfide exposure. These two amino acids may function as nontoxic sulfide storage compounds. Inhibition of symbiont and host protein synthesis and host ammonia assimilation blocked sulfide-stimulated taurine synthesis; in contrast, only the inhibition

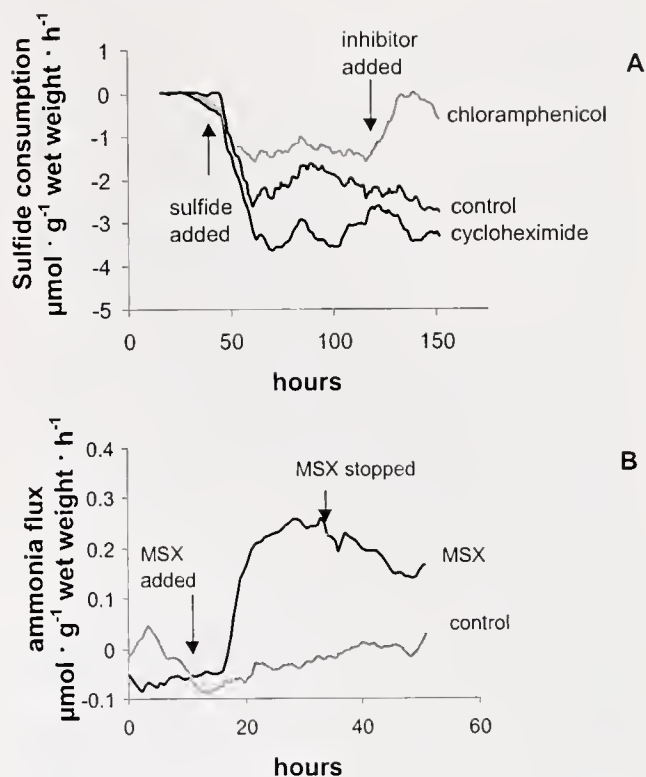


**Figure 2.** Effect of inhibitors on *Solemya velum* ammonia and sulfide fluxes. (A). Chloramphenicol (0.9 mM), an inhibitor of prokaryotic protein synthesis, blocked sulfide consumption. Cycloheximide (0.02 mM), an inhibitor of eukaryotic protein synthesis, had no effect. (B). Methionine sulfoximine (MSX, 0.25 mM), an inhibitor of ammonia assimilation, blocked ammonia uptake and resulted in ammonia excretion. Negative fluxes denote uptake from the medium.

of symbiont metabolism decreased the sulfide-stimulated thiotaurine synthesis. The maintenance of free amino acid pools depended upon the presence of functioning symbionts, sulfide consumption, and host ammonia assimilation. Thus, sulfur-containing free amino acids also may be a link between cycling of nitrogen and sulfur in chemoautotrophic symbioses.

The magnitude of changes in taurine and thiotaurine pools observed in the present study is sufficient for these amino acids to be physiologically significant sulfide storage compounds. In experiments in which clams were exposed to sulfide for 24 h, the increases in taurine and thiotaurine levels corresponded to synthesis rates of  $0.89 \mu\text{mol} \cdot \text{g}^{-1}$  wet weight  $\cdot \text{h}^{-1}$  and  $0.22 \mu\text{mol} \cdot \text{g}^{-1} \cdot \text{h}^{-1}$ , respectively. Since taurine contains one S atom and thiotaurine contains two S atoms, this corresponds to a potential sulfide incorporation rate of  $1.33 \mu\text{mol} \cdot \text{g}^{-1} \cdot \text{h}^{-1}$ . The average rate of whole animal sulfide consumption measured under the control (no inhibitor) conditions was  $2.57 \mu\text{mol} \cdot \text{g}^{-1} \cdot \text{h}^{-1}$ , which is similar to the sulfide consumption rate of *Solemya reidi* under similar experimental conditions (Anderson *et al.*, 1987). Therefore, the contribution of taurine and thio-

taurine to sulfide detoxification could account for up to 50% of the total sulfide flux.

Treatment with chloramphenicol, cycloheximide, and MSX prevented the sulfide-induced increases in taurine levels exhibited by the control clams. The lack of detectable taurine synthesis in chloramphenicol-treated clams likely can be attributed to the chloramphenicol-induced cessation of sulfide consumption. Additionally, chloramphenicol may act to prevent synthesis of mitochondrial proteins that are not nuclear encoded. Therefore, effects of chloramphenicol treatment might also be ascribed to impairment of mitochondrial metabolism. However, in preliminary experiments, *S. velum* tolerated treatment with 0.9 mM chloramphenicol for at least 9 days, suggesting that the effects due to chloramphenicol treatment are most likely the result of disrupted symbiont metabolism rather than toxicity to the host. Treatment with cycloheximide, which inhibits eukaryotic protein synthesis (Burnap and Trench, 1989) and is functionally analogous to chloramphenicol, decreased taurine synthesis in the presence of sulfide, but did not affect sulfide consumption. These results suggest that taurine is synthesized by the host and that the cycloheximide treatment did not affect any sulfide consumption which may occur in host tissues (Powell and Somero, 1986). Exposure to MSX blocked ammonia assimilation, probably contributing to the decreased taurine levels in MSX-treated clams. These results mirror those reported by Lee and coworkers (Lee *et al.*, 1997), who found a direct relationship between external ammonia availability and taurine levels in *S. reidi*.

Hypotaurine levels were not altered by exposure to sulfide or the metabolic inhibitors. These results suggest that hypotaurine is not directly involved in sulfide detoxification, nor is it an intermediate in the taurine synthesis pathway in *S. velum* (Cavallini *et al.*, 1976). Alternatively, hypotaurine could have protective functions, such as by serving as a compatible osmolyte (Yin *et al.*, 2000) or by scavenging free radicals (Huxtable, 1992).

Thiotaurine levels were greater in the gills of sulfide-exposed clams than in non-sulfide-exposed clams, regardless of exposure to metabolic inhibitors. Treatment with chloramphenicol reduced, but did not prevent, sulfide-induced thiotaurine synthesis. This reduction likely resulted from the chloramphenicol-induced cessation of sulfide consumption. Inhibition of host metabolic activity with cycloheximide did not affect thiotaurine levels in sulfide-exposed clams. Thiotaurine may be produced abiotically in host tissues, in which case host enzymatic pathways may not be necessary. Despite the MSX-induced inhibition of ammonia assimilation, thiotaurine levels in MSX-treated clams increased following sulfide exposure. Again, these results suggest that thiotaurine may be produced abiotically from precursors already present in the gill tissue and depend less upon ammonia availability.

#### *Taurine and thiotaurine synthesis in S. velum*

It is not known whether symbiotic bivalves maintain free amino acid pools by absorbing amino acids from the environment or by synthesizing them. We do know that *S. reidi* can take up free amino acids from sediment interstitial water (Lee *et al.*, 1992). However, sulfur-containing amino acids were not detected in the pore water samples from *S. reidi* burrows (Lee *et al.*, 1992) and were not present in the incubation medium in the experiments presented here, suggesting that solemyid clams synthesize taurine and thiotaurine. The biosynthesis pathways of taurine and thiotaurine in solemyid clams are unknown, but the results from this study suggest that these pathways require ammonia assimilation, sulfide consumption, and active symbiont metabolism.

Ammonia is present at elevated levels in the burrow environment of solemyid clams (Lee *et al.*, 1992; Krueger, 1996), and the clams assimilate it into amino acids, which may then serve as precursors for sulfur-containing amino acids (Lee and Childress, 1994). The present study indicates that glutamine synthetase is the primary enzyme in the assimilation pathway, since MSX treatment blocked ammonia uptake and caused ammonia excretion, similar to what was demonstrated in an algal-cnidarian symbiosis (Rees, 1987). The product of ammonia assimilation, glutamate, can then be used as a precursor in the production of taurine, which is a major product of ammonia assimilation in *S. reidi* tissues (Lee *et al.*, 1997; thiotaurine production was not tested for). Therefore, in *S. velum*, taurine and thiotaurine production in response to sulfide, as demonstrated in this study, may be facilitated by the ability of the bacterium-mollusc association to synthesize glutamate from inorganic nitrogen.

Just as glutamate likely contributes organic nitrogen to the synthesis of taurine and thiotaurine, the probable source of organic sulfur is cysteine. All of the demonstrated taurine synthesis pathways in mammalian and invertebrate tissues incorporate cysteine (Jacobsen and Smith, Jr., 1968; Bender, 1975; Bishop *et al.*, 1983; Huxtable, 1992), which apparently cannot be synthesized by molluscs (Bishop *et al.*, 1983). Although some intertidal molluscs utilize external cysteine sources to maintain taurine pools (Allen and Awapara, 1960; Jacobsen and Smith, Jr., 1968; Allen and Garrett, 1972; Bender, 1975), it is unlikely that solemyid clams take up cysteine from their environment (Lee *et al.*, 1992). Therefore, the most likely source of cysteine or other taurine precursors is the symbiotic bacteria. Gram-negative bacteria cannot synthesize hypotaurine, taurine, or thiotaurine (Jacobsen and Smith, Jr., 1968; Huxtable, 1992), but can make cysteine (Kredich, 1996). Cysteine synthesis in *E. coli* requires sulfur in the form of sulfide or thiosulfate (Stauffer, 1996) and assimilated ammonia in the form of glutamate (Reitzer, 1996). Translocation of the essential

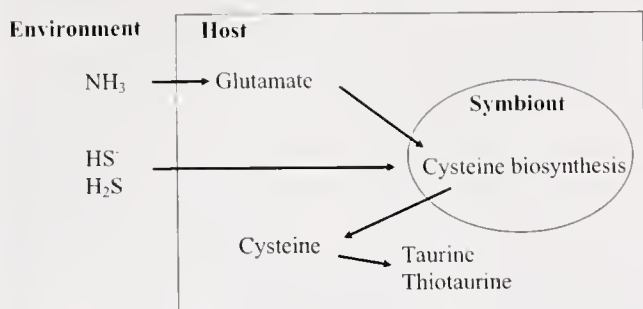


**Figure 3.** Proposed model of taurine and thiotaurine biosynthesis in *Solemya velum*. The clams extract ammonia and sulfides from the burrow environment. Ammonia is assimilated into glutamate, which is probably utilized by the symbionts in cysteine synthesis. Cysteine is translocated to the host and utilized in the synthesis of taurine and thiotaurine.

amino acid cysteine from gram-negative symbionts to host may occur in *S. velum* gill tissue as modeled in Figure 3. Such translocations have been demonstrated in bacteria-aphid and algal-cnidarian associations (Wang and Douglas, 1999; Douglas *et al.*, 2001).

The results of this study suggest that *S. velum* relies upon its symbionts as a source of taurine precursors, as modeled in Figure 3. The inhibition of symbiont metabolism with chloramphenicol, therefore, may equate to a loss of cysteine metabolism, thus decreasing sulfide consumption and taurine and thiotaurine synthesis by the host. Ammonia limitation, either by MSX treatment or reduced exogenous ammonia resources, may limit glutamate availability in *S. velum* tissues, thereby limiting cysteine production in the symbionts (Fig. 3). This could result in the lower taurine levels seen in the solemyid clams in this study and in previous work (Lee *et al.*, 1997). Thus, taurine and thiotaurine may be a link between nitrogen and sulfur cycling in chemoautotrophic symbioses and serve as nontoxic sulfide storage and transport compounds. The absence of similar patterns in nonsymbiotic sulfide-tolerant molluscs (*Geukensia demissa* and *Yoldia limatula*) suggests these functions of sulfur-containing free amino acids may be limited to symbiotic molluscs.

### Acknowledgments

We thank Gerhard Munske of Washington State University for his aid in conducting the amino acid analyses. We also thank David Julian, Stephanie Wohlgemuth, Michael J. Greenberg, and two anonymous reviewers for helpful comments on the manuscript. The Marine Resources Center of the Marine Biological Laboratory at Woods Hole collected all of the clams and provided the information on water temperature. Ray Romjue of the WSU Technical Services constructed the respirometry chambers. This work was funded by grants from the National Science Foundation (IBN0076604) and the National Undersea Research Pro-

gram to R.W.L. and the Western Society of Malacologists to J.L.J.

### Literature Cited

- Atheric, P., and J. Boulegue. 1990. Unusual amino compounds in the tissues of *Calyptogena phaseoliformis* (Japan Trench): possible link to symbiosis. *Prog. Oceanogr.* **24**: 89–101.
- Allen, J. A., and M. R. Garrett. 1971. Taurine in marine invertebrates. *Adv. Mar. Biol.* **9**: 205–253.
- Allen, J. A., and M. R. Garrett. 1972. Studies on taurine in the euryhaline bivalve *Mya arenaria*. *Comp. Biochem. Physiol.* **41A**: 307–317.
- Allen, K., and J. Awapara. 1960. Metabolism of sulfur amino acids in *Mytilus edulis* and *Rangia cuneata*. *Biol. Bull.* **118**: 173–182.
- Anderson, A. E., J. J. Childress, and J. A. Favuzzi. 1987. Net uptake of  $\text{CO}_2$  driven by sulphide and thiosulphate oxidation in the bacterial symbiont-containing clam *Solemya reidi*. *J. Exp. Biol.* **133**: 1–31.
- Bender, D. A. 1975. *Amino Acid Metabolism*. John Wiley & Sons, New York.
- Bishop, S. H., L. L. Ellis, and J. M. Burcham. 1983. Amino acid metabolism in molluscs. Pp. 243–327 in *The Mollusca: Metabolic Biochemistry and Molecular Biomechanics*, P. W. Hochachka, ed. Academic Press, New York.
- Burnap, R. L., and R. K. Trench. 1989. The biogenesis of the cyanellae of *Cyanophora paradoxa*. II. Pulse-labeling of cyanellar polypeptides in the presence of transcriptional and translational inhibitors. *Proc. R. Soc. Lond. B* **238**: 73–87.
- Carrico, R. J., W. E. Blumberg, and J. Peisach. 1978. The reversible binding of oxygen to solfhemoglobin. *J. Biol. Chem.* **253**: 7212–7215.
- Cavallini, D., B. Mondovi, and C. de Marco. 1963. Hypotaurine and thiotaurine. *Biochem. Prep.* **10**: 72–75.
- Cavallini, D., R. Scandurra, S. Dupré, G. Federici, L. Santoro, G. Ricci, and D. Barra. 1976. Alternative pathways of taurine biosynthesis. Pp. 59–66 in *Taurine*, R. J. Huxtable and A. Barbeau, eds. Raven Press, New York.
- Cavanaugh, C. M. 1983. Symbiotic chemoautotrophic bacteria in marine invertebrates from sulphide-rich habitats. *Nature* **302**: 58–61.
- Cavanaugh, C. M. 1994. Microbial symbiosis: patterns of diversity in the marine environment. *Am. Zool.* **34**: 79–89.
- Chien, C.-C., E. R. Leadbetter, and W. Godchaux, III. 1999. *Rhodococcus* spp. utilize taurine (2-aminoethanesulfonate) as sole source of carbon, energy, nitrogen, and sulfur for aerobic respiratory growth. *FEMS Microbiol. Lett.* **176**: 333–337.
- Conway, N. M., and J. E. McDowell Capuzzo. 1992. High taurine levels in the *Solemya velum* symbiosis. *Comp. Biochem. Physiol.* **102B**: 175–185.
- Conway, N. M., B. L. Howes, J. E. McDowell Capuzzo, R. D. Turner, and C. M. Cavanaugh. 1992. Characterization and site description of *Solemya borealis* (Bivalvia: Solemyidae), another bivalve-bacteria symbiosis. *Mar. Biol.* **112**: 601–613.
- Cook, A. M., H. Laue, and F. Junker. 1999. Microbial desulfonation. *FEMS Microbiol. Rev.* **22**: 399–419.
- Denis, W., and L. Reed. 1927. The action of blood on sulfides. *J. Biol. Chem.* **72**: 385–394.
- Doeller, J. E., D. W. Kraus, J. M. Colacino, and J. B. Wittenberg. 1988. Gill hemoglobin may deliver sulfide to bacterial symbionts of *Solemya velum* (Bivalvia, Mollusca). *Biol. Bull.* **175**: 388–396.
- Douglas, A. E., L. B. Minto, and T. L. Wilkinson. 2001. Quantifying nutrient production by the microbial symbionts in an aphid. *J. Exp. Biol.* **204**: 349–358.
- Felbeck, H. 1983. Sulfide oxidation and carbon fixation by the gutless clam *Solemya reidi*: an animal-bacteria symbiosis. *J. Comp. Physiol.* **152B**: 3–11.

- Felbeck, H. 1985.** CO<sub>2</sub> fixation in the hydrothermal vent tube worm *Riftia pachyptila* (Jones). *Physiol. Zool.* **58**: 272–281.
- Felbeck, H., J. J. Childress, and G. N. Somero. 1981.** Calvin-Benson cycle and sulphide oxidation enzymes in animals from sulphide-rich habitats. *Nature* **293**: 291–293.
- Fenchel, T. M., and R. J. Riedl. 1970.** The sulfide system: a new biotic community underneath the oxidized layer of marine sand bottoms. *Mar. Biol.* **7**: 255–268.
- Frey, R. W. 1968.** The Lebensspuren of some common marine invertebrates near Beaufort, North Carolina. I. Pelecypod burrows. *J. Paleontol.* **42**: 570–574.
- Huxtable, R. J. 1992.** Physiological actions of taurine. *Physiol. Rev.* **72**: 101–163.
- Jacobsen, J. G., and L. H. Smith, Jr. 1968.** Biochemistry and physiology of taurine and taurine derivatives. *Physiol. Rev.* **48**: 424–511.
- Julian, D., and A. J. Arp. 1992.** Sulfide permeability in the marine invertebrate *Urechis caupo*. *J. Comp. Physiol.* **162B**: 59–67.
- King, J. E., and J. P. Quinn. 1997.** The utilization of organosulphonates by soil and freshwater bacteria. *Lett. Appl. Microbiol.* **24**: 474–478.
- Kraus, D. W., J. E. Doeller, and J. B. Wittenberg. 1992.** Hydrogen sulfide reduction of symbiont cytochrome *c*<sub>552</sub> in gills of *Solemya reidi* (Mollusca). *Biol. Bull.* **182**: 435–443.
- Kredich, N. M. 1996.** Biosynthesis of cysteine. Pp. 514–527 in *Escherichia coli and Salmonella: Cellular and Molecular Biology*, F. C. Neidhardt, ed. ASM Press, Washington, D.C.
- Krueger, D. M. 1996.** Ecology and evolution of *Solemya* spp., marine bivalves living in symbiosis with chemoautotrophic bacteria. Ph.D. dissertation, Harvard University, Cambridge, MA.
- Lee, P. L. Y., and R. H. Slocum. 1988.** A high-resolution method for amino acid analysis of physiological fluids containing mixed disulfides. *Clin. Chem.* **34**: 719–723.
- Lee, R. W., and J. J. Childress. 1994.** Assimilation of inorganic nitrogen by marine invertebrates and their chemoautotrophic and methanotrophic symbionts. *Appl. Environ. Microbiol.* **60**: 1852–1858.
- Lee, R. W., E. V. Thuesen, and J. J. Childress. 1992.** Ammonium and free amino acids as nitrogen sources for the chemoautotrophic symbiosis *Solemya reidi* Bernard (Bivalvia: Protobranchia). *J. Exp. Mar. Biol. Ecol.* **158**: 75–91.
- Lee, R. W., J. J. Childress, and N. T. Desaulniers. 1997.** The effects of exposure to ammonia on ammonia and taurine pools of the symbiotic clam *Solemya reidi*. *J. Exp. Biol.* **200**: 2797–2805.
- Lee, R. W., J. J. Robinson, and C. M. Cavanaugh. 1999.** Pathways of inorganic nitrogen assimilation in chemoautotrophic bacteria-marine invertebrate symbioses: expression of host and symbiont glutamine synthetase. *J. Exp. Biol.* **202**: 289–300.
- Lovatt Evans, C. 1967.** The toxicity of hydrogen sulphide and other sulphides. *Q. J. Exp. Physiol.* **52**: 231–248.
- Nicholls, P. 1975.** The effect of sulphide on cytochrome *aa3*: isosteric and allosteric shifts of the reduced alpha-peak. *Biochim. Biophys. Acta* **396**: 24–35.
- Pierce, S. K. 1982.** Invertebrate cell volume control mechanisms: a coordinated use of intracellular amino acids and inorganic ions as osmotic solute. *Biol. Bull.* **163**: 405–419.
- Powell, M. A., and A. J. Arp. 1989.** Hydrogen sulfide oxidation by abundant nonhemoglobin heme compounds in marine invertebrates from sulfide-rich habitats. *J. Exp. Zool.* **249**: 121–132.
- Powell, M. A., and G. N. Somero. 1985.** Sulfide oxidation occurs in the animal tissue of the gutless clam, *Solemya reidi*. *Biol. Bull.* **169**: 164–181.
- Powell, M. A., and G. N. Somero. 1986.** Hydrogen sulfide oxidation is coupled to oxidative phosphorylation in mitochondria of *Solemya reidi*. *Science* **233**: 563–566.
- Pranal, V., A. Fiala-Médioni, and J.-C. Colomines. 1995.** Amino acid and related compound composition in two symbiotic mytilid species from hydrothermal vents. *Mar. Ecol. Prog. Ser.* **119**: 155–166.
- Pruski, A. M. 2001.** Carrier of reduced sulfur is a possible role for thiotaurine in symbiotic species from hydrothermal vents with thiotrophic symbionts. *Hydrobiologia* **461**: 9–13.
- Pruski, A. M., A. Fiala-Médioni, and J.-C. Colomines. 1997.** High amounts of sulphur-amino acids in three symbiotic mytilid bivalves from deep benthic communities. *C. R. Acad. Sci. Paris.* **320**: 791–796.
- Pruski, A. M., A. Fiala-Médioni, R. Prudon, and J.-C. Colomines. 2000.** Thiotaurine is a biomarker of sulfide-based symbiosis in deep-sea bivalves. *Limnol. Oceanogr.* **45**: 1860–1867.
- Rau, G. H. 1981.** Hydrothermal vent clam and tube worm <sup>13</sup>C/<sup>12</sup>C: further evidence of nonphotosynthetic food sources. *Science* **213**: 338–339.
- Rees, T. A. V. 1987.** The green hydra symbiosis and ammonium. I. The role of the host in ammonium assimilation and its possible regulatory significance. *Proc. R. Soc. Lond. B.* **229**: 299–314.
- Reichenhecher, W., and J. C. Murrell. 1999.** Linear alkanesulfonates as carbon and energy sources for gram-positive and gram-negative bacteria. *Arch. Microbiol.* **171**: 430–438.
- Reitzer, L. J. 1996.** Ammonia assimilation and the biosynthesis of glutamine, glutamate, aspartate, asparagine, L-alanine, and D-alanine. Pp. 391–407 in *Escherichia coli and Salmonella: Cellular and Molecular Biology*, F. C. Neidhardt, ed. ASM Press, Washington, D.C.
- Rice, M. A., and G. C. Stephens. 1988.** Influx, net flux and transepithelial flux of amino acids in the hardshell clam *Mercenaria mercenaria* (Linne): influence of salinity. *Comp. Biochem. Physiol.* **89A**: 631–636.
- Ruby, E. G., C. O. Wirsén, and H. W. Jannasch. 1981.** Chemolithotrophic sulfur-oxidizing bacteria from the Galápagos Rift hydrothermal vents. *Appl. Environ. Microbiol.* **42**: 317–324.
- Seitz, A. P., E. R. Leadbetter, and W. Godchaux, III. 1993.** Utilization of sulfonates as sole sulfur sources by soil bacteria including *Comamonas acidovorans*. *Arch. Microbiol.* **159**: 440–444.
- Smiley, D. W., and B. J. Wilkinson. 1983.** Survey of taurine uptake and metabolism in *Staphylococcus aureus*. *J. Gen. Microbiol.* **129**: 2421–2428.
- Southward, A. J., E. C. Southward, P. R. Dando, G. H. Rau, H. Felbeck, and H. Flügel. 1981.** Bacterial symbionts and low <sup>13</sup>C/<sup>12</sup>C ratios in tissues of *Pogonophora* indicate unusual nutrition and metabolism. *Nature* **293**: 616–620.
- Stapley, E. O., and R. L. Starkey. 1970.** Decomposition of cysteine acid and taurine by soil micro-organisms. *J. Gen. Microbiol.* **63**: 77–84.
- Stauffer, G. V. 1996.** Biosynthesis of serine, glycine, and one-carbon units. Pp. 506–513 in *Escherichia coli and Salmonella: Cellular and Molecular Biology*, F. C. Neidhardt, ed. ASM Press, Washington, D.C.
- Svenson, A. 1980.** A rapid and sensitive spectrophotometric method for determination of hydrogen sulfide with 2,2'-dipyridyl disulfide. *Anal. Biochem.* **107**: 51–55.
- Wang, J. T., and A. E. Douglas. 1999.** Essential amino acid synthesis and nitrogen recycling in an alga-invertebrate symbiosis. *Mar. Biol.* **135**: 219–222.
- Willason, S. W., and K. S. Johnson. 1986.** A rapid, highly sensitive technique for the determination of ammonia in seawater. *Mar. Biol.* **91**: 285–290.
- Yancey, P. H., M. E. Clark, S. C. Hand, R. D. Bowlus, and G. N. Somero. 1982.** Living with water stress: evolution of osmolyte systems. *Science* **217**: 1214–1222.
- Yin, M., H. R. Palmer, A. L. Fyfe-Johnson, J. J. Bedford, R. A. J. Smith, and P. H. Yancey. 2000.** Hypotaurine, N-methyltaurine, taurine, and glycine betaine as dominant osmolytes of vestimentiferan tubeworms from hydrothermal vents and cold seeps. *Physiol. Biochem. Zool.* **73**: 629–637.

# Localization of a Symbiosis-Related Protein, Sym32, in the *Anthopleura elegantissima*–*Symbiodinium muscatinei* Association

J. A. SCHWARZ\* AND V. M. WEIS

*Department of Zoology, 3029 Cordley Hall, Oregon State University, Corvallis, Oregon 97331*

**Abstract.** Cnidarian–dinoflagellate symbioses are widespread in the marine environment. Growing concern over the health of coral reef ecosystems has revealed a fundamental lack of knowledge of how cnidarian–algal associations are regulated at the cellular and molecular level. We are interested in identifying genes that mediate interactions between the partners, and we are using the temperate sea anemone *Anthopleura elegantissima* as a model. We previously described a host gene, *sym32*, encoding a fasciclin domain protein, that is differentially expressed in symbiotic and aposymbiotic *A. elegantissima*. Here, we describe the subcellular localization of the *sym32* protein. In aposymbiotic (symbiont-free) hosts, *sym32* was located in vesicles that occur along the apical edges of gastrodermal cells. In symbiotic hosts, such vesicles were absent, but *sym32* was present within the symbiosome membranes. Sym32 (or a cross-reactive protein) was also present in the accumulation bodies of the symbionts. Although the anti-*sym32* antiserum was not sufficiently specific to detect the target protein in cultured *Symbiodinium bermudense* cells, Western blots of proteins from two *Symbiodinium* species revealed a protein doublet of 45 and 48 kDa, suggesting that the symbionts may also produce a fasciclin domain protein. We suggest that host *sym32* is relocated from gastrodermal vesicles to the symbiosome membrane when symbionts are taken into host cells by phagocytosis.

## Introduction

Intracellular associations between eukaryotic microorganisms and animal hosts encompass a wide range of interactions ranging from parasitic to mutualistic. Most eukaryotic microbes that infect animals reside within a membrane-bound vacuole within the cytoplasm of host cells (Hackstadt, 2000). The formation of the vacuole is a dynamic process that is initiated either by active invasion of the host cell by the microbe—for example, the parasite *Toxoplasma* (Dobrowolski and Sibley, 1996)—or by phagocytic uptake of the microbe by the host cell—for example, the parasite *Leishmania* (Courret *et al.*, 2002) and the symbiont *Symbiodinium* (Fitt and Trench, 1983).

Studies on eukaryotic microbial parasites show that, in the vast majority of cases, the nascent vacuole that contains the microbe fails to continue through the complete endocytic pathway that culminates in acidification of the vacuole and fusion with lysosomes. Instead, the microbial inhabitant actively interferes with one or more steps in the normal process of fusion between the vacuole and endocytic organelles that direct the vacuole through the phagocytic process (Mellman, 1996). The result is that the microbe successfully transforms what would have been a phagolysosome into a compartment that is hospitable for growth, replication, or differentiation into various life-history stages (Hackstadt, 2000; and for examples, see Mukkada *et al.*, 1985; Sinai and Joiner, 1997).

In the marine environment, associations between animals and eukaryotic microbes include mutualistic as well as parasitic interactions. One prevalent mutualistic association occurs between cnidarians (most commonly sea anemones and corals) and photosynthetic dinoflagellates (usually *Symbiodinium* spp.). These associations are characterized by reciprocal nutritional interactions between host and

Received 14 April 2003; accepted 27 August 2003.

\* To whom correspondence should be addressed. Current address: Department of Microbiology and Immunology, D305 Fairchild Building, 299 Campus Drive, Stanford University, Stanford, CA 94305. E-mail: jschwarz@stanford.edu

symbiont (Falkowski *et al.*, 1984; Muller-Parker and D'Elia, 1998). The photosynthetic symbionts contribute glycerol and other organic compounds to host metabolism (Lewis and Smith, 1971; Battey and Patton, 1987; Muscatine, 1992), and the host contributes nitrogen (Wang and Douglas, 1998, 1999) and carbon dioxide (Weis, 1993) for algal photosynthesis. These associations occur in the photic zones of both temperate and tropical benthic habitats, and they thrive in nutrient-poor tropical marine environments because they conserve and recycle nutrients.

In its associations with dinoflagellates, the host cnidarian most commonly houses symbionts within gastrodermal cells, in a vacuole of phagosomal origin. The initial infection, during which the dinoflagellate symbionts are internalized, typically occurs when dinoflagellates that enter the host's mouth are taken into phagocytic gastrodermal cells that line the gastric cavity (Colley and Trench, 1983; Fitt and Trench, 1983; Schwarz *et al.*, 1999, 2002). The phagosome, through unknown mechanisms, fails to fuse with lysosomes (Fitt and Trench, 1983), and the dinoflagellates remain undigested within the vacuole. Ultimately, the dinoflagellates reside within a compartment delineated by multiple membranes (Taylor, 1968, 1987; Wakefield *et al.*, 2000). Historically, the origin of the multiple membranes that surround the symbiont has been uncertain. Recently, immunolocalization studies using host-specific and dinoflagellate-specific monoclonal antibodies suggest that only the outermost membrane originates from the host, and all of the inner membranes originate from the dinoflagellates, perhaps accumulating from repeated cycles of ecdysis within the host vacuole (Wakefield and Kempf, 2001).

We have been interested in identifying host genes that play roles in symbiotic interactions in cnidarian–dinoflagellate symbioses (Weis and Levine, 1996; Weis and Reynolds, 1999; Reynolds *et al.*, 2000). We have used as a model system the temperate symbiotic sea anemone *Anthopleura elegantissima* (Brandt, 1835), which is abundant in the intertidal region of the eastern Pacific, from Mexico through Alaska. This species is able to form associations with two species of dinoflagellates, *Symbiodinium californium* and *S. muscatinei*. The presence of one or more of the symbionts within a particular host depends upon microhabitat differences that are created along temperature and light gradients that occur along latitudinal and intertidal ranges. Along the Oregon coast, most hosts contain only a single symbiont, *S. muscatinei* (LaJeunesse and Trench, 2000).

Using biochemical and molecular approaches, we have identified a number of host genes that are likely to function in mediating host-symbiont interactions (Reynolds *et al.*, 2000; Weis and Levine, 1996; Weis and Reynolds, 1999). One of these, *sym32*, encodes a protein that belongs to a class of cell adhesion proteins called fasciadin domain proteins (Reynolds *et al.*, 2000). Fasciadin domain proteins share low overall sequence identity, but all possess between

one and four repeats of three highly conserved "fasciadin" domains that are believed to function as adhesive domains in cell–cell and cell–extracellular matrix interactions (Hu *et al.*, 1998). Members of this family have been identified in organisms as diverse as mycobacteria (Harboe and Nagai, 1984; Harboe *et al.*, 1995; Terasaka *et al.*, 1989), *Volvox* (Huber and Sumper, 1994), insects (Zinn *et al.*, 1988), sea urchins (Brennan and Robinson, 1994), and humans (Skonier *et al.*, 1992; Takeshita *et al.*, 1993).

To further investigate the role played by *sym32* in symbiotic interactions between cnidarian hosts and dinoflagellate symbionts, we used immunocytochemical techniques to examine the distribution of the *sym32* protein within the *A. elegantissima*–*S. muscatinei* association. In this paper we demonstrate that *sym32* protein is differentially distributed in symbiotic and aposymbiotic *A. elegantissima* both at the cellular and subcellular level. Of particular interest, *sym32* antiserum labels the multiple layers of membrane that surround the symbiont within the host cell. We also show that anti-*sym32* antiserum specifically labels the accumulation body of dinoflagellates residing within host gastroderm. Western blots of proteins from two *Symbiodinium* species revealed a protein doublet of 45 and 48 kDa (45/48 kDa) that cross reacts with the *sym32* antiserum; but in immunolocalization studies, the antiserum was insufficiently specific to detect the target protein in cultured specimens of *S. bermudense*. Possibly, both the host and symbiont produce fasciadin domain proteins that interact *via* the fasciadin adhesive domain.

## Materials and Methods

### Animal maintenance

Symbiotic and aposymbiotic specimens of *A. elegantissima* were collected at low tide from the intertidal zone at Seal Rock, Oregon. Aposymbiotic anemones were taken from under rock overhangs or crevices where there was little or no light to support the growth of symbiotic dinoflagellates. Symbiotic anemones were taken from the open rock benches that are exposed to light. Anemones were transported to the laboratory, where they were maintained in an 11 °C recirculating seawater aquarium on a 12:12 h light:dark cycle. Anemones were fed previously frozen adult brine shrimp about once a week.

### Light-level immunocytochemistry

*Anemones.* Tentacles from both symbiotic and aposymbiotic specimens of *A. elegantissima* were clipped and immediately transferred to tissue freezing medium (Triangle Biomedical Sciences) and frozen at –80 °C. Tentacles were cryosectioned at –20 °C on a Reichert-Jung cryostat (20- $\mu$ m sections) and placed on polylysine slides, then immersed in 4% paraformaldehyde fixative in phosphate

buffered saline (PBS: 10 mM phosphate buffer, pH 7.2, + 150 mM NaCl) for 1.5 h. Sections on slides were rinsed three times, 5 min each time, in PBS with 0.5% BSA; dehydrated in a methanol series (25%, 50%, 75%, 100%, 75%, 50%, 25%); and rinsed again in PBS/BSA. Sections were incubated in a blocking solution of 1:200 dilution of goat serum:PBS/BSA for 30 min at room temperature and then rinsed three times, 5 min each time, in PBS/BSA. Slides were incubated for 1 h in either a 1:2000 dilution of sym32 antiserum from rabbit (antibody development described in Reynolds *et al.*, 2000) in PBS/BSA or in a 1:2000 dilution of preimmune serum from the same rabbit. Sections were rinsed three times, 5 min each time, in PBS/BSA and then incubated for 1 h in a 1:200 dilution of goat anti-rabbit IgG–5-nm colloidal gold conjugate (Ted Pella). Slides were rinsed as above. Gold particle labeling was silver-enhanced using a silver enhancement kit (Ted Pella). To stop color development, slides were washed in ePure water. Coverslips were affixed with a glycerol mount and sealed with fingernail polish.

*Cultured Symbiodinium bermudense cells.* Immunofluorescence was used to investigate whether the symbiont-produced 45/48 kDa cross-reactive protein (identified from Western blots, described below) could be localized to symbionts free from host cells. Cells of *S. bermudense* (CCMP830) were grown in sterile filtered seawater enriched with f/2-Si media at about 100  $\mu$ E light on a cycle of 12 h light to 12 h dark at 25 °C. Cells were collected by centrifugation from liquid media and resuspended into 3% paraformaldehyde in PBS. After fixation for 30 min, cells were given two 10-min washes in PBS and transferred to PBS. Cells were incubated 30 min in blocking solution (PBS + 3% BSA); 30 min in PBS/BSA/0.2% Triton X-100; 1 h in preimmune serum or anti-sym32 antiserum diluted with PBS/BSA/Triton X to 1:50, 1:200, 1:2000; 5 min in PBS, repeated five times; 1 h in 1:200 Alexa Fluor 488 goat anti-rabbit IgG in PBS/BSA; and 5 min in PBS, repeated five times. After incubation, the cells were viewed under an Olympus BX-60 fluorescence microscope.

#### *EM-level immunocytochemistry*

*Anemones.* Immunocytochemistry was performed on three occasions using symbiotic anemones collected at different times and on one aposymbiotic anemone. Tentacles from aposymbiotic and symbiotic anemones were clipped and immersed in 1% paraformaldehyde, 1% glutaraldehyde fixative in PBS for 1.5 h. Tentacles were rinsed three times, 10 min each time, in PBS and then dehydrated for 15 min in each concentration of a methanol (MeOH) series (15%, 30%, 50%, 85%, 95%, 100%, 100%). Tentacles were infiltrated with LR White resin on a rotating table in a series of MeOH dilutions (1:3 LR White:MeOH overnight, 1:1 overnight, 100% LR White for 3 h), and then placed in gelatin

capsules in fresh LR White. LR White was allowed to polymerize at 52 °C for 2 days.

Ultra-thin, gold–silver sections were cut with a diamond knife and placed onto Formvar-coated nickel grids. These grids were processed for immunocytochemistry as follows: they were immersed in blocking solution (PBS + 5% BSA) for 15 min, incubated in a 1:1000 dilution of sym32 antiserum or a 1:1000 dilution of preimmune serum in PBS for 1.5 h, rinsed 3 times, 10 min each time, in PBS/BSA + 0.1% Tween 20, incubated in a 1:75 dilution of EM grade goat anti-rabbit IgG–15-nm colloidal gold (Ted Pella) in PBS for 1 h, rinsed as above, rinsed in ePure water for 5 min, and then allowed to dry. Grids were stained in 2% uranyl acetate for 5 min, rinsed by dipping in water 10 times each in three changes of water, then immediately stained in 0.4% lead acetate for 3 min, with water rinses as above, and then air dried. Between 5 and 10 grids of each type of anemone were viewed under 60 kV using a CM-12 Phillips transmission electron microscope.

*Cultured Symbiodinium bermudense cells.* Cells were collected as described in the light microscopy section, fixed as described for anemone tentacles, and processed essentially as described for anemone tentacles. Several dilutions of anti-sym32 antiserum and preimmune serum were tested (1:10, 1:50, 1:200, 1:500, 1:1000, 1:2000), as well as various dilutions of either Tween-20 or Triton X (0%, 0.1%, 1%) in the following solutions: blocking solution, primary antibody solution, wash solution.

#### *Preparation of anemone and dinoflagellate proteins: one- and two-dimensional SDS-PAGE and Western analysis*

Proteins were isolated from the host as follows: a host anemone was removed from an 11 °C recirculating aquarium and flash-frozen in liquid nitrogen. The anemone was minced with a razor blade, and placed into a glass grinder with a Teflon pestle driven by a hand drill in four volumes ice-cold grinding buffer (100 mM Tris, 100 mM NaCl, 10 mM EDTA) with protease inhibitors (Sigma: 5  $\mu$ l per 10 ml buffer). The homogenate was placed into a centrifuge tube and the grinder was rinsed with two volumes of buffer (v:w anemone tissue), which was added to the tube and mixed well. The remaining homogenate was centrifuged at 16,000  $\times$  g for 10 min at 4 °C to remove algal cells and host cell debris and membranes from the homogenized anemone tissue. The supernatant was removed to a new tube and centrifuged again. Protein concentration was determined on this cleared homogenate using the Bradford assay (Pierce Coomassie reagent). Host proteins prepared according to this protocol are free from contamination by symbiont proteins (Weis and Levine, 1996).

Proteins were isolated from symbionts that had been either continuously maintained in culture with no host contact for many generations or freshly isolated from an

*A. elegantissima* host. Many species of *Symbiodinium* can be isolated from their hosts and brought into culture in nutrient-supplemented seawater. These symbionts are therefore free from any host cell contact. We obtained frozen pelleted symbionts from cultures of *S. bermudense*, which was originally isolated from the tropical sea anemone *Aiptasia pallida*. A chunk of the pelleted symbionts (about 100  $\mu$ l in volume) was briefly ground in a glass tissue grinder with a Teflon pestle in an equal volume of grinding buffer with a protease inhibitor cocktail. Examination under a light microscope revealed that nearly all symbionts were still intact after this step. An equal volume of acid-rinsed glass beads (Sigma: 425–600  $\mu$ m) was added and the mixture alternately vortexed for 15–30 s and placed on ice for about 30 s, for a total of 20 times. With repeated vortexing, the homogenate became intensely orange, likely indicating the release of the major water-soluble accessory pigment, peridinin-chlorophyll protein. By this means, at least 75% of symbionts were broken open, as determined by light microscopy. With a syringe and a 24-gauge needle, the homogenate was removed from the glass beads and centrifuged at  $16,000 \times g$  for 10 min at 4 °C to remove cellular debris. The supernatant was placed into a new tube and again centrifuged. This cleared supernatant fraction was then assayed for protein concentration, as described above, and then prepared for one-dimensional or two-dimensional SDS-PAGE, as described below.

Proteins from freshly isolated symbionts were prepared by isolating symbionts from a host and then extracting proteins using glass beads to fracture the symbiont cell wall and release the contents of the cytoplasm. A host anemone weighing about 2 g was removed from an 11 °C recirculating aquarium and flash-frozen in liquid nitrogen. The anemone was minced with a razor blade and placed into a glass grinder with 3 ml of grinding buffer plus protease inhibitor. All subsequent steps were performed on ice. The anemone was ground with a Teflon pestle instead of a ground glass pestle to homogenize the animal tissues without shearing the cell walls of the symbionts. This homogenate was centrifuged at  $2000 \times g$  for 10 min to pellet the symbionts. The pellet, about 300  $\mu$ l in volume, was partially cleaned of anemone debris by regrinding the pellet in grinding buffer using a glass tissue grinder with a Teflon pestle (this regrinding step was sufficient to break up the pellet, but not break open the symbionts) and reconcentrating the symbionts by centrifugation. The partially cleaned pellet was ground a final time before adding 500  $\mu$ l of buffer with protease inhibitor cocktail and an equal volume of prerinsed glass beads. This resuspended pellet contained a significant amount of host tissue, as revealed by the presence of numerous nematocysts. We then followed the same vortexing and centrifugation protocol as described above. The cleared supernatant fraction (intensely orange in color) was used for one-dimensional SDS-PAGE, as described below.

One-dimensional SDS-PAGE with 10% Nu-PAGE Bis-Tris gels (Invitrogen) was performed on proteins from host tissue and from freshly isolated, and cultured symbiont proteins. Samples were denatured and prepared for electrophoresis using LDS buffer + DTT (Invitrogen) according to manufacturer's instructions; 10  $\mu$ g of protein was loaded for each sample. Electrophoresis was performed in MOPS buffer according to the manufacturer's instructions. Gels were transferred to 12.5 mM Tris, 100 mM glycine, 10% MeOH for 20 min, and proteins were electrophoretically transferred onto nitrocellulose membrane for 1.25 h at 100 V in a BioRad chamber.

Two-dimensional SDS-PAGE was performed using proteins extracted from freshly isolated symbionts. Proteins were extracted as described above, except that no NaCl was used in the buffer, as salt interferes with isoelectric focusing. The SDS-PAGE was carried out on a Multiphor II system (Amersham Pharmacia), according to the manufacturer's instructions and as described in Reynolds *et al.* (2000). Thirty microliters of symbiont homogenate containing 60  $\mu$ g of protein was used for isoelectric focusing on an 180-mm IPG strip, pH 3–10. After isoelectric focusing, the IPG strip was equilibrated and placed on a 12% ExcelGel; electrophoresis was performed according to manufacturer's instructions. After electrophoresis, the gel was placed into transfer buffer (50 mM Tris, 40 mM glycine, 0.04% SDS, 20% methanol) for 20 min. The gel was removed from the plastic backing, and proteins were transferred to a nitrocellulose membrane under a discontinuous buffer system (Multiphor II system from Amersham).

For Western analysis, the membranes from one- and two-dimensional SDS-PAGE were incubated at 4 °C overnight in blocking buffer (TBS: 20 mM Tris, 500 mM NaCl, Ph 7.5, + 5% powdered milk + 0.1% Tween-20). The following morning, the membrane was washed for 15 min in TBS + 0.5% Tween-20 (TBST); incubated for 45 min in a 1:1500 dilution of anti-sym32 antiserum: block buffer; rinsed 10 min each in TBS, TBST, TBS; incubated 45 min in a 1:5000 dilution of HRP-antirabbit IgG (Amersham Pharmacia); and washed as before. Sym32 protein was detected by chemiluminescence using ECL detection reagents (Amersham Pharmacia) and exposing membranes to film for 1 min.

## Results

### *Microscopy of anemone tentacles*

*Cryosectioned tentacles.* Cryosectioned tentacles of aposymbiotic and symbiotic anemones were incubated with (1) preimmune serum as a negative control for endogenous staining or (2) sym32 antiserum. Staining for sym32 in aposymbiotic tentacles was distinct from that in symbiotic tentacles, relative to preimmune controls (Fig. 1). In both symbiotic and aposymbiotic tentacles, preimmune controls

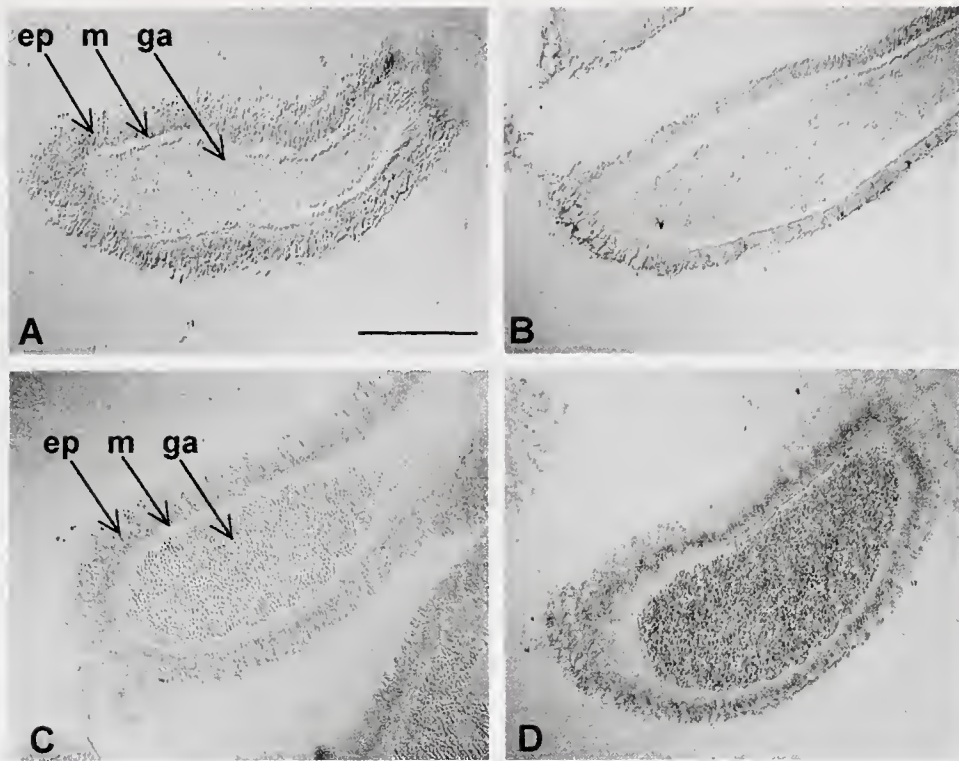


**Figure 1.** Light micrographs showing immunolocalization of sym32 protein within cryosections of tentacles from aposymbiotic (A and B) and symbiotic (C and D) *Anthopleura elegantissima*. The spherical symbionts can be clearly seen within the gastroderm of symbiotic tentacles. Sections were incubated in either preimmune serum (A and C) or sym32 anti-serum (B and D), and sym32 was visualized using silver enhancement of colloidal gold labeling. Sym32 levels are high in the gastrodermis of symbiotic anemones, low in the gastrodermis of aposymbiotic anemones, faint in the epidermis of both types of anemones, and absent in the mesoglea of both types of anemones. Host tissue layers are marked as ep = epidermis, ga = gastrodermis, m = mesoglea. Scale bar = 0.3 mm for all panels.

showed light brown staining in epidermal and gastrodermal tissues, and no staining in the mesoglea. In aposymbiotic tentacles incubated in sym32 antiserum, staining in the epidermal and gastrodermal layers was slightly darker than in the preimmune controls. In symbiotic tentacles, staining in the epidermis was also slightly darker than in the preimmune controls, and in the gastrodermis, where dinoflagellates are housed, it was significantly darker. The mesogleal layer of both aposymbiotic and symbiotic tentacles remained unstained.

**Electron microscopy.** To further examine the location of sym32 within the host-symbiont association, we performed EM-level colloidal gold immunocytochemistry using sym32 antiserum to label the sym32 protein within thin sections of resin-embedded tentacles from one aposymbiotic and three symbiotic anemones (Figs. 2–4). We examined between 15 and 25 sections from each anemone. We also performed negative controls with preimmune serum to check for non-specific labeling of the tissues. In all cases, the preimmune controls were almost completely free of gold-sphere labeling (data not shown).

In aposymbiotic tentacles, sym32 gold-sphere labeling was associated exclusively with medium-density vesicles located within both epidermal and gastrodermal cells (Fig. 2). There was no evidence of any sym32 label within the mesogleal layer, and the pattern of distribution of the sym32-containing vesicles in the epidermal cells was distinct from that in the gastrodermis. The vesicles were relatively uncommon in the epidermis (Fig. 2A, B) but more abundant in the gastrodermis, where they were concentrated along the apical end of the gastroderm, near the interface between the gastroderm and the gastric cavity (Fig. 2C, D).

In symbiotic tentacles, the pattern of distribution in the epidermis was the same as in aposymbiotic tentacles; sym32 gold-sphere labeling was contained within vesicles that were relatively sparsely distributed, most commonly occurring near nematocysts. In contrast, the distribution of sym32 within the gastrodermis was dramatically different. The sym32-containing vesicles that were so abundant in aposymbiotic gastroderm were not present in symbiotic gastroderm. Instead, the sym32

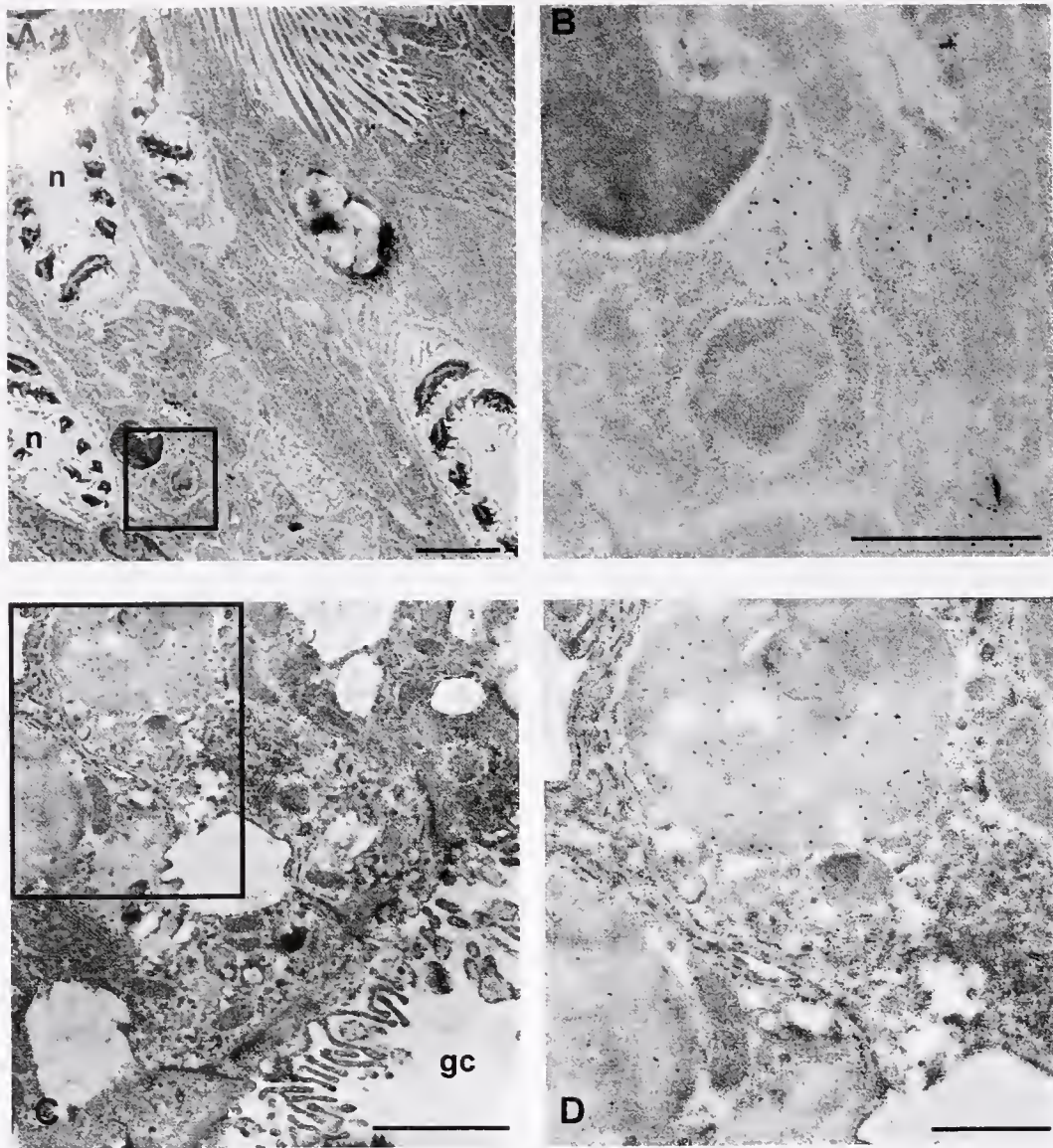


**Figure 2.** Transmission electron micrographs of immunogold-labeled sections from tentacles of aposymbiotic anemones. Gold spheres, visible as black dots, indicate the presence of sym32. (A) Epidermal cells with nematocysts (n). (B) Enlargement of the boxed section of A, with gold spheres labeling vesicles located near nematocysts. (C) Gastrodermal cells adjacent to the gastric cavity (gc). (D) Enlargement of the boxed section of C, showing gold spheres within vesicles in the gastrodermal cells. Scale bars = 2  $\mu\text{m}$  (A, C) and 1  $\mu\text{m}$  (B, D).

label was associated with the multiple membranes that enclose the dinoflagellate symbiont within the host cell (Fig. 3A, B). Gold spheres were diffusely arranged within these membranes, not clearly associated with any single membrane layer. To confirm that this labeling was specific to the membranous layers, we quantified the staining relative to areas outside the membranes. The membranous layers contained an average of  $12.2 \pm 4.65$  (SD),  $n = 19$ , while equivalent areas outside the membranous layers contained an average of  $1.0 \pm 1.1$ ,  $n = 19$ .

*Symbiodinium within host cells.* In addition to the sym32 labeling within the membranes that surround the symbionts, there was a significant amount of labeling within the symbionts themselves (Fig. 4). Specifically, gold spheres were located within the accumulation body, a poorly described organelle that is believed to function in the endocytic pathways of dinoflagellates. The density of labeling within the accumulation bodies was highly variable: some contained only a few gold spheres, while others contained hundreds (average =  $56.4 \pm 83.2$  [SD] gold spheres/ $\mu\text{m}^2$ ,  $n = 18$ ).

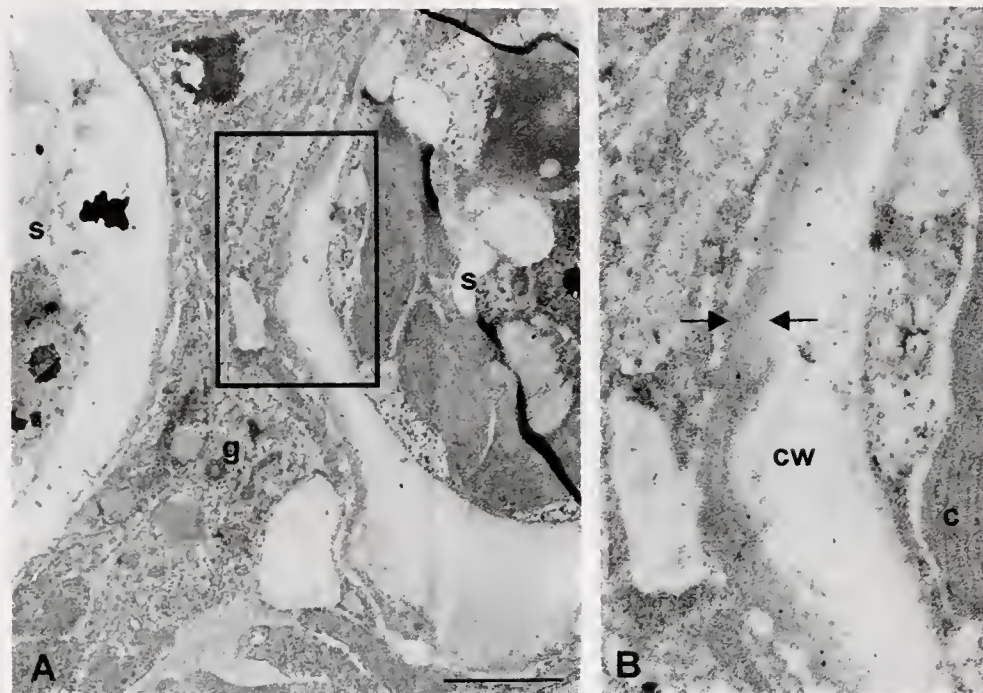


**Figure 3.** Transmission electron micrographs of immunogold-labeled sections of tentacles from symbiotic *Anthopleura elegantissima*. (A) Illustrates the presence of dinoflagellates within host gastrodermal cells. (B) Enlargement of boxed area in A, showing gold spheres associated with the multiple layers of membrane that surround the dinoflagellates. The arrows delineate the margins of the multiple membranes surrounding the dinoflagellate. Preimmune controls showed virtually no gold-sphere labeling (not shown). c = symbiont chloroplast, cw = symbiont cell wall, g = gastrodermal cell of the host, s = dinoflagellate symbiont. Scale bar = 2  $\mu$ m.

### Western blots

The presence of gold-sphere label within the accumulation bodies of the symbionts suggested that the symbionts were producing a sym32 homolog. We performed Western analysis using anti-sym32 antiserum to look for cross-reactive proteins in homogenates from symbionts freshly removed from a host anemone and from cultured symbionts that were not in contact with host cells. Anti-sym32 Western blots of one-dimensional gels from homogenates of freshly isolated *Symbiodinium muscatinei* revealed three bands (Fig. 5A, lane 2). The 32-kDa band, identical in size to a band in host-only homogenate (lane 1), is probably due to contamination from host sym32. This was expected, as protein preparations of the symbionts are invariably contaminated by host proteins (Weis *et al.*, 1998). A 48-kDa band and a faint 45-kDa band below it suggest the presence of cross-reactive proteins that are produced by the symbionts. Homogenates of cultured algae (*Symbiodinium bermudense*) that were never in contact with host tissues (lane 3) also contained the same 45/48-kDa doublet but lacked the 32-kDa host band. Western blots of two-dimensional gels of freshly isolated *S. muscatinei* homogenates revealed two spots

with distinctly different molecular weights and isoelectric points (pI) (Fig. 5B). A cross-reactive spot at 32 kDa, 8.2 pI, corresponds exactly with host sym32 (Reynolds *et al.*, 2000), and again is probably due to host contamination. In addition there was a 48-kDa spot with a pI range of 4.3 to 4.5. The 45/48-kDa protein doublet that is present in cultured *S. bermudense* and in *S. muscatinei* freshly harvested from a host, and is also faintly visible in the host lane, therefore represents a protein produced by *Symbiodinium* both when it is in symbiosis with a host, and when it is free-living.

### Microscopy of cultured *Symbiodinium bermudense* cells

We were interested in determining the location of the symbiont-produced 45/48-kDa protein doublet. We therefore used the anti-sym32 antiserum (which was developed against recombinant host sym32 protein), to localize the target protein in cultured specimens of *S. bermudense*. We used two immunolocalization methods. For intact cells, we used immunofluorescence, in which a fluorescent secondary antibody is detected by fluorescence microscopy. For sectioned cells, immunoelectron microscopy allowed us to detect any patterns in staining

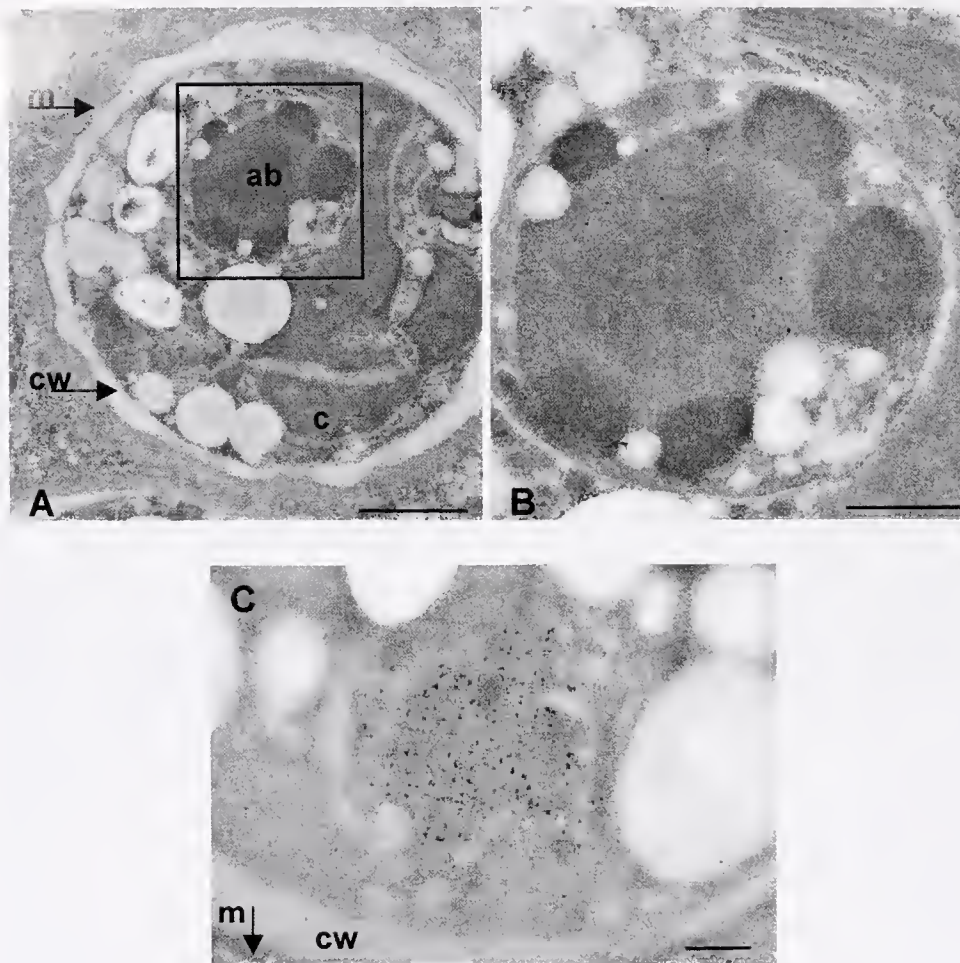


**Figure 4.** Transmission electron micrographs of immunogold-labeled sections of dinoflagellate symbionts contained within host gastrodermal cells. (A) Dinoflagellate contained within a host gastrodermal cell. (B) Enlargement of the accumulation body, shown boxed in A, illustrating sparse gold labeling of the dinoflagellate accumulation body. (C) Region around the accumulation body of another symbiont (section not counterstained) showing intense labeling specific to the accumulation body. The cell wall (cw) and membrane layers (m) are visible as concentric gray rings around the symbiont. Sections incubated with preimmune serum showed virtually no gold-sphere labeling (data not shown). m = membranes surrounding the dinoflagellate, cw = dinoflagellate cell wall, c = dinoflagellate chloroplast, ab = accumulation body of the dinoflagellate. Scale bar = 2.5  $\mu\text{m}$  (A), 1.0  $\mu\text{m}$  (B, C).

at the subcellular level. Despite testing many concentrations of antiserum and buffer solutions, we were unable to detect a pattern of staining of the target protein in cultured cells of *S. bermudense*. With the immunofluorescence method, preimmune controls looked identical to antiserum-incubated specimens at all dilutions of serum that we tested. With immunoelectron microscopy, we could detect no specific staining to any particular compartment within the cell, even though the background staining varied from almost no gold-sphere labeling at the 1:2000 dilutions to heavy labeling at the 1:10 dilutions. In the preimmune controls, labeling was restricted to a few, widely scattered spheres.

## Discussion

The sym32 protein is distributed among different subcellular compartments in symbiotic and aposymbiotic anemones. Most notably, the sym32-containing vesicles that are so abundant in the gastroderm of aposymbiotic hosts are absent from symbiotic hosts; instead, sym32 localizes to the symbiosome membranes. This suggests that the internalization of symbionts is accompanied by a transfer of sym32 from gastrodermal vesicles to the symbiosome membranes. This would most likely occur during phagocytic uptake of the symbiont, by fusion of the sym32 vesicles with the phagosome.

The presence of sym32 within the dinoflagellates them-

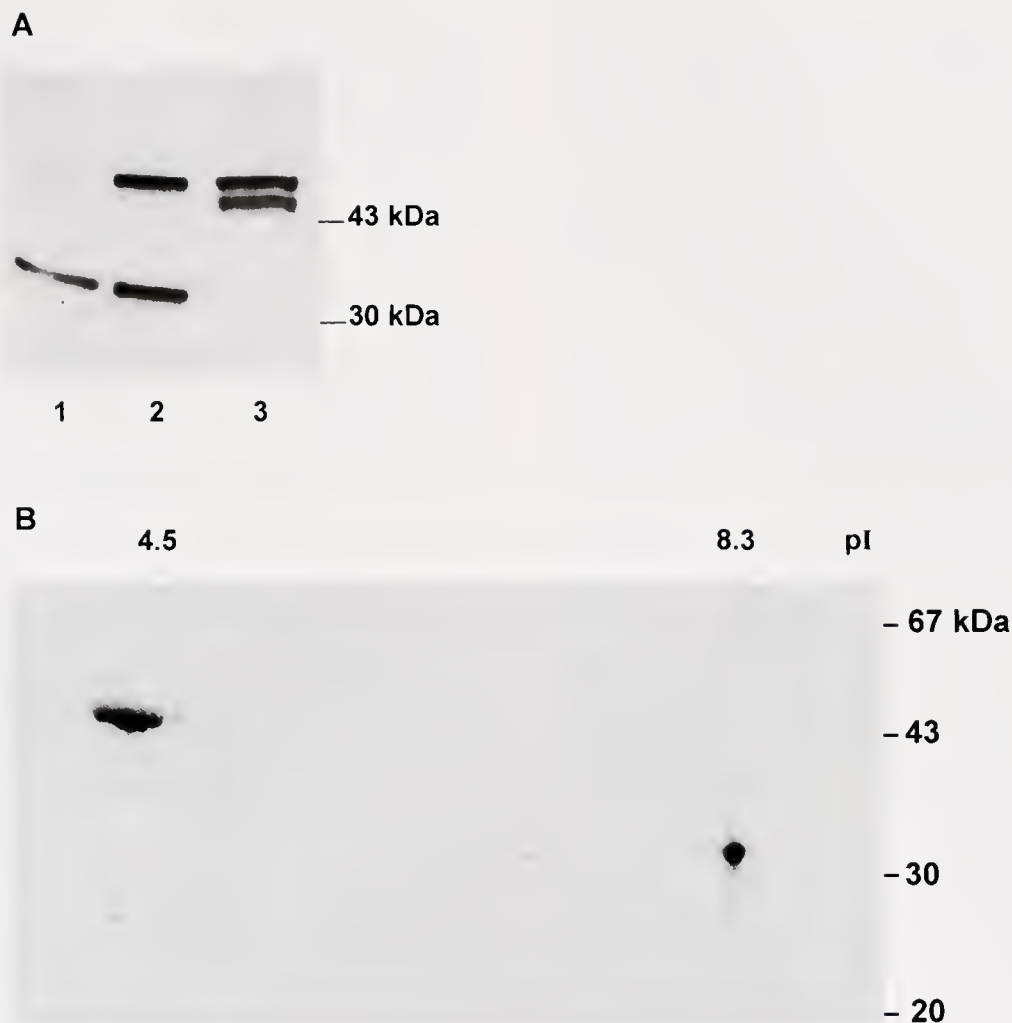


**Figure 5.** Anti-sym32 Western blots of protein homogenates from *Symbiodinium*. (A) Western blot of a one-dimensional gel. All lanes contained 10  $\mu\text{g}$  of soluble protein. Lane 1, host-only proteins, shows a 32-kDa band and a faint 48-kDa band. Lane 2, *Symbiodinium muscatinei* freshly harvested from a host anemone (and therefore contaminated with host tissues), shows three bands: a strongly staining 32-kDa band, a strongly staining 48-kDa band, and a faint 45-kDa band. Lane 3, cultured *Symbiodinium bermudense*, contains two equal intensity bands at 45-kDa and 48-kDa. (B) Western blot of a two-dimensional gel of protein homogenate (60  $\mu\text{g}$ ) from *S. muscatinei* freshly harvested from an anemone host. Two spots are present: a 32-kDa, pI 8.2, spot, identifiable as sym32, presumably from contaminating host tissue, and a 48-kDa spot, pI range 4.3–4.5.

selves complicates the picture and adds a new dimension to our studies of sym32. The accumulation body in dinoflagellates is postulated to function as a lysosome, although this organelle has not been studied in many species, and its function has not been examined in *Symbiodinium*. The free-living dinoflagellate *Prorocentrum* has multiple accumulation bodies with features characteristic of eukaryotic lysosomes. These bodies contain electron-dense material, fibrous material, and membranous material, and they possess acid phosphatase activity, react positively with the periodic acid/Schiff reagent, and stain with acridine orange (Zhou and Fritz, 1994). *Symbiodinium* has a single accumulation body that varies in size and is postulated to function

as a molecular “trash dump” (Taylor, 1987; Wakefield *et al.*, 2000). We observed that the accumulation body is invariably located adjacent to the nucleus, often appearing to displace the edge of the nucleus. If the accumulation body is a lysosome or a trash dump, host sym32 may be transported from the vacuolar membranes, across the dinoflagellate cell wall, and into a degradative pathway within the dinoflagellate. This ability to transport molecules from the host cell, across the vacuolar membrane, into the cytosol or organelles of an intracellular inhabitant is common in parasitic protozoans, and there are many mechanisms by which this occurs (Schwab *et al.*, 1994; Raibaud *et al.*, 2001; Goodyer *et al.*, 1997).

It is also possible, however, that the protein detected in the accumulation body is not a host protein but a symbiont protein. To determine whether the symbionts also produce a sym32 cross-reactive protein, we performed anti-sym32 Western analysis on symbiont proteins separated by one- or two-dimensional SDS-PAGE. Anti-sym32 antiserum labeled a 45/48-kDa cross-reactive protein doublet in both cultured *S. bermudense* (free from any host cell contact) and *S. muscatinei* that we removed from host cells (Fig. 5). The presence of a 32-kDa band in the lane containing *S. muscatinei* proteins almost certainly results from the presence of contaminating host proteins. It is highly likely that the symbiont 45/48-kDa protein is, in fact, a sym32 homolog. Its size is consistent with the fasciclin domain proteins, which consist of between one and four repeats of an approximately 15-kDa domain (thus symbiont p45/48 might consist of three repeats of the 15-kDa-domain). Furthermore, fasciclin domain proteins are diversely distributed and have been identified in bacteria (Paulsrud and Lindblad, 2002; Terasaka *et al.*, 1989), photosynthetic algae (Huber and Sumper, 1994), invertebrate animals (Bastiani *et al.*, 1987; Zinn *et al.*, 1988; Brennan and Robinson, 1994; Bostic and Strand, 1996; Reynolds *et al.*, 2000), and humans (Skonier *et al.*, 1992). To confirm that symbiont p45/48 is in fact a fasciclin domain protein, we are attempting to sequence this gene.

We attempted to immunolocalize the 45/48-kDa symbiont protein in fixed specimens from cultures of *S. bermudense*, by using the anti-sym32 antiserum to detect the 45/48-kDa target protein. Two methods (immunofluorescence to examine intact cells, and immunoelectron microscopy to examine sectioned cells) failed to detect any pattern of staining. This suggests that the anti-sym32 antiserum, although able to recognize epitopes in denatured symbiont proteins on a Western blot (Fig. 4), was not specific enough to detect epitopes in the native protein within *S. bermudense* (data not shown). Occasionally, antibodies can work in Western analysis but not immunolocalization, especially when the antibody is being used to detect a protein other than that to which it was developed (Harlow and Lane, 1999). These results strengthen the conclusion that the protein that we observed within the symbiosome membranes and the symbiont accumulation body is the host-derived protein and not the symbiont-derived protein. If true, this indicates that the symbiont has an active role in modifying the structure or design of the symbiosome membranes. However, this possibility will remain untested until antibodies that can distinguish between the host and symbiont proteins are developed.

Interest in fasciclin domain proteins appears to be gaining momentum judging from the many recent reports that describe the functions or structures of these proteins in diverse organisms (for example, Kim *et al.*, 2002; Tamura *et al.*, 2002; Carr *et al.*, 2003; Clout *et al.*, 2003). These reports

greatly expand upon the initial description of the fasciclin I protein as a homophilic cell adhesion molecule in insects (Elkins *et al.*, 1990). It is now known that, while all fasciclin domain proteins contain at least one 15-kDa fasciclin binding domain, they may also contain a variety of other functional domains that lend diversity to their functions. All, however, share the common role, *via* the fasciclin domain, of mediating recognition and specificity events in cell-cell or cell-extracellular matrix interaction. The mechanisms by which they do so have yet to be elucidated, but clues may be provided by their structures, as in the insect fasciclin I protein (domains 3 and 4) and the *Mycobacteria tuberculosis* complex MBP70 protein (Carr *et al.*, 2003; Clout *et al.*, 2003). Although the mycobacterial MBP70 protein consists of a single fasciclin domain, and the insect fasciclin I protein contains four domains, the structures of the individual domains are strikingly similar. Each domain appears to fold to produce two functional faces on opposite sides of the protein, each of which probably binds independently to other molecules (Carr *et al.*, 2003). Mutations within these functional faces in the human protein  $\beta$ ig-h3 are known to be associated with corneal dystrophy, suggesting that specificity in binding of these molecules to their targets is mediated by small changes in amino acid composition along the functional faces (Carr *et al.*, 2003). This has important implications for the possible role of a fasciclin domain protein in a symbiosis, where specificity in molecular interactions between host and symbiont likely mediates the establishment and regulation of the partnership.

Recent evidence suggests that fasciclin domain proteins function in mediating symbiotic interactions in other associations. In both the rhizobium-plant association and the cyanobacterial-fungal lichen association, homologs have been identified from the symbiont genomes, and in plants, deletion of this gene reduces its ability to fix nitrogen (Oke and Long, 1999; Paulsrud and Lindblad, 2002). This is the first report to suggest that both partners in a symbiosis may produce fasciclin domain proteins.

The sym32 story is complex. The sym32 protein apparently has functions in multiple biological processes within the host: both in symbiotic interactions with dinoflagellates (as evidenced by the presence of sym32 within the membranes surrounding the dinoflagellates), and in other non-symbiosis-related processes (as evidenced by the presence of sym32 in the epidermis of both aposymbiotic and symbiotic anemones). Furthermore, the presence of a cross-reactive protein in both free-living *Symbiodinium* and *Symbiodinium* freshly isolated from a host suggests that the symbionts possess a sym32 homolog. Still to be elucidated are the degree to which the host and symbiont proteins interact and the roles that each plays in the biology of each partner separately and of the partners in symbiosis.

## Acknowledgments

Thanks to Mike Nesson for his assistance with the electron microscopy, Santiago Perez for cultures of *Symbiodinium bermudense*, and Kim Koch for her assistance with the light-level immunocytochemistry. This research was supported by an EPA STAR graduate fellowship to JAS (915432) and an NSF award (9728405-IBN) to VMW.

## Literature Cited

- Bastiani, M. J., A. L. Harrelson, P. M. Snow, and C. S. Goodman. 1987. Expression of fasciclin I and II glycoproteins on subsets of axon pathways during neuronal development in the grasshopper. *Cell* **48**: 745–755.
- Batley, J. F., and J. S. Patton. 1987. Glycerol translocation in *Condylactis gigantea*. *Mar. Biol.* **95**: 37–46.
- Bostic, J. R., and M. Strand. 1996. Molecular cloning of a *Schistosoma mansoni* protein expressed in the gynecophoral canal of male worms. *Mol. Biochem. Parasitol.* **79**: 79–89.
- Brennan, C., and J. J. Robinson. 1994. Cloning and characterization of HLC-32, a 32-kDa protein component of the sea urchin extraembryonic matrix, the hyaline layer. *Dev. Biol.* **165**: 556–565.
- Carr, M. D., M. J. Bloemink, E. Dentten, A. O. Whelan, S. V. Gordon, G. Kelly, T. A. Frenkiel, R. G. Hewinson, and R. A. Williamson. 2003. Solution structure of the *Mycobacterium tuberculosis* complex protein MPB70: from tuberculosis pathogenesis to inherited human corneal disease. *J. Biol. Chem.* **10.1074/jbc.M307235200**.
- Clout, N. J., D. Tisi, and E. Hohenester. 2003. Novel fold revealed by the structure of a FAS1 domain pair from the insect cell adhesion molecule fasciclin I. *Structure* **11**: 197–203.
- Colley, N. J., and R. K. Trench. 1983. Selectivity in phagocytosis and persistence of symbiotic algae by the scyphistoma stage of the jellyfish *Cassiopeia xamachana*. *Proc. R. Soc. Lond. B* **219**: 61–82.
- Corrret, N., C. Frehel, N. Goubier, M. Pouchelet, E. Prina, P. Roux, and J. C. Antoine. 2002. Biogenesis of *Leishmania*-harbouring parasitophorous vacuoles following phagocytosis of the metacyclic promastigote or amastigote stages of the parasites. *J. Cell Sci.* **115**: 2303–2316.
- Dobrowolski, J. M., and L. D. Sibley. 1996. *Toxoplasma* invasion of mammalian cells is powered by the actin cytoskeleton of the parasite. *Cell* **84**: 933–939.
- Elkins, T., M. Hortsch, A. J. Bieber, P. M. Snow, and C. S. Goodman. 1990. *Drosophila* fasciclin I is a novel homophilic adhesion molecule that along with fasciclin III can mediate cell sorting. *J. Cell Biol.* **110**: 1825–1832.
- Falkowski, P. G., Z. Dubinsky, and L. Muscatine. 1984. Light and the bioenergetics of a symbiotic coral. *Bioscience* **34**: 705–709.
- Fitt, W. K., and R. K. Trench. 1983. Endocytosis of the symbiotic dinoflagellate *Symbiodinium microadriaticum* Freudenthal by endodermal cells of the scyphistomae of *Cassiopeia xamachana* and resistance of the algae to host digestion. *J. Cell Sci.* **64**: 195–212.
- Goodyer, I. D., B. Pouvelle, T. G. Schneider, D. P. Treika, and T. F. Taraschi. 1997. Characterization of macromolecular transport pathways in malaria-infected erythrocytes. *Mol. Biochem. Parasitol.* **87**: 13–28.
- Hackstadt, T. 2000. Redirection of host vesicle trafficking pathways by intracellular parasites. *Traffic* **1**: 93–99.
- Harhoe, M., and S. Nagai. 1984. MPB70, a unique antigen of *Mycobacterium bovis* BCG. *Am. Rev. Respir. Dis.* **128**: 444–452.
- Harhoe, M., S. Nagai, H. G. Wilker, K. Stetten, and S. Haga. 1995. Homology between the MPB70 and MPB83 proteins of *Mycobacterium bovis* BCG. *Scand. J. Immunol.* **42**: 46–51.
- Harlow, E., and D. P. Lane. 1999. Antibody-antigen interactions. Pp. 21–39 in *Using Antibodies: A Laboratory Manual*. Cold Spring Harbor Laboratory Press, Cold Spring Harbor, NY.
- Hu, S., M. Sonnenfeld, S. Stahl, and S. T. Crews. 1998. Midline fasciclin: a *Drosophila* fasciclin-I-related membrane protein localized to the CNS midline cells and trachea. *J. Neurobiol.* **3**: 77–93.
- Huber, O., and M. Sumper. 1994. Algal-CAMs: isoforms of a cell adhesion molecule in embryos of the alga *Volvox* with homology to *Drosophila* fasciclin I. *EMBO* **13**: 4212–4222.
- Kim, J.-E., H.-W. Jeong, J.-O. Nam, B.-H. Lee, J.-Y. Choi, R.-W. Park, J.-Y. Park, and I.-S. Kim. 2002. Identification of motifs in the fasciclin domains of the transforming growth factor- $\beta$ -induced matrix protein  $\beta$ ig-h3 that interact with the  $\alpha$ v $\beta$ 5 integrin. *J. Biol. Chem.* **277**(48): 46159–46165.
- LaJeunesse, T. C., and R. K. Trench. 2000. Biogeography of two species of *Symbiodinium* (Freudenthal) inhabiting the intertidal sea anemone *Anthopleura elegantissima* (Brandt). *Biol. Bull.* **199**: 126–134.
- Lewis, D. H., and D. C. Smith. 1971. The autotrophic nutrition of symbiotic marine coelenterates with special reference to hermatypic corals. I. Movement of photosynthetic products between the symbionts. *Proc. R. Soc. Lond. B* **178**: 111–129.
- Mellman, I. 1996. Endocytosis and molecular sorting. *Annu. Rev. Cell Dev. Biol.* **12**: 575–625.
- Mukkada, A. J., J. C. Meade, T. A. Glaser, and P. F. Bonventre. 1985. Enhanced metabolism of *Leishmania donovani* amastigotes at acid pH: an adaptation for intracellular growth. *Science* **229**: 1099–1101.
- Muller-Parker, G., and C. F. D'Elia. 1998. Interactions between corals and their symbiotic algae. Pp. 96–113 in *Life and Death of Coral Reefs*, C. Birkeland, ed. Chapman and Hall, New York.
- Muscatine, L. 1990. The role of symbiotic algae in carbon and energy flux in reef corals. Pp. 75–87 in *Coral Reefs*, Z. Dubinsky, ed. Elsevier, Amsterdam.
- Oke, V., and S. R. Long. 1999. Bacterial genes induced within the nodule during the *Rhizobium*-legume symbiosis. *Mol. Microbiol.* **32**: 837–849.
- Paulsrud, P., and P. Lindblad. 2002. Fasciclin domain proteins are present in *Nostoc* symbionts of lichens. *Appl. Environ. Microbiol.* **68**: 2036–2039.
- Raibaud, A., P. Lupetti, R. E. Paul, D. Mercati, P. T. Brey, R. E. Sinden, J. E. Heuser, and R. Dallai. 2001. Cryofracture electron microscopy of the ookinete pellicle of *Plasmodium gallinaceum* reveals the existence of novel pores in the alveolar membranes. *J. Struct. Biol.* **135**: 47–57.
- Reynolds, W. S., J. A. Schwarz, and V. M. Weis. 2000. Symbiosis-enhanced gene expression in cnidarian-algal associations: cloning and characterization of a cDNA, sym32, encoding a possible cell adhesion protein. *Comp. Biochem. Physiol. A* **126**: 33–44.
- Schwah, J. C., C. J. Beckers, and K. A. Joiner. 1994. The parasitophorous vacuole membrane surrounding intracellular *Toxoplasma gondii* functions as a molecular sieve. *Proc. Natl. Acad. Sci. USA* **91**: 509–513.
- Schwarz, J. A., D. A. Krupp, and V. M. Weis. 1999. Late larval development and onset of symbiosis in the scleractinian coral *Fungia scutaria*. *Biol. Bull.* **196**: 70–79.
- Schwarz, J. A., D. C. Potts, and V. M. Weis. 2002. Feeding behavior and acquisition of zooxanthellae by planula larvae of the sea anemone *Anthopleura elegantissima*. *Mar. Biol.* **140**: 471–478.
- Sinai, A. P., and K. A. Joiner. 1997. Safe haven: the cell biology of nonfusogenic pathogen vacuoles. *Annu. Rev. Microbiol.* **51**: 415–462.
- Skonier, J., M. Neubauer, M. Madisen, K. Bennet, G. Plowman, and A. F. Purchio. 1992. cDNA cloning and sequence analysis of  $\beta$ ig-h3, a novel gene induced in an adenocarcinoma cell line after treatment with transforming growth factor- $\beta$ . *DNA Cell Biol.* **11**: 511–522.

- Takeshita, S., R. Kikuchi, K. Tezuka, and E. Amann. 1993. OSF-2: cloning and characterization of a novel protein expressed in bone with sequence homology to the insect protein fasciclin I. *Biochem J.* **294**: 271–278.
- Tamura, F., S. Adachi, J. Osuga, K. Ohashi, N. Yahagi, M. Sekiya, H. Okazaki, S. Tomita, Y. Iizuka, H. Shimano, R. Nagai, S. Kimura, M. Tsujimoto, and S. Ishibashi. 2003. FEEL-1 and FEEL-2 are endocytic receptors for advanced glycation end products. *J. Biol. Chem.* **278**(15): 12613–12617.
- Taylor, D. L. 1968. *In situ* studies of the cytochemistry and ultrastructure of a symbiotic marine dinoflagellate. *J. Mar. Biol. Assoc. UK* **48**: 349–366.
- Taylor, F. J. R., ed. 1987. *The Biology of Dinoflagellates*. Botanical Monographs, Vol. 21. Blackwell Scientific Publications, Oxford.
- Terasaka, K., R. Yamaguchi, K. Matsuo, A. Yamazaki, S. Nagai, and T. Yamada. 1989. Complete nucleotide sequence of immunogenic protein MPB70 from *Mycobacterium bovis* BCG. *FEMS Microbiol. Lett.* **49**: 273–276.
- Wakefield, T. S., and S. C. Kempf. 2001. Development of host- and symbiont-specific monoclonal antibodies and confirmation of the origin of the symbiosome membrane in a cnidarian-dinoflagellate symbiosis. *Biol. Bull.* **200**: 127–143.
- Wakefield, T. S., M. A. Farmer, and S. C. Kempf. 2000. Revised description of the fine structure of *in situ* "Zooxanthellae" genus *Symbiodinium*. *Biol. Bull.* **199**: 76–84.
- Wang, J. T., and A. E. Douglas. 1998. Nitrogen recycling or nitrogen conservation in an alga-invertebrate symbiosis? *J. Exp. Biol.* **201**: 2443–2453.
- Wang, J. T., and A. E. Douglas. 1999. Essential amino acid synthesis and nitrogen recycling in an alga-invertebrate symbiosis. *Mar. Biol.* **135**: 219–222.
- Weis, V. M. 1993. The effect of dissolved inorganic carbon on the photosynthesis of the symbiotic sea anemone *Aiptasia pulchella*: role of carbonic anhydrase. *J. Exp. Mar. Biol. Ecol.* **174**: 209–225.
- Weis, V. M., and R. P. Levine. 1996. Differential protein profiles reflect the different lifestyles of symbiotic and aposymbiotic *Anthopleura elegantissima*, a sea anemone from temperate waters. *J. Exp. Biol.* **199**: 883–892.
- Weis, V. M., and W. S. Reynolds. 1999. Carbonic anhydrase expression and synthesis in the sea anemone *Anthopleura elegantissima* are enhanced by the presence of dinoflagellate symbionts. *Physiol. Biochem. Zool.* **72**: 307–316.
- Weis, V. M., J. von Kampen, and R. P. Levine. 1998. Techniques for exploring symbiosis-specific gene expression in cnidarian-algal associations. Pp 435–448 in *Some Molecular Approaches to the Study of the Ocean*. K. E. Cooksey, ed. Chapman and Hall, London.
- Zhou, J., and L. Fritz. 1994. The PAS/accumulation bodies in *Prorocentrum lima* and *Prorocentrum maculosum* (Dinophyceae) are dinoflagellate lysosomes. *J. Phycol.* **30**: 39–44.
- Zinn, K., L. McAllister, and C. S. Goodman. 1988. Sequence analysis and neuronal expression of fasciclin I in grasshopper and *Drosophila*. *Cell* **53**: 577–587.

# Columellar Muscle of Neogastropods: Muscle Attachment and the Function of Columellar Folds

REBECCA M. PRICE

*Department of Geophysical Sciences, University of Chicago, 5734 S. Ellis Ave., Chicago, Illinois 60637*

**Abstract.** Malacologists often assume that ornamentation on snail shells is functional, and therefore adaptive. I conducted the first comprehensive test of the widely accepted hypothesis that columellar folds, a type of internal ornamentation, enhance the performance of the columellar muscle, which attaches the snail to its shell. Careful dissections of live, non-relaxed specimens reveal that the physical attachment between the columellar muscle and the columella is not restricted to a small, circular patch located deep within the shell. Instead, the attachment is long and narrow, extending approximately a full whorl along the length of the columella. I developed a novel technique for preparing three-dimensional reconstructions from photographs documenting the dissections. These reconstructions were then used to measure four parameters that describe the muscle: (1) the surface area of the physical attachment between the muscle and columella, (2) the total contact area between the muscle and the columella, (3) the depth of attachment, and (4) the length of attachment. None of these parameters differed significantly between species with and without folds. In light of the biomechanics of muscular hydrostats, values of the first parameter indicate that columellar folds probably do not guide the columellar muscle as the animal moves in and out of its shell. Values of the other parameters indicate that columellar folds neither increase an animal's ability to maneuver its shell nor facilitate deeper withdrawal. These results, and the fact that folds have evolved convergently several times, might indicate that folds are an easily evolvable solution to many functional problems, none of which are currently understood.

## Introduction

Malacologists often assume that gastropod shell ornamentation is adaptive, but experiments that demonstrate the function of these presumed adaptations are rare (Morton, 1967; for notable tests of ornamentation function, see Palmer, 1977, 1979; Bertness and Cunningham, 1981; Appleton and Palmer, 1988; Marko and Palmer, 1991; West *et al.*, 1991; Carefoot and Donovan, 1995; Donovan *et al.*, 1999). Columellar folds, plications on the columella, or central column of a gastropod shell (see Fig. 1), are particularly intriguing ornaments because they evolved repeatedly in a number of clades, such as the Caenogastropoda, Opisthobranchia, and Pulmonata (Price, 2001). In the subclade Neogastropoda of the caenogastropods, the columellar folds may be an adaptation that is intimately related to the columellar muscle (Fig. 1). In fact, the muscle does attach the animal to the columella (Signor and Kat, 1984; Fretter and Graham, 1994) and has grooves that fit between each fold. In this paper, I test three hypotheses that purport to explain a functional relationship between the columellar folds and the columellar muscle.

Columellar folds are readily visible on the inner lip of many shells, and systematists have used the impressive diversity of fold shapes to distinguish species and higher taxa. I consider a fold to be any ridge on the inner lip of the aperture that extends along the columella for a number of whorls, usually extending all the way to the apex. Some folds occur at the bottom edge of the aperture, as in *Nassarius vibex*, whereas others, such as those in *Terebra dislocata*, are located in the center of the inner lip. Folds can be wide (*Triplofusus giganteus*) or narrow (*Nassarius vibex*), subtle (*Busycon contrarium*) or prominent (*Vasum muricatum*).

The columellar muscle conforms exactly to the shape of the folds where it lies over them, and this conformation has inspired the hypotheses that are most commonly cited to

explain the function of folds. These hypotheses must be considered in light of the fact that the columellar muscle functions as a muscular hydrostat (Thompson *et al.*, 1998), controlling protraction from, and retraction into, the shell. Like hydrostatic skeletons in general, the volume of a muscular hydrostat remains constant, so a contraction in one direction induces elongation in an opposing direction (Kier and Smith, 1985). The columellar muscle is composed of muscle fibers that are oriented longitudinally, transversely, and obliquely with respect to the long axis of the columellar muscle (Thompson *et al.*, 1998). Thus, the columellar muscle controls its own twisting, shortening, and elongating in addition to protraction and retraction.

Dall (1894; restated by Fretter and Graham, 1994) published the only nonfunctional explanation of folds. His explanation does not pertain to the columellar muscle, relying instead on the nature of the mantle, the tissue that secretes the shell. Dall surmised that folds, and all other internal ornamentation including the parietal ridge, lirae, and teeth on the outer lip, were deposited in the wrinkles that would form when an overly large mantle retracted into the shell. This idea predicts that ornamentation would be more pronounced at the aperture (Dall, 1894), but ornamentation around the aperture where the mantle is largest is exaggerated only in some species with determinate growth (Paul, 1991; Vermeij and Signor, 1992; Vermeij, 2001a); furthermore, contrary to Dall's prediction, not all of these animals have columellar folds. Indeed, the internal morphology of gastropods is highly stereotyped, not random, and it is unlikely that the mantle would always wrinkle uniformly (Signor and Kat, 1984). There are also no obvious differences in mantle size between species with and without internal ornamentation in general, or columellar folds in particular (pers. obs.).

Three interrelated hypotheses have been presented to explain how the folds affect the function of the columellar muscle, thereby explaining both why folds have evolved and why so many neogastropod lineages maintain them:

1. *Guidance*. Columellar folds guide the columellar muscle as the animal moves in and out of its shell (Signor and Kat, 1984; Ponder, 1972). The analogy here is that the folds act like a railroad track guiding a train; that is, they prevent the animal from slipping in its shell. One manner in which the folds may guide the muscle is by protruding far into the columellar muscle, restricting the muscle movement *along* the folds. In this event, the area of contact should be greater in species with folds than in those without. I test this prediction.

Signor and Kat (1984) limited their guidance hypothesis to high-spired, narrow (turritelliform) species, implying that the columellar muscle would slip within the shell unless folds guided its movement. Any attempt to extend this hypothesis to low-spired

shell shapes must account for the absence of folds in some large neogastropods, such as *Syrinx aruanus*, whose shell can reach almost a meter in length (Harasewych and Petit, 1989).

2. *Maneuverability*. Columellar folds enhance a snail's ability to maneuver its shell (Fretter and Graham, 1962; Vermeij, 1978). A number of authors have assumed that the shape of the muscle's physical attachment to the columella is small and circular, like the adductor muscle attachment in bivalves (*e.g.*, Linsley, 1978; Signor and Kat, 1984; Morita, 1993; Thompson *et al.*, 1998). Vermeij (1978) assumed that the attachment occurs immediately over the folds and predicted that animals with folds would consequently have a larger surface area of muscle attachment. An animal with greater attachment area might be better at maneuvering its shell, for example when it swings the shell back and forth to fend off a predator (Thompson *et al.*, 1998), or when it pries open the shells of prey (Taylor *et al.*, 1980). This hypothesis has remained untested because dissections usually begin by removing and discarding the shell, and because the muscle easily detaches from a cracked shell.
3. *Predator avoidance*. Snails with columellar folds can withdraw more deeply into their shells (Dall, 1894), increasing their ability to escape from predators. Dall (1894) commented that snails with columellar folds retract more deeply, but presented no data in support of this idea. Since then, others have documented that snails that retract more deeply are better at escaping predators: they are harder to reach, and they take so long to handle that the predator eventually abandons the task (Vermeij, 1978, 1987). Although it is not immediately obvious why these behaviors might be associated with columellar folds, the data required to confirm Dall's claim are easy to collect.

I have developed procedures for dissecting gastropods while keeping the columellar muscle intact; employed a novel mathematical algorithm that converts a photograph of a snail into a three-dimensional surface from which I can measure areas; and examined neogastropod species that represent a range of columellar fold morphologies, as well as species with smooth columellae. Contrary to what has been assumed, the muscle attachment to the columella is complex and leaves no scar. None of the three hypotheses outlined above adequately explain the functional relationship between the columellar folds and the columellar muscle.

## Materials and Methods

### Sample

Quantitative data on the columellar muscle were collected from seven species with folds (from five genera and

four families) and five species lacking them (from five genera and three families), affording phylogenetic breadth (Table 1). One of the species without folds, *Strombus alatus*, is not a neogastropod; it is a caenogastropod (a clade that contains the neogastropods) with shell shape similar to other species considered here. At least two and up to five specimens were studied for each species, for a total of 31 specimens for most measurements (36 specimens for attachment depth). These data were supplemented with qualitative observations from an additional nine species. All specimens were stored in 70% ethanol and deposited at the Field Museum of Natural History (FMNH), Chicago, Illinois. Except for *Oliva sayana*, all species have a functional operculum, eliminating any possible bias introduced by a relationship between folds and an operculum.

The sample includes species with a variety of columellar fold shapes and numbers (Table 2), but all have fairly modest folds. Prominent folds, such as those in the Mitridae, Volutidae, and Cancellariidae could not be included, because they were too difficult to collect or purchase alive. *Oliva sayana* has plications on the inner lip of the aperture

that some authors describe as columellar folds (e.g., Abbott, 1974), but these do not continue inside the shell, and they therefore do not contact the columellar muscle, even when the animal is fully protracted. As such, these apertural plications cannot affect the function of the columellar muscle, so I consider *Oliva sayana* to be without folds.

#### Terminology describing orientation

A description of fold morphology requires terms that orient the reader to the snail shell (Fig. 1). In this paper, all terms refer to a snail shell in a standard orientation, with apex up and aperture visible (and on the right for dextral species). *Top* and *bottom* refer to positions along the coiling axis. The *bottom* of a whorl is farthest from the apex, whereas the *top* of the whorl is closest to the apex. The *width* of a feature is measured along a line parallel to the *top-bottom* axis, following the convention that the short axis of the columellar muscle represents *width*, whereas the long axis of the columellar muscle represents *length* (Fig. 1A, E, Fig. 2E). *Apical* and *apertural* refer to directions along the

Table 1

#### Species examined

Species	Collection site*	Family	Folds	Museum ID	Data type
<i>Busycon contrarium</i> (Conrad, 1840)	FS	Melongenidae	Yes	299449, 299459	Quantitative
<i>Busycon spiratum</i> (Lamarck, 1816)	FS	Melongenidae	Yes	299444, 299463, 299468, 299472	Quantitative
<i>Fasciolaria hunteria</i> (Perry, 1811)	FS, WFS, SM	Fascioliariidae	Yes	299450, 299492, 299493	Quantitative
<i>Fasciolaria tulipa</i> (Linnaeus, 1758)	HT	Fascioliariidae	Yes	299448, 299456	Quantitative
<i>Nassarius vibex</i> (Say, 1822)	FS, WFS	Nassariidae	Yes	299475, 299477	Quantitative
<i>Triplofusus giganteus</i> (Kiener, 1840)	HT	Fascioliariidae	Yes	299441, 299442	Quantitative
<i>Cantharus cancellarius</i> (Conrad, 1846)†	DIR	Muricidae	Yes	299486, 299487	Quantitative
<i>Chicoreus florifer distans</i> (Adams, 1855)	WFS	Muricidae	No	299451, 299458	Quantitative
<i>Melongena corona</i> (Gmelin, 1791)	FS, WFS	Melongenidae	No	299453, 299457	Quantitative
<i>Stramonita haemastoma</i> (Linnaeus, 1767)	WFS	Muricidae	No	299452, 299454, 301941	Quantitative
<i>Strombus alatus</i> (Gmelin, 1791)	P	Strombidae	No	301942, 301943	Quantitative
<i>Urosalpinx perrugata</i> (Conrad, 1846)	WFS, SM, ST	Muricidae	No	299481, 299482, 299483, 299484, 299485	Quantitative
<i>Columbella rusticooides</i> (Heilprin, 1886)	DIR	Columbellidae	Yes	299473, 299474	Qualitative
<i>Leucozonia nassa</i> (Gmelin, 1791)	S	Fascioliariidae	Yes	299506, 299520, 299521, 299522, 299526, 299527, 299530, 299531	Qualitative
<i>Opeatostoma pseudodon</i> (Burrow, 1815)	IV	Fascioliariidae	Yes	299496	Qualitative
<i>Pleuroploca salmo</i> (Wood, 1928)	B	Fascioliariidae	Yes	299494	Qualitative
<i>Terebra dislocata</i> (Say, 1822)	HT	Terebridae	Yes	299488, 299489, 299490, 299491	Qualitative
<i>Vasum muricatum</i> (von Born, 1778)	G	Vasidae	Yes	299500	Qualitative
<i>Cypraea cervus</i> (Linnaeus, 1771)	G	Cypraeidae	No	299495	Qualitative
<i>Oliva sayana</i> (Ravenel, 1834)	SM, HT	Olividae	No	299460, 299461, 299466, 299469	Qualitative‡
<i>Polystira nobilis</i> (Hinds, 1843)	GC	Turridae	No	299497, 299499	Qualitative

\* Collection sites: B, Bique, Panama (Pacific Ocean); DIR, Dog Island Reef, Florida (Gulf of Mexico); FS, Florida State University Marine Lab, Turkey Bayou, Florida (Gulf of Mexico); G, Galeta, Panama (Caribbean Sea); GC, Golfo de Chiriquí, Panama (Pacific Ocean); HT, Hammock Trail, near St. Joseph Bay, Gulf County, Florida (Gulf of Mexico); IV, Isla Venado near Playa Veracruz, Panama (Pacific Ocean); P, Purchased from Gulf Specimen Aquarium and Marine Biological Supply, Panama, Florida; S, Sebastian, Florida (Indian River County); SM, St. Mark's Wildlife Refuge, Florida (Gulf of Mexico); ST, Beach at St. Teresa, Florida (Gulf of Mexico); WFS, West side of Florida State University Marine Lab on oyster bar.

† Tentatively placed in *Soleneistra* by Vermeij (2001b).

‡ Only the attachment depth was measured.

Table 2

Fold morphology: in *st.ect.* examined

Species	Fold morphology
<i>Busycos contrarium</i>	1 subtle fold at the bottom of the whorl, distinguished by a groove and angled obliquely; difficult to observe at aperture, but more prominent in older whorls
<i>Busycos spiratum</i>	As in <i>B. contrarium</i> , but slightly more defined
<i>Cantharus cancellarius</i>	1 fold at the bottom of the whorl, angled obliquely; broader than in other species
<i>Columbella rusticooides</i>	1 fold immediately at the bottom of the whorl
<i>Fasciolaria hunteria</i>	2 folds at the bottom of the whorl, angled obliquely; the lower edge of the bottom fold coincides with the edge of the columella
<i>Fasciolaria tulipa</i>	As in <i>F. hunteria</i> , but with 3 folds
<i>Leucozonia nassa</i>	3 folds, angled obliquely and closely spaced
<i>Nassarius vibex</i>	1 well-defined fold at the bottom of the whorl, angled obliquely; square, rather than rounded, profile
<i>Opeatostoma pseudodon</i>	As in <i>L. nassa</i>
<i>Pleuroploca salmo</i>	As in <i>F. tulipa</i>
<i>Terebra dislocata</i>	2 large, broad folds spread throughout whorl; the bottom fold is more prominent than the top one
<i>Triplofusus giganteus</i>	As in <i>F. tulipa</i> , but top fold is more subtle than the others
<i>Vasum muricatum</i>	5 folds in "1 prominent—1 weak—1 prominent—1 weak—1 prominent" pattern; folds angled more perpendicular to coiling axis than in any of the other species and spread throughout the bottom two-thirds of the whorl

spiral of the shell towards the tip or opening respectively: the columellar muscle narrows apically, but is *wide* aperturally. A *junction* occurs where the bottom of one whorl meets the top of another. The *depth* of a feature indicates the number of revolutions between it and the aperture, where one revolution is 360°; for example, the columellar muscle attachment might begin at a depth of 300°.

### Dissections

Dissections were performed on live, untreated animals. Surprisingly, any treatment of animals, such as freezing, storing in ethanol, or relaxing in magnesium sulfate (Epsom salts), caused the muscle to detach from the shell, even when tugged only slightly. Fresh material is therefore essential to study columellar muscle attachment.

To expose the soft tissues while keeping them and the columella intact, I used a Dremel rotary tool with a 1.6-mm-diameter carborundum abrasive wheel to cut away the exterior. The size of the blade limited the specimens that could be dissected with precision to those with whorls larger than half a centimeter. Thus, the

attachment morphology could be quantified in the largest specimens of *Nassarius vibex*, but the available specimens of *Columbella rusticooides* were too small. The largest whorl of *Terebra dislocata*, a high-spined species, is only a few millimeters tall, so it could not be quantified with these methods. Although the most apertural point of the attachment was documented in *Oliva sayana*, the morphology of attachment throughout the rest of its length was inaccessible, because the delicate columella cannot withstand even slight pressure.

To distinguish between muscle that was physically attached and muscle that was simply pressed against the columella, I used a blunt but flexible 34-gauge copper wire to probe between the tissue and columella. In all cases, only the top of the muscle (that closest to the junction between two whorls; see Figs. 1, 2) was physically attached. Since the bottom of the muscle was free, the attachment was not disturbed when probed.

### Measurements

The measurements required to test the hypotheses (Table 3) were the standardized (see below) total area of muscle physically attached to the columella, the standardized total area of muscle in contact with the columella throughout the attachment, the depth of attachment, and the length of the attachment.

It was especially difficult to measure the total area of muscle physically attached to the columella (ATT in Figs. 1, 2). In these species, the columellar muscle attachment does not scar the shell, so the attachment area had to be observed directly. I tried removing strips of columellar muscle that were not attached to determine how much muscle was left on the columella, but this procedure inevitably destroyed the attachment. However, the attachment was so narrow relative to the total width of the columellar muscle that, when measured from digital photographs, it could be reasonably estimated as a thin but long box, only one pixel wide but many degrees long. The small bias introduced by this approximation should be the same in species with and without folds.

Another challenge was to measure the surface area of contact between the columellar muscle and the columella (CM in Figs. 1, 2G). The apertural end of the muscle grades into the foot (Voltzow, 1990; Thompson *et al.*, 1998), so the only point that could be consistently identified at the apertural end of the columellar muscle was the point at which the muscle *attachment* began (ATT in Fig. 2E). I measured the total area of muscle in contact with the columella: beginning with the attachment, extending down the width of the muscle to the bottom of the whorl, and extending across the columella to include the most apical part of the muscle (CM in Figs. 1, 2G). Because the muscle always spanned the columella between the attachment and the

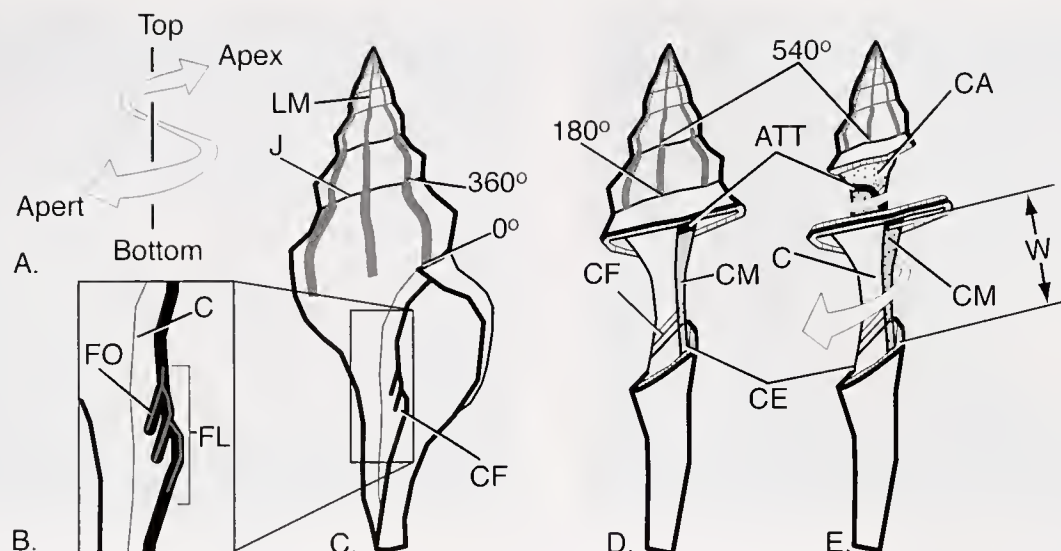


**Figure 1.** Definition of terms describing columellar morphology illustrated with *Triplofusus giganteus*. (A) *Top* refers to the part of a whorl relatively closer to the apex along a vertical axis (*adapical* in some literature, e.g., Vermeij, 1978); *bottom* refers to the lower part of that same axis (*abapical*). The open arrows wrap around the axis from the aperture to the apex. The *apertural* point of the muscle attachment is that closest to the aperture (also see D), and the *apical-most* point is that immediately after the attachment crosses the folds (also see E). *Width* (*W*) is the dimension from the *top* and to the *bottom* of a structure (e.g., the muscle is shown at its widest point in D and E; see also Fig. 2E). (B) Close-up of the inner lip of the aperture. The fold modifier is calculated as the ratio of FO:FL, where FL is the minimum length between folds, and FO is the outline of the folds (see Equation 1 in Materials and Methods). (C) Intact shell. (D) Same shell rotated 180° with sections of the shell exterior removed. (E) Same view as in D, but another 360° of shell exterior has been removed, and open arrows indicate the apertural-apical axis. Cut surfaces are indicated by fine, vertical hatching. Degrees indicate the *depth* of the landmark (LM); i.e., the number of degrees between the landmark and the aperture. The columellar muscle is shaded gray and passes over the columellar folds; the attachment area is a thick black line that is slightly exaggerated for illustrative purposes; stipples mark the area of the columella throughout the length of the attachment (CA). *Abbreviations:* Apert, aperture; ATT, columellar muscle attachment; C, columella; CA, columellar area; CE, edge of the columella; CF, columellar folds; CM, area of contact between columellar muscle and columella; FO, length of fold outline; FL, minimum length of folds; J, junction between two whorls; LM, landmark line; W, width.

bottom of the whorl, this measurement could be made in relaxed, contracted, and protracted animals. The position and length of the muscle attachment and the area under the attachment remain the same regardless of the animal's behavior. The exclusion of the area between the foot and the initial attachment was justifiable: it never included muscle that conformed to the morphology of the folds and was therefore not relevant to the present study; there was no reason to assume that it varied differently in species with and without folds.

Both the attachment area and the contact area were standardized to the columellar area (CA in Fig. 1; Table 3) to remove the effect of size. Columellar area is the area of the columella above, below, and including the length of attachment.

I used the depth of attachment as a proxy for depth of retraction, measured as the number of degrees behind the aperture. The two depths are intuitively related, because an animal cannot retract deeper than its attachment.

Depth of attachment was much easier to measure, and it is not subject to behavioral variation. This proxy assumes that the amount of space between the columellar muscle attachment of the contracted animal and its operculum varies equally among species with folds and those without.

The length of attachment was defined as the number of degrees between the depth of attachment and the apical edge of the attachment, which occurred in the crease between the columella and the rest of the shell (Fig. 2F, G). Some muscle fibers and connective tissue extended even farther apically beyond this point, but they were small and thus likely to function differently from the rest of the muscle. My methods were too coarse to dissect this tiny strand of tissue accurately.

Because the length of attachment and the depth of attachment were both measured as the number of revolutions behind the aperture (in degrees), they were independent of size and did not need to be standardized.

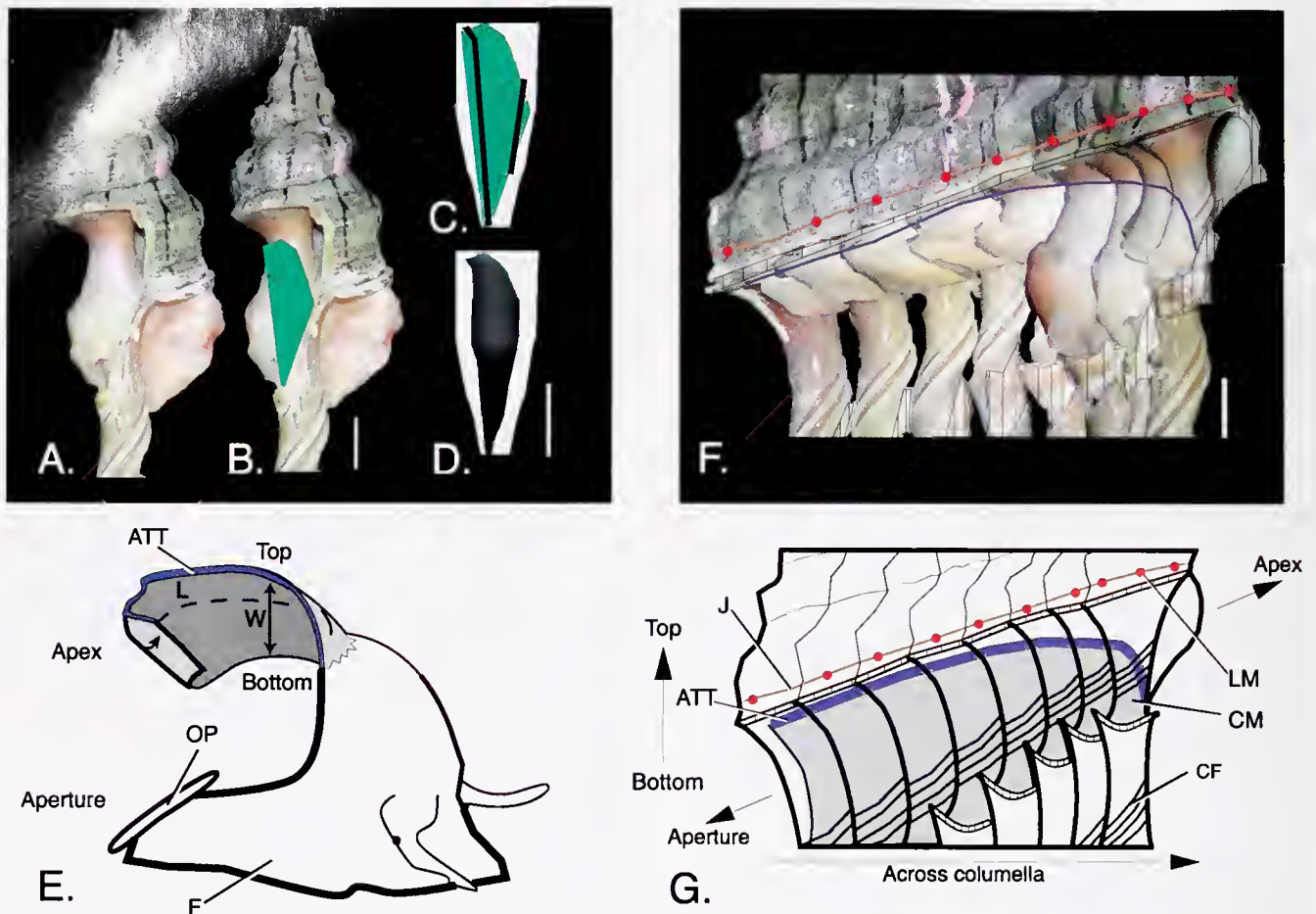


**Figure 2.** (A–D) An example illustrating the image processing technique. One photograph is shown from a series that documents the whole dissection. In this example, the contact area of *Triplofusus giganteus* (FMNH 299441) is reconstructed. The central landmark in this view has a depth of  $540^\circ$  (see Fig. 1D, E). (B) Contact area is highlighted (in green). (C) Comparison between contact area and a reference area (white). The reference area is a symmetrical stack of circles centered on the coiling axis (see Appendix). The black lines mark the middle  $90^\circ$  sector with the image ( $45^\circ$  on either side of the landmark line), or “target area” as described in the Appendix. (D) Reconstructed contact area. Read the reconstruction as a topographic map: lighter points on the image are farther from the plane of the page. (E) Generic neogastropod with shell and viscera removed to illustrate the attachment and the manner in which the columellar muscle (in gray) coils throughout its length. The broken edge indicates that the columellar muscle grades into the musculature of the foot. Drawing based on figure 2 in Thompson, J. T., A. D. Lowe, and W. M. Kier. 1998. The columellar muscle of prosobranch gastropods: morphological zonation and its functional implications. *Invertebr. Biol.* 117: 45–56. (F) Photographic montage and (G) graphic representation of the columellar muscle attachment in the same specimen illustrated in A and B. F and G are constructed from a series of photographs spliced together by aligning the attachment, and thus creating a single image that looks like an uncoiled, flattened shell. As indicated by the blue line, the attachment begins at the top of the whorl and gradually slides down the columella. Towards the apical end of the muscle, the angle of attachment changes dramatically, and the attachment crosses the folds. In F, much of the muscle has been removed to expose the columellar folds, but it remains largely intact in two of the views, demonstrating that the area of contact extends from the attachment to the bottom of the whorl. Hatching indicates shell broken to expose the columella and columellar muscle. All scale bars, 1 cm. *Abbreviations:* F, foot; L, length; OP, operculum; W, width; other abbreviations as in Figure 1.

### Image processing

All measurements were taken from a series of digital photographs that documented each dissection. However, photographs distort three-dimensional data into two dimen-

sions, so the surface areas in the photographs under-represent true areas. I therefore developed a procedure to process the series of photographs for each dissection, as well as a geometric algorithm that calculates the three-dimensional

Table 3

Summary of measurements required to test hypotheses

Measurement	Hypothesis	Use modifier to adjust for fold topography?
Standardized total area of muscle physically attached to the columella (ATT/CA in Fig. 1)	Maneuverability	Yes
Standardized surface area of contact between columella and columellar muscle throughout attachment when animal is relaxed (CM/CA in Fig. 1)	Guidance	Yes
Depth of attachment, in degrees	Retraction depth	No
Length of attachment, in degrees	Maneuverability	No

area projected into each photograph. The algorithm is presented in the Appendix.

Photographs were taken with a Nikon CoolPix 950 digital camera. The image plane of each photograph was parallel to the coiling axis, to which the optic axis was perpendicular. Each photograph also included a scale bar, was centered on a landmark, and showed the muscle attachment and the edge of the columella.

The outside of each shell was marked with radial lines running perpendicular to the junctions between whorls (LM in Fig. 1) every quarter of a whorl for small specimens and every eighth of a whorl for larger specimens (generally, those with shells longer than 2 cm). These landmark lines were used to locate the image within the series.

Each series consisted of between 4 and 12 photographs, with at least one photograph per quarter whorl. To create each series, all images were scaled and oriented identically. Only the middle 90° sector within each photograph was measured (45° on either side of the landmark line), thus eliminating overlap among the images (Fig. 2C).

The algorithm employed to estimate surface area converted tracings of photographs into three-dimensional surfaces (Fig. 2A–C). I used a mouse or mouse tablet (Wacom Graphire2) to trace the surface areas of the muscle attachment, the muscle in contact with the shell, and the columella within each image. Tracings were transformed according to the procedure described in the Appendix (implemented in MATLAB ver. 6.0; Fig. 2D), and then areas were summed from each image in the series. The procedure used to calculate the number of degrees from the aperture to the apertural and apical ends of the attachment is also described in the Appendix.

The 20 largest specimens were used to determine the precision of each measurement. I had two quarter-whorl series for these specimens, because they were photographed every eighth of a whorl; one series, for example, depicted the attachment centered on landmarks at 135°, 225°, 315°,

and 405°, and the other centered on landmarks at 180°, 270°, 360°, and 450°. I averaged the final measurements from the two series.

### Fold modifier

The three-dimensional reconstruction technique employed here did not take into account the presence of folds. To account for folds, I employed a scale factor (“modifier”) defined as the length of the projected outline of the folds divided by the minimum distance between the two endpoints of the folds (Fig. 1B; Eq. 1):

$$\text{modifier} = \frac{\text{Length}_{\text{outline}}}{\text{Length}_{\text{minimum}}} \quad (1)$$

When there are no folds, the minimum length equals the length of the outline, so the lower limit of the modifier is 1.

I measured the fold modifier in each of the photographs of a series that clearly showed the folds’ silhouette. This measurement is highly sensitive to shell orientation and to the endpoints of the fold outline, for which I used inflection points. To compensate for this sensitivity, I always used the maximum fold modifier; this approach favored finding a statistical difference between groups with and without folds. Although there was considerable variability in fold modifier values within a species, the variance for the entire sample of species with folds was low (fold modifier variance, 0.003; range, 1.0 to 1.2; 114 measurements over 17 specimens).

After measuring the surface area of the columellar folds, and transforming it according to the algorithm in the Appendix, I applied Equation 2:

$$\text{Area}_{\text{final}} = A_T - A_{JT} + (A_{JT} \times \text{modifier}) \quad (2)$$

where  $A_T$  is the area transformed by the algorithm into an estimate of the area of a three-dimensional surface (either attachment area or contact area), and  $A_{JT}$  is the similarly transformed area of the folds. In other words, I subtracted the transformed fold area from the attachment area, multiplied it by the fold modifier, added the product back to the attachment area, and then repeated the adjustment for the contact area.

The total surface area of the columella was not adjusted, because that measurement is used to standardize the other metrics. If fold surface area were added to columellar area, the difference between species with and without folds would be erased.

### Statistics

Statistical comparisons between species with folds and those lacking them were performed with a Mann-Whitney  $U$  test using StatView 5.0 for Windows.

## Results

### Morphology of columellar muscle attachment

These dissections demonstrated that the columellar muscle attachment in neogastropods is far more complex than previously assumed (by authors such as Linsley, 1978; Signor and Kat, 1984; Morita, 1993; Thompson *et al.*, 1998). The muscle did not leave a scar, so there was no macroscopic feature on the columella that approximated attachment shape. The shape of the attachment was similar in all species, regardless of the presence of folds (Fig. 2E–G). In most of the species examined, the attachment began about three-quarters of a whorl ( $\sim 275^\circ$ ) back from the aperture (Fig. 3C, raw data for the histogram is in Table 4). The depth of attachment might be much deeper in high-spired shells. In *Terebra dislocata*, attachments began about two whorls back from the aperture (pers. obs.). *T. maculata* and *T. subulata*, muscles were previously reported to attach more deeply at about 2.5 and 4.5 whorls back from the aperture, respectively (Signor and Kat, 1984). In general, the attachment was long and sometimes extended for more than one revolution; it was restricted to the upper edge of the muscle (blue line is ATT in Fig. 2E–G).

The relative position of the attachment changed as it

moved from the apertural edge of the muscle across to the apical edge. At its most apertural end, the attachment lay immediately under the junction of the two whorls. Tracing it apically along the rising junction, the attachment shifted in position progressively downward and across the columella toward the bottom of the whorl, with the rate of descent gradually increasing. Shortly before reaching the bottom of the whorl, the angle of the attachment changed dramatically, becoming more oblique to the junction and curving sharply down to the base of the whorl; this is where the attachment crossed the folds when they were present. Here the muscle was remarkably less robust than elsewhere along its length. Farther apically, the muscle was only a thin extension situated in the crease between the columella and the base of the whorl. Within the area where the muscle was attached, the muscle width was maximal at its apertural end and minimal towards the apex.

### Functional hypotheses

Contrary to the prediction drawn from the functional hypotheses outlined in the Introduction, no significant differences were found between species with and without folds with respect to the surface area of muscle attachment ( $P =$

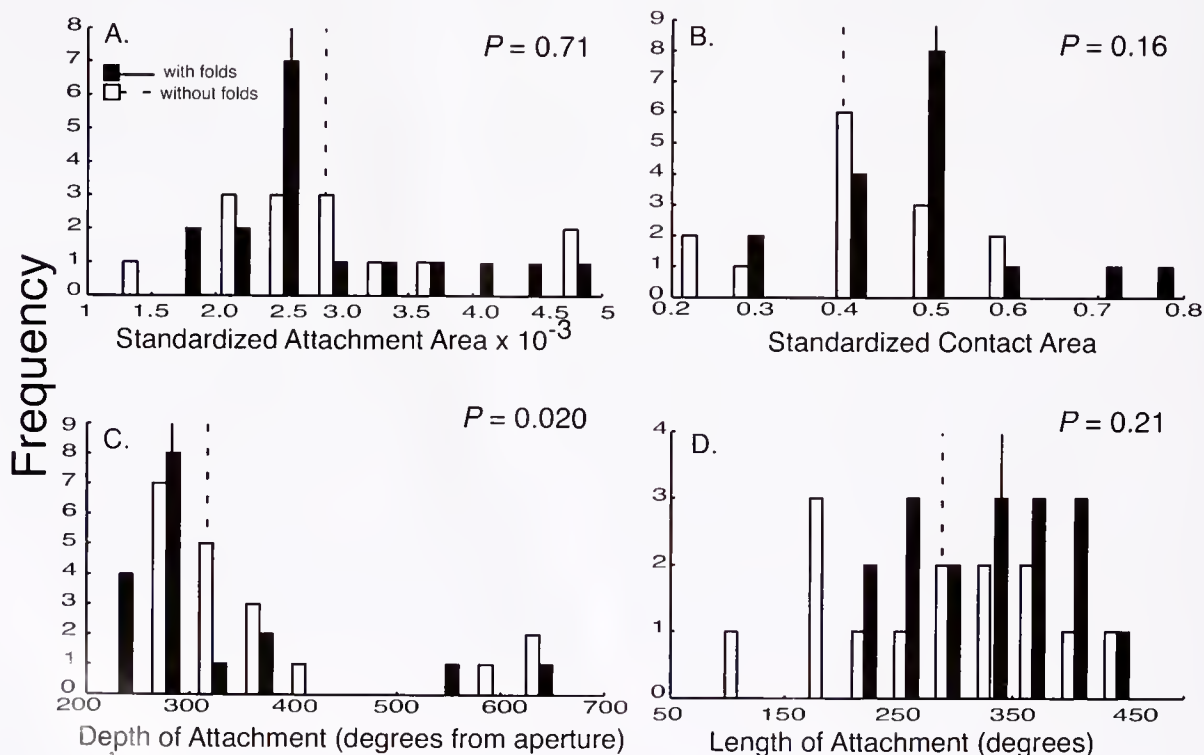


**Figure 3.** Frequency distribution of (A) attachment area, (B) contact area, (C) depth of attachment, and (D) length of attachment. Values for species with folds are indicated with black bars, and their median is a solid line; those without have white bars, median is dotted line.  $P$  values from Mann-Whitney  $U$  test. Raw data are provided in Table 4.

Table 4

Measurements for all specimens

Species	Museum ID	Folds	Standardized attachment area ( $\times 10^{-3}$ )	Standardized contact area	Depth of attachment (degrees)	Length of attachment (degrees)
<i>Busycon contrarium</i>	299449	Yes	3.0	0.5	210	330
<i>Busycon contrarium</i>	299459	Yes	2.7	0.5	240	330
<i>Busycon spiratum</i>	299444	Yes	2.2	0.4	280	230
<i>Busycon spiratum</i>	299463	Yes	1.8	0.3	270	290
<i>Busycon spiratum</i>	299468	Yes	2.3	0.4	270	450
<i>Busycon spiratum</i>	299472	Yes	2.4	0.4	250	270
<i>Cantharus cancellarius</i>	299486	Yes	3.6	0.5	350	330
<i>Cantharus cancellarius</i>	299487	Yes	3.4	0.3	360	230
<i>Fasciolaria hunteria</i>	299450	Yes	2.5	0.5	310	290
<i>Fasciolaria hunteria</i>	299492	Yes	2.4	0.5	280	370
<i>Fasciolaria hunteria</i>	299493	Yes	2.4	0.5	260	390
<i>Fasciolaria tulipa</i>	299448	Yes	2.5	0.6	260	390
<i>Fasciolaria tulipa</i>	299456	Yes	2.7	0.5	230	420
<i>Nassarius vibex</i>	299475	Yes	1.9	0.5	630	250
<i>Nassarius vibex</i>	299477	Yes	4.6	0.4	570	240
<i>Triplofusus giganteus</i>	299441	Yes	3.9	0.7	290	360
<i>Triplofusus giganteus</i>	299442	Yes	4.7	0.8	280	370
<i>Chicoreus florifer distans</i>	299451	No	3.1	0.4	270	190
<i>Chicoreus florifer distans</i>	299458	No	3.1	0.4	330	260
<i>Melongena corona</i>	299453	No	2.7	0.6	270	460
<i>Melongena corona</i>	299457	No	2.3	0.5	320	400
<i>Oliva sayana</i>	299460	No	ND	ND	280	ND
<i>Oliva sayana</i>	299461	No	ND	ND	260	ND
<i>Oliva sayana</i>	299465	No	ND	ND	370	ND
<i>Oliva sayana</i>	299466	No	ND	ND	300	ND
<i>Oliva sayana</i>	299469	No	ND	ND	290	ND
<i>Stramonita haemastoma</i>	299452	No	2.3	0.4	320	370
<i>Stramonita haemastoma</i>	299454	No	2.2	0.4	280	350
<i>Stramonita haemastoma</i>	301941	No	3.0	0.4	660	90
<i>Strombus alatus</i>	301942	No	2.4	0.2	590	210
<i>Strombus alatus</i>	301943	No	2.6	0.2	650	170
<i>Urosalpinx perrugata</i>	299481	No	1.2	0.4	310	300
<i>Urosalpinx perrugata</i>	299482	No	4.7	0.5	330	330
<i>Urosalpinx perrugata</i>	299483	No	3.4	0.3	360	320
<i>Urosalpinx perrugata</i>	299484	No	3.5	0.6	420	170
<i>Urosalpinx perrugata</i>	299485	No	5.0	0.5	360	310

ND—not determined. Measurements could not be taken because the columella is too delicate to survive dissection.

0.71), the amount of contact between muscle and columella ( $P = 0.16$ ), or the length of muscle attachment ( $P = 0.21$ ) (Fig. 3; Table 4). The depth of attachment in species with folds was significantly closer to the aperture than in species without folds ( $P = 0.020$ ), which is opposite to what was predicted.

Three specimens (*Busycon contrarium* FMNH299449, *B. contrarium* FMNH299459, and *Cantharus cancellarius* FMNH299487) had fold modifier values close to unity (1.02, 1.00, and 1.04, respectively), meaning that the folds were almost flush with the columella and thus did not protrude enough to increase the topographic relief above that of specimens lacking folds. The data were consequently re-analyzed categorizing these three specimens as lacking

folds. Results were identical for the contact area, attachment area, and length of attachment. However, the depth of attachment was no longer significantly different between species with folds and those lacking them ( $P = 0.19$ ).

## Discussion

Using novel methods to examine the columellar muscle *in situ*, I have described, for the first time, the surprisingly complex attachment of the columellar muscle in neogastropods. This attachment is remarkable for its delicate structure, lack of discernible muscle scars, and considerable length. The data presented here do not support any of the previously published hypotheses thought to explain the

function of columellar folds, although the species included do not exhibit the most exuberantly developed folds. These data cast doubt on the hypothesis that folds act as struts, guiding the columellar muscle as the animal protracts from, and retracts into, its shell. Furthermore, the muscle probably does not need to be guided, because it is a muscular hydrostat. The muscle probably mirrors the morphology of the folds simply because it is physically adjacent to them. I reject the hypotheses that animals with folds maneuver better because their attachment area is larger, and that these animals avoid predators by retracting deeper. While I reject these hypotheses as general explanations for columellar fold function in neogastropods as a whole, future work may demonstrate that some of them adequately explain function within groups of species with similarly shaped folds.

### Methodology

I developed two novel methods in this research: one is a practical dissection technique, and the other is an analytical approach for measuring distances and areas from photographs of specimens. With the dissection technique, I described the columellar muscle attachment in 20 neogastropods and one caenogastropod (Table 1). The soft tissues of other gastropods can be dissected without damaging the columella, and future applications of this approach will provide a more general understanding of how soft tissues are situated within the shell. With the analytical approach, I determined the relative position of soft tissues and shell features. I quantitatively characterized the columellar muscle in 11 species of neogastropods and one caenogastropod (Tables 1, 3, 4). This algorithm will work for any organism arranged as a stack of circles—echinoderms, cnidarians, foraminifera, diatoms, and mushrooms, for example.

The measurements and their analysis rest on three assumptions. First, to measure the area of contact between the columellar muscle and the columella, I assumed that the amount of muscle apertural to the attachment varies equally in species with and without folds. Second, I also assumed that the attachment area was only one pixel wide, which seems justified by the observation that the attachment was quite thin relative to the total width of the muscle. Third, areas were inflated by the algorithm that transformed the two-dimensional data, because the columella was assumed to be perfectly symmetrical (see Appendix). All of these assumptions were justified, especially in this first attempt to quantify differences in the columellar muscle. Furthermore, there is no *a priori* reason to believe that they would affect species with folds differently than species lacking them.

Note that the measurements are coarse (Table 4), and that subtle differences in contact area, attachment area, depth of attachment, and length of attachment cannot be resolved with these methods.

### Columellar muscle attachment

The complexity and extent of the columellar muscle attachment has gone unrecognized because the attachment itself is remarkably delicate. A slight tug in the wrong direction (away from the aperture, toward the apex) tore the muscle from the columella, and the strength of the attachment deteriorated rapidly in preserved or relaxed animals. Its tenuous nature probably reflects the interplay between the physical mechanism of adhesion and the shape of the adhesive surface. Although the muscle was easily detached from the columella, the animal never naturally experiences a force pulling on the attachment from the angle or location I used during dissection; if the shell is opened as I have opened it, the animal is already too exposed to save itself from predators. An adhesive joint that can withstand large shear stresses will frequently fail when peeled (Portelli, 1986). The muscle attachment is analogous to a long piece of tape on a tabletop. When peeled backward, perpendicular to the table, the tape detaches easily, but when pulled along its length, it has great strength.

Surprisingly, none of the species studied here have muscle scars, even though scars are found in all major groups of shelled molluscs throughout their history (*e.g.*, Abbott, 1974; Lindberg, 1985; Pojeta, 1985; Doguzhaeva and Mutvei, 1996; Isaji *et al.*, 2002). In vertebrates, however, muscles frequently do not leave attachment scars (McGowan, 1982; Bryant and Seymour, 1990), especially when they insert directly into bone instead of attaching to a tendon which inserts into bone. In snails, the columellar muscle inserts into an epithelium that in turn inserts into the shell (Tompa and Watabe, 1976). Additional work is required to determine whether neogastropods and vertebrates lack muscle scars for similar reasons.

The fact that the muscle attachment is so much longer than previously thought (by authors such as Linsley, 1978; Morita, 1993; Thompson *et al.*, 1998) has interesting implications for how the columellar muscle functions. Thompson *et al.* (1998) calculated, on theoretical considerations, the force required to buckle the columellar muscle and the amount of torsion the muscle could exert. The muscle, which has a crescentic cross section, buckled more easily and could not exert as much torsional force as a cylindrical muscle with a circular cross section. However, these authors assumed that the muscle was attached at only one end rather than throughout its length. The true, side-long attachment should help the muscle resist compressive forces (J. T. Thompson, St. Joseph's University, pers. comm.), so that the mechanical disadvantage due to buckling may not be so severe. Similarly, the net torsion exerted must be reconsidered in light of the new attachment data.

### Guidance

I hypothesized that folds guide the columellar muscle during protraction and retraction by protruding far into the columellar muscle, compelling the muscle to move along the folds. I reasoned further that, if folds act as struts, then they should protrude far enough into the muscle to significantly increase the amount of contact between the muscle and columella. For the species analyzed here, however, there was no significant difference in the contact area or length of attachment between species with folds and those lacking them. Therefore, the folds-as-struts hypothesis, as explained here, was not supported.

From another perspective, the methods were relatively coarse, and the data were poorly resolved. If these methods are applied to species with a subtle fold topology, then no significant increase in the contact area may be detectable. In species with folds, I compared the unadjusted contact area to the contact area after it had been adjusted with the fold modifier. The two metrics differed by more than 2% in only one specimen, and the average difference was only 0.2% ( $n = 17$ ). This difference is less than the precision of the measurement of contact area, which is only to one decimal place. Therefore, although the topography of folds does not increase the contact area in the specimens considered here, the contact area may be greater in species with more prominent folds, such as those in the Volutidae, Mitridae, and Cancellariidae. Thus, additional work with these species and with methods providing higher resolution may lend support to the guidance hypothesis and its corollary that folds act as struts.

A consideration of the association between the area of contact and the presence of folds suggests other functional relationships. For example, if the advantage offered by strut-like folds were offset by the benefit of a large contact area, species with folds should have a significantly smaller area of contact than those without. Similarly, species with folds could have the same area of contact as species without folds, provided that the increase in contact due to the protruding folds was offset by a shorter attachment length. However, no such significant differences were observed.

The guidance hypothesis assumes that, without the resistance offered by folds, the muscle would slip along the columella during both retraction and protraction, presumably causing the animal to expend more energy. However, the arrangement of fibers within the muscle, including some fibers that are wound obliquely around the robust, apertural end of the muscle, suggests that the fibers, and not the columellar folds, control the path of the muscle when it contracts (Thompson *et al.*, 1998). Because the muscle is attached along its top edge (Fig. 2), it will shift across the columella when the oblique fibers contract. In light of this newer evidence about the columellar muscle in particular and the muscular hydrostats of molluscs in general (Kier

and Smith, 1985, 1990; Hodgson and Trueman, 1987; Kier, 1988; Marshall *et al.*, 1989), the muscle seems to function in the way that was previously thought inefficient (Signor and Kat, 1984).

Signor and Kat (1984) formulated the guidance hypothesis in part because Signor (1982) correlated burrowing behavior in high-spired gastropods with columellar folds: 55 of 59 burrowing species had folds, but only 1 in 46 non-burrowing species did. He concluded that columellar folds guide the columellar muscle in burrowing animals (Signor and Kat, 1984). However, 40 of his 59 burrowers were in the Terebridae, and only 4 of his 11 families included non-burrowing species. Thus, his results may be explained by phylogenetic bias and should be reanalyzed with comparative methods based on phylogenetic contrasts (as in Harvey and Pagel, 1991) once the appropriate estimates of relationship are available. The advantage of folds to burrowing animals is not obvious, especially if the guidance hypothesis is not true. Furthermore, many species with folds do not burrow (G. J. Vermeij, University of California, Davis, pers. comm.). The species considered here cannot be used to explore the relationship between folds and burrowing behavior, because species were not sampled randomly across burrowing and non-burrowing habitats.

In conclusion, since the inner surface of the columellar muscle is an exact impression of the columellar folds, it is only reasonable to assume that the muscle moves along the folds. This assumption does not require, however, that the folds dictate the muscle's motion. I suspect that the similarity in the shape of the muscle and folds is due simply to their proximity, and that the direction the muscle moves is governed instead by attachment morphology and muscle fiber orientation.

### Maneuverability

As with contact area, the folds added insignificantly to the attachment area. The attachment was so long, and so much of it was distant from the folds, that the folds would need to protrude into the muscle six times more than they do (*i.e.*, multiply the fold modifier by 6) to significantly increase attachment area in species with folds at the  $\alpha < 0.05$  level. If animals with folds are better able to maneuver their shells, it is not because they have a greater surface area of muscle attachment.

Signor and Kat (1984) suggested that the columellar muscle is divided by the folds into functionally discrete units joined only by connective tissue. However, judging by the observations presented here, the divisions they describe are probably part of a gradation between the robust, most apertural, part of the muscle and the weak, more apical part (left and right sides of Fig. 2E–G). Since Signor and Kat (1984) did not mention the frequency or placement of their histological sections, nor illustrate their results, it is difficult

to reevaluate their conclusions in the light of the newly recognized attachment morphology. The muscle histology of high-spired species with and without folds should be compared to determine whether the muscle is subdivided, and if so, whether those subdivisions are constrained by, or at least correspond to, columellar folds.

Maneuverability in a number of terrestrial pulmonates does appear to be enhanced by physically distinct subdivisions of the columellar muscle (Suvorov, 1993, 1999a, b, c). In these taxa, the columellar muscle originates from the most apical point (this is the only part of the muscle that is attached) and is divided into left and right pedal retractors, and left and right buccal mass retractors. These four branches continue to subdivide closer to the aperture. The four functional groups of the muscle are separated by a septum of connective tissue, but apertural teeth and columellar folds may play a secondary role in keeping subsets of branches separated. Thus, columellar ornamentation in pulmonates apparently evolved for a different reason than it did in neogastropods.

#### *Predator avoidance*

I was unable to substantiate Dall's (1894) claim that animals with folds retract deeper into their shells. Instead, animals lacking folds retract more deeply, because they have a significantly deeper attachment site. A larger sample of species is required to confirm this conclusion. Because all of the specimens from which quantitative data were obtained were collected in spring, seasonal variability in growth rate and attachment site were not considered. Variability in growth rate may be especially important to consider in genera such as *Busycon*, which exhibit highly episodic growth.

The depth of attachment was surprisingly constant among most species considered here (median depth = 295°;  $n = 36$ ). Interestingly, the distribution of attachment depth was bimodal, with medians at 280° ( $n = 31$ ) and 630° ( $n = 5$ ) (Fig. 3), although, admittedly, there were few specimens in the higher mode. One species, *Stramonita haemastoma*, had specimens in both modes. This bimodality may reflect episodicity in growth.

Despite these overall similarities, the shallower attachment depth of species with folds implies that columellar folds do not help gastropods to escape from their predators by retracting into their shell. Moreover, my qualitative laboratory and field observations suggest that neogastropods are not subject to particularly intense predation. For example, a number of species (*Leucozonia nassa*, *Stramonita haemastoma*, *S. rustica*, *Pisania tinctoria*, and *Melongena corona*) neither retract quickly nor re-orient themselves quickly when their shells are overturned (pers. obs.). I have found wild specimens of *Latirus mediamericus* (fascio-

lariid, with folds) lying on coral, each with the aperture pointed upward and the foot hanging outside the aperture.

#### *Do folds have a single function?*

Although the function of columellar folds remains unidentified, there are potentially fruitful paths for future research. As discussed above, the correlation between the presence of folds and burrowing habit in high-spired gastropods (Signor, 1982) must be studied in more detail. Also, columellar folds might strengthen the shell, thereby protecting the animal from predators. External features of the shell, such as thickness and the presence of spines, have been shown to increase resistance to predators, making it more difficult for a durophagous predator to break a snail's shell (reviewed in Vermeij, 1993; Kohn, 1999). In fact, some species have a corrugated shell, which presumably increases strength while minimizing the costs associated with building and moving a heavy shell (Vermeij, 1993). Perhaps, in a similar manner, columellar folds protect against predators by increasing the strength of the inner lip while minimizing the cost of thickening the entire columella. Supporting this idea, Hughes and Elner (1979) report that crabs open *Nuccella lapillus* shells that have thin columellae by snapping the inner lip, breaking the shell in half. In contrast, *N. lapillus* individuals with thickened columellae are attacked at the apex of the shell. Both *N. lapillus* phenotypes lack folds, but these observations imply that strengthening the inner lip makes the columella harder to break more apically. However, predators of gastropods rarely break the inner lip. Most predators either crush the shell at its apex or peel back the shell at the outer lip (Vermeij, 1982; Johannesson, 1986); folds are simply ill-placed to affect either of these actions directly. There may be no evidence of damage on columella, as there are with failed attempts at predation in other parts of the shell, because when these attacks succeed, the shell fails catastrophically (G. J. Vermeij, pers. comm.).

Vermeij (1978) has observed that, within at least the families Vasidae and Mitridae, columellar folds are more common in tropical species, suggesting that the presence of folds might be correlated with latitude and increased predation intensity. This observation should certainly be tested quantitatively, although it is difficult to interpret the meaning of latitudinal diversity trends (Roy *et al.*, 1998).

Columellar folds may not have a function. Still, convergence is considered to be some of the best evidence for adaptation (Raup and Gould, 1974; Harvey and Pagel, 1991; Larson and Losos, 1996), and columellar folds have evolved at least six times within different families of neogastropods (Price, 2001). Direct observations on how fold shape has evolved over time may reveal patterns of evolution that are consistent with adaptation. This approach would require a phylogenetic context (Harvey and Pagel, 1991; Larson and Losos, 1996), although there are currently no well-resolved

phylogenies that include a sufficiently large number of species with and without folds to give power to such an analysis. With the phylogenetic comparative method, it would be possible to determine whether folds evolved by "hitchhiking" along with demonstrably adaptive characters (Maynard Smith and Haigh, 1974).

On the other hand, folds may have evolved as a common solution to a number of problems, especially because the function of folds in pulmonates obviously differs from that in neogastropods. Functional experiments on species from a number of smaller clades that contain closely related species with and without folds should be conducted to identify functions unique to those smaller clades. If columellar folds serve different functions in different clades, then they might be an easy-to-evolve, flexible solution to a number of problems.

### Conclusions

Columellar folds probably do not guide the columellar muscle. Rather, the motion of the muscle is likely determined by muscle fiber orientation and by the attachment to the shell, which is along the upper edge of the muscle. The geometry of the attachment is probably responsible for its adhesive strength, and the weak physical connection between muscle and shell is not. The methods employed here show no association between the presence of folds and the length of columellar muscle attachment, surface area of attachment, or depth of attachment. The widely observed similarity in morphology between the folds and the columellar muscle may be due simply to their physical juxtaposition rather than to any functional relationship, with folds having some other and presently unknown functions. Because folds have evolved multiple times, the most plausible explanation for their existence might be that they are an easy-to-evolve solution to a number of functional demands.

### Acknowledgments

I thank Dan Reuman, Moon Duchin, and Chris Degni for generously devoting their time to help develop the algorithm to reconstruct the 3-D surface of the shell. Jason Goodman and Gidon Eshel helped debug the programs that implemented the algorithm. Deirdre Gonsalves-Jackson, Greg Farley, Cheryl Swanson, Jessica Cande, the Smithsonian Marine Station, and the Florida State University Marine Lab helped with field collections. Jochen Gerber, Janeen Jones, and Martin Prydzia at the Field Museum of Natural History helped deposit specimens. Additional thanks to Michael LaBarbera, David Jablonski, Rüdiger Bieler, Susan Kidwell, Peter Wagner, and colleagues at the University of Chicago for support throughout this research and helpful comments on the manuscript. Geerat J. Vermeij, two anonymous reviewers, and especially Michael J. Green-

berg provided helpful suggestions that greatly improved this paper. This material is based upon work supported by the National Science Foundation under Grant No. 0073248. NSF grant 9903030 to David Jablonski, the Conchologists of America, the Link Foundation and Smithsonian Marine Station, and the University of Chicago Hinds and Gurley Funds provided additional support.

### Literature Cited

- Abbott, R. T. 1974.** *American Seashells*, 2nd ed. Van Nostrand Reinhold, New York.
- Appleton, R. D., and A. R. Palmer. 1988.** Water-borne stimuli released by predatory crabs and damaged prey induce more predator-resistant shells in a marine gastropod. *Proc. Natl. Acad. Sci. USA* **85**: 4387–4391.
- Bertness, M. D., and C. Cunningham. 1981.** Crab shell-crushing predation and gastropod architectural defense. *J. Exp. Mar. Biol. Ecol.* **50**: 213–230.
- Bryant, H. N., and K. L. Seymour. 1990.** Observations and comments on the reliability of muscle reconstruction in fossil vertebrates. *J. Morphol.* **206**: 109–117.
- Carefoot, T. H., and D. A. Donovan. 1995.** Functional significance of varices in the muricid gastropod *Ceratostoma foliatum*. *Biol. Bull.* **189**: 59–68.
- Dall, W. H. 1894.** The mechanical cause of folds in the aperture of the shell of Gastropoda. *Am. Nat.* **28**: 909–914.
- Doguzhaeva, L., and H. Mutvei. 1996.** Attachment of the body to the shell in ammonoids. Pp. 43–63 in *Ammonoid Paleobiology*, N. H. Landman, K. Tanabe, and R. A. Davis, eds. Plenum Press, New York.
- Donovan, D. A., J. P. Danko, and T. H. Carefoot. 1999.** Functional significance of shell sculpture in gastropod molluscs: test of a predator-deterrent hypothesis in *Ceratostoma foliatum* (Gmelin). *J. Exp. Mar. Biol. Ecol.* **236**: 235–251.
- Fretter, V., and A. Graham. 1962.** *British Prosobranch Molluscs: Their Functional Anatomy and Ecology*. 1st ed. Ray Society, London.
- Fretter, V., and A. Graham. 1994.** *British Prosobranch Molluscs: Their Functional Anatomy and Ecology*, 2nd ed. Ray Society, London.
- Harasewych, M. G., and R. E. Petit. 1989.** The nomenclatural status and phylogenetic affinities of *Syrinx aruanus* Linné 1758 (Prosobranchia: Turbellinellidae). *Nautilus* **103**: 83–84.
- Harvey, P. H., and M. D. Pagel. 1991.** *The Comparative Method in Evolutionary Biology*. Oxford University Press, New York.
- Hodgson, A. N., and E. R. Trueman. 1987.** The siphons of *Scrobicularia plana* (Bivalvia; Tellinacea). Observations on movement and extension. *J. Zool.* **194**: 445–459.
- Hughes, R. N., and R. W. Elner. 1979.** Tactics of a predator, *Carcinus maenas*, and morphological responses of the prey, *Nucella lapillus*. *J. Anim. Ecol.* **48**: 65–78.
- Isaji, S., T. Kase, K. Tanabe, and K. Uchiyama. 2002.** Ultrastructure of muscle-shell attachment in *Nautilus pompilius* Linnaeus (Mollusca: Cephalopoda). *Veliger* **45**: 316–330.
- Johannesson, B. 1986.** Shell morphology of *Littorina saxatilis* Otivi: the relative importance of physical factors and predation. *J. Exp. Mar. Biol. Ecol.* **102**: 183–196.
- Kier, W. M. 1988.** The arrangement and function of molluscan muscle. Pp. 211–252 in *Form and Function*, E. R. Trueman and M. R. Clarke, eds. Academic Press, New York.
- Kier, W. M., and A. M. Smith. 1990.** The morphology and mechanics of octopus suckers. *Biol. Bull.* **178**: 126–136.
- Kier, W. M., and K. K. Smith. 1985.** Tongues, tentacles and trunks: the biomechanics of movement in muscular-hydrostats. *J. Linn. Soc. Lond. Zool.* **83**: 307–324.

- Kohn, A. J. 1999.** Anti-predatory defences of shelled gastropods. Pp. 169–181 in *Functional Morphology of the Invertebrate Skeleton*, E. Savazzi, ed. Wiley and Sons, New York.
- Larson, A., and J. B. Losos. 1996.** Phylogenetic systematics of adaptation. Pp. 187–220 in *Adaptation*, M. R. Rose and G. V. Lauder, eds. Academic Press, New York.
- Lindberg, D. R. 1985.** Aplacophorans, monoplacophorans, polyplacophorans, scaphopods: the lesser classes. Pp. 230–247 in *Mollusks: Notes for a Short Course*, D. J. Bottjer, C. S. Hickman, and P. D. Ward, eds. The University of Tennessee, Knoxville.
- Linsley, R. M. 1978.** Shell form and the evolution of gastropods. *Am. Nat.* **66**: 432–441.
- Marko, P. B., and A. R. Palmer. 1991.** Responses of a rocky shore gastropod to the effluents of predatory and non-predatory crabs: avoidance and attraction. *Biol. Bull.* **181**: 363–370.
- Marshall, D. J., A. N. Hodgson, and E. R. Trueman. 1989.** The muscular hydrostat of a limpet tentacle. *J. Molluscan Stud.* **55**: 421–422.
- Maynard Smith, J., and J. Haigh. 1974.** The hitch-hiking effect of a favourable gene. *Genet. Res.* **23**: 23–35.
- McGowan, C. 1982.** The wing musculature of the brown kiwi *Apteryx australis* Mantelli and its bearing on ratite affinities. *J. Zool.* **197**: 173–219.
- Morita, R. 1993.** Development mechanics of retractor muscles and the “Dead Spiral Model” in gastropod shell morphogenesis. *Neues Jahrb. Geol. Palaeontol. Abh.* **190**: 191–217.
- Morton, J. E. 1967.** *Molluscs*. Hutchinson University Library, London.
- Palmer, A. R. 1977.** Function of shell sculpture in marine gastropods: hydrodynamic destabilization in *Ceratosstoma foliatum*. *Science* **197**: 1293–1295.
- Palmer, A. R. 1979.** Fish predation and the evolution of gastropod shell sculpture—experimental and geographic evidence. *Evolution* **33**: 697–719.
- Paul, C. R. C. 1991.** The functional morphology of gastropod apertures. Pp. 127–140 in *Constructional Morphology and Evolution*, N. Schmidt-Kittler and K. Vogel, eds. Springer-Verlag, Berlin.
- Pojeta, J., Jr. 1985.** Early evolutionary history of diosome mollusks. Pp. 102–121 in *Mollusks: Notes for a Short Course*, D. J. Bottjer, C. S. Hickman, and P. D. Ward, eds. The University of Tennessee, Knoxville.
- Ponder, W. F. 1972.** The morphology of some mitriform gastropods with special reference to their alimentary and reproductive systems (Neogastropoda). *Malacologia* **11**: 295–342.
- Portelli, G. B. 1986.** Testing, analysis, and design of structural adhesive joints. Pp. 447–449 in *Structural Adhesives: Chemistry and Technology*, S. R. Hartshorn, ed. Plenum Press, New York.
- Price, R. M. 2001.** Using constructional data to detect convergence: an underutilized approach to studying adaptation in the fossil record. *Paleobios* **21**: 105–106.
- Raup, D. M., and S. J. Gould. 1974.** Stochastic simulation and evolution of morphology—towards a nomothetic paleontology. *Syst. Zool.* **23**: 305–322.
- Roy, K., D. Jahlonski, J. W. Valentine, and G. Rosenberg. 1998.** Marine latitudinal diversity gradients: tests of causal hypotheses. *Proc. Natl. Acad. Sci. USA* **95**: 3699–3702.
- Signor, P. W., III. 1982.** Resolution of life habits using multiple morphologic criteria: shell form and life-mode in turrilliform gastropods. *Paleobiology* **8**: 378–388.
- Signor, P. W., III, and P. W. Kat. 1984.** Functional significance of columellar folds in turrilliform gastropods. *J. Paleontol.* **58**: 210–216.
- Suvorov, A. N. 1993.** Some aspects of functional morphology of the aperture in the Pupillina suborder (Gastropoda Pulmonata). *Ruthenica* **3**: 141–152.
- Suvorov, A. N. 1999a.** The conflict between operative and conservative subsystems of organism in the evolution of terrestrial snails (Sylommatophora, Pulmonata). *Russ. J. Zool.* **3**: 401–409.
- Suvorov, A. N. 1999b.** Functional interrelations between aperture structures and soft organs in lower Geophila: 1. Pupillina, Oleacinina. *Russ. J. Zool.* **3**: 5–15.
- Suvorov, A. N. 1999c.** Some mechanisms of adaptation to the wet microhabitats in higher *Geophila* (Mollusca, Pulmonata). *J. Gen. Biol. (Moscow)* **60**: 177–188.
- Taylor, J. D., N. J. Morris, and C. N. Taylor. 1980.** Food specialization and the evolution of predatory prosobranch gastropods. *Palaeontology* **23**: 375–409.
- Thomas, G. B., Jr., and R. L. Finney. 1984.** *Calculus and Analytical Geometry*, 6th ed. Addison-Wesley, Reading, MA.
- Thompson, J. T., A. D. Lowe, and W. M. Kier. 1998.** The columellar muscle of prosobranch gastropods: morphological zonation and its functional implications. *Invertebr. Biol.* **117**: 45–56.
- Tompa, A. S., and N. Watabe. 1976.** Ultrastructural investigation of the mechanism of muscle attachment to the gastropod shell. *J. Morphol.* **149**: 339–352.
- Vermeij, G. J. 1978.** *Biogeography and Adaptation: Patterns of Marine Life*. Harvard University Press, Cambridge, MA.
- Vermeij, G. J. 1982.** Gastropod shell form, breakage, and repair in relation to predation by the crab *Calappa*. *Malacologia* **23**: 1–12.
- Vermeij, G. J. 1987.** *Evolution and Escalation: an Ecological History of Life*. Princeton University Press, Princeton, NJ.
- Vermeij, G. J. 1993.** *A Natural History of Shells*. Princeton University Press, Princeton, NJ.
- Vermeij, G. J. 2001a.** Innovation and evolution at the edge: origins and fates of gastropods with a labral tooth. *Biol. J. Linn. Soc.* **72**: 461–508.
- Vermeij, G. J. 2001b.** Taxonomy, distribution, and characters of Pre-Oligocene members of the *Cantharus* group of Pisaniiinae (Neogastropoda: Buccinoidea). *J. Paleontol.* **75**: 295–309.
- Vermeij, G. J., and P. W. Signor. 1992.** The geographic, taxonomic, and temporal distribution of determinate growth in marine gastropods. *Biol. J. Linn. Soc.* **47**: 233–247.
- Voltzow, J. 1990.** The functional morphology of the pedal musculature of the marine gastropods *Busycon contrarium* and *Haliotis kamtschatkana*. *Veliger* **33**: 1–19.
- West, K., A. Cohen, and M. Baron. 1991.** Morphology and behavior of crabs and gastropods from Lake Tanganyika, Africa—implications for lacustrine predator-prey coevolution. *Evolution* **45**: 589–607.

Appendix

Measuring True Surface Area and Location on a Shell from a Series of Photographs

Measuring surface area

A photograph defines an *XY*-plane that contains an object (Appendix Fig. 1A), and the pixels within the object are "on," whereas those outside the object are "off." That object is a projection of a surface, *Z*, onto the *XY*-plane. The projected surface area,  $SA_Z$ , is defined as

$$SA_Z = \int_x \int_y \left( 1 + \left( \frac{\partial z}{\partial x} \right)^2 + \left( \frac{\partial z}{\partial y} \right)^2 \right) dx dy \quad (A1)$$

(equation 6a in Thomas and Finney, 1984).

Because a digital photograph is pixelated, I approximated  $SA_Z$  by calculating the surface area of each pixel, *i*, then summing those values over all *n* pixels:

$$SA_Z = \sum_{i=1}^n \sqrt{1 + \left( \frac{\Delta z}{\Delta x_i} \right)^2 + \left( \frac{\Delta z}{\Delta y_i} \right)^2} A_i dx dy, \quad (A2)$$

where  $A_i$  is the area of the pixel. Since the area of a pixel is 1, Equation A2 reduces to

$$SA_Z = \sum_{i=1}^n \sqrt{1 + \left( \frac{\Delta z}{\Delta x_i} \right)^2 + \left( \frac{\Delta z}{\Delta y_i} \right)^2} dx dy. \quad (A3)$$

I found the partial derivative of *Z* with respect to *x* and the partial derivative of *Z* with respect to *y* by assuming that the object was a series of circles stacked on top of each other. Each row in the object corresponded to one circle, and all circles were centered about the *Y*-axis, which is also the coiling axis. Anyone familiar with the shape of neogastropods will recognize that the columella is somewhat asymmetrical. Imposing symmetry on the columella inflated true surface area, but this deviation was uniform across randomly sampled specimens with and without folds (28% inflation, st. dev. = 15%, *n* = 10).

Consider one row of pixels, *i*, of the photograph. The number of "on" pixels in that row equals the diameter of the circle, because the circle was projected straight onto that row. Thus, the circle's radius and origin were both known, the surface function,  $z_i$ , for a given row was

$$x_i^2 + z_i^2 = r_i^2 \quad (A4)$$

(Appendix Fig. 1B), and the partial derivative was

$$\frac{\partial z_p}{\partial x_p} = \frac{-x_p}{\sqrt{r_i^2 + x_p^2}} \quad (A5)$$

where *p* was any pixel in row *i* of the object.

The partial derivative of *Z* in the *x*-direction represented the distortion of the projection due to the curvature of the circle about the coiling axis. Therefore, a pixel located immediately on or above the coiling axis did not have any horizontal distortion, and the two pixels 90° from the coiling axis were the most severely distorted.

To calculate the partial derivative of *Z* with respect to *y*, I expressed the edge of the image as  $f(y) = r$ . Rewriting Equation A4 gives:

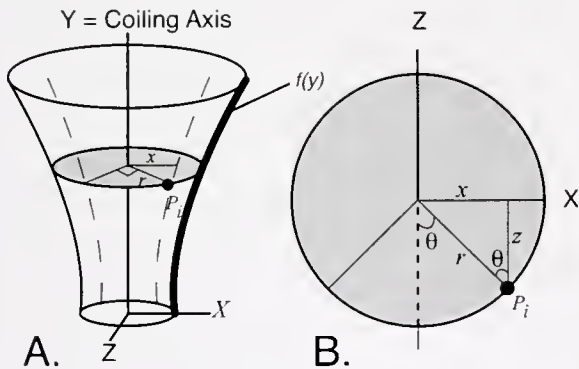
$$x_i^2 + y_i^2 = f(y_i)^2. \quad (A6)$$

where  $f(y)$  was found empirically by fitting a second-degree polynomial to the edge. The partial derivative  $\partial z/\partial y$  was evaluated from this polynomial.

The resulting area was measured in pixels.

Identifying a target region

A curved surface projects a 180° sector onto a row, so when a series contains photographs taken every 90° about a coiling axis, the photographs overlap. I eliminated overlap by using only the middle of each image (dashed lines in Appendix Fig. 1). This approach has the added benefit of using the region of the photograph with the best focus and least distortion.



Appendix Figure 1. (A) A shell in a photograph can be thought of as a stack of circles centered on a coiling axis, *Y*. *r* is the radius of a circle, measured as one-half the number of "on" pixels in a row. Dashed lines define the target region, 45° on either side of the coiling axis; *x* is the distance from the coiling axis to the edge of the target region. The curve in bold is  $f(y) = z$ . (B) The projection of a circle onto the *XZ*-plane. The *Y*-axis is perpendicular to the page.  $\theta$  is the angle from the coiling axis, and the coiling axis always corresponds to a landmark line in these photographs. Since *r* is known, and *x* is the projected distance from the coiling axis to  $P_i$ , both *z* (the surface function) and  $\theta$  (the angle between  $P_i$  and the landmark) can be calculated.

One row of "on" pixels represented a circle projected onto its diameter. The coiling axis marked the midpoint of the diameter, and the end points of the row were  $45^\circ$  and  $-45^\circ$  from the coiling axis. If we draw the circle, we can see that its radius is the hypotenuse of an isosceles right triangle (Appendix Fig. 1B). The sides of this triangle equal the  $x$ -coordinate for the boundary of the target region.

#### *Measuring degrees from aperture*

I used the same circle to locate point  $P_i$  relative to the aperture (Appendix Fig. 1), to calculate the edges of the attachment. In this case, I determined the  $X$ -coordinate of the point from the photograph, which is simply the distance

between the coiling axis and  $P_i$ . Here, the  $X$ -coordinate was known, but the triangle was not necessarily isosceles, so the angle,  $\theta$ , was not known. The angle that defined the arc between the coiling axis and  $P_i$  was calculated:

$$\theta = \text{asin}\left(\frac{x}{r}\right) \quad (\text{A7})$$

If  $P_i$  was apertural to the nearest landmark, I subtracted  $\theta$  from the landmark's depth. Suppose, for example, that  $P_i$  was depth of attachment, the curve  $f(y)$  in Appendix Figure 1 was coincident with the landmark at  $270^\circ$ , and  $\theta$  equals  $20^\circ$ . The value of attachment depth would be  $290^\circ$ . If  $P_i$  were apical to the nearest landmark, then I would have added  $\theta$  to the landmark's depth.

# Response in Nematocyst Uptake by the Nudibranch *Flabellina verrucosa* to the Presence of Various Predators in the Southern Gulf of Maine

KINSEY FRICK

*NOAA Fisheries, Northwest Fisheries Science Center, Fish Ecology Division,  
2725 Montlake Boulevard East, Seattle, Washington 98112*

**Abstract.** Aeolid nudibranchs maintain nematocysts sequestered from their cnidarian prey for protection against predators. Selection for nematocyst incorporation is a function of diet and prey choice, but ratios vary among nudibranchs feeding on a given diet, indicating that other factors may be involved. It is proposed that the presence of predators influences nematocyst incorporation. Nematocyst uptake in the nudibranch *Flabellina verrucosa* collected from the southern Gulf of Maine was examined in response to various potential predators, including *Crossaster papposus*, *Tautogolabrus adspersus*, and *Carcinus maenas*. Nudibranchs in individual flow-through containers feeding on a diet of the hydroids *Tubularia* spp. and *Obelia geniculata* were subjected to tanks containing a predator, then their nematocyst distribution was examined. Although most of the changes over the experimental period were attributable to diet, *F. verrucosa* responded to both *T. adspersus* and *C. papposus* by significantly increasing microbasic mastigophore incorporation. No differential uptake was seen with *C. maenas*. Response was evident in the nudibranchs both for predators present in the collection area and for those with which they had no previous exposure, indicating that *F. verrucosa* modulates nematocyst incorporation in response to the presence of predators as well as to diet. A coevolution of nudibranchs and potential predators may govern changes in nematocyst uptake.

## Introduction

Prey anti-predator responses are crucial to prey survival, though studies of predator-prey coexistence often focus on predator characteristics (for reviews see Murdoch and Oaten, 1975; Hassell, 1978; Taylor, 1984). Prey species reduce their mortality from predation by using a variety of tactics. Mobile animals may be protected by armored or cryptic morphologies, noxious chemicals, and a variety of escape behaviors (Edmunds, 1974; Pianka, 1983; Havel, 1987). In marine communities, opisthobranch nudibranchs would seem a likely prey item since they are not protected against predation by the shell employed by prosobranch gastropods. To compensate for the lack of a natural physical refuge, nudibranchs have developed various defensive strategies, including avoidance behaviors, cryptic or aposematic coloration, spicules, toxic secretions, and stinging nematocysts (summarized by Harris, 1973). They are slow-moving and often flamboyantly colored or on contrasting substrate, but despite their being seemingly easy prey, there are few reports of predation on nudibranchs (Thompson, 1976; Karuso, 1987; Faulkner, 1992; Proksch, 1994), thus demonstrating the efficacy of nudibranch defense tactics.

An aspect of predator-prey interactions unique to the defensive strategies of some aeolid nudibranchs is their use of cnidarian nematocysts. For armament against predators, these nudibranchs maintain an arsenal of functional stinging nematocysts that they acquire, through ingestion, from their cnidarian prey (Thompson, 1960; Edmunds, 1966; Thompson and Bennett, 1969; Greenwood and Mariscal, 1984a, b). Nematocysts pass through the digestive tract to the tips of the dorsal cerata, where they are incorporated into specialized cavities called cnidosacs and are maintained in a functional state (Conklin and Mariscal, 1977; Greenwood and

Received 11 October 2002; accepted 15 September 2003.

E-mail: Kinsey.Frick@noaa.gov.

*Abbreviations:* BI, basitrichous isorhizas; DS, desmosomes; HeA, heterotrichous anisorhizas; HI, holotrichous isorhizas; HME, heterotrichous microbasic euryteles; HoA, holotrichous anisorhizas; MA, microbasic amastigophores; MM, microbasic mastigophores; ST, stenoteles.

Mariscal, 1984a). The nematocysts are then available to be ejected by the nudibranch, presumably as a defense mechanism.

While it is well understood that aeolid nudibranchs store cnidarian nematocysts from their prey, the dynamics of nematocyst selection are not explicit. There are more than 25 types of nematocysts in cnidarians (see Mariscal, 1974), each with different functions in prey acquisition and defense, and those present in a given cnidarian are a function of the species. Therefore, specific nematocysts are present in varying combinations and proportions among nudibranch prey species (Mariscal, 1974; Calder, 1988). Nudibranch nematocyst incorporation is a function of availability in the diet, so depending on the cnidarian prey they consume and on which parts of the prey, nudibranchs sequester different kinds of nematocysts within their cnidosacs. Additionally, they can preferentially select specific types from what is available (Grosvenor, 1903; Day and Harris, 1978). The nematocyst complement serves as a measure of feeding history, as nudibranchs incorporate a small number of all nematocyst types found in the prey they have been consuming. However, individuals of a given nudibranch species feeding on the same diet sequester varying proportions of those nematocyst types (pers. obs.), indicating that factors other than strict availability must be involved in selection.

Predation pressure may influence nematocyst uptake, and therefore different nematocyst types may be selected in response to specific predators. Since nudibranch nematocysts purportedly function as predator deterrents, predator cues may affect nematocyst incorporation such that nudibranchs maintain weapons capable of combating predators specific to the area in which they live. Edmunds (1966) suggested that certain nematocyst types may be more effective against some predators—penetrants for use against fish and adherents against crustaceans, for example—so nematocyst incorporation may be based on nudibranch predators in the vicinity. Despite studies of individual species populations, few studies have examined variation with respect to the predation pressure encountered by the organism in question. The objective of this study was to identify changes in nematocyst uptake by nudibranchs in response to chemical cues from potential predators. My work examines the incorporation of nematocysts by nudibranchs in response to individual predator species and considers both predation pressure and the nudibranch's previous experience. To further elucidate the relationship between nematocysts in nudibranch cnidosacs and predation pressures, I examined nematocyst uptake in the nudibranch *Flabellina verrucosa* with and without exposure to potential predators. I hypothesize that (a) the presence of specific predators differentially affects nematocyst uptake, (b) response depends on the nudibranch's previous exposure to the predator, and (c) response depends on the predator's ability to prey on the nudibranch. By testing these hypotheses I will determine

whether population-level variation in nematocysts sequestered by *F. verrucosa* provides a link between nematocyst incorporation and predation pressure.

## Materials and Methods

### Study organisms

*Flabellina* (formerly *Coryphella*) *verrucosa* (= *rufibranchialis*) (Sars, 1829) is a common aeolid nudibranch in the shallow marine subtidal throughout the Gulf of Maine. Its distribution is circumboreal: in the Atlantic its range includes northern Europe (British Isles, Norway, and Iceland) and Greenland south to the Gulf of Maine; in the Pacific *F. verrucosa* can be found off British Columbia and the coast of Russia (Bleakney, 1996). A generalist predator, *F. verrucosa* consumes numerous athecate hydroid species, scyphistomae, and tunicates (Kuzirian, 1979). No predators are known to prey primarily on this nudibranch.

In the following experiments, *F. verrucosa* was exposed to a variety of predators, and nematocyst uptake was compared with uptake in the absence of predator cues. The predators to which *F. verrucosa* was exposed included the wrasse *Tautoglabrus adspersus* (Walbaum, 1792), the sea star *Crossaster papposus* (Linnaeus, 1767), and the green crab *Carcinus maenas* (Linnaeus, 1758). *Crossaster papposus* is present in cold deep waters in the southern Gulf of Maine collection area, though none were observed at the depths where nudibranchs were collected for this study. While not a nudibranch specialist, *C. papposus* feeds on nudibranchs, including *F. verrucosa*, when they are encountered in the field (Mauzey *et al.*, 1968) (pers. obs.). Among its other prey, the wrasse *T. adspersus* (cunner) is known to feed voraciously on some nudibranch species, but shows an aversion to consuming *F. verrucosa* (Harris, 1986; pers. obs.). Cunner are seasonally abundant in the southern Gulf of Maine in the summer and fall when water temperatures are mild, but they are absent during the colder winter and spring seasons. The omnivorous green crab *Carcinus maenas* is common both intertidally and subtidally throughout the Gulf of Maine, but unlike some crab species reported to prey on certain nudibranchs (Harris, 1970; Ajeska, 1971), *C. maenas* is not a known nudibranch predator.

The experience that specimens of *F. verrucosa* collected in the southern Gulf of Maine have had with the predators used in this study ranges from common exposure (*C. maenas* and *T. adspersus*) to no probable exposure (*C. papposus*) for nudibranchs of the collected generation. Depending on collection location, there may be differences in exposure to cunner: nudibranchs collected from mooring chains at Shoals are less likely to have encountered *T. adspersus* than those from Nubble (description below). At Nubble, fish forage and live on the wall where nudibranchs were collected, but at Shoals, the mooring lines do not support substantial populations of the predatory fish. For all collec-

tion sites, nudibranchs are unlikely to be found deep enough to have been exposed to *C. papposus* prior to collection. However, parental generations of *F. verrucosa* may have been exposed to the entire suite of experimental predators in other areas within the species' range, presenting the possibility that nematocyst uptake could be influenced by a coevolutionary response based on exposure of previous generations to the predators used in this study.

#### Specimen collection

Nudibranchs were collected from two locations within the southern Gulf of Maine: Cape Neddick (Nubble) in York, Maine (43°9'54"N, 70°35'29"W), and Gosport Harbor near Appledore and Lunging Islands of the Isles of Shoals island group located about 10 km off the coast of New Hampshire (42°59'21"N, 70°36'54"W). The shallow subtidal of Cape Neddick and the Isles of Shoals are both algal-dominated, gradual slopes containing vertical rock surfaces and undercuts dominated by animal communities. Nudibranch populations at these sites are of the same genetic stock due to site proximity and widespread dispersal of planktonic veliger larvae, but their post-settlement feeding histories may differ due to the availability of prey items at the two locations.

Between 30 and 50 specimens of *Flabellina verrucosa* were collected from vertical rock wall surfaces at Nubble in 3–8 m of water, and also from blooms of the hydroid *Tubularia crocea* on mooring ball lines near the Isles of Shoals (Appledore and Lunging Islands) in October and November 2001 and January 2002. Animals were maintained following collection and for the duration of all experiments at 10 °C in a constant-temperature room at the University of New Hampshire. Tanks were filled with natural seawater obtained from the Coastal Marine Laboratory at the Portsmouth Coast Guard Station at the mouth of Portsmouth Harbor (43°4'20"N, 70°42'37"W). Animals for each site were kept together and used separately in each experiment.

#### Experimental setup

Experimental tanks containing a predator were established 1–2 days before experiment inception. Control tanks did not contain a predator. Following initial nematocyst counts (procedure described below) for each nudibranch population, nudibranchs were placed in individual flow-through containers with two hydroid food sources. The hydroids used were *Obelia geniculata* (Linnaeus, 1758) and *Tubularia* spp. (*crocea* and/or *indivisa*), each present in excess so that food was not a limiting factor. Examination of the tissues of these cnidarian prey species revealed mutually exclusive nematocyst complements (Table 1), so they offer a variety of nematocyst types. *Tubularia* spp. were collected from the nudibranch collection sites at the Isles of Shoals,

Table 1

*Nematocyst types found upon examination of cnidarian prey tissues*

Hydroid species	Nematocysts apparent in tissue*
<i>Obelia geniculata</i>	MM, MA
<i>Tubularia indivisa</i> , <i>T. crocea</i>	ST, DS, HeA, HME, BI

\* Nematocyst types are abbreviated as follows: MM, microbasic mastigophores; MA, microbasic amastigophores; ST, stenoteles; DS, desmonemes; HeA, heterotrichous anisorhizas; HME, heterotrichous microbasic euryteles; BI, basitrichous isorhizas.

and *O. geniculata* from pilings at the Portsmouth Coast Guard Station. The hydroids used as prey were not fed during the experiment and have no direct ecological relationships with the predators used in the study.

Experimental flow-through containers remained in the tanks for 2 weeks, with a fresh replacement of hydroid food and a partial water change in the tanks after 7 days. Control tanks had five containers for each nudibranch population randomly distributed among the tanks. After 2 weeks of exposure to the experimental conditions, the nematocyst content of each nudibranch was evaluated by examining ceras squashes for three cerata per animal *via* light microscopy. Cerata were removed from the anterior region in the first or second ceratal cluster by using forceps combined with the animals' propensity to autotomize these projections. For each ceras, 100 nematocysts (identification according to Mariscal, 1974; see reference for visual representations) were categorized on the basis of visual characteristics (if the field of view included more than 100 nematocysts, all in the field were counted). Counts included both fired and encapsulated (unfired) nematocysts. The setup was repeated with each predator and for each nudibranch collection site, adjusted as described below. The numbers of replicates for each experiment are summarized in Table 2.

For the *C. papposus* experiment, ten 2.5-gallon tanks containing a sea star measuring 2.7–6.5 cm and three 2.5-gallon tanks without a sea star were established. Each tank contained one container for each nudibranch collection site. The sea stars were starved for the duration of the experiment because they refused to eat regularly once brought into the laboratory. The experiment using the cunner *T. adspersus* was conducted similarly, but due to limited numbers of captive fish, it involved six 10-gallon tanks, each containing two flow-through containers for each experimental site. The cunner in the tanks measured between 7 and 17 cm and were fed locally collected *Mytilus edulis* meat every other day. When the green crab *Carcinus maenas* was used as the predator, tank setup and size was equivalent to that used for the *C. papposus* experiment, with crab carapace size ranging from 5.5 to 7.0 cm. Crabs were fed frozen cooked

Table 2

Summary of experimental design, including number of replicate flow-through containers for each population and each treatment

Predator treatment	Number of experimental containers	Number of experimental tanks	Number of control containers	Number of control tanks
<i>Crossaster papposus</i>	10	10	5	3
<i>Tautoglabrus adspersus</i>	12	6	6	3
<i>Carcinus maenas</i>	10	10	5	4

shrimp two to three times weekly for the duration of the experiment.

Total numbers of nematocysts for each condition were analyzed using chi-square tests of independence to identify differences in the distribution of nematocysts. Pairwise ANOVA analyses were performed on average nematocyst proportions for each nudibranch using the PC program Systat 9.0 to determine the nematocyst types that were exhibiting changes for each comparison of conditions.

## Results

Southern Gulf of Maine populations of *Flabellina verrucosa* responded to the presence of some experimental predators by changing which nematocyst types they incorporated. Field-collected nudibranchs showed a wide range of incorporated nematocysts and high variability between individuals and between sites (Fig. 1), with stenoteles (ST), desmonemes (DS), and heterotrichous microbasic euryteles (HME) sharing dominant percentages. The results for predator exposure are subdivided below, and nematocyst incorporation response for all predators is summarized in Table 3. All results marked as being significant are based on *P* values less than 0.05.

### Southern Gulf of Maine predator responses

*Flabellina verrucosa* responded to the presence of *Crossaster papposus* with significantly increased incorporation of microbasic mastigophores (MM) and depressed uptake of heterotrichous anisorhizas (HeA) (Fig. 2A). In response to *Tautoglabrus adspersus* (cunner), incorporation of MM was also significantly increased (Fig. 2B), while uptake of heterotrichous microbasic euryteles (HME) and stenoteles (ST) was depressed. The presence of the green crab *Carcinus maenas* evoked no significant differences in nematocyst incorporation compared to control nudibranchs (Fig. 2C); all differences were attributable only to change due to the provided diet.

### Site-dependent responses

Trends in nematocyst incorporation depended on the predator used, not the site where the nudibranchs were

collected. However, these trends were not always significant.

When exposed to the sea star *Crossaster papposus*, nudibranchs from Shoals significantly adjusted their nematocyst incorporation, (Fig. 3A) following the same trends as the combined data for the two sites (Fig. 2). Those from Nubble showed no significant differences attributable to the presence of *C. papposus*, but showed a propensity for increased incorporation of MM (Fig. 3B).

Exposure to the cunner *T. adspersus* also triggered significantly increased incorporation of MM in the Shoals population when compared to the control group (Fig. 4A), while uptake of three other nematocyst types was depressed. Nudibranchs from Nubble showed similar trends of increasing nematocyst incorporation, but the only significant difference was lower uptake of microbasic amastigophores (MA) in the experimental nudibranchs (Fig. 4B).

As in the combined test (see Fig. 2C), the presence of *Carcinus maenas* did not elicit differences in nematocyst incorporation for experimental nudibranchs in comparison with control animals for either the Shoals or Nubble populations.

### Control comparison

Individual southern Gulf of Maine populations incorporated nematocysts similarly from the provided hydroid diets, yet exhibited some differences in nematocyst uptake in the absence of predator cues. However, results were not consistent between experiments when comparing control groups from the different collection sites (Fig. 5). In the experiment with *C. papposus*, nudibranchs collected from Shoals had significantly higher incorporation of ST (Fig. 5A). In the *T. adspersus* experiment, Nubble nudibranchs retained a significantly higher percentage of desmonemes (DS) than the Shoals population, and significantly fewer HME and holotrichous anisorhizas (HoA) (Fig. 5B). Conversely, the control comparison from the *Carcinus maenas* experiment showed that nudibranchs from Shoals kept more DS (Fig. 5C).

## Discussion

The animal world offers numerous illustrations of predator incorporation of prey defense mechanisms. Some of the

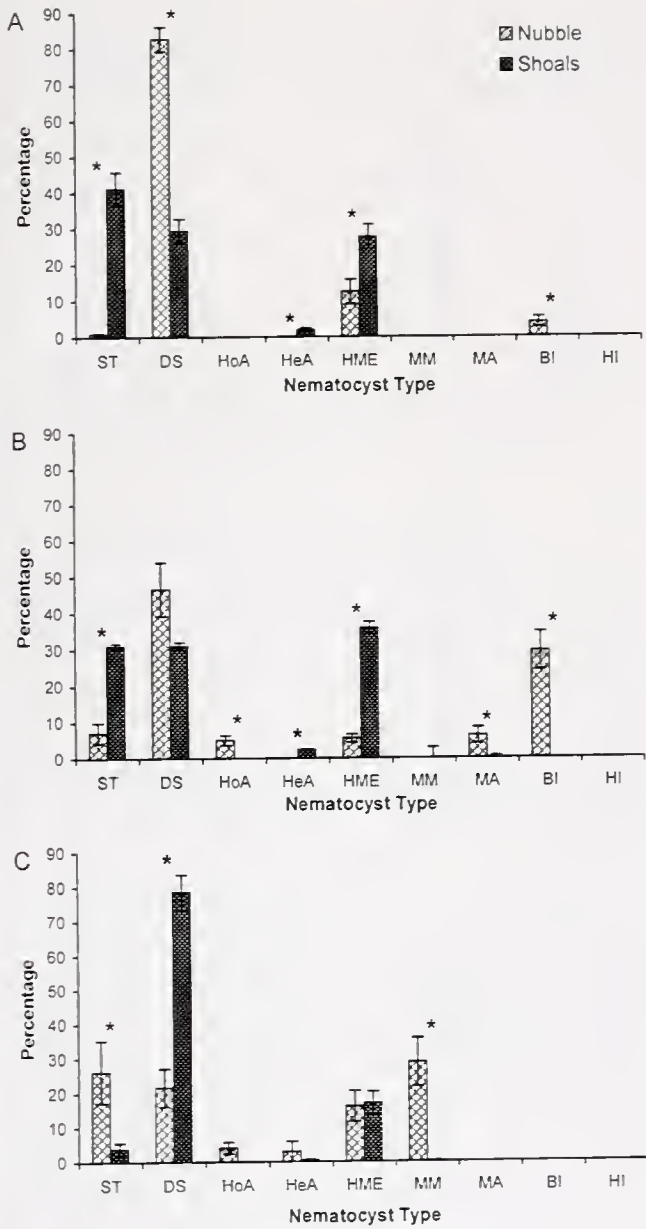


**Figure 1.** Initial distribution of nematocyst types in *Flabellina verrucosa* collected from two sites in the southern Gulf of Maine. Results are presented according to the predator experiment for which the nudibranchs were collected: (A) *Crossaster papposus*, (B) *Tautogolabrus adspersus*, and (C) *Carcinus maenas*. \*Indicates significant differences.  $P < 0.05$ . Nematocyst types: ST, stenoteles; DS, desmosomes; HoA, holotrichous anisorhizas; HeA, heterotrichous anisorhizas; HME, heterotrichous microbasal euryteles; MM, microbasal mastigophores; MA, microbasal amastigophores; BI, basitrichous isorhizas; HI, holotrichous isorhizas.

most specialized species store prey-derived toxins and use them for their own chemical defenses against predators at the third trophic level (Rowell-Rahier and Pasteels, 1992). Among the many examples in insects and vascular plants (Rothschild, 1973; Rowell-Rahier and Pasteels, 1992), the most famous involves monarch butterflies utilizing carde-

nolides from milkweed host plants (Brower *et al.*, 1972, 1975; Brower and Moffitt, 1974; Dixon *et al.*, 1978; Calvert *et al.*, 1979; Seiber *et al.*, 1986; Malcolm and Brower, 1989; Malcolm and Zalucki, 1996). In the marine realm, some dorid nudibranchs sequester chemical compounds from sponges for defense against predators (Karuso, 1987; Scheuer, 1990; Faulkner, 1992; Proksch, 1994). With both monarch butterflies and dorid nudibranchs, the uptake process is selective in that the predator incorporates specific compounds from those available in the host (monarchs: Seiber *et al.*, 1986; nudibranchs: Proksch, 1994). However, while the process is discriminatory, there is no evidence that selectivity can be modified in response to environmental cues. In the case of *Flabellina verrucosa* and its incorporation of cnidarian nematocysts, the animal not only has choices as to the specific defensive structure to sequester, but as shown in this study, the selection can also be based on chemical cues from specific predators. This is an instance of secondary induction, where the nudibranch responds to the presence of predators by altering incorporation of defensive organelles from the cnidarian prey.

*Flabellina verrucosa* from the southern Gulf of Maine responded to both *Crossaster papposus* and *Tautogolabrus adspersus* by increasing incorporation of one type of penetrating nematocyst, the microbasal mastigophore. In cnidarians, this nematocyst has been suggested to be an effective defense against predation by the nudibranch *Cratena pilata* (Kepner, 1943); when incorporated by a nudibranch, it may also be effective against a diverse suite of predators. For nudibranchs, as for cnidarians, use of a single type of nematocyst against many predators may be more efficient than needing a different nematocyst for each potential predator.

Given the experimental nudibranchs' lack of field exposure to some of the predators used in this study, the uptake of a single nematocyst type (MM) in response to multiple predators could reflect an inducible defensive selectivity. Such selectivity may be attributable to a variety of factors, including the long-term coevolution of nudibranchs with these predators, genetic control over nematocyst response to predator cues, or a propensity to take up a particularly noxious nematocyst when any potential predators are present. The ability of *F. verrucosa* to respond to *C. papposus* and *T. adspersus* can be explained in two ways: either nudibranchs in this generation have had prior experience with these predators, or they are demonstrating a coevolutionary response based on exposure to these predators over time. Individuals of *F. verrucosa* collected from the southern Gulf of Maine are likely to have been exposed to *T. adspersus*, and they responded strongly by increasing uptake of a potent nematocyst (Fig. 2B). Nudibranchs from the two collection sites showed the same trends when exposed to cunner, but the response was not significant for the specimens from Nubble (Fig. 4, Table 3). The ecological

Table 3

Significant change in nematocyst incorporation between experimental and control *Flabellina verrucosa* when exposed to each predator for each individual collection site and the combined southern Gulf of Maine

Population	Significant changes in nematocyst incorporation	Predator		
		<i>Crossaster papposus</i>	<i>Tautogolabrus adspersus</i>	<i>Carcinus maenas</i>
Combined southern Gulf of Maine	Increased	MM ( $P = 0.004$ )	MM ( $P = 0.001$ )	(NR)
	Decreased	HeA ( $P = 0.006$ )	HME ( $P = 0.033$ ), ST ( $P = 0.003$ )	(NR)
Nubble	Increased	(NR)	(NR)	(NR)
	Decreased	(NR)	MA ( $P = 0.009$ )	(NR)
Shoals	Increased	MM ( $P = 0.038$ )	MM ( $P = 0.000$ )	(NR)
	Decreased	HeA ( $P = 0.003$ )	HME ( $P = 0.000$ ), ST ( $P = 0.000$ ), HeA ( $P = 0.047$ )	(NR)

Nematocyst types are abbreviated as follows: MM, microbasic mastigophores; HeA, heterotrichous anisorhizas; HME, heterotrichous microbasic caryteles; ST, stenoteles; MA, microbasic amastigophores. (NR) indicates no significant response.

context of nudibranchs and cunner at this site may explain the lack of significance: although the nudibranchs settle among a dense population of cunner and may be nipped at, they may recognize that these fish do not represent a valid threat; thus they are less likely to significantly change their incorporation of nematocysts. However, the nudibranchs used in this study are unlikely to have encountered *C. papposus* at the shallow subtidal sites where they were collected, yet they still modified their nematocyst incorporation (Fig. 2A). By increasing incorporation of a formidable penetrant, specimens of *F. verrucosa* are probably demonstrating a response due to their long-term coevolution with both experimental predators in other parts of their circumboreal distribution. In this study, regardless of the likelihood of previous individual exposure to the potential predator, *F. verrucosa* countered by incorporating larger percentages of the penetrating microbasic mastigophore.

Conversely, *Carcinus maenas* is a common crab in the Gulf of Maine and also co-occurs with *F. verrucosa* in Europe, but it is not known to actually prey upon *F. verrucosa*. Therefore, the nudibranch's failure to modify the type of nematocysts it sequesters when exposed to chemical cues from the green crab is not surprising. Thus, incorporation of specific nematocyst types is increased in response only to realistic potential predators and can be modified depending on the specific predator cue the nudibranch receives.

This system is unique in that nudibranchs selectively incorporate the defenses of another organism for specialized adapted defense against their predators. The indirect interactions in the system are analogous to trait-mediated indirect effects. Such effects arise when one species modifies the way two other species interact by causing changes in the behavior of the intervening species (Abrams, 1995; Abrams *et al.*, 1996; Werner and Anholt, 1996; Schmitz and Suttle, 2001). In interactions involving *Flabellina verrucosa*, the presence of a predator elicits a response from the nudibranch, but the cascade continues down the food web to the

level of the nudibranch's cnidarian prey. Responses to increased predation that result in changes in prey use are examples of trait-mediated indirect effects (*e.g.*, Messina, 1981; Power *et al.*, 1985; Turner and Mittelbach, 1990; Huang and Sih, 1991; McIntosh and Townsend, 1996; Peacor and Werner, 1997; Beckerman *et al.*, 1997; Turner *et al.*, 1999). *Flabellina verrucosa*'s increased incorporation of microbasic mastigophores from its cnidarian prey in the presence of the predators *Crossaster papposus* and *Tautogolabrus adspersus* is a unique example of such an interaction.

The hydroid species used in this study were abundant at both collection sites. *Flabellina verrucosa* is more often found associated with the *Tubularia* spp. (pers. obs.), though the nudibranchs collected had nematocysts representative of both experimental prey species (Fig. 1). However, the trends in preferential uptake of specific nematocysts shown between nudibranch populations collected from different sites and substrates may be related to pre-collection feeding differences. In addition to post-experimental changes in nematocyst uptake in response to the presence of some predators, the populations considered here incorporated somewhat different nematocysts from the provided diet even when no predator was present, as seen in the control comparisons (see Fig. 5).

The differences observed may demonstrate acquired tendencies of incorporation as a result of feeding history or disparities in the populations' ingestive conditioning. Ingestive conditioning affects selection of prey species in other aeolids such that they will preferentially prey upon species they have been feeding upon recently (Hall *et al.*, 1982; Hall and Todd, 1984), but it has never been considered with respect to nematocyst selection. However, all nematocyst types that were significantly different in the control populations at the end of the experiment (Fig. 5) had also been significantly different when the nudibranchs were collected (Fig. 1). The original nematocyst complement may still

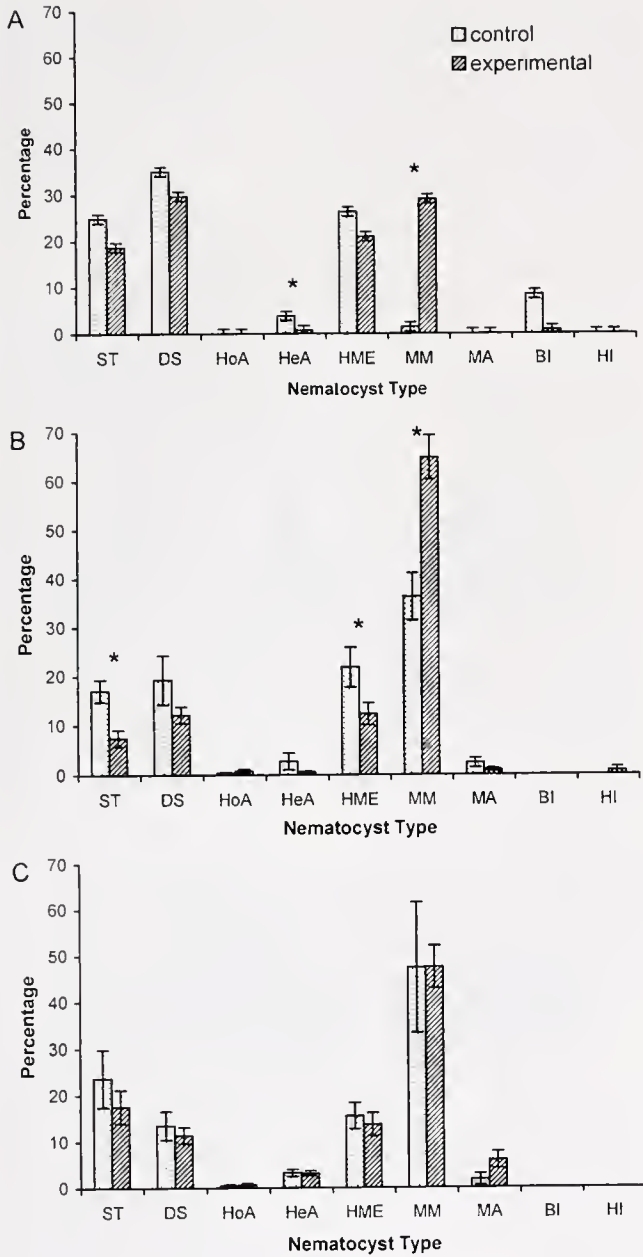


**Figure 2.** Changes in nematocyst uptake by *Flabellina verrucosa* collected in the southern Gulf of Maine in response to predator cues: (A) *Crossaster papposus*, (B) *Tautoglabrus adspersus*, (C) *Carcinus maenas*. \*Indicates significant differences,  $P < 0.05$ . Nematocyst types as in Figure 1.

have been affecting the cnidom, though nematocysts in *F. verrucosa* are replaced quickly, with complete exchanges occurring within 12 days of switching diets (Day and Harris, 1978). These results indicate that ingestive conditioning may play a role in nematocyst preference in subsequent feeding trials, though directed responses to predator cues are possible despite such tendencies.

Preferential feeding on *Obelia geniculata* by *F. verrucosa* in the presence of *T. adspersus* and *C. papposus* could

explain the observed increase in MM, as *O. geniculata* is the source of this nematocyst type for the experiment. However, nematocysts from the *Tubularia* spp. tissue (ST, DS, and HME) were also present at high levels in these animals. Although nudibranch feeding preference was not quantified, when the experiments were monitored or cnidarian prey were changed, nudibranchs were observed more often on the *Tubularia* hydroids. This observation and the presence of tubularian nematocysts suggest that a superficial preference for consuming *O. geniculata* in the face of predators cannot solely explain the increase in microbasic mastigophores.

The ability of a prey species to react by optimizing specific defense mechanisms against a given predator increases its fitness by decreasing mortality by predation. While this study has not shown any particular nematocyst to be an effective weapon against a specific predator, the nudibranchs' change in nematocyst selectivity suggests a directed response in which choices about prey use and nematocyst incorporation are made in response to predator cues. However, work on the specifics of that response and on its effectiveness against the predators is still lacking.

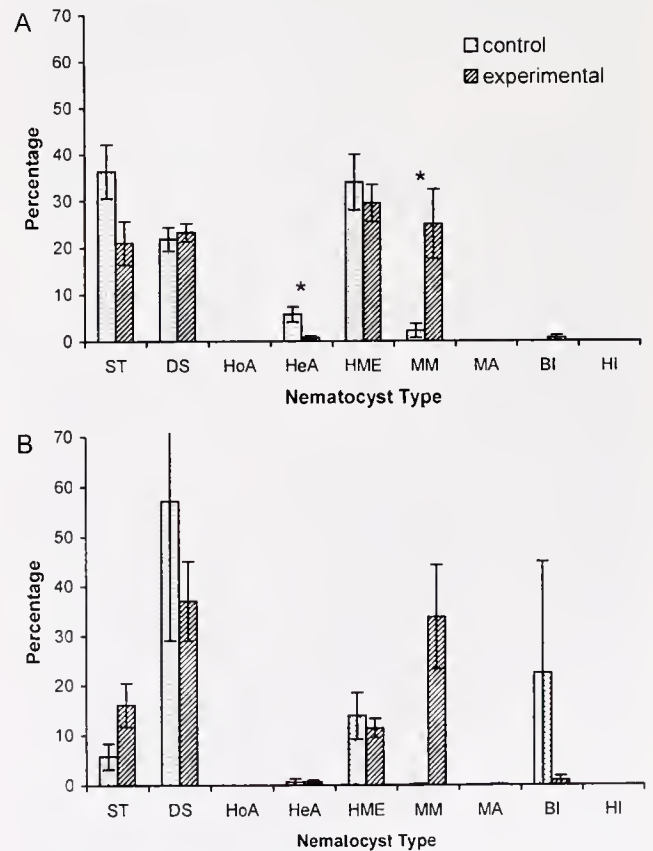


**Figure 3.** Site-dependent responses in nematocyst uptake by *Flabellina verrucosa* caused by cues from *Crossaster papposus* for nudibranchs collected from (A) Isles of Shoals and (B) Nubble. \*Indicates significant differences,  $P < 0.05$ . Nematocyst types as in Figure 1.

perspective of both predator and prey. These concepts provide avenues of further study to elucidate the dynamics that control nematocyst uptake and the potential for predator response by aeolid nudibranchs. Determining how such predilection operates and its efficacy in deterring predation will help us better understand ecological communities and

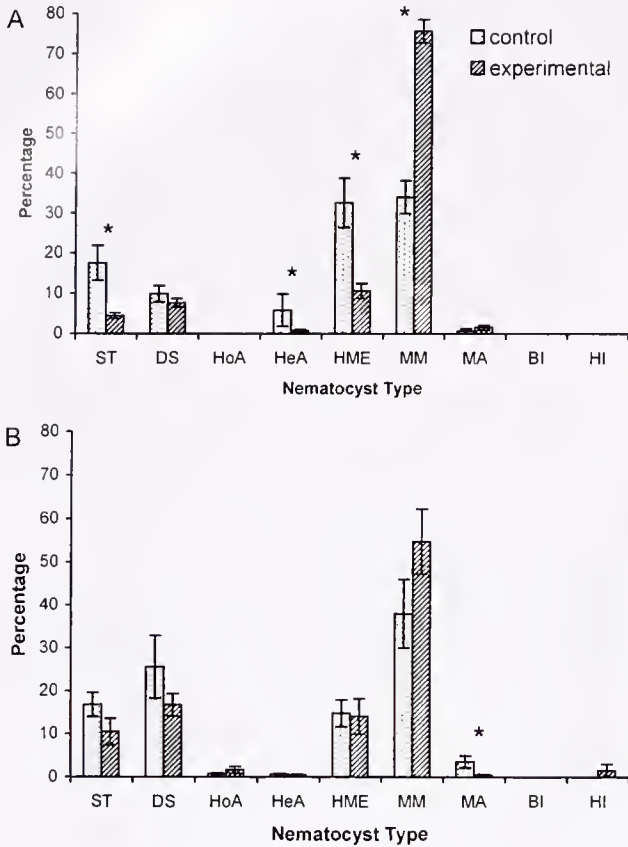


**Figure 4.** Modification of nematocyst uptake by nudibranchs exposed to *Tautoglabrus adspersus* when collected from (A) Isles of Shoals and (B) Nubble. \*Indicates significant differences,  $P < 0.05$ . Nematocyst types as in Figure 1.

Work should continue on the mechanism of selection (prey choice vs. active cellular selection by the nudibranch), variation in the types or proportions of nematocysts produced by the cnidarian prey in response to nudibranch predation, and differences in selective incorporation by other nudibranch species in the face of changing predation pressures.

The phenomenon of aeolid nudibranchs changing their defensive nematocyst regime may be widespread, though that has yet to be determined. Since the ability of a nudibranch to choose noxious organelles depends upon the variety of nematocysts available in the prey species, then the nudibranch's ability to respond to external cues is influenced by whether it is a specialist with a definite nematocyst array contained within its prey or a generalist capable of acquiring a wider range of nematocyst types from a variety of prey species. It may also be that large or potent nematocysts can only be incorporated at certain life-history stages due to physical limitations. Obviously the hydroid prey does not passively provide its defenses, and the nudibranch is not merely an adapted consumer that can choose from among an array of weapons without cost. The interaction is dynamic in its intricacies and malleable from the

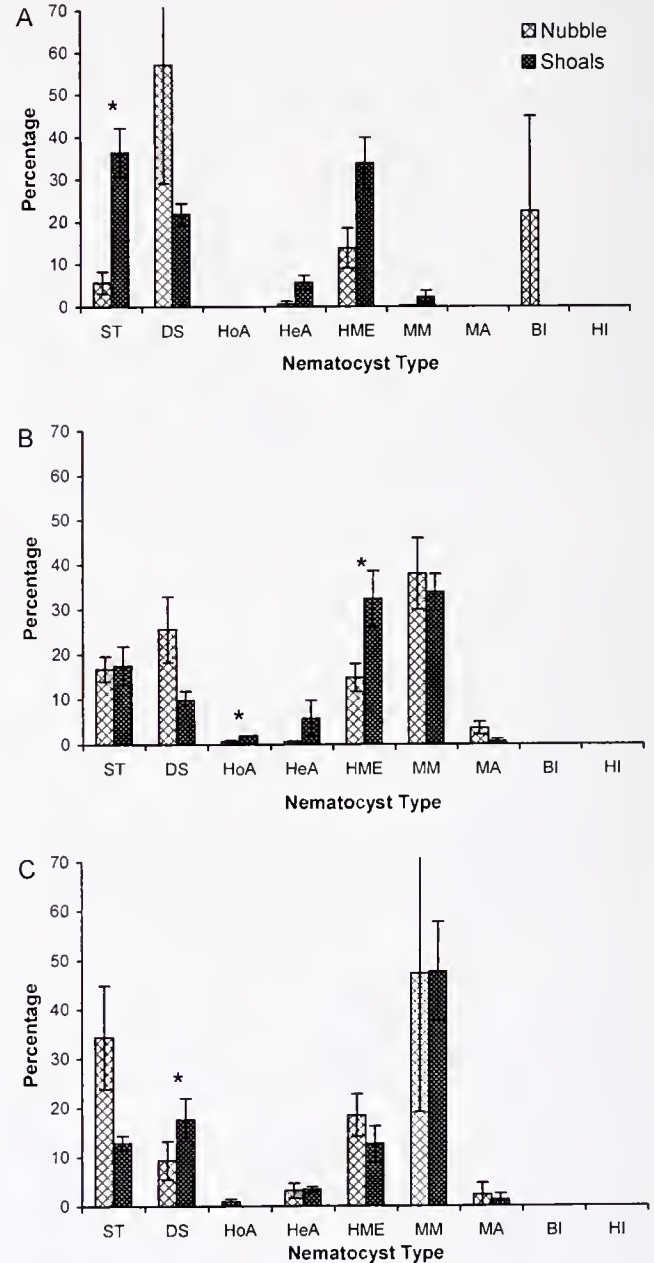


**Figure 5.** Comparison of control groups of *Flabellina verrucosa* collected from two sites in the southern Gulf of Maine. Results for each predator treatment are presented separately: (A) *Crossaster papposus*, (B) *Tautoglabrus adspersus*, and (C) *Carcinus maenas*. \*Indicates significant differences,  $P < 0.05$ . Nematocyst types as in Figure 1.

the selective pressures that have brought about their formation.

### Acknowledgments

This project was possible thanks to support, space, and funding through the University of New Hampshire. Larry Harris and Rebecca Toppin helped with formulating ideas and collecting specimens for this work. Additional thanks go to Glen Rice for hydroid collection and Chris Neefus for statistical advice. Comments from Lauralyn Dyer and Jenn Dijkstra improved the experimental design, and Larry Harris, Anne Stork, and the members of the writing seminar made helpful suggestions on earlier drafts of this paper. This research was supported by funds from the University of New Hampshire Center for Marine Biology; the National Sea Grant College Program of the National Oceanic and Atmospheric Administration, Department of Commerce, under grant number NA56RG0159 to the University of New Hampshire/University of Maine Sea Grant College Program; and by additional funds provided by the Open Ocean Aquaculture project component of the NOAA UNH Cooperative Institute for New England Mariculture and Fisheries (CINEMAR), NOAA grant number NA16RP1718.

### Literature Cited

- Abrams, P. A. 1995. Implications of dynamically-variable traits for identifying, classifying, and measuring direct and indirect effects in ecological communities. *Am. Nat.* **146**: 112–134.
- Abrams, P. A., B. A. Menge, G. G. Mittelbach, D. Spiller, and P. Yodzis. 1996. The role of indirect effects in food webs. Pp. 371–195 in *Food Webs: Integration of Patterns and Dynamics*, G. Polis and K. Winemiller, eds. Chapman & Hall, New York.
- Ajeska, R. 1971. Some aspects of the biology of *Melibe leonina*. *Abstr. Proc. West. Soc. Malacol.* **4**: 13.
- Beckerman, A. P., M. Uriarte, and O. J. Schmitz. 1997. Experimental evidence for a behavior-mediated trophic cascade in a terrestrial food chain. *Proc. Natl. Acad. Sci. USA* **94**: 10,735–10,738.
- Bleakney, J. S. 1996. *Sea Slugs of Atlantic Canada and the Gulf of Maine*, S. Lucy, ed. Nimbus Publishing and the Nova Scotia Museum, Halifax, Nova Scotia. Pp. 113–126.
- Brower, L. P., and C. M. Moffitt. 1974. Palatability dynamics of cardenolides in the monarch butterfly. *Nature* **249**: 280–283.
- Brower, L. P., P. B. McEvoy, K. L. Williamson, and M. A. Flannery. 1972. Variation in cardiac glycoside content of monarch butterflies from natural populations in eastern North America. *Science* **177**: 426–429.
- Brower, L. P., M. Edmunds, and C. M. Moffitt. 1975. Cardenolide content and palatability of a population of *Danaus chrysippus* butterflies from West Africa. *J. Entomol. Ser. A* **49**: 183–196.
- Calder, D. R. 1988. Shallow-water hydroids of Bermuda: the Athecatae. *R. Ont. Mus. Life Sci. Cont.* 148.
- Calvert, W. H., L. E. Hedrick, and L. P. Brower. 1979. Mortality of the monarch butterfly (*Danaus plexippus* L.): avian predation at five overwintering sites in Mexico. *Science* **204**: 847–851.
- Conklin, E. J., and R. N. Mariscal. 1977. Feeding behavior, ceras structure, and nematocyst storage in the aeolid nudibranch, *Spirilla neapolitana* (Mollusca). *Bull. Mar. Sci.* **27**: 658–667.
- Day, R. M., and L. G. Harris. 1978. Selection and turnover of coelenterate nematocysts in some aeolid nudibranchs. *Veliger* **21**: 104–109.
- Dixon, C. A., J. M. Erickson, D. N. Kelleff, and M. Rothschild. 1978. Some adaptations between *Danaus plexippus* and its food plant, with notes on *Danaus chrysippus* and *Euploea core* (Insecta: Lepidoptera). *J. Zool.* **185**: 437–467.
- Edmunds, M. 1966. Protective mechanisms in the Eolidacea (Mollusca, Nudibranchia). *J. Linn. Soc. Lond. Zool.* **46**: 46–71.
- Edmunds, M. 1974. *Defence in Animals*. Longman, New York.
- Faulkner, D. J. 1992. Chemical defenses of marine mollusks. Pp. 119–163 in *Ecological Roles of Marine Natural Products*, V. J. Paul, ed. Comstock, Ithaca, NY.
- Greenwood, P. G., and R. N. Mariscal. 1984a. Immature nematocyst incorporation by the aeolid nudibranch *Spirilla neapolitana*. *Mar. Biol.* **80**: 35–38.
- Greenwood, P. G., and R. N. Mariscal. 1984b. The utilization of cnidarian nematocysts by aeolid nudibranchs: nematocyst maintenance and release in *Spirilla*. *Tissue Cell* **16**: 719–730.
- Grosvenor, G. H. 1903. On the nematocysts of aeolids. *Proc. R. Soc. Lond. B* **72**: 462–486.
- Hall, S. J., and C. D. Todd. 1984. Prey-species selection by the anemone predator *Aeolidia papillosa* (L.): the influence of ingestive conditioning and previous dietary history, and a test for switching behaviour. *J. Exp. Mar. Biol. Ecol.* **82**: 11–33.
- Hall, S. J., C. D. Todd, and A. D. Gordon. 1982. The influence of ingestive conditioning on the prey species selection in *Aeolidia papillosa* (Mollusca: Nudibranchia). *J. Anim. Ecol.* **51**: 907–921.
- Harris, L. G. 1970. Studies on the aeolid nudibranch, *Ph استثilla melanobranchia* (Bergh, 1874). Ph.D. dissertation, University of California, Berkeley.
- Harris, L. G. 1973. Nudibranch associations. Pp. 275–277 in *Current Topics in Comparative Pathobiology*, T. C. Cheng, ed. Academic Press, New York.
- Harris, L. G. 1986. Size-selective predation in a sea anemone, nudibranch, and fish food chain. *Veliger* **29**: 38–47.
- Hassell, M. P. 1978. *The Dynamics of Arthropod Predator-Prey Systems*. Princeton University Press, Princeton, NJ.
- Havel, J. E. 1987. Predator-induced defenses: a review. P. 263–278 in *Predation: Direct and Indirect Impacts on Aquatic Communities*, W. D. Kerfoot and A. Sih, eds. University Press of New England, Hanover, NH.
- Huang, C., and A. Sih. 1991. Experimental studies on direct and indirect interactions in a three trophic-level system. *Oecologia* **85**: 530–536.
- Karuso, P. 1987. Chemical ecology of the nudibranchs. Pp. 32–60 in *Bioorganic Marine Chemistry*, Vol. 1. P. J. Scheuer, ed. Springer, Berlin.
- Kepner, W. A. 1943. The manipulation of the nematocysts of *Pennaria tiarella* by *Aeolis pilata*. *J. Morphol.* **73**: 297–311.
- Kuzirian, A. M. 1979. Taxonomy and biology of four New England coryphellid nudibranchs (Gastropoda: Opisthobranchia). *J. Molluscan Stud.* **45**: 239–261.
- Malcolm, S. B., and L. P. Brower. 1989. Evolutionary and ecological implications of cardenolide sequestration in the monarch butterfly. *Experientia* **45**: 284–295.
- Malcolm, S. B., and M. P. Zalucki. 1996. Milkweed latex and cardenolide induction may resolve the lethal plant defence paradox. *Entomol. Exp. Appl.* **80**: 193–196.
- Mariscal, R. N. 1974. Nematocysts. Pp. 129–178 in *Coelenterate Biology: Reviews and New Perspectives*, L. Muscatine and H. M. Lenhoff, eds. Academic Press, New York.
- Mauzey, K. P., C. Birkeland, and P. K. Dayton. 1968. Feeding behavior of asteroids and escape responses of their prey in the Puget Sound region. *Ecology* **49**: 603–619.
- McIntosh, A. R., and C. R. Townsend. 1996. Interactions between fish,

- grazing invertebrates and algae in a New Zealand stream: trophic cascade mediated by fish-induced changes to grazer behavior? *Oecologia* **108**: 174–177.
- Messina, F. J. 1991. Plant protection as a consequence of an ant-membracid mutualism: interactions on goldenrod (*Solidago* sp.). *Ecology* **62**: 1433–1440.
- Murdoch, W. W., and A. Oaten. 1975. Predation and population stability. *Adv. Ecol. Res.* **9**: 1–131.
- Peacor, S., and E. E. Werner. 1997. Trait-mediated indirect interactions in a simple aquatic food web. *Ecology* **78**: 1146–1156.
- Pianka, E. R. 1983. *Evolutionary Ecology*. Harper and Row, New York.
- Power, M. E., W. J. Matthews, and A. J. Stewart. 1985. Grazing minnows, piscivorous bass, and stream algae: dynamics of a strong interaction. *Ecology* **66**: 1448–1456.
- Proksch, P. 1994. Defensive roles for secondary metabolites from marine sponges and sponge-feeding nudibranchs. *Toxicon* **32**: 639–655.
- Rothschild, M. 1973. Secondary plant substances and warning colouration in insects. *Symp. R. Entomol. Soc. Lond.* **6**: 59–83.
- Rowell-Rahier, M., and J. M. Pasteels. 1992. Third trophic level influences of plant allelochemicals. Pp. 243–277 in *Herbivores: Their Interactions With Secondary Plant Metabolites, Vol. II: Ecological and Evolutionary Processes*, 2nd ed. G. A. Rosenthal and M. R. Berenbaum, eds. Academic Press, San Diego, CA.
- Scheuer, P. J. 1990. Some marine ecological phenomena: chemical basis and biomedical phenomena. *Science* **248**: 173–177.
- Schmitz, O. J., and K. B. Suttle. 2001. Effects of top predator species on direct and indirect interactions in a food web. *Ecology* **82**: 2072–2081.
- Seiber, J. N., L. P. Brower, S. M. Lee, M. M. McChesney, H. T. A. Cheung, C. J. Nelson, and T. R. Watson. 1986. Cardenolide connection between overwintering monarch butterflies from Mexico and their larval food plant, *Asclepias syriaca*. *J. Chem. Ecol.* **12**: 1157–1170.
- Taylor, R. J. 1984. *Predation*. Chapman and Hall, New York.
- Thompson, T. E. 1960. Defensive adaptations in opisthobranchs. *J. Mar. Biol. Assoc. UK* **39**: 123–134.
- Thompson, T. E. 1976. *Biology of Opisthobranch Mollusks*. The Ray Society, London.
- Thompson, T. E., and I. Bennett. 1969. *Physalia* nematocysts: utilized by mollusks for defense. *Science* **166**: 1532–1533.
- Turner, A. M., and G. G. Mittelbach. 1990. Predator avoidance and community structure: interactions among piscivores, planktivores, and plankton. *Ecology* **71**: 2241–2254.
- Turner, A. M., S. A. Fetterolf, and R. J. Bernot. 1999. Predator identity and consumer behavior: differential effects of fish and crayfish on habitat use of a freshwater snail. *Oecologia* **118**: 242–247.
- Werner, E. E., and B. R. Anholt. 1996. Predator-induced behavioral indirect effects: consequences to competitive interactions in anuran larvae. *Ecology* **77**: 157–169.

## INDEX

### A

- ABRAHAM, D. M., M. A. CHARETTE, M. C. ALLEN, A. RAGO, AND K. D. KROEGER, Radiochemical estimates of submarine groundwater discharge to Waquoit Bay, Massachusetts, 246
- Actin, 195  
ring, 192
- S-adenosyl-L-methionine:farnesoic acid *O*-methyl transferase, 308
- Aggregation, 1
- Aggregations of egg-brooding deep-sea fish and cephalopods on the Gorda Escarpment: a reproductive hot spot, 1
- Aggression, 26
- AGNEW, A. M., D. H. SHULL, AND R. BUCHSBAUM, Growth of a salt marsh invertebrate on several species of marsh grass detritus, 238
- AGUIAR, A. B., see J. A. Morgan, 252
- AGUIAR, A. B., J. A. MORGAN, M. TEICHBERG, S. FOX, AND I. VALIELA, Transplantation and isotopic evidence of the relative effects of ambient and internal nutrient supply on the growth of *Ulva lactuca*, 250
- Alexandrium*, 231
- Alkaline phosphatase, 230
- ALKON, D. L., see F. M. Child, 218; A. M. Kuzirian, 220
- ALLEN, M. C., see J. M. Talbot, 244; D. M. Abraham, 246
- Allogenic interaction, 133
- Ammonia, 331
- Ammonium, 244
- Amphipod, 252
- An experimental approach to the study of gap-junction-mediated cell death, 197
- Anadara*, 73
- ANDERSON, DONALD M., see Madeline Galac, 231
- Animation, 225
- Antarctica, 93
- Anthopleura*, 66, 339
- Aplysia*, 16
- Apoptosis, 197, 199  
in *Microciconia prolifera* allografts, 199
- Aquifer, 244, 246
- ARMSTRONG, MARGARET T., see Peter B. Armstrong, 201
- ARMSTRONG, PETER B., AND MARGARET T. ARMSTRONG, The decorated clot: binding of agents of the innate immune system to the fibrils of the *Limulus* blood clot, 201
- Armstrong, Peter B., see Victoria Isakova, 203; John M. Harrington, 205
- Ascidian, 133
- Aster, 193
- Astogeny, 330
- ATEMA, J., see Anna Savage, 222; K. D. Mann, 224
- Attractin, 16
- Axon, 187, 188, 190
- Axonal transport, 188, 190
- Axoplasm, 188
- Axotomy, 187
- Axotomy inhibits the slow axonal transport of tubulin in the squid giant axon, 187

### B

- Bacteria, 228, 233
- Bacteriolysis, 203
- BAIRD, KRISTAL D., HEMANT M. CHIKARMANE, ROXANNA SMOLOWITZ, AND KEVIN R. UHLINGER, Detection of *Edwardsiella* infections in *Opsanus tau* by polymerase chain reaction, 235
- BAKER, ROBERT, see Edwin Gilland, 176
- BARNES, D. K. A., see J. J. Bell, 144

- Behavior, 218, 222, 225
- Behavioral characterization of attractin, a water-borne peptide pheromone in the genus *Aplysia*, 16
- BELL, J. J., AND D. K. A. BARNES, Effect of disturbance on assemblages: an example using Porifera, 144
- BENINGER, PETER G., GAËL LE PENNEC, AND MARCEL LE PENNEC, Demonstration of nutrient pathway from the digestive system to oocytes in the gonad intestinal loop of the scallop *Pecten maximus* L., 83
- BERGMAN, DANIEL A., AND PAUL A. MOORE, Field observations of intraspecific agonistic behavior of two crayfish species, *Orconectes rusticus* and *Orconectes virilis*, in different habitats, 26
- Bindin, 8
- Biological beam, 36
- Bioluminescence, 102
- Biosensor, 207
- Bivalve, 83  
gills, 73
- BLACK, SARA, see Sherry D. Painter, 16
- Blastoderm, 179
- Blob sculpin, 1
- Blood clotting, 201, 203
- BOGORFF, DANIEL J., MARK A. MESSERLI, ROBERT P. MALCHOW, AND PETER J. S. SMITH, Development and characterization of a self-referencing glutamate-selective micro-biosensor, 207
- BOLLER, MICHAEL L., see Howard R. Lasker, 330
- BONAVENTURA, CELIA, see Ana Beardsley Christensen, 54
- Bottom-up, 252
- BOYER, BARBARA C., see Susan D. Hill, 182
- Brachiolaria, 285
- Brittle star, 54
- BROWN, JEREMIAH R., see John Delacruz, 188; Carl J. DeSelm, 190
- BUCHSBAUM, R., see A. M. Agnew, 238
- Building a database of historic land cover to detect landscape change, 257
- BURGER, M. M., see S. Tepsuporn, 199
- BURTON, O. T., see S. J. Zottoli, 211
- BYRNE, MARIA, MICHAEL HART, ANNA CERRA, AND PAULA CISTERNAS, Reproduction and larval morphology of broadcasting and viviparous species in the *Cryptasterina* species complex, 285
- Bystander cell death, 197

### C

- C-reactive protein, 201
- Calcium, 176, 215  
mobilization, 185
- Calcectin, 220
- Capitella*, 182
- CARMICHAEL, R. H., see C. W. O'Connell, 254
- Cascading trophic impacts of reduced biomass in the Ross Sea, Antarctica: Just the tip of the iceberg?, 93
- Caspase-3, 199
- CASTANARO, JOHN, see Howard R. Lasker, 330
- Catalase in microsporidian spores before and during discharge, 236
- Catch connective tissue, 261
- CAVATORTA, J. R., see M. E. Johnston, 248
- CAVATORTA, JASON R., MORGAN JOHNSTON, CHARLES HOPKINSON, AND VINTON VALENTINE, Patterns of sedimentation in a salt marsh-dominated estuary, 239
- Cecum, 47
- Cell  
adhesion, 220  
cycle, 195  
division, unequal, 192

- Centrosome, 193  
 Cephalopod, 1, 47, 192  
 Cercaria, 110  
 CERRA, ANNA, see Maria Byrne, 285  
 CHADWICK-FURMAN, NANETTE E., AND IRVING L. WEISSMAN, Effects of allogeneic contact on life-history traits of the colonial ascidian *Botryllus schlosseri* in Monterey Bay, 133  
 CHAMBERS, J. A., see S. J. Zottoli, 211  
 CHAPPELL, R. L., see S. Redenti, 213  
 CHAPPELL, R. L., J. ZAKEVICIUS, AND H. RIPPS, Zinc modulation of hemichannel currents in *Xenopus* oocytes, 209  
 Characterization of phosphorus-regulated genes in *Trichodesmium* spp., 230  
 CHARETTE, M. A., see J. M. Talbot, 244; D. M. Abraham, 246  
 Chemoautotrophy, 331  
 Chemoreception, 222  
 CHENEY, DANIEL P., see Amro M. Hamdoun, 160  
 CHERR, GARY N., see Amro M. Hamdoun, 160  
 CHIKARMANE, HEMANT M., see Krystal D. Baird, 235  
 CHILD, F. M., see A. M. Kuzirian, 220  
 CHILD, F. M., H. T. EPSTEIN, A. M. KUZIRIAN, AND D. L. ALKON, Memory reconsolidation in *Hemissenda*, 218  
 CHRISTENSEN, ANA BEARDSLEY, JAMES M. COLACINO, AND CELIA BONAVENTURA, Functional and biochemical properties of the hemoglobins of the burrowing brittle star *Hemiphysalis elongata* Say (Echinodermata, Ophiuroidea), 54  
 Cilia, 182  
 CISTERNAS, PAULA, see Maria Byrne, 285  
 Cleavage, 179  
 Cloning, characterization, and developmental expression of a putative farnesic acid *O*-methyl transferase in the female edible crab *Cancer pagurus*, 308  
 CLOUGH, BRET, see Sherry D. Painter, 16  
 COHEN, W. D., see R. M. Pielak, 192  
 COLACINO, JAMES M., see Ana Beardsley Christensen, 54  
 Colonial invertebrate, 133  
 Colony growth, 330  
 Columellar  
   fold, 351  
   muscle, 351  
 Columellar muscle of neogastropods: muscle attachment and the function of columellar folds, 351  
 Community composition, 144  
 Competition, 133  
 Conditioning, associative, 220  
 Connective tissue  
   catch, 261  
   mutable, 261  
 Connexin, 197, 209  
 Cooperativity, 54  
 Coral, 339  
 Coral reef, 330  
*Corbicula*, 73  
 CRAWFORD, K., Lithium chloride inhibits development along the animal-vegetal axis and anterior midline of the squid embryo, 181  
 CRAWFORD, K., see P. H. Wadson, 179  
 Crustacea, 26, 308  
*Cryptasterina*, 285  
 Cryptic species, 285  
 CUSATO, K., J. ZAKEVICIUS, AND H. RIPPS, An experimental approach to the study of gap-junction-mediated cell death, 197  
 Cuttlefish, 233  
 Cx35, 209  
 Cx38, 209  
 Cyclopia, 181  
 Cytochrome *c*, 197  
 Cytokinesis, 192  
 Cytoskeletal events preceding polar body formation in activated *Spisula* eggs, 192  
 Cytoskeleton, 192
- D**
- DAVIDSON, E., see C. Walker, 256  
 DAVY, SIMON K., AND JOHN R. TURNER, Early development and the acquisition of zooxanthellae in the temperate symbiotic sea anemone *Anthopleura ballii* (Cocks), 66  
 Decapod, 26  
 The decorated clot: binding of agents of the innate immune system to the fibrils of the *Limulus* blood clot, 201  
 Deep-sea, 102  
 DELACRUZ, JOHN, JEREMIAH R. BROWN, AND GEORGE M. LANGFORD, Interactions between recombinant conventional squid kinesin and native myosin-V, 188  
 Demonstration of nutrient pathway from the digestive system to oocytes in the gonad-intestinal loop of the scallop *Pecten maximus* L., 83  
 Denitrification, 242  
 DENK, WINFRIED, see Edwin Gilland, 176  
 DEPINA, ANA S., see Torsten Wöllert, 195  
 Description of *Vibrio alginolyticus* infection in cultured *Sepia officinalis*, *Sepia apama*, and *Sepia pharaonis*, 233  
 DESELM, CARL J., see Torsten Wöllert, 195  
 DESELM, CARL J., JEREMIAH R. BROWN, RENNE LU, AND GEORGE M. LANGFORD, Rab-GDI inhibits myosin V-dependent vesicle transport in squid giant axon, 190  
 Detection of *Edwardsiella* infections in *Opsanus tau* by polymerase chain reaction, 235  
 Determinate growth and modularity in a gorgonian octocoral, 330  
 Detritivore, 238  
 Detritus, 26  
 Development, 181, 182, 285  
   nonfeeding, 295  
 Development and characterization of a self-referencing glutamate-selective micro-biosensor, 207  
 DIERSSEN, HEIDI M., see Brad A. Scibel, 93  
 Digestive gland, 47  
 Dinoflagellate, 231  
 Disease, 233, 235  
 DON, 256  
 Dorsal cell, 211  
 DRAZEN, JEFFREY C., SHANA K. GOFFREDI, BRIAN SCHLINING, AND DEBRA S. STAKES, Aggregations of egg-brooding deep-sea fish and cephalopods on the Gorda Escarpment: a reproductive hot spot, 1  
*Dreissena*, 73  
 DYHRMAN, SONYA, see Elizabeth Orchard, 230; Madeline Galac, 231  
 Dynamic mechanical properties of body-wall dermis in various mechanical states and their implications for the behavior of sea cucumbers, 261
- E**
- Early development and the acquisition of zooxanthellae in the temperate symbiotic sea anemone *Anthopleura ballii* (Cocks), 66  
 Echinoderm, 54, 261  
*Edwardsiella tarda*, 235  
 Effect of disturbance on assemblages: an example using Porifera, 144  
 Effects of allogeneic contact on life-history traits of the colonial ascidian *Botryllus schlosseri* in Monterey Bay, 133  
 Electron microscopy, 177  
 Embryonic development, 308  
 Epizootic lobster shell disease, 228  
 EPSTEIN, H. T., see F. M. Child, 218; A. M. Kuzirian, 220  
 ERDNER, DEANA, see Madeline Galac, 231  
 ESEH, R., see S. J. Zottoli, 211  
 Estuary, 110  
 ETNIER, SHELLY A., Twisting and bending of biological beams: distribution of biological beams in a stiffness mechanospace, 36  
 Eutrophication, 242, 252  
 Expressed sequence tag, 227  
 Expressed sequence tag analysis of genes expressed in the bay scallop, *Argopecten irradians*, 227  
 Extracellular lipid droplets in *Diosepius notoides*, the Southern pygmy squid, 47  
 Extrinsic factors, 26

EYSTER, L. S., AND L. M. VAN CAMP, Extracellular lipid droplets in *Diosepius notoides*, the Southern pygmy squid, 47

## F

Fasciclin, 339  
Feeding, 93  
  opposed-band, 295  
FERNANDEZ-BUSQUETS, X., see S. Tepsuporn, 199  
Fertilization, 8  
Field observations of intraspecific agonistic behavior of two crayfish species, *Orconectes rusticus* and *Orconectes virilis*, in different habitats, 26  
Filament  
  distal growth, 73  
  formation, 73  
FINDLEY, ANN, see Earl Weidner, 236  
FINGERUT, JONATHAN T., CHERYL ANN ZIMMER, AND RICHARD K. ZIMMER, Patterns and processes of larval emergence in an estuarine parasite system, 110  
Fish, 211  
*Flabellina verrucosa*, 367  
Flatworm, 110  
Flexibility, 36  
FOREMAN, K. H., see T. Thoms, 242  
Formation of the blastoderm and yolk syncytial layer in early squid development, 179  
FOX, S., see A. B. Aguiar, 250; J. A. Morgan, 252  
FRICK, KINSEY, Response in nematocyst uptake by the nudibranch *Flabellina verrucosa* to the presence of various predators in the southern Gulf of Maine, 367  
Functional and biochemical properties of the hemoglobins of the burrowing brittle star *Hemiphysalis elongata* Say (Echinodermata, Ophiuroidea), 54  
Functional morphology, 351

## G

GALAC, MADELINE, DEANA ERDNER, DONALD M. ANDERSON, AND SONYA DYHRMAN, Molecular quantification of toxic *Alexandrium fundyense* in the Gulf of Maine, 231  
GALLANT, P. E., Axotomy inhibits the slow axonal transport of tubulin in the squid giant axon, 187  
Gamete recognition, 8  
Gap junction, 197  
Gastropod, 93, 276, 351  
Gastrulation, 176  
GAYSINSKAYA, V. A., see R. M. Pielak, 192  
Geffen, Audrey, see Carolyn J. Ruddell, 308  
Geographic information system, 257  
GERLACH, G., see K. D. Mann, 224; E. R. Turnell, 225  
GIBSON, A. E., see T. Thoms, 242  
GIBSON, GLENYS D., Larval development and metamorphosis in *Pleurobranchaea maculata*, with a review of development in the Notaspidea (Opisthobranchia), 121  
GILEADI, OPHER, AND ALON SABBAN, Squid sperm to clam eggs: imaging wet samples in a scanning electron microscope, 177  
GILLAND, EDWIN, ROBERT BAKER, AND WINFRIED DENK, Long duration three-dimensional imaging of calcium waves in zebrafish using multiphoton fluorescence microscopy, 176  
GIS, 257  
GIUFFRIDA, B. A., see L. M. Palmer, 216  
Glutamate, 207  
GOETZ, F. W., see S. B. Roberts, 227  
GOFFREDI, SHANA K., see Jeffrey C. Drazen, 1  
Gonad, 83  
GRADY, S. P., see C. W. O'Connell, 254  
*Graneledone*, 1  
Grazing, 252  
Groundwater, 242, 244  
Growth, 133, 238

  algal, 250, 252  
  Growth of a salt marsh invertebrate on several species of marsh grass detritus, 238  
  Gulf of Maine, 231  
  GUTIÉRREZ, L. M., see S. J. Zottoli, 211

## H

HADDOCK, STEVEN H. D., see Bruce H. Robison, 102  
HAMDOUN, AMRO M., DANIEL P. CHENEY, AND GARY N. CHERR, Phenotypic plasticity of HSP70 and HSP70 gene expression in the Pacific oyster (*Crassostrea gigas*): implications for thermal limits and induction of thermal tolerance, 160  
HAMMAR, KATHERINE, see Anthony J. A. Molina, 215  
HARRINGTON, JOHN M., AND PETER B. ARMSTRONG, A liposome-permeating activity from the surface of the carapace of the American horseshoe crab, *Limulus polyphemus*, 205  
HART, MICHAEL, see Maria Byrne, 285  
Heat-shock protein, 160, 276  
Heat-shock protein 70 (Hsp70) as a biochemical stress indicator: an experimental field test in two congeneric intertidal gastropods (Genus: *Tegula*), 276  
HECK, D. E., AND J. D. LASKIN, Ryanodine-sensitive calcium flux regulates motility of *Arbacia punctulata* sperm, 185  
Hemichannel, 209  
Hemoglobin, 54  
Hemolysis, 205  
*Hermisenda*, 218, 220  
Heterochrony, 121  
HILL, SUSAN D., AND BARBARA C. BOYER, HNK-1/N-CAM immunoreactivity correlates with ciliary patterns during development of the polychaete *Capitella* sp. 1, 182  
Histidine, 213  
Histopathology, 233  
HNK-1/N-CAM immunoreactivity correlates with ciliary patterns during development of the polychaete *Capitella* sp. 1, 182  
HOLDEN, M. T., C. LIPPITT, R. G. PONTIUS, JR., AND C. WILLIAMS, Building a database of historic land cover to detect landscape change, 257  
*Homarus americanus*, 222, 228  
HOPKINSON, C. S., see Jason R. Cavatorta, 239; M. E. Johnston, 248  
Horizontal cell, 215  
HSP70 family, 160  
HSU, A. C., AND R. M. SMOLOWITZ, Scanning electron microscopy investigation of epizootic lobster shell disease in *Homarus americanus*, 228  
HUNT, JAMES C., see Bruce H. Robison, 102  
Hydrothermal vent, 98

## I

Iceberg, 93  
*Idiosepius*, 47  
Imaging, 177  
Immunity  
  cutaneous, 205  
  innate, 201, 203, 205  
  invertebrate, 199  
Immunolabeling, 177  
Immunolocalization, 339  
Importance of metabolism in the development of salt marsh ponds, 248  
Imprisonment in a death-row cell: the fates of microbes entrapped in the *Limulus* blood clot, 203  
Incubation conditions of forest soil yielding maximum dissolved organic nitrogen concentrations and minimal residual nitrate, 256  
Induced protein, 160  
Interactions between recombinant conventional squid kinesin and native myosin-V, 188  
Intertidal zone, 166  
Intracellular release of caged calcium in skate horizontal cells using fine optical fibers, 215  
Invasive species, 238  
ISAKOVA, VICTORIA, AND PETER B. ARMSTRONG, Imprisonment in a death-

row cell: the fates of microbes entrapped in the *Limulus* blood clot, 203

## J

- JOHNSTON, M. E., J. R. CAVATORTA, C. S. HOPKINSON, AND V. VALENTINE, Importance of metabolism in the development of salt marsh ponds, 248  
 JOHNSTON, MORGAN, see Jason R. Cavatorta, 239  
 JOYNER, JOANNA L., SUZANNE M. PEYER, AND RAYMOND W. LEE, Possible roles of sulfur-containing amino acids in a chemoautotrophic bacterium–mollusc symbiosis, 331

## K

- KALTENBACH, J. C., see S. Tepsuporn, 199  
 KAPPES, HEIKE, see Dietrich Neumann, 73  
 Kin recognition, 224  
 Kin recognition in juvenile zebrafish (*Danio rerio*) based on olfactory cues, 224  
 Kinesin, 188  
 KINGERLEE, W., see C. Walker, 256  
 KROEGER, K. D., see J. M. Talbot, 244; D. M. Abraham, 246  
 KRON, M. M., see S. J. Zottoli, 211  
 KUHNS, W. J., see S. Tepsuporn, 199  
 KUZIRIAN, A. M., see F. M. Child, 218  
 KUZIRIAN, A. M., F. M. CHILD, H. T. EPSTEIN, M. E. MOTTA, C. E. OLDENBURG, AND D. L. ALKON, Training alone, not the tripeptide RGD, modulates calcitonin in *Hemissenda*, 220

## L

- Landscape change, 257  
 LANGFORD, GEORGE M., see John Delacruz, 188; Carl J. DeSelm, 190; Torsten Wöllert, 195  
 Larva, 110, 121, 285, 295  
 Larval development and metamorphosis in *Pleurobranchaea maculata*, with a review of development in the Notaspidea (Opisthobranchia), 121  
 LASKER, HOWARD R., MICHAEL L. BOLLER, JOHN CASTANARO, AND JUAN ARMANDO SÁNCHEZ, Determinate growth and modularity in a gorgonian octocoral, 330  
 LASKIN, J. D., see D. E. Heck, 185  
 Lateral line, 216  
 LE PENNEC, GAËL, see Peter G. Beninger, 83  
 LE PENNEC, MARCEL, see Peter G. Beninger, 83  
 Learning, 218  
 LEE, RAYMOND W., see Joanna L. Joyner, 331  
 LEE, RAYMOND W., Thermal tolerances of deep-sea hydrothermal vent animals from the Northeast Pacific, 98  
 LESCHEN, A. S., see C. W. O'Connell, 254  
 LESSIOS, H. A., see Kirk S. Zigler, 8  
 Light production by the arm tips of the deep-sea cephalopod *Vampyroteuthis infernalis*, 102  
*Limulus*, 201, 203, 205, 254  
 Lipid, 47  
 Liposome, 205  
 A liposome-permeating activity from the surface of the carapace of the American horseshoe crab, *Limulus polyphemus*, 205  
 LIPPITT, C., see M. T. Holden, 257  
 Lithium chloride, 181  
 Lithium chloride inhibits development along the animal vegetal axis and anterior midline of the squid embryo, 181  
 Lobster, 222, 228  
 Localization of a symbiosis-related protein, Sym32, in the *Anthopleura elegantissima*–*Symbiodinium muscatinei* association, 339  
 Long duration three-dimensional imaging of calcium waves in zebrafish using multiphoton fluorescence microscopy, 176  
 Lough Hyne, 144  
 LU, RENNE, see Carl J. DeSelm, 190

## M

- d2-macroglobulin, 201  
 Macrophytes, 26  
 MALCHOW, ROBERT P., see Daniel J. Bogorff, 207; Anthony J. A. Molina, 215  
 Mandibular organ, 308  
 MANN, K. D., see E. R. Turnell, 225  
 MANN, K. D., E. R. TURNELL, J. ATEMA, AND G. GERLACH, Kin recognition in juvenile zebrafish (*Danio rerio*) based on olfactory cues, 224  
 Mantle formation, 121  
 Marine Biological Laboratory  
 Annual Report, v. 205(1), R1  
 General Scientific Meetings, 171  
 Map, digital land-cover, 257  
 Mate choice, 225  
 Mate choice in zebrafish (*Danio rerio*) analyzed with video-stimulus techniques, 225  
 Mechanical properties, 261  
 Memory, 218  
 consolidated long-term, 218  
 long-term, 220  
 reconsolidation, 218  
 Memory reconsolidation in *Hemissenda*, 218  
 MENSINGER, A. F., see L. M. Palmer, 216  
 MESSERLI, MARK A., see Daniel J. Bogorff, 207  
 Metabolic rate, 93  
 Methyl farnesoate, 308  
 Methyl transferase, 308  
 Microscope, polarizing-aperture scanning, 193  
 Microsporidian catalase, 236  
 Microtubule, 193  
 Modularity, 330  
 Molecular chaperone, 160  
 Molecular quantification of toxic *Alexandrium fundyense* in the Gulf of Maine, 231  
 Molecule, 220  
 MOLINA, ANTHONY J. A., KATHERINE HAMMAR, RICHARD SANGER, PETER J. S. SMITH, AND ROBERT P. MALCHOW, Intracellular release of caged calcium in skate horizontal cells using fine optical fibers, 215  
 Mollusc, 16  
 MOORE, PAUL A., see Daniel A. Bergman, 26  
 MORGAN, J. A., A. B. AGUIAR, S. FOX, M. TEICHBERG, AND I. VALIELA, Relative influence of grazing and nutrient supply on growth of the green macroalga *Ulva lactuca* in estuaries of Waquoit Bay, Massachusetts, 252  
 MORGAN, J. A., see A. B. Aguiar, 250  
 Morphology, 330  
 Mortality, 133  
 MOTOKAWA, TATSUO, AND AKIFUMI TSUCHI, Dynamic mechanical properties of body-wall dermis in various mechanical states and their implications for the behavior of sea cucumbers, 261  
 MOTTA, M. E., see A. M. Kuzirian, 220  
 Multiphoton fluorescence, 176  
 Multiple approaches to tracing nitrogen loss in the West Falmouth wastewater plume, 242  
 Myosin  
 -II, 195  
 -V, 188, 190

## N

- N-CAM, 182  
<sup>15</sup>N label, 256  
 NAGLE, GREGG T., see Sherry D. Painter, 16  
 Nematocyst, 367  
 NEUMANN, DIETRICH, AND HEIKE KAPPES, On the growth of bivalve gills initiated from a lobule-producing budding zone, 73  
 Neural recordings from the lateral line in free-swimming toadfish, *Opsanus tau*, 216  
 Neurochemical modulation of behavioral response to chemical stimuli in *Homarus americanus*, 222

Neuromodulator, 222  
 Neuron, supramedullary, 211  
 Nitrate, 244  
 Nitric oxide, 185  
 Nitrogen, 242, 244, 256  
 Nitrogen flux and speciation through the subterranean estuary of Waquoit Bay, Massachusetts, 244  
 Nuclear envelope, 177  
*Nucula*, 73  
 Nudibranch, 16, 218, 220, 367  
 Nutrient  
   supply, 250  
   transfer, 83  
 Nutrition, larval, 295

## O

O'CONNELL, C. W., S. P. GRADY, A. S. LESCHEN, R. H. CARMICHAEL, AND I. VALIELA, Stable isotopic assessment of site loyalty and relationships between size and trophic position of the Atlantic horseshoe crab, *Limulus polyphemus*, within Cape Cod estuaries, 254  
 Octopus, 1  
 OLDENBOURG, RUDOLF, see Michael Shribak, 194  
 OLDENBURG, C. E., see A. M. Kuzirian, 220  
 Olfaction, 224  
 On the growth of bivalve gills initiated from a lobule-producing budding zone, 73  
 Oocyte, 83, 192  
 Ophiuroid, 54  
*Opsanus tau*, 216, 235  
 ORCHARD, ELIZABETH, ERIC WEBB, AND SONYA DYHRMAN, Characterization of phosphorus-regulated genes in *Trichodesmium* spp., 230  
*Orchestia grillus*, 238  
 Oxygen binding equilibrium, 54  
 Oyster, 160

## P

Pain, 211  
 PAINTER, SHERRY D., BRET CLOUGH, SARA BLACK, AND GREGG T. NAGLE, Behavioral characterization of attractin, a water-borne peptide pheromone in the genus *Aplysia*, 16  
 PALMER, L. M., B. A. GIUFFRIDA, AND A. F. MENSINGER, Neural recordings from the lateral line in free-swimming toadfish, *Opsanus tau*, 216  
 Paralytic shellfish poisoning, 231  
 Parasite, 110  
*Patiriella*, 285  
 Patterns and processes of larval emergence in an estuarine parasite system, 110  
 Patterns of sedimentation in a salt marsh-dominated estuary, 239  
 PCR, 231, 235  
 Peptide pheromone, 16  
 PERNET, BRUNO, Persistent ancestral feeding structures in nonfeeding annelid larvae, 295  
 Persistent ancestral feeding structures in nonfeeding annelid larvae, 295  
 PEYER, SUZANNE M., see Joanna L. Joyner, 331  
 Phenotypic plasticity of HSP70 and HSP70 gene expression in the Pacific oyster (*Crassostrea gigas*): implications for thermal limits and induction of thermal tolerance, 160  
 Pheromone, peptide, 16  
 Phosphorus, 230  
 Phylogeny, opisthobranch, 121  
 PIELAK, R. M., V. A. GAYSINSKAYA, AND W. D. COHEN, Cytoskeletal events preceding polar body formation in activated *Spisula* eggs, 192  
*Pisidium*, 73  
 Polar body, 192  
 Polychaete, 182, 295  
 PONTIUS, R. G. JR., see M. T. Holden, 257  
 Porifera, 144  
 Possible roles of sulfur-containing amino acids in a chemoautotrophic bacterium-mollusc symbiosis, 331

Predator, 367  
 PRICE, REBECCA M., Columellar muscle of neogastropods: muscle attachment and the function of columellar folds, 351  
 Productivity, 93  
 Prototroch, 182  
*Psychrolutes*, 1  
 Pteropoda, 93

## R

Rab-GDI inhibits myosin V-dependent vesicle transport in squid giant axon, 190  
 Rabs, 190  
 Radiochemical estimates of submarine groundwater discharge to Waquoit Bay, Massachusetts, 246  
 Radiochemical tracer, 246  
 Radium, 246  
 Radon, 246  
 RAGO, A., see J. M. Talbot, 244; D. M. Abraham, 246  
 Ratio, twist-to-bend, 36  
 REDENTI, S., AND R. L. CHAPPELL, Zinc chelation enhances the sensitivity of the ERG b-wave in dark-adapted skate retina, 213  
 REES, HUW H., see Carolyn J. Ruddell, 308  
 REISENBICHLER, KIM R., see Bruce H. Robison, 102  
 Relative influence of grazing and nutrient supply on growth of the green macroalga *Ulva lactuca* in estuaries of Waquoit Bay, Massachusetts, 252  
 Remote sensing, 93  
 Reproduction, 83, 133, 285, 308  
 Reproduction and larval morphology of broadcasting and viviparous species in the *Cryptasterina* species complex, 285  
 Reproductive hot spot, 1  
 Resource holding power, 26  
 Response in nematocyst uptake by the nudibranch *Flabellina verrucosa* to the presence of various predators in the southern Gulf of Maine, 367  
 Retina, 213, 215  
 RGD, 220  
 Rho-kinase, 195  
 Rho-kinase is required for myosin-II-mediated vesicle transport during M-phase in extracts of clam oocytes, 195  
 RIPPS, H., see K. Cusato, 197; R. L. Chappell, 209  
 ROBERTS, S. B., AND F. W. GOETZ, Expressed sequence tag analysis of genes expressed in the bay scallop, *Argopecten irradians*, 227  
 ROBISON, BRUCE H., KIM R. REISENBICHLER, JAMES C. HUNT, AND STEVEN H. D. HADDOCK, Light production by the arm tips of the deep-sea cephalopod *Vampyroteuthis infernalis*, 102  
 ROSENTHAL, G. G., see E. R. Turnell, 225  
 RUDDELL, CAROLYN J., GEOFFREY WAINWRIGHT, AUDREY GEFFEN, MICHAEL R. H. WHITE, SIMON G. WEBSTER, AND HUW H. REES, Cloning, characterization, and developmental expression of a putative farnesoic acid O-methyl transferase in the female edible crab *Cancer pagurus*, 308  
 Ryanodine, 185  
 Ryanodine-sensitive calcium flux regulates motility of *Arbacia punctulata* sperm, 185

## S

SABBAN, ALON, see Opher Gileadi, 177  
 Sabellid, 295  
 Salt marsh, 238, 239, 248  
   accretion, 239  
   metabolism, 248  
   pond, 239, 248  
 SÁNCHEZ, JUAN ARMANDO, see Howard R. Lasker, 330  
 SANFORD, ERIC, see Lars Tomanek, 276  
 SANGER, RICHARD, see Anthony J. A. Molina, 215  
 SANGSTER, C. R., AND R. M. SMOLOWITZ, Description of *Vibrio alginolyticus* infection in cultured *Sepia officinalis*, *Sepia apama*, and *Sepia pharaonis*, 233

SAVAGE, ANNA, AND JELLE ATEMA, Neurochemical modulation of behavioral response to chemical stimuli in *Homarus americanus*, 222

SAVAGE, K., see C. Walker, 256

Scallop, 83, 227

Scanning electron microscopy, 228

Scanning electron microscopy investigation of epizootic lobster shell disease in *Homarus americanus*, 228

SCHLNING, BRIAN, see Jeffrey C. Drazen, 1

SCHWARZ, J. A., AND V. M. WEIS, Localization of a symbiosis-related protein, Sym32, in the *Anthopleura elegantissima*-*Symbiodinium muscatinei* association, 339

Scuba, 26

Sea anemone, 66, 339

Sea cucumber, 261

Sea level rise, 239

Sea star, 285

Sea urchin, 8, 185

Sedimentation, 239

SEIBEL, BRAD A., AND HEIDI M. DIERSSEN, Cascading trophic impacts of reduced biomass in the Ross Sea, Antarctica: Just the tip of the iceberg?, 93

Self-recognition, 199

Self-referencing, 207

*Sepia*, 233

Sewage, 242

Shell

- lesions, 228
- loss, 121

Shelters, 26

SHRIBAK, MICHAEL, AND RUDOLF OLDENBOURG, Three-dimensional birefringence distribution in reconstituted asters of *Spisula* oocytes revealed by scanned aperture polarized light microscopy, 194

SHULL, D. H., see A. M. Agnew, 238

Site loyalty, 254

*Solemya*, 331

Skate, 213

SMITH, PETER J. S., see Daniel J. Bogorff, 207; Anthony J. A. Molina, 215

SMOLOWITZ, R. M., see A. D. Hsu, 228; C. R. Sangster, 233; Krystal D. Baird, 235

Soil, 256

Sperm motility, 185

*Spisula*, 192

Sponge, 144, 199

Spore discharge, 236

Squid, 47, 179

- embryo, 181
- giant axon, 187, 188, 190

Squid sperm to clam eggs: imaging wet samples in a scanning electron microscope, 177

Stable isotope, 250, 254

Stable isotopic assessment of site loyalty and relationships between size and trophic position of the Atlantic horseshoe crab, *Limulus polyphemus*, within Cape Cod estuaries, 254

STAKES, DEBRA S., see Jeffrey C. Drazen, 1

Stiffness

- flexural, 36
- torsional, 36

Stress protein, 160

Submarine groundwater discharge, 244, 246

Sulfide, 54

Supramedullary neuron, 211

*Symbiodinium*, 339

Symbiosis, 66, 331, 339

## T

TALBOT, J. M., K. D. KROEGER, A. RAGO, M. C. ALLEN, AND M. A. CHARETTE, Nitrogen flux and speciation through the subterranean estuary of Waquoit Bay, Massachusetts, 244

Taurine, 331

*Tegula*, 276

TEICHBERG, M., see J. A. Morgan, 252; A. B. Aguiar, 259

Telencephalic hemisphere, removal of, 211

Telotroch, 182

TEPSUPORN, S., J. C. KALTENBACH, W. J. KUHN, M. M. BURGER, AND X. FERNANDEZ-BUSQUETS, Apoptosis in *Microciconia prolifera* allografts, 199

Thermal tolerances of deep-sea hydrothermal vent animals from the North-east Pacific, 98

Thermotolerance, 98, 160, 276

Thiotaurine, 331

THOMS, T., A. E. GIBSON, AND K. H. FOREMAN, Multiple approaches to tracing nitrogen loss in the West Falmouth wastewater plume, 242

Three-dimensional birefringence distribution in reconstituted asters of *Spisula* oocytes revealed by scanned aperture polarized light microscopy, 194

3-D

- reconstruction, 351
- stimulus, 225

Time-lapse, 179

Toadfish, 216, 235

TOMANEK, LARS, AND ERIC SANFORD, Heat-shock protein 70 (Hsp70) as a biochemical stress indicator: an experimental field test in two congeneric intertidal gastropods (Genus: *Tegula*), 276

Top-down, 252

Training alone, not the tripeptide RGD, modulates calcitonin in *Hermisenda*, 220

Trait-mediated indirect interaction, 367

Transient use of tricaine to remove the telencephalon has no residual effects on physiological recordings of supramedullary/dorsal neurons of the cunner, *Tautoglabrus adspersus*, 211

Transplantation and isotopic evidence of the relative effects of ambient and internal nutrient supply on the growth of *Ulva lactuca*, 250

Transport, 187

Trematode, 110

Tricaine, 211

*Trichodesmium*, 230

Trochophore, 182

Trophic

- ecology, 93
- position, 254

TSUCHI, AKIFUMI, see Tatsuo Motokawa, 261

Tubulin, 187

TURNELL, E. R., see K. D. Mann, 224

TURNELL, E. R., K. D. MANN, G. G. ROSENTHAL, AND G. GERLACH, Mate choice in zebrafish (*Danio rerio*) analyzed with video-stimulus techniques, 225

TURNER, JOHN R., see Simon K. Davy, 66

Twist-to-bend ratio, 36

Twisting and bending of biological beams: distribution of biological beams in a stiffness mechanospace, 36

250 million years of bindin evolution, 8

## U

UHLINGER, KEVIN R., see Krystal D. Baird, 235

*Ulva lactuca*, 250, 252

*Unio*, 73

## V

VALENTINE, VINTON, see Jason R. Cavatorta, 239; M. E. Johnston, 248

VALIELA, I., see A. B. Aguiar, 250; J. A. Morgan, 252; C. W. O'Connell, 254

*Vampyroteuthis infernalis*, 102

VAN CAMP, L. M., see L. S. Eyster, 47

Veliger, 121

Vesicle transport, 188, 190, 195

*Vibrio alginolyticus*, 233

Vision, 225

Visual sensitivity, 213

Viviparity, 285

## W

- WADESON, P. H., AND K. CRAWFORD. Formation of the blastoderm and yolk syncytial layer in early squid development, 179
- WAINWRIGHT, GEOFFREY, see Carolyn J. Ruddell, 308
- WALKER, C., E. DAVIDSON, W. KINGERLEE, AND K. SAVAGE. Incubation conditions of forest soil yielding maximum dissolved organic nitrogen concentrations and minimal residual nitrate, 256
- WEBB, ERIC, see Elizabeth Orchard, 230
- WEBSTER, SIMON G., see Carolyn J. Ruddell, 308
- WEIDNER, EARL, AND ANN FINDLEY. Catalase in microsporidian spores before and during discharge, 236
- WEIS, V. M., see J. A. Schwarz, 339
- WEISSMAN, IRVING L., see Nanette E. Chadwick-Furman, 133
- WHITE, MICHAEL R. H., see Carolyn J. Ruddell, 308
- WILLIAMS, C., see M. T. Holden, 257
- WÖLLERT, TORSTEN, ANA S. DEPINA, CARL J. DESELM, AND GEORGE M. LANGFORD. Rho-kinase is required for myosin-II-mediated vesicle transport during M-phase in extracts of clam oocytes, 195

## X

- Xenopus* oocytes, 209

## Y

- Yolk syncytial nuclear collapse, 179

## Z

- ZAKEVICIUS, J., see K. Cusato, 197; R. L. Chappell, 209
- Zebrafish, 176, 224, 225
- ZIGLER, KIRK S., AND H. A. LESSIOS. 250 million years of binding evolution, 8
- ZIMMER, CHERYL ANN, see Jonathan T. Fingerut, 110
- ZIMMER, RICHARD K., see Jonathan T. Fingerut, 110
- Zinc, 209, 213
- Zinc chelation enhances the sensitivity of the ERG b-wave in dark-adapted skate retina, 213
- Zinc modulation of hemichannel currents in *Xenopus* oocytes, 209
- Zooplankton, 93
- Zooxanthella, 66, 339
- ZOTTOLI, S. J., O. T. BURTON, J. A. CHAMBERS, R. ESEH, L. M. GUTIÉRREZ, AND M. M. KRON. Transient use of tricaine to remove the telencephalon has no residual effects on physiological recordings of supramedullary/dorsal neurons of the cunner, *Tautoglabrus adspersus*, 211

THE BIOLOGICAL BULLETIN  
(www.biolbull.org)  
2004 SUBSCRIPTION FORM  
(VOLUMES 206-207, 6 ISSUES)

(please print)

NAME: \_\_\_\_\_

INSTITUTION: \_\_\_\_\_

ADDRESS: \_\_\_\_\_

CITY: \_\_\_\_\_ STATE: \_\_\_\_\_

POSTAL CODE: \_\_\_\_\_ COUNTRY: \_\_\_\_\_

TELEPHONE: \_\_\_\_\_ FAX: \_\_\_\_\_

E-MAIL ADDRESS \_\_\_\_\_

All subscriptions run on the calendar year; price includes both print and online journals

Please send me a 2004 subscription to *The Biological Bulletin* at the rate indicated below:

Individual: \$120.00 (6 ISSUES)

Institutional : \$325.00 (6 ISSUES)

Individual: \$70.00 (3 ISSUES)

Institutional : \$165.00 (3 ISSUES)

Check one:  February April June or  August October December

Please send me the following back issue(s): \_\_\_\_\_

Individual: at \$25.00 (PER ISSUE)  Institutional : at \$75.00 (PER ISSUE)

### Delivery Options

\_\_\_\_\_ Surface Delivery (Surface delivery is included in the subscription price.)

\_\_\_\_\_ Air delivery (Please add the correct amount to your payment.)

U.S. and Canada: \$46.00  Mexico: \$60.00  All other locations: \$100.00

### Payment Options

\_\_\_\_\_ Enclosed is my check or U.S. money order for \$ \_\_\_\_\_ payable to The Marine Biological Laboratory

\_\_\_\_\_ Please charge my  VISA,  MasterCard  Discover Card \$ \_\_\_\_\_

\_\_\_\_\_ Please send me an invoice. (Note: Payment must be received before subscription commences.)

Account No.: \_\_\_\_\_ Exp. Date: \_\_\_\_\_

Signature: \_\_\_\_\_ Date: \_\_\_\_\_

Return this form with your check or credit information to:

Marine Biological Laboratory

Subscription Office ♦ The Biological Bulletin ♦ 7 MBL Street ♦ Woods Hole, MA 02543-1015

5034 57

# MARINE RESOURCES CENTER

MARINE BIOLOGICAL LABORATORY • WOODS HOLE, MA 02543 • (508)289-7700

WWW.MBL.EDU/SERVICES/MRC/INDEX.HTML



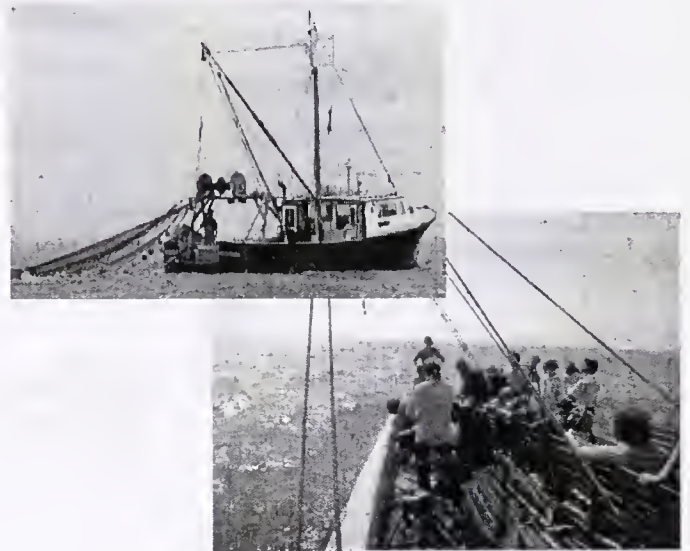
zebrafish facilities

## Animal and Tissue Supply for Education & Research

- 150 aquatic species available for shipment via online catalog: <<http://www.mbl.edu/animals/index.html>>; phone: (508)289-7375; or e-mail: [specimens@mbi.edu](mailto:specimens@mbi.edu)
- zebrafish colony containing limited mutant strains
- custom dissection and furnishing of specific organ and tissue samples

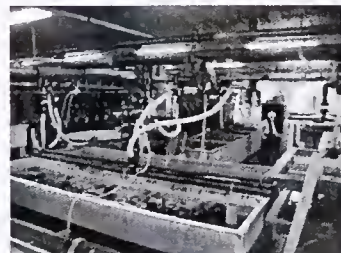
## MRC Services Available

- basic water quality analysis
- veterinary services (clinical, histopathologic, microbial services, health certificates, etc.)
- aquatic systems design (mechanical, biological, engineering, etc.)
- educational tours and collecting trips aboard the R/V Gemma



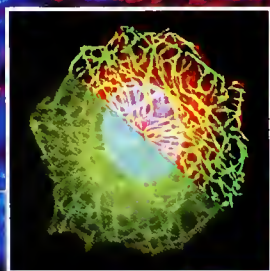
## Using the MRC for Your Research

- capability for advanced animal husbandry (temperature, light control, etc.)
- availability of year-round, developmental life stages
- adaptability of tank system design for live marine animal experimentation



# The Bar Has Been Raised

## Axioplan 2 Research Microscope.



A digital microscope designed for the future, Zeiss Axioplan 2 Imaging is a marvel of modern engineering. With new optics of high light transmission, precision of its innovative components and infinite flexibility, Axioplan 2 is a reliable partner that meets

the latest demanding requirements today and for the years to come. No wonder the Axioplan 2 Imaging has become the best selling research microscope in America!

For information about Zeiss products please call 800-233-2343 or visit us online: [zeiss.com/micro](http://zeiss.com/micro).

Carl Zeiss MicroImaging, Inc. • Thornwood, NY 10594 • [micro@zeiss.com](mailto:micro@zeiss.com)



We make it visible.





MBL/WHOI LIBRARY



WH LARS T

